

Final Scientific Report

Fenestration System Performance Research, Testing, and Evaluation

Award Number: DE-FC26-04NT42109

Award Recipient: The National Fenestration Rating Council

Project Director: Jim Benney

Team members: Carli, Inc, Architectural Testing, Inc., Center for the Built Environment, Enermodal, Sunergy, Solar Consulting Services, WinBuild, Lingnell Associates, Sunpine Consulting, Tait Solar, Heschong Mahone Group

DISCLAIMER

This report was prepared as an account of work sponsored by an agency of the United States Government. Neither the United States Government nor any agency thereof, nor any of their employees, makes any warranty, express or implied, or assumes any legal liability or responsibility for the accuracy, completeness, or usefulness of any information, apparatus, product, or process disclosed, or represents that its use would not infringe privately owned rights. Reference herein to any specific commercial product, process, or service by trade name, trademark, manufacturer, or otherwise does not necessarily constitute or imply its endorsement, recommendation, or favoring by the United States Government or any agency thereof. The views and opinions of authors expressed herein do not necessarily state or reflect those of the United States Government or any agency thereof.

Table of Contents

Executive Summary 3
NFRC Introduction 5
Accomplishments versus Goals and Objectives 6
Project Activities and Summary Developed 8
Product Developed 28
Computer Modeling Developments 34
Summary 36

Executive Summary

The research conducted by the NFRC and its contractors adds significantly to the understanding of several areas of investigation. NFRC enables manufacturers to rate fenestration energy performance to comply with codes, participate in ENERGY STAR, and compete fairly. NFRC continuously seeks to improve its ratings and also seeks to simplify the rating process. Several research projects investigated rating improvement potential such as

- Three Dimensional Corner Heat Transfer Effects in Fenestration Products
- Heat Transfer Effects of Sloped, Ventilated Cavities Framing
- Revision of Standard Spectral Weighting Function for Calculation of Solar Optical Properties and Solar Heat Gain
- Window 6 and Therm 6 Validation Research Project
- Tubular Daylighting Devices U-factor Rating

Conclusions from these research projects led to important changes and increased confidence in the existing NFRC rating process. Conclusions from the Window 6/Therm 6 project will enable window manufacturers to rate an expanded array of projects and improve existing ratings.

Some research lead to an improved new rating method called the Component Modeling Approach. A primary goal of the CMA was a simplification of the commercial energy rating process to increase participation and make the commercial industry more competitive and code compliant. The project below contributed towards CMA development:

- Component Modeling Approach Frame Grouping Research
- Component Modeling Approach Condensation Resistance Research
- Component Modeling Approach-Non Standard Products Research Project

Results from each of these completed projects were quickly integrated into the developing CMA software tool to ensure accurate ratings and a reasonable array of product rating potential.

Some projects served to open up the potential for new ratings in the near future:

- Effect of Surface Heat Transfer Coefficients on U-factor for Highly conductive and Projecting Products
- Thermal Comfort Rating
- Glass Block Solar Heat Gain Research
- Angle Dependence of Fenestration Attachments
- Development of a Procedure and a Model for U-factor Rating of Domed Skylights
- Complex Product VT Rating Research Project

Currently, NFRC cannot rate attachments (blinds, shades), glass block (diffuse glazings), highly projecting products (garden windows, domed skylights) or accurately measure visible light in some applications. The projects listed above are a basis to build upon towards new ratings for these products. NFRC is actively working with the attachment industry towards ratings. Diffuse glazing measurements will expand NFRC's rating capabilities to popular products such as frits and glass block. NFRC continues to pursue all these areas with industry towards expansion of its rating capabilities.

NFRC completed the development of the Component Modeling Approach program. The program includes the CMA software tool, CMAST, and several procedural documents to govern the certification process. This significant accomplishment was a response the commercial fenestration industry's need for a simplification of the present NFRC energy rating method (named site built). To date, most commercial fenestration is self rated by a variety of techniques. The CMA enables commercial fenestration manufacturers to rate according to the NFRC 100/200 as most commercial energy codes require. As of this writing, the CMA program has been launched and NFRC is working towards full implementation.

NFRC carefully considers the technical effectiveness and economic feasibility of existing and potential new ratings. Much of the research becomes the technical basis for ratings. The NFRC membership carefully considers this prior to moving forward with a rating. NFRC requires full industry participation prior to considering future energy ratings.

NFRC achieved significant international harmonization success by licensing the Australian Fenestration Rating Council and the Association of Architectural Aluminum Manufacturers of South Africa (AAAMSA) to product NFRC certified product ratings in their respective nations. NFRC worked in several other nations to introduce the NFRC ratings system:

- India
- China
- Jordan
- Kuwait
- Japan

NFRC attended or hosted several meetings in each of these nations establishing academic, commercial, industrial, and governmental contacts. NFRC presented the NFRC process and then necessary infrastructure steps necessary to achieve harmonization with the NFRC labeling system. Each of these nations is in various stages of becoming an NFRC licensee with India the most likely to do so first. NFRC looks forward to continued work toward harmonization in these nations and potentially others.

The public benefit NFRC offers is significant. ENERGY STAR, USGBC-LEED, ASHRAE 90.1, and IECC all reference NFRC 100 and NFRC 200 exclusively for fenestration energy compliance. NFRC operates a significant qualify control program involving third party certification for all product ratings. Consumers can easily identify the most energy efficient products for their homes based on NFRC ratings. NFRC publishes all participating manufacturer ratings on its web site via a certified product directory accessible to the public and updated frequently.

NFRC Introduction

The National Fenestration Rating Council (NFRC) is a non-profit, public/private organization created by the window, door, and skylight industry. It consists of representatives from many aspects of the energy and fenestration sectors:

- fenestration product manufacturers and suppliers
- major trade organizations
- state energy officials
- research organizations
- utilities
- specifiers
- testing laboratories
- energy consultants
- public interest groups
- building and code industry representatives
- government agencies

On June 25, 1989, a group of fenestration industry professionals gathered at an ASHRAE meeting in Vancouver, BC to discuss the founding of the NFRC. The lack of a credible and fair energy rating system at that time had caused confusion in the marketplace. Industry experts agreed about the need for a third party to rate fenestration performance. Additionally, these experts agreed the administering entity needed to be comprised of a broad array of fenestration interests thus the diverse list shown above. This diversity ensures that no single interest in the industry is catered to unfairly. On December 4, 1989, the first NFRC meeting was held in Orlando, Florida to sketch out the details of the organization and its goals.

Today, the National Fenestration Rating Council lists over 2.5 million fenestration product energy ratings. Over eight hundred manufacturers participate in the ongoing committee sessions to refine the energy rating process continuously for the consumer. Today, the National Fenestration Rating Council energy ratings are referenced by the International Energy Conservation Code to which most state legislatures enact reference. The National Fenestration Rating Council continues to be primary energy rating entity for the nation. The National Fenestration Rating Council also continues to pursue international harmonization with many nations including China, India, the European Union, and Canada.

The US DOE supported the 1989 foundation of the organization and provided initial funding. NFRC now operates independently and is fully funded by membership and participation fees. The US DOE continues to provide cooperative agreements with NFRC for research, international harmonization, and new rating development. The US DOE funding were and are instrumental in the NFRC's continued success.

NFRC is a consumer organization. Independent ratings are essential. A system of test labs, simulating labs and independent agencies exists to ensure these features. Simulating labs gather manufacturer supplied energy performance data for input into fenestration simulation programs. These simulations produce whole product U-factor ratings, visible transmittance (VT), and solar heat gain coefficients (SHGC). Next, manufacturers are required to confirm their simulated U-factor ratings by physically testing one product per product line every four years. An NFRC accredited testing laboratory performs these tests. U-factors indicate the heat loss of a window from inside

to out. The simulated and tested U-factor ratings are sent to an independent agency for comparison and validation. Once the ratings were compared and confirmed to be within the required tolerance, the manufacturer is then authorized to put an NFRC label on their product line. Note the legal liability for the rating lies with the manufacturer, not the independent agency or NFRC.

NFRC Process



Accomplishments versus Goals and Objectives

NFRC-DOE Cooperative Agreement Original Goal and Objective:

The National Fenestration Rating Council (NFRC) is a broad coalition of organizations representing the fenestration industry, other segments of the building industry, state governments, utilities, and public interest groups. The purpose of NFRC is to establish a fair, accurate and credible rating system for fenestration products and to coordinate certification and labeling activities to ensure their uniform application.

NFRC's mission regarding a "fair, accurate and credible" rating system, as well as the Federal Trade Commission's requirements for a rating system which is "open to innovation" and has a "sound technical basis" poses significant research requirements. Also, the acceptance of the technical basis for the rating system by the international scientific community (and subsequently by the International Organization for Standardization) requires a high degree of technical excellence. Further, research is required to extend the rating system to address all key thermal and optical properties and the energy and peak load impacts of fenestration on buildings (and utility systems). New or improved simulation tools and test procedures are needed to address a broader scope of technologies. These tools would be more accurate, more "friendly," less costly to use and capable of interfacing with the design process.

The NFRC pursued three primary tasks for this project to achieve this goal:

1. Fenestration Research
2. Software Tool Improvement
3. International Harmonization

The NFRC operates a Research Program using its Research Program Manual[1] that requires the development of RFPs, bid solicitation and award, and result presentation to the NFRC membership. Results from the research are then put into practice by modifying the various NFRC technical documents. These modifications serve to continuously improve the NFRC fenestration energy rating system.

NFRC's goal to maintain and improve its fenestration energy rating systems was accomplished by developing, awarding, and integrated results from several research projects.

Since 2005 and with the US DOE's assistance, NFRC has achieved the following:

- New commercial energy rating method created an launched (task 6)
  - Component Modeling Approach
  - January 1, 2010 effective date
- New applied film rating developed (task 1)
  - Ten manufacturer participants to date
- Completed several research projects (task 1)
- Added South African and Australian licensees (task 3)
- Developed fenestration rating facilities in India (likely to become licensee in 2010) (task 3)
- NFRC ratings remain essential in residential and commercial building energy codes (IECC, ASHRAE)
- NFRC ratings for at least 90% of all residential window and door products
- 300% manufacturer participation increase (200 to 800 window manufacturer participants)
- 166% annual operating budget increase ($1.5 to $4.0 million)
- 33% operating efficiency increase
  - $7500/manufacturer participant in 2005 to $5,000/participant in 2009
- NFRC ratings remain as the exclusive required referenced for the ENERGY STAR windows program
- Annual Energy Rating process formalized, but voluntary

More detailed information is contained in the next section of this report.

[1] NFRC 703-2010-Research Program Manual

Project Activities

NFRC and its contractors conducted numerous activities to accomplish this agreements goal. Below is a summary of project activities and summaries of the actual accomplishments. For more detailed explanations of the research tasks (number 1.X.X) see the full research reports referenced in the next report section titled, Product Developed.

Statement of Work Task	Project	Goal	Actual Accomplishment
1.1.1	Effect of Surface Heat Transfer Coefficients on U-factor for Highly conductive and Projecting Products	The main objective of the proposed research project is to develop more accurate boundary conditions for use in projecting and highly conductive fenestration products	This research confirmed that ISO 15099 boundary conditions will work on projecting products. The research recommends that new simulation methods would need to be developed to accurately measure the U-factor for projecting products. The research achieved the goal of determining the effect of heat transfer coefficients on projecting products and made recommendations to further investigate more accurate testing models involving a projecting CTS.

Statement of Work Task	Project	Goal	Actual Accomplishment
1.1.2	Three Dimensional Corner Heat Transfer Effects in Fenestration Products	The objectives of this project are to develop procedures consisting of formulas, correlations, or correction factors, or their combinations, which will be applied to two-dimensional computer models to properly account for the three-dimensional effects in fenestration systems.	The first conclusion from this study is that for present day frame, spacer and glazing materials, 3-D corner conduction heat transfer effects are fairly small and can be ignored in existing fenestration computer modeling tools. For insulating frames and super insulating glazing, the difference between 2-D and 3-D heat transfer effects becomes more pronounced and significant and it exceeds 2% for smaller size windows. Spacer conductivity does not play significant role in the level of differences between 3-D and 2-D conduction heat transfer models. On an individual component level, there were more significant differences, going up to 10%. These differences, would however often cancel each other as the frame and edge of glass sections would usually have different sign in front of the difference.
1.1.3	Thermal Comfort Rating	This research project will deliver a practical procedure for a pilot Window Comfort Rating that could be applied by the NFRC.	The researchers achieved the research goal of determining potential equations for a summer and winter comfort ratings using computer modeling techniques.
1.1.6	Heat Transfer Effects of Sloped, Ventilated Cavities Framing	To develop new set of correlations for sloped frame cavities and criteria and correlations for ventilated frame cavities. The correlations would be used in 2-D computer	1. Newly developed experimental techniques for measuring heat transfer in vertical and tilted frame cavities (i.e., modified C518 apparatus for horizontal frame members and modified hot box apparatus for vertical frame members)

Statement of Work Task	Project	Goal	Actual Accomplishment
1.1.6	Heat Transfer Effects of Sloped, Ventilated Cavities Framing	tools for determining U-Factor and CI for fenestration products.	can be used for research level validation of numerical modeling of heat transfer by convection in these cavities. 2. The 2-D modeling assumption is appropriate to predict natural convection heat transfer in frame cavities tilted around the long axis, such as the ones found in sill, head and horizontal meeting rail and mullion cross-sections (i.e., horizontal frame members). 3. The 2-D modeling assumption is not appropriate to predict natural convection heat transfer in frame cavities tilted around the short axes, such as the ones found in jambs, and vertical meeting rail and mullion cross-sections (i.e., vertical frame members) and full 3-D models need to be utilized. 4. From 3-D modeling results it can be concluded that for vertical frame members, frame cavity correlation equations suggested by ISO 15099 do not match well the results of this study and new correlations will have to be proposed. 5. Numerical modeling of ventilated frame cavities produced experimentally validated results. The new correlations are proposed for the calculation of convection heat transfer in these cavities.

Statement of Work Task	Project	Goal	Actual Accomplishment
1.1.7	Development of a Procedure and a Model for U-factor Rating of Domed Skylights	To develop methods and procedures to simulate and validate domed skylights for their nighttime thermal performance.	The principal investigator did develop methods and procedures to measure U-factors for domed skylights and achieved the research's goals. Several equations were developed for integration into NFRC 100 (U-factor calculation) and can be found in the full research report (Appendix G). NFRC 100 instructs the WINDOW5/THERM5 software on how to make the calculation.
1.1.8	Tubular Daylighting Devices U-factor Rating	To develop a standard test method and procedure to measure the thermal transmittance (U-Factor) of TDD products under typical residential application conditions.	The researcher achieved the goal of developing a U-factor transmittance measurement method for Tubular Daylighting Devices. This method will supersede the current method and will go into effect in 2012.
na	Entrance Door Systems Rating Simplification	Develop a simplified door rating method based on analysis of existing door ratings where components might be extracted and used to predict common component performance.	The principal investigator was able to determine door rating trends and integrate the finding into NFRC Technical documents. The research goals were achieved and a modest simplification of the rating method was achieved as well.

Statement of Work Task	Project	Goal	Actual Accomplishment
1.1.13	Component Modeling Approach Frame Grouping Research	Develop frame grouping rules considering non-residential products, in addition to residential products, so that new frame grouping rules can include most fenestration products, either residential or non-residential. In addition to whole product grouping rules, investigate and develop frame grouping rules specific to frame component submission in the new CMA as being the basis for the new non-residential NFRC procedure.	This research concluded with several recommendations for frame grouping. The recommendations were integrated into the new CMA software tool (CMAST). The new CMAST is commercial available now and using the results from this research. The research goals were achieved.
1.1.14	Component Modeling Approach Condensation Resistance Research	Develop a Component Modeling Approach (CMA) simulation procedure for Condensation Resistance so it can be used in conjunction with the CMA methodology currently being developed for U-factor, SHGC, and VT. Review and comment on the AAMA test-only procedure for CRF. Investigate if some hybrid procedure can be developed that produces a CRF like number, and is applicable to CMA methodology.	The researcher has achieved the primary goals of the project to identify the best methods to calculated condensation resistance within the CMA method. Results of the research will be integrated into the CMA software tool in the near future. The researcher has also made recommendations on potential CR harmonization with the AAMA CR standard.

Statement of Work Task	Project	Goal	Actual Accomplishment
1.1.15	Component Modeling Approach-Non Standard Products Research Project	Simulate selected group of non-standard products using both standard THERM/WINDOW and CMA methodology, so that it can be confirmed that these products can be covered by CMA methodology. In case that for some or all of these products CMA methodology does not produce satisfactory answers, propose course of action and provide recommendations for further research to resolve discrepancies. These products include: -Single Glazing Structural glazing Sloped Glazing -IG incorporating a laminate layer Double Sash Configuration	The results from the both conventional (THERM/WINDOW) and CMA based simulations were compared. All of the U-Factor results are within the expected discrepancies (i.e., less than 0.02 Btu/(hr-ft2-F), with the majority being below 0.01 Btu/(hr-ft2-F). SHGC results are all within 0.01 while VT results are identical in both procedures. The results are summarized in Table 1 of the final research report (appendix L). From the results, it can be concluded that current CMA procedure can be confidently used for all the non standard products. The research goals were achieved.
1.1.16	Revision of Standard Spectral Weighting Function for Calculation of Solar Optical Properties and Solar Heat Gain	To provide a recommended spectrum to NFRC by assessing the impact of a potential change in the reference spectrum that is used to properly weigh the spectral transmission calculations through glazing.	The researcher achieved the primary goal to investigate the effects of modifying the spectrum that NFRC ratings use. The project evaluated several NFRC ratings with the latest ASTM spectrum developed. The results presented would modify all NFRC ratings, particularly the SHGC ratings making them somewhat higher.

Statement of Work Task	Project	Goal	Actual Accomplishment
1.1.17	Complex Product VT Rating Research Project	Establish VT rating conditions for TDDs and determine if a goniophotometer can be used to determine NFRC-ratable visible transmittance (VT) for TDDs.	Lawrence Berkeley National Labs and two Tubular Daylighting Devices manufacturers are completing testing and compiling results. Preliminary results indicated good agreement for the testing of a common product.
1.1.18	Window 6 and Therm 6 Validation Research Project	This research project will gather and generate about 20 SHGC and 20 U-Factor physical test results for comparison with the results from simulating these complex glazing systems using newly developed WINDOW 6 and THERM 6 simulation software.	All U-factor and SHGC physical tests are complete and only a few U-factor and SHGC simulations remain. This research includes several attachment products (blinds, shades). The researcher achieved several interim goals of the research and reports are included in appendix O.
2.0	Development of NFRC 101-Thermonphysical Properties of Materials for use in NFRC approved Software	To continuously update the NFRC 101 to capture the latest thermophysical properties available in the marketplace	NFRC 101, *Thermophysical Properties of Materials for Use in NFRC Approved Software* is a repository for non glazing thermophysical properties for use in NFRC approved Software WINDOW 5/THERM5. Frequently, manufacturers want specific materials to be added beyond the more common, generic material. NFRC amended this document via a peer reviewed process to include manufacture specific properties. NFRC worked with the University of Massachusetts do continuously develop this document. From 2005 to 2009, approximately 26 peer reviewed materials were added to the document.

Statement of Work Task	Project	Goal	Actual Accomplishment
3.1	International Standard Organization	Attend relevant ISO meetings to promote and harmonize NFRC rating procedures and monitor ISO procedures that could be or are currently NFRC referenced.	Carli, an NFRC contractor, attended two ISO TC163 meetings each year from 05 to 09 regarding ISO 18292-Energy performance of fenestration systems - Calculation procedure. This procedure calculates the energy consumption of a window based on how it is used in a typical home. NFRC has developed a similar procedure, NFRC 901-Annual Energy Performance and is working with ISO towards potential harmonization or minimally good understanding of the various assumptions that ISO is making to for the calculation procedure. Work continues on ISO 18292 towards publication and implementation/adoption.
3.2	International Harmonization	Work with Australian, South African, Chinese, Indian, Japanese, Kuwaiti, Korean, and Jordanian Fenestration industry authorities to harmonize NFRC rating system. South Africa	NFRC established the Australian Fenestration Rating Council, AFRC that is licensed to produce NFRC certified ratings. AFRC has trained simulators and is developing test facilities as required by the program. NFRC licensed the Association of Architectural Aluminum Manufacturers of South Africa (AAAMSA) to produce NFRC ratings and continues to develop infrastructure prior to full implementation. NFRC also accredited a thermal testing lab and trained simulators in South Africa as they move towards a full NFRC certification system.

Statement of Work Task	Project	Goal	Actual Accomplishment
	International Harmonization	South Africa Chinese Harmonization	NFRC attended numerous conferences to introduce the NFRC rating system to China. They are listed here: The Glass Processing Days China conference, April 9th, 2008: Presented a paper at the conference entitled "Energy performance calculation for fenestration product using different environmental conditions adopted by various country codes and its impact". On April 10th: Visit to China Glass Show meeting with Mr. Mo WenYi, Director, China Ceramic Society, the organizer of the China Glass show, to discuss future cooperation. Visited key Chinese glazing manufacturers along with him at the show. April 11th: Visit to China Building Material Academy (CBMA), Certification Testing Center (CTC) and China Building Research Academy (CBRA) to discuss future cooperation regarding development of an energy efficiency rating and labeling program in China. The CBMA delegation included their Mrs. Yao Yen president, Mr. Shi Xinyong assistant President, Ma Zhenzhu vice director, Dr. Sui Tongbo and others. Visited the China Building Material Test and Certification Center which is a subsidiary of CBMA and is

Statement of Work Task	Project	Goal	Actual Accomplishment
	International Harmonization	Harmonization with China	in the same facility as CBMA. The centers insulating glass testing facility has received IGCC accreditation. April 12th, USA-China Conference on Energy Efficiency in Building Envelope, Beijing, China: Workshop/Conference involving Chinese association, institute and government officials to discuss Window energy ratings and labeling. Over 90 selected representatives from US and Chinese government, institutes, association and manufacturers attended the conference. The MOC, CBMA, CBRA, CCMSA, CAIGA and CRECC provided information about the Chinese energy efficiency standards requirement and a synopsis of the window energy rating and labeling program. US-DOE, NFRC and IWFA provided information about the USA codes and window energy rating and labeling program and areas of cooperation. April 13th, Meeting with Ministry of Construction: Mr. Marc Lafrance (US-DOE), James Benney (NFRC), Darrell Smith (IWFA), and Bipin Shah (WinBuild Inc) met with Mr. Liang Jungiang, the Director of the Division of Building Energy Efficiency, The Ministry of Construction and Mr. Shi Xinyong

Statement of Work Task	Project	Goal	Actual Accomplishment
	International Harmonization	Kick off meeting with the Chinese *Research Institute of Standards and Norms (RISN)*	assistant President CBMA. The main topic of discussion was to submit a "Flagship" proposal to the APP for financial support of a Chinese Fenestration Ratings Council. In November 2008, NFRC attended a kick of meeting Beijing China with Chinese partners RSIN Research Institute of Standards & Norms (RISN) of Ministry of Housing Urban-Rural Development (MOHURD, used to be Ministry of Construction) and CBMA for planning tasks and its execution for the APP project, 'Building Energy Performance Certification'. Representative of NAIMA, Ron Pickering (CSR group) and David Tang (Owens Corning) also participated in the meeting.
		Present Harmonization information at the *Fenestration China Conference*	NFRC presented at the Fenestration China Conference, November 16-17, 2008. In November NFRC met with CAM, China Association of Mayors and CADRG, China Architecture Design & Research Group for planning USA-China Building Envelope Energy Efficiency and Safety Technology conference, March 2009.
		Develop Simulation Manual in Chinese language with China	In November 2008, NFRC visited the CBMA laboratory to access the needs for upgrading the testing laboratory hot box and Air infiltration testing chambers.

Statement of Work Task	Project	Goal	Actual Accomplishment
	International Harmonization	Building Material Academy Attend USA-China Building Envelop Energy Efficiency and Safety Conference Harmonization work in India Train Indian technical persons on NFRC simulation software operation Meet with several Indian technical persons to work toward CEPT establishment	March 23-24, 2009: Worked with China Building Material Academy (CBMA) to develop simulation manual in Chinese which lists the USA and the Chinese simulation modeling requirements. March 26, 2009: USA-China Building envelope Energy Efficiency and Safety conference where more than 150 people attended. March 27, 2009: Visited the US Pavilion at the China Green Building Expo in Beijing, China: March 27, 2009: Meeting with Yang Shichao, Vice President, Guangdong Provincial Academy of Building Research. NFRC conducted and attended several meetings in India to introduce and begin to establish the NFRC rating system in India. Design Builder workshop: December 3-4, 2008: Coordinated and arranged a Design Building, Building simulation software training program. Dr. Mahabir Bhandari of DesignBuilder-USA provided the training to 8 people, of which one was an ECO-III engineer Mr. Anurag Mathur. December 5, 2008 Meeting with Glazing Industry Representatives. Attending:

Statement of Work Task	Project	Goal	Actual Accomplishment
	International Harmonization	HOst USA Pavilion at the Door and Window Trade Show in New Delhi	Mr. Shah of WinBuild, Jim Benney (NFRC Executive Director), Werner Lichtenberger (NFRC Board of Director, Ex-offico), Mr. met with Mr. Anand Jain and Mr. Subramanian (Saint Gobain), and Rajan Rawal (CEPT) to discuss the status of the industry funding support for the establishment of energy center at CEPT. USA Pavilion at Door and Window Trade Show: December 5-7, 2008 NFRC organized the US-Pavilion where US-DOE, NAIMA, CRRC, IWFA and NFRC participated at the Door and Window trade show in New Delhi and demonstrated advanced building envelope components and fenestration technologies.
		Organize the Building Envelop Energy Efficiency Technologies Conference	Conference on Building Envelope Energy Efficiency Technologies: December 7, 2008. NFRC and WinBuild organized the Building Envelop Energy Efficiency Technologies working with BEE, IRG, and CEPT. The conference was organized by the Zak trade show. NFRC, NAIMA, CRRC and IWFA sponsored the event and companies such as True Seal, 3M, CP Film, Owens Corning, Saint Gobain, TRACO, Technoform and Design Builder-USA participated in the conference. Several key Indian companies, such as
		Meet with the Indian Ministry of New and Renewable Energy	

Statement of Work Task	Project	Goal	Actual Accomplishment
	International Harmonization	Meet with the Glazing Society of India to begin to discuss the establishment of an NFRC based rating system at this association/society.	Reliance, also participated. Initiative with Ministry of New and Renewable Energy: December 8th, 2008 Mr. Shah had a Meeting with Dr. Ashwini Kumar, Director MNRE, on December 8th, 2008. MNRE is interested in collaborating with US-DOE and NFRC in establishing an energy rating for residential buildings. August 18th -20th and 22nd-25th meetings held at Indian Center for Environmental Planning and Technology (CEPT). August 22nd meeting held with Glazing Society of India (GSI): Meetings were held with Dr. R.N Vakil, Mr. Mukul Doctor and Mr. Rajan of CEPT for planning installation of the Air Leakage chamber, Solar Calorimeter, and other equipment in the Regional Energy Efficiency Center (REEC). These equipments are part of the REEC requirements to test the building envelope component energy performance. Further discussions were held with Dr. Patel of CEPT on documenting the equipment procedure, quality control, and operations procedure. Mr. Shah will work with CEPT for these documentation and providing the design and construction guidelines.
		Continued GSI and CEPT meetings	August 22nd Meeting held

Statement of Work Task	Project	Goal	Actual Accomplishment
	International Harmonization	towards NFRC rating system establishment	with CEPT and the Glazing Society of India which was represented by the new Executive Director, Mr. A. Kumarasamy, Chairman Mr. Subramanian and Saint Gobain representative Mr. Anand Jain. Discussions were related to identifying the steps and goals to expediting the formation of rating program in India for fenestration products and signing of the Memorandum of Understanding (MoU) between CEPT and GSI for testing service for certification program. Tentative date for signing the MoU is September 5th, 2009.
		Ministry of New and Renewable Energy and ECO III meetings to continues work towards NFRC rating system establishment	August 21st -22nd meeting held with the Ministry of New and Renewable Energy (MoNRE) and ECO-III. Ms. Gauri Singh (Joint Secretary Government of India, MoNRE), Dr. Ashvini Kumar, Director (Solar Thermal), Mr. Bipin Shah (representing WinBuild Inc and NFRC), met and discussed the further needs for the establishment of the REEC at CEPT in Ahmedabad and cool roof rating center at International Institute of Information and Technology (IIIT) in Hyderabad. Discussions were held to finalize the visit by MoNRE and industry representatives to USA to discuss research and technology collaboration. Tentative dates of September 28 to October 2nd, 2009 were

Statement of Work Task	Project	Goal	Actual Accomplishment
			finalized.
	International Harmonization		Met with Mr. Satish Kumar of ECO-III team to discuss the upcoming Indian delegation visit to the USA, which will focus on demonstrating the working of National Fenestration Rating Council working in the USA. Mr. Shah will coordinate the NFRC administrative office, test and simulation laboratory, NFRC licensed inspection agency and a manufacturer visit.
		Harmonization discussed with the Indian Applied Film representatives	Meeting was held with the Indian applied film representatives, August 26th, 2009: Met with Mr. Rahul Batija of Hanita Inc, and Meeta Zaveri of Lumar Inc. Discussions focused on how to educate consumers in India about the application of the applied films for Energy Efficiency retrofit solutions.
		Several Indian industry experts visited NFRC Headquarters in Greenbelt, MD and test facilities in PA	In October 2009, 10 Indian Fenestration and building industry experts visited the NFRC HQ in Greenbelt and toured NFRC accredited test labs and inspection facilities in York, PA.
		Meet with Japanese officials to discuss potential international harmonization work with the Japanese government and industry.	NFRC worked in Japan meeting with industrial, governmental, and commercial authorities, but the Japanese are reluctant to pursue NFRC harmonization presently. One Japanese company may pursue NFRC ratings to demonstrate the value in the

Statement of Work Task	Project	Goal	Actual Accomplishment
	International Harmonization	Meet with Jordanian Industry experts to begin harmonization efforts in the Middle Eastern Region.	marketplace. NFRC traveled to Jordan twice to attend the U.S.-Jordanian Joint Committee Meeting (JCM) on Science & Technology (S&T) Cooperation, July 9–10, 2008, in Amman. NFRC, with support from US-DOE, conducted a Jordan-American Building Envelope Energy Efficiency Technology Cooperation Workshop where all key stakeholders from Jordan attended on October 25th, 2008. NFRC provided basic training in THERM, WINDOWS and OPTICS software on October 26 and 27 to 16 attendees for the workshop. An NFRC representative visited the Jordan higher Council research center and testing laboratory, October 28, 2008, to access the set-up and to determine the needs for establishment of building envelope testing center.
		Attend the GCREEDER conference in Amman, Jordan to discuss potential international harmonization work.	The National Fenestration Rating Council (NFRC) participated at the GCREEDER-2009 conference in Amman Jordan, March 31st -April 2nd, 2009. The NFRC worked with Higher Council for Science & Technology (HCST) to coordinate and host a workshop on April 1st, 2009 in Amman Jordan that included 4 regional countries, Jordan, Kuwait, Yemen, and Lebanon

Statement of Work Task	Project	Goal	Actual Accomplishment
	International Harmonization	Work with USAID and the Higher Council for Science and Technology to develop energy efficient building component strategies.	participating along with regional US manufacturers' participation. The key US building envelope stakeholders participating included NFRC, the International Window Film Manufacturer Association (IWFA). Mr. Ross Hagan, Director, Energy Office, USAID/Jordan also participated in the meeting. USAID has keen interest to work with US-DOE to develop of regional codes and promote energy efficiency building envelope product in the region. General Secretary of HCST, Dr. Anwar M. Battikhi and Energy Advisor to the Council Dr. Mohammad Hamdan pledged the needed support for the effort. Future activities will likely include study of different regional building codes, case study of building construction, simulation training for fenestration, building energy efficiency and window film and other component installation. Final goal of this effort is to develop a regional energy building energy efficiency code for Middle Eastern countries which will help USA manufacturers to sell energy efficient product in the region without barriers to comply with different codes. US-DOE, NFRC and HCST meeting with USAID April 2nd, 2009: A representative of the (NFRC), US-DOE and the Higher Council for

Statement of Work Task	Project	Goal	Actual Accomplishment
	International Harmonization	Meet with Kuwait Institute of Scientific Research to establish a potential building envelope energy efficiency rating system.	Science & Technology met with USAID to discuss future project. April 3rd, 2009; Meeting with Maisam architect and engineering firm to discuss the case study for application of newly developed Jordan building energy efficiency for a building in Amman Jordan. Kuwait, September 21-23, 2008: Significant progress was made with the Kuwait Institute for Scientific Research (KISR) to establish building envelope energy rating program. KISR would like to work with US-DOE, NFRC, NAIMA, CRRC and other USA association in expediting the implementation. They will be preparing a proposal for obtaining funding from their government and then would like our assistance in upgrading their Laboratory and development of the Rating program.

Statement of Work Task	Project	Goal	Actual Accomplishment
4 (2008 only)	IG Durability and Applied Film Status Harmonization (low-e technology promotion)	NFRC and its contractor will work towards instituting IG durability requirements as part of fenestration energy ratings. The contractor will gather standards and determine existing state of any IG durability code and energy rating systems in the countries of interest. Applied films are a good solution for aftermarket energy efficiency on existing buildings. NFRC and its contractor will work with APP and NFRC countries to harmonize applied film standards.	China has adopted the European procedure for testing Insulated Glazing units (IGU). The contractor participated in several experts meeting, and concluded that the efforts to convince the Chinese to adopt North American practice is futile, and therefore recommends ending the efforts for IGU standards harmonization with China.
5 (2008 only)	IG and Applied Film ISO Activities	NFRC and its contractor will begin to reinvigorate efforts at ISO by bringing forward NFRC's requirements as a proposed international standard. NFRC and its contractor will participate in harmonization efforts with China, India, and Australia to significantly improve sealed insulated glass durability requirements.	The China National Centre for Quality Supervision & Testing of Glass (CCQTG) is in the process of finalizing the applied film standards by end of 2010. Gaining importance, the standard has been elevated to a National Standard status. It is recommended to monitor this activity and assisting CCQTG with any additional information required. NFRC hosted an industry meeting including Chinese and American attendees to gather input for Chinese applied film standards.

Statement of Work Task	Project	Goal	Actual Accomplishment
6 (2008 only)	Component Modeling Approach (CMA)	NFRC will work on three primary CMA tasks: 1. Software Development 2. Pilot Implementation and Training Program 3. Marketing and Education	NFRC completed development of the Component Modeling Approach Program. This new calculation method is integrated into NFRC's existing rating program conforming to the fundamental rating requirements in NFRC 100 (U-factor) and NFRC 200 (SHGC, VT). This new rating calculation method is online enabling users to more simply calculate commercial fenestration energy performance. NFRC conducted CMAST user training sessions throughout the US and officially launched the CMA program in January 2010. NFRC hired Heschong Mahone to market the CMAST in California where energy codes are more robustly enforced. Please note the CMA method produces U-factors, SHGC, and VTs according to NFRC 100 and 200. This fact enables CMA to become pertinent to ASHRAE 90.1 code requirements immediately since NFRC 100/200 is directly referenced. California's Title 24 codes also directly references NFRC 100/200. As of May 2010, NFRC has achieved five label certificates, trained

Product Developed

Task 1, fenestration research, resulted in one final paper for each completed project. Projects not yet complete do have interim reports and these are provided. NFRC posts

the final paper on its own website for public review of its most current research and archives older research papers making them available upon request to NFRC members and the public. For convenience, hyperlinks to local files in the folder are provided for the reader to open the full, final research report PDF documents. Web links are also provided for additional information.

All individual project activities are summarized within the final report and include original hypothesis, approaches used, problems encountered, and assessment of impact on final results. Applicable facts, figures, analyses, and assumptions are contained within the reports as well.
Tasks 2-6 are described in the table below also. Networks, collaborations, technologies, and license agreements did result while performing these tasks are included below.

Task 6, Component Modeling Approach, is a large task that was partially funded during 2008. Since this project resulted in software development, it is summarized in this paper under the section titled, Computer Modeling Developments. Other supporting items for this task are listed below as well.

Statement of Project Objective Task #	Project	Final Report, Publications, Web Links, Networks and collaborations established, license agreements
1.1.1	Effect of Surface Heat Transfer Coefficients on U-factor for Highly conductive and Projecting Products	Link to appendix 1.1.1-full report
1.1.2	Three Dimensional Corner Heat Transfer Effects in Fenestration Products	Link to appendix 1.1.2-full report
1.1.3	Thermal Comfort Rating	Link to appendix 1.1.3-full report
1.1.6	Heat Transfer Effects of Sloped, Ventilated Cavities Framing	Link to appendix 1.1.6-full report
1.1.7	Development of a Procedure and a Model for U-factor Rating of Domed Skylights	Link to appendix 1.1.7-full report
1.1.8	Tubular Daylighting Devices U-factor Rating	Link to appendix 1.1.8-full report
na	Entrance Door Systems Rating Simplification	Link to appendix na-full report
1.1.13	Component Modeling Approach Frame Grouping Research	Link to appendix 1.1.13-full report

Statement of Project Objective Task #	Project	Final Report, Publications, Web Links, Networks and collaborations established, license agreements
1.1.14	Component Modeling Approach Condensation Resistance Research	Link to appendix 1.1.14-full report
1.1.15	Component Modeling Approach Non- Standard Products Research Project	Link to appendix 1.1.15-full report
1.1.16	Revision of Standard Spectral Weighting Function for Calculation of Solar Optical Properties and Solar Heat Gain	Link to appendix 1.1.16-full report
1.1.17	Complex Product VT Rating Research Project	Link to appendix 1.1.17-full report
1.1.18	Window 6 and Therm 6 Validation Research Project	Link to appendix 1.1.18-full report
2	Development of NFRC 101-Thermonphysical Properties of Materials for use in NFRC approved Software	Link to appendix 2-full report
3.1	International Standard Organization	Carli, an NFRC contractor, attended two ISO TC163/SC2/WG11 meetings each year from 05 to 09 regarding ISO 18292- *Energy performance of fenestration systems - Calculation procedure*. This procedure calculates the energy consumption of a window based on how it is used in a typical home. Carli maintains an ISO relationship for the NFRC and monitors developments with the ISO18292 procedure to enable NFRC to consider similar process related to its comparable standard, NFRC 901-*Guidelines to Estimate the Effects of Fenestration on Heating and Cooling Energy Consumption in Single Family Residences*. Link to appendix 3.1-full report
3.2	International Harmonization-South Africa	NFRC has a license agreement with the Association of Architectural Aluminum Manufacturers of South Africa (AAAMSA) to begin developing NFRC ratings for fenestration products. NFRC conducted

Statement of Project Objective Task #	Project	Final Report, Publications, Web Links, Networks and collaborations established, license agreements
		fenestration simulation training and accredited Thermal Testing Labs in South Africa (a thermal testing facility for fenestration), an important first step towards a full NFRC certification program. Link to appendix 3.2 South Africa – NFRC-AAAMSA License Agreement
	Australia	NFRC continues to work with the Australian Fenestration Rating Council (AFRC, a new NFRC licensee) as they begin to certify fenestration products according to NFRC procedures. Their website contains numerous technical documents that were jointly developed with NFRC: www.afrc.org.au NFRC works with the Australian Window Association (AWA) closely to continue work toward NFRC harmonization. Link to appendix 3.2 Australia (a) – Australian Fenestration Rating Council procedures Link to appendix 3.2 Australia (b) – NFRC-AFRC License Agreement
	India	NFRC attended and hosted several events in India and hosted India Visitors to the NFRC in the US to work towards harmonization: Link to appendix 3.2 India (a) – Summary and booth information for US-Pavilion and Building Envelope Conference Link to appendix 3.2 India (b) – WinBuild presentation for Indian Visitors
	China	NFRC attended several events in China working towards window labeling harmonization: Link to appendix 3.2 China (a) – Presentation for Glass Processing Days Beijing, China Link to appendix 3.2 China (b) – NFRC presentation at Building Envelope

Statement of Project Objective Task #	Project	Final Report, Publications, Web Links, Networks and collaborations established, license agreements
		Link to appendix 3.2 China (c) – presentation for US-China Building Conference on Energy Efficiency Link to appendix 3.2 China (d) – US Green Building Technology Seminar agenda and invitation
	Jordan	NFRC attended the U.S.-Jordanian Joint Committee Meeting (JCM) on Science & Technology (S&T) Cooperation, July 9–10, 2008, in Amman. NFRC, with support from US-DOE, conducted a Jordan-American Building Envelope Energy Efficiency Technology Cooperation Workshop where all key stakeholders from Jordan attended on October 25th, 2008. NFRC provided basic training in THERM, WINDOWS and OPTICS software on October 26 and 27 to 16 attendees for the workshop. An NFRC representative visited the Jordan higher Council research center and testing laboratory, October 28, 2008, to access the set-up and to determine the needs for establishment of building envelope testing center. The National Fenestration Rating Council (NFRC) participated at the GCREEDER-2009 conference in Amman Jordan, March 31st - April 2nd, 2009. The NFRC worked with Higher Council for Science & Technology (HCST) to coordinate and host a workshop on April 1st, 2009 in Amman Jordan that included 4 regional countries, Jordan, Kuwait, Yemen, and Lebanon participating along with regional US manufacturers' participation. The key US building envelope stakeholders participating included NFRC, the International Window Film Manufacturer Association (IWFA). Mr. Ross Hagan, Director, Energy Office, USAID/Jordan also participated in the meeting. USAID has keen interest to work with US-DOE to develop of regional codes and promote energy efficiency building envelope product in the region.

Statement of Project Objective Task #	Project	Final Report, Publications, Web Links, Networks and collaborations established, license agreements
		General Secretary of HCST, Dr. Anwar M. Battikhi and Energy Advisor to the Council Dr. Mohammad Hamdan pledged the needed support for the effort. On April 2, 2009, a representative of the National Fenestration Rating Council (NFRC), US-DOE and the Higher Council for Science & Technology met with USAID to discuss future project. April 3, 2009, NFRC met with Maisam architect and engineering firm to discuss the case study for application of newly developed Jordan building energy efficiency for a building in Amman Jordan. Link to appendix 3.2 Jordan (a) – brochure for Global Conference on Renewables and Energy Efficiency for Desert Regions Link to appendix 3.2 Jordan (b) – NFRC presentation to Jordan visitors Link to appendix 3.2 Jordan (c) – agenda for Building Envelope Energy Efficiency Technology Cooperation
	Japan	NFRC hosted a Japanese delegation in September 2008 for the following participants: • Mr. Tatsumi Nakamura, the president of Shannon (PVC window manufacture), Chairman of PVC window manufactures association • Mr. Yukitoshi Hashimoto, General Manager, Development & Technical Dept. of Shanon • Mr. Nozomi Suzuki, Sales Director of Nihon Fukuso (IGU manufacture) • Ms. Mieko Goto, Consultant, Goto Tomorrow Co., Ltd Several presentations were given (click to view) Link to appendix 3.2 Japan (a) – NFRC presentation to Japanese visitors

Statement of Project Objective Task #	Project	Final Report, Publications, Web Links, Networks and collaborations established, license agreements
		Link to appendix 3.2 Japan (b) – presentation on Japanese vinyl market Link to appendix 3.2 Japan (c) – presentation on Japanese window market
4 (2008 only)	IG Durability and Applied Film Status Harmonization (low-e technology promotion)	China has adopted the European procedure for testing Insulated Glazing units (IGU). The contractor participated in several experts meeting, and concluded that the efforts to convince the Chinese to adopt North American practice is futile, and therefore recommends ending the efforts for IGU standards harmonization with China. Link to appendix 4 (a) – agenda for IG Durability and Applied Film Meeting Link to appendix 4 (b) – presentation for International Window Film Harmonization
5 (2008 only)	IG and Applied Film ISO Activities	The China National Centre for Quality Supervision & Testing of Glass (CCQTG) is in the process of finalizing the applied film standards by end of 2010. Gaining importance, the standard has been elevated to a National Standard status. It is recommended to monitor this activity and assisting CCQTG with any additional information required.

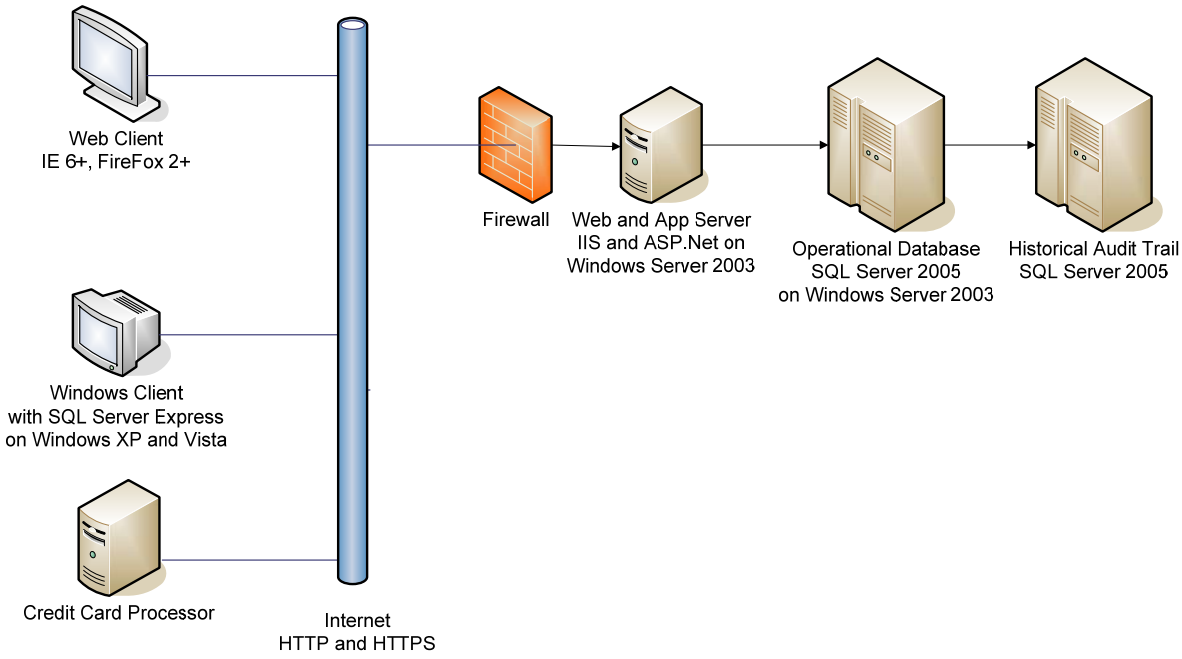
Statement of Project Objective Task #	Project	Final Report, Publications, Web Links, Networks and collaborations established, license agreements
6 (2008 only)	Component Modeling Approach (CMA)	NFRC has completed and launched its new rating procedure, the Component Modeling Approach. The calculation tool named the Component Modeling Approach Software Tool (CMAST), is found on the NFRC web site and is available for commercial use. It may be downloaded here: http://cmast.nfrc.org/ Below are links to several materials developed to support the CMA program. Link to appendix 6 (a) – CMAST User Manual Link to appendix 6 (b) – CMA Marketing Plan Link to appendix 6 (c) – CMA Information Brochure Link to appendix 6 (d) – CMA Information Packet

Computer Modeling Developments

NFRC developed the Component Modeling Approach Software Tool (CMAST). This tool calculates commercial fenestration energy performance using NFRC's existing rating program principles. CMAST uses a three-tier architecture that divides an application into distinct layers: presentation (user interface), middle (business logic), and database (storage).

The three tier architecture is used when an effective distributed client/server design is needed that provides (when compared to the two tier) increased performance, flexibility, maintainability, reusability, and scalability, while hiding the complexity of distributed processing from the user. These characteristics have made three layer architectures a popular choice for Internet applications and net-centric information systems.[2]

[2] Carnegie-Mellon University, Software Engineering Institute. http://www.sei.cmu.edu/str/descriptions/threetier.html.



The user interface layer is implemented in both a Windows and a Web application. The Web client is primarily read-only and works closely with the application server business objects. The Windows client has its own local database and also implements product configuration, energy calculations, and interfaces to WINDOW and THERM. It synchronizes with the server database at the user's request.

Other details of the program are listed below.

- Software titled THERM6.0, a 2D heat transfer simulation program provides thermal models for framing and spacer components
- Software titled WINDOW6.0 provides center of glass U-factor, SHGC, and VT calculations and also combines THERM6.0 frame and spacer calculations to product final product energy ratings. WINDOW 6.0 calculations are embedded in CMAST.
- Window Product energy ratings are restricted to NFRC standard sizes as written in NFRC 100-2010, table 4.3. Actual size ratings are generated, but they are not intended for NFRC certification.
- All rating conditions, assumptions, and performance criteria are controlled by NFRC 100-2010 (U-factor) and NFRC 200 (SHGC and VT).
- Current CMAST version, as of this writing, is 1.1.11.
- ISO 15099 equations used for fundamental window energy performance calculations and are coded into WINDOW 6.0
- CMAST has been tested against the most current versions of WINDOW and THERM in August of 2009. Comparison between THERM6.0/WINDOW6.0 and CMAST produced differences that, for vast majority of products, particularly at NFRC size, were less than 0.01 for all indices (i.e., U, SHGC, VT). For a few products at sizes other than NFRC, differences in U-factor reached 0.02, while for SHGC and VT they consistently remain below 0.01.
- CMAST model code is proprietary

Summary

The US DOE was and is instrumental to NFRC's beginning and its continued success. The 2005 to 2009 funding enables NFRC to continue expanding and create new, improved ratings procedures. Research funded by the US DOE enables increased fenestration energy rating accuracy. International harmonization efforts supported by the US DOE allow the US to be the global leader in fenestration energy ratings. Many other governments are working with the NFRC to share its experience and knowledge toward development of their own national fenestration rating process similar to the NFRC's.

The broad and diverse membership composition of NFRC allows anyone with a fenestration interest to come forward with an idea or improvement to the entire fenestration community for consideration. The NFRC looks forward to the next several years of growth while remaining the nation's resource for fair, accurate, and credible fenestration product energy ratings.

NFRC continues to improve its rating system by considering new research, methodologies, and expanding to include new fenestration products. Currently, NFRC is working towards attachment energy ratings. Attachments are blinds, shades, awnings, and overhangs. Attachments may enable a building to achieve significant energy savings. An NFRC rating will enable fair competition, a basis for code references, and a new ENERGY STAR product category. NFRC also is developing rating methods to consider non specular glazing such as fritted glass. Commercial applications frequently use fritted glazing, but no rating method exists. NFRC is testing new software that may enable this new rating and contribute further to energy conservation.

Around the world, many nations are seeking new energy conservation methods and NFRC is poised to harmonize its rating system assisting these nations to better manage and conserve energy in buildings by using NFRC rated and labeled fenestration products. As this report has shown, much more work needs to be done to continues research to improve existing ratings and develop new ones. NFRC needs to continue the work it has begun in several nations to implement the NFRC rating system that has been introduced. Many nations are eager to accept the expertise NFRC can offer to achieve energy conservation goals. NFRC looks forward to a continues partnership with the US Department of Energy to cooperatively achieve both

Project 1.1.1

Project Name: Effect of Surface Heat Transfer Coefficients on U-factor for Highly Conductive and Projecting Products

Date: January 31, 2005

Purpose: See title

Project Summary:

All of the final products have been modeled according to NFRC 100-2001 and NFRC 200-2001 in THERM 5.2 and WINDOW 5.2. In addition to NFRC standard boundary conditions, which include advanced radiation model on the indoor side, the newly developed convective boundary conditions have been also applied and results included. The investigation of improved convective surface heat transfer coefficients is presented in the second half of the report.

Click here for view final report

Carli, Inc.

18 Tanglewood Rd.
Amherst, MA 01002

TEL: (413) 256-4647
FAX: (413) 256-4823

home@fenestration.com
http://www.fenestration.com

Final Technical Report:

Effect of Surface Heat Transfer Coefficients on U-Factors for Projecting and Highly Conducting Fenestration Products

Report prepared for:

National Fenestration Rating Council, Inc.

1300 Spring Street, Suite 500
Silver Spring, MD 20910

January 31, 2005

TABLE OF CONTENTS

TABLE OF CONTENTS 2
EXECUTIVE SUMMARY 3
SPECIMENS 4
MODELING RESULTS 20
CONVECTIVE FILM COEFFICIENT DEVELOPMENT 20
Previously Published Correlations 20
Numerical Simulations: 26
Natural Convection in a LBNL IR Thermal Chamber 26
Projecting CTS and Natural Convection in a Typical Hot Box Setup 31
THERM MODELING RESULTS 43
DISCUSSION OF RESULTS and CONCLUSIONS 45
RECOMMENDATIONS: 57
REFERENCES 57
APPENDIX A: THERM Models and Selected Results 59
Appendix B: Mounting Details 66

EXECUTIVE SUMMARY

This technical report provides final results for the research project: “Effect of Surface Heat Transfer Coefficients on U-Factors for Projecting and Highly Conducting Fenestration Products”. All of the final products have been modeled according to NFRC 100-2001 and NFRC 200-2001 in THERM 5.2 and WINDOW 5.2. In addition to NFRC standard boundary conditions, which include advanced radiation model on the indoor side, the newly developed convective boundary conditions have been also applied and results included. For six specimens, either no test results were available or the specimens were duplicative with other specimens or they belonged to a category not covered with this research project (e.g., domed skylights), so they have been eliminated from this research project. These products are shown in Table 2 as strike-through fields.

Available test results for majority of specimens were issued by commercial test laboratories, using NFRC 100-1997 procedures. Couple of test results were research level testing and it did not necessarily provided standardized U-factors, but rather temperature profiles (i.e., FGW) or field measurement data (i.e., Rlang). For those test results that were done according to NFRC 100-1997, the new standardized U-factors were calculated using NFRC 100-2001 test procedure (i.e., NFRC 102-2001, which is identical to NFRC100-2004) procedure, so that they could be better compared to the modeling results with THERM 5.2 and WINDOW 5.2, which are done according to NFRC 100-2001 simulation procedures. In addition, and as a result of this research project Task 4, modification to the test procedure has been proposed for projecting products and results using this modified test procedure has been presented.

The investigation of improved convective surface heat transfer coefficients is presented in the second half of the report. Theoretical analysis and resulting correlations for the average convective surface heat transfer coefficient are presented and plotted for different window heights and temperature differentials. Selected numerical modeling of air flow and convective heat transfer on the warm side of the test chamber had been performed and presented here.

New convective heat transfer coefficients have been applied to all of THERM and WINDOW models and their results were compared to the simulation results using standard boundary conditions and all of the test results.

Test results were analyzed critically and corrected standardized U-factors were calculated including the potentially new projecting CTS method.

New modeling procedure for extreme projecting products, like garden house windows is presented and validated and recommended for future use at NFRC.

SPECIMENS

Originally, 16 projecting products and 4 flat/highly conducting products were considered. Tables 1 and 2 list all the products and also indicate the ones that are not included in the final analysis. The tables give specimen descriptions, sizes, and projections.

Table 1. Original List of Projecting Specimens

Number	Manufacturer	Model	Description	Size (outer) in	RO Size (in.)	Projection (in.)
~~1~~	~~Wasco~~	~~DDRA 2246~~	~~Domed Skylight w/ integral curb, double dome~~	~~24.38x48.38~~	~~22.25x46.25~~	~~7.91~~
~~2~~	~~ODL~~	~~EC 2852~~	~~Al w/ thermal break. Wood curb, dome and flat~~	~~26.36x50.36~~	~~23.36x47.36~~	~~9.03~~
~~3~~	~~ODL~~	~~EC 5252~~	~~Al w/ thermal break. Wood curb, dome and flat~~	~~50.36x50.36~~	~~47.36x47.36~~	~~12.03~~
~~4~~	~~ODL~~	~~OG2840~~	~~Vinyl Skylights~~		~~30x42~~	
5	Milgard	780	Al clad vinyl. Wood curb, dg low E-0.2 / 0.625" Air	27.25x51.25	22.5x46.5	6.84
6	Velux	1 06/ FS87	Al clad wood. Intergral curb dg low E (0.118) 0.378" Air	21.57x51.75	19.48x44.05	4.13
7	Velux	FS95	Al clad wood. Intergral curb	30.75x55.13	28.04x52.05	4.13
8	Velux	VS98	Al clad wood. Intergral curb	30.75x55.13	28.09x52.22	5.57
~~9~~	~~Velux~~	~~FCM~~	~~Al clad wood. Intergral curb~~			
~~10~~	~~Bristolite~~	~~GAL SF~~	~~Al Integral curb, single dome~~	~~27.75x51.75~~	~~22.25x46.25~~	~~4.3~~
11	R. Lang	Truframe "J" Series	Al greenhouse window, dg low E, 0.5" Air	60x36	59x35	16
12	LBNL	Foam GHW	Foam w/ Plexiglas green house window	37.375x37.375	37.375x37.375	12.938
13	NFRC (Rollin)	Projecting CTS	Foam sandwiched between layers of glass w/ proj	23.85x47.25	23.85x47.25	4.25
14	Kawneer	1600 System 1	Al curtain wall	80x80	75x75	N/A
15	Kawneer	1600 System 5	Al curtain wall	80x80	75x75	N/A
16	Kawneer	6000IB	Al curtain wall	80.38x80	75.38x75	N/A

Notes: For Units tested at Intertek (A, B, C, etc.) indicate Intertek's Testing Labeling System
Sizes of Products are as Tested
* Measured in Mowitt facility
** Measured in IR Thermographic facility
*** Partial measurements

Table 2. Original List of Flat/Conducting Specimens

Number	Manufacturer	Model	Description	Size (in.)	RO Size (in.)	Projection (in.)
1	Milgard	NFRC TRR99	Aluminum horizontal slider	60x36	N/A	N/A
2	TRACO	NFRC TRR01	Thermally Broken Aluminum Fixed Window	40x40	N/A	N/A
4	NFRC	Flat CTS	Foam sandwiched between layers of glass - Flat	23x47	N/A	N/A
~~5~~	~~Custom~~	~~Conducting CTS~~	~~Thin foam rubber sandwiched between layers of glass~~		~~N/A~~	~~N/A~~

Table 3 and **Table 4** list details about the availability of drawings, dxf standard graphics exchange files, test results, test result sources and detailed test reports. The specimens that are crossed-out either do not apply to this project (i.e., Wasco, ODL and Bristolite domed skylights) or the sample was not measured (Conducting CTS).

Table 3. Listing of Availability of Drawings and Test Results for Projecting Products

					TESTS				
Number	**Manufacturer**	**Model**	**Have .DWGs**	**Have .DXFs**	**Intertek**	**LBL**	**ORNL**	**Other**	**Test Reports**
~~1~~	~~Wasco~~	~~DDRA 2246~~	~~No~~	~~No~~	~~X (A)~~				~~X~~
~~2~~	~~ODL~~	~~EC 2852~~	~~Yes~~	~~Yes~~	~~X (B)~~				~~X~~
~~3~~	~~ODL~~	~~EC 5252~~	~~Yes~~	~~Yes~~	~~X (B_1)~~				~~X~~
~~4~~	~~ODL~~	~~OG2840~~	~~Yes~~	~~Yes~~					
5	Milgard	780	Yes	No	X (C)				X
6	Velux	1 06/ FS87	Yes	No	X (D)				X
7	Velux	FS95	Yes	Yes				ATI	X
8	Velux	VS98	Yes	Yes				ATI	X
~~9~~	~~Velux~~	~~FCM~~	~~Yes~~	~~Yes~~				~~ATI~~	
~~10~~	~~Bristolite~~	~~GAL SF~~	~~Yes~~	~~No~~	~~X (E)~~				~~X~~
11	R. Lang	Truframe "J" Series	Yes	Yes		X*			
12	LBNL	Foam GHW	Yes	Yes		X**			
13	NFRC (Rollin)	Projecting CTS	Yes	Yes			X***		
14	Kawneer	1600 System 1	Yes	Yes				ATI	X
15	Kawneer	1600 System 5	Yes	Yes				ATI	X
16	Kawneer	6000IB	Yes	Yes				ATI	X

Table 4. Listing of Availability of Drawings and Test Results for Conducting Products

					TESTS				
Number	**Manufacturer**	**Model**	**Have .DWGs**	**Have .DXFs**	**Intertek**	**LBL**	**ORNL**	**Other**	**Test Reports**
1	Milgard	NFRC TRR99	Yes	Yes				8 Labs	X
2	TRACO	NFRC TRR01	Yes	Yes				8 Labs	X
4	NFRC	Flat CTS	No	No	X				X
~~5~~	~~Custom~~	~~Conducting CTS~~	~~No~~	~~No~~					

These specimens were tested with individual glazing options, and they were also modeled with the same set of glazing options in order to provide appropriate validation points. Details of glazing options are all listed in **Table 5**.

Table 5. Glazing Options for Analyzed Specimens

			Thicknesses					Emissivity							
Number	**Manufacturer**	**Model**	**Layer 1**	**Gap 1**	**Layer 2**	**Gap2**	**Layer 3**	**Side 1**	**Side 2**	**Side 3**	**Side 4**	**Side 5**	**Side 6**	**Gap Contents**	**Spacer Info**
~~1~~	~~Wasco~~	~~DDRA 2246~~				~~N/A~~	~~N/A~~					~~N/A~~	~~N/A~~		~~No Spacer~~
~~2~~	~~ODL~~	~~EC 2852~~	~~0.1"~~	~~NA~~	~~.08"~~	~~N/A~~	~~N/A~~	~~0.84~~	~~0.84~~	~~0.84~~	~~0.84~~	~~N/A~~	~~N/A~~	~~Air~~	~~No Spacer~~
~~3~~	~~ODL~~	~~EC 5252~~	~~0.125"~~	~~NA~~	~~.08"~~	~~N/A~~	~~N/A~~	~~0.84~~	~~0.84~~	~~0.84~~	~~0.84~~	~~N/A~~	~~N/A~~	~~Air~~	~~No Spacer~~
~~4~~	~~ODL~~	~~OG2840~~	~~0.125"~~	~~0.5"~~	~~0.25"~~	~~N/A~~	~~N/A~~	~~0.84~~	~~0.84~~	~~0.84~~	~~0.84~~	~~N/A~~	~~N/A~~	~~Air~~	~~Allmetal Aluminum~~
5	Milgard	780	0.185"	0625"	0.185"	N/A	N/A	0.84	0.2	0.84	0.84	N/A	N/A	Air	Intercept
6	Velux	FS87/FS Type 75	0.124"	0.386"	0.122"	N/A	N/A	0.84	0.038	0.84	0.84	N/A	N/A	95% Argon, 5% Air	Steel Allmetal
7	Velux	FS95/FS Type 75	0.124"	0.386"	0.122"	N/A	N/A	0.84	0.038	0.84	0.84	N/A	N/A	95% Argon, 5% Air	Steel Allmetal
8	Velux	VS98/VS Type 75	0.124"	0.428"	0.122"	N/A	N/A	0.84	0.038	0.84	0.84	N/A	N/A	95% Argon, 5% Air	Steel Allmetal
~~9~~	~~Velux~~	~~FCM Type 75~~	~~0.124"~~	~~0.428"~~	~~0.122"~~	~~N/A~~	~~N/A~~	~~0.84~~	~~0.038~~	~~0.84~~	~~0.84~~	~~N/A~~	~~N/A~~	~~95% Argon, 5% Air~~	~~Steel Allmetal~~
~~10~~	~~Bristolite~~	~~GAL SF~~				~~N/A~~	~~N/A~~					~~N/A~~	~~N/A~~		~~No spacer~~
11	R. Lang	Truframe "J" Series	0.118"	.264"	.118"	N/A	N/A	0.84	0.84	0.84	0.84	N/A	N/A	Air	Swiggle Strip
12	LBNL	Foam GHW	None	0.75"	0.1875"	N/A	N/A	N/A	0.9	N/A	0.9	N/A	N/A	Foam	No spacer - continuous foam
13	NFRC (Rollin)	Projecting CTS	0.22"	0.488"	0.22"	N/A	N/A	0.84	N/A	N/A	0.84	N/A	N/A	Foam	No spacer - continuous foam
14	Kawneer	1600 System 1	0.22"	0.51"	0.22"	N/A	N/A	0.84	0.84	0.84	0.84	N/A	N/A	Air	Allmetal Aluminum
15	Kawneer	1600 System 5	0.22"	0.51"	0.22"	N/A	N/A	0.84	0.84	0.84	0.84	N/A	N/A	Air	Allmetal Aluminum
16	Kawneer	6000IB	0.22"	0.5"	0.22"	N/A	N/A	0.84	0.84	0.84	0.84	N/A	N/A	Air	Allmetal Aluminum
1	Milgard	NFRC TRR99	0.129"	0.244"	0.003"	0.244"	0.129"	0.84	0.84	0.772	0.088	0.23	0.84	Air	Allmetal Steel
2	TRACO	NFRC TRR01	0.122	.338"	0.003"	0.338"	0.122"	0.84	0.204	0.759	0.052	0.204	0.84	Air	Allmetal Aluminum
3	NFRC	Flat CTS	0.177"	0.5"	0.177"	N/A	N/A	0.84	N/A	N/A	0.84	N/A	N/A	Foam	No spacer - continuous foam

Geometry, construction of the specimens, and relevant materials are shown in **Error! Reference source not found.** to Figure 13.

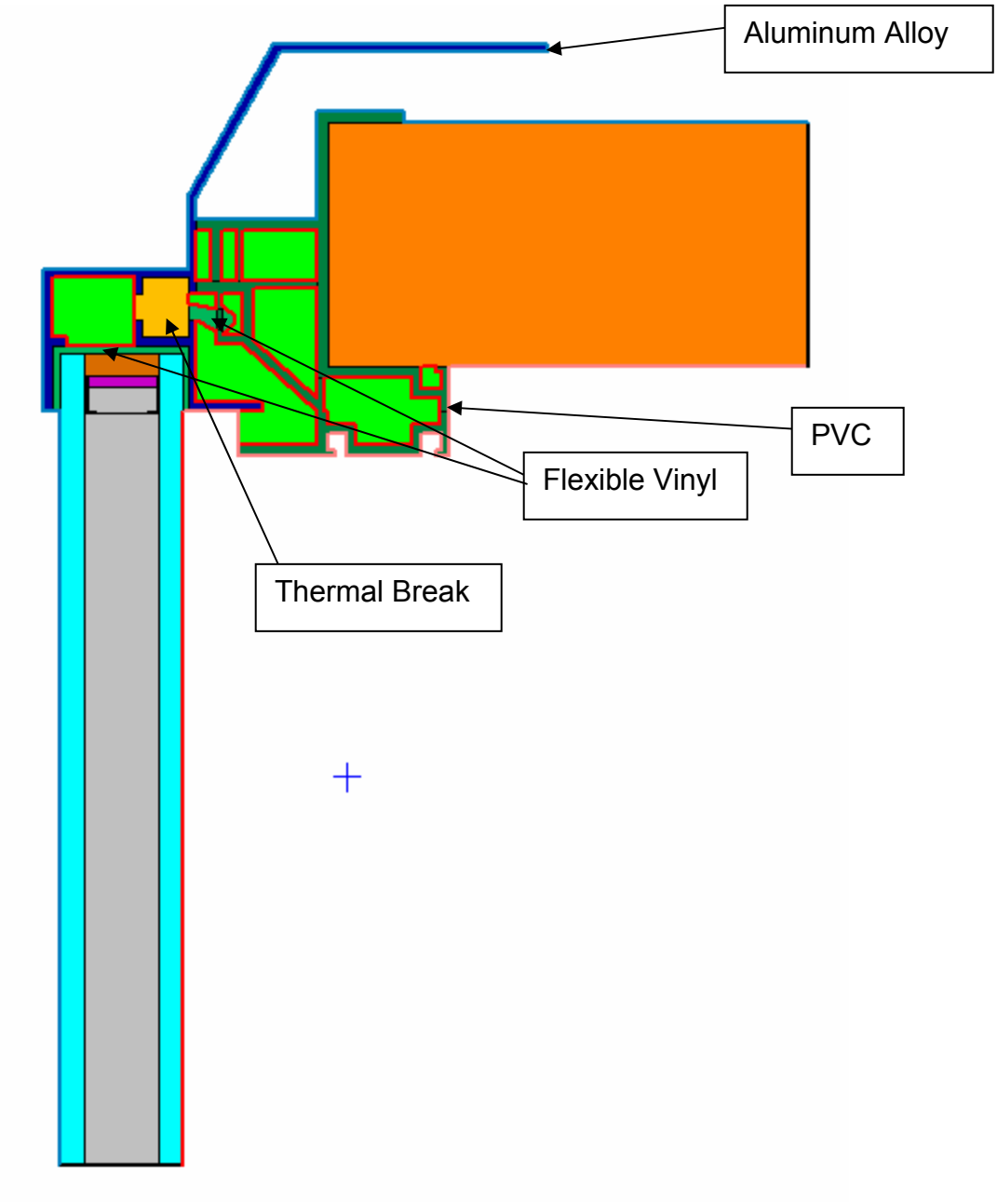


Figure 1. Milgard 780 Skylight

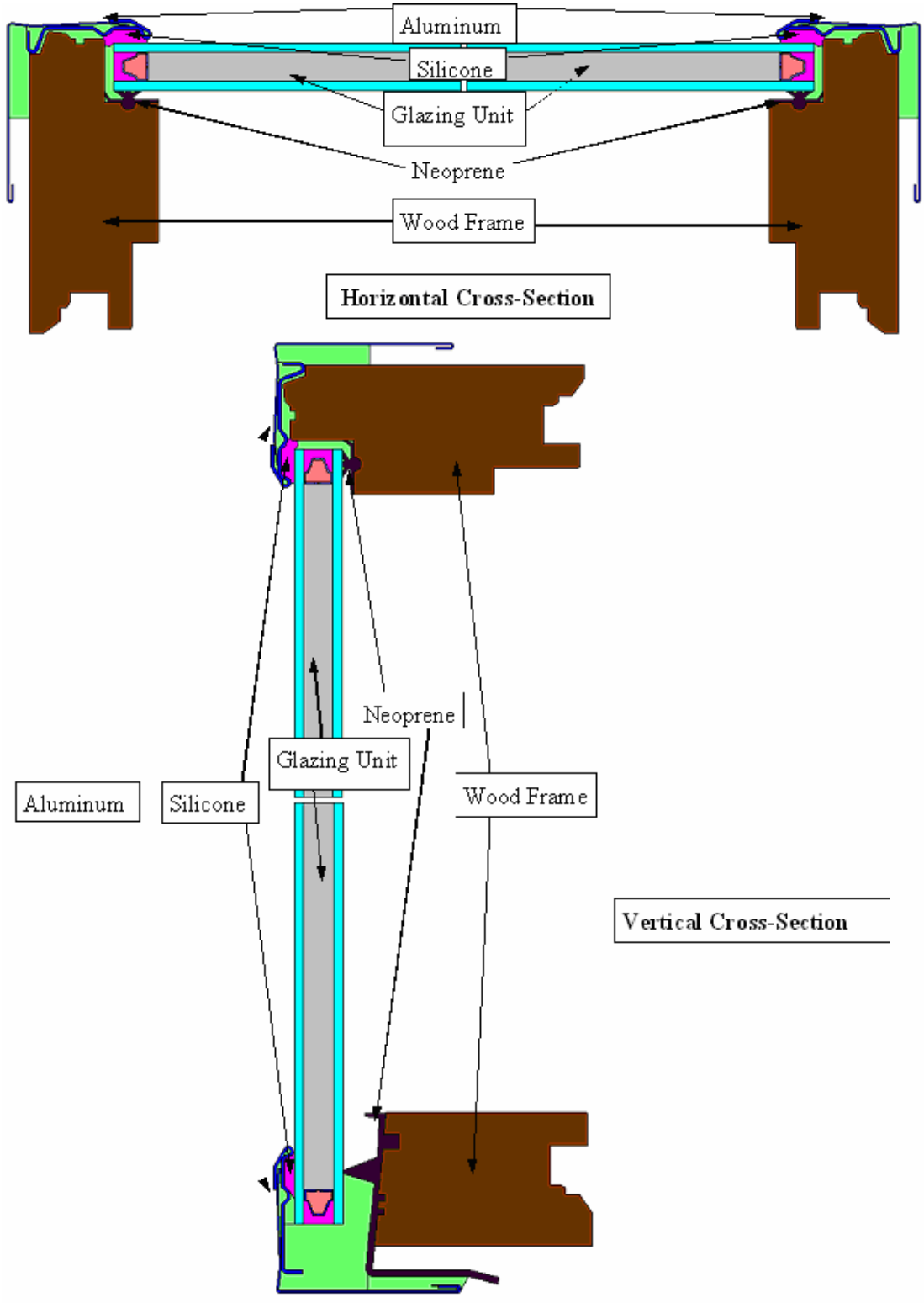


Figure 2. Velux FS87 Skylight

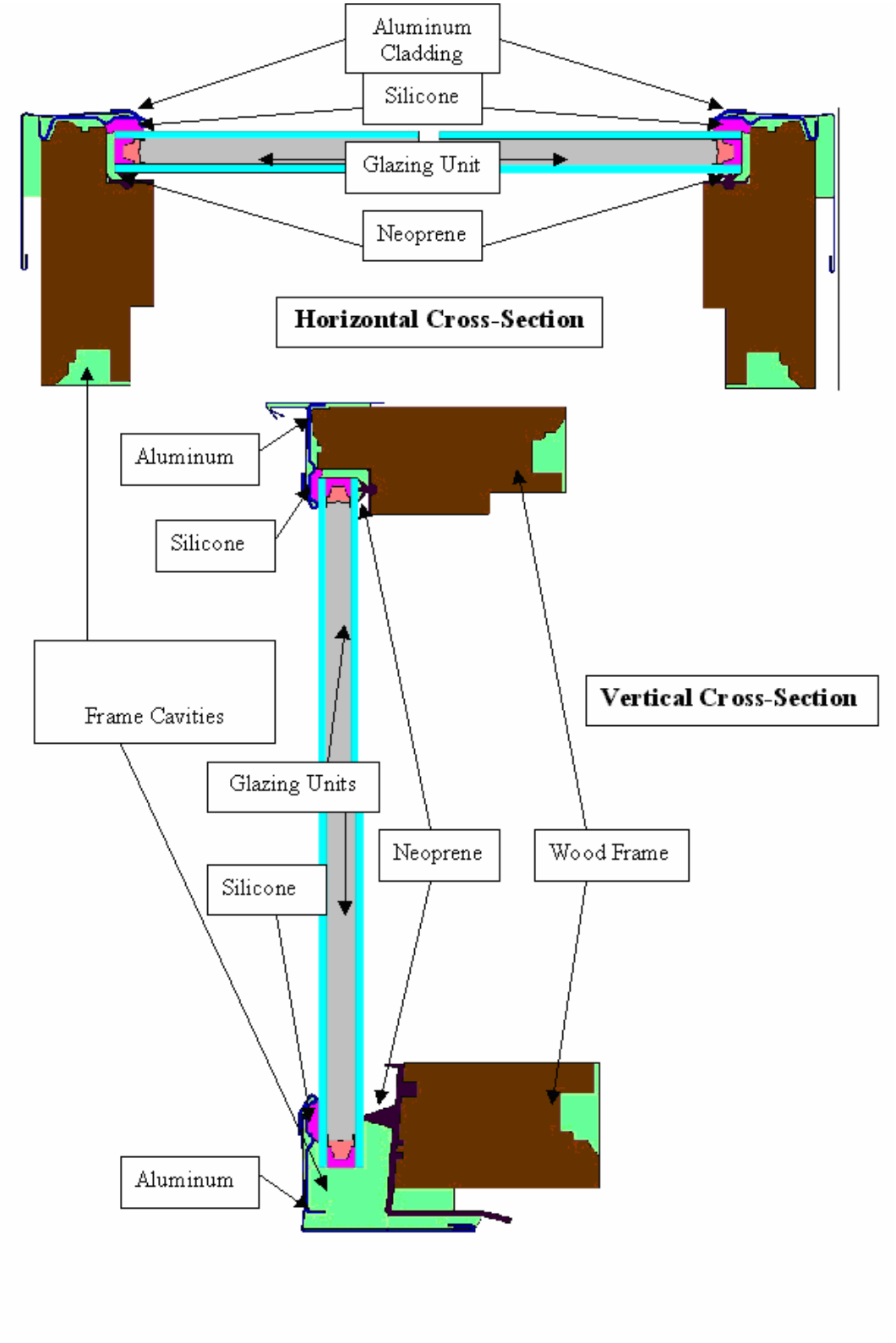


Figure 3. Velux FS95 Skylight

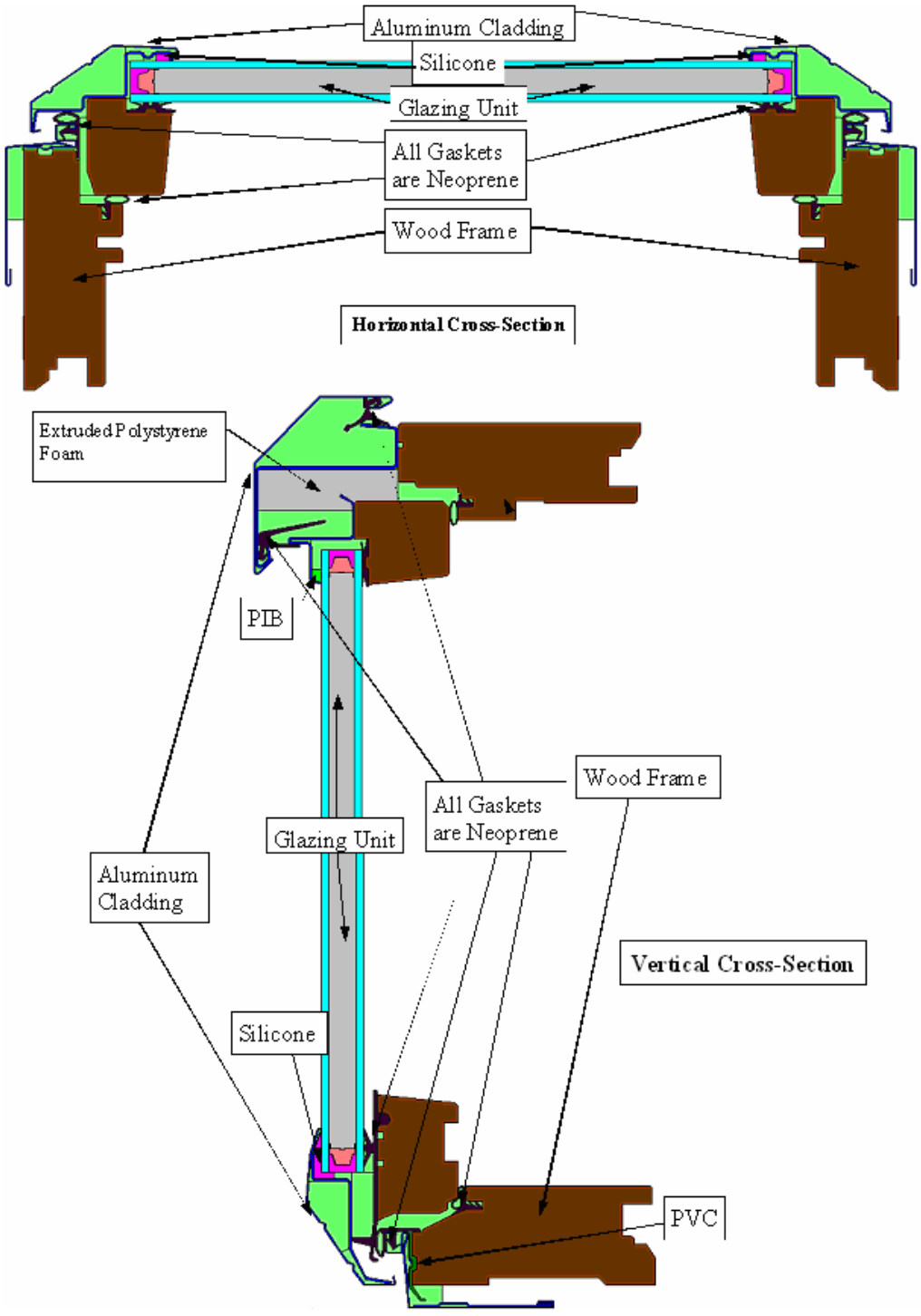


Figure 3. Velux VS98 Skylight

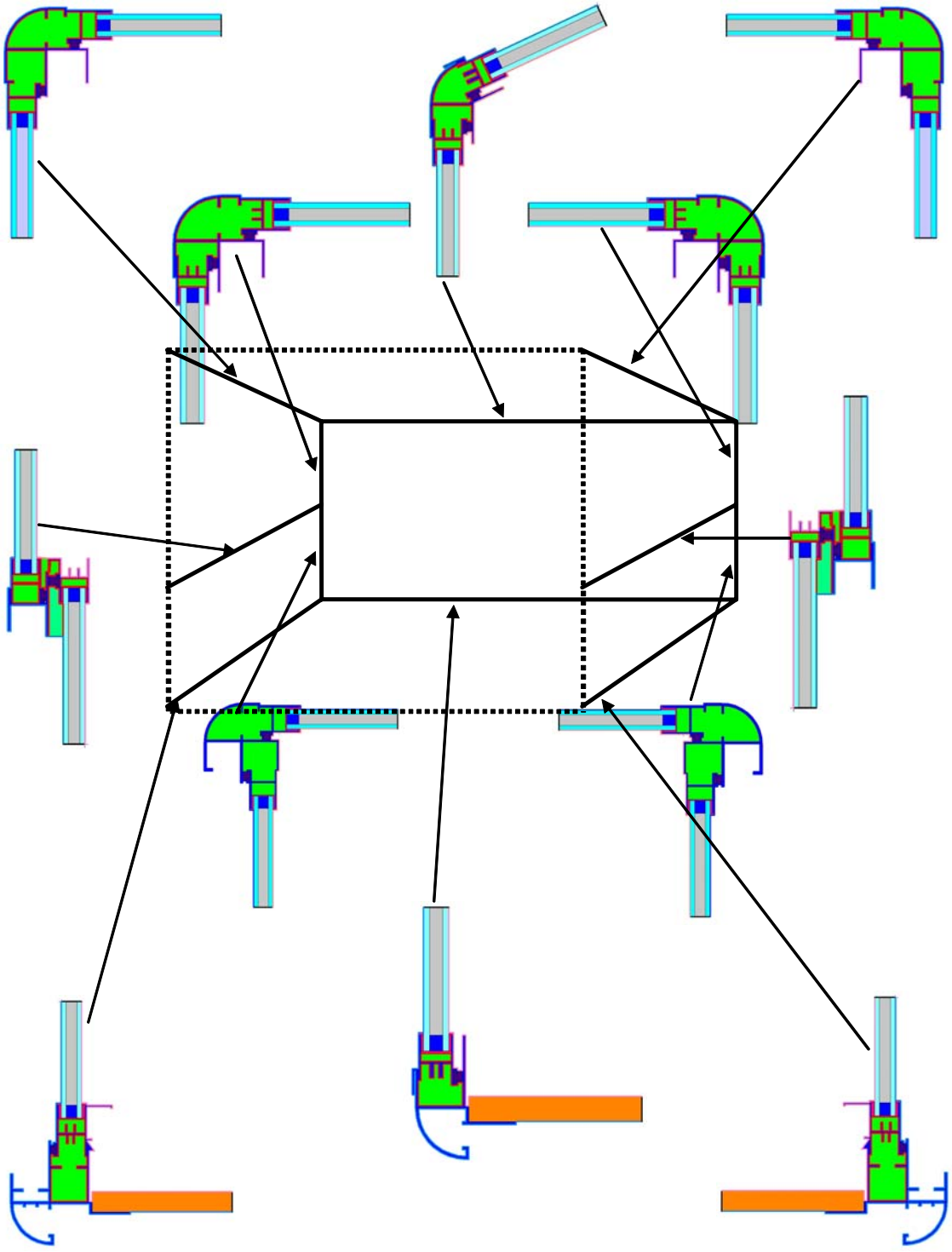


Figure 4. RLang Truframe J series Garden House Window – Front Side

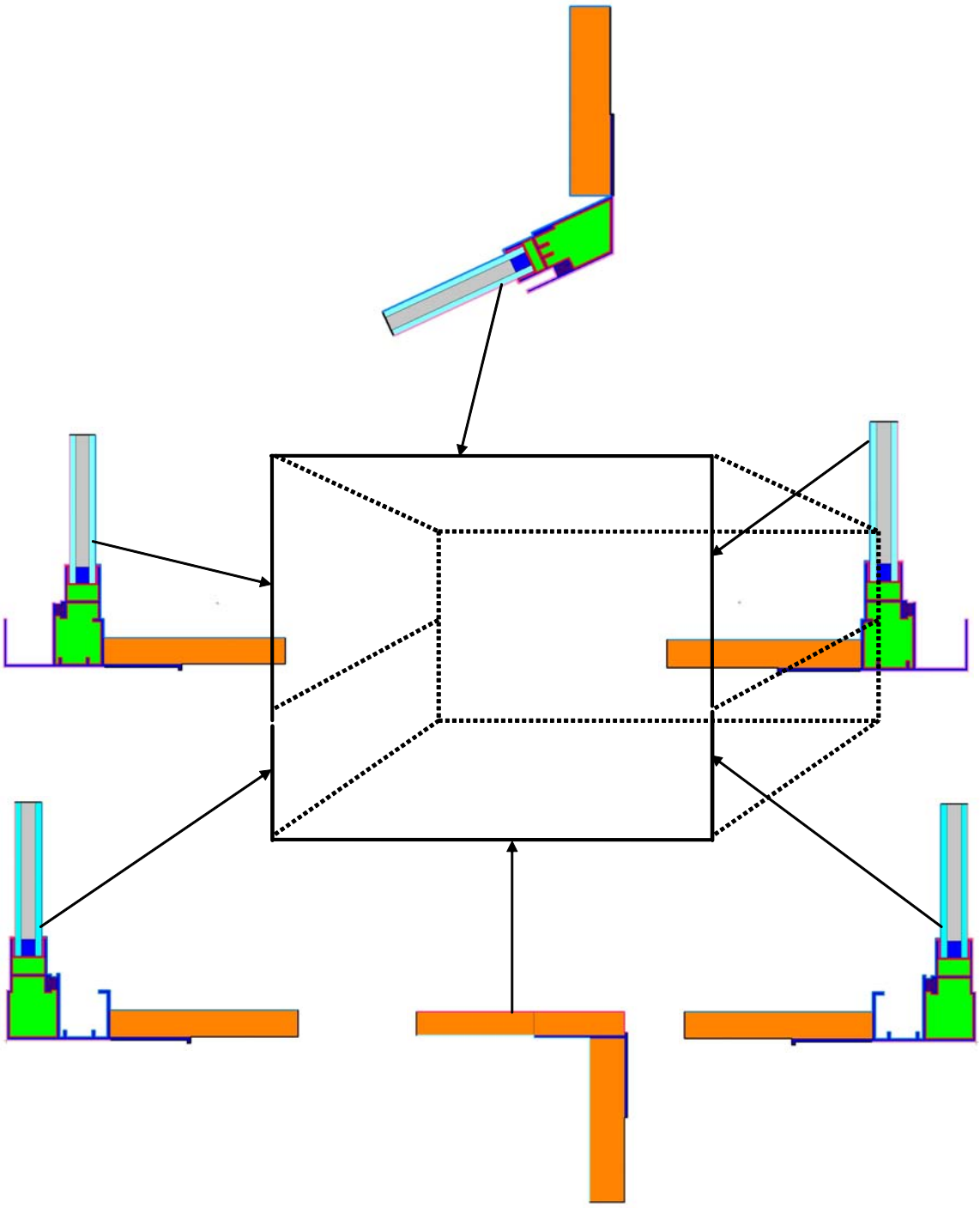


Figure 5. RLang Truframe J series Garden House Window – Back Side

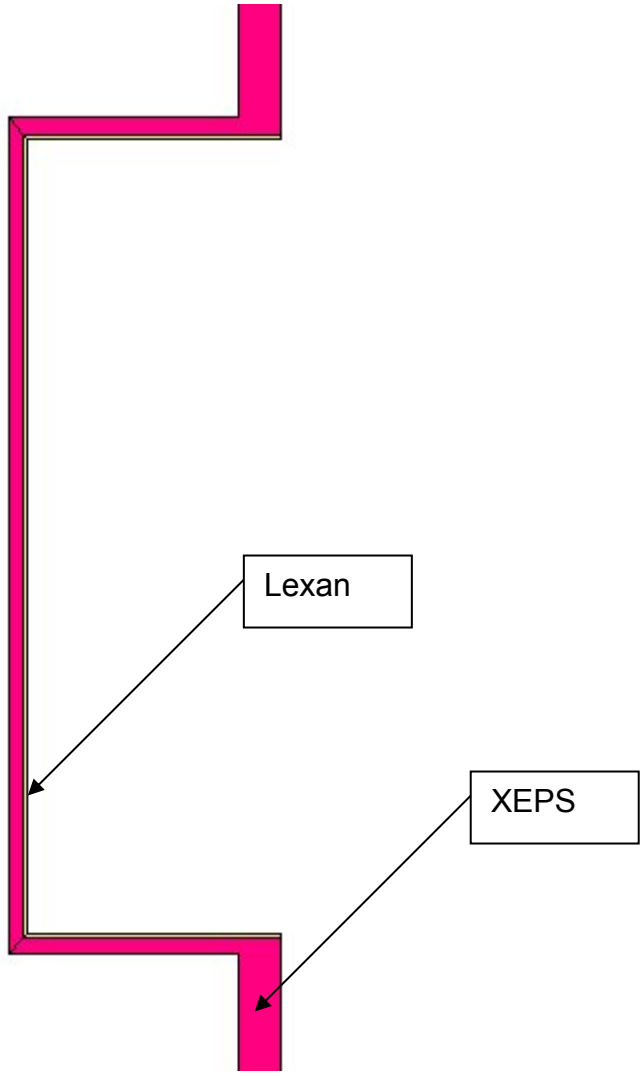


Figure 6. LBNL Foam Garden Window

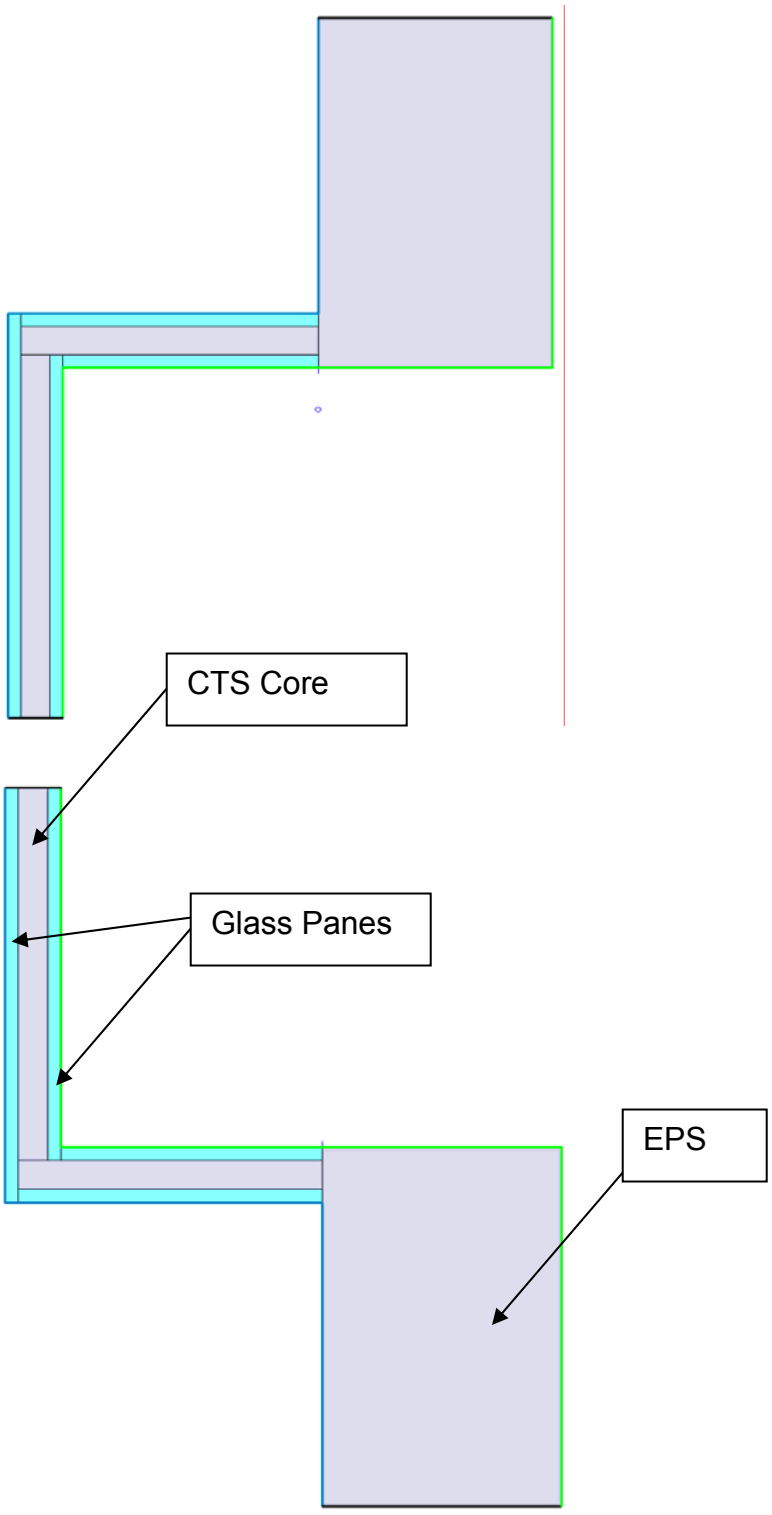


Figure 7. Projecting CTS

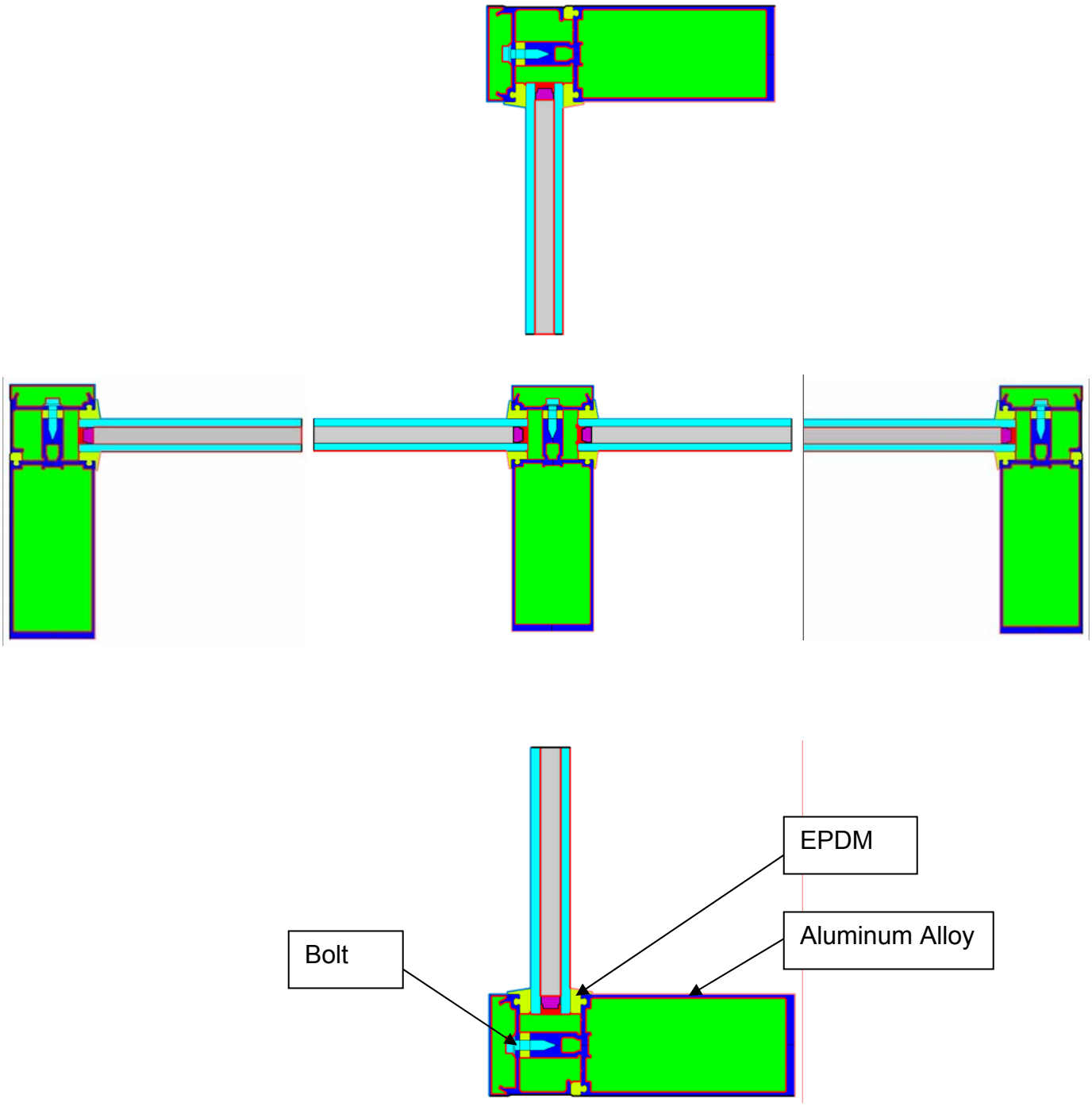


Figure 8. Kawneer 1600 System 1

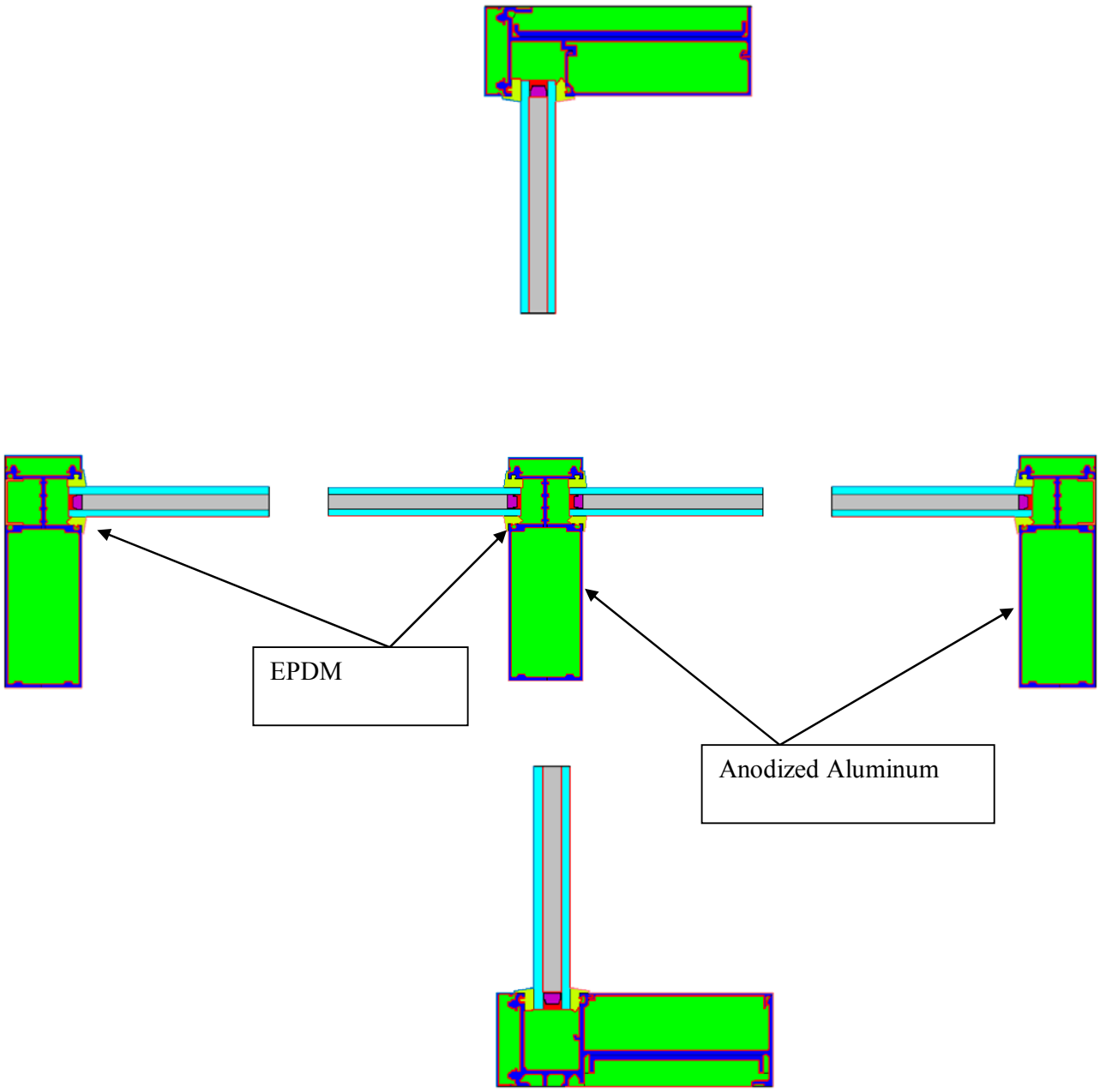


Figure 9. Kawneer 1600 System 5

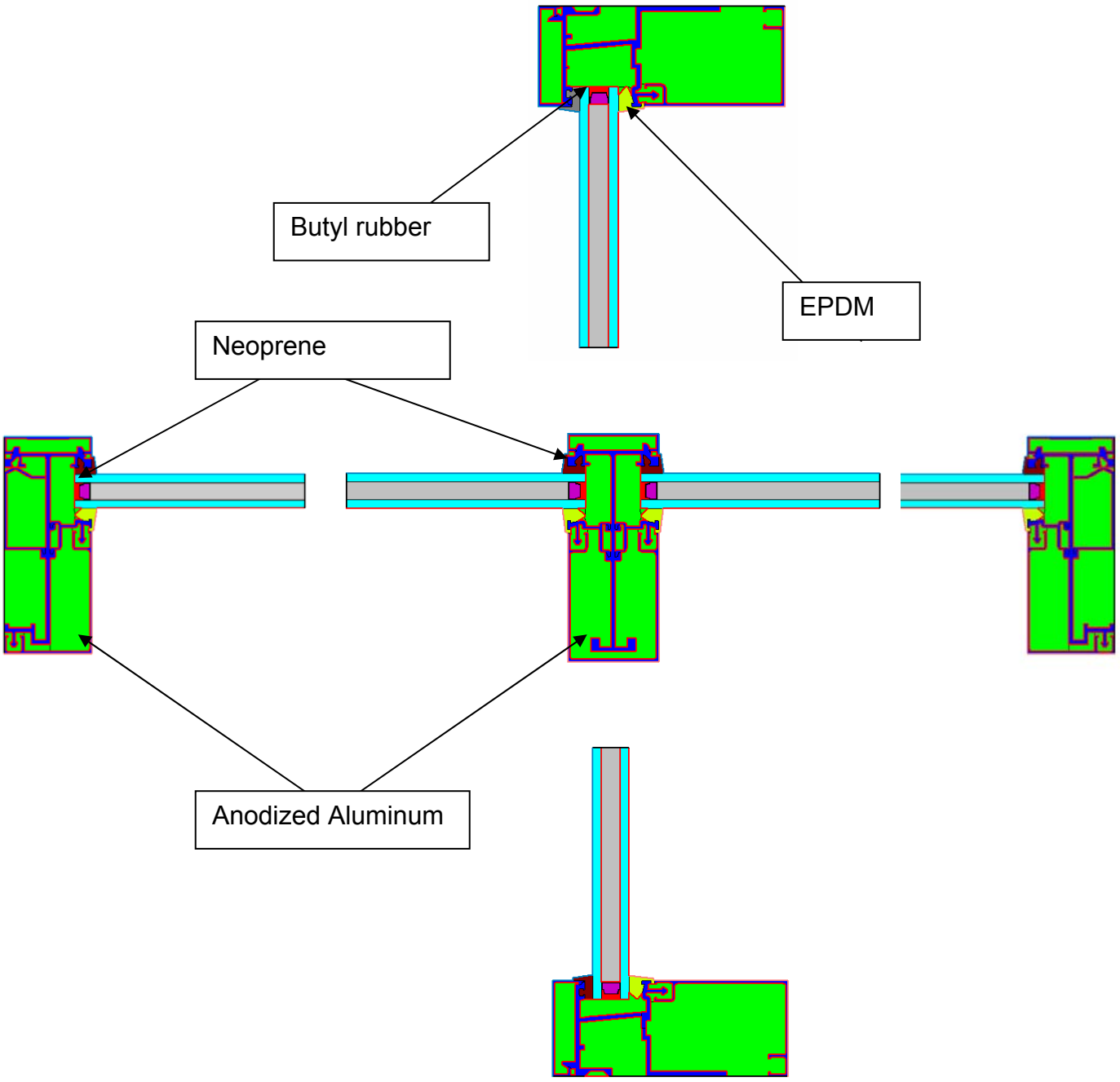


Figure 10. Kawneer 6000 IB

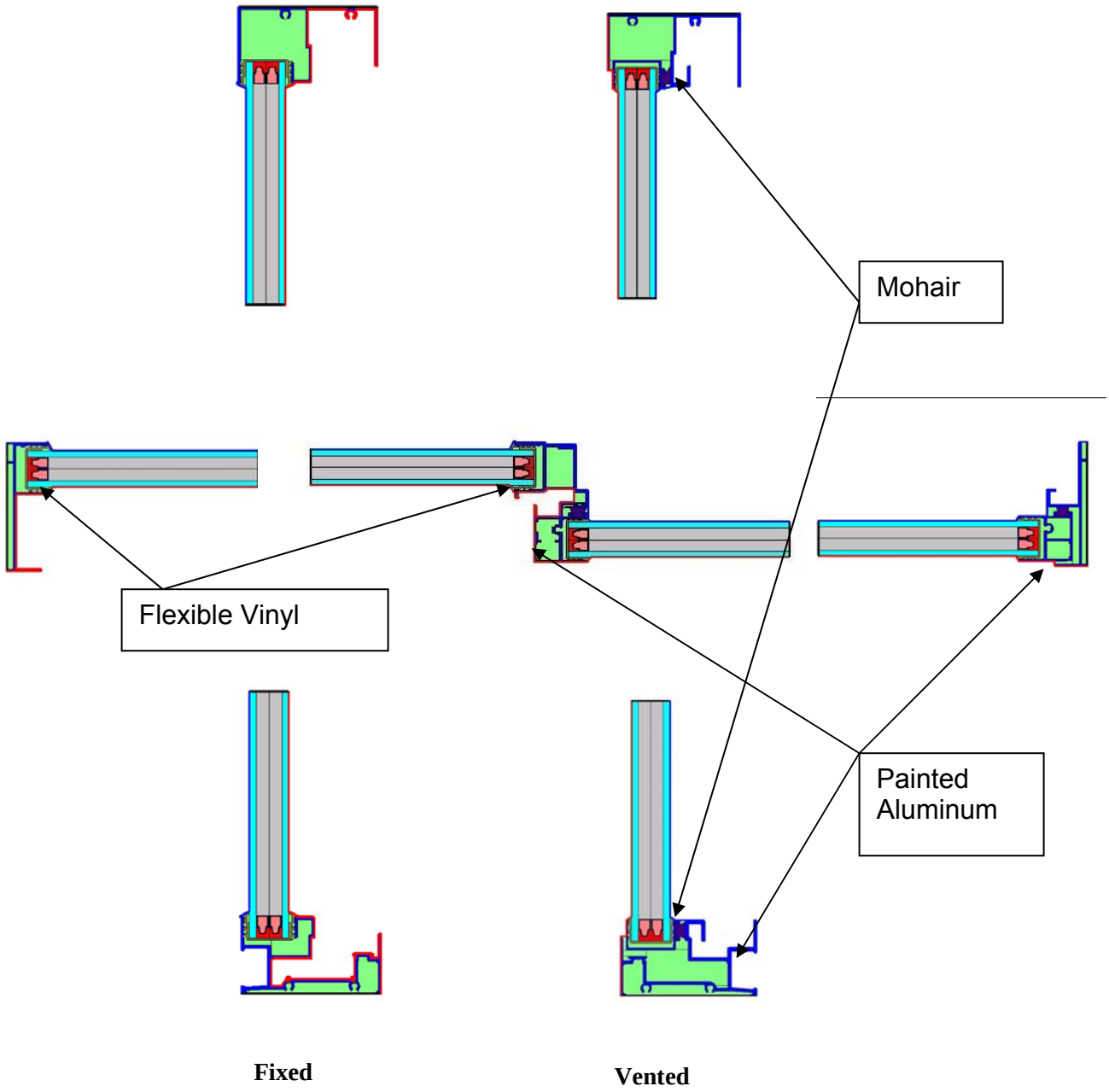


Figure 11. NFRC Testing Round Robin 1999 (TRR99)

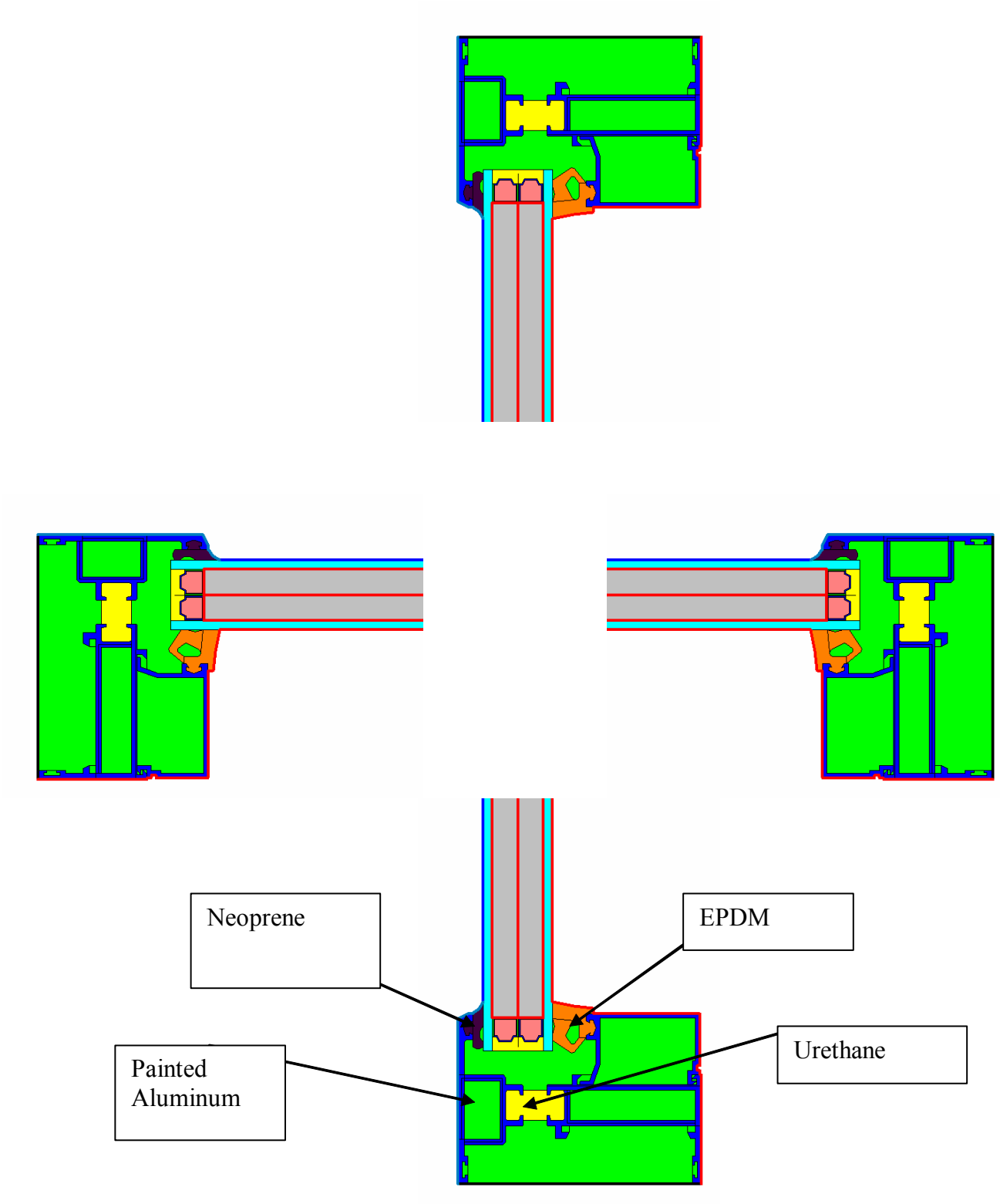


Figure 12. NFRC Testing Round Robin 2001 (TRR01)

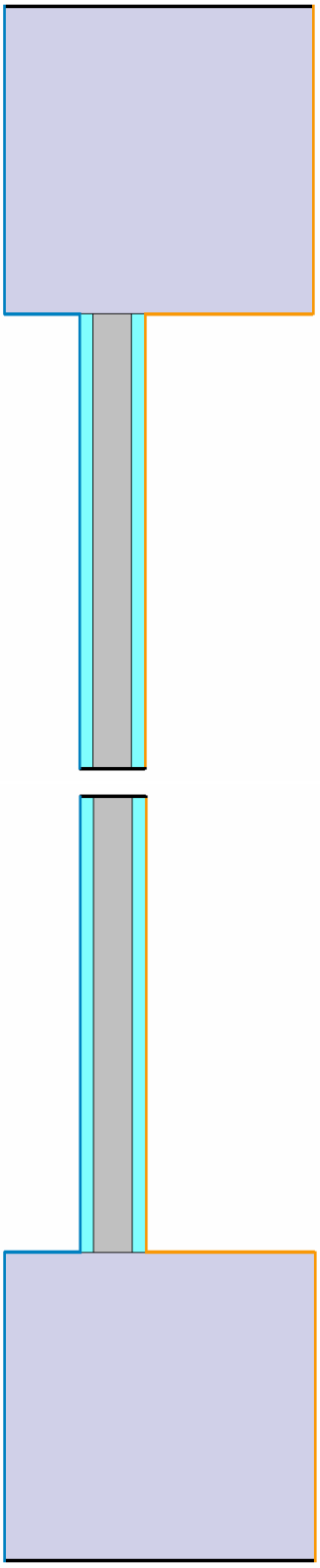


Figure 13. Flat CTS

MODELING RESULTS

All of the models had been simulated using THERM 5.2 and WINDOW 5.2, using NFRC 100-2001 and NFRC 200-2001 procedures. In addition, modeling was also done using convective heat transfer coefficient developed from the detailed computer modeling using FLUENT (Fluent 2004), in combination with the existing published work, both numerical and experimental. The following sections present results of the development of convective heat transfer coefficient.

CONVECTIVE FILM COEFFICIENT DEVELOPMENT

Existing convective film coefficient correlations are critically examined and new correlations based on theoretical analysis and numerical simulations were investigated. Two theoretical correlations, based on experimental work of the flow in square open channel, more representative of the hot box configuration, where baffle and surround panel form channel flow.

Previously Published Correlations

Fresh look was taken at the problem of natural convective heat transfer on indoor fenestration surfaces. Concern was that current correlations are developed for flat plate in infinite medium, while in reality windows are placed in a hot box where there is a "channel" usually 6 in. wide. Because of the close proximity of two boundary layers, from two parallel surfaces forming a "channel", concern was that actual heat transfer rates may be substantially different than for flat plate in infinite medium. **Figure 14** shows geometry and natural convection flow conditions for a typical hot box setup on the warm side.

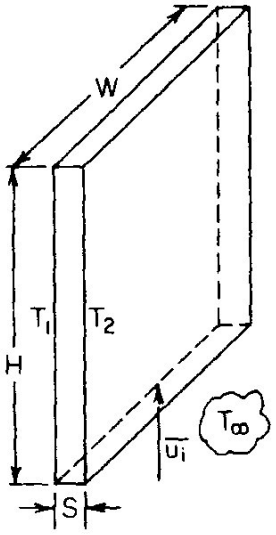


Figure 14. Geometry and Flow Conditions in a Hot Box Setting

Bar-Cohen/Rohsenow Correlations:

Extensive review of the literature pointed to the two important papers, which provide experimental correlations for the flow in a vertical channel, like the one on Figure 14. First reference is correlation by Bar-Cohen and Rohsenow (1984). They investigated effects of temperature differential, channel height, and channel width on heat transfer rates. The correlation is presented in equation (1). Assuming channel width of 6 in., **Figure 15** shows graphs of convective heat transfer coefficients based on surface-to-air temperature differential and window height.

$$\overline{Nu_s} = \left[\frac{C_1}{\left(Ra_s \frac{S}{H} \right)^2} + \frac{C_2}{\left(Ra_s \frac{S}{H} \right)^{\frac{1}{2}}} \right]^{-\frac{1}{2}} \qquad (1)$$

Where:

C_1 = 144

C_2 = 2.87

$Ra_s \frac{S}{H} \le 10$ *;* For fully developed flow

$Ra_s \frac{S}{H} \ge 100$ *;* Isolated plate limits

$$Ra_s = \frac{g\beta(T_s - T_\infty)S^3}{\alpha\nu}$$

$$\beta = \frac{1}{T_m}$$

Properties of the air are calculated at T_m, where:

$$T_m = \frac{T_s + T_\infty}{2}$$

$$\overline{h_s} = \frac{\overline{Nu_s} \cdot k}{S}$$

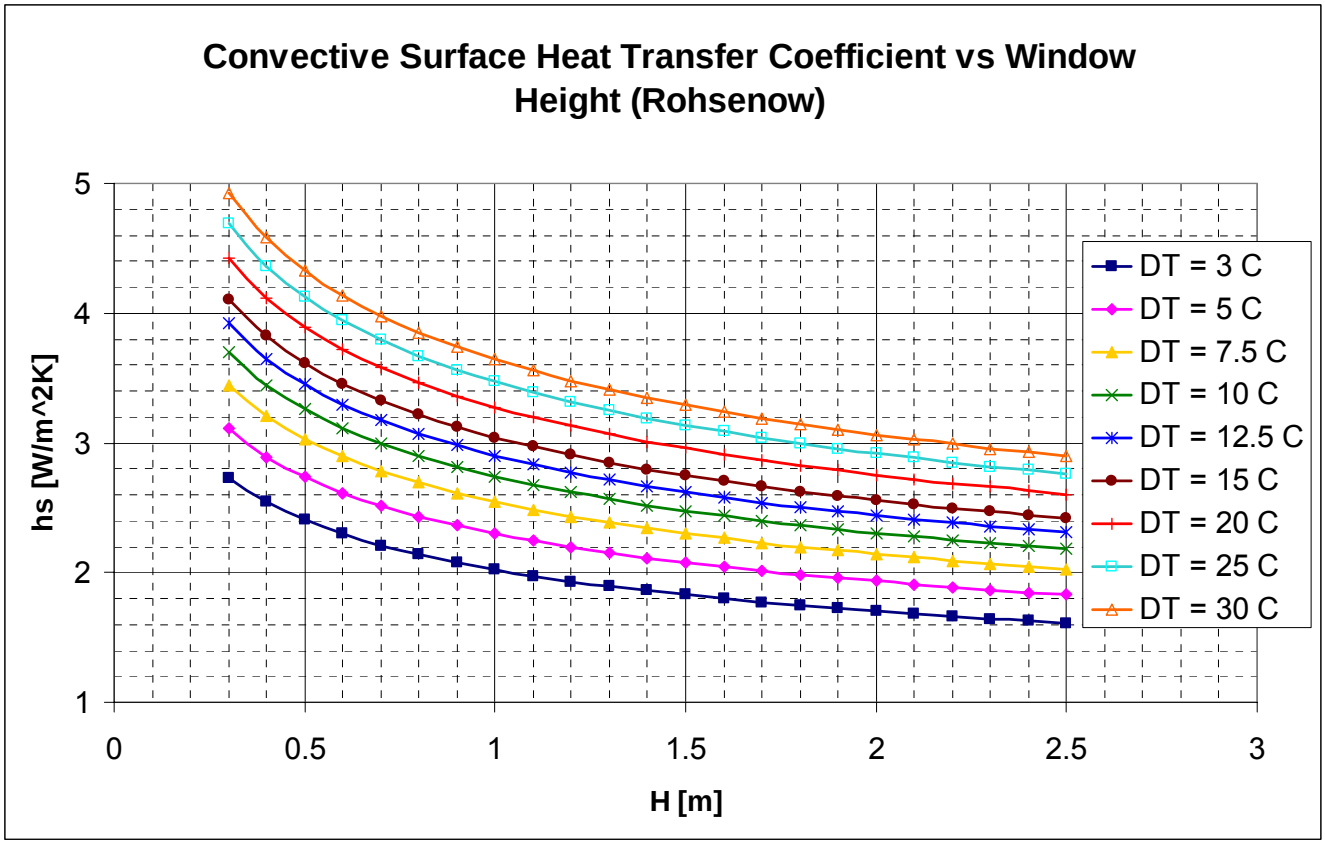


Figure 15. Average convective heat transfer coefficient as a function of window height and temperature difference – Bar-Cohen & Rohsenow correlations

Aung Correlations:

Second reference that was selected is by Aung (1972). He looked at the same type of configuration and conditions. Aung has additionally looked at the dependence of both surface temperatures on heat transfer rates. Correlations, based on this reference are presented by equations 2 and 3. **Figure 16** shows curves of heat transfer coefficient as a function of surface-to-air temperature differential and window height. Width of the channel was assumed to be 6 in. as well as surface temperature of the second surface being equal to the free stream air temperature, which are both reasonable assumptions for hot box environment.

$$Nu_{fd} = \frac{4T^{*2} + 7T^{*} + 4}{90\left(1+T^{*}\right)^{2}} Ra\,;\; Ra \le 10^{3} \qquad (2)$$

Where:

$$Ra = \frac{g\beta\left(\overline{T_w} - T_\infty\right)S^3}{\alpha\nu}\frac{S}{H}$$

$\overline{T_w} = \frac{1}{2}(T_1 + T_2)$; where T_1 = Window surface temperature and T_2 = baffle temperature

$$T^* = \frac{T_\infty - T_2}{T_\infty - T_1}$$

$$\beta = \frac{1}{T_m}$$

properties are evaluated at $T_m = \frac{1}{2}(\overline{T_w} + T_\infty)$

$Nu_l = c\overline{C_l}Ra^{1/4}$; $10^3 < Ra \le 10^5$

Where:

c = 1.2 – 1.32 (use 1.2)

$\overline{C_l} =$ 0.515 (for air)

$$\overline{Nu_s} = \left[(Nu_{fd})^m + \left(c\overline{C_l}Ra^{1/4}\right)^m \right]^{1/m}; \; Ra \le 10^5 \qquad (3)$$

Where:

m = -1.9

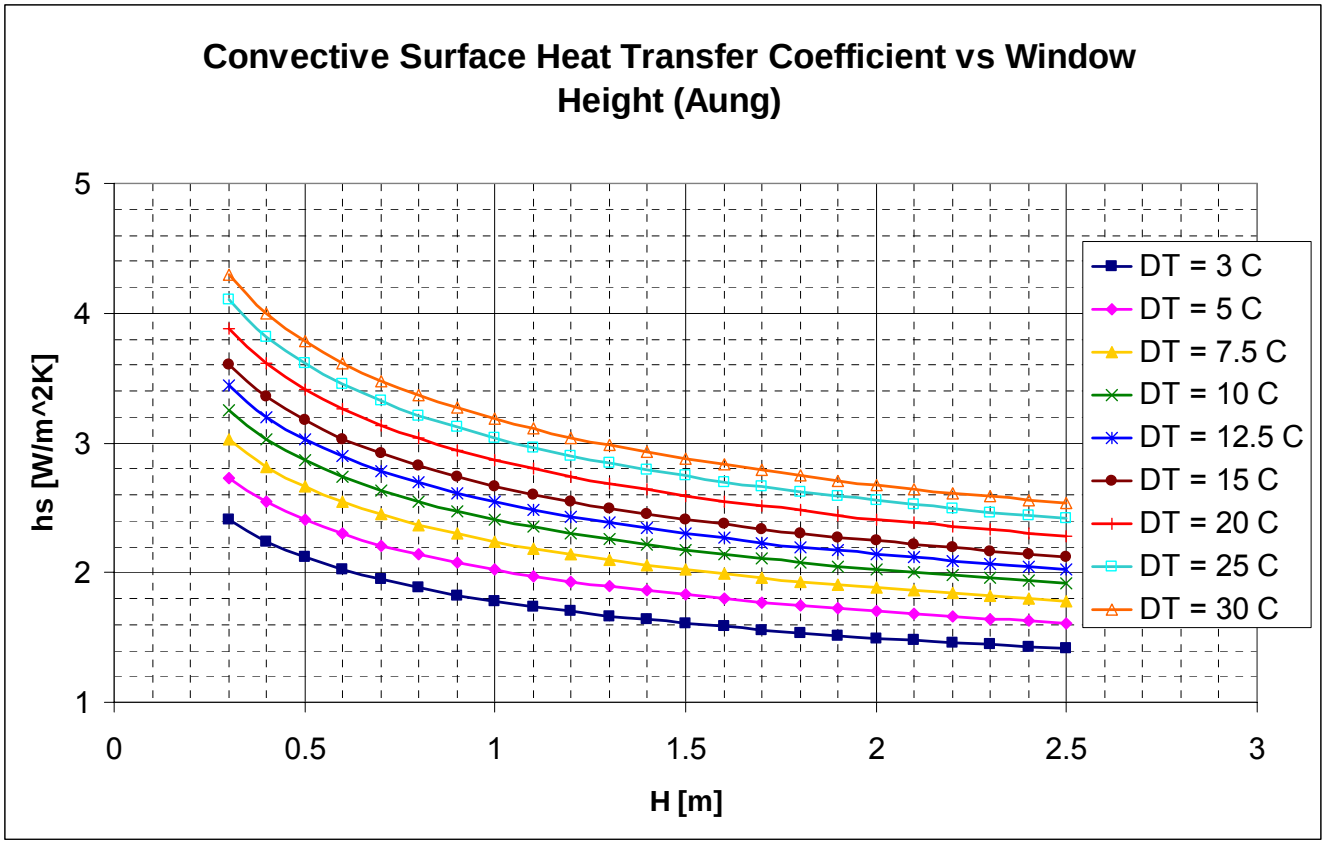


Figure 16. Average convective heat transfer coefficient as a function of window height and temperature difference – Aung correlations

ISO 15099 Correlations (Currently used correlations):

In order to provide comparison with the two new correlations, currently used correlations in NFRC 100 and 200 are presented here in equations 4 to 6. Graph with convective heat transfer curves is presented in**Figure 17**.

$$Ra_C = 2.5 \cdot 10^5 \left(\frac{e^{0.72 \cdot \theta}}{\sin \theta} \right)^{1/5} \quad ; \theta \text{ in degrees} \tag{5}$$

$$h_{c,in} = N_u \frac{k}{H}$$

where,

N_u – Nusselt number

k – thermal conductivity of air

H – height of the fenestration system

Windows inclined from 15^o to 90^o $(15^o \le \theta \le 90^o)$

$$Ra_C = 2.5 \cdot 10^5 \left(\frac{e^{0.72 \cdot \theta}}{\sin \theta} \right)^{1/5} \quad ; \theta \text{ in degrees} \tag{5}$$

$$N_u = 0.56 \cdot (Ra_H \sin\theta)^{1/4} \; ; Ra_H \le Ra_C \tag{6}$$

$$N_u = 0.13 \cdot (Ra_H^{1/3} - Ra_C^{1/3}) + 0.56 \cdot (Ra_C \sin\theta)^{1/4} \; ; Ra_H > Ra_C \tag{7}$$

where,

Ra_H – Rayleigh number based on the height of the fenestration system, defined as:

$$Ra_H = \frac{\rho^2 H^3 g C_p (T_{in} - T_{b,n})}{T_{mf} \mu k}$$

Air properties (i.e. density, specific heat, viscosity and thermal conductivity) are evaluated at the mean film temperature:

$$T_{mf} = T_{in} + \frac{1}{4}(T_{b,n} - T_{in})$$

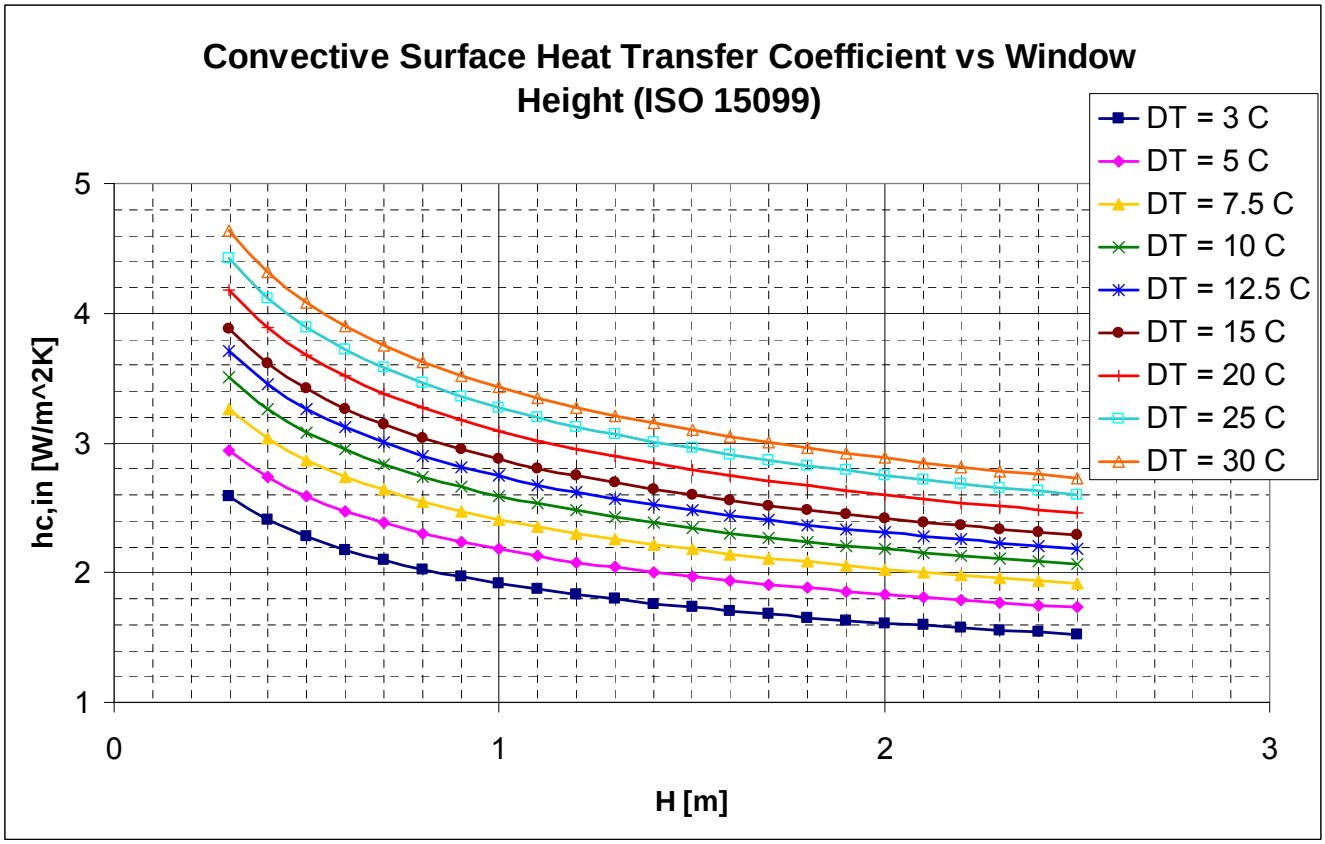


Figure 17. Average convective heat transfer coefficient as a function of temperature difference – ISO 15099 correlations

Additionally, graph comparing the three sets of correlations for selected temperature differentials is shown in **Figure 18**.

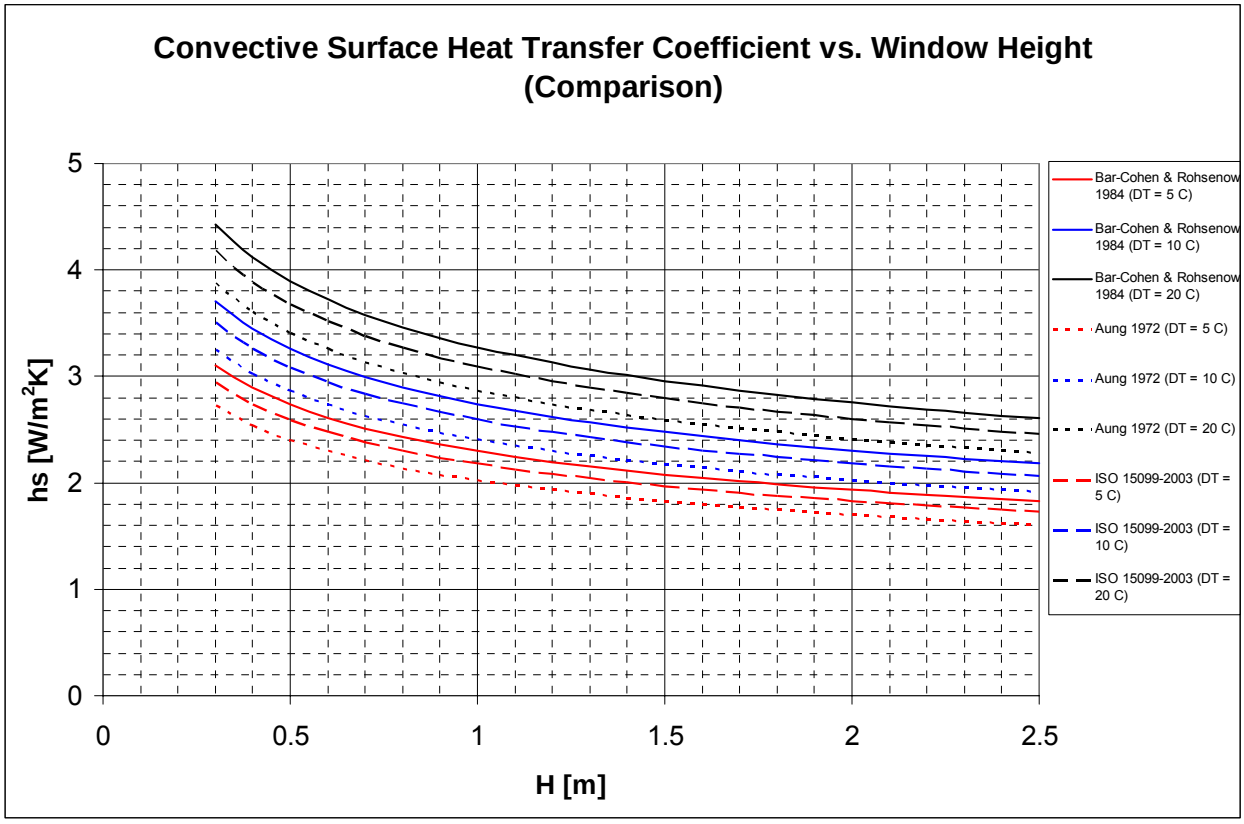


Figure 18. Comparison of Convective Surface Heat Transfer Coefficients for Different Correlations

Numerical Simulations:

Numerical simulations are done for two samples placed in two different thermal chambers. One sample is typical fixed window placed in a LBNL IR thermography chamber. The other sample is projecting CTS, placed in a typical hot box environment. Both sides of thermal chamber, cold and warm were modeled, however, only the results from the warm side are presented in detail here.

Natural Convection in a LBNL IR Thermal Chamber

Typical wood window has been modeled in a LBNL IR Thermal chamber setting using FLUNET software. Natural convection, aided by small fans on the warm side (in a plenum under the floor of the chamber), has been modeled using FLUNET turbulent model. The modeling results have been compared to measurements of temperature and velocity profiles on the vertical cross-section. The model description and results of validation are presented here:

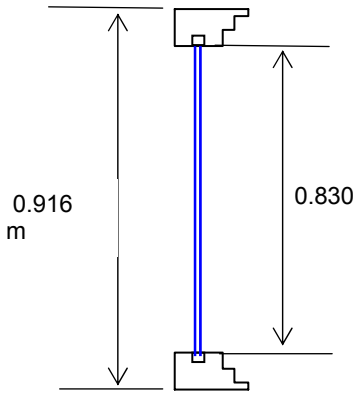


Figure 19. Geometry of the validation specimen

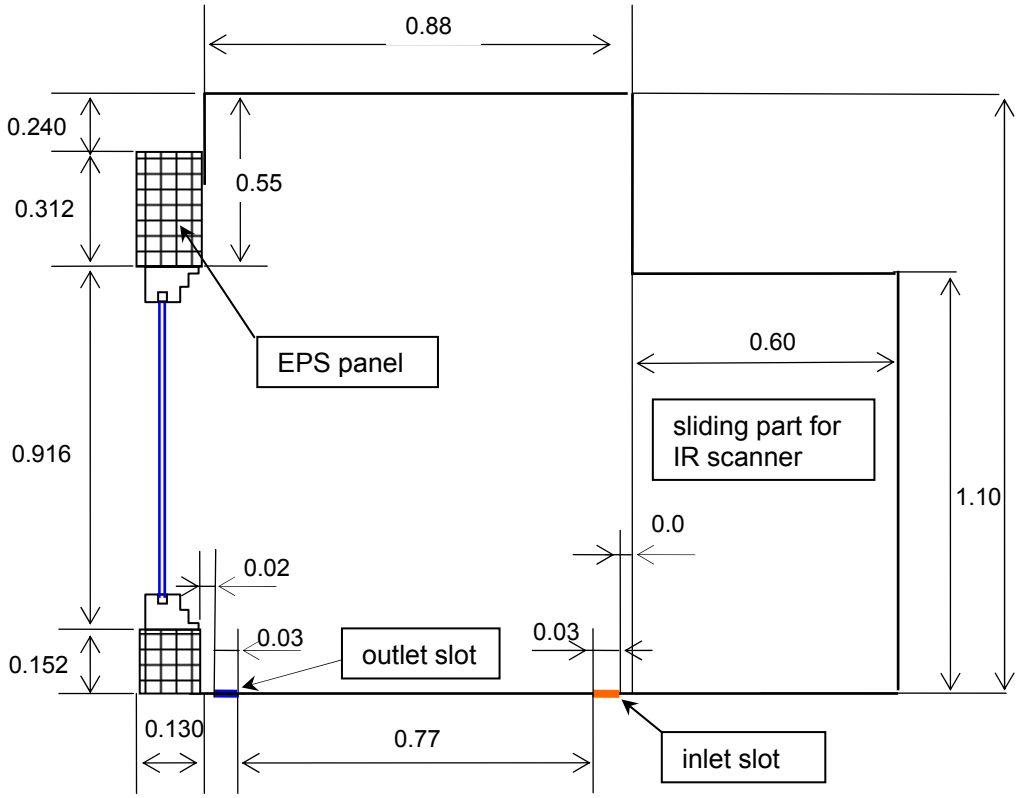


Figure 20. Geometry of the test chamber setup and specimen location

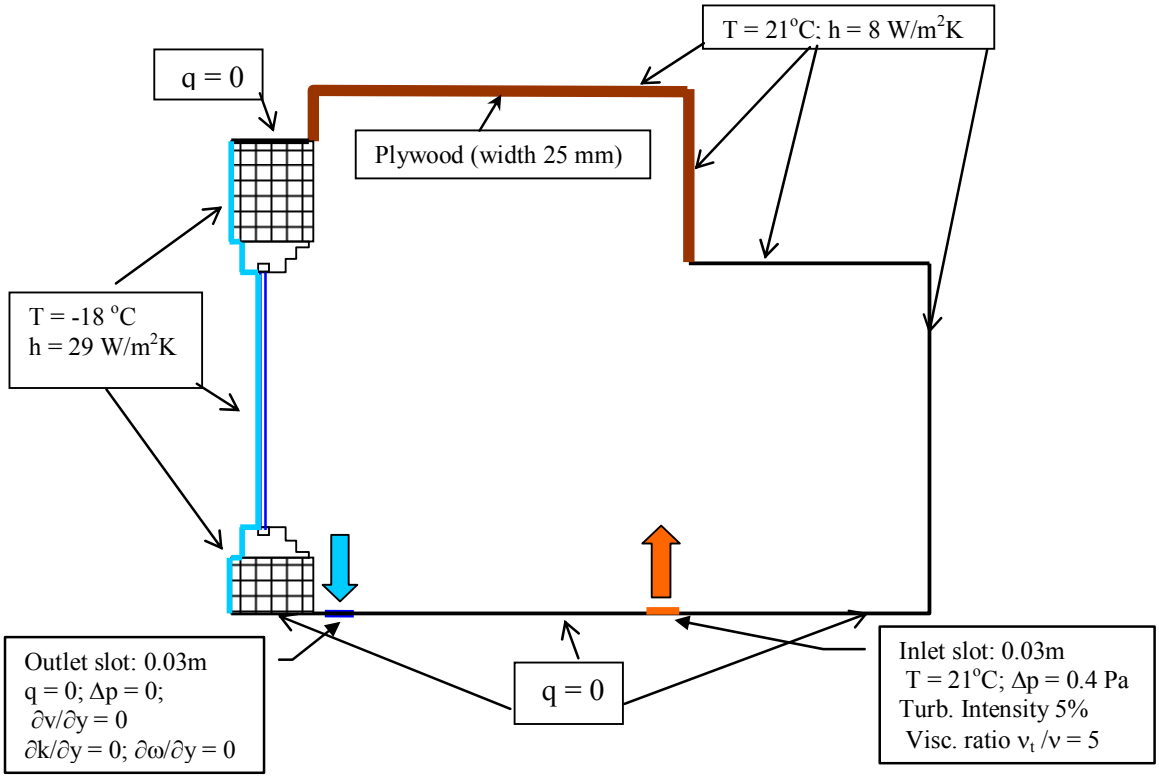


Figure 21. Schematic of the mathematical model

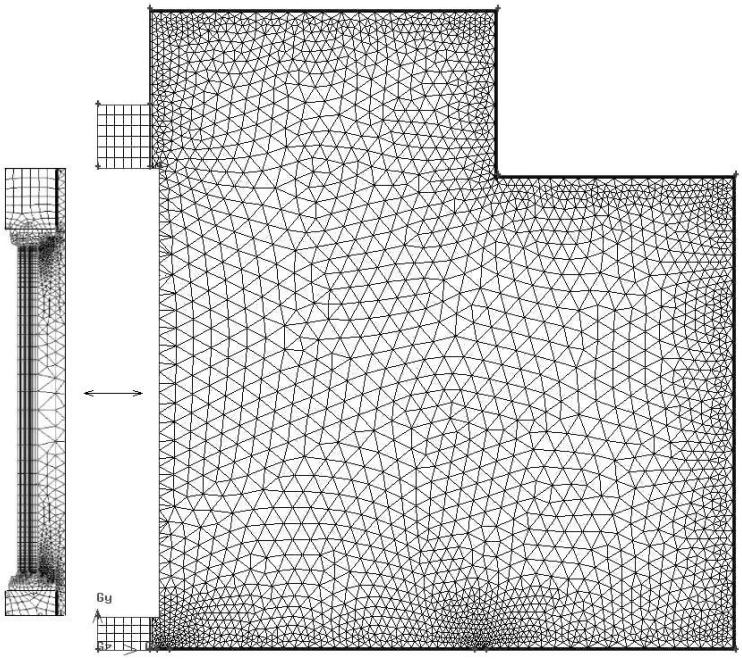


Figure 22. Numerical model of the thermal test chamber and specimen setup

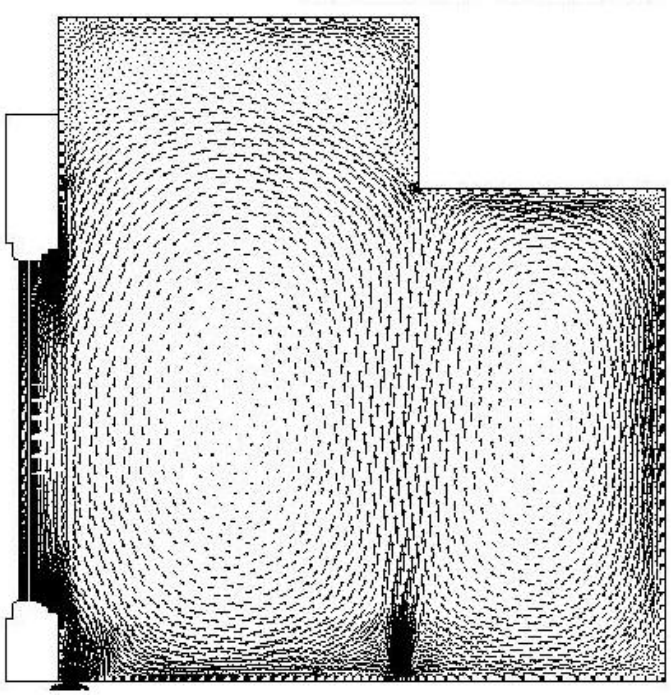


Figure 23. Velocity vectors for the flow in thermal test chamber

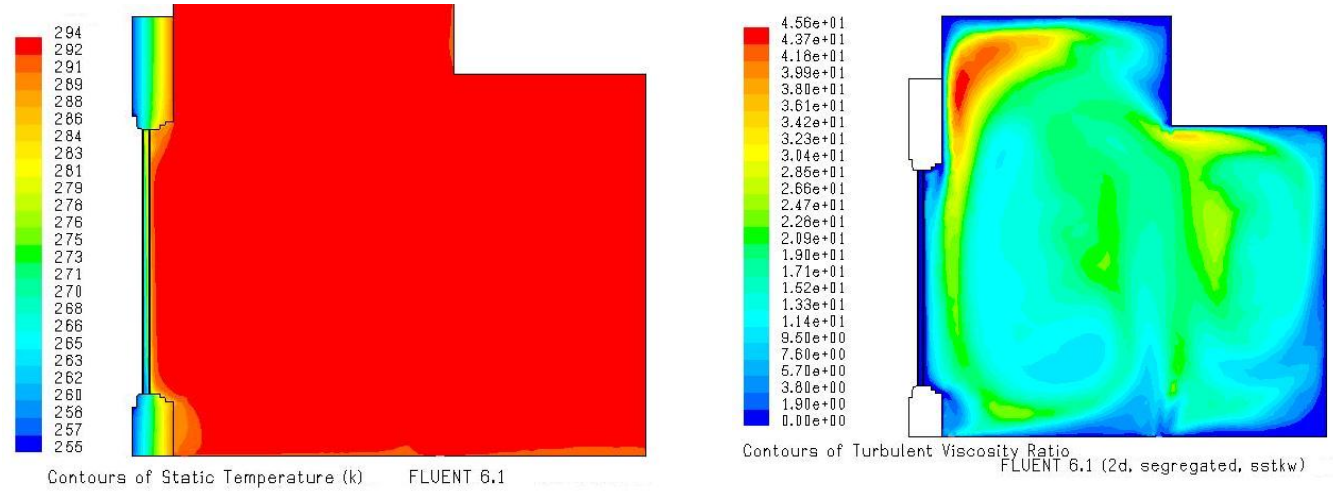


Figure 24. Temperature and turbulent viscosity fields in thermal test chamber

The comparison predicted and measured vertical velocities at the specific height from the bottom of the PFM window glazing is given in **Figure 25**. Predicted maximal value

(0.26 m/s) is less than measured one (0.28 m/s) by 7 %. Predicted thickness of inner part of boundary layer (between surface and maximum) is 6 cm and measured one is 7.5 cm.

The comparison between predicted and measured distributions of convective heat transfer coefficients along glazing surface is presented in **Figure 26**. The calculated average convection film coefficient on window glazing is 3.04 W/(m^{2o}C) that is very close to the average value obtained in experimental work [5]: h_c = 3 W/(m^{2o}C).

Thus, results of the numerical model compare excellent with available experiment results for the sample window (PFM01).

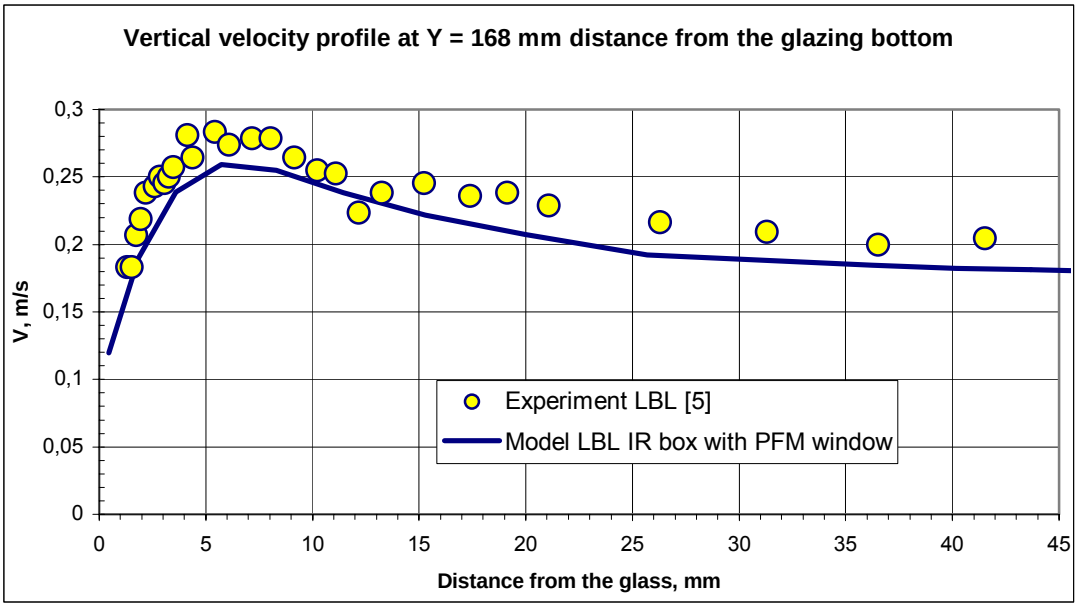


Figure 25. The predicted and measured vertical velocity profiles.

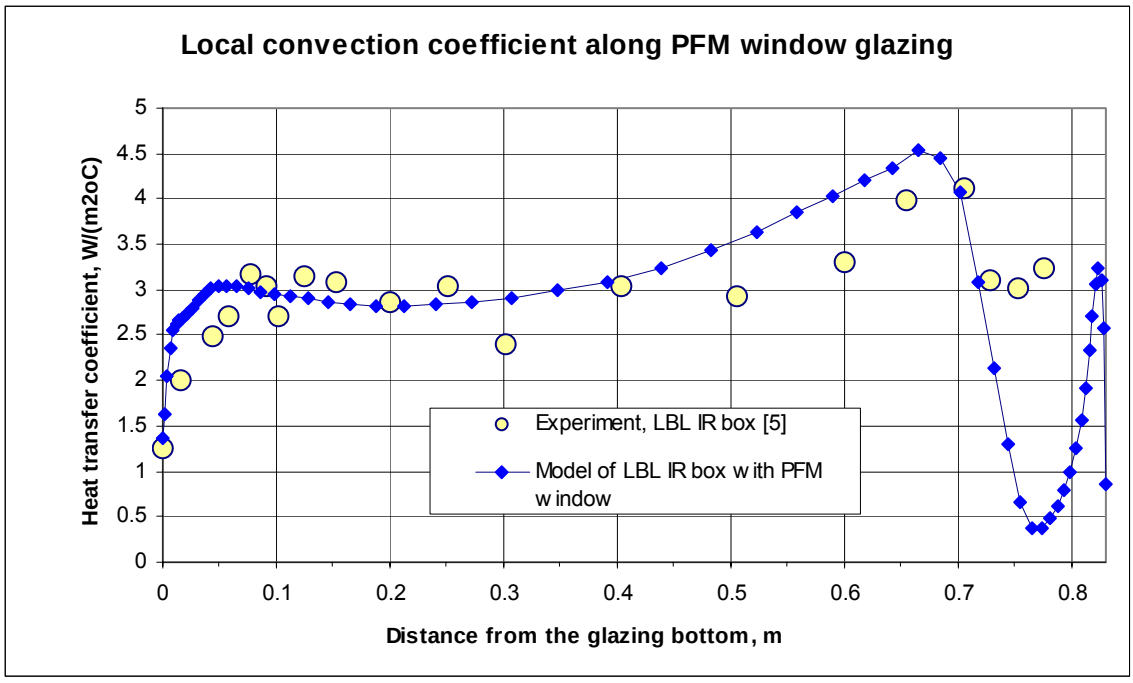


Figure 26. The comparison between predicted and measured distributions of convective heat transfer coefficients on glazing surface

Projecting CTS and Natural Convection in a Typical Hot Box Setup

Projecting CTS, originally measured by Intertek Testing and given in Table 2, has been modeled as installed in a hot box and natural convection heat transfer, coupled with detailed radiation heat transfer, as well as cold side forced convection have been modeled using FLEUNT. Again, appropriate turbulent models are applied to each side and described in the following section. Geometry and boundary conditions were specified in order to duplicate conditions present during the physical test.

The results are shown in terms of temperature and turbulence kinetic energy fields, velocity profiles, and local film coefficient distributions. Also, integrated film coefficients are tabulated.

Description of The Modeling Geometry And Boundary Conditions

Characteristic sections of the climatic and warm-side chambers of a hot box were modeled. Projecting CTS panel was installed in the surround panel. Baffles and spaces between surround panel and baffles were modeled as well. The main goal of this modeling was to obtain distribution of local heat transfer coefficient along projecting CTS surfaces. Also, temperatures and velocities around CTS, under the typical conditions of a hot box were recorded, so that comparison with physical test could be made. **Figure 27.** Schematic of geometry, including dimensions of the modeled projecting CTS panel installed in hotbox (not to scale). shows geometry of the model.

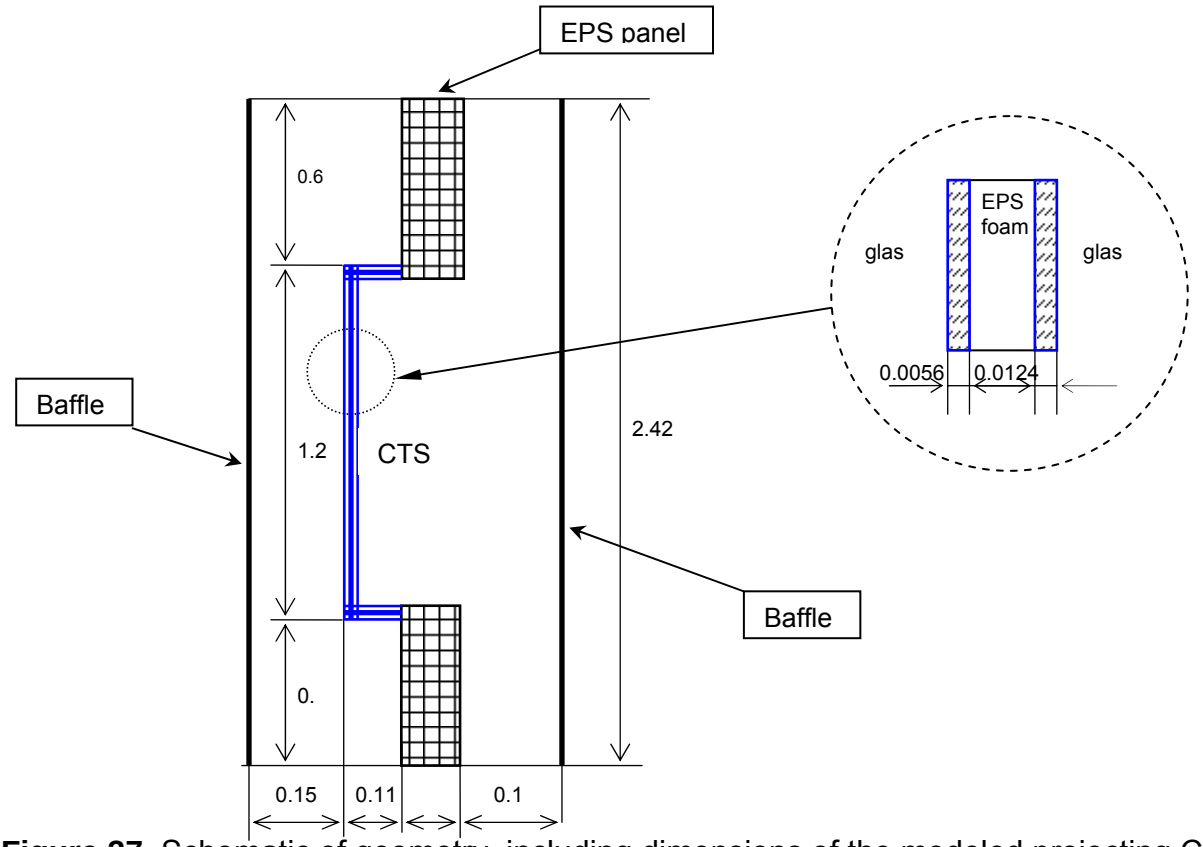


Figure 27. Schematic of geometry, including dimensions of the modeled projecting CTS panel installed in hotbox (not to scale).

Boundary conditions were defined for the model of a hot box with installed projecting CTS and shown in **Figure 28**.

Thermo-physical properties of air were treated as constants and were evaluated at the temperature of –17.8°C for air for the cold side and at the temperature of 21.1°C for the warm side. Boussinesq approximation was used in viscous turbulent model.

Material thermo-physical properties are given in **Table 6**.

Table 6. Material thermo-physical properties

Material/Component	Conductivity, W/(m-K)	Emissivity
Glass	0.90	0.84
EPS foam core of CTS panel	0.0325	0.90
Insulated surround panel (EPS)	0.038	0.90
Steel (baffle)	50	0.90

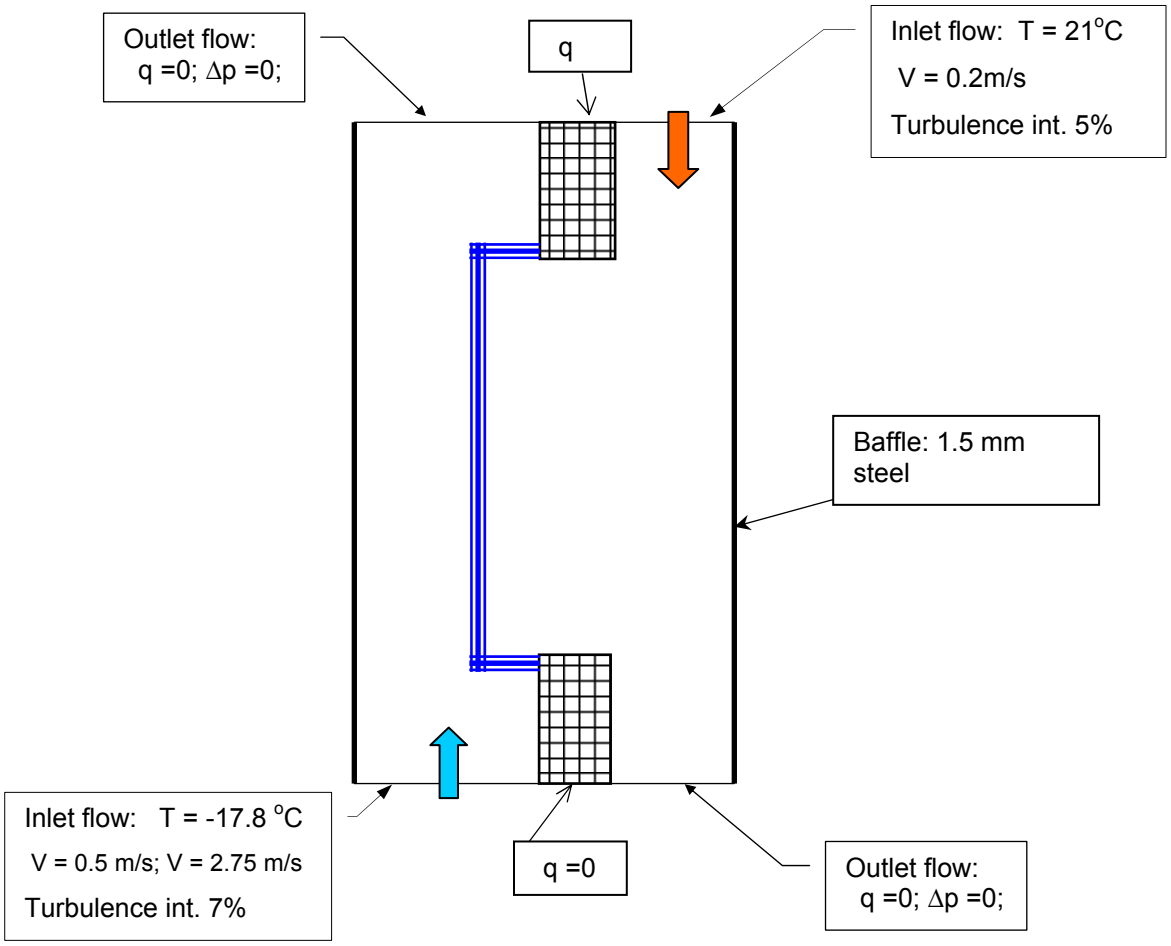


Figure 28. Boundary conditions for the model.

MODELING RESULTS

The mesh of the model was created by using Fluent's software Gambit 1.3 [3] and shown in **Figure 29**. The main boundary layer along CTS and insulated panels has parameters: 9 - element number, first element size 0.0005 m, increasing ratio coefficient 1.3 and summary layer thickness 0.017 m.

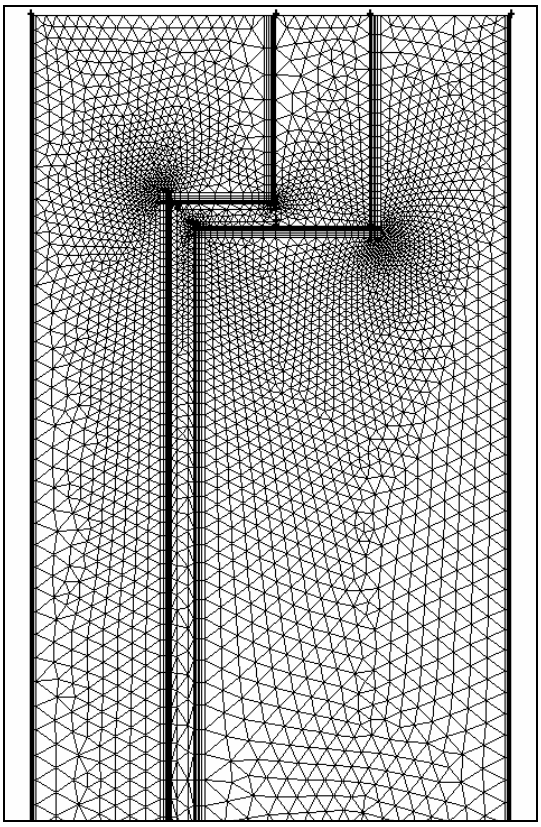


Figure 29. Finite Volume Mesh of the Model's Top Part. (Gambit [3]).

SOLUTION PROCEDURE

Segregated solver was used with the following settings:

- implicit formulation,
- steady calculation,
- energy equation was included,
- Viscous model was defined as shear-stress transport (SST) k-ω turbulence model with option *transitional flows,*
- Radiation model was defined as Discrete Transfer Radiation Model (DTRM) with angle parameters: theta divisions θ = 6, phi divisions φ = 6,
- *Solution controls*: under-relaxation factors (RF) for all equations (variables) were defined with default settings and for energy equation as RF = 0.8,
- *Method discretization*: pressure equation – PRESTO; pressure-velocity coupling – SIMPLEC; momentum – First Order; energy – First Order Scheme,
- The solution reached convergence after approximately 2000 iterations.

PRESENTATION OF RESULTS

Predicted temperature and turbulent kinetic energy fields in the computational domain are shown in **Figure 30**. Predicted temperature distribution in computational domain shows that, except for the limited domain of the boundary layer and corners on the warm side, the rest of the domain contains air at inlet temperatures of -17.8 and 21.1., respectively. At the top part of the warm side of projected CTS there are several vortices being formed, but turbulence intensity is not high. Maximum turbulent kinetic energy obtained in the cold side of the model is 1.4 m^2/s^2 at air velocity 5.5 m/s.

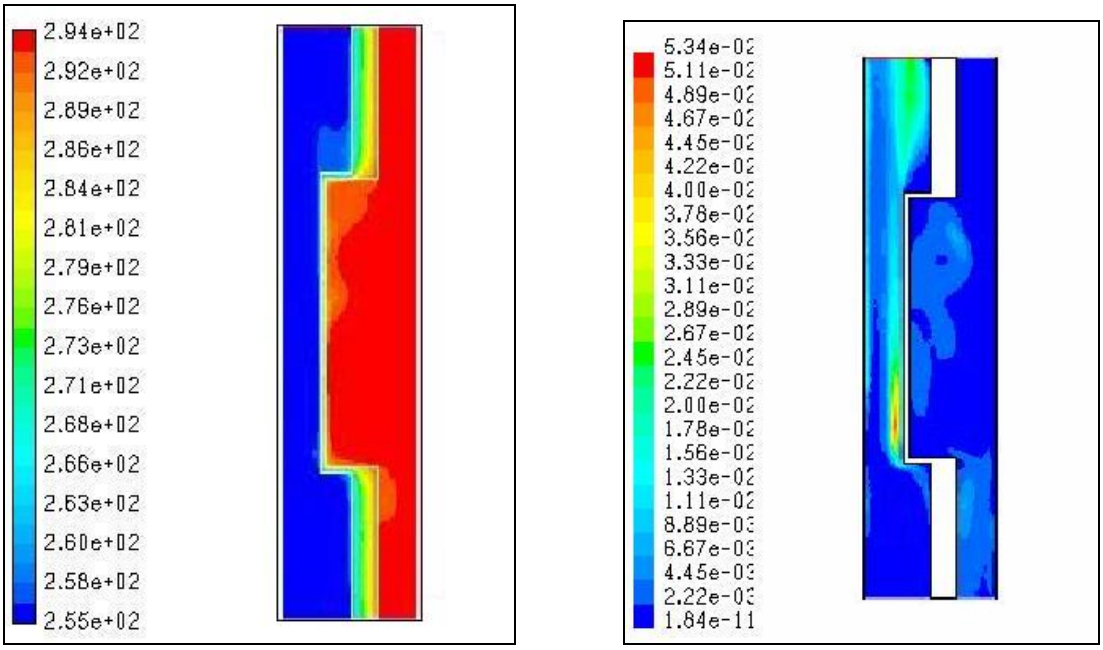


Figure 30. Contours of temperature and turbulent kinetic energy (m^2/s^2) in computational domain at cold side air velocity of 1.0 m/s. (Fluent 6.1 [1]).

Figure 31 shows the location of lines along which vertical velocities in physical test were measured. The choice of placement for these measurement points were made without any input from numerical simulations and it appears that their placement could have been done better. Figure 30 shows that turbulence intensity is quite high at the place where velocity and temperature sensors are usually located. If the sensors are located at the true free stream location, which is normally located immediately after the flow entry into the space (i.e., lower portion of the cold side and upper portion on the warm side), the sensors would measure true free stream fluid properties, which are necessary to compare to correlation that are used for standardizing results and that are also used in NFRC simulation tools. This recommendation could also be extended to the future standard revision so that the placement of measurement sensors is moved from the typical middle of the height to the location of the fluid entry into the space, shifted by the entry length, normally 2-3 opening widths long (i.e., 12-18 in.).

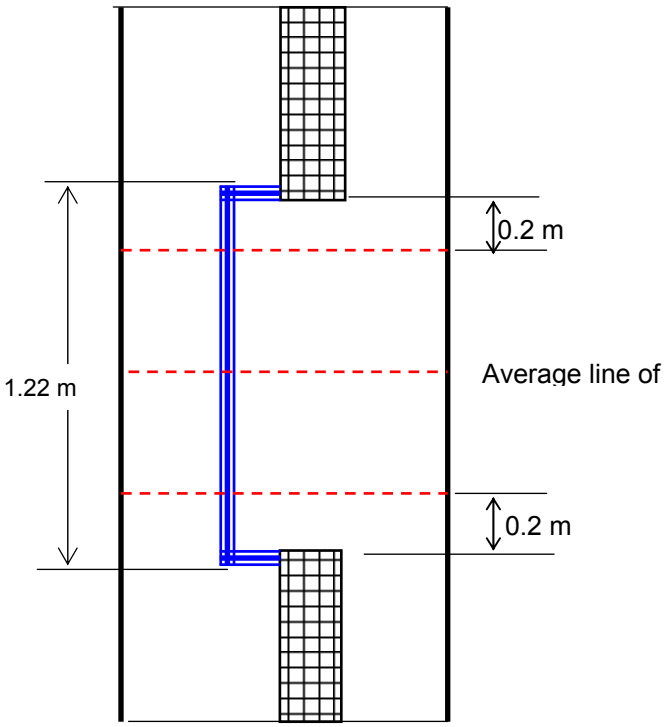


Figure 31. Schematic of location of lines along which velocities were measured.

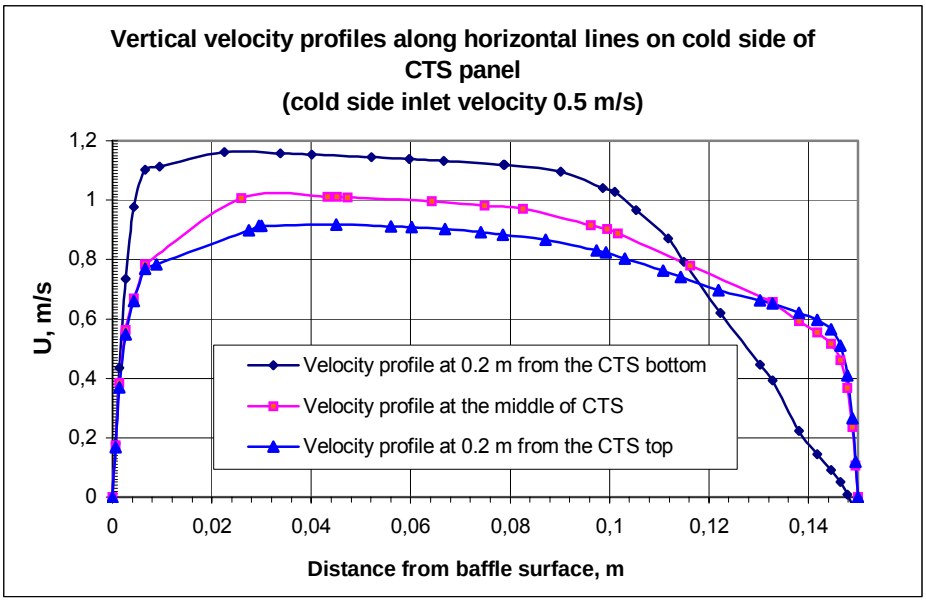


Figure 32. Vertical velocity profiles on the cold side at an air velocity 0.5 m/s.

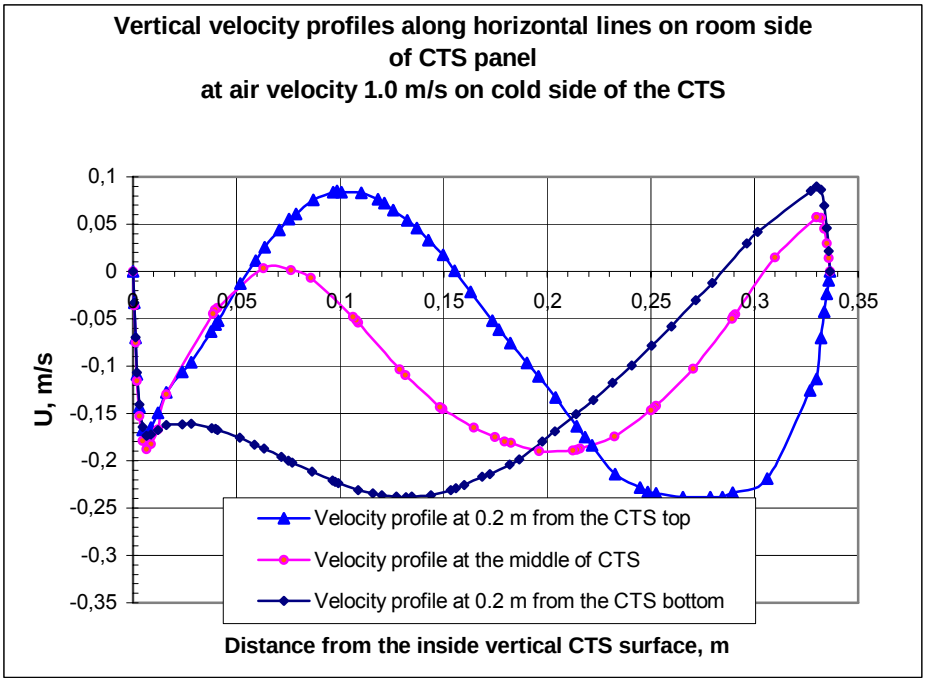


Figure 33. Vertical velocity profiles at warm side at the cold side air velocity of 1.0 m/s.

Vertical velocity profiles along the specified horizontal lines (see **Figure 31**) are presented in **Figure 33** and **Figure 35** for cases of air velocity 1 m/s and 5.5 m/s, respectively, on the cold side of the projecting CTS. In both cases inlet velocity on the warm side of the model was 0.2 m/s, as evidenced from the velocity profile near the PCTS surface at all three vertical locations. This is expected result being representative of natural convection (see **Figure 28**). Further analysis of velocity profiles shown in **Figure 33**, indicate that at the top portion of the Projecting CTS, there is stronger recirculation, as evidenced by upward velocity (0.1 m/s) further away from the vertical CTS surface. This upward flow diminishes as flow reaches mid section and at that point this upward velocity is nearly 0 and further away from the vertical CTS surface the flow again approaches 0.2 m/s in the downward direction. Finally, for the location 0.2 m from the bottom there is almost uniform flow downward at about 0.2-0.25 m/s.

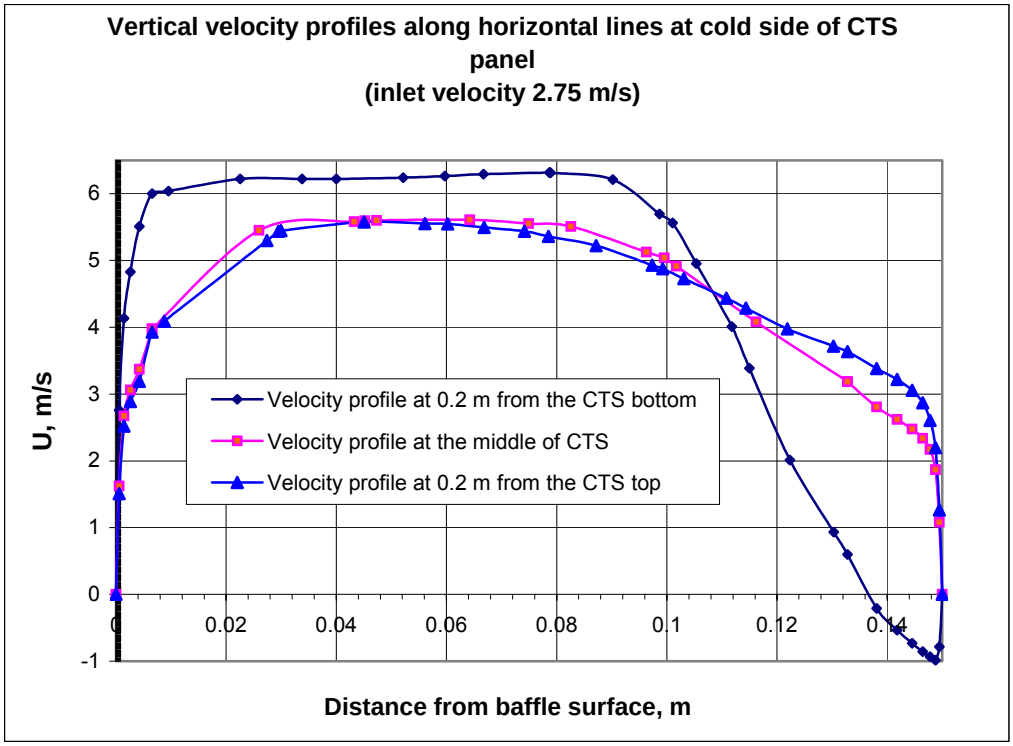


Figure 34. Vertical velocity profiles on the cold side at an air velocity 2.75 m/s.

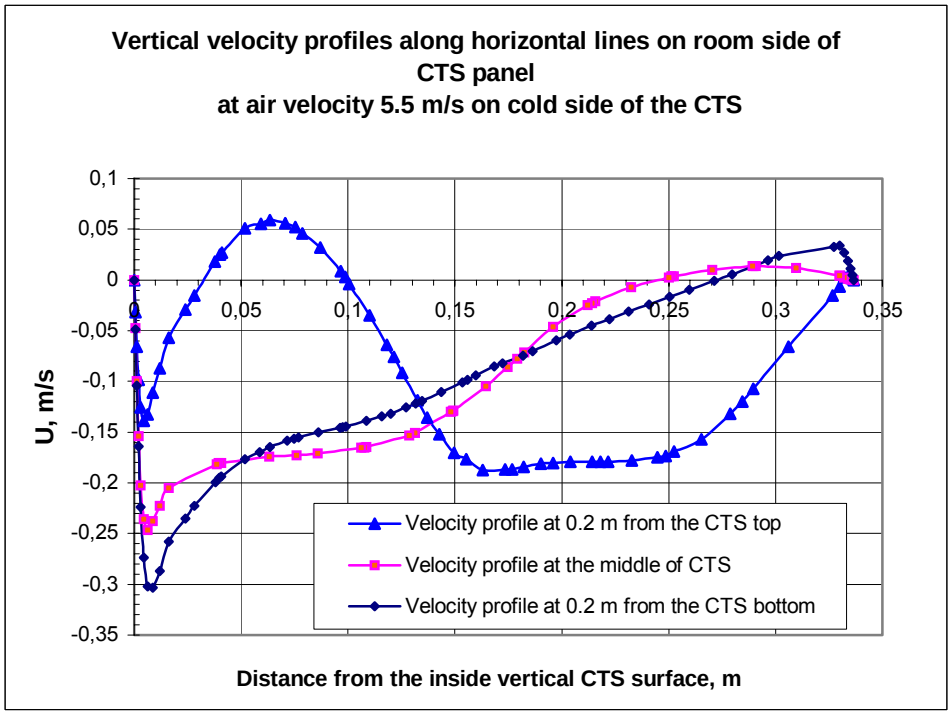


Figure 35. Vertical velocity profiles at warm side at the cold side air velocity of 5.5 m/s.

Figure 36 gives predicted temperature distribution along CTS surfaces for two values of cold side air velocity (1 m/s and 5.5 m/s, respectively).

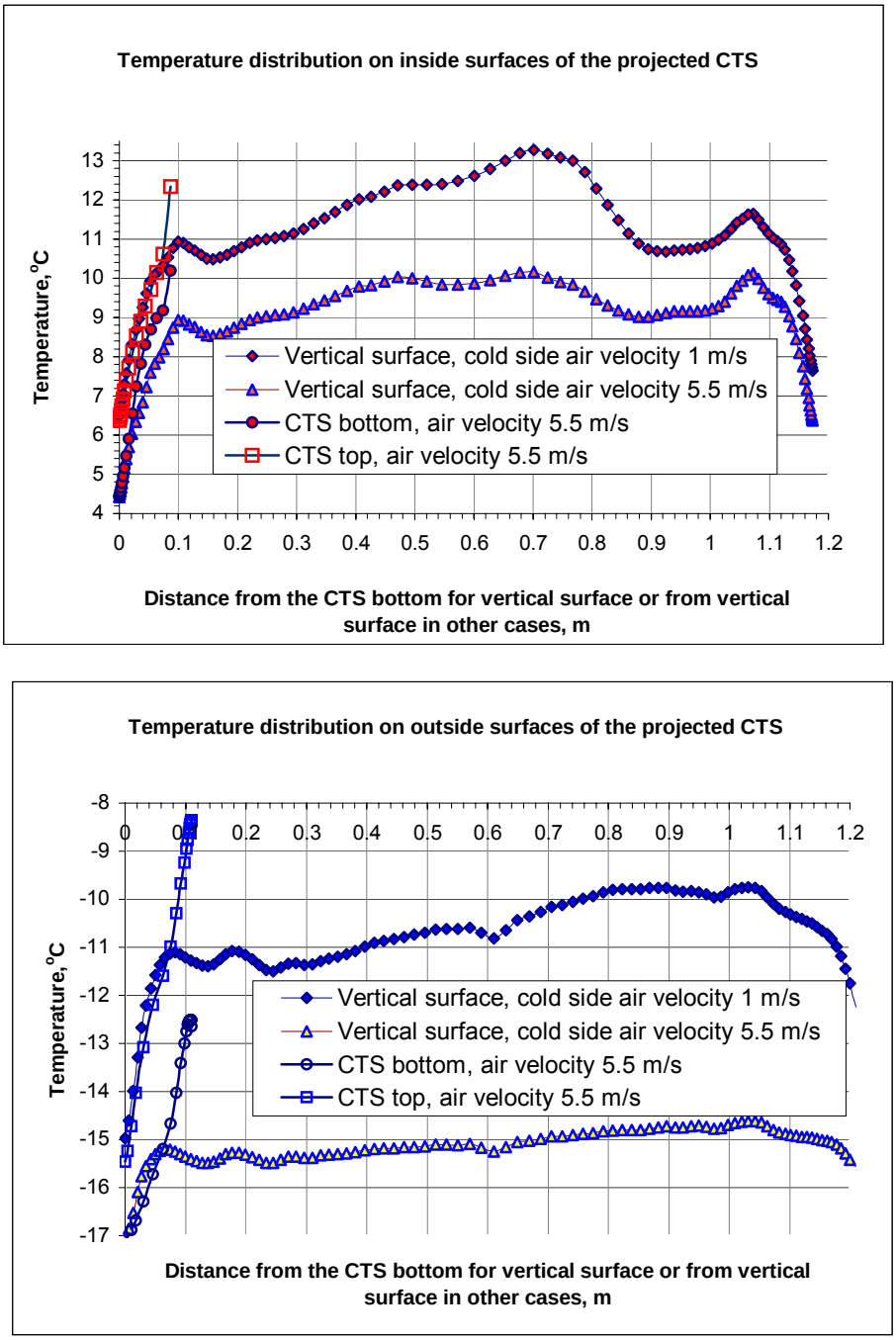


Figure 36. Temperature distributions on warm and cold surfaces of projected CTS at the two values of cold side air velocity.

Figure 37 shows predicted distribution of the local film coefficient along CTS surfaces for two values of cold side air velocity (1 m/s and 5.5 m/s, respectively)..

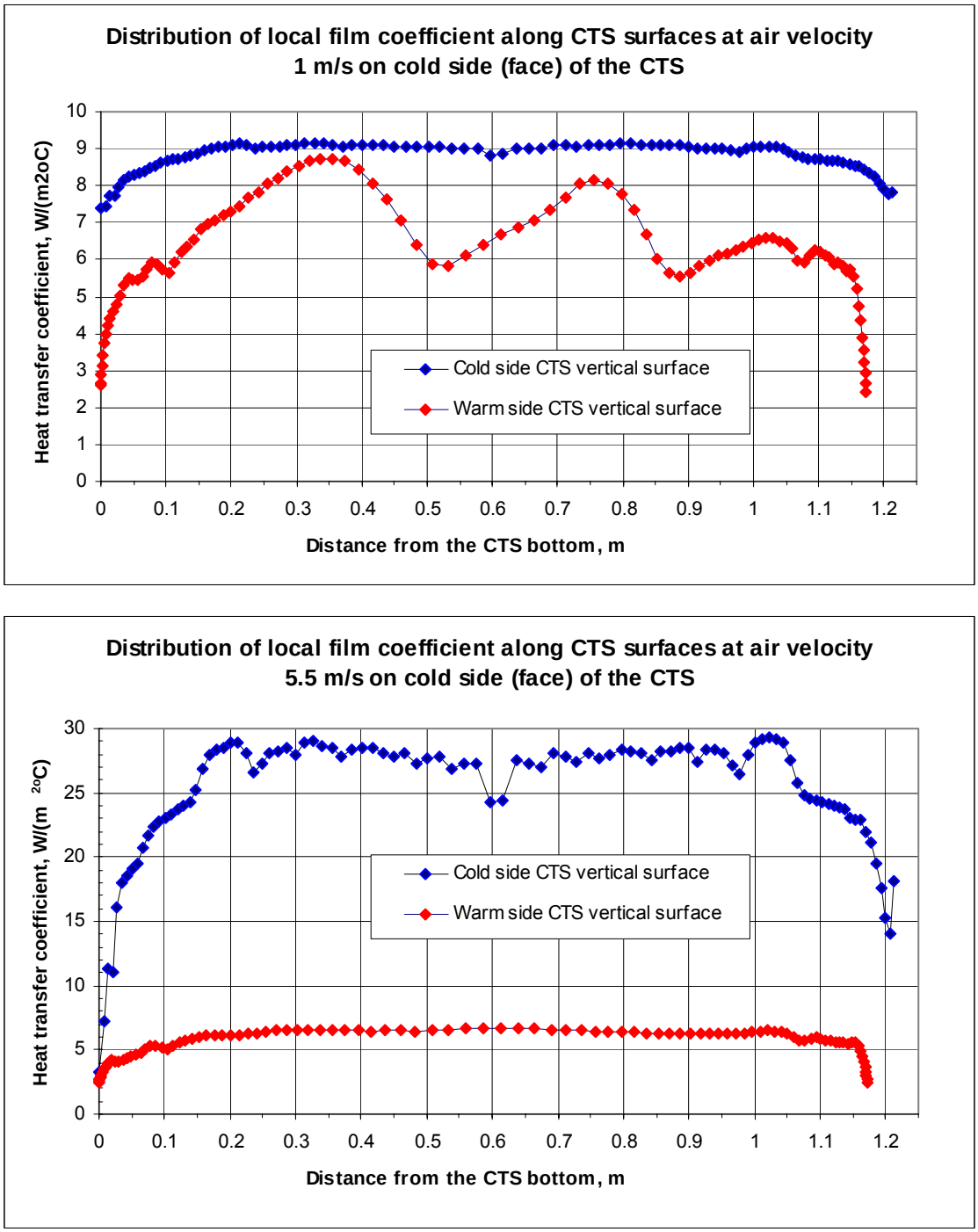


Figure 37. Distribution of film coefficient along warm and cold surfaces of the projecting CTS for 1 m/s and 5.5 m/s cold side air velocities.

Predicted values of average film coefficients on CTS surfaces at air velocities 1 m/s and 5.5 m/s along the projecting CTS are summarized in **Table 7**.

Table 7. Average (Area Weighted) **total heat transfer coefficient, h [W/(m^{2}K)]**, on Projected CTS (PCTS) surfaces at the cold side air velocity of 1m/s and 5.5 m/s.

Surface	Warm side of CTS		Cold side of CTS	
	$U_{cold\ side}$ = 1 m/s	$U_{cold\ side}$ = 5.5 m/s	$U_{cold\ side}$ = 1 m/s	$U_{cold\ side}$ = 5.5 m/s
Vertical	6.8	6.2	8.9	26.1
Top of CTS	5.1	4.8	5.3	8.1
Bottom of CTS	4.5	4.8	9.8	26.6

Table 7 shows total surface heat transfer coefficients (convection and radiation) as calculated on both, warm and cold side of the PCTS. Further on, three values were calculated on each side, one for vertical surface and one for top and bottom horizontal surface each. This was done for two cold side wind velocities. It is clear from the Table that warm side surface heat transfer coefficient is much less sensitive on the cold side velocity, while cold side film coefficient depends strongly on the wind speed. This is expected result, because cold side surface heat transfer coefficient is directly affected by wind velocity, being forced convection value. It should be noted that in NFRC we use 5.5 m/s velocity, so these results are more representative and more interesting. It should also be noted that the horizontal surface produce somewhat lower values on the warm side.

Table 8. Convective Heat Transfer Coefficient, hc [W/(m^{2}K)], on projected CTS surfaces at the cold side air velocity of 5.5 m/s

Surface	$U_{cold\ side}$ = 5.5 m/s
Vertical	2.40
Top of CTS	2.52
Bottom of CTS	2.50

However, examination of convective only portion of surface heat transfer coefficient shown in **Table 8** indicates that convection heat transfer is actually slightly higher on horizontal surfaces, which would mean that because overall values are lower for horizontal surfaces that radiation heat transfer is somewhat lower on horizontal surfaces. These convective portions on the warm side are of our particular interest in this study and we can conclude from the calculated values that they are very close to each other and that no separate value would be warranted for horizontal vs. vertical surfaces. These values compare excellent with the currently used ISO 15099 correlations, which would produce average warm side convective heat transfer coefficient for this CTS to be hc = 2.48 W/(m^{2}K).

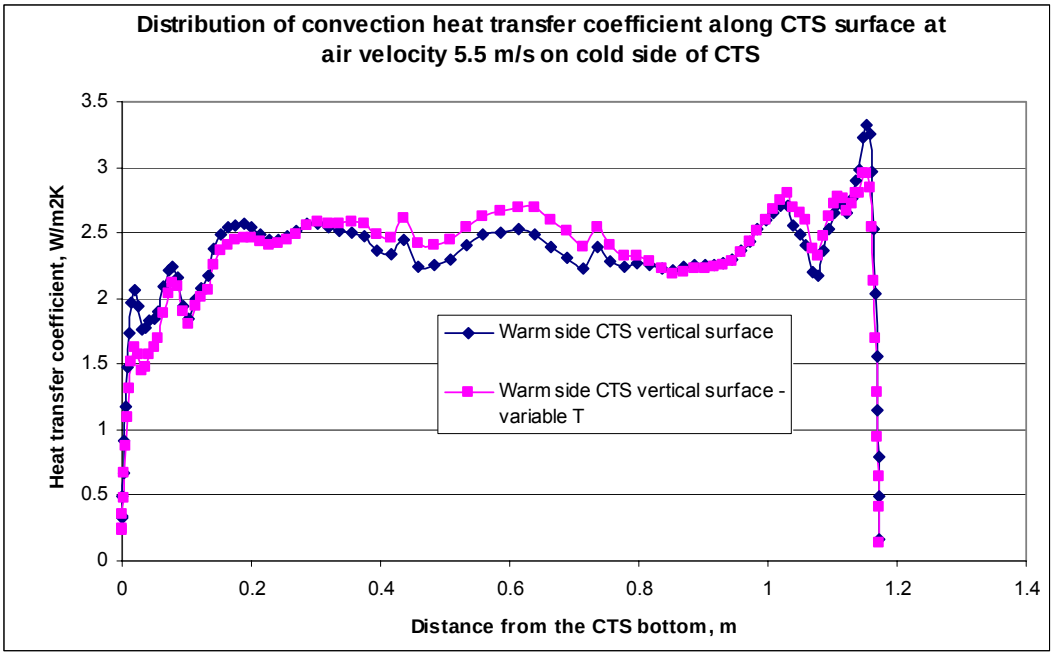


Figure 38. Distribution of Local Convective Heat Transfer Coefficient on the Warm side of Projecting CTS.

THERM MODELING RESULTS

All of the models had been simulated using THERM 5.2 and WINDOW 5.2, using NFRC 100-2004 and NFRC 200-2004 procedures. In addition, modeling was also done using correlations from the work presented in the previous section. The modeling results are shown in **Error! Reference source not found.**.

The thermo-physical properties of materials, used in models are shown in **Table 9**.

Table 9. Material Properties

	Material	Conductivity, *k* W/(m·K)
1	Extruded Polystyrene Foam	0.028
2	Wood(Pine, Spruce, Fir)	0.14
3	Silicone	0.36
4	EPS Used in ATI Kawneer Tests	0.027
5	Stainless Steel	14.3
6	Neoprene	0.19
7	Polyisobutylene	0.24
8	Aluminum	160
9	ABS Plastic Filler	0.223
10	Silica Gel (Desiccant)	0.03
11	Acrylite Extruded Acrylic	1.557
12	EPDM Dense Rubber	0.143
13	Butyl Rubber	0.24
14	Polysulphide	0.19
15	Polyurethane	0.121
16	Vinyl (Flexible)	0.12

For ISO 15099 correlations, which are currently used in NFRC procedures, convective heat transfer coefficients for glazing were calculated by WINDOW program and the values were function of indoor surface temperature and window height for indoor side and function of wind speed on the outdoor side, respectively. For frame surfaces, convective heat transfer coefficients on indoor side are pre-calculated for four typical frame material types and applied correspondingly, while for outdoor side they are identical to the glazing value for outdoor side. The natural heat transfer correlations for

the “channel” flow, by Rohsenow and Aung, which are also function of surface temperature (i.e., air-surface temperature differential) and window height, were also applied to each of the models.

For radiation heat transfer, on indoor side detailed view-factor based radiation modeling was applied in all of the cases. This means that radiation heat transfer boundary condition was calculated in real time as a function of surface temperature, emissivity and view factors between window surfaces and environment, by the THERM program. On the outdoor side, constant value, which is a function of wind speed, had been applied in all of the cases.

Most of physical testing was done in a hot box. Only one specimen was measured in an IR thermal chamber at LBNL. Several specimens were measured as a part of NFRC research project by Intertek Testing Services. Several specimens were measured by ATI, Inc. and two samples were measured by several (eight) laboratories as a part of NFRC Testing Round Robin (TRR). The distribution of testing by laboratory was given in **Table 3** and **Table 4**.

Test results in **Table 10** are given in four columns, first two columns contain originally reported testing results, where first column gives un-standardized (so called air-to-air) U-factor, U_s. Second column gives standardized U-factor, U_{st} according to CTS method. While most of reports also list area weighted method U_{st}, this U-factor was not analyzed or reported here because NFRC 100-2001 and beyond does not specify use of any standardization method other than CTS method. Further inspection of testing results reveals that NFRC 100-1997 CTS method was not applied correctly. Instead of calculating equivalent surface temperature from the set of equations, test results from some of the laboratories use measured surface temperature, instead. Some of the test report contained erroneous calculations, in addition to the application of wrong methodology. For these reasons, all of the NFRC 100-1997 results were recalculated and reported in a third column of test results. Finally, fourth column contains results of NFRC 100-2001 test method. This test method uses similar CTS method as NFRC 100-1997, except that the indoor side standard surface heat transfer coefficient is calculated using updated formulas (i.e., ISO 15099). These additional calculations of standardized results were done from the raw test data, where available. New NFRC 100-2004 uses the identical method to NFRC 100-2001, so these results will be applicable top the latest NFRC standards as well. Test results according to NFRC 100-2001 were used to compare to simulation results. Some of the samples were modeled, using the surround panel section as well, so that specimen flanking losses could be accounted for. These results were also included in a comparison.

Table 11 shows the additional details of the test results. In addition to standardized U-factors calculated from the standard convection constant K_c, reported by the lab, for some specimens test results were calculated using convection constant calculated from the projecting CTS, as measured by Intertek Testing Services.

Table 10. Test and simulation results for projecting and highly conducting products

			Test Results				W5/THERM5 Simulations							
Number	Manufacturer	Model	Original		Corrected		ISO 15099 Correlations (2001)				Rohsenow		Aung	
			Us	Ust	1997	2001	w/o SP	% Diff	with SP	% Diff	w/o SP	% diff	w/o SP	% diff
5	Milgard C	780	0.661	0.558	0.558	0.608	0.582	*-4.31*	0.576	*-5.30*	0.583	*-4.07*	0.580	*-4.56*
6	Velux D	1 06/ FS87	0.525	0.493	0.493	0.495	0.446	*-9.84*	0.439	*-11.26*	0.447	*-9.71*	0.445	*-10.07*
7	Velux	FS95	0.400	0.400	0.410	0.396	0.393	*-0.76*	0.388	*-2.02*	0.394	*-0.47*	0.396	*-0.07*
8	Velux	VS98	0.410	0.410	0.421	0.406	0.433	*6.65*	0.420	*3.45*	0.434	*6.93*	0.433	*6.54*
11	R. Lang	Truframe "J" Series	1.347	-	-	-	1.336	*-0.85*	-	-	1.351	*0.30*	1.329	*-1.34*
12	LBNL	Foam GHW	-	-	-	-	0.411	*N/A*	0.419	*N/A*	0.414	*N/A*	0.408	*N/A*
13	NFRC (Rollin)	Projecting CTS	0.494	0.443	0.485	0.473	0.527	*6.67*	0.527	*6.74*	0.531	*7.46*	0.522	*5.60*
14	Kawneer	1600 System 1	0.660	0.570	0.687	0.636	0.675	*6.13*	-	-	0.677	*6.50*	0.672	*5.62*
15	Kawneer	1600 System 5	0.740	0.640	0.766	0.702	0.637	*-9.29*	-	-	0.640	*-8.84*	0.635	*-9.64*
16	Kawneer	6000IB	0.640	0.580	0.646	0.601	0.655	*8.94*	-	-	0.658	*9.50*	0.653	*8.56*
1	NFRC TRR99	Horizontal slider	0.580	0.570	0.570	0.545	0.546	*0.18*	-	-	0.548	*0.47*	0.545	*0.06*
2	NFRC TRR01	TB Al fixed	0.410	0.410	0.408	0.395	0.403	*2.03*	-	-	0.403	*2.14*	0.402	*1.89*
3	NFRC	Flat CTS	0.316	0.314	0.315	0.310	0.306	*-1.29*	0.307	*-0.97*	0.308	*-0.65*	0.304	*-1.94*

Note * All skylights are curb mounted and tested at vertical position
** These standardized results don't make any sense. Kc is listed as 0.108, but when standirdized with that Kc, it produces Ust=0.528
*** Standardizing done using flat CTS Kc

1997 means NFRC 100-1997; and 2001 means NFRC 100-2001.

Table 11. Results of Additional Analysis of Test vs. Simulation Results

			Test Results		W5/THERM5 Simulations							
Number	Manufacturer	Model	Corrected		ISO 15099 Correlations (2001)				Rohsenow		Aung	
			1997	2001	w/o SP	% Diff	with SP	% Diff	w/o SP	% diff	w/o SP	% diff
5	Milgard C	780	0.589	0.563	0.582	*3.37*	0.576	*2.31*	0.583	*3.64*	0.580	*3.11*
6	Velux D	1 06/ FS87	0.469	0.454	0.446	*-1.77*	0.439	*-3.31*	0.447	*-1.63*	0.445	*-2.02*

Note: SP means that THERM and WINDOW modeling were done with window isnatlled in a surround panel as the one typical for hot box testing.

DISCUSSION OF RESULTS AND CONCLUSIONS

Review of additional heat transfer correlations for geometries and setups that better correspond to the hot box setup, along with the FLUENT modeling results for a specific test configuration (i.e., projecting CTS), reveals that currently used set of correlations as given in ISO 15099 agree quite well with these additional sources of data. This has also been corroborated from practice where there are far less non-validating projecting products than before the application of NFRC 100-2001 standard. Column 1 of the THERM/WINDOW results show currently used methodology and it is clear that none of samples shows disagreement greater than 10%. Some of the results are close to 10%, although that is not the case with any of the more carefully done measurements, like Testing round robin measurements.

One of principal problems in this study has been the lack of testing samples done specifically as a part of this study. The funding for the project did not allow resources for additional testing and it was hoped that the results of testing done previously was of good quality. However, careful review of the testing data revealed a number of deficiencies in the testing done by the two commercial labs. Furthermore, straight use of their published testing data would be inaccurate and misleading.

FLUENT modeling results for projecting CTS were also compared to the flat plate correlations that are basis for ISO 15099 and presented in **Figure 39**.

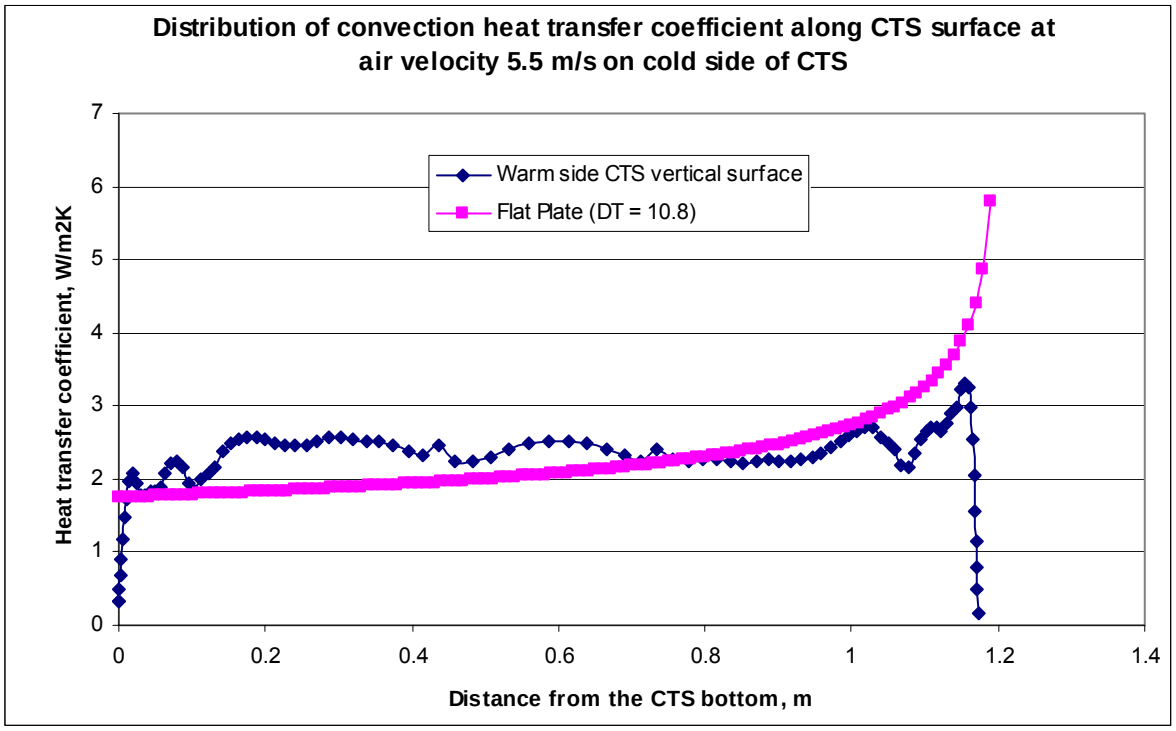


Figure 39. Comparison of Local Convective Heat Transfer Coefficient Distribution For Flat Plate and Projecting CTS modeled in FLUENT

The closer inspection of **Figure 39** shows that modeling results for projecting CTS are somewhat flatter in the middle section, than flat plate results (i.e., flat plate results have monotonous decrease, while projecting CTS curve is more constant in the middle section). The overall agreement is pretty close in both average and local sense, except for those departures discussed above, which are due to projections.

Because the average heat transfer coefficient is very close between all of the investigated correlations, our recommendation is to keep the current NFRC convective heat transfer boundary condition for U-factor calculations for both “Flat” and “Projecting” products, as well as highly conducting products. The ISO 15099 correlations provide good choice for all of fenestration products.

Extreme projecting products, like garden house windows, are currently not modeled in NFRC system, but this study shows that their modeling is also reliable and accurate. We believe that they should also be included in an NFRC system, while applying the following modeling rules:

- Model individual cross-sections as shown in **Figure 40** to **Figure 45.** Enclosure Radiation Definition for the Right Front Corner of the Horizontal Garden House Window Cross-Section., with the following exceptions:
    - Draw the radiation enclosure beyond the end of glazing system so that outline of garden house window in 2-D is shown

  - Apply temperature of center of glass and emissivity of the glass surface to the portion of the radiation enclosure where there would normally be garden house window surfaces
  - Apply air temperature and emissivity of 1.0 to the rest of radiation enclosure surfaces
- Do the area-weighting of calculated results based on 5 sided garden window envelope
- Divide area weighted U-factors by the opening of the garden house window

Figure 40 to **Figure 45** illustrate this recommendation using the example of Rlang garden window's cross-sections. **Figure 40** shows the entire front vertical cross-section of the garden house window, while **Figure 41** shows only upper left modeled cross-section with the rest of surfaces treated as radiation enclosure. **Figure 42** shows lower left modeled cross-section with the rest of surfaces treated as radiation enclosure. **Figure 43** to **Figure 45** show the same methodology for selected individual cross-sections applied to the entire horizontal cross-section.

Convective film coefficient applied in the modeling of Rlang garden house window was the same ISO 15099 film coefficient applied to other products. The agreement to testing results is obviously excellent.

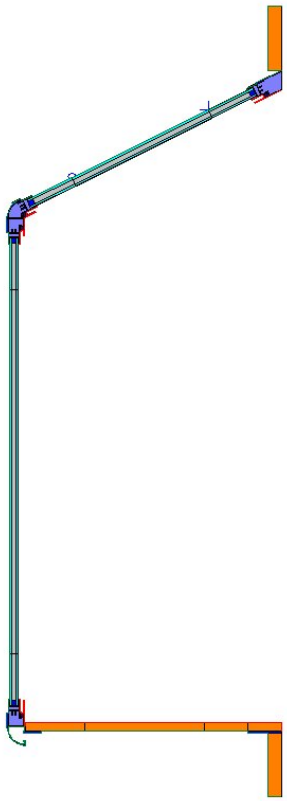


Figure 40. Vertical Cross-section of garden house window through the front of the window.

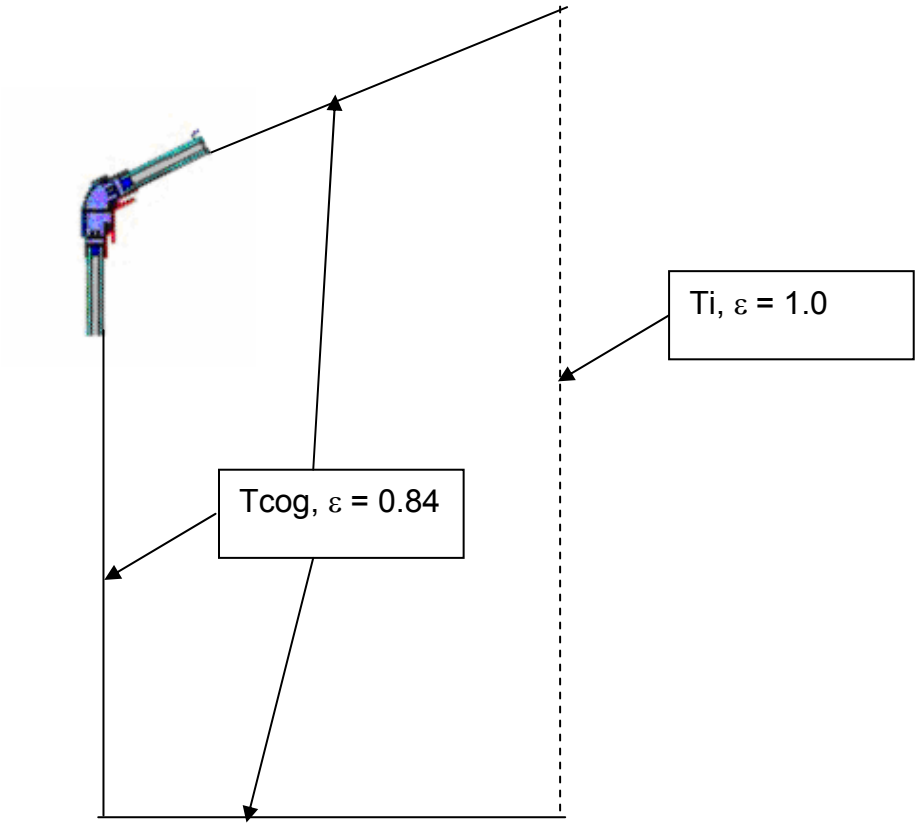


Figure 41. Enclosure Radiation Definition for the Upper Left Corner of the Front Garden House Window Cross-Section

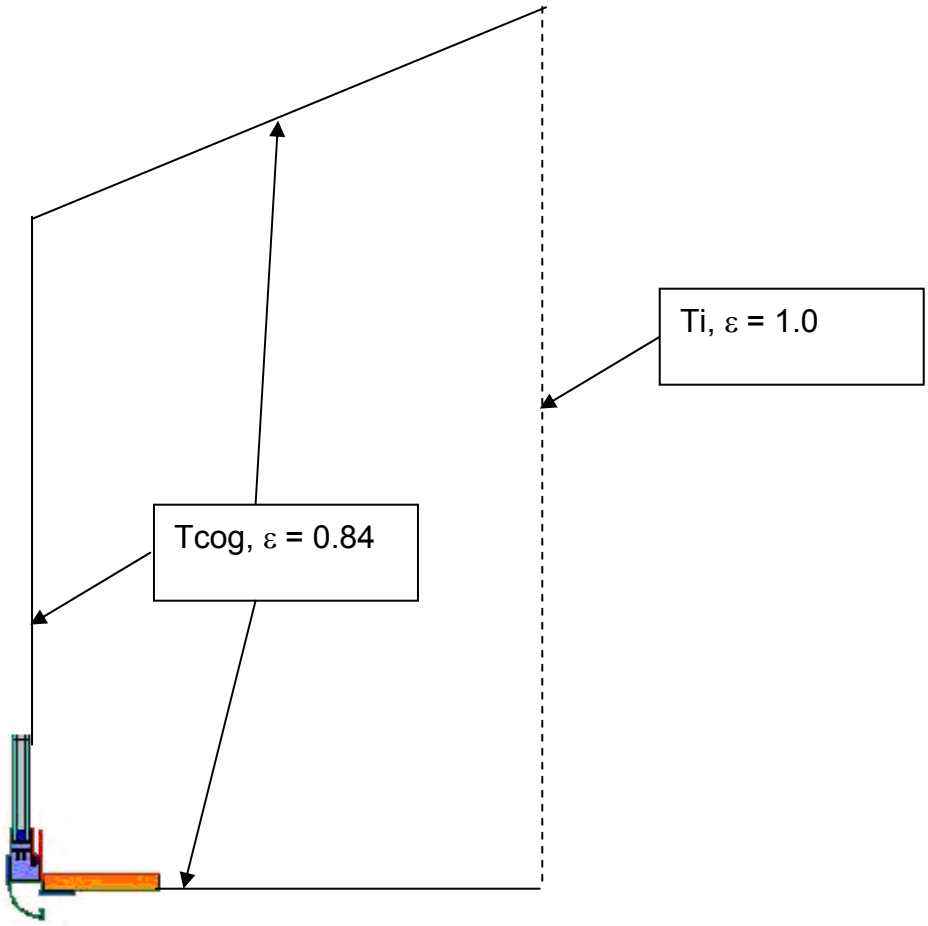


Figure 42. Enclosure Radiation Definition for the Lower Left Corner of the Front Garden House Window Cross-Section



Figure 43. Horizontal Cross-section of Garden House Window Through the Front of the Window.

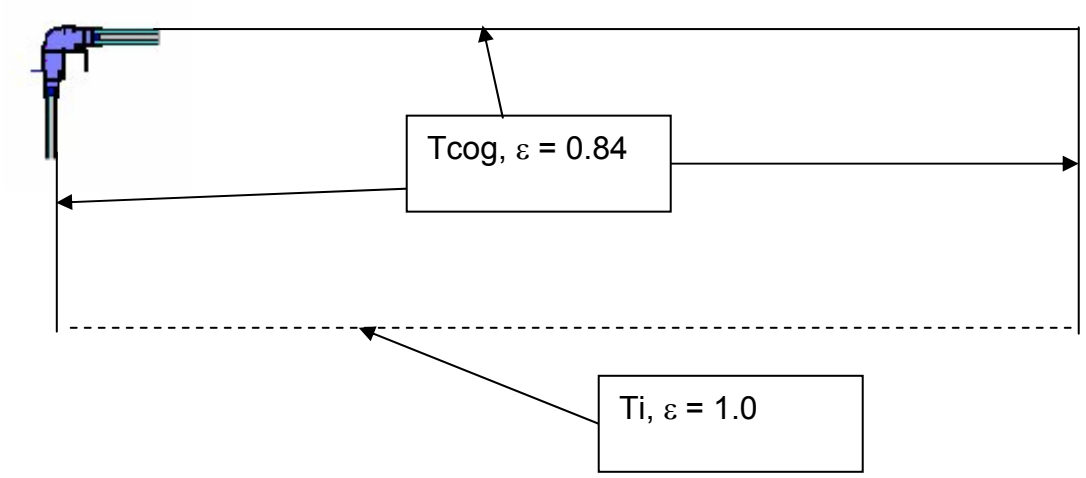


Figure 44. Enclosure Radiation Definition for the Left Front Corner of the Horizontal Garden House Window Cross-Section.

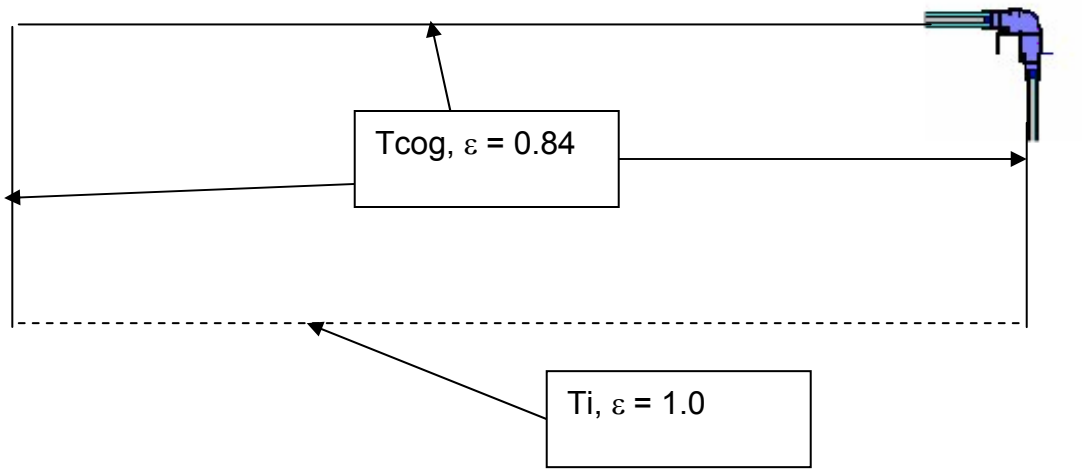


Figure 45. Enclosure Radiation Definition for the Right Front Corner of the Horizontal Garden House Window Cross-Section.

Test Results Analysis: Detailed analysis and study of test results indicate possibility to improve standardization of test results. For limited number of specimens, alternative standardization method had been applied. **Table 10** shows results of this alternate standardization along with the comparisons to the THERM and WINDOW results. Convection constant Kc, calculated from the projecting CTS has been applied to two of the specimens, for which detailed reports were available and for both specimens, application of projecting CTS Kc has produced improved agreement between testing

and simulation. The value of Kc, has been calculated as 0.247 for flat glass CTS in the parallel flow configuration, while it was 0.371 for projecting CTS in parallel flow configuration.

Because of limited data available and uncertainty in the way the Kc for projecting CTS was calculated by now defunct Intertek Testing Services laboratory, this finding it does not warrant recommendation to change the way testing results are standardized for projecting products, but it is recommended to explore this methodology through the separate research project.

Another test method that is specific to the projecting products is ISO 12567-2 standard (ISO 2004). This standard has been completed and published only recently. While it is desirable to work with International Standard Organization committee ISO TC163/WG14 in further development and harmonization of this and associated standard for flat windows ISO 12567-1 (ISO 2000) and general hot box standard ISO 8990 (ISO 1994), this was not done as a part of this project due to lack of interest in North America in using these standards. ISO 12567-2 uses flat CTS method to standardize testing results, in a similar manner as we do in North America at the present time. The biggest difference is that ISO standard does not attempt to calculate average surface temperatures to be used in the standardization process, but uses corrections based on heat flux through the specimen. ISO standard also attempts to account for specimen flanking losses, which North American standard does not do. It is difficult to say which method is better or more accurate without further research into the testing standards, but it should be noted that since NFRC adopted CTS only method, that agreement between testing and simulation became better.

We recommend further research to be done as a separate research project in conjunction with the development effort at ASTM to update and possibly harmonize North American and ISO standards. Notwithstanding technical hurdles and divergence of these standards for many years, political realities of the voting block from EU countries should also be considered in the decision to try to harmonize our and ISO standards.

Condensation Resistance Implications: While the application of the existing average convective heat transfer coefficient proves to be appropriate and accurate for U-factor calculations of projecting products, there is indication that local variation in surface convective heat transfer coefficient would be more appropriate for condensation resistance simulations.

Based on earlier work by Curcija (1993), the distribution of local convective heat transfer coefficient was derived and plotted vs. the simulated performance in Figure

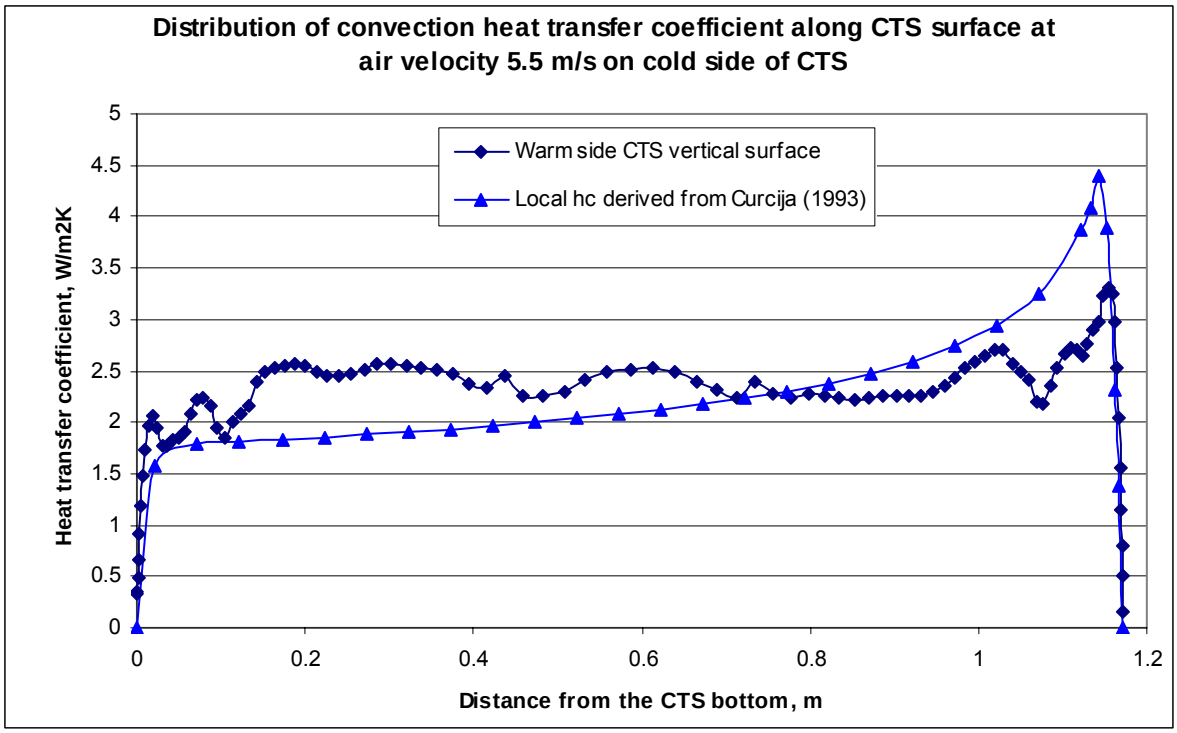


Figure 46. Comparison of Simulated Local hc for PCTS vs. Curcija (1993)

It appears that the two local convective heat transfer coefficients agree quite well, except for the lower part of the vertical surface, which is most likely due to recirculation of the flow in the lower part, or some other phenomena caused by the actual hot box configuration for which the projecting CTS results were modeled. However, inspection of the regions near the corner reveals remarkable agreement between the two results. It appears that the use of these linear distributions on the glass surface near the corners would improve results of condensation resistance calculations.

Because at NFRC we use fixed value of local convective surface heat transfer coefficient, and center of glass performance is done as a 1-D model, it is proposed to apply local variation in a form of linear distribution only near the sightline (1 in. or 25 mm in length, as suggested by the FLUENT simulation result. Further inspection of the local distribution indicate that at the head region, the local value is higher than average and then drops in the last 1 in., so it is expected that these two effects would be a wash. This was also indicated by an earlier work by Curcija et al. (1998) when he compared THERM simulation results with the IR thermography measurements. The proposed distribution is shown in **Figure 47**.

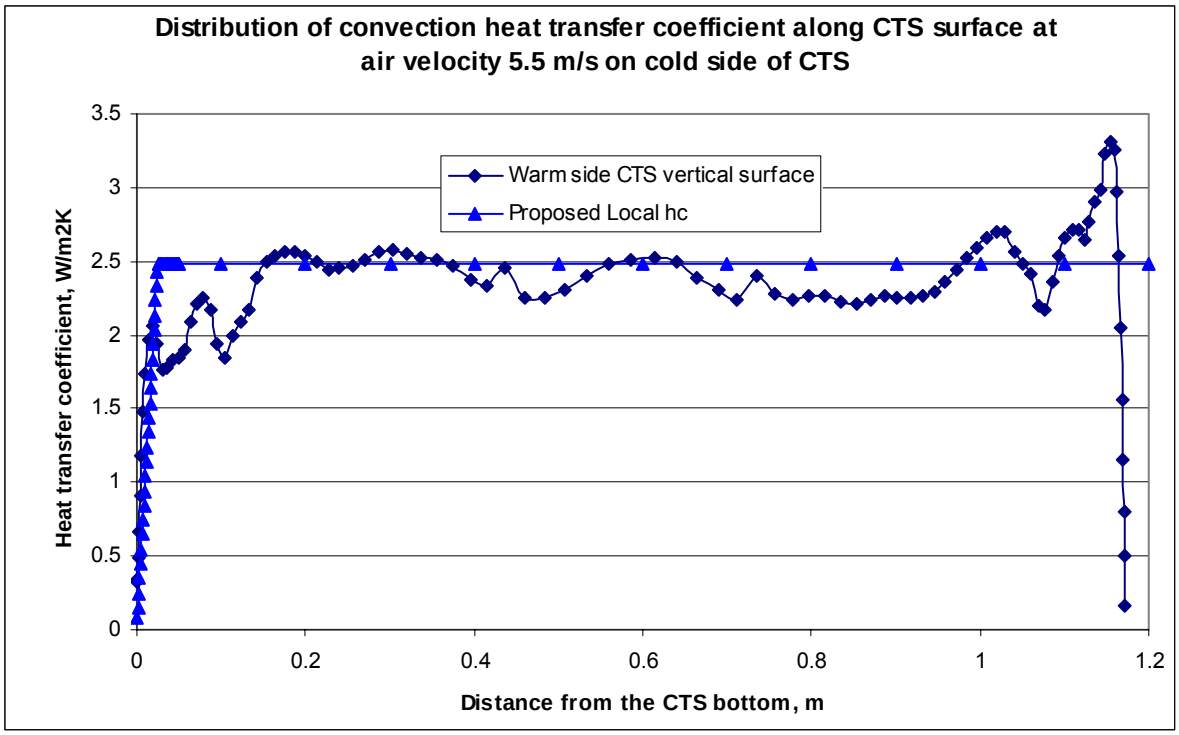


Figure 47. Comparison of Simulated Local hc for PCTS vs. proposed distribution

Local Heat Transfer Coefficient Modeling:

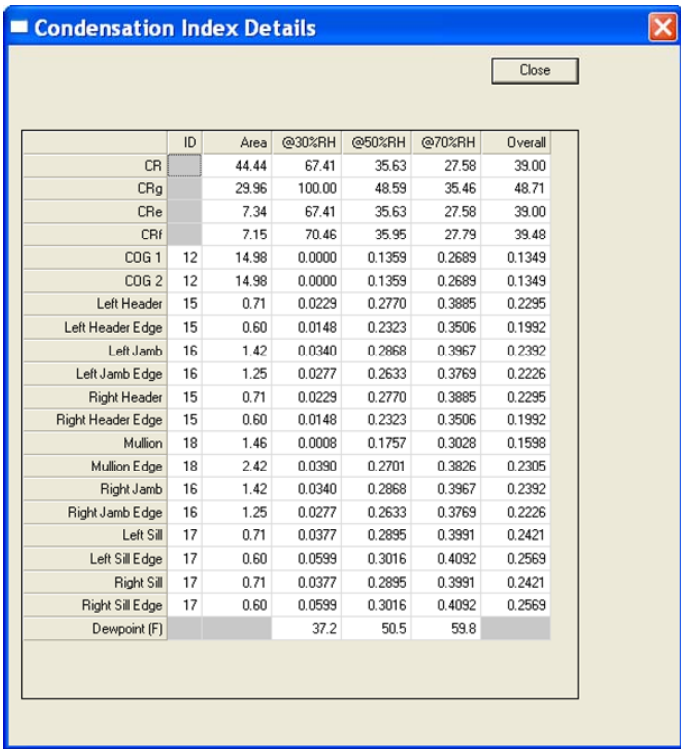
For two fenestration products, Kawneer 1600 Sys1 and TRR01, modeling was done using proposed local convective surface heat transfer coefficient proposed in Figure 47. In order to produce results with more signal, TRR01 window was modeled with double glazed, instead of triple glazed window. For windows with triple and quadruple glazing, local variation of convective surface heat transfer coefficient is not expected to produce significant variation, due to multiple air spaces, with gap gas flows going in opposite direction, therefore diminishing any local effects on the warm side.

Both, U-factor and condensation resistance indices were analyzed in order to examine effects of applying local distribution of convective surface heat transfer coefficients.

Table 12. Effects of Local Convective Surface Heat Transfer Coefficients

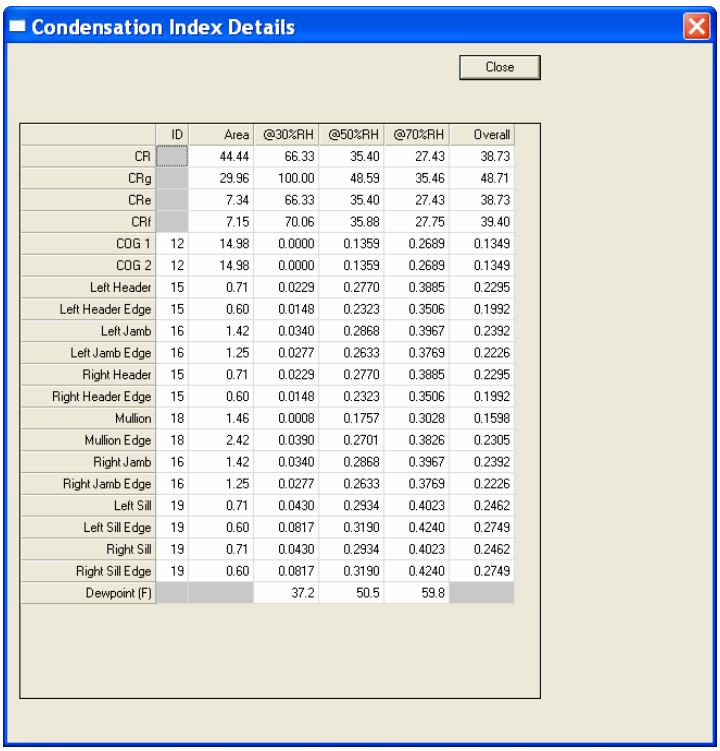
	Kawneer 1600 Sys1		TRR01	
	Fixed hc	Local hc	Fixed hc	Local hc
U-Factor	0.675	0.674	0.424	0.424
CR*	39.00	38.73	42.27	42.18

*Note: CR numbers are reported as integers in NFRC, but for the purpose of identifying differences, they are reported to two decimal points here.



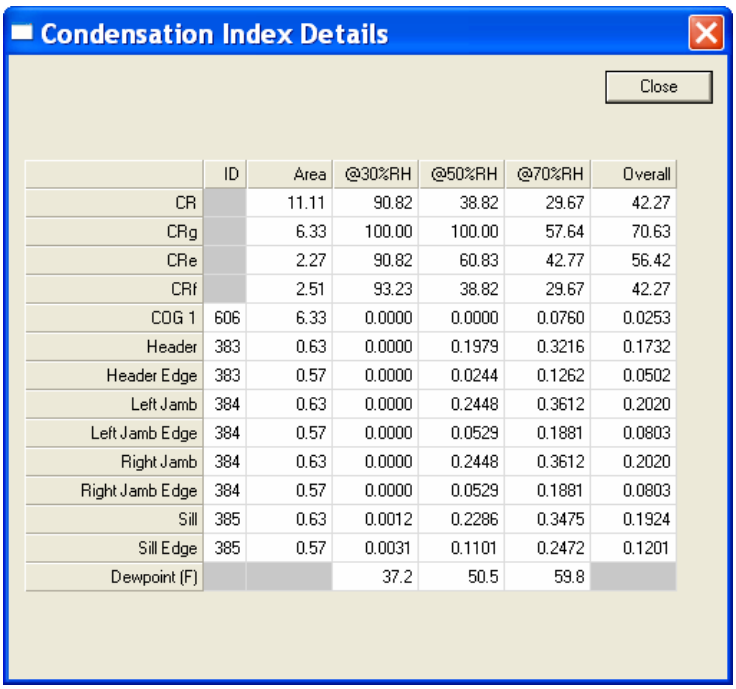
	ID	Area	@30%RH	@50%RH	@70%RH	Overall
CR		44.44	67.41	35.63	27.58	39.00
CRg		29.96	100.00	48.59	35.46	48.71
CRe		7.34	67.41	35.63	27.58	39.00
CRf		7.15	70.46	35.95	27.79	39.48
COG 1	12	14.98	0.0000	0.1359	0.2689	0.1349
COG 2	12	14.98	0.0000	0.1359	0.2689	0.1349
Left Header	15	0.71	0.0229	0.2770	0.3885	0.2295
Left Header Edge	15	0.60	0.0148	0.2323	0.3506	0.1992
Left Jamb	16	1.42	0.0340	0.2868	0.3967	0.2392
Left Jamb Edge	16	1.25	0.0277	0.2633	0.3769	0.2226
Right Header	15	0.71	0.0229	0.2770	0.3885	0.2295
Right Header Edge	15	0.60	0.0148	0.2323	0.3506	0.1992
Mullion	18	1.46	0.0008	0.1757	0.3028	0.1598
Mullion Edge	18	2.42	0.0390	0.2701	0.3826	0.2305
Right Jamb	16	1.42	0.0340	0.2868	0.3967	0.2392
Right Jamb Edge	16	1.25	0.0277	0.2633	0.3769	0.2226
Left Sill	17	0.71	0.0377	0.2895	0.3991	0.2421
Left Sill Edge	17	0.60	0.0599	0.3016	0.4092	0.2569
Right Sill	17	0.71	0.0377	0.2895	0.3991	0.2421
Right Sill Edge	17	0.60	0.0599	0.3016	0.4092	0.2569
Dewpoint (F)			37.2	50.5	59.8	

Figure 48. CR Details for the Kawneer 1600 Sys1, with fixed hc



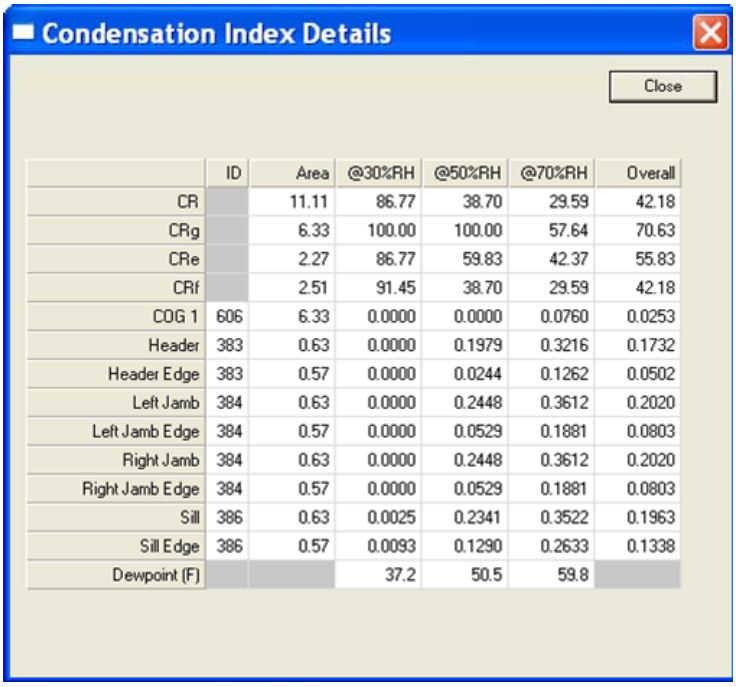
	ID	Area	@30%RH	@50%RH	@70%RH	Overall
CR		44.44	66.33	35.40	27.43	38.73
CRg		29.96	100.00	48.59	35.46	48.71
CRe		7.34	66.33	35.40	27.43	38.73
CRf		7.15	70.06	35.88	27.75	39.40
COG 1	12	14.98	0.0000	0.1359	0.2689	0.1349
COG 2	12	14.98	0.0000	0.1359	0.2689	0.1349
Left Header	15	0.71	0.0229	0.2770	0.3885	0.2295
Left Header Edge	15	0.60	0.0148	0.2323	0.3506	0.1992
Left Jamb	16	1.42	0.0340	0.2868	0.3967	0.2392
Left Jamb Edge	16	1.25	0.0277	0.2633	0.3769	0.2226
Right Header	15	0.71	0.0229	0.2770	0.3885	0.2295
Right Header Edge	15	0.60	0.0148	0.2323	0.3506	0.1992
Mullion	18	1.46	0.0008	0.1757	0.3028	0.1598
Mullion Edge	18	2.42	0.0390	0.2701	0.3826	0.2305
Right Jamb	16	1.42	0.0340	0.2868	0.3967	0.2392
Right Jamb Edge	16	1.25	0.0277	0.2633	0.3769	0.2226
Left Sill	19	0.71	0.0430	0.2934	0.4023	0.2462
Left Sill Edge	19	0.60	0.0817	0.3190	0.4240	0.2749
Right Sill	19	0.71	0.0430	0.2934	0.4023	0.2462
Right Sill Edge	19	0.60	0.0817	0.3190	0.4240	0.2749
Dewpoint (F)			37.2	50.5	59.8	

Figure 49. CR Details for the Kawneer 1600 Sys1, with local hc



	ID	Area	@30%RH	@50%RH	@70%RH	Overall
CR		11.11	90.82	38.82	29.67	42.27
CRg		6.33	100.00	100.00	57.64	70.63
CRe		2.27	90.82	60.83	42.77	56.42
CRf		2.51	93.23	38.82	29.67	42.27
COG 1	606	6.33	0.0000	0.0000	0.0760	0.0253
Header	383	0.63	0.0000	0.1979	0.3216	0.1732
Header Edge	383	0.57	0.0000	0.0244	0.1262	0.0502
Left Jamb	384	0.63	0.0000	0.2448	0.3612	0.2020
Left Jamb Edge	384	0.57	0.0000	0.0529	0.1881	0.0803
Right Jamb	384	0.63	0.0000	0.2448	0.3612	0.2020
Right Jamb Edge	384	0.57	0.0000	0.0529	0.1881	0.0803
Sill	385	0.63	0.0012	0.2286	0.3475	0.1924
Sill Edge	385	0.57	0.0031	0.1101	0.2472	0.1201
Dewpoint (F)			37.2	50.5	59.8	

Figure 50. CR Details for the TRR01 with Dbl Argon glazing, with fixed hc



	ID	Area	@30%RH	@50%RH	@70%RH	Overall
CR		11.11	86.77	38.70	29.59	42.18
CRg		6.33	100.00	100.00	57.64	70.63
CRe		2.27	86.77	59.83	42.37	55.83
CRf		2.51	91.45	38.70	29.59	42.18
COG 1	606	6.33	0.0000	0.0000	0.0760	0.0253
Header	383	0.63	0.0000	0.1979	0.3216	0.1732
Header Edge	383	0.57	0.0000	0.0244	0.1262	0.0502
Left Jamb	384	0.63	0.0000	0.2448	0.3612	0.2020
Left Jamb Edge	384	0.57	0.0000	0.0529	0.1881	0.0803
Right Jamb	384	0.63	0.0000	0.2448	0.3612	0.2020
Right Jamb Edge	384	0.57	0.0000	0.0529	0.1881	0.0803
Sill	386	0.63	0.0025	0.2341	0.3522	0.1963
Sill Edge	386	0.57	0.0093	0.1290	0.2633	0.1338
Dewpoint (F)			37.2	50.5	59.8	

Figure 51. CR Details for the TRR01 with Dbl Argon glazing, with local hc

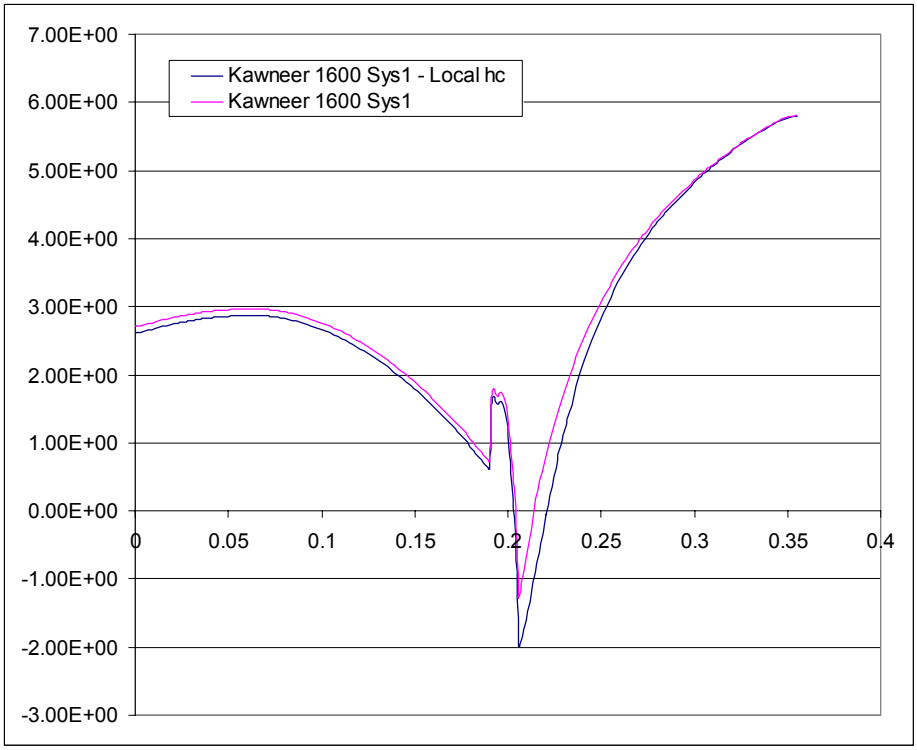


Figure 52. Temperature Distribution for the Sill Region of Kawneer 1600 Sys1.

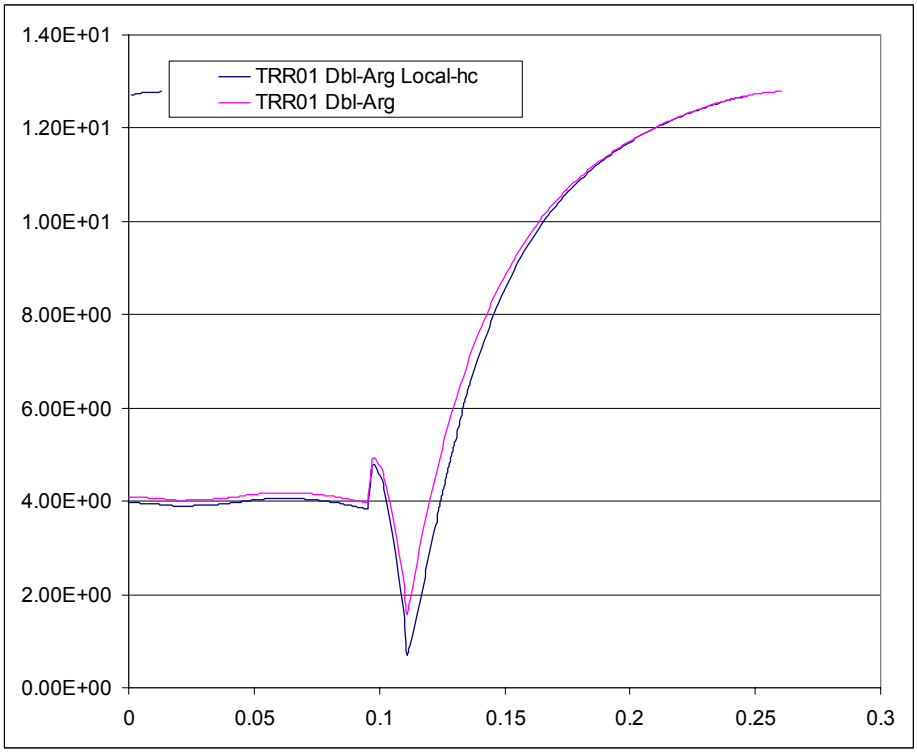


Figure 53. Temperature Distribution for the Sill Region of TRR01 Dbl Argon.

Review of differences that result from the use of local hc in THERM models reveal that the application of local hc in only small region near the sightline does not have substantial impact on either U-factor or CR. **Figure 52** and **Figure 53** show temperature distribution in the sill region and one can observe that there is a drop of about 1.5 F at the sightline, due to the use of local hc.

RECOMMENDATIONS:

- For the calculation of U-factors of projecting and highly conducting products, keep the boundary conditions that are currently in use (ISO 15099)
- Adopt newly developed procedure for modeling garden house windows. It is recommended to extend validation to at least one more garden house product so that the new procedure can be recommended with higher confidence.
- Develop improved testing procedure for projecting products incorporating projecting CTS method. It is recommended that new research project be developed that will consider existing ASTM and ISO methods and current NFRC practice and develop recommendations for future directions in developing test methods. Include location of sensors as an integral part of this research project.
- Use local distribution of convective heat transfer coefficient in the form that was analyzed here is not recommended, however further, more systematic study of local convective surface heat transfer coefficients is recommended in order to fully understand the impact of local distributions on condensation resistance and unification of CR and U-factor models into a single methodology.

REFERENCES

Arasteh, D.K.; Finlayson, E.; Curcija, D.; Baker, J.; and Huizenga, C. 1998. “Guidelines for Modeling Projecting Fenestration Products”. *ASHRAE Transactions*. Vol. 104, Part I. January, 1998.

Aung, W. 1972. “Fully Developed Laminar Free Convection Between Vertical Plates Heated Asymmetrically.” *International Journal of Heat and Mass Transfer*. Vol. 15. pp. 1577 to 1580.

Bar-Cohen, A.; and Rohsenow, W.M. 1984. “Thermally Optimum Spacing of Vertical Natural Convection Cooled, Parallel Plates.” *Journal of Heat Transfer*. Vol. 106, pp. 116.

Curcija, D.; and Goss, W.P. 1993. "Two Dimensional Natural Convection Over the Isothermal Indoor Fenestration Surface - Finite Element Numerical Solution." *ASHRAE Transactions*, Vol. 99, Part I, January 1993.

Curcija, D.; Zhao, Y.; and Goss, W.P. 1998. “The Effect of Realistic Boundary Conditions in Computer Modeling of Condensation Resistance for Fenestration

Systems" *Thermal Performance of Building Envelopes VII*, Clearwater, FL. December, 1998

ISO. 1994. "ISO 8990: Thermal Insulation – Determination of Steady State Thermal Transmission Properties – Calibrated and Guarded Hot Box" *International Standardization Organization*.

ISO. 2000. "ISO 12567-1: Thermal Performance of Windows and Doors – Determination of Thermal Resistance by Hot Box Method – Part 1: Complete Windows and Doors" *International Standardization Organization*. First Edition.

ISO. 2003. "ISO 15099: Thermal Performance of Windows, Doors, and Shading Devices – Detailed Calculations." *International Standardization Organization*. First Edition.

ISO. 2004. "ISO 12567-2: Thermal Performance of Windows and Doors – Determination of Thermal Resistance by Hot Box Method – Part 2: Roof Windows and Other Projecting Products" *International Standardization Organization*. First Edition.

FDI 2003. FLUENT 6.5. Users and Reference Manual. Fluid Dynamics International, Fluid Dynamics Analysis Package. Fluent Inc.

FDI 2000. "Gambit 2.0 Users and Reference Manual". Fluid Dynamics International, Fluid Dynamics Analysis Package Revision 1.3.2, Evanston, IL.

Griffith, B.; Curcija, D.; Turler, D.; Arasteh, D. 1998. "Improving Computer Simulations of Heat Transfer for Projecting Fenestration Products: Using Radiation Viw-Factor Models. *ASHRAE Transactions*. Vol. 104, Part I. January, 1998.

APPENDIX A: THERM MODELS AND SELECTED RESULTS

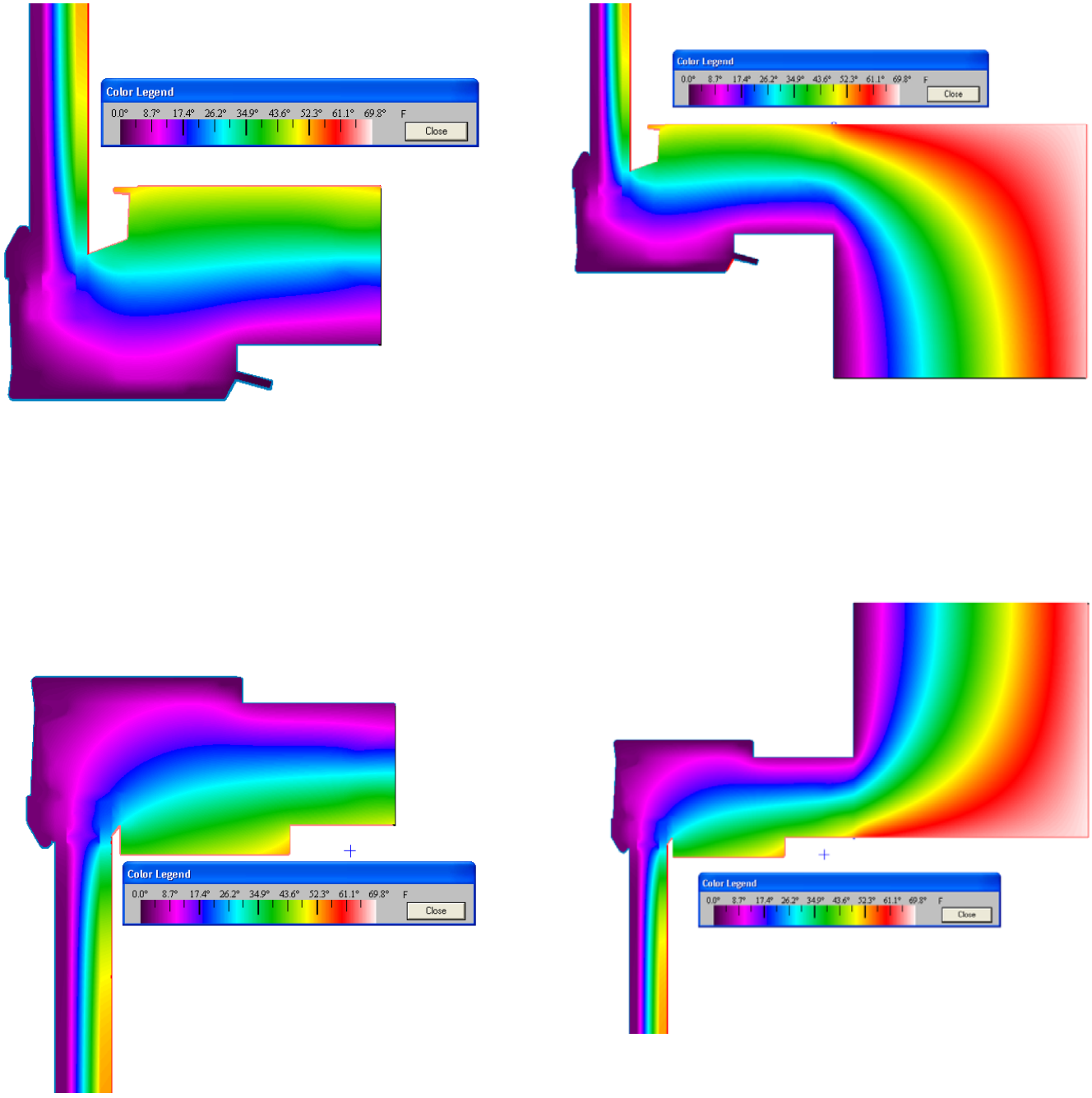


Figure A 1: Velux FS95- infrared plots (a) sill cross-section with and without SP and (b) head cross-section with and without SP

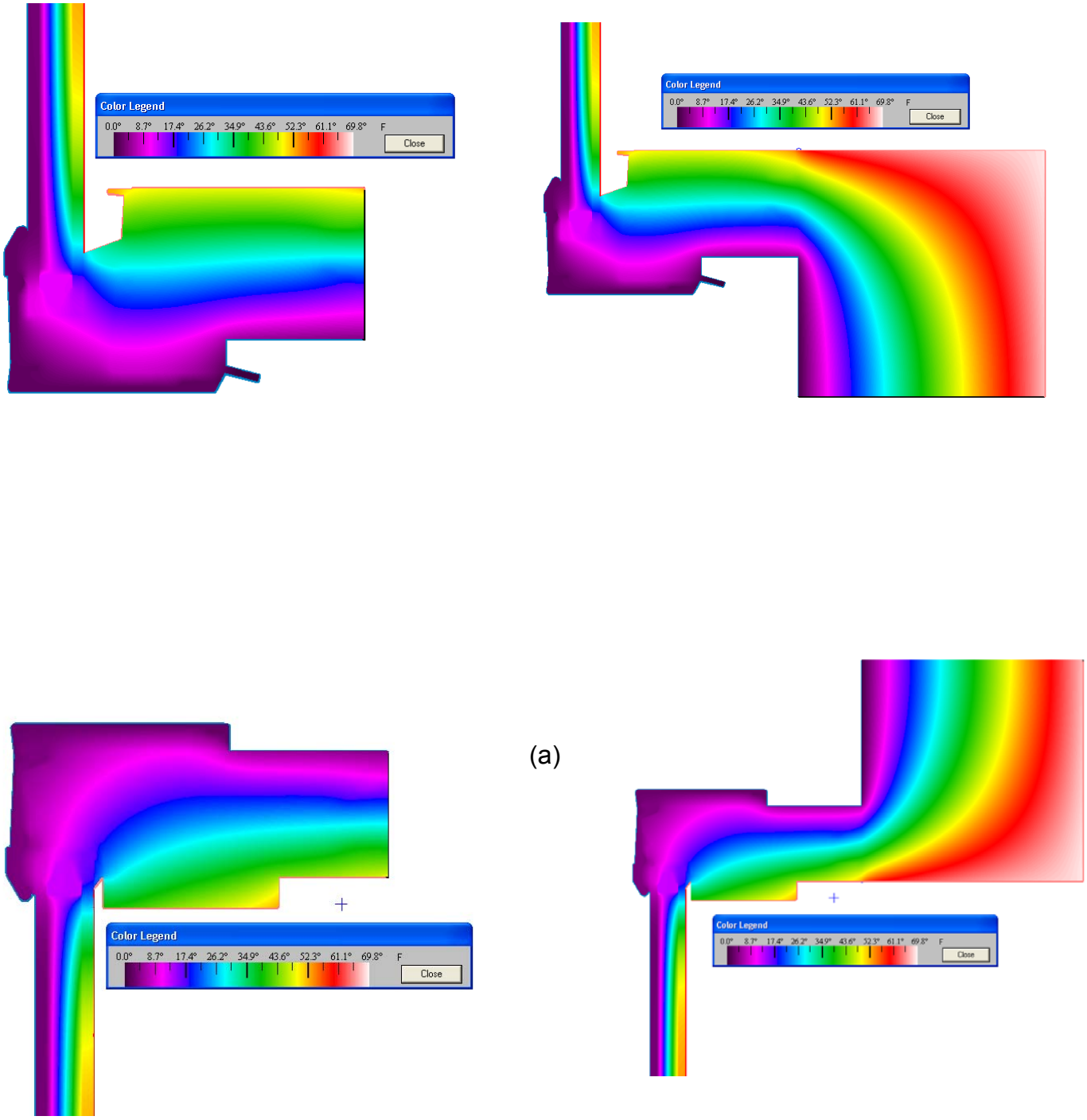


Figure A 2: Velux FS87- infrared plots (a) sill cross-section with and without SP and (b) head cross-section with and without SP

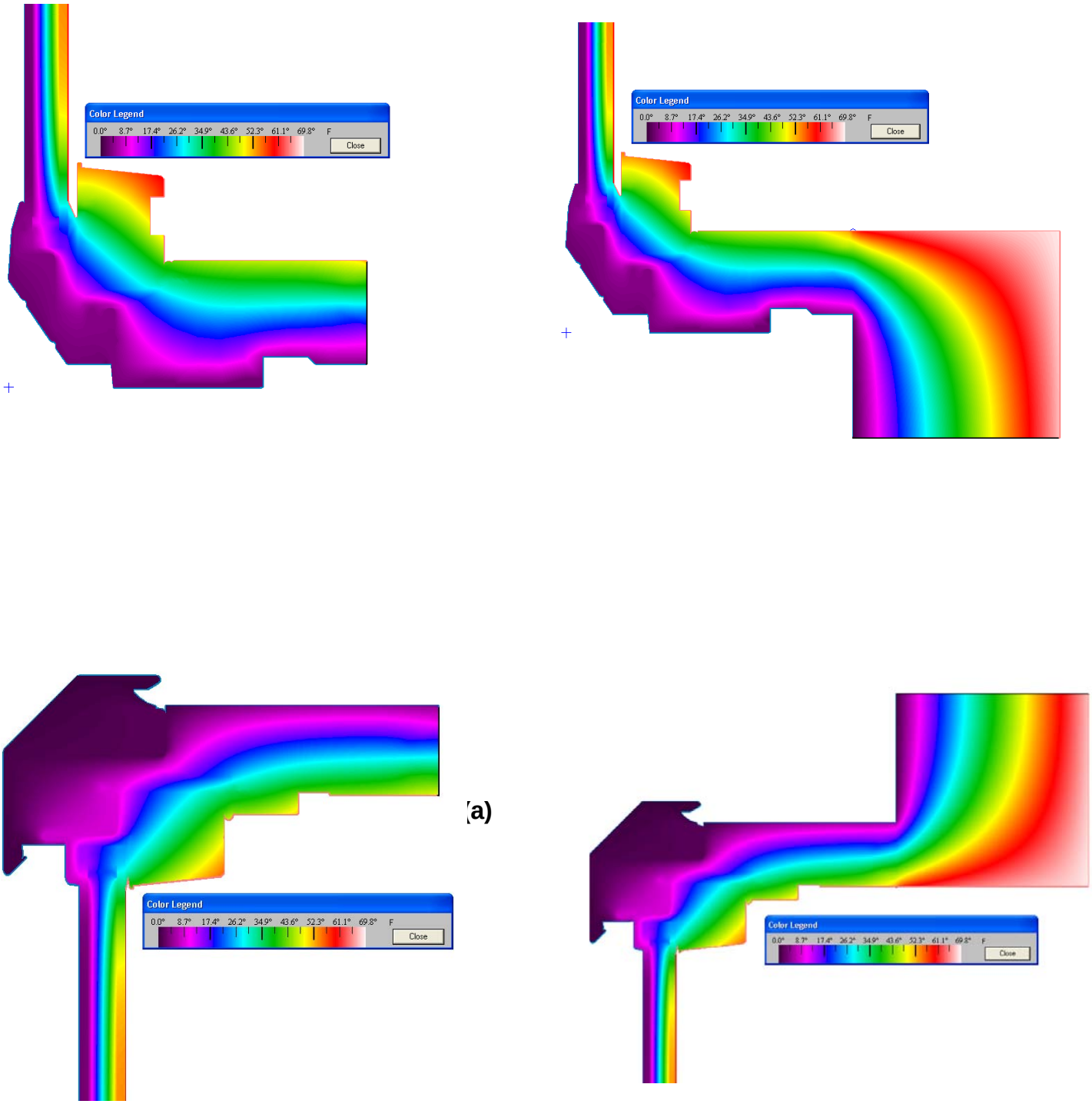
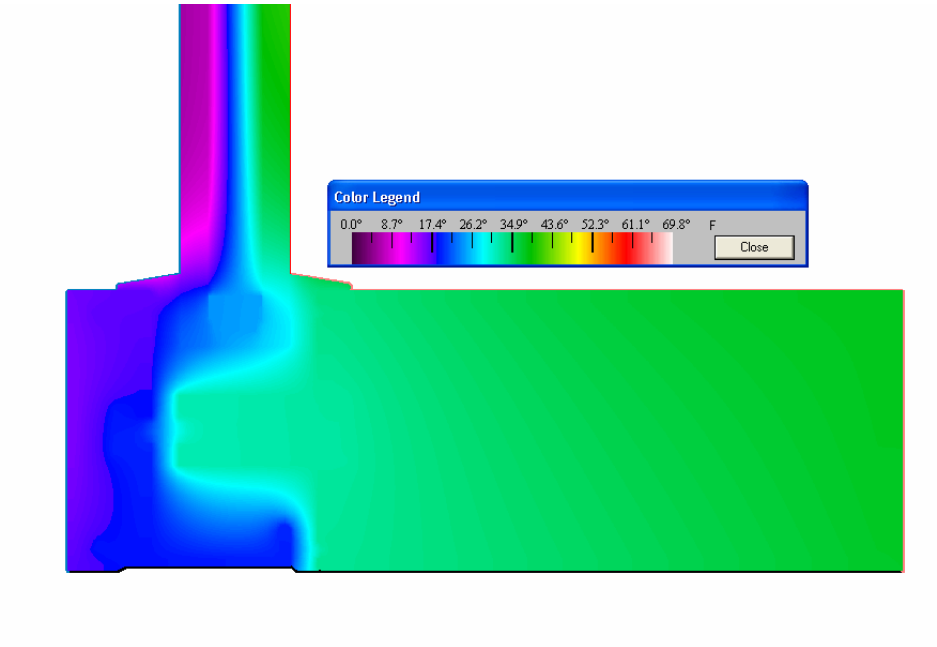
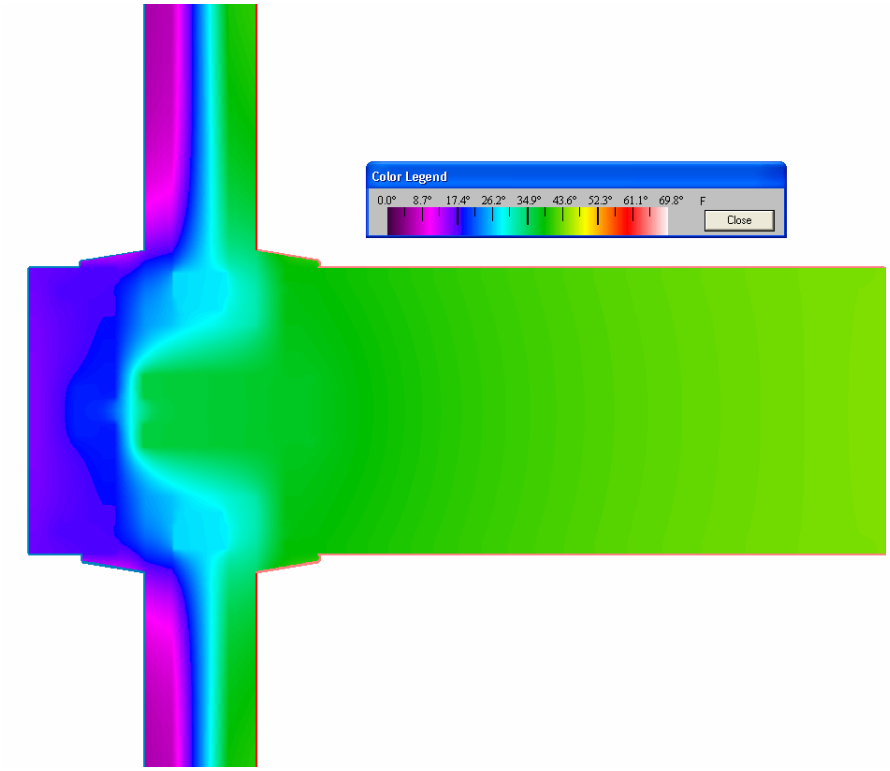


Figure A 3: Velux VS98- infrared plots (a) sill cross-section with and without SP, and (b) head cross-section with and without SP



(a)



(b)

Figure A 4: Kawneer 1600 Sytem 1- infrared plots (a) sill and (b) meeting rail

Kawneer system 1 contains a bolt. The keff of bolt is calculated as per the procedure as follows:

Bolt (keff) Calculations

k (W/mK)

Notation	Materials	Conductivity (W/mK)
k_1	Air Cavity	0.024
k_2	Aluminum Alloy	160
k_3	EPDM	0.25
k_4	Air Cavity	0.024

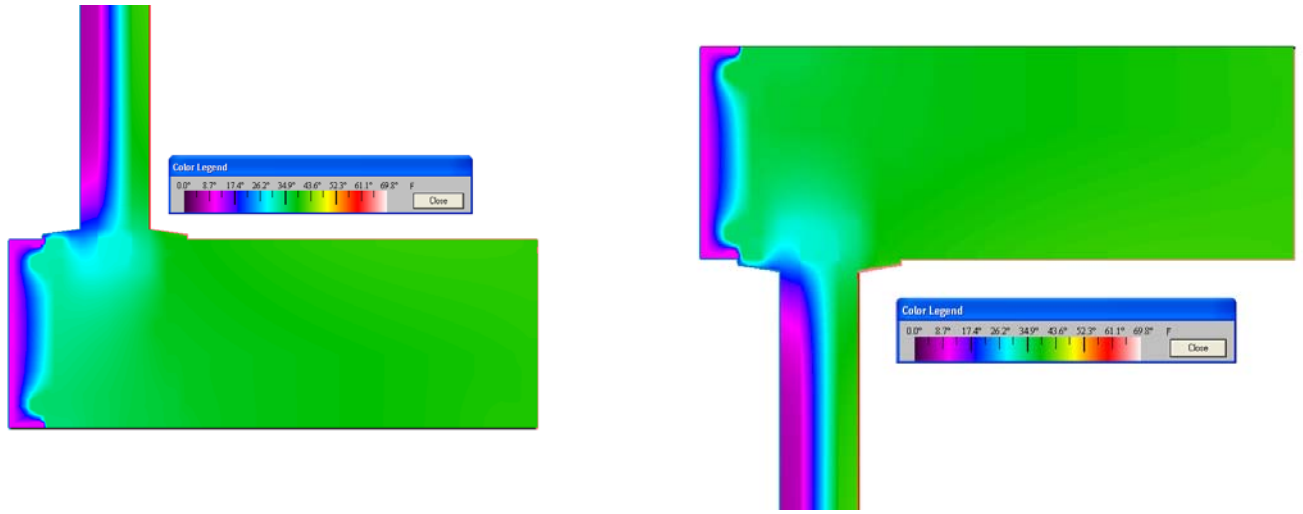
d (m)

Lengths (of parts of the bolt)	(m)
d_1	0.00545
d_2	0.003175
d_3	0.00635
d_4	0.01717

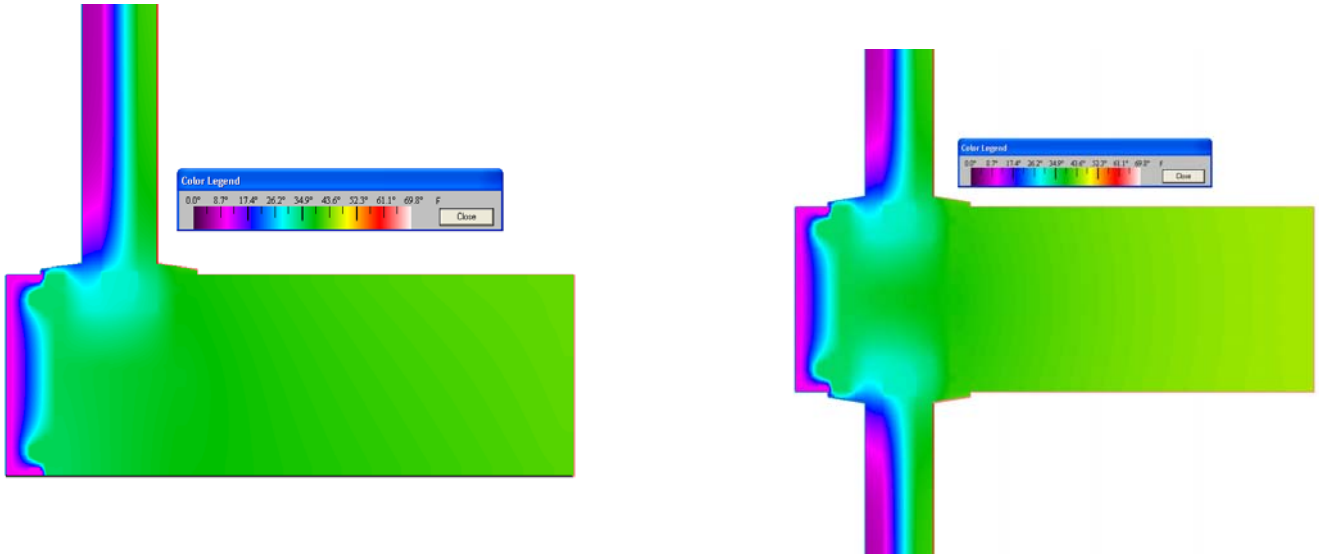
R (d/k) (m2k/W)

Heat transfer resistance	(m^2k/W)
R_1	0.227083333
R_2	1.98438E-05
R_3	0.0254
R_4	0.715416667

4. $R_t=R_1+R_2+R3+R_4$ (m^2k/W)	0.967919844	
$D_{t=}$ d_1 +d_2 +d_3 +d_4(m) Total length of the bolt	0.032145	
5.K_n=Dt/Rt (W/mK) Average conductivity	0.033210395	
K_b (W/mK) Conductivity of bolt material (galvanized steel)	50	
6. W_b (mm) Width of the bolt head	12.7	
Sb (mm) Spacing of the bolts (9")	228.6	
F_b =W_b/S_b (%)	0.055555556	5.555556
F_n=1-F_b (%)	0.944444444	94.44444
7.Keff= F_b***** K_b+ F_n* K_n (W/mK) or (Btu/hr-ft-F)	2.809143151 (W/mK)	1.622282 Btu/hr-ft-F)



(a) (b)



(c) **(d)**

Figure A 5: Kawneer 1600 System 5- infrared plots (a) sill, (b) meeting rail, (c) jamb and (d) meeting rail

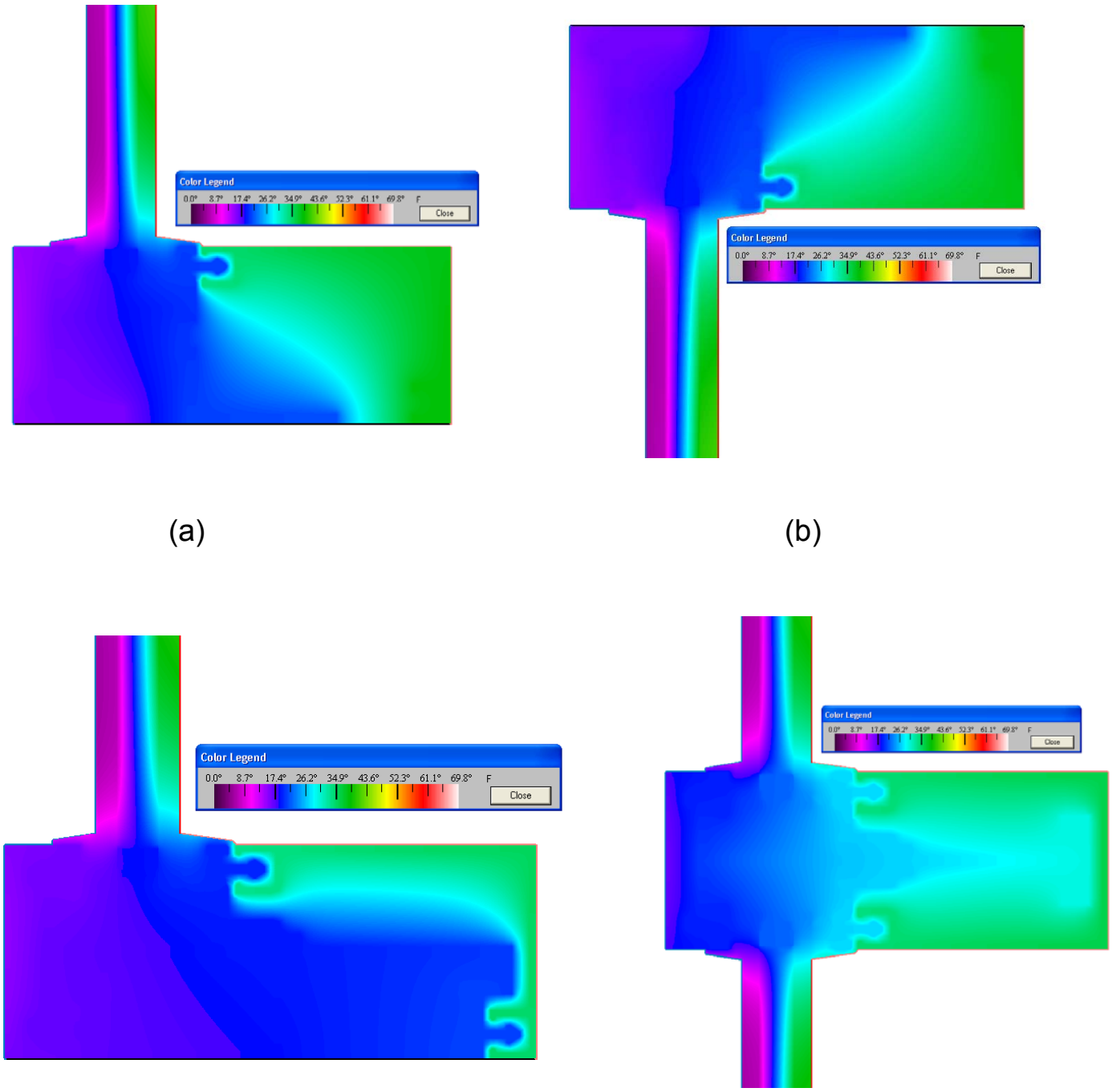


Figure A 6: Kawneer 6000 IB- infrared plots (a) sill, (b) meeting rail, (c) jamb and (d) meeting rail

APPENDIX B: MOUNTING DETAILS

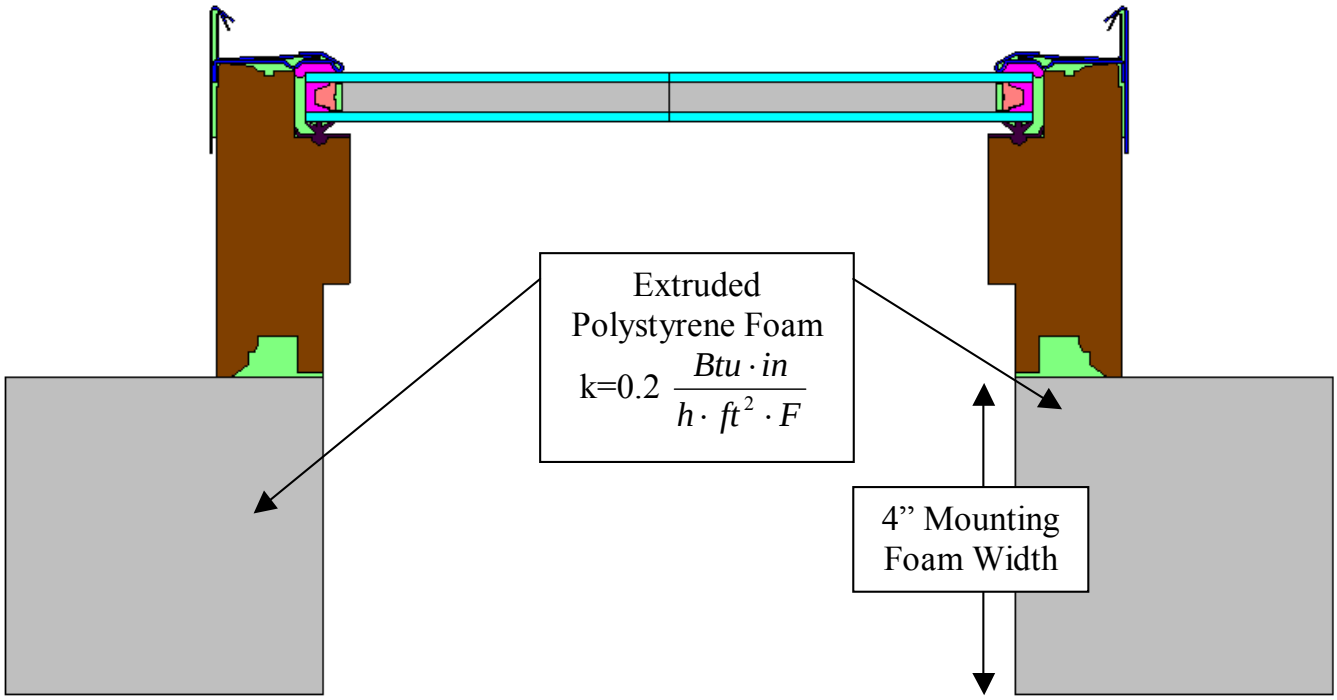


Figure B1: Architectural Testing Inc. Curb Mounting

Project 1.1.2

Project Name:	Three-Dimensional Heat Transfer Effects in Fenestration Systems
Date:	March 4, 2005
Purpose:	The main goal of this research project was to investigate 3-D corner conduction heat transfer effects in windows and to provide recommendations for improvements to 2-D fenestration models.

Project Summary:

This study is the first of its kind of looking in 3-D corner heat transfer effects in fenestration systems in a systematic way. Four different frame materials, covering practically entire range of present day frame materials, were considered, three spacer types, covering the entire range of present day and future spacer materials and designs, and four different glazing systems, covering the entire range of present day and future glazing designs, except for single glazing, were investigated and reported in this study.

Click here for final report

Carli, Inc.

18 Tanglewood Rd.
Amherst, MA 01002

TEL: (413) 256-4647
FAX: (413) 256-4823

carli@fenestration.com
http://www.fenestration.com

Technical Report:

Three-Dimensional Heat Transfer Effects in Fenestration Systems

Report prepared for:

National Fenestration Rating Council, Inc.

8484 Georgia Ave., Suite 320

Silver Spring, MD 20910

Report prepared by:

Dr. Charlie Curcija

March 4, 2005

TABLE OF CONTENTS

TABLE OF CONTENTS 2
EXECUTIVE SUMMARY 3
BACKGROUND 3
DESCRIPTION OF SPECIMENS: 4
MODELING ASSUMPTIONS: 12
MATHEMATICAL MODELS 17
RESULTS 17
DISCUSSION OF RESULTS 28
CONCLUSIONS AND RECOMMENDATIONS 29
APPENDIX A: 30
APPENDIX B: 42
APPENDIX C: 54
APPENDIX D: 66

EXECUTIVE SUMMARY

This technical report is a final deliverable on an NFRC research project “Three-Dimensional Heat Transfer Effects in Fenestration Systems “ and it presents full set of results of this research project. The main goal of this research project was to investigate 3-D corner conduction heat transfer effects in windows and to provide recommendations for improvements to 2-D fenestration models. First part of the report contains detailed description of analyzed specimens and methodology employed. Second part of the report contains detailed and summarized results and proposed modification to existing algorithms to account for 3-D effects in 2-D fenestration heat transfer tools.

Four windows were analyzed, employing four major material types, representing broad range of fenestration products on the market today. Wood, Aluminum, Thermally-broken Aluminum, and PVC materials were analyzed. These materials represent vast majority of fenestration products on the market today, and even the ones that are not included in this study could be well approximated by these 4 materials (e.g., fiberglass poltrusions have very similar performance as PVC extrusions, etc.). In addition to varying frame materials, variations of glazing options and spacer design and product geometry have been also considered in order to develop corrections that would cover most of the products in the market.

The results are presented in the form of 4 tables, where each table represents one material type. Each table presents matrix of options, consisting of variations in glazing, spacer and product sizes. Also, included are plots of relative differences between 3-D and 2-D models vs. glazing performance. Three such plots are given for each product, representing variations in spacer effective conductivity. These plots and data are used for the final conclusions and development of recommendations to account for 3-D effects in 2-D fenestration models, like THERM (LBNL 2003).

Individual component results are also provided in the form of tables and graphs for each window type and size, glazing and spacer option. These results are presented in Appendices A to D.

This research project has dealt with the topic of 3-D conduction heat transfer corner effects in order to quantify the level of simplification due to the use of 2-D conduction model instead of 3-D conduction model. Future work should include 3-D convection and radiation heat transfer effects.

BACKGROUND

Three-Dimensional (3-D) heat transfer computer tools are effective means of investigating the 3-D heat transfer through fenestration systems. However, their use is still prohibitively expensive in terms of both the cost of these computer programs, and time needed to generate the model of an actual window and obtain heat transfer results (e.g., overall U-factors). Currently accepted simulation methods typically perform two-dimensional (2-D) heat transfer modeling of characteristic cross sections of frame and edge-of-glass area and one-dimensional (1-D) heat transfer of center-of-glass area and then area-weight those results into an overall U-factor that is representative of the complete 3-D product. Other indices, like SHGC and VT have negligible or no 3-D effects (in fact, VT has no 2-D or 3-D effects, as all visible portion of solar radiation

takes place through IGU without any secondary corner effects), therefore they were not investigated as a part of this research.

3-D heat transfer effects are mostly present in the corner regions of fenestration systems, where the assumption of 2-D heat transfer, or infinite extension of the model in z direction, ceases to exist. In North America, the overall U-factor of a fenestration system is calculated by area-weighting the 2-D conduction and radiation heat transfer results for each of the different frame and edge-of-glass cross sections (e.g., sill, jamb, head, meeting rail, and corresponding edge of glass areas). Corner 3-D effects could be added as an additional quantity to the overall results, and this quantity could either be negative or positive. In the current procedure (ISO 2004), this effect is entirely ignored.

The assumption in 1-D and 2-D models are that there is no corner 3-D effect, or that it is negligible. Some studies done in the past (Curcija and Goss 1995, Svendsen 2000) suggest that these effects may not be negligible, but there was no focused effort to determine the level of effect for different types of windows. Curcija and Goss (1995) have used computer models to analyze the 3-D heat transfer of a wood picture window incorporating a double glazed Insulated Glazing Unit (IG). Their results indicate that 3-D heat transfer effects accounted for approximately 3% difference in total U-factor for that particular window. No attempt had been made to develop universal correction that would account for 3-D effects, because only one type and one size of window was analyzed. For higher conducting frames and for projecting products, this difference could be larger.

This research project takes systematic approach at the problem, by considering matrix of typical options representing majority of products on the market today and analyzing both 2-D/1-D and full 3-D conduction heat transfer for the matrix of products.

NFRC approved software tool THERM incorporates finite element method for analyzing 2-D conduction and radiation heat transfer of frames and glazing system in the vicinity of frame cross-sections, where 2-D and 3-D heat transfer effects dominate over 1-D. WINDOW program is used in conjunction with THERM to calculate overall product performance by area weighting center-of-glass (1-D simulations) and frame/edge-of-glass (2-D simulations).

In this work, four different material types for windows were considered; incorporating matrix of glazing and spacer options, covering the entire range of performance of both today's and anticipated future fenestration products. All of the products have been analyzed for three different sizes.

DESCRIPTION OF SPECIMENS:

For this study, four fenestration specimens have been analyzed:

1. Wood window
2. Thermally broken Aluminum window (T/B AL)
3. Aluminum window (AL)
4. PVC window

The choice of sample specimens was based on the availability of test results and detailed drawings for the computer modeling. It was decided that existing NFRC testing round robins and THERM sample windows would make very good choice for this study, as the performance of these systems have been thoroughly investigated and validated against scrutinized test results. Table 1 lists the products that are considered in this study:

Glazing options, spacer types and product geometry have been also varied in order to provide matrix of options that represent entire range of performance, typical of both today's and future technology. Systematic analysis of matrix of product options, covering all of existing and future products allows for the development of recommendations for accounting of 3-D effects in existing computer tools, without the need to run expensive 3-D heat transfer models in everyday practice.

Table 1. List of fenestration systems analyzed

Window Type	Description
Wood	Marvin sample (prototype) fenestration model - PFM
T/B AL	NFRC test round robin 2001 - TRR01
AL	Modified TRR01 (thermal break replaced with Al)
PVC	Modified TRR01 (Al walls replaced with PVC)

Table 2. Matrix of glazing options and spacer designs

Window		Double Clear	Double HC Low-e	Double SC Low-e	R-10**
Wood	Gas Fill:	Air	Argon*, Air	Argon*, Air	Modified Krypton
	Spacer:	Al, Steel, Foam	Al, Steel, Foam	Al, Steel, Foam	Al, Steel, Foam
TB-AL	Gas Fill:	Air	Argon*, Air	Argon*, Air	Modified Krypton
	Spacer:	Al, Steel, Foam	Al, Steel, Foam	Al, Steel, Foam	Al, Steel, Foam
AL	Gas Fill:	Air	Argon*, Air	Argon*, Air	Modified Krypton
	Spacer:	Al, Steel, Foam	Al, Steel, Foam	Al, Steel, Foam	Al, Steel, Foam
PVC	Gas Fill:	Air	Argon*, Air	Argon*, Air	Modified Krypton
	Spacer:	Al, Steel, Foam	Al, Steel, Foam	Al, Steel, Foam	Al, Steel, Foam

Note: * Argon composition is 5% Air / 95% Argon and is present in Low-e glazing only

** Hypothetical gas was created by modifying properties of Krypton to approximate R-10 glazing

In addition to the originally planned three glazing systems (Double Clear, Double HC Low-e, and Double SC Low-e), one theoretical R-10 (i.e., U = 0.10 Btu/hr-ft^{2}F) glazing system was also added to the matrix. This glazing system represents anticipated high performance limit, with a U-factor value close to that of a wall. In order to create IGU which would fit in the existing glazing pocket, while keeping double glazing configuration and spacer thickness, an artificial gap fill gas was created to achieve R-10 glazing by modifying the properties of a Krypton gas.

1. Wood Window:

Figures 1-2 show geometry and details of the wood window.

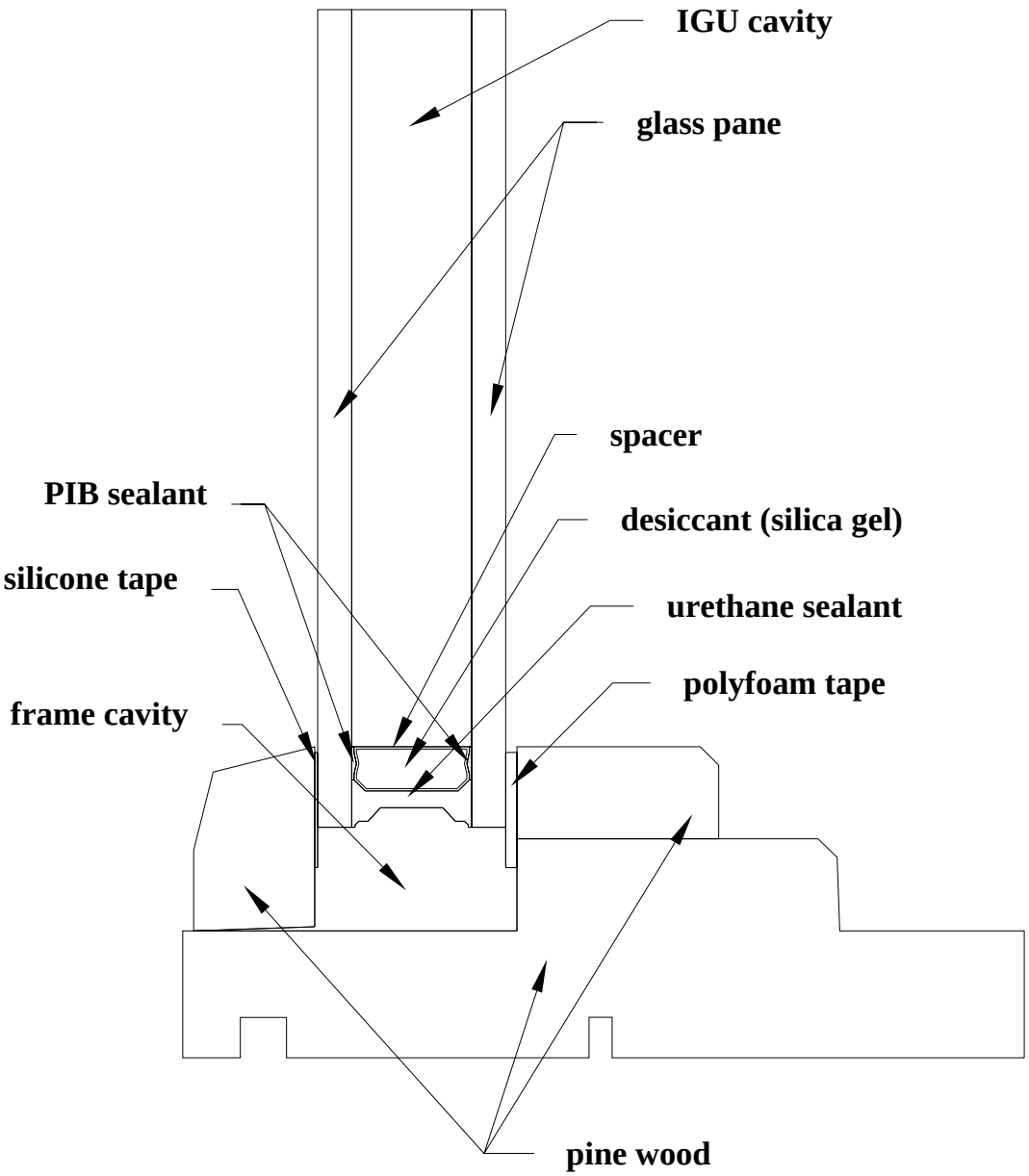


Figure 1. Typical Cross-Section of the Wood Window and List of Materials

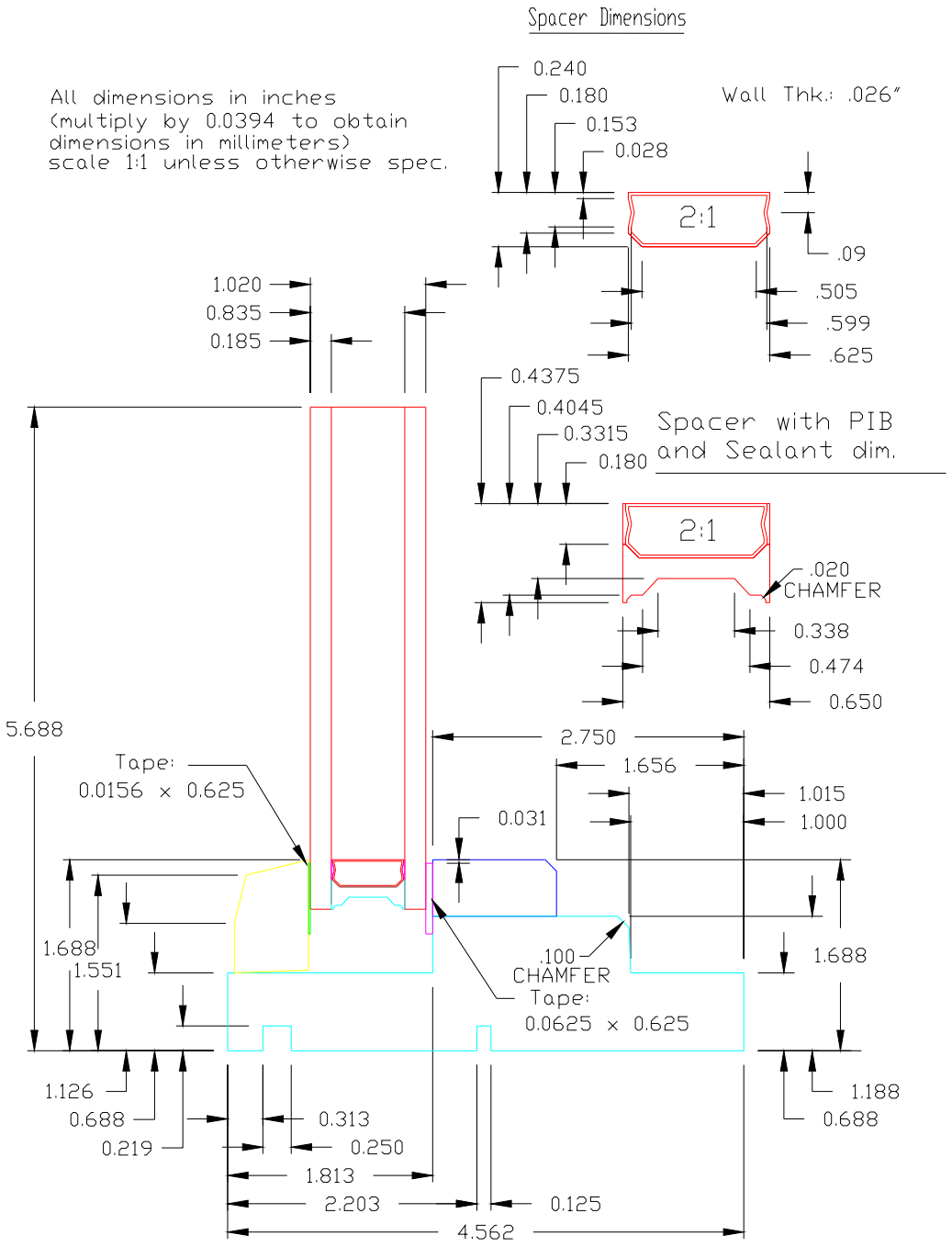


Figure 2. Dimensioned Drawing of the Sill Cross-Section of the Wood Window

2, 3, 4. Al, T/B Al, PVC Windows:

TRR01 window was used as a basis for the creation of Thermally Broken Aluminum window ”T/B AL”, Aluminum window (non-thermally broken), “AL”, and Polyvinylchloride window, “PVC”. TRR01 window was a NFRC 2001 Testing Round Robin sample. It was manufactured by TRACO Company and is of fixed window type. The round robin testing of this window was done by 8 different laboratories, so its performance is well documented and validated.

Thermally-broken Aluminum window was created as a direct model of TRR01 window. For Aluminum and PVC windows, TRR01 geometry was utilized, but material conductivities were changed. Aluminum window was created from TRR01 window by simply replacing the conductivity of thermal break material with solid Aluminum conductivity. Separate validation in THERM was done to prove that this change was equivalent to replacing the thermal break with the Aluminum extrusion wall, which would be normal way that Al window would be manufactured.

PVC window was created by modifying conductivity of all of Aluminum materials with the conductivity of PVC. Because PVC windows incorporate extrusions similar to the ones found in Aluminum windows, with the only significant difference of having conductivity of extrusion walls substantially lower, this is considered to be very good approximation of the actual PVC window.

Figure 3 shows detailed geometry and different view of cross-sections of the actual TRR01 window. Figure 4 shows geometry and bill of materials for the sill cross-section of the TRR01 window. This window was modeled as a part of the testing round robin evaluation and the THERM and WINDOW models agreed quite well with the measurements. Based on this geometry, slightly modified geometry was developed, mostly to simplify details around spacer, weather-strips, internal extrusion walls, thermal break, etc. so that 3-D geometry would not become overly complicated. Prior to finalizing simplifications to the T/B AL window, THERM models were run for both windows, TRR01 and T/B AL to confirm that final results did not show any appreciable difference. Figure 5 shows modified geometry of the T/B AL window, while Table 3 shows comparison of heat transfer results between TRR01 and T/B AL windows. It is apparent that the difference between the two models is miniscule and therefore acceptable. On the positive side, this simplification has reduced the number of 3-D elements by more than half, resulting in tens of thousand less elements and substantially improved running time. Figures 6-7 show the modified models of AL and PVC windows.

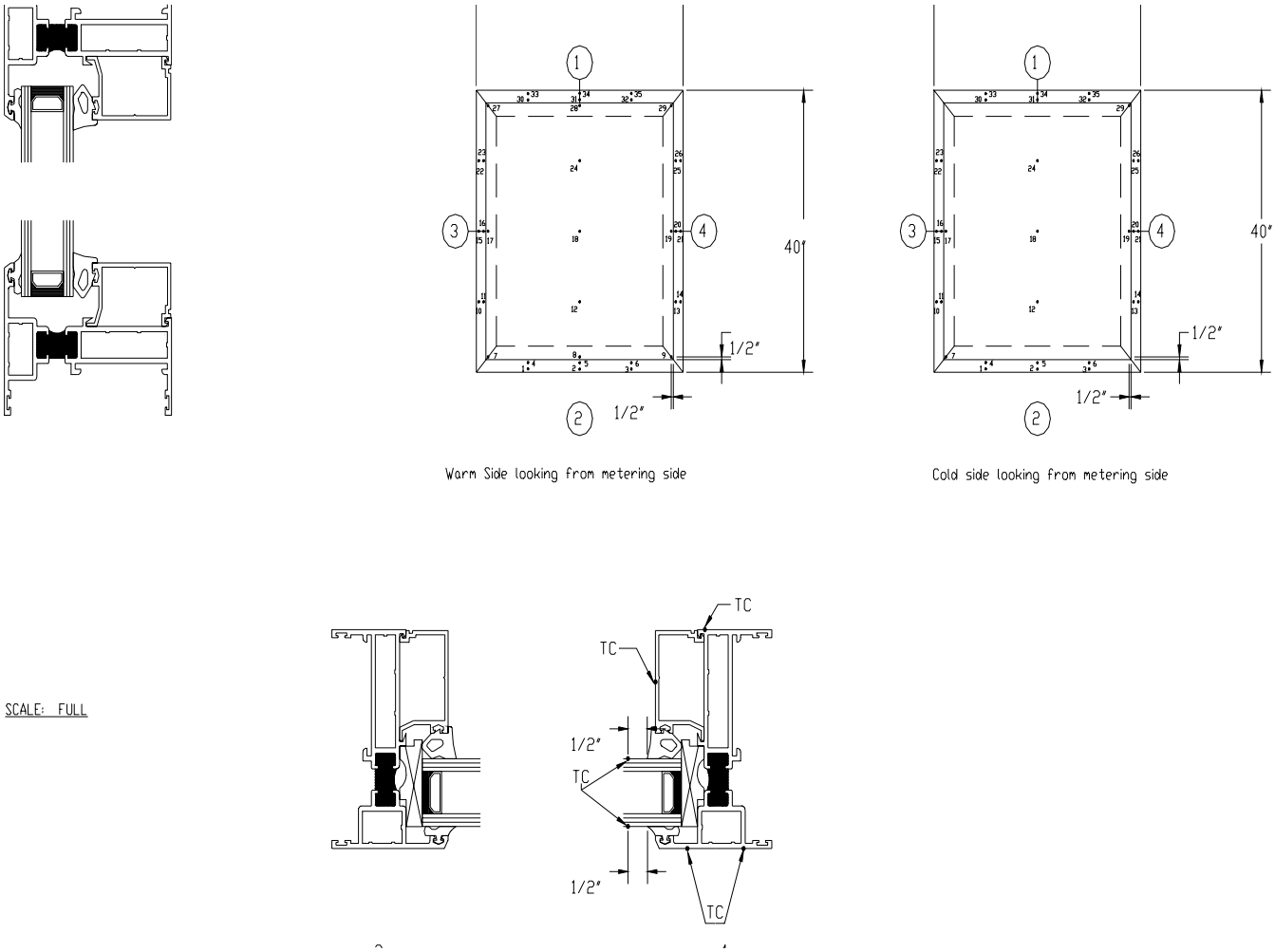


Figure 3. Geometry and Cross-Sections of TRR01 Window

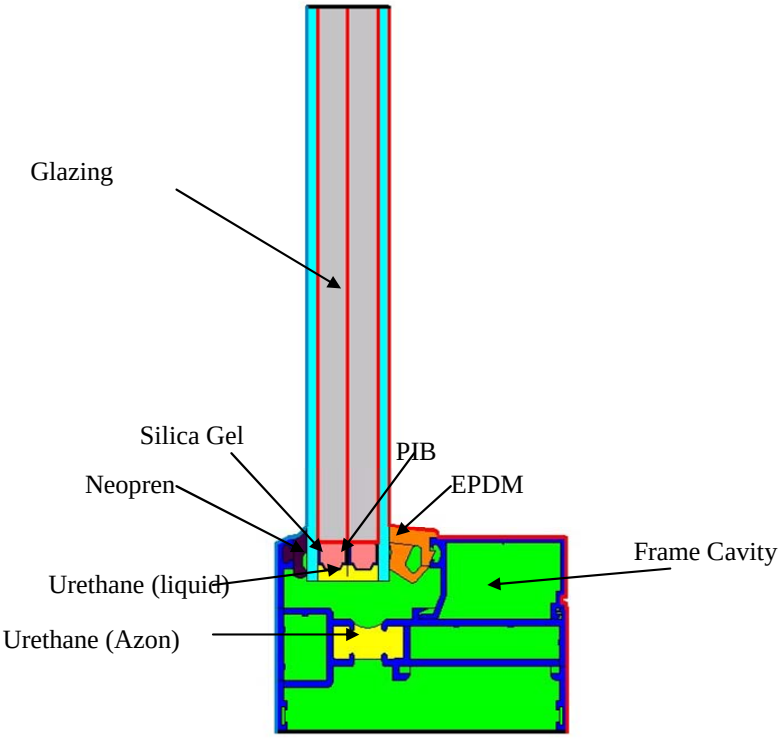


Figure 4. Geometry and List of Materials for the Sill Cross-Section of the TRR01 Window

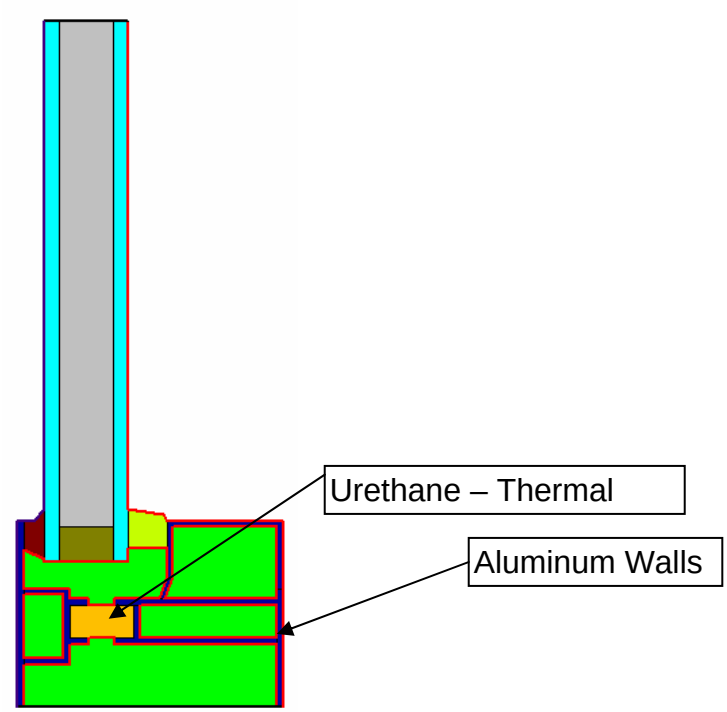


Figure 5. Geometry for the Sill Cross-Section of the T/B AL Window

Table 3. Comparison of U-Factors between TRR01 and T/B Al

	Relative Difference
Edge U-Factor	-0.1%
Frame U-Factor	-2.8%
Whole Window U-Factor	-0.08%

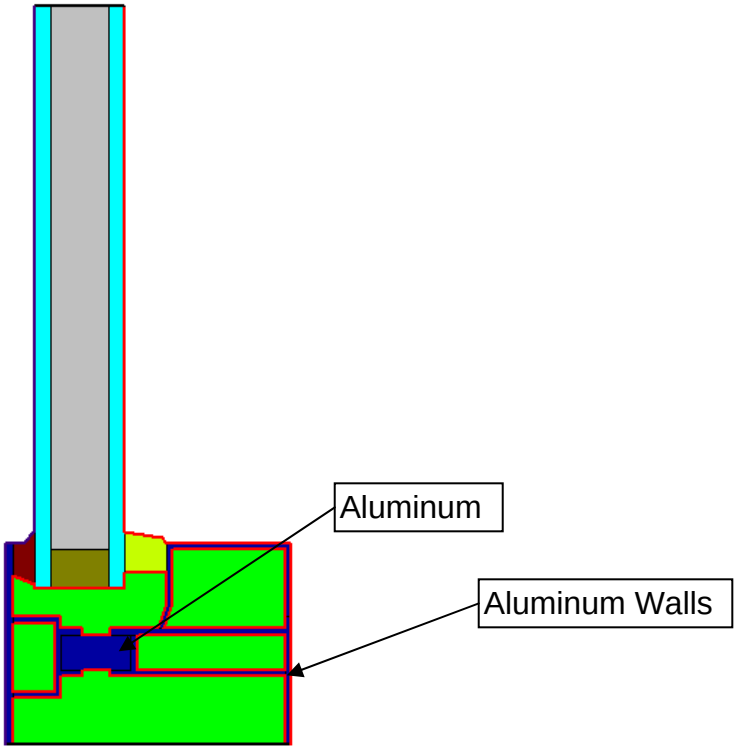


Figure 6. Geometry, for the Sill Cross-Section of the AL Window

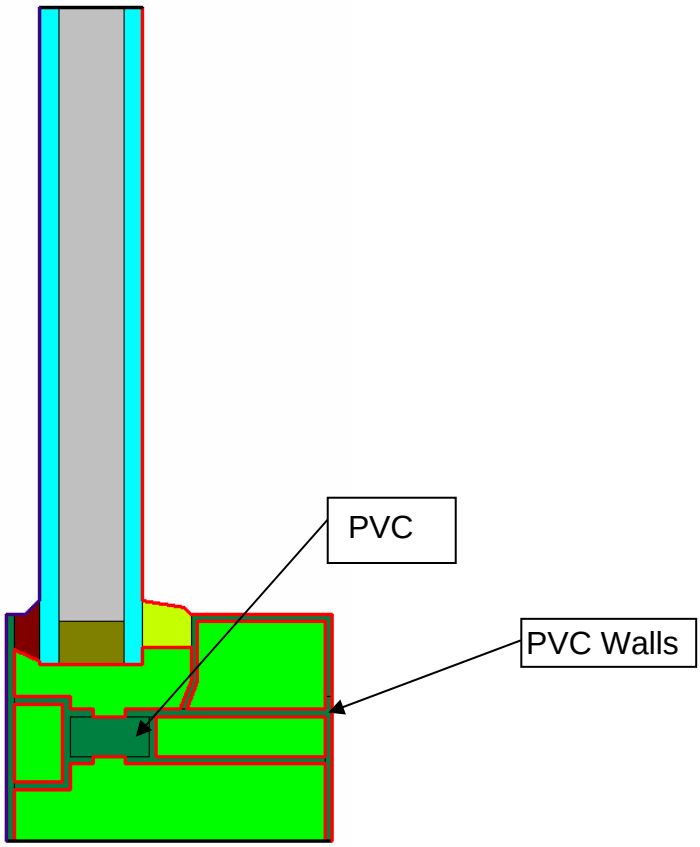


Figure 7. Geometry, for the Sill Cross-Section of the PVC Window

MODELING ASSUMPTIONS:

Actual spacer designs were replaced by block of material with effective thermal conductivity, calculated from the actual spacer configurations. This assumption was also checked in THERM program to confirm that it does not create larger discrepancies. Simplification of spacer geometry allowed for more effective numerical meshes, while preserving the accuracy of results. At the same time, this approach also allows for easy analysis of an arbitrary spacer design by simply replacing effective conductivity of one spacer assembly with the one of the other spacer assembly. It has been proven that this approach produces valid results not only for U-factors but also for condensation resistance results as well.

This model was compared in THERM with the model where thermal break geometry was replaced by Aluminum profile, which is how typical Aluminum window configuration would be. This was done in order to confirm that the simplification of replacing conductivity of thermal break material was valid.

Each of window models utilized horizontal symmetry, so only one half of the window, divided at the vertical centerline, was modeled. Figure 8 shows the example of left half of the wood window and location of the symmetry plane.

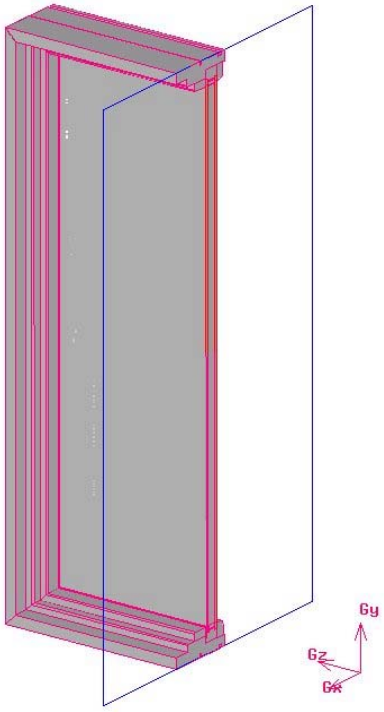


Figure 8. Geometry of One Half of the Wood Window and Location of Symmetry Plane

3-D models of wood window are shown in figures 9 and 10. 3-D models of Aluminum and PVC windows are shown in figures 11 and 12. 2-D model of Aluminum and PVC windows are shown in Figure 13. Figures 14 and 15 show THERM finite element mesh in 2-D.

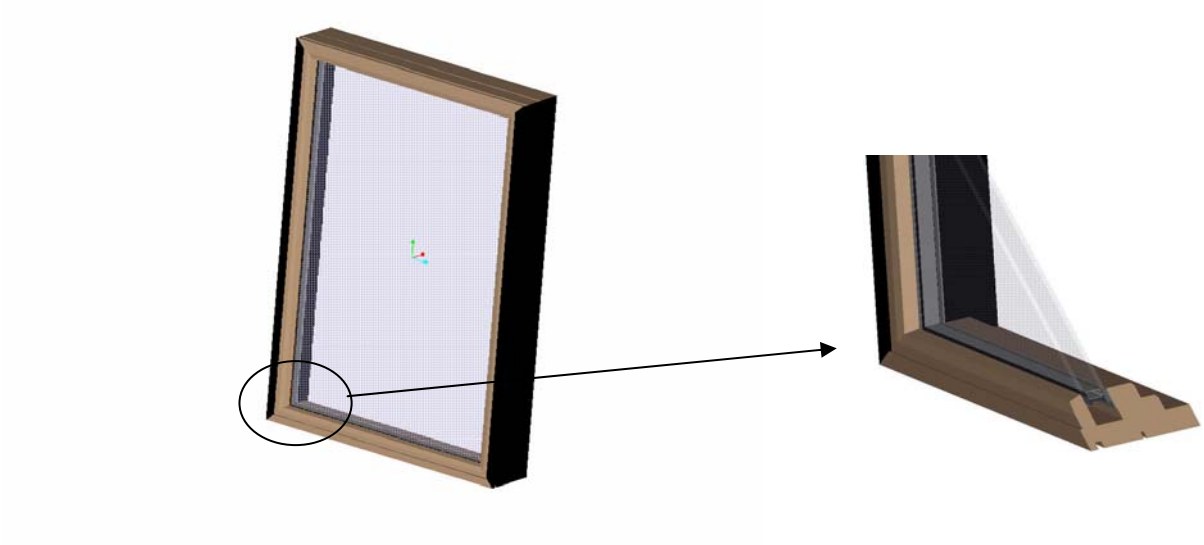


Figure 9. 3-D Model of Wood Window

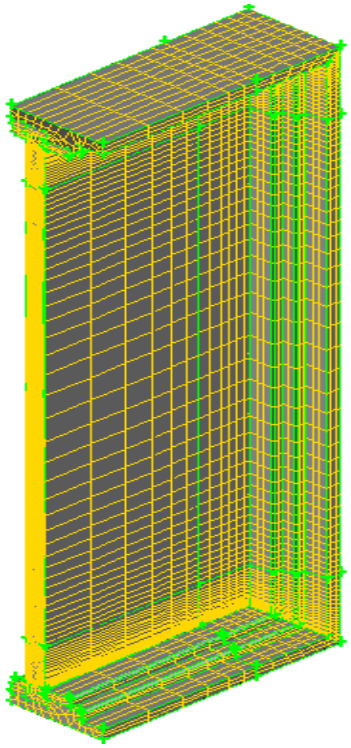


Figure 10. Finite Volume Mesh of the Wood Window

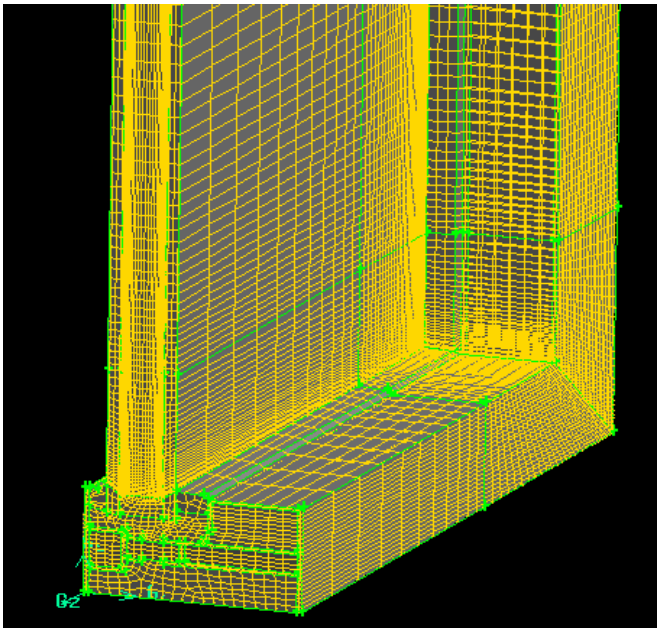


Figure 11. Finite Volume Mesh of the Aluminum and PVC windows

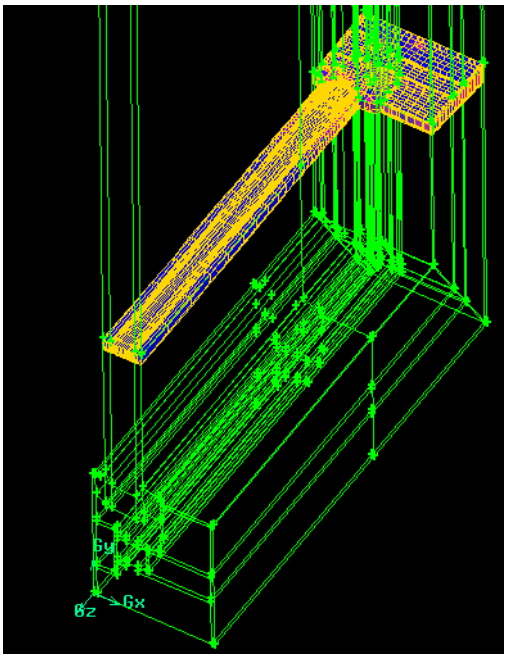


Figure 12. 2-D Cross-Section From the 3-D Model of the Aluminum and PVC windows

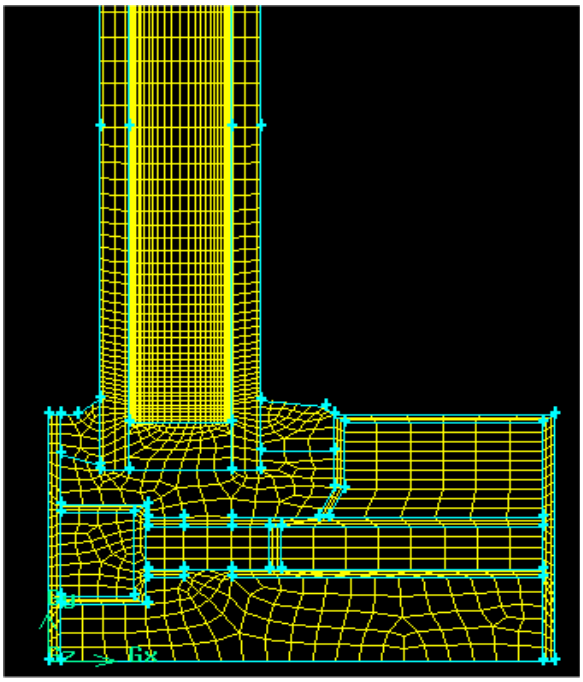


Figure 13. 2-D Finite Volume Model of Aluminum and PVC Windows

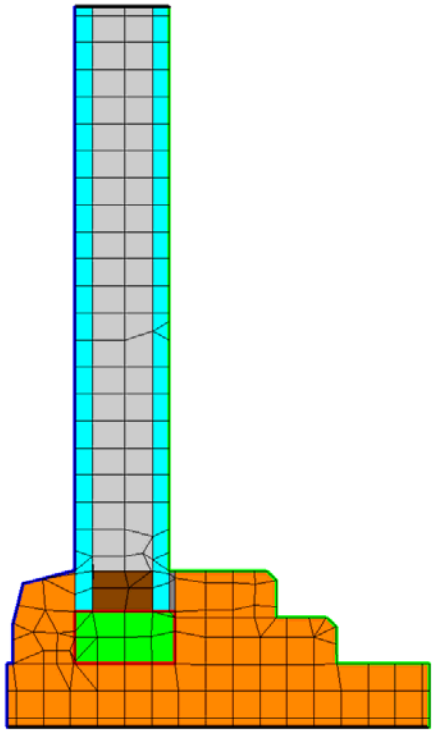


Figure 14. Finite Element Mesh of the Wood Window Sill Cross-Section in THERM

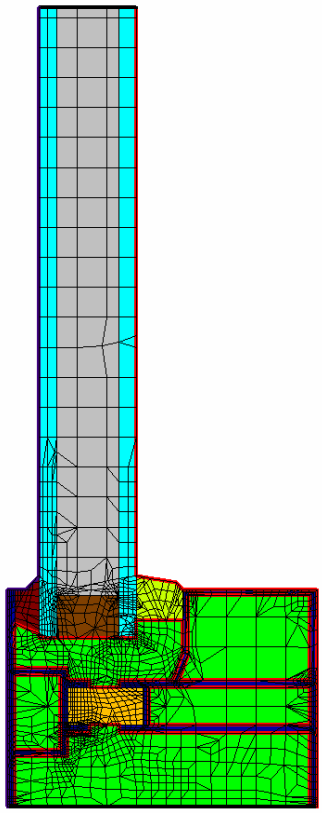


Figure 15. Finite Element Mesh of the T/B AL Window Sill Cross-Section in THERM

MATHEMATICAL MODELS

All of the windows and their options were run in FLUENT (Fluent 2004) and THERM 5.2 (LBNL 2003a) and WINDOW 5.2 (LBNL 2003b) computer programs.

FLUENT is general purpose computational fluid dynamic and heat transfer software, which utilizes finite volume numerical method for solving governing fluid flow and energy equations. In this work, FLUENT was used to solve 2-D and 3-D conduction heat transfer equation in steady state without internal heat generation. This equation is obtained from the energy equation, where velocity terms, temporal terms and internal heat generation terms are eliminated, resulting in Laplace type of equation:

In 3-D:

$$\frac{\partial^2 T}{\partial x^2} + \frac{\partial^2 T}{\partial y^2} + \frac{\partial^2 T}{\partial z^2} = 0$$

And in 2-D:

$$\frac{\partial^2 T}{\partial x^2} + \frac{\partial^2 T}{\partial y^2} = 0$$

The following additional assumptions were used:

- All materials are considered homogeneous and isotropic
- The material properties are constant (not temperature dependent)

The air in frame cavities and gas fills in glazing cavities are modeled like a solid, whose conductivity includes effects of conduction, convection and radiation heat transfer. This conductivity is referred to as effective conductivity or k_{eff}. The effective conductivity was calculated in WINDOW and THERM programs and input into FLUENT program.

Mathematical models incorporated into the THERM and WINDOW programs are described in detail in ISO 15099 standard (ISO 2004) and rules for using these programs in modeling fenestration heat transfer are described in an NFRC Simulation Manual (NFRC 2003). These documents also explain how is effective conductivity calculated.

RESULTS

FLUENT models were done in 2-D and 3-D, so that effective comparison between results could be achieved. THERM and WINDOW models were run first and effective conductivities of frame cavities and glazing cavities were utilized in FLUENT models.

FLUENT 3-D results were compared to FLUENT 2-D results for the final conclusion about the 3-D heat transfer effects. This was done because it is the true “apples-to-apples” comparison that exposes 3-D effects and most effectively eliminates noise in results. In other words, any small differences between THERM and FLUENT 2-D results will not affect comparison between 2-D and 3-D heat transfer results. On the other hand, results from THERM and WINDOW were compared to FLUENT 2-D results to make sure that FLEUNT models were sound and accurate representation of the fenestration models. Side benefit was further verification and validation of the accuracy of THERM program.

The window geometry has been divided-up into several regions (see Figure 16), so that each contribution to 3-D heat transfer can be separately accounted for. For example, sill portion of the frame is divided into the region farther from the corner, where pure 2-D effects dominate, while the corner region, which looks like trapezoid when viewed facing the window, is evaluated separately in order to understand the corner effects. Edge of glass near the corner and near the center of glass is also separately considered. This allows for better resolution of results and better understanding of 3-D heat transfer effects. Figure 17 shows full listing of all of subdivisions that were used for calculating heat transfer.

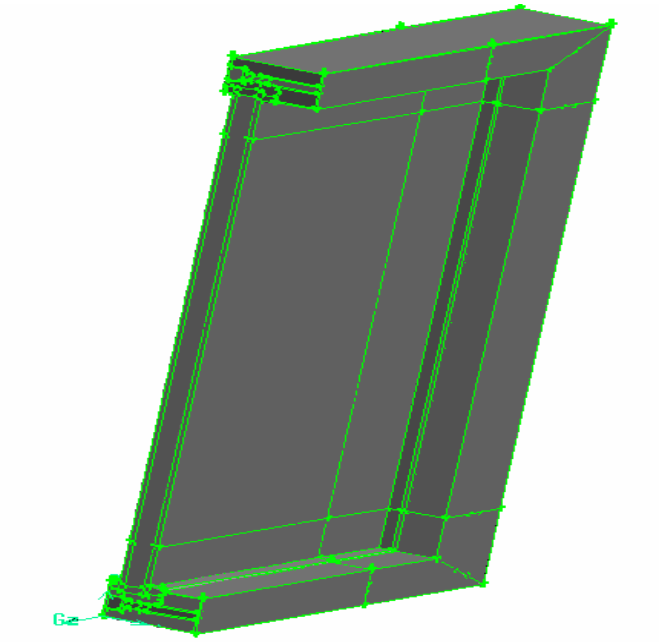


Figure 16. Sub-division of 3-D Geometry for Better Resolution of Results

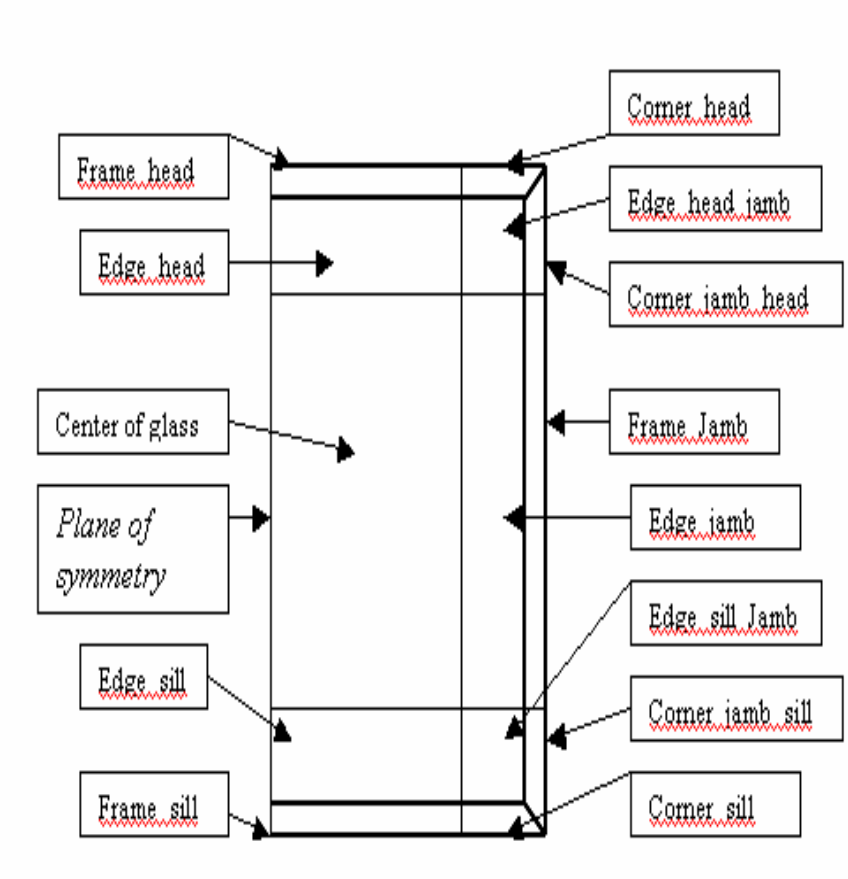


Figure 17. Listing of Individual Areas on Indoor Side

Tables 4 to 7 give results for all of the analyzed products and options on the level of the whole window. Each table is organized into three major groups, characterized by size. Each of these sections is further subdivided into three sub-groups for spacer performance and finally, each of these spacer subgroups is then sub-divided into 3 or 4 (depending on the size) groups for each IGU. This provides 33 options for each window material, or 132 options for all 4 windows.

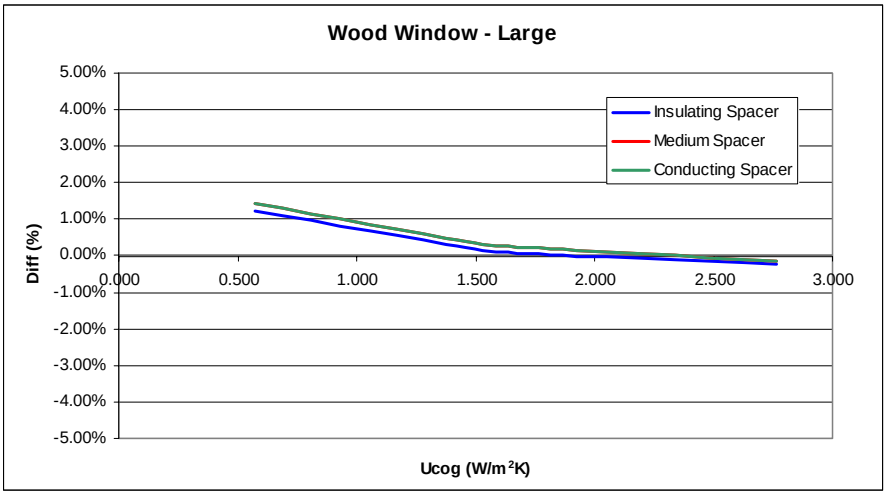
The results are presented for W5/T5 (WINDOW 5.2 and THERM 5.2 programs), FLUENT 2-D, and FLUENT 3-D. Differences between FLUENT 2-D vs. W5/T5 and FLUENT 3-D vs. FLUENT 2-D are calculated and are provided in the table. Therefore, each table has 5 columns of numbers, of which 3 are simulated U-factors and 2 are calculated differences.

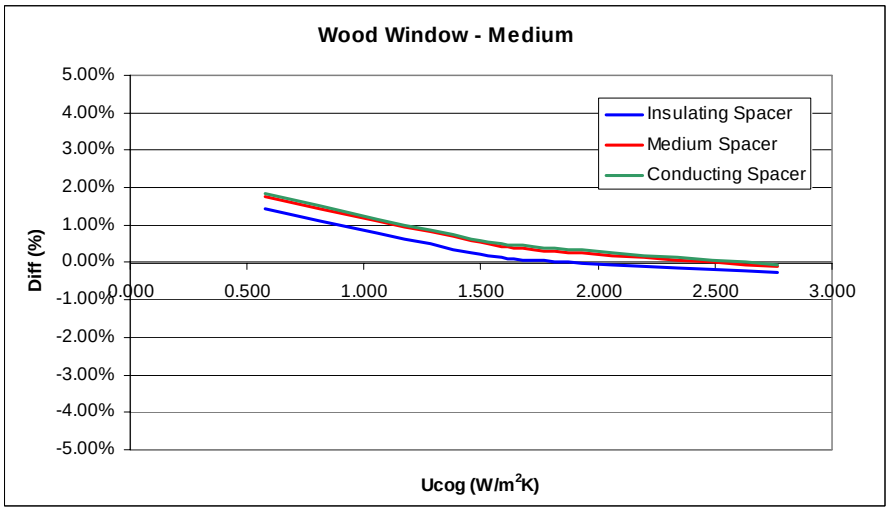
Figures 18 to 21 show differences between FLUENT 3-D and FLUENT 2-D results, by plotting the percentage difference vs. IGU performance for each spacer and window size.

Table 4: Wood Window Results:

Size	Spacer cond. (W/mK)	Fill gas	Glazing	U-factor (W/m^{2}K)				
				W5 / T5	FLUENT 2-D	*% diff.*	FLUENT 3-D	***% diff. (3D-2D)***
Large (0.6 x 1.5)	Low (0.05)	Air	Clear-clear	2.60	2.58	-0.52%	2.58	-0.21%
		Argon	Clear-low-e HC	1.76	1.75	-0.23%	1.76	0.07%
			Clear-low-e SC	1.55	1.53	-1.42%	1.53	0.22%
		Hypothetic	R10	0.86	0.84	-2.45%	0.85	1.24%
	Medium (0.674)	Air	Clear-clear	2.76	2.76	-0.06%	2.75	-0.13%
		Argon	Clear-low-e HC	1.96	1.97	0.57%	1.98	0.23%
			Clear-low-e SC	1.76	1.76	-0.31%	1.77	0.40%
		Hypothetic	R10	1.12	1.11	-0.81%	1.12	1.45%
	High (1.9)	Air	Clear-clear	2.83	2.82	-0.33%	2.82	-0.14%
		Argon	Clear-low-e HC	2.04	2.05	0.58%	2.05	0.21%
			Clear-low-e SC	1.84	1.84	-0.24%	1.85	0.39%
		Hypothetic	R10	1.21	1.20	-1.31%	1.21	1.41%
Medium (0.6 x 1.2)	Low (0.05)	Air	Clear-clear	2.59	2.57	-0.54%	2.57	-0.26%
		Argon	Clear-low-e HC	1.76	1.76	-0.24%	1.76	0.08%
			Clear-low-e SC	1.56	1.53	-1.47%	1.54	0.26%
		Hypothetic	R10	0.88	0.86	-2.37%	0.87	1.42%
	Medium (0.674)	Air	Clear-clear	2.76	2.75	-0.07%	2.75	-0.11%
		Argon	Clear-low-e HC	1.97	1.98	0.57%	1.99	0.35%
			Clear-low-e SC	1.78	1.77	-0.28%	1.79	0.57%
		Hypothetic	R10	1.14	1.14	-0.73%	1.16	1.77%
	High (1.9)	Air	Clear-clear	2.83	2.82	-0.36%	2.82	-0.08%
		Argon	Clear-low-e HC	2.05	2.07	0.59%	2.07	0.41%
			Clear-low-e SC	1.86	1.86	-0.15%	1.87	0.64%
		Hypothetic	R10	1.25	1.23	-1.17%	1.25	1.83%
Small (0.6 x 0.9)	Low (0.05)	Air	Clear-clear	2.57	2.55	-0.64%	2.55	-0.28%
		Argon	Clear-low-e HC	1.76	1.76	-0.35%	1.76	0.11%
			Clear-low-e SC	1.56	1.54	-1.49%	1.54	0.34%
	Medium (0.674)	Air	Clear-clear	2.75	2.75	-0.09%	2.74	-0.16%
		Argon	Clear-low-e HC	1.99	2.00	0.53%	2.01	0.34%
			Clear-low-e SC	1.80	1.80	-0.25%	1.81	0.58%
	High (1.9)	Air	Clear-clear	2.83	2.82	-0.40%	2.82	-0.17%
		Argon	Clear-low-e HC	2.08	2.09	0.55%	2.09	-0.02%
			Clear-low-e SC	1.90	1.89	-0.19%	1.90	0.58%

Note: HC: ε = 0.16; SC: ε = 0.03; Argon = 95% Argon & 5% Air





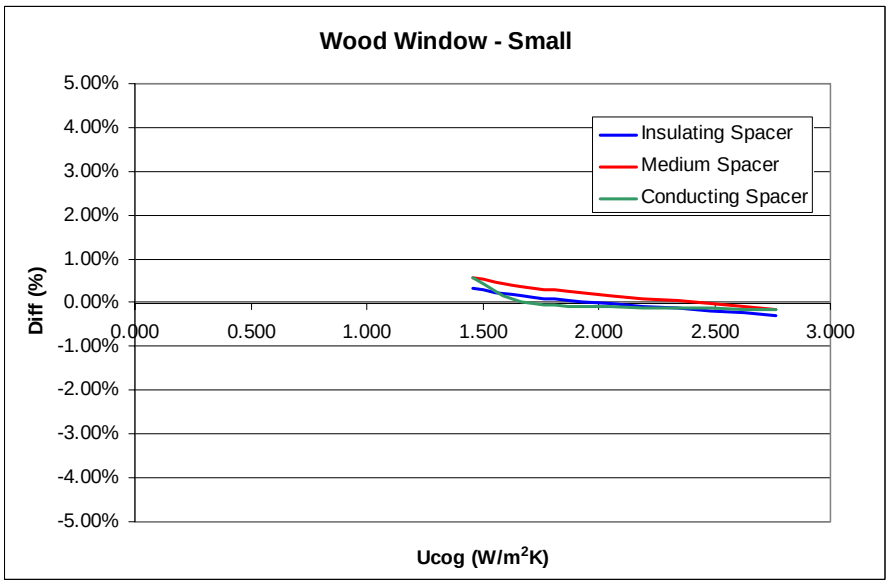
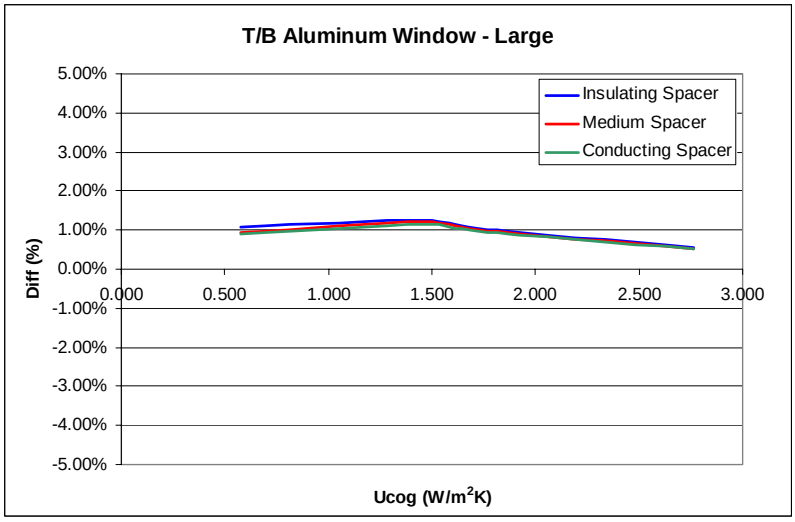


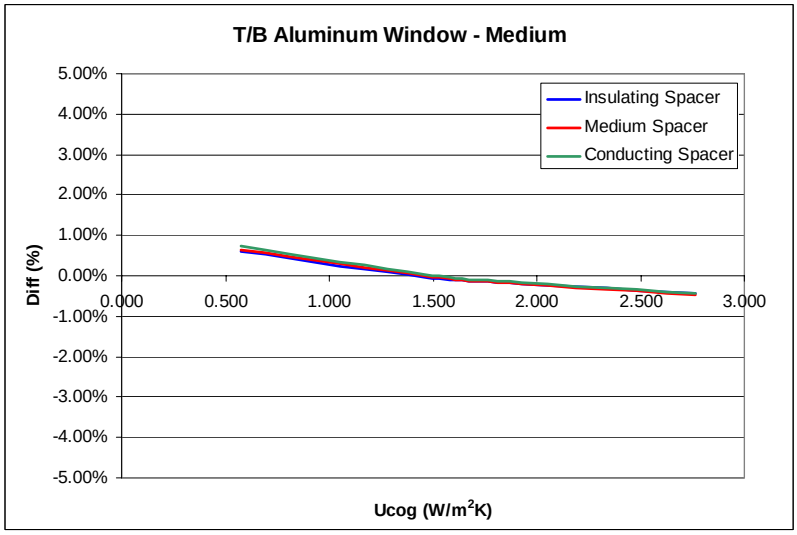
Figure 18. 3-D vs 2-D Differences for Wood Window

Table 5: Thermally-Broken Aluminum (T/B AL) Window Results:

Size	Spacer cond. (W/mK)	Fill gas	Glazing	U-factor (W/m^{2}K)				
				W5 / T5	FLUENT 2-D	*% diff.*	FLUENT 3-D	***% diff. (3D-2D)***
Large (0.6 x 1.5)	Low (0.05)	Air	Clear-clear	3.48	3.41	-2.07%	3.43	0.54%
		Argon	Clear-low-e HC	2.70	2.65	-2.11%	2.67	1.03%
			Clear-low-e SC	2.51	2.44	-2.99%	2.47	1.25%
		Hypothetic	R10	1.87	1.83	-2.44%	1.85	1.07%
	Medium (0.674)	Air	Clear-clear	3.61	3.55	-1.62%	3.57	0.53%
		Argon	Clear-low-e HC	2.86	2.82	-1.85%	2.85	1.01%
			Clear-low-e SC	2.68	2.62	-2.29%	2.65	1.23%
		Hypothetic	R10	2.07	2.03	-1.57%	2.05	0.93%
	High (1.9)	Air	Clear-clear	3.68	3.62	-1.61%	3.64	0.51%
		Argon	Clear-low-e HC	2.94	2.89	-1.54%	2.92	0.96%
			Clear-low-e SC	2.76	2.70	-2.26%	2.73	1.14%
		Hypothetic	R10	2.16	2.12	-1.62%	2.14	0.91%
Medium (0.6 x 1.2)	Low (0.05)	Air	Clear-clear	3.52	3.47	-1.51%	3.45	-0.43%
		Argon	Clear-low-e HC	2.75	2.71	-1.38%	2.71	-0.15%
			Clear-low-e SC	2.57	2.51	-2.21%	2.51	-0.02%
		Hypothetic	R10	1.94	1.90	-2.50%	1.91	0.60%
	Medium (0.674)	Air	Clear-clear	3.65	3.62	-1.00%	3.60	-0.48%
		Argon	Clear-low-e HC	2.92	2.90	-0.80%	2.89	-0.15%
			Clear-low-e SC	2.74	2.70	-1.44%	2.70	-0.01%
		Hypothetic	R10	2.15	2.11	-1.61%	2.13	0.62%
	High (1.9)	Air	Clear-clear	3.72	3.68	-0.98%	3.67	-0.44%
		Argon	Clear-low-e HC	3.00	2.98	-0.81%	2.98	-0.09%
			Clear-low-e SC	2.83	2.79	-1.41%	2.79	0.05%
		Hypothetic	R10	2.24	2.21	-1.61%	2.22	0.74%
Small (0.6 x 0.9)	Low (0.05)	Air	Clear-clear	3.57	3.52	-1.58%	3.52	0.24%
		Argon	Clear-low-e HC	2.83	2.79	-1.53%	2.81	0.85%
			Clear-low-e SC	2.65	2.59	-2.27%	2.61	0.53%
	Medium (0.674)	Air	Clear-clear	3.72	3.68	-1.02%	3.68	0.01%
		Argon	Clear-low-e HC	3.01	2.99	-0.83%	3.00	0.42%
			Clear-low-e SC	2.84	2.80	-1.42%	2.83	0.88%
	High (1.9)	Air	Clear-clear	3.79	3.76	-1.01%	3.75	-0.17%
		Argon	Clear-low-e HC	3.10	3.08	-0.84%	3.09	0.37%
			Clear-low-e SC	2.93	2.89	-1.41%	2.91	0.55%

Note: HC: ε = 0.16; SC: ε = 0.03; Argon = 95% Argon & 5% Air





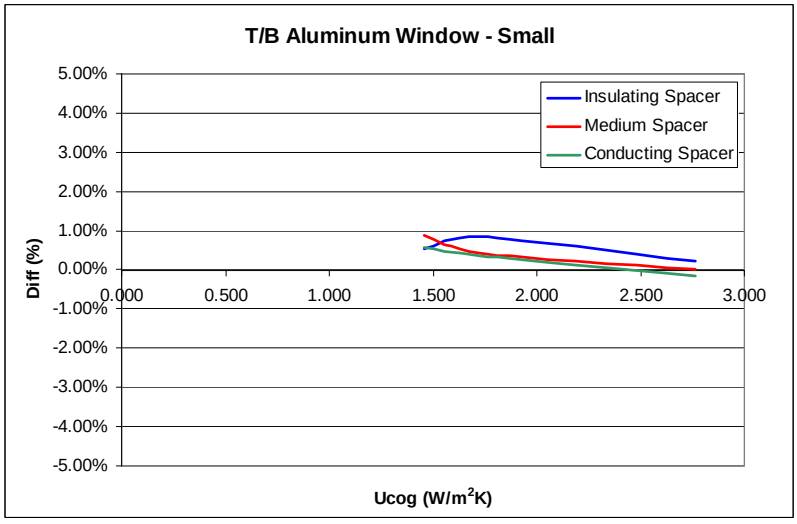
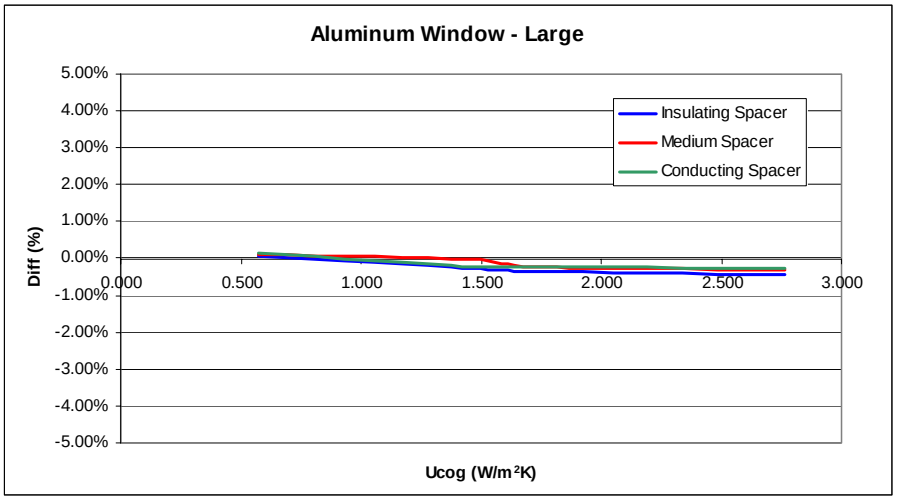


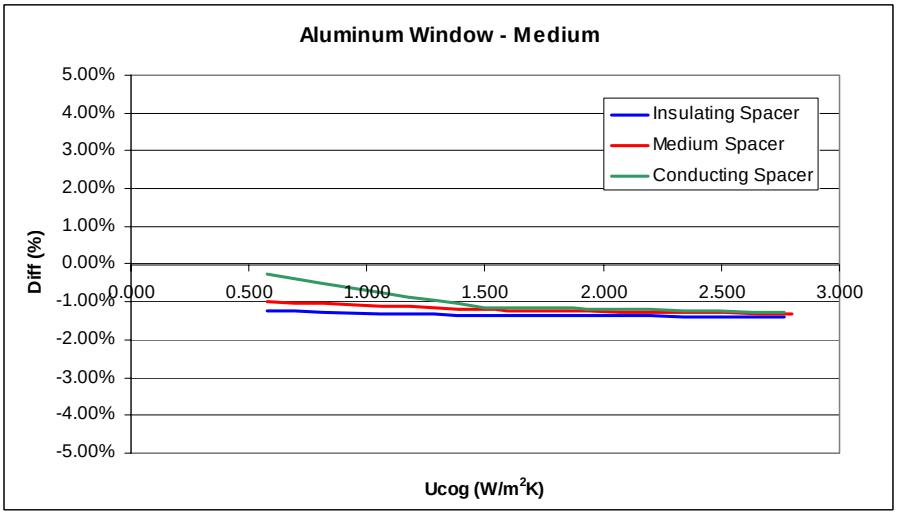
Figure 19. 3-D vs 2-D Differences for T/B AL Window

Table 6: Aluminum (AL) Window Results:

Size	Spacer cond. (W/mK)	Fill gas	Glazing	U-factor (W/m^{2}K)				
				W5 / T5	FLUENT 2-D	*% diff.*	FLUENT 3-D	***% diff. (3D-2D)***
Large (0.6 x 1.5)	Low (0.05)	Air	Clear-clear	4.47	4.47	0.02%	4.45	-0.42%
		Argon	Clear-low-e HC	3.72	3.74	0.45%	3.73	-0.34%
			Clear-low-e SC	3.54	3.54	0.09%	3.53	-0.28%
		Hypothetic	R10	2.91	2.94	0.80%	2.94	0.05%
	Medium (0.674)	Air	Clear-clear	4.51	4.50	-0.18%	4.49	-0.30%
		Argon	Clear-low-e HC	3.78	3.79	0.05%	3.78	-0.25%
			Clear-low-e SC	3.61	3.59	-0.39%	3.59	-0.02%
		Hypothetic	R10	3.00	3.00	-0.27%	3.00	0.11%
	High (1.9)	Air	Clear-clear	4.53	4.52	-0.28%	4.51	-0.29%
		Argon	Clear-low-e HC	3.81	3.81	-0.09%	3.80	-0.23%
			Clear-low-e SC	3.63	3.62	-0.51%	3.61	-0.22%
		Hypothetic	R10	3.04	3.02	-0.52%	3.03	0.14%
Medium (0.6 x 1.2)	Low (0.05)	Air	Clear-clear	4.57	4.57	-0.01%	4.51	-1.38%
		Argon	Clear-low-e HC	3.84	3.86	0.38%	3.80	-1.35%
			Clear-low-e SC	3.66	3.66	0.01%	3.61	-1.37%
		Hypothetic	R10	3.05	3.08	0.79%	3.04	-1.24%
	Medium (0.674)	Air	Clear-clear	4.61	4.60	-0.22%	4.54	-1.31%
		Argon	Clear-low-e HC	3.90	3.90	-0.01%	3.86	-1.23%
			Clear-low-e SC	3.73	3.71	-0.41%	3.67	-1.19%
		Hypothetic	R10	3.14	3.14	-0.22%	3.10	-1.01%
	High (1.9)	Air	Clear-clear	4.64	4.62	-0.33%	4.56	-1.26%
		Argon	Clear-low-e HC	3.93	3.93	-0.15%	3.88	-1.15%
			Clear-low-e SC	3.76	3.74	-0.58%	3.70	-1.10%
		Hypothetic	R10	3.18	3.15	-1.13%	3.14	-0.25%
Small (0.6 x 0.9)	Low (0.05)	Air	Clear-clear	4.72	4.72	0.03%	4.69	-0.71%
		Argon	Clear-low-e HC	4.02	4.04	0.40%	4.02	-0.49%
			Clear-low-e SC	3.85	3.85	0.10%	3.84	-0.35%
	Medium (0.674)	Air	Clear-clear	4.77	4.76	-0.16%	4.73	-0.71%
		Argon	Clear-low-e HC	4.09	4.09	0.01%	4.07	-0.48%
			Clear-low-e SC	3.92	3.91	-0.34%	3.89	-0.39%
	High (1.9)	Air	Clear-clear	4.80	4.78	-0.25%	4.75	-0.72%
		Argon	Clear-low-e HC	4.12	4.12	-0.10%	4.10	-0.56%
			Clear-low-e SC	3.96	3.94	-0.47%	3.92	-0.51%

Note: HC: ε = 0.16; SC: ε = 0.03; Argon = 95% Argon & 5% Air





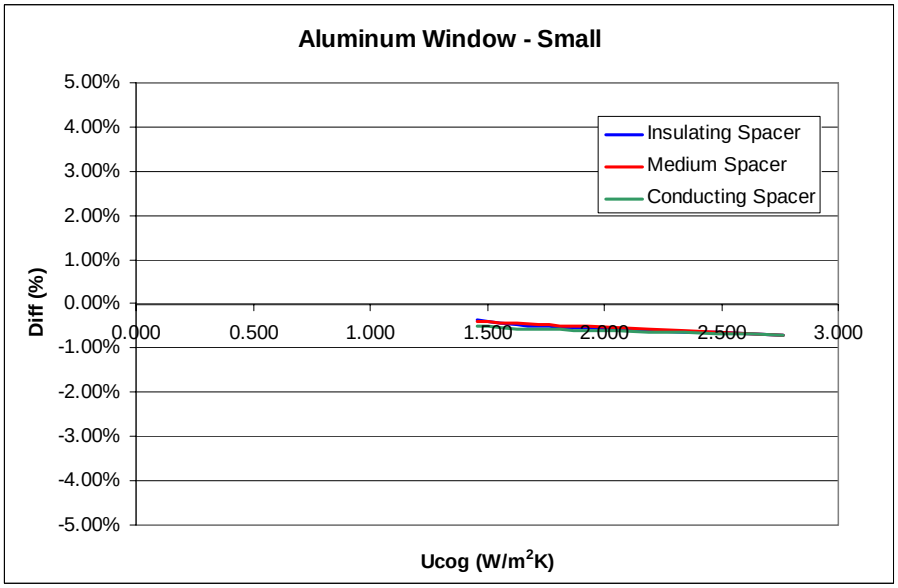
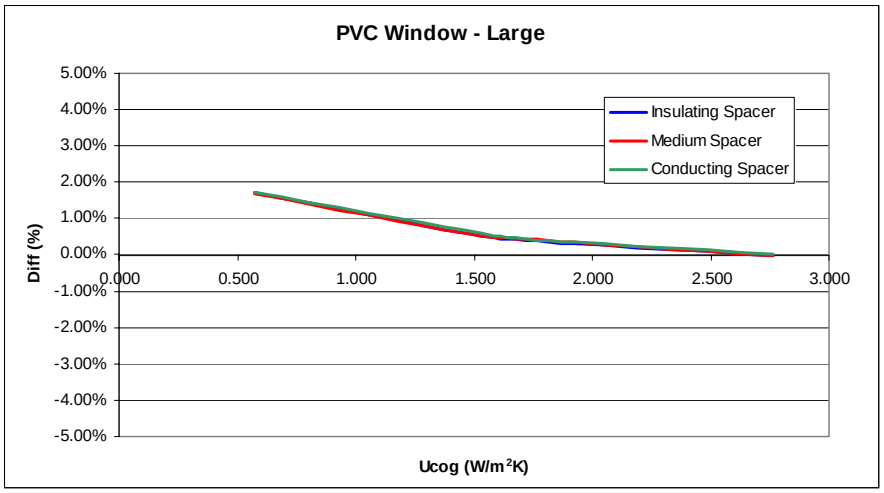


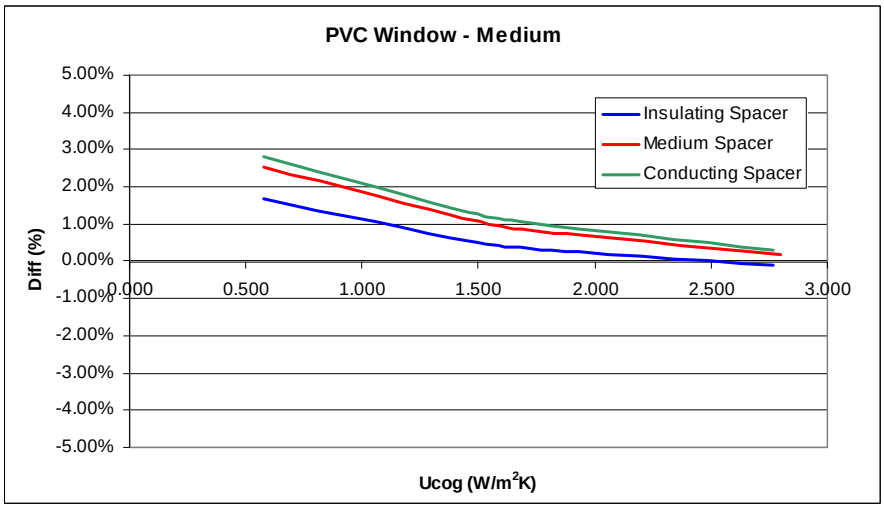
Figure 20. 3-D vs 2-D Differences for AL Window

Table 7: Polyvinylchloride (PVC) Window Results:

Size	Spacer cond. (W/mK)	Fill gas	Glazing	U-factor (W/m^{2}K)				
				W5 / T5	FLUENT 2-D	*% diff.*	FLUENT 3-D	***% diff. (3D-2D)***
Large (0.6 x 1.5)	Low (0.05)	Air	Clear-clear	2.66	2.64	-0.85%	2.64	-0.03%
		Argon	Clear-low-e HC	1.88	1.86	-0.64%	1.87	0.40%
			Clear-low-e SC	1.68	1.65	-1.73%	1.66	0.59%
		Hypothetic	R10	1.01	1.01	0.24%	1.03	1.73%
	Medium (0.674)	Air	Clear-clear	2.82	2.80	-0.84%	2.80	-0.01%
		Argon	Clear-low-e HC	2.07	2.06	-0.59%	2.07	0.44%
			Clear-low-e SC	1.89	1.86	-1.52%	1.87	0.61%
		Hypothetic	R10	1.24	1.25	0.94%	1.27	1.70%
	High (1.9)	Air	Clear-clear	2.89	2.86	-1.00%	2.86	0.01%
		Argon	Clear-low-e HC	2.16	2.14	-0.98%	2.14	0.45%
			Clear-low-e SC	1.98	1.94	-1.88%	1.95	0.69%
		Hypothetic	R10	1.34	1.34	0.40%	1.36	1.72%
Medium (0.6 x 1.2)	Low (0.05)	Air	Clear-clear	2.65	2.63	-0.81%	2.63	-0.09%
		Argon	Clear-low-e HC	1.88	1.87	-0.54%	1.88	0.33%
			Clear-low-e SC	1.69	1.66	-1.59%	1.67	0.53%
		Hypothetic	R10	1.03	1.04	0.66%	1.05	1.70%
	Medium (0.674)	Air	Clear-clear	2.82	2.79	-0.82%	2.80	0.20%
		Argon	Clear-low-e HC	2.09	2.07	-0.56%	2.09	0.84%
			Clear-low-e SC	1.91	1.88	-1.47%	1.90	1.11%
		Hypothetic	R10	1.27	1.29	1.18%	1.32	2.52%
	High (1.9)	Air	Clear-clear	2.89	2.86	-1.02%	2.87	0.31%
		Argon	Clear-low-e HC	2.17	2.15	-0.96%	2.18	1.02%
			Clear-low-e SC	2.00	1.96	-1.85%	1.99	1.32%
		Hypothetic	R10	1.37	1.38	0.57%	1.42	2.80%
Small (0.6 x 0.9)	Low (0.05)	Air	Clear-clear	2.63	2.61	-0.93%	2.61	-0.14%
		Argon	Clear-low-e HC	1.89	1.87	-0.72%	1.88	0.41%
			Clear-low-e SC	1.70	1.67	-1.74%	1.68	0.65%
	Medium (0.674)	Air	Clear-clear	2.81	2.79	-0.90%	2.78	-0.13%
		Argon	Clear-low-e HC	2.11	2.09	-0.68%	2.10	0.38%
			Clear-low-e SC	1.94	1.91	-1.51%	1.92	0.64%
	High (1.9)	Air	Clear-clear	2.89	2.86	-1.09%	2.85	-0.15%
		Argon	Clear-low-e HC	2.20	2.18	-1.06%	2.19	0.47%
			Clear-low-e SC	2.03	2.00	-1.90%	2.01	0.68%

Note: HC: ε = 0.16; SC: ε = 0.03; Argon = 95% Argon & 5% Air





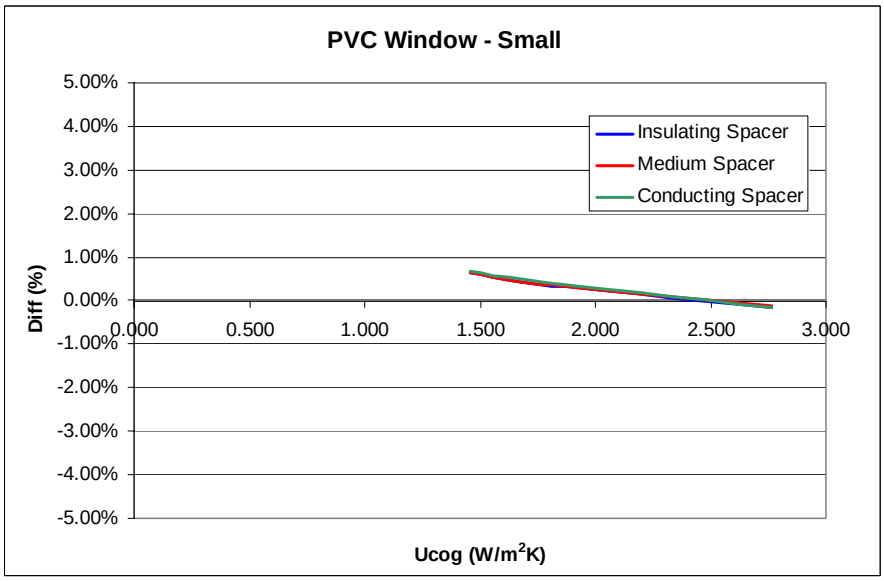


Figure 21. 3-D vs 2-D Differences for PVC Window

DISCUSSION OF RESULTS

One of the most striking results of this study is the validity of the assumption in 2-D models that 3-D conduction heat transfer corner effects are relatively small for present day frame and glazing materials. Close inspection of Tables 4-7 and Figures 18-21, reveal that for highly conducting frames, the difference is literally hovering around 0% for the whole product U-factor. For more insulating frames, like Wood and PVC, this difference becomes larger for super insulating glazing systems (i.e., R10), while it is still fairly small for standard glazing systems, including present day good insulating glazing (i.e., Argon, SC Low-e), for which the difference is hovering around 0.5% for the whole product U-factor. For R-10 glazing, the difference for wood and PVC frames exceeds 2% for smaller frames. This is still relatively small difference but for very small windows may become important and may need to be included in THERM and WINDOW as a correction.

Another interesting observation is that spacer conductivity did not play significant role in the level of differences between 3-D and 2-D conduction heat transfer models. The most significant factors were level of glazing insulation, frame conductance and to some extent, size.

In order to better understand differences on the whole product level, each of the windows were subdivided into the individual regions and their differences were investigated separately. These detailed results are presented in appendices A to D, in Tables A1-A9, B1-B9, C1-C9, and D1-D9, as well as Figures A1-A3, B1-B3, C1-C3, and D1-D3.

Based on detailed analysis of these individual component results, an overall conclusion can be drawn that small differences between 2-D and 3-D conduction heat transfer results are due to somewhat canceling effect of the summation of individual components effects. The most common canceling effect exists between frame cross-sections and jamb cross-sections. They are usually at the opposite side of y axis. Individual component U-factor differences were quite significant for some of the components going up to 10% for some window designs.

As expected sill and head heat transfer effects were very similar due to their symmetric location wrt. jamb cross-section, while jamb had different results, depending on the size and type of window. Jamb had the same design as head and sill in all of the models, which was another attempt to limit variables in this study. The difference is due only to the position within the window, not because of the arbitrary differences in individual geometries. On the other hand, this is also a limiting factor because most slider and projecting windows would have different sill and head designs.

Center of glass differences go up to around 4% very consistently for smaller size windows, which is somewhat expected result, indicating that for smaller windows, center of glass area, includes some 2-D and 3-D effects.

Providing that 3-D radiation and convection heat transfer effects were not analyzed in this study, future work should include systematic study of these effects. The current work at the University of Massachusetts includes the study of 3-D convection heat transfer effects and once published, these results should be analyzed and compared to the conduction heat transfer effects from this work.

CONCLUSIONS AND RECOMMENDATIONS

This study is the first of its kind of looking in 3-D corner heat transfer effects in fenestration systems in a systematic way. Four different frame materials, covering practically entire range of present day frame materials, were considered, three spacer types, covering the entire range of present day and future spacer materials and designs, and four different glazing systems, covering the entire range of present day and future glazing designs, except for single glazing, were investigated and reported in this study.

The first conclusion from this study is that for present day frame, spacer and glazing materials, 3-D corner conduction heat transfer effects are fairly small and can be ignored in existing fenestration computer modeling tools.

For insulating frames and super insulating glazing, the difference between 2-D and 3-D heat transfer effects becomes more pronounced and significant and it exceeds 2% for smaller size windows.

Spacer conductivity does not play significant role in the level of differences between 3-D and 2-D conduction heat transfer models.

On an individual component level, there were more significant differences, going up to 10%. These differences, would however often cancel each other as the frame and edge of glass sections would usually have different sign in front of the difference.

Future work should include 3-D convection and radiation heat transfer effects, for the same complete range of window, spacer, and glazing types, so that definitive answer could be drawn on the overall 3-D effects.

Future windows will be more insulating than present day ones, approaching the performance of R-10 glazing and more insulating frames, and based on this work, for these windows the differences are more pronounced and may require correlations to be applied to 2-D models, or may necessitate the development of dedicated 3-D fenestration heat transfer computer programs.

APPENDIX A: COMPONENT LEVEL RESULTS AND COMPARISONS FOR WOOD WINDOW:

Table A1. Wood Window – Large Size, Insulating Spacer

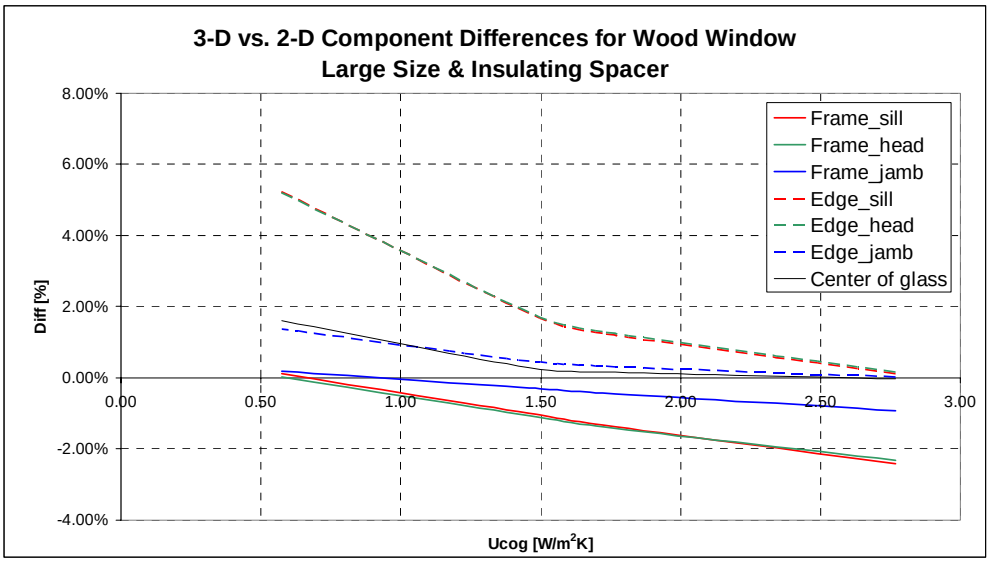
Dbl Clear	**Spacer keff =**		**0.050**	**W/mK**			
Section	**T5/W5**	**2-D**	**% diff**	**2-D***	**% diff**	**3-D**	**% diff**
	W/m^{2}K	**W/m^{2}K**	**2D vs T5/W5**	**W/m^{2}K**	**2D* vs T5/W5**	**W/m^{2}K**	**3D vs 2-D**
Frame_sill	1.87	1.83	-2.36%	1.83	-2.31%	1.78	-2.41%
Frame_head	1.87	1.83	-2.36%	1.80	-3.91%	1.78	-2.31%
Frame_jamb	1.89	1.83	-3.51%	1.80	-5.20%	1.81	-0.93%
Center of glass	2.77	2.77	0.00%	2.77	0.00%	2.77	-0.01%
Edge_sill	2.76	2.75	-0.35%	2.75	-0.34%	2.75	0.11%
Edge_head	2.76	2.75	-0.35%	2.75	-0.34%	2.75	0.15%
Edge_jamb	2.77	2.75	-0.64%	2.75	-0.63%	2.75	0.03%
TOTAL	**2.60**	**2.58**	**-0.52%**	**2.58**	**-0.71%**	**2.58**	**-0.21%**
Dbl Low-e HC	**Spacer keff =**		**0.050**	**W/mK**			
Section	**T5/W5**	**2-D**	**% diff**	**2-D***	**% diff**	**3-D**	**% diff**
	W/m^{2}K	**W/m^{2}K**	**2D vs T5/W5**	**W/m^{2}K**	**2D* vs T5/W5**	**W/m^{2}K**	**3D vs 2-D**
Frame_sill	1.68	1.64	-2.59%	1.64	-2.54%	1.61	-1.33%
Frame_head	1.68	1.64	-2.46%	1.61	-4.23%	1.62	-1.38%
Frame_jamb	1.72	1.64	-5.28%	1.61	-6.97%	1.63	-0.42%
Center of glass	1.72	1.74	0.79%	1.74	0.79%	1.74	0.16%
Edge_sill	1.88	1.88	-0.04%	1.88	-0.03%	1.91	1.26%
Edge_head	1.88	1.88	-0.03%	1.88	-0.04%	1.91	1.29%
Edge_jamb	1.89	1.88	-0.51%	1.88	-0.59%	1.89	0.33%
TOTAL	**1.76**	**1.75**	**-0.23%**	**1.75**	**-0.49%**	**1.76**	**0.07%**
Dbl Low-e SC	**Spacer keff =**		**0.050**	**W/mK**			
Section	**T5/W5**	**2-D**	**% diff**	**2-D***	**% diff**	**3-D**	**% diff**
	W/m^{2}K	**W/m^{2}K**	**2D vs T5/W5**	**W/m^{2}K**	**2D* vs T5/W5**	**W/m^{2}K**	**3D vs 2-D**
Frame_sill	1.63	1.59	-2.95%	1.59	-2.90%	1.57	-0.99%
Frame_head	1.63	1.59	-2.76%	1.56	-4.56%	1.57	-1.06%
Frame_jamb	1.66	1.59	-4.34%	1.56	-6.01%	1.58	-0.28%
Center of glass	1.46	1.45	-0.61%	1.45	-0.60%	1.46	0.28%
Edge_sill	1.67	1.65	-1.23%	1.65	-1.23%	1.68	1.82%
Edge_head	1.67	1.65	-1.23%	1.65	-1.23%	1.68	1.85%
Edge_jamb	1.68	1.65	-1.78%	1.65	-1.90%	1.66	0.48%
TOTAL	**1.55**	**1.53**	**-1.42%**	**1.52**	**-1.73%**	**1.53**	**0.22%**
Hypothetical R10	**Spacer keff =**		**0.050**	**W/mK**			
Section	**T5/W5**	**2-D**	**% diff**	**2-D***	**% diff**	**3-D**	**% diff**
	W/m^{2}K	**W/m^{2}K**	**2D vs T5/W5**	**W/m^{2}K**	**2D* vs T5/W5**	**W/m^{2}K**	**3D vs 2-D**
Frame_sill	1.48	1.45	-1.97%	1.45	-1.93%	1.45	0.11%
Frame_head	1.47	1.45	-1.77%	1.42	-3.65%	1.45	0.03%
Frame_jamb	1.50	1.45	-3.56%	1.42	-5.24%	1.45	0.19%
Center of glass	0.58	0.58	-0.07%	0.58	-0.05%	0.58	1.60%
Edge_sill	1.00	0.96	-4.39%	0.95	-4.41%	1.01	5.23%
Edge_head	1.00	0.96	-4.23%	0.95	-4.30%	1.01	5.20%
Edge_jamb	1.01	0.96	-5.65%	0.95	-6.10%	0.97	1.38%
TOTAL	**0.86**	**0.84**	**-2.45%**	**0.84**	**-3.01%**	**0.85**	**1.24%**

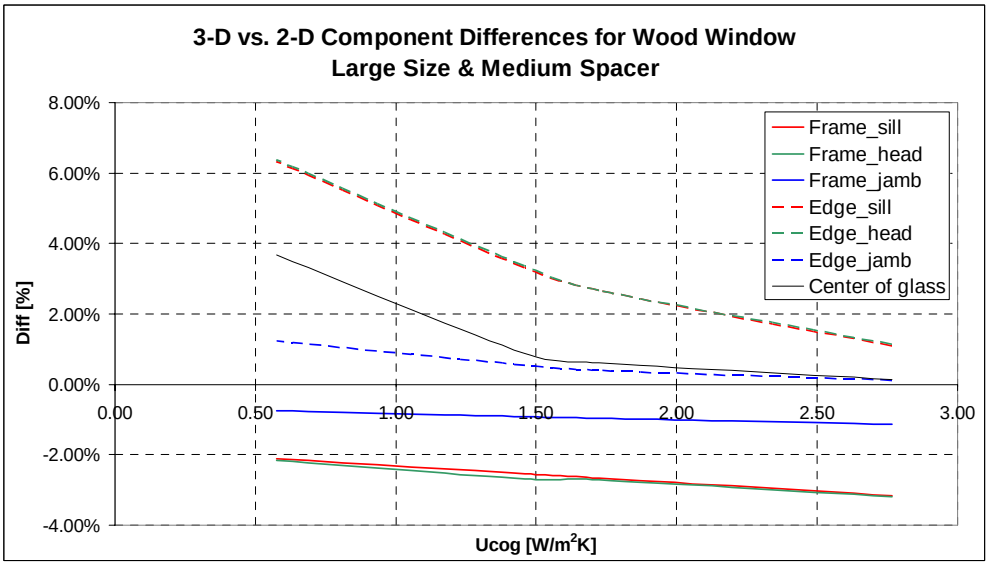
Table A2. Wood Window – Large Size, Medium Conducting Spacer

Dbl Clear	**Spacer keff =**		**0.674**	**W/mK**			
Section	**T5/W5**	**2-D**	**% diff**	**2-D***	**% diff**	**3-D**	**% diff**
	W/m^{2}K	**W/m^{2}K**	**2D vs T5/W5**	**W/m^{2}K**	**2D* vs T5/W5**	**W/m^{2}K**	**3D vs 2-D**
Frame_sill	2.33	2.31	-0.83%	2.31	-0.78%	2.24	-3.15%
Frame_head	2.33	2.32	-0.50%	2.28	-2.03%	2.24	-3.20%
Frame_jamb	2.33	2.31	-0.70%	2.28	-2.17%	2.29	-1.14%
Center of glass	2.77	2.77	0.05%	2.77	0.06%	2.77	0.15%
Edge_sill	3.05	3.05	0.29%	3.05	0.29%	3.09	1.10%
Edge_head	3.05	3.05	0.31%	3.05	0.30%	3.09	1.15%
Edge_jamb	3.05	3.05	0.23%	3.05	-0.03%	3.06	0.11%
TOTAL	**2.76**	**2.76**	**-0.06%**	**2.75**	**-0.31%**	**2.75**	**-0.13%**
Dbl Low-e HC	**Spacer keff =**		**0.674**	**W/mK**			
Section	**T5/W5**	**2-D**	**% diff**	**2-D***	**% diff**	**3-D**	**% diff**
	W/m^{2}K	**W/m^{2}K**	**2D vs T5/W5**	**W/m^{2}K**	**2D* vs T5/W5**	**W/m^{2}K**	**3D vs 2-D**
Frame_sill	2.23	2.21	-0.68%	2.21	-0.63%	2.16	-2.67%
Frame_head	2.23	2.22	-0.38%	2.18	-1.94%	2.16	-2.71%
Frame_jamb	2.25	2.21	-1.54%	2.18	-3.04%	2.19	-0.96%
Center of glass	1.72	1.74	0.92%	1.74	0.93%	1.75	0.61%
Edge_sill	2.27	2.29	1.04%	2.29	1.03%	2.36	2.68%
Edge_head	2.27	2.29	1.06%	2.29	1.05%	2.36	2.67%
Edge_jamb	2.27	2.29	0.90%	2.28	0.40%	2.30	0.41%
TOTAL	**1.96**	**1.97**	**0.57%**	**1.96**	**0.19%**	**1.98**	**0.23%**
Dbl Low-e SC	**Spacer keff =**		**0.674**	**W/mK**			
Section	**T5/W5**	**2-D**	**% diff**	**2-D***	**% diff**	**3-D**	**% diff**
	W/m^{2}K	**W/m^{2}K**	**2D vs T5/W5**	**W/m^{2}K**	**2D* vs T5/W5**	**W/m^{2}K**	**3D vs 2-D**
Frame_sill	2.20	2.19	-0.73%	2.19	-0.69%	2.13	-2.53%
Frame_head	2.20	2.19	-0.35%	2.16	-1.91%	2.13	-2.69%
Frame_jamb	2.22	2.19	-1.65%	2.16	-3.15%	2.17	-0.91%
Center of glass	1.46	1.45	-0.42%	1.45	-0.41%	1.47	0.89%
Edge_sill	2.08	2.09	0.43%	2.09	0.43%	2.16	3.32%
Edge_head	2.08	2.09	0.41%	2.09	0.40%	2.16	3.37%
Edge_jamb	2.09	2.09	0.29%	2.08	-0.32%	2.10	0.55%
TOTAL	**1.76**	**1.76**	**-0.31%**	**1.75**	**-0.75%**	**1.77**	**0.40%**
Hypothetical R10	**Spacer keff =**		**0.674**	**W/mK**			
Section	**T5/W5**	**2-D**	**% diff**	**2-D***	**% diff**	**3-D**	**% diff**
	W/m^{2}K	**W/m^{2}K**	**2D vs T5/W5**	**W/m^{2}K**	**2D* vs T5/W5**	**W/m^{2}K**	**3D vs 2-D**
Frame_sill	2.10	2.12	0.82%	2.12	0.87%	2.07	-2.10%
Frame_head	2.10	2.12	0.99%	2.09	-0.57%	2.08	-2.16%
Frame_jamb	2.12	2.12	-0.08%	2.08	-1.57%	2.10	-0.74%
Center of glass	0.58	0.58	0.61%	0.58	0.66%	0.60	3.67%
Edge_sill	1.53	1.48	-3.37%	1.48	-3.35%	1.58	6.33%
Edge_head	1.54	1.48	-3.45%	1.48	-3.48%	1.58	6.36%
Edge_jamb	1.54	1.48	-3.64%	1.47	-4.70%	1.50	1.23%
TOTAL	**1.12**	**1.11**	**-0.81%**	**1.10**	**-1.53%**	**1.12**	**1.45%**

Table A3. Wood Window – Large Size, Highly Conducting Spacer

Dbl Clear	**Spacer keff =**		**1.900**	**W/mK**			
Section	**T5/W5**	**2-D**	**% diff**	**2-D***	**% diff**	**3-D**	**% diff**
	W/m^{2}K	**W/m^{2}K**	**2D vs T5/W5**	**W/m^{2}K**	**2D* vs T5/W5**	**W/m^{2}K**	**3D vs 2-D**
Frame_sill	2.53	2.49	-1.73%	2.49	-1.68%	2.41	-3.47%
Frame_head	2.53	2.49	-1.37%	2.46	-2.88%	2.41	-3.64%
Frame_jamb	2.55	2.49	-2.45%	2.45	-4.01%	2.46	-1.34%
Center of glass	2.77	2.77	0.07%	2.77	0.08%	2.77	0.21%
Edge_sill	3.18	3.17	-0.20%	3.17	-0.20%	3.22	1.39%
Edge_head	3.18	3.17	-0.16%	3.17	-0.16%	3.22	1.40%
Edge_jamb	3.18	3.17	-0.23%	3.16	-0.65%	3.17	0.06%
TOTAL	**2.83**	**2.82**	**-0.33%**	**2.81**	**-0.63%**	**2.82**	**-0.14%**
Dbl Low-e HC	**Spacer keff =**		**1.900**	**W/mK**			
Section	**T5/W5**	**2-D**	**% diff**	**2-D***	**% diff**	**3-D**	**% diff**
	W/m^{2}K	**W/m^{2}K**	**2D vs T5/W5**	**W/m^{2}K**	**2D* vs T5/W5**	**W/m^{2}K**	**3D vs 2-D**
Frame_sill	2.42	2.41	-0.38%	2.42	-0.35%	2.34	-3.14%
Frame_head	2.42	2.42	-0.23%	2.38	-1.70%	2.35	-3.13%
Frame_jamb	2.44	2.41	-1.16%	2.38	-2.75%	2.39	-1.25%
Center of glass	1.72	1.74	0.97%	1.74	0.98%	1.75	0.76%
Edge_sill	2.42	2.44	0.88%	2.44	0.86%	2.52	2.98%
Edge_head	2.42	2.44	0.86%	2.44	0.83%	2.52	3.04%
Edge_jamb	2.43	2.44	0.80%	2.43	0.07%	2.45	0.31%
TOTAL	**2.04**	**2.05**	**0.58%**	**2.04**	**0.12%**	**2.05**	**0.21%**
Dbl Low-e SC	**Spacer keff =**		**1.900**	**W/mK**			
Section	**T5/W5**	**2-D**	**% diff**	**2-D***	**% diff**	**3-D**	**% diff**
	W/m^{2}K	**W/m^{2}K**	**2D vs T5/W5**	**W/m^{2}K**	**2D* vs T5/W5**	**W/m^{2}K**	**3D vs 2-D**
Frame_sill	2.41	2.40	-0.38%	2.40	-0.34%	2.33	-3.04%
Frame_head	2.41	2.40	-0.18%	2.36	-1.70%	2.33	-3.08%
Frame_jamb	2.43	2.40	-1.21%	2.36	-2.80%	2.37	-1.21%
Center of glass	1.46	1.45	-0.35%	1.46	-0.34%	1.47	1.10%
Edge_sill	2.25	2.25	0.22%	2.25	0.23%	2.34	3.65%
Edge_head	2.25	2.25	0.25%	2.25	0.19%	2.33	3.61%
Edge_jamb	2.25	2.25	0.18%	2.23	-0.64%	2.26	0.46%
TOTAL	**1.84**	**1.84**	**-0.24%**	**1.83**	**-0.76%**	**1.85**	**0.39%**
Hypothetical R10	**Spacer keff =**		**1.900**	**W/mK**			
Section	**T5/W5**	**2-D**	**% diff**	**2-D***	**% diff**	**3-D**	**% diff**
	W/m^{2}K	**W/m^{2}K**	**2D vs T5/W5**	**W/m^{2}K**	**2D* vs T5/W5**	**W/m^{2}K**	**3D vs 2-D**
Frame_sill	2.33	2.34	0.61%	2.34	0.68%	2.28	-2.71%
Frame_head	2.33	2.34	0.81%	2.31	-0.67%	2.28	-2.75%
Frame_jamb	2.34	2.34	-0.16%	2.30	-1.70%	2.32	-1.07%
Center of glass	0.58	0.58	0.84%	0.58	0.91%	0.61	4.36%
Edge_sill	1.75	1.67	-4.71%	1.67	-4.66%	1.78	6.45%
Edge_head	1.75	1.67	-4.74%	1.67	-4.72%	1.79	6.52%
Edge_jamb	1.75	1.67	-4.77%	1.65	-6.07%	1.69	1.07%
TOTAL	**1.21**	**1.20**	**-1.31%**	**1.19**	**-2.12%**	**1.21**	**1.41%**





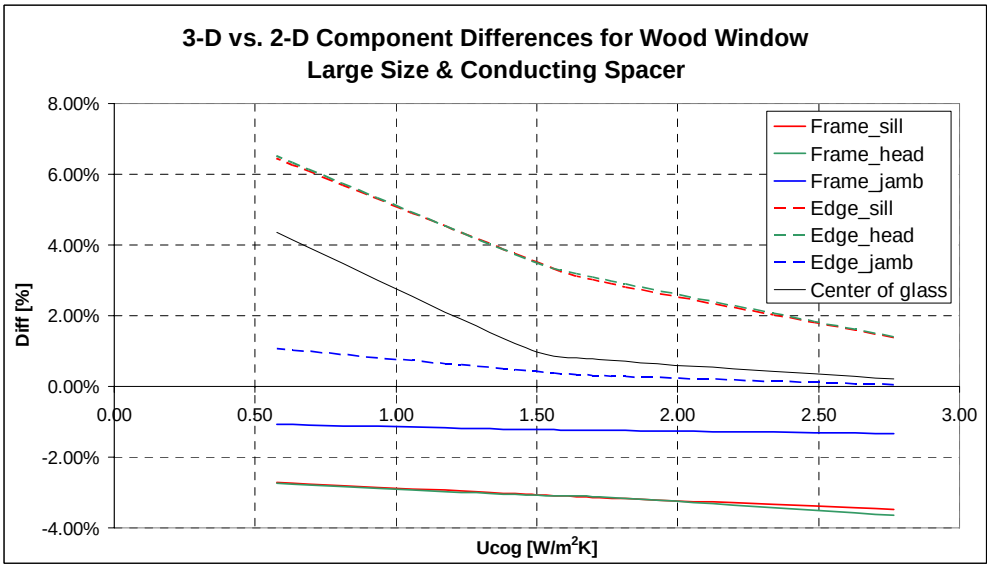


Figure A1. Component Level Difference Graphs for Large Size Wood Window

Table A4. Wood Window – Medium Size, Insulating Spacer

Dbl Clear	**Spacer keff =**		**0.050**	**W/mK**			
Section	**T5/W5**	**2-D**	**% diff**	**2-D***	**% diff**	**3-D**	**% diff**
	W/m^{2}K	**W/m^{2}K**	**2D vs T5/W5**	**W/m^{2}K**	**2D* vs T5/W5**	**W/m^{2}K**	**3D vs 2-D**
Frame_sill	1.87	1.83	-2.37%	1.83	-2.30%	1.78	-2.43%
Frame_head	1.87	1.83	-2.22%	1.80	-3.90%	1.78	-2.46%
Frame_jamb	1.89	1.83	-3.52%	1.79	-5.41%	1.81	-1.13%
Center of glass	2.77	2.77	0.00%	2.77	0.00%	2.77	-0.01%
Edge_sill	2.76	2.75	-0.34%	2.75	-0.34%	2.75	0.09%
Edge_head	2.76	2.75	-0.35%	2.75	-0.33%	2.75	0.11%
Edge_jamb	2.77	2.75	-0.63%	2.75	-0.62%	2.75	0.04%
TOTAL	**2.59**	**2.57**	**-0.54%**	**2.57**	**-0.75%**	**2.57**	**-0.26%**
Dbl Low-e HC	**Spacer keff =**		**0.050**	**W/mK**			
Section	**T5/W5**	**2-D**	**% diff**	**2-D***	**% diff**	**3-D**	**% diff**
	W/m^{2}K	**W/m^{2}K**	**2D vs T5/W5**	**W/m^{2}K**	**2D* vs T5/W5**	**W/m^{2}K**	**3D vs 2-D**
Frame_sill	1.68	1.64	-2.58%	1.64	-2.52%	1.61	-1.37%
Frame_head	1.68	1.64	-2.45%	1.61	-4.20%	1.62	-1.41%
Frame_jamb	1.70	1.64	-3.93%	1.61	-5.91%	1.63	-0.62%
Center of glass	1.72	1.74	0.80%	1.74	0.80%	1.74	0.15%
Edge_sill	1.88	1.88	-0.04%	1.88	0.02%	1.91	1.26%
Edge_head	1.88	1.88	-0.04%	1.88	0.02%	1.91	1.23%
Edge_jamb	1.89	1.88	-0.51%	1.88	-0.45%	1.89	0.58%
TOTAL	**1.76**	**1.76**	**-0.24%**	**1.75**	**-0.51%**	**1.76**	**0.08%**
Dbl Low-e SC	**Spacer keff =**		**0.050**	**W/mK**			
Section	**T5/W5**	**2-D**	**% diff**	**2-D***	**% diff**	**3-D**	**% diff**
	W/m^{2}K	**W/m^{2}K**	**2D vs T5/W5**	**W/m^{2}K**	**2D* vs T5/W5**	**W/m^{2}K**	**3D vs 2-D**
Frame_sill	1.63	1.59	-2.95%	1.59	-2.90%	1.57	-1.04%
Frame_head	1.63	1.59	-2.76%	1.56	-4.55%	1.57	-1.05%
Frame_jamb	1.66	1.59	-4.34%	1.56	-6.34%	1.58	-0.45%
Center of glass	1.46	1.45	-0.58%	1.45	-0.58%	1.46	0.26%
Edge_sill	1.67	1.65	-1.25%	1.65	-1.23%	1.68	1.80%
Edge_head	1.67	1.65	-1.25%	1.65	-1.17%	1.68	1.82%
Edge_jamb	1.68	1.65	-1.80%	1.65	-1.70%	1.66	0.85%
TOTAL	**1.56**	**1.53**	**-1.47%**	**1.53**	**-1.78%**	**1.54**	**0.26%**
Hypothetical R10	**Spacer keff =**		**0.050**	**W/mK**			
Section	**T5/W5**	**2-D**	**% diff**	**2-D***	**% diff**	**3-D**	**% diff**
	W/m^{2}K	**W/m^{2}K**	**2D vs T5/W5**	**W/m^{2}K**	**2D* vs T5/W5**	**W/m^{2}K**	**3D vs 2-D**
Frame_sill	1.48	1.45	-1.97%	1.45	-1.91%	1.45	0.04%
Frame_head	1.47	1.45	-1.78%	1.42	-3.63%	1.45	0.02%
Frame_jamb	1.50	1.45	-3.57%	1.42	-5.64%	1.45	0.07%
Center of glass	0.58	0.58	0.08%	0.58	0.07%	0.58	1.45%
Edge_sill	1.00	0.95	-4.44%	0.96	-4.24%	1.01	5.34%
Edge_head	1.00	0.95	-4.30%	0.96	-4.13%	1.01	5.33%
Edge_jamb	1.01	0.95	-5.74%	0.96	-5.46%	0.98	2.55%
TOTAL	**0.88**	**0.86**	**-2.37%**	**0.85**	**-2.87%**	**0.87**	**1.42%**

Table A5. Wood Window – Medium Size, Medium Conducting Spacer

Dbl Clear	**Spacer keff =**		**0.674**	**W/mK**			
Section	**T5/W5**	**2-D**	**% diff**	**2-D***	**% diff**	**3-D**	**% diff**
	W/m^{2}K	**W/m^{2}K**	**2D vs T5/W5**	**W/m^{2}K**	**2D* vs T5/W5**	**W/m^{2}K**	**3D vs 2-D**
Frame_sill	2.33	2.31	-0.84%	2.31	-0.79%	2.24	-3.16%
Frame_head	2.33	2.31	-0.71%	2.28	-2.03%	2.24	-2.99%
Frame_jamb	2.33	2.31	-0.71%	2.27	-2.38%	2.28	-1.46%
Center of glass	2.77	2.77	0.06%	2.77	0.07%	2.77	0.13%
Edge_sill	3.05	3.05	0.27%	3.06	0.30%	3.09	1.13%
Edge_head	3.05	3.05	0.30%	3.05	0.32%	3.09	1.14%
Edge_jamb	3.05	3.05	0.20%	3.06	0.24%	3.07	0.51%
TOTAL	**2.76**	**2.75**	**-0.07%**	**2.75**	**-0.28%**	**2.75**	**-0.11%**

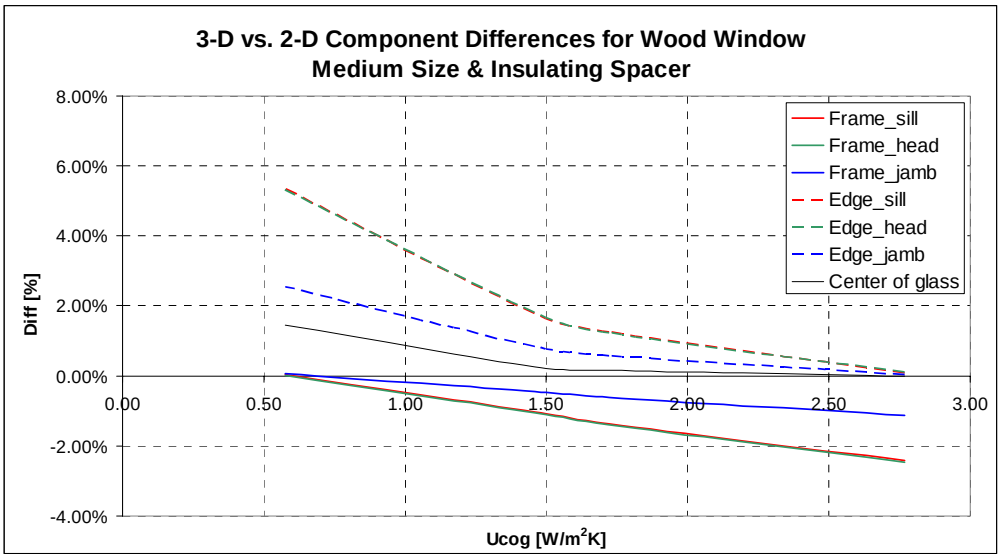
Dbl Low-e HC	**Spacer keff =**		**0.674**	**W/mK**			
Section	**T5/W5**	**2-D**	**% diff**	**2-D***	**% diff**	**3-D**	**% diff**
	W/m^{2}K	**W/m^{2}K**	**2D vs T5/W5**	**W/m^{2}K**	**2D* vs T5/W5**	**W/m^{2}K**	**3D vs 2-D**
Frame_sill	2.23	2.21	-0.70%	2.21	-0.64%	2.15	-2.68%
Frame_head	2.23	2.22	-0.40%	2.18	-1.94%	2.16	-2.69%
Frame_jamb	2.25	2.21	-1.55%	2.18	-3.25%	2.19	-1.22%
Center of glass	1.72	1.74	0.97%	1.74	0.97%	1.75	0.55%
Edge_sill	2.27	2.29	0.95%	2.29	1.09%	2.36	2.78%
Edge_head	2.27	2.29	1.00%	2.29	1.11%	2.36	2.73%
Edge_jamb	2.27	2.29	0.82%	2.30	0.97%	2.32	1.29%
TOTAL	**1.97**	**1.98**	**0.57%**	**1.98**	**0.31%**	**1.99**	**0.35%**

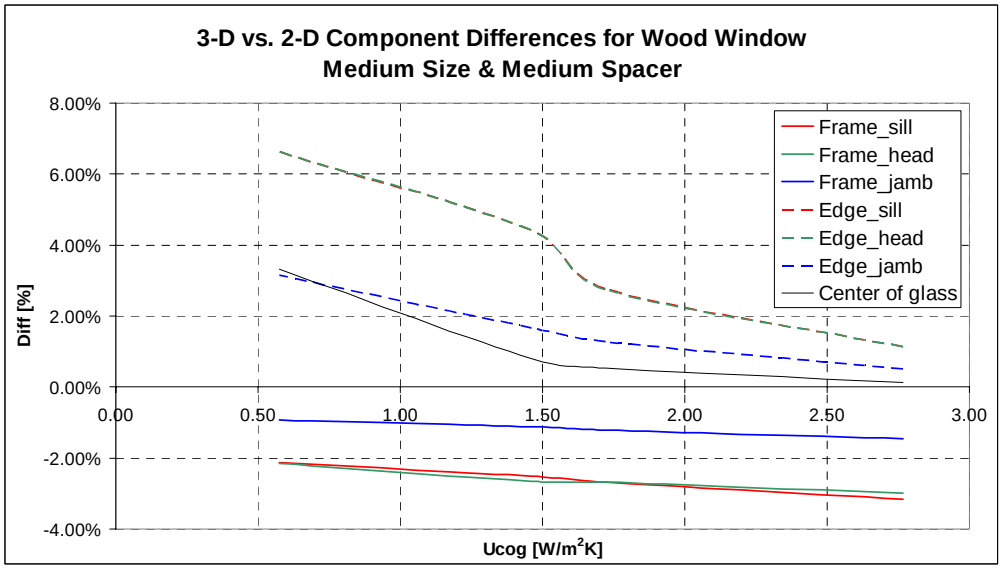
Dbl Low-e SC	**Spacer keff =**		**0.674**	**W/mK**			
Section	**T5/W5**	**2-D**	**% diff**	**2-D***	**% diff**	**3-D**	**% diff**
	W/m^{2}K	**W/m^{2}K**	**2D vs T5/W5**	**W/m^{2}K**	**2D* vs T5/W5**	**W/m^{2}K**	**3D vs 2-D**
Frame_sill	2.20	2.19	-0.75%	2.19	-0.68%	2.13	-2.51%
Frame_head	2.20	2.19	-0.37%	2.16	-1.89%	2.14	-2.67%
Frame_jamb	2.22	2.19	-1.67%	2.15	-3.35%	2.16	-1.12%
Center of glass	1.46	1.46	-0.34%	1.46	-0.34%	1.47	0.80%
Edge_sill	2.08	2.09	0.36%	2.09	0.53%	2.19	4.42%
Edge_head	2.08	2.09	0.34%	2.09	0.51%	2.19	4.42%
Edge_jamb	2.09	2.09	0.22%	2.09	0.40%	2.12	1.66%
TOTAL	**1.78**	**1.77**	**-0.28%**	**1.77**	**-0.57%**	**1.79**	**0.57%**

Hypothetical R10	**Spacer keff =**		**0.674**	**W/mK**			
Section	**T5/W5**	**2-D**	**% diff**	**2-D***	**% diff**	**3-D**	**% diff**
	W/m^{2}K	**W/m^{2}K**	**2D vs T5/W5**	**W/m^{2}K**	**2D* vs T5/W5**	**W/m^{2}K**	**3D vs 2-D**
Frame_sill	2.10	2.12	0.81%	2.12	0.89%	2.07	-2.12%
Frame_head	2.10	2.12	0.97%	2.09	-0.56%	2.08	-2.14%
Frame_jamb	2.12	2.12	-0.09%	2.07	-2.23%	2.10	-0.93%
Center of glass	0.58	0.58	0.96%	0.58	0.95%	0.60	3.33%
Edge_sill	1.53	1.48	-3.46%	1.49	-3.12%	1.59	6.63%
Edge_head	1.54	1.48	-3.55%	1.49	-3.23%	1.59	6.62%
Edge_jamb	1.54	1.48	-3.73%	1.40	-9.60%	1.53	3.15%
TOTAL	**1.14**	**1.14**	**-0.73%**	**1.11**	**-2.68%**	**1.16**	**1.77%**

Table A6. Wood Window – Medium Size, Highly Conducting Spacer

Dbl Clear	**Spacer keff =**		**1.900**	**W/mK**			
Section	**T5/W5**	**2-D**	**% diff**	**2-D***	**% diff**	**3-D**	**% diff**
	W/m^{2}K	**W/m^{2}K**	**2D vs T5/W5**	**W/m^{2}K**	**2D* vs T5/W5**	**W/m^{2}K**	**3D vs 2-D**
Frame_sill	2.53	2.49	-1.75%	2.49	-1.68%	2.41	-3.46%
Frame_head	2.53	2.49	-1.39%	2.46	-2.89%	2.41	-3.62%
Frame_jamb	2.55	2.49	-2.47%	2.45	-4.12%	2.45	-1.60%
Center of glass	2.77	2.77	0.09%	2.77	0.09%	2.77	0.19%
Edge_sill	3.18	3.17	-0.25%	3.17	-0.18%	3.22	1.43%
Edge_head	3.18	3.17	-0.21%	3.17	-0.14%	3.22	1.45%
Edge_jamb	3.18	3.17	-0.28%	3.17	-0.21%	3.19	0.66%
TOTAL	**2.83**	**2.82**	**-0.36%**	**2.81**	**-0.57%**	**2.82**	**-0.08%**
Dbl Low-e HC	**Spacer keff =**		**1.900**	**W/mK**			
Section	**T5/W5**	**2-D**	**% diff**	**2-D***	**% diff**	**3-D**	**% diff**
	W/m^{2}K	**W/m^{2}K**	**2D vs T5/W5**	**W/m^{2}K**	**2D* vs T5/W5**	**W/m^{2}K**	**3D vs 2-D**
Frame_sill	2.42	2.41	-0.42%	2.42	-0.34%	2.34	-3.08%
Frame_head	2.42	2.42	-0.23%	2.38	-1.69%	2.35	-3.12%
Frame_jamb	2.44	2.41	-1.21%	2.38	-2.82%	2.38	-1.41%
Center of glass	1.72	1.74	1.05%	1.74	1.04%	1.75	0.69%
Edge_sill	2.42	2.44	0.78%	2.45	0.95%	2.52	3.22%
Edge_head	2.42	2.44	0.76%	2.45	0.92%	2.52	3.18%
Edge_jamb	2.43	2.44	0.70%	2.45	0.87%	2.48	1.50%
TOTAL	**2.05**	**2.07**	**0.59%**	**2.06**	**0.33%**	**2.07**	**0.41%**
Dbl Low-e SC	**Spacer keff =**		**1.900**	**W/mK**			
Section	**T5/W5**	**2-D**	**% diff**	**2-D***	**% diff**	**3-D**	**% diff**
	W/m^{2}K	**W/m^{2}K**	**2D vs T5/W5**	**W/m^{2}K**	**2D* vs T5/W5**	**W/m^{2}K**	**3D vs 2-D**
Frame_sill	2.41	2.39	-0.43%	2.40	-0.33%	2.33	-2.98%
Frame_head	2.41	2.40	-0.23%	2.37	-1.69%	2.33	-3.02%
Frame_jamb	2.43	2.39	-1.26%	2.36	-2.87%	2.36	-1.33%
Center of glass	1.46	1.46	-0.24%	1.46	-0.25%	1.47	0.99%
Edge_sill	2.25	2.25	0.13%	2.25	0.34%	2.34	3.89%
Edge_head	2.25	2.25	0.10%	2.25	0.31%	2.34	3.89%
Edge_jamb	2.25	2.25	0.09%	2.25	0.30%	2.29	1.83%
TOTAL	**1.86**	**1.86**	**-0.15%**	**1.86**	**-0.43%**	**1.87**	**0.64%**
Hypothetical R10	**Spacer keff =**		**1.900**	**W/mK**			
Section	**T5/W5**	**2-D**	**% diff**	**2-D***	**% diff**	**3-D**	**% diff**
	W/m^{2}K	**W/m^{2}K**	**2D vs T5/W5**	**W/m^{2}K**	**2D* vs T5/W5**	**W/m^{2}K**	**3D vs 2-D**
Frame_sill	2.33	2.34	0.58%	2.34	0.69%	2.28	-2.70%
Frame_head	2.33	2.34	0.79%	2.31	-0.66%	2.28	-2.73%
Frame_jamb	2.34	2.34	-0.19%	2.30	-1.78%	2.31	-1.19%
Center of glass	0.58	0.58	1.27%	0.58	1.25%	0.61	3.97%
Edge_sill	1.75	1.67	-4.84%	1.67	-4.43%	1.79	6.82%
Edge_head	1.75	1.67	-4.86%	1.67	-4.47%	1.79	6.81%
Edge_jamb	1.75	1.67	-4.90%	1.67	-4.49%	1.72	3.27%
TOTAL	**1.25**	**1.23**	**-1.17%**	**1.23**	**-1.54%**	**1.25**	**1.83%**





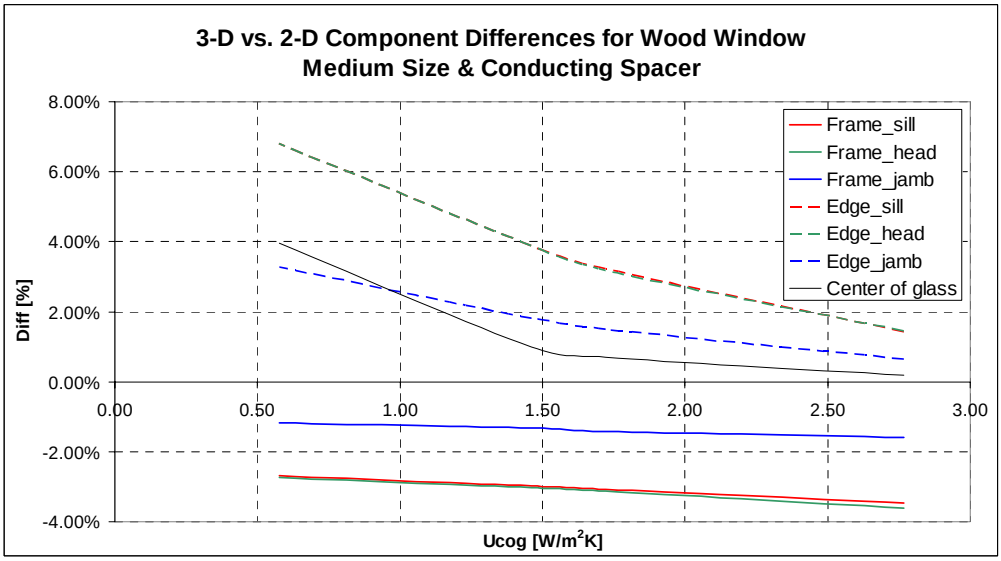


Figure A2. Component Level Difference Graphs for Medium Size Wood Window

Table A7. Wood Window - Small Size, Insulating Spacer

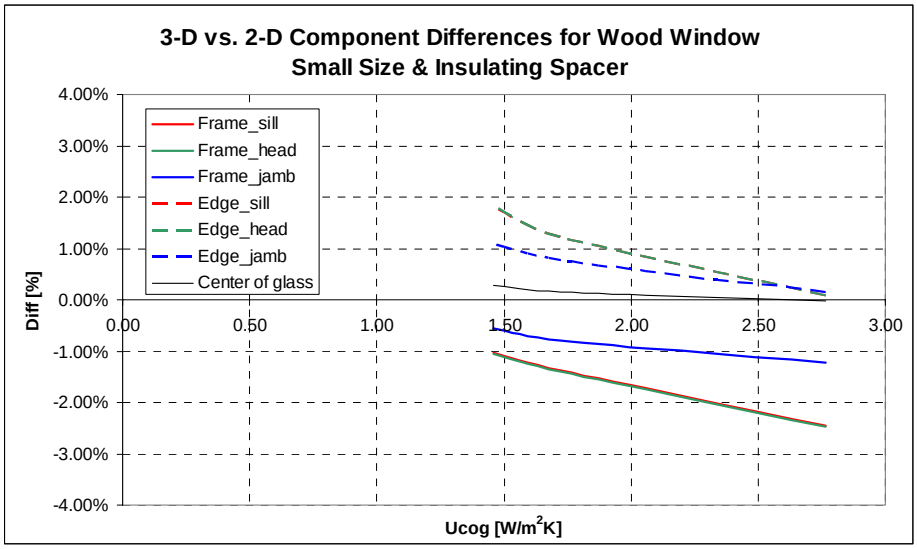
Dbl Clear	Spacer keff =		0.050	W/mK			
Section	**T5/W5**	**2-D**	**% diff**	**2-D***	**% diff**	**3-D**	**% diff**
	W/m^{2}K	**W/m^{2}K**	**2D vs T5/W5**	**W/m^{2}K**	**2D* vs T5/W5**	**W/m^{2}K**	**3D vs 2-D**
Frame_sill	1.87	1.83	-2.36%	1.83	-2.31%	1.78	-2.45%
Frame_head	1.87	1.83	-2.21%	1.80	-3.91%	1.78	-2.47%
Frame_jamb	1.89	1.82	-3.81%	1.80	-5.20%	1.80	-1.24%
Center of glass	2.77	2.77	0.00%	2.77	0.00%	2.77	-0.02%
Edge_sill	2.76	2.75	-0.34%	2.75	-0.34%	2.75	0.08%
Edge_head	2.76	2.75	-0.34%	2.75	-0.34%	2.75	0.09%
Edge_jamb	2.77	2.75	-0.61%	2.75	-0.63%	2.76	0.15%
TOTAL	**2.57**	**2.55**	**-0.64%**	**2.55**	**-0.82%**	**2.55**	**-0.28%**
Dbl Low-e HC	**Spacer keff =**		**0.050**	**W/mK**			
Section	**T5/W5**	**2-D**	**% diff**	**2-D***	**% diff**	**3-D**	**% diff**
	W/m^{2}K	**W/m^{2}K**	**2D vs T5/W5**	**W/m^{2}K**	**2D* vs T5/W5**	**W/m^{2}K**	**3D vs 2-D**
Frame_sill	1.68	1.64	-2.58%	1.64	-2.55%	1.61	-1.38%
Frame_head	1.68	1.64	-2.45%	1.61	-4.24%	1.62	-1.41%
Frame_jamb	1.72	1.64	-5.27%	1.61	-7.00%	1.62	-0.79%
Center of glass	1.72	1.74	0.83%	1.74	0.83%	1.74	0.16%
Edge_sill	1.88	1.88	-0.04%	1.88	-0.05%	1.91	1.22%
Edge_head	1.88	1.88	-0.03%	1.88	-0.05%	1.91	1.23%
Edge_jamb	1.89	1.88	-0.51%	1.88	-0.58%	1.90	0.78%
TOTAL	**1.76**	**1.76**	**-0.35%**	**1.75**	**-0.64%**	**1.76**	**0.11%**
Dbl Low-e SC	**Spacer keff =**		**0.050**	**W/mK**			
Section	**T5/W5**	**2-D**	**% diff**	**2-D***	**% diff**	**3-D**	**% diff**
	W/m^{2}K	**W/m^{2}K**	**2D vs T5/W5**	**W/m^{2}K**	**2D* vs T5/W5**	**W/m^{2}K**	**3D vs 2-D**
Frame_sill	1.63	1.59	-2.95%	1.59	-2.90%	1.57	-1.04%
Frame_head	1.63	1.59	-2.76%	1.56	-4.55%	1.57	-1.05%
Frame_jamb	1.66	1.59	-4.34%	1.57	-5.68%	1.58	-0.56%
Center of glass	1.46	1.45	-0.54%	1.45	-0.53%	1.46	0.29%
Edge_sill	1.67	1.65	-1.25%	1.65	-1.23%	1.68	1.80%
Edge_head	1.67	1.65	-1.25%	1.65	-1.22%	1.68	1.82%
Edge_jamb	1.68	1.65	-1.80%	1.64	-2.46%	1.67	1.10%
TOTAL	**1.56**	**1.54**	**-1.49%**	**1.53**	**-1.87%**	**1.54**	**0.34%**

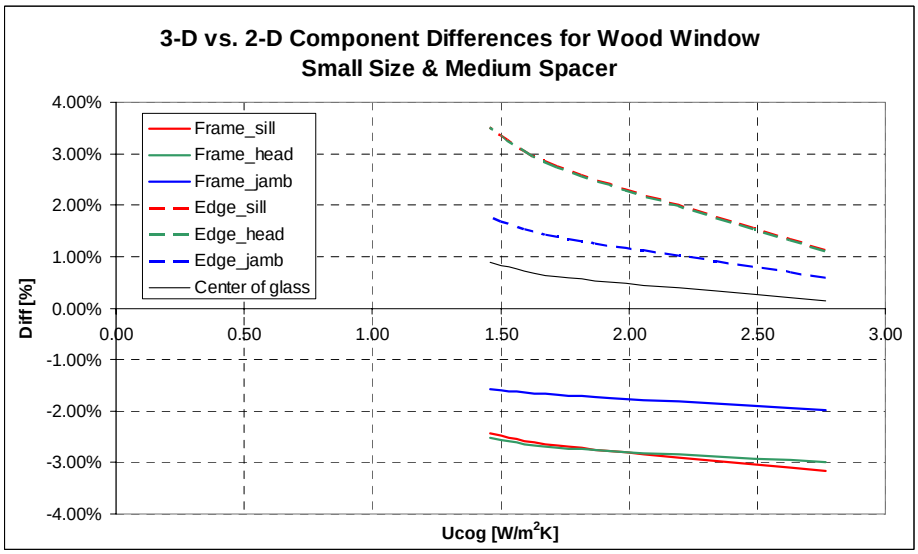
Table A8. Wood Window – Small Size, Medium Conducting Spacer

Dbl Clear	**Spacer keff =**		**0.674**	**W/mK**			
Section	**T5/W5**	**2-D**	**% diff**	**2-D***	**% diff**	**3-D**	**% diff**
	W/m^{2}K	**W/m^{2}K**	**2D vs T5/W5**	**W/m^{2}K**	**2D* vs T5/W5**	**W/m^{2}K**	**3D vs 2-D**
Frame_sill	2.33	2.31	-0.84%	2.31	-0.78%	2.24	-3.16%
Frame_head	2.33	2.31	-0.71%	2.28	-2.03%	2.24	-2.98%
Frame_jamb	2.33	2.31	-0.71%	2.28	-2.21%	2.27	-1.97%
Center of glass	2.77	2.77	0.09%	2.77	0.09%	2.77	0.15%
Edge_sill	3.05	3.05	0.27%	3.05	0.29%	3.09	1.12%
Edge_head	3.05	3.05	0.30%	3.05	0.31%	3.09	1.11%
Edge_jamb	3.05	3.05	0.20%	3.05	0.01%	3.07	0.59%
TOTAL	**2.75**	**2.75**	**-0.09%**	**2.74**	**-0.34%**	**2.74**	**-0.16%**
Dbl Low-e HC	**Spacer keff =**		**0.674**	**W/mK**			
Section	**T5/W5**	**2-D**	**% diff**	**2-D***	**% diff**	**3-D**	**% diff**
	W/m^{2}K	**W/m^{2}K**	**2D vs T5/W5**	**W/m^{2}K**	**2D* vs T5/W5**	**W/m^{2}K**	**3D vs 2-D**
Frame_sill	2.23	2.21	-0.70%	2.21	-0.64%	2.15	-2.68%
Frame_head	2.23	2.22	-0.40%	2.18	-1.94%	2.16	-2.71%
Frame_jamb	2.25	2.21	-1.55%	2.18	-3.10%	2.18	-1.68%
Center of glass	1.72	1.74	1.08%	1.74	1.09%	1.75	0.61%
Edge_sill	2.27	2.29	0.95%	2.29	1.03%	2.36	2.75%
Edge_head	2.27	2.29	1.00%	2.29	1.06%	2.36	2.73%
Edge_jamb	2.27	2.29	0.82%	2.28	0.46%	2.32	1.39%
TOTAL	**1.99**	**2.00**	**0.53%**	**2.00**	**0.17%**	**2.01**	**0.34%**
Dbl Low-e SC	**Spacer keff =**		**0.674**	**W/mK**			
Section	**T5/W5**	**2-D**	**% diff**	**2-D***	**% diff**	**3-D**	**% diff**
	W/m^{2}K	**W/m^{2}K**	**2D vs T5/W5**	**W/m^{2}K**	**2D* vs T5/W5**	**W/m^{2}K**	**3D vs 2-D**
Frame_sill	2.20	2.19	-0.75%	2.19	-0.69%	2.14	-2.43%
Frame_head	2.20	2.19	-0.36%	2.16	-1.91%	2.14	-2.53%
Frame_jamb	2.22	2.19	-1.66%	2.15	-3.22%	2.15	-1.57%
Center of glass	1.46	1.46	-0.19%	1.46	-0.18%	1.47	0.89%
Edge_sill	2.08	2.09	0.36%	2.09	0.43%	2.17	3.51%
Edge_head	2.08	2.09	0.34%	2.09	0.41%	2.17	3.51%
Edge_jamb	2.09	2.09	0.22%	2.08	-0.23%	2.13	1.78%
TOTAL	**1.80**	**1.80**	**-0.25%**	**1.79**	**-0.66%**	**1.81**	**0.58%**

Table A9. Wood Window – Small Size, Highly Conducting Spacer

Dbl Clear	**Spacer keff =**		**1.900**	**W/mK**			
Section	**T5/W5**	**2-D**	**% diff**	**2-D***	**% diff**	**3-D**	**% diff**
	W/m^{2}K	**W/m^{2}K**	**2D vs T5/W5**	**W/m^{2}K**	**2D* vs T5/W5**	**W/m^{2}K**	**3D vs 2-D**
Frame_sill	2.53	2.49	-1.75%	2.49	-1.68%	2.41	-3.46%
Frame_head	2.53	2.49	-1.39%	2.46	-2.88%	2.41	-3.62%
Frame_jamb	2.55	2.49	-2.47%	2.45	-4.06%	2.43	-2.25%
Center of glass	2.77	2.77	0.13%	2.77	0.13%	2.78	0.21%
Edge_sill	3.18	3.17	-0.25%	3.17	-0.20%	3.22	1.43%
Edge_head	3.18	3.17	-0.21%	3.17	-0.16%	3.22	1.45%
Edge_jamb	3.18	3.17	-0.28%	3.16	-0.60%	3.19	0.65%
TOTAL	**2.83**	**2.82**	**-0.40%**	**2.81**	**-0.70%**	**2.82**	**-0.17%**
Dbl Low-e HC	**Spacer keff =**		**1.900**	**W/mK**			
Section	**T5/W5**	**2-D**	**% diff**	**2-D***	**% diff**	**3-D**	**% diff**
	W/m^{2}K	**W/m^{2}K**	**2D vs T5/W5**	**W/m^{2}K**	**2D* vs T5/W5**	**W/m^{2}K**	**3D vs 2-D**
Frame_sill	2.42	2.41	-0.42%	2.42	-0.35%	2.34	-3.10%
Frame_head	2.42	2.42	-0.23%	2.38	-1.70%	2.35	-3.13%
Frame_jamb	2.44	2.41	-1.21%	2.38	-2.81%	2.37	-2.05%
Center of glass	1.72	1.74	1.17%	1.74	1.09%	1.76	0.77%
Edge_sill	2.42	2.44	0.78%	2.44	0.84%	2.52	3.10%
Edge_head	2.42	2.44	0.76%	2.44	0.86%	2.52	3.10%
Edge_jamb	2.43	2.44	0.70%	2.43	0.17%	2.48	1.45%
TOTAL	**2.08**	**2.09**	**0.55%**	**2.08**	**0.10%**	**2.09**	**-0.02%**
Dbl Low-e SC	**Spacer keff =**		**1.900**	**W/mK**			
Section	**T5/W5**	**2-D**	**% diff**	**2-D***	**% diff**	**3-D**	**% diff**
	W/m^{2}K	**W/m^{2}K**	**2D vs T5/W5**	**W/m^{2}K**	**2D* vs T5/W5**	**W/m^{2}K**	**3D vs 2-D**
Frame_sill	2.41	2.39	-0.43%	2.40	-0.34%	2.33	-3.00%
Frame_head	2.41	2.40	-0.23%	2.36	-1.70%	2.33	-3.03%
Frame_jamb	2.43	2.39	-1.26%	2.36	-2.87%	2.35	-1.99%
Center of glass	1.46	1.46	-0.06%	1.46	-0.05%	1.48	1.10%
Edge_sill	2.25	2.25	0.13%	2.25	0.23%	2.34	3.75%
Edge_head	2.25	2.25	0.10%	2.25	0.21%	2.33	3.75%
Edge_jamb	2.25	2.25	0.09%	2.23	-0.52%	2.29	1.77%
TOTAL	**1.90**	**1.89**	**-0.19%**	**1.88**	**-0.65%**	**1.90**	**0.58%**





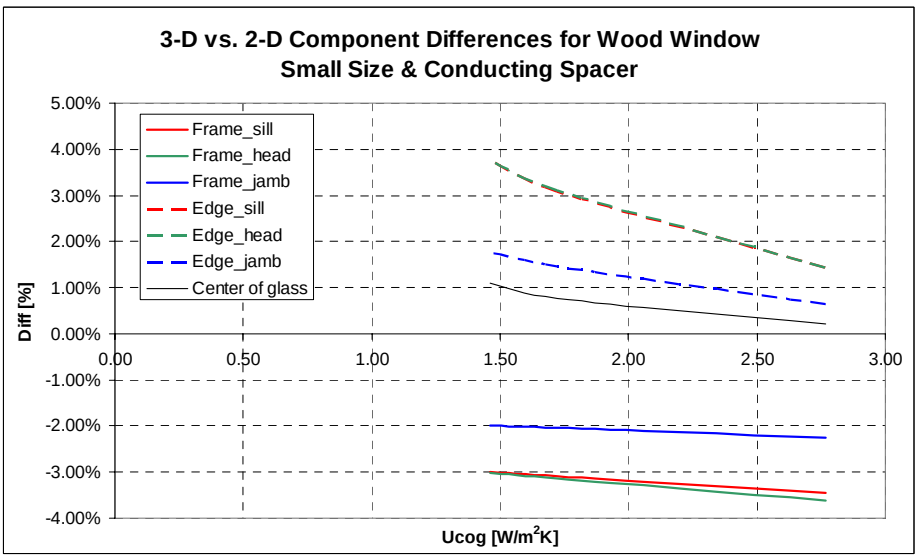


Figure A3. Component Level Difference Graphs for Small Size Wood Window

APPENDIX B: COMPONENT LEVEL RESULTS AND COMPARISONS FOR THERMALLY-BROKEN ALUMINUM (T/B AL) WINDOW:

Table B1. T/B AL Window – Large Size, Insulating Spacer

Dbl Clear	**Spacer keff =**		**0.050**	**W/mK**			
Section	**T5/W5**	**2-D**	**% diff**	**2-D***	**% diff**	**3-D**	**% diff**
	W/m^{2}K	**W/m^{2}K**	**2D vs T5/W5**	**W/m^{2}K**	**2D* vs T5/W5**	**W/m^{2}K**	**3D vs 2-D**
Frame_sill	5.02	4.84	-3.70%	5.08	1.21%	4.92	1.68%
Frame_head	4.99	4.84	-3.29%	5.08	1.68%	4.92	1.77%
Frame_jamb	5.38	5.10	-5.40%	5.10	-5.40%	5.15	0.95%
Center of glass	2.80	2.79	-0.07%	2.79	-0.11%	2.79	0.01%
Edge_sill	2.87	2.85	-0.63%	2.87	-0.04%	2.88	1.07%
Edge_head	2.87	2.85	-0.60%	2.87	0.02%	2.88	1.11%
Edge_jamb	2.90	2.88	-0.64%	2.88	-0.64%	2.83	-1.54%
TOTAL	**3.48**	**3.41**	**-2.07%**	**3.43**	**-1.53%**	**3.43**	**0.54%**
Dbl Low-e HC	**Spacer keff =**		**0.050**	**W/mK**			
Section	**T5/W5**	**2-D**	**% diff**	**2-D***	**% diff**	**3-D**	**% diff**
	W/m^{2}K	**W/m^{2}K**	**2D vs T5/W5**	**W/m^{2}K**	**2D* vs T5/W5**	**W/m^{2}K**	**3D vs 2-D**
Frame_sill	4.83	4.66	-3.68%	4.92	1.74%	4.78	2.40%
Frame_head	4.83	4.65	-3.75%	4.92	1.79%	4.77	2.51%
Frame_jamb	5.19	4.94	-5.06%	4.94	-5.06%	4.99	1.10%
Center of glass	1.73	1.75	0.80%	1.75	0.77%	1.75	0.30%
Edge_sill	2.00	1.99	-0.42%	2.01	0.61%	2.05	2.92%
Edge_head	2.00	1.99	-0.50%	2.01	0.58%	2.05	2.98%
Edge_jamb	2.03	2.02	-0.38%	2.02	-0.38%	2.04	0.60%
TOTAL	**2.70**	**2.65**	**-2.11%**	**2.67**	**-1.34%**	**2.67**	**1.03%**
Dbl Low-e SC	**Spacer keff =**		**0.050**	**W/mK**			
Section	**T5/W5**	**2-D**	**% diff**	**2-D***	**% diff**	**3-D**	**% diff**
	W/m^{2}K	**W/m^{2}K**	**2D vs T5/W5**	**W/m^{2}K**	**2D* vs T5/W5**	**W/m^{2}K**	**3D vs 2-D**
Frame_sill	4.79	4.62	-3.75%	4.88	1.91%	4.74	2.69%
Frame_head	4.79	4.61	-3.88%	4.88	1.85%	4.74	2.75%
Frame_jamb	5.16	4.90	-5.25%	4.90	-5.25%	4.96	1.15%
Center of glass	1.47	1.46	-0.59%	1.46	-0.61%	1.47	0.49%
Edge_sill	1.79	1.76	-1.52%	1.78	-0.26%	1.83	3.78%
Edge_head	1.79	1.76	-1.61%	1.78	-0.30%	1.83	3.84%
Edge_jamb	1.82	1.80	-1.46%	1.80	-1.46%	1.81	0.81%
TOTAL	**2.51**	**2.44**	**-2.99%**	**2.46**	**-2.13%**	**2.47**	**1.25%**
Hypothetical R10	**Spacer keff =**		**0.050**	**W/mK**			
Section	**T5/W5**	**2-D**	**% diff**	**2-D***	**% diff**	**3-D**	**% diff**
	W/m^{2}K	**W/m^{2}K**	**2D vs T5/W5**	**W/m^{2}K**	**2D* vs T5/W5**	**W/m^{2}K**	**3D vs 2-D**
Frame_sill	4.65	4.49	-3.56%	4.77	2.43%	4.64	3.20%
Frame_head	4.65	4.48	-3.75%	4.76	2.38%	4.64	3.32%
Frame_jamb	5.02	4.88	-2.81%	4.78	-4.99%	4.84	-0.82%
Center of glass	0.58	0.58	0.30%	0.58	0.34%	0.59	2.43%
Edge_sill	1.11	1.07	-3.16%	1.10	-0.80%	1.17	8.34%
Edge_head	1.11	1.07	-3.40%	1.10	-0.89%	1.17	8.49%
Edge_jamb	1.15	1.12	-3.02%	1.12	-3.14%	1.14	1.88%
TOTAL	**1.87**	**1.83**	**-2.44%**	**1.83**	**-2.33%**	**1.85**	**1.07%**

Table B2. T/B AlLWindow – Large Size, Medium Conducting Spacer

Dbl Clear	**Spacer keff =**		**0.674**	**W/mK**			
Section	**T5/W5**	**2-D**	**% diff**	**2-D***	**% diff**	**3-D**	**% diff**
	W/m^{2}K	**W/m^{2}K**	**2D vs T5/W5**	**W/m^{2}K**	**2D* vs T5/W5**	**W/m^{2}K**	**3D vs 2-D**
Frame_sill	5.35	5.22	-2.41%	5.45	1.90%	5.27	0.90%
Frame_head	5.35	5.22	-2.50%	5.45	1.82%	5.27	0.88%
Frame_jamb	5.69	5.45	-4.26%	5.45	-4.26%	5.50	0.87%
Center of glass	2.80	2.79	-0.04%	2.79	-0.07%	2.80	0.11%
Edge_sill	3.05	3.04	-0.51%	3.05	-0.08%	3.09	1.52%
Edge_head	3.05	3.04	-0.50%	3.05	-0.07%	3.09	1.52%
Edge_jamb	3.07	3.05	-0.54%	3.05	-0.54%	3.06	0.37%
TOTAL	**3.61**	**3.55**	**-1.62%**	**3.57**	**-1.13%**	**3.57**	**0.53%**
Dbl Low-e HC	**Spacer keff =**		**0.674**	**W/mK**			
Section	**T5/W5**	**2-D**	**% diff**	**2-D***	**% diff**	**3-D**	**% diff**
	W/m^{2}K	**W/m^{2}K**	**2D vs T5/W5**	**W/m^{2}K**	**2D* vs T5/W5**	**W/m^{2}K**	**3D vs 2-D**
Frame_sill	5.22	5.10	-2.30%	5.36	2.50%	5.18	1.49%
Frame_head	5.23	5.11	-2.29%	5.36	2.40%	5.18	1.38%
Frame_jamb	5.57	5.35	-4.01%	5.35	-4.01%	5.40	0.96%
Center of glass	1.73	1.75	0.88%	1.75	0.85%	1.76	0.56%
Edge_sill	2.25	2.24	-0.40%	2.25	0.34%	2.32	3.47%
Edge_head	2.25	2.24	-0.38%	2.25	0.34%	2.32	3.46%
Edge_jamb	2.26	2.25	-0.36%	2.25	-0.36%	2.28	0.89%
TOTAL	**2.86**	**2.82**	**-1.55%**	**2.84**	**-0.88%**	**2.85**	**1.01%**
Dbl Low-e SC	**Spacer keff =**		**0.674**	**W/mK**			
Section	**T5/W5**	**2-D**	**% diff**	**2-D***	**% diff**	**3-D**	**% diff**
	W/m^{2}K	**W/m^{2}K**	**2D vs T5/W5**	**W/m^{2}K**	**2D* vs T5/W5**	**W/m^{2}K**	**3D vs 2-D**
Frame_sill	5.20	5.07	-2.47%	5.33	2.47%	5.16	1.65%
Frame_head	5.20	5.08	-2.31%	5.33	2.44%	5.16	1.46%
Frame_jamb	5.54	5.33	-4.09%	5.33	-4.09%	5.38	0.98%
Center of glass	1.47	1.46	-0.47%	1.46	-0.42%	1.47	0.93%
Edge_sill	2.05	2.03	-1.31%	2.05	-0.33%	2.12	4.38%
Edge_head	2.05	2.03	-1.28%	2.04	-0.35%	2.12	4.33%
Edge_jamb	2.07	2.05	-1.14%	2.05	-1.14%	2.07	1.15%
TOTAL	**2.68**	**2.62**	**-2.29%**	**2.64**	**-1.52%**	**2.65**	**1.23%**
Hypothetical R10	**Spacer keff =**		**0.674**	**W/mK**			
Section	**T5/W5**	**2-D**	**% diff**	**2-D***	**% diff**	**3-D**	**% diff**
	W/m^{2}K	**W/m^{2}K**	**2D vs T5/W5**	**W/m^{2}K**	**2D* vs T5/W5**	**W/m^{2}K**	**3D vs 2-D**
Frame_sill	5.11	5.01	-1.90%	5.25	2.80%	5.09	1.53%
Frame_head	5.11	5.00	-2.14%	5.25	2.79%	5.09	1.76%
Frame_jamb	5.45	5.36	-1.72%	5.25	-3.84%	5.30	-1.00%
Center of glass	0.58	0.58	0.72%	0.58	0.77%	0.60	3.65%
Edge_sill	1.43	1.39	-2.87%	1.41	-1.61%	1.51	7.89%
Edge_head	1.43	1.39	-2.97%	1.41	-1.61%	1.51	7.97%
Edge_jamb	1.45	1.41	-2.92%	1.41	-2.97%	1.45	2.24%
TOTAL	**2.07**	**2.03**	**-1.57%**	**2.03**	**-1.67%**	**2.05**	**0.93%**

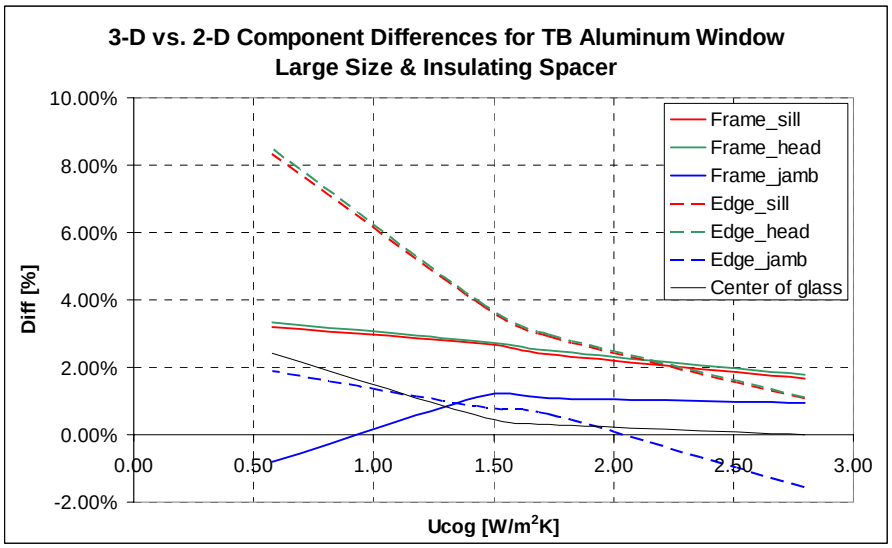
Table B3. T/B AL Window – Large Size, Highly Conducting Spacer

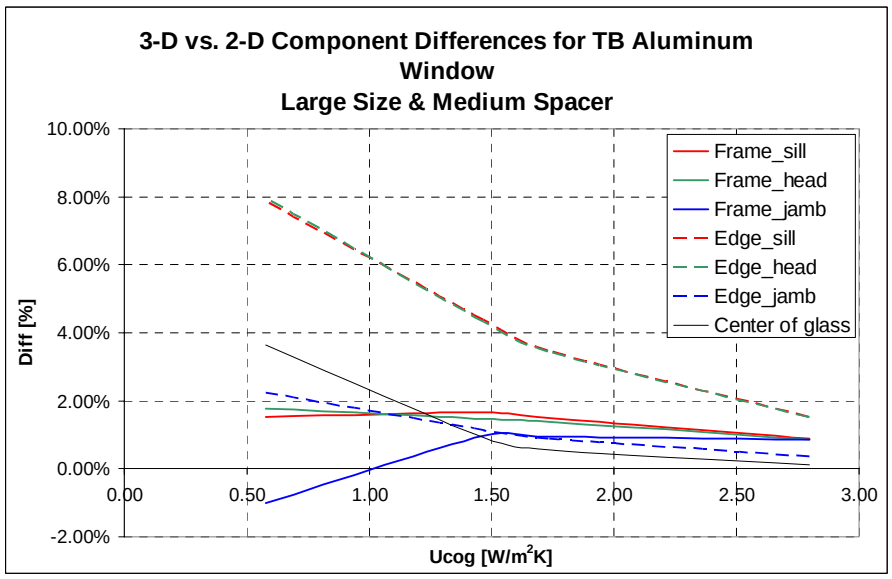
Dbl Clear	**Spacer keff =**		**1.900**	**W/mK**			
Section	**T5/W5**	**2-D**	**% diff**	**2-D***	**% diff**	**3-D**	**% diff**
	W/m^{2}K	**W/m^{2}K**	**2D vs T5/W5**	**W/m^{2}K**	**2D* vs T5/W5**	**W/m^{2}K**	**3D vs 2-D**
Frame_sill	5.52	5.39	-2.49%	5.62	1.73%	5.42	0.64%
Frame_head	5.51	5.40	-2.12%	5.62	1.90%	5.42	0.46%
Frame_jamb	5.85	5.62	-4.07%	5.62	-4.07%	5.67	0.77%
Center of glass	2.80	2.80	-0.02%	2.79	-0.06%	2.80	0.16%
Edge_sill	3.15	3.12	-0.72%	3.13	-0.33%	3.18	1.71%
Edge_head	3.14	3.12	-0.67%	3.03	-3.89%	3.18	1.70%
Edge_jamb	3.15	3.13	-0.69%	3.13	-0.69%	3.15	0.45%
TOTAL	**3.68**	**3.62**	**-1.61%**	**3.62**	**-1.47%**	**3.64**	**0.51%**

Dbl Low-e HC	**Spacer keff =**		**1.900**	**W/mK**			
Section	**T5/W5**	**2-D**	**% diff**	**2-D***	**% diff**	**3-D**	**% diff**
	W/m^{2}K	**W/m^{2}K**	**2D vs T5/W5**	**W/m^{2}K**	**2D* vs T5/W5**	**W/m^{2}K**	**3D vs 2-D**
Frame_sill	5.42	5.31	-2.02%	5.54	2.21%	5.35	0.78%
Frame_head	5.41	5.31	-1.91%	5.54	2.38%	5.35	0.84%
Frame_jamb	5.76	5.54	-3.91%	5.54	-3.91%	5.59	0.86%
Center of glass	1.73	1.75	0.92%	1.75	0.89%	1.76	0.69%
Edge_sill	2.37	2.35	-0.73%	2.36	-0.14%	2.44	3.62%
Edge_head	2.36	2.35	-0.71%	2.36	-0.09%	2.44	3.64%
Edge_jamb	2.38	2.36	-0.72%	2.36	-0.72%	2.38	1.02%
TOTAL	**2.94**	**2.89**	**-1.54%**	**2.91**	**-0.93%**	**2.92**	**0.96%**

Dbl Low-e SC	**Spacer keff =**		**1.900**	**W/mK**			
Section	**T5/W5**	**2-D**	**% diff**	**2-D***	**% diff**	**3-D**	**% diff**
	W/m^{2}K	**W/m^{2}K**	**2D vs T5/W5**	**W/m^{2}K**	**2D* vs T5/W5**	**W/m^{2}K**	**3D vs 2-D**
Frame_sill	5.40	5.29	-2.04%	5.52	2.20%	5.34	0.81%
Frame_head	5.39	5.29	-1.92%	5.52	2.42%	5.33	0.93%
Frame_jamb	5.74	5.52	-3.98%	5.52	-3.98%	5.57	0.88%
Center of glass	1.47	1.46	-0.42%	1.46	-0.44%	1.48	1.01%
Edge_sill	2.18	2.14	-1.61%	2.16	-0.95%	2.24	4.37%
Edge_head	2.18	2.14	-1.65%	2.16	-0.94%	2.24	4.40%
Edge_jamb	2.19	2.15	-1.62%	2.15	-1.62%	2.18	1.25%
TOTAL	**2.76**	**2.70**	**-2.26%**	**2.72**	**-1.59%**	**2.73**	**1.14%**

Hypothetical R10	**Spacer keff =**		**1.900**	**W/mK**			
Section	**T5/W5**	**2-D**	**% diff**	**2-D***	**% diff**	**3-D**	**% diff**
	W/m^{2}K	**W/m^{2}K**	**2D vs T5/W5**	**W/m^{2}K**	**2D* vs T5/W5**	**W/m^{2}K**	**3D vs 2-D**
Frame_sill	5.33	5.23	-1.87%	5.46	2.48%	5.28	1.01%
Frame_head	5.31	5.22	-1.83%	5.46	2.75%	5.28	1.25%
Frame_jamb	5.65	5.57	-1.59%	5.45	-3.66%	5.51	-1.07%
Center of glass	0.58	0.58	0.89%	0.58	0.95%	0.61	4.18%
Edge_sill	1.58	1.53	-3.71%	1.54	-2.62%	1.66	7.87%
Edge_head	1.58	1.53	-3.81%	1.54	-2.62%	1.66	7.95%
Edge_jamb	1.60	1.54	-3.71%	1.54	-3.66%	1.58	2.40%
TOTAL	**2.16**	**2.12**	**-1.62%**	**2.12**	**-1.75%**	**2.14**	**0.91%**





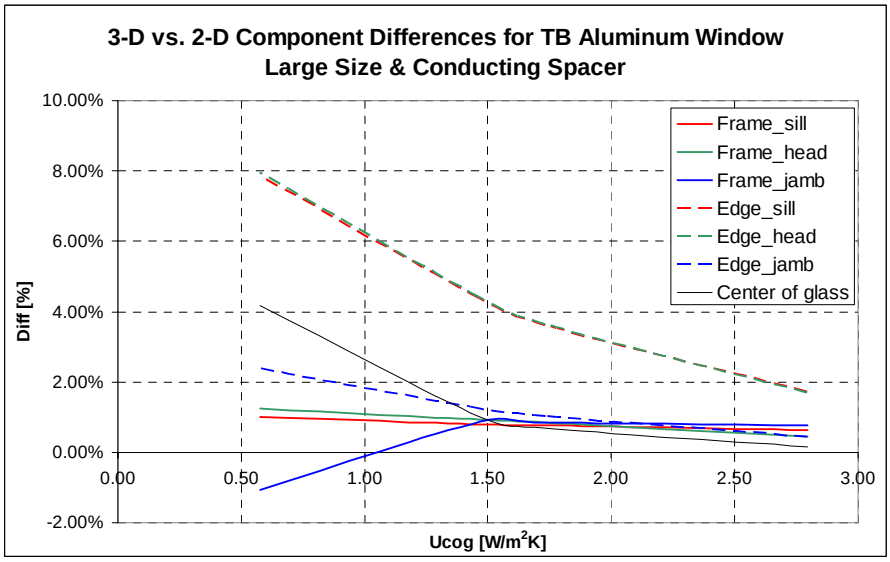


Figure B1. Component Level Difference Graphs for Large Size T/B AL Window

Table B4. T/B AL Window – Medium Size, Insulating Spacer

Dbl Clear	**Spacer keff =**		**0.050**	**W/mK**			
Section	**T5/W5**	**2-D**	**% diff**	**2-D***	**% diff**	**3-D**	**% diff**
	W/m^{2}K	**W/m^{2}K**	**2D vs T5/W5**	**W/m^{2}K**	**2D* vs T5/W5**	**W/m^{2}K**	**3D vs 2-D**
Frame_sill	5.02	4.84	-3.68%	5.11	1.84%	4.96	2.30%
Frame_head	4.99	4.83	-3.34%	5.11	2.35%	4.96	2.48%
Frame_jamb	5.38	5.21	-3.22%	5.14	-4.59%	5.04	-3.37%
Center of glass	2.80	2.79	-0.11%	2.79	-0.10%	2.79	0.06%
Edge_sill	2.87	2.85	-0.62%	2.88	0.32%	2.89	1.50%
Edge_head	2.87	2.85	-0.60%	2.88	0.38%	2.89	1.55%
Edge_jamb	2.90	2.88	-0.59%	2.89	-0.20%	2.90	0.57%
TOTAL	**3.52**	**3.46**	**-1.51%**	**3.48**	**-1.03%**	**3.45**	**-0.43%**
Dbl Low-e HC	**Spacer keff =**		**0.050**	**W/mK**			
Section	**T5/W5**	**2-D**	**% diff**	**2-D***	**% diff**	**3-D**	**% diff**
	W/m^{2}K	**W/m^{2}K**	**2D vs T5/W5**	**W/m^{2}K**	**2D* vs T5/W5**	**W/m^{2}K**	**3D vs 2-D**
Frame_sill	4.83	4.66	-3.68%	4.95	2.46%	4.81	3.08%
Frame_head	4.83	4.66	-3.67%	4.95	2.54%	4.81	3.14%
Frame_jamb	5.19	5.04	-2.83%	4.98	-4.08%	4.89	-3.16%
Center of glass	1.73	1.75	0.78%	1.75	0.80%	1.75	0.35%
Edge_sill	2.00	1.99	-0.42%	2.02	1.06%	2.06	3.45%
Edge_head	2.00	1.99	-0.49%	2.02	1.05%	2.06	3.53%
Edge_jamb	2.03	2.03	-0.29%	2.04	0.23%	2.05	1.25%
TOTAL	**2.75**	**2.71**	**-1.38%**	**2.73**	**-0.65%**	**2.71**	**-0.15%**
Dbl Low-e SC	**Spacer keff =**		**0.050**	**W/mK**			
Section	**T5/W5**	**2-D**	**% diff**	**2-D***	**% diff**	**3-D**	**% diff**
	W/m^{2}K	**W/m^{2}K**	**2D vs T5/W5**	**W/m^{2}K**	**2D* vs T5/W5**	**W/m^{2}K**	**3D vs 2-D**
Frame_sill	4.79	4.62	-3.76%	4.91	2.51%	4.77	3.26%
Frame_head	4.79	4.61	-3.86%	4.91	2.49%	4.77	3.32%
Frame_jamb	5.16	5.00	-3.10%	4.94	-4.32%	4.85	-3.10%
Center of glass	1.47	1.46	-0.59%	1.46	-0.56%	1.47	0.54%
Edge_sill	1.79	1.76	-1.53%	1.79	0.19%	1.84	4.31%
Edge_head	1.79	1.76	-1.62%	1.79	0.18%	1.84	4.41%
Edge_jamb	1.82	1.80	-1.40%	1.81	-0.80%	1.83	1.56%
TOTAL	**2.57**	**2.51**	**-2.21%**	**2.53**	**-1.39%**	**2.51**	**-0.02%**
Hypothetical R10	**Spacer keff =**		**0.050**	**W/mK**			
Section	**T5/W5**	**2-D**	**% diff**	**2-D***	**% diff**	**3-D**	**% diff**
	W/m^{2}K	**W/m^{2}K**	**2D vs T5/W5**	**W/m^{2}K**	**2D* vs T5/W5**	**W/m^{2}K**	**3D vs 2-D**
Frame_sill	4.65	4.49	-3.63%	4.80	3.07%	4.67	3.85%
Frame_head	4.65	4.48	-3.71%	4.80	3.07%	4.67	3.91%
Frame_jamb	5.02	4.88	-2.84%	4.83	-3.96%	4.74	-2.90%
Center of glass	0.58	0.58	0.47%	0.58	0.57%	0.59	2.46%
Edge_sill	1.11	1.07	-3.19%	1.10	-0.22%	1.18	9.02%
Edge_head	1.11	1.07	-3.39%	1.10	-0.23%	1.18	9.24%
Edge_jamb	1.15	1.12	-3.04%	1.13	-2.13%	1.16	3.26%
TOTAL	**1.94**	**1.90**	**-2.50%**	**1.92**	**-1.28%**	**1.91**	**0.60%**

Table B5. T/B AL Window – Medium Size, Medium Conducting Spacer

Dbl Clear	Spacer keff =		0.674 W/mK				
Section	**T5/W5**	**2-D**	**% diff**	**2-D***	**% diff**	**3-D**	**% diff**
	W/m²K	**W/m²K**	**2D vs T5/W5**	**W/m²K**	**2D* vs T5/W5**	**W/m²K**	**3D vs 2-D**
Frame_sill	5.35	5.23	-2.19%	5.49	2.54%	5.31	1.37%
Frame_head	5.35	5.22	-2.46%	5.49	2.48%	5.31	1.56%
Frame_jamb	5.69	5.57	-2.05%	5.50	-3.48%	5.39	-3.48%
Center of glass	2.80	2.79	-0.07%	2.79	-0.06%	2.80	0.16%
Edge_sill	3.05	3.04	-0.48%	3.07	0.45%	3.10	2.10%
Edge_head	3.05	3.04	-0.50%	3.07	0.44%	3.10	2.12%
Edge_jamb	3.07	3.05	-0.47%	3.07	0.06%	3.08	1.01%
TOTAL	**3.65**	**3.62**	**-1.00%**	**3.63**	**-0.61%**	**3.60**	**-0.48%**

Dbl Low-e HC	Spacer keff =		0.674 W/mK				
Section	**T5/W5**	**2-D**	**% diff**	**2-D***	**% diff**	**3-D**	**% diff**
	W/m²K	**W/m²K**	**2D vs T5/W5**	**W/m²K**	**2D* vs T5/W5**	**W/m²K**	**3D vs 2-D**
Frame_sill	5.22	5.12	-1.94%	5.39	3.09%	5.21	1.79%
Frame_head	5.23	5.11	-2.27%	5.39	2.99%	5.21	1.99%
Frame_jamb	5.57	5.46	-1.90%	5.39	-3.21%	5.29	-3.30%
Center of glass	1.73	1.75	0.89%	1.75	0.92%	1.76	0.63%
Edge_sill	2.25	2.24	-0.32%	2.27	1.13%	2.34	4.29%
Edge_head	2.25	2.24	-0.37%	2.27	1.12%	2.34	4.34%
Edge_jamb	2.26	2.26	-0.31%	2.28	0.61%	2.30	2.05%
TOTAL	**2.92**	**2.90**	**-0.80%**	**2.92**	**-0.19%**	**2.89**	**-0.15%**

Dbl Low-e SC	Spacer keff =		0.674 W/mK				
Section	**T5/W5**	**2-D**	**% diff**	**2-D***	**% diff**	**3-D**	**% diff**
	W/m²K	**W/m²K**	**2D vs T5/W5**	**W/m²K**	**2D* vs T5/W5**	**W/m²K**	**3D vs 2-D**
Frame_sill	5.20	5.09	-2.04%	5.36	3.09%	5.19	1.91%
Frame_head	5.20	5.08	-2.27%	5.36	3.08%	5.19	2.11%
Frame_jamb	5.54	5.44	-1.98%	5.37	-3.26%	5.26	-3.24%
Center of glass	1.47	1.46	-0.44%	1.46	-0.40%	1.48	0.91%
Edge_sill	2.05	2.03	-1.22%	2.06	0.46%	2.14	5.17%
Edge_head	2.05	2.03	-1.27%	2.06	0.45%	2.14	5.24%
Edge_jamb	2.07	2.04	-1.20%	2.07	-0.13%	2.10	2.48%
TOTAL	**2.74**	**2.70**	**-1.44%**	**2.72**	**-0.74%**	**2.70**	**-0.01%**

Hypothetical R10	Spacer keff =		0.674 W/mK				
Section	**T5/W5**	**2-D**	**% diff**	**2-D***	**% diff**	**3-D**	**% diff**
	W/m²K	**W/m²K**	**2D vs T5/W5**	**W/m²K**	**2D* vs T5/W5**	**W/m²K**	**3D vs 2-D**
Frame_sill	5.11	5.01	-1.93%	5.29	3.45%	5.13	2.25%
Frame_head	5.11	5.00	-2.14%	5.29	3.46%	5.13	2.45%
Frame_jamb	5.45	5.36	-1.75%	5.29	-2.91%	5.20	-3.07%
Center of glass	0.58	0.58	1.01%	0.58	1.15%	0.60	3.73%
Edge_sill	1.43	1.39	-2.89%	1.43	-0.16%	1.54	9.35%
Edge_head	1.43	1.39	-2.98%	1.43	-0.17%	1.54	9.47%
Edge_jamb	1.45	1.41	-2.94%	1.44	-1.12%	1.48	4.52%
TOTAL	**2.15**	**2.11**	**-1.61%**	**2.13**	**-0.56%**	**2.13**	**0.62%**

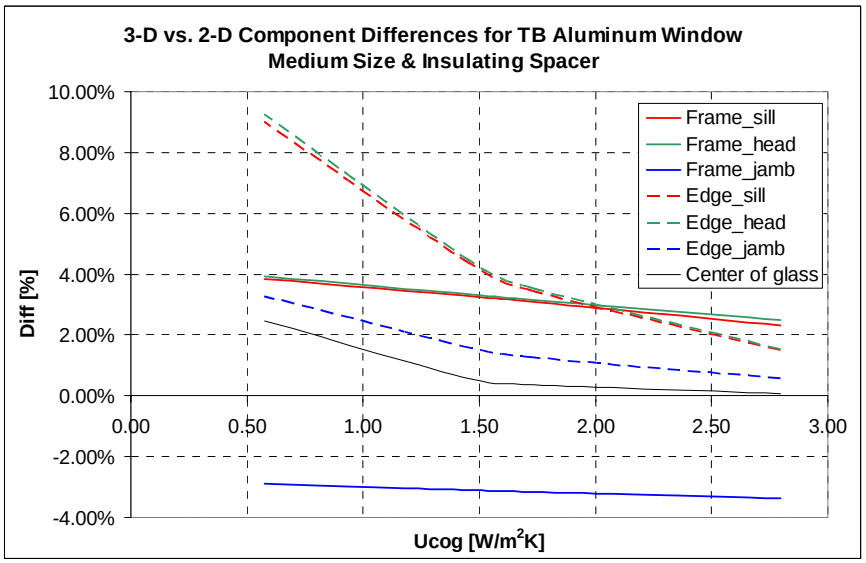
Table B6. T/B AL Window – Medium Size, Highly Conducting Spacer

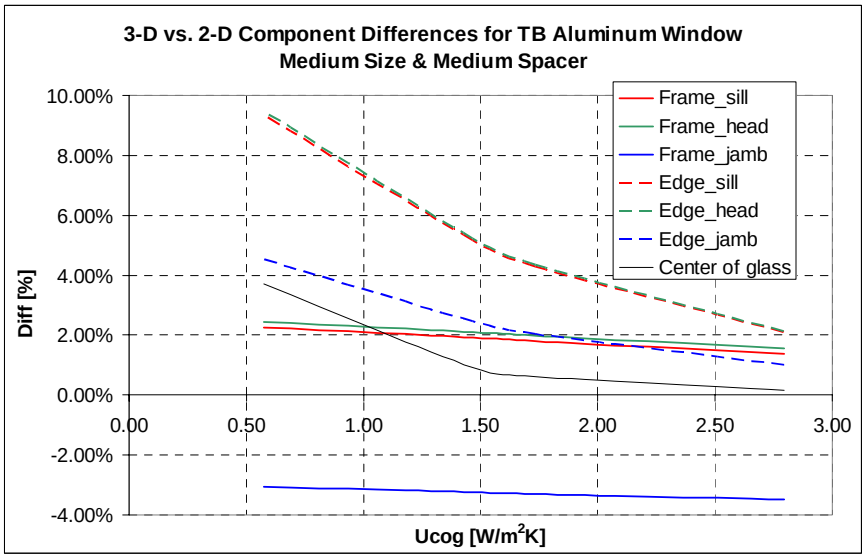
Dbl Clear	**Spacer keff =**		**1.900**	**W/mK**			
Section	**T5/W5**	**2-D**	**% diff**	**2-D***	**% diff**	**3-D**	**% diff**
	W/m^{2}K	**W/m^{2}K**	**2D vs T5/W5**	**W/m^{2}K**	**2D* vs T5/W5**	**W/m^{2}K**	**3D vs 2-D**
Frame_sill	5.52	5.41	-2.13%	5.66	2.45%	5.47	1.12%
Frame_head	5.51	5.40	-2.09%	5.66	2.69%	5.47	1.32%
Frame_jamb	5.85	5.74	-1.91%	5.67	-3.24%	5.55	-3.42%
Center of glass	2.80	2.79	-0.05%	2.79	-0.04%	2.80	0.21%
Edge_sill	3.15	3.12	-0.67%	3.15	0.24%	3.20	2.35%
Edge_head	3.14	3.12	-0.66%	3.15	0.27%	3.20	2.36%
Edge_jamb	3.15	3.13	-0.64%	3.15	-0.01%	3.17	1.21%
TOTAL	**3.72**	**3.68**	**-0.98%**	**3.70**	**-0.56%**	**3.67**	**-0.44%**

Dbl Low-e HC	**Spacer keff =**		**1.900**	**W/mK**			
Section	**T5/W5**	**2-D**	**% diff**	**2-D***	**% diff**	**3-D**	**% diff**
	W/m^{2}K	**W/m^{2}K**	**2D vs T5/W5**	**W/m^{2}K**	**2D* vs T5/W5**	**W/m^{2}K**	**3D vs 2-D**
Frame_sill	5.42	5.32	-1.90%	5.58	2.94%	5.40	1.47%
Frame_head	5.41	5.31	-1.92%	5.58	3.14%	5.40	1.68%
Frame_jamb	5.76	5.65	-1.81%	5.59	-3.02%	5.47	-3.24%
Center of glass	1.73	1.75	0.94%	1.75	0.97%	1.76	0.75%
Edge_sill	2.37	2.35	-0.71%	2.38	0.75%	2.46	4.60%
Edge_head	2.36	2.35	-0.72%	2.38	0.79%	2.46	4.65%
Edge_jamb	2.38	2.36	-0.70%	2.38	0.34%	2.42	2.31%
TOTAL	**3.00**	**2.98**	**-0.81%**	**3.00**	**-0.16%**	**2.98**	**-0.09%**

Dbl Low-e SC	**Spacer keff =**		**1.900**	**W/mK**			
Section	**T5/W5**	**2-D**	**% diff**	**2-D***	**% diff**	**3-D**	**% diff**
	W/m^{2}K	**W/m^{2}K**	**2D vs T5/W5**	**W/m^{2}K**	**2D* vs T5/W5**	**W/m^{2}K**	**3D vs 2-D**
Frame_sill	5.40	5.30	-1.98%	5.56	2.94%	5.38	1.57%
Frame_head	5.39	5.28	-1.94%	5.56	3.19%	5.38	1.79%
Frame_jamb	5.74	5.63	-1.89%	5.57	-3.05%	5.46	-3.18%
Center of glass	1.47	1.46	-0.32%	1.46	-0.33%	1.48	1.02%
Edge_sill	2.18	2.14	-1.62%	2.18	0.07%	2.27	5.49%
Edge_head	2.18	2.14	-1.68%	2.18	0.07%	2.27	5.55%
Edge_jamb	2.19	2.15	-1.63%	2.18	-0.40%	2.22	2.77%
TOTAL	**2.83**	**2.79**	**-1.41%**	**2.81**	**-0.68%**	**2.79**	**0.05%**

Hypothetical R10	**Spacer keff =**		**1.900**	**W/mK**			
Section	**T5/W5**	**2-D**	**% diff**	**2-D***	**% diff**	**3-D**	**% diff**
	W/m^{2}K	**W/m^{2}K**	**2D vs T5/W5**	**W/m^{2}K**	**2D* vs T5/W5**	**W/m^{2}K**	**3D vs 2-D**
Frame_sill	5.33	5.23	-1.90%	5.51	3.25%	5.33	1.87%
Frame_head	5.31	5.22	-1.82%	5.51	3.55%	5.33	2.09%
Frame_jamb	5.65	5.56	-1.61%	5.51	-2.64%	5.40	-3.01%
Center of glass	0.58	0.58	1.24%	0.58	1.40%	0.61	4.27%
Edge_sill	1.58	1.53	-3.72%	1.57	-0.95%	1.69	9.51%
Edge_head	1.58	1.53	-3.81%	1.57	-0.96%	1.69	9.63%
Edge_jamb	1.60	1.54	-3.72%	1.57	-1.63%	1.62	4.86%
TOTAL	**2.24**	**2.21**	**-1.61%**	**2.23**	**-0.50%**	**2.22**	**0.74%**





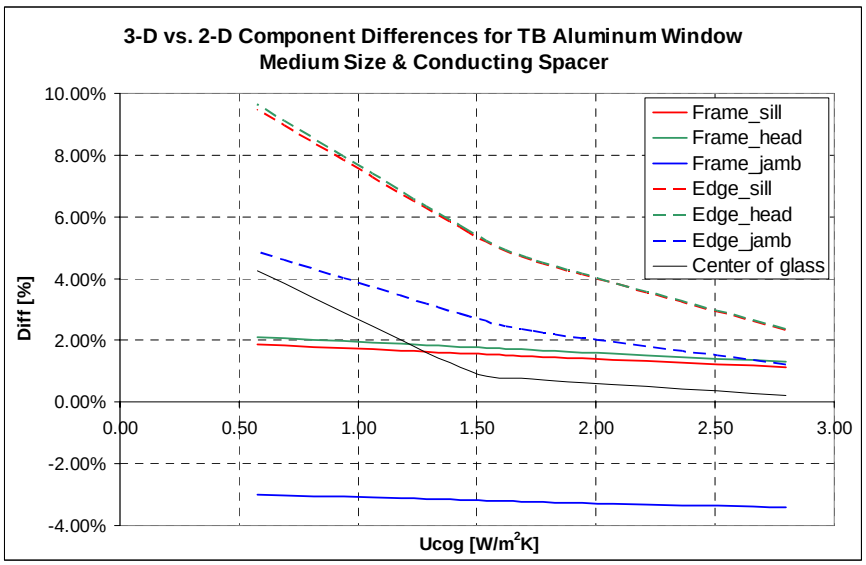


Figure B2. Component Level Difference Graphs for Medium Size T/B AL Window

Table B7. T/B AL Window – Small Size, Insulating Spacer

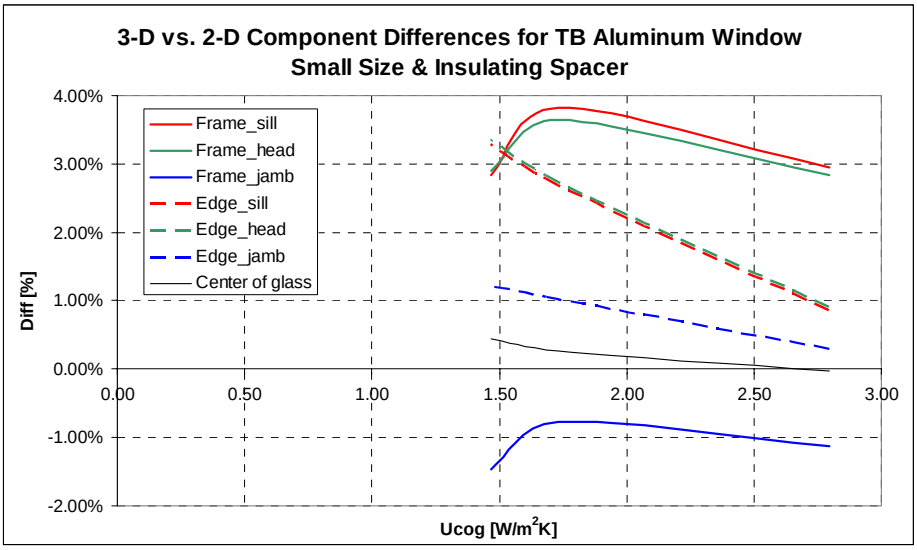
Dbl Clear	**Spacer keff =**		**0.050**	**W/mK**			
Section	**T5/W5**	**2-D**	**% diff**	**2-D***	**% diff**	**3-D**	**% diff**
	W/m^{2}K	**W/m^{2}K**	**2D vs T5/W5**	**W/m^{2}K**	**2D* vs T5/W5**	**W/m^{2}K**	**3D vs 2-D**
Frame_sill	5.02	4.83	-3.88%	5.14	2.33%	4.98	2.94%
Frame_head	4.99	4.83	-3.40%	5.13	2.64%	4.97	2.83%
Frame_jamb	5.38	5.21	-3.26%	5.16	-4.28%	5.15	-1.12%
Center of glass	2.80	2.80	-0.02%	2.79	-0.10%	2.79	-0.02%
Edge_sill	2.87	2.85	-0.65%	2.87	-0.10%	2.88	0.87%
Edge_head	2.87	2.85	-0.62%	2.87	-0.01%	2.88	0.91%
Edge_jamb	2.90	2.88	-0.58%	2.88	-0.60%	2.89	0.30%
TOTAL	**3.57**	**3.52**	**-1.58%**	**3.54**	**-0.80%**	**3.52**	**0.24%**
Dbl Low-e HC	**Spacer keff =**		**0.050**	**W/mK**			
Section	**T5/W5**	**2-D**	**% diff**	**2-D***	**% diff**	**3-D**	**% diff**
	W/m^{2}K	**W/m^{2}K**	**2D vs T5/W5**	**W/m^{2}K**	**2D* vs T5/W5**	**W/m^{2}K**	**3D vs 2-D**
Frame_sill	4.83	4.65	-3.92%	4.98	3.01%	4.83	3.83%
Frame_head	4.83	4.65	-3.82%	4.97	2.87%	4.83	3.65%
Frame_jamb	5.19	5.04	-2.91%	5.00	-3.74%	5.00	-0.77%
Center of glass	1.73	1.75	0.90%	1.75	0.85%	1.75	0.27%
Edge_sill	2.00	1.99	-0.49%	2.00	0.45%	2.04	2.69%
Edge_head	2.00	1.99	-0.53%	2.01	0.47%	2.04	2.74%
Edge_jamb	2.03	2.02	-0.30%	2.02	-0.39%	2.05	1.03%
TOTAL	**2.83**	**2.79**	**-1.53%**	**2.82**	**-0.36%**	**2.81**	**0.85%**
Dbl Low-e SC	**Spacer keff =**		**0.050**	**W/mK**			
Section	**T5/W5**	**2-D**	**% diff**	**2-D***	**% diff**	**3-D**	**% diff**
	W/m^{2}K	**W/m^{2}K**	**2D vs T5/W5**	**W/m^{2}K**	**2D* vs T5/W5**	**W/m^{2}K**	**3D vs 2-D**
Frame_sill	4.79	4.62	-3.76%	4.89	2.06%	4.75	2.83%
Frame_head	4.79	4.61	-3.88%	4.89	2.00%	4.75	2.90%
Frame_jamb	5.16	5.00	-3.18%	4.92	-4.72%	4.93	-1.46%
Center of glass	1.47	1.46	-0.44%	1.46	-0.49%	1.47	0.45%
Edge_sill	1.79	1.76	-1.53%	1.77	-0.58%	1.82	3.28%
Edge_head	1.79	1.76	-1.62%	1.77	-0.58%	1.82	3.37%
Edge_jamb	1.82	1.80	-1.41%	1.79	-1.63%	1.82	1.22%
TOTAL	**2.65**	**2.59**	**-2.27%**	**2.61**	**-1.50%**	**2.61**	**0.53%**

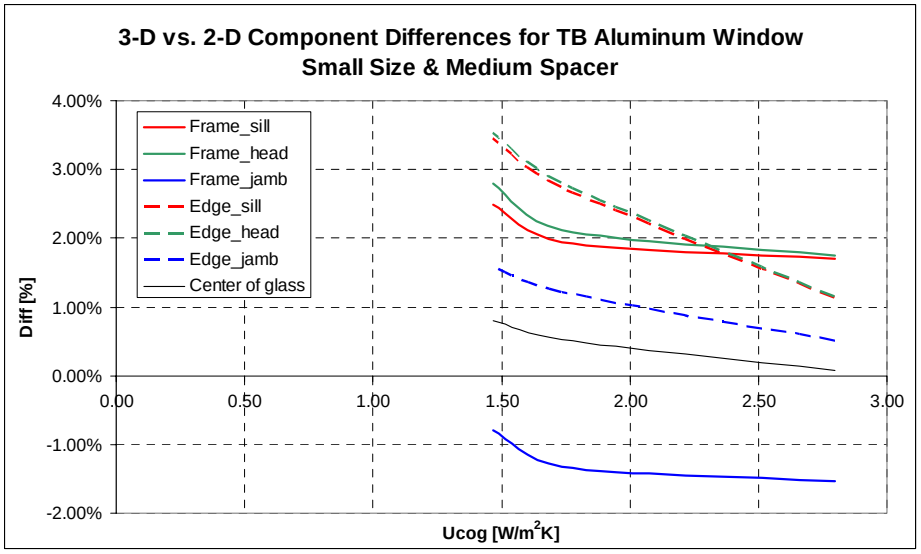
Table B8. T/B AL Window – Small Size, Medium Conducting Spacer

Dbl Clear	Spacer keff =		0.674	W/mK			
Section	**T5/W5**	**2-D**	**% diff**	**2-D***	**% diff**	**3-D**	**% diff**
	W/m^{2}K	**W/m^{2}K**	**2D vs T5/W5**	**W/m^{2}K**	**2D* vs T5/W5**	**W/m^{2}K**	**3D vs 2-D**
Frame_sill	5.35	5.22	-2.48%	5.50	2.67%	5.31	1.70%
Frame_head	5.35	5.22	-2.47%	5.50	2.72%	5.32	1.75%
Frame_jamb	5.69	5.57	-2.03%	5.50	-3.31%	5.49	-1.53%
Center of glass	2.80	2.80	0.04%	2.79	-0.04%	2.80	0.07%
Edge_sill	3.05	3.04	-0.51%	3.05	-0.27%	3.07	1.13%
Edge_head	3.05	3.04	-0.50%	3.05	-0.23%	3.07	1.16%
Edge_jamb	3.07	3.05	-0.46%	3.05	-0.66%	3.07	0.51%
TOTAL	**3.72**	**3.68**	**-1.02%**	**3.70**	**-0.50%**	**3.68**	**0.01%**
Dbl Low-e HC	**Spacer keff =**		**0.674**	**W/mK**			
Section	**T5/W5**	**2-D**	**% diff**	**2-D***	**% diff**	**3-D**	**% diff**
	W/m^{2}K	**W/m^{2}K**	**2D vs T5/W5**	**W/m^{2}K**	**2D* vs T5/W5**	**W/m^{2}K**	**3D vs 2-D**
Frame_sill	5.22	5.11	-2.08%	5.39	3.17%	5.22	1.94%
Frame_head	5.23	5.11	-2.25%	5.40	3.19%	5.22	2.12%
Frame_jamb	5.57	5.46	-1.91%	5.40	-3.06%	5.39	-1.32%
Center of glass	1.73	1.75	1.07%	1.75	1.00%	1.76	0.52%
Edge_sill	2.25	2.24	-0.35%	2.24	-0.15%	2.30	2.74%
Edge_head	2.25	2.24	-0.36%	2.25	-0.08%	2.30	2.81%
Edge_jamb	2.26	2.26	-0.30%	2.25	-0.73%	2.28	1.22%
TOTAL	**3.01**	**2.99**	**-0.83%**	**3.01**	**-0.14%**	**3.00**	**0.42%**
Dbl Low-e SC	**Spacer keff =**		**0.674**	**W/mK**			
Section	**T5/W5**	**2-D**	**% diff**	**2-D***	**% diff**	**3-D**	**% diff**
	W/m^{2}K	**W/m^{2}K**	**2D vs T5/W5**	**W/m^{2}K**	**2D* vs T5/W5**	**W/m^{2}K**	**3D vs 2-D**
Frame_sill	5.20	5.09	-2.15%	5.39	3.63%	5.22	2.49%
Frame_head	5.20	5.08	-2.26%	5.41	3.83%	5.23	2.80%
Frame_jamb	5.54	5.44	-1.99%	5.40	-2.66%	5.39	-0.80%
Center of glass	1.47	1.46	-0.22%	1.46	-0.28%	1.48	0.79%
Edge_sill	2.05	2.03	-1.23%	2.03	-1.01%	2.10	3.45%
Edge_head	2.05	2.03	-1.26%	2.03	-0.94%	2.10	3.54%
Edge_jamb	2.07	2.04	-1.19%	2.04	-1.67%	2.08	1.59%
TOTAL	**2.84**	**2.80**	**-1.42%**	**2.83**	**-0.37%**	**2.83**	**0.88%**

Table B9. T/B AL Window – Small Size, Highly Conducting Spacer

Dbl Clear	Spacer keff =		1.900 W/mK				
Section	**T5/W5**	**2-D**	**% diff**	**2-D***	**% diff**	**3-D**	**% diff**
	W/m^{2}K	**W/m^{2}K**	**2D vs T5/W5**	**W/m^{2}K**	**2D* vs T5/W5**	**W/m^{2}K**	**3D vs 2-D**
Frame_sill	5.52	5.39	-2.40%	5.65	2.21%	5.45	1.05%
Frame_head	5.51	5.40	-2.10%	5.65	2.49%	5.45	1.04%
Frame_jamb	5.85	5.74	-1.92%	5.66	-3.44%	5.63	-1.88%
Center of glass	2.80	2.80	0.06%	2.80	-0.01%	2.80	0.12%
Edge_sill	3.15	3.12	-0.71%	3.13	-0.56%	3.16	1.28%
Edge_head	3.14	3.12	-0.67%	3.13	-0.49%	3.16	1.30%
Edge_jamb	3.15	3.13	-0.63%	3.13	-0.86%	3.15	0.62%
TOTAL	**3.79**	**3.76**	**-1.01%**	**3.77**	**-0.67%**	**3.75**	**-0.17%**
Dbl Low-e HC	**Spacer keff =**		**1.900 W/mK**				
Section	**T5/W5**	**2-D**	**% diff**	**2-D***	**% diff**	**3-D**	**% diff**
	W/m^{2}K	**W/m^{2}K**	**2D vs T5/W5**	**W/m^{2}K**	**2D* vs T5/W5**	**W/m^{2}K**	**3D vs 2-D**
Frame_sill	5.42	5.31	-2.06%	5.58	2.92%	5.39	1.52%
Frame_head	5.41	5.31	-1.91%	5.59	3.22%	5.40	1.68%
Frame_jamb	5.76	5.65	-1.82%	5.59	-2.99%	5.57	-1.44%
Center of glass	1.73	1.75	1.13%	1.75	1.07%	1.76	0.64%
Edge_sill	2.37	2.35	-0.74%	2.35	-0.58%	2.42	2.94%
Edge_head	2.36	2.35	-0.71%	2.35	-0.60%	2.42	3.00%
Edge_jamb	2.38	2.36	-0.69%	2.35	-1.12%	2.39	1.42%
TOTAL	**3.10**	**3.08**	**-0.84%**	**3.10**	**-0.22%**	**3.09**	**0.37%**
Dbl Low-e SC	**Spacer keff =**		**1.900 W/mK**				
Section	**T5/W5**	**2-D**	**% diff**	**2-D***	**% diff**	**3-D**	**% diff**
	W/m^{2}K	**W/m^{2}K**	**2D vs T5/W5**	**W/m^{2}K**	**2D* vs T5/W5**	**W/m^{2}K**	**3D vs 2-D**
Frame_sill	5.40	5.29	-2.11%	5.57	2.95%	5.38	1.62%
Frame_head	5.39	5.28	-1.95%	5.57	3.32%	5.38	1.84%
Frame_jamb	5.74	5.63	-1.90%	5.57	-2.98%	5.56	-1.34%
Center of glass	1.47	1.47	-0.12%	1.47	-0.18%	1.48	0.95%
Edge_sill	2.18	2.14	-1.64%	2.14	-1.58%	2.22	3.60%
Edge_head	2.18	2.14	-1.67%	2.14	-1.50%	2.22	3.69%
Edge_jamb	2.19	2.15	-1.62%	2.14	-2.12%	2.19	1.76%
TOTAL	**2.93**	**2.89**	**-1.41%**	**2.91**	**-0.69%**	**2.91**	**0.55%**





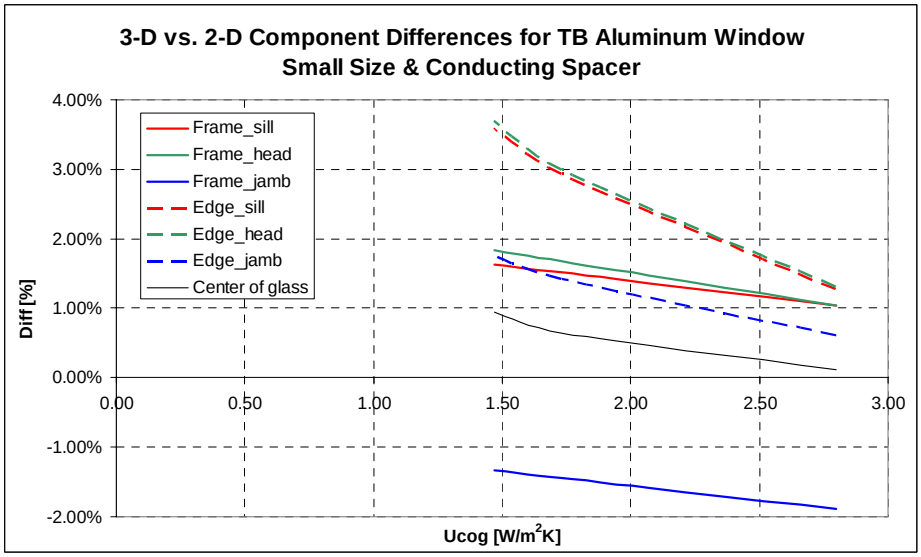


Figure B3. Component Level Difference Graphs for Small Size T/B AL Window

APPENDIX C: COMPONENT LEVEL RESULTS AND COMPARISONS FOR ALUMINUM (AL) WINDOW:

Table C1. AL Window – Large Size, Insulating Spacer

Dbl Clear	**Spacer keff =**		**0.050**	**W/mK**			
Section	**T5/W5**	**2-D**	**% diff**	**2-D***	**% diff**	**3-D**	**% diff**
	W/m^{2}K	**W/m^{2}K**	**2D vs T5/W5**	**W/m^{2}K**	**2D* vs T5/W5**	**W/m^{2}K**	**3D vs 2-D**
Frame_sill	8.80	8.75	-0.51%	8.88	0.90%	8.53	-2.62%
Frame_head	8.80	8.75	-0.58%	8.88	0.90%	8.53	-2.54%
Frame_jamb	8.80	8.77	-0.36%	8.61	-2.16%	8.71	-0.65%
Center of glass	2.80	2.80	-0.02%	2.79	-0.07%	2.80	0.15%
Edge_sill	3.08	3.11	1.03%	3.12	1.33%	3.16	1.72%
Edge_head	3.08	3.11	0.96%	3.12	1.28%	3.16	1.76%
Edge_jamb	3.08	3.12	1.26%	3.12	1.30%	3.14	0.55%
TOTAL	**4.47**	**4.47**	**0.02%**	**4.45**	**-0.44%**	**4.45**	**-0.42%**
Dbl Low-e HC	**Spacer keff =**		**0.050**	**W/mK**			
Section	**T5/W5**	**2-D**	**% diff**	**2-D***	**% diff**	**3-D**	**% diff**
	W/m^{2}K	**W/m^{2}K**	**2D vs T5/W5**	**W/m^{2}K**	**2D* vs T5/W5**	**W/m^{2}K**	**3D vs 2-D**
Frame_sill	8.72	8.67	-0.49%	8.79	0.84%	8.45	-2.63%
Frame_head	8.72	8.66	-0.66%	8.79	0.82%	8.45	-2.47%
Frame_jamb	8.72	8.69	-0.31%	8.52	-2.27%	8.63	-0.75%
Center of glass	1.73	1.75	0.90%	1.75	0.88%	1.76	0.65%
Edge_sill	2.24	2.30	2.58%	2.31	3.02%	2.39	3.60%
Edge_head	2.24	2.30	2.42%	2.31	2.94%	2.39	3.69%
Edge_jamb	2.25	2.32	3.02%	2.32	3.07%	2.34	1.15%
TOTAL	**3.72**	**3.74**	**0.45%**	**3.72**	**-0.15%**	**3.73**	**-0.34%**
Dbl Low-e SC	**Spacer keff =**		**0.050**	**W/mK**			
Section	**T5/W5**	**2-D**	**% diff**	**2-D***	**% diff**	**3-D**	**% diff**
	W/m^{2}K	**W/m^{2}K**	**2D vs T5/W5**	**W/m^{2}K**	**2D* vs T5/W5**	**W/m^{2}K**	**3D vs 2-D**
Frame_sill	8.70	8.65	-0.50%	8.77	0.83%	8.43	-2.62%
Frame_head	8.70	8.64	-0.63%	8.77	0.82%	8.43	-2.49%
Frame_jamb	8.70	8.67	-0.32%	8.50	-2.29%	8.61	-0.75%
Center of glass	1.47	1.46	-0.45%	1.46	-0.45%	1.48	0.97%
Edge_sill	2.04	2.09	2.27%	2.10	2.80%	2.18	4.38%
Edge_head	2.04	2.08	2.11%	2.10	2.69%	2.18	4.47%
Edge_jamb	2.04	2.10	2.77%	2.10	2.85%	2.13	1.42%
TOTAL	**3.54**	**3.54**	**0.09%**	**3.52**	**-0.56%**	**3.53**	**-0.28%**
Hypothetical R10	**Spacer keff =**		**0.050**	**W/mK**			
Section	**T5/W5**	**2-D**	**% diff**	**2-D***	**% diff**	**3-D**	**% diff**
	W/m^{2}K	**W/m^{2}K**	**2D vs T5/W5**	**W/m^{2}K**	**2D* vs T5/W5**	**W/m^{2}K**	**3D vs 2-D**
Frame_sill	8.61	8.59	-0.19%	8.71	1.21%	8.38	-2.48%
Frame_head	8.61	8.58	-0.27%	8.71	1.19%	8.38	-2.42%
Frame_jamb	8.57	8.60	0.36%	8.44	-1.45%	8.55	-0.56%
Center of glass	0.58	0.58	0.78%	0.58	0.83%	0.60	3.87%
Edge_sill	1.40	1.44	2.77%	1.45	3.60%	1.57	8.04%
Edge_head	1.40	1.44	2.53%	1.45	3.42%	1.57	8.15%
Edge_jamb	1.39	1.46	4.68%	1.46	4.82%	1.50	2.67%
TOTAL	**2.91**	**2.94**	**0.80%**	**2.92**	**0.14%**	**2.94**	**0.05%**

Table C2. AL Window – Large Size, Medium Conducting Spacer

Dbl Clear	Spacer keff =		0.674	W/mK			
Section	**T5/W5**	**2-D**	**% diff**	**2-D***	**% diff**	**3-D**	**% diff**
	W/m^{2}K	**W/m^{2}K**	**2D vs T5/W5**	**W/m^{2}K**	**2D* vs T5/W5**	**W/m^{2}K**	**3D vs 2-D**
Frame_sill	8.86	8.81	-0.55%	8.94	0.97%	8.59	-2.54%
Frame_head	8.86	8.80	-0.69%	8.94	0.96%	8.59	-2.41%
Frame_jamb	8.86	8.82	-0.47%	8.68	-2.09%	8.77	-0.49%
Center of glass	2.80	2.80	-0.01%	2.80	-0.03%	2.80	0.22%
Edge_sill	3.19	3.20	0.21%	3.21	0.51%	3.26	1.92%
Edge_head	3.19	3.19	0.15%	3.21	0.47%	3.26	1.95%
Edge_jamb	3.19	3.20	0.29%	3.20	0.35%	3.22	0.65%
TOTAL	**4.51**	**4.50**	**-0.18%**	**4.49**	**-0.54%**	**4.49**	**-0.30%**

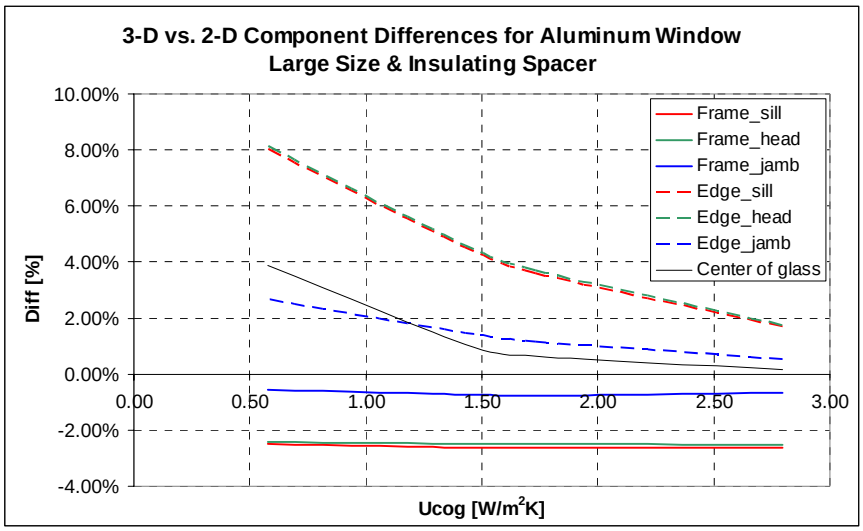
Dbl Low-e HC	Spacer keff =		0.674	W/mK			
Section	**T5/W5**	**2-D**	**% diff**	**2-D***	**% diff**	**3-D**	**% diff**
	W/m^{2}K	**W/m^{2}K**	**2D vs T5/W5**	**W/m^{2}K**	**2D* vs T5/W5**	**W/m^{2}K**	**3D vs 2-D**
Frame_sill	8.79	8.74	-0.63%	8.86	0.74%	8.51	-2.64%
Frame_head	8.79	8.72	-0.81%	8.86	0.73%	8.51	-2.48%
Frame_jamb	8.80	8.75	-0.52%	8.59	-2.39%	8.69	-0.69%
Center of glass	1.73	1.75	0.95%	1.75	0.92%	1.76	0.78%
Edge_sill	2.41	2.42	0.76%	2.43	1.19%	2.52	3.81%
Edge_head	2.41	2.42	0.65%	2.43	1.13%	2.52	3.87%
Edge_jamb	2.41	2.43	0.94%	2.43	1.02%	2.46	1.27%
TOTAL	**3.78**	**3.79**	**0.05%**	**3.76**	**-0.51%**	**3.78**	**-0.25%**

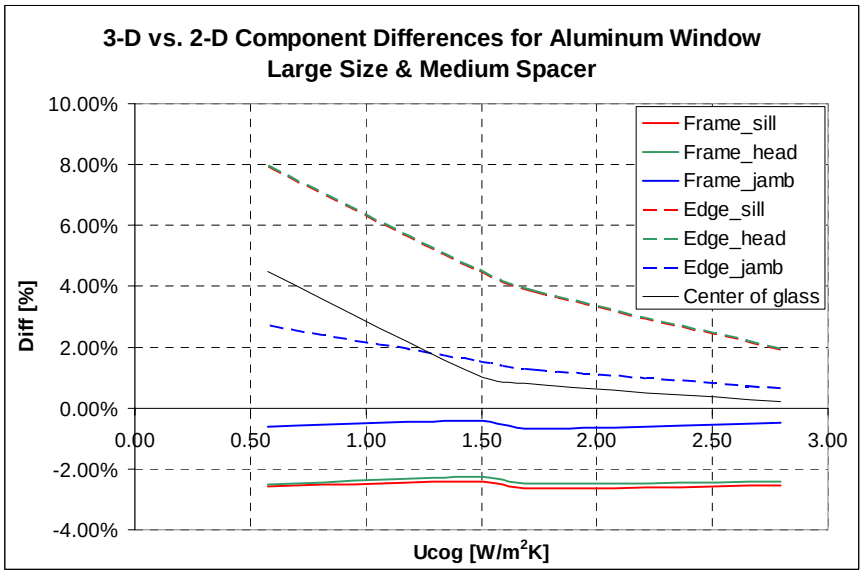
Dbl Low-e SC	Spacer keff =		0.674	W/mK			
Section	**T5/W5**	**2-D**	**% diff**	**2-D***	**% diff**	**3-D**	**% diff**
	W/m^{2}K	**W/m^{2}K**	**2D vs T5/W5**	**W/m^{2}K**	**2D* vs T5/W5**	**W/m^{2}K**	**3D vs 2-D**
Frame_sill	8.78	8.72	-0.64%	8.86	0.95%	8.52	-2.41%
Frame_head	8.78	8.71	-0.79%	8.86	0.95%	8.52	-2.26%
Frame_jamb	8.78	8.73	-0.55%	8.59	-2.17%	8.69	-0.43%
Center of glass	1.47	1.46	-0.39%	1.46	-0.41%	1.48	1.13%
Edge_sill	2.22	2.22	0.15%	2.23	0.65%	2.32	4.57%
Edge_head	2.22	2.22	0.03%	2.23	0.58%	2.32	4.63%
Edge_jamb	2.22	2.22	0.30%	2.23	0.43%	2.26	1.57%
TOTAL	**3.61**	**3.59**	**-0.39%**	**3.58**	**-0.81%**	**3.59**	**-0.02%**

Hypothetical R10	Spacer keff =		0.674	W/mK			
Section	**T5/W5**	**2-D**	**% diff**	**2-D***	**% diff**	**3-D**	**% diff**
	W/m^{2}K	**W/m^{2}K**	**2D vs T5/W5**	**W/m^{2}K**	**2D* vs T5/W5**	**W/m^{2}K**	**3D vs 2-D**
Frame_sill	8.70	8.67	-0.37%	8.79	1.00%	8.45	-2.59%
Frame_head	8.70	8.66	-0.46%	8.79	0.98%	8.45	-2.52%
Frame_jamb	8.70	8.67	-0.35%	8.52	-2.17%	8.62	-0.60%
Center of glass	0.58	0.58	0.99%	0.58	1.05%	0.61	4.48%
Edge_sill	1.62	1.60	-1.23%	1.62	-0.44%	1.74	7.94%
Edge_head	1.62	1.60	-1.36%	1.61	-0.56%	1.74	7.98%
Edge_jamb	1.63	1.61	-0.89%	1.61	-0.72%	1.66	2.72%
TOTAL	**3.00**	**3.00**	**-0.27%**	**2.98**	**-0.93%**	**3.00**	**0.11%**

Table C3. AL Window – Large Size, Highly Conducting Spacer

Dbl Clear	Spacer keff =		1.900	W/mK			
Section	**T5/W5**	**2-D**	**% diff**	**2-D***	**% diff**	**3-D**	**% diff**
	W/m^{2}K	**W/m^{2}K**	**2D vs T5/W5**	**W/m^{2}K**	**2D* vs T5/W5**	**W/m^{2}K**	**3D vs 2-D**
Frame_sill	8.89	8.82	-0.70%	8.97	0.95%	8.61	-2.44%
Frame_head	8.89	8.83	-0.57%	8.97	0.95%	8.61	-2.57%
Frame_jamb	8.89	8.84	-0.48%	8.70	-2.10%	8.80	-0.51%
Center of glass	2.80	2.80	0.00%	2.80	-0.02%	2.80	0.24%
Edge_sill	3.25	3.24	-0.24%	3.25	0.07%	3.31	2.02%
Edge_head	3.25	3.24	-0.29%	3.25	0.03%	3.31	2.04%
Edge_jamb	3.25	3.24	-0.27%	3.24	-0.20%	3.26	0.69%
TOTAL	**4.53**	**4.52**	**-0.28%**	**4.50**	**-0.64%**	**4.51**	**-0.29%**
Dbl Low-e HC	**Spacer keff =**		**1.900**	**W/mK**			
Section	**T5/W5**	**2-D**	**% diff**	**2-D***	**% diff**	**3-D**	**% diff**
	W/m^{2}K	**W/m^{2}K**	**2D vs T5/W5**	**W/m^{2}K**	**2D* vs T5/W5**	**W/m^{2}K**	**3D vs 2-D**
Frame_sill	8.83	8.77	-0.68%	8.89	0.70%	8.54	-2.68%
Frame_head	8.83	8.76	-0.84%	8.89	0.69%	8.54	-2.53%
Frame_jamb	8.83	8.78	-0.57%	8.62	-2.43%	8.72	-0.71%
Center of glass	1.73	1.75	0.96%	1.75	0.94%	1.76	0.85%
Edge_sill	2.48	2.48	0.04%	2.49	0.50%	2.58	3.93%
Edge_head	2.48	2.48	-0.01%	2.49	0.48%	2.58	3.97%
Edge_jamb	2.48	2.48	0.13%	2.49	0.23%	2.52	1.33%
TOTAL	**3.81**	**3.81**	**-0.09%**	**3.79**	**-0.64%**	**3.80**	**-0.23%**
Dbl Low-e SC	**Spacer keff =**		**1.900**	**W/mK**			
Section	**T5/W5**	**2-D**	**% diff**	**2-D***	**% diff**	**3-D**	**% diff**
	W/m^{2}K	**W/m^{2}K**	**2D vs T5/W5**	**W/m^{2}K**	**2D* vs T5/W5**	**W/m^{2}K**	**3D vs 2-D**
Frame_sill	8.82	8.76	-0.68%	8.87	0.62%	8.52	-2.75%
Frame_head	8.82	8.74	-0.84%	8.87	0.61%	8.52	-2.60%
Frame_jamb	8.82	8.77	-0.56%	8.60	-2.53%	8.70	-0.80%
Center of glass	1.47	1.46	-0.36%	1.46	-0.38%	1.48	1.21%
Edge_sill	2.30	2.28	-0.66%	2.29	-0.17%	2.39	4.65%
Edge_head	2.30	2.28	-0.75%	2.29	-0.23%	2.39	4.69%
Edge_jamb	2.30	2.28	-0.56%	2.29	-0.45%	2.32	1.58%
TOTAL	**3.63**	**3.62**	**-0.51%**	**3.59**	**-1.15%**	**3.61**	**-0.22%**
Hypothetical R10	**Spacer keff =**		**1.900**	**W/mK**			
Section	**T5/W5**	**2-D**	**% diff**	**2-D***	**% diff**	**3-D**	**% diff**
	W/m^{2}K	**W/m^{2}K**	**2D vs T5/W5**	**W/m^{2}K**	**2D* vs T5/W5**	**W/m^{2}K**	**3D vs 2-D**
Frame_sill	8.75	8.71	-0.40%	8.83	0.95%	8.49	-2.65%
Frame_head	8.75	8.70	-0.54%	8.83	0.92%	8.49	-2.55%
Frame_jamb	8.75	8.71	-0.41%	8.56	-2.24%	8.66	-0.64%
Center of glass	0.58	0.58	1.08%	0.58	1.15%	0.61	4.77%
Edge_sill	1.72	1.68	-2.70%	1.69	-1.89%	1.82	7.95%
Edge_head	1.72	1.68	-2.82%	1.69	-1.99%	1.82	7.99%
Edge_jamb	1.72	1.68	-2.49%	1.69	-2.27%	1.73	2.77%
TOTAL	**3.04**	**3.02**	**-0.52%**	**3.00**	**-1.18%**	**3.03**	**0.14%**





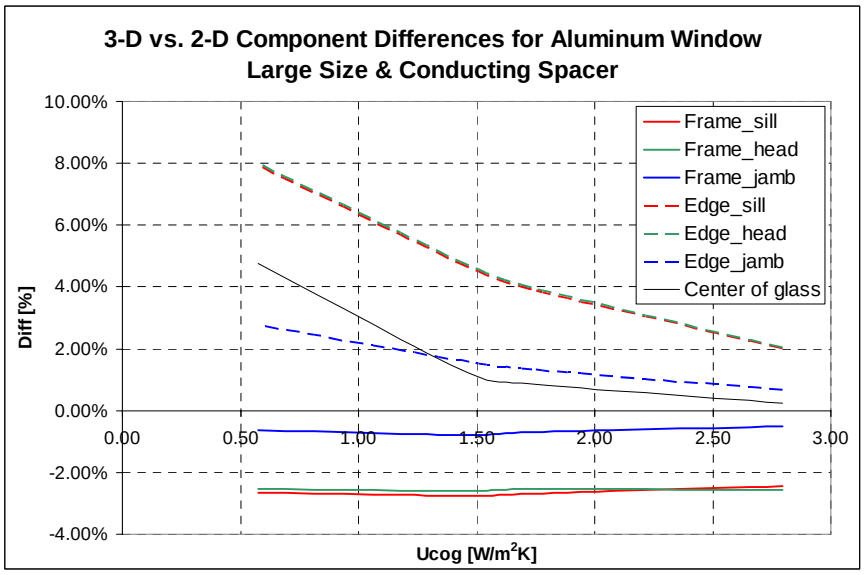


Figure C1. Component Level Difference Graphs for Large Size AL Window

Table C4. AL Window – Medium Size, Insulating Spacer

Dbl Clear	**Spacer keff =**		**0.050**	**W/mK**			
Section	**T5/W5**	**2-D**	**% diff**	**2-D***	**% diff**	**3-D**	**% diff**
	W/m^{2}K	**W/m^{2}K**	**2D vs T5/W5**	**W/m^{2}K**	**2D* vs T5/W5**	**W/m^{2}K**	**3D vs 2-D**
Frame_sill	8.80	8.76	-0.48%	8.89	1.09%	8.54	-2.56%
Frame_head	8.80	8.75	-0.57%	8.89	1.09%	8.54	-2.46%
Frame_jamb	8.80	8.76	-0.44%	8.65	-1.77%	8.48	-3.29%
Center of glass	2.80	2.79	-0.05%	2.79	-0.04%	2.80	0.20%
Edge_sill	3.08	3.11	1.04%	3.12	1.47%	3.17	1.87%
Edge_head	3.08	3.11	0.96%	3.12	1.46%	3.17	1.96%
Edge_jamb	3.08	3.12	1.26%	3.13	1.54%	3.15	0.88%
TOTAL	**4.57**	**4.57**	**-0.01%**	**4.56**	**-0.15%**	**4.51**	**-1.38%**
Dbl Low-e HC	**Spacer keff =**		**0.050**	**W/mK**			
Section	**T5/W5**	**2-D**	**% diff**	**2-D***	**% diff**	**3-D**	**% diff**
	W/m^{2}K	**W/m^{2}K**	**2D vs T5/W5**	**W/m^{2}K**	**2D* vs T5/W5**	**W/m^{2}K**	**3D vs 2-D**
Frame_sill	8.72	8.67	-0.48%	8.82	1.16%	8.47	-2.41%
Frame_head	8.72	8.67	-0.57%	8.82	1.16%	8.47	-2.32%
Frame_jamb	8.72	8.68	-0.45%	8.57	-1.73%	8.41	-3.19%
Center of glass	1.73	1.75	0.92%	1.75	0.94%	1.76	0.68%
Edge_sill	2.24	2.30	2.58%	2.32	3.18%	2.39	3.77%
Edge_head	2.24	2.30	2.45%	2.32	3.18%	2.39	3.92%
Edge_jamb	2.25	2.32	3.01%	2.33	3.41%	2.36	1.69%
TOTAL	**3.84**	**3.86**	**0.38%**	**3.85**	**0.26%**	**3.80**	**-1.35%**
Dbl Low-e SC	**Spacer keff =**		**0.050**	**W/mK**			
Section	**T5/W5**	**2-D**	**% diff**	**2-D***	**% diff**	**3-D**	**% diff**
	W/m^{2}K	**W/m^{2}K**	**2D vs T5/W5**	**W/m^{2}K**	**2D* vs T5/W5**	**W/m^{2}K**	**3D vs 2-D**
Frame_sill	8.70	8.65	-0.51%	8.80	1.16%	8.45	-2.37%
Frame_head	8.70	8.65	-0.59%	8.80	1.16%	8.43	-2.59%
Frame_jamb	8.70	8.66	-0.47%	8.55	-1.74%	8.39	-3.17%
Center of glass	1.47	1.46	-0.40%	1.46	-0.38%	1.48	0.97%
Edge_sill	2.04	2.09	2.26%	2.10	2.93%	2.19	4.54%
Edge_head	2.04	2.08	2.11%	2.10	2.93%	2.19	4.72%
Edge_jamb	2.04	2.10	2.74%	2.11	3.19%	2.14	2.02%
TOTAL	**3.66**	**3.66**	**0.01%**	**3.66**	**-0.10%**	**3.61**	**-1.37%**
Hypothetical R10	**Spacer keff =**		**0.050**	**W/mK**			
Section	**T5/W5**	**2-D**	**% diff**	**2-D***	**% diff**	**3-D**	**% diff**
	W/m^{2}K	**W/m^{2}K**	**2D vs T5/W5**	**W/m^{2}K**	**2D* vs T5/W5**	**W/m^{2}K**	**3D vs 2-D**
Frame_sill	8.61	8.59	-0.18%	8.74	1.54%	8.40	-2.26%
Frame_head	8.61	8.58	-0.27%	8.74	1.54%	8.40	-2.15%
Frame_jamb	8.57	8.60	0.37%	8.49	-0.88%	8.34	-3.12%
Center of glass	0.58	0.58	1.09%	0.58	1.20%	0.61	3.83%
Edge_sill	1.40	1.44	2.77%	1.46	3.75%	1.57	8.18%
Edge_head	1.40	1.44	2.52%	1.46	3.74%	1.57	8.50%
Edge_jamb	1.39	1.46	4.69%	1.47	5.30%	1.52	3.60%
TOTAL	**3.05**	**3.08**	**0.79%**	**3.07**	**0.68%**	**3.04**	**-1.24%**

Table C5. AL Window – Medium Size, Medium Conducting Spacer

Dbl Clear	Spacer keff =		0.674	W/mK			
Section	**T5/W5**	**2-D**	**% diff**	**2-D***	**% diff**	**3-D**	**% diff**
	W/m²K	**W/m²K**	**2D vs T5/W5**	**W/m²K**	**2D* vs T5/W5**	**W/m²K**	**3D vs 2-D**
Frame_sill	8.86	8.81	-0.58%	8.95	1.04%	8.59	-2.55%
Frame_head	8.86	8.80	-0.67%	8.95	1.03%	8.59	-2.46%
Frame_jamb	8.86	8.81	-0.57%	8.70	-1.83%	8.53	-3.23%
Center of glass	2.80	2.80	-0.03%	2.80	-0.02%	2.80	0.24%
Edge_sill	3.19	3.20	0.20%	3.21	0.70%	3.27	2.14%
Edge_head	3.19	3.19	0.15%	3.21	0.70%	3.27	2.20%
Edge_jamb	3.19	3.20	0.29%	3.21	0.67%	3.23	1.06%
TOTAL	**4.61**	**4.60**	**-0.22%**	**4.60**	**-0.31%**	**4.54**	**-1.31%**

Dbl Low-e HC	Spacer keff =		0.674	W/mK			
Section	**T5/W5**	**2-D**	**% diff**	**2-D***	**% diff**	**3-D**	**% diff**
	W/m²K	**W/m²K**	**2D vs T5/W5**	**W/m²K**	**2D* vs T5/W5**	**W/m²K**	**3D vs 2-D**
Frame_sill	8.79	8.74	-0.62%	8.89	1.07%	8.53	-2.42%
Frame_head	8.79	8.73	-0.71%	8.89	1.07%	8.53	-2.32%
Frame_jamb	8.80	8.74	-0.61%	8.64	-1.83%	8.47	-3.15%
Center of glass	1.73	1.75	0.98%	1.75	1.00%	1.76	0.81%
Edge_sill	2.41	2.42	0.76%	2.44	1.51%	2.53	4.14%
Edge_head	2.41	2.42	0.68%	2.44	1.50%	2.53	4.24%
Edge_jamb	2.41	2.43	0.94%	2.44	1.54%	2.48	2.00%
TOTAL	**3.90**	**3.90**	**-0.01%**	**3.90**	**-0.06%**	**3.86**	**-1.23%**

Dbl Low-e SC	Spacer keff =		0.674	W/mK			
Section	**T5/W5**	**2-D**	**% diff**	**2-D***	**% diff**	**3-D**	**% diff**
	W/m²K	**W/m²K**	**2D vs T5/W5**	**W/m²K**	**2D* vs T5/W5**	**W/m²K**	**3D vs 2-D**
Frame_sill	8.78	8.72	-0.67%	8.87	1.05%	8.52	-2.38%
Frame_head	8.78	8.71	-0.74%	8.87	1.07%	8.52	-2.29%
Frame_jamb	8.78	8.72	-0.64%	8.62	-1.85%	8.46	-3.12%
Center of glass	1.47	1.46	-0.33%	1.46	-0.30%	1.48	1.15%
Edge_sill	2.22	2.22	0.12%	2.24	0.98%	2.33	4.92%
Edge_head	2.22	2.22	0.04%	2.24	0.98%	2.33	5.04%
Edge_jamb	2.22	2.22	0.30%	2.24	0.99%	2.28	2.37%
TOTAL	**3.73**	**3.71**	**-0.41%**	**3.71**	**-0.45%**	**3.67**	**-1.19%**

Hypothetical R10	Spacer keff =		0.674	W/mK			
Section	**T5/W5**	**2-D**	**% diff**	**2-D***	**% diff**	**3-D**	**% diff**
	W/m²K	**W/m²K**	**2D vs T5/W5**	**W/m²K**	**2D* vs T5/W5**	**W/m²K**	**3D vs 2-D**
Frame_sill	8.70	8.67	-0.38%	8.83	1.42%	8.48	-2.26%
Frame_head	8.70	8.66	-0.46%	8.83	1.42%	8.48	-2.17%
Frame_jamb	8.70	8.67	-0.35%	8.58	-1.50%	8.42	-3.04%
Center of glass	0.58	0.58	1.36%	0.58	1.49%	0.61	4.46%
Edge_sill	1.62	1.60	-1.23%	1.62	0.11%	1.75	8.45%
Edge_head	1.62	1.60	-1.36%	1.62	0.11%	1.75	8.64%
Edge_jamb	1.63	1.61	-0.89%	1.63	0.21%	1.68	4.08%
TOTAL	**3.14**	**3.14**	**-0.22%**	**3.14**	**-0.18%**	**3.10**	**-1.01%**

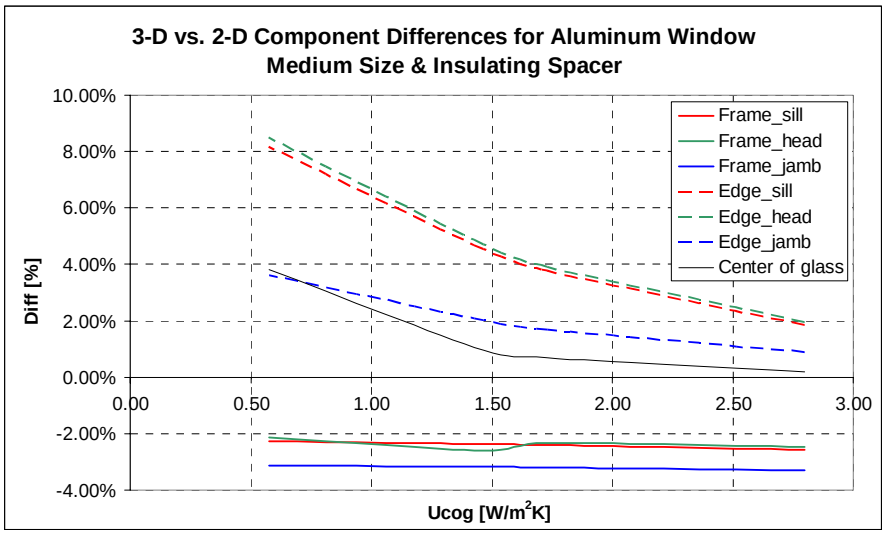
Table C6. AL Window – Medium Size, Highly Conducting Spacer

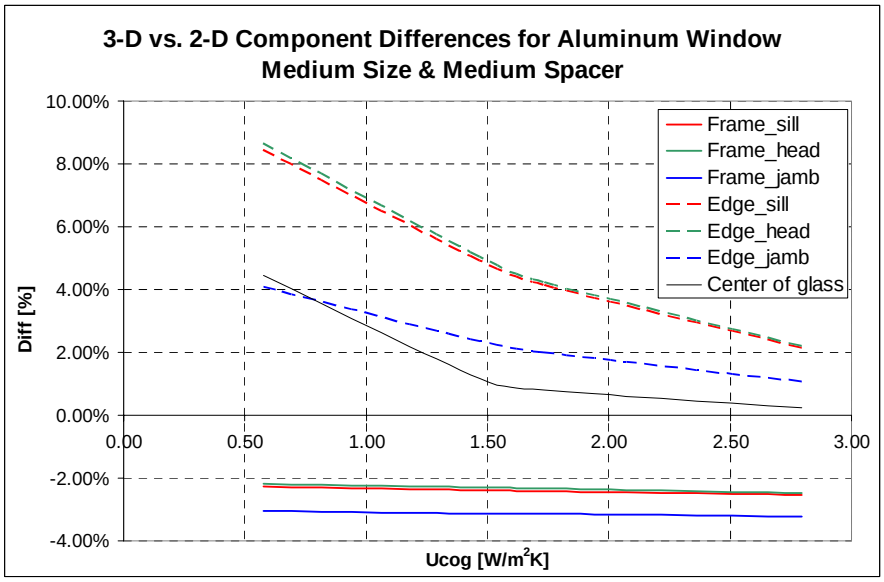
Dbl Clear	**Spacer keff =**		**1.900**	**W/mK**			
Section	**T5/W5**	**2-D**	**% diff**	**2-D***	**% diff**	**3-D**	**% diff**
	W/m^{2}K	**W/m^{2}K**	**2D vs T5/W5**	**W/m^{2}K**	**2D* vs T5/W5**	**W/m^{2}K**	**3D vs 2-D**
Frame_sill	8.89	8.83	-0.59%	8.98	1.06%	8.62	-2.54%
Frame_head	8.89	8.83	-0.66%	8.98	1.07%	8.62	-2.45%
Frame_jamb	8.89	8.84	-0.58%	8.73	-1.79%	8.56	-3.19%
Center of glass	2.80	2.80	-0.02%	2.80	-0.01%	2.80	0.27%
Edge_sill	3.25	3.24	-0.24%	3.26	0.29%	3.31	2.27%
Edge_head	3.25	3.24	-0.28%	3.26	0.29%	3.31	2.32%
Edge_jamb	3.25	3.24	-0.27%	3.26	0.16%	3.28	1.15%
TOTAL	**4.64**	**4.62**	**-0.33%**	**4.62**	**-0.38%**	**4.56**	**-1.26%**

Dbl Low-e HC	**Spacer keff =**		**1.900**	**W/mK**			
Section	**T5/W5**	**2-D**	**% diff**	**2-D***	**% diff**	**3-D**	**% diff**
	W/m^{2}K	**W/m^{2}K**	**2D vs T5/W5**	**W/m^{2}K**	**2D* vs T5/W5**	**W/m^{2}K**	**3D vs 2-D**
Frame_sill	8.83	8.77	-0.67%	8.93	1.08%	8.57	-2.39%
Frame_head	8.83	8.76	-0.76%	8.93	1.07%	8.57	-2.31%
Frame_jamb	8.83	8.77	-0.67%	8.67	-1.83%	8.51	-3.10%
Center of glass	1.73	1.75	1.00%	1.75	1.03%	1.77	0.88%
Edge_sill	2.48	2.48	0.03%	2.50	0.88%	2.59	4.34%
Edge_head	2.48	2.48	0.02%	2.50	0.92%	2.59	4.42%
Edge_jamb	2.48	2.48	0.13%	2.50	0.84%	2.54	2.15%
TOTAL	**3.93**	**3.93**	**-0.15%**	**3.93**	**-0.15%**	**3.88**	**-1.15%**

Dbl Low-e SC	**Spacer keff =**		**1.900**	**W/mK**			
Section	**T5/W5**	**2-D**	**% diff**	**2-D***	**% diff**	**3-D**	**% diff**
	W/m^{2}K	**W/m^{2}K**	**2D vs T5/W5**	**W/m^{2}K**	**2D* vs T5/W5**	**W/m^{2}K**	**3D vs 2-D**
Frame_sill	8.82	8.76	-0.72%	8.91	1.06%	8.55	-2.35%
Frame_head	8.82	8.75	-0.79%	8.91	1.06%	8.55	-2.28%
Frame_jamb	8.82	8.76	-0.71%	8.66	-1.85%	8.50	-3.07%
Center of glass	1.47	1.46	-0.29%	1.46	-0.26%	1.48	1.24%
Edge_sill	2.30	2.28	-0.69%	2.30	0.29%	2.40	5.13%
Edge_head	2.30	2.28	-0.75%	2.30	0.29%	2.40	5.23%
Edge_jamb	2.30	2.28	-0.58%	2.30	0.26%	2.34	2.55%
TOTAL	**3.76**	**3.74**	**-0.58%**	**3.74**	**-0.55%**	**3.70**	**-1.10%**

Hypothetical R10	**Spacer keff =**		**1.900**	**W/mK**			
Section	**T5/W5**	**2-D**	**% diff**	**2-D***	**% diff**	**3-D**	**% diff**
	W/m^{2}K	**W/m^{2}K**	**2D vs T5/W5**	**W/m^{2}K**	**2D* vs T5/W5**	**W/m^{2}K**	**3D vs 2-D**
Frame_sill	8.75	8.71	-0.43%	8.87	1.42%	8.52	-2.24%
Frame_head	8.75	8.70	-0.53%	8.87	1.41%	8.52	-2.14%
Frame_jamb	8.75	8.67	-0.86%	8.62	-1.51%	8.46	-2.55%
Center of glass	0.58	0.58	1.49%	0.59	1.63%	0.61	4.76%
Edge_sill	1.72	1.68	-2.72%	1.70	-1.15%	1.84	8.63%
Edge_head	1.72	1.68	-2.82%	1.70	-1.15%	1.84	8.80%
Edge_jamb	1.72	1.61	-7.04%	1.70	-1.14%	1.76	8.36%
TOTAL	**3.18**	**3.15**	**-1.13%**	**3.17**	**-0.37%**	**3.14**	**-0.25%**





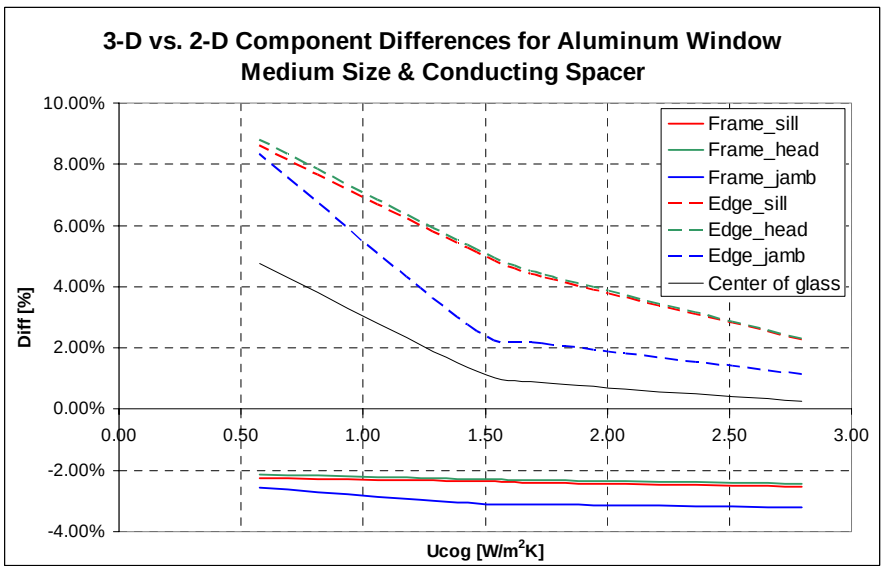


Figure C2. Component Level Difference Graphs for Medium Size AL Window

Table C7. AL Window – Small Size, Insulating Spacer

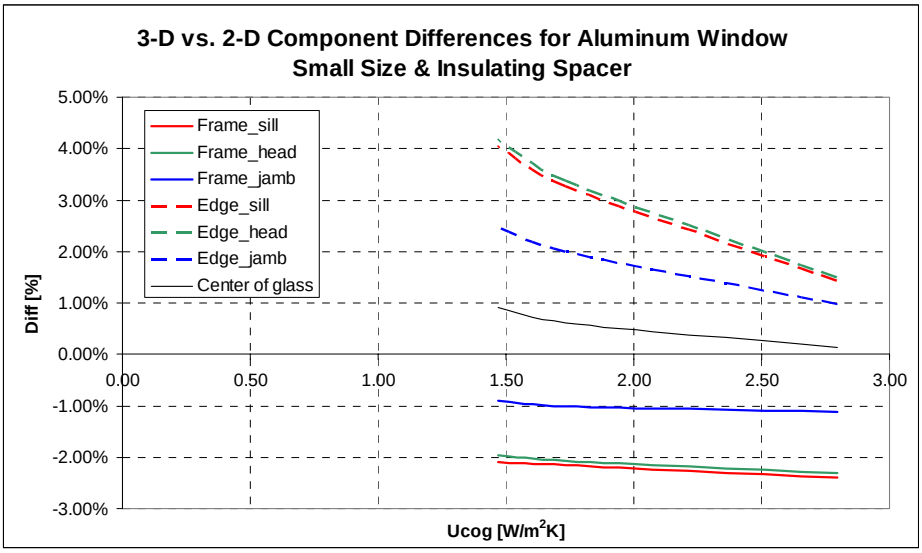
Dbl Clear	Spacer keff =		0.050	W/mK			
Section	**T5/W5**	**2-D**	**% diff**	**2-D***	**% diff**	**3-D**	**% diff**
	W/m^{2}K	**W/m^{2}K**	**2D vs T5/W5**	**W/m^{2}K**	**2D* vs T5/W5**	**W/m^{2}K**	**3D vs 2-D**
Frame_sill	8.80	8.76	-0.47%	8.90	1.17%	8.55	-2.39%
Frame_head	8.80	8.75	-0.57%	8.90	1.15%	8.55	-2.31%
Frame_jamb	8.80	8.76	-0.43%	8.66	-1.57%	8.66	-1.13%
Center of glass	2.80	2.80	0.06%	2.80	-0.01%	2.80	0.12%
Edge_sill	3.08	3.11	1.04%	3.12	1.22%	3.15	1.43%
Edge_head	3.08	3.11	0.96%	3.12	1.22%	3.15	1.50%
Edge_jamb	3.08	3.12	1.26%	3.12	1.33%	3.15	0.99%
TOTAL	**4.72**	**4.72**	**0.03%**	**4.72**	**0.02%**	**4.69**	**-0.71%**
Dbl Low-e HC	**Spacer keff =**		**0.050**	**W/mK**			
Section	**T5/W5**	**2-D**	**% diff**	**2-D***	**% diff**	**3-D**	**% diff**
	W/m^{2}K	**W/m^{2}K**	**2D vs T5/W5**	**W/m^{2}K**	**2D* vs T5/W5**	**W/m^{2}K**	**3D vs 2-D**
Frame_sill	8.72	8.67	-0.52%	8.83	1.29%	8.49	-2.16%
Frame_head	8.72	8.66	-0.62%	8.83	1.27%	8.49	-2.08%
Frame_jamb	8.72	8.68	-0.39%	8.59	-1.47%	8.60	-1.01%
Center of glass	1.73	1.75	1.11%	1.75	1.05%	1.76	0.61%
Edge_sill	2.24	2.30	2.56%	2.31	2.84%	2.38	3.26%
Edge_head	2.24	2.30	2.43%	2.31	2.82%	2.38	3.37%
Edge_jamb	2.25	2.32	3.02%	2.32	3.10%	2.36	1.99%
TOTAL	**4.02**	**4.04**	**0.40%**	**4.04**	**0.47%**	**4.02**	**-0.49%**
Dbl Low-e SC	**Spacer keff =**		**0.050**	**W/mK**			
Section	**T5/W5**	**2-D**	**% diff**	**2-D***	**% diff**	**3-D**	**% diff**
	W/m^{2}K	**W/m^{2}K**	**2D vs T5/W5**	**W/m^{2}K**	**2D* vs T5/W5**	**W/m^{2}K**	**3D vs 2-D**
Frame_sill	8.70	8.65	-0.50%	8.82	1.35%	8.48	-2.09%
Frame_head	8.70	8.64	-0.64%	8.81	1.33%	8.47	-1.97%
Frame_jamb	8.70	8.66	-0.42%	8.58	-1.41%	8.58	-0.89%
Center of glass	1.47	1.47	-0.17%	1.46	-0.22%	1.48	0.91%
Edge_sill	2.04	2.09	2.26%	2.09	2.64%	2.17	4.08%
Edge_head	2.04	2.08	2.09%	2.09	2.59%	2.17	4.20%
Edge_jamb	2.04	2.10	2.75%	2.10	2.88%	2.15	2.47%
TOTAL	**3.85**	**3.85**	**0.10%**	**3.86**	**0.23%**	**3.84**	**-0.35%**

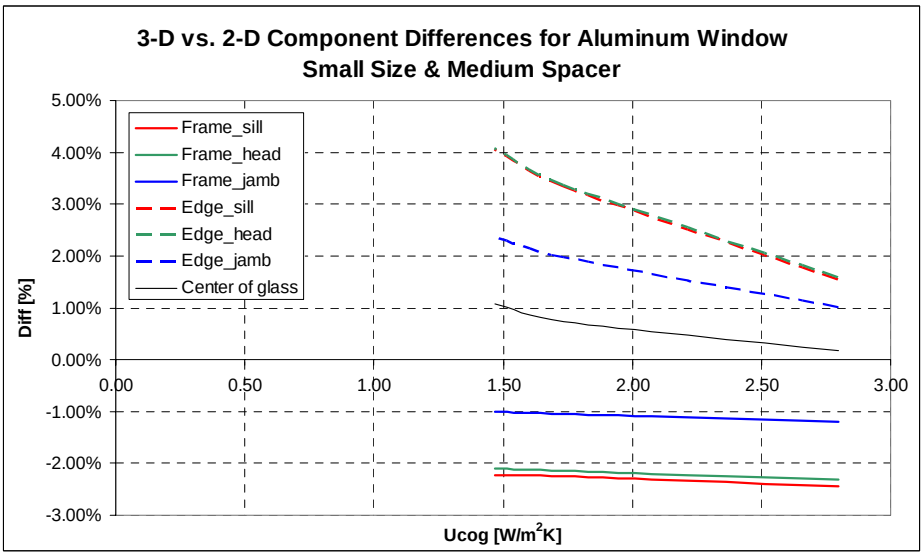
Table C8. AL Window – Small Size, Medium Conducting Spacer

Dbl Clear	**Spacer keff =**		**0.674**	**W/mK**			
Section	**T5/W5**	**2-D**	**% diff**	**2-D***	**% diff**	**3-D**	**% diff**
	W/m^{2}K	**W/m^{2}K**	**2D vs T5/W5**	**W/m^{2}K**	**2D* vs T5/W5**	**W/m^{2}K**	**3D vs 2-D**
Frame_sill	8.86	8.81	-0.57%	8.95	1.08%	8.60	-2.44%
Frame_head	8.86	8.80	-0.70%	8.95	1.07%	8.60	-2.31%
Frame_jamb	8.86	8.82	-0.49%	8.71	-1.67%	8.71	-1.20%
Center of glass	2.80	2.80	0.09%	2.80	0.03%	2.80	0.18%
Edge_sill	3.19	3.20	0.20%	3.20	0.32%	3.25	1.55%
Edge_head	3.19	3.19	0.14%	3.20	0.30%	3.25	1.59%
Edge_jamb	3.19	3.20	0.29%	3.20	0.26%	3.23	1.02%
TOTAL	**4.77**	**4.76**	**-0.16%**	**4.76**	**-0.20%**	**4.73**	**-0.71%**
Dbl Low-e HC	**Spacer keff =**		**0.674**	**W/mK**			
Section	**T5/W5**	**2-D**	**% diff**	**2-D***	**% diff**	**3-D**	**% diff**
	U-value	**U-value**	**2D vs T5/W5**	**U-value**	**2D* vs T5/W5**	**U-value**	**3D vs 2-D**
Frame_sill	8.79	8.74	-0.66%	8.89	1.13%	8.54	-2.24%
Frame_head	8.79	8.73	-0.77%	8.89	1.12%	8.54	-2.14%
Frame_jamb	8.80	8.75	-0.57%	8.65	-1.64%	8.65	-1.04%
Center of glass	1.73	1.75	1.18%	1.75	1.12%	1.77	0.74%
Edge_sill	2.41	2.42	0.74%	2.43	0.89%	2.51	3.35%
Edge_head	2.41	2.42	0.66%	2.43	0.83%	2.51	3.37%
Edge_jamb	2.41	2.43	0.94%	2.43	0.83%	2.48	1.98%
TOTAL	**4.09**	**4.09**	**0.01%**	**4.09**	**0.04%**	**4.07**	**-0.48%**
Dbl Low-e SC	**Spacer keff =**		**0.674**	**W/mK**			
Section	**T5/W5**	**2-D**	**% diff**	**2-D***	**% diff**	**3-D**	**% diff**
	U-value	**U-value**	**2D vs T5/W5**	**U-value**	**2D* vs T5/W5**	**U-value**	**3D vs 2-D**
Frame_sill	8.78	8.72	-0.67%	8.88	1.13%	8.53	-2.22%
Frame_head	8.78	8.71	-0.79%	8.88	1.12%	8.53	-2.10%
Frame_jamb	8.78	8.73	-0.60%	8.64	-1.64%	8.64	-1.00%
Center of glass	1.47	1.47	-0.06%	1.47	-0.11%	1.48	1.07%
Edge_sill	2.22	2.22	0.12%	2.22	0.20%	2.31	4.05%
Edge_head	2.22	2.22	0.02%	2.22	0.20%	2.31	4.08%
Edge_jamb	2.22	2.22	0.30%	2.22	0.17%	2.28	2.37%
TOTAL	**3.92**	**3.91**	**-0.34%**	**3.91**	**-0.29%**	**3.89**	**-0.39%**

Table C9. AL Window – Small Size, Highly Conducting Spacer

Dbl Clear	**Spacer keff =**		**1.900**	**W/mK**			
Section	**T5/W5**	**2-D**	**% diff**	**2-D***	**% diff**	**3-D**	**% diff**
	U-value	**U-value**	**2D vs T5/W5**	**U-value**	**2D* vs T5/W5**	**U-value**	**3D vs 2-D**
Frame_sill	8.89	8.83	-0.58%	8.98	1.06%	8.62	-2.47%
Frame_head	8.89	8.82	-0.70%	8.98	1.07%	8.62	-2.34%
Frame_jamb	8.89	8.84	-0.48%	8.74	-1.68%	8.74	-1.24%
Center of glass	2.80	2.80	0.10%	2.80	0.04%	2.80	0.20%
Edge_sill	3.25	3.24	-0.24%	3.24	-0.16%	3.29	1.61%
Edge_head	3.25	3.24	-0.29%	3.24	-0.18%	3.29	1.64%
Edge_jamb	3.25	3.24	-0.27%	3.24	-0.34%	3.28	1.04%
TOTAL	**4.80**	**4.78**	**-0.25%**	**4.78**	**-0.30%**	**4.75**	**-0.72%**
Dbl Low-e HC	**Spacer keff =**		**1.900**	**W/mK**			
Section	**T5/W5**	**2-D**	**% diff**	**2-D***	**% diff**	**3-D**	**% diff**
	U-value	**U-value**	**2D vs T5/W5**	**U-value**	**2D* vs T5/W5**	**U-value**	**3D vs 2-D**
Frame_sill	8.83	8.77	-0.70%	8.92	1.02%	8.57	-2.35%
Frame_head	8.83	8.76	-0.82%	8.92	1.02%	8.57	-2.23%
Frame_jamb	8.83	8.78	-0.54%	8.68	-1.75%	8.68	-1.22%
Center of glass	1.73	1.75	1.22%	1.75	1.16%	1.77	0.79%
Edge_sill	2.48	2.48	0.03%	2.48	0.04%	2.57	3.30%
Edge_head	2.48	2.48	0.00%	2.48	0.03%	2.56	3.33%
Edge_jamb	2.48	2.48	0.13%	2.48	-0.07%	2.53	1.94%
TOTAL	**4.12**	**4.12**	**-0.10%**	**4.12**	**-0.15%**	**4.10**	**-0.56%**
Dbl Low-e SC	**Spacer keff =**		**1.900**	**W/mK**			
Section	**T5/W5**	**2-D**	**% diff**	**2-D***	**% diff**	**3-D**	**% diff**
	U-value	**U-value**	**2D vs T5/W5**	**U-value**	**2D* vs T5/W5**	**U-value**	**3D vs 2-D**
Frame_sill	8.82	8.75	-0.72%	8.91	0.99%	8.55	-2.34%
Frame_head	8.82	8.74	-0.85%	8.91	0.98%	8.55	-2.23%
Frame_jamb	8.82	8.77	-0.57%	8.66	-1.80%	8.66	-1.22%
Center of glass	1.47	1.47	-0.01%	1.47	-0.07%	1.48	1.15%
Edge_sill	2.30	2.28	-0.69%	2.28	-0.79%	2.37	3.90%
Edge_head	2.30	2.28	-0.77%	2.28	-0.81%	2.37	3.95%
Edge_jamb	2.30	2.28	-0.57%	2.28	-0.84%	2.34	2.29%
TOTAL	**3.96**	**3.94**	**-0.47%**	**3.93**	**-0.54%**	**3.92**	**-0.51%**





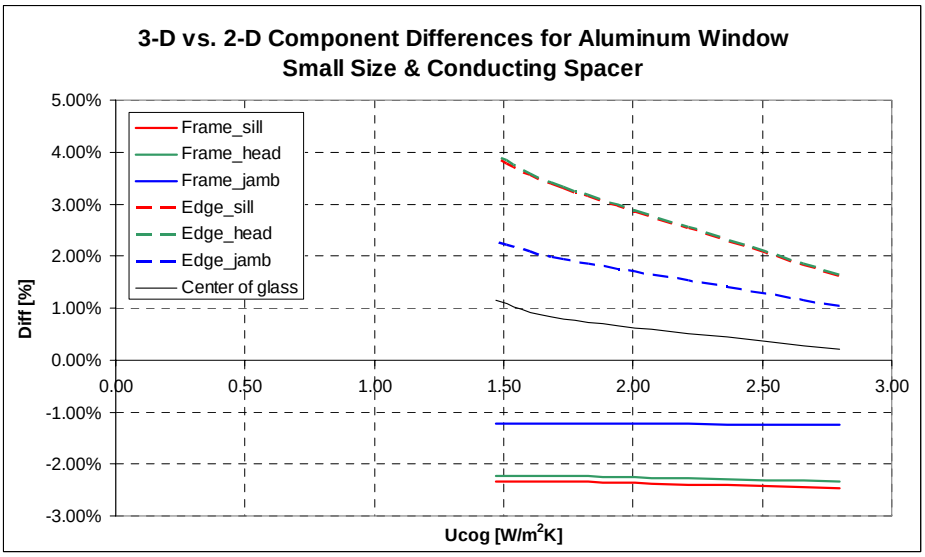


Figure C3. Component Level Difference Graphs for Small Size AL Window

APPENDIX D: COMPONENT LEVEL RESULTS AND COMPARISONS FOR POLYVINYLCHLORIDE (PVC) WINDOW:

Table D1. PVC Window – Large Size, Insulating Spacer

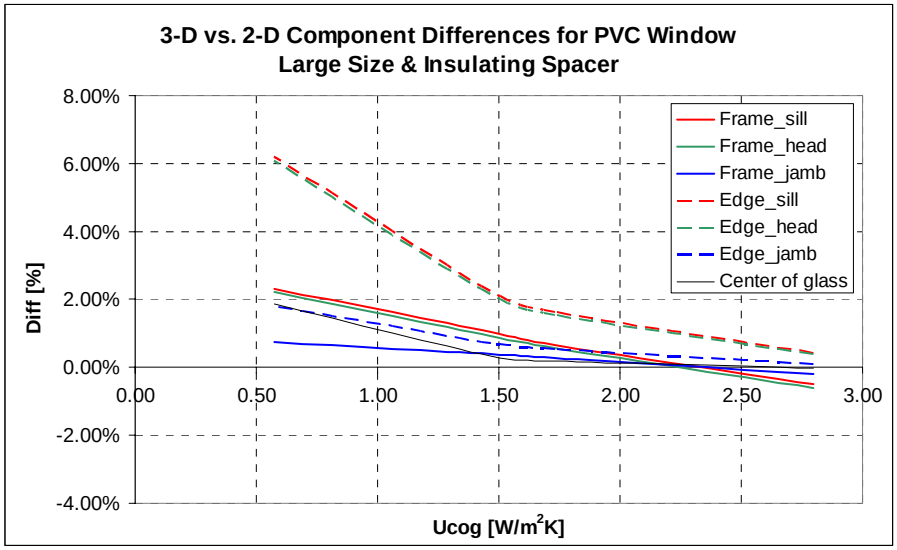
Dbl Clear	**Spacer keff =**		**0.050**	**W/mK**			
Section	**T5/W5**	**2-D**	**% diff**	**2-D***	**% diff**	**3-D**	**% diff**
	W/m^{2}K	**W/m^{2}K**	**2D vs T5/W5**	**W/m^{2}K**	**2D* vs T5/W5**	**W/m^{2}K**	**3D vs 2-D**
Frame_sill	2.11	2.03	-3.52%	2.04	-3.01%	2.02	-0.50%
Frame_head	2.11	2.04	-3.49%	2.04	-3.12%	2.02	-0.60%
Frame_jamb	2.33	2.23	-4.18%	2.17	-7.17%	2.23	-0.19%
Center of glass	2.80	2.79	-0.07%	2.79	-0.11%	2.79	-0.02%
Edge_sill	2.82	2.83	0.22%	2.83	0.22%	2.84	0.41%
Edge_head	2.82	2.83	0.25%	2.83	0.23%	2.84	0.39%
Edge_jamb	2.83	2.84	0.14%	2.83	0.11%	2.84	0.08%
TOTAL	**2.66**	**2.64**	**-0.85%**	**2.63**	**-1.32%**	**2.64**	**-0.03%**
Dbl Low-e HC	**Spacer keff =**		**0.050**	**W/mK**			
Section	**T5/W5**	**2-D**	**% diff**	**2-D***	**% diff**	**3-D**	**% diff**
	W/m^{2}K	**W/m^{2}K**	**2D vs T5/W5**	**W/m^{2}K**	**2D* vs T5/W5**	**W/m^{2}K**	**3D vs 2-D**
Frame_sill	1.93	1.86	-3.57%	1.87	-3.17%	1.87	0.67%
Frame_head	1.93	1.86	-3.52%	1.87	-3.27%	1.87	0.56%
Frame_jamb	2.15	2.06	-4.35%	2.00	-7.49%	2.06	0.27%
Center of glass	1.73	1.75	0.79%	1.75	0.75%	1.75	0.20%
Edge_sill	1.91	1.93	1.06%	1.93	0.92%	1.96	1.63%
Edge_head	1.91	1.93	1.13%	1.93	0.92%	1.96	1.56%
Edge_jamb	1.93	1.94	0.59%	1.94	0.60%	1.95	0.54%
TOTAL	**1.88**	**1.86**	**-0.64%**	**1.85**	**-1.28%**	**1.87**	**0.40%**
Dbl Low-e SC	**Spacer keff =**		**0.050**	**W/mK**			
Section	**T5/W5**	**2-D**	**% diff**	**2-D***	**% diff**	**3-D**	**% diff**
	W/m^{2}K	**W/m^{2}K**	**2D vs T5/W5**	**W/m^{2}K**	**2D* vs T5/W5**	**W/m^{2}K**	**3D vs 2-D**
Frame_sill	1.88	1.81	-3.83%	1.82	-3.42%	1.83	1.05%
Frame_head	1.88	1.82	-3.77%	1.82	-3.52%	1.83	0.92%
Frame_jamb	2.10	2.01	-4.59%	1.95	-7.79%	2.02	0.39%
Center of glass	1.47	1.46	-0.60%	1.46	-0.64%	1.46	0.34%
Edge_sill	1.69	1.69	0.00%	1.69	-0.15%	1.73	2.25%
Edge_head	1.69	1.69	0.09%	1.69	-0.15%	1.73	2.17%
Edge_jamb	1.72	1.71	-0.45%	1.71	-0.44%	1.72	0.73%
TOTAL	**1.68**	**1.65**	**-1.73%**	**1.64**	**-2.45%**	**1.66**	**0.59%**
Hypothetical R10	**Spacer keff =**		**0.050**	**W/mK**			
Section	**T5/W5**	**2-D**	**% diff**	**2-D***	**% diff**	**3-D**	**% diff**
	W/m^{2}K	**W/m^{2}K**	**2D vs T5/W5**	**W/m^{2}K**	**2D* vs T5/W5**	**W/m^{2}K**	**3D vs 2-D**
Frame_sill	1.65	1.68	1.65%	1.69	2.13%	1.72	2.32%
Frame_head	1.65	1.68	1.75%	1.69	2.10%	1.72	2.21%
Frame_jamb	1.83	1.88	2.81%	1.82	-0.36%	1.89	0.74%
Center of glass	0.58	0.58	0.18%	0.58	0.17%	0.59	1.86%
Edge_sill	1.00	0.97	-3.18%	0.97	-3.27%	1.04	6.19%
Edge_head	1.01	0.97	-3.17%	0.97	-3.38%	1.04	6.09%
Edge_jamb	1.04	1.00	-4.74%	1.00	-4.85%	1.02	1.81%
TOTAL	**1.01**	**1.01**	**0.24%**	**1.00**	**-0.89%**	**1.03**	**1.73%**

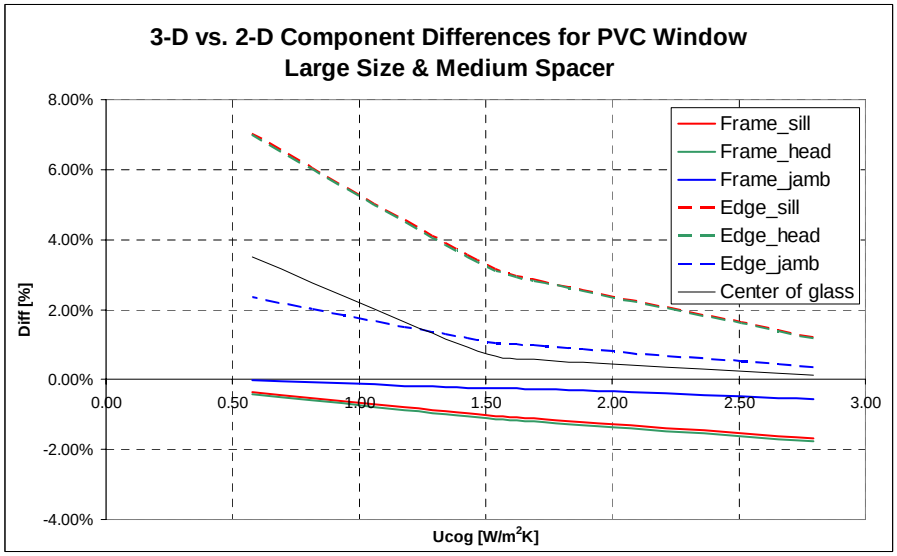
Table D2. PVC Window – Large Size, Medium Conducting Spacer

Dbl Clear	**Spacer keff =**		**0.674**	**W/mK**			
Section	**T5/W5**	**2-D**	**% diff**	**2-D***	**% diff**	**3-D**	**% diff**
	W/m^{2}K	**W/m^{2}K**	**2D vs T5/W5**	**W/m^{2}K**	**2D* vs T5/W5**	**W/m^{2}K**	**3D vs 2-D**
Frame_sill	2.50	2.41	-3.76%	2.43	-3.22%	2.37	-1.67%
Frame_head	2.50	2.41	-3.75%	2.42	-3.36%	2.37	-1.77%
Frame_jamb	2.71	2.61	-3.74%	2.55	-6.42%	2.60	-0.56%
Center of glass	2.80	2.80	-0.03%	2.79	-0.07%	2.80	0.11%
Edge_sill	3.05	3.06	0.33%	3.06	0.34%	3.09	1.20%
Edge_head	3.05	3.06	0.36%	3.06	0.35%	3.09	1.17%
Edge_jamb	3.04	3.05	0.30%	3.05	0.26%	3.06	0.35%
TOTAL	**2.82**	**2.80**	**-0.84%**	**2.78**	**-1.30%**	**2.80**	**-0.01%**
Dbl Low-e HC	**Spacer keff =**		**0.674**	**W/mK**			
Section	**T5/W5**	**2-D**	**% diff**	**2-D***	**% diff**	**3-D**	**% diff**
	W/m^{2}K	**W/m^{2}K**	**2D vs T5/W5**	**W/m^{2}K**	**2D* vs T5/W5**	**W/m^{2}K**	**3D vs 2-D**
Frame_sill	2.40	2.32	-3.52%	2.33	-3.05%	2.29	-1.14%
Frame_head	2.40	2.32	-3.52%	2.32	-3.19%	2.29	-1.23%
Frame_jamb	2.61	2.51	-3.79%	2.45	-6.48%	2.50	-0.29%
Center of glass	1.73	1.75	0.89%	1.75	0.86%	1.76	0.55%
Edge_sill	2.23	2.25	0.94%	2.25	0.85%	2.31	2.80%
Edge_head	2.23	2.25	0.98%	2.25	0.85%	2.31	2.76%
Edge_jamb	2.23	2.24	0.69%	2.24	0.71%	2.27	0.96%
TOTAL	**2.07**	**2.06**	**-0.59%**	**2.05**	**-1.19%**	**2.07**	**0.44%**
Dbl Low-e SC	**Spacer keff =**		**0.674**	**W/mK**			
Section	**T5/W5**	**2-D**	**% diff**	**2-D***	**% diff**	**3-D**	**% diff**
	W/m^{2}K	**W/m^{2}K**	**2D vs T5/W5**	**W/m^{2}K**	**2D* vs T5/W5**	**W/m^{2}K**	**3D vs 2-D**
Frame_sill	2.37	2.29	-3.63%	2.30	-3.19%	2.27	-0.98%
Frame_head	2.37	2.29	-3.62%	2.30	-3.33%	2.27	-1.08%
Frame_jamb	2.58	2.48	-3.92%	2.42	-6.67%	2.48	-0.26%
Center of glass	1.47	1.46	-0.46%	1.46	-0.50%	1.47	0.81%
Edge_sill	2.03	2.03	0.16%	2.03	0.00%	2.11	3.42%
Edge_head	2.03	2.03	0.22%	2.03	0.00%	2.11	3.36%
Edge_jamb	2.03	2.03	-0.15%	2.03	-0.18%	2.05	1.14%
TOTAL	**1.89**	**1.86**	**-1.52%**	**1.85**	**-2.20%**	**1.87**	**0.61%**
Hypothetical R10	**Spacer keff =**		**0.674**	**W/mK**			
Section	**T5/W5**	**2-D**	**% diff**	**2-D***	**% diff**	**3-D**	**% diff**
	W/m^{2}K	**W/m^{2}K**	**2D vs T5/W5**	**W/m^{2}K**	**2D* vs T5/W5**	**W/m^{2}K**	**3D vs 2-D**
Frame_sill	2.17	2.22	1.87%	2.23	2.43%	2.21	-0.35%
Frame_head	2.17	2.21	2.03%	2.23	2.47%	2.21	-0.43%
Frame_jamb	2.31	2.41	4.04%	2.35	1.50%	2.41	-0.03%
Center of glass	0.58	0.58	0.71%	0.58	0.74%	0.60	3.52%
Edge_sill	1.42	1.39	-2.73%	1.39	-2.71%	1.49	7.02%
Edge_head	1.43	1.39	-2.85%	1.39	-2.85%	1.49	7.00%
Edge_jamb	1.44	1.38	-3.99%	1.39	-3.96%	1.42	2.37%
TOTAL	**1.24**	**1.25**	**0.94%**	**1.24**	**0.05%**	**1.27**	**1.70%**

Table D3. PVC Window – Large Size, Highly Conducting Spacer

Dbl Clear	**Spacer keff =**		**1.900**	**W/mK**			
Section	**T5/W5**	**2-D**	**% diff**	**2-D***	**% diff**	**3-D**	**% diff**
	W/m^{2}K	**W/m^{2}K**	**2D vs T5/W5**	**W/m^{2}K**	**2D* vs T5/W5**	**W/m^{2}K**	**3D vs 2-D**
Frame_sill	2.66	2.56	-3.90%	2.58	-3.30%	2.51	-2.08%
Frame_head	2.66	2.56	-3.88%	2.57	-3.42%	2.51	-2.17%
Frame_jamb	2.88	2.77	-4.12%	2.70	-6.66%	2.75	-0.67%
Center of glass	2.80	2.80	-0.02%	2.79	-0.06%	2.80	0.16%
Edge_sill	3.15	3.15	-0.02%	3.15	0.03%	3.20	1.50%
Edge_head	3.15	3.15	0.03%	3.15	0.07%	3.20	1.49%
Edge_jamb	3.14	3.14	-0.02%	3.14	-0.02%	3.16	0.48%
TOTAL	**2.89**	**2.86**	**-1.00%**	**2.85**	**-1.44%**	**2.86**	**0.01%**
Dbl Low-e HC	**Spacer keff =**		**1.900**	**W/mK**			
Section	**T5/W5**	**2-D**	**% diff**	**2-D***	**% diff**	**3-D**	**% diff**
	W/m^{2}K	**W/m^{2}K**	**2D vs T5/W5**	**W/m^{2}K**	**2D* vs T5/W5**	**W/m^{2}K**	**3D vs 2-D**
Frame_sill	2.58	2.49	-3.82%	2.50	-3.31%	2.44	-1.72%
Frame_head	2.58	2.48	-3.85%	2.49	-3.47%	2.44	-1.79%
Frame_jamb	2.80	2.69	-4.27%	2.62	-6.82%	2.67	-0.48%
Center of glass	1.73	1.75	0.93%	1.75	0.89%	1.76	0.68%
Edge_sill	2.36	2.37	0.23%	2.37	0.15%	2.45	3.13%
Edge_head	2.36	2.37	0.30%	2.37	0.19%	2.45	3.10%
Edge_jamb	2.36	2.36	0.04%	2.36	0.08%	2.39	1.09%
TOTAL	**2.16**	**2.14**	**-0.98%**	**2.12**	**-1.55%**	**2.14**	**0.45%**
Dbl Low-e SC	**Spacer keff =**		**1.900**	**W/mK**			
Section	**T5/W5**	**2-D**	**% diff**	**2-D***	**% diff**	**3-D**	**% diff**
	W/m^{2}K	**W/m^{2}K**	**2D vs T5/W5**	**W/m^{2}K**	**2D* vs T5/W5**	**W/m^{2}K**	**3D vs 2-D**
Frame_sill	2.56	2.46	-3.94%	2.48	-3.35%	2.43	-1.53%
Frame_head	2.56	2.46	-3.96%	2.47	-3.52%	2.43	-1.61%
Frame_jamb	2.78	2.66	-4.39%	2.60	-6.90%	2.65	-0.38%
Center of glass	1.47	1.46	-0.40%	1.46	-0.43%	1.48	1.01%
Edge_sill	2.18	2.16	-0.64%	2.16	-0.63%	2.25	3.93%
Edge_head	2.17	2.16	-0.55%	2.16	-0.59%	2.25	3.88%
Edge_jamb	2.17	2.15	-0.84%	2.16	-0.71%	2.18	1.42%
TOTAL	**1.98**	**1.94**	**-1.88%**	**1.93**	**-2.46%**	**1.95**	**0.69%**
Hypothetical R10	**Spacer keff =**		**1.900**	**W/mK**			
Section	**T5/W5**	**2-D**	**% diff**	**2-D***	**% diff**	**3-D**	**% diff**
	W/m^{2}K	**W/m^{2}K**	**2D vs T5/W5**	**W/m^{2}K**	**2D* vs T5/W5**	**W/m^{2}K**	**3D vs 2-D**
Frame_sill	2.38	2.40	1.02%	2.42	1.70%	2.38	-1.05%
Frame_head	2.37	2.40	1.23%	2.42	1.79%	2.38	-1.11%
Frame_jamb	2.51	2.61	3.66%	2.54	1.32%	2.60	-0.24%
Center of glass	0.58	0.58	0.91%	0.58	0.94%	0.61	4.14%
Edge_sill	1.60	1.54	-3.98%	1.54	-3.79%	1.66	7.32%
Edge_head	1.60	1.54	-4.11%	1.54	-3.92%	1.66	7.32%
Edge_jamb	1.61	1.53	-5.13%	1.53	-4.96%	1.57	2.56%
TOTAL	**1.34**	**1.34**	**0.40%**	**1.33**	**-0.36%**	**1.36**	**1.72%**





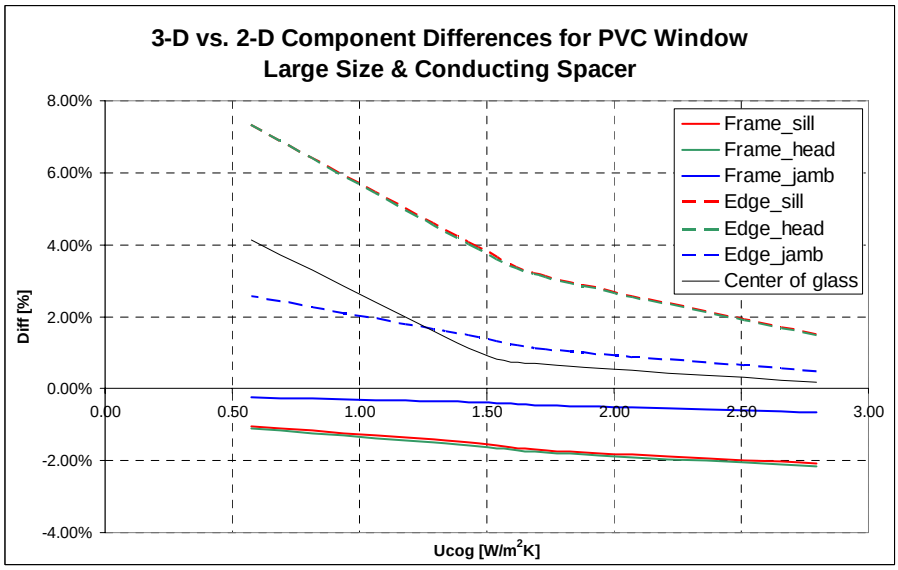


Figure D1. Component Level Difference Graphs for Large Size PVC Window

Table D4. PVC Window – Medium Size, Insulating Spacer

Dbl Clear	**Spacer keff =**		**0.050**	**W/mK**			
Section	**T5/W5**	**2-D**	**% diff**	**2-D***	**% diff**	**3-D**	**% diff**
	W/m^{2}K	**W/m^{2}K**	**2D vs T5/W5**	**W/m^{2}K**	**2D* vs T5/W5**	**W/m^{2}K**	**3D vs 2-D**
Frame_sill	2.11	2.04	-3.03%	2.04	-2.99%	2.02	-0.96%
Frame_head	2.11	2.04	-3.01%	2.04	-3.00%	2.02	-0.98%
Frame_jamb	2.33	2.24	-3.80%	2.17	-7.19%	2.23	-0.70%
Center of glass	2.80	2.79	-0.11%	2.79	-0.11%	2.79	0.03%
Edge_sill	2.82	2.83	0.34%	2.83	0.43%	2.85	0.56%
Edge_head	2.82	2.83	0.37%	2.83	0.43%	2.85	0.53%
Edge_jamb	2.83	2.84	0.23%	2.84	0.37%	2.85	0.31%
TOTAL	**2.65**	**2.63**	**-0.81%**	**2.62**	**-1.29%**	**2.63**	**-0.09%**
Dbl Low-e HC	**Spacer keff =**		**0.050**	**W/mK**			
Section	**T5/W5**	**2-D**	**% diff**	**2-D***	**% diff**	**3-D**	**% diff**
	W/m^{2}K	**W/m^{2}K**	**2D vs T5/W5**	**W/m^{2}K**	**2D* vs T5/W5**	**W/m^{2}K**	**3D vs 2-D**
Frame_sill	1.93	1.87	-3.14%	1.87	-3.20%	1.87	0.23%
Frame_head	1.93	1.87	-3.09%	1.87	-3.21%	1.87	0.20%
Frame_jamb	2.15	2.06	-3.89%	1.99	-7.54%	2.06	-0.24%
Center of glass	1.73	1.75	0.76%	1.75	0.76%	1.75	0.24%
Edge_sill	1.91	1.93	1.08%	1.93	1.04%	1.97	1.80%
Edge_head	1.91	1.93	1.12%	1.93	1.03%	1.97	1.76%
Edge_jamb	1.93	1.95	0.77%	1.95	0.85%	1.96	0.76%
TOTAL	**1.88**	**1.87**	**-0.54%**	**1.86**	**-1.27%**	**1.88**	**0.33%**
Dbl Low-e SC	**Spacer keff =**		**0.050**	**W/mK**			
Section	**T5/W5**	**2-D**	**% diff**	**2-D***	**% diff**	**3-D**	**% diff**
	W/m^{2}K	**W/m^{2}K**	**2D vs T5/W5**	**W/m^{2}K**	**2D* vs T5/W5**	**W/m^{2}K**	**3D vs 2-D**
Frame_sill	1.88	1.82	-3.39%	1.82	-3.47%	1.83	0.58%
Frame_head	1.88	1.82	-3.34%	1.82	-3.48%	1.83	0.55%
Frame_jamb	2.10	2.02	-4.12%	1.95	-7.84%	2.02	-0.09%
Center of glass	1.47	1.46	-0.63%	1.46	-0.62%	1.46	0.38%
Edge_sill	1.69	1.69	0.04%	1.69	-0.06%	1.74	2.40%
Edge_head	1.69	1.69	0.08%	1.69	-0.07%	1.74	2.36%
Edge_jamb	1.72	1.71	-0.25%	1.71	-0.19%	1.73	0.98%
TOTAL	**1.69**	**1.66**	**-1.59%**	**1.65**	**-2.42%**	**1.67**	**0.53%**
Hypothetical R10	**Spacer keff =**		**0.050**	**W/mK**			
Section	**T5/W5**	**2-D**	**% diff**	**2-D***	**% diff**	**3-D**	**% diff**
	W/m^{2}K	**W/m^{2}K**	**2D vs T5/W5**	**W/m^{2}K**	**2D* vs T5/W5**	**W/m^{2}K**	**3D vs 2-D**
Frame_sill	1.65	1.69	2.21%	1.69	2.07%	1.72	1.75%
Frame_head	1.65	1.69	2.32%	1.69	2.12%	1.72	1.71%
Frame_jamb	1.83	1.89	3.27%	1.82	-0.38%	1.90	0.39%
Center of glass	0.58	0.58	0.31%	0.58	0.34%	0.59	1.87%
Edge_sill	1.00	0.98	-2.80%	0.97	-3.25%	1.04	6.04%
Edge_head	1.01	0.98	-2.79%	0.97	-3.36%	1.04	5.98%
Edge_jamb	1.04	1.00	-4.37%	1.00	-4.45%	1.02	2.36%
TOTAL	**1.03**	**1.04**	**0.66%**	**1.02**	**-0.69%**	**1.05**	**1.70%**

Table D5. PVC Window – Medium Size, Medium Conducting Spacer

Dbl Clear	**Spacer keff =**		**0.674**	**W/mK**			
Section	**T5/W5**	**2-D**	**% diff**	**2-D***	**% diff**	**3-D**	**% diff**
	W/m^{2}K	**W/m^{2}K**	**2D vs T5/W5**	**W/m^{2}K**	**2D* vs T5/W5**	**W/m^{2}K**	**3D vs 2-D**
Frame_sill	2.50	2.42	-3.43%	2.44	-2.57%	2.39	-1.41%
Frame_head	2.50	2.42	-3.43%	2.44	-2.57%	2.39	-1.40%
Frame_jamb	2.71	2.62	-3.52%	2.56	-5.74%	2.61	-0.41%
Center of glass	2.80	2.79	-0.06%	2.79	-0.05%	2.80	0.16%
Edge_sill	3.05	3.06	0.41%	3.07	0.80%	3.11	1.67%
Edge_head	3.05	3.06	0.43%	3.07	0.80%	3.11	1.65%
Edge_jamb	3.04	3.05	0.33%	3.07	0.81%	3.08	1.00%
TOTAL	**2.82**	**2.79**	**-0.01**	**2.79**	**-1.01%**	**2.80**	**0.20%**
Dbl Low-e HC	**Spacer keff =**		**0.674**	**W/mK**			
Section	**T5/W5**	**2-D**	**% diff**	**2-D***	**% diff**	**3-D**	**% diff**
	W/m^{2}K	**W/m^{2}K**	**2D vs T5/W5**	**W/m^{2}K**	**2D* vs T5/W5**	**W/m^{2}K**	**3D vs 2-D**
Frame_sill	2.40	2.32	-3.32%	2.34	-2.33%	2.31	-0.68%
Frame_head	2.40	2.32	-3.32%	2.36	-1.47%	2.31	-0.67%
Frame_jamb	2.61	2.52	-3.56%	2.47	-5.70%	2.52	0.00%
Center of glass	1.73	1.75	0.90%	1.75	0.91%	1.76	0.61%
Edge_sill	2.23	2.25	0.87%	2.26	1.50%	2.33	3.63%
Edge_head	2.23	2.25	0.90%	2.26	1.50%	2.33	3.61%
Edge_jamb	2.23	2.24	0.73%	2.26	1.55%	2.29	2.03%
TOTAL	**2.09**	**2.07**	**-0.01**	**2.07**	**-0.68%**	**2.09**	**0.84%**
Dbl Low-e SC	**Spacer keff =**		**0.674**	**W/mK**			
Section	**T5/W5**	**2-D**	**% diff**	**2-D***	**% diff**	**3-D**	**% diff**
	W/m^{2}K	**W/m^{2}K**	**2D vs T5/W5**	**W/m^{2}K**	**2D* vs T5/W5**	**W/m^{2}K**	**3D vs 2-D**
Frame_sill	2.37	2.30	-3.42%	2.32	-2.39%	2.28	-0.48%
Frame_head	2.37	2.30	-3.41%	2.32	-2.39%	2.28	-0.48%
Frame_jamb	2.58	2.49	-3.67%	2.44	-5.79%	2.49	0.11%
Center of glass	1.47	1.46	-0.43%	1.46	-0.41%	1.47	0.88%
Edge_sill	2.03	2.03	0.09%	2.05	0.83%	2.13	4.43%
Edge_head	2.03	2.03	0.09%	2.05	0.82%	2.13	4.44%
Edge_jamb	2.03	2.03	-0.09%	2.05	0.88%	2.08	2.45%
TOTAL	**1.91**	**1.88**	**-0.01**	**1.88**	**-1.62%**	**1.90**	**1.11%**
Hypothetical R10	**Spacer keff =**		**0.674**	**W/mK**			
Section	**T5/W5**	**2-D**	**% diff**	**2-D***	**% diff**	**3-D**	**% diff**
	W/m^{2}K	**W/m^{2}K**	**2D vs T5/W5**	**W/m^{2}K**	**2D* vs T5/W5**	**W/m^{2}K**	**3D vs 2-D**
Frame_sill	2.17	2.22	2.14%	2.25	3.25%	2.23	0.16%
Frame_head	2.17	2.22	2.33%	2.25	3.43%	2.23	0.17%
Frame_jamb	2.31	2.41	4.26%	2.37	2.39%	2.43	0.47%
Center of glass	0.58	0.58	1.00%	0.58	1.11%	0.60	3.58%
Edge_sill	1.42	1.39	-2.64%	1.40	-1.38%	1.51	8.32%
Edge_head	1.43	1.39	-2.74%	1.40	-1.52%	1.51	8.31%
Edge_jamb	1.44	1.39	-3.91%	1.41	-2.20%	1.45	4.54%
TOTAL	**1.27**	**1.29**	**1.18%**	**1.29**	**1.11%**	**1.32**	**2.52%**

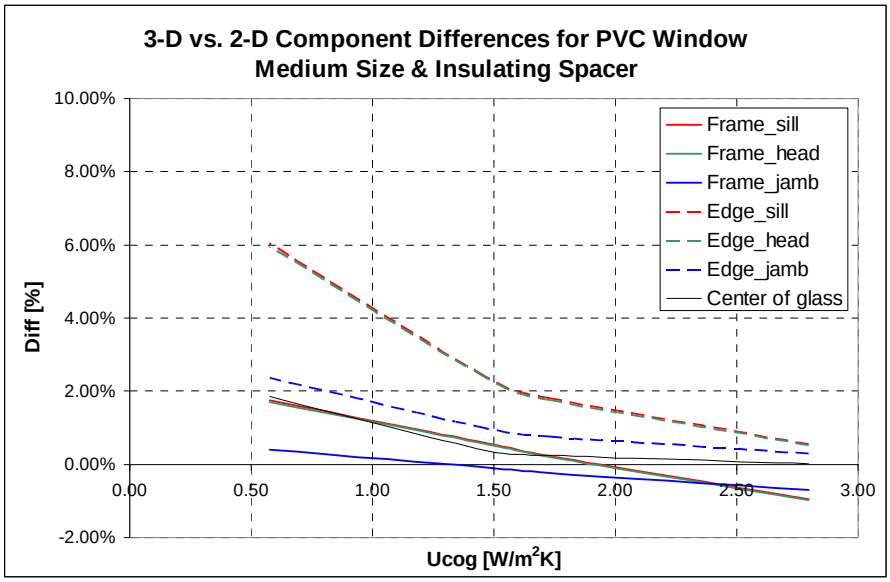
Table D6. PVC Window – Medium Size, Highly Conducting Spacer

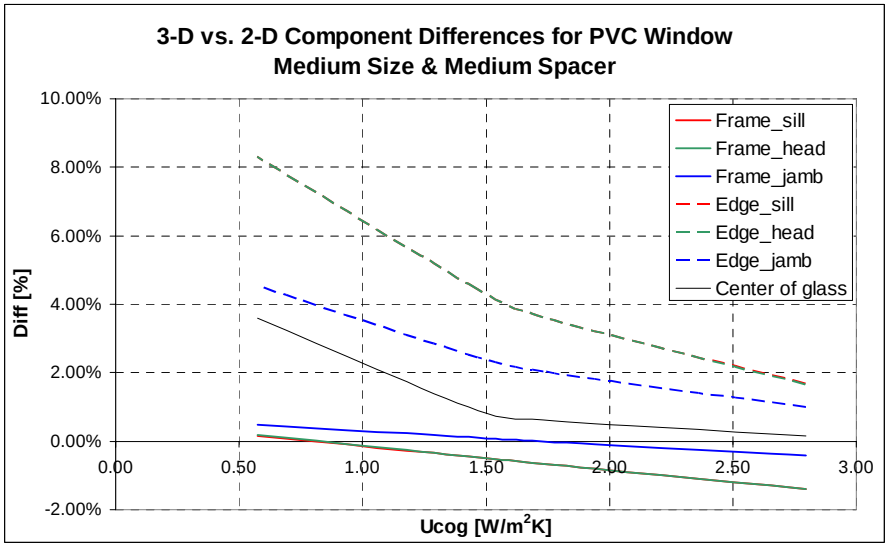
Dbl Clear	Spacer keff =		1.900	W/mK			
Section	**T5/W5**	**2-D**	**% diff**	**2-D***	**% diff**	**3-D**	**% diff**
	W/m^{2}K	**W/m^{2}K**	**2D vs T5/W5**	**W/m^{2}K**	**2D* vs T5/W5**	**W/m^{2}K**	**3D vs 2-D**
Frame_sill	2.66	2.57	-3.62%	2.60	-2.41%	2.53	-1.51%
Frame_head	2.66	2.57	-3.60%	2.60	-2.38%	2.53	-1.48%
Frame_jamb	2.88	2.77	-3.92%	2.73	-5.65%	2.76	-0.24%
Center of glass	2.80	2.79	-0.04%	2.80	-0.03%	2.80	0.22%
Edge_sill	3.15	3.15	0.04%	3.17	0.51%	3.22	2.02%
Edge_head	3.15	3.15	0.09%	3.17	0.54%	3.22	2.00%
Edge_jamb	3.14	3.14	0.00%	3.16	0.59%	3.18	1.21%
TOTAL	**2.89**	**2.86**	**-0.01**	**2.86**	**-1.07%**	**2.87**	**0.31%**

Dbl Low-e HC	Spacer keff =		1.900	W/mK			
Section	**T5/W5**	**2-D**	**% diff**	**2-D***	**% diff**	**3-D**	**% diff**
	W/m^{2}K	**W/m^{2}K**	**2D vs T5/W5**	**W/m^{2}K**	**2D* vs T5/W5**	**W/m^{2}K**	**3D vs 2-D**
Frame_sill	2.58	2.49	-3.68%	2.52	-2.25%	2.47	-0.86%
Frame_head	2.58	2.49	-3.70%	2.52	-2.25%	2.47	-0.84%
Frame_jamb	2.80	2.69	-4.07%	2.65	-5.62%	2.70	0.17%
Center of glass	1.73	1.75	0.95%	1.75	0.97%	1.76	0.75%
Edge_sill	2.36	2.37	0.14%	2.39	0.95%	2.47	4.13%
Edge_head	2.36	2.37	0.19%	2.39	0.99%	2.47	4.12%
Edge_jamb	2.36	2.36	0.07%	2.39	1.09%	2.42	2.36%
TOTAL	**2.17**	**2.15**	**-0.01**	**2.15**	**-0.89%**	**2.18**	**1.02%**

Dbl Low-e SC	Spacer keff =		1.900	W/mK			
Section	**T5/W5**	**2-D**	**% diff**	**2-D***	**% diff**	**3-D**	**% diff**
	W/m^{2}K	**W/m^{2}K**	**2D vs T5/W5**	**W/m^{2}K**	**2D* vs T5/W5**	**W/m^{2}K**	**3D vs 2-D**
Frame_sill	2.56	2.47	-3.79%	2.50	-2.30%	2.45	-0.69%
Frame_head	2.56	2.47	-3.81%	2.50	-2.30%	2.45	-0.66%
Frame_jamb	2.78	2.67	-4.20%	2.63	-5.69%	2.68	0.28%
Center of glass	1.47	1.46	-0.36%	1.46	-0.33%	1.48	1.07%
Edge_sill	2.18	2.16	-0.73%	2.18	0.23%	2.27	4.97%
Edge_head	2.17	2.16	-0.67%	2.18	0.27%	2.27	4.96%
Edge_jamb	2.17	2.15	-0.80%	2.18	0.41%	2.22	2.83%
TOTAL	**2.00**	**1.96**	**-0.02**	**1.96**	**-1.72%**	**1.99**	**1.32%**

Hypothetical R10	Spacer keff =		1.900	W/mK			
Section	**T5/W5**	**2-D**	**% diff**	**2-D***	**% diff**	**3-D**	**% diff**
	W/m^{2}K	**W/m^{2}K**	**2D vs T5/W5**	**W/m^{2}K**	**2D* vs T5/W5**	**W/m^{2}K**	**3D vs 2-D**
Frame_sill	2.38	2.41	1.25%	2.45	2.85%	2.41	-0.14%
Frame_head	2.37	2.41	1.47%	2.45	3.10%	2.41	-0.09%
Frame_jamb	2.51	2.61	3.84%	2.58	2.62%	2.63	0.63%
Center of glass	0.58	0.58	1.25%	0.58	1.39%	0.61	4.22%
Edge_sill	1.60	1.54	-3.93%	1.56	-2.26%	1.69	8.79%
Edge_head	1.60	1.54	-4.06%	1.56	-2.37%	1.69	8.84%
Edge_jamb	1.61	1.53	-5.10%	1.56	-2.97%	1.61	4.98%
TOTAL	**1.37**	**1.38**	**0.57%**	**1.39**	**0.95%**	**1.42**	**2.80%**





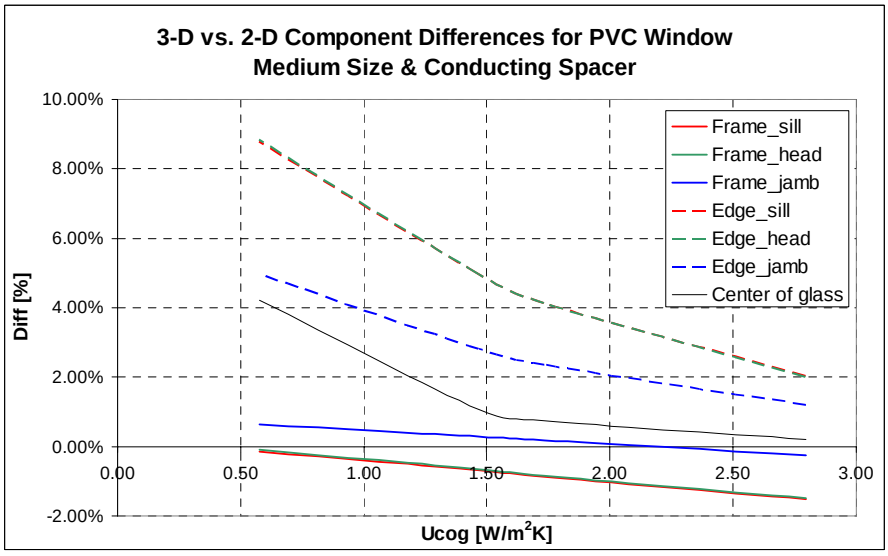


Figure D2. Component Level Difference Graphs for Medium Size PVC Window

Table D7. PVC Window – Small Size, Insulating Spacer

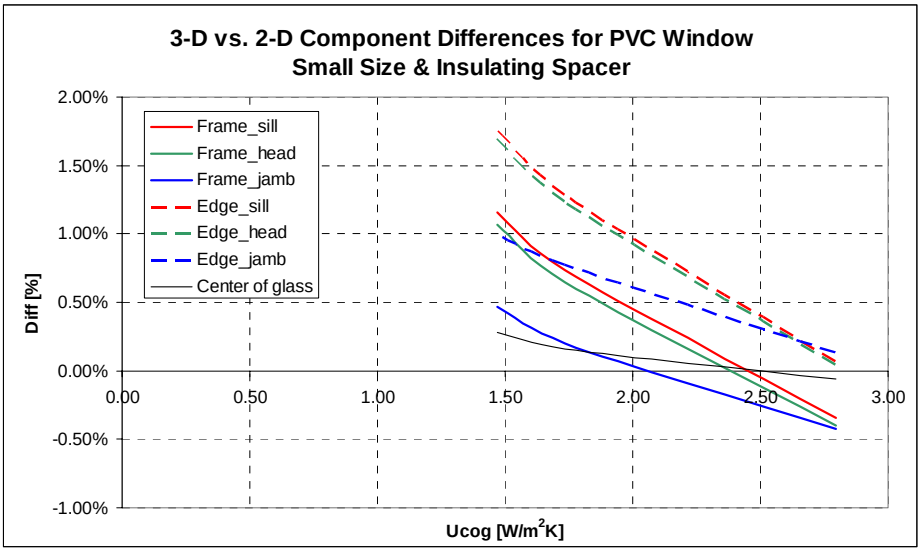
Dbl Clear	Spacer keff =		0.050	W/mK			
Section	**T5/W5**	**2-D**	**% diff**	**2-D***	**% diff**	**3-D**	**% diff**
	W/m^{2}K	**W/m^{2}K**	**2D vs T5/W5**	**W/m^{2}K**	**2D* vs T5/W5**	**W/m^{2}K**	**3D vs 2-D**
Frame_sill	2.11	2.03	-3.49%	2.05	-2.81%	2.03	-0.35%
Frame_head	2.11	2.03	-3.49%	2.05	-2.89%	2.03	-0.40%
Frame_jamb	2.33	2.23	-4.17%	2.17	-7.01%	2.22	-0.43%
Center of glass	2.80	2.80	-0.03%	2.79	-0.11%	2.79	-0.06%
Edge_sill	2.82	2.83	0.24%	2.82	0.10%	2.83	0.07%
Edge_head	2.82	2.83	0.27%	2.82	0.11%	2.83	0.05%
Edge_jamb	2.83	2.84	0.15%	2.83	0.02%	2.84	0.13%
TOTAL	**2.63**	**2.61**	**-0.01**	**2.60**	**-1.38%**	**2.61**	**-0.14%**
Dbl Low-e HC	**Spacer keff =**		**0.050**	**W/mK**			
Section	**T5/W5**	**2-D**	**% diff**	**2-D***	**% diff**	**3-D**	**% diff**
	W/m^{2}K	**W/m^{2}K**	**2D vs T5/W5**	**W/m^{2}K**	**2D* vs T5/W5**	**W/m^{2}K**	**3D vs 2-D**
Frame_sill	1.93	1.86	-3.59%	1.87	-3.11%	1.87	0.74%
Frame_head	1.93	1.86	-3.55%	1.87	-3.18%	1.87	0.65%
Frame_jamb	2.15	2.06	-4.33%	2.00	-7.44%	2.06	0.20%
Center of glass	1.73	1.75	0.88%	1.75	0.80%	1.75	0.16%
Edge_sill	1.91	1.93	1.03%	1.93	0.78%	1.96	1.29%
Edge_head	1.91	1.93	1.07%	1.93	0.76%	1.96	1.23%
Edge_jamb	1.93	1.94	0.61%	1.94	0.40%	1.96	0.78%
TOTAL	**1.89**	**1.87**	**-0.01**	**1.86**	**-1.38%**	**1.88**	**0.41%**
Dbl Low-e SC	**Spacer keff =**		**0.050**	**W/mK**			
Section	**T5/W5**	**2-D**	**% diff**	**2-D***	**% diff**	**3-D**	**% diff**
	W/m^{2}K	**W/m^{2}K**	**2D vs T5/W5**	**W/m^{2}K**	**2D* vs T5/W5**	**W/m^{2}K**	**3D vs 2-D**
Frame_sill	1.88	1.81	-3.86%	1.82	-3.29%	1.84	1.16%
Frame_head	1.88	1.81	-3.80%	1.82	-3.36%	1.83	1.07%
Frame_jamb	2.10	2.01	-4.57%	1.95	-7.66%	2.02	0.47%
Center of glass	1.47	1.46	-0.47%	1.46	-0.57%	1.47	0.28%
Edge_sill	1.69	1.69	-0.04%	1.69	-0.44%	1.72	1.77%
Edge_head	1.69	1.69	0.02%	1.69	-0.46%	1.72	1.70%
Edge_jamb	1.72	1.71	-0.44%	1.70	-0.79%	1.72	0.99%
TOTAL	**1.70**	**1.67**	**-0.02**	**1.66**	**-2.48%**	**1.68**	**0.65%**

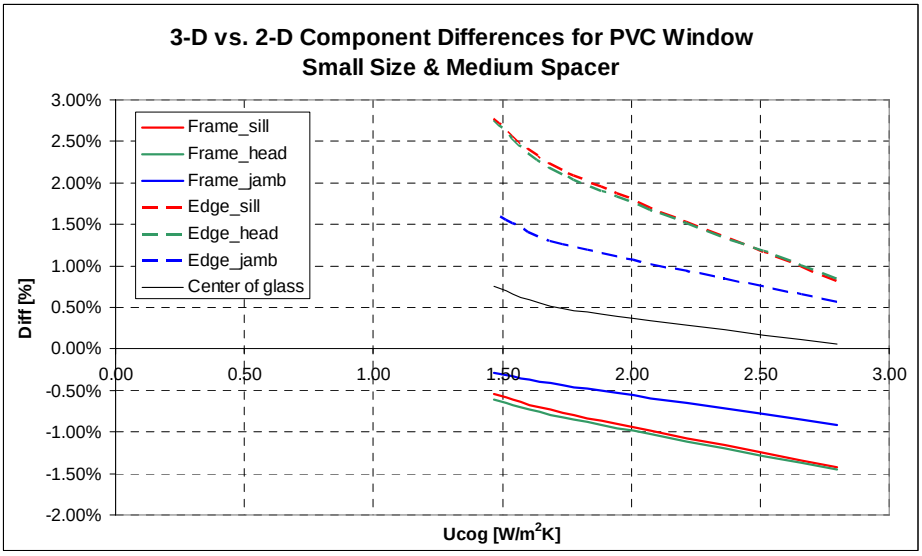
Table D8. PVC Window – Small Size, Medium Conducting Spacer

Dbl Clear	**Spacer keff =**		**0.674**	**W/mK**			
Section	**T5/W5**	**2-D**	**% diff**	**2-D***	**% diff**	**3-D**	**% diff**
	W/m^{2}K	**W/m^{2}K**	**2D vs T5/W5**	**W/m^{2}K**	**2D* vs T5/W5**	**W/m^{2}K**	**3D vs 2-D**
Frame_sill	2.50	2.41	-3.72%	2.43	-2.92%	2.38	-1.42%
Frame_head	2.50	2.41	-3.74%	2.43	-2.99%	2.38	-1.45%
Frame_jamb	2.71	2.61	-3.74%	2.56	-6.10%	2.59	-0.91%
Center of glass	2.80	2.80	0.04%	2.79	-0.04%	2.80	0.06%
Edge_sill	3.05	3.06	0.38%	3.05	0.21%	3.08	0.83%
Edge_head	3.05	3.06	0.34%	3.05	0.21%	3.08	0.85%
Edge_jamb	3.04	3.05	0.30%	3.05	0.11%	3.07	0.57%
TOTAL	**2.81**	**2.79**	**-0.01**	**2.77**	**-1.31%**	**2.78**	**-0.13%**
Dbl Low-e HC	**Spacer keff =**		**0.674**	**W/mK**			
Section	**T5/W5**	**2-D**	**% diff**	**2-D***	**% diff**	**3-D**	**% diff**
	W/m^{2}K	**W/m^{2}K**	**2D vs T5/W5**	**W/m^{2}K**	**2D* vs T5/W5**	**W/m^{2}K**	**3D vs 2-D**
Frame_sill	2.40	2.32	-3.54%	2.34	-2.66%	2.30	-0.77%
Frame_head	2.40	2.32	-3.53%	2.33	-2.73%	2.30	-0.83%
Frame_jamb	2.61	2.51	-3.78%	2.46	-6.08%	2.50	-0.44%
Center of glass	1.73	1.75	1.08%	1.75	1.00%	1.76	0.49%
Edge_sill	2.23	2.25	0.91%	2.24	0.40%	2.30	2.16%
Edge_head	2.23	2.25	0.95%	2.24	0.39%	2.30	2.11%
Edge_jamb	2.23	2.24	0.69%	2.23	0.21%	2.27	1.26%
TOTAL	**2.11**	**2.09**	**-0.01**	**2.08**	**-1.25%**	**2.10**	**0.38%**
Dbl Low-e SC	**Spacer keff =**		**0.674**	**W/mK**			
Section	**T5/W5**	**2-D**	**% diff**	**2-D***	**% diff**	**3-D**	**% diff**
	W/m^{2}K	**W/m^{2}K**	**2D vs T5/W5**	**W/m^{2}K**	**2D* vs T5/W5**	**W/m^{2}K**	**3D vs 2-D**
Frame_sill	2.37	2.29	-3.65%	2.31	-2.71%	2.28	-0.55%
Frame_head	2.37	2.29	-3.64%	2.31	-2.79%	2.28	-0.61%
Frame_jamb	2.58	2.48	-3.92%	2.43	-6.18%	2.48	-0.29%
Center of glass	1.47	1.47	-0.20%	1.46	-0.27%	1.48	0.76%
Edge_sill	2.03	2.03	0.18%	2.02	-0.44%	2.09	2.78%
Edge_head	2.03	2.03	0.18%	2.02	-0.45%	2.09	2.76%
Edge_jamb	2.03	2.03	-0.15%	2.02	-0.68%	2.06	1.64%
TOTAL	**1.94**	**1.91**	**-0.02**	**1.90**	**-2.10%**	**1.92**	**0.64%**

Table D9. PVC Window – Small Size, Highly Conducting Spacer

Dbl Clear	**Spacer keff =**		**1.900**	**W/mK**			
Section	**T5/W5**	**2-D**	**% diff**	**2-D***	**% diff**	**3-D**	**% diff**
	W/m^{2}K	**W/m^{2}K**	**2D vs T5/W5**	**W/m^{2}K**	**2D* vs T5/W5**	**W/m^{2}K**	**3D vs 2-D**
Frame_sill	2.66	2.56	-3.87%	2.59	-2.79%	2.52	-1.63%
Frame_head	2.66	2.56	-3.84%	2.59	-2.84%	2.52	-1.68%
Frame_jamb	2.88	2.77	-4.10%	2.71	-6.14%	2.74	-0.97%
Center of glass	2.80	2.80	0.07%	2.80	-0.03%	2.80	0.10%
Edge_sill	3.15	3.15	0.00%	3.14	-0.36%	3.17	0.73%
Edge_head	3.15	3.15	0.05%	3.14	-0.31%	3.18	0.88%
Edge_jamb	3.14	3.14	0.00%	3.13	-0.33%	3.16	0.53%
TOTAL	**2.89**	**2.86**	**-0.01**	**2.85**	**-1.47%**	**2.85**	**-0.15%**
Dbl Low-e HC	**Spacer keff =**		**1.900**	**W/mK**			
Section	**T5/W5**	**2-D**	**% diff**	**2-D***	**% diff**	**3-D**	**% diff**
	W/m^{2}K	**W/m^{2}K**	**2D vs T5/W5**	**W/m^{2}K**	**2D* vs T5/W5**	**W/m^{2}K**	**3D vs 2-D**
Frame_sill	2.58	2.48	-3.84%	2.51	-2.71%	2.46	-1.16%
Frame_head	2.58	2.48	-3.86%	2.51	-2.75%	2.46	-1.16%
Frame_jamb	2.80	2.69	-4.26%	2.64	-6.15%	2.67	-0.53%
Center of glass	1.73	1.75	1.16%	1.75	1.08%	1.76	0.63%
Edge_sill	2.36	2.37	0.20%	2.36	-0.19%	2.43	2.64%
Edge_head	2.36	2.37	0.26%	2.36	-0.19%	2.43	2.57%
Edge_jamb	2.36	2.36	0.05%	2.35	-0.34%	2.40	1.58%
TOTAL	**2.20**	**2.18**	**-0.01**	**2.17**	**-1.48%**	**2.19**	**0.47%**
Dbl Low-e SC	**Spacer keff =**		**1.900**	**W/mK**			
Section	**T5/W5**	**2-D**	**% diff**	**2-D***	**% diff**	**3-D**	**% diff**
	W/m^{2}K	**W/m^{2}K**	**2D vs T5/W5**	**W/m^{2}K**	**2D* vs T5/W5**	**W/m^{2}K**	**3D vs 2-D**
Frame_sill	2.56	2.46	-3.96%	2.49	-2.76%	2.44	-0.96%
Frame_head	2.56	2.46	-3.98%	2.49	-2.82%	2.44	-0.99%
Frame_jamb	2.78	2.66	-4.40%	2.62	-6.26%	2.65	-0.41%
Center of glass	1.47	1.47	-0.09%	1.47	-0.17%	1.48	0.93%
Edge_sill	2.18	2.16	-0.67%	2.15	-1.25%	2.23	3.15%
Edge_head	2.17	2.16	-0.60%	2.15	-1.22%	2.23	3.12%
Edge_jamb	2.17	2.15	-0.83%	2.14	-1.34%	2.19	1.87%
TOTAL	**2.03**	**2.00**	**-0.02**	**1.99**	**-2.36%**	**2.01**	**0.68%**





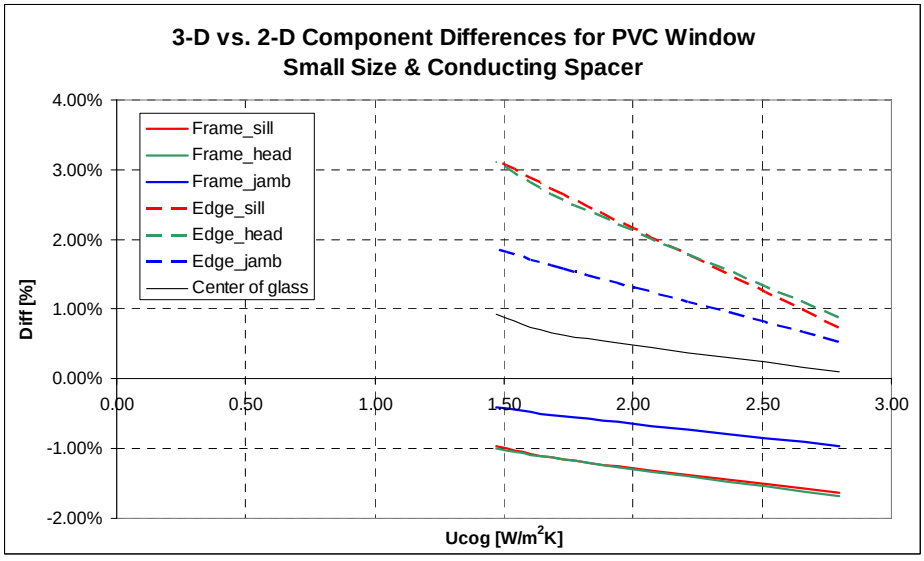


Figure D3. Component Level Difference Graphs for Small Size PVC Window

Project 1.1.3

Project Name: Thermal Comfort Rating

Date: February 7, 2006

Purpose: The purpose of this study was to; (1) Review the literature to identify relevant work relating to windows and thermal comfort, (2) Develop an improved understanding of the impact of windows on thermal comfort and to propose an analytical method for evaluating this impact. The method could form the basis for a future NFRC window comfort rating method that could be used by both designers and consumers.

Project Summary:

In this report, we provided a thorough literature study on the impacts of windows on thermal comfort and more generally on comfort in asymmetrical environments, such as environments with cool or warm ceilings, walls, or floors.

In evaluating comfort in highly asymmetrical environments, such as the environment with cold or hot windows, local discomfort is very important. The UCB comfort model predicts comfort for 16 body parts, as well as for the whole body. The model is therefore well-suited to evaluate nonuniform thermal environments.

A single index for rating the thermal comfort performance of a window is not practical because the winter and summer performance are dependent on largely unrelated characteristics of the window. We therefore have identified several possible ratings for winter and summer and have recommended one of these for each season.

To illustrate how the methods we describe in this report could be applied to a comfort rating, we chose geometries with large view factors. This assumption will show larger differences between window products than if a geometry with a smaller view factor is used.

Click here for final report



WINDOW PERFORMANCE FOR HUMAN THERMAL COMFORT

FINAL REPORT TO THE NATIONAL FENESTRATION RATING COUNCIL

FEBRUARY 2006

CENTER FOR THE BUILT ENVIRONMENT

CHARLIE HUIZENGA
HUI ZHANG
PIETER MATTELAER
TIEFENG YU
EDWARD ARENS

UNIVERSITY OF CALIFORNIA, BERKELEY
390 WURSTER HALL
UNIVERSITY OF CALIFORNIA, BERKELEY
BERKELEY, CA 94720-1839

ARUP

PETER LYONS

ARUP FAÇADE ENGINEERING
LEVEL 17
1 NICHOLSON STREET
MELBOURNE
VIC 3000
AUSTRALIA

TABLE OF CONTENTS

EXECUTIVE SUMMARY ..... **I**
1 INTRODUCTION **5**
2 OBJECTIVE **5**
3 LITERATURE REVIEW **5**
3.1 HOW WINDOWS INFLUENCE COMFORT 5
3.2 SHORT-WAVE RADIATION 7
3.3 LONG-WAVE RADIATION 8
3.4 UNWANTED AIR MOVEMENT (DRAFT) 17
3.5 THERMAL COMFORT MODELS 22
3.6 LOCAL DISCOMFORT 25
4 UC BERKELEY COMFORT MODEL **26**
4.1 MODEL DESCRIPTION 26
4.2 MODEL COMPARISON 29
5 ASSESSMENT OF WINDOW COMFORT **32**
5.1 PRIMARY FACTORS INFLUENCING WINDOW COMFORT 32
5.2 INTERIOR AIR TEMPERATURE VS. WINDOW SURFACE TEMPERATURE 34
5.3 IMPACT OF WINDOW TEMPERATURE ON INTERIOR AIR TEMPERATURE 35
5.4 IMPACT OF GEOMETRY 35
5.5 FRAME AND EDGE EFFECT 41
5.6 IMPACT OF DIFFUSE RADIATION 44
5.7 IMPACT OF DIRECT RADIATION 49
5.8 MAXIMUM ALLOWABLE SOLAR RADIATION 50
5.9 WINDOW OPTICAL PROPERTY CHARACTERIZATION 54
6 RATING METHODS FOR WINDOW COMFORT **56**
6.1 POSSIBLE ALTERNATIVES 56
6.2 WINTER RATING METHOD 56
6.3 SUMMER RATING METHOD 62
7 SUMMARY **65**
8 ANNOTATED BIBLIOGRAPHY **66**
9 REFERENCES **76**

TABLE OF FIGURES

Figure 1: Winter window comfort rating – Minimum allowable exterior temperature 3
Figure 2: Window impacts on thermal comfort: solar radiation, long-wave radiation, convective drafts 6
Figure 3: Percentage of comfort in relation to thermal sensation (McNall and Biddison 1970) 10
Figure 4: Local thermal discomfort caused by radiant asymmetry (ASHRAE Standard 55 – 2004, same figure as presented by Fanger et al. 1985) 11
Figure 5: Local discomfort caused by warm and cold floors (ASHRAE 55 – 2004) 16
Figure 6: Allowable mean air speed as a function of air temperature and turbulence intensity (Fountain and Arens 1993) 18
Figure 7: Air speed required to offset increased temperature (Fountain and Arens 1993) 18
Figure 8: Range of velocity requirements (Fountain and Arens 1993) 19
Figure 9: Openings in window sill to reduce draft down flow (Ruegg et al. 2004) 21
Figure 10: EHT piste and ideal profiles for a driver in winter (left) and summer (right) (Wyon 2004) 25
Figure 11: Subdivision into 16 body parts used in UCB comfort model 26
Figure 12: Polygons used to calculate radiation heat exchange in UCB comfort model 27
Figure 13: Prediction of local as well as overall sensation/comfort in UCB comfort model 27
Figure 14: Screenshot of UCB comfort model interface 28
Figure 15: Screenshots of "room editor" and boundary conditions from UCB comfort model 29
Figure 16: Geometric input data for comfort simulation 29
Figure 17: Overall sensation – PMV vs. UCB model 30
Figure 18: Comfort limits – PMV vs. UCB model 31
Figure 19: Factors influencing window comfort 32
Figure 20: Schematic diagram illustrating how geometry influences view factor 33
Figure 21: Interior air temperature at which maximum comfort occurs for different window surface temperatures 34
Figure 22: Window geometry for simulated cases 36
Figure 23: View factor data for a seated person in one-foot increments for a vertical wall. 37
Figure 24: Effect of window/room geometry 39
Figure 25: Depth of zone of discomfort for different view factors 40
Figure 26: Spatial distribution of comfort 41
Figure 27: Influence of window components on overall window comfort 42
Figure 28: Explicit modeling of window components vs. uniform window temperature 42
Figure 29: Different window configurations considered for calculation of overall window comfort 43
Figure 30: Diffuse solar radiation from the sky and reflected from the ground 45
Figure 31: Calculation of diffuse radiation - Assume entire view is sky 46
Figure 32: Calculation of diffuse radiation - Assume entire view is ground 47

Figure 33: Calculation of diffuse radiation - Weighted glass temperature 48
Figure 34: Impact of direct solar radiation, case B geometry 50
Figure 35: Scenario 1 – Maximum allowable direct solar radiation to maintain indoor comfort 52
Figure 36: Scenario 2 – Maximum allowable direct solar radiation to maintain indoor comfort 53
Figure 37: Comparison – Maximum allowable direct solar radiation with/without direct exposure 54
Figure 38: Regression of Maximum allowable solar radiation with Tsol and $SHGC_{indirect}$ 55
Figure 39: Winter glazing comfort rating - Minimum allowable outdoor temperature 58
Figure 40: Winter window comfort rating - Minimum allowable outdoor temperature 59
Figure 41: Linear regression between window R-value (1/U-factor) and minimum allowable outdoor temperature 60
Figure 42: Energy Star climate zones and recommended window performance 61
Figure 43: Diffuse radiation – Summer comfort index as a function of solar transmittance and SHGC 64
Figure 44: Direct radiation - Summer comfort index as a function of solar transmittance and SHGC 64

TABLE OF TABLES

Table 1: Winter rating – Boundary conditions 2
Table 2: Summer comfort ratings for example glass types 4
Table 3: Advanced glazing (Clarke et al. 1998) 8
Table 4: Allowable radiant temperature asymmetry (ASHRAE 55 – 2004) 12
Table 5: Example window temperature impact for different window types 35
Table 6: Inside window surface temperature required to be comfortable (1m from window) 40
Table 7: Calculation of area-weighted window temperature (low performance frame) 43
Table 8: Local hand comfort for different window configurations (low performance frame) 43
Table 9: Calculation of area-weighted window temperature (high performance frame) 44
Table 10: Local hand comfort for different window configurations (high performance frame) 44
Table 11: Equivalent glass temperature increase due to diffuse radiation 49
Table 12: Range of glazing systems 51
Table 13: Glazing build-up and performance 57
Table 14: Window build-up and performance 59
Table 15: Window comfort assessment vs. Energy Star recommendations 62
Table 16: Comfort SHGC for different glazing systems – diffuse / direct radiation 63

EXECUTIVE SUMMARY

Anyone who has ever sat near a cold window on a winter day or in direct sunlight on a hot day recognizes that windows can cause thermal discomfort. In spite of this broad recognition there is no standard method to quantify the extent of such discomfort. The purpose of this study was to:

1. Review the literature to identify relevant work relating to windows and thermal comfort.
2. Develop an improved understanding of the impact of windows on thermal comfort and to propose an analytical method for evaluating this impact. The method could form the basis for a future NFRC window comfort rating method that could be used by both designers and consumers.

Literature review. We identified nearly 200 papers, articles and books that contain relevant information to the topic. This report summarizes the conclusions in some detail and also includes an annotated bibliography of 42 of the most important of these sources. We hope that this review serves as an excellent primer on the ways in which windows affect thermal comfort.

In brief, while there has been considerable work done on the fundamental issues related to windows and thermal comfort (e.g. long-wave radiant heat transfer, solar transmittance, induced convection) there is a lack of research that specifically addresses how to evaluate comfort at a level of detail sufficient to compare one window product to another that could be used as a basis for a rating system.

Analysis. Thermal comfort is influenced by a combination of physical, physiological and psychological factors. ASHRAE Standard 55 defines thermal comfort as "that state of mind which expresses satisfaction with the thermal environment." Over the last century, considerable research has been undertaken on the factors that influence thermal comfort. The basis for our analysis in this report was simulation rather than physical testing with human subjects. Human subject testing is both expensive and difficult to carry out. Fortunately, models of thermal comfort have been developed that can be used to predict subjective comfort assessment and these models have been validated against human subject studies. The PMV model (Fanger 1970) is the most widely used thermal comfort model. However, this model was developed using tests that were done in uniform thermal environments and windows almost always create asymmetric thermal environments. Because of this and other limitations of the PMV model, UC Berkeley has developed a more sophisticated thermal comfort model that is capable of assessing comfort in non-uniform, non-steady-state conditions (Zhang 2003, Huizenga 2001). This model is capable of predicting *local* discomfort such as what is typically caused by a hot or cold window.

We used the UCB Comfort Model to assess a wide range of conditions that might be created by a wide range of window products. The two most significant aspects of windows and comfort that we focused on are 1) the effect of window surface temperature on long-wave radiation heat exchange between the body and the window, and 2) the effect of solar radiation transmitted by the window and absorbed by the body. With respect to solar radiation, we considered only diffuse radiation based on notion that direct sun falling on the body will cause discomfort in all but the coolest environments and that some action will be taken by the occupant to mitigate direct sun. Diffuse solar still has a significant effect on comfort, though significantly less than direct solar. To simplify the analysis process, we developed a method to represent the effect of diffuse solar radiation as an equivalent rise in temperature of the window that would result in the same overall heat gain to the body from the window. This method, detailed in the report, allowed us to model both effects by changing the window surface temperature.

Another key factor in determining the impact of a window on comfort is geometry. Obviously, the closer a person is to a window, or the larger the window, the greater the impact on comfort.

These two parameters, distance to the window and window size, combine to define the *view factor* between the person and the window. The greater the view factor, the greater the impact on comfort the window can have. We created some standard geometries to define a range of view factors. These included distance from the window of 1m, 2m, and 4m; window sizes from a single double-hung window (1.2m x 1.5m) to a fully-glazed façade; and windows on a single wall or windows on two adjacent walls. To illustrate how the methods we describe in this report could be applied to a comfort rating, we chose geometries with large view factors to calculate possible indices. This was done to clearly differentiate between different window products. In any rating method that might be adopted by NFRC, these assumptions will need to be considered carefully to meet the objectives of the council.

Comfort effects of windows are fundamentally different in summer and winter. The winter effect is largely driven by inside window surface temperature, which in turn is tightly correlated with window U-factor and outside temperature. The summer effect is driven by a combination of the inside surface temperature and transmitted solar radiation, both of which are heavily influenced by the optical properties of the window. As a result, our recommendation is to include both a winter and summer comfort rating, akin to the U-factor (nominally a winter rating) and SHGC (nominally a summer rating) currently used.

Winter Rating. The winter comfort impact is driven by the inside glass surface temperature. As such, we propose that this rating be based on the U-factor of the glass, which correlates well with inside surface temperature for almost all window products. The rating we propose is the minimum outside temperature for which an occupant would still be comfortable sitting near the window. The advantage of this rating is that is easy to understand and also differentiates between typical window types on the market. There are a range of possible configurations and assumptions that could be used (with respect to window size, distance from the window, etc.) but we provide example ratings based on the assumptions described in Table 1.

Distance from the window:	1 meter
View factor:	0.26
Metabolic rate:	1.2 met
Clothing:	0.59 clo (typical indoor clothing)
Inside temperature:	23.5°C

Table 1: Winter rating – Boundary conditions

Based on these assumptions, the winter comfort rating is defined as:

$$\text{Winter comfort rating (°C)} = [-45.3/\text{U-factor (W/m}^2\text{-K)}] + 23.5°C$$

Example ratings for some typical window types are shown in Figure 1.

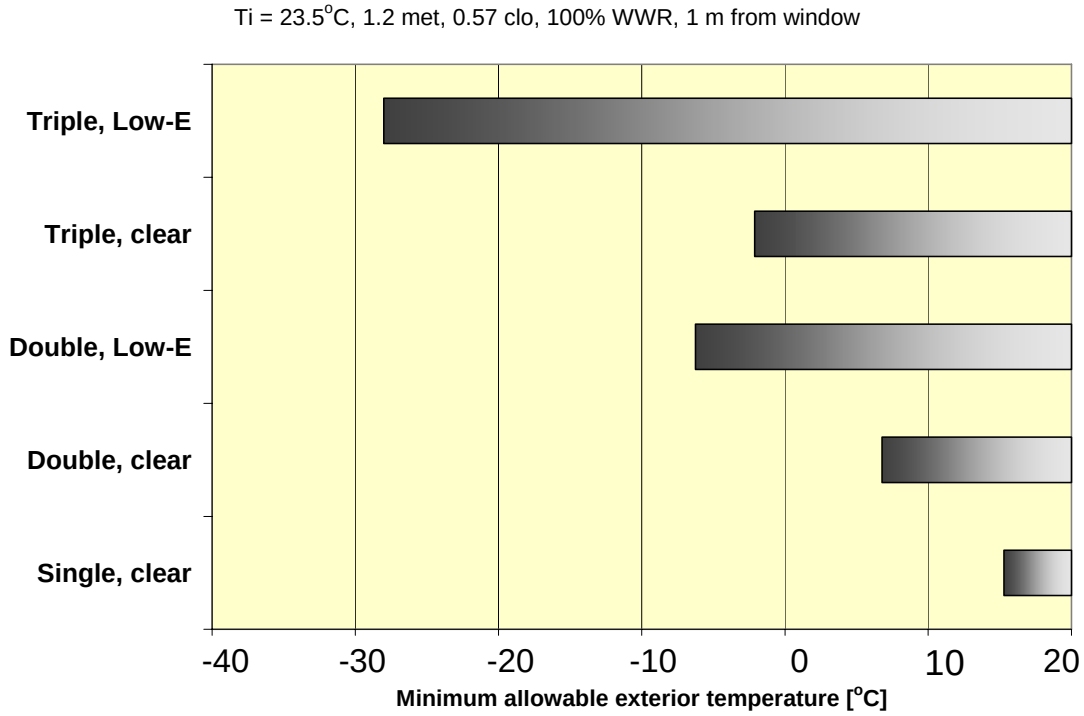


Figure 1: Winter window comfort rating – Minimum allowable exterior temperature

Summer rating: In summer, solar radiation and the optical properties of the window most heavily influence the inside surface temperature of the window. As a result, exterior temperature does not characterize the effect of the window on comfort as it does in winter and using a summer rating akin to the winter rating would have little value. The two important characteristics of a window with respect to warm season comfort are Tsol (direct solar transmittance) and $SHGC_{indirect}$ (defined as SHGC – Tsol, or the portion of SHGC that is absorbed by the window and then retransmitted to the interior). Tsol determines how much solar radiation is transmitted directly through the window that could fall on the body.

In our analysis, we considered two scenarios: (1) a case where the occupant is only exposed to diffuse radiation, making the assumption that direct sun is such a strong effect that an occupant would take action to correct a situation where direct sun was falling on them (by adjusting a blind or shade or even repositioning themselves) and (2) a case where the occupant is exposed to direct solar radiation. $SHGC_{indirect}$ characterizes the increase in the inside window surface temperature due to solar radiation being absorbed by the glazing system. The absorbed energy is then emitted to the inside environment by convection and radiation from the interior glazing surface.

Our analysis shows that for scenario 1 – occupant only exposed to diffuse radiation – $SHGC_{indirect}$ is approximately 4.4 times more important in its impact on comfort as Tsol. However, for scenario 2 – occupant exposed to direct radiation – $SHGC_{indirect}$ is only approximately 2.4 times more important in its impact on comfort as Tsol.

This suggests that a reasonable index that captures the impact of a window on summer comfort could be defined by as a combination of Tsol and SHGC, which we call the *Summer Comfort Index*. This can be thought of as the effective solar gain from the perspective of thermal comfort.

The relative importance of $SHGC_{indirect}$ depends on the assumptions one makes about direct solar radiation.

Scenario 1 – only diffuse radiation: *Summer Comfort Index* = Tsol + 4.4* $SHGC_{indirect}$

Scenario 2 –direct radiation: *Summer Comfort Index* = Tsol + 2.4* $SHGC_{indirect}$

Table 2 shows example comfort ratings for some selected glass types. A lower rating indicates a lower negative impact in comfort. Note that a single absorbing glass (e.g., bronze) and the clear triple glazing have the highest value in the table since they both have a high $SHGC_{indirect}$.

Glazing system	Tsol	SHGC	$SHGC_{indirect}$	*Summer Comfort Index*
bronze, single	0.49	0.62	0.13	1.06
clear, triple	0.49	0.62	0.13	1.06
low-e, double	0.47	0.59	0.12	1.00
clear, double	0.61	0.70	0.09	1.01
clear, single	0.77	0.82	0.05	0.99
low-e, triple	0.34	0.45	0.11	0.82
low-e, selective, double	0.31	0.36	0.05	0.53
low-e, selective, triple	0.25	0.31	0.06	0.51

Table 2: Summer comfort ratings for example glass types

1 INTRODUCTION

Anyone who has ever sat near a cold window on a winter day or in direct sunlight on a hot day recognizes that windows can cause thermal discomfort. In spite of this broad recognition there is no standard method to quantify the extent of such discomfort. HVAC systems are designed to respond to the air temperature sensors, which in fact do not reflect the radiation problems caused by windows. Even when HVAC designers specify dedicated perimeter heating and cooling systems to mitigate window-related comfort problems, they use simplified assumptions that may not solve the comfort problems or that might lead to designs that are energy-inefficient. Window manufacturers promote the positive impact on comfort of high performance glazing, yet they have no real way of quantifying this impact, nor do consumers have a way to compare products with respect to comfort.

The Fenestration chapter of the 2005 ASHRAE Handbook of Fundamentals offers basic guidance about windows and comfort for the designer:

> *"In heating-dominated climates, windows with the lowest U-factor tend to give the best comfort outcomes... In cooling-dominated climates or for orientations where cooling loads are of concern, windows with the lowest rise in surface temperature (for a given SHGC) tend to give the best comfort outcomes."*

This rather limited advice does not provide any explicit way to evaluate whether a given product will produce satisfactory results. No basis for this recommendation is provided, nor does it makes any reference to the wide range of modern products such as low-e glazing, the current standard in high performance glazing systems.

2 OBJECTIVE

The objective of the research project is to develop an improved understanding of the impact of windows on thermal comfort and to propose an analytical method for evaluating this impact. The method could form the basis for a future NFRC window comfort rating method that could be used by both designers and consumers. It would also provide useful information for an improved treatment of the comfort impacts windows in ASHRAE *Standard* 55.

3 LITERATURE REVIEW

This section provides the results of a detailed literature search of work related to windows and comfort. It reviews the studies about the comfort impact from short wave, long wave radiation asymmetry (including the asymmetry from ceilings, walls, windows, and floors), and the comfort limits developed for standards. An annotated bibliography of the most relevant literature is presented in Section 8 and a complete bibliography in Section 9.

3.1 HOW WINDOWS INFLUENCE COMFORT

A window influences thermal comfort in three ways (Figure 2):

- long-wave radiation from the warm or cold interior glass surface
- transmitted solar radiation
- induced air motion (convective drafts) caused by a difference between the glass surface temperature and the adjacent air temperature

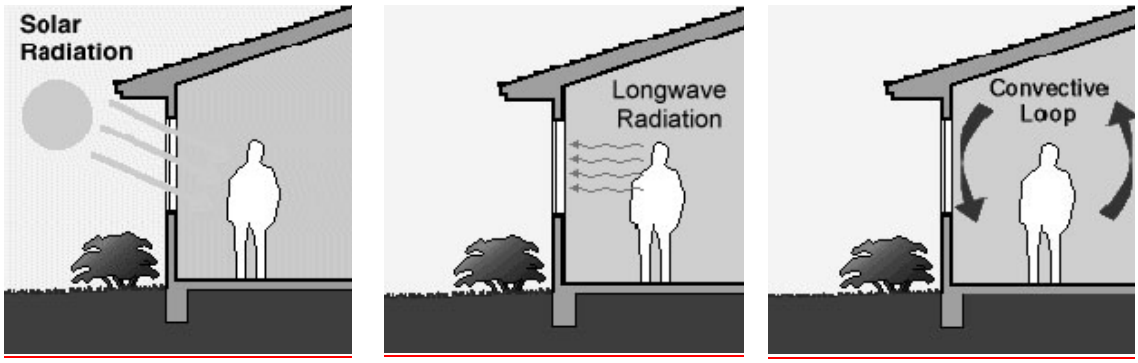


Figure 2: Window impacts on thermal comfort: solar radiation, long-wave radiation, convective drafts

Windows absorb and transmit a significant amount of solar radiation. *Absorbed* radiation influences the temperature of the glass; the inside surface of heat absorbing glass can routinely reach temperatures above 120°F (50°C) in summer conditions, raising MRT by as much as 15°F (8°C). *Transmitted* radiation often causes discomfort if it falls directly on the occupant. A person sitting near a window in direct solar radiation can experience heat gain equivalent to a 20°F (11°C) (Arens et al. 1986) rise in mean radiant temperature. These radiant heating and cooling effects act on the occupant's body *asymmetrically*, causing some parts of the body to be considerably cooler or warmer than a uniform model like MRT can describe. Models need to consider the effect on *local* skin temperature in order to be sensitive to discomfort caused by windows.

The inside surface temperature of a window is heavily influenced by exterior conditions and this temperature can significantly affect the radiant heat exchange between an occupant and the environment. If this heat exchange becomes greater than or less than the acceptable range, discomfort will result. Mean radiant temperature (MRT), defined as the uniform temperature of an imaginary enclosure in which the net radiation heat exchange between the occupant and the enclosure equals the net radiation heat exchange in the actual environment, is commonly used to simplify the characterization of the radiant environment. On a cold day the inside surface temperature can easily drop below 15°F (-9°C) for a clear single pane window and below 40°F (4°C) for a clear, double pane window. If the occupant is sitting sufficiently near the window, MRT could drop to 55°F (13°C) for the single pane case and 62°F (17°C) for the double pane case. Based on ASHRAE *Standard* 55, even the use of the double pane window could result in discomfort.[1] In addition to the MRT effect, a cold inside glass surface can induce a downward draft that increases air movement, contributing to further discomfort.

Understanding the influence of windows on thermal comfort is important not only to help designers create comfortable buildings, it will also help evaluate the benefits of improved windows. Although it is well understood how high-performance windows can reduce building energy consumption, a better understanding of how they affect comfort might lead to even greater savings. For example, a study (Hawthorne and Reilly 2000) suggests that there are significant energy implications to the standard practice of using perimeter duct distribution in houses to mitigate potential discomfort caused by windows. They found that perimeter heating is often not necessary when high performance windows are installed, and that heating energy savings of 10% to 15% could result from installing a simpler, less expensive duct system.

[1] This example assumes an outdoor air temperature of 0°F (-18°C), indoor air temperature of 72°F (22°C), non-window surface temperatures of 72°F (22°C), occupant-window view factor of 0.3, 0.9 clo (standard winter indoor clothing), activity level of 1 met.

3.2 SHORT-WAVE RADIATION

In a cold winter morning, direct sunlight on a person's body may be perceived as a pleasant presence. However, in summer daytime, solar radiation will almost certainly cause discomfort. Short-wave radiation causes thermal discomfort directly when it is absorbed by the body (or clothing) and indirectly by increasing the air and surface temperatures in a space. This latter impact is in theory moderated by the HVAC system. In our analysis, we assume that the HVAC system controls the air and surface temperatures in the space to compensate for solar gain. In practice, HVAC systems rarely achieve perfect control and as a result, solar gain often raises the operative temperature in perimeter zones.

Hausler and Berger (2002) found that when the air temperature is 22ºC or above, direct solar radiation on the body causes discomfort. Schutrum et al. (1968) tested subject thermal sensation with solar radiation transmitted through a window whose glass temperature was separately controlled. When the glass temperature increased from 3ºC to 48ºC (room air temperature increased from 23.7 to 24.3ºC) on a cloudy day, overall sensation elevated 1.1 units (from slightly cool to neutral, 7-point scale,). On a clear day with solar radiation on the body, the window temperature increased to 31.7ºC and the overall sensation became 2.5 units warmer (from slightly cool to above slightly warm).

In summer, thermal comfort is mostly uncorrelated with U-value but is closely related to solar transmittance (Lyons et al. 1999). In fact, solar transmittance is the controlling factor with respect to the effect a particular glazing system will have on comfort. The Tsol of the glass determines the amount of solar gain that is transmitted into the space. Simulations show that replacing single 3mm clear glass (Tsol = 0.83) with double 3mm low-E glass (Tsol = 0.53) can reduce discomfort by more than half (Lyons et al.1999). Sengupta et al. (2005) simulated comfort in a room and the results demonstrated that in summer daytime (780 W/m^2 solar radiation) the change from clear single glazing to clear double glazing did not significantly improve thermal comfort. However, reducing the window size (from 40% to 20% glass-to-floor area ratio) significantly improved the comfortable floor area. Olesen & Parsons (2002) also discuss radiant discomfort and state that "direct solar radiation should be avoided in the occupied zone, by means of building design or solar shading devices".

Because solar transmittance is a major factor in determining comfort, a logical way to reduce solar radiation is to use glazing with a spectrally selective coating. Although glass temperature normally increases because of the higher solar absorptance of the film coating compared to normal glass, the reduction in solar transmittance can be more than 50% (Arasteh et al. 1987, Alvarez et al. 1998, Karlson et al. 1988, Estrada-Gasca et al. 1993a and 1993b, Howthorne and Reilly 2000). Ideally, a spectrally selective coating should have a small effect on visible transmittance, to preserve daylight and views, but will be near-opaque at other wavelengths. This is especially critical in the automobile industry where for safety reasons the visible transmittance must be 70% or above (Bohm et al. 2002, Nair and Nair 1991). Clarke et al. (1998) provided a summary for the performance of the advanced glazing systems that is presented in Table 3.

Insulating glazing	The insulating properties of a window can be improved by including multiple glass layers, by applying low-ε coatings to layers surfaces, or by using a low-conductivity gas such as argon or krypton instead of air (Arasteh *et al.*, 1987).
Spectrally selective coatings	Spectrally selective coatings can be applied to the glass to reduce transmission at specific wavelengths. Of foremost interest are those coatings which give solar control with little adulteration of view, i.e. glazings that have minimum effect on visible light but are opaque at other wavelengths, particularly within the infrared portion of the solar spectrum (e.g. a typical advanced glazing product will have a visible transmittance of 67% for a total solar transmittance of only 37%).
Edge spacers	These provide the seal for multiple glazing and are invariably made of aluminium or steel to provide mechanical strength under thermal stress. Because such materials give rise to a high conductivity thermal bridge, low-conductivity spacers are being developed (Aschehoug and Baker, 1995; Svendsen and Fritzel, 1995).
Insulating frames	Typical double glazing frames have higher *U*-values than the corresponding centre pane *U*-values for low-ε double glazing. With frames comprising some 20–25% of the aperture area, or 10% in the case of a curtain walling system, improved frame systems are required to achieve a low, overall component *U*-value (Beck and Arasteh, 1992).
Variable transmittance	Adjustable glazing systems offers the best prospect for providing an optimum solution as occupant and system needs vary throughout the year and daily. Blinds or louvers operated under automatic or manual control offer one option. An elegant alternative, which is currently under development, is electrochromic glazing whereby the transmittance can be varied by the application of a small voltage, which changes the oxidation state of the electrochromic coating. Both visible and total solar transmittance can be varied from their normal value (say 60%) down to some lower value (say 10%). The time taken to change (from the maximum to minimum values) is typically about 5 min. Because the voltage is only required to effect the change, and need not be sustained thereafter, the power consumption is small. The effective integration of this technology will require the development of appropriate control algorithms (Sullivan *et al.*, 1994).

Table 3: Advanced glazing (Clarke et al. 1998)

In buildings, ways of blocking solar radiation can also be achieved by applying shading elements, such as overhangs or curtains, (e.g. the Phoenix Public Library designed by William Bruder, and the Arup Campus designed by Arup Associates). They both used shading devices and the results are very good in terms of keeping both thermal and visual comfort). There are many studies carried out at Lawrence Berkeley National Laboratory (LBNL) that look at thermal and visual performance of shading systems. For example, a study by Lee et al. (1998) compared the energy and lighting performance of an automated venetian blind with a static venetian system. The automated blind was operated in synchronization with a dimmable electric lighting system to: block direct sun, provide the design workplace illuminance, and maximize view. Through a year-monitoring, they found that the energy consumption (used in cooling and lighting) and peak demand were significantly reduced compared to the static blind.

The impact of direct solar radiation on occupant comfort also depends on the absorptance of clothing skin. Solar absorptance of clothing depends on the color and property of the fabric. Morton and Hearle (1993) give a detailed description of solar properties based on the structure of the fabric. The absorptivity of skin varies with color in the visible and the near-infrared spectra. For visible wavelengths (0.4 – 0.7μm), white skin is about 0.5, while black skin is 0.74 (Houdas and Ring 1982). In the near infrared (0.8 – 2μm), the absoptivity of black skin is also higher than the white skin. For ultraviolet (<0.4μm) and far infrared (>2μm), there is no significant difference. Narita et al. (2001) tested human skin for thermal sensitivity to radiation at different wavelengths and found that human skin is more sensitive to the visible (0.3 – 0.8μm) and middle-infrared (1.7 – 2.3μm) than to near-infrared (0.8 – 1.35μm) wavelengths.

3.3 LONG-WAVE RADIATION

Long-wave radiation from a warm or a cold window affects occupant comfort in two ways. First, it influences the overall radiative heat exchange between the body and the surroundings, affecting the body's heat balance and therefore comfort. Second, even when there is a neutral overall heat balance, local discomfort of one or more body part may result from asymmetric radiation fields near windows.

ASHRAE and ISO standards define a comfort zone for the body based on overall heat balance, however thermal neutrality is not the only condition to ensure thermal comfort. A person may feel thermally neutral for the body as a whole, but he may not be comfortable if one part of the body is warm and another cold. A further requirement to comfort is that no local warm or cold discomfort exists at any part of the body. Local discomfort can be caused by radiation temperature asymmetry such as a warm or cold window, ceiling, wall, or floor; excessive air motion (draft); or vertical air temperature stratification. Comfort standards prescribe limits for these parameters. This section reviews the literature addressing radiation asymmetry caused by ceilings, walls, floor, and windows, and for limits on asymmetry as prescribed in comfort standards.

3.3.1 RADIATION ASSYMETRY FROM WALL AND CEILING

In a uniform environment, the relative contribution of mean radiant temperature on comfort is considered approximately equal to that of the air temperature (Fanger et al. 1980, Fanger 1972), or slightly smaller (McNall and Schlegel 1968, McIntyre and Griffiths 1975). McIntyre and Griffiths (1972) give the relative influence of radiant and convective heat transfer as 0.44 and 0.56, respectively. When the radiation on the body is asymmetric, the geometry and shape of local body parts influence the relative importance of radiation and convection.

Radiation exchange with the surrounding environment is commonly defined in terms of radiant temperature. Radiation from the hemisphere surrounding a plane surface can be defined in terms of 'plane radiant temperature', the uniform temperature of an enclosure in which the irradiance on the plane is the same as in the existing non-uniform environment. The vector radiant temperature (VRT) proposed by McIntyre (1974) is used to measure the asymmetry. It is equal to the difference in plane radiant temperature on opposite sides of a small plane element, when the element has been oriented so as to make the difference a *maximum*. Instead of getting the maximum difference, by fixing the orientation of the plane, Fanger et al. (1980) proposed radiant temperature asymmetry (RTA). It is the difference between the plane radiant temperatures on two opposite sides of a small plane element of a *fixed* orientation. For a heated ceiling, Fanger positions the plane horizontally 0.6m above the floor. Therefore, for measuring the vertical radiant asymmetry between floor and ceiling, the vector radiant temperature (VRT) and radiant temperature asymmetry (RTA) are equivalent. The effects of asymmetric radiation on thermal comfort have been extensively investigated through human subject tests at Kansas State University in the 1960s. Under non-extreme conditions (overall sensation between cool and warm), Schlegel and McNall (1968) found that a wall with 6.7ºC (warm and cool) surface temperature difference from the rest of the surfaces (the chamber was 12 ft and 24 ft in plan and an 8 ft ceiling height, five subjects stayed 3.5 to 4.5 ft from the wall whose temperature was changed, a view factor of 0.2) created no noticeable difference from comfort results under uniform test conditions. The authors then examined the impact of hot and cool walls and ceilings, with a wider range of radiation asymmetries (McNall and Biddison 1970). The cool wall temperature was 9ºC, 11ºC lower than the surface temperature of the rest of the space (the view factor was again 0.2). The hot wall temperature was fixed at 54ºC, 41ºC warmer than the rest of the surfaces, a quite extreme condition. The cool ceiling was 10.5ºC, 16ºC lower than the rest surfaces (view factor 0.12). The hot ceiling was 54ºC, 38ºC higher than the space. The room air temperatures were designed at various levels. A control test was also conducted with a neutral uniform environment (25.5ºC). Each test lasted three hours and the thermal questionnaires were answered in 30-minute intervals. The human subjects were asked both sensation and comfort questions, and the results are presented in terms of sensation and percentage of subjects feeling comfortable (Figure 3). A total of 170 subjects participated in these tests.

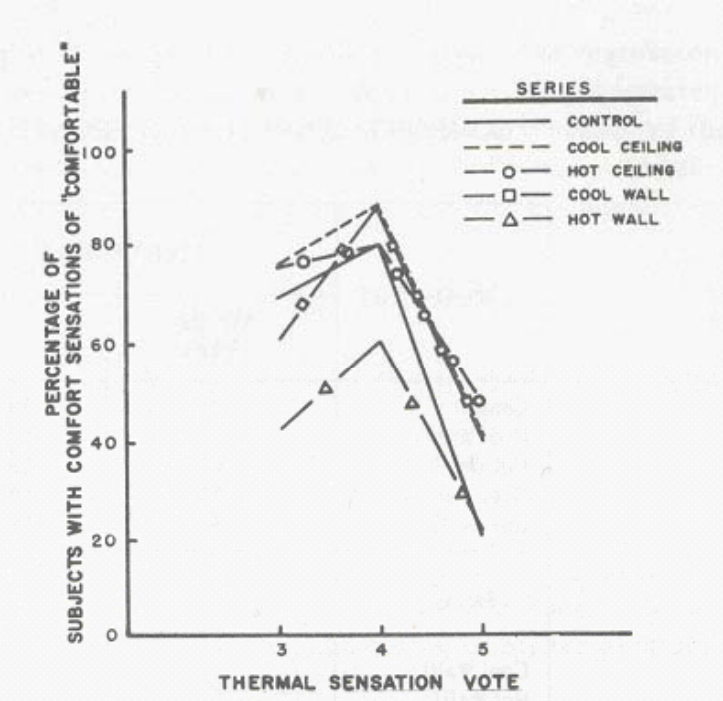


Figure 3: Percentage of comfort in relation to thermal sensation (McNall and Biddison 1970)

In Figure 3, we see that a larger percentage of subjects felt uncomfortable with the hot wall than with the other three radiation asymmetries. The three asymmetries (cool ceiling, cool wall, and hot ceiling) were also more comfortable than the uniform neutral condition (control test). At the neutral overall sensation (value of 4), the percentage of subjects feeling comfortable with the cool wall and cool ceiling is 7% higher than in the uniform control condition.

In order to eliminate discomfort due to whole-body warmth or cool discomfort, the authors used only comfort responses when thermal sensation was neutral for their analysis of impact from asymmetrical radiation. Statistically, only the hot wall has a significantly lower probability of resulting in a "comfortable" vote than those of the control tests. When the overall sensation is neutral, the cool wall as low as 9ºC, cool ceiling as low as 10.5ºC, and the hot ceiling as high as 54ºC, would not cause discomfort due to asymmetric radiation. With the overall whole body thermally neutral, subjects exposed to the 54.4ºC warm wall experienced significant discomfort due to asymmetric radiation. The subjects showed a larger tolerance for the hot ceiling than the hot wall. This might be because in the test chamber, the view factor for the ceiling (0.12) is smaller than for the wall (0.2).

A series of tests were carried out at the Technical University of Denmark (DTU) in the late1970s regarding the impact of radiation asymmetry on comfort. In examining impact from a heated ceiling (Fanger et al. 1980), the test was conducted in a chamber (4.7 x 6 x 2.4 m). A light ceiling (2.2 x 2.2 m) was suspended at a height 2 m above the floor, giving a view factor of 0.11. In examining the impact from a heated/cooled wall (Fanger et al. 1985), 4 panels (2 x 1.6 m), 0.5 m away from the center of the person (view factor 0.25) was installed. The cooled ceiling size was 2 x 1.6 m, plus 2 x 0.9 m vertical sections on both sides (view factor 0.2). The authors reached different conclusions than the KSU tests: the subjects were most tolerant with the warm wall (radiant temperature asymmetry up to 23ºC) and the least with the warm ceiling (radiant temperature asymmetry up to 4ºC).

In the DTU tests, the subjects first stayed in the chamber for an hour. Then the environment was changed five times in the following 2.5 hours to correspond to five radiation asymmetries.

Sixteen females and sixteen males participated in the "cool wall" test (wall temperature from 0.4ºC to 17.8ºC) and eight females and eight males participated in the "warm wall" (32.6 to 70.1ºC), "cool ceiling" (0.8 to 16.0ºC) and "warm ceiling" (34 to 69ºC) tests. The air temperature was adjusted according to the subjects' requests to keep their feelings neutral. The results are presented as the radiant asymmetry vs. percentage of dissatisfied (PPD) (Figure 4). Because people showed more sensitivity to a cool wall than to a warm wall, the authors state that local cooling of the body seems to more frequently cause discomfort than local heating. Comparing the subjects' sensitivity to the warm/cool wall to that of the ceiling, the authors conclude that people are more sensitive to vertical radiation than to lateral radiant asymmetry. To explain the differences between their results and those of McNall and Biddison (1970), the authors propose that in the studies carried out at Kansas State University only the surface temperatures in the chamber were controlled to maintain a constant MRT. The authors explained that the air temperature was not adjusted in a way to keep a neutral temperature for the subjects. Therefore, the discomfort values measured in the Kansas study were due to both the overall discomfort and to local discomfort caused by radiation asymmetry.

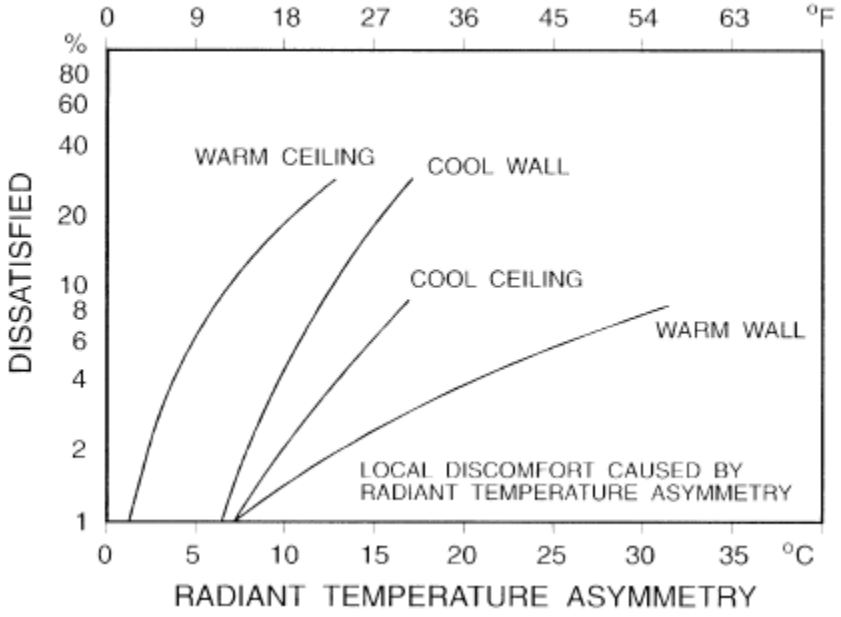


Figure 4: Local thermal discomfort caused by radiant asymmetry (ASHRAE Standard 55 – 2004, same figure as presented by Fanger et al. 1985)

This explanation does not seem sufficient. McNall and Biddison (1970) examined the results by restricting their statistical analysis to data when overall sensation was perceived as neutral, to eliminate the effect of general thermal discomfort. The results still showed that only the warm wall has a significantly lower probability of being "comfortable" than the uniform condition.

A possible explanation lies in the different approaches of the two studies. In McNall's study, when increasing a wall temperature, the remaining five surfaces were simultaneously reduced in temperature so as to keep the same overall MRT. When the warm wall temperature was 54ºC, the rest of the surfaces were at 12.8ºC, while the room air temperature was 25.6ºC. Therefore, subjects felt stronger asymmetry (from both warm and cold walls) than in Fanger's test condition, where the warm wall was 52ºC and the remaining surfaces and the air temperature were kept at 22.3ºC to preserve the neutral sensation. At the cool environment in Fanger's study, the warm wall was perceived as pleasant and therefore was found to have bigger tolerance limits. However,

this did not appear in Fanger's warm ceiling test. From Fanger's study, it seems that people are more sensitive to warm ceilings than warm walls. Local discomfort was found either as warm head or cool feet. The room air and the five surface temperatures were low in order to balance the heated ceiling to keep subject neutral. From the results, cool feet discomfort happened more than warm head discomfort when the ceiling temperature was between 34ºC and 52ºC (operative temperatures were the same, around 24.1ºC). It was only with ceiling temperature as high as 63ºC to 69ºC that warm head discomfort occurred more often than cool feet discomfort. So in a way Fanger's resulting limit for heated ceiling was caused partially by cool feet. That is probably why the limit for cool ceiling (14ºC radiant temperature asymmetry, the air and the five surfaces warmer) is higher than the heated ceiling (4ºC radiant temperature asymmetry, the air and the five surfaces cooler) if we assume that people in general are more sensitive to cool feet than warm head. The heated tests cover the radiant temperature asymmetry from 4.5 to 23.6ºC, so in fact the limit of 4ºC radiant temperature asymmetry based on 5% dissatisfied for warm ceiling is not supported by any of the test conditions. There are two other major differences between the two tests. One is that in Fanger's study, subjects stayed in one asymmetric condition for half an hour. During that half-hour, the radiation conditions were changed, and so did the room temperature according to the subjects' requirements. Six subjective surveys were conducted in five-minute intervals. It is not easy to meet subjects' requirements in that short period of time and therefore whole-body discomfort might still exist. Therefore the dissatisfaction might not be totally due to asymmetric radiation. In McNall's study, the test duration was three hours. Another difference was that the comfort rating scales employed in the two studies were different. The questions (comfortable, slightly uncomfortable, uncomfortable, very uncomfortable, intolerable) were asked in McNall's study, while in Fanger's study, if at least twice as much local discomfort was reported during the last three votes, the person was considered uncomfortable.

The ASHRAE (2004) and ISO (1994) standards define the allowable radiant temperature asymmetry categorized as warm/cool ceiling and warm/cool wall. The limits are presented in Table 4. These limits are obtained from Figure 4 with 5% dissatisfied due to radiant asymmetry. These limits are determined based on studies conducted by Fanger et al. (1985, 1980).

Radiant Temperature Asymmetry °C (°F)			
Warm Ceiling	Cool Wall	Cool Ceiling	Warm Wall
< 5 (9.0)	< 10 (18.0)	< 14 (25.2)	< 23 (41.4)

Table 4: Allowable radiant temperature asymmetry (ASHRAE 55 – 2004)

There have been other studies that tried to find the limits for the asymmetric radiation but the results are not consistent. The first investigation of discomfort from a heated ceiling was performed in the 1950s in England by Chrekon (1953). The heated ceiling increased MRT by up to 12ºC, while the air temperature was kept constant. The percentage dissatisfied was higher compared to Fanger's (1980) study. The reason for this is probably that the subjects experienced an overall sensation of warmth because the temperature of the chamber's other surfaces and the air temperature was not changed along with the heated ceiling. Chrekon recommended a limit corresponding to a VRT of about 6ºC. From the early 1970s McIntyre and Griffiths in England did extensive studies on radiation asymmetry and comfort. Griffiths and McIntyre (1974) exposed 24 subjects to a control condition and three different ceiling temperatures. The method is similar to that of McNall and Biddison (1970) where the air temperature was kept constant and the temperature of the rest of the surfaces were adjusted while the ceiling was heated. They found that a vector radiant temperature of 20ºC did not produce any significant worsening of subjective responses when compared with a uniform control condition and therefore a VRT of 20ºC was recommended. This finding is similar to what was found by McNall and Biddison (1970) when the ceiling temperature was 54ºC and the VRT was 24ºC. However this was

significantly higher than the results from Fanger (1980), where the radiant temperature asymmetry limit for heated ceiling was 4ºC. McIntyre (1977) did a follow-up study to change both the temperatures of the remaining surfaces and the air while increasing the ceiling temperature (a similar approach to Fanger's), and found that not only did the heated ceiling produce no discomfort, but indeed it was preferred when the ceiling temperature was high and the air and other surfaces were cooler. This confirms our earlier explanation about the difference between Fanger et al. (1985) and McNall and Biddison (1970) regarding the warm wall. We explained that in Fanger's test, when the wall was warm (52ºC), the rest of the surfaces and the air temperature was 22.3ºC, and the warm wall was perceived as pleasant and therefore allows bigger tolerance limits. In McIntyre's similar test configuration (1977), he invited subjects to attribute discomfort specifically to the overhead radiation, the answers show a significant increase of discomfort with ceiling temperature. This is a contradictory result. It appears that people are ready to attribute discomfort to unusual aspects of their environment. For that reason, because people clearly notice the asymmetrical radiation at VRT of 10ºC, although no one was actually more uncomfortable than in the uniform environment, McIntyre and Griffiths (1977, 1975) recommended a VRT of 10ºC as the limit, which is also similar to the recommendations by Schroder and Steek (1973), 9ºC, and Banhidi (1972), who recommended a VRT in the range 8.5 to 13ºC.

Olesen et al. (1972) exposed nude subjects to a lateral asymmetry and found the tolerable limit of radiant temperature asymmetry to be 10ºC. He recommended limits for asymmetry for closed subjects based on heat transfer calculation, which agreed well with the recommendation of a VRT of 20ºC by McIntyre and Griffiths (1972), within the range of recommendations given by Fanger et al. (1985, cold wall: 10ºC, warm wall: 23ºC). Olesen and Nielsen (1981) tested the spot cooling effect from a cold vertical panel (1m x 2m, 0ºC) in a warm environment (30ºC). The cold panel was placed 0.5m behind the back of the subjects (view factor 0.25). The overall sensation was a cooling from 1.68 to 1.12, a 0.5-unit scale reduction. The overall comfort was still around "uncomfortable", from 2.10 to 1.78[2]. The subjects' overall thermal acceptability increased from 38% to 50%, but was smaller than the values for uniform conditions. The author explained that the rather limited increase in acceptability due to cooling was reduced due to the radiant asymmetry. Looking at the local sensation votes, the coldest sensation came from the body parts which were most exposed to the cold radiation: back (-0.18) and neck (0.33), while the non-radiant body parts felt slightly warm: face 1.24, chest 1.26. This suggests it would be preferable if the view factor were also calculated for these most exposed body parts (e.g. back and neck)

Displacement ventilation has the advantage of saving energy and providing better air quality for the breathing zone. However, it is limited in its ability to convectively remove the heat loads encountered in offices. Additional mechanisms such as chilled ceilings may become necessary, which also have the effect of reducing the air stratification in the occupied zone (Feustel and Stetiu, 1995). Kuelpmann (1993) tested the performance of displacement ventilation with a cooled ceiling under several typical configurations and found a radiant temperature asymmetry of 8ºC, smaller than the limits set up by the standard. Hodder et al. (1998) examined thermal comfort in a more sophisticated thermal environment with a chilled ceiling and displacement ventilation. A typical ceiling tile surface temperature is normally in a range of 16ºC to 19ºC. He tested ceiling temperatures of 12.4, 14, 18 and 22ºC and found that ceiling temperatures in this range had no significant influence on overall comfort and local discomfort. His experiments involved eight female subjects because in their early investigations they had found female subjects to be more thermally sensitive to their environment than males. Another study by the

[2] Scale: 1 - comfortable, 2 - slightly uncomfortable, 3 - uncomfortable, and 4 - very uncomfortable

same authors (Loveday et al. 1997, 2002) involving a larger number of subjects (184) also showed that no significant local discomfort happened in the cool-ceiling and displacement-ventilation environments. Kitagawa et al. (1999) examined the effect of humidity and low levels of air motion on thermal comfort under a cool-ceiling environment and found that better comfort votes were obtained in the condition when thermal sensation vote was not neutral but near –0.5.

Summarizing: Many studies have been conducted to define limits for radiant asymmetry caused by cooled/heated ceilings and walls. For heated ceilings, most of the literature suggests a much higher acceptable radiant asymmetry limit (10ºC to 20ºC) than the 5ºC provided by the standard. For warm walls, there is a large difference between the limits provided by McNall and Biddison (1970) and Fanger et al. (1980). Cool ceilings and walls seem to have similar limits. ASHRAE standard 55-2004 defines limits for a warm- or a cool wall (radiant asymmetry temperature <10ºC for a cool wall, <23ºC for a warm wall). Radiant cooling or heating of floors (which will be discussed in a separate section later), ceilings, and walls provide energy-efficient approaches to space conditioning (Roulet et al. 1999). Therefore, these studies about radiant asymmetry and comfort have great value in practical applications. The studies of heated or cooled ceilings also provide useful information for evaluating the impact of skylights.

3.3.2 RADIANT ASSYMMETRY FROM WINDOWS

Many studies emphasize the importance of a warm or a cold window on comfort. By simulating the thermal impacts of ten generic glazing systems ranging from single-pane window to high performance window, Lyons et al. (1999) concluded that except in the case where the body is directly in the sun, long-wave radiation to and from the window is the most significant factor affecting thermal comfort. When applying advanced glazing, a secondary phenomenon occurs. The inside glass temperature rises. It causes a positive effect in winter, but increases discomfort in summer. Under NFRC summer test conditions, single bronze glazing is 13ºC hotter than single clear glazing because of the higher solar absorptance, which corresponds to a calculated increase of discomfort from 36% to 45% due to long-wave radiation. Sengupta et al. (2005) and Chapman et al. (2004) simulated window impacts on comfort for eight cases covering different glass areas and window configurations. By displaying PMV contours on a plane 1.25 m above the floor, the authors showed very large variations due to the existence of the windows. In summer with solar radiation, the presence of two windows (40% of the wall area) and one window (20% of the wall area) results in only 7% and 25% of the floor area being comfortable (with PMV within –0.5 to +0.5). Large glazed façades are essential features of modern architecture. Gan's simulations (2001) showed that when outdoor air temperature is –4ºC, room air temperature 21ºC, the radiant asymmetry temperature exceeds 10ºC when the location is 1m from the window (room size 5 x 4 x 3 m with a window 3.5 m wide and 2 m high). That means the area within 1 m distance from the window would not meet the ASHRAE standard. Ge and Fazio (2004) measured the inside glass temperatures of a large glass panel when outdoor temperature was –18ºC (NFRC winter condition), and Montreal's worst winter condition, –32ºC. The inside glass temperatures were 10ºC and 3.8ºC, respectively.

Improving window performance reduces thermal discomfort. Sengupta et al. (2005) showed that in winter nighttime conditions, changing a single-pane window to double-pane greatly improved the comfortable floor area. Gan (2001) examined a series of factors regarding the window properties, sizes, and shapes. For a single-pane window, a 10ºC radiant asymmetry exists at 1m from window at an outdoor temperature of –4ºC. A double-glazed window has the same asymmetry 0.15 m from the window at an outdoor temperature of –10ºC. He also demonstrated that square windows are more likely to cause thermal discomfort than narrow windows and when a large window is replaced by several smaller windows (keeping the same window area), the discomfort is greatly lowered.

Although radiant temperature is as important as air temperature, conventional practice is to use air temperature as the measure for controlling mechanical systems. Gan (2001) recommends that, in circumstances where a large radiant asymmetry exists (e.g. a room with a large window), sensors are more effective if they respond to the combination of air temperature and radiant temperature rather than air temperature alone.

3.3.3 FLOOR SURFACE TEMPERATURE

An early study of foot thermal comfort that concerned the effect of floor material was carried out in 1948 by Munro and Chrenko (1948). The subjects were exposed to air temperatures of 12.8ºC and 18.3ºC for 60 minutes. It was found that the floor material had only a very small influence on the preferred floor temperature for people with shoes. The air temperature was the dominant factor determining foot thermal comfort. After that, Muncey and Hutson (1953) and Muncey (1954) also conducted subject tests and also found no influence of the flooring material on foot thermal comfort.

In early 1950s, a study was undertaken at Kansas State University to determine the effect of floor surface temperature on foot and whole-body thermal comfort. Nevins et al. tested the effect of different floor temperatures on thermal comfort for young men and young women seated (reading) and standing (writing and sorting bibliography cards to simulate light office work) three hours with shoes, and concluded that a floor temperature as low as 15.5ºC and as high as 29.4ºC did not cause significant discomfort when air temperatures was 23.9ºC (Nevins et al. 1958, Nevins et al. 1964, Michaels et al. 1964, Nevins et al. 1967). Except for seated women (Michael et al. 1964), a floor temperature of 32.2ºC did not make the subjects uncomfortable. For seated women, the upper temperature limit was lower, 29.4ºC. Their greater sensitivity could be caused by the women's lightweight cotton smocks exposed bare skin of the lower legs to radiation from the floor, and the lower muscular activity in the legs due to sitting may have reduced blood circulation and the removal of the absorbed radiant gain. Later on the authors did a study to examine floor surface temperature on comfort for elderly. They found that at the same floor temperatures, female elderly feels warmer than the male elderly (Springer et al. 1966). No obvious difference in thermal sensation was seen for male between floor temperature 23.9 to 37.8ºC. For female, no obvious difference in thermal sensation was seen between 23.9 – 35ºC, but a jump in thermal sensation at floor temperature 37.8ºC.

Olesen did studies evaluating floor temperature for bare feet (1977a) and for feet with shoes (1975, 1977b). The tests were carried out for standing and sedentary people. Sixteen subjects (eight females and eight males) occupied the floor for 10 minutes with bare feet and gave an evaluation of their foot comfort. Eighty-five subjects were tested with shoes, keeping their feet on the floor for three hours. For floors occupied by people with bare feet, the author found that the floor material is important. The optimal floor temperature for 10 minutes occupancy ranged from 26 – 29ºC for several typical flooring materials. For floors occupied by people with normal indoor footwear, flooring material had an insignificant effect, the same as found in the early studies mentioned above by Chrenko, Muncey and Hutson, and Muncey. Optimal floor temperatures of 25ºC for sedentary and 23ºC for standing or walking people were recommended. At floor temperatures below 20 – 22ºC the percentage of people experiencing cold feet increased rapidly (Olesen 1975). The results are presented in a figure showing the floor temperature and percentage of dissatisfied (1977b). The optimal floor temperature for seated/standing people ranges from 20 – 28ºC with shoes and 23 – 30ºC with bare feet (Olesen 1997a &b). The minimum temperature can be reduced for higher activity levels. Figure 5 shows a similar figure adopted by the ASHRAE and ISO standards to define acceptable floor temperatures. The allowable range of the floor temperature is 19 – 29ºC for the 10% dissatisfaction criterion. The upper limit is in fact the same as the limit provided by the 1956 edition of the ASHAE Guide.

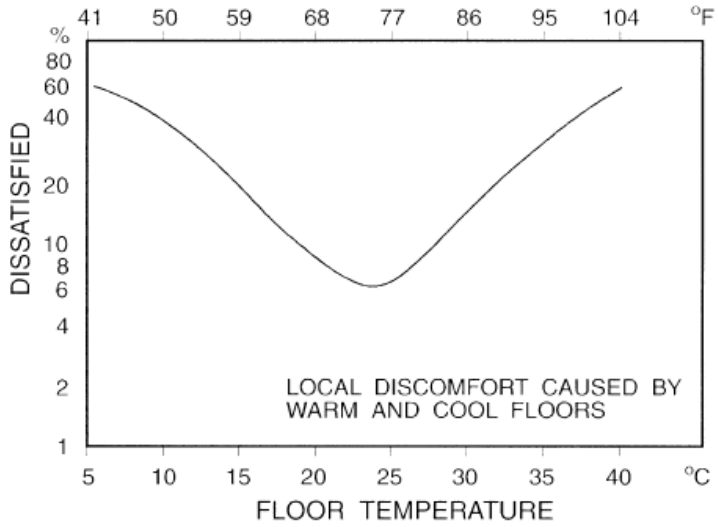


Figure 5: Local discomfort caused by warm and cold floors (ASHRAE 55 – 2004)

A heated floor is regarded as a low-energy heating strategy which provides a high comfort level because of the reduced perception of draft due to the smaller vertical air temperature difference when the floor is heated. Occupants find it pleasant to receive direct thermal radiation from the heated floor (Eijdems 1994, Boerstra et al. 2000, Watanabe 2001). It was popular in Britain during the Roman Empire (Winslom et al. 1949), and is culturally preferred for heating in Korea and Japan (Yoon 1992, Hashiguchi 2004).

Hashiguchi et al. (2004) tested thermal-comfort reactions to floor heating for both elderly and young people and found that the percentage of subjects who felt comfortable was higher for the heated floor (air 21ºC, floor 29ºC) than for the neutral room (25ºC) for both age groups, although the differences were not significant. Sohn (1986) recommends 33.6 – 38.8ºC as the comfortable floor surface temperature, much higher than the value provided by standards. After reviewing a large number of studies about the optimal floor surface temperature in Japan, Zhang et al. (1998) proposed that the optimal floor surface temperature should be within 26 – 30ºC in Japan. The lower limit is also considerably higher than the standards. Katahira et al. (2005) examined thermal comfort in a space with floor heating (no floor surface temperature provided) at air temperatures of 18, 20 and 22ºC, and in air-conditioned space at air temperatures 20, 22, 24ºC. Although the test conditions were generally evaluated as cool and no significant differences were found between the floor-heating and the air-conditioned conditions, the chilliest feeling did go to the 20ºC air-conditioned room. The desire for higher floor temperatures was higher in the air-conditioned spaces than the floor-heating spaces. Tarano et al. (1996, 1997, 2000) conducted a series of studies to examine the comfort impact by heating the sole or legs in a cool environment. One study (1996) showed that in a cool environment (18ºC), a 38ºC hot panel for heating soles (sole sensation was between ‘slightly hot’ to ‘hot’) can remove whole body discomfort. In the study (2000), the authors showed that in a cool environment, a warm thermal sensation of sole at 2 of the ASHRAE 7-point scale seemed to provide the most satisfactory with the sole sensation. In the study (1996), the authors showed that when the lower legs, not only the bottom of the feet, were warmed by both bottom and side heating panels, whole body comfort was achieved in a cool environment (18ºC).

Cooling floors are also considered as an alternative low energy technology for buildings and it has been applied in a large airport (Simmonds 1994, Simmonds et al. 2000), and in residences [Davis Energy Group, personal communication].

3.4 UNWANTED AIR MOVEMENT (DRAFT)

Air motion can be viewed as a pleasant breeze when people are warm, as it is traditionally used for cooling and stimulation in natural ventilated buildings, or it can be considered as an unacceptable cool draft when people are neutral or cool. Draft is defined as an unwanted local cooling of the body caused by air motion. It usually occurs when the body's heat balance is neutral or cold.

3.4.1 DRAFT STUDIES

The sensation of draft from air motion depends on the body's thermal state. The percentage of dissatisfied population is a function of room air temperature (representing the whole-body thermal state), air velocity, and turbulence intensity. Convective heat transfer is roughly proportional to the square root of mean air velocity.

The turbulent intensity, representing the velocity fluctuation which is defined as the standard deviation of the instantaneous velocities divided by the mean velocity, was identified as an important factor on the occurrence of draft sensation (Mayer 1987). Fanger and Pederson (1977) found that the percentage of dissatisfied was much higher for a fluctuating velocity than a constant velocity. Maximum discomfort appears at the air velocity fluctuated at a frequency between 0.3 – 0.5 Hz (Fanger and Pederson 1977, Zhou and Melikov 2002). Fanger et al. (1989) investigated the effect of turbulence intensity on the sensation of draft and developed a draft model (Eq. 1) to predict the percentage of dissatisfied population (DR).

$$DR = (34 - t_a) \cdot (V - 0.05)^{0.62} \cdot (0.37VT_u + 3.14) \qquad \text{(Eq. 1)}$$

The 1989 study was conducted for sedentary people at an air temperature of 23ºC. The draft model was developed by interpolating results from this study and an earlier test (Fanger P.O. and Christensen 1986) done at 20ºC, 23ºC, and 26ºC under moderate to high turbulent intensity.

The air flow in the tests came from behind the subjects, directed toward the back of the neck because this direction was judged to be the most sensitive direction. In the first hour of the tests before the air flow was applied, the subjects modified their clothing to keep themselves neutral. In the following 90 minutes, their clothing was kept constant and the subjects experienced six different levels of velocity from 0.05 m/s to 0.4 m/s, increasing in15 minute time steps. As the velocity increased, the subject's thermal sensation decreased and was lower than neutral.

Because the test conditions were neutral to cool, the draft model should apply only to sedentary, thermally neutral or cool people. It should also apply only to air flows directed toward the back of the neck. Neither of these restrictions are specified in the standards which have adopted the draft model.

The draft model is presented in Figure 6, as it appears in ASHRAE 55 and ISO standards. ASHRAE standard 55 – 2004 also allows elevated air speed to be used to increase the maximum temperature. Figure 7 (from Fountain and Arens 1993) shows the air velocities that can be used to offset the comfort effects of a rise in air temperature. The velocities are much greater than in the draft model. However, this figure can be used only if affected occupants have control of the air speed, usually through an operable window or fan. This leaves Figure 6 covering all other conditions, regardless of the fact that the original tests were conducted under neutral to slightly cool environments and the air motion towards the back of the neck. Field measurements carried out to characterize turbulence occurring in ventilated spaces in a wide variety of buildings by Hanzawa et al. (1987) show that the turbulence intensity is in a range of 10% to 70%. If applying 50% turbulence intensity, the acceptable air velocity is about 0.2 m/s.

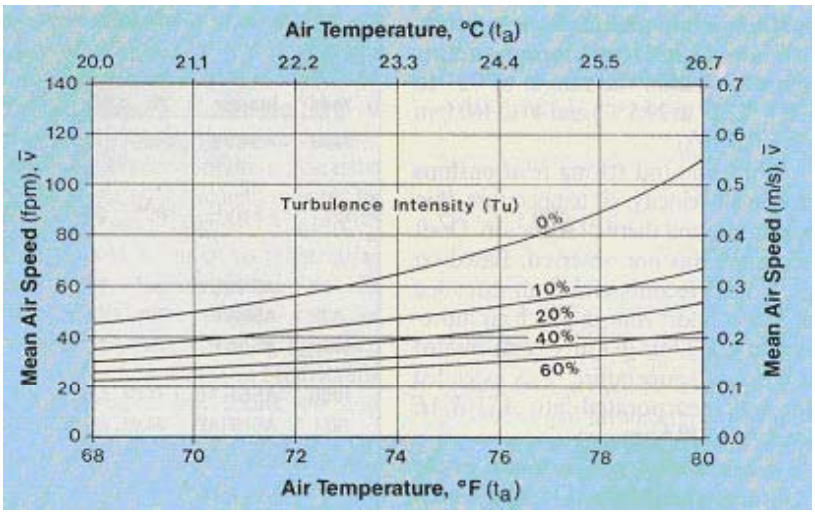


Figure 6: Allowable mean air speed as a function of air temperature and turbulence intensity (Fountain and Arens 1993)

The limit of the air motion and the risk of the draft should be considered under different environments. Under neutral or slight cool environments, the risk of draft sensation is high (Houghten et al. 1938, Fanger at al. 1974, Fanger and Pedersen 1977, Fanger and Christensen 1986, Fanger el al. 1988). Toftum (1994a, 1996, 2003) found that as the overall sensation moves toward cool from neutral, the risk of draft increased two to three times. Toftum (2002) cites the work of Berglund & Fobelets (1987) and states that subjective responses to air velocity and radiant asymmetry are independent. He draws attention to the finding that, in cold weather, "the percent of subjects experiencing a draught approximately doubled in the cool environment as compared to the neutral environment".

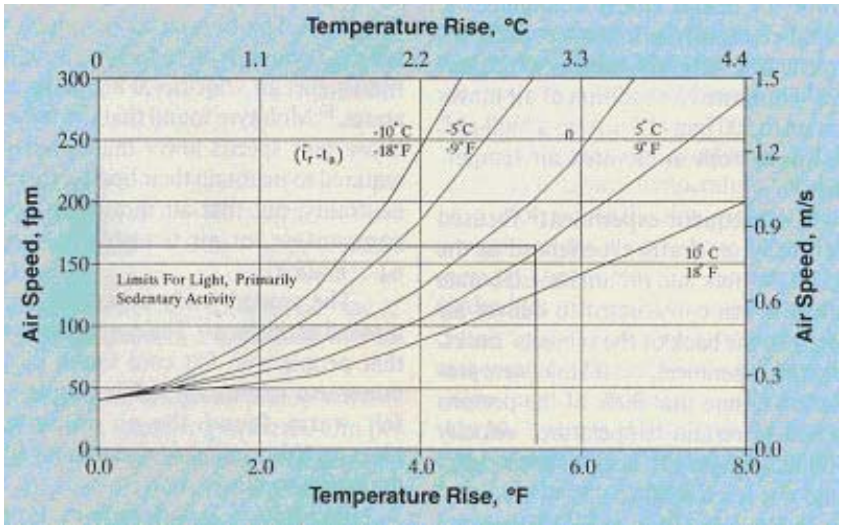


Figure 7: Air speed required to offset increased temperature (Fountain and Arens 1993)

In warmer environments, many studies show that higher velocities (up to 0.8 m/s by Roles et al. 1974, 1983, 1.0 m/s by Scheatzle et al. 1989, Busch 1990, and Tanabe and Kimura 1987, 1.2 m/s by Kontz et al. 1983, 1.6 m/s by Tanabe et al.) were preferable or perceived as pleasant and no unpleasant draft was perceived. A literature review examining air motion, comfort, and standard was provided by Fountain and Arens (1993). The paper provides a figure to consolidate several

studies to show the different ranges for preferred velocities and the limits at different environments (Figure 8).

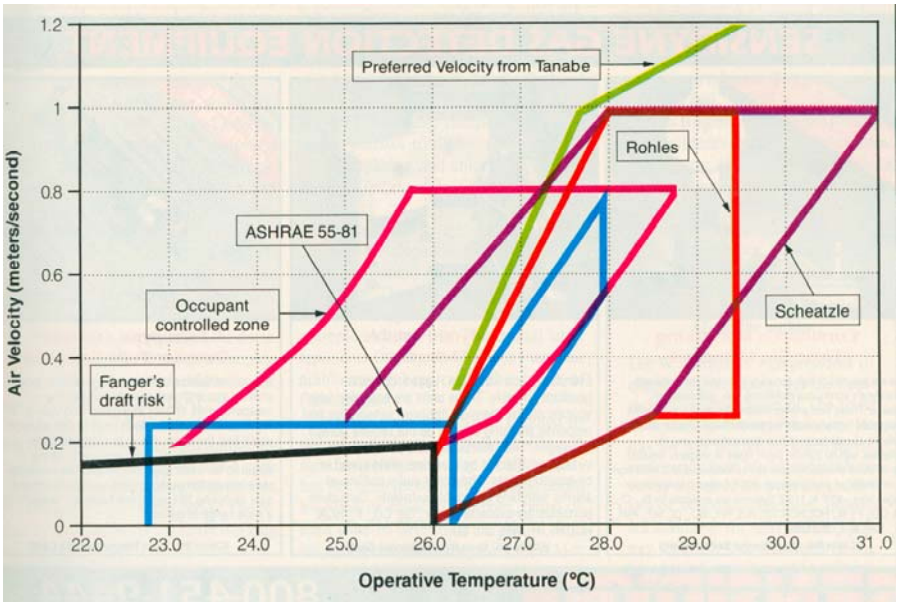


Figure 8: Range of velocity requirements (Fountain and Arens 1993)

The studies of many researchers show that in a warm environment, higher air movement provides comfort. Arens et al. (1998) did a laboratory study where 119 people participated. It found that subjects considered air motion pleasant up to 1 m/s at 29.5ºC, desiring no change to temperature or air movement. It was possible to make people comfortable by air motion up to 1.4 m/s at air temperature up to 31ºC (1 met) or 29ºC (1.2 met). Crossing the entire test conditions (24.5 – 31.5ºC), in most cases, the air velocity was above 0.4 m/s and up to 1.4 m/s, but very few people wanted less air movement. Fountain et al. (1994) found that the air motion can make 91% people comfortable up to an air temperature of 28.5ºC. However, based on the draft model, 63.2% of these comfortable votes would have been predicted to be "unacceptable". At the upper limit of the draft model (0.2 m/s at a turbulence intensity of 40%), 50% of the people wanted more air movement. The authors point out that the draft model is not designed to make the greatest number of people satisfied with the air movement in warm environment, just to protect 20% from being dissatisfied in slightly cool environment. So instead of examining discomfort, the authors defined an index of predicted Percent Satisfied (PS) which can be used to predict the percentage of satisfaction in a warm environment by applying higher air motion. The model is developed based on an experiment that encouraged people to use air motion to make them comfortable. McIntyre did two studies (1978) to examine the acceptable velocity at warm room temperatures. He found that the subjects chose an air motion lower than the value necessary for heat balance, but that the air motion could compensate for air temperature up to 28.5ºC. In another test examining the draft directed at the face (McIntyre 1989), the author found that when the whole body was warm, people considered the air motion pleasant. When the whole body was cool the air motion was considered unpleasant. Toftum et al. (1997) also examined effect of air direction on draft. They found that at an air temperature of 20ºC and 23ºC, the air motion from below was perceived as most uncomfortable. At air temperature 26ºC, air movement from above was perceived as uncomfortable. The authors also recommended taking air direction into account when providing design guidelines for air movement.

Recent studies indicate that the draft model has to be modified to take into account additional parameters such as the activity level, length of exposure and velocity directions (Jorn and Nielsen

1996a & b, Jorn et al. 2000, Griefhana 1999). People with higher activity levels were found to be not so sensitive to draft (Jones et al. 1986, Toftum and Nielsen 1996, Griefahn et al. 2001)). Toftum (1994) proposed an extension of the draft model which specifies much higher velocity corresponding to the high activity level.

Toftum (2004) examined the literature and provides a good summary for the desirable air motion vs. draft sensation under different environmental conditions. "At temperature up to 22 – 23ºC, at sedentary activity and with occupants feeling neutral or cooler, there is a risk of air motion being perceived as unacceptable even at low velocities. In particular, a cool overall thermal sensation negatively influences the subjective perception of air movement. With occupants feeling warmer than neutral, at temperature above 23ºC or at raised activity levels, humans generally do not feel draught at air velocities typical for indoor environments (up to around 0.4 m/s). In the higher temperature range, very high air velocities up to around 1.6 m/s have been found to be acceptable at air temperatures around 30ºC" (Toftum 2004).

3.4.2 DRAFT CAUSED BY COLD WINDOWS

Cool drafts are a common complaint near windows. Although a warm window can also induce air motion, because the air movement is upward and not near the occupied zone, and also because the warm air temperature has little heat removal potential, it has little effect. Most studies focus on the downward air motion induced by a cool window and its impact on comfort (draft). A cold window causes draft discomfort through increased velocity, lowered air temperature, and increased turbulence intensity.

Ge and Fazio (2004) measured velocity and temperature profiles with large tall (3.8m x 6.7m) glass panels. Near the window, the cold window-induced air motion could be as large as 1 m/s (0.6 m above floor). When measured at 1.2 m away from the window, the velocity reduced to 0.15 m/s. The air temperature at 1.2 m away was about 0.8ºC lower than the room air temperature. Near the floor (0.1 m above) and close to the window, the maximum air velocity reached 0.4 m/s. Rueegg et al. (2001) measured velocity profiles due to cold windows. When the outdoor temperature was below –10ºC, a well insulated window (U-value of 1.4 W/m^2 K) created an air movement greater than 0.2 m/s within 0.2m of the window at height 0.13m above the window frame. When the outdoor air temperature was higher but near –10ºC, at 1m away from the window, the maximum velocity was smaller than 0.15 m/s at the height 0.1 m above the floor. People have footwear so normally 0.1 m above floor is considered an appropriate measurement height (Manz and Frank 2004). Manz and Frank also recommend 1m away from the window as the occupied zone. ASHRAE Standard 55 defines 0.6 m away from the window as the occupied zone. Compared with long-wave and short-wave radiations, Lyons et al. (1999) demonstrated that for most residential-size windows, draft effects are generally small. Through CFD analysis of a room 3 x 3 x 5 m with one cold wall, Manz and Frank (2004) found that draft is more critical and caused more discomfort than reduced operative temperature or strong radiation asymmetry. A PPD of 20% due to draft occurs 1 m away from a 15ºC wall and 2m away from a 10ºC wall.

Heiselberg (1994, 1995) developed a set of empirical equations to calculate the maximum velocity and temperature changes of the cold draft along the floor after it flows off the surface and penetrates into the occupied zone. Rueegg et al. (2001) measured the air velocity profile along the floor and compared with the predicted value from Heiselberg's equation and found that the equation provides satisfactory results, even for windows with a sill. Ge and Fazio (2004) compared their velocity and temperature measurements for large tall glass panels with the predictions from the empirical equations developed by Heiselberg. The authors also proved that Heiselherg's equations provide close estimations of the measured data for cases having a frame projection, providing the height of the glazing is used in the calculation. Manz and Frank (2004) used CFD simulations to show that an increase of the internal heat load leads to higher downdraft

air speed, and they modified Heiselberg's equation to account for the internal heat load. They explained that the momentum of the buoyancy flow at the heat source boosts the motion of the downward flow near the cold wall. However, Rueegg et al. (2001) measured the velocity profile of a draft near a cold window and found that as the internal heat load increased, the boundary layer thickness increased but the peak velocity decreased. The author's explanation was that the plumes from the heat load spread at the ceiling and circulated down, and mixed together with the draft layer so the temperature of the layer was raised and the draft was reduced.

As the cool air flows downward next to a cold window, the thickness of the air layer to which the vertical motion is confined increases from the top to the bottom. At a certain distance the airflow will become turbulent. By simulation, Manz and Frank (2004) found that in a room (with an entire wall being cold), the turbulent intensity could reach 50%, although a lower turbulent intensity was found in a similar setting (Olesen 2002).

To counteract downdrafts, a common solution is to install a radiator underneath the window, which costs energy (Lyons 1999), but does improve comfort. Gan's simulation (2001) showed that keeping the 10ºC radiant asymmetry, by applying a radiator under the window sill, the discomfort area originally extending to 1m from the window was reduced to 0.75 m from the window. However, care should be taken at ankle level (being hot from the radiator) and cool at the upper body level. With the window performance improved, the effect of the draft is reduced. A few studies have examined the possibility of removing the heating source by increasing the window performance, in some cases finding that it is possible to maintain comfort without additional radiators (Rueegg et al. 2001, Larson and Moshfegh 2002). Measurements by Rueegg et al. also showed that it was critical to insulate the frame of advanced windows. They also tested the effect of increasing the roughness on top of the windowsill, which showed little influence reducing the draft. However, openings on the windowsill (as shown in Figure 9) can significantly reduce the draft because they take up the downdraft and release it again at a lower speed. Heiseberg et al. (1995) found however that with turbulent flow obstacles larger than the boundary-layer thickness can break down the boundary layer to reduce the downward cold draft from large glazed surface. The risk of thermal discomfort due to downdraft was reduced considerably.

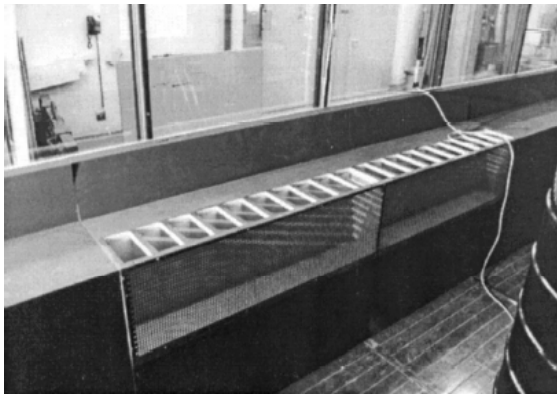


Figure 9: Openings in window sill to reduce draft down flow (Ruegg et al. 2004)

Although the draft model is used in the ASHRAE and ISO standards for any direction or location of air motion, it is based only on tests in which airflow affected the back of subjects' necks (Fanger and Christensen 1986, Fanger et al. 1988). Although the back of the neck may be the most sensitive part of a building occupant, airflows in this direction and location do not happen each time there is measurable air movement. For example, the probability of air coming through an open window and hitting the back of the neck is relatively small given the way people orient

themselves. The probability is particularly small in the case of the downward airflow induced by a cold window, where the highest air movement is within inches of the glass or at ankle level along the floor. The sensitivity to draft at ankle is much less than at back of neck (Fanger and Pedersen 1977). Therefore, the draft model should be used carefully in cases with cold windows, although at this time there is no other evaluation method available (except the UCB Comfort Model which we will discuss later). The evaluations by other researchers (Manz and Frank 2004, Rueegg et al. 2001, Ge and Fazio 2004) about the discomfort induced by drafts from cold windows may also need to be reexamined, since they applied the draft model.

3.4.3 OPERABLE WINDOWS

In a general and recurring theme, a number of papers discuss the value of operable windows for increasing summer comfort and reducing air-conditioning energy consumption. Nicol & Humphreys (2002) discuss "adaptive opportunity", meaning "the ability to open a window, draw a blind, use a fan and so on", and the beneficial effect this has on an occupant's perception of comfort. They also remind us that solar control (to reduce PMV) is orientation-specific and therefore so is the specification of the appropriate glazing solar transmittance. McCartney & Nicol (2002), Humphreys & Nicol (2002), de Dear & Brager (2002), and Fanger & Toftum (2002) describe the mechanisms by which operable windows and natural ventilation can offset mechanical cooling.

It may be possible to acknowledge the potential contribution of operable windows in a quantified 'window comfort rating'. Clearly, correctly-operated windows should improve comfort through much of the occupied space. It may be feasible to include a conservative "operable window/natural ventilation" term in the comfort calculation, if such a quantity is integrated over a year of operation. Any such algorithm would need to be climate-sensitive.

3.5 THERMAL COMFORT MODELS

The most common method for evaluating thermal comfort is the Predicted Mean Vote (PMV) model proposed by Fanger (1973). The PMV method predicts thermal comfort based on overall heat loss from the body.

The thermal comfort index (PMV) is calculated using Eq. 2.

$$PMV = \left[0.303^{-0.036M} + 0.028\right] \cdot L \qquad \text{(Eq. 2)}$$

L represents the thermal load on the body, defined as the difference between the internal heat production and the heat loss to the actual environment for a person hypothetically kept at a comfortable value of skin temperature and sweat rate. The thermal load L is calculated from air temperature, mean radiant temperature (MRT), air velocity, humidity, clothing level and metabolic heat production.

Fountain and Huizenga (1995) developed an ASHRAE Thermal Comfort Tool software to allow consistent calculation of thermal comfort indices including PMV, PPD, and Effective Temperature (ET*). ET* is based on a two-node physiological model of the body, with core and skin as the two nodes (Gagge et al., 1970).

There are several models to predict thermal sensation in uniform but transient environments, such as models developed by Fiala (1998) and Wang (1994). These models predict sensation under transient condition by incorporating a dynamic factor in the model. Ring and de Dear (1991) developed a sophisticated skin model which divides the skin and clothing into 40 layers to calculate thermal sensation response to fast changes in environmental conditions. Tanabe et al (2002) used their 65-node thermoregulation model to investigate a room having a window at one end and/or a cooled ceiling panel. This model incorporates a CFD model developed by

Murakami et al. (1998) and a radiation model (which considers the differing sensitivity of the skin to various wavelengths, Marita et al. (2001)). PMV is used as the thermal comfort evaluation index.

Using these uniform condition models, when windows are warmer or cooler than the air temperature, mean radiant temperature (MRT) has to be determined. MRT is defined as the uniform temperature of an imaginary uniform enclosure in which radiant heat transfer from the human body equals the radiant heat transfer in the actual non-uniform environment. Measured air temperature, globe temperature, and air velocity can be combined to calculate MRT (ASHRAE Handbook 1997). When surface temperatures can be measured, MRT can be calculated from these temperatures along with view factors of the person to each surface. In buildings with windows, the glass and frame temperatures can be calculated by software WINDOW and THERM based on outdoor air temperature and solar radiation. Both WINDOW and THERM are developed by the Windows and Daylighting Group at Lawrence Berkeley National Laboratory (LBNL). There exist other models (e.g. Gan 1994) to deal with the non-uniform radiation field. Gan's model divides non-isothermal walls into isothermal segments and then calculates the MRT based on the surface temperatures of the segments and their view factors. Another way to deal with the long-wave radiation asymmetry is to directly calculate the radiative heat transfer between the person and his/her surroundings based on the view factors, as is done in the UCB Comfort Model (Huizenga et al. 2000). In the UCB Comfort Model, the human body and the environments were divided into thousands of polygons to derive detailed view factors to calculate the radiant heat exchange.

Kansas State University (KSU) produced a program (Building Comfort Analysis Program, BCAP) sponsored by ASHRAE to determine radiant heat exchange of the human body with his/her surrounding (Jones and Chapman 1994, Chapman and De Greef 1997). The current BCAP model links the properties obtained from the WINDOW program and includes the impact from the window frames. The PMV, PPD and operative temperature calculations are conducted for each node point of the room so the results are presented as the contour of PMV, PPD, or operative temperature (Chapman et al. 2004, Sengupta et al. 2005a & b, Chapman and Sengupta 2003). The authors proposed "Penetration depth" and "Fenestration performance map" to evaluate the window performance. Penetration depth is defined as the distance into the room from a window, beyond that thermal comfort condition exists. The fenestration map can be used as a design tool to determine the correct window wall ratio to ensure comfort at a defined distance from the window.

When solar radiation is present, the PMV calculation has to consider this load. One way is to put the solar load as an additional load into the thermal load L calculation, which is used to calculate the PMV as shown in Eq. 2. The alternative way is to calculate an MRT equivalent to surrounding temperatures plus the solar radiation, such as a method provided by Arens et al. (1986). Sullivan provided a linearized expression to calculate the sensitivity of PMV to the solar flux (Sullivan 1986a and 1986b). By applying both Arens and Sullivan's methods, Lyons et al. (1999) demonstrated that every unit of incident solar radiation (W/m^2) (derived from the product of solar irradiance and direct solar transmittance of a window) corresponds to +0.0024 increment in PMV (thermal sensation vote).

The PMV evaluation method treats the entire body as one object. It does not distinguish between different parts of the body. If one side is warm and the other cold, the PMV calculation would calculate a zero thermal load and therefore yield a neutral thermal sensation (PMV=0).

The PMV model is basis for most current standards prescribing methods for evaluating thermal comfort in buildings. The model was developed based on data from uniform thermal environments (Fanger 1970). Because it only calculates the heat transfer for the entire body, it

cannot predict local discomfort. Clothing is assumed to cover the entire body uniformly which results in one equal skin temperature across the entire body. Obviously, the local effects of asymmetric conditions, such as an environment with a hot or a cold window, or local air motion around a person's face provided by a fan, are lost in this whole-body model. Calculating MRT in an asymmetric radiation environment averages the influence to the whole body and makes the influence on a specific body part, which has a bigger view factor, less sensitive.

The non-uniformity of the environment with the presence of warm or cold windows not only provides an asymmetric radiant field, but also causes a variation in the air velocity and the temperature over a person's height. Several examples from measurements of a large tall glass panel are shown by Ge and Fazio (2004). Obviously it is difficult to directly apply the PMV method in complex situations with a warm or cold window. In automobile industry, researchers adopted a few ways to deal with the asymmetrical environment. Ingersoll et al. (1992) applied the PMV model individually to head, torso, and feet. Their whole-body PMV is an area weighted average of the PMV from the three body parts. Matsunaga et al. (1993) calculated the weighted equivalent temperature from head, abdomen, and feet and used the equivalent temperature to calculate PMV. Kori et al. (1995) applied the two-node model (which treats the whole body as one uniform unit) to eleven body parts to calculate the SET* individually. The KSU clothing model (Jones and Ogawa 1992) combines the two-node model with a detailed clothing model to deal with radiant asymmetry. Because the PMV model and the 2-node model treat the whole body as one object, all the above methods have difficulties really separating the body into more parts in order to deal with asymmetry. Hagino and Hara (1992) predict whole-body thermal sensation using sensations from a few body parts which experience environmental changes in their test conditions (forehead, upper arm on window side, thigh on window side and instep on window side). Because their experiment didn't examine other body parts, the model can only be used in situations similar to the test condition. Taniguchi et al. (1992) developed a model to predict thermal sensation based on face skin temperatures. Again because the model was based on the test in which asymmetry only appears on the head with air motion, the model can only be used in situations similar to the test condition.

Wyon et al. (1989) proposed to use Equivalent Homogeneous Temperature (EHT) to express heat loss for each body part individually. The EHT for one body part is defined as the temperature in a uniform environment where the heat loss from the body part is the same as his/her heat loss in an actual (non-uniform) environment. The acceptable comfort range for each body part is presented as a "piste"[3] shown in Figure 10(Wyon et al. 1989). Between the upper and lower temperature limits is the ideal profile.

The EHT evaluation method has been used in automobile industry (Bohm et al. 1990, 2004, Nilsson 2005) to address non-uniform environments. EHT defines an acceptable temperature range for each body part, but it does not quantify local comfort levels and the *overall* thermal comfort. In other words, it does not tell how comfortable or uncomfortable a body part feels, and it does not tell the overall comfort when all parts are slightly cool vs. some parts are slightly cool and other parts are slightly warm, all within the acceptable range defined by the piste. In addition, the piste developed from each study only applies to the environmental and the clothing and metabolic conditions tested. So, its use is limited to the specific conditions tested in the studies where it was applied.

[3] so-called because the diagram looks somewhat like a ski run (piste) on a mountainside.

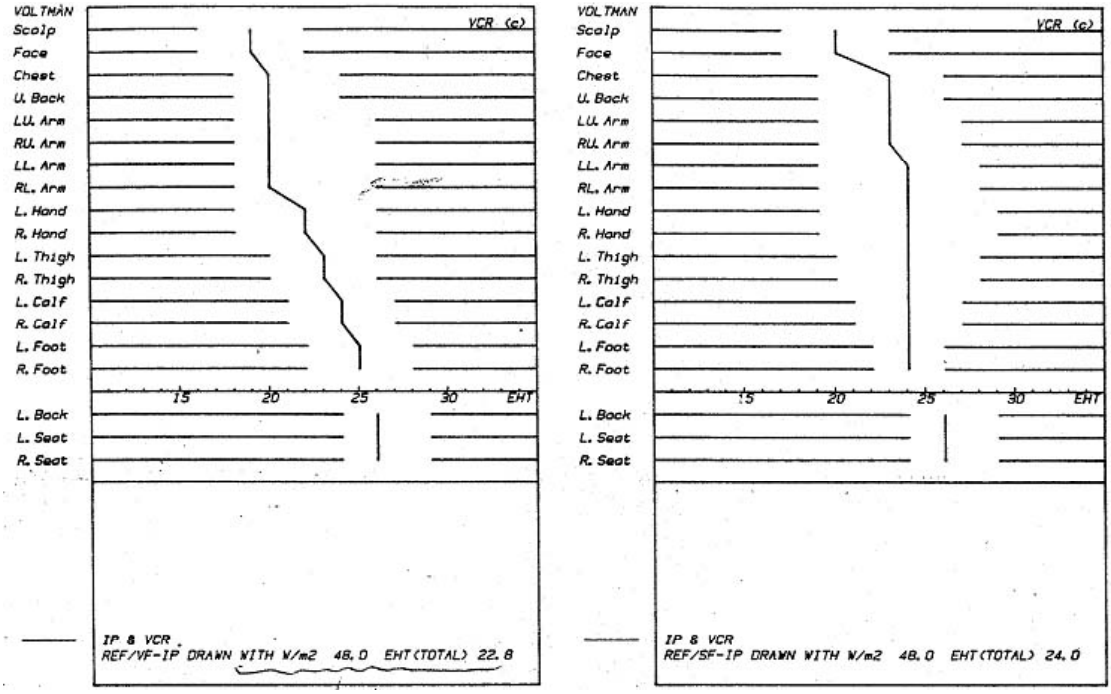


Figure 10: EHT piste and ideal profiles for a driver in winter (left) and summer (right) (Wyon 2004)

3.6 LOCAL DISCOMFORT

Over $80 billion is spent annually in the United States to heat and cool buildings, in order to provide comfortable, productive environments for their occupants. The heating, ventilating, and air conditioning (HVAC) equipment used to create and maintain these indoor environments is energy-intensive, but is not particularly successful at keeping occupants truly comfortable. Studies have shown that about 75% of all occupant complaints in buildings are thermal-comfort-related (Martin et al. 2002). These complaints are largely caused by discomfort in local body parts such as feet, hands, and neck, based on field survey in displacement ventilated office buildings (Melikov et al. 2005). Even in the studies presented early in the literature section for investigating the limits with asymmetric walls and ceilings (Fanger et al. 1980, 1985), and the other study defining the acceptable air temperature stratification (Olesen et al. 1979), the authors all pointed out that the discomfort was due to warm head or cool feet, i.e. local discomfort.

In the highly asymmetric environments such as the ones with large windows or very high or low glass temperatures, the discomfort for local body parts are likely to happen. Identifying how these phenomena of local discomfort occur and removing the driving forces that create them is the key to improve sustained comfort in office buildings. A principal weakness in current building practice is exactly the absence of analytical methods to quantify and evaluate local discomfort in the context of thermally asymmetric environments. Most of the existing analytical models (PMV, Fanger 1970, Fiala 1998, Wang 1994) were all developed for uniform conditions (models developed by Fiala and Wang predict thermal sensation under transient conditions). The UCB Comfort Model is the only model existed which predicts thermal sensation and comfort for local body parts.

4 UC BERKELEY COMFORT MODEL

This section introduces the UCB Comfort Model and explains its capabilities in terms of the assessment of thermal comfort in thermally asymmetric environments. A comparison between the comfort indicators provided by the PMV model and the UCB model is presented. The suitability of both models with respect to analyzing the impact of window performance on thermal comfort is discussed.

4.1 MODEL DESCRIPTION

The University of California at Berkeley developed a thermal comfort model (UC Berkeley Comfort Model) that predicts local comfort for different body parts, and integrates local comfort levels to yield whole-body thermal comfort (Zhang et al. 2004). The model is developed based on a large number of human subject tests under different asymmetric and transient thermal environments (Zhang 2003, Huizenga 2004). When simulating an indoor environment with windows, the UCB comfort model predicts the local comfort for all body parts, which is influenced by radiant heat exchange with the window, solar gain, air motion, and non-uniform air temperatures, and provides a whole body comfort level by integrating the local comfort of the various body parts.

The UCB comfort model divides the body into 16 body parts (Figure 11). Each part is divided into core, muscle, fat, and skin layers. An underlying model of the blood circulation system simulates the heat exchanges between the tissue layers, such as muscle and skin. A detailed description of the physiology modeling and the validation results can be found in Huizenga et al. 2001.

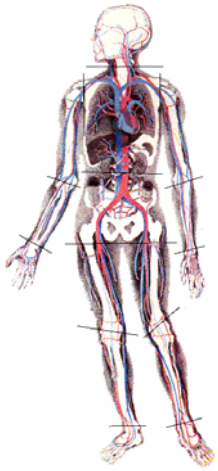


Figure 11: Subdivision into 16 body parts used in UCB comfort model

The model divides the surface of the human body into more than five thousand polygons to calculate the radiation heat transfer between the body and the environment (Figure 12). Therefore, the heat transfer between the body and thermally asymmetric surfaces, such as walls containing windows, can be calculated in great detail. The solar load on the body is also calculated based on the relative geometric position of the sun, the environment, and the polygons mapping the body surface.

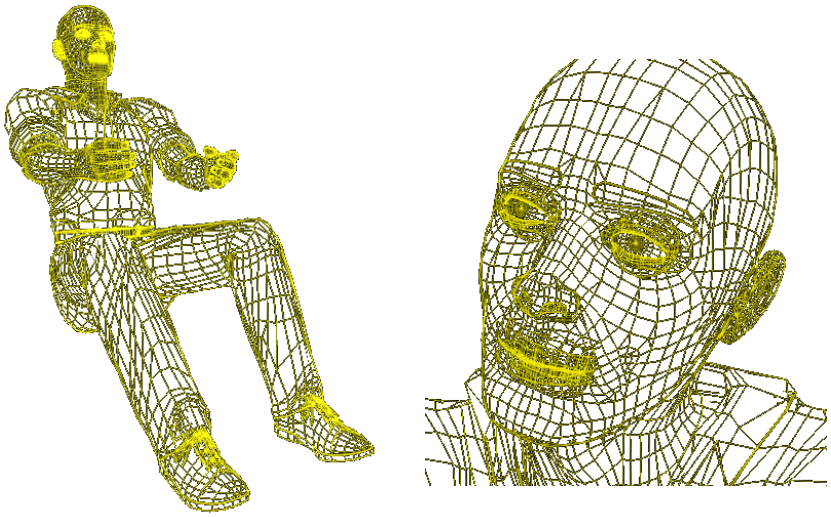


Figure 12: Polygons used to calculate radiation heat exchange in UCB comfort model

Local sensation (e.g. left hand feels cold) is calculated based on the local skin temperature of the body part and the mean skin temperature, which represents the whole-body thermal state. In transient conditions, the derivatives of local skin and core temperatures are included. Local comfort (e.g. face feels comfortable) is calculated based on local and overall sensations. For example, face cooling could be interpreted either as comfortable or uncomfortable depending on whether the whole-body thermal state is warm or cool. Separate local sensation and comfort models are provided for each of the 16 body parts. The local sensation and comfort levels are integrated to get an overall sensation (e.g. whole-body feels hot) and an overall comfort (whole-body is very comfortable). A description of the local and overall sensation and comfort models is presented in Zhang et al. 2004. Figure 13 illustrates the concepts of local sensation and comfort, whole-body sensation and comfort. Because the UCB comfort model simulates the heat transfer between each individual body part and its microclimate in order to predict sensation and comfort for individual body parts, it is well-suited for complex thermal environment where thermal asymmetry and transience exist. It is the currently the only existing model that provides local sensation and local comfort for individual body parts.



Figure 13: Prediction of local as well as overall sensation/comfort in UCB comfort model

Figure 14 shows the interface of the UCB comfort model. The example shown depicts that due to solar radiation (shown in the big image at the center), hands, lower and upper arms, and head feel warmer (right lower bottom image, warmer color presenting warm sensation). As a result, these body parts are uncomfortable (right middle image, yellow to black presenting discomfort from just uncomfortable to very uncomfortable). The overall sensation is shown at the top middle figure (red color representing hot), and the overall comfort is uncomfortable (dark figure on the top left). The overall sensation and comfort levels are also presented numerically next to the figures. The data on the top right shows the values of sensation and comfort for each body part and the whole-body. The data can also show skin, core, muscle, fat temperatures, heat loss, skin wettedness etc based on user's selections. The graph at the middle bottom shows the transient results for the parameters that the user can select.

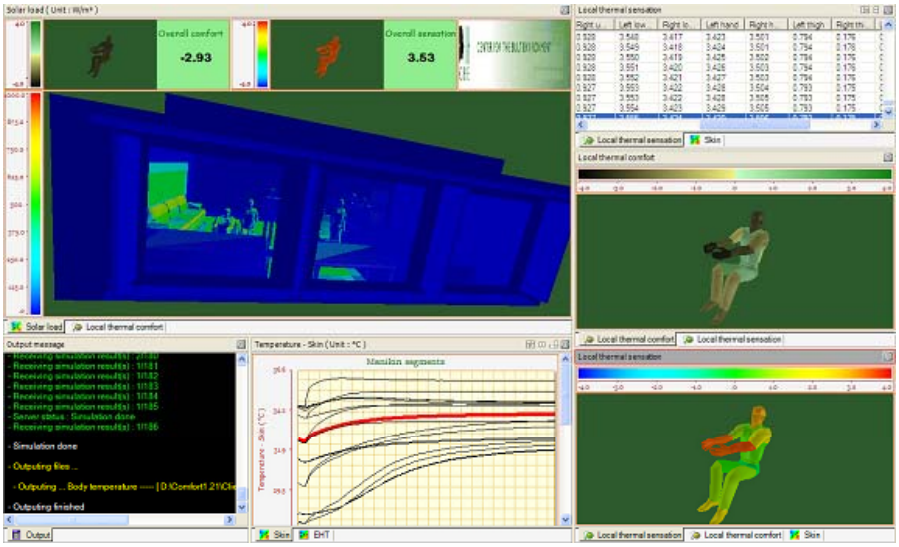


Figure 14: Screenshot of UCB comfort model interface

The model allows users to define their own room and window geometries through a "room editor". Figure 15 shows an example. Because the person can be located at any place, the model can be used to evaluate comfort at any given location of the room, such as a location in a perimeter zone or at a center zone. The surface temperatures of the environment, such as the window or a wall, are individually defined so the window can have the different temperature from the other surfaces. Each surface (such as a wall or a window) can be further divided into small surfaces to assign different component surface temperatures, such as window frame, edge of glass and center of glass temperature. The database with glazing products from WINDOW has been incorporated in the model.

Because of the functionality and the capabilities with respect to the simulation of local discomfort, the UCB comfort model has been used in this research project to predict the effect of window performance on human thermal comfort.

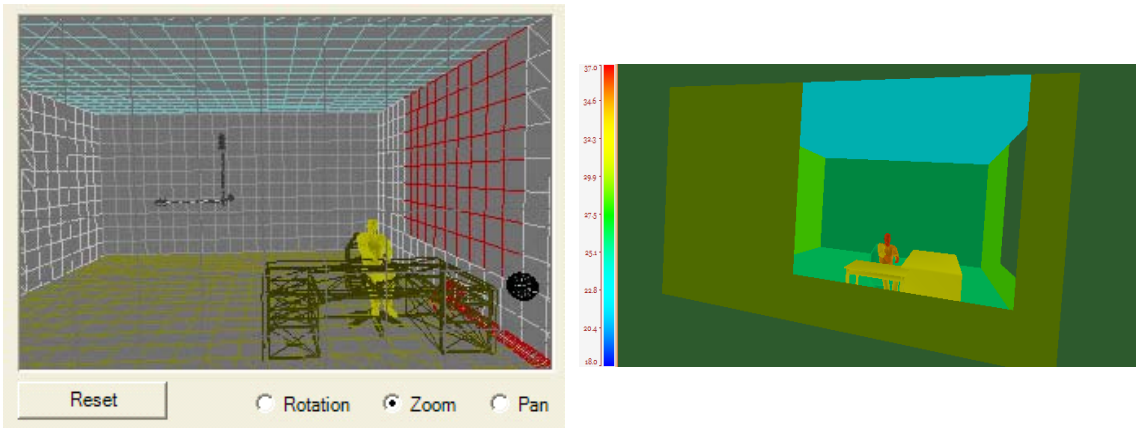


Figure 15: Screenshots of "room editor" and boundary conditions from UCB comfort model

4.2 MODEL COMPARISON

The following paragraphs provide an overview of how the results from both PMV and UCB comfort models compare to each other in particular in assessing the comfort effect of windows.

4.2.1 OVERALL THERMAL SENSATION

The simulations were carried out for a test room measuring 6m wide, 6m deep and 3m high. One elevation of the room is assumed fully glazed (6m x 3m window) and the occupant is positioned 1m away from the window along the center line of the window (Figure 16). The air temperature in the room was set at 25.7ºC and was assumed to be uniform throughout the room. This temperature represents the neutral temperature (i.e. the temperature which yields an overall sensation equal to 0) for a person (1 met, 0.6 clo) seated in the center of a room at uniform temperature (i.e. air temperature equal to internal surface temperature, no windows). We varied the interior surface temperature of the window from –10ºC to 56ºC. The analysis was carried out using both the PMV model and the UCB comfort model and the results are presented in Figure 17 and Figure 18.

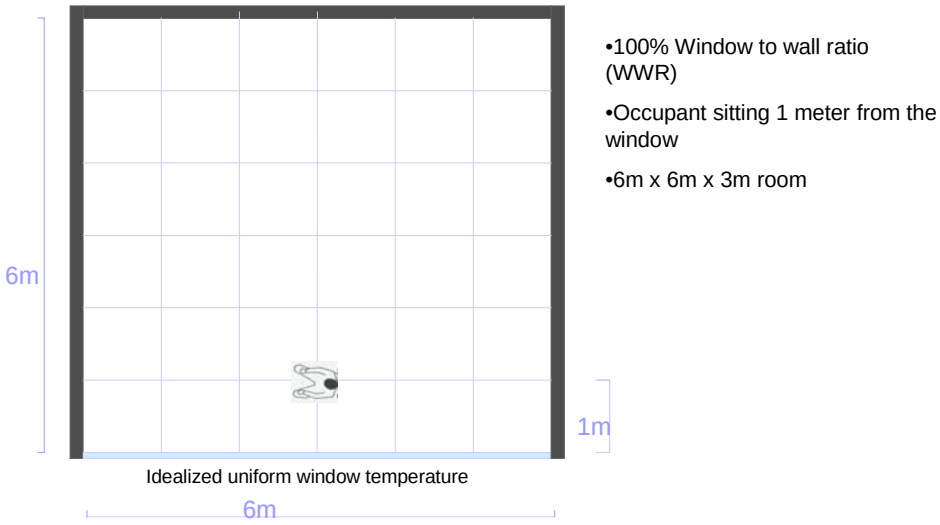


Figure 16: Geometric input data for comfort simulation

When the window surface temperature stays approximately in the center of the temperature range (e.g. between 15ºC and 35º when –0.5 < PMV <0.5), the difference between the PMV and the UCB comfort model is relatively small, less than 0.5 unit of the scale (Figure 17). However, as the window surface temperature becomes more pronounced cold or hot (below 15ºC or above 35ºC), the difference between the two models becomes larger. Because the PMV model only assesses the overall heat transfer between the body and the environment, it is less sensitive to the asymmetry and the local effects caused by the window. The PMV model averages the heat exchange over the whole body and thereby under predicts the effects of thermal asymmetries on comfort. The UCB model calculates the variation in local sensation for the different body parts caused by the window and factors their individual influence into the assessment of overall sensation. The overall heat transfer approach predicts the overall energy balance, but ignores the impact of local discomfort which clearly influences the general assessment of comfort.

The zone in the overall sensation curve which is flattened out (and where the UCB model overlaps with the PMV model) is caused by the adaptation of the thermal receptors in the skin to the environmental temperature. There is a temperature band, centered around the neutral skin temperature (skin temperature under neutral thermal condition, i.e. 25.7ºC), in which the skin temperature can be altered without significantly impacting the thermal sensation. Within this temperature range, the skin is fairly insensitive to thermal stimuli and thermal adaptation occurs. Thermal adaptation occurs more pronounced on the cold side of the neutral temperature than on the warm side (McIntyre 1980, Stevens 1960). This explains why the thermal sensation curve is flattened out more when the window temperature is cooler than the neutral temperature compared to warmer window temperatures.

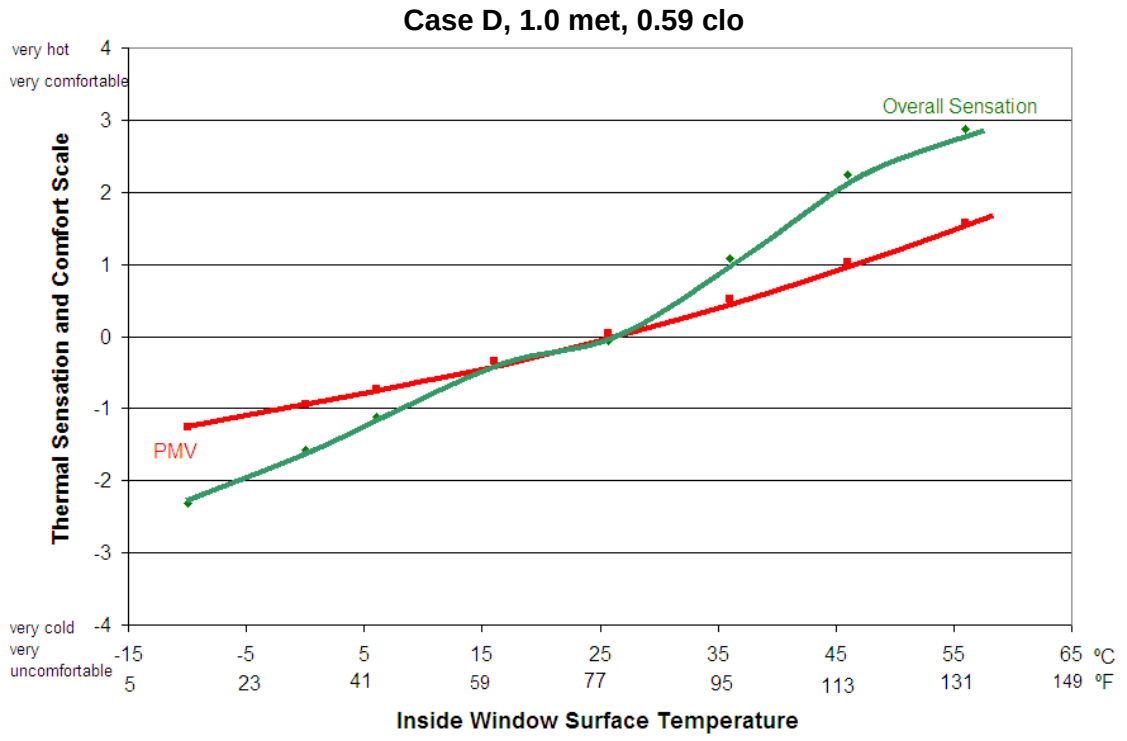


Figure 17: Overall sensation – PMV vs. UCB model

4.2.2 COMFORT LIMITS

The comfort limits for the PMV model are typically defined as –0.5 < PMV < 0.5, which corresponds to a Predicted Percent Dissatisfied (PPD) of 10%. The thermal comfort standards developed by ASHRAE and ISO provide additional limits for the difference between room surface temperatures and the air temperature. For a cold vertical surface, the radiant temperature asymmetry needs to be below 10ºC. For a warm vertical surface, the asymmetry limit is somewhat larger, i.e. 23ºC.

Figure 18 shows the comfort metrics of both the PMV and the UCB model for the boundary conditions described in Section 4.2.1. The PPD curve relates to the PMV curve, in the sense that the PPD attains a minimum value when PMV is equal to 0 (i.e. neutral sensation) and the PPD starts to rise as the PMV moves away from the neutral point. The red shaded area bound by PPD ≤ 10% at the bottom of the graph indicates the limits on the acceptable interior surface temperature of the window. The PMV reaches a value of ±0.5 at 12.5ºC and 37ºC respectively. The comfort limits determined by the UCB comfort model are indicated by the green shaded area at the top of Figure 18.

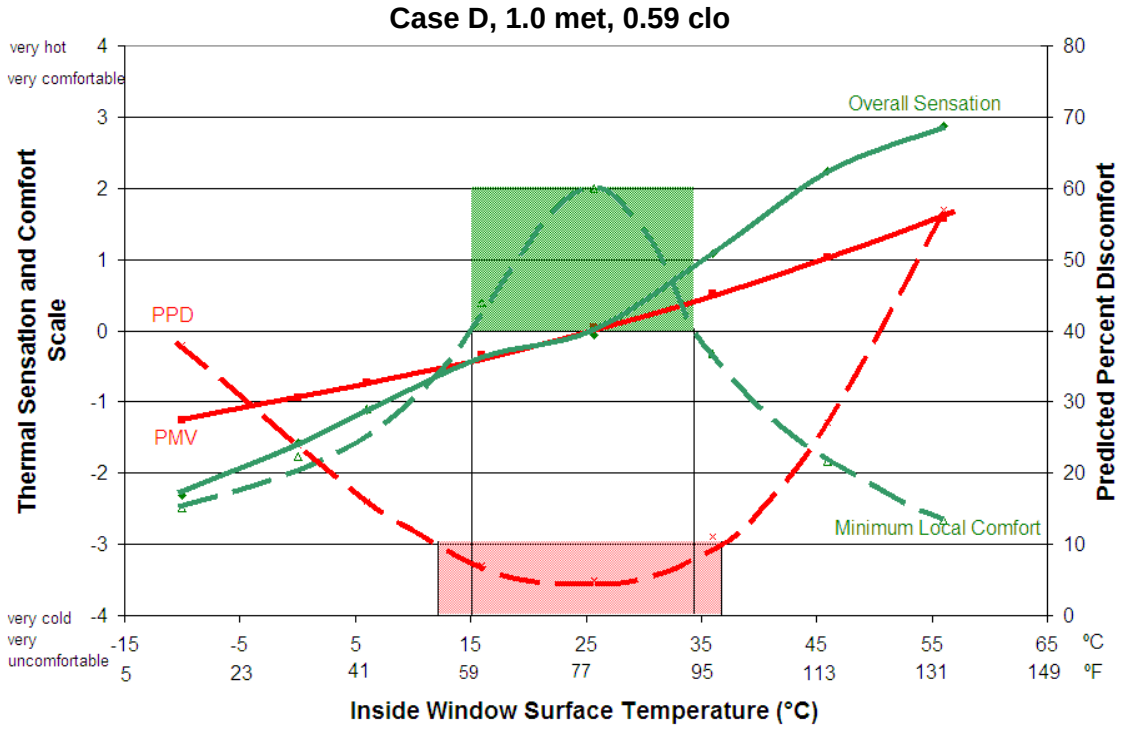


Figure 18: Comfort limits – PMV vs. UCB model

Because studies show that thermal discomfort is mainly caused by local discomfort (Melikov 2005, Wyon 1996), we have defined comfort according to the criteria that 'no *local* discomfort' may occur. The overall comfort value is an integration of the local comfort sensations of all body parts. When a particular body part experiences discomfort, a person might still be overall comfortable. Therefore, an overall comfort does not guarantee no local discomfort happening. However, a situation where no local discomfort occurs does guarantee overall comfort. Therefore, the criterion requiring 'no *local* discomfort' sets stricter limits for acceptable comfort conditions. The UCB comfort limits are defined by the intersections of the curve of the minimum local comfort (of all body parts) and the neutral line (equal to 0). Thermal comfort is guaranteed when the minimum local comfort (of all body parts) stays above zero, i.e. for window surfaces between 15ºC and 34ºC. These comfort limits are about 3ºC higher/lower than the limits provided by the

PMV model, i.e. the comfort band decreases with approximately 6ºC. These comfort limits ensure that no local body part experiences local discomfort.

4.2.3 CONCLUSIONS

Avoiding local discomfort is key to ensure thermal comfort, especially in thermally asymmetric environments such as rooms with cold or warm window surfaces. The PMV model is not only insensitive to the effects of thermal asymmetry, but does also not provide any information regarding possible discomfort of local body parts. The UCB comfort model is currently the only existing model that provides information on overall comfort as well as on local comfort of the individual body parts. Therefore, the model appears appropriate for evaluating thermal comfort in complex thermal environments.

5 ASSESSMENT OF WINDOW COMFORT

This section provides an overview of the primary factors influencing window comfort and the different approaches that can be used to evaluate the impact of different window systems on the thermal comfort in the indoor environment. The UCB comfort model has been used in the various analysis examples, using the criterion 'no *local* discomfort' as the comfort evaluation.

5.1 PRIMARY FACTORS INFLUENCING WINDOW COMFORT

Figure 19 provides a list of the primary factors influencing window comfort, organized according to those factors which impact the view factors between the person and the surroundings, the factors that determine the interior surface temperature of the window and the human factors:

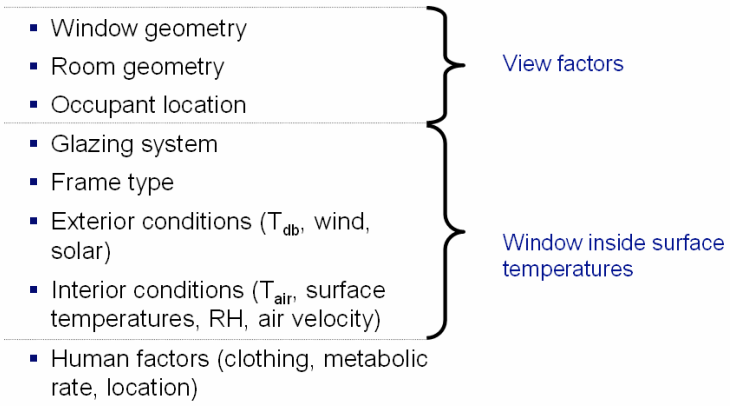
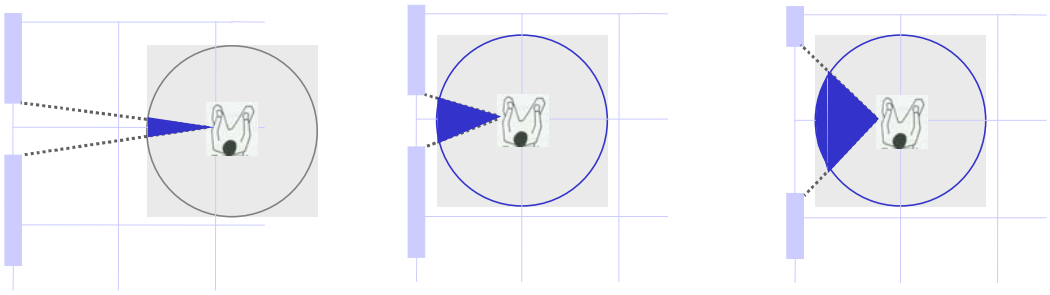


Figure 19: Factors influencing window comfort

To evaluate window thermal comfort, one must evaluate how the window affects the heat balance between the person and the environment. The differential heat exchange across a person's body will result in different skin temperatures for individual body parts and a resulting core temperature, a combination of which invokes different thermal sensations and comfort. As indicated above, there are three areas that affect window thermal comfort:

View factor: The view factor describes how much a person "sees" a surface. It indicates how much the person is influenced by the temperature of a particular surface when calculating the radiation heat exchange between the person and the surrounding surfaces. The bigger the view factor is, the larger the influence on the person. It is determined by the geometry of a surface and its orientation/position relative to the person. Figure 20 shows the qualitative effect of distance and window size on view factor. A more detailed discussion of view factor follows insect Section 5.4.



View factor is used to quantify the amount of radiation energy leaving the body that reaches the window.

View factor is increased by moving closer to the window.

View factor is increased with a larger window.

Figure 20: Schematic diagram illustrating how geometry influences view factor

Window inside surface temperature: The window temperature is affected by the glazing system, frame type, exterior environmental conditions, such as dry-bulb temperature, wind, solar radiation, and interior conditions which include air and surface temperatures, relative humidity, and air velocity. Most window products have an inside surface emissivity of approximately 0.84. Products that have a lower emissivity could be used to reduce heat transfer between the window surface and the occupant. Such products are not common due to difficulties in keeping the surface clean and dry. If the surface becomes dirty, the effect of the low-e coating is reduced. Although the method we describe in this report is fully capable of addressing low-e interior surfaces, we have not included any data on the performance of such products.

Draft caused by cold windows: The sensation of draft due to air motion can be caused by two primary factors: induced air motion from a cold interior window surface temperature and infiltration. Lyon et al. (1999) showed that in general the impact from surface temperature induced draft on comfort is small except in cases with a very tall, low-performance window. A common way to reduce the draft impact on comfort is to install a heater under the window sill, which can easily remove the discomfort caused by the draft.

The impact of infiltration of comfort can be much more significant, however it is extremely difficult to characterize. The effect of infiltration is dependent on whether a space is positively or negatively pressurized with respect to outdoors and also on the details of air flow patterns in the space. These are very difficult to predict and depend heavily on the HVAC system configuration and operation. In most modern window installations, air leakage is generally assumed to be quite low. Based on these reasons, we do not include the effects of air motion in our assessment of window comfort.

Human factors, such as clothing, metabolic heat production: Factors inherent to the human body such as its metabolic heat production and inherent to human behavior such as one's clothing greatly influence a person's state of thermal comfort. The metabolic heat production is a measure of how much heat the body creates internally. The higher one's metabolic heat production, the warmer a person feels. The amount of heat the body produces is closely linked to the level of activity the body engages in. The insulation level provided by the clothing determines how easy it is for the body to exchange heat with the environment (i.e. the rate at which a thermal imbalance can be corrected). The lower the clothing level, the higher the heat transfer rate between the body and the environment. As such, the person feels cooler when the environment is either cool or warm. With respect to the effect of windows on comfort, higher clothing levels will generally lessen the impact. Most of the analysis on this report was done with a clothing ensemble consisting of underwear, slacks, long-sleeve shirt, shoes and socks (0.59 clo). For both clothing

and metabolic rate, the most important factor is that they be appropriate for the air temperature being considered. For example, if the clothing or metabolic rate is increased without adjusting the air temperature, the person will be in a warm thermal state. If the effects of a cold window were being considered, the window might actually increase thermal comfort by counteracting the overall warm state of the body. Conversely, if the air temperature was low with respect to clothing and metabolic rate, the body will be in a cool thermal state and the effects of a cold window will be magnified. This balance between air temperature and clothing is probably more important than either the choice of clothing or metabolic rate.

5.2 INTERIOR AIR TEMPERATURE VS. WINDOW SURFACE TEMPERATURE

The impact of a variation in window surface temperature on occupant comfort can be offset by modifying the interior air temperature. As such, the cooling/heating effect of a cold/warm window can be compensated by increasing/lowering the air temperature inside the room.

Figure 21 shows how the minimum local comfort varies as a function of the interior air temperature. The four curves correspond to different window temperatures (i.e. 10, 20, 30 and 40°C), and each curve reveals an interior air temperature at which a maximum for the minimum local comfort is reached. For a window temperature of 10°C, maximum comfort is obtained at an interior air temperature of 25.5ºC, whereas for a window temperature of 40ºC, the optimal interior air temperature drops to approximately 21.5ºC. The shift in optimal air temperatures at which maximum comfort is obtained illustrates how the thermal effect of windows can be offset by a change in air temperature.

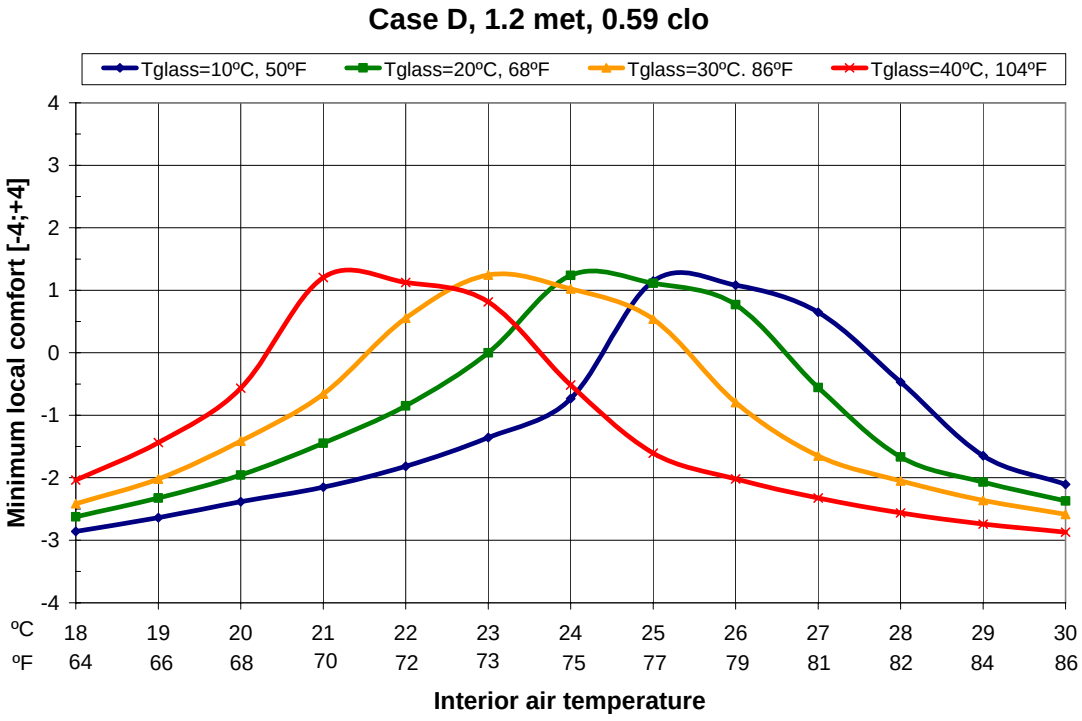


Figure 21: Interior air temperature at which maximum comfort occurs for different window surface temperatures

5.3 IMPACT OF WINDOW TEMPERATURE ON INTERIOR AIR TEMPERATURE

Another way of quantifying the performance of a window with respect to indoor comfort is to assess the change in air temperature in a space that would have the same impact on thermal comfort as the window. The window temperature impact expresses the effect of the temperature difference between the 'actual' window surface temperature and the 'neutral' window surface temperature in terms of an equivalent change in air temperature. The neutral window temperature is defined as the condition where the window temperature is equal to the air temperature that provides a neutral thermal experience for the building occupant.

The extent to which the actual window temperature diverges from the neutral temperature is converted into a change in air temperature which has an equivalent impact on thermal comfort. Hence, the impact of the window on thermal comfort is rectified or accommodated by an equivalent change in indoor air temperature. As such, an ideal window has a value of 0ºC, i.e. it has an actual surface temperature equal to the neutral temperature. The window temperature impact could be calculated for NFRC summer/winter conditions or also for a whole year. The approach could also be used to calculate the energy required to offset the temperature impact (i.e. by changing the heating/cooling setpoint).

Table 5 provides some example data calculated for the typical reference space with geometry case D, a person sitting 1m away from window at 1.2met, 0.9 clo (winter clothing) for winter rating, and 0.6 clo (typical indoor clothing) for summer rating).

Window	Winter rating [ºF] [ºC]	Summer rating, w/o diffuse solar [ºF] [ºC]	Summer rating w/ diffuse solar [ºF] [ºC]
Single, poor frame	-5.1 (2.8)	2.7 (1.5)	5.4 (3.0)
Double, clear, poor frame	-2.7 (1.5)	2.9 (1.6)	5.0 (2.8)
Double, clear, good frame	-2.3 (1.3)	2.2 (1.2)	3.8 (2.1)
Double, selective low-e, good frame	-1.6 (0.9)	1.1 (0.6)	2.2 (2.2)
Triple, clear, good frame	-1.6 (0.9)	2.5 (1.4)	3.8 (2.1)
Triple, selective low-e, good frame	-1.1 (0.6)	1.3 (0.7)	2.2 (1.2)

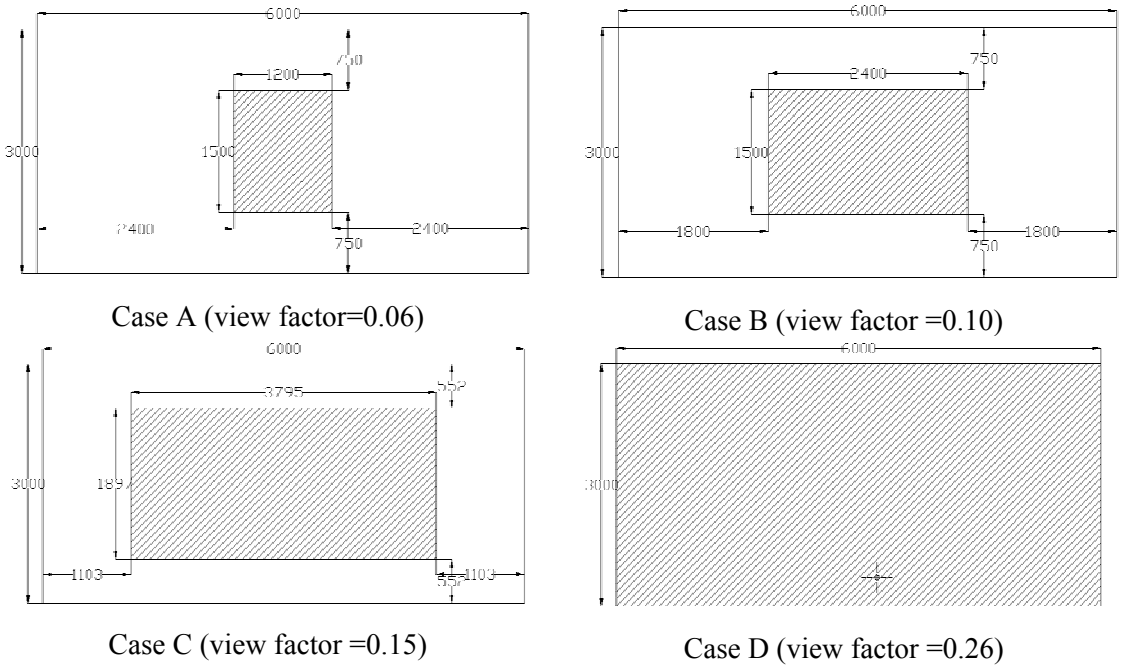
Table 5: Example window temperature impact for different window types

5.4 IMPACT OF GEOMETRY

The following paragraphs explore the impact of geometry on the assessment of thermal comfort, both in terms of the relative position of windows to the building occupant as well as the spatial variation of thermal comfort throughout a room.

5.4.1 WINDOW / ROOM GEOMETRY

The relative position of windows to a person determines the view factor and hence the magnitude of the (long-wave) radiation heat exchange between the person and the windows. We define four window geometries, shown in Figure 22, that are used in the analyses that follow. The most important attribute of each of the geometries is the view factor, shown in Table 6**.**



Case A (view factor=0.06)

Case B (view factor =0.10)

Case C (view factor =0.15)

Case D (view factor =0.26)

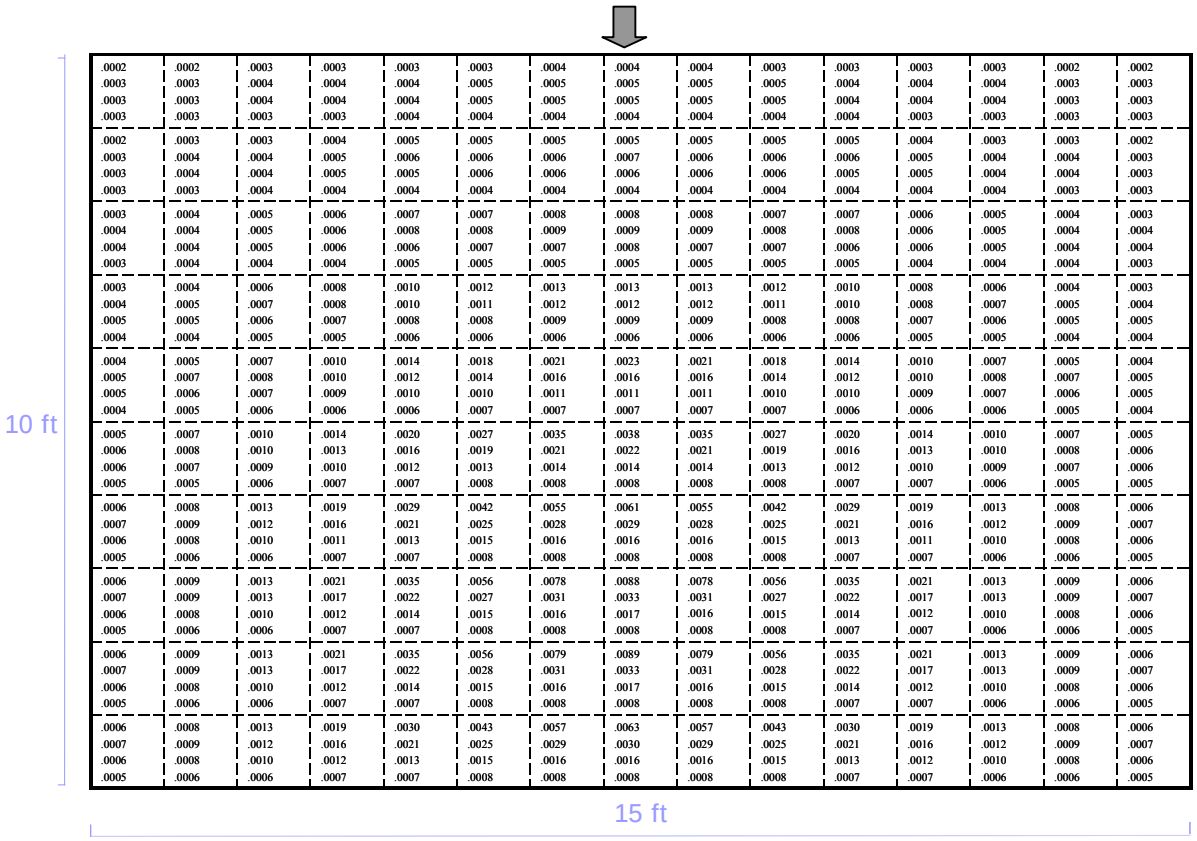
Figure 22: Window geometry for simulated cases

Geometry	Window size	Distance from window			
		1m	1.5m	2m	4m
Case A	1.2m x 1.5m	0.06	0.04	0.03	0.01
Case B	2.4m x 1.5m	0.10	0.07	0.05	0.02
Case C	3.8m x 1.9m	0.15	0.11	0.08	0.03
Case D	6.0m x 3.0m	0.26	0.20	0.16	0.07

Table 6: View factors for reference geometry cases (see **Figure 22**)

For reference, view factors for six addition geometries are provided in **Table 7**. Note that a person sitting in the corner of a façade with a 1.8m high strip window has the same view factor as a fully glazed façade.

The view factors in these tables were calculated according the method proposed by Fanger (1973) and implemented in a computer program. View factors are for a seated person, and the orientation is the average of the four orthogonal orientations with respect to the wall. Although the method can be carried out by hand, it is somewhat tedious. Figure 23 presents a graphical method for calculating view factor for most window configurations.



.0002 .0003 .0003 .0003	.0002 .0003 .0003 .0003	.0003 .0004 .0004 .0003	.0003 .0004 .0004 .0003	.0003 .0004 .0004 .0004	.0003 .0005 .0005 .0004	.0004 .0005 .0005 .0004	.0004 .0005 .0005 .0004	.0004 .0005 .0005 .0004	.0003 .0005 .0005 .0004	.0003 .0004 .0004 .0004	.0003 .0004 .0004 .0003	.0003 .0004 .0004 .0003	.0002 .0003 .0003 .0003	.0002 .0003 .0003 .0003
.0002 .0003 .0003 .0003	.0003 .0004 .0004 .0003	.0003 .0004 .0004 .0004	.0004 .0005 .0005 .0004	.0005 .0006 .0006 .0004	.0005 .0006 .0006 .0004	.0005 .0006 .0006 .0004	.0005 .0007 .0006 .0004	.0005 .0006 .0006 .0004	.0005 .0006 .0006 .0004	.0005 .0006 .0005 .0004	.0004 .0005 .0005 .0004	.0003 .0004 .0004 .0004	.0003 .0004 .0004 .0003	.0002 .0003 .0003 .0003
.0003 .0004 .0004 .0003	.0004 .0004 .0004 .0004	.0005 .0005 .0005 .0004	.0006 .0006 .0006 .0004	.0007 .0008 .0006 .0005	.0007 .0008 .0007 .0005	.0008 .0009 .0008 .0005	.0008 .0009 .0008 .0005	.0008 .0009 .0007 .0005	.0007 .0008 .0007 .0005	.0007 .0008 .0006 .0005	.0006 .0006 .0006 .0004	.0005 .0005 .0005 .0004	.0004 .0004 .0004 .0004	.0003 .0004 .0004 .0003
.0003 .0004 .0005 .0004	.0004 .0005 .0005 .0004	.0006 .0007 .0006 .0005	.0008 .0008 .0007 .0005	.0010 .0010 .0008 .0006	.0012 .0011 .0008 .0006	.0013 .0012 .0009 .0006	.0013 .0012 .0009 .0006	.0013 .0012 .0009 .0006	.0012 .0011 .0008 .0006	.0010 .0010 .0008 .0006	.0008 .0008 .0007 .0005	.0006 .0007 .0006 .0005	.0004 .0005 .0005 .0004	.0003 .0004 .0005 .0004
.0004 .0005 .0005 .0004	.0005 .0007 .0006 .0005	.0007 .0008 .0007 .0006	.0010 .0010 .0009 .0006	.0014 .0012 .0010 .0006	.0018 .0014 .0010 .0007	.0021 .0016 .0011 .0007	.0023 .0016 .0011 .0007	.0021 .0016 .0011 .0007	.0018 .0014 .0010 .0007	.0014 .0012 .0010 .0006	.0010 .0010 .0009 .0006	.0007 .0008 .0007 .0006	.0005 .0007 .0006 .0005	.0004 .0005 .0005 .0004
.0005 .0006 .0006 .0005	.0007 .0008 .0007 .0005	.0010 .0010 .0009 .0006	.0014 .0013 .0010 .0007	.0020 .0016 .0012 .0007	.0027 .0019 .0013 .0008	.0035 .0021 .0014 .0008	.0038 .0022 .0014 .0008	.0035 .0021 .0014 .0008	.0027 .0019 .0013 .0008	.0020 .0016 .0012 .0007	.0014 .0013 .0010 .0007	.0010 .0010 .0009 .0006	.0007 .0008 .0007 .0005	.0005 .0006 .0006 .0005
.0006 .0007 .0006 .0005	.0008 .0009 .0008 .0006	.0013 .0012 .0010 .0006	.0019 .0016 .0011 .0007	.0029 .0021 .0013 .0007	.0042 .0025 .0015 .0008	.0055 .0028 .0016 .0008	.0061 .0029 .0016 .0008	.0055 .0028 .0016 .0008	.0042 .0025 .0015 .0008	.0029 .0021 .0013 .0007	.0019 .0016 .0011 .0007	.0013 .0012 .0010 .0006	.0008 .0009 .0008 .0006	.0006 .0007 .0006 .0005
.0006 .0007 .0006 .0005	.0009 .0009 .0008 .0006	.0013 .0013 .0010 .0006	.0021 .0017 .0012 .0007	.0035 .0022 .0014 .0007	.0056 .0027 .0015 .0008	.0078 .0031 .0016 .0008	.0088 .0033 .0017 .0008	.0078 .0031 .0016 .0008	.0056 .0027 .0015 .0008	.0035 .0022 .0014 .0007	.0021 .0017 .0012 .0007	.0013 .0013 .0010 .0006	.0009 .0009 .0008 .0006	.0006 .0007 .0006 .0005
.0006 .0007 .0006 .0005	.0009 .0009 .0008 .0006	.0013 .0013 .0010 .0006	.0021 .0017 .0012 .0007	.0035 .0022 .0014 .0007	.0056 .0028 .0015 .0008	.0079 .0031 .0016 .0008	.0089 .0033 .0017 .0008	.0079 .0031 .0016 .0008	.0056 .0028 .0015 .0008	.0035 .0022 .0014 .0007	.0021 .0017 .0012 .0007	.0013 .0013 .0010 .0006	.0009 .0009 .0008 .0006	.0006 .0007 .0006 .0005
.0006 .0007 .0006 .0005	.0008 .0009 .0008 .0006	.0013 .0012 .0010 .0006	.0019 .0016 .0012 .0007	.0030 .0021 .0013 .0007	.0043 .0025 .0015 .0008	.0057 .0029 .0016 .0008	.0063 .0030 .0016 .0008	.0057 .0029 .0016 .0008	.0043 .0025 .0015 .0008	.0030 .0021 .0013 .0007	.0019 .0016 .0012 .0007	.0013 .0012 .0010 .0006	.0008 .0009 .0008 .0006	.0006 .0007 .0006 .0005

(a)

(b)

Figure 23: View factor data for a seated person in one-foot increments for a vertical wall. (a)The arrow at the center column represents the horizontal location for the person. The four numbers in each column represent the view factors for a perpendicular distance from the window of 3', 5', 7' and 10', from top to bottom, respectively. The window(s) can be sketched on this figure and the view factors enclosed by the window added up to determine the view factor for the window. The procedure can be used for multiple wall orientations, summing the view factor for each window. (b) Graphical representation of the tabular data for a distance of 3 feet. Lighter shades represent larger view factors.

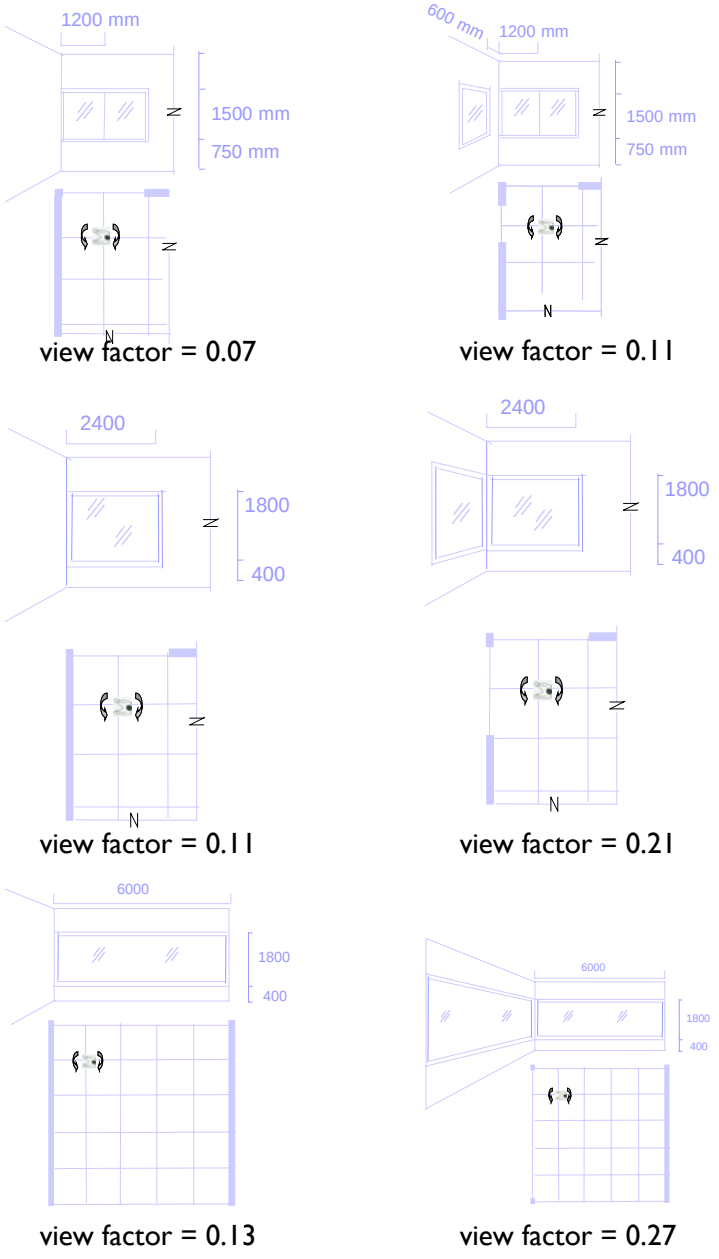
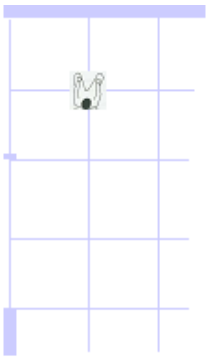


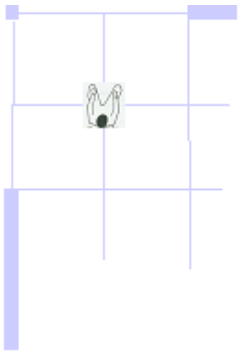
Table 7: Example geometries and view factors

In order to demonstrate the impact of window configurations with the same total window surface area but different window locations, we carried out a comfort assessment for the two geometries shown in Figure 24. Two identical windows, measuring 2m x 1.8m, are positioned either next to each other on one side, or next to each other on the two sides of a corner. The person is sitting (1.0 met) 1m away from the window, wearing typical indoor clothing (0.59 clo). The window has

a uniform temperature of -9ºC, which corresponds closely to the performance of single clear glazing under NFRC winter condition (–18ºC outdoor air temperature).

The simulation results show that placing the windows on two sides greatly decreases the overall comfort of the person, because the person feels a lot colder due to the increased view factor to the cold window. The left hand discomfort significantly decreased from –0.6 (left hand sensation –1.5, between slightly cool to cool) to –2.1 (left hand sensation –2.5, between cool to cold). When the windows are located at a corner relative to the person, not only the left hand is more exposed to the cold window, but the entire body feels also cooler, therefore the hand feels cooler, and the cool hand is perceived as much more uncomfortable.





Windows on one side (view factor = 0.11)		Windows on two sides side (view factor = 0.20)	
Left hand sensation	= -1.5	Left hand sensation	= -2.5
Left hand comfort	= -0.6	Left hand comfort	= -2.1
Overall sensation	= -0.7	Overall sensation	= -1.4
Overall comfort	= -0.1	Overall comfort	= -1.3

Figure 24: Effect of window/room geometry

5.4.2 DEPTH OF ZONE OF DISCOMFORT

This approach looks at the distance from the window that is required to maintain comfort for different inside window surface temperatures, and for different window sizes. The closer to the window an occupant is, the bigger the influence from the window on the occupant. As such, we can define the required distance away from the window necessary to maintain comfort as the "depth of zone of discomfort". The geometry of the room is same as shown in Figure 16. Figure 22 illustrates the window geometries for the different window sizes.

Figure 25 indicates that when the window temperature is kept constant, the depth of zone of discomfort increases with increasing window size. When the window size is kept constant, the depth of zone of discomfort increases for more extreme window temperatures.

If we require the zone up to 1 meter away from the window to remain comfortable, stringent limits are required for the interior surface temperature of the glazing for increasing window view factors. The temperature range defined by the dashed vertical lines in Figure 25 decreases with increasing view factor. These temperature ranges are presented further in Table 8. The allowable temperature range proves to be very sensitive to the view factor.

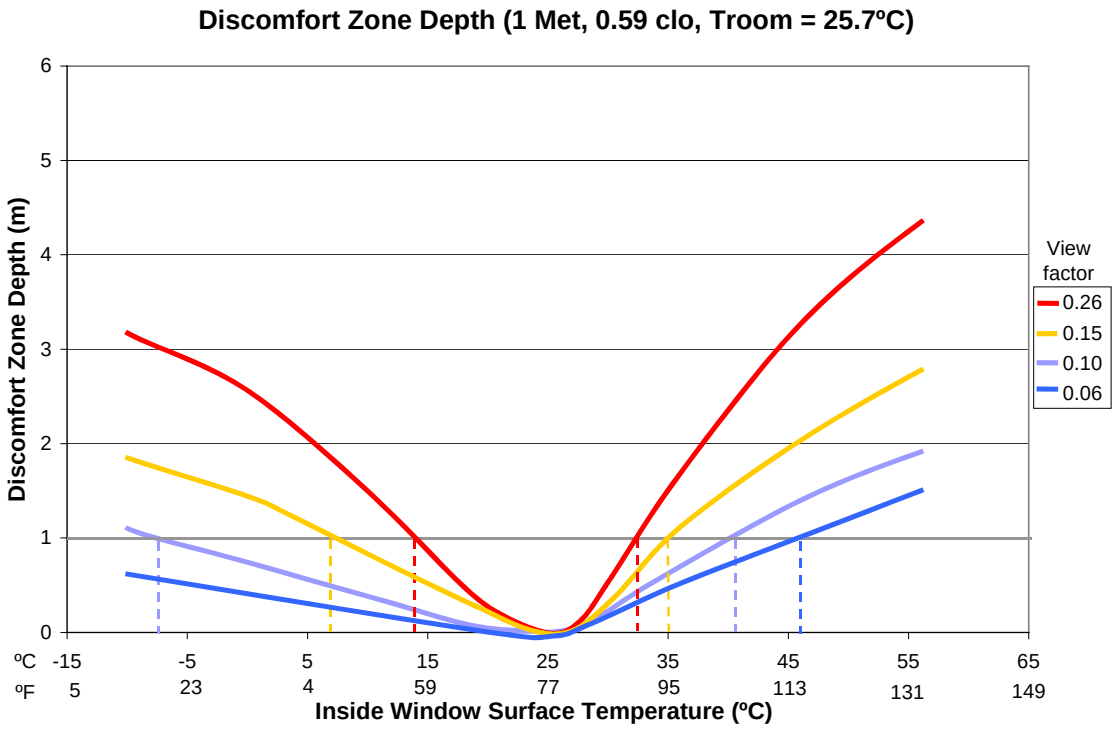


Figure 25: Depth of zone of discomfort for different view factors

For example, to maintain comfort up to 1m away from the window for a view factor of 0.10, the window temperature can be as low as –7ºC and as high as 41ºC. As the view factor increase to 0.15, the range of inside window surface temperatures changes to 7ºC to 35ºC to maintain comfort. When we want to maintain comfort in the space up to 2m away from the window, the limits imposed on the required temperature range are significantly relaxed. For example, for a view factor of 0.26, the required window temperature drops from 14 ºC to 5.5ºC on the cold side and 32.5ºC to 37.5ºC on the warm side.

View factor	Cool window – Minimum allowable Tsi [ºC]	Warm window – Maximum allowable Tsi [ºC]
Case A: 0.06	-20	46
Case B: 0.10	-7	41
Case C: 0.15	7	35
Case D: 0.26	14	32.5

Table 8: Inside window surface temperature required to be comfortable (1m from window)

5.4.3 SPATIAL DISTRIBUTION OF COMFORT

Another way to appreciate the impact of the relative position between person and window is to plot the variation in thermal comfort over the floor plan of a room (Figure 26). We positioned the person along various points on a rectangular grid on the floor plate and evaluated the person's thermal comfort at every location. As such, we obtained an understanding of the special distribution of the thermal comfort throughout the space (in 2 dimensions).

The geometry of the room is same as shown in Figure 16. One of the elevations has a window and three different window sizes are considered (cases B, C and D). The person is wearing typical indoor clothing (0.59 clo), and has an activity level of 1.2 met. The charts plot the minimum local comfort for an interior air temperature of 24°C (summer time) and an averaged window surface temperature of 40°C, representing a tinted glass exposed to solar radiation.

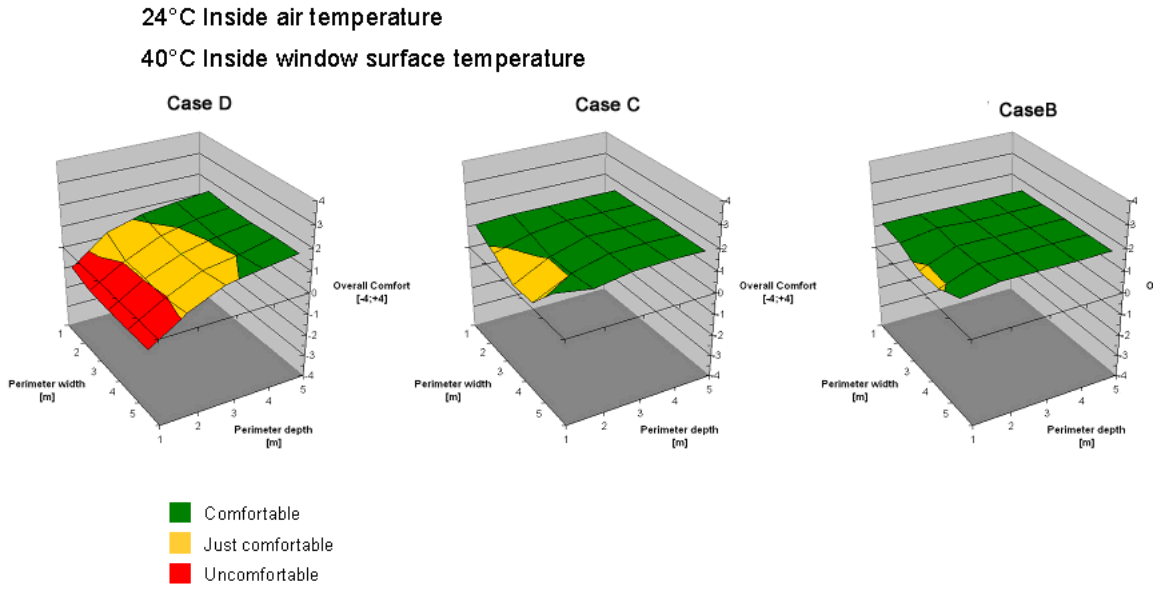


Figure 26: Spatial distribution of comfort

The figures indicate that the larger the window area, the greater the influence of the window on the spatial comfort distribution. A larger window causes the zone of discomfort to penetrate much deeper into the space.

5.5 FRAME AND EDGE EFFECT

We have investigated the impact of the contribution of frame, edge- and center of glass temperatures on the overall assessment of comfort. The objective was to answer the following two questions:

1) Is it important to consider the differences in temperature between the different window components (i.e. center of glass, edge of glass and frame)?
2) Is it an acceptable approximation to use an area-weighted window temperature instead of explicitly modeling each window component with a different temperature?

Figure 27 shows a window and its division into frame, edge- and center of glass. We have used WINDOW to calculate the center of glass temperature and THERM to calculate the edge of glass and frame temperatures.

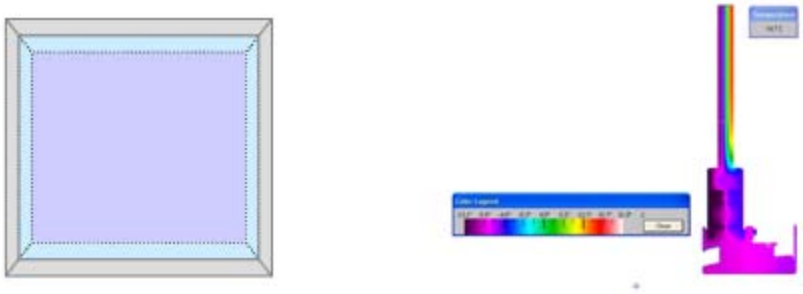


Figure 27: Influence of window components on overall window comfort

The UCB comfort model allows us to model the different window components and define the temperatures for frame, edge- and center glass explicitly. We have compared the predicted comfort values obtained using three different modeling approaches (Figure 28):

- explicit modeling of the three window components with each their own temperature;
- area-weighted approach by calculating an average window temperature;
- modeling the entire window at the center of glass temperature and ignoring the presence of the edge of glass and frame.



Figure 28: Explicit modeling of window components vs. uniform window temperature

The differences between the different modeling approaches have been assessed by carrying out some sample window simulations.

A window unit with the following specifications was used: 1.5m wide by 1.2m high, double IGU, low-e coating, argon filling, 75mm wide aluminum frame. For the first simulations, the premise was to combine a well performing glazing type with a low quality frame to obtain a large temperature difference between the center of the glazing and the frame and hence emphasize the frame effect. The typical room geometry was used as simulation environment and the air temperature was held at 24.5 ^{o}C, which is the neutral temperature for a person wearing typical indoor clothing (0.59 clo), doing light office work (1.2met) while seated along the center line of the window, 1 m away from the window. Three different window configurations were considered (Figure 29):

Table 9 allows the comparison of the results obtained using the three different modeling approaches for the window with a low-performance frame. Standard NFRC winter boundary conditions (outdoor air temperature –18ºC) were used in the calculation of the interior surface temperature of the window components.

The influence of the overall window temperature on the local hand comfort (i.e. the body part most sensitive to environmental changes in this simulation environment) is given in Table 10:

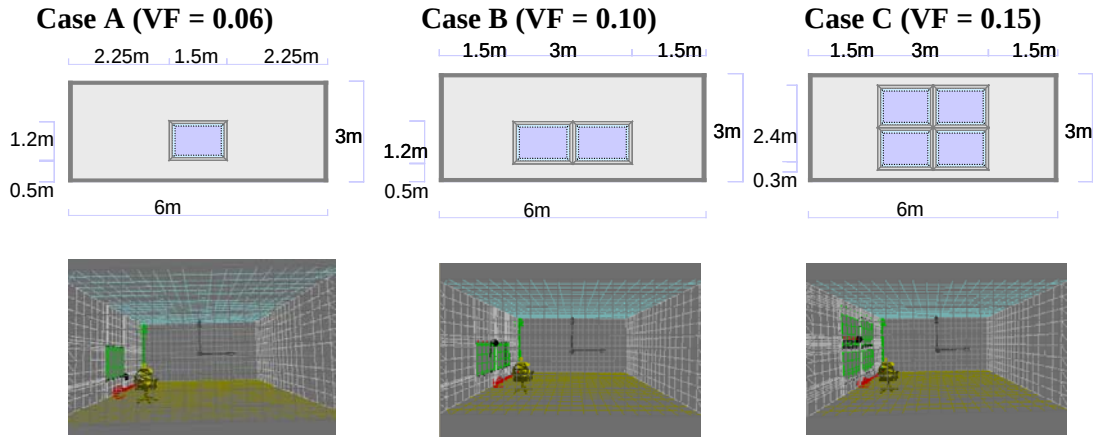


Figure 29: Different window configurations considered for calculation of overall window comfort

Window element	Temperature [°C]	Dimension
center of glass	14.7	1225mm x 925mm
edge of glass	6	62.5mm depth
frame	-5	75mm width
Overall window (area-weighted average)	9.1	1500mm x 1200mm

Table 9: Calculation of area-weighted window temperature (low performance frame)

	Case A (VF = 0.06)	Case B (VF = 0.10)	Case C (VF = 0.15)
reference case with no window	1.97	1.97	1.97
ignoring effect of frame and edge of glass	1.5	1.3	1.0
explicit modeling of frame and edge of glass	1.4	0.9	0.4
area-weighted average window temperature	1.3	0.8	0.3

Table 10: Local hand comfort for different window configurations (low performance frame)

The simulation results indicate that the different modeling approaches with respect to window temperature yield similar results when the window size is small (case A). However, as the window size increases (cases B and C), the impact of the frame and the edge of glass temperature becomes significant and can no longer be ignored. The lower temperature of the low performance frame starts to impact the overall window temperature compared to the relatively warm center of glass temperature of the good performing glazing system. Local hand comfort is reduced by about 0.5 when considering the effect of the frame and the edge of glass temperature (from 1.3 to 0.9 for case B, and from 1.0 to 0.4 for case C). We note however that the difference between the results obtained with the explicit modeling approach and the area-weighted average approach are small, with 0.1 comfort level reduction for the area-weighted modeling.

The same comparison of analysis results has also been carried out for a window with a good performing frame and the temperature of the window components is shown in Table 11. In this

case, the temperature difference between the frame and the center of glass is smaller comparing the window with a poor performing frame.

Window element	Temperature [°C]	Dimension
center of glass	14.7	1225mm x 925mm
edge of glass	10	62.5mm depth
frame	5	75mm width
Overall window (area-weighted average)	11.9	1500mm x 1200mm

Table 11: Calculation of area-weighted window temperature (high performance frame)

The influence of the overall window temperature on the local hand comfort is given in Table 12. As expected, the impact of the frame and edge of glass on the comfort assessment is smaller. However, we still see that with case C the frame and edge of glass temperatures cannot be ignored (-0.3 reduction in local hand comfort). The comfort levels obtained by explicit modeling of the window components and the area-weighted modeling approach are identical. Again, the simulations were carried out for NFRC winter conditions.

	Case A	Case B	Case C
reference case with no window	1.97	1.97	1.97
ignoring effect of frame and edge of glass	1.5	1.3	1.0
explicit modeling of frame and edge of glass	1. 4	1.2	0.7
area-weighted average window temperature	1.4	1.2	0.7

Table 12: Local hand comfort for different window configurations (high performance frame)

We conclude that (1) the effects of the frame and edge of glass temperature on the overall window temperature and the resulting impact on local comfort should not be ignored, (2) the difference between the results obtained using the area-weighted average window temperature and explicitly modeled window component temperatures is small and (3) the comfort levels calculated using the area-weighted method result in slightly lower comfort compared to the explicit method due to the spreading of the lower frame temperature over a larger area. As such, we recommend adopting an area-weighted calculation of the average window temperature to assess the overall impact of the window on occupant comfort.

5.6 IMPACT OF DIFFUSE RADIATION

5.6.1 GENERAL APPROACH

In typical conditions, when direct solar radiation reaches the body it will almost always cause discomfort. Exceptions to this include cases where the air temperature is very cold, the solar radiation falls on only a small portion of the body, or the solar transmittance of the window is extremely low. [to do: add an example analysis of solar radiation falling on the body]. Because direct solar radiation almost always causes discomfort, we make the assumption in our analysis that the occupant will take steps to avoid this condition by relocating or adjusting blinds or shades. It would be possible to include direct solar radiation in a rating system, although specific assumptions about how much of the body received radiation would need to be made and these are very specific to the details of a particular building. In the rating approach we describe below, we

only evaluate the effect of diffuse solar radiation falling on the body. However, we do consider the effect of direct radiation on the glass surface temperature.

A common way to account for the solar radiation impact on the human body is to convert the direct and diffuse solar radiation to an equivalent mean radiation temperature (Arens at al. 1986, Matzarakis et al. 2000). Here we adopted a similar approach, converting diffuse radiation into an equivalent glass surface temperature rise.

The approach entails the calculation of an equivalent temperature increase of the inside surface of the window that would result in the same net heat transfer to the person (by long-wave radiation) as the diffuse radiation. As such, the calculation method accounts for the transmitted diffuse radiation by estimating a temperature increase of the window surface equivalent to the impact of the diffuse radiation.

The approach considers the diffuse radiation arriving from the sky as well as the diffuse radiation reflected from the ground surface (Figure 30). Part of the diffuse radiation incident on the window is transmitted (proportional to the solar transmittance of the glazing) and a portion of the transmitted radiation gets absorbed by the building occupant (proportional to the absorptance of the occupant's clothing).

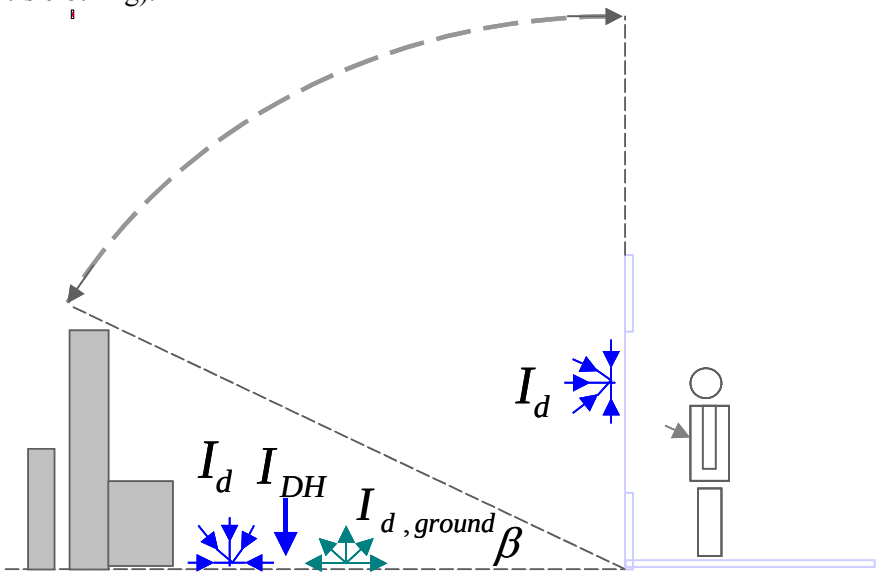


Figure 30: Diffuse solar radiation from the sky and reflected from the ground

The calculation of the glass temperature increase which is equivalent to the impact of diffuse radiation is carried out in three steps:

1. Calculate 'sky' temperature increment of the window assuming the person sees radiation from the sky only;
2. Calculate 'ground' temperature increment of the window assuming the person sees reflected radiation from the ground only;
3. Calculate weighted average of 'sky' and 'ground' temperature increments, factoring in how much a person sees of sky and ground to obtain an 'overall' glass temperature increment.

The calculation process of each of the three steps is discussed further in the following paragraphs.

5.6.2 STEP 1 – DIFFUSE RADIATION FROM SKY

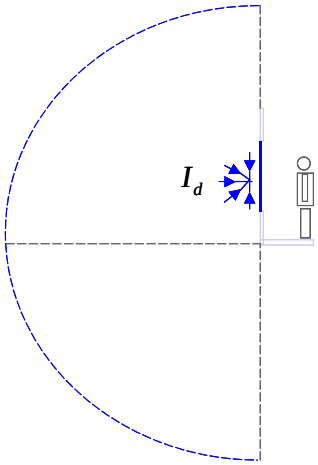


Figure 31: Calculation of diffuse radiation - Assume entire view is sky

The calculation of the portion of diffuse solar radiation coming from the sky which gets absorbed by a person, under the assumption that the entire view (half-sphere) is seen as sky, can be derived as follows:

Diffuse solar radiation	=	I_d	[W/m^2]
Portion transmitted through glass	=	$I_d A_g \tau_{sol}$	(Eq. 3)
Portion absorbed by person	=	$I_d A_g \tau_{sol} F_{g-p} \alpha_{clo}$	(Eq. 4)

With

A_g	=	area of glazing	[m^2]
τ_{sol}	=	solar transmittance of glazing	[-]
F_{g-p}	=	viewfactor glazing - person	[-]
α_{clo}	=	clothing absorptance	[-]

Then,

Radiation between glass and person	=	$\sigma \varepsilon_g \left[T_g^4 - T_p^4\right] A_g F_{g-p}$	(Eq. 5)

And,

Radiation between glass and person after glass has absorbed diffuse radiation from sky	=	$\sigma \varepsilon_g \left[\left(T_g + \delta T_{g-sky}\right)^4 - T_p^4\right] A_g F_{g-p}$	(Eq. 6)

Hence,

Radiation increase after glass has absorbed diffuse radiation from sky (Eq. 6 – Eq. 5)	=	$\sigma \varepsilon_g \left[\left(T_g + \delta T_{g-sky}\right)^4 - T_g^4\right] A_g F_{g-p}$	(Eq.7)

If we say that

Diffuse solar radiation absorbed by person	=	Increased radiation heat transfer between glass and person

Then,

$$I_d \tau_{sol} \alpha_{clo} A_g F_{g-p} = \sigma \varepsilon_g \left[\left(T_g + \delta T_{g-sky} \right)^4 - T_g^4 \right] A_g F_{g-p} \quad \text{(Eq.8)}$$

or

$$\frac{I_d \tau_{sol} \alpha_{clo}}{\sigma \varepsilon_g} = \left(T_g - \delta T_{g-sky} \right)^4 - T_g^4 \quad \text{(Eq.9)}$$

Equation 9 allows the temperature increment due to the diffuse radiation coming from the sky to be written in function of the diffuse radiation and a series of known variables, such as the solar transmittance of the glazing, the absorptance of the clothing and the emissivity of the glazing surface.

5.6.3 STEP 2 – GROUND REFLECTED DIFFUSE RADIATION

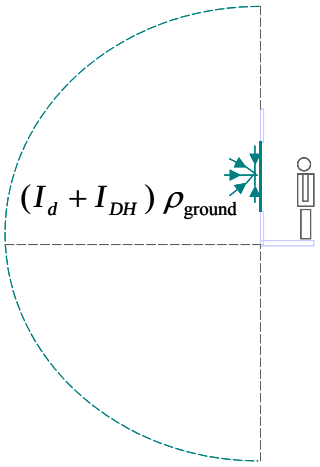


Figure 32: Calculation of diffuse radiation - Assume entire view is ground

The calculation of the ground reflected solar radiation (sky diffuse + horizontal direct) which gets absorbed by a person, under the assumption that the entire view (half-sphere) is seen as the ground, can be derived as follows:

Ground reflected diffuse solar radiation	=	$\left(I_d + I_{DH}\right)\rho_{ground}$	[W/m^2]
Portion transmitted through glass	=	$\left(I_d + I_{DH}\right)\rho_{ground} A_g \tau_{sol}$	(Eq. 10)
Portion absorbed by person	=	$\left(I_d + I_{DH}\right)\rho_{ground} A_g \tau_{sol} F_{g-p} \alpha_{clo}$	(Eq. 11)

With

I_{DH}	=	horizontal direct radiation, which upon reflection of the ground is transformed into diffuse radiation	[W/m^2]
ρ_{ground}	=	ground reflectance	[-]

Then,

Radiation increase after glass has absorbed ground reflected radiation	=	$\sigma \varepsilon_g \left[\left(T_g + \delta T_{g-ground} \right)^4 - T_g^4 \right] A_g F_{g-p}$	(Eq.12)

If we say again that

Ground reflected solar radiation absorbed by person	=	Increased radiation heat transfer between glass and person

Then,

$$\left(I_d + I_{DH}\right)\rho_{ground} A_g \tau_{sol} F_{g-p} \alpha_{clo} = \sigma\varepsilon_g \left[\left(T_g + \delta T_{g-ground}\right)^4 - T_g^4\right] A_g F_{g-p} \quad \text{(Eq.13)}$$

or

$$\frac{\left(I_d + I_{DH}\right)\rho_{ground} \tau_{sol} \alpha_{clo}}{\sigma\varepsilon_g} = \left(T_g - \delta T_{g-ground}\right)^4 - T_g^4 \quad \text{(Eq.14)}$$

Equation 14 allows the temperature increment due to the ground-reflected diffuse radiation to be written in function of the diffuse radiation and a series of known variables, such as the solar transmittance of the glazing, the absorptance of the clothing and the emissivity of the glazing surface.

5.6.4 STEP 3 – WEIGHTED GLASS TEMPERATURE INCREASE

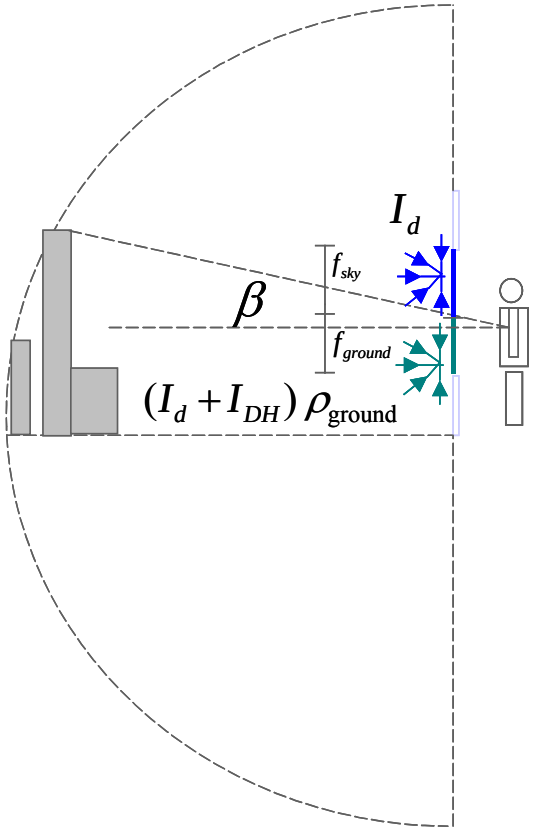


Figure 33: Calculation of diffuse radiation - Weighted glass temperature

The calculation of the weighted glass temperature increase, which combines the effects of both the temperature increment due to the diffuse radiation coming from the sky as well as the ground reflected diffuse radiation, can be summarized as follows:

First, we divide the glazing in two portions: a sky fraction f_{sky} receiving the diffuse radiation from the sky and a ground fraction $f_{ground} = 1 - f_{sky}$ receiving the diffuse radiation reflected by the ground. We obtain a resulting combined temperature increment by calculating the weighted average of both temperature increments calculated in sections 5.6.2 and 5.6.3.

$$\delta T_g = \delta T_{g-sky} f_{sky} + \delta T_{g-ground} f_{ground} \quad \text{(Eq. 15)}$$

5.6.5 SAMPLE CALCULATION RESULTS

Some sample calculations of the glass temperature increase δT_g [°C] that results in long-wave heat transfer which is equivalent to the impact of short-wave diffuse radiation are provided in Table 13. The following values for the variables are assumed: $f_{sky} = 0.5$, $\rho_{ground} = 0.2$, $\alpha_{clo} = 0.5$.

τ_{sol}	0.1	0.2	0.3	0.4	0.5	0.6	0.7	0.8
I_d = 165 W/m^2 I_{DH} = 165 W/m^2	1.4	2.7	4.0	5.3	6.6	7.9	9.2	10.4
I_d = 300 W/m^2 I_{DH} = 0 W/m^2	1.6	3.2	4.8	6.3	7.8	9.3	10.7	12.1

Table 13: Equivalent glass temperature increase due to diffuse radiation

The benefits of converting the impact of diffuse radiation in an equivalent glass temperature increase are (1) that the complex impact of diffuse solar radiation is separated from the comfort model and the effect re-inserted in the comfort assessment in a more straightforward way, (2) the approach allows a simpler rating of window comfort while still considering diffuse radiation, and (3) the approach allows the evaluation of windows with curtains. One would only need to provide a curtain temperature (under direct and diffuse solar radiation) to calculate the impact on comfort.

5.7 IMPACT OF DIRECT RADIATION

5.7.1 GENERAL APPROACH

The UCB Comfort Model is capable of including the effect of direct solar radiation in the comfort calculations. The model has a feature to specify the sun position (altitude and azimuth) and the amount of direct and diffuse radiation, and consecutively calculates the sun penetration into the space (including the effect of any shading elements). On the basis of these geometric relations, the amount of solar radiation that is transmitted by the glazing and absorbed by the occupant is calculated. The model allows the specification of the optical properties of the glazing and the absorption of the occupant. The amount of direct radiation is geometrically calculated for the polygons mapping the body surface and the diffuse radiation is evenly spread throughout the space.

5.7.2 SAMPLE CALCULATIONS

Sample calculations were carried out for an occupant positioned in the room shown in Figure 16 and 1m away from a window. The case B geometry (view factor=0.10) was assumed to illustrate the effect of geometry, i.e. the relationship between the person and the sun as seen through a particular window. The window was south facing and the sun was positioned directly south (azimuth = 180º) at 45º altitude. NFRC Summer environmental boundary conditions were assumed (outdoor temperature = 32ºC, indoor temperature = 24ºC and solar radiation = 783 W/m^2). Comfort boundary conditions of 1.2met and 0.6clo were assumed. The glazing was assumed to be clear double glazing with a clear low-e coating on face 3. Other glazing systems were considered in Section 5.8.3. Under NFRC Summer boundary conditions, the interior surface temperature of the glazing is 36.8ºC.

Figure 34 illustrates the direct sun beam penetrating the window and hitting the occupant. The screenshot also shows that the Overall Sensation of the person is +2.76 (very warm) which yields an Overall Comfort vote of -2.40 (very uncomfortable). Although, the applied direct solar radiation is quite high (783 W/m^2), the maximum amount of radiation hitting the occupant (on the left thy) is only about 350 W/m^2 because the clear double low-e glazing only has a solar

transmittance of 0.47. This example shows that in most cases, exposure to direct solar radiation tends to cause significant discomfort. The maximum allowable amount of direct solar radiation that can be accommodated by different glazing systems whilst maintaining occupant comfort is explored in section 5.8.3.

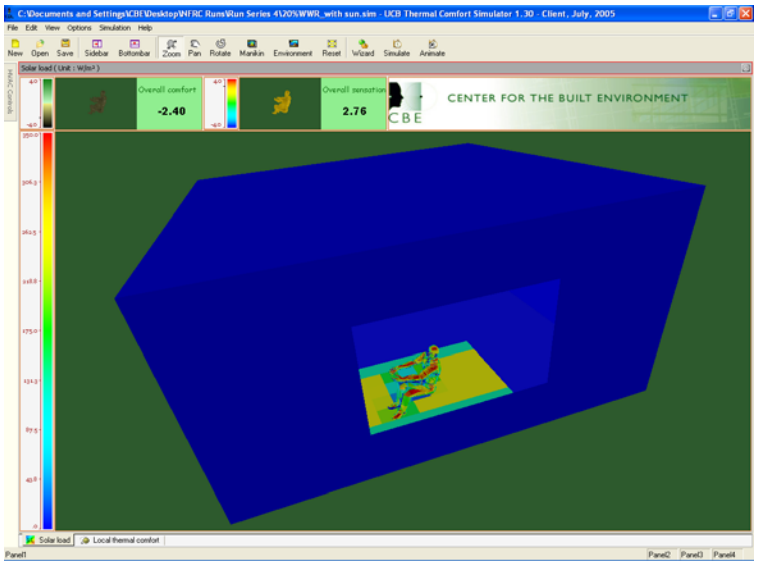


Figure 34: Impact of direct solar radiation, case B geometry

5.8 MAXIMUM ALLOWABLE SOLAR RADIATION

5.8.1 GENERAL CONSIDERATIONS

The dominant factor affecting summer indoor comfort in the vicinity of windows is solar radiation. The impact of solar radiation on window performance is determined by the optical properties of the window. The effect can be divided into two components: transmitted radiation and absorbed radiation. The transmitted radiation impacts how much shortwave radiation reaches the body and the absorbed radiation effects how much the window temperature will increase. The increase of the interior window temperature causes radiant asymmetry as the glazing becomes warm compared to other indoor surfaces such as walls. As such, glazing can become a source of discomfort when it is heated up by solar radiation, because it will act as a radiator emitting heat to the building occupant.

A way to look at the summer-time performance of glazing is to assess the maximum allowable solar radiation that can be tolerated for it to remain comfortable within the room. However, a building occupant will likely be more uncomfortable when he is in the direct path of the sun (exposed to direct solar radiation). In this situation, it is likely that the building occupant will mitigate the discomfort due to the direct exposure to solar radiation by either moving out of the direct solar beam or by pulling a blind down that blocks most of the direct radiation.

As such, our goal was to assess the impact of solar radiation on occupant comfort in two different scenarios. The first scenario assumes that the building occupant is not exposed to direct solar radiation, but is only receiving diffuse radiation transmitted through the glazing and the long-wave radiation due to the glass temperature increase (caused by the glass being exposed to direct and diffuse radiation). A second scenario assumes that the building occupant is exposed to a beam of direct solar radiation penetrating the window and the long-wave radiation of the glazing system which is heated up by the sun.

5.8.2 SCENARIO 1: OCCUPANT NOT EXPOSED TO DIRECT SOLAR RADIATION

This method assumes that the building occupant is not exposed to direct solar radiation and only considers transmitted diffuse radiation and the effect of direct and diffuse radiation absorbed by the glazing system. For this analysis we assumed diffuse radiation to be 20% of the direct radiation, typical of clear sky conditions. Our approach is to calculate a resultant interior surface temperature on the basis of (1) the temperature difference between inside and outside, (2) the increase in glazing temperature due to the exposure to direct solar radiation and (3) the glazing temperature increment due to the impact of diffuse radiation (as per section 5.6). Using this approach, windows can the be characterized in terms of the maximum amount of solar radiation they can tolerate while maintaining comfort for a building occupant seated 1m away from a fully glazed façade (case D).

The maximum allowable solar radiation for a glazing system is calculated in an iterative process:

Step 1: we calculate the interior surface temperature of the glazing (using WINDOW) due to ΔT inside-outside (assuming NFRC summer temperature conditions) and direct solar radiation;

Step 2: we apply 20% of the direct radiation as diffuse radiation and calculate the increase in interior surface temperature δT_g it causes (using the approach explained in Section 5.6);

Step 3: we sum the original interior surface temperature as calculated with WINDOW5 with the temperature increase δT_g due to diffuse radiation to obtain a 'resultant' interior surface temperature of the glazing;

Step 4: we increase the direct solar radiation iteratively (maintaining diffuse radiation equal to 20% of direct radiation) in order to obtain the maximum allowable window interior surface temperature as predicted by the UCB comfort model.

This step-by-step iterative calculation has been carried out for a number of glazing systems exposed to NFRC summer boundary conditions (Ti = 24ºC and Te = 32ºC). Other simulation variables included case D geometry, activity level of 1.2met, typical indoor clothing level of 0.59 clo. These boundary conditions yield a maximum allowable interior surface temperature of the glazing of 36ºC for a person seated 1m away from a very large window.

Table 14 provides a range of glazing systems within a wide band of performances, from single clear glazing to clear and coated double glazing and then to clear and coated triple glazing.

CODE	GLAZING DESCRIPTION
G1	Clear single glazing, 6mm
G2	Bronze single glazing, 6mm
G3	Clear double glazing, air cavity, 6/16/6mm
G4	Low-ε double glazing, air cavity, ε = 0.08 face 3, 6/16/6mm
G5	Spectrally selective low-ε double glazing, air cavity, ε = 0.04 face 2, 6/16/6mm
G6	Clear triple glazing, air cavities, 6/16/6/16/6mm
G7	Low-ε triple glazing, air cavity, ε = 0.08 face 2&4, 6/16/6/16/6mm
G8	Spectrally selective low-ε triple glazing, air cavity, ε = 0.04 face 2 & ε = 0.08 face 4, 6/16/6/16/6mm

Table 14: Range of glazing systems

The maximum allowable solar radiation (in W/m²) is calculated for each of the glazing systems described in Table 14 and the results are presented in Figure 35. The data provides a ranking of

the glazing systems in terms of their solar performance expressed as the maximum allowable solar radiation to maintain indoor comfort 1m away from a fully glazed façade. As expected, glazing system G5, which is the double glazing with a spectrally selective coating on face 2, performs best by allowing the highest maximum solar radiation. The tined single glass (G2) cannot tolerate as much solar radiation as the single clear glazing (G1), because it absorbs the solar radiation which causes it to heat up which results in radiant discomfort. A clear low- ε coating does not have a significant impact on the solar performance of double and triple glazing, because it only reduces the solar transmission of the window panes slightly. However, a spectrally selective low- ε coating (G5 and G8) greatly improves the solar performance of the glazing in terms of maximum allowable solar radiation.

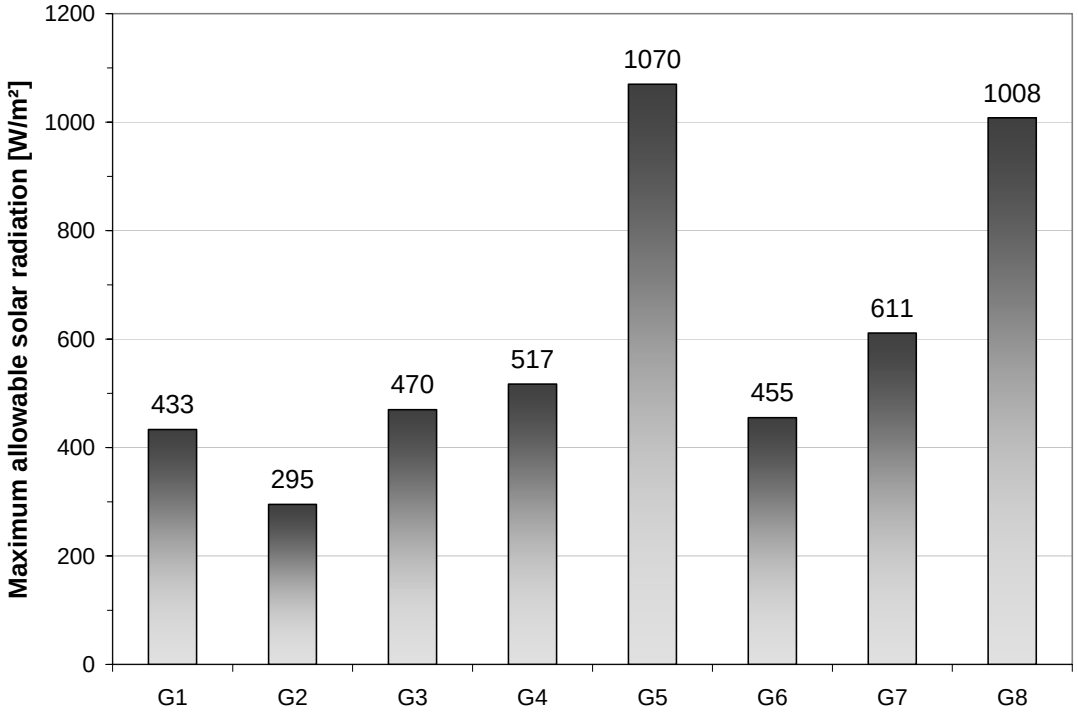


Figure 35: Scenario 1 – Maximum allowable direct solar radiation to maintain indoor comfort

5.8.3 SCENARIO 2: OCCUPANT EXPOSED TO DIRECT SOLAR RADIATION

The performance of the different glazing systems outlined in Table 14 has also been assessed for the scenario where the occupant is exposed to direct solar radiation. The person is positioned 1m away from a fully glazed façade (case D - geometry as per Figure 16). Once again, NFRC Summer boundary conditions (Ti = 24ºC and Te = 32ºC) have been assumed with varying levels of solar radiation (0, 250, 500, 750, 783 W/m^2). The comfort boundary conditions are again an activity level of 1.2met, and a typical indoor clothing level of 0.59 clo. The interior surface temperature of the different glazing systems exposed to different levels of solar radiation was calculated using WINDOW. For every glazing system, we calculated how much direct solar radiation could be allowed whilst maintaining indoor comfort for the occupant. A local comfort above 0 for every body segment was used as the comfort criterion in this evaluation.

Figure 36 illustrates that the maximum allowable solar radiation for the different glazing systems is much lower when considering a scenario where the occupant is exposed to direct solar radiation. However, the relative order of the performance of the different glazing systems is quite

similar with only glazing systems G1/G2 (clear/bronze single glazing) and G5/G8 (spectrally selective low-ε double/triple glazing) changing their performance relative to each other.

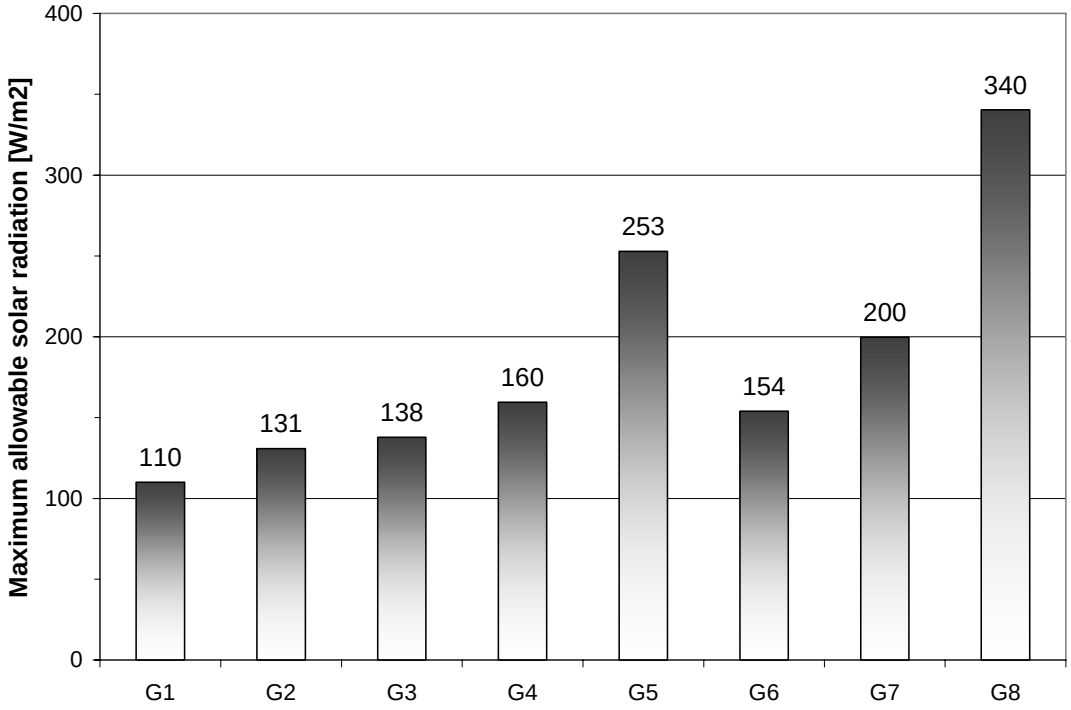


Figure 36: Scenario 2 – Maximum allowable direct solar radiation to maintain indoor comfort

5.8.4 COMPARISON: WITHOUT/WITH DIRECT SOLAR RADIATION

Figure 40 compares the maximum allowable solar radiation in order to maintain indoor comfort for a person seated at 1m away from a fully glazed façade (case D). It is clear that the scenario where the occupant is exposed to direct solar radiation yields discomfort at much lower radiation levels compared to the scenario where the occupant is not exposed to any direct radiation. The case without direct exposure assesses the effect of the temperature increase of the glazing by absorption, combined with the effect of diffuse radiation (assumed equal to 20% of the direct radiation) which is translated into an equivalent temperature rise of the interior glass surface following the method outlined in section 5.6. The case with direct exposure assesses the effect of the temperature increase of the glazing by absorption, combined with the effect of the direct solar radiation that is transmitted through the glazing and absorbed by the occupant. As such, the first scenario puts much more emphasis on those glazing properties that govern the indirect heat transfer of radiation to the indoor space (such as solar absorption and U-value), whereas the second scenario puts more importance on those glazing properties that govern direct transfer of radiation into the space (solar transmission). As mentioned, both approaches lead to slightly different metrics for the maximum allowable solar radiation and hence provide a somewhat different ordering of the solar performance of the different glazing systems with respect to summer indoor comfort.

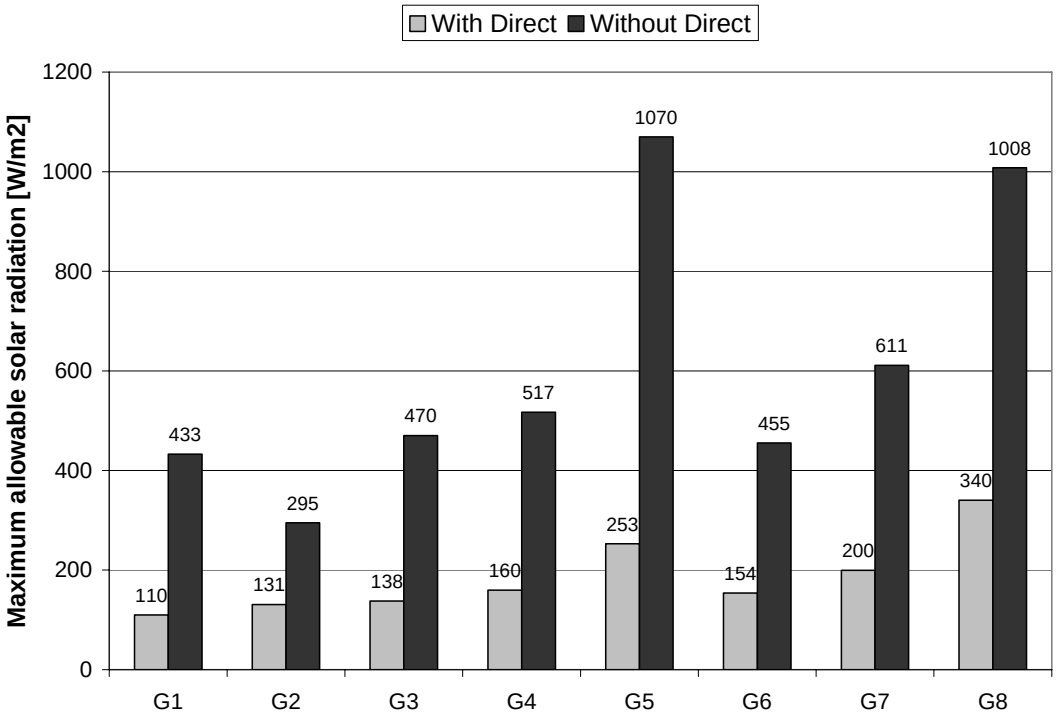


Figure 37: Comparison – Maximum allowable direct solar radiation with/without direct exposure

5.9 WINDOW OPTICAL PROPERTY CHARACTERIZATION

The two effects described above, transmitted direct/diffuse solar radiation and the temperature increase of the window due to absorbed radiation, are characterized by existing rating metrics. The solar heat gain coefficient (SHGC) is defined as:

$$SHGC = Tsol + NA$$

where:
Tsol = overall solar transmittance
N = inward-flowing fraction of absorbed solar radiation
A = solar absorbtance

With respect to thermal comfort, SHGC has the relevant attributes of the window but the relative importance of Tsol and the window surface temperature increase due to the absorbed solar radiation are dependent on a specific condition. Two examples illustrate this point. For a person located very far from a small window, yet with direct solar radiation falling on them, Tsol is the important characteristic of the window with respect to comfort. Since the person is far from a small window, the view factor is small and therefore the longwave radiant exchange is small. Another example is a person sitting very close to a large window, but with no direct sun falling on them. In this case, the surface temperature of the window becomes important. It is a rare case where Tsol becomes unimportant, since even if direct sun does not fall on the body, diffuse radiation would still play a role.

Because Tsol and SHGC are easily obtained values for window products, we can easily determine the quantiy N*A* by the following:

$$NA = SHGC_{indirect} = SHGC - Tsol$$

We use the term $SHGC_{indirect}$ to refer to the fraction of solar energy absorbed by the window and subsequently transmitted to the inside by convection and radiation.

It can be shown that the data in Figure 38, which is the maximum allowable solar radiation calculated for scenario 1 – occupant not exposed to direct solar radiation – from section 5.8.2, can be well predicted by a linear regression of Tsol and $SHGC_{indirect}$ of the form:

$$\text{Maximum allowable solar radiation} = C_1 Tsol + C_2\, SHGC_{indirect} + C_3$$

The result of a linear regression (shown in Figure 38) yields:

$C_1 = -1200$
$C_2 = -5280$
$C_3 = 1600$

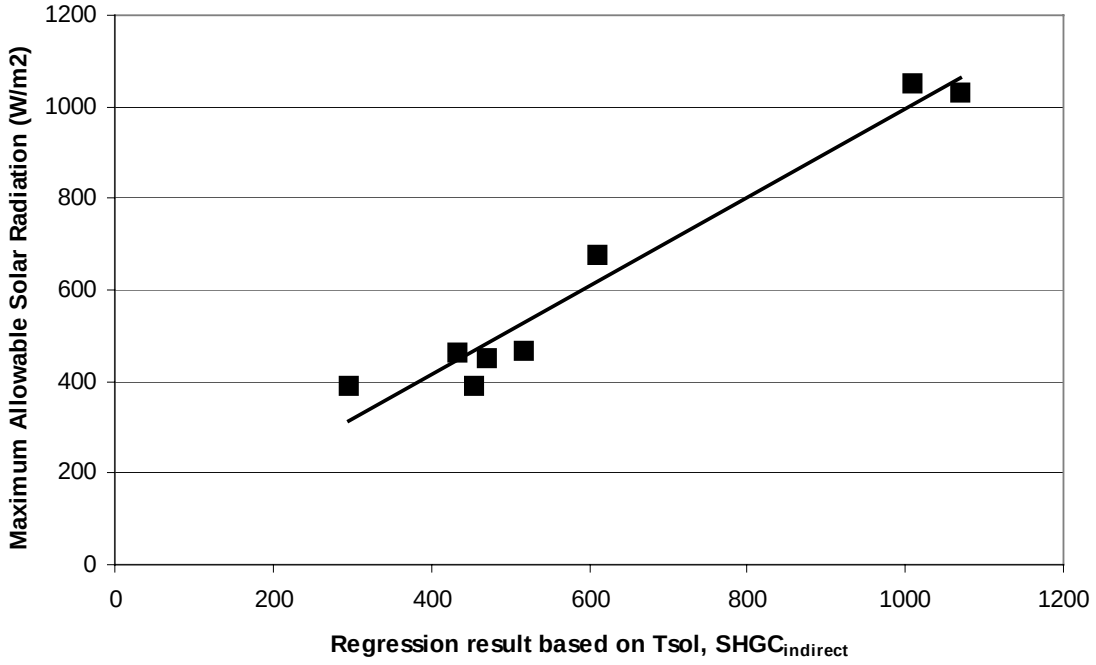


Figure 38: Regression of Maximum allowable solar radiation with Tsol and $SHGC_{indirect}$

This analysis suggests that for the conditions used for the analysis above, $SHGC_{indirect}$ is approximately 4.4 times (5280/1200) more important than Tsol in its impact on thermal comfort. We propose a new index, the **comfort solar heat gain coefficient**, defined as:

$$SHGC_{comfort} = Tsol + k * SHGC_{indirect}$$

The term *k* is a weighting factor on the indirect heat gain, which for the case of diffuse radiation falling on a person 1 meter from a large window (as in section 5.8.2) is of the order 4.4:

$$SHGC_{comfort} = Tsol + 4.4 * SHGC_{indirect}$$

For cases where only diffuse radiation (no direct radiation) falls on the occupant, *k* is very sensitive to the view factor between the occupant and the window. This is because both the transmitted diffuse radiation and the longwave radiation exchange are impacted by the viewfactor. The value of k should be smaller if the person receives direct solar radiation, and smaller still if they receive direct radiation and the view factor window becomes smaller. For scenario 2

described earlier of an occupant sitting 1 meter from a large window in direct sun (section 5.8.3), the value of *k* is approximately 2.4.

6 RATING METHODS FOR WINDOW COMFORT

In Section 5 we provided a discussion on the several parameters which are involved in the evaluation of window comfort. The following section proposes some methods which could be used to rate windows with respect to thermal comfort, to assess both winter and summer window comfort.

6.1 POSSIBLE ALTERNATIVES

The previous sections have discussed several methods to assess window thermal comfort. However, the list of different performance evaluators was by no means exhaustive. To illustrate this, we have provided a list of possible alternatives for the evaluation of window comfort. Our report has focused exclusively on the performance of windows at a specific point in time, under a static set of environmental conditions.

Some possible point-in-time indices to evaluate window comfort for a specific assessment geometry (space and window size, window and occupant location) are:

- Thermal comfort index (e.g. minimum local comfort) for NFRC summer and winter conditions;
- Required indoor air temperature to achieve comfort for NRFC summer and winter outdoor conditions;
- Window temperature impact expressed as the change in indoor air temperature which has a comfort impact equivalent to the window;
- Minimum distance from the window that a person can still be comfortable in the space;
- Minimum outside temperature that remains comfortable for the building occupant;
- Solar heat gain coefficient for comfort.

These point-in-time indices could also be evaluated over a longer period of time and even converted into annual indices, such as:

- Annual average comfort index;
- Number of hours outside the comfort zone;
- Annual energy required to modify room air temperature to maintain comfort;
- Percent of floor area of a specified room that remains comfortable to a certain level over the year;
- Percentage of time the outside temperature drops below the minimum outside temperature required to maintain comfort.

However, given the difficulties associated with the large number of (debatable) assumptions that would inherently be incorporated into an annual index, we have chosen not to pursue this path further in this report and only focus on point-in-time indices for window comfort.

6.2 WINTER RATING METHOD

The comfort index we propose for the assessment of window comfort in winter conditions is the minimum outdoor temperature that can be sustained while maintaining indoor comfort. The

calculation of the minimum outdoor temperature is carried out for a specific set of geometric and environmental boundary conditions. The simulation space is the previously defined standard room measuring 6m wide by 6m deep and 3m high. One of the elevations is fully glazed (case D) and the building occupant is positioned sideways 1m away from the window along the center line of the room. The indoor air temperature is maintained at 23.5ºC and the seated occupant has a clothing level of 0.59 and a metabolic activity level of 1.2met.

To illustrate this approach, we have calculated the minimum allowable outdoor temperature for the 8 glazing systems previously mentioned in section 5.7. Table 15 provides the window properties and performance of the 8 glazing types, as calculated with WINDOW in accordance to NFRC 100-2002. As mentioned, the glazing systems have been chosen to represent a broad range of window performance that can be found in practice.

CODE	GLAZING DESCRIPTION
G1	Clear single glazing, 6mm
G2	Bronze single glazing, 6mm
G3	Clear double glazing, air cavity, 6/16/6mm
G4	Low-ε double glazing, air cavity, ε = 0.08 face 3, 6/16/6mm
G5	Spectrally selective low-ε double glazing, air cavity, ε = 0.04 face 2, 6/16/6mm
G6	Clear triple glazing, air cavities, 6/16/6/16/6mm
G7	Low-ε triple glazing, air cavity, ε = 0.08 face 2&4, 6/16/6/16/6mm
G8	Spectrally selective low-ε triple glazing, air cavity, ε = 0.04 face 2 & ε = 0.08 face 4, 6/16/6/16/6mm

GLAZING	VISIBLE LIGHT			SOLAR ENERGY				U-FACTOR
SYSTEM	Tvis	Rfvis	Rbvis	Tsol	Rfsol	Abs	SHGC	[W/(m^2.K)]
G1	0.88	0.08	0.08	0.77	0.07	0.16	0.82	5.8
G2	0.53	0.06	0.06	0.49	0.05	0.46	0.62	5.8
G3	0.79	0.14	0.14	0.61	0.11	0.28	0.70	2.7
G4	0.75	0.12	0.11	0.47	0.21	0.32	0.59	1.8
G5	0.67	0.12	0.12	0.31	0.32	0.37	0.36	1.7
G6	0.70	0.19	0.19	0.49	0.14	0.37	0.62	1.7
G7	0.65	0.14	0.14	0.34	0.23	0.43	0.45	0.9
G8	0.58	0.14	0.15	0.25	0.33	0.42	0.31	0.9

Table 15: Glazing build-up and performance

The minimum allowable outdoor temperature calculated for the 8 different types of glazing systems are shown in Figure 39. The minimum allowable outdoor temperature is directly related to the U-factor of the window, which is a measure of the heat loss through the window.

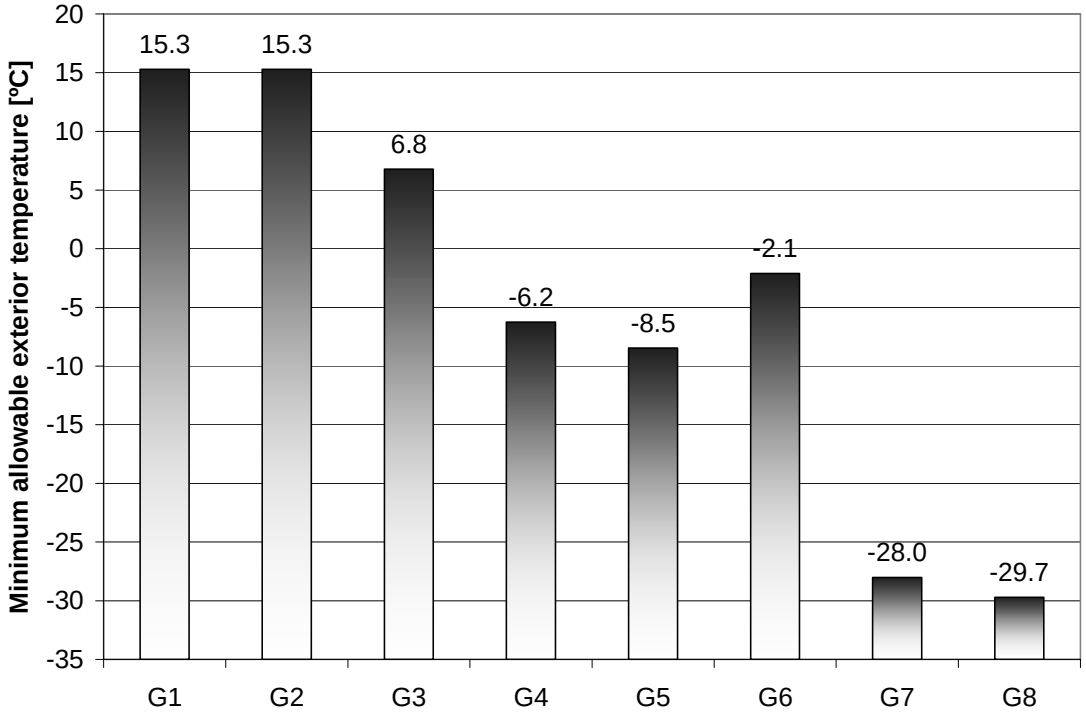


Figure 39: Winter glazing comfort rating - Minimum allowable outdoor temperature

To evaluate whole-window performance with respect to comfort, we have combined the above glazing systems with some typical window frames to obtain an overall window U-factor and the corresponding minimum allowable exterior temperature for the window. The window has been assumed to consist of 20% framing and 80% glazing, but this ratio obviously varies between window geometries. The U-factor of wood framing was assumed to be 2.3 W/(m^2.K), that of vinyl framing 3.4 W/(m^2.K) and of thermally broken aluminum framing 5.7 W/(m^2.K). Ten different window combinations of glazing and framing are shown in Table 16, combining a variation of low and high performance glazing systems with low and high performance window frames.

CODE	WINDOW DESCRIPTION
W1	Clear single glazing, wood frame
W2	Clear single glazing, thermally-broken aluminum frame
W3	Clear double glazing, wood frame
W4	Clear double glazing, thermally-broken aluminum frame
W5	Low-ε double glazing, wood frame
W6	Low-ε double glazing, vinyl frame
W7	Low-ε double glazing, thermally-broken aluminum frame
W8	Low-ε triple glazing, wood frame
W9	Low-ε triple glazing, vinyl frame
W10	Low-ε triple glazing, thermally-broken aluminum frame

WINDOW SYSTEM	GLAZING U-FACTOR [W/(m^2.K)]	FRAME U-FACTOR [W/(m^2.K)]	WINDOW U-FACTOR [W/(m^2.K)]	$T_{ex,min}$ [ºC]
W1	5.8	2.3	5.1	14.6
W2	5.8	5.7	5.8	15.7
W3	2.7	2.3	2.6	6.2
W4	2.7	5.7	3.3	9.7
W5	1.8	2.3	1.9	-0.4
W6	1.8	3.4	2.1	2.1
W7	1.8	5.7	2.6	5.9
W8	0.9	2.3	1.2	-15.1
W9	0.9	3.4	1.4	-8.8
W10	0.9	5.7	1.9	-0.9

Table 16: Window build-up and performance

Figure 40 displays the results for the calculated minimum allowable outdoor temperature for the different window systems listed in Table 16. In general, the frame performance is lower than the glazing performance (i.e. window framing has a higher U-factor than glazing), except when combining single and uncoated double glazing with a wooden frame. As such, the results show that the minimum allowable outdoor temperature to maintain indoor comfort increases to higher temperatures. For example, the minimum allowable outdoor temperature for glazing system G4 (low-ε double glazing) increases from -6.2ºC for the glazing alone, to -0.4ºC when combined with wooden framing and even to 2.1ºC when combined with thermally broken aluminum framing.

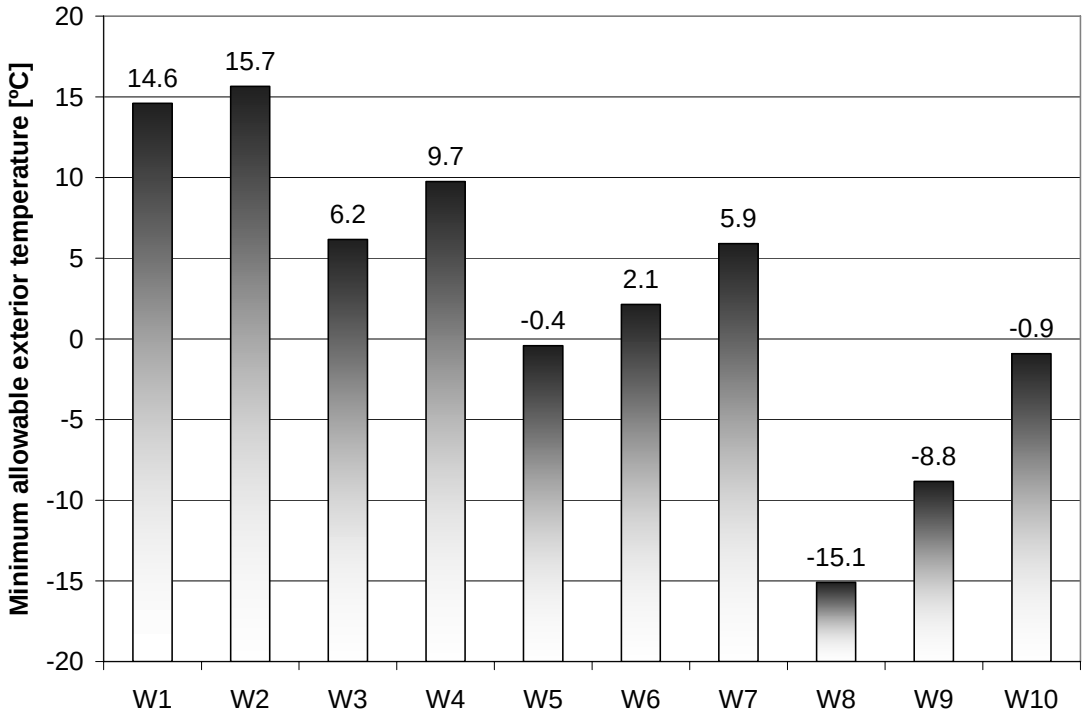


Figure 40: Winter window comfort rating - Minimum allowable outdoor temperature

The direct relationship between the window comfort indices and the U-factor of the windows is illustrated in Figure 41, which provides the regression relationship that allows the prediction of winter window comfort based on the window U-factor.

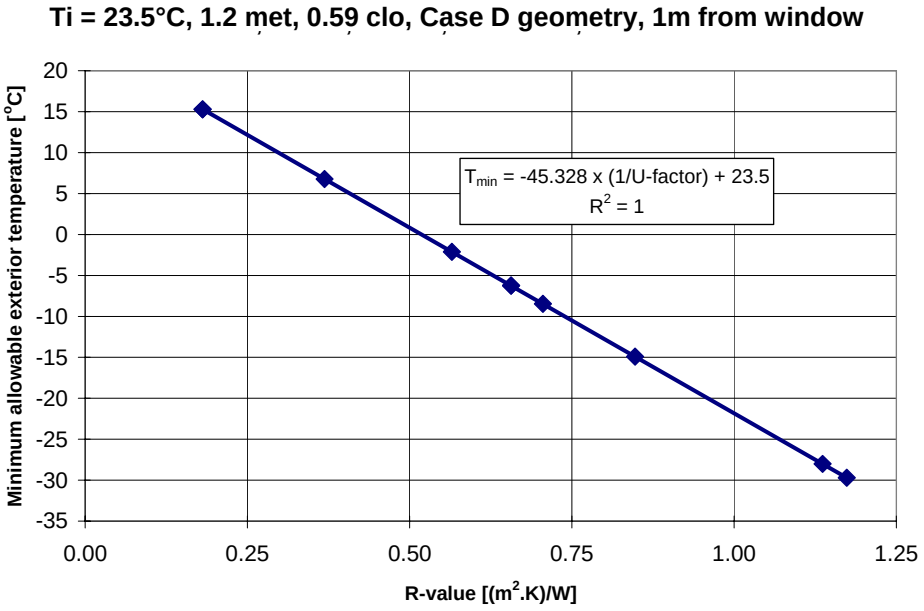
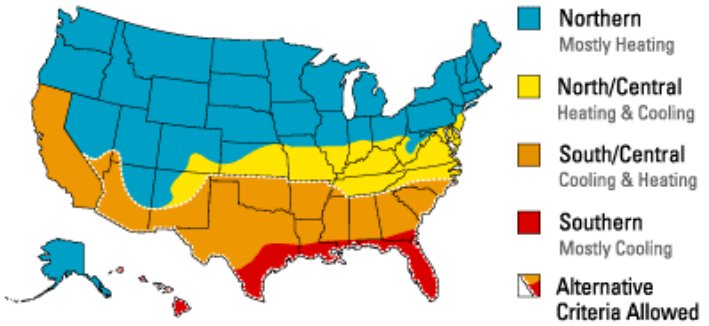


Figure 41: Linear regression between window R-value (1/U-factor) and minimum allowable outdoor temperature

The minimum allowable outdoor temperature index can also be compared to the window performance recommended by the Energy Star program run by EPA/DOE. The Energy Star criteria for residential windows, doors, and skylights are tailored to four Climate Zones, as shown in Figure 42. A product's energy efficiency for a given climate is based on its impact on heat gain and loss in cold weather and heat gain in warm weather.

On the basis of ASHRAE winter time (97.5%) design data, we have selected a number of cities lying within the four Energy Star climate zones to represent the variation in minimum outdoor temperatures experienced within each climate zone. From this minimum winter design temperature we have calculated the window U-factor required to maintain indoor comfort using the approach explained above. We then compared the U-factor we calculated with the window U-factor that is recommended by Energy Star for the different climate zones. The results are presented in Table 17. It becomes clear that the maximum window U-factors Energy Star recommends from the perspective of energy conservation are significantly higher than those calculated to maintain indoor comfort for the geometry we used. If a smaller window (and/or a larger distance from the window) was used, windows with higher U-factors would be acceptable.



Windows & Doors

Climate Zone	U-Factor[1]	SHGC[2]	
Northern	≤ 0.35	Any	
North/Central	≤ 0.40	≤ 0.55	
South/Central	≤ 0.40	≤ 0.40	Prescriptive
	≤ 0.41	≤ 0.36	Equivalent Performance *(Excluding CA)*
	≤ 0.42	≤ 0.31	
	≤ 0.43	≤ 0.24	*Products meeting these criteria also qualify in the Southern zone.*
Southern	≤ 0.65	≤ 0.40	Prescriptive
	≤ 0.66	≤ 0.39	Equivalent Performance
	≤ 0.67		
	≤ 0.68	≤ 0.38	
	≤ 0.69	≤ 0.37	
	≤ 0.70		
	≤ 0.71	≤ 0.36	
	≤ 0.72	≤ 0.35	
	≤ 0.73		
	≤ 0.74	≤ 0.34	
	≤ 0.75	≤ 0.33	

Skylights

Climate Zone	U-Factor[1] 2001 NFRC rated at 20°[3]	U-Factor[1] RES97 rated at 90°[4]	SHGC[2]
Northern	≤ 0.60	≤ 0.45	Any
North/Central	≤ 0.60	≤ 0.45	≤ 0.40
South/Central	≤ 0.60	≤ 0.45	≤ 0.40
Southern	≤ 0.75	≤ 0.75	≤ 0.40

[1] *Btu/h.ft².°F*

[2] *Fraction of incident solar radiation.*

[3] *U-Factor qualification criteria based on 2001 NFRC simulation and certification procedures that rate skylights at a 20-degree angle. Although reported U-Factor is higher than RES97 rated products, energy performance at the ENERGY STAR minimum qualifying level is equivalent.*

[4] *NFRC certification using the 1997 NFRC procedures for residential windows (RES 97) that rated skylights at a 90-degree angle. Skylights rated under this procedure may be present in the marketplace until March 31, 2008. NFRC labels for products using this procedure state: "RES97 rated at 90 degrees."*

Figure 42: Energy Star climate zones and recommended window performance

Table 17 illustrates that the minimum allowable outdoor temperature approach can be used to derive a maximum allowable window U-factor to maintain indoor comfort from a winter design temperature for a specific climatic region. As such, the approach can be used to develop a map of the US displaying the maximum allowable window U-factor to maintain indoor comfort, in parallel to the window performance map provided by Energy Star. The resolution of such map can be improved by considering a larger number of climatic sites. This kind of map would provide more detailed information on the window U-factor that is required to maintain indoor comfort for a set of pre-defined assessment variables.

ZONE	CITY	WINTER DESIGN TEMPERATURE [97.5%]	WINDOW U-FACTOR	ENERGY STAR U-FACTOR	ENERGY STAR ALLOWABLE $T_{ex,min}$
		[ºC]	[W/(m^2.K)]		
N	Bemidji, MN	-32	0.8	2.0	0.7
N	Fairbanks, AK	-44	0.7	2.0	0.7
N	Salt Lake, UT	-13	1.2	2.0	0.7

N	Winslow, AZ	-12	1.3	2.0	0.7
N/C	La Junta, CO	-16	1.1	2.3	3.6
N/C	Norfolk, VA	-6	1.6	2.3	3.6
S/C	Los Angeles, CA	6	2.6	2.3	3.6
S/C	Mt Shasta, CA	-7	1.5	2.3	3.6
S	Tallahassee, FL	-1	1.8	3.7	3.6
S	Key West, FL	14	4.7	3.7	11.2

Table 17: Window comfort assessment vs. Energy Star recommendations

6.3 SUMMER RATING METHOD

In summer, solar radiation and the optical properties of the window most heavily influence the inside surface temperature of the window. As a result, exterior temperature does not characterize the effect of the window on comfort as it does in winter and using a summer rating akin to the winter rating would have little value. The rating method we propose for the summer is the **comfort solar heat gain coefficient**, which is defined as:

$$SHGC_{comfort} = Tsol + k*SHGC_{indirect}$$

The term *k* is a weighting factor on the indirect heat gain, which value is dependent on the extent to which the occupant is exposed to direct and/or diffuse radiation.

Section 5.8 discussed the summer time performance of glazing systems in terms of the maximum allowable solar radiation which could be accommodated without causing discomfort. The occupant was seated 1m away from a fully glazed façade. Standard NFRC Summer boundary conditions were assumed for external and internal environmental temperature.

Two scenarios were considered: (1) a scenario where the occupant was not exposed to direct radiation but only to diffuse radiation (equal to 20% of the direct radiation), and (2) a scenario where the occupant was exposed to direct radiation. Both scenarios considered the effect of longwave radiation caused by the temperature increase of the glazing due to absorption of solar radiation. Scenario 1 added the effect of diffuse radiation as an equivalent temperature increase of the glazing surface as per section 5.6. Scenario 2 used the functionality of the UCB Comfort Model to directly calculate the direct solar radiation falling on the building occupant for a specific sun position.

The data from section 5.8 was used to derive a correlation between the maximum allowable solar radiation and the optical properties of the glazing (Tsol and SHGC) in section 5.9. On the basis of this correlation, the concept of a *summer comfort index* was introduced which could be calculated from a linear combination of the solar transmission and the regular SHGC.

The weighting factor *k* varies between the situations whether the occupant is exposed to only diffuse or direct solar radiation. Scenario 1 – considering only diffuse radiation – yields the following relationship:

$$\textit{Summer Comfort Index} = Tsol + 4.4*SHGC_{indirect}$$

Scenario 2 – considering direct radiation – yields the following relationship:

$$\textit{Summer Comfort Index} = Tsol + 2.4*SHGC_{indirect}$$

As mentioned, for cases where only diffuse radiation falls on the occupant, *k* is very sensitive to the view factor between the occupant and the window. This is because both the transmitted diffuse radiation and the longwave radiation exchange are impacted by the viewfactor. The value of *k* is smaller if the person receives direct solar radiation, and smaller still if they receive direct radiation and the view factor window becomes smaller.

These relationships allow ranking glazing performance in terms of the *summer comfort index*, once a set of specific boundary conditions is fixed, such as room geometry, window geometry, occupant position and environmental/comfort boundary conditions (met, clo, etc).

Table 18 provides the relevant properties of the different glazing systems and the calculated comfort SHGC for both scenarios, i.e. only diffuse and direct radiation.

GLAZING	OPTICAL PROPERTIES			U-FACTOR	DIFFUSE	DIRECT
SYSTEM	Tsol	SHGC	$SHGC_{indirect}$	[W/(m^2.K)]	*summer comfort index*	*summer comfort index*
G1	0.77	0.82	0.05	5.8	0.99	0.89
G2	0.49	0.62	0.13	5.8	1.06	0.80
G3	0.61	0.70	0.09	2.7	1.01	0.83
G4	0.47	0.59	0.12	1.8	1.00	0.76
G5	0.31	0.36	0.05	1.7	0.53	0.43
G6	0.49	0.62	0.13	1.7	1.06	0.80
G7	0.34	0.45	0.11	0.9	0.82	0.60
G8	0.25	0.31	0.06	0.9	0.51	0.39

Table 18: Comfort SHGC for different glazing systems – diffuse / direct radiation

Figure 43 and Figure 44 plot the *summer comfort index* as linear functions of varying solar transmission and SHGC. Both figures are made up of a series of curves, each curve representing a specific SHGC and varying solar transmission. Physically impossible combinations of SHGC and solar transmission have been excluded by stopping each SHGC curve at its corresponding minimum solar transmission value. For example, a glass with a solar transmission of 0.5 cannot have a SHGC below 0.5.

Figure 43 provides the relationships for scenario 1 – the case where the occupant is only exposed to diffuse radiation, whereas Figure 44 provides the curves for scenario 2 – the case where the occupant is exposed to direct radiation. The actual *summer comfort index* values for the different glazing systems of Table 18 are also shown on Figure 43 and Figure 44. For these types of graphs, it would be possible to color in zones of approximate glazing performance corresponding to the different classes of glazing performance (such as single clear, single absorbing, double low-ε, etc) to represent the variation in performance between products from different glazing manufacturers caused by slight differences in optical properties.

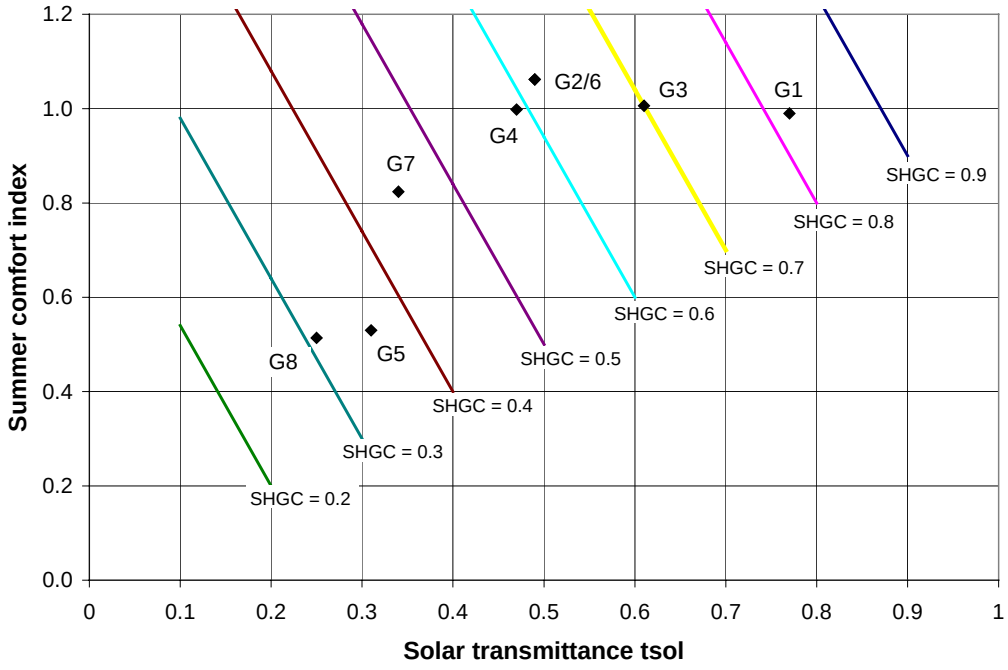


Figure 43: Diffuse radiation – Summer comfort index as a function of solar transmittance and SHGC

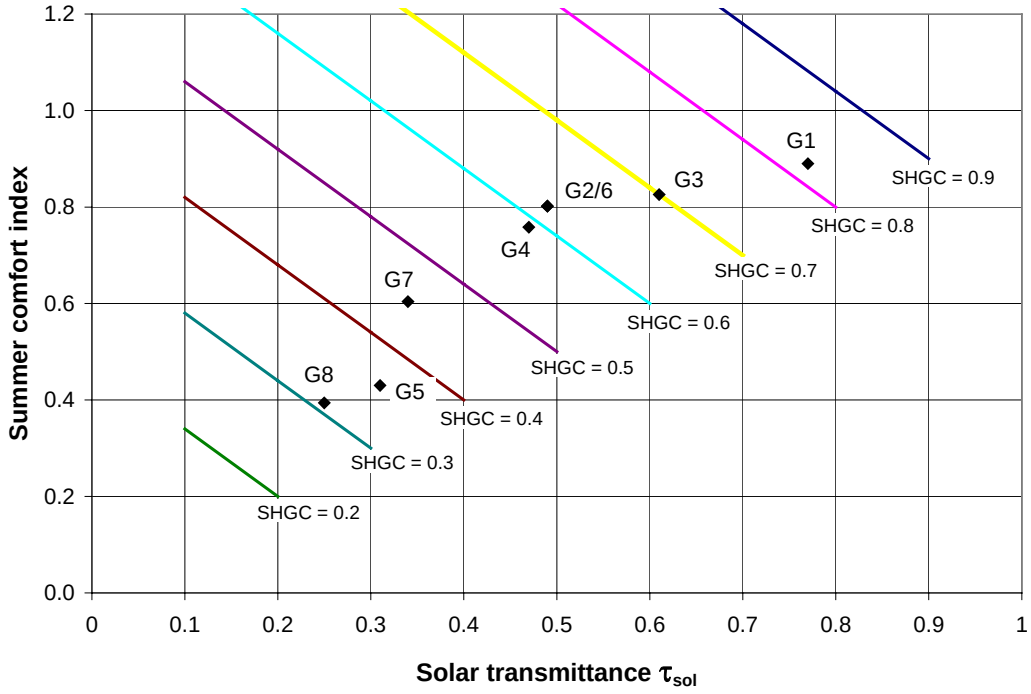


Figure 44: Direct radiation - Summer comfort index as a function of solar transmittance and SHGC

7 SUMMARY

In this report, we provided a thorough literature study on the impacts of windows on thermal comfort and more generally on comfort in asymmetrical environments, such as environments with cool or warm ceilings, walls, or floors.

In evaluating comfort in highly asymmetrical environments, such as the environment with cold or hot windows, local discomfort is very important. The UCB comfort model predicts comfort for 16 body parts, as well as for the whole body. The model is therefore well-suited to evaluate non-uniform thermal environments.

A single index for rating the thermal comfort performance of a window is not practical because the winter and summer performance are dependent on largely unrelated characteristics of the window. We therefore have identified several possible ratings for winter and summer and have recommended one of these for each season.

The winter rating is based on the window u-factor and the summer rating is based on a combination of solar transmittance and solar heat gain coefficient.

For winter, the minimum outdoor air temperature to ensure no discomfort happening for any body part is used as the index. This minimum allowable outdoor air temperature is directly related to the U-factor of the window, and a regression of the window comfort index with the U-value for winter condition is provided. The advantage of this index is that it provides guidance for designers when they choose windows for a specific climate.

In summer, however, the dominant factor is not the outdoor air temperature, but the solar radiation. The solar performance of glazing is determined by the optical properties of the glass, the solar transmission, reflection and absorption. Because the solar absorptance increases the surface temperature of the glass, the index is a combination of the transmittance and the absorptance of solar radiation, which is characterized by SHGC and Tsol (overall solar transmittance).

To illustrate how the methods we describe in this report could be applied to a comfort rating, we chose geometries with large view factors. This assumption will show larger differences between window products than if a geometry with a smaller view factor is used.

8 ANNOTATED BIBLIOGRAPHY

1) **Arens, E.A., Xu, T., Miura, K., Zhang, H., Fountain, M.E. and Bauman, F. 1998, "A Study of Occupant Cooling by Personally Controlled Air Movement". Building and Energy 27: 45 - 59.**

The authors (Center for the Environmental Design Research, UC Berkeley) did a laboratory study of thermal comfort under user-controlled air movement. 119 subjects participated. The results show that subjects considered air motion pleasant up to 1 m/s at 29.5ºC. Across the entire range of test conditions (24.5 – 31.5ºC), the chosen air velocity was in most cases above 0.4 m/s and up to 1.4 m/s, and very few people wanted less air movement. It is possible to make people comfortable by air motion at air temperatures 31ºC (1 met) or 29ºC (1.2 met). Based on the results, the authors proposed a "zone of likely use" for locally controlled air movement, which recommends air movement to provide comfort in warm environments.

2) **Bohm, M., Browen, A. et al. 1990, Evaluation of Vehicle Climate with a Thermal Manikin - The Relationship between Human Temperature Experience and Local Heat Loss, Swedish Institute of Agricultural Engineering.**

This report provides Equivalent Homogeneous Temperature (EHT) pistes for winter and summer conditions. The tests were conducted at the Swedish Institute of Agricultural Engineering, Ultuna, Uppsala. The pistes are widely used in automobile industry to evaluate thermal comfort in highly asymmetrical vehicle environments.

3) **Chapman, K.S., Sengupta, J. 2004, "Window Performance for Human Thermal Comfort". Final Report of ASHRAE Research Project RP-1162, Atlanta: ASHRAE Inc.**

This is a project funded by ASHRAE to evaluation window thermal comfort for human. The authors (Kansas State University) further developed the BCAP (Building Comfort Analysis Program, BCAP) model, which calculates the radiant heat exchange of the human body with his surrounding by calculating radiant intensity field. The current BCAP model links the properties obtained from the Window 5.1 program and includes the impact from window frames. The PMV, PPD and operative temperature are presented as contours.

The report explains the methods to calculate heat transfer of the room in great detail and provides calculation equations. It defines thermal comfort fenestration length as an evaluation parameter to evaluate window thermal comfort. The penetration length is defined as the distance into the room from the fenestration system, beyond which thermally comfortable conditions exist. At the end the authors provides 8 case studies to show the impact of fenestration system on comfort based on the simulation results. The authors proposed "Penetration depth" and "Fenestration performance map" to evaluate the window performance. Penetration depth is defined as the distance into the room from a window, beyond that thermal comfort condition exists. The fenestration map can be used as a design tool to determine the correct window wall ratio to ensure comfort at a defined distance from the window.

4) **Fanger, P.O. 1967, "Calculation of Thermal Comfort: Introduction of a Basic Comfort equation". ASHRAE Transactions 73 (2), 4.0 – 4.20.**

This paper provides a complete set of heat transfer equations to calculate the heat exchange between a human body and his surroundings.

5) **Fanger, P.O. 1973, Thermal Comfort. McGraw-Hill Book Co., New York, 244p.**

This book is based on the five-year research carried out at the Laboratory of Heating and Air-conditioning, Technical University of Denmark, and at the Institute for Environmental Research, Kansas State University, where the author worked for a period in year 1966 – 1967.

The book describes the thermal comfort evaluation indices, Predicted Mean Vote (PMV), and the Predicted Percentage of Dissatisfied (PPD) developed from a large number of human subject tests carried out by the author and other researchers..

The book offers heat transfer calculations between a human body and his surroundings, considers impacts on comfort from many aspects such as body builder, food, circadian rhythm, provides radiant view factors of a person within a room.

6) Fanger, P.O. and Christensen, N.K. 1986, "Perception of Draught in Ventilated Spaces". Ergonomics, 29, 215 - 235.

This study examined the perception of draft at air temperatures 20º, 23ºC and 26ºC, air movement from 0.05 to 0.4 m/s, under moderate and high levels of turbulent intensity. The results are presented as draft chart which predicts percentage of dissatisfied due to draft as a function of air velocity and air temperature. The data from this measurement, together with the data from another study by Fanger et al. (1988) were used to develop the draft model. The model was adopted by ASHRAE and ISO standards to define limits for air velocity and turbulent intensity.

7) Fanger, P.O., Banhidi, L., Olesen, B.W. and Langkilde, G. 1980, "Comfort Limits for Heated Ceilings". ASHRAE Trans., 86 (2), 141 – 156.

The purpose of the study was to determine the temperature limits for heated ceilings, to which people in thermal neutrality can be exposed without feeling discomfort. Researchers from the Laboratory of Heating and Air Conditioning, Technical University of Denmark conducted human subject tests using 8 male + 8 female college students. To eliminate discomfort caused by whole-body thermal imbalance,, neutral condition was maintained by asking subject's temperature preference and making changes of the chamber air temperature accordingly. During the first hour the ceiling was unheated. In the following five half-hour periods the subject was exposed to five different ceiling temperatures ranging from 34ºC to 69ºC (corresponding to a radiant temperature asymmetry from 4.5ºC to 23.6º). The thermal comfort questionnaires were presented in 5 minutes intervals.

If a subject reported twice out of the last three surveys that local discomfort happened, the subject was considered uncomfortable. Local discomfort was found either as a warm head or cool feet. In heated- ceiling tests, because the room air and the rest of the surface temperatures were low in order to balance the heated ceiling to keep subject neutral, the cool-feet discomfort happened more than warm head when ceiling temperature was between 34 – 52ºC (operative temperatures were same, around 24.1ºC). It was when ceiling temperature were between 63 – 69ºC that warm head discomfort happened more than cool feet discomfort. So in a way the limit for heated ceiling was based on cool feet discomfort. That is probably why the limit for cool ceiling (warmer the rest surfaces and air) is higher (14ºC from another paper by Fanger et al. 1985) than the heated ceiling (cooler the rest surfaces and air, 4ºC from this study) if we assume that people in general are more sensitive to cool feet than warm head. The heated ceiling tests cover the radiant temperature asymmetry from 4.5 – 23.6º, which in fact were all outside of the proposed limit, 4ºC for warm ceiling.

8) Fanger, P.O., Ipsen, B.M., Langkilde, G., Olesen, B.W., Christensen N.K. and Tanabe, S. 1985, "Comfort Limits for Asymmetric Thermal Radiation". Energy and Buildings, 8, 225 – 236.

The purpose of the study is to define limits for cool ceiling, hot/cool walls to which man in neutrality can be exposed without discomfort. The researchers from the Laboratory of Heating and Air Conditioning, Technical University of Denmark conducted the study.

A similar method as the study "Comfort Limits for Heated Ceilings" (Fanger et al. 1980) was applied. 16(F) + 16(M) college subjects participated in cool wall test, and 8 (F) + 8 (M) college subjects in warm wall and cool ceiling tests. The subjects first stayed in the chamber for an hour. Then his environment was changed 5 times in the following 2.5 hours to corresponding to 5 radiation asymmetries (cool wall: 17.8ºC to – 0.4ºC, warm wall: 32.6ºC to 70.1ºC, cool ceiling: 16.0ºC to – 0.8ºC). The room air and the rest of the surface temperatures were adjusted based on

subject's requirement to keep an overall neutral feeling. The votes were asked every 5 minutes and only the last three (votes on 20, 25, 30 minutes) were used.

The limits are presented as the radiant asymmetry temperature, for cool ceiling, 14ºC, cool wall, 10ºC, warm ceiling 23ºC. Because people seem more sensitive to cool wall than the warm wall, the authors stated that local cooling of the body is more frequently causing discomfort than local heating. Comparing with the larger allowed warm/cool wall then ceiling, the authors concluded that men seem more sensitive to radiation asymmetry from head to feet than from left to right.

The results from this paper and the limit from the heated ceiling are adopted by ASHRAE Standard 55 – 2004 and ISO 3370.

9) Fanger, P.O., Milikov, A.K., Hanzawa, H.and Ring, J. 1988, "Air Turbulence and Sensation of Draught". Energy and Buildings, 12, 21 – 29.

This research was conducted at the Laboratory of Heating and Air Conditioning, Technical University of Denmark. The purpose is to investigate the sensation of draught caused by the air turbulent. Fifty subjects (mostly college students, 25 females and 25 males) were exposed to three different turbulent intensity levels (low turbulence Tu<12%, medium turbulence 20%<Tu<35%, high turbulence >55%) and four air velocities (from 0.05 m/s to 0.4 m/s). The room air temperature was kept at a constant value, 23ºC.

The subjects stayed for an hour during which the subjects were encouraged to change clothing to keep them neutral. Then the air velocity changed every 15 minutes in the following one and half hours to present 6 velocity levels (the participants became cooler as the velocity increased). The subjects answered questions every 5 minutes about whether he felt an air movement, whether it is uncomfortable, and where it was felt.

The study found that at the same air velocity and temperature, airflow with higher turbulence causes more people to feel the draught. Women seem slightly more sensitive to the turbulent intensity than men at lower velocity. A draft model to predict percentage dissatisfied using velocity, air temperature and turbulent intensity was proposed based on this study together with another study conducted at air temperatures 20ºC, 23ºC and 26ºC and under higher turbulence levels (Fanger and Christensen 1986).

Because the draft model is based on data under neutral test conditions (20ºC, 23ºC, and 26ºC for sedentary people), it should only be applied for sedentary people in neutral to cool environment.

The draft model is adopted by ASHRAE and ISO standards to define limits for air velocity and turbulence to eliminate draft.

10) Fanger, P.O. and Pedersen, C.J.K. 1977, "Discomfort due to Air Velocities in Spaces". Proc. of the Meeting of Commissions B1, B2, E1 of the IIR, 4, Belgrade, 289 - 296.

Ten college-age subjects (five females and five males) participated in this experiment to examine draft sensitivity to turbulent intensity. The ten subjects were chosen as the most draft-sensitive from one hundred subjects. The air was designed directly blown to the back of the subject's neck.

The author found that the fluctuation of the air flow is an important factor causing draft. At the same percentage of dissatisfaction, the draft limit for constant flow is much higher than the limit for a fluctuating velocity. The discomfort is maximum at frequencies around 0.3 – 0.5 Hz for air velocity at 0.3 m/s. People are less sensitive to the draft at the ankle than at the neck. When the author blow the air to the bare skin of the ankle, the draft limit is 50 – 100% increased.

11) Fountain, M. and Huizenga, C. 1995, A Thermal Sensation Model for Use by the Engineering Profession. Environmental Anylitics, Piedmont, California, U.S.A.

The authors (Environmental Analytics and Center for Environmental Design Research at UC Berkeley) developed a thermal comfort prediction tool for ASHRAE. In this menu, the authors summarized the thermal comfort evaluation methods, evaluated different comfort models, described the tool developed for this project, and presented the detailed equations to carry out the heat transfer and to predict thermal comfort.

12) Fountain, M.E. and Arens, E.A. 1993, "Air Movement and Thermal Comfort". ASHRAE Journal, August 26 – 30.

This paper reviewshistorical studies of air movement and comfort since the beginning of the 20th century, summarizes the findings. The authors (from Center for the Environmental Design Research, UC Berkeley) argue that the draft model was developed based on laboratory studies at the lower end of the comfort zone (23º). In the higher temperature range (above 23ºC) the draft model was obtained by extrapolations to conditions where data were not collected and where other research is in disagreement.

The authors also provide a figure which shows the preferred air movements at higher temperatures by several studies. The figure shows that the draft model and the ASHRAE standard 55-81 allows the significantly lower velocities than the other studies.

13) Fountain, M.E., Arens, E.A., de Dear, R., Bauman, F. and Miura, K. 1994, "Locally Controlled Air Movement Preference in Warm Isothermal Environments". ASHRAE Transactions 100: 937 - 952.

The objective of the study is to examine the air movement preference in warm environment. Fifty-four human subjects participated in this test (in Center for the Environmental Design Research , UC Berkeley). The room temperature was set at 25.5 – 28.5ºC. The subjects were asked to adjust the air movement from local supply systems to make them comfortable. The thermal questionnaire includes sensation, preference, air movement preference, acceptability, and local sensation.

By providing air motion in this temperature range, the subjects in only 8.8% of the tests (out of 158 tests) responded that their overall sensation was not between –1 and +1, or voted that the present air movement was unacceptable. That means that air motion can make 91% people comfortable up to air temperature 28.5ºC. However, the draft model would predict that 63.2% of these comfortable votes are "unacceptable". At the upper limit of the draft model (0.2 m/s at turbulent intensity 40%), 50% of the people wanted more air movement. The preferred air movement is significantly higher than the draft limit. When the room temperature was 28ºC, 50% people chose air velocity higher than 0.4m/s to make themselves comfortable. The preferred velocity went as high as 0.8 m/s.

The authors pointed out that the draft model is not designed to make a maximum number of people satisfied with the air movement, but rather to protect a small percentage (15%) from feeling draft discomfort. The authors developed a converse model forpredicting percentage of satisfied (PS model).

14) Gan, G. 2001, "Analysis of Mean Radiant Temperature and Thermal Comfort". Building Serv. Eng. Research Technology 22.2: 95 – 101.

The author (Institute of Building Technology, School of the Built Environment, University of Nottingham, UK) examined a series of comfort impacts of windows by simulating more than 20 window design cases. The variables in these 20 cases include the size of the window, shape of the window (height vs. width), type of the glazing, and the effect of a radiator. The author found that for the same size glazing, a tall and a narrow window is preferable than a square window. Replacing a large window with several smaller windows improves comfort. Double-glazing and a radiator installed under a window improve comfort.

15) Ge, H. and Fazio, P. 2004, "Experimental Investigation of Cold Draft Induced by Two Different Types of Glazing Panels in Metal Curtain Walls". Building and Environment 39, 115 – 125.

The authors (Building Envelope Performance Laboratory, Center for Building Studies, Department of Building, Civil and Environmental Engineering, Concordia University, Montreal, Quebec, Canada) measured velocity and temperature profiles with large tall glass panels. Near the window, the cold window-induced air motion could be as large as 1 m/s. When the location was 1.2 m away from the window, the velocity reduced to 0.15 m/s. The air temperature 1.2 m away from the window was about 0.8ºC lower than the room air temperature. The velocity and temperature also vary with the height, so not only radiation, but temperature and velocity are also

not uniform. The authors also found that the empirical equations developed by Heiselberg (1994) provide close estimations of the measured data for cases having projecting window frames.

16) Griffinths, I.S. and McIntyre, D.A. 1974, "Subjective Response to Overhead Thermal Radiation". Human Factors, 16 (3), 415 – 422.

The authors (Electricity Council Research Centre, Capenhurst, Chester, UK) exposed 24 subjects to a neutral condition and three different ceiling temperatures. The method is similar to McNall and Biddison (1970) where the air temperature was kept constant and the temperature of the rest of the surfaces was adjusted to balance the temperature of the heated ceiling to keep the same MRT. They found that a vector radiant temperature of 20ºC did not produce any significant worsening of subjective responses when compared with a uniform control condition, and therefore a v.r.t of 20ºC was recommended. This finding is similar to what was found by McNall and Biddison (1970) when ceiling temperature was 54ºC corresponding to v,r,t = 24ºC, but significantly higher than the results from Fanger's (1980) where the radiant temperature asymmetry limit for heated ceiling is 4ºC.

17) Heiselberg, P., Overby, H. and Bjorn, E. 1995, "Energy-efficient Measures to Avoid Downdraft from Large Glazed Façade". ASHRAE Transactions 101 (2), 1127 - 1135.

To counter-react to the downdraft caused by cold glass, the conventional way is to provide convectors placed down to the façade, but that increases the energy use. This study (Department of Building Technology and Structural Engineering, Aalborg University, DK-9000 Aalborg, Denmark) examined effect from obstacles on the downdraft and found that with turbulent flow and an obstacle larger than the boundary layer thickness, the flow separated from the surface and a new boundary layer was established below the obstacle. The risk of thermal discomfort due to downdraft was reduced significantly.

18) Heiselberg, P 1994, "Draught Risk from Cold Vertical Surfaces". Building and Environment, 29: 297 – 301.

In this paper, the author (Department of Building Technology and Structural Engineering, Aalborg University, DK-9000 Aalborg, Denmark) examined the temperature and velocity profiles along the floor which is cause by vertical cold surfaces and penetrates into the occupied zone, and provided the prediction equations. These equations are widely used since they were proposed. The percentage of dissatisfied occupants was also examined. It reduces rapidly after 2 m away from the cold window because of the reduction in maximum air velocity.

19) Huizenga, C., Zhang, H., Arens, E. and Wang, D. 2004, "Skin and Core Temperature Responses in Uniform and Non-Uniform, Steady-State and Transient Thermal Environments". Journal of Thermal Biology, 29, 549 – 558. Accepted by The 1st Symposium on Physiology and Pharmacology of Thermal Biology and Temperature Regulation, Rhodes Greece, October, 2004.

This paper describes a large set of human subject tests carried out at the Center for the Built Environment at UC Berkeley. The tests were designed to investigate and develop models to predict human thermal comfort responses under transient and asymmetrical environment. This paper gives an overall description of the experiment set up, together with the skin and core temperature responses of people during the tests.

20) Huizenga, C., Zhang, H., Arens, E. and Duan, T. 2001, "A Model of Human Physiology and Comfort for Assessing Complex Thermal Environments". Building and Environment 36(6): 691 - 699.

This paper describes the advanced thermal physiology model that was developed at Center for Environmental Design Research, UC Berkeley. The model is based on the Stolwijk multi-node model, but has included significant changes - considering blood counter-current heat exchange, adding details view factor to calculate the radiative heat transfer of the human body with his surrounding, incorporating the solar radiation load on people. It divides the human body into 16 parts, each part is divided into core, muscle, fat, and skin layers. The model is able to calculate human thermal responses in transient and non-uniform environments.

21) Jones, B.W., Hsieh, K. and Hashinaga, M. 1986, "The Effect of Air Velocity on Thermal Comfort at Moderate Activity Levels". ASHRAE Transaction, 92(2B), 761 – 769.

The study examined the effect by air motion on people with higher metabolic level. The tests were for working people (2.3 metabolic level) with 0.65 clo and 1.09 clo, with velocity 0.2 m/s and 1.2 m/s, temperature over a range. The results show that comfort can be good with high air velocity.

22) Loveday, D.L., Parsons, K.C., Taki, A.H. and Hodder, S.G. 2002, "Displacement Ventilation Environments with Chilled Ceiling: Thermal Comfort Design within the Context of the BS EN ISO 7730 versus Adaptive Debate". Energy and Buildings, 34: 573 – 579.

Displacement ventilation saves energy. However, its ability to balance the heat load is limited. A common method is to apply a chilled ceiling. This introduces a more complex thermal environment. The authors, from Loughborough University and De Montfort University in UK, examined whether the ISO standard is applicable under this condition.

Total 184 subjects participated the tests in a chamber set up with the chilled ceiling/displacement ventilation. The ceiling temperatures were 14, 16, 18, and 21ºC, the supply air temperature from the displacement ventilation was 19ºC. The air supply flow rates were at 2.5, 3.9, 6.0, and 8.0 changes/hour. The subjects stayed in the test chamber for 3 hours to carry out the office work (1.2 met). The PMV predictions and the actual votes were close, so the author concluded that the PMV calculation method can be used in such complex thermal environment.

23) Lyons, P.R.A., Arasteh, D. and Huizenga, C. 1999, "Window Performance for Human Thermal Comfort". ASHRAE Transactions 73 (2), 4.0 – 4.20.

In this study, the authors (Windows and Day Lighting Group of Lawrence Berkeley National Laboratory and Center for Environmental Design Research at UC Berkeley) evaluate the window performance for 10 different window systems by simulation. The simulation results show that except in the situation where the human body is in the direct sun, the long-wave radiation is most important in determining thermal comfort. The impact of draft on comfort for residential size windows is small.

24) Manz, H. and Frank, T. 2004, "Analysis of Thermal Comfort near Cold Vertical Surfaces by Means of Computational Fluid Dynamics". Indoor Built Environment, 13: 233 – 242.

By CFD simulation, the authors (Swiss Federal Laboratories for Materials testing and research (EMPA), Duebendorf) showed that Heiselberg's empirical equations predicting maximum air speed near the floor due to cold windows works well in an empty room. However, with the presencet of internal heat gains, the predicted air velocity is smaller. The reason that the air speed increasedin a room with internal heat load is that the momentum of the buoyancy flows above heat sources boosts the motion of the downward flow near the cold wall. The author provided the modification to the Heiselberg's equations for situations with internal heat load. The simulation results also show that by improving the U-value of the windows, heating devices may not be necessary.

25) McIntyre, D.A. 1980, Indoor Climate. Applied Science Publishers LTD., London, 443p.

The author (Electricity Council Research Centre, Capenhurst, Chester, UK) provides knowledge basically covering all the areas that an indoor thermal environment and air quality study needs to deal with. It includes fundamental topics such as heat transfer, thermoreceptors and thermal sensation, and thermoregulation, to the summary of different indices used to describe thermal comfort, the comparison of laboratory study vs. field measurements.

26) McIntyre, D.A. 1977, "Sensation and Discomfort Associated with Overhead Thermal Radiation". Ergonomics, 20 (3): 287 – 296.

McIntyre (1977) did a following study (after Grinfinths and McIntyre 1974) to study heated ceiling on comfort. In this study, the author increases the ceiling temperature, but reduces both the

air temperature and the temperatures of the rest of the test chamber surfaces, in order to keep the same operative temperature, a similar approach to that of Fanger. He found not only thatthe heated ceiling produced no discomfort, but indeed was preferred when the ceiling temperature was high and the air and other surfaces were cooler. However, in the test, when subjects were invited to attribute discomfort specifically to the heated ceiling, the answers show a significant increase of discomfort with ceiling temperature, a contradictory answer from the pleasantness and discomfort questions in the test. It appears that people are ready to attribute discomfort to unusual aspects of the environments. For that reason, and because people clearly noticed the asymmetry radiation at v.r.t 10º, although no one was actually more uncomfortable than in the uniform environment, McIntyre recommended a v.r.t of 10ºC as the limit, which is also similar to the recommendations by Schroder and Steek (1973), 9ºC, and Banhidi (1972), a v.r.t between 8.5 – 13ºC.

27) McNall, Jr.P.E. and Biddison, R.E, 1970, "Thermal and Comfort Sensations of Sedentary Persons Exposed to Asymmetric Radiant Fields". ASHRAE Transactions, 76 (1), 123 – 136.

The effects of asymmetric radiation on thermal comfort was extensively investigated in Kansan State University in 1960s. In this study, the authors conducted a series of tests to examine the impact from warm and cool walls and ceilings covering large degree of radiation asymmetry. The cold wall temperature reached 9ºC (view factor 0.2) and it was 11ºC lower than the surface temperature of the rest. The warm wall temperature was fixed at 54ºC and it was 41ºC warmer than the rest. The cold ceiling reached 10.5ºC (view factor 0.12), 16ºC lower than the rest. The warm ceiling was kept at 54ºC and the difference from the rest was 38ºC. A control test was also conducted under neutral uniform environment (25.5ºC) in order to carry out the comparison.

Subjects exposed to warm wall had significant small satisfaction rate than the rate in other test conditions. When overall sensation was neutral, radiation asymmetry up to 9ºC wall, 10.5ºC ceiling, and 54ºC wall did not create significant discomfort, but did for the 54ºC warm wall. Under overall neutral condition, people with cool ceiling and cool wall received a 7% high percentage of satisfaction than under neutral condition.

The results are different from the results of Fanger et al. (1985) where the warm ceiling was perceived as the least tolerable while the warm wall had the largest allowable surface temperature. The major cause could be due to the different approaches. In Fanger's tests, both temperatures of the remaining surfaces and the air were lowered to balance the heated ceiling or wall. Therefore, a warm wall in a cool environment was perceived as acceptable and therefore has a larger allowable limit. In McNall's study, only the temperature of the rest surfaces was lowered to balance the heated ceiling or wall to keep the same MRT. The air temperature wasn't adjusted. As the results, the subjects experienced a stronger radiation than in Fanger's test condition. The discomfort could be caused by both warm or cool walls (we cannot tell because this information is not provided in the paper). The reason for a much smaller acceptable limit for heated ceiling in Fanger's study could also be caused by the experiment method. For ceiling temperature up to 52ºC (the rest of the room temperature was 22.3ºC), the discomfort from cool feet occurred more than from warm head. In normal temperature range people are more sensitive to cool feet than warm head. Therefore, the limit found was smaller, but it may not be specifically for the heated ceiling.

The two other differences are the scales to define discomfort and the test durations (please see the report).

28) Michaels, K.B., Nevins, R.G. and Feyerherm, A.M. 1964, "The Effect of Floor Surface Temperature on Comfort. Part II: College Age Females". ASHRAE Trans., 70, 37 – 43.

This test belongs to a series of tests conducted at the Kansas State University to determine the effect of floor surface temperature on foot and whole body thermal comfort. This paper focuses on the studies for college female subjects.

Eighteen female college students participated in the seated tests and eighteen participated in standing tests (with light work). The duration of the tests was 3 hours. The room air temperature was kept at 23.9ºC and floor temperature was changed from 23.9ºC to 37.8ºC. The floor

temperature as high as 32.2ºC did not cause much discomfort for standing female. For seated, the upper limit was 29.4ºC.

29) Narita, C., Tanabe, S., Ozeki, Y. and Konishi, M. 2001, "Effects of spectral property of solar radiation on thermal sensation at back of hands". Moving Thermal Comfort Standards into the 21st Century Conference Proceedings, 393 – 400.

This paper showed that human skin reacts differently to different wavelength. The skin is more sensitive to visible (0.30 – 0.80 um) and middle-infrared (1.70 – 2.30 um) than near-infrared (0.80 – 1.35 um). The results are from tests which different wavelength radiation was applied on the back of hands. Twenty subjects participated in the test. It was conducted in the Waseda University and Asahi Glass Co, Ltd. in Japan.

30) Nevins, R.G. and Feyerherm, A.M. 1967, "Effect of Floor Surface Temperature on Comfort. Part IV: Cold Floors". ASHRAE Trans., 73, III.2.1 – III. 2.8

This test also belongs to a series of tests conducted at the Kansas State University to determine the effect of floor surface temperature on foot and whole body thermal comfort. This paper focuses on the studies about the cold floors.

Twenty-four male and twenty-four female college students participated in the 3 hour long seated test. The room air temperature was kept at 23.9ºC and floor temperature changes from 15.5ºC to 23.9ºC. The floor temperature as low as 15.5ºC did not cause serious discomfort for the subjects.

31) Nevins, R.G. and Flinner, A.O. 1958, "Effect of Heated Floor Temperature on Comfort". ASHVE Trans., 64, p. 175.

Starting early 1950s, a series of studies were undertaken at the Kansas State University to determine the effect of floor surface temperature on foot and whole body thermal comfort. This paper focuses on the effect of heated floor on comfort.

College students (108 male, 21 female) were exposed to different heated floors for 60 minutes. The results show that covering air temperature from 18.3ºC to 29.4ºC, the floor temperature range from 26.7ºC to 35ºC did not create significantly effect on sensation. The subject sensation became warmer as the floor temperature increased from 35ºC to 37.8ºC, although the actual value of vote indicated comfort. Therefore, the upper limit is considered as 35ºC.

32) Nevins, R.G., Michaels, K.B. and Feyerherm, A.M. 1964, "The Effect of Floor Surface Temperature on Comfort. Part I: College Age Males". ASHRAE Trans., 70, 29 – 36.

This test belongs to a series of tests conducted at the Kansas State University to determine the effect of floor surface temperature on foot and whole body thermal comfort. The previous study (Nevins and Flinner 1958) had subjects seat in an environment for 1 hour. Now the exposures continued for 3 hours for both seated and standing. This paper focuses on the studies for college male subjects.

Total 45 male college students participated in the tests (25 seated and 21 standing with light work). The room air temperature was kept at 23.9ºC and floor temperature changes from 23.9ºC to 37.8ºC. The floor high as 32.2ºC did not cause much discomfort.

33) Olesen, B.W. 1977, "Thermal Comfort Requirements for Floors". Proc. Of the meeting of commissions B1, B2, E1 of the IIR, Belgrade, 1977/4, 337 - 343.

The study was conducted at the Laboratory of Heating and Air Conditioning, Technical University of Denmark. The objective is to define the limits for floor temperatures. Eighty-five subjects participated in the test, keeping the feet (with shoes) on the floor for 3 hours. The impact from flooring material is insignificant. The optimal temperature of 25ºC for sedentary and 23ºC for standing or walking people are recommended. At floor temperature below 20 – 22ºC the percentage of people experiencing cold feet increases rapidly (Olesen 1975). For 10% dissatisfied, the floor temperature should be within 20 – 28ºC. The ASHRAE and ISO standards specify 19 – 29ºC floor temperature for 10% dissatisfaction based on this study.

34) Ruegg, T., Dorer, V. and Steinemann, U. 2001, "Must Cold Air Down Draughts Be Compensated When Using Highly Insulating Windows?" Energy and Buildings 33: 489 – 493.

The authors (EMPA Swiss Federal Laboratories for Materials Tsting and Research, Duebendorf CH, Switzerland and US Engineering, Wollerau CH, Switzerland) measured air velocity profiles along the floor next to a cold window. They compared the measured data with the predicted values from Heiselberg's equation and found that the equation provides satisfactory results, even for windows with a sill. The measured velocity profile shows that as the internal heat load increased, the boundary layer thickness increased but the peak velocity decreased. The author explained that the plumes from the heat load spread at the ceiling and circulated down, mixed together with the draft layer so the temperature of the layer was raised and the draft was reduced. They also tested effect of increasing the roughness on top of a windowsill which showed little influence reducing the draft. However, openings on a windowsill can significantly reduce the draft because they take up the down draft and release it again at a lower speed. It is possible to remove the heat compliance by increasing the window property as far as the window frame is well insulated.

35) Sengupta, J, Chapman, K.S. and Keshavarz, A. 2005a, "Window Performance for Human Thermal Comfort". ASHRAE Transactions, 111 (1).

The authors (Kansas State University) further developed the BCAP (Building Comfort Analysis Program, BCAP) model, which determines radiant heat exchange of the human body with his surrounding. The current BCAP model links the properties obtained from the Window 5.1 program and includes the impact from window frames. The PMV, PPD and operative temperature are presented as contours.

The authors examined window performance on comfort for 8 cases covering different glass areas and window configurations. In summer with solar radiation, the present of two windows (40% of the wall area) and one window (20% of the wall area) only provides 7% - 25% floor area that is comfortable.

36) Sengupta, J, Chapman, K.S. and Keshavarz, A. 2005b, "Development of A Methodology to Incorporate Fenestration Systems into Occupant Thermal Comfort Calculations". ASHRAE Transactions, 111 (1).

The authors (Kansas State University) described the further development of the BCAP (Building Comfort Analysis Program, BCAP) model. The authors proposed a parameter "penetration depth" to describe the window impact on comfort. The penetration depth is defined as the distance into the room from a window, beyond which thermally comfortable conditions exist.

37) Schutrum, L.F., Stewart, J.L and Nevins, R.G. 1968, "A Subjective Evaluation of Effects of Solar Radiation and Raradiation from Windows on the Thermal Comfort of Women. ASHRAE Transactions, 74 (2), 115 – 128.

The authors (Pittsburgh Plate Glass Co., Harmaville, Pa, and Kansas State University) tested subject thermal sensation with solar radiation transmitted through a window. The glass temperature was separately controlled. The results show that in cloudy day, when the glass temperature increased from 3ºC to 48ºC, overall sensation elevated 1.1 unit. In clear day, the window temperature increased to 31.7ºC and the overall sensation became 2.5 units warmer. In clear day, the glass temperature influence on overall sensation is small because solar radiation is the dominant factor.

38) Toftum, J. 2004, "Air Movement – Good or Bad?" Indoor Air 14: 40 – 45.

The author (from International Centre for Indoor Environment and Energy, Technical University of Denmark) reviewed a large number of literature regarding the impact of air movement on comfort provides a summary. With people feeling neutral or cooler (temperature up to 22ºC to 23ºC, at sedentary activity), there is a risk of draft, even at low velocities. With occupants feeling warmer than neutral (air temperature above 23ºC or at higher activity level), people normally do not feel draft in normal indoor air velocities (up to 0.4 m/s). At high temperature around 30ºC, air

velocity up to 1.6 m/s was fond to be acceptable, although such high velocity may not be desirable for other reasons.

39) Toftum, J., Zhou, G., Melikov, A. 1997, "Effect of airflow direction on human perception of draught" Clima2000.

Forty subjects, 20 women and 20 men, were exposed to airflows from five different directions: horizontally towards the front, the back, and the left side and vertically upwards and downwards, at three temperature levels 20, 23 and 26oC. The results showed that airflow direction has an impact on perceived discomfort due to draught. At 20oC and 23oC, airflow from below was perceived as most uncomfortable followed by airflows towards the back and front. At 26oC airflow from above and towards the back caused most dissatisfaction due to draught, but generally only a few of the subjects perceived discomfort at this temperature. The authors also recommended to take air direction into account when providing design guidelines for air movement.

40) Window 5.1 2001, User Manual, A PC Program for Analyzing Windows Thermal Performance, LBNL – 44789.

WINDOW 5.2 is a publicly available computer program for calculating total window thermal performance indices (i.e. U-values, solar heat gain coefficients, shading coefficients, and visible transmittances). WINDOW 5.2 provides a versatile heat transfer analysis method consistent with the updated rating procedure developed by the National Fenestration Rating Council (NFRC) that is consistent with the ISO 15099 standard. The program can be used to design and develop new products, to assist educators in teaching heat transfer through windows, and to help public officials in developing building energy codes.

41) Wyon, D. P., Larsson, S. 1989, "Standard Procedures for Assessing Vehicle Climate with a Thermal Manikin". SAE Technical Paper Series 890049: 1-11.

David Wyon (Human Criteria Laboratory, National Swedish Institute for Building Research, Gavle, Sweden) proposed a method to evaluate asymmetrical thermal environment – Equivalent Homogeneous Temperature (EHT). The EHT is the temperature of a reference environment where the heat loss for a body part is the same as in the real asymmetrical environment. It is measured by a thermal manikin which shows the dry heat loss and skin temperature for individual body parts. The acceptable EHT range for all body parts are presented as a "piste". The EHT method is widely used in automobile industry to evaluate thermal comfort in asymmetrical environment. The piste only corresponds to the levels of the clothing and metabolic level that tested. It only defines the acceptable temperature range for each individual body part, does not tell local body thermal sensation and does not integrate local body information into the whole body thermal status.

42) Zhang, H., Huizenga, C., Arens, E., and Wang, D. 2004, "Thermal Sensation and Comfort in Transient Non-Uniform Thermal Environments". European Journal of Applied Physiology, Vol. 92, 728 – 733. Also presented in 5th International Meeting on Thermal Manikin and Modeling, Strasbourg France, September, 2003.

This paper summarizes the human thermal comfort prediction models developed from the human subject tests carried out at the Center for the Built Environment at UC Berkeley. An overall description of the test was presented by Huizenga et al. (2004). The models predict sensation and comfort under transient and asymmetrical environment. The models have been incorporated into the physiology model developed by the group (Huizenga et al. 2001) so the model now is able to predict the human comfort under complex thermal environments.

9 REFERENCES

1. Alvarez, G., Flores, J.J. and Estrada, C.A. 1998, "The Thermal Response of Laminated Glass with Solar Control Coating". J. Phys. D: Appl. Phys. 31, 3057 – 3065.
2. Arasteh, D., Hartmann, J. and Rubin, M. 1987, "Experimental Verification of a Model of Heat Transfer through Windows". ASHRAE Transactions 93, 1425 - 1431.
3. ASHRAE Handbook – Fundamentals, 1997. ASHRAE Inc.
4. ASHRAE *Standard 55-2004*, Thermal Environmental Conditions for Human Occupancy, Atlanta: ASHRAE Inc.
5. Arens, E., Gonzalez, R., and Berglund, L. 1986, "Thermal Comfort under an Extended Range of Environmental Conditions", ASHRAE Transactions 92 (1).
6. Arens, E.A., Xu, T., Miura, K., Zhang, H., Fountain, M.E. and Bauman, F. 1998, "A Study of Occupant Cooling by Personally Controlled Air Movement". Building and Energy 27: 45 - 59.
7. Banhidi, L. 1972, "Thermal Comfort Surveys in Buildings". Symposium 'Thermal Comfort and Moderate Heat Stress', CIB Commission W45, BRE, Watford, England.
8. Beck, F.A. and Arasteh, A. 1992, "Improving the Thermal Performance of Vinyl-framed Windows". Proc. 5th Conf. On Thermal Performance of the Exterior Envelopes of Buildings, Clearwater Beach, FL, U.S.A.
9. Bedford, T. 1964, Basic Principles of Ventilation and Heating. 2nd Ed., H.K. Lewis, London.
10. Bedford, T. and Warner, C.G. 1939, "Subjective Impressions of Freshness in Relation to Environmental Condition". J. Hyg. Comb. 39, 498.
11. Berglund, L. and Fobelets, A. 1987, "Subjective human response to low-level air currents and asymmetric radiation". ASHRAE Transactions 93 (1), 497-523.
12. Boerstra, A., Op 't Veld, P.J.M., Eijdems, H.H.E. 2000, "The Health, Safety and Comfort Advantages of Low Temperature Heating Systems: A literature Review". Proceedings, Healthy Building, 2000
13. Bohm, M., Holmer, I., Nilsson, H. and Noren, O. 2002, Thermal Effect of Glazing in Driver's Cabs, JTI-Report, Lantbruk & Industri 305, Uppsala, Sweden.
14. Bohm, M., A. Browen, et al. 1990, Evaluation of Vehicle Climate with a Thermal Manikin - The Relationship between Human Temperature Experience and Local Heat Loss, JTI-Report, Swedish Institute of Agricultural Engineering.
15. Brager, G. S. and de Dear R. 2000, "A Standard for Natural Ventilation". ASHRAE Journal: 21-28.
16. Brager, G. S., Paliaga G. et al. 2003a, The Effect of Personal Control and Thermal Variability on Comfort and Acceptability, RP-1161 Final Report, ASHRAE Inc.
17. Brager, G. S., Paliaga G. et al. 2003b, "Operable Windows, Personal Control & Occupant Comfort (RP-1161)". ASHRAE Transactions 110.
18. Butch, J. 1990, "Thermal Sensation to the Thai Office Environment". ASHRAE Transactions 96 (1), 859– 872.

19. Cabanac, M., Guillaume, J. et al. 2002, "Pleasure in Decision-Making Situations". BMC Psychiatry 2(7).

20. Candas, V. 2002, "To Be or Not to Be Comfortab1e: Basis and Prediction". The 10th International Conference on Environmental Ergonomics, Fukuoka, Japan.

21. Chapman, K.S. and DeGreef, J.M. 1997, Design Factor Development to Obtain Thermal Comfort with Combined Radiant and Convective In-space Heating and Cooling Systems, Final Report of ASHRAE Research Project RP-907, Atlanta: ASHRAE Inc.

22. Chapman, K.S. and Sengupta, J. 2003, Development of A Simplified Methodology to Quantify the Impact of Fenestration Systems on Human Thermal Comfort, Final Report of ASHRAE Research Project 1071, ASHRAE Inc.

23. Chapman, K.S., Sengupta, J. 2004, "Window Performance for Human Thermal Comfort". Final Report of ASHRAE Research Project RP-1162, Atlanta: ASHRAE Inc.

24. Chapman, K. S. 2005, "Methodology to Incorporate the Effect of Wavelength Dependency of Thermal and Optical Properties of Window Glass into In-Space Thermal Comfort Calculations". ASHRAE Winter Meeting, Orlando FL, January.

25. Chrenko, F.A. 1953, "Heated Ceiling and Comfort". Journal of the Inst. Of Heating and Ventilating Enginers, 20: 375 – 396, 21:145 – 154.

26. Clarke, J.A., Janak, M. and Ruyssevelt, P. 1998, "Assessing the Overall Performance of Advanced Glazing Systems". Solar Energy, 63 (4), 231 – 241.

27. de Dear, R. and Brager, G. S. 2001, "The Adaptation Model of Thermal Comfort and Energy Conservation in Built Environment". International Journal of Biometerology 45(2): 100 - 108.

28. de Dear, R. and Brager G. S. 2002, "Thermal comfort in naturally ventilated buildings: revisions to ASHRAE Standard 55". Energy and Buildings, Volume 34, Issue 6.

29. Eijdems, H.H.E., Boerstra, A.C., Op 't Veld, P.J.M.1994, "Low Temperature Heating Systems Impact on IAQ, Thermal Comfort and Energy Consumption". Proceedings, Healthy Building 94

30. Estrada-Gasca, C.A., Alvarez-Garcia, G and Nair, P.K. 1993, "Theoretical Analysis of the Thermal Performance of Chemically Deposited Solar Control Coatings". J. Phys. D: Appl. Phys. 26, 1304 - 1309.

31. Estrada-Gasca, C.A., Alvarez-Garcia, G. and Nair, P.K. 1993, "Thermal Performance of an Architectural Window with Chemically Deposited SnS-CuxS Solar Control Coating". Renewable Energy 3: 683 – 690.

32. Evin, F. and Edouard, S. 2002, "Sensory evaluation of heating and air conditioning systems". Energy and Buildings, Volume 34, Issue 6.

33. Fanger. P.O. 1967, "Calculation of Thermal Comfort: Introduction of a Basic Comfort equation". ASHRAE Transactions 73 (2), 4.0 – 4.20.

34. Fanger, P.O. 1973, Thermal Comfort. McGraw-Hill Book Co., New York, 244p.

35. Fanger, P.O. and Christensen, N.K. 1986, "Perception of Draught in Ventilated Spaces". Ergonomics, 29, 215 - 235.

36. Fanger, P.O. and Pedersen, C.J.K. 1977, "Discomfort due to Air Velocities in Spaces". Proc. of the Meeting of Commissions B1, B2, E1 of the IIR, 4, Belgrade, 289 - 296.

37. Fanger, P.O., Banhidi, L., Olesen, B.W. and Langkilde, G. 1980, "Comfort Limits for Heated Ceilings". ASHRAE Trans., 86 (2), 141 – 156.

38. Fanger, P.O., Ipsen, B.M., Langkilde, G., Olesen, B.W., Christensen, N.K. and Tanabe S. 1985, "Comfort Limits for Asymmetric Thermal Radiation". Energy and Buildings, 8, 225 – 236.

39. Fanger, P.O., Melikov, A.K., Hanzawa, H.and Ring, J. 1988, "Air Turbulence and Sensation of Draught". Energy and Buildings, 12, 21 – 29.

40. Fanger, P.O., Ostergaard, J., Olesen, S. and Madsen, L.1974, "The Effect on Man's Comfort of a Uniform Airflow from Different Directions". ASHRAE Trans., 80, 142 – 157.

41. Fanger, P. O. and Toftum, J. 2002, "Extension of the PMV model to non-air-conditioned buildings in warm climates". Energy and Buildings, Volume 34, Issue 6.

42. Feustrel, H. and Stetiu, C. 1995, "Hydronic Radiant Cooling – Preliminary Assessment". Energy and Buildings 22: 193 – 205.

43. Fiala, D. 2002, "First Principles Modeling of Thermal Sensation Responses in Steady State and Transient Conditions". ASHRAE Transactions.

44. Fiala, D. 1998, Dynamic Simulation of Human Heat Transfer and Thermal Comfort. Ph. D. Thesis, Institute of Energy and Sustainable Development, De Montfort University, Leicester.

45. Fountain, M. and Huizenga, C. 1995, A Thermal Sensation Model for Use by the Engineering Profession. Environmental Anylitics, Piedmont, California, U.S.A.

46. Fountain, M.E. and Arens, E.A. 1993, "Air Movement and Thermal Comfort". ASHRAE Journal, August 26 – 30.

47. Fountain, M.E., Arens, E.A., de Dear R., Bauman F. and Miura, K. 1994, "Locally Controlled Air Movement Preference in Warm Isothermal Environments". ASHRAE Transactions 100: 937 - 952.

48. Gagge, A.P., Stolwijk, J. and Nishi Y. 1970, "An Effective Temperature Scale Based on A Simple Model of Human Physiological Regulatory Response". ASHRAE Transactions.

49. Gan, G. 1994, "Numerical Method for a Full Assessment of Indoor Thermal Comfort". Indoor Air, 4: 154 – 168.

50. Gan, G. 2001, "Analysis of Mean Radiant Temperature and Thermal Comfort". Building Serv. Eng. Research Technology 22.2: 95 – 101.

51. Ge, H. and Fazio, P. 2004, "Experimental Investigation of Cold Draft Induced by Two Different Types of Glazing Panels in Metal Curtain Walls". Building and Environment 39, 115 – 125.

52. Goto, T., Toftum, J. et al. 2002, "Thermal Sensation and Comfort with Transient Metabolic Rates". Proceedings of Indoor Air Conference, Monterey. USA. June 30 - July 5.

53. Griefahn, B., Kunemund, C. and Gering, U. 2001, "The Impact of Draught Related to Air Velocity, Air Temperature and Workload". Applied Ergonomics, 32, 407 – 417.

54. Griefhahn, B. 1999, "Assesment of Draught at Workplaces (in German)". Fb 828, Dortmund, Schriftenreihe der Bundesanstalt fur Arbeitsschutz und Arbeitsmedizin.

55. Griffinths, I.S. and McIntyre, D.A. 1974, "Subjective Response to Overhead Thermal Radiation". Human Factors, 16 (3), 415 – 422.

56. Guan, Y., Hosni, M. H. et al. 2003, "Investigation of Human Thermal Comfort under Highly Transient Conditions for Automobile Applications - Part1: Experimental Design and Human Subject Testing Implementation". ASHRAE Transactions 109(2).

57. Guan, Y., Hosni, M. H. et al. 2003, "Investigation of Human Thermal Comfort under Highly Transient Conditions for Automobile Applications - Part2: Thermal Sensation Modeling". ASHRAE Transactions 109(2).

58. Hagino, M. and Hara, J. 1992, "Development of a Method for Predicting Comfortable Airflow in the Passenger Compartment". SAE Technical Paper Series 922131: 1 - 10.

59. Hashiguchi, N., Tochihara, Y., Ohnaka, T., Tsuchida, C., Otsuki, T. 2004, "Physiological and Subjective Responses in the Elderly When Using Floor Heating and Air Conditioning Systems". Journal of Physiological Anthropology and Applied Human Science, 23, 205 – 213.

60. Hausler, T. and Beregr, U. 2002, "Determination of Thermal Comfort and Amount of Daylight". Air Conditioning, Air Protection & District Heating, Szklarska Poreba, Juni 2002, Zusammenfassung.

61. Havenith, G., Holmér, I. and Parsons, K. 2002, "Personal factors in thermal comfort assessment: clothing properties and metabolic heat production". Energy and Buildings, Volume 34, Issue 6.

62. Hawthorne, W. and Reilly, M.S. 2000, "The Impact of Glazing Selection on Residential Duct Design and Comfort". ASHRAE Transactions 106 (1).

63. Heating, Ventilating, Air Conditioning Guide 1956, Chapter 24 – Panel Heating, p. 581. ASHAE Inc.

64. Heidari, S. and Sharples S. 2002, "A comparative analysis of short-term and long-term thermal comfort surveys in Iran". Energy and Buildings, Volume 34, Issue 6.

65. Heiselberg, P 1994, "Draught Risk from Cold Vertical Surfaces". Building and Environment, 29: 297 – 301.

66. Heiselberg, P., Overby, H. and Bjorn, E. 1995, "Energy-efficient Measures to Avoid Downdraft from Large Glazed Façade". ASHRAE Transactions 101 (2), 1127 - 1135.

67. Hodder, S.G., Loveday, D.L., Parsons, K.C. and Taki, A.H. 1998, "Thermal Comfort in Chilled Ceiling and Displacement Ventilation Environments: Vertical Radiant Temperature Asymmetry Effects". Energy and Buildings, 27: 167 – 173

68. Höppe, P. 2002, "Different aspects of assessing indoor and outdoor thermal comfort". Energy and Buildings, Volume 34, Issue 6.

69. Houdas, Y. and Ring, E.F.J. 1982, "Human Body Temperature: Its Measurement and Regulation". Plenum Press, New York, London.

70. Houghten, F.C., Guyberlet, C. and Witkowski, E. 1938, "Draft Temperatures and Velocities in Relation to Skin Temperature and Feeling of Warmth". ASH and VE Transactions, 44: 289 – 308.

71. Huizenga, C., Zhang, H., Arens, E. and Wang, D. 2004, "Skin and Core Temperature Responses in Uniform and Non-Uniform, Steady-State and Transient Thermal Environments". Journal of Thermal Biology, 29, 549 – 558. Accepted by *The 1st Symposium on Physiology and Pharmacology of Thermal Biology and Temperature Regulation*, Rhodes Greece, October, 2004.

72. Huizenga, C., Zhang H., Arens E. and Duan T. 2001, "A Model of Human Physiology and Comfort for Assessing Complex Thermal Environments". Building and Environment 36(6): 691 - 699.

73. Humphreys, M. A. and Nicol, J. F. 2002, "The validity of ISO-PMV for predicting comfort votes in every-day thermal environments". Energy and Buildings, Volume 34, Issue 6.

74. Ingersoll, J. G., Kalman, T. G. et al. 1992, "Automobile Passenger Compartment Thermal Comfort Model - Part II: Human Thermal Comfort Calculation". SAE Technical Paper Series 920266: 1-11.

75. ISO 7730, 1994, Moderate Thermal Environments – Determination of the PMV and PPD Indices and Specification of the Conditions for Thermal Comfort

76. Jones, B. and Chapman, K.S. 1994, Simplified Method to Factor Mean Radiant Temperature (MRT) into Building and HVAC System Design, Final Report of ASHRAE Research Project RP-657. Atlanta: ASHRAE Inc.

77. Jones, B.W., Hsieh, K. and Hashinaga, M. 1986, "The Effect of Air Velocity on Thermal Comfort at Moderate Activity Levels". ASHRAE Transaction, 92(2B), 761 – 769.

78. Jones, B. W. 2002, "Capabilities and Limitations of Thermal Models for Use in Thermal Comfort Standards". Energy and Buildings, Volume 34, Issue 6.

79. Jones, B.W. and Ogawa, Y. 1992, "Transient Interaction between the Human and the Thermal Environment". ASHRAE Transaction 98, Pt.1.

80. Karlson, T., Ribbing, C.G., Ross, A. and Valkonen, E. 1988, "Window Coating for efficient Energy Control". Int. J. Energy Res. 12: 23 – 29

81. Katahira, D., Akimoto, T., Kuwasawa, Y. and Emura, K. 2005, "Heating Thermal Comfort in Highly Air-Tight and Insulated House". The 10th International Conference on Indoor Air Quality and Climate, Beijing, Sept. 4 – 9.

82. Kitagawa, K., Komoda, N., Hayano, H. and Tanabe S. 1999, "Effect of Humidity and Small Air Movement on Thermal Comfort under a Radiant Cooling Ceiling by Subjective Experiments". Energy and Buildings, 30: 185 – 193

83. Kontz, S. et al.1983, "The Effect of Air Velocity on the Thermal Comfort". Proceedings of the 27th Annual Meeting of the Human Factor Socienty. Norfolk, Virginia. New York, New York: The Human Factor Society.

84. Kohri, I., Kataoka, T. et al. 1995, "Evaluation Method of Thermal Comfort in a Vehicle by SET* Using Thermal Manikin and Theoretical Thermoregulation Model in Man". IMechE C496(022): 357 - 363.

85. Kuelpmann, R. 1993, "Thermal Comfort and Air Quality in Rooms with Cooled Ceilings – Results from Scientific Investigations". ASHRAE Transactions, 99(2).

86. Larsson, U. and Moshfegh, B. 2002," Experimental Investigation of Downdraught from Well-insulated Windows". Energy and Buildings 37: 1073 - 1082.

87. Lee, E.S., DiBartolomeo, D.L. and Selkowitz, S.E. 1998, "Thermal and daylighting performance of an automated venetian blind and lighting system in a full-scale private office". Energy and buildings. 29(1): 47 – 63.

88. Loveday, D.L., Parsons, K.C., Hodder, S.G. and Taki, A.H. 1997, "Chilled Ceiling and Displacement Ventilation Environments: Air Flow, Radiant Asymmetry and Thermal

Comfort Effects". Proc. BEPAC/EPSRC Mini-conference Sustainable Building, Abingdon (ISBN 0-1872126-12-X).

89. Loveday, D.L., Parsons, K.C., Taki, A.H. and Hodder, S.G. 2002, "Displacement Ventilation Environments with Chilled Ceiling: Thermal Comfort Design within the Context of the BS EN ISO 7730 versus Adaptive Debate". Energy and Buildings, 34: 573 – 579.

90. Loveday, D.L. and Parsons, K. C., Taki, A. H. and Hodder, S. G. 2002, "Displacement ventilation environments with chilled ceilings: thermal comfort design within the context of the BS EN ISO 7730 versus adaptive debate". Energy and Buildings, Volume 34, Issue 6.

91. Lyons, P.R.A., Arasteh D. and Huizenga, C. 1999, "Window Performance for Human Thermal Comfort". ASHRAE Transactions 73 (2), 4.0 – 4.20.

92. Manz, H. and Frank, T. 2004, "Analysis of Thermal Comfort near Cold Vertical Surfaces by Means of Computational Fluid Dynamics". Indoor Built Environment, 13: 233 – 242.

93. Matzarakis, A., Rutz, F. and Mayer, F. 2000, "Estimation and Calculation of the Mean Radiant Temperature within Urban Structures", in Biometeorology and Urban Climatology at the Turn of the Millennium, ed. by R.J. de Dear, J.D. Kalma, T.R. Oke and A. Auliciems. Selected papers from the Conference ICB-ICUC'99, Sydney, WCASP-50, WMO/TD No. 1026, 273 – 278.

94. Martin, R. A., Federspiel, C. C., Auslander, D. M., "Responding to Thermal Sensation Complaints in Buildings". ASHRAE Transactions 112 (1), 407 – 412.

95. Matsunaga, K., Sudo, F. et al. 1993, "Evaluation and Measurement of Thermal Comfort in the Vehicles with a New Thermal Manikin". SAE Paper Series, 931958.

96. Mayer, E. 1987, "Physical Causes for Draught: Some New Finding". ASHRAE Transactions 93 (1), 540 - 540.

97. McCartney, K. J. and Nicol, J. F. 2002, "Developing an adaptive control algorithm for Europe". Energy and Buildings, Volume 34, Issue 6.

98. McIntyre, D. 1978, "Preferred Air Speed for Comfort in Warm Conditions". ASHRAE Transactions 84 (2), 264 – 277.

99. McIntyre, D. 1979, "The Effect of Air Movement on Thermal Comfort and Sensation". Indoor Climate, P.O. Fanger and O. Valbjorn, eds. Copenhagen, Denmark: Denish Building Research Institute, pp. 541 - 560.

100. McIntyre, D.A. 1974, "The Thermal Radiation Field". Building Sciences 9: 247 – 262.

101. McIntyre, D.A. 1980, Indoor Climate. Applied Science Publishers LTD., London, 443p.

102. McIntyre, D.A. 1977, "Sensation and Discomfort Associated with Overhead Thermal Radiation". Ergonomics 20 (3): 287 – 296.

103. McIntyre, D.A. and Griffinths, I.S. 1972, "Radiant Temperature and Thermal Comfort". Symposium 'Thermal Comfort and Moderate Heat Stress', CIB Commission W45, BRE, Watford, England.

104. McIntyre, D.A. and Griffiths, I.D. 1975, "The Effect of Uniform and Asymmetric Thermal Radiation on Comfort". Proc. Of the 6th International Congress of Climatistics "CLIMA 2000", Milan, March 1975.

105. McNall Jr.P.E. and Biddison R.E, 1970, "Thermal and Comfort Sensations of Sedentary Persons Exposed to Asymmetric Radiant Fields," *ASHRAE Transactions,* 76 (1), 123 – 136.

106. McNall, Jr.P.E. and Schlegel, J. 1968, "The Relative Effect of Convection and Radiation Heat Transfer on Thermal Comfort (Thermal Neutrality) for Sedentary and Active Human Subjects". ASHRAE Transactions, 74, 131 – 142.

107. Melikov, A., Pitchurov, G., Naydenov, K., Langkilde, G., 2005, "Field Study on Occupant Comfort and the Office Thermal Environment in Rooms with Displacement Ventilation". Indoor Air, 15, 205 – 214.

108. Michaels, K.B., Nevins, R.G., Feyerherm, A.M. 1964, "The Effect of Floor Surface Temperature on Comfort. Part II: College Age Females". ASHRAE Trans., 70, 37 – 43.

109. Morton, W.E. and Hearle, J.W.S. 1993, 3rd edition, "Physical Properties of Testile Fibres". The Textile Institure, UK

110. Muncey, R.W. and Hutson, J.M.1953, "The Effect of the Floor on Foot Temperature". Australia Journal of Applied Science, 4 (3), p. 395.

111. Muncey, R.W.1954, "The Temperature of the Foot and Its Thermal Comfort". Australia Journal of Applied Science, 5, p. 36.

112. Munro, A.F. and Chrenko, F.A., "The Effect of Air Temperature and Velocity and of Various Flooring Materials on the Thermal Sensation and Skin Temperature of the Feet". Journal of Hyg. Comb, 46, p. 451.

113. Murakami, S., Kato, S. and Zeng, J. 1998, "Numerical Simulation of Contaminant Distribution around a Modelled Human Body: CFD Study on Computational Thermal Manikin". ASHRAE Transactions 104 (2).

114. Nagano, K., Takaki, A. et al. 2002, "Thermal Responses to Temperature Steps in Summer". The 10th International Conference on Environmental Ergonomics, Fukuoka, Japan.

115. Nair, M.T.S. and Nair, P.K. 1991, "SnS-Cu_xS Thin Film Combination: A Desirable Solar Control Coatings for Architectural and Automobile Glazing". Journal of Phys. D: Applied Phys. 24: 450

116. Nakano, J., Tanabe, S. and Kimura K. 2002, "Differences in perception of indoor environment between Japanese and non-Japanese workers". Energy and Buildings, Volume 34, Issue 6.

117. Narita, C., Tanabe S., Ozeki Y. and Konishi, M. 2001, "Effects of spectral property of solar radiation on thermal sensation at back of hands". Moving Thermal Comfort Standards into the 21st Century Conference Proceedings, 393 – 400.

118. Nevins, R.G., Feyerherm, A.M. 1967, "Effect of Floor Surface Temperature on Comfort. Part IV: Cold Floors". ASHRAE Trans., 73, III.2.1 – III. 2.8

119. Nevins, R.G., Flinner, A.O. 1958, "Effect of Heated Floor Temperature on Comfort". ASHVE Trans., 64, p. 175.

120. Nevins, R.G., Michaels, K.B., Feyerherm, A.M. 1964, "The Effect of Floor Surface Temperature on Comfort. Part I: College Age Males". ASHRAE Trans., 70, 29 – 36.

121. Nicol, J.F. and Humphreys, M. A. 2002, "Adaptive thermal comfort and sustainable thermal standards for buildings". Energy and Buildings, Volume 34, Issue 6.

122. Nilsson, H. O. 2003, "Evaluation and Visualisation of Perceived Thermal Conditions". The 5th International Meeting on Thermal Manikin and Modeling, Centre d'Etudes de Physiologie Appliquee, Strasbourg, France, September 29 - 30.

123. Nilsson, H. O. 2005, "Thermal Comfort Evaluation with Virtual Manikin Methods". The 10th International Conference on Indoor Air Quality and Climates, Beijing, China, September 4 - 9.

124. Oguro, M., E. Arens, et al. (2002). "Convective Heat Transfer Coefficients and Clothing Insulation for Each Part of the Clothed Human Body under Air Flow Conditions." Journal of Architectural Planning and Environmental Engineering AIJ, No. 561, 31 – 39.

125. Olesen, B.W. 1977, "Thermal Comfort Requirements for Floors". Proc. Of the meeting of commissions B1, B2, E1 of the IIR, Belgrade, 1977/4, 337 - 343.

126. Olesen, B.W. 1977a, "Thermal Comfort Requirements for Floors Occupied by People with Bare Feet". ASHRAE Trans., 83 (2).

127. Olesen, B.W. 1977b, "Thermal Comfort Requirements for Floors". Proc. Of the meeting of commissions B1, B2, E1 of the IIR, Belgrade, 1977/4, 337 - 343.

128. Olesen B.W., Scholer M., and Fanger P.O. 1979. "Discomfort caused by vertical air temperature differences," *Indoor Climate*, Fanger P.O. and Valbjorn O. eds., Danish Building Institute, Copenhagen

129. Olesen, B.W. 1997, "Flachenheizung und Kuhlung; Einsatzbereiche fur Fussboden-, Wand- und Deckensysteme". Proceedings Velta Congress '97, pp. 35, Norderstedt, Germany

130. Olesen, B.W. 1997, "Possibilities and Limitations of Radiant Floor Cooling". ASHRAE Transaction, 103 (1), 42 - 48.

131. Olesen, B.W. 1997, Thermiske Komfort Krav til Gulve (Thermal Comfort Requirements for Floors). Ph.D. Thesis, Laboratory of Heating and Air Conditioning, Technical University of Denmark.

132. Olesen, B.W. 2002, "Are 'Cold' Window Surfaces A Problem with Regard to Thermal Comfort Nowadays (in Germany)". Proc. Of Velta Kongress, 81 - 96.

133. Olesen, B.W. and Nielsen, R. 1981, "Radiant Spot Cooling of Hot Working Places". ASHRAE Transactions, 87 (1)

134. Olesen, S., Bassing, J.J. and Fanger, P.O. 1972, "Physiological Comfort Conditions at Sixteen Combinations of Activity, Clothing, Air Velocity and Ambient Temperature". ASHRAE Trans., 78 (2), 199 - 206.

135. Olesen, B.W. and Parsons, K. C. 2002, "Introduction to thermal comfort standards and to the proposed new version of EN ISO 7730". Energy and Buildings, Volume 34, Issue 6.

136. Oseland, N.A. 1994, "A Review of Thermal Comfort and Its Relevance to Future Design Models and Guidance". Proceedings of the BEPAC Conference Building Environmental Performance: Facing the Future, York, UK, 205 – 216.

137. Oseland, N.A. and Humphereys M.A.1994, Trends in Thermal Comfort Research. Garston, Watford, UK: Building Research Establishment .

138. Parsons, K.C 2002, "The effects of gender, acclimation state, the opportunity to adjust clothing and physical disability on requirements for thermal comfort". Energy and Buildings, Volume 34, Issue 6.

139. Pellerin, N., Deschuyteneer, A. et al. 2003, "Local Thermal Unpleasantness and Discomfort Prediction in the Vicinity of Themoneutrality". The 5th International Meeting on Thermal Manikin and Modeling, Centre d'Etudes de Physiologie Appliquee, Strasbourg, France, September 29 - 30.

140. Ring. J. W. and de Dear. R. J. 1991, "Temperature Transients: A Model for Heat Diffusion through the Skin, Thermoreceptor Response and Thermal Sensation". Indoor Air 1(4): 448-456.

141. Roles, F. et al 1974, "The Effect of Air Movement and Temperature on the Thermal Sensations of Sedentary Man". ASHRAE Transactions 80 (1), 101 – 119.

142. Roles, F. et al 1974, "The Effect of Air Movement and Temperature on the Thermal Sensations of Sedentary Man". ASHRAE Transactions 80 (1), 101 – 119.

143. Roles, F., Kontz S. and Jones, B. 1983, "Ceiling Fans as Extenders of the Summer Comfort Envelope". ASHRAE Transactions 89 (1), 245 – 263.

144. Roulet, C. A., Rossy, J.P. and Roulet, Y. 1999, "Using Large Radiant Panels for Indoor Climate Conditioning". Energy and Buildings 30: 121 – 126.

145. Rueegg, T., Dorer, V. and Steinemann, U. 2001, "Must cold air down draughts be compensated when using highly insulating windows?" Energy and Buildings 33: 489 – 493.

146. Scheatzle, D. et al. 1989, "Extending the Summer Comfort Envelope with Ceiling Fans in Hot, Arid Climates". ASHRAE Transactions 95 (1), 169 – 280.

147. Schlegel, J. and McNall, Jr.P.E. 1968, "The Effect of Asymmetric Radiation on the Thermal and Comfort Sensations of Sedentary Subjects". ASHRAE Transactions, 74, 144 – 152.

148. Schroder, G. and Steck, B. 1973, "Die Empfindungsgenniisse Bowertung der Gesimtbestrah". Inngsstarke von Beleuehtnngsanlagen mit Leuchtstofflampen, Lichttechnik, 25: 17 – 21

149. Schutrum, L.F., Stewart, J.L and Nevins, R.G. 1968, "A Subjective Evaluation of Effects of Solar Radiation and Raradiation from Windows on the Thermal Comfort of Women. ASHRAE Transactions, 74 (2), 115 – 128.

150. Segre, G. 2002, A Matter of Degrees. New York, Viking Penguin.

151. Sengupta, J, Chapman, K.S. and Keshavarz, A. 2005a, "Window Performance for Human Thermal Comfort". ASHRAE Transactions, 111 (1).

152. Sengupta, J, Chapman, K.S. and Keshavarz, A. 2005b, "Development of A Methodology to Incorporate Fenestration Systems into Occupant Thermal Comfort Calculations". ASHRAE Transactions, 111 (1).

153. Simmonds, P. 1994, "Control Strageties for Combined Heating Cooling Radiant Systems". ASHRAE Transactions 100 (1), 1031 – 1039

154. Simmonds, P., Holst, S., Reuss, S. and Gaw, W. 2000, "Using Radiant Cooled Floors to Condition Large Spaces and Maintain Comfort Conditions". ASHRAE Transactions 106 (1), 695 – 701.

155. Sohn, J. 1986, "The State of Thermal Sensation Researches in Korea and Thermal Comfort in Ondol Space". Proceedings of the 10th Symposium on Human-Environment System, 93 – 96.

156. Springer, W.E., Nevins, R.G., Feyerherm, A.M., and Michaels, K.B., 1966, "The Effect of Floor Surface Temperature on Comfort. Part I: College Age Males". ASHRAE Trans., 72 (I), 292 – 300.

157. Stevens, J. C. and Stevens, S. S. 1960, "Warmth and Cold: Dynamics of Sensory Intensity". Journal of Experimental Psychology, Vol. 60, No. 3, 183 – 192.

158. Sullivan, R., Lee, E., Papamichael, K., Rubin, M. and Selkowitz ,S. 1994, "Effect of Switching Control Strategies on the Energy Performance of Electrochromic Windows". Proc. XIII SPIE Int. Symp. On Optical Materials Technology for Energy Efficiency and Solar Energy Conversion, Friedrichsbau, Freiburg, Germany.

159. Svedsen, S. and Fritzel, P. 1995, "Spaces for Highly Insulating Windows". Proc. Window Innovations'95. Natural Resource Canada, CTEC Bldgs Group, Ottawa, Canada, 90 - 97.

160. Tanabe, S. and Kimura, K. 1987, "Thermal Comfort Requirements Under Hot and Humid Conditions". Proceedings of the First ASHRAE Far East Conference on Air Conditioning in Hot Climates, Singapore, Atlanta, Georgia: ASHRAE.

161. Tanabe, S., Kimura, K. and Hara, T. 1987, "Thermal Comfort Requirements during the Summer Season in Japan". ASHRAE Transactions 93 (1), 564 - 577.

162. Tanabe, S., Kobayashi, K., Nakano, J., Ozeki, Y. and Konishi, M, 2002, "Evaluation of thermal comfort using combined multi-node thermoregulation (65MN) and radiation models and computational fluid dynamics (CFD)". Energy and Buildings, 34 (6), 637 – 646.

163. Taniguchi, Y., Aoki, H. et al. 1992, "Study on Car Air Conditioning System Controlled by Car Occupants' Skin Temperatures - Part 1: Research on a Method of Quantitative Evaluation of Car Occupants' Thermal Sensations by Skin Temperatures". SAE Technical Paper Series 920169: 13-19.

164. Terano, M., Nomura, K., Kamaya, S., and Kuno, S. 1997, "Study on Thermal Comfort When Soles Are Heated by a Hot Panel". Healthy Buildings, Washington DC.

165. Terano, M., Sakamori, N., Kamaya, S., and Kuno, S. 1996, "Study on Thermal Comfort When Legs Are Heated by a Horizataku System". Indoor Air.

166. Terano, M., Yasuhito, S., and Kuno, S. 2000, "Study on the Effect of Heating Soles of the Feet in Slightly Cool or Cool Conditionsl". Clima 2000/Napoli 2001 World Congress – Napoli (I), 15 – 18, September 2001.

167. Toftum, J. 1994a, Draught Complaints in the Industrial Work Environment, Ph.D. dissertation, Laboratory of Heating and Air-conditioning, Technical University of Demark.

168. Toftum, J. 1994b, "A Field Study on Draught Complaints in the Industrial Environment". ICEE'94, 6th International Conference on Environmental Ergonomics, Quebec, Canada, pp. 252 - 254.

169. Toftum, J. and Nielsen, R. 1996a, "Draught Sensitivity is Influenced by General Thermal Sensation". International Journal of Industrial Ergonomics, 18: 295 – 305.

170. Toftum, J. and Nielsen, R. 1996b, "Impact of Metabolic Rate on Human Response to Air Movements During Work in Cool Environments". International Journal of Industrial Ergonomics, 18: 307 – 316.

171. Toftum, J., Zhou, G., Melikov, A. 1997, "Effect of airflow direction on human perception of draught" Clima2000.

172. Toftum, J., Melikov, A., Tynel, A., Bruzda, M.A. and Fanger P.O. 2003, "Human Response to Air Movement – Evaluation of ASHRAE's Draft Criteria". International Journal of Heating, Ventilation, Air-conditioning and Refrigeration Research, 9: 187 – 202.

173. Toftum, J., Remann, G. et al. 2002, "Perceived Air Quality, Thermal Comfort, and BS Symptoms at Low Air Temperature and Increased Radiant Temperature". Inddor Air 2002, Monterey, California, June 30 – July 5.

174. Toftum, J. 2002, "Human response to combined indoor environment exposures". Energy and Buildings, Volume 34, Issue 6.

175. Toftum, J. 2004, "Air Movement – Good or Bad?" Indoor Air 14: 40 – 45.

176. Wang X. L. 1994, "Thermal Comfort and Sensation under Transient Conditions". Department of Energy Technology. Stockholm, The Royal Institute of Technology.

177. Watanabe S. 2001, "A Review of Floor Heating Research in Japan". Journal of the Human-Environmental System, 5 13 – 23

178. Window 5.1 2001, User Manual, A PC Program for Analyzing Windows Thermal Performance, LBNL – 44789.

179. Winslom, C. and Herrington, L. 1949, Temperature and Human Life, Princeton University Press.

180. Wu, H. 1989, "The Use of Oscillating Fans to Extend the Summer Comfort Envelope in Hot Arid Climates". 2nd ASHRAE Far East Conference on Air Conditioning in Hot Climates, 5 – 14.

181. Wyon, D. Larsson, P.S. 1989, "Standard Procedures for Assessing Vehicle Climate with a Thermal Manikin". SAE Technical Paper Series 890049: 1-11.

182. Xu, G., Kuno, S., Mizutani, S., and Saito, T. 1996, "Experimental Study og Physiological and Psychological Responses to Fluctuating Air Movement". In Yoshizawa, S., Kimura, K., Ikelda, K., Tanabe, S. and Iwata, T. (Eds.), Indoor Air '96: The 7th International Conference on Indoor Air Quality and Climate, 2: 547 – 552, Tokyo, Japan.

183. Xu, X., Tikuisis, P. et al. 2003, "Thermoregulatory Model for Prediction of Long-Term Cold Exposure". J. Appl. Physiol. In press.

184. Yoon, Y.J., Park, S.D., Sohn, J.Y. 1992, "Optimum Comfort Limits Determination Through the Characteristics of Asymmetric Thermal Radiation in a Heated Floor Space, 'Ondol'". Ann. Physiological Anthropology, 11 (5), 517 – 522.

185. Zhang, L, Emura, K., Nakane, Y. 1998, "A Proposal of Optimal Floor Surface Temperature Based on Survey of Literatures Related to Floor Heating Environment in Japan". Applied Human Science, 17, 61 – 66

186. Zhang, H., Huizenga, C., Arens, E. and Wang, D. 2004, "Thermal Sensation and Comfort in Transient Non-Uniform Thermal Environments". European Journal of Applied Physiology, Vol. **92**, 728 – 733. Also presented in *5th International Meeting on Thermal Manikin and Modeling*, Strasbourg France, September, 2003.

187. Zhang, H. 2003, "Human Thermal Sensation and Comfort in Transient and Non-Uniform Thermal Environments", Ph. D. Thesis, CEDR, University of California at Berkeley, pp415

188. Zhang, H., Huizenga, C., Arens E., and Yu T. 2001, "Considering Individual Physiological Differences in a Human Thermal Model". Journal of Thermal Biology 26(4-5): 401-408.

189. Zhou, G. and Melikov, A. 2002, "Equivalent Frequency – A New Parameter for Description of Frequency Characteristics of Airflow Fluctuations". Proceedings of Roomvent 2002, September, Copenhagen, Denmark, pp. 357 – 360.

Project 1.1.6

Project Name:	Heat Transfer Effect of Sloped, Ventilated Cavities Framing
Date:	February 27, 2007
Purpose:	The main purpose of this project was to develop set of convection heat transfer correlations for sloped and closed window frame cavities oriented at several discrete angles from horizontal. The second purpose is to develop criteria and heat transfer correlations for sill cavities with slots/holes in the walls and ventilated from outside.

Project Summary:

These criteria and correlations should be obtained on the basis of results of numerical modeling convection heat transfer in frame cavities selected configurations and sizes.

In experimental part, the present research project should provide guidelines for thermal properties measurement of sloped cavities and ventilated cavities and experimental validation of proposed numerical models.

Click here for final report

C E E R E

Center for Energy Efficiency and Renewable Energy

Building Energy Efficiency Program



University of Massachusetts

Engineering Laboratory Building
160 Governor's Dr
Amherst, MA 01003-9265

Final Report:

Investigation of Heat Transfer Effects of Sloped and Ventilated Internal Cavities of Framing Systems

Submitted by: *Dr. Alexander Fomichev*
Dr. D. Charlie Curcija
Balraj Balagurunathan
Michel Stocki

February 27, 2007

TABLE OF CONTENTS

1. Introduction 4

1.1 Background 4

1.2 Objectives 4

2. Literature Review 5

2.1 Laminar Natural Convection in Inclined Cavities 5

2.2 Natural Convection in Cavities with Opening 9

3. Convective heat transfer in closed frame sill/head cavity 10

3.1 Introduction 10

3.2 Numerical study 10

3.2.1 2-D Study 10

3.2.1.1 Mesh density analysis and validation of 2D model 14

3.2.1.2 Results and Discussion 20

3.2.2 3-D Study 27

3.2.2.1 Results and Discussion 29

3.3 Experimental study 35

3.3.1 Description of apparatus 35

3.3.2 Description of cavity specimen and test method 35

3.3.3 Results and Discussion 37

3.4 Heat transfer correlations for frame sill cavities 41

3.5 Summary 44

4. Convective heat transfer in closed frame jamb cavity 45

4.1 Introduction 46

4.2 Numerical Study 46

4.2.1 Mesh analysis of the numerical model 48

4.2.2 Results and Discussion 50

4.3 Experimental Study 61

4.3.1 Description of equipment and sensors 61

4.3.2 Calibration procedure 63

4.3.3 Description of cavity specimen and test method 65

4.3.4 Results and Discussion 68
4.4 Heat transfer correlations for tilted frame jamb cavity 74
4.5 Summary 78
5. Convective heat transfer in ventilated frame sill cavity 78
5.1 Introduction 78
5.2 Numerical Study 78
5.2.1 Description of numerical model 78
5.2.2 Results and Discussion 81
5.3 Experimental Study 88
5.3.1 Description of the cavity specimen installation 88
5.3.2 The test results 90
5.3.3 Numerical model and comparison 91
5.4 Heat transfer correlations for ventilated frame sill cavity 94
5.5 Summary 94
6. Overall Summary 95
7. Conclusions 96
8. Recommendations 97
9. References 98
Appendix A: 101
Appendix B: 102
Appendix C: 103
Appendix D: 105

1. INTRODUCTION

This document is the final report on the research project on sloped and ventilated frame cavities in fenestration systems. This report supersedes prior progress reports.

This research was undertaken under the grant with National Fenestration Rating Council in an effort to develop more accurate correlations for sloped and ventilated frame cavities in fenestration systems.

1.1 Background

Frame cavities in most of fenestration products (i.e., windows, doors, curtain walls, etc.) are normally oriented in a horizontal direction (sill, head, etc.) or vertical direction (jamb, vertical meeting rails, etc.). However, in limited number of systems, like skylights, roof windows, some commercial fenestration products, garden windows, etc. they may be tilted at various angles.

Currently NFRC and international standards (ISO 15099, ISO 10292) do not give us any heat transfer correlations for sloped frame cavities that are tilted around shorter axis, so that their longer axis is tilted. (e.g., jamb cross-sections tilted from vertical orientation). For frame cavities, which are essentially horizontal (i.e., cavities tilted around their longer axis so that shorter axis is tilted), right now we use “rectangularization” rule (process of transforming arbitrarily shaped polygon into an equivalent rectangle with its axis parallel and perpendicular to the direction of gravity vector. This rule is explained in ISO (2003). Numerous studies have investigated convection heat transfer in sloped cavities and enclosures, however studied cavities do not correspond in size and configuration to fenestration frame cavities.

In addition, fenestration systems may also have some of its frame cavities connected with outdoor environment by slots or holes (e.g., weep holes), which can make thermal performance of such fenestration products worse than if the holes did not exist. This phenomenon is sometimes referred to as “air washing”, due to the effect of cold outdoor air entering frame cavities through one hole or slot and exiting through another, sweeping the interior of the cavity and effectively increasing heat transfer due to both increased surface heat transfer coefficient and reduced air temperature.

International standard ISO 15099 describes this case as ventilated or slightly ventilated cavities and has rule how to define thermal properties of these cavities. Problem is that this rule is not documented and not confirmed by corresponding numerical and experimental research works and it is unknown how accurate is this rule particularly in the case of vertical oriented jamb cavities.

1.2 Objectives

The main objective of the present research project is to develop set of convection heat transfer correlations for sloped and closed window frame cavities oriented at several discrete angles from horizontal.

The second objective is to develop criteria and heat transfer correlations for sill cavities with slots/holes in the walls and ventilated from outside.

These criteria and correlations should be obtained on the basis of results of numerical modeling convection heat transfer in frame cavities selected configurations and sizes.

In experimental part, the present research project should provide guidelines for thermal properties measurement of sloped cavities and ventilated cavities and experimental validation of proposed numerical models.

2. LITERATURE REVIEW

2.1 Laminar Natural Convection in Inclined Cavities

The definition of the boundary conditions and the coordinate system and the geometry of an inclined sill/head and jamb frame cavities are shown in Figure 2.1. Tilt angle θ is defined as the angle between the hot wall and the horizontal surface. The cavity can be treated as 3-D or 2-D depending on the width (W) size. Most of the researches dealing with inclined cavities make the basic assumption of an infinite width enabling them to treat it as a 2-D cavity.

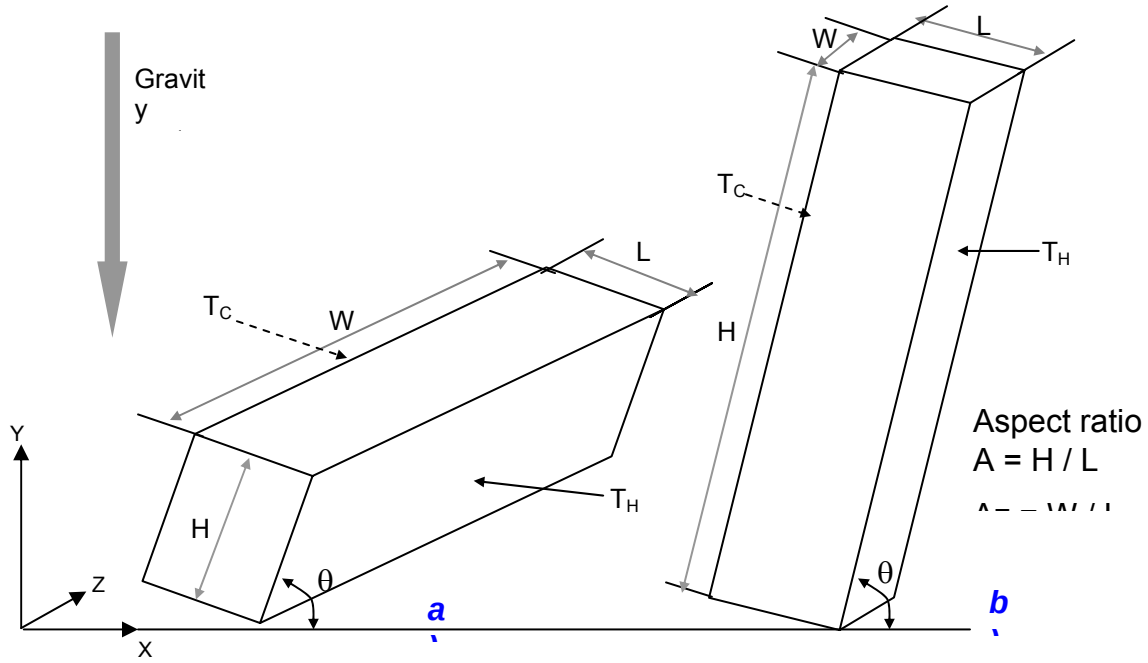


Figure 2.1: Problem Description for an Inclined Sill (a) and Jamb (b) Frame Cavities.

The general agreement among researchers is that an inclined cavity exhibits a behavior that is similar to the horizontal (heated from below) case up to a certain angle θ_c and to the vertical case for $\theta_c < \theta < 90$. For $\theta < \theta_c$, the flow is roll-like with the axis in the up slope

direction and is characterized by a critical Rayleigh number, independent of the Prandtl number. For $\theta > \theta_c$, the hydrodynamic instabilities of the vertical case in the form of a transverse roll with its axis along the Z direction are found.

For a vertical cavity heated from one side, Unny (1972) describes that the resulting pressure difference in the horizontal direction causes a circular motion in the fluid layer as soon as heating begins. He describes the flow as 'base flow' which is unicellular and completely filling the whole vertical cavity. As the angle of inclination to the horizontal is decreased, the magnitude of the base flow is reduced and the effect of secondary flow in cellular form becomes more and more dominant. He concluded that the stability phenomena in inclined layers are strongly Prandtl number dependent.

Ayyaswamy and Catton (1973) investigated the boundary layer regime for tilted rectangular cavities and showed that for sufficiently high Ra a rescaling of the results for 90° could be applied for tilt angles between 70° and 90°. They gave a relation for *Nu* in terms of θ:

$$Nu(\theta) = Nu(\theta = 90)\,\mathrm{Sin}^{1/4}\theta; \quad \text{For } 70^\circ < \theta < 90^\circ \tag{2.7}$$

Hollands and Konicek (1973) studied various flow regimes in terms of the range of values of the critical Rayleigh numbers closely related to the stability of the horizontal, vertical and inclined air layers of high aspect ratio cavities (in this case, A = 44). The principal modes of flow were discussed. For the horizontal mode, heat is transferred by conduction across the fluid layer, when Ra is less than the critical value ($Ra_c < 1708$). For the inclined cases, two types of instabilities should be considered, the static "top-heavy" instability associated with the horizontal case and the gravitational buoyancy or the hydrodynamic instability associated with the vertical case. The relative magnitude of each depends on the angle of inclination. At the critical angle heat transfer changes from one mode to the other.

Catton, Ayyaswamy and Clever (1974) theoretically investigated natural convection in an inclined rectangular enclosure and reported a pronounced aspect ratio dependency. Their solutions were two-dimensional and limited to angles 60° and 90°. They presented predictions for aspect ratios from 0.2 to 20 and for Ra up to 10^6. Their results were restricted to the case of infinite Prandtl number.

Ozoe et al (1974a) studied the rate of heat transfer and the mode of circulation in a long, inclined, square channel both experimentally and numerically and found that the heat transfer rate goes through a maximum and a minimum value as the tilt angle was decreased from the vertical position to the horizontal position. The maximum and minimum heat flux occurred at approximate angles of 50° and 10° respectively. The point of minimum heat flux corresponded to a change in the flow mode from a long roll-cell to a series of oblique roll-cells with axes normal to the long dimension. They subsequently reported (Ozoe at al, 1974b) the same pattern of maximum and minimum heat transfer for rectangular enclosures with A = 2, 3 and 4 and observed that the experimental and numerical results agree very well except at small angle of inclination. The angle of inclination depended strongly on the aspect ratio and was almost invariant with Ra. Ozoe et al (1975) extended the prediction of Ozoe et al (1974b) up to A = 8.4 and Ra up to 10^5.

Studies of Ozoe et al (1975) and Arnold et al (1976) for heat transfer across tilted enclosures showed a distinct local minimum heat transfer which is presumed to coincide with the transition from the boundary layer mode of flow to a series of oblique roll cell mode of flow. Arnold et al. (1976) experimentally investigated natural convection heat transfer in inclined rectangular cavities with aspect ratios 1, 3, 6, and 12, and Ra up to 10^6. They observed that the highest heat transfer occurs at 0° and as θ increases, *Nu* first decreases to a local minimum value and then as θ approaches 90° a local maximum heat transfer is reached. They also reported that the angle of minimum heat transfer shifts towards the horizontal as the Ra number decreases and is different for different aspect ratios. In general, their results showed reasonable agreement with those of Ozoe et al. (1975).

Meyer et al (1979) have concluded from their experimental work with air that convective heat transfer is a strong function of aspect ratio for aspect ratios < 4. Their work was on an array of enclosures inclined at 45°, 60° and 90°. They observed that as A is increased from 0.1 to 2, the heat transfer increased and then decreased for further increase in A. They concluded that perfectly conducting sidewalls caused lower heat transfer than adiabatic sidewalls.

Linthorst et al (1981) carried out flow visualization experiments to study natural convection in inclined enclosures. Observations were made for aspect ratios 0.25 to 7, tilt angles from 0° to 90°, and Rayleigh numbers between 5×10^3 and 2.5×10^5. They reported that the transition from stationary two-dimensional to stationary three-dimensional flow occurs at increasing θ with increasing A, when aspect ratio is larger than 1. For A < 1 the transition occurs for increasing θ with decreasing A (E.g., θ = 40° for A = 0.5, θ = 60° for A = 0.25 at 2.5×10^5). The angle of transition is only slightly dependent on Rayleigh number.

Symons and Peck (1984) classified the cavities in their experimental work as 'transverse' slots for a cavity with A = 0.17 and Az = 18 and 'longitudinal' slots for cavities with A = 7.5 to 18 and Az = 0.08 to 0.17. These configurations are, to an extent, similar to frame sill and frame jamb cavities respectively. They have compared heat transfer rates between these two cavities at different angles of inclination for Ra between 10^5 and 10^7 with a linear temperature profile on the end walls.

Zhong et al (1985) and Yang et al (1986) have applied numerical analysis to study the effects of variable thermal properties, namely: thermal conductivity, viscosity and heat capacity. Flow patterns and heat transfer were analyzed for a complete set of inclination angles. Transition from uni-cell to three-dimensional oblique rolls was reported at critical angles between 30° and 0°.

Hoogendoorn (1986) has reviewed research dealing with mixed boundary conditions. The aim of his work was to emphasize the importance of boundary conditions and 3-D geometry on natural convection in enclosures. He concluded that the sidewalls thermally interact with the isothermal walls through radiation and/or by conduction in the wall material. Heat transfer results split into conductive/convective and radiative fluxes for a cavity with A = 0.1 were given. He has compared numerically calculated heat transfer results obtained for small vertical aspect ratio cavities ($0.1 \leq A \leq 0.5$) given by Shiralkar et al (1981) and Sernas and Lee (1981). The Ra number was in the range of 10^5 to 4×10^7. He has also reviewed the

work of Linthorst (1985) on the role of 3-D effects in inclined narrow cavities. Linthorst (1985) had compared 2-D numerical results with 3-D experimental results for A = 0.1, 0.125, 0.25 and 0.5 and angle of inclination at 45^0. He had concluded that at critical Ra value convection starts to shift to a lower value in the case of 3-D simulation.

The numerical work of Yang et al (1987) is by far an important work from the perspective of the current research. They have used the longitudinal cavity (A = 7.5 and Az = 0.17) problem from Symons and Peck (1984) to verify their three-dimensional numerical procedure. In addition, they carried out simulation with Az = 0.5 and 1 to determine the effect of W/L on the uni-cell to multi-cell flow transition. They concluded that: (1) the flow transition is abrupt for Az = 0.17 while it is more gradual for cases of Az = 0.5 and 1, and, (2) the increase in heat transfer is substantial for Az changing from 0.17 to 0.5 while it is relatively low beyond Az = 0.5. This work complemented an earlier work done by Yang et al (1986) for 'transverse' slots.

Fath et al (1988) reported the effect of Prandtl number and different boundary conditions on heat transfer inside enclosures for different aspect ratios and tilt angles from 90^0 to 0^0. Calculations were reported for Pr values of 10, 0.72, 0.1, 0.01 and 0.001, Aspect ratios 1, 5, 10 and 20, and, Rayleigh numbers between 10^3 and 10^7. Their results indicated that the maximum heat transfer occur at tilt angles between 60^0 and 20^0 depending upon Ra. The influence of Prandtl number is more pronounced at low aspect ratio and high Ra numbers and the computed values of Nusselt number for adiabatic sidewall conditions were higher than that for conducting sidewall conditions.

Hamady et al (1989) obtained measurements of local and average Nusselt numbers at various tilt angles for Rayleigh numbers between 10^4 and 10^6, and compared their experimental data to the numerical data. Their aspect ratio A is 1 and the secondary aspect ratio A_z is 10. Their experimental results showed that the heat transfer rate continues to increase from 180° (heated from above) until a maximum value is reached at an angle between 70° and 60°. Below this point a decrease in tilt angle resulted in a decrease of the average heat transfer rate until a local minimum between 30° and 20°. Then the heat transfer increases and reaches a weak maximum value at 0°. The minimum occurs when the flow exhibits a transition from longitudinal rolls to a three-dimensional cellular flow configuration. Their 2-D numerical results showed good agreement with the experimental data beyond 30°. The numerical scheme became unstable at inclination angles smaller than 30°. Catton et al (1974) and Reddy (1981) reported similar instabilities in their numerical schemes for angles less than 30°.

Asako et al (1990) have performed a numerical study on hexagonal honeycomb core structure utilizing an algebraic co-ordinate transformation, which maps an irregular cross-section into a rectangle. Three different boundary conditions: perfectly conducting, adiabatic and no-thickness thermal boundary conditions were studied. Results for inclined cavities with aspect ratios 0.25, 0.5, 1, 2, 5, and, with Ra number between 10^3 and 10^5 were given. They have reported that 2-D and 3-D results agree very well for A = 2 and A = 5 whereas slight differences are found for A = 0.5 and 1 because of sidewall end effects. Among the

three boundary types used, the adiabatic boundary condition yielded the highest average Nusselt number. Their results compared favorably with Ozoe et al (1974a, 1974b).

Kuyper et al (1993) performed detailed numerical simulations for an inclined square cavity for both laminar and turbulent flows (Ra number between 10^6 and 10^{10}). They concluded that steady two-dimensional results could be obtained up to a minimal angle of 20°. This is close to the results reported by Hamady et al (1989) in which case the minimum angle was 30°. The three-dimensional, highly unstable flow at angles smaller than 20° was not considered.

Yang (2003) studied the buoyancy flow in inclined cavities with high aspect ratio typical of a window-glazing cavity. Two-dimensional finite element model was initially used and found unable to predict correct heat transfer results. Different types of non-ideal boundary conditions on hot and cold vertical walls like non-constant temperature distribution, time-dependent boundary conditions and wall roughness were tried to account for the discrepancy between the 2-D numerical results and the compared experimental results. It was concluded that the difference was because of the three dimensionality of buoyancy flow in inclined cavities and hence 3-D modeling is the effective way to understand transition in flow patterns and predict accurate heat transfer.

Literature study shows that enclosures and cavities studied in these investigations do not correspond in size and configuration (aspect ratio) to fenestration frame cavities.

2.2 Natural Convection in Cavities with Opening

Most of the studies involving ventilated cavities deal with free convection in cavities, which are partially or fully open on one of the vertical walls. Studies considering boundary conditions encountered similar to ventilated frame sill/head cavities, which are exposed to airflow at low velocities from the exterior with a small slot width, are limited.

Miyamoto et al (1989) have analyzed numerically the effects of aperture and cavity orientation on natural convection heat transfer in partially and fully open square cavities with all three walls isothermal. In case of partially open cavity, the dimensionless aperture size was 0.5 and it was centrally located. The Ra number was from 0.7 to 7 x 10^5 and they have used an extended computation domain, similar to Chan and Tien (1985). They have reported that for a fully open cavity with three equally heated walls, the average Nusselt number is approximately half that obtained for a cavity with a heated sidewall and insulated top and bottom walls. The difference between the overall, average Nu number in the partially and fully open cavities is reduced as the Rayleigh number decreases.

Elsayed and Chakroun (1999) experimentally investigated free convection in a square, partially open cavity with four different slit opening arrangements: high wall, low wall, centered wall and uniform wall slots. The ratio of opening height to cavity height ranged from 0.25 to 0.75. The vertical wall facing the wall with the slot was at a constant high temperature and all other walls were adiabatic. They have reported that for an opening ratio of 0.25 no definite trend could be seen when heat transfer was compared for the four arrangements.

Bilgen and Oztop (2004) have found that the average Nu number is an increasing function of Rayleigh number, aperture size and generally aperture position. Their conclusion was based on a numerical study on inclined partially open square cavities, which are formed, by adiabatic walls and a partial opening. The wall facing the partial opening is an isothermal wall. Rayleigh number was from 10^3 to 10^6. The aperture size and position was similar to Elsayed and Chakroun (1999).

Literature study shows that use of extended computation domain allows to define the boundary conditions at the ventilated walls more accurately and similar to the actual conditions that will exist in an experimental study.

The current study on ventilated frame cavity study is different from the studies shown in the literature review in the following ways: (a) airflow outside the ventilated cavities is wind induced and cannot be modeled as laminar natural convection, hence, turbulence modeling needs to be taken up; (b) the ratio of slot width to cavity height is much less than those mentioned in the literature review.

3. CONVECTIVE HEAT TRANSFER IN CLOSED FRAME SILL/HEAD CAVITY

3.1 Introduction

The range of study was determined by identifying suitable 2D Frame Sill cavities and the angle of inclination that are commonly used. Aspect ratios (ratio of cavity height to its width) 1:2, 2:1 and 5:1 were chosen. For each of the aspect ratio, 2 different geometries were chosen such that a large range of Rayleigh numbers from 2,316 to 92,625 are covered for a particular aspect ratio while the difference in temperature between hot and cold side is within a maximum of 10^0 C.

3.2 Numerical study

3.2.1 2-D Study

The boundary conditions and geometry of the frame sill cavity model are shown in Figure 3.2.

The geometry consists of two isothermal vertical sidewalls, T_h (hot wall on the right) and T_c (cold wall on the left) with $T_h > T_c$. The top and bottom walls are adiabatic. The cavity is assumed to be infinitely long in the z-direction, which will enable us to treat the model as two-dimensional. Heat is transferred from the hot wall to the cold wall by convective motion of the air and conduction across the cavity.

The boundary conditions used in the simulation of the Frame sill cavity are:

1) Fixed cavity wall temperatures on the indoor and outdoor surfaces. The temperatures on the hot and cold side (T_h and T_c respectively) were determined based on the Ra number at which the simulation was done. The air cavity was assumed to have a mean temperature of the wall temperatures (T_h and T_c). The properties of air in the cavity are calculated at the mean temperature

2) The top and bottom surfaces of the model are adiabatic and have zero heat flux across them.

3) No-slip velocity condition on all four surfaces

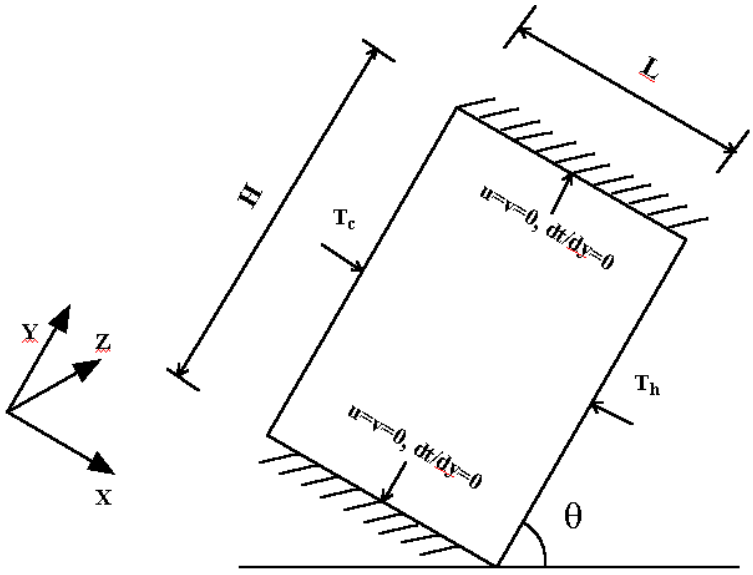


Figure 3.2: Geometry and Boundary Conditions of the Sill/Head Cavity Specimen.

The following approximations are used in the present study:

1) The cavity air fluid motion is assumed to be an incompressible flow. The fluid motion driven by natural convection is accounted for by making the Boussinesq approximation (approximation of the density change while maintaining the incompressible flow).

2) Due to low temperature differences between hot and cold surfaces (a maximum difference of 10 ^{0}C), constant property values are assumed for all materials.

3) There is no internal heat generation, and viscous dissipation and compressibility effects are negligible.

For optimization of the thermal performance of the frame sill cavity model, the flow within the cavity is studied under laminar conditions. The range of Aspect ratio chosen is such that the study is limited to laminar flow. Turbulent flow is more often found within rectangular cavities having high aspect ratios

Material Properties

The property values of the air inside the cavity were calculated based on ISO 15099 correlations at the mean temperature of 273K. Table 3.1 lists the material properties for air.

Table 3.1: Material Properties

Material: air (Fluid)			
Property	*Units*	*Method*	*Value(s)*
Density	Kg/m3	Boussinesq	1.2874
Cp (Specific Heat)	J/kg-K	Constant	1006.1
Thermal Conductivity	W/m-K	Constant	0.02406
Viscosity	Kg/m-s	Constant	1.721E-05
Thermal Expansion Coefficient	1/K	Constant	0.003663

Fluent Settings

Solver	Segregated
Formulation	Implicit
Space	2D
Time	Steady
Velocity formulation	Absolute
Viscous	Laminar
Energy	Enabled
Radiation	Off
Gravity	Enabled

Solution scheme Used:

Pressure	PRESTO
Pressure-Velocity Coupling	SIMPLE
Momentum	QUICK
Energy	QUICK

Convergence Criteria

The following criteria were used to determine model convergence:

A1) Area weighted average heat flux on Hot AND Cold wall (rounded to 3 decimals) is constant over 100 iterations.

OR

A2) Area weighted average heat flux on Hot AND Cold wall (rounded to 2 decimals) is constant over 500 iterations.

AND

B) Percent difference between area weighted average heat flux hot & cold wall is less than 1%.

The value of area weighted average heat flux on the hot and cold wall sides at the converged solution was used further in the calculation of average Nusselt number on the hot and cold side.

Description of Mesh

The 2-D Frame Sill Cavity interior was modeled and meshed using quadratic elements in Gambit (Fluent software). The number of elements in the cavity differs based on the size of the cavity and size of the mesh being used. An optimum mesh size was used to obtain the best possible convergence while minimizing the CPU time.

Appropriate boundary growth layers were applied to the interior side of the edges of the frame cavity to obtain a finer mesh near the corners of the horizontal and vertical edges so that edge effects can be captured accurately. Figure 3.3 shows a typical mesh in a model used in the simulation.

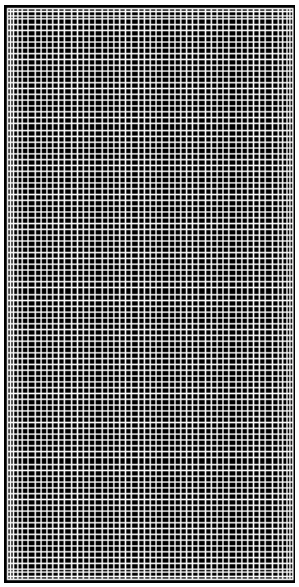


Figure 3.3: Typical Mesh of a Model (A=1:2).

3.2.1.1 Mesh density analysis and validation of 2D model

The following representative models were used for simulation for each of the Aspect ratios 1:2, 2:1 and 5:1, for 90 degrees. The average Nusselt numbers from the simulation were compared with the Nusselt number obtained from appropriate ISO 15099 correlations. Optimum mesh densities were selected for each of the Aspect ratios 1:2, 2:1 and 5:1.

1) A=H:L=1:2 (H = 0.01m, L = 0.02m) and Ra = 11,578 (with ΔT 10K)

Mesh's Analyzed

- 25X50
- 50X100
- 100X200
- 200X400

ISO Convergence

- Mesh 25X50 and Mesh 50X100 produced nearly identical results within 5% of ISO values

Since a mesh density of 50x100 showed the best possible convergence of all the mesh densities chosen, this mesh density has been recommended for further use in other angles for A=1:2.

2) A=H:L=2:1 (H = 0.08m, L = 0.04m) and Ra = 92,625 (with ΔT 10K)

Mesh's Analyzed

- 50x25
- 100x50
- 200x100

ISO Convergence

- Mesh 100x50 and Mesh 200x100 produced identical results within 2% of ISO values

Since a mesh density of 100x50 showed the best possible convergence of all the mesh densities chosen, this mesh density has been recommended for further use in other angles for A=2:1.

3) A=H:L=5:1 (H = 0.20m, L = 0.04m) and Ra = 92,625 (with ΔT 10K)

Mesh's Analyzed

- 100x20
- 200x40
- 400x80

ISO Convergence

- Mesh 200x40 and Mesh 400x80 produced identical results within 4% of ISO values.

Since a mesh density of 200x40 showed the best possible convergence of all the mesh densities chosen, this mesh density has been recommended for further use in other angles for A=5:1.

Table 3.2 provides the calculated Nusselt number from current simulation for 90^0, which has been compared with Nusselt number values from the correlation equations in ISO 15099.

The Nusselt number values for aspect ratio 1:2, at 90^o orientation, has a maximum deviation of 18% at Ra=92,625. For A=2:1, the Nusselt number values for 90^o orientation show a significant difference between current simulation and the ISO 15099 results. The ISO 15099 result has been obtained by a straight-line interpolation between the results of A=1:2 and A=5:1. The deviation may be caused by some extent by the interpolation. For A=5:1, the Nusselt number values for 90^o inclination compare very well with the ISO 15099 results and a maximum deviation of close to 6% is observed at Ra=18,525.

Figure 3.4 through Figure 3.6 show the comparison between Nusselt number from the current study and the ISO 15099 standards for 90 degrees oriented frame sill cavities.

Table 3.2: Nusselt Number Comparison Current Study Results Versus ISO 15099 Correlations 2D Frame Sill Cavities Oriented at 90 degrees

Aspect Ratio	**Rayleigh number**	**Comparison of Nusselt Number**		
A	Ra	**θ = 90°**		
		Nu [A] (Hot Wall)	ISO 15099 Nu [B]	% Difference
A = H:L = 1:2	2,316	1.03	1.04	-0.20%
	4,631	1.09	1.11	-2.44%
	6,947	1.17	1.21	-3.27%
	9,262	1.27	1.31	-3.59%
	11,578	1.37	1.42	-3.85%
	18,525	1.68	1.77	-4.55%
	37,050	2.37	2.61	-9.23%
	55,575	2.89	3.32	-13.02%
	74,100	3.30	3.92	-15.77%
	92,625	3.65	4.44	-17.82%
A = H:L = 2:1	2,316	1.51	1.12	34.96%
	4,631	1.88	1.26	49.12%
	6,947	2.12	1.39	53.10%
	9,262	2.31	1.51	53.22%
	11,578	2.45	1.62	51.64%
	18,525	2.79	1.94	44.00%
	37,050	3.33	2.66	25.31%
	55,575	3.70	3.24	14.13%
	74,100	3.98	3.73	6.96%
	92,625	4.22	4.14	1.98%
A = H:L = 5:1	2,316	1.30	1.29	0.28%
	4,631	1.60	1.56	2.22%
	6,947	1.81	1.75	3.68%
	9,262	1.97	1.89	4.44%
	11,578	2.10	2.01	4.86%
	18,525	2.41	2.28	5.56%
	37,050	2.91	2.76	5.51%
	55,575	3.23	3.08	4.79%
	74,100	3.46	3.33	4.02%
	92,625	3.66	3.54	3.34%

A) Computed from Fluent output of total surface heat flux

B) ISO 15099 NU Values calculated via equations #88 or #90/91/92 in ISO 15099 Standards for 90 degrees (Vertical orientation)

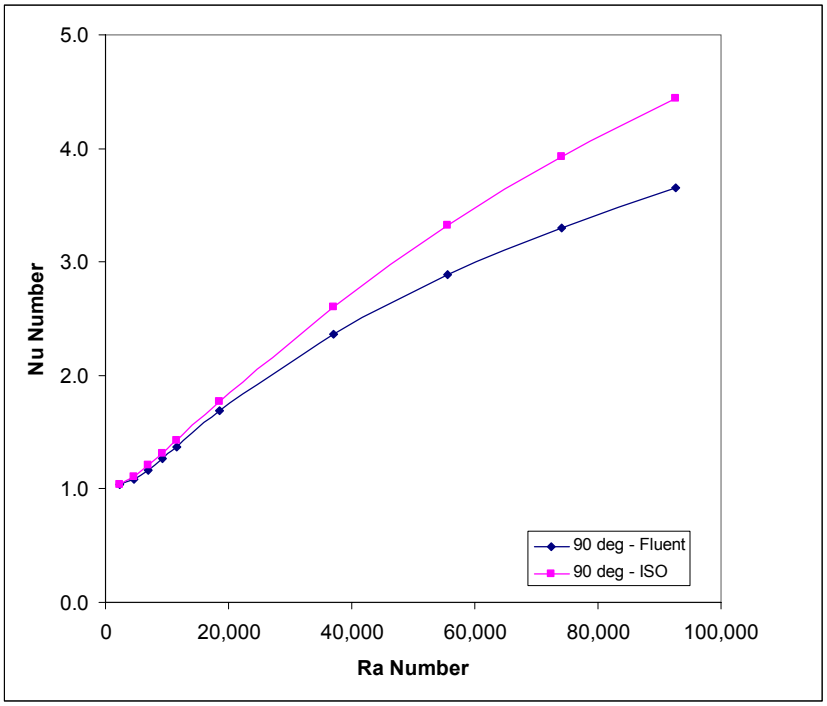


Figure 3.4: *Nu* From Current Study vs. ISO15099 for 2D Frame Sill Cavities at 90 Degrees for A=1:2

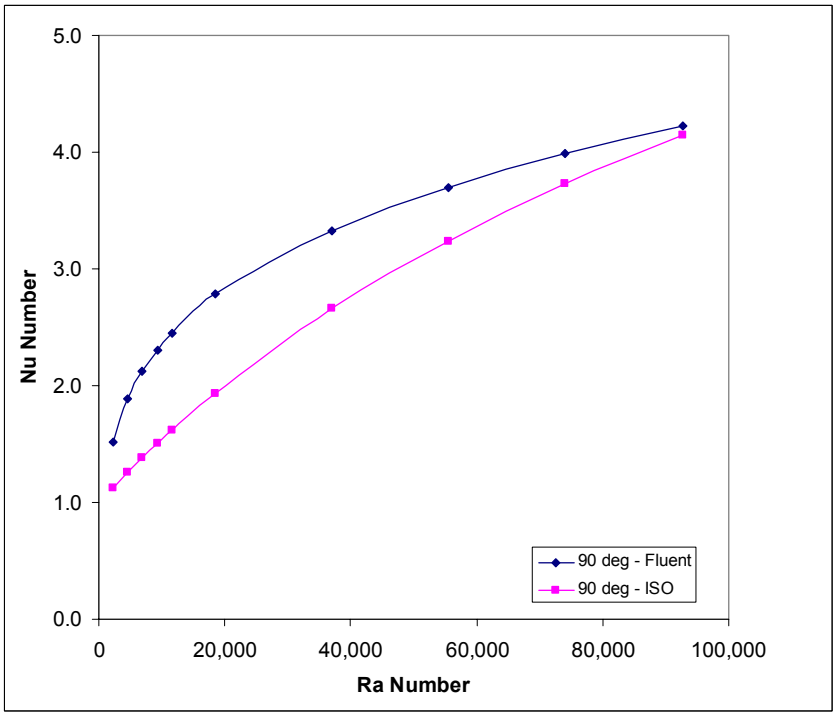


Figure 3.5: *Nu* From Current Study vs. ISO15099 for 2D Frame Sill cavities at 90 degrees for A=2:1

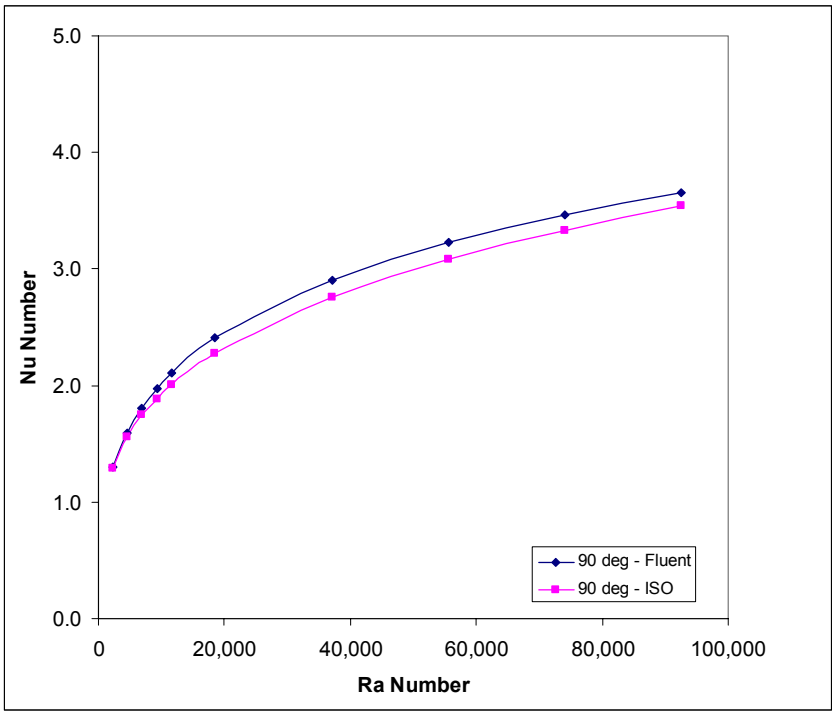


Figure 3.6: Nusselt number from current study Vs ISO 15099 for 2D Frame Sill cavities at 90 degrees for A=5:1

Following the results from the mesh analysis, the following combination of Frame Sill Cavity geometry, Raleigh (Ra) number and temperature difference (ΔT) between the hot and cold walls was used for each aspect ratio and angle of inclination combination. Hence, a total of 10 (Ra number) X 3 (Aspect Ratio) X 4 (Angle of inclination) = 120 simulations were performed. This constitutes the matrix of models for which heat transfer results are obtained and tabulated. Table 3.3 shows this range of the analysis.

Table 3.3: Range of Sloped Frame Study

Aspect Ratio	Mesh Density	Temperature Conditions		Geometry		Rayleigh Number
		Tm (K)	ΔT	L (m)	H (m)	Ra
A = H: L = 1:2	50X100	273 K	2 K	0.02 m	0.01 m	2,316
	50X100	273 K	4 K	0.02 m	0.01 m	4,631
	50X100	273 K	6 K	0.02 m	0.01 m	6,947
	50X100	273 K	8 K	0.02 m	0.01 m	9,262
	50X100	273 K	10 K	0.02 m	0.01 m	11,578
	50X100	273 K	2 K	0.04 m	0.02 m	18,525
	50X100	273 K	4 K	0.04 m	0.02 m	37,050
	50X100	273 K	6 K	0.04 m	0.02 m	55,575
	50X100	273 K	8 K	0.04 m	0.02 m	74,100
	50X100	273 K	10 K	0.04 m	0.02 m	92,625
A = H:L = 2:1	100X50	273 K	2 K	0.02 m	0.04 m	2,316
	100X50	273 K	4 K	0.02 m	0.04 m	4,631
	100X50	273 K	6 K	0.02 m	0.04 m	6,947
	100X50	273 K	8 K	0.02 m	0.04 m	9,262
	100X50	273 K	10 K	0.02 m	0.04 m	11,578
	100X50	273 K	2 K	0.04 m	0.08 m	18,525
	100X50	273 K	4 K	0.04 m	0.08 m	37,050
	100X50	273 K	6 K	0.04 m	0.08 m	55,575
	100X50	273 K	8 K	0.04 m	0.08 m	74,100
	100X50	273 K	10 K	0.04 m	0.08 m	92,625
A = H: L = 5:1	200x40	273 K	2 K	0.02 m	0.10 m	2,316
	200x40	273 K	4 K	0.02 m	0.10 m	4,631
	200x40	273 K	6 K	0.02 m	0.10 m	6,947
	200x40	273 K	8 K	0.02 m	0.10 m	9,262
	200x40	273 K	10 K	0.02 m	0.10 m	11,578
	200x40	273 K	2 K	0.04 m	0.20 m	18,525
	200x40	273 K	4 K	0.04 m	0.20 m	37,050
	200x40	273 K	6 K	0.04 m	0.20 m	55,575
	200x40	273 K	8 K	0.04 m	0.20 m	74,100
	200x40	273 K	10 K	0.04 m	0.20 m	92,625

3.2.1.2 Results and Discussion

As no experimental results and hence no correlation data exists for 2D Sloped Frame sill cavities at angles other than 0 and 90 degrees, the results are being discussed in comparison with the results of other aspect ratios and angles under study. The results for 90^0 were compared with the ISO 15099 correlation results. There were some differences in the results, which were discussed in the earlier section.

A summary of the average Nusselt number data obtained from the simulation for each of the aspect ratio is provided. The average Nusselt number values are given for the hot side of the cavity. Although as described in the convergence criteria, the percentage difference of heat flux between hot and cold wall is less than 1%.

The frame cavities oriented in the vertical direction (90 degrees) exhibit single cell convection throughout the range of Ra numbers and for all aspect ratios. The cells can be described to have a central core where the temperature is almost constant across the length of the cavity and the velocity is close to zero. The thickness of the core increases with increasing Ra number as the air rises along the entire height of the cavity indicating that heat transfer by convection is more prominent.

For the frame cavities oriented at angles between the vertical and horizontal, the behavior exhibited is either that of horizontal orientation or vertical orientation. Lower angles tend to resemble the horizontal case while higher angles resemble the vertical case. The transition angle is where the flow starts showing a multi-cellular behavior. From the results, it is believed that for A=5:1, the angle lies between 20 and 45 degrees and, for A=2:1, it could be between 0 and 20 degrees. For A=1:2, the flow is single celled throughout and hence no transition in the flow detected. The transition angle needs to be determined as there is a fluctuation in the trend of the Nusselt number at these angles, which will impact the way the heat transfer correlations are derived.

From the results obtained by the 2-D model simulation, preliminary heat transfer correlations were derived for aspect ratios 1:2, 2:1 and 5:1. The correlation equations are functions of Rayleigh number only. The angle of inclination has not been included in the correlations though the possibility of including it exists as the correlations develop into a more concrete form. Statistical software *Datafit* was used to determine the best model that provided the closest correlation. Regression analysis parameters like residual sum of squares and co-efficient of multiple determination (R^2) were checked for values close to 0 and 1 respectively for each of the correlation developed.

The following section discusses the results for each Aspect ratio separately and provides the correlation equations developed for aspect ratios 1:2, 2:1 and 5:1

Results and Correlation Equation for Aspect Ratio A=1:2, Angle=90 degrees

The average Nusselt number calculated for A=1:2 at various angles has been tabulated in Table 3.4. For purposes of comparing the flow pattern between the various angles at this ratio, Figure 3.7 has been plotted between average Nusselt number (on the hot side) and Ra number.

For this aspect ratio, the average Nusselt number increases as the angle of inclination is increased and then after reaching a peak value at an angle in between 20^o and 90^o the Nusselt number starts to decrease. Contour plots (Appendix A) indicate that the stagnant core in the cavity elongates as the angle of inclination and Ra number is increased. The fluid motion is predominantly single celled for all the angles. At a particular angle between 20^o and 90^o the heat transfer is more because of the direction of the velocity vector, which is inclined at angles towards the cold side and hence a peak Nusselt number at this angle. As the angle of inclination approaches 90^o flow is mostly parallel to the walls. This is not effective in transferring the heat from the hot side to the cold side.

Table 3.4: Calculated Average Nusselt Number for 2D Sloped Frame Sill Cavity with A=1:2

Temperature Conditions		Geometry		Rayleigh number	Calculated Nusselt number from Fluent results		
Tm (K)	ΔT	L (m)	H (m)	Ra	$\theta = 90^o$	$\theta = 70^o$	$\theta = 45^o$
273	2	0.02	0.01	2,316	1.03	1.03	1.03
273	4	0.02	0.01	4,631	1.09	1.10	1.08
273	6	0.02	0.01	6,947	1.17	1.21	1.20
273	8	0.02	0.01	9,262	1.27	1.35	1.37
273	10	0.02	0.01	11,578	1.37	1.49	1.55
273	2	0.04	0.02	18,525	1.68	1.94	2.09
273	4	0.04	0.02	37,050	2.37	2.83	2.99
273	6	0.04	0.02	55,575	2.89	3.44	3.50
273	8	0.04	0.02	74,100	3.30	3.89	3.84
273	10	0.04	0.02	92,625	3.65	4.24	4.10

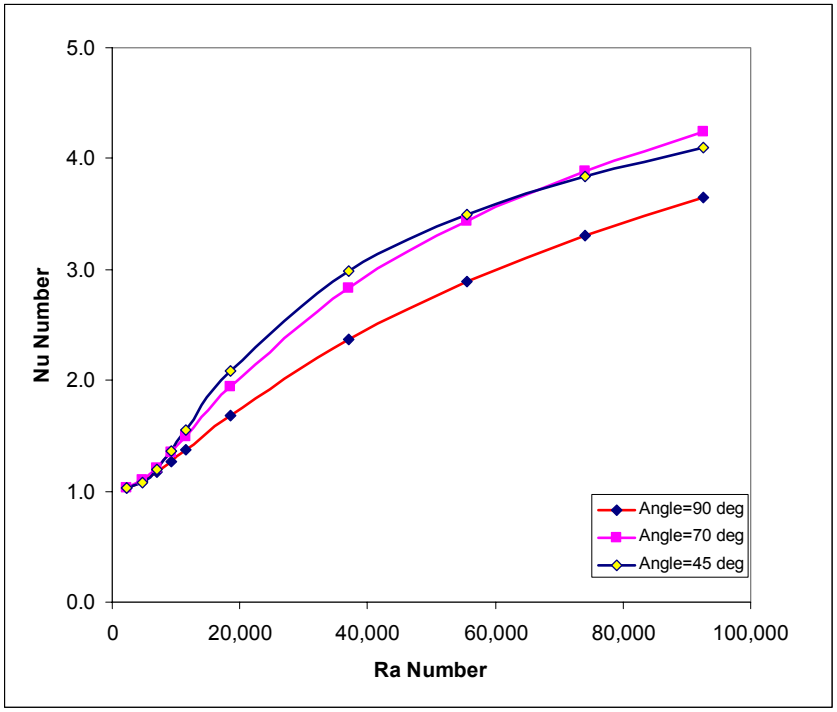


Figure 3.7: *Nu* vs. *Ra* for Aspect Ratio 1:2

The correlation equation number 88 from ISO 15099 standards document was used as a template. The equation derived here is of a similar form but with different correlation coefficients. Table 3.5 shows a comparison between the Fluent results and the Nusselt values obtained from the following correlation.

$$Nu = \{(a * Ra^{b})^{c} + (d * Ra^{e})^{f}\}^{g}, \quad (3.1)$$

Where

a = 0.65
b = 0.3
c = 0.6
d = 0.061
e = 0.33
f = 30.24
g = 0.0424

Table 3.5: Comparison of Nusselt number obtained from current study with Nusselt number from new heat transfer correlation developed – A=1:2, 90 degrees

Rayleigh number	Nusselt number	Comparison of Nusselt number with fluent results	
		θ = 90°	
Ra	Nu from new correlation equation	Nu From Fluent	% Difference
2,316	1.049	1.034	*-1.474%*
4,631	1.063	1.086	*2.066%*
6,947	1.174	1.169	*-0.468%*
9,262	1.319	1.267	*-4.089%*
11,578	1.452	1.370	*-5.990%*
18,525	1.772	1.685	*-5.147%*
37,050	2.375	2.368	*-0.325%*
55,575	2.820	2.887	*2.340%*
74,100	3.185	3.304	*3.612%*
92,625	3.500	3.651	*4.141%*
Regression Analysis parameter			Regression Analysis results
			θ = 90°
Residual Sum of Squares			0.03228
Co-efficient of Multiple determination (R^2)			0.99634

Correlation Equation for A=1:2, Angle=70 and 45 degrees

The Nusselt number variation showed a similar trend for angles of orientation of 70^0 and 45^0. Hence one correlation equation was derived to get the closest data fit. The correlation equation number 88 from ISO 15099 was used as a template and the equation derived here is of a similar form but with different correlation coefficients. Table 2.6 shows a comparison between the fluent results and the Nusselt values obtained from the following correlation.

$$Nu = \{(a * Ra^{b})^{c} + (d * Ra^{e})^{f}\}^{g}, \quad (3.2)$$

Where:

a = 0.45
b = 0.3
c = 0.6

d = 0.0619
e = 0.33
f = 35.24
g = 0.0424

Table 3.6: Comparison of *Nu* Obtained from Current Study with *Nu* from new heat transfer correlation developed – A=1:2, 70 and 45 degrees.

Ra	*Nu*	Comparison of Nusselt number with fluent results			
		θ = 70°		**θ = 45°**	
Ra	Nu from new correlation equation	Nu From Fluent	% Difference	Nu From Fluent	% Difference
2,316	1.040	1.032	*-0.701*	1.026	*-1.293%*
4,631	1.060	1.098	*3.544*	1.080	*1.859%*
6,947	1.228	1.208	*-1.698*	1.198	*-2.439%*
9,262	1.414	1.345	*-4.888*	1.365	*-3.469%*
11,578	1.579	1.494	*-5.389*	1.551	*-1.744%*
18,525	1.990	1.940	*-2.511*	2.087	*4.844%*
37,050	2.801	2.834	*1.175*	2.991	*6.773%*
55,575	3.421	3.440	*0.560*	3.497	*2.217%*
74,100	3.943	3.886	*-1.446*	3.838	*-2.647%*
92,625	4.401	4.240	*-3.671*	4.098	*-6.878%*
Regression Analysis parameter				Regression Analysis results	
				θ = 70°	**θ = 45°**
Residual Sum of Squares				0.028857	0.13347
Coefficient of Multiple determination (R^2)				0.9979	0.98996

Results for Aspect Ratio 2:1

The average Nusselt number calculated for A=2:1 at various angles has been tabulated in Table 3.7. For purposes of comparing the flow pattern between the various angles at this ratio, Figure 3.8 has been plotted between average Nusselt number (on the hot side) and Ra number.

The flow pattern and the heat transfer distribution is similar to A=1:2. The flow is single cell for all angles. The Nusselt number varies in a pattern similar to that of A=1:2, where there is a peak value of Nu at an angle in between 0^o and 90^o.

Table 3.7: Calculated Average *Nu* for 2D Sloped Frame Sill Cavity with A=2:1

Temperature Conditions		Geometry		*Ra*	Calculated Nusselt number from Fluent results		
Tm (K)	ΔT	L (m)	H (m)	Ra	θ = 90^o	θ = 70^o	θ = 45^o
273	2	0.02	0.01	2,316	1.51	1.56	1.53
273	4	0.02	0.01	4,631	1.88	1.96	1.95
273	6	0.02	0.01	6,947	2.12	2.22	2.22
273	8	0.02	0.01	9,262	2.31	2.41	2.41
273	10	0.02	0.01	11,578	2.45	2.57	2.57
273	2	0.04	0.02	18,525	2.79	2.91	2.92
273	4	0.04	0.02	37,050	3.33	3.46	3.45
273	6	0.04	0.02	55,575	3.70	3.83	3.80
273	8	0.04	0.02	74,100	3.98	4.12	4.06
273	10	0.04	0.02	92,625	4.22	4.36	4.28

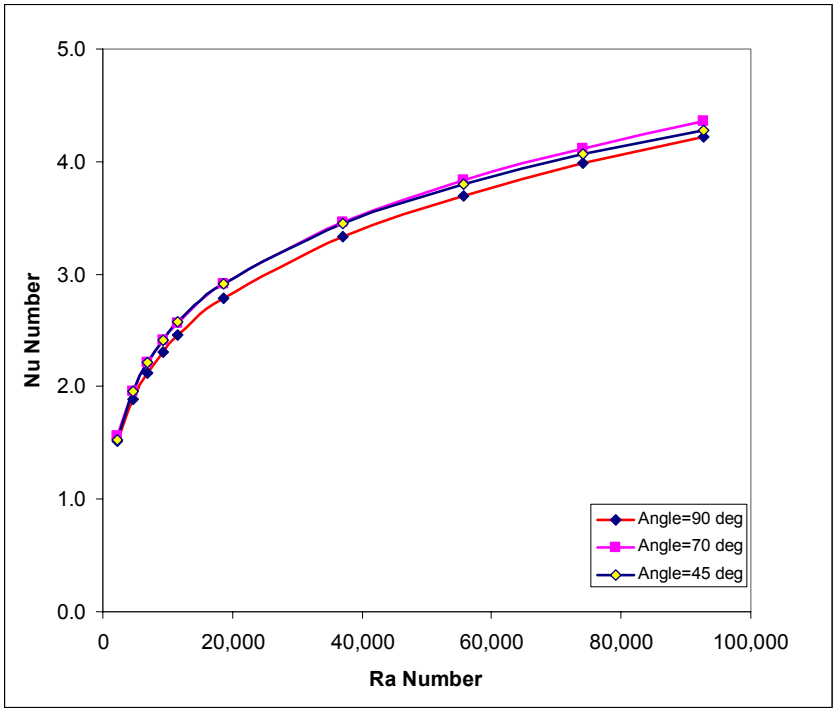


Figure 3.8: *Nu* vs. *Ra* for Aspect Ratio 2:1

Correlation Equation for A=2:1, Angle=90, 70 and 45 degrees

The Nusselt number variation showed a similar trend for angle of inclination 90, 70 and 45 for Aspect ratio 2:1 and hence one equation was derived to get the closest data fit. The correlation equation number 90 from ISO 15099 was used as a template and the equation derived here is of a similar form but with different correlation coefficients. Table 8 shows a comparison between the fluent results and the Nusselt values obtained from the following correlation.

$$Nu = \{1+[(a * Ra^{b}) / (1+(c / Ra)^{d})]^{e}\}^{f}, \quad (3.3)$$

Where:

a = 0.0025
b = 1.02
c = 8250
d = 0.12
e = 0.54
f = 0.5

Table 3.8: Comparison of Nusselt number from current study with Nusselt number from new heat transfer correlation developed – A=2:1, 90, 70 and 45 degrees

Ra	*Nu*	Comparison of *Nu* with fluent results					
		θ = 90°		**θ = 70°**		**θ = 45°**	
Ra	*Nu* from new correlation equation	*Nu* From Fluent	% Difference	*Nu* From Fluent	% Difference	*Nu* From Fluent	% Difference
2,316	1.688	1.514	*11.50*	1.562	*8.07*	1.53	*10.24*
4,631	1.956	1.883	*3.91*	1.962	*-0.28*	1.95	*0.11*
6,947	2.144	2.124	*0.96*	2.218	*-3.33*	2.22	*-3.37*
9,262	2.295	2.306	*-0.48*	2.411	*-4.79*	2.41	*-4.95*
11,578	2.423	2.454	*-1.26*	2.566	*-5.54*	2.57	*-5.73*
18,525	2.727	2.789	*-2.22*	2.911	*-6.31*	2.92	*-6.49*
37,050	3.272	3.330	*-1.75*	3.459	*-5.42*	3.45	*-5.24*
55,575	3.651	3.697	*-1.25*	3.829	*-4.65*	3.80	*-3.85*
74,100	3.951	3.985	*-0.85*	4.119	*-4.09*	4.06	*-2.73*
92,625	4.203	4.224	*-0.50*	4.361	*-3.63*	4.28	*-1.85*

Regression Analysis parameter	Regression Analysis results		
	θ = 90°	**θ = 70°**	**θ = 45°**
Residual Sum of Squares	0.04608	0.04944	0.07880
Coefficient of Multiple determination (R^2)	0.99411	0.99411	0.99008

3.2.2 3-D Study

3-D numerical modeling of frame sill cavities was carried out to verify convective heat transfer results for frame sill cavities, which were obtained using 2-D numerical. Heat transfer results from 2-D numerical modeling of frame sill cavities tilted at 90^0, 70^0 and 45^0 from the horizontal position were presented above. Heat transfer results for frame sill cavities tilted at 20^0 was not included, as detailed analysis on this case is required using a 3-D numerical model. This section will describe the difference in the heat transfer predicted between 2-D and 3-D numerical model.

The temperature difference between hot and cold wall ranged from 2K to 10K (Ra number from 2,316 to 92,625). Aspect ratio of cavities model:

- A = 0.5 (H x L = 1 cm x 2 cm and 2 cm x 4 cm),

- A = 2 (H x L = 4 cm x 2 cm and 8 cm x 4 cm), and,
- A = 5 (H x L = 10 cm x 2 cm and 20 cm x 4 cm)

Figure 3.9 shows the mid-width and mid-height cavity cross-sections of the frame sill cavity specimen, which are used to analyze heat transfer effects using a 3-D model. Effect of inclination angle on local heat flux along line 1-2 and temperature distribution and vertical velocity distribution along line a-b are compared between the 2-D and 3-D numerical models. Figure 3.10 shows the single cell flow pattern in frame sill cavities. Figure 3.11 shows the mode of convective heat transfer in the form of multi-cells, which were detected using 3-D models.

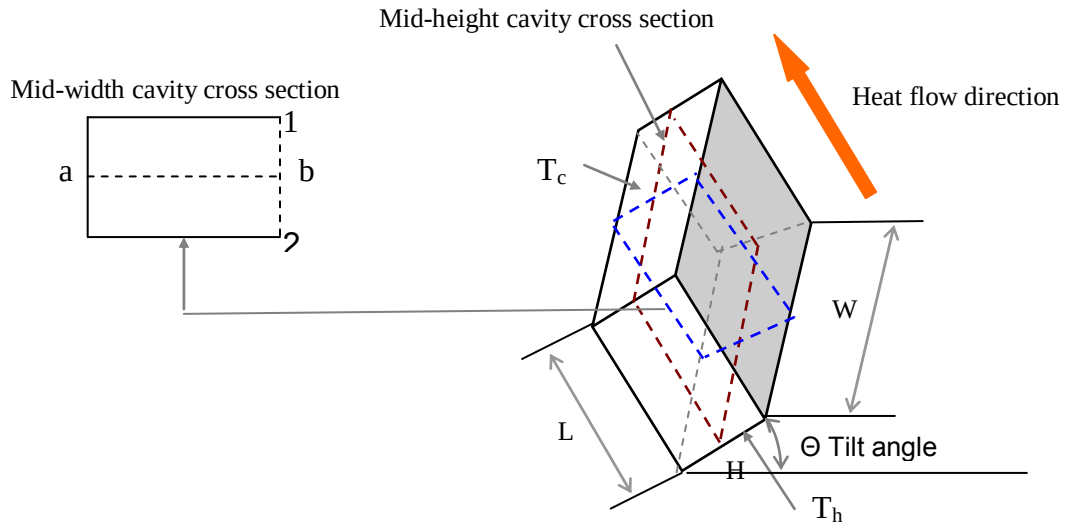


Figure 3.9: Frame Sill Cavity Specimen

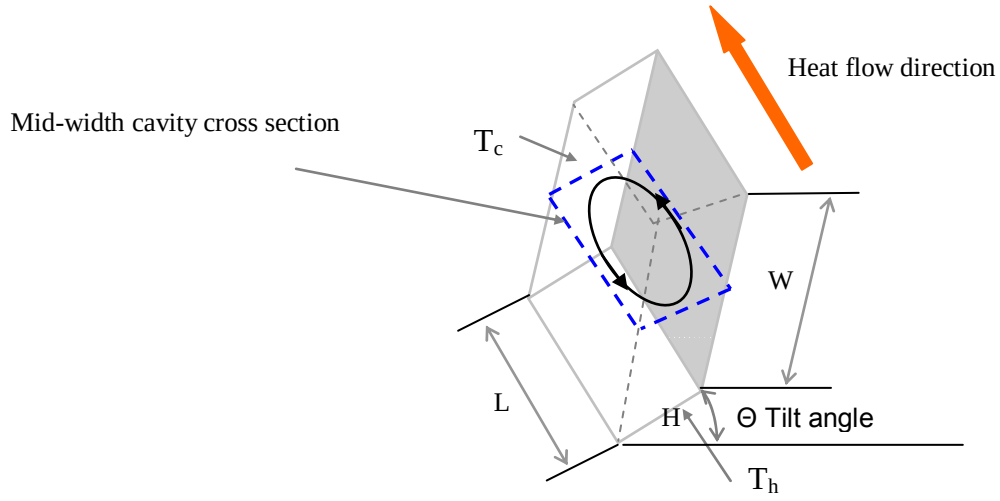


Figure 3.10: Frame Sill Cavity Specimen Showing a Single-Cell Flow Pattern

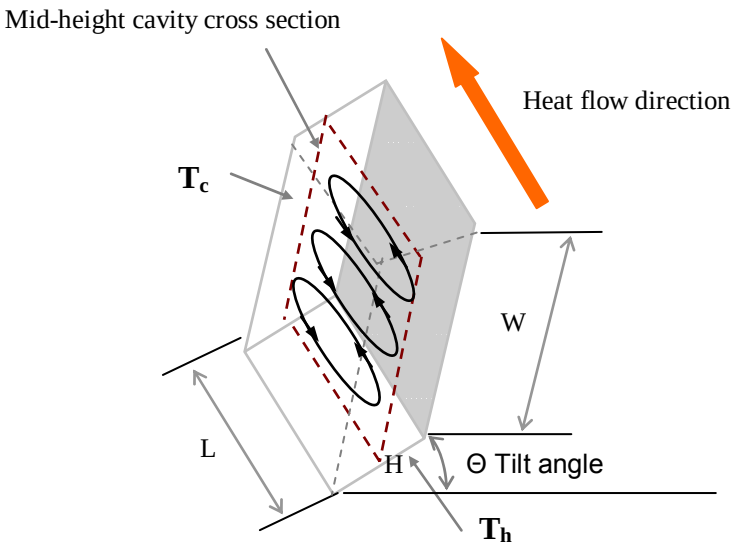


Figure 3.11: Frame Sill Cavity Specimen Showing Multi-Cell Flow Pattern

3.2.2.1 Results and Discussion

The width (W in Figure 3.9) of 3-D numerical models in the current study is chosen to be six times more than the largest size of the cavity cross section to provide a stable 2-D flow in the middle part of the cavity. A factor greater than six has not shown any significant improvement in the results. The 2-D and 3-D models are discussed with A = H : L as the aspect ratio for the reason mentioned above.

Heat transfer results using 3-D models were obtained for A = 2 cm : 4 cm with a temperature difference of 10K (Ra=92,625) between hot and cold wall. Figure 3.12 shows the dependence of Nusselt number on tilt angle between 2-D and 3-D numerical models. The difference in the average Nusselt number between the 2-D and the 3-D model is more than 20% for tilt angle 20^0. For 90^0 and 45^0, the difference is within an acceptable limit of 3%. Further simulation was done using 3-D models to obtain results for cavity with A = 0.5 tilted at 20^0 for the entire range of Rayleigh numbers and is presented in Table 3.9.

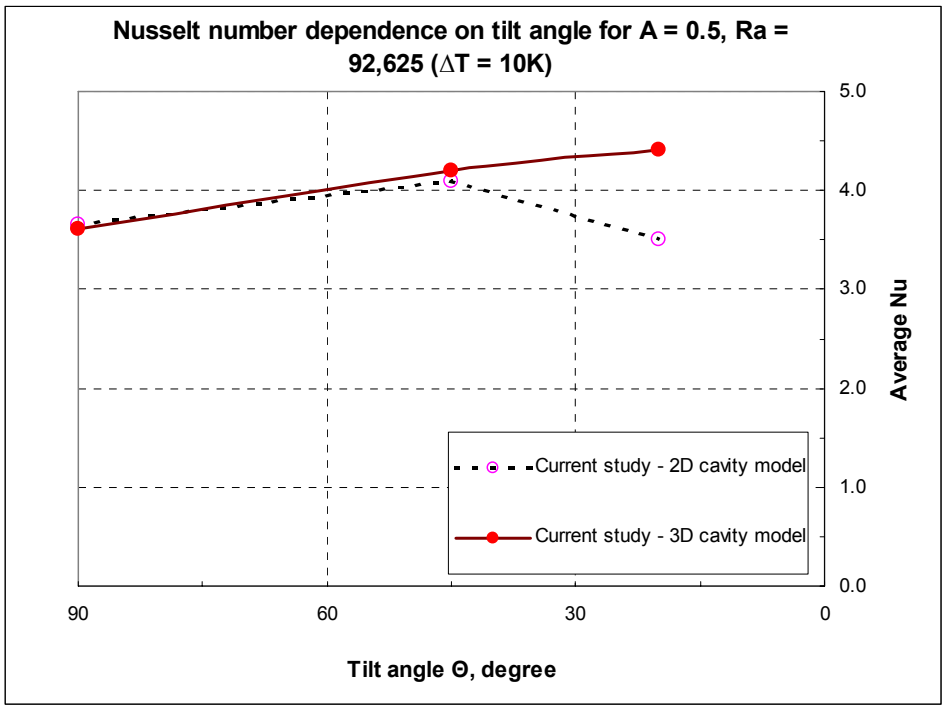


Figure 3.12: *Nu* Dependence on Tilt Angle Between 2D and 3D Cavity Models for A = 0.5 (*Ra* = 92,625, ΔT = 10K)

Table 3.9: Comparison of Heat Transfer Results Between 2-D and 3-D Numerical Models for A = 0.5 and Tilt Angle 20^0

Cavity size H x L (cm)	*Ra*	ΔT (K)	Average heat flux on hot wall (W/m^2)		Average *Nu* on hot wall		% Difference in average *Nu* between 2D and 3D models
			2D Model	3D Model	2D Model	3D Model	
1 x 2	2316	2	2.44	2.46	1.01	1.02	-0.8%
	4631	4	4.96	5.07	1.03	1.05	-2.2%
	6947	6	7.88	10.29	1.09	1.43	**-23.4%**
	9262	8	11.81	16.26	1.23	1.69	**-27.4%**
	11578	10	17.01	23.21	1.41	1.93	**-26.7%**
2 x 4	18575	2	2.35	2.85	1.95	2.37	**-17.5%**
	37050	4	6.58	7.73	2.74	3.21	**-14.9%**
	55575	6	11.18	13.43	3.10	3.72	**-16.7%**
	74100	8	16.00	19.78	3.33	4.11	**-19.1%**
	92625	10	21.03	26.55	3.50	4.41	**-20.8%**

The results from Table 3.9 indicate that for Rayleigh numbers greater than 4,631 the difference in average Nu number between 2D and 3D model is significant for this aspect ratio at this tilt angle. Velocity magnitude contours on a cross section at mid height of the cavity in Figure 3.13 shows the presence of multi-cell flow pattern. The difference in the heat transfer results is attributed to the presence of such multi-cell flow pattern. This is evident only when 3D modeling is used.

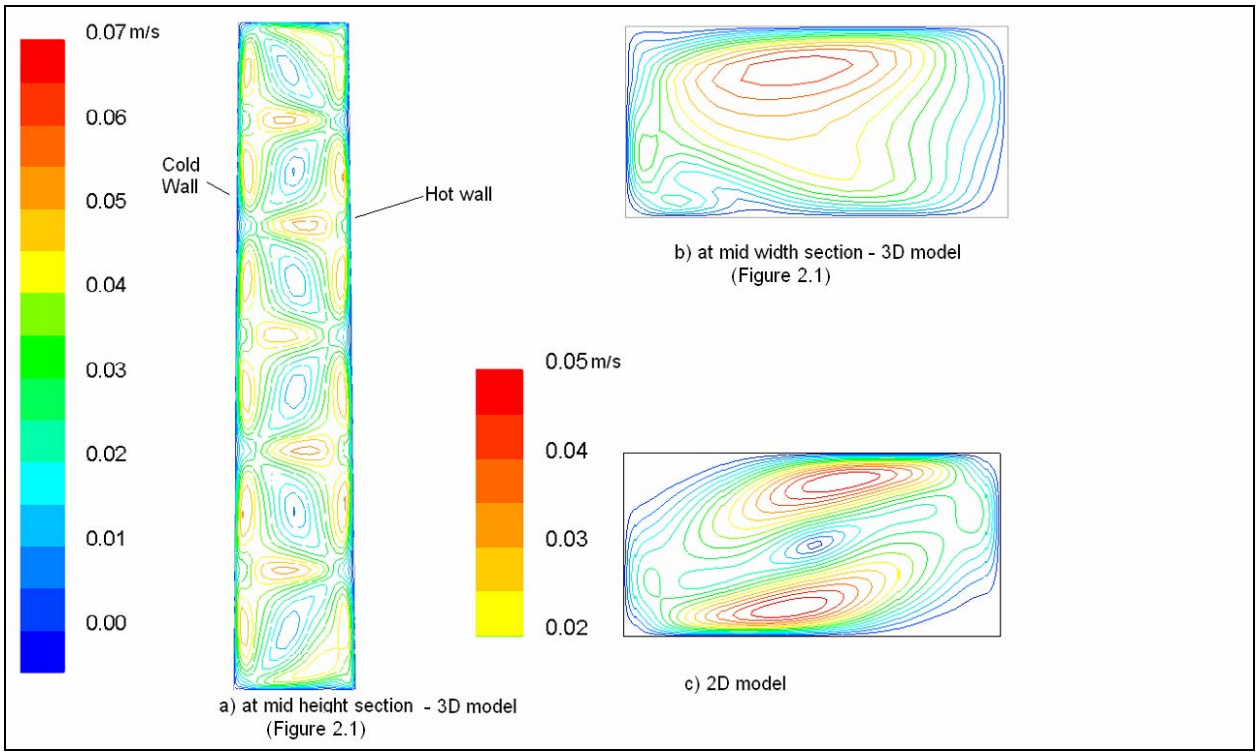


Figure 3.13: Velocity Contours for H x L = 2 cm x 4 cm, *Ra*=92,625 at Tilt Angle = 20^0

In Figure 3.14 the distributions of local heat flux on the hot wall compared between the 2D and 3D cavity models. The local heat flux for the 3D model is taken along line 1-2 as shown in Figure 3.9. Effect of tilt angle on the temperature distribution and vertical velocity distribution between the 2D and 3D models for A=0.5 have been provided in Appendix B. The values for temperature and vertical velocity component are taken along line a-b as shown in Figure 3.9. It is seen by above comparisons that for 20^0 there is a significant difference in the way heat transfer is predicted by using 2-D and 3-D numerical model. The difference is due to the three-dimensional effects imposed by the narrow cavity and cannot be neglected when modeling heat transfer through frame sill cavities.

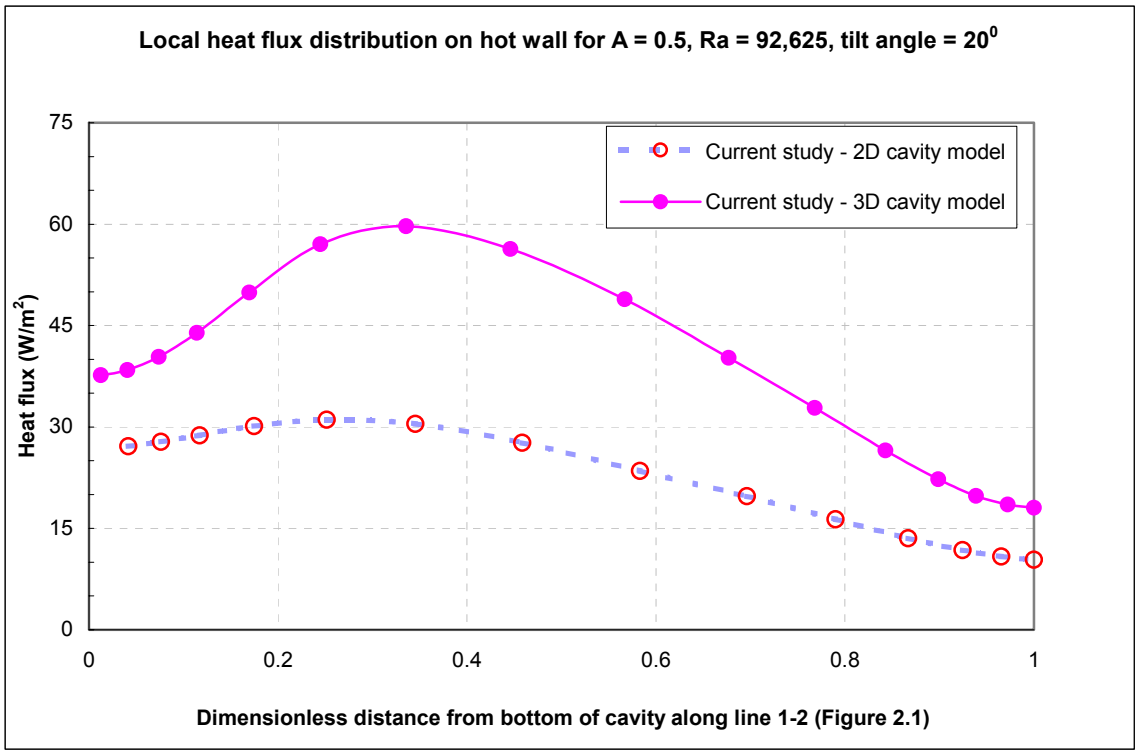


Figure 3.14: Dependence of Heat Flux on Tilt Angle for H x L = 2 cm x 4 cm, *Ra* = 92,625

A similar study, as done for A = 0.5, has been done for A = 2 to determine if 3-D numerical model predicted different heat transfer results than the 2-D model. The results, shown in Table 3.10 indicate that the difference in the predicted average heat flux on the hot wall between the 2D and the 3D model is negligible. The heat flow pattern in the 3D model is in single cell mode for the cavity at all tilt angles in the current study.

Table 3.10: Comparison of Average *Nu* on Hot Wall Between 2D and 3D Numerical Model for H x L = 8 cm x 4 cm (A = 2)

Ra	ΔT (K)	Angle of tilt (Deg)	Average heat flux on hot wall (W/m^2)		Average *Nu* on hot wall		% Difference in average *Nu* between 2D and 3Dmodels
			2D Model	3D Model	2D Model	3D Model	
92625	10	90	25.41	25.60	4.22	4.26	-0.7%
		45	25.75	25.91	4.28	4.31	-0.6%
		20	24.60	24.51	4.09	4.08	0.4%

The results for A=5, shown in Table 3.11, indicate that the predicted average heat fluxes on the hot wall from the 2D and the 3D model show negligible difference for all the tilt angles under study.

Table 3.11: Comparison of Average *Nu* on Hot Wall Between 2D and 3D Numerical Model for H x L = 20 cm x 4 cm (A = 5)

Ra	ΔT (K)	Angle of tilt (Deg)	Average heat flux on hot wall (W/m^2)		Average *Nu* on hot wall		% Difference in average *Nu* between 2D and 3D models
			2D Model	3D Model	2D Model	3D Model	
92625	10	90	21.67	21.49	3.60	3.57	0.8%
		45	21.16	21.09	3.52	3.51	0.3%
		20	19.14	18.93	3.18	3.15	1.1%

Further research was done to determine the range of aspect ratios for which the three-dimensional nature of flow in frame sill cavities is not significant and hence a 2D numerical model would be sufficient. 2D and 3D numerical simulation was done for cavities with A = 0.25, 0.625, 0.75, 1 and 4 apart from cavities with A = 0.5, 2 and 5 for which results have been obtained. The objective was to determine the tilt angle at which the flow pattern existed in the form of multi-cells for the above cavities for Ra number = 92,625. The results are graphically represented in Figure 3.15 and the average Nu number obtained is presented in Appendix B.

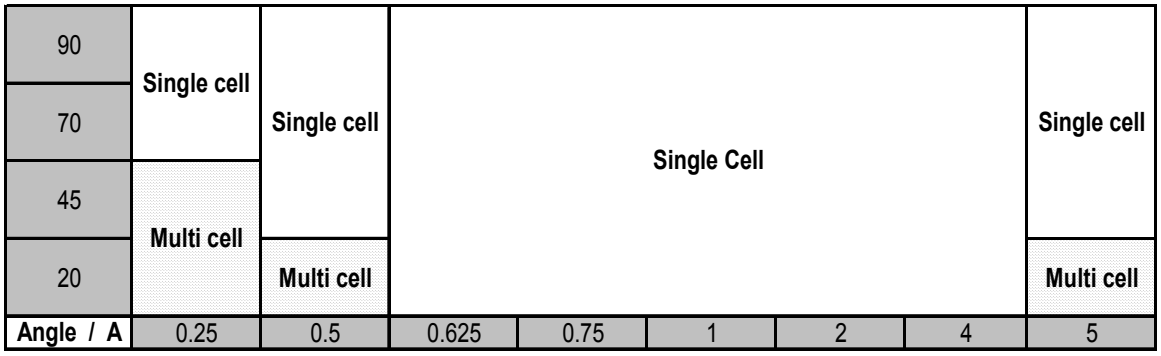


Figure 3.15: Type of Flow Pattern Seen for All Aspect Ratios Using a 3D Cavity Model (at *Ra* = 92,625)

The Nusselt number dependence on the range of Rayleigh number under current study for frame sill cavities with aspect ratios and tilt angles mentioned earlier is shown in Appendix C. New heat transfer correlations for frame sill cavities tilted at 70^0, 45^0 and 20^0 will be proposed based on the results given in these appendices.

3.3 Experimental study

The *main goal* of this work stage is to validate results of numerical 2-D and 3-D modeling convection heat transfer in frame cavities against experiment results. The numerical modeling gives us information about temperature and heat flux distribution on frame cavity walls that could be compared with test values under similar conditions. It is necessary to find out a degree of conformity between numerical models of heat transfer in cavities (Fluent's software) and experimental results. Thus we can validate also correlations for convection heat transfer in frame cavities, which are the result of the numerical simulations in this work.

The main goal in this experimental work is to obtain value of total heat flow through the tilted rectangular cavity specimen H x L x W = 2 cm x 4 cm x 24 cm (A = H:L = 0.5) and H x L x W = 4 cm x 2 cm x 24 cm (A = H:L = 2) for further comparison with values predicted by simulation. These experimental results will be compared with Fluent's 2-D and 3-D simulation results of cavity tilted at 40^{o} and 20^{o}, and subject to the same set of boundary conditions.

3.3.1 Description of apparatus

The measurements in this research project were done using innovative technique involving ASTM C518 apparatus [5], which is normally used for the measurement of conductivity of homogenous specimens. The C518 apparatus was used for measuring heat flow through the specimen under steady state conditions. The instrument is calibrated using NIST SRM 1450b (Standard Reference Material of National Institute of Standards and Technology). Accuracy (total uncertainty) for this apparatus and conditions is 1% [5].

Upper and lower plates of the instrument contain heat flux meters (transducers) and temperature sensors (thermocouples). The actual measuring area size is 102 mm x 102 mm in the central area of each plate. The lower plate can move up to conform to the thickness of the specimen. Temperatures of the plates can be independently maintained at specified temperature with accuracy +/- 0.02 C^{o}. The chamber size is approximately 12" x 12".

3.3.2 Description of cavity specimen and test method

Figure 3.16 shows the experimental setup. A thin film (tape) was used as front and back walls of cavity (not shown in Figure 3.16), while EPS foam was used for side wall, making the "cavity specimen". The space between instrument plates outside of the "cavity specimen" is filled with the foam insulation to minimize lateral losses. The heat flow through the measuring area of the instrument is caused by convection and radiation in a cavity and thermal conduction process through walls of the "cavity specimen" and surrounding foam insulation. Assuming that the effect of convection and radiation heat transfer on the cavity walls is negligible, the total heat flow Q_{MA} through the measuring area will the sum of heat flow due to convection and radiation heat transfer in the cavity Q_{cav} and the conduction through cavity walls Q_{wall} and through foam insulation Q_{foam}:

$$Q_{MA} = Q_{cav} + Q_{wall} + Q_{foam} \quad (3.4)$$

Where:

Q_{MA} = total heat flow

Q_{cav} = convection and radiation heat transfer in the cavity

Q_{wall} = conduction through cavity walls

Q_{foam} = conduction through the foam insulation

The assumption accepted above means also that temperature fields in cavity walls and foam insulation assumed to be one-dimensional ones and heat flow through the measuring area of these members could be calculated using Fourier law:

$$Q_{wall} = A_{wall}\, k_{wall}\, \Delta T/L, \quad (3.5)$$

Where,

A_{wall} = total area of wall cross section in measuring area, m;

k_{wall} = thermal conductivity of wall material, W/(m·K);

ΔT = temperature difference between cold and warm plates, K;

L = cavity size along heat flow direction (see Figure 3.1), m;

and

$$Q_{foam} = A_{foam}\, k_{foam}\, \Delta T/L, \quad (3.6)$$

Where,

A_{foam} = total area of foam insulation in measuring area, m;

k_{foam} = thermal conductivity of foam material, W/(m·K);

ΔT = temperature difference between cold and warm plates, K;

L = cavity size along heat flow direction, m.

Thus, using measured average heat flux through measuring area and equations (1)-(3) heat flow due to convection and radiation heat transfer in the cavity Q_{cav} is calculated.

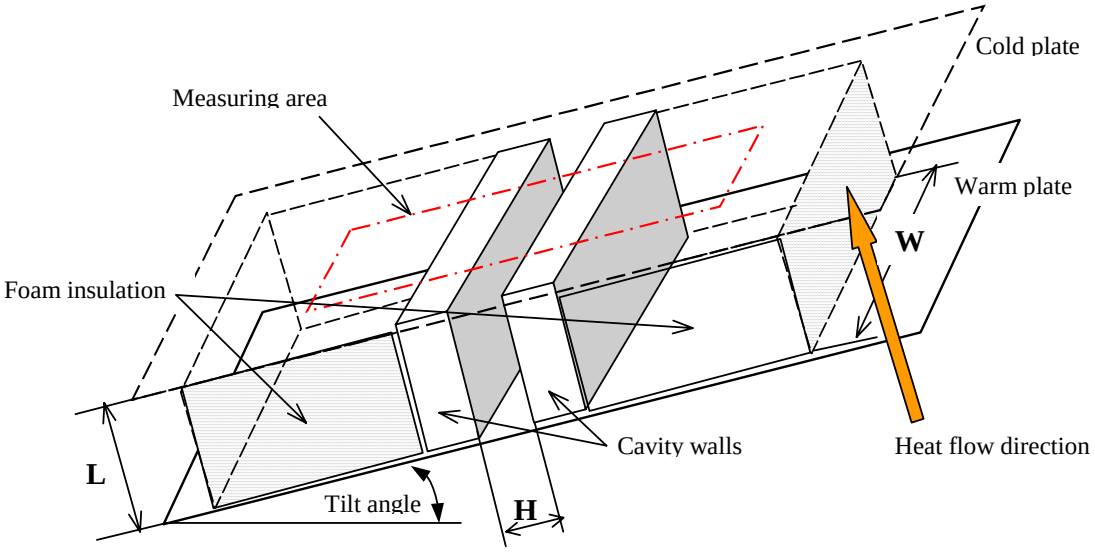


Figure 3.16: Schematic of the Frame Cavity Specimen Installation in the Instrument Tilted at the Specified Angle.

3.3.3 Results and Discussion

In Figure 3.16, the geometry and boundary conditions of 3-D cavity numerical model, are shown. They are consistent with conditions of the actual measurement in the C518 apparatus. Two isothermal walls with temperature T_h and T_c (T_h - T_c = 25 ^oC) are modeled in order to duplicate the hot and cold plates of the instrument. Another four walls are specified as adiabatic, as an approximation of the heavy insulation around the specimen.

For simulation of convection and radiation heat transfer in “cavity specimen”, laminar viscous model with Boussinesq approximation and Discrete Transfer Radiation Model (DTRM) with angle parameters: theta divisions θ = 6, phi divisions φ = 6. Emissivity of wall surfaces was specified as ε = 0.9, were used.

Thermal conductivity of the "cavity specimen" wall material and of foam insulation around the specimen was measured using FOX304 instrument in accordance with requirements of standard ASTM C 518 - 98 [1] under testing conditions:

Cold plate temperature: –10 ^{o}C;

Warm plate temperature: +15 ^{o}C;

Mean specimen temperature: +2.5 ^{o}C;

Vertical heat flow (Up);

Thermal conductivity of cavity wall material is k_{wall} = 0.0292, W/(m·K).

Thermal conductivity of foam insulation is k_{foam} = 0.0349, W/(m·K).

Case of cavity specimen H x L x W = 4 cm x 2 cm x 24 cm

In this case 2-D model and 3-D model predicted very close results, as shown in Table 3.12. Both models predict one-vortex or one-cell pattern structure of airflow in the cavity. Experimental results for the same set of test conditions are more close to 3-D model, where the difference between predicted and experimental values of heat flow through cavity is not more than 3.1%.

Table 3.12: Comparison of Experimental and Predicted Results of Heat Transfer in Sill/Head Cavity Specimen H x L x W = 4 cm x 2 cm x 24 cm (A = H:L = 2) at Angles 20^{o} and 40^{o} and Boundary Temperatures t_w = 15 ^{o}C and t_c = -10 ^{o}C.

Tilt angle	Average heat flow through the measuring area of the cavity, W			
	Present numerical study		Present Experiment	Difference between 3-Dim model and experiment
	2-Dim model	3-Dim model		
40^{o}	0.7088	0.6992	0.6783	-3.1 %
20^{o}	0.6885	0.6776	0.6586	-2.9 %

Case of cavity specimen H x L x W = 4 cm x 4 cm x 24 cm

In this case both numerical models also predict close results (difference less than 2%). Both models predict one-vortex or one-cell pattern structure of airflow in the cavity. Both models predict decrease of 3% for heat flow through cavity for the tilt angle of 20^{o} in comparing with the case with angle of 40^{o}. The experiment does not confirm this prediction and gives almost same values of heat flow for both tilt angles.

Table 3.13: Comparison of Experimental and Predicted results of Heat Transfer in Sill/Head Cavity Specimen H x L x W = 4 cm x 4 cm x 24 cm (A = H:L = 1) at Angles 20^o and 40^o and Boundary Temperatures t_w = 15 ^oC and t_c = -10 ^oC.

Tilt angle	Average heat flow through the measuring area of the cavity, W			
	Present numerical study		Present Experiment	Difference between 3-Dim model and experiment
	2-Dim model	3-Dim model		
40^o	0.6037	0.6024	0.6171	+2.2 %
20^o	0.5865	0.5853	0.6214	+5.6 %

Case of cavity specimen H x L x W = 2 cm x 4 cm x 24 cm

This case demonstrates significant difference between heat flow values predicted by 2-D and 3-D models for tilt angle of 20^o. 3-D model predicts heat flow through cavity due to convection, which is 21% higher than in 2-D model. This difference is a consequence of different predicted airflow patterns for 2-D and 3-D models. If 2-D model predicts one-cell airflow pattern in the cavity tilted under angle 20^o than 3-D model predicts complex multi-cell airflow motion in this cavity. In Figure 3.17 velocity magnitude distribution is shown in mid-height cross section of the tilted cavity obtained from 3-D model. In this figure we can observe presence of three identical cells, each of them consisting of two large vortices extended along size *H* (see Figure 3.16) and rotating in opposite directions. There are also several small vortices present.

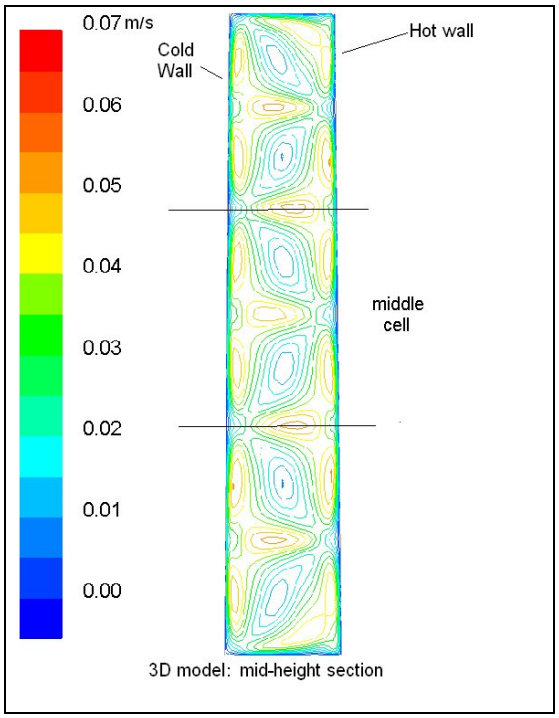


Figure 3.17: Predicted Velocity Magnitude at Mid-Height Cross Section of the Cavity Tilted at Angle 20^{o}.

To decide which model gives correct result to this heat transfer problem it is necessary to compare predicted heat transfer rate with the result of the experiment. Results of numerical modeling and the experiment are summarized in Table 3.14.

Table 3.14: Comparison of Experiment and Predicted results of Heat Transfer in Sill/Head Cavity Specimen H x L x W = 2 cm x 4 cm x 24 cm (A = H:L = 0.5) at Angles 20^{o} and 40^{o} and Boundary Temperatures t_w = 15 ^{o}C and t_c = -10 ^{o}C.

Tilt angle	Average heat flow through the measuring area of the cavity, W			
	Present numerical study		Present Experiment	Difference between 3-D model and experiment
	2-Dim model	3-Dim model		
40^{o}	0.2443	0.2567	0.2631	+2.4 %
20^{o}	0.2185	0.2774	0.2753	-0.7 %

From these results it is obvious that 3-D model is in a good agreement with the experiment and 2-D model cannot catch features of convection heat transfer for this case for tilt angle of 20^{o}.

3.4 Heat transfer correlations for frame sill cavities

In this section all derived correlations for sill/head frame cavities in the range of aspect ratio from A = 0.5 to A = 5 and Rayleigh number from Ra = $4.5*10^3$ to Ra = $9.2*10^4$ are summarized in the Table 3.14.

Table 3.14: Convection Heat Transfer correlations for Frame Sill Cavities

Aspect ratio	Tilt angle	Correlation equation	Equation number
A = 0.5	90^o	$Nu_{(\theta=90)} = 5.58 - 4.63/[1 + Ra/71497)^{1.26}]$	3.7a
	$70^o \le \theta \le 20^o$	$Nu_{(\theta)} = 0.08 + [1.147*(Nu_{(\theta=90)})]^{0.975} + 0.008*(70 - \theta)$, where $Nu_{(\theta=90)}$ = Nu from equation 3.7a	3.7b
	$90^o < \theta < 70^o$	Linear interpolation on angle θ between endpoints 3.7a and 3.7b at $\theta = 70^o$	3.7c
A = 1	$90^o \le \theta \le 20^o$	$Nu = 0.1944*(Ra)^{0.2732}$	3.8
0.5 < A < 1	$90^o \le \theta \le 20^o$	Linear interpolation on aspect ratio A between endpoints of 3.8 and 3.7(a, b, c)	
A = 5	$90^o \le \theta \le 45^o$	$Nu = Nu_{(ISO)}$, where $Nu_{(ISO)}$ is Nu number from equations (90)-(92) of ISO 15099 (2003) for calculation Nu number in frame sill cavities	3.9a
	$45^o < \theta \le 20^o$	$Nu = Nu_{(ISO)} - 0.28*COS(\theta)$	3.9b
1 < A < 5	$90^o \le \theta \le 45^o$	Linear interpolation between endpoints of 3.8 and 3.9a	
	$45^o < \theta \le 20^o$	Linear interpolation between endpoints of 3.8 and 3.9b	

The average Nu number from the proposed correlations are plotted as a function of Rayleigh number and shown in Figure 3.18 – Figure 3.22 for the aspect ratios mentioned above. The corresponding Nu number obtained from the numerical study is also plotted for comparison. The correlation equations are able to fit the data within an accuracy of 6% for all considered cases.

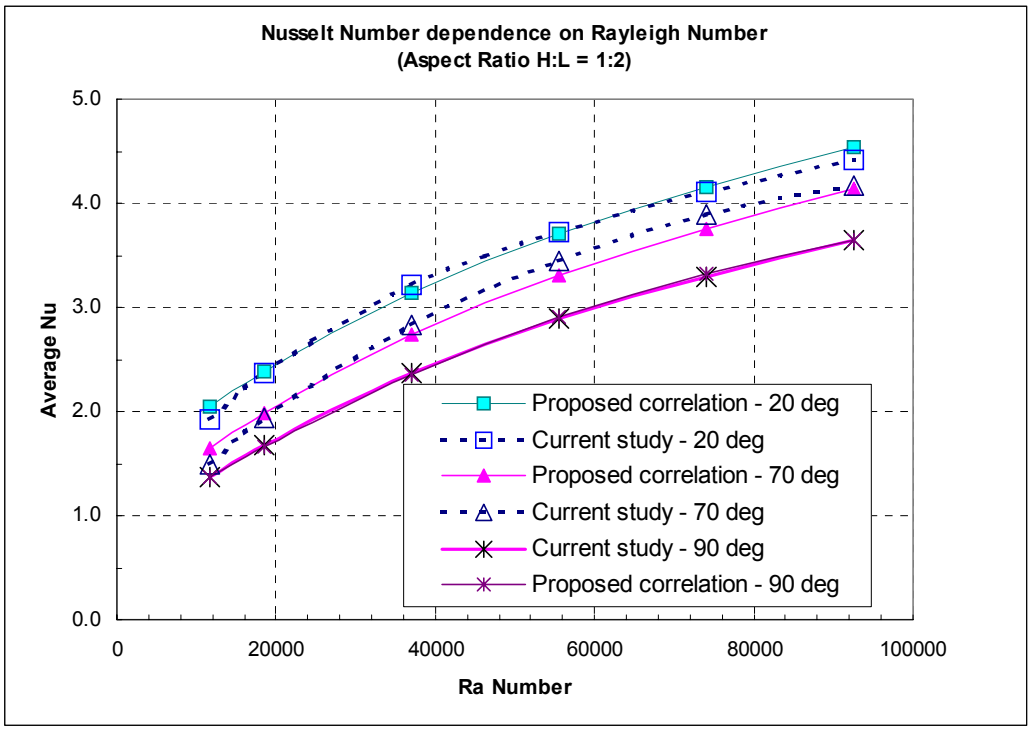


Figure 3.18: *Nu* vs. *Ra* for cavity A = 0.5

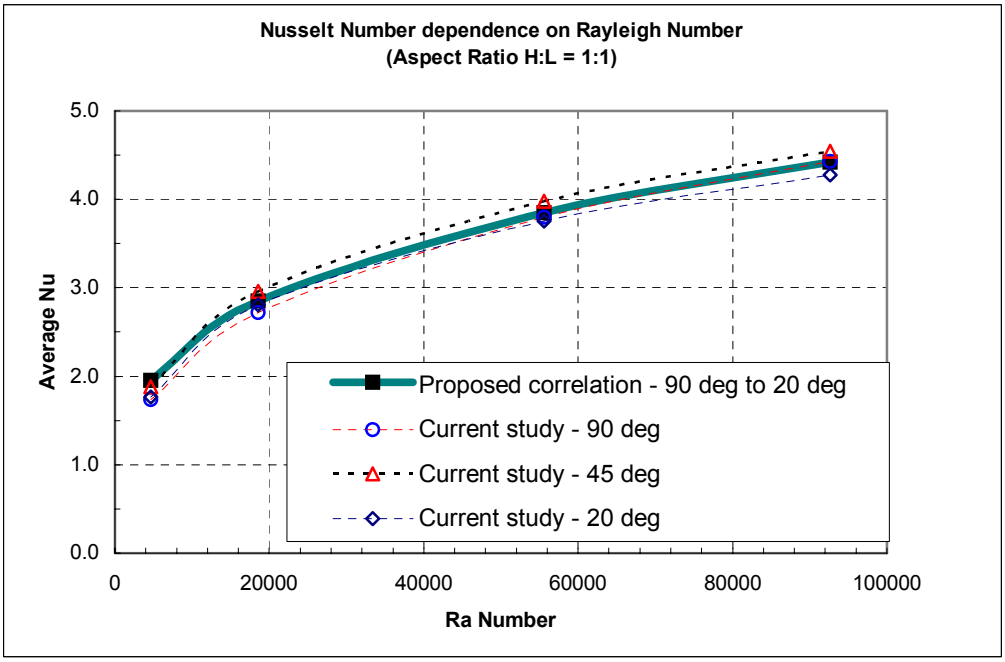


Figure 3.19: *Nu* vs. *Ra* for cavity A = 1.0

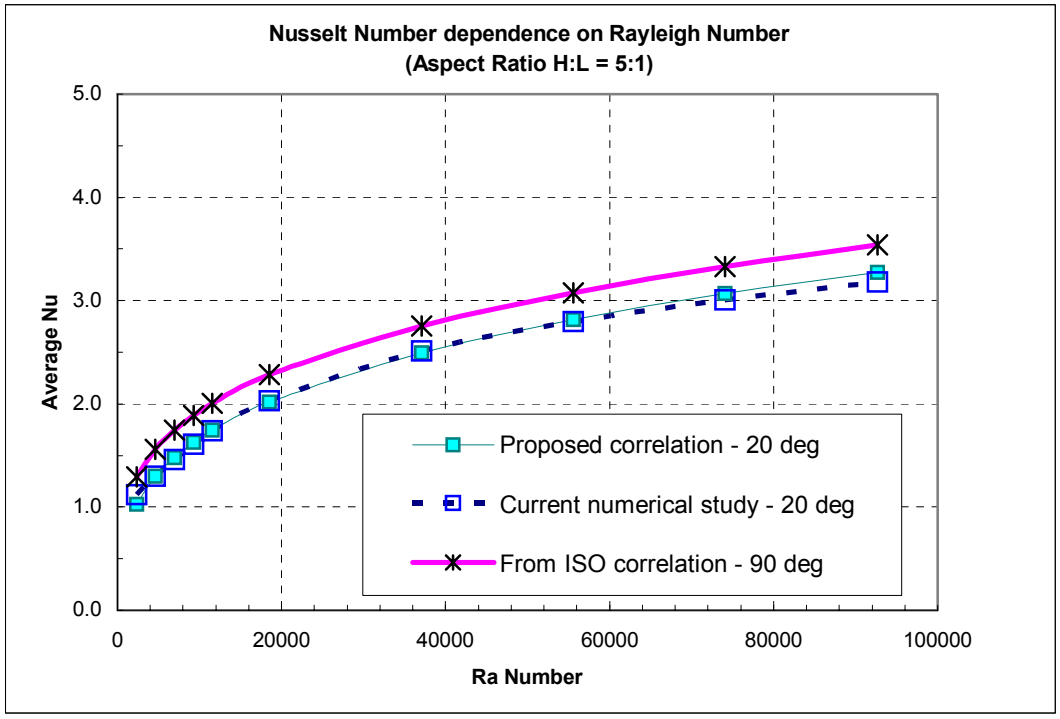


Figure 3.20: *Nu* vs. *Ra* for cavity A = 5.0

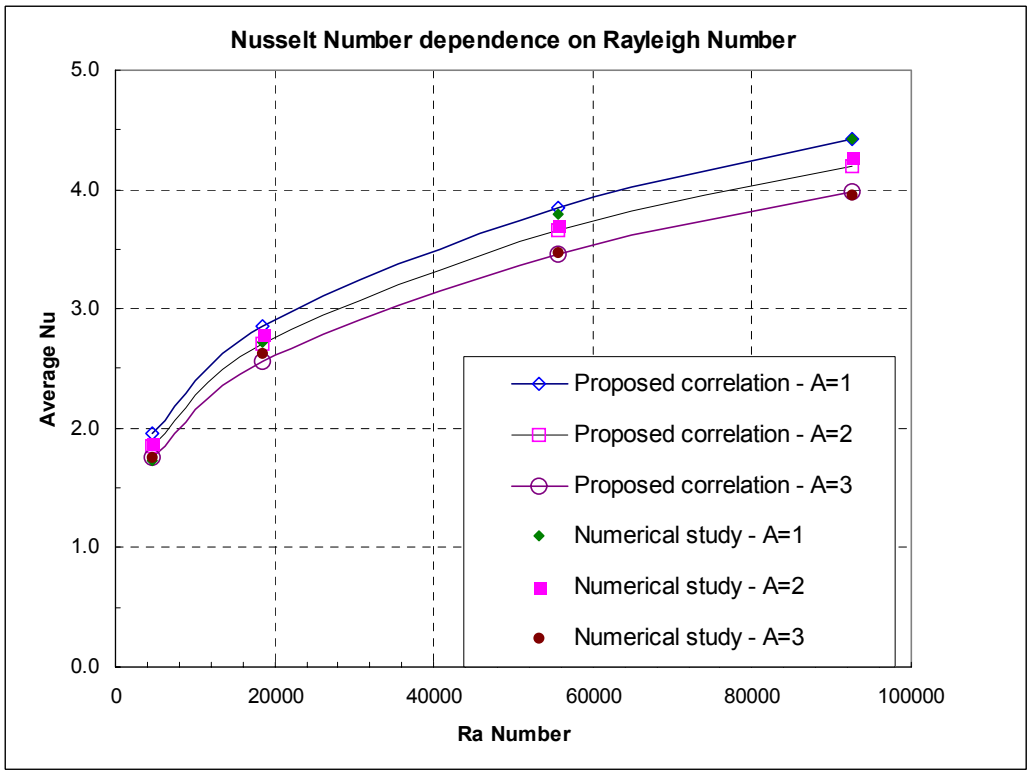


Figure 3.21: *Nu* vs. *Ra* for cavity 1< A < 5

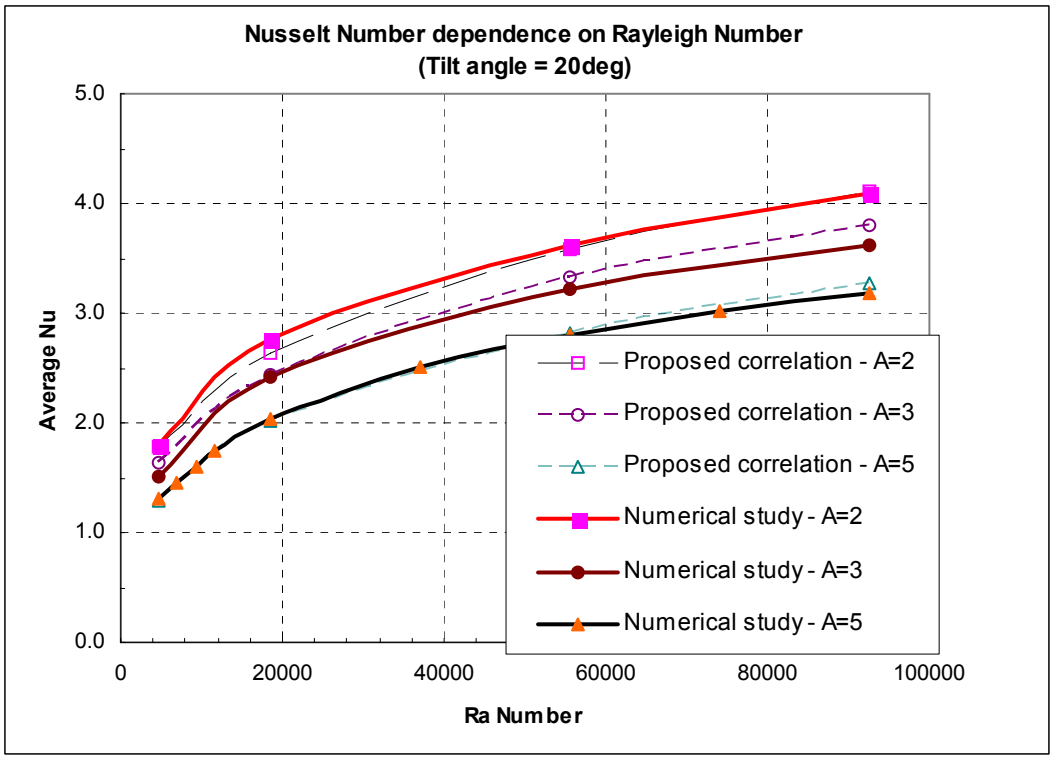


Figure 3.22: *Nu* vs. *Ra* for cavity 1< A < 5 – Tilt angle 20°

3.5 Summary

- Heat transfer results using 3D models indicate that for A=0.5, multi-cells exists for frame sill cavities tilted at 20^0 for Ra numbers beyond a certain limit. The limit of the Ra number depends on the actual size of the cavity. The 3D nature of the flow is seen to occur at higher Ra numbers as the size of the cavity is increased. In the current study, for cavity with sizes H x L = 1 cm x 2 cm and 2 cm x 4 cm, three-dimensional effects are seen for Ra numbers higher than 4,631 and 11,578 respectively.
- For A=0.5, the results from 2D modeling of frame sill cavities tilted at 20^0 should be replaced with results from 3D modeling presented in this section.
- For A=2 and A=5, the 3D models predict similar results as 2D models for all tilt angles in the current study. Heat transfer correlations can be derived using results obtained from 2D numerical modeling.
- The test method for the measurement of heat flow rate through tilted sill/head frame cavity specimens, using the ASTM C518 instrument was developed.
- Three frame cavity specimens with various cross section sizes (H x L: 2 cm x 4 cm, 4 cm x 4 cm, 4 cm x 2 cm) were tested under temperature difference 25 °C (–10 °C; +15 °C) and tilt angles 20° and 40°. Obtained results of heat flow through the cavity were compared with 2-D and 3-D simulation results under the same boundary conditions.

- 3-D numerical model of heat transfer in tilted sill/head frame cavities gives predictions in good accordance with the experiment. Difference between predicted and experimental values of heat flow through the cavity of no more than 3.1% were observed, except for the case of frame cavity 4 cm x 4 cm under tilt angle of 20^{o} where the experiment result differs from simulation one by 5.6%. This is still very acceptable agreement.
- 2-D model of convection heat transfer in tilted sill/head frame cavities predicts close results to the 3-D model and the experiment but it fails to predict complex multi-vortices convection regime and heat transfer intensity for any cavities tilted under angles close to 20^{o}.

4. CONVECTIVE HEAT TRANSFER IN CLOSED FRAME JAMB CAVITY

Figure 4.1 shows the flow pattern of convective heat flow in a frame jamb cavity. The heat transfer correlations that are currently in use for frame jamb cavities have been derived using heat transfer results obtained for the cross section shown in the figure. These correlations have been developed with the assumption that the fluid flow is two-dimensional as in the case of frame sill cavities. However, in relation to the frame jamb cavity with a large vertical aspect ratio (H/L) and a small horizontal aspect ratio (W/L), the three-dimensional nature of the flow cannot be neglected and only 3-D natural convection modeling can provide adequate results.

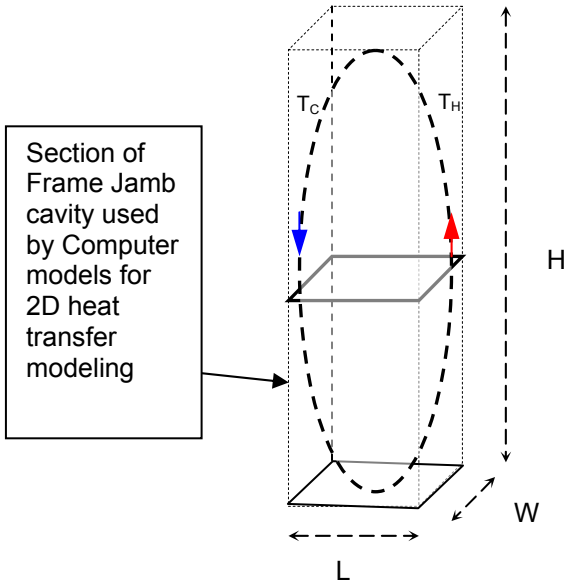


Figure 4.1: Heat Flow Pattern in a Vertical Frame Jamb Cavity

4.1 Introduction

Detailed 3-D numerical simulation of convective heat transfer in sloped jamb frame cavities was performed. Simulation was carried out for three different cavities with vertical aspect ratio and horizontal aspect ratio (A = H/L and A_h = W/L) as 20:1, 1:2; 25:1, 1:1 and 25:1, 2:1 respectively. The range of Rayleigh numbers was between 18,525 and 144,726 and the tilt angles were 90^0, 70^0, 45^0 and 20^0 from the horizontal direction. The present section also provides the heat transfer correlation that was derived for frame jamb cavities.

4.2 Numerical Study

Figure 4.2 represents the geometry and boundary conditions of the frame jamb cavity, which has been created using Gambit. The geometry consists of two isothermal vertical sidewalls, T_H (hot wall on the right) and T_C (cold wall on the left) with $T_H > T_C$. The remaining four walls are adiabatic.

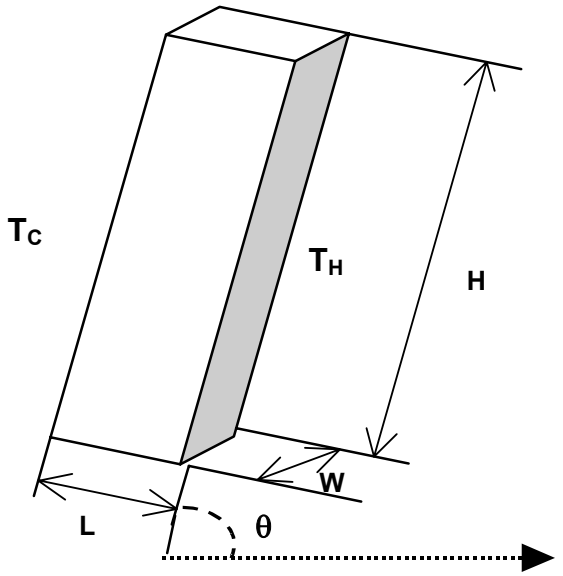


Figure 4.2: Boundary Conditions and Configuration of Sloped Frame Jamb Cavity Specimen.

The following approximations are used in the present study:

a) The cavity air fluid motion is assumed to be an incompressible flow. The fluid motion driven by natural convection is accounted for by making the Boussinesq assumption (assumption of density change while maintaining the incompressible flow).

b) Due to low temperature differences between hot and cold surfaces (a maximum difference of 10 ^{0}C), constant property values are assumed for air. The constant

property values of air inside the cavity were calculated based on ISO 15099 correlations at mean temperature of 273K. Table 1 lists some of the properties of air.

c) There is no internal heat generation, and viscous dissipation and compressibility effects are negligible.

d) The flow within the cavity is studied under laminar conditions. The range of aspect ratio and temperature difference across the isothermal walls chosen for this study is such that fluid flow in the cavity is limited to laminar conditions.

Table 4.1: Material Properties

Material: air (Fluid)			
Property	*Units*	*Method*	*Value(s)*
Density	Kg/m3	Boussinesq	1.2874
Cp (Specific Heat)	J/kg-K	Constant	1006.1
Thermal Conductivity	W/m-K	Constant	0.02406
Viscosity	Kg/m-s	Constant	1.721E-05
Thermal Expansion Coefficient	1/K	Constant	0.003663

The numerical simulation is performed using the finite volume CFD software Fluent (2001). Fluent uses a control-volume based technique to convert the governing conservation equations of mass, momentum and energy into algebraic equations that can be solved numerically. This control volume technique consists of integrating the governing equations about each control volume, yielding discrete equations that conserve each quantity on a control volume basis. Segregated solver along with appropriate discretization schemes are chosen for solving the governing equations. A First-order upwind scheme is used for the momentum and energy variables. The PRESTO (Pressure Staggering Option) scheme is used for obtaining the pressure values and SIMPLEC (Semi-Implicit Method for Pressure-Linked Equations Consistent) is used to couple the interaction between pressure and velocity.

Natural convection in such frame jamb cavity models is buoyancy induced. Hence, suitable schemes for the laminar flow in a rectangular cross section cavity, modeled using hexahedral meshes have been chosen. Optimal computational time and acceptable degree of accuracy while yielding a better-converged solution have all been taken into account before deciding on the above numerical model.

4.2.1 Mesh analysis of the numerical model

The frame jamb cavity was modeled and meshed using hexahedral elements in Gambit. The number of elements in the cavity differs based on the size of the cavity and size of the mesh being used. A mesh density study of the frame jamb cavity oriented at vertical position was performed to determine a suitable frame jamb cavity model that could be used in the numerical simulation. An optimum mesh size was selected to obtain the best possible convergence while minimizing the CPU time.

The selection of mesh density was based on several considerations. Frame jamb cavity models with sizes (H, W and L) as 100 cm, 4 cm, 4 cm (A=25:1:1) and 80 cm, 4 cm, 4 cm (A=20:1:1) were chosen to check for dependency of the height of the cavity on the average Nusselt number. For frame cavity model A=25:1:1, different mesh densities were considered starting with a mesh size of 74 x 20 x 16 (H x W x L). The mesh sizes were varied in such a way as to determine the dependence of mesh density in a particular direction upon the heat transfer results. The results for A=25:1:1 are given in Table 4.2.

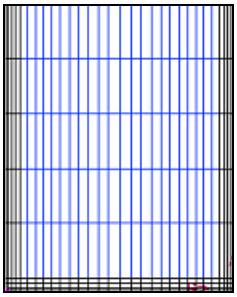
The mesh density study shows that increasing the overall mesh size beyond a certain limit does not show any significant improvement in the average Nusselt number predicted. It can be seen from Table 4.2 that mesh size 111 x 30 x 24 is the coarsest mesh, which provides us with equivalent results when compared with a finer mesh like 129 x 35 x 28. Hence mesh density of 111 x 30 x 24 has been recommended for further analysis in sloped frame jamb cavities.

The height of the frame jamb cavity modeled in this project has been fixed to 100 cm because the difference in average Nusselt number of the two models with height 100 cm and 80 cm studied in mesh analysis is less than 3% and frame jamb cavity of height 100 cm is a more commonly occurring size.

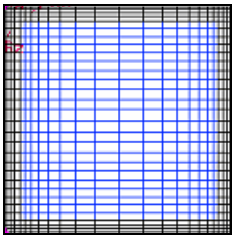
Table 4.2: Nusselt Number for Different Mesh Sizes for *A*=25:1:1 and *Ra*=92,625

Mesh size (H x W x L)	**Avg *Nu* from current study**	**% Difference with previous mesh**
74 x 2 0x 16	2.2463	NA
111 x 30 x 24	2.2828	1.60%
129 x 35 x 28	2.2877	0.21%

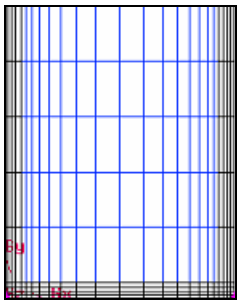
Figure 4.3 shows a typical mesh at the three cross sections of the frame jamb cavity for the case of A=25:1:1. Appropriate boundary growth layers were applied to the interior side of the edges of the frame jamb cavity to obtain a finer mesh near the corners of the horizontal and vertical edges so that edge effects can be captured accurately.



(a) H: W (Bottom part)



(b) W: L



(c) H: L (Bottom part)

Figure 4.3: Different views of the mesh for cavity with A=25:1, Az=1:1

Range of study

Three different frame jamb cavity models have been simulated in the current study. Commonly occurring sizes of frame jamb cavities have been chosen. The height of the cavity is typically set at 1m for these models. Table 4.3 lists the frame jamb cavity models used and temperature conditions applied.

Table 4.3: Geometry of Frame Jamb Cavity Models and Boundary Conditions Applied

Aspect Ratio	Mesh Density	Geometry	*Ra*	Temperature Conditions
	H x W x L	H (cm) x W (cm) x L (cm)	Ra	ΔT, K
A = H: L = 20:1 Az = W: L = 1:2	111 x 32 x 22	100 x 2.5 x 5	27,136	1.5
			36,181	2
			72,363	4
			108,544	6
			144,726	8
A = H: L = 25:1 Az = W: L = 1:1	111 x 30 x 24	100 x 4 x 4	18,525	2
			37,050	4
			55,575	6
			74,100	8
			92,625	10
A = H: L = 25:1 Az = W: L = 2:1	200 x 38 x 22	100 x 8 x 4	18,525	2
			37,050	4
			55,575	6
			74,100	8
			92,625	10
			39,100	10

4.2.2 Results and Discussion

Results for Aspect ratio A=20:1, Az=1:2 (H x W x L = 100 cm x 2.5 cm x 5 cm)

Predicted temperature and velocity distributions at the mid width plane section of the frame cavity specimen for Ra number 108,544 (with ΔT = 6K) is shown in Figure 4.1 and Figure 4.5 respectively. The heat transfer results in values of average Nusselt number and heat flux are given in Table 4.4. The results were compared with numerical results from Yang et al (1986). The Aspect ratio and Ra number in Yang et al. (1986) are different from the ones used in current simulation but the prediction of single-cell to multi-cell transition at angles between 45-60 degrees in Yang et al. (1986) is in agreement with results in this study.

The current study predicts a single-cell behavior for cavities oriented at 90^0 and 70^0. Whereas, for 45^0 the single-cell pattern changes to multi-cell at Ra=36,181. The single-cell

is characterized with one vortex of fluid flow rising at the hot wall and descending at the cold wall. The multi-cell is characterized with one vortex of fluid flow in each cell, but the direction of the fluid flow is in opposite directions in each of the adjacent cells.

The basic two-dimensional cell pattern, familiar at angles 90^0 and 70^0, starts to break down because of the separation of flow at the middle of the cavity. The single longitudinal cell is split into two short cells at the middle and two elongated cells at the top and bottom end of the cavity. The axis of these cells is tilted in a direction opposite to that of the tilt angle of the cavity. These cells indicate secondary flows with axis not exactly parallel to the shorter side of the cavity (which could be width or length of cavity) but deflected towards the height of the cavity. The two elongated cells at the top and bottom ends of the cavities exhibit a two-dimensional pattern until Ra numbers 108,544, beyond which the flow becomes three dimensional in nature. This pattern of flow is similar to that obtained by Yang et al (1986).

At 20^0, the flow pattern is different from the one at 45^0. Multi-cells begin to form at lower Ra numbers with two cells being formed one each at the top and bottom end of the cavity whereas the flow in the remaining part of the cavity is essentially in the form of a single elongated cell. As the Ra number is increased further, the heat transfer is enhanced by the formation of additional cells. As high as 6 cells are formed at the highest Ra number simulated.

The average Nusselt number predicted by current study for this frame cavity model oriented at 90^0 and 70^0 is essentially the same. Arnold et al. (1976) have experimentally observed for cavities of different aspect ratios that a minimum heat transfer rate occurs at the transition angle where there is a change in the flow pattern between the vertical and horizontal orientation. Current study indicates that the actual transition in the flow pattern from single-cell to multi-cells occurs at an angle between 70^0 and 45^0.

The heat transfer results for this cavity oriented at the vertical position are compared with Gustavsen (2001) whose numerical procedure using CFD simulation for frame cavities has been validated with experimental result in Gustavsen et al (2001). Figure 8 shows that the average Nusselt number predicted is in very close agreement with current study.

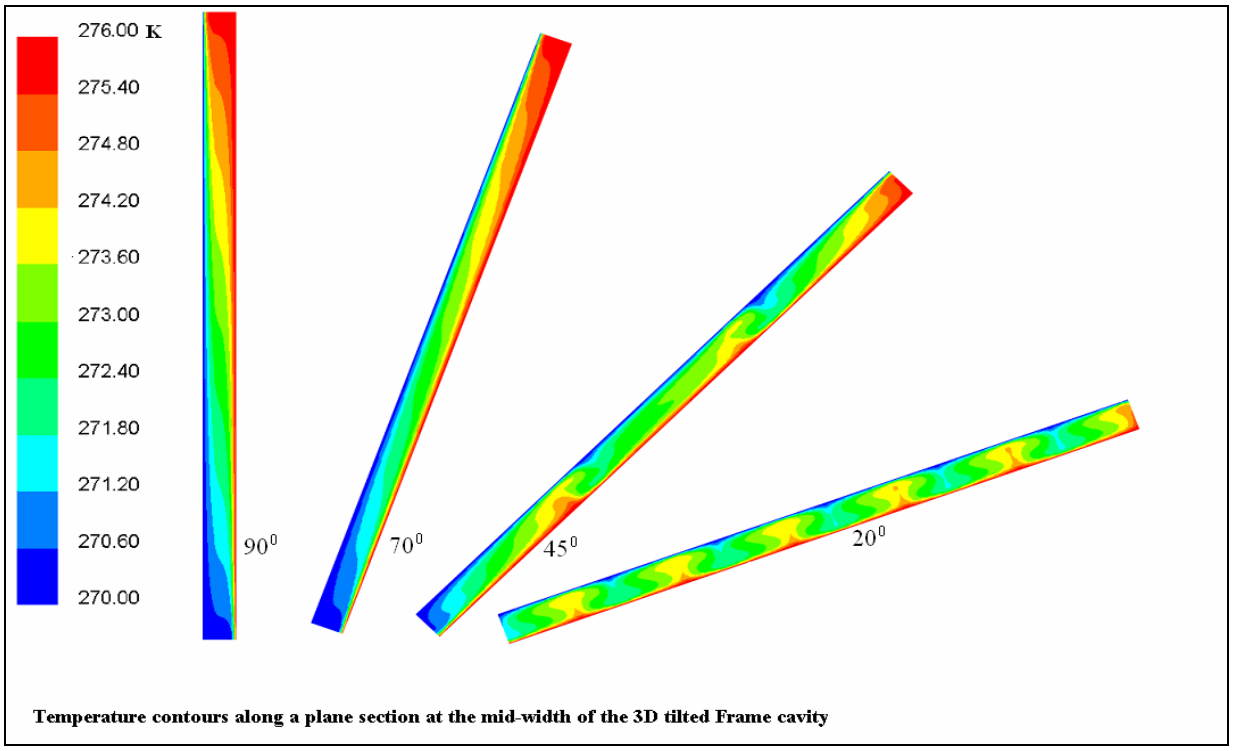


Figure 4.4: Contours of Temperature Distribution in the Mid Plane Section of Frame Cavity Model *A*=20:1, *Az*=1:2 for *Ra*=108,544.

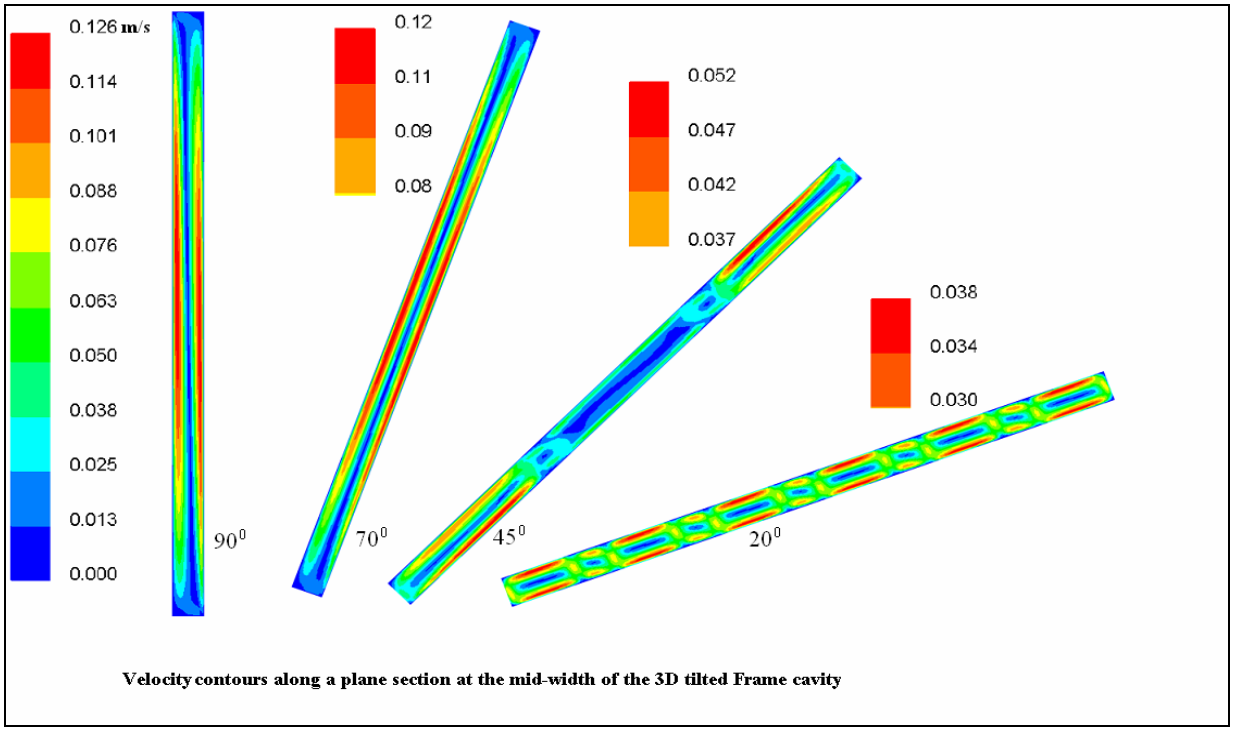


Figure 4.5: Contours of Velocity Magnitude in the Mid Plane Section of Frame Cavity Model *A*=20:1, *Az*=1:2 for *Ra*=108,544

Note: Velocity magnitude scales are different for each of the tilted frame cavity.

Table 4.4: Predicted Average Heat Flux and *Nu* for Frame Jamb Cavity *A*=20:1, *Az*=1:2 (*H* x *W* x *L* = 100 cm x 2.5 cm x 5 cm)

ΔT, K	*Ra*	**Θ** = 90°		**Θ** = 70°		**Θ** = 45°		**Θ** = 20°	
		Nu	*q*, W/m^2	*Nu*	*q*, W/m^2	*Nu*	*q*, W/m^2	*Nu*	*q*, W/m^2
1.5	27,136	1.47	1.06	1.45	1.05	1.65	1.19	2.35	1.70
2	36,181	1.61	1.55	1.59	1.53	1.93	1.85	2.58	2.48
4	72,363	2.02	3.89	2.00	3.85	2.65	5.11	3.20	6.15
6	108,544	2.30	6.65	2.29	6.62	2.76	7.98	3.59	10.38
8	144,726	2.52	9.69	2.53	9.73	2.94	11.32	3.84	14.79

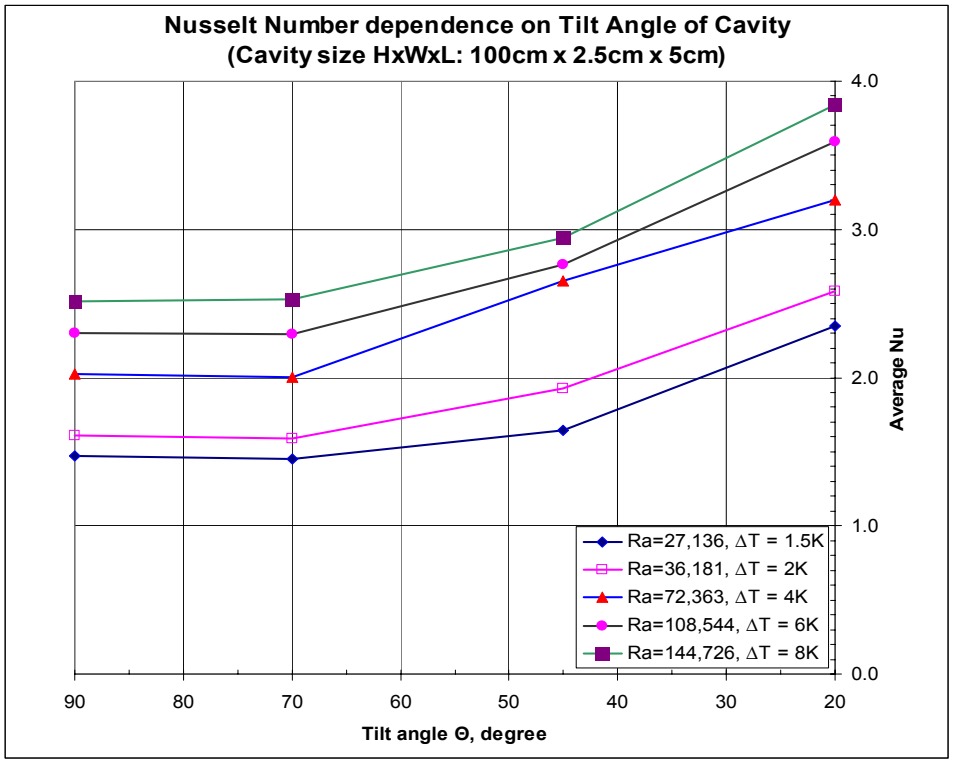


Figure 4.6: *Nu* vs. Tilt Angle for Frame Jamb Cavity *A*=20:1, *Az*=1:2 (*H* x *W* x *L* = 100 cm x 2.5 cm x 5 cm)

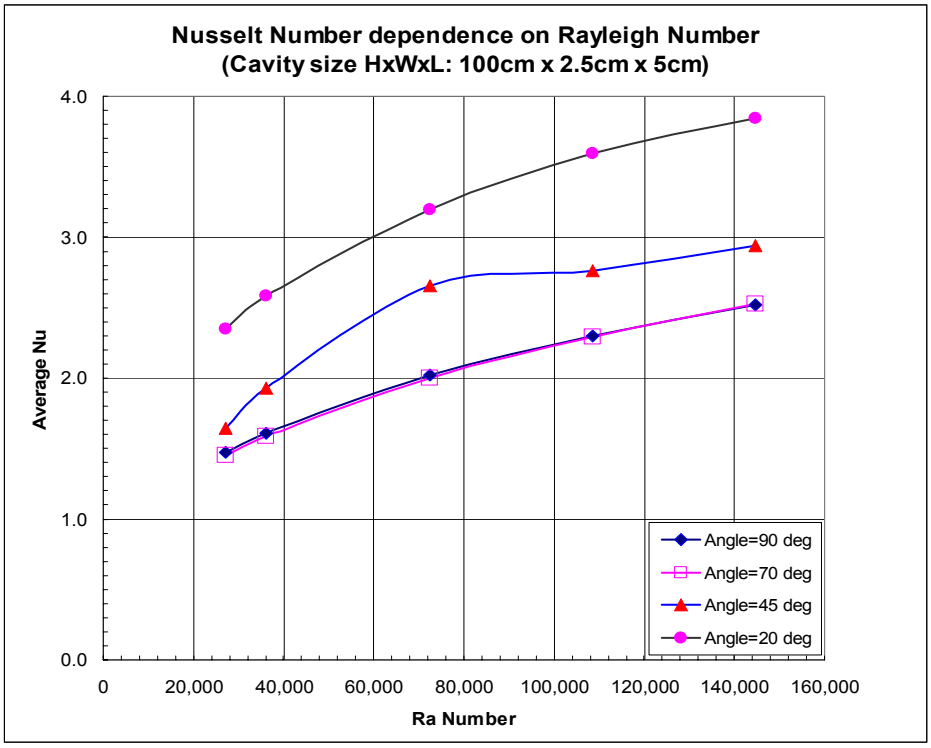


Figure 4.7: *Nu* vs. *Ra* for Frame Jamb Cavity *A*=20:1, *Az*=1:2 (*H* x *W* x *L* = 100 cm x 2.5 cm x 5 cm)

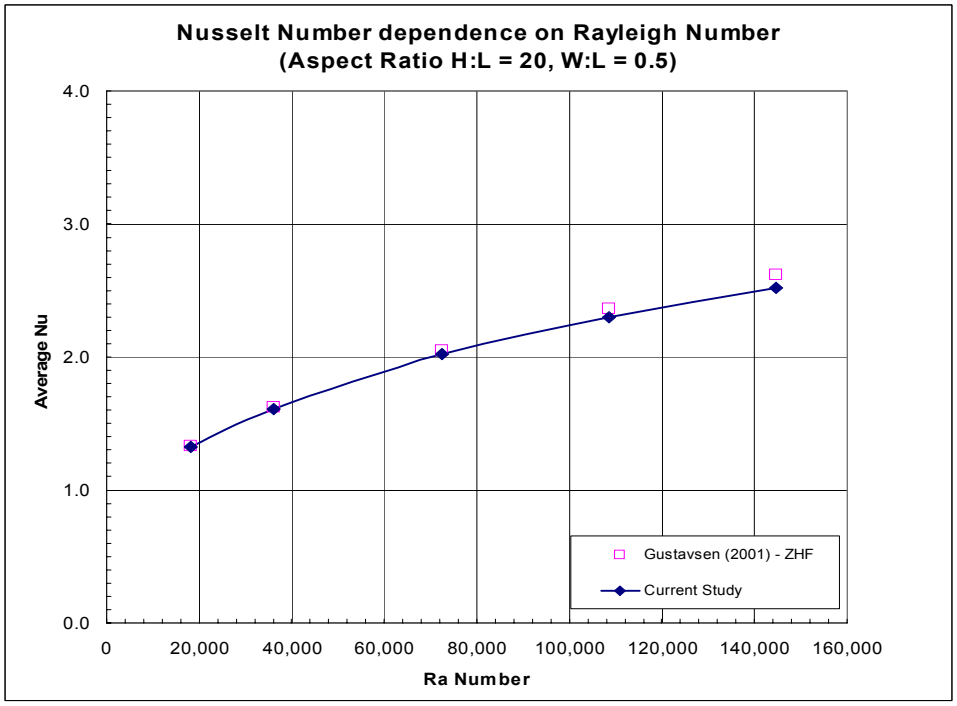


Figure 4.8: Comparison of average *Nu* for *A*=20, *Az*=0.5 with Numerical Results of Gustavsen (2001)

Results for Aspect ratio A=25:1, Az=1:1 (H x W x L = 100 cm x 4 cm x 4 cm)

Predicted temperature and velocity distributions on a vertical plane at the mid width of the frame cavity for Ra number 92,625 (with ΔT = 10K) are shown in Figure 4.9 and Figure 4.10 respectively. The heat transfer results in values of average Nusselt number and heat flux are given in Table 4.5.

The current study predicts a single cell behavior for 90^0 and 70^0. The flow pattern at 70^0, for higher Ra numbers, indicates the onset of the three dimensional nature of flow. The velocity profile indicates waviness in the airflow pattern. At 45^0, cells begin to form at the top and bottom ends of the cavity while the elongated cell in the middle of the cavity starts to exhibit secondary flow. At 20^0, formation of multi-cells is more pronounced even at lower Ra numbers.

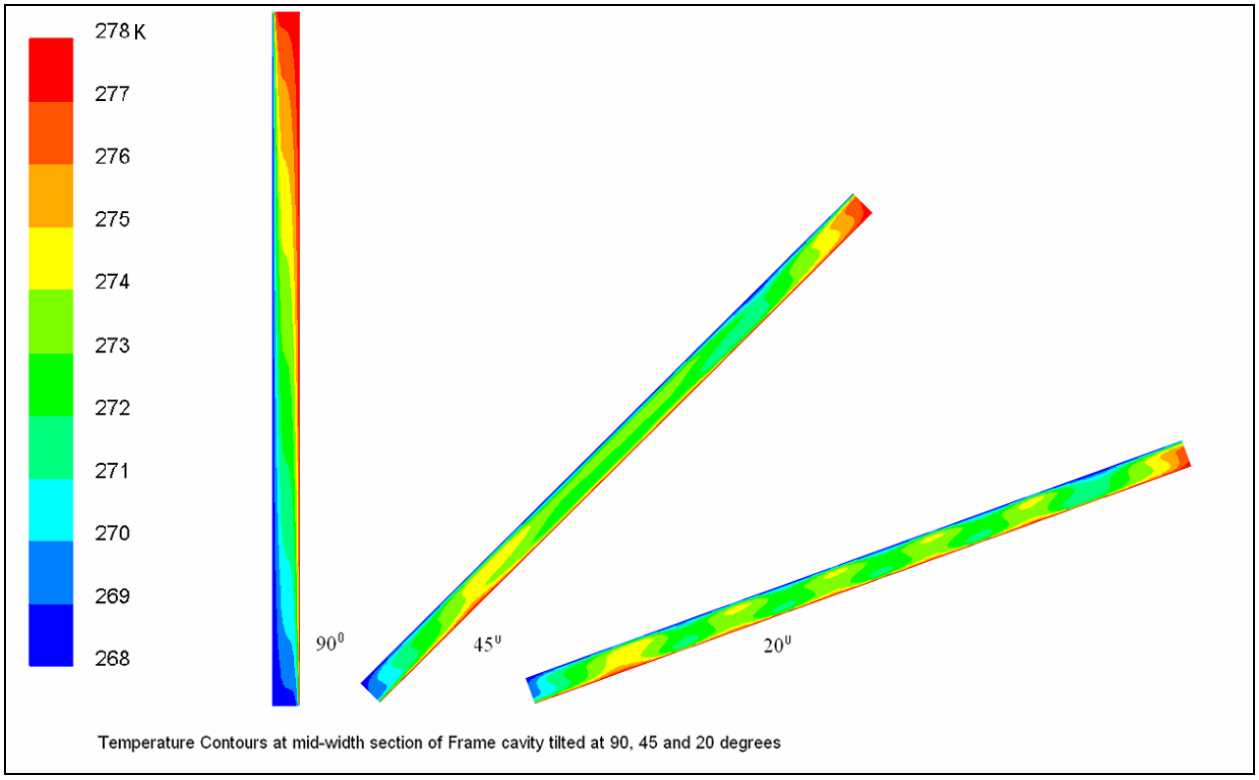


Figure 4.9: Contours of temperature distribution in mid plane section of frame cavity model A=25:1, Az=1:1 for Ra=92,625.

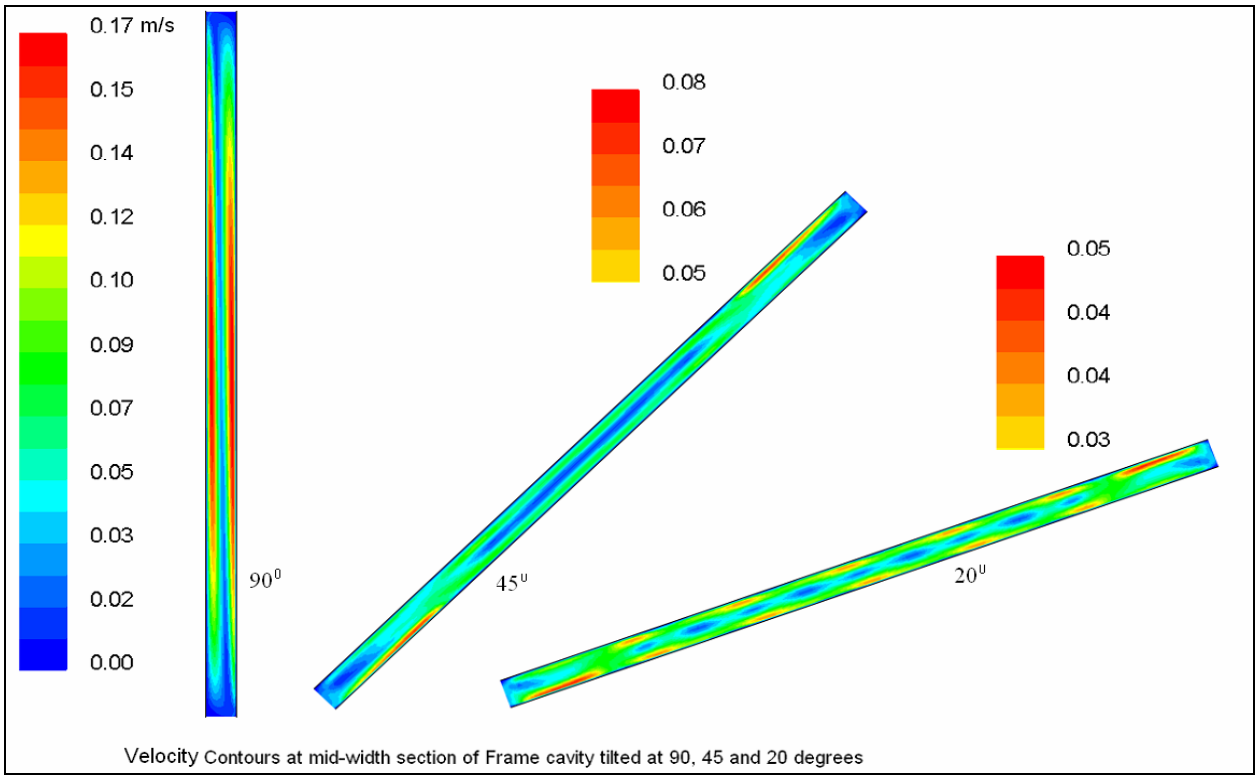


Figure 4.10: Contours of Velocity Magnitude in the Mid Plane Section of Frame Cavity Model *A*=25:1, *Az*=1:1 for *Ra*=92,625.

Note: Velocity magnitude scales are different for each of the tilted frame cavity.

Table 4.5: Predicted Average Heat Flux and *Nu* for Frame Jamb Cavity *A*=25:1, *Az*=1:1 (*H* x *W* x *L* = 100 cm x 4 cm x 4 cm).

ΔT, K	Ra	**Θ** = 90°		**Θ** = 70°		**Θ** = 45°		**Θ** = 20°	
		Nu	Q, W/m²	Nu	q, W/m²	Nu	q, W/m²	Nu	q, W/m²
2	18,525	1.41	1.69	1.39	1.67	2.25	2.70	2.46	2.96
4	37,050	1.73	4.15	1.70	4.10	2.67	6.41	2.91	6.99
6	55,575	1.96	7.06	1.95	7.04	2.92	10.53	3.20	11.54
8	74,100	2.14	10.27	2.14	10.32	3.12	15.01	3.40	16.34
10	92,625	2.28	13.73	2.31	13.87	3.30	19.82	3.56	21.43

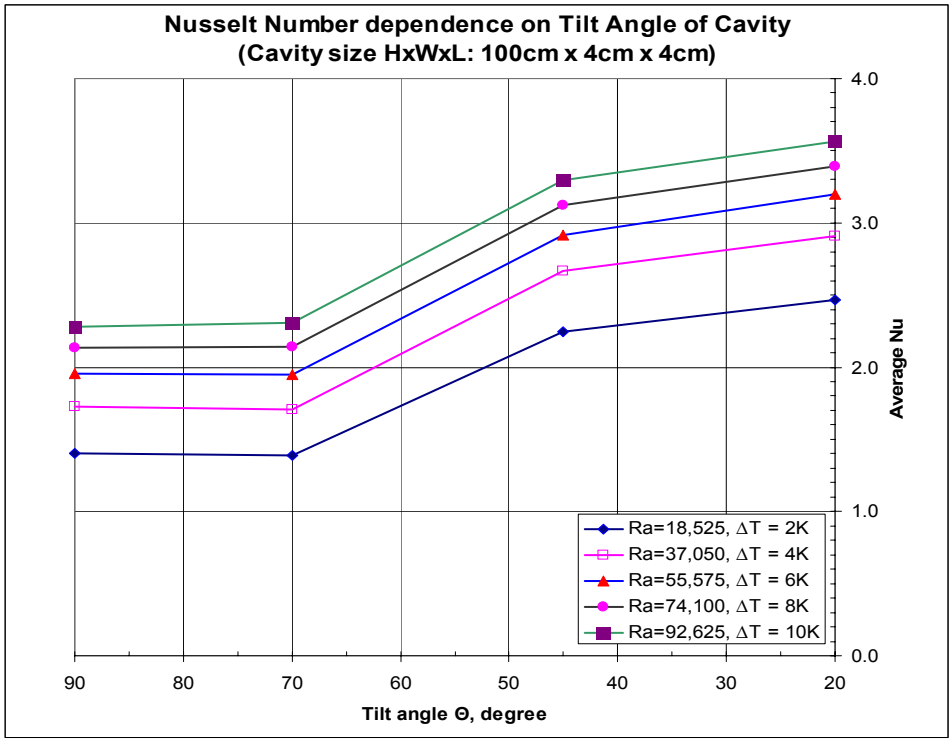


Figure 4.11: *Nu* vs. Tilt Angle for Frame Jamb Cavity *A*=25:1, *Az*=1:1 (*H* x *W* x *L* = 100 cm x 4 cm x 4 cm).

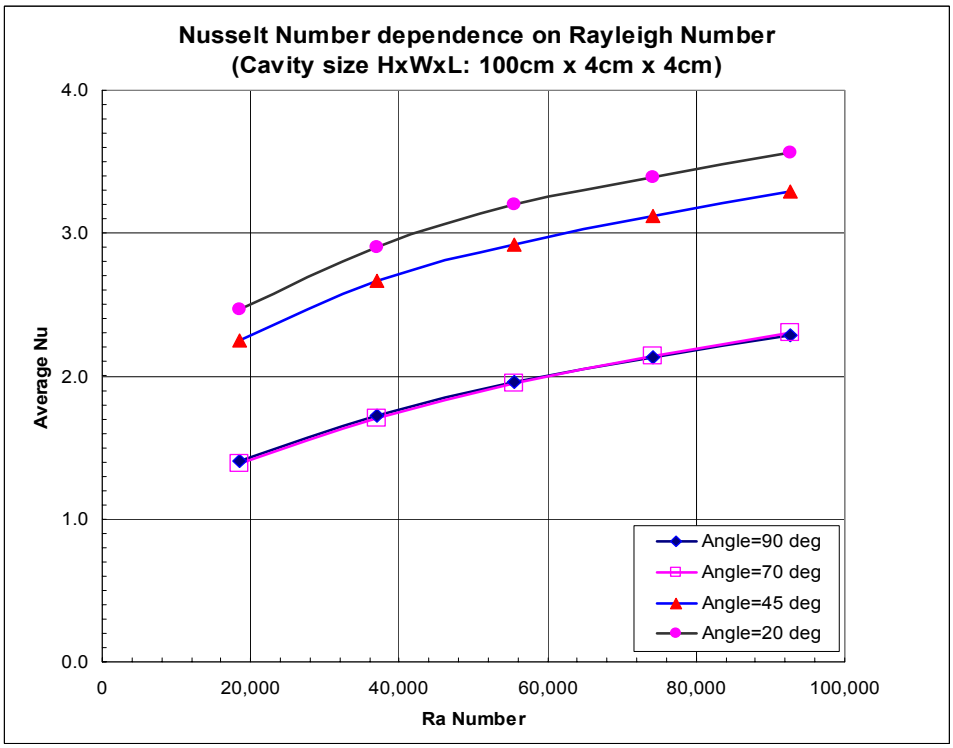


Figure 4.12: *Nu* vs. *Ra* for Frame Jamb cavity *A*=25:1, *Az*=1:1 (*H* x *W* x *L* = 100 cm x 4 cm x 4 cm).

Results for Aspect ratio A=25:1, Az=2:1 (H x W x L = 100 cm x 8 cm x 4 cm)

Predicted temperature and velocity distributions on a vertical plane at the mid width of the frame cavity model for Ra number 92,625 (with ΔT = 10K) are shown in Figure 4.13 and Figure 4.14 respectively. The heat transfer results in values of average Nusselt number and heat flux are given in Table 4.6.

The current study predicts a single cell behavior for 90^0 and 70^0. Whereas, for 45^0 and 20^0, the flow pattern for the entire range of Ra number is multi-cellular. Flow pattern is much more complex at 45^0 and 20^0 than the earlier model with Az=1. Getting convergence under steady state conditions was an issue for this case. Hence, transient solver was used to obtain the results by allowing the calculations to run for a fixed period of time and then taking the time-averaged Nusselt number.

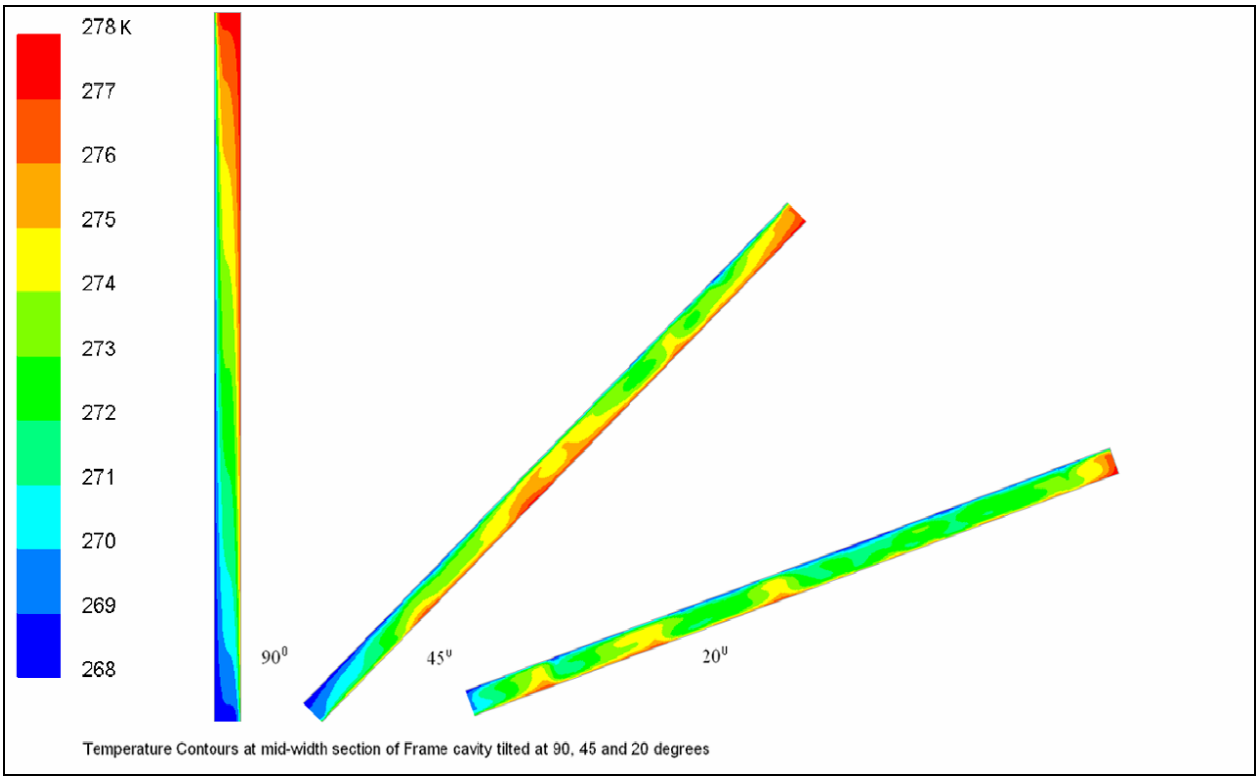


Figure 4.13: Contours of Temperature Distribution in Mid Plane Section of Frame Cavity Model *A*=25:1, *Az*=2:1 for *Ra*=92,625.

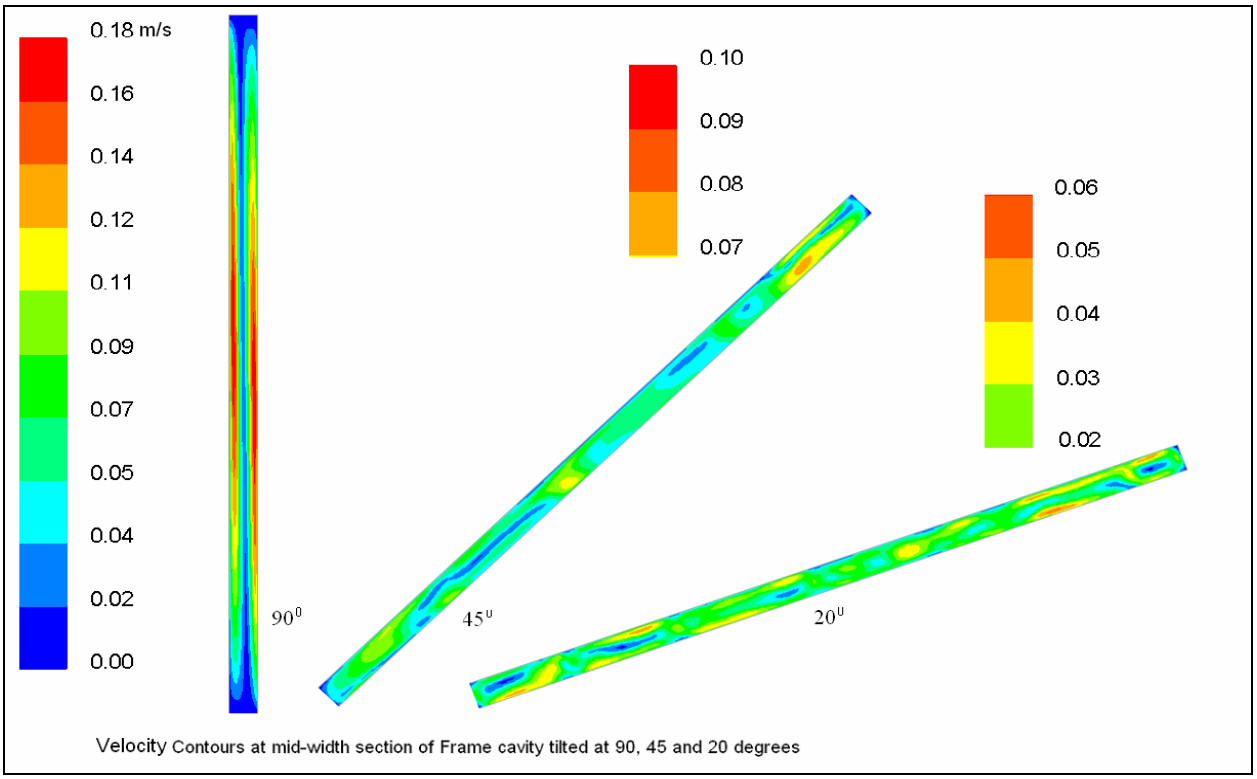


Figure 4.14: Contours of Velocity Magnitude in the Mid Plane Section of Frame Cavity Model *A*=25:1, *Az*=2:1 for *Ra*=92,625.

Note: Velocity magnitude scales are different for each of the tilted frame cavity.

Table 4.6: Predicted Average Heat Flux and *Nu* for Frame Jamb Cavity *A*=25:1, *Az*=2:1 (*H* x *W* x *L* = 100 cm x 8 cm x 4 cm).

ΔT, K	*Ra*	**Θ** = 90°		**Θ** = 70°		**Θ** = 45°		**Θ** = 20°	
		Nu	*q*, W/m^2	*Nu*	*q*, W/m^2	*Nu*	*q*, W/m^2	*Nu*	*q*, W/m^2
2	18,525	1.49	1.79	1.48	1.78	2.34	2.82	2.66	3.20
4	37,050	1.84	4.42	1.82	4.37	2.91	7.00	3.09	7.44
6	55,575	2.08	7.50	2.07	7.47	3.05	11.02	3.16	11.41
8	74,100	2.26	10.88	2.26	10.87	3.12	15.04	3.46	16.64
10	92,625	2.41	14.52	2.42	14.53	3.40	20.44	3.61	21.68

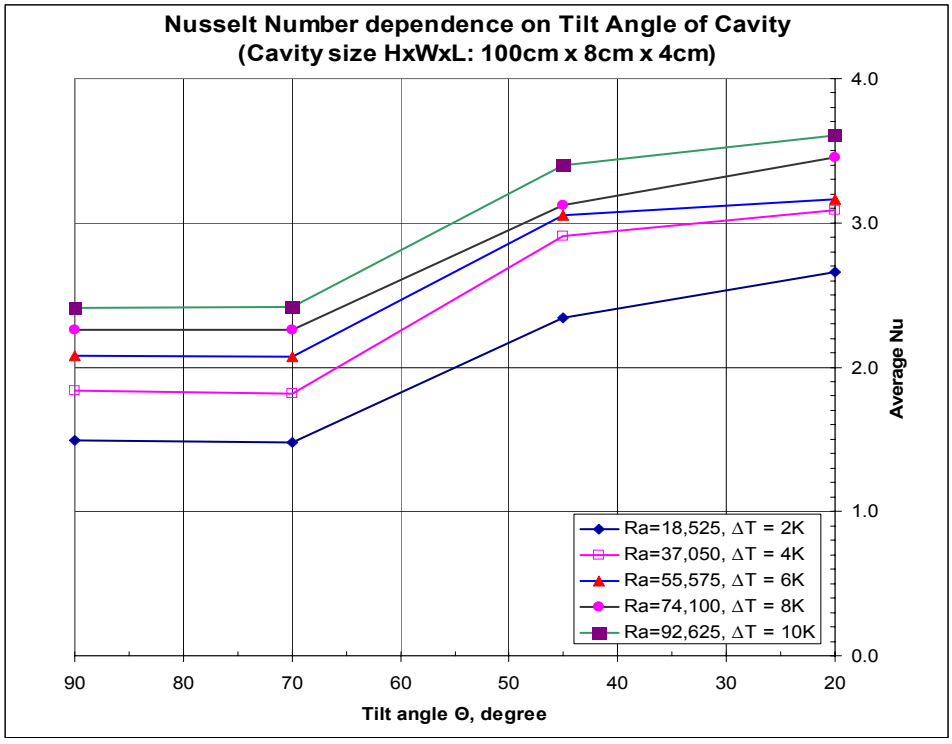


Figure 4.15: *Nu* vs. Tilt Angle for Frame Jamb Cavity *A*=25:1, *Az*=2:1 (*H* x *W* x *L* = 100 cm x 8 cm x 4 cm).

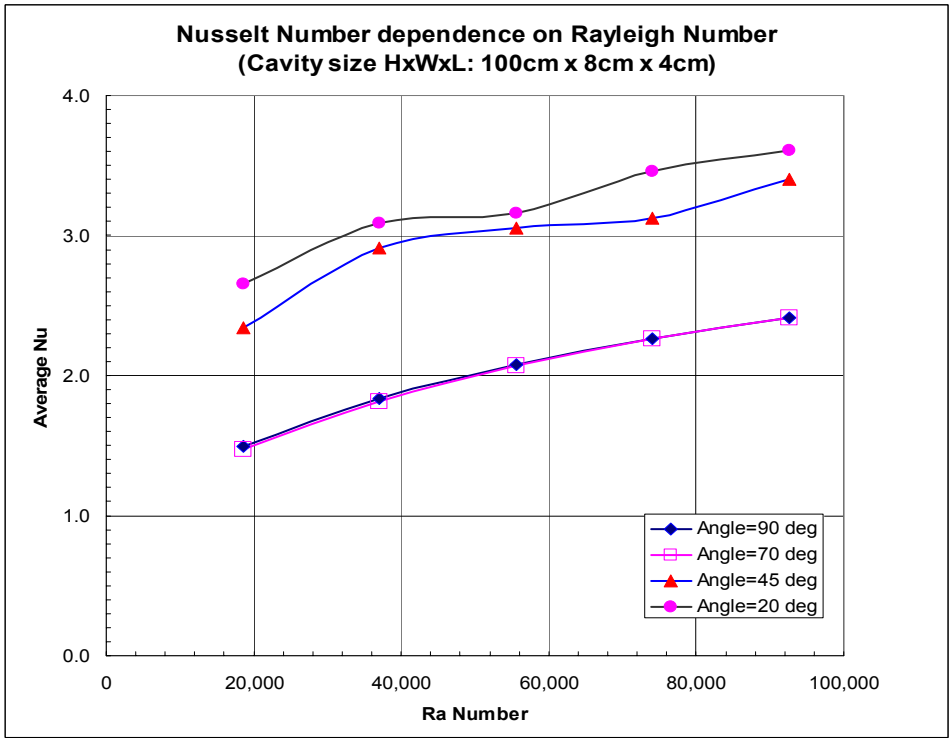


Figure 4.16: *Nu* vs. *Ra* for Frame Jamb Cavity *A*=25:1, *Az*=2:1 (*H* x *W* x *L* = 100 cm x 8 cm x 4 cm).

Conclusions

1) Results from the current study indicate that with reasonable degree of accuracy, it can be assumed that until angle of orientation is 70^0, there is no change in the heat transfer compared with the vertical orientation.
2) The average Nusselt number predicted at each angle of orientation shows a consistent trend for each of the geometries modeled. From the results, it can be seen that there is a marked increase in the heat transfer rate at which the flow transition from one-vortex pattern to multi-vortices occurs. This happens at an angle between 60^0 and 45^0. Further, the heat transfer increases to a higher rate for frame jamb cavities sloped at 20^0 angle of orientation.
3) In all the three geometries investigated, the average Nusselt number predicted by the 3-D numerical model for the case of vertical orientation is smaller than the Nusselt number calculated from 2-D frame cavity correlations available in ISO 15099. As the horizontal aspect ratio increases from 0.5 to 2, the difference in the Nusselt number value predicted by current study and the ISO 15099 correlations decreases. This is an indication that as the W/L ratio, Az increases 3-D numerical results approach two-dimensional ones and for Az going to the limit of infinity, the two should produce the same results.

4.3 Experimental Study

The *goal* of this study was to validate results of numerical 3-D modeling convection heat transfer in the vertical and tilted frame jamb cavities against experiment results. The numerical modeling gives us information about temperature and heat flux distribution on frame cavity walls that could be compared with test values under similar conditions. Thus, by verifying some of the numerical results, we are validating the subsequent correlations that are developed from these numerical results.

During the experimental measurements, heat flux values and surface temperatures on walls were taken. Rectangular cavity specimen with H x L x W = 80 cm x 5 cm x 5 cm (A = H:L = 16) was considered for further comparison with numerical modeling values. These results should be compared with Fluent's 3-D simulation results of the cavity in vertical orientation at the same boundary conditions.

4.3.1 Description of equipment and sensors

Climatic chamber

For the climatic chamber, standard upright large freezer was used with dimensions of inside opening H x W = 115 cm x 86 cm. The freezer is depicted in Figure 4.17. The opening 114 cm x 85 cm was cut in the freezer door and insulation panel from polyisocyanurate material was installed from backside of the door.



Figure 4.17: Standard Upright Freezer, Customized for the Purpose of Heat Transfer Measurements.

The instrument for thermal conductivity measurement

The ASTM C518 instrument was used for measuring thermal conductivity of insulation panel material under steady state conditions. The instrument is calibrated using NIST SRM 1450b (Standard Reference Material of National Institute of Standards and Technology). Accuracy (total uncertainty) for this apparatus and conditions is 1%.

Temperature sensors

The T-type thermocouples have been used for the temperature measurement. Six thermocouples were fabricated from copper and constantan wires. The accuracy and quality of thermocouples were checked using Omega thermometer (model CL23A) and the method of comparing with standard T-type thermocouple in three temperature points: -18 C^o, 0 C^o and 24 C^o. The measured temperature difference between standard thermocouple and reference ones was not more than 0.1 C^o. Taking into account accuracy of Omega thermometer 0.25 C^o the total absolute uncertainty of used thermocouples can be estimated as 0.35 C^o.

Heat flux sensors

The 3 heat flux meters (transducers) have been used for the measurements of heat flux on surfaces of the cavity specimen. The heat flux meters are of the integrating type with 40 mm x 8 mm active area and have thickness 2 mm. The heat flux meters are using a T-type thermocouples.

Electronic control

The digital multi-meter (Keithley, model 175) with resolution 0.01 mV was used for measuring electrical signals from heat flux meters.

4.3.2 Calibration procedure

The goal of calibration procedure is to determine transducer coefficient of heat flux meters (in W/(m^2·mV) units) for specific conditions of natural convection around heat flux meters in metering area. The scheme of sensors allocation is shown in Figure 4.18 and general view of metering area is depicted in Figure 4.19.

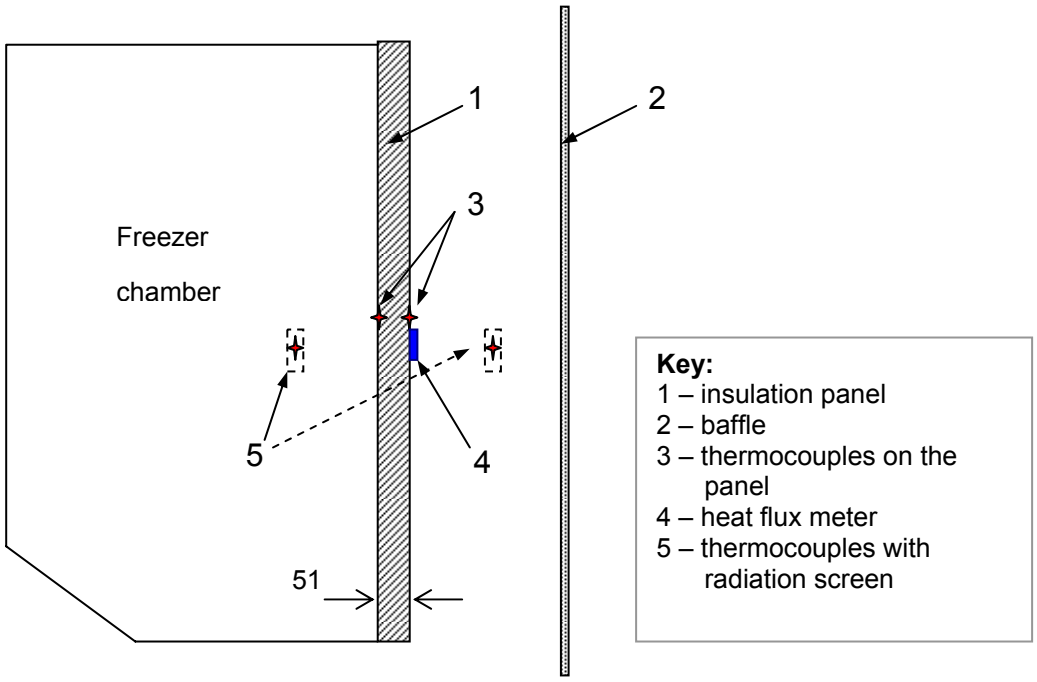


Figure 4.18: The Schematic of Sensor Installation for Calibration of Heat Flux Meters.

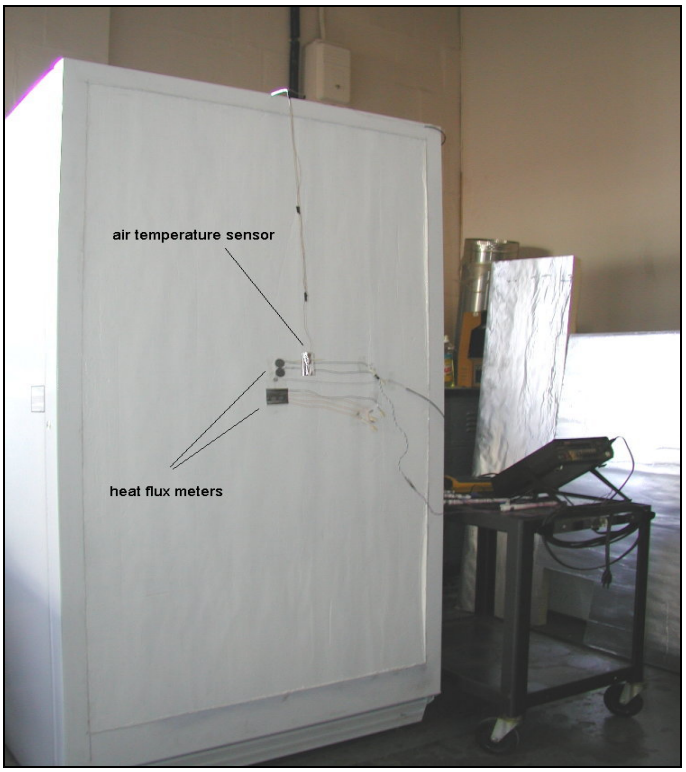


Figure 4.19: The Insulation Panel With Installed the Heat Flux Meters for Calibration.

The temperature field in the central area of the insulation panel (Figure 4.18) is assumed to be one-dimensional and the heat flux through the measuring area of the panel can be calculated using Fourier law:

$$q_{panel} = k_{panel} \Delta T/d, \quad (4.1)$$

where,

k_{panel} = 0.024 W/(m·K) - thermal conductivity of polyisocyanurate material, obtained using the ASTM C518 instrument;

ΔT = temperature difference between cold and warm surfaces of the panel, K, measured by attached thermocouples;

d = 0.051 m average thickness of the panel.

Calibration coefficient of heat flux meter C_{HFM} (W/(m^2·mV) calculated from the following expression:

$$C_{HFM} = q_{panel}/E_{HFM}, \quad (4.2)$$

Where,

q_{panel} = heat flux obtained from (4), W/m2;

E_{HFM} = measured electrical drive force of heat flux meter, mV.

Obtained calibration coefficients were checked in repeated test with the other panel from polyisocyanurate insulation with total thickness of 68 mm. Heat flux q_{HFM} through heat flux meter was calculated using equation:

$$q_{HFM} = C_{HFM} * E_{HFM}, \quad (4.3)$$

where C_{HFM} and E_{HFM} are the same as in (4.2).

The maximum difference between heat flux values obtained from (4.1) and the one obtained when using calibration coefficient from (4.3) was 1.9%.

To estimate the total uncertainty of heat flux meter in this calibration procedure it is necessary to sum up obtained maximum difference (1.9%) with uncertainty of each component on the right side of expression (4.1): Thermal conductivity *k* (1%), temperature difference ΔT (1%) and thickness *d* (1%). Thus, the total uncertainty of heat flux meter in this calibration procedure is 4.9%.

4.3.3 Description of cavity specimen and test method

Jamb cavity specimen with air cavity dimensions H x W x D = 80 cm x 5 cm x 5 cm was formed from rigid polyvinyl chloride (PVC) material with wall thickness 3.2 mm as shown in Figure 4.20. A thin film was used as top and bottom walls of the cavity (not shown in Figure 4.20).

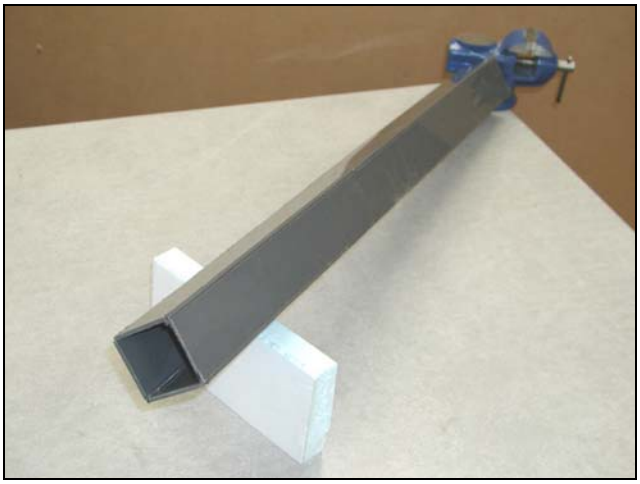


Figure 4.20: PVC Jamb Cavity Specimen.

The PVC cavity specimen was inserted in the opening of the insulation panel and sealed by silicone glue. The PVC cavity specimen installed in surround insulation panel is shown in Figure 4.21.



Figure 4.21: PVC Jamb Cavity Specimen With Attached Thermocouples and Heat Flux Meters in the Insulation Panel. The Baffle is Not Shown.

The PVC cavity specimen with air cavity dimensions H x W x D = 80 cm x 5 cm x 5 cm was inserted in the opening of the insulation panel of the climatic chamber (freezer) tilted under the angle 45^{o} from vertical position. The tilted climatic chamber with PVC cavity specimen is shown in Figure 4.22.

The schedule of sensors for the measurement of the heat transfer of the jamb cavity specimen is shown in Figure 4.22. Three heat flux meters (designated as HF1, HF2 and HF3 in Figure 4.23) were used for measuring local heat flux on outside cavity specimen wall.



Figure 4.22: The Tilted PVC Jamb Cavity Specimen With Attached Thermocouples and Heat Flux Meters on the Insulation Panel. The Baffle is Not Shown.

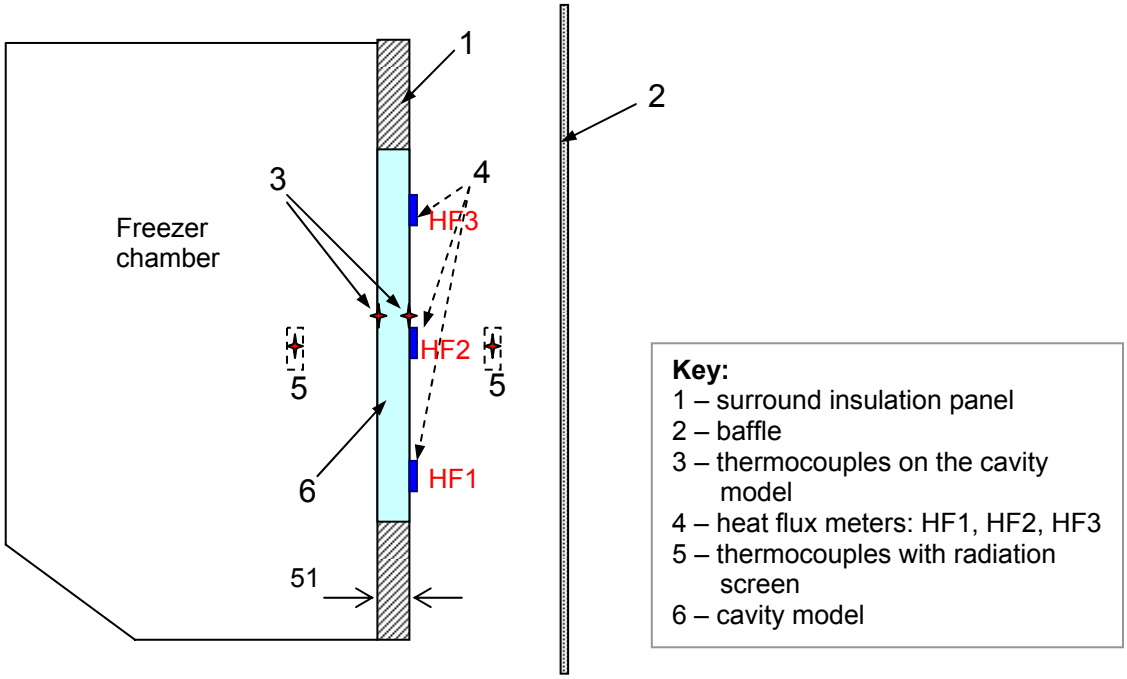


Figure 4.24: The Schematic of Sensor Installation for Heat Transfer Testing of the Jamb Cavity Specimen.

The schematic of sensors installation for the measurements of heat transfer of the tilted jamb cavity specimen is shown in Figure 4.24. Three heat flux meters (designated as HF1, HF2 and HF3 in Figure 4.25) were used for measuring local heat flux on outside cavity specimen wall.

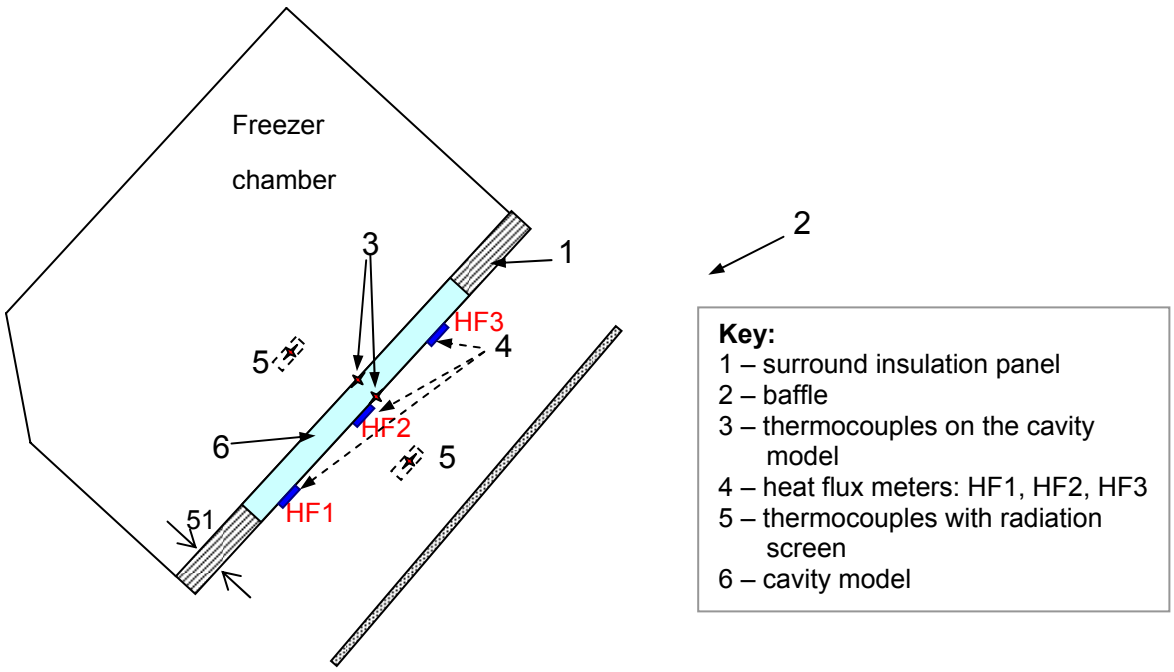


Figure 4.24: The Schematic of Sensor Locations for the Test Setup for Heat Transfer Measurements of the Tilted Jamb Cavity Specimen.

The inside and outside local heat transfer coefficients (film coefficients) $h_{i/o}$ on wall surfaces in the middle of the model height (area HF2) were calculated from the equation:

$$h_{i/o} = q_{HF2}/(t_{i/o} - t_{i/o}), \quad (4.4)$$

where q_{HF2} = heat flux measured by heat flux meter HF2, W/m^2;

$t_{i/o}$ = air temperature (inside/outside), C^o;

$t_{i/o}$ = surface temperature (inside/outside), C^o.

4.3.4 Results and Discussion

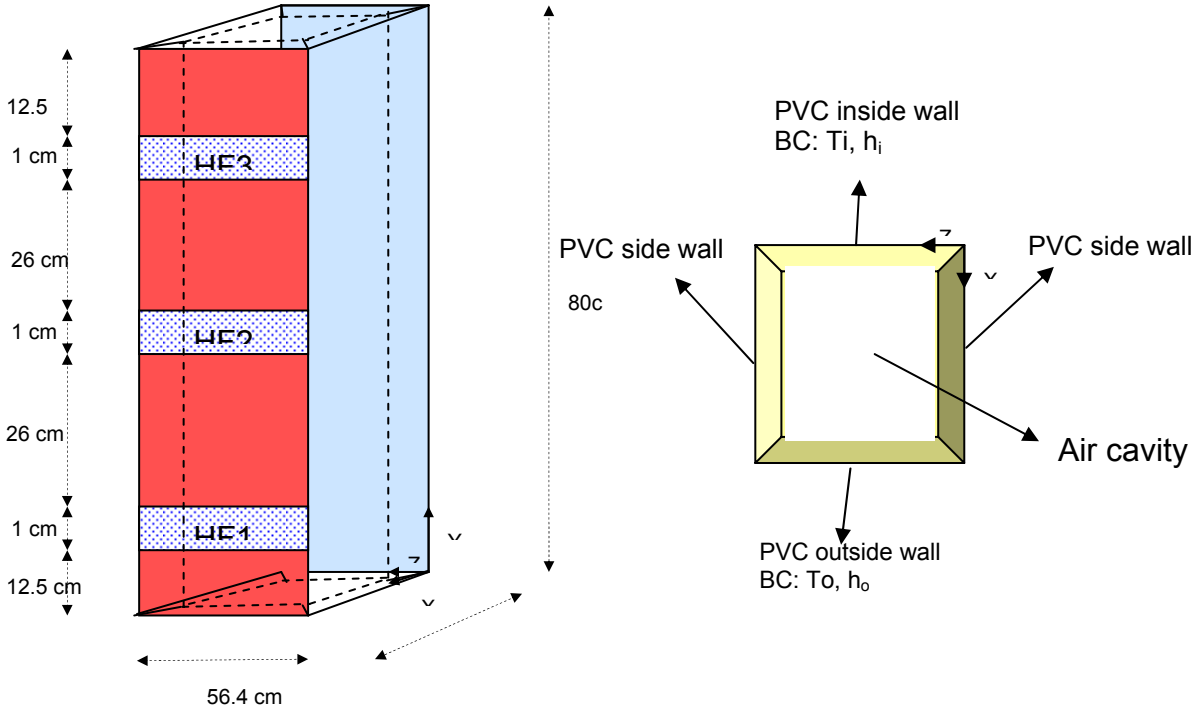
Here we are using the method of comparing local values of heat fluxes and surface temperatures on cavity specimen walls, obtained from the measurements and numerical

modeling. The boundary conditions applied to the numerical model are based on values obtained during the test. In particular, inside and outside film coefficients were calculated using equation (4.4).

Description of the numerical model:

The geometry of the model was created and meshed using Gambit 2.1. The main boundary layer along the air cavity walls has parameters: 6 - element number, first element size 0.0005 m, and increasing ratio coefficient 1.3. The air cavity was meshed using hexahedral elements.

Figure 4.25 shows the frame jamb cavity specimen along with the PVC walls. Three heat flux meters are located on the PVC outside wall. The location of the heat flux meters on the PVC outside wall is determined by analyzing the numerical results of a frame jamb cavity with size 100 cm x 4 cm x 4 cm modeled in an earlier task. The top and bottom locations of the heat flux meter, H1 and H3 respectively on Figure 1, are chosen such that the edge effects at the top and bottom of the cavity are excluded. The position of top and bottom heat flux meters is approximated to be 2.5 times the length of the cavity, which is 12.5 cm for the current jamb cavity specimen. The other heat flux meter is located at the center of the PVC outside wall.



(a) Frame Jamb Cavity specimen with 3 heat flux meters on the warm wall

(b) Cross section of the cavity model

Figure 4.25: The Numerical Model of Frame Jamb Cavity with PVC walls.

Material Properties:

Table 4.7: Material Properties

Material: air (Fluid)			
Property	Units	Method	Value(s)
Density	Kg/m3	Boussinesq	1.2755
Cp (Specific Heat)	J/kg-K	Constant	1006.13
Thermal Conductivity	W/m-K	Constant	0.0243
Viscosity	Kg/m-s	Constant	1.734E-05
Thermal Expansion Coefficient	1/K	Constant	0.003663
Material: PVC (Solid)			
Property	Units	Method	Value(s)
Density	Kg/m3	Constant	1400
Thermal Conductivity	W/m-K	Constant	0.17

Boundary Conditions:

The following boundary conditions, corresponding to the test conditions, were specified for the frame jamb cavity specimen:

- PVC outside wall (Hot wall): Convective heat transfer coefficient h_o = 8.8 W/(m^2·K) and temperature to = 19 ^oC (292 K)
- PVC inside wall (Cold wall): Convective heat transfer coefficient h_i = 7.8 W/(m^2·K) and temperature ti = -13.9 ^oC (259.1K)
- PVC Side walls: adiabatic (zero heat flux)
- Jamb cavity top and bottom wall: Adiabatic (Zero heat flux)
- Internal emissivity of 0.9 on all walls of the enclosed jamb cavity

Solution procedure:

Segregated solver was used with the following settings:

- implicit formulation,
- unsteady,
- laminar viscous model in the cavity;

- radiation model was defined as Discrete Transfer Radiation Model (DTRM) with angle parameters: theta divisions θ = 6, phi divisions φ = 6,
- *Solution controls*: under-relaxation factors (RF) for all equations (variables) were defined with default settings and for energy equation as RF = 0.99,
- *Method discretization*: pressure equation – PRESTO; pressure-velocity coupling – SIMPLEC; momentum – First Order Scheme; energy – First Order Scheme,

Convergence is achieved when the heat flow percentage difference on the PVC inside and outside wall is less than 3%.

Results:

Results of the simulation and the experiment are summarized in Table 4.8. Figure 4.26 shows the heat flux distribution on the outside cavity wall along vertical mid-line obtained from simulation and the test.

Table 4.8: The Comparison Between Experimental and Modeled Results for the Vertical PVC Jamb Cavity specimen H x W x L = 80 cm x 5 cm x 5 cm

Method	Boundary conditions		Hot wall surface temperature at middle height T_{in}, ^0C	Cold wall surface temperature at middle height T_{out}, ^0C	Ra	ΔT across inside cavity surfaces, (^0C)	Heat flux, (W/m^2)		
	Outside air h_{in} = 8.8 $W/(m^2 \cdot K)$ T_{out}	Inside air h_{out} = 7.8 $W/(m^2 \cdot K)$ T_{in}					Area HF1	Area HF2	Area HF3
Test	19 ^{o}C	-13.9 ^{o}C	11.6	-5.5	NA	NA	74.70	65.30	56.50
Simulation	19 ^{o}C	-13.9 ^{o}C	11.0	-5.0	244,552	16.0	79.24	66.35	56.90
Δq (%)							5.7%	1.6%	0.7%

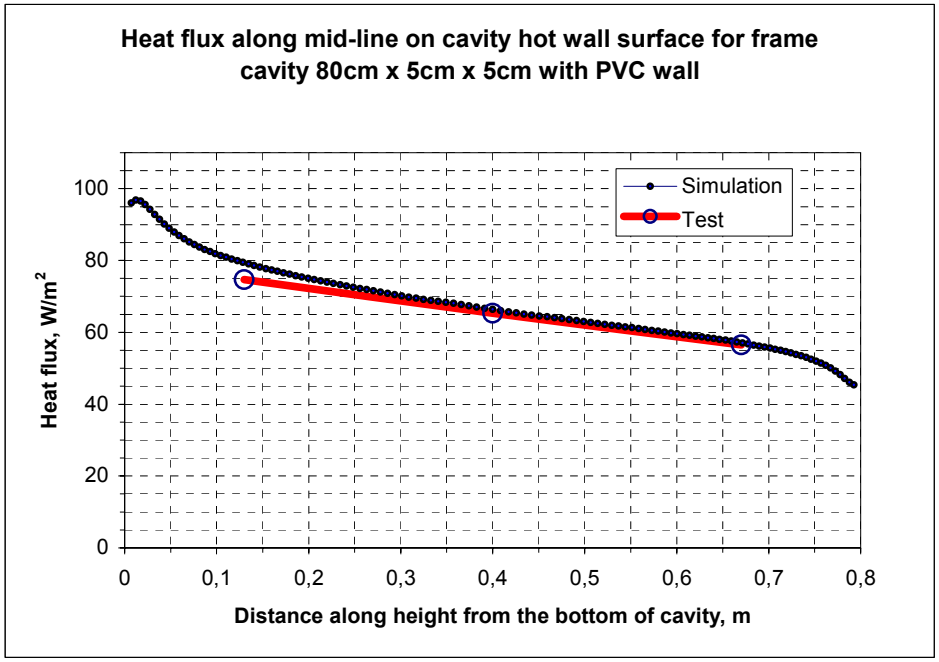


Figure 4.26: Comparison Between Heat Flux Values Obtained from the Test and the Numerical Modeling.

From the results it is obvious that 3-D model is in good agreement with the experimental results. The difference in surface temperatures at the middle height of the specimen is not more than 0.6 ^{o}C.

The difference between measured and predicted heat fluxes (5.7%) at the bottom part of the model (location HF1 in Fig. 4.25 and Fig. 4.24) is more than estimated total uncertainty (4.9%) in the test method, but only marginally and within other uncertainties, such as non-homogeneity of boundary conditions during the test, etc..

Results of the simulation and the experiment for tilted jamb cavity specimen are summarized in Table 4.9. Figure 4.27 shows the heat flux distribution on the outside cavity wall surface along vertical mid-line, obtained from simulation and the test.

Table 4.9: The Comparison Between Experimental and Modeled Results for the PVC Jamb Cavity Specimen H x W x L = 80 cm x 5 cm x 5 cm Tilted at 45°

Method	Boundary conditions		Hot wall surface temperature in middle height T_{in}, ^0C	Cold wall surface temperature in middle height T_{out}, ^0C	Ra	ΔT between inside cavity surfaces, (^0C)	Heat flux, (W/m^2)		
	Outside air h_{in} = 8.2 $W/(m^2 \cdot K)$ T_{out}	Inside air h_{out} = 8.7 $W/(m^2 \cdot K)$ T_{in}					Area HF1	Area HF2	Area HF3
Test	21 °C	-14.7 °C	11.4	-5.6	NA	NA	76.7	78.3	68.3
Simulation	21 °C	-14.7 °C	10.8	-6.1	250,000	16.4	80.2	82.9	68.3
Δq (%)							-4.6%	-5.9%	0.0%

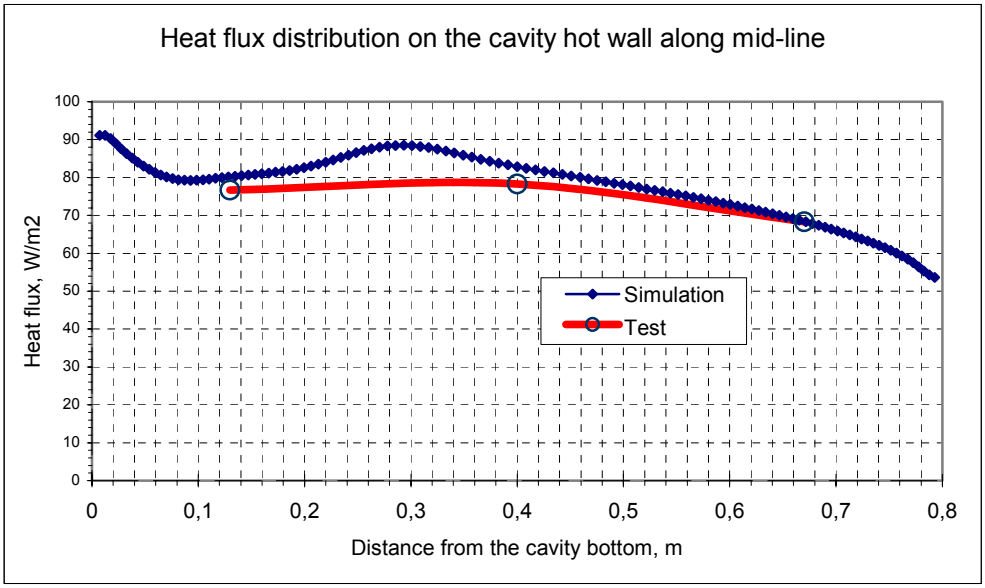


Figure 4.27: Comparison Between Measured and Modeled Heat Flux Values for PVC Jamb Cavity Specimen Tilted at 45°.

From the presented results it is obvious that 3-D model is in a good agreement with the experimental results. The difference in surface temperatures at the middle height of the model is not more than 0.6 °C.

The difference between measured and predicted heat fluxes is within total uncertainty of the test method and Fluent simulation. The maximum obtained difference is at the middle part of the specimen.

4.4 Heat transfer correlations for tilted frame jamb cavity

The following correlation is proposed for vertical frame jamb cavities. This correlation equation uses the Nusselt number derived from 2D frame cavity correlations given in ISO 15099 (2003).

$$Nu_{3D} = 1 + 0.4[Nu_{2D} - 1 - (0.0047 * A_h^{(1/A_h)} * Ra * 10^{1.1})][1 + \sqrt{A_h}\,(0.8 - A/100)](\mathrm{ATAN}\sqrt{A_h})$$

for $20 \le A \le 40$; $0.5 \le A_h \le 2$; $15{,}000 \le Ra < 120{,}000$

(4.5)

Where:

Nu_{2D} = Nusselt number in eq. 88–92 in ISO 15099 (2003) for 2-D frame cavities

A = Vertical aspect ratio of cavity, H/L

A_h = Horizontal aspect ratio of cavity, W/L

Ra = Rayleigh number

The average *Nu* from the proposed correlation and vertical frame cavity correlation (Equations 90–92) from ISO 15099 (2003) are plotted as a function of Rayleigh number in Figure 4.28 and Figure 4.29 for aspect ratios mentioned above. The corresponding *Nu* obtained from the numerical study are also plotted for comparison. The proposed correlation equation gives much better conformity with results from numerical study than correlation in ISO 15099.

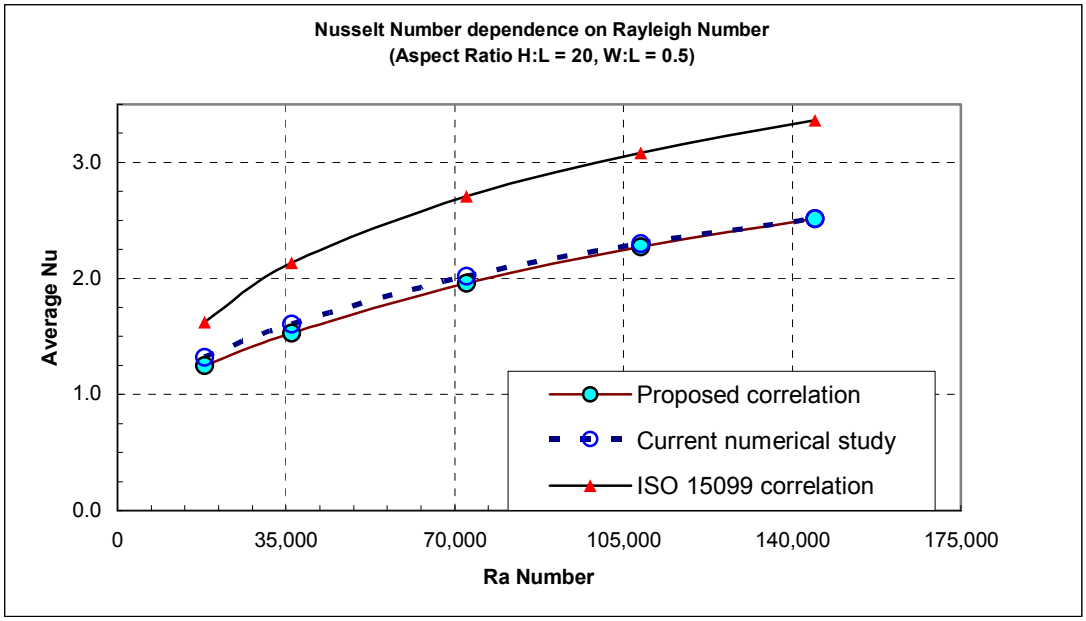


Figure 4.28: Average *Nu* vs. *Ra* From Proposed Correlation and Corresponding Values From the Current Numerical Study and ISO 15099 (A=20:1, A_h=1:2)

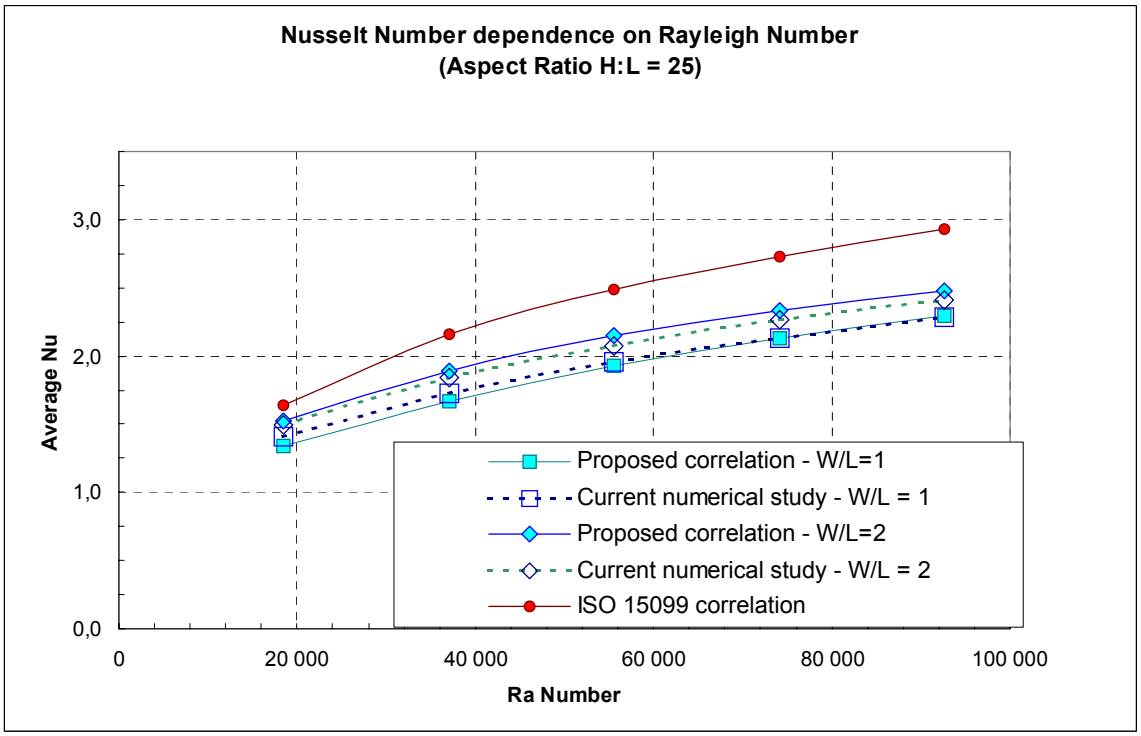


Figure 4.29: Average Nu vs. *Ra* From Proposed Correlation and Corresponding Values From the Current Numerical Study and ISO 15099 (A=25:1, A_h=1 and 2).

The vertical frame cavity correlation (4.5) is used as the base for creating correlations for tilted jamb cavity in the range of tilt angles θ from 90^o to 20^o and aspect ratio W/L from 0.5 to 2.

This correlation is expressed as follows:

a) for θ from 20^o to 45^o:

$$Nu(\theta) = [Nu_{(\theta=90)}] + 1.1 - 0.1 \cdot A_h \cdot (45 - \theta) \text{ ; for } 1 \le A_h \le 2 \quad (4.6)$$

$$Nu(\theta) = [Nu_{(\theta=90)}] + \sqrt{[0.045 \cdot (45 - \theta) + 3.5 \cdot Ra \cdot 10^{(-6)}]} \text{ ; for } A_h = 0.5 \le A_h < 1 \quad (4.7)$$

b) for θ from 45^o to 70^o:

Nusselt number is found using a linear interpolation between the endpoints of equation (4.5) and (4.6) or (4.7) based on required aspect ratio W/L.

c) for θ from 70^o to 90^o:

Correlation (1) should be used.

The average *Nu* from the proposed correlations are plotted as a function of *Ra* in Figures 4.30, 4.31, and 4.32, for the aspect ratios mentioned above. The corresponding *Nu* obtained from the numerical study is also plotted for comparison. The tables with source data for presented diagrams are given in Appendix D.

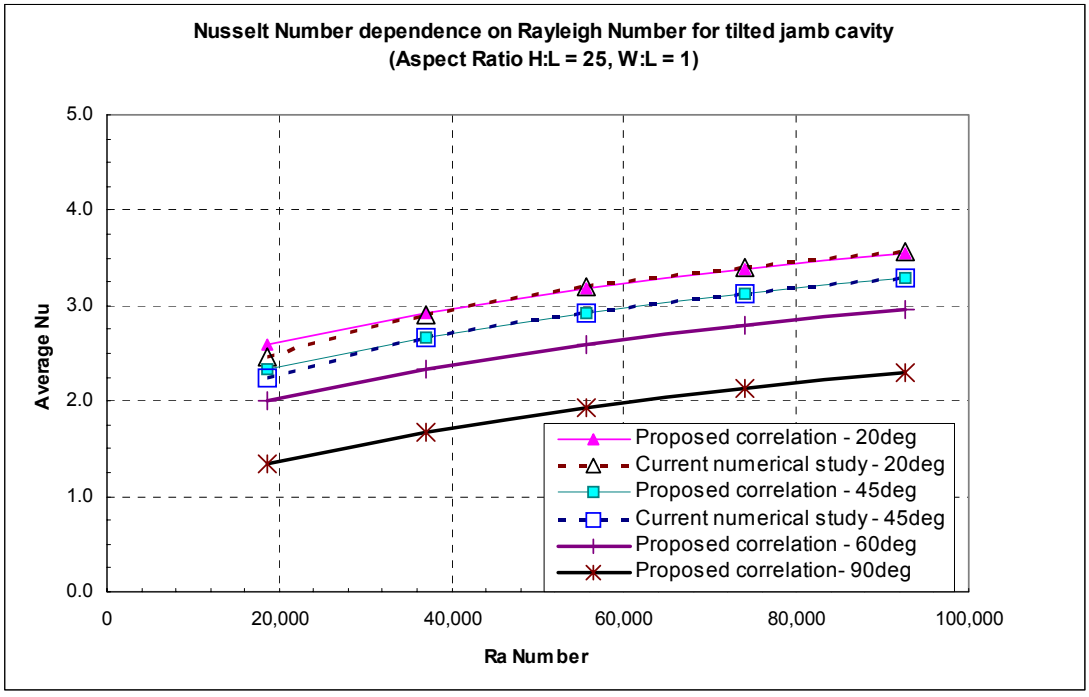


Figure 4.30: *Nu* vs. *Ra*r for Cavity *A*=25:1, A_h=1:1

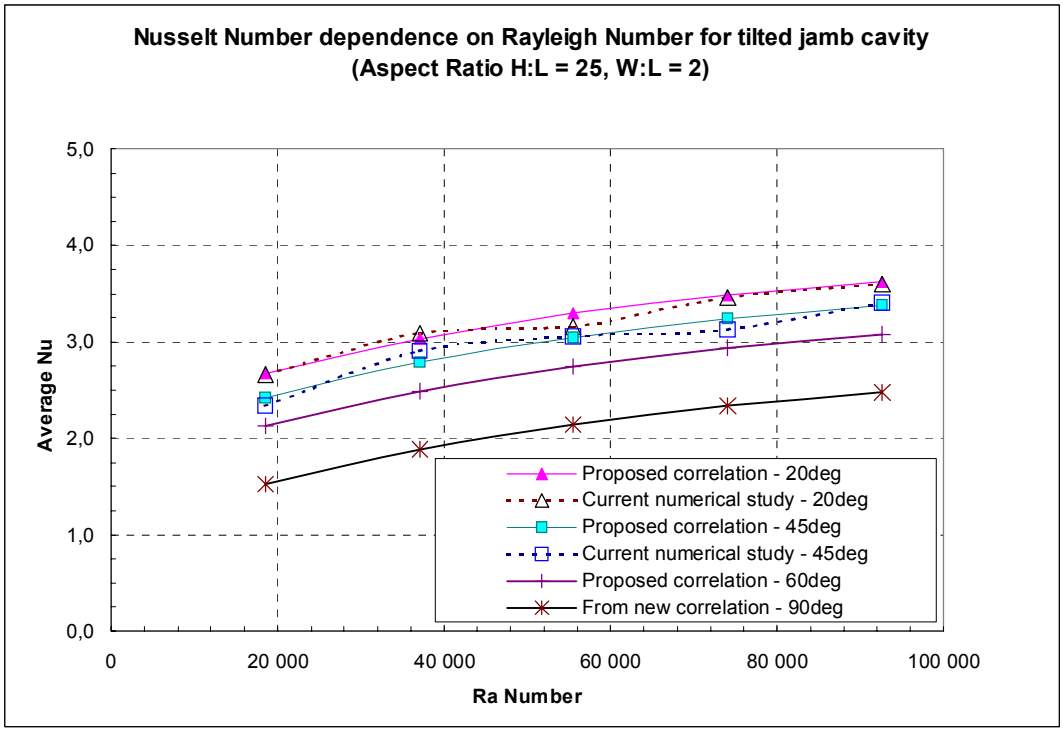


Figure 4.31: *Nu* vs. *Ra* for cavity *A*=25:1, A_h=2:1

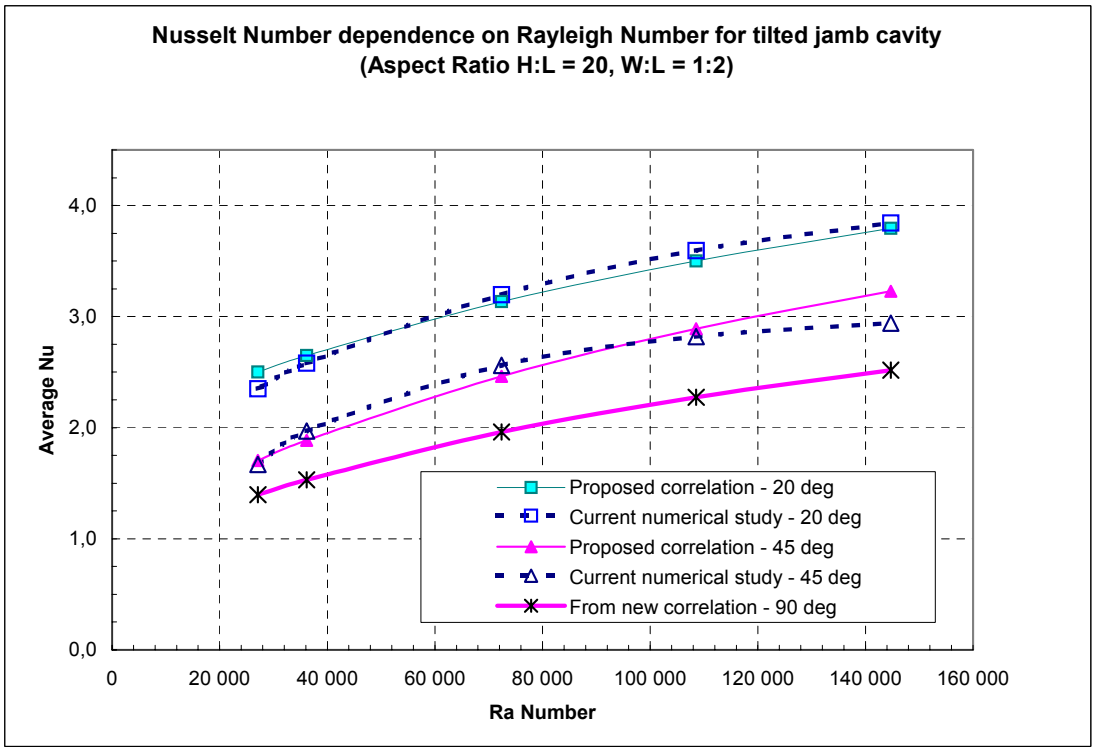


Figure 4.32: *Nu* vs. *Ra* for cavity *A*=20:1, A_h=1:2

4.5 Summary

- A test method for estimating heat transfer through jamb frame cavity specimen using the freezer chamber as a climatic chamber providing cold air area was developed.
- The PVC jamb cavity specimen tilted under the angle 45^{o} with dimensions H x W x D = 80 cm x 5 cm x 5 cm and wall thickness 3.2 mm was tested under temperature difference of 35.7 ^{o}C (–14.7 ^{o}C; +21 ^{o}C). Obtained results of heat flux through the wall cavity and surface temperature were compared with 3-D numerical simulation results under the same boundary conditions.
- The 3-D numerical model results of heat transfer rate in jamb frame cavity agreed well with the experimental results. The difference between predicted and measured surface temperatures less than 0.6 ^{o}C. The difference between predicted and experimental values of heat flux through the cavity wall in specified locations is less than 6%
- The heat transfer correlations for tilted frame jamb cavity, in the aspect ratio range of $20 \le A \le 40$ and $0.5 \le A_h \le 2$, tilt angles from 90^{o} to 20^{o}, and *Ra* between 15,000 and 120,000, were developed.

5. CONVECTIVE HEAT TRANSFER IN VENTILATED FRAME SILL CAVITY

5.1 Introduction

This part of the report provides results of modeling detailed convective heat transfer through ventilated cavity, i.e. cavity with a slot in outside wall. FLUENT software tool was used for this modeling. Geometry and boundary conditions were specified in order to reproduce conditions during the physical test in a test apparatus. The results are shown in terms of heat transfer rate through cavity and temperature and velocity and turbulence quantities fields.

The current study on ventilated frame cavity is different from the other published studies, reviewed in the literature review section in following ways: (a) airflow outside the ventilated cavities is wind induced and cannot be modeled as laminar natural convection, hence, turbulence modeling was undertaken; (b) the ratio of slot width to cavity height is much less than those in other published studies.

5.2 Numerical Study

5.2.1 Description of numerical model

Cavity specimen was installed in the surround panel of the test apparatus. This condition was numerically modeled. Baffle and space between surround panel and baffle were modeled as well. The main goal of this modeling was to obtain heat transfer rate due to convection in cavity with slot in the outer (cold side) wall. Figure 5.1 shows geometry of the model.

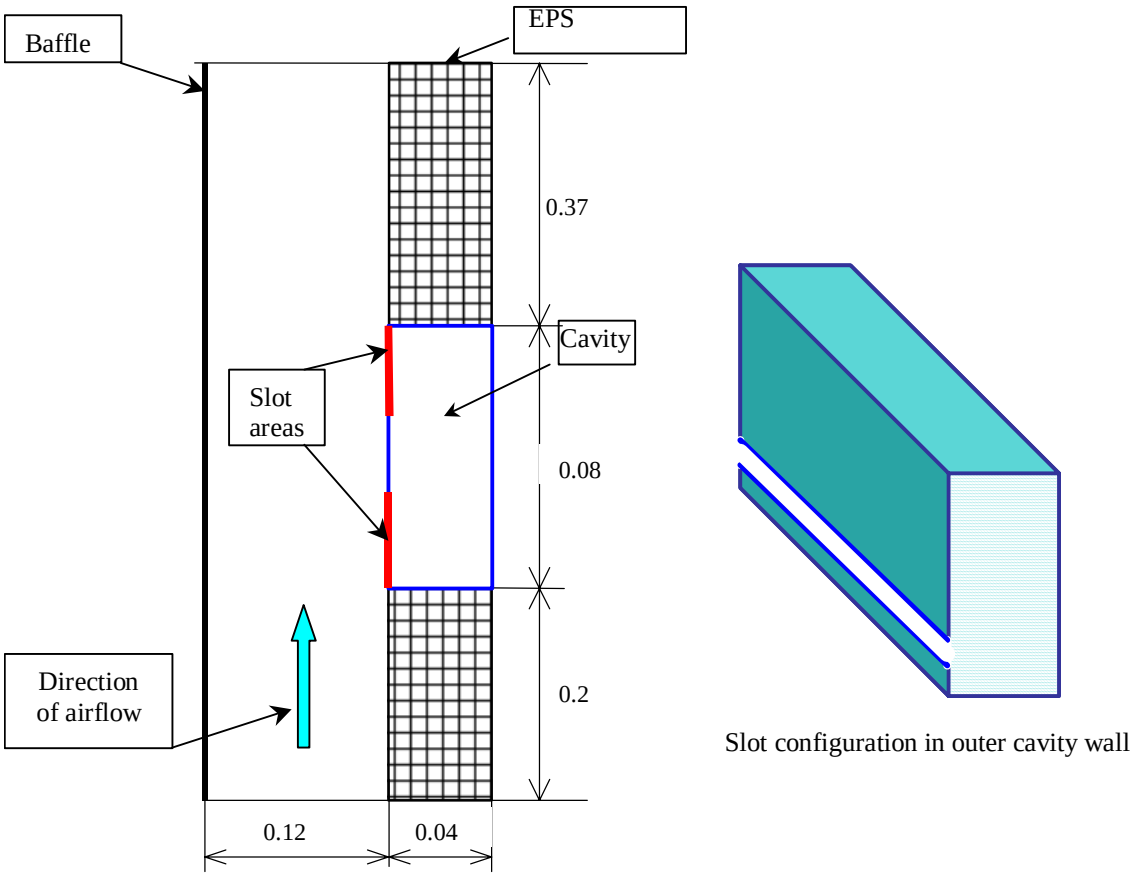


Figure 5.1: Schematic of the Ventilated Cavity Specimen (Not to Scale).

Boundary conditions were defined for the model of cavity installed in insulation panel and subject to forced airflow, at velocity V_c and temperature T_c on the outside wall and shown in Figure 5.2.

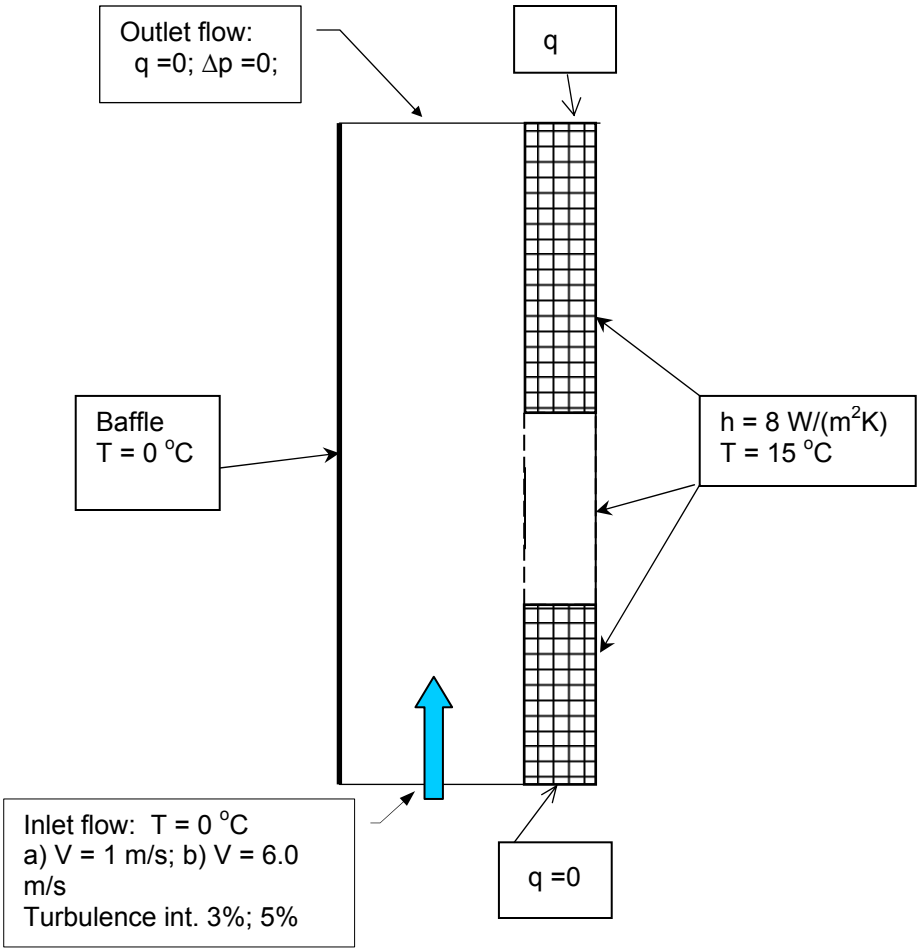


Figure 5.2: Boundary Conditions for the Numerical Model.

Thermo-physical properties of air were treated as constants and were evaluated at the temperature of 0 °C for air for the cold side and at the temperature of 7 °C for the warm side. Thermal conductivity of insulation panel material was k = 0.029 W/(m·K). Boussinesq approximation was used in viscous turbulent model.

The mesh of the model was created by using Fluent's software Gambit 1.3 and shown in Figure 5.3. The main boundary layer along insulated panel has parameters: 6 - element number, first element size 0.0005 m, and increasing ratio coefficient 1.3.

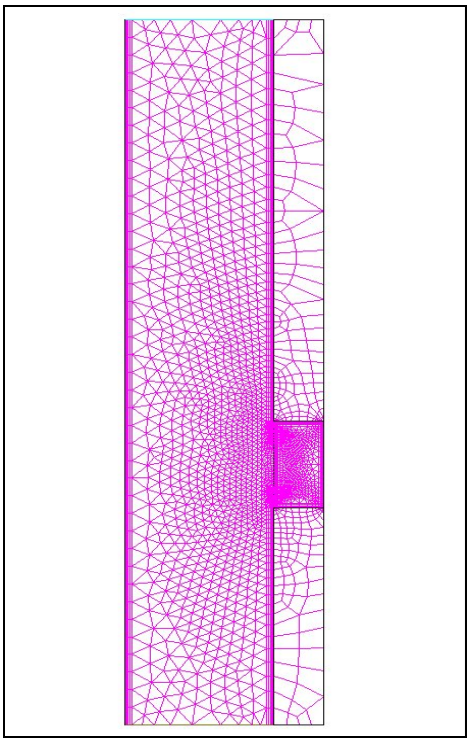


Figure 5.3: Finite Volume Mesh of the Computational Domain.

Segregated solver was used with the following settings:

- Implicit formulation,
- Steady calculation,
- Viscous model was defined as shear-stress transport (SST) k-ω turbulence model with option *transitional flows*, and in case of closed cavity was used laminar viscous model in the cavity;
- Radiation model was defined for case of closed cavity as Discrete Transfer Radiation Model (DTRM) with angle parameters: theta divisions θ = 6, phi divisions φ = 6,
- *Solution controls*: under-relaxation factors (RF) for all equations (variables) were defined with default settings and for energy equation as RF = 0.9,
- *Method discretization*: pressure equation – PRESTO; pressure-velocity coupling – SIMPLEC; momentum – First Order; energy – First Order Scheme,
- The solution reached convergence after approximately 350 iterations.

5.2.2 Results and Discussion

Closed cavity. Comparing with THERM5 results.

Three models were used in this modeling: turbulent and laminar viscous models, with radiation model DTRM in FLUENT and conduction/detailed radiation model THERM5.

In the turbulent model, with the inlet velocity of 6 m/s, the average heat transfer coefficient on the cold side is estimated at h_c = 33 W/(m^2·K) and temperature t_c = 0 ºC. On the warm side, combined heat transfer coefficient of h_w = 8 W/(m^2·K) and temperature t_w = 15 0 ºC were applied. Emissivity of all surfaces was 0.9. Results in terms of heat flow through inside (warm) wall are summarized in Table 5.1.

Table 5.1: Predicted Heat Flow Through the Warm Wall of Closed Cavity.

Inlet velocity	Heat flow through warm wall of closed cavity specimen, W		
	Viscosity model		Conductive model THERM5
	Laminar	Turbulent	
6 m/s (convection + radiation)	3.53	3.73	3.33
6 m/s (only convection)	2.14	2.12	N/A
1 m/s (only convection)	1.90	2.02	N/A

Predicted temperature and velocity fields in the cavity are shown in Figure 5.4 and turbulent viscosity ratio distribution within the computational domain is shown in Figure 5.5 for the case of cold side velocity of 6 m/s. These distributions are typical for laminar regime in closed cavity and for turbulence flow of low turbulent intensity in a channel. Obtained maximum turbulent kinetic energy in the channel is 0.24 m^2/s^2.

a) b)

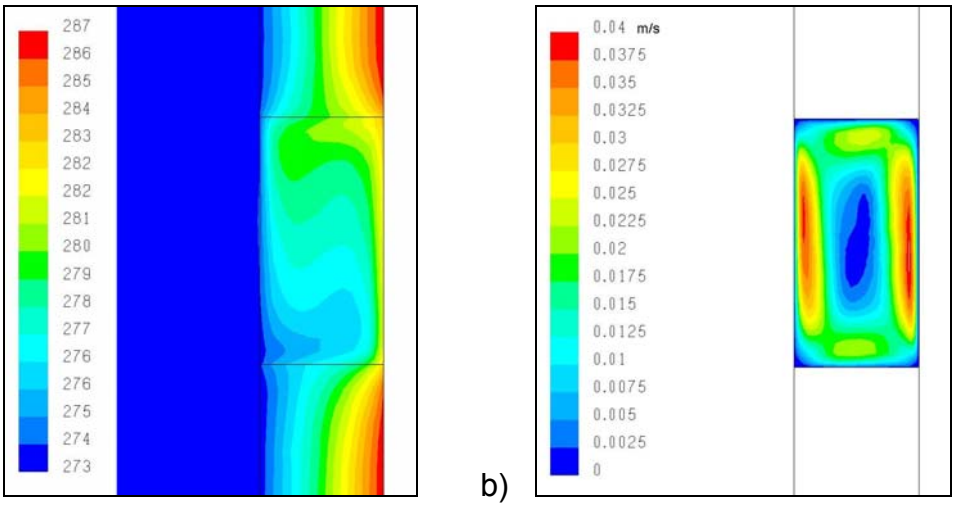


Figure 5.4: Temperature (a) and Velocity Magnitude (b) Distribution in Closed Cavity - Turbulent Model.

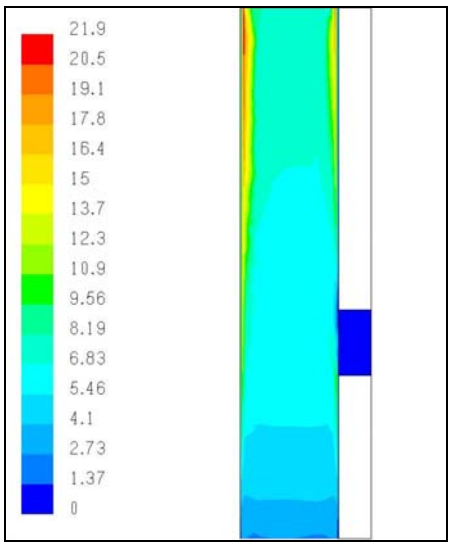


Figure 5.5: Turbulent Viscosity Ratio Distribution in Computational Domain. The Case of Closed Cavity.

Ventilated cavity.

For the case of ventilated cavity, the dependence of convection heat transfer through cavity vs. location and width of slot opening was studied. Two airflow velocities were considered; 1) 1 m/s and 2) 6 m/s. There were two sizes of slot opening under consideration: 5 mm and 10 mm.

Predicted temperature and velocity distributions in computational domain are presented in Figures 5.6 and 5.7 for slots on the bottom and top of the cavity. These results show that ventilated effect distorts temperature and velocities fields in comparison with the closed cavity (see Figure 5.4).

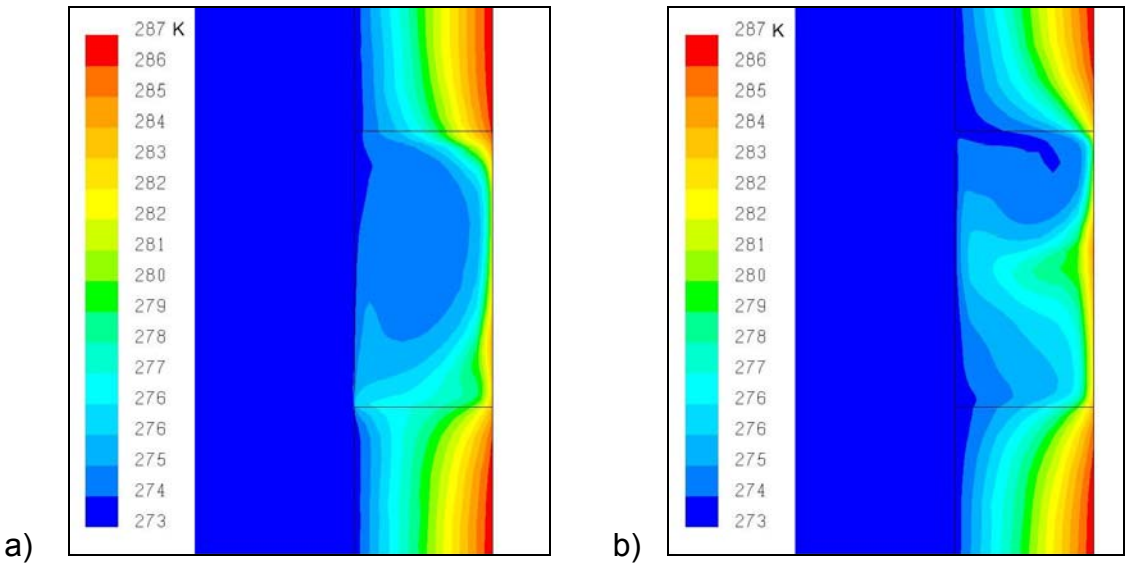


Figure 5.6: Predicted Temperature Distribution in Ventilated Cavity With 5 mm slot: (a) slot at the bottom; (b) slot at the top of cavity wall.

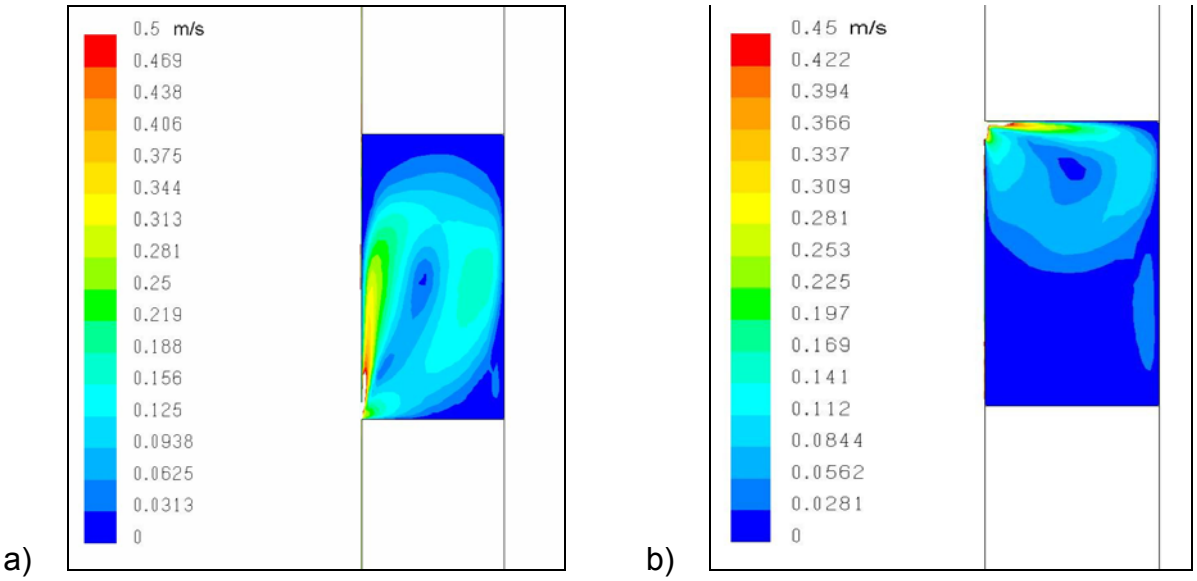


Figure 5.7: Predicted Velocity Magnitude Distribution in Ventilated Cavity With 5 mm slot: (a) slot at the bottom; (b) slot at the top of cavity wall.

Inside the cavity we can also observe presence of turbulence quantities with values close to values in the mainstream. As an example, predicted turbulent viscosity ratio distributions in computational domain are shown in Figure 5.8. This distribution coincides with the distribution of turbulent thermal effective conductivity of air in the cavity that has maximum value of about 0.04 W/(m·K).

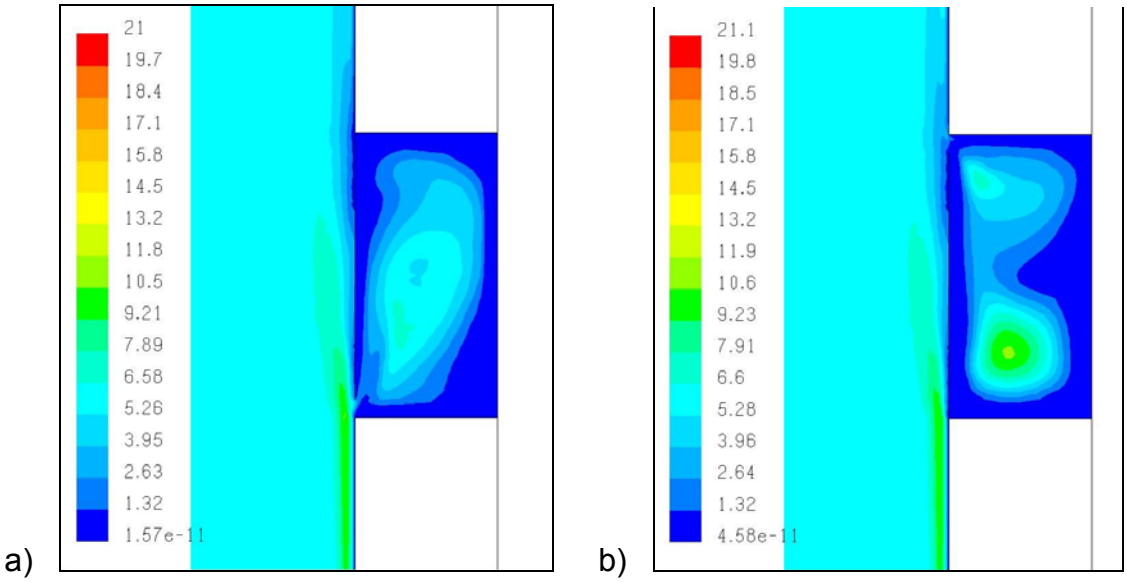


Figure 5.8: Predicted Turbulent Viscosity Ratio Distribution in Ventilated Cavity With 5 mm slot: (a) Slot at the Bottom; (b) Slot at the Top of Cavity Wall.

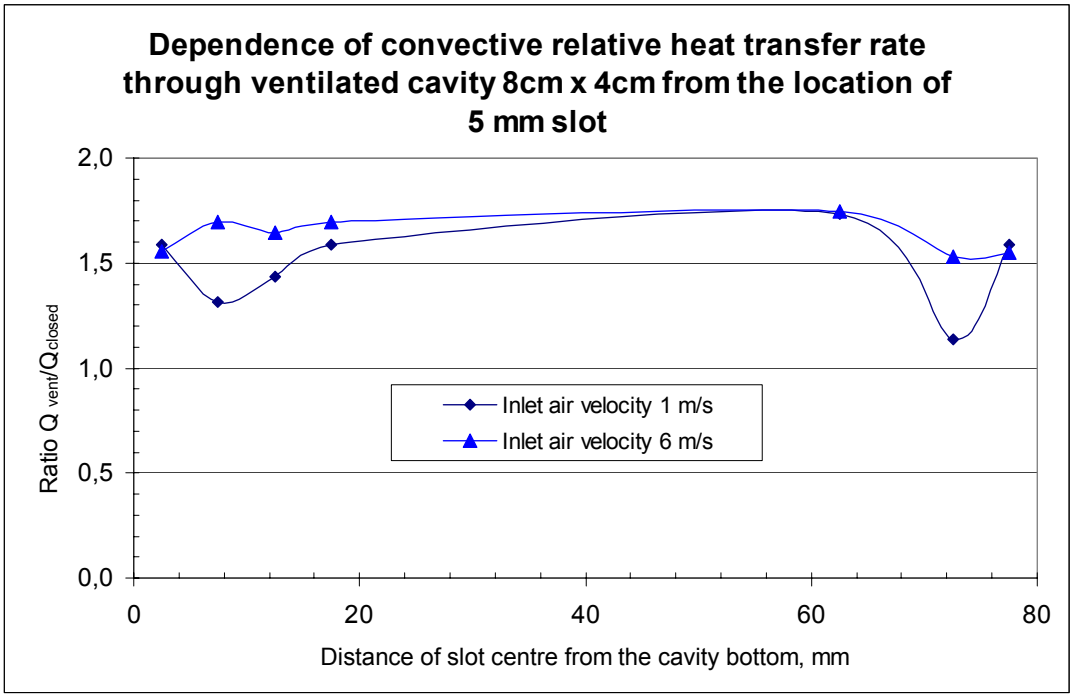


Figure 5.9: Dependence of Ventilation Effect on the Location of the Slot in the Cavity.

For inlet velocity of 6 m/s, the location of cavity slot changes ventilation effect in cavity no more than 14 %. For this cavity case the maximum increase of heat flow through ventilated cavity with 5 mm width slots due ventilated effect is about 70%.

Simulation results for seven cavity models are summarized in Appendix E. Predicted increasing convective heat transfer intensity in ventilated cavities with slot of 5 mm width is in the range from 20% to 120% in comparison with the closed cavity under same conditions. From results of modeling it follows that increasing width of slot opening from 5 mm to 10 mm increases convective heat transfer flow through cavity from 15% to 35%. The effect of slot opening increase is less pronounced for smaller cavities. In Figure 5.10 dependence of cavity ventilation effect vs .*Ra* is shown for slot width of 5 mm.

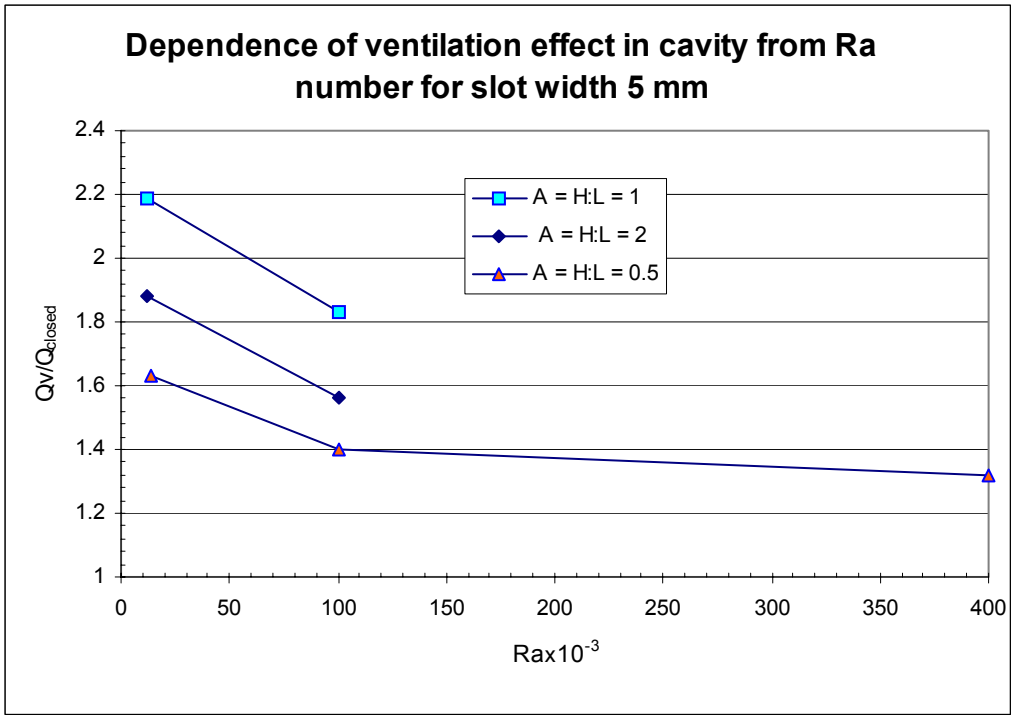


Figure 5.10: Cavity Ventilation Effect vs *Ra*.

From the obtained results it follows that the ventilation effect decreases with increase of *Ra* almost equally for all studied cavity aspect ratios.

Dependence of ventilation effect from the depth of a slot

Above results are obtained under the assumption that the depth of a slot opening is not larger than the thickness of the cavity wall (about 2 mm). In practice it is possible to have cases where this is not the case, as shown in Figure 5.11.

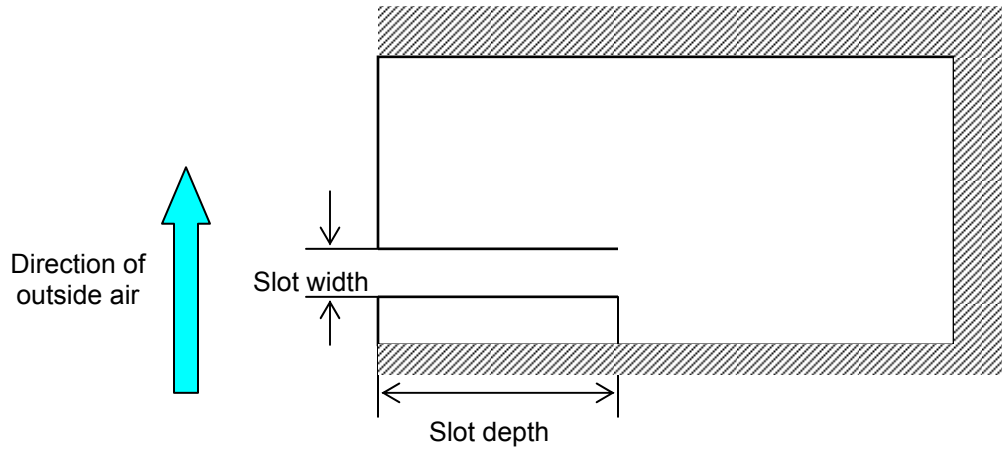


Figure 5.11: Schematic of the Cavity With Slot Width Smaller then the Slot Depth.

Simulation results for cavities H x L = 4 cm x 8 cm and H x L = 4 cm x 4 cm with slot depth of 10 mm and 25 mm and slot width 5 mm are given in Table 5.2 and these results are plotted vs. the ventilation effect from the slot depth (see Figure 5.12).

Table 5.2: Predicted Heat Flow Through Warm Wall of Ventilated Cavity with the Air Velocity of 6 m/s From the Cold Side and Slots with depth 10 mm and 25 mm

Cavity size H x L	Cavity type	Slot width, mm	Slot distance from the cavity bottom, mm	**Slot depth, mm**	Relative heat transfer rate of the cavity, Q_{vent}/Q_{closed}	Heat flow through cavity hot wall, W
4 cm x 8 cm	*closed*	-	-		-	*0.96*
	ventilated	5	5	**10**	1.11	1.07
	ventilated	5	5	**25**	1.04	1.00
4 cm x 4 cm	*closed*	-	-	-	-	*1.06*
	ventilated	5	5	**10**	1.16	1.23
	ventilated	5	5	**25**	1.0	1.06

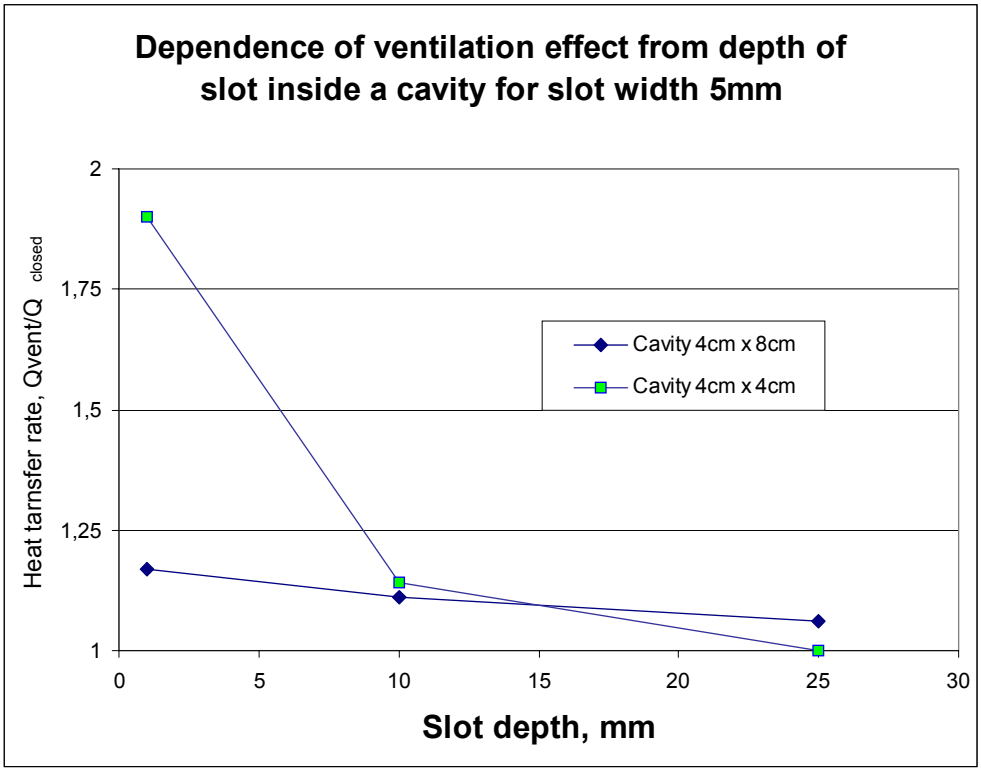


Figure 5.12:. Slot Ventilation Effect for Slot Width of 5 mm and Various Slot Depths.

From these results it can be concluded that for cavities with larger size *L* (8 cm) and slot depth equal to width (5 mm) ventilation effect can be about 50 % (Figure 5.12) and only for slots with depth twice more than width ventilation effect from slot drops to 11% - 14%.

5.3 Experimental Study

In this section, experimental setup for the study of convection heat transfer in ventilated cavities is presented. The goal is to obtain heat flux values and surface temperatures on the warm wall of the rectangular PVC cavity specimen with H x L x W = 60 cm x 5 cm x 5 cm with hole/slot for comparison with modeled values. These results are compared with the Fluent's simulation results at the same boundary conditions.

5.3.1 Description of the cavity specimen installation

The PVC cavity specimen with air cavity dimensions H x W x D = 60 cm x 5 cm x 5 cm was inserted in the opening of the insulation panel of the climatic chamber. The climatic chamber with cavity specimen is shown in Figure 5.13.



Figure 5.13: The PVC Sill Cavity Specimen With Attached Thermocouples and Heat Flux Meters in the Insulation Panel. The Baffle is not Shown.

The schematic of sensors installation for this test and basic dimensions are presented in Figure 5.14. Three heat flux meters were used for measuring local heat flux on outside cavity wall.

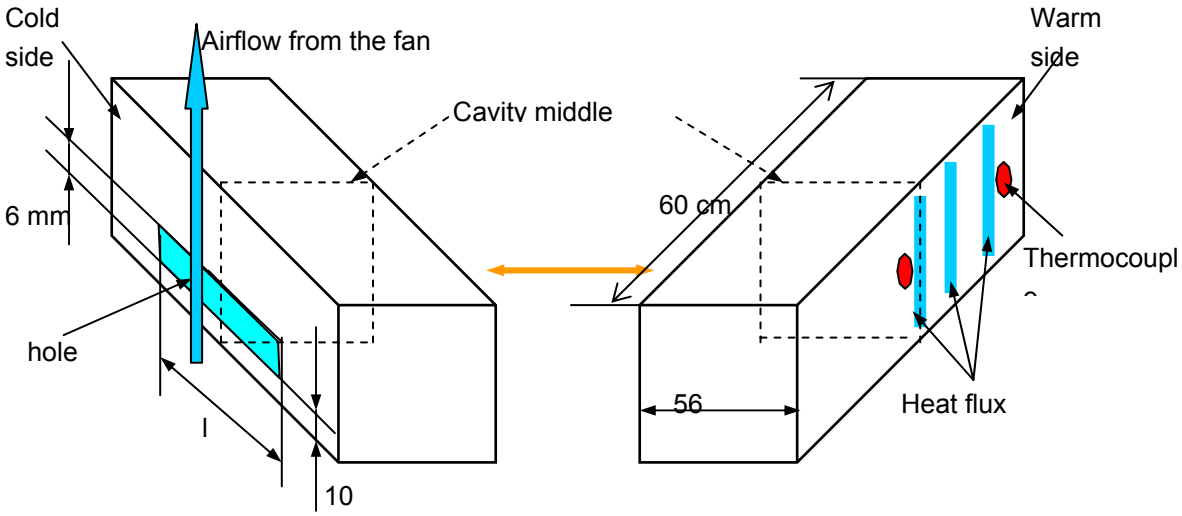


Figure 5.14: The Schematic of Sensor Installation for Heat Transfer Measurements of the Ventilated PVC Cavity Specimen.

Electronic control and air velocity sensor

The Agilent (model 34970A) Data Acquisition/Switch Unit was used for measuring temperature and electrical signals from heat flux meters.

The Air-velocity meter VelociCalc®Plus (model 8384) was used for measuring air velocity produced by double fan.

5.3.2 The test results

The stages of the experiment

1. Closed cavity model. During the first stage the closed cavity specimen was tested,
2. The same cavity with hole size 6 mm x 24 mm in central area of cold wall (see Fig. 3),
3. The same cavity with hole size 6 mm x 50 mm,
4. The same cavity with slot 6 mm x 370 mm.

This testing plan was developed in order to provide validation of the numerical model of the same setup.

Test conditions

During experiments the fan provided average air velocity about 1m/s during the first three tests and 1.2 m/s during the last test. The velocity was measured along the vertical centerline of the insulation panel. Warm side air temperature was 24ºC on average.

Results and discussion

Figure 5.15 shows the results of heat flux measurements for cavity specimen with and without hole.

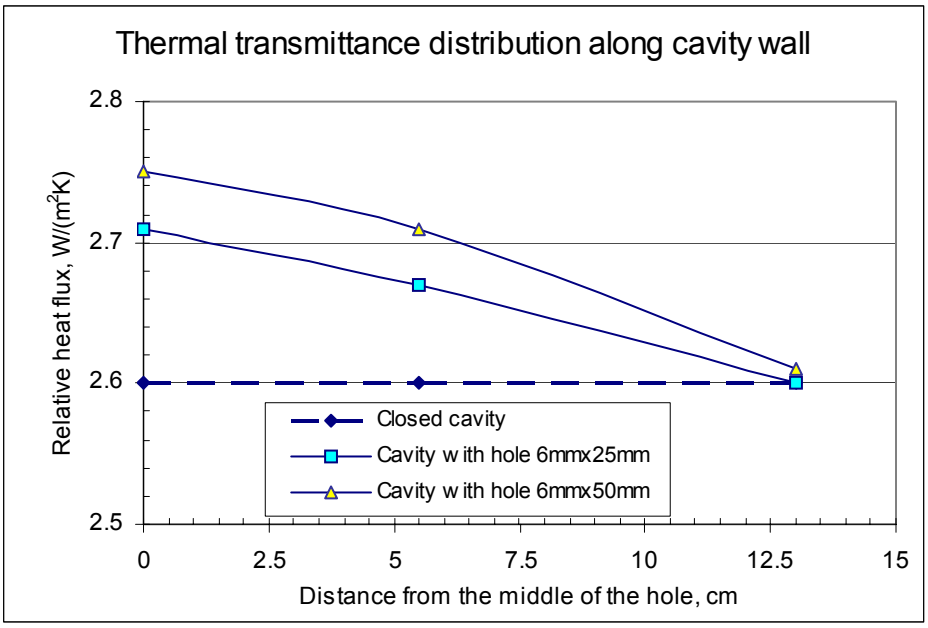


Figure 5.15:. Comparison of Heat Flux Distributions Along Warm Cavity Wall.

Inspection of Figure 5.15 shows that the presence of the hole increases local heat transfer rate by 6% for airflow velocity 1 m/s in comparison with the closed cavity.

For the test of the cavity with slot, different values of heat flux and surface temperatures for different locations on wall surface of the cavity specimen were obtained. This points to the presence of 3-D airflow patterns in the cavity. Heat flux values were obtained in the range from 116 W/(m^2·K) to 166 W/(m^2·K). The average value q = 142 W/(m^2·K) was used for comparing with numerical model.

5.3.3 Numerical model and comparison

Here we are using the method of comparing local values of heat flux and surface temperature on the cavity walls obtained from the test and numerical modeling. The boundary conditions applied to the numerical model are based on values obtained during the test.

The inside and outside local heat transfer coefficients (film coefficients) $h_{i/o}$ on wall surface in the middle of the model and on the panel surfaces were calculated from equation (4.4).

Boundary Conditions:

Boundary conditions were defined for the numerical turbulence model of cavity with slot width 6 mm and airflow with specified velocity and temperature values determined from the test as shown in Figure 5.16.

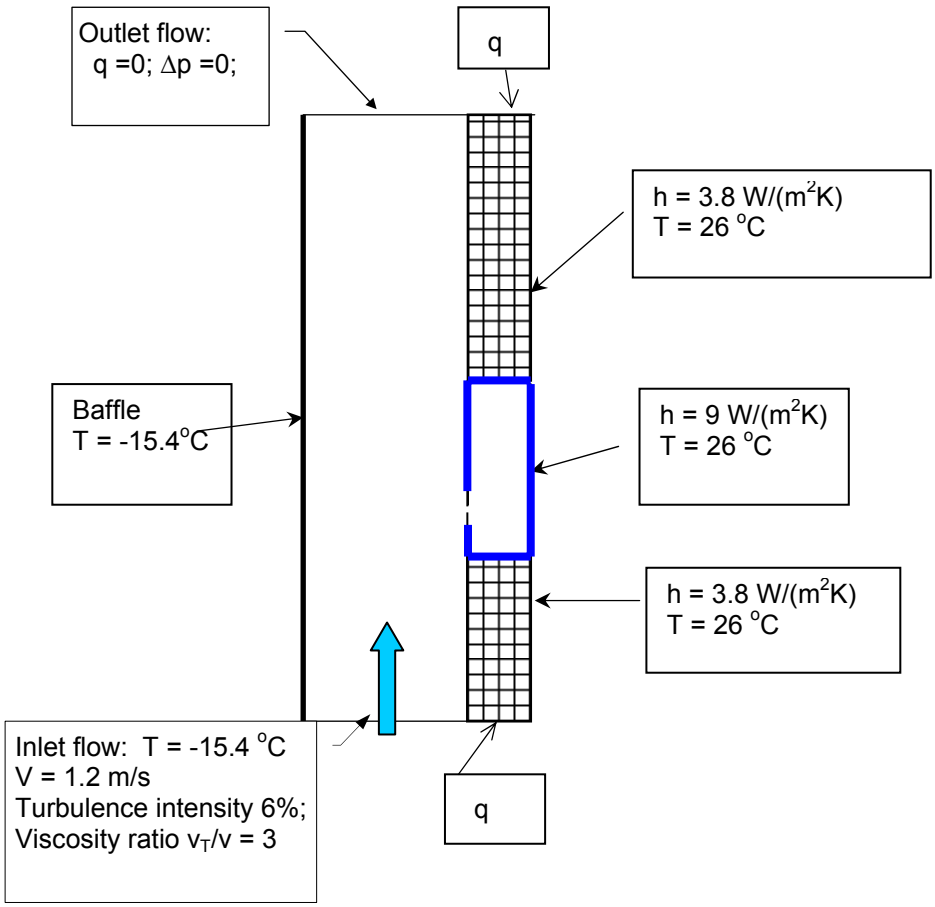


Figure 5.16: Boundary Conditions for the Numerical Model.

Thermo-physical properties of air were treated as constants and were evaluated at the temperature of –15.4 °C for air. Thermal conductivity of insulation panel material was specified as k = 0.024 W/(m·K). Boussinesq approximation was used in viscous turbulent model. Radiation heat transfer was calculated using Fluent DTRM radiation model.

A viscous model was defined as shear-stress transport (SST) k-ω turbulence model with option *transitional flows*.

Results:

Predicted temperature and velocity and turbulence intensity fields in the cavity are shown in Figure 5.17.

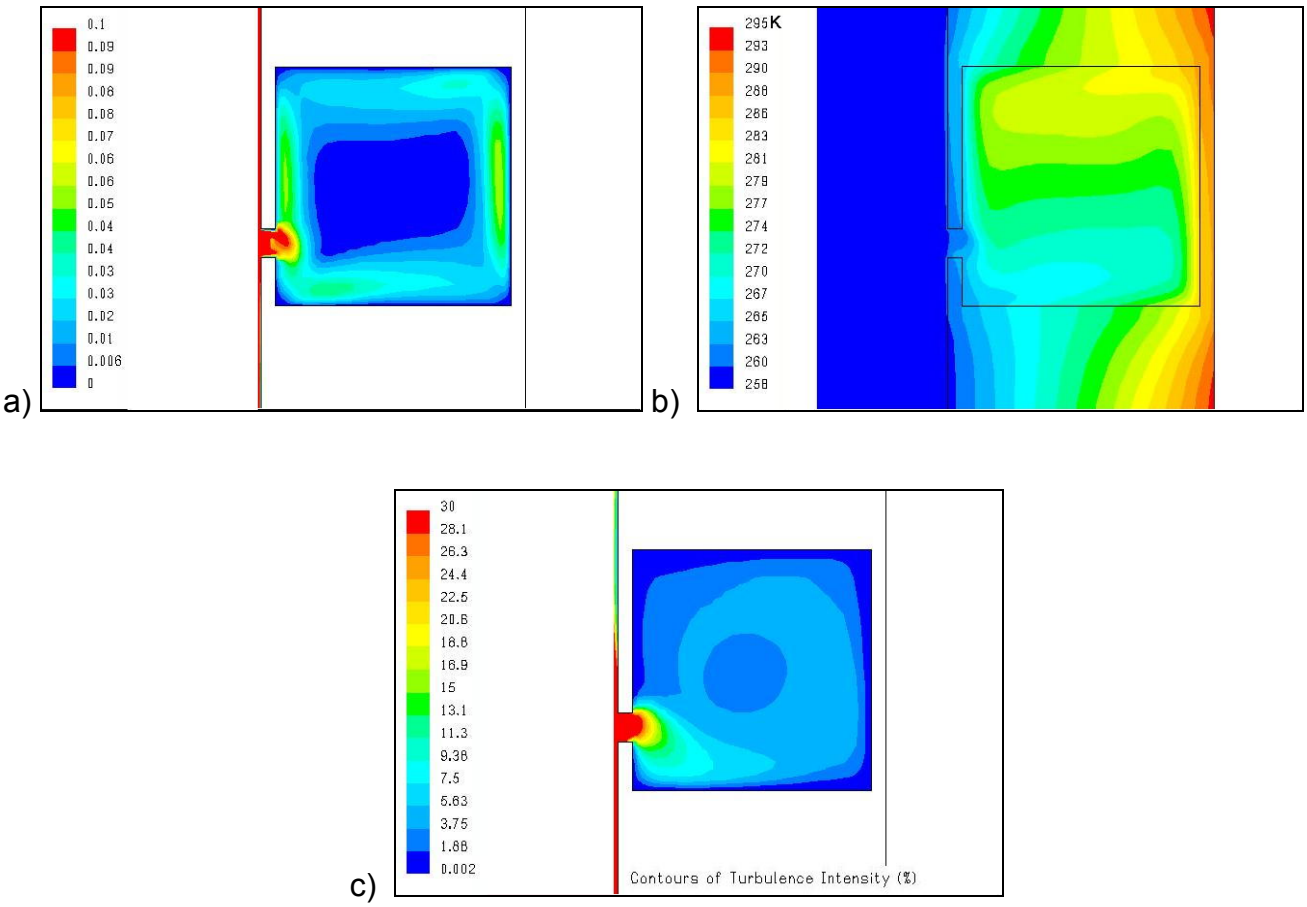


Figure 5.17: Predicted Temperature (a), Velocity (b), and Turbulence Intensity (c) Distributions in the Cavity With Slot.

Results of the simulation and the experiment for ventilated sill cavity specimen with horizontal slot (width 6 mm) are summarized in Table 5.3.

Table 5.3: The Comparison Between Experimental and Predicted Results for the PVC Sill Cavity Specimen H x W x L = 60 cm x 5 cm x 5 cm with horizontal slot 6 mm wide.

Method	Boundary conditions		Hot wall model surface temperature T_{in} , ^0C	Average heat flux on hot wall, (W/m^2)
Test	26.2 °C	-15.4 °C	11.5	116
Simulation	26.2 °C	-15.4 °C	9.6	108
Δq (%)				-6.9%

From the results, presented in Table 5.3, it is obvious that 2-D model makes good prediction of the heat transfer in the cavity with the slot. The difference between measured and predicted average heat fluxes is within 7% in the central area of the slot and only in edge area the difference is so mush as 24% that could be explained by existing 3-D airflow pattern of airflow and convection heat transfer in this area. Study of 3-D convection heat transfer effects in corners is beyond the scope of this study, so these effects are not going to be further investigated here.

Conclusions

- The test for measuring heat transfer through the frame cavity specimen with hole/slot in the cold sidewall was conducted.
- From obtained results it follows that the presence of the hole (6 mm wide and 25/50 mm long) increases local heat transfer rate about 6% for airflow velocity 1 m/s in comparison with the closed cavity.
- Measured heat flux through the wall cavity with slot (6 mm wide and 370 mm long) and surface temperatures were compared with 2-D numerical simulation results under the same boundary conditions. The presence of 3-D airflow and convection heat transfer in the cavity corners was found out during experiment. The 2-D turbulence model can predict accurately heat fluxes and surface temperatures at the central area of the cavity specimen. The difference in predicted and measured average heat fluxes is within 7% and temperature difference is 1.9 ^{o}C.

5.4 Heat transfer correlations for ventilated frame sill cavity

Based on simulation results the heat transfer correlations for ventilated cavities for $Ra < 10^5$ were derived:

$$Nu_{vent} = Nu_{closed}\,(2.24 - 4.1{*}10^{-6}\,Ra) \quad \text{for aspect ratio A = H:L = 1} \quad (5.1)$$

$$Nu_{vent} = Nu_{closed}\,(1.92 - 4.1{*}10^{-6}\,Ra) \quad \text{for aspect ratio A = H:L = 2} \quad (5.2)$$

$$Nu_{vent} = Nu_{closed}\,(1.7 - 3{*}10^{-6}\,Ra) \quad \text{for aspect ratio A = H:L = 0.5} \quad (5.3)$$

For intermediate aspect ratio, a linear interpolation for *Nu* between endpoints of (5.1) – (5.3) can be used.

5.5 Summary

- Modeling convection heat transfer and airflows around and inside ventilated cavities with aspect ratio A = H : L = 2 and A = 1 and A =0.5 under conditions similar to hotbox conditions was accomplished.
- Turbulent 2-D model and method for the calculation of convection heat transfer in ventilated cavities is developed.
- The dependence of ventilated effect from location of a slot in outer cavity wall is obtained.

- The dependence of ventilated effect from *Ra* and from depth of a slot in the cavity wall is obtained.
- Predicted increasing convective heat transfer intensity in ventilated cavities with slot of 5 mm width is in the range from 20 % to 120 % in comparison with closed cavity under same conditions.
- Increasing width of slot opening from 5 mm to 10 mm increases convective heat transfer flow through cavity from 15% to 35% and this increasing depends from cavity size: for smaller cavities it is less.
- Measurements of heat flux through the warm side of the cavity wall with slot (6 mm width and 370 mm length) and surface temperatures were compared with 2-D numerical simulation results under the same boundary conditions. The presence of 3-D airflow and convection heat transfer in the cavity corners was found out during experiment. The 2-D turbulence model can predict accurately heat fluxes and surface temperatures on the cavity wall in the central area. Difference in predicted and measured average heat fluxes is within 7% and temperature difference is 1.9 ^{o}C.
- Heat transfer correlations for ventilated cavities for $Ra < 10^5$ were derived from results of modeling.

6. OVERALL SUMMARY

1. Two Innovative, research level test methods were developed for validating numerical heat transfer modeling in fenestration products and components.
2. Experimental validation of numerical modeling for enclosed sill and head type frame cavities, tilted at an arbitrary angle, using ASTM C518 instrument was accomplished. This experimental validation has also led to the development of the innovative experimental technique for measuring and validating numerical modeling of this class of heat transfer problems (i.e., heat transfer in enclosed rectangular cavities tilted around their long axis).
3. Experimental validation of numerical modeling for enclosed jamb type frame cavities, tilted at an angle of 20 º, using modified hot box apparatus was accomplished. This experimental validation has also led to the development of alternate methodology for research level hot box measurements.
4. Numerical modeling of enclosed sill and head type of frame cavities, tilted around the long axis (i.e., cavities whose long axis is horizontal and when tilted their short axes are tilted while long axis remains horizontal) was done in both 2-D and 3-D modeling space. Numerical modeling has produced experimentally validated results that can be used for the development of heat transfer correlations.
5. New heat transfer correlations for sill, head and horizontal meeting rail type cavities were developed from the 2-D numerical modeling results and they are proposed to replace existing correlations from ISO 15099.

6. Numerical modeling of enclosed jamb type of frame cavities (i.e., cavities whose long axis is vertical in vertically oriented windows and sloped at 20º from horizontal in skylights and sloped fenestration) was done in both 2-D and 3-D modeling space. Ensuing 3-D numerical modeling of these cavities has produced experimentally validated results that can be used for the development of heat transfer correlations.
7. New heat transfer correlations for vertical frame jamb cavities and for frame jamb cavities tilted at other angles have been derived from 3-D modeling results
8. Numerical modeling of enclosed jamb type of frame cavities (i.e., cavities whose long axis is vertical in vertically oriented windows and sloped at 20º from horizontal in skylights and sloped fenestration) was done in both 2-D and 3-D modeling space. Ensuing 3-D numerical modeling of these cavities has produced experimentally validated results that can be used for the development of heat transfer correlations.
9. The 3-D numerical model results of heat transfer rates in vertical and sloped jamb frame cavities agreed well with the experimental results. The difference between predicted and measured surface temperatures was less than 0.6 ºC. The difference between predicted and experimental values of heat flux through the cavity wall in specified locations is less than 6%.
10. Turbulent 2-D model and method for estimation of convection heat transfer in ventilated sill/head cavities are developed. The dependences of ventilated effect from Rayleigh number and location of a slot in outer cavity wall were obtained.
11. Turbulent 2-D model and method for estimation of convection heat transfer in ventilated sill/head cavities are developed. The dependences of ventilated effect from Rayleigh number and location of a slot in outer cavity wall were obtained.

7. CONCLUSIONS

1. Newly developed experimental techniques for measuring heat transfer in vertical and tilted frame cavities (i.e., modified C518 apparatus for horizontal frame members and modified hot box apparatus for vertical frame members) can be used for research level validation of numerical modeling of heat transfer by convection in these cavities.
2. The 2-D modeling assumption is appropriate to predict natural convection heat transfer in frame cavities tilted around the long axis, such as the ones found in sill, head and horizontal meeting rail and mullion cross-sections (i.e., horizontal frame members).
3. The 2-D modeling assumption is not appropriate to predict natural convection heat transfer in frame cavities tilted around the short axes, such as the ones found in jambs, and vertical meeting rail and mullion cross-sections (i.e., vertical frame members) and full 3-D models need to be utilized.

4. From 3-D modeling results it can be concluded that for vertical frame members, frame cavity correlation equations suggested by ISO 15099 do not match well the results of this study and new correlations will have to be proposed.
5. Numerical modeling of ventilated frame cavities produced experimentally validated results. The new correlations are proposed for the calculation of convection heat transfer in these cavities.

8. RECOMMENDATIONS

1. New set of heat transfer correlations is developed for natural convection heat transfer in rectangular frame cavities of the sill, head and horizontal meeting rail type. The set of correlations is presented below:

Aspect ratio	Tilt angle	Correlation
A = 0.5	90°	$Nu_{(\theta=90^\circ)} = 5.58 - 4.63 \cdot \left[1 + \left(\frac{Ra}{71497}\right)^{1.26}\right]$
	70° ≤ θ ≤ 20°	$Nu_{(\theta)} = 0.08 + \left[1.147 \cdot \left(Nu_{(\theta=90^\circ)}\right)^{0.975} + 0.008 \cdot (70 - \theta)\right]$
	90° < θ < 70°	Linear interpolation between endpoints $Nu_{(\theta=90^\circ)}$ and $Nu_{(\theta=70^\circ)}$
A = 1	90° ≤ θ ≤ 20°	$Nu = 0.194 \cdot Ra^{0.2732}$
0.5 < A < 1	90° ≤ θ ≤ 20°	Linear interpolation between in aspect ratio A between endpoints of $Nu_{A=0.5}$ and $Nu_{A=1}$
A = 5	90° ≤ θ ≤ 45°	$Nu = Nu_{(ISO)}$, where $Nu_{(ISO)}$ is Nusselt numbers from eq. 90-92 in ISO 15099
	45° < θ ≤ 20°	$Nu = Nu_{(ISO)} - 0.28 * cos(\theta)$
1<A<5	90° ≤ θ ≤ 20°	Linear interpolation between endpoints of $Nu_{A=1}$ and $Nu_{A=5}$

2. New heat transfer correlation is developed for natural convection heat transfer in rectangular frame cavities of the jamb and vertical meeting rail and mullion type. The correlation is presented below

$$N_{3D} = 1 + 0.4\left[Nu_{2D} - 1 - \left(0.0047 \cdot A_h^{1/A_h} \cdot Ra \cdot 10^{1.1}\right)\right] \cdot \left[1 + \sqrt{A_h \cdot \left(0.8 - \frac{A}{100}\right)}\right] Arc\tan\sqrt{A_h}$$

The application range for the above equation is:

$20 \le A \le 40$; $0.5 \le A_h \le 2$; $15{,}000 \le Ra < 120{,}000$

Where:

Nu_{2D} = Nusselt number as defined in eq. 88–92 from ISO 15099

A = Vertical aspect ratio of cavity, H/L

A_h = Horizontal aspect ratio of cavity, W/L

Ra = Rayleigh number

3. New set of heat transfer correlations are developed for convection heat transfer in ventilated frame cavities. The correlation is presented below:

$Nu_{vent} = Nu_{closed} \cdot \left(2.24 - 4.1 \cdot 10^{-6} \cdot Ra\right)$; $A = H{:}L = 1$, $Ra < 10^5$

$Nu_{vent} = Nu_{closed} \cdot \left(1.92 - 4.1 \cdot 10^{-6} \cdot Ra\right)$; $A = H{:}L = 2$, $Ra < 10^5$

$Nu_{vent} = Nu_{closed} \cdot \left(1.70 - 3.0 \cdot 10^{-6} \cdot Ra\right)$; $A = H{:}L = 0.5$, $Ra < 10^5$

For intermediate aspect ratios, a linear interpolation for *Nu* between endpoints should be used.

9. REFERENCES

Arnold, J. N., Catton, I., and Edwards, D. K., 1976, "Experimental Investigation of Natural Convection in Inclined Rectangular Regions of Differing Aspect Ratios," Journal of Heat Transfer, Vol. 98, pp. 67-71

Asako, Y., Nakamura, H., Chen, Z., 1990, "Three-Dimensional Laminar Natural Convection in an Inclined Air Slot with a Hexagonal Honeycomb Core", AIAA/ASME Thermophysics and Heat Transfer Conference, Seattle, ASME HTD-Vol. 140, pp. 9-16.

ASTM C 518 – 98, 1998, "Standard Test Method for Steady-State Thermal Transmission Properties by Means of the Heat Flow Meter Apparatus".

Ayyaswamy, P.S., and Catton, I. 1973. "The boundary-layer regime for natural convection in a differentially heated, tilted rectangular cavity," Journal of Heat Transfer, Vol. 95, pp. 543-545.

Batchelor, G.K., 1954, "Heat Transfer by Free Convection Across a Closed Cavity Between Vertical Boundaries at Different Temperatures," Quarterly of Applied Mathematics, Vol. 12, pp. 209-223.

Bejan, A., and Tien, C.L., 1978, " Laminar Natural Convection Heat Transfer in a Horizontal Cavity With Different End Temperatures," Journal of Heat Transfer, Vol. 100, pp. 641-647.

Bilgen, E., and Oztop, H., 2004, “Natural convection heat transfer in partially open inclined square cavities”, International Journal of Heat and Mass Transfer, Vol. 48, pp. 1470-1479.

Bonacina, C., Giacomin, G., and Strada, .M., 1981, “A numerical analysis of free convection in inclined square enclosures”, La Termotecnica, Vol. 35, pp. 574-588.

Catton, I., Ayyaswamy, P.S., and Clever, R.M., 1974, “Natural Convection Flow in a Finite, Rectangular Slot Arbitrarily Oriented with Respect to the Gravity Vector,” International Journal of Heat and Mass Transfer, Vol. 17, pp. 173-184.

Chan, Y.L., Tien, C.L., 1985, “A numerical study of two-dimensional laminar convection in shallow open cavities”, International Journal of Heat and Mass Transfer, Vol. 28, pp. 603-612.

Chen, C.J., and Talaie, V., 1985, “Finite Analytic Numerical Solutions of Laminar Natural Convection in Two-Dimensional Inclined Rectangular Enclosures,” ASME paper 85-HT-10.

Cormack, D.E., Leal, L.L., and Seinfield, J.H., 1974, "Natural Convection in a Shallow Cavity with Differentially Heated End Walls: Part 2 - Numerical Solutions," Journal of Fluid Mechanics, Vol. 65, pp. 231-246.

Curcija, D., 1992. “Three-Dimensional Finite Element Model of Overall Night Time Heat Transfer Through Fenestration Systems”, PhD Thesis, University of Massachusetts, Amherst.

Datafit 8.1, Oakdale Engineering, http://www.curvefitting.com.

De Vahl Davis, G., 1968, “Laminar Natural Convection in a Rectangular Cavity,” International Journal of Heat and Mass Transfer, Vol. 11, pp.1675-1693.

De Vahl Davis, G., 1983, “Natural Convection of Air in a square cavity: A Bench mark numerical solution,” International Journal for Numerical methods in Fluids, Vol. 3, pp.249-264.

OMEGA. 2002. “Digital Calibrator/Thermometer CL23A, 24, 25, 26, 27. User’s Guide.” OMEGA Corporation.

Elsayed, M.M., Chakroun, W., 1999, “Effect of Aperture Geometry on Heat Transfer in Tilted Partially Open Cavities”, Journal of Heat Transfer, Vol. 121, pp. 819-827

Elsherbiny, S.M., Raithby, G. D., and Hollands, K. G. T., 1982, “Heat Transfer by Natural Convection across Vertical and Incline Air Layers,” Transactions of the ASME, Vol. 104, pp. 96-102

Fluent. 2001. Fluent 6. Fluent Inc, Nashua, NH.

FOX. 2004. “FOX200 and FOX300 Series Instruments Manual”. LaserComp, Inc., 1999-2004

Fusegi, T., Hyun, J.M., Kuwahara, K., and Farouk, B., 1991, “A numerical study of three-dimensional natural convection in a differentially heated cubical enclosure”, International Journal of Heat and Mass Transfer, Vo. 34, pp. 1543-1557

Gustavsen, A., 2001, “Heat transfer in window frames with internal cavities”, PhD Dissertation, Department of Building and Construction Engineering, Norwegian University of Science and Technology, Norway

Gustavsen, A., Griffith, T.B., and Arasteh, D., 2001, “Three-Dimensional conjugate computational fluid dynamics simulations of internal window frame cavities validated using Infrared Thermography”, ASHRAE Transactions, Vol. #107, Part 2, pp. 538-549

Hollands, K.G.T., and Konicek, L., 1973, “Experimental Study of the Stability of Differentially Heated Inclined Air Layers,” International Journal of Heat and Mass Transfer, Vol. 16, pp.1467-1476.

Hollands, K. G. T., Unny, T. E., Raithby, G. D., and Konicek, L., 1976, “Free Convective Heat Transfer across Incline Air Layers,” Journal of Heat Transfer, Vol. 98, pp.189- 193.

Hoogendoorn, C.J., 1986, “Natural convection in enclosures”, Proceedings of the Eight International Heat Transfer Conference, Vol. 1, pp. 111-120.

HP. 2000. “HP 34970A Data Acquisition/Switch Unit. User’s Guide”. Hewlett Packard.

ISO. 2003, “Thermal Performance of Windows, Doors and Shading Devices – Detailed Calculations,” ISO 15099:2003(E)

Miyamoto, M., Kuehn, T.H., Goldstein, J., Katoh, Y., 1989, “Two-dimensional laminar natural convection heat transfer from a fully or partially open square cavity”, Numerical Heat Transfer, Part A, Vol. 15, pp. 411-430

Ozoe, H., Sayama, H., and Churchill, S. W., 1975, “Natural Circulation in an Inclined Rectangular Channel at Various Aspect Ratios and Angles—Experimental Measurements,” International Journal of Heat and Mass Transfer, Vol.18, pp.1425-1420

TSI. 2000. *Airvelocity meter VelociCalc®Plus*. TSI Incorporated. Operation and service manual. 2000.

Yang, H.Q., Yang, K.T., and Lloyd, J.R., 1986, "Flow Transition in Laminar Buoyant flow in a three dimensional tilted rectangular enclosure", Proceedings of 8th International Heat Transfer Conference. Vol. 4, pp. 1495-1500

Yang, Y., 2003, “Natural convective flow and heat transfer in vertical and inclined glazing cavities,” M.S. Thesis, Department of Mechanical and Industrial Engineering, University of Massachusetts, Amherst

Zhao, Y., Curcija, D., and Goss, W.P., 1999, “Convective Heat Transfer Correlations for Fenestration Glazing Cavities: A Review,” ASHRAE Transactions, Vol. 105, Part 2

APPENDIX A:

Velocity vector contours for sill cavity A = 1:2

a) 90 deg

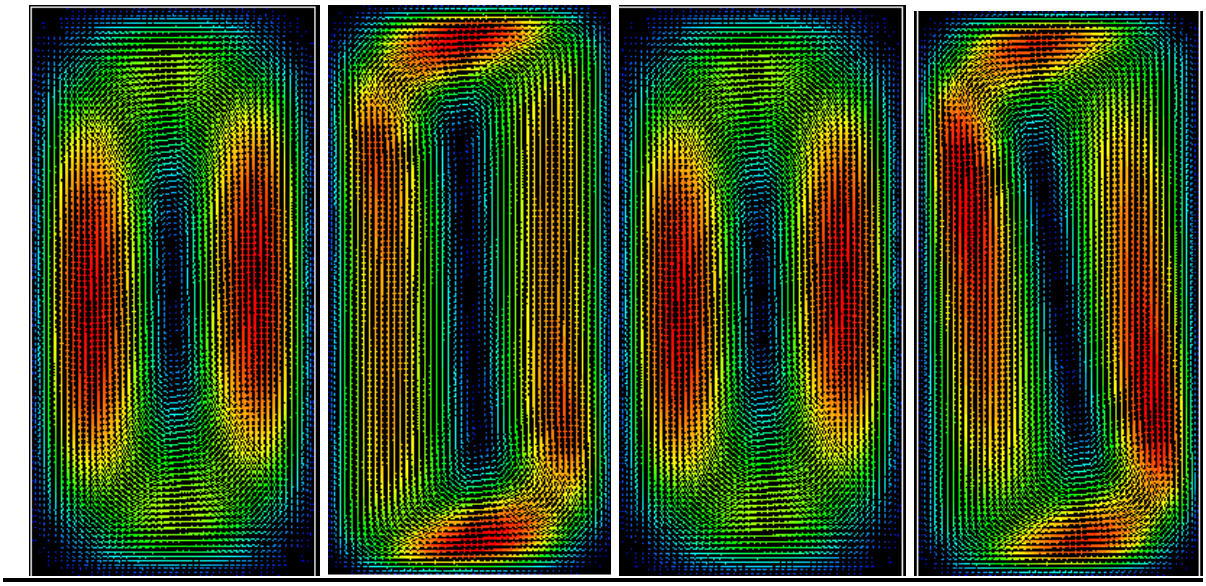
Gravity vector: ⇦

Ra = 2316 Ra = 92625

b) 70 deg

Gravity vector: ⇙

Ra = 2316 Ra = 92625



c) 45 deg

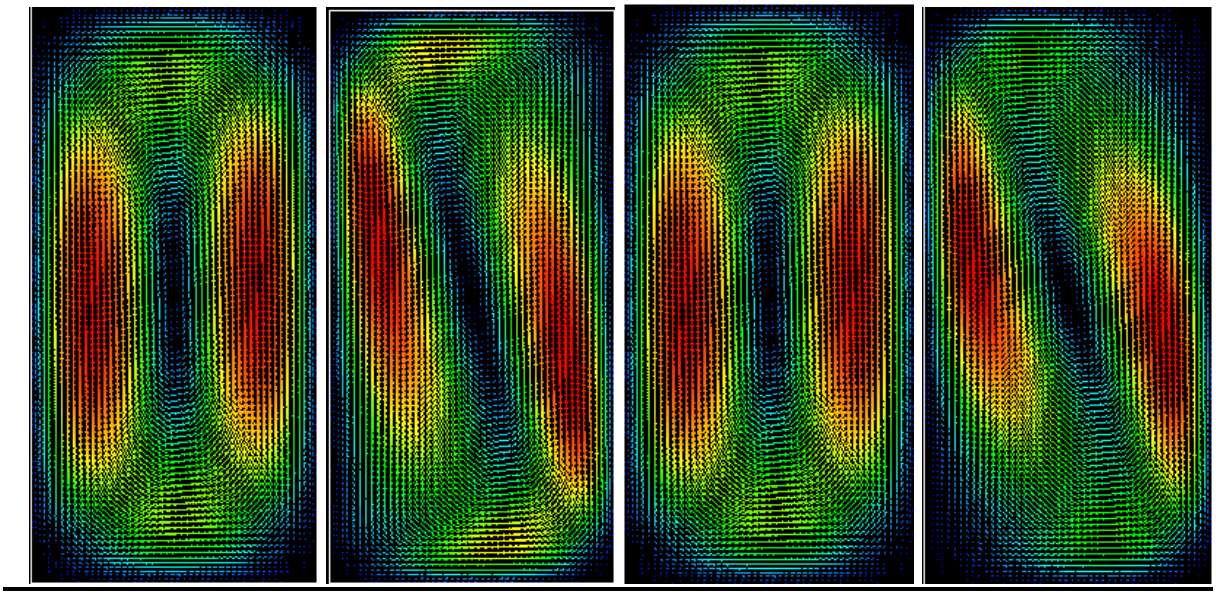
Gravity vector: ⇙

Ra = 2316 Ra = 92625

d) 20 deg

Gravity vector: ⇓

Ra = 2316 Ra = 92625



APPENDIX B:

Table B1: Comparison of heat transfer rate between 2D and 3D silll cavity models with A = 0.25, 0.5, 0.625, 0.75, 1, 2, 4 and 5, RA= 92,625, $\Theta = 90^0$, 45^0 and 20^0

Tilt angle (Degrees)	Aspect ratio (H/L)	Cavity size H x L (cm)	Average heat flux on hot wall (W/m^2)		Average Nu on hot wall		% Difference in average Nu between 2D and 3D Models	Comments on flow pattern
			2D Model	3D Model	2D Model	3D Model		
90^0	0.25	1 x 4	8.20	8.14	1.36	1.35	0.7%	Single cell
	0.5	2 x 4	21.96	21.71	3.65	3.61	1.2%	Single cell
	0.625	2.5 x 4	24.93	24.49	4.15	4.07	1.8%	Single cell
	0.75	3 x 4	26.05	25.61	4.33	4.26	1.7%	Single cell
	1	4 x 4	26.63	26.45	4.43	4.40	0.7%	Single cell
	2	8 x 4	25.41	25.60	4.22	4.26	-0.7%	Single cell
	4	16 x 4	22.61	22.57	3.76	3.75	0.2%	Single cell
	5	20 x 4	21.67	21.49	3.60	3.57	0.8%	Single cell
45^0	*0.25*	*1 x 4*	*8.65*	*19.98*	*1.44*	*3.32*	***-56.7%***	***Multi cell***
	0.5	2 x 4	24.65	25.28	4.10	4.20	-2.5%	Single cell
	0.625	2.5 x 4	26.67	26.27	4.43	4.37	1.5%	Single cell
	0.75	3 x 4	27.13	26.71	4.51	4.44	1.6%	Single cell
	1	4 x 4	27.35	27.25	4.55	4.53	0.4%	Single cell
	2	8 x 4	25.75	25.91	4.28	4.31	-0.6%	Single cell
	4	16 x 4	22.24	22.21	3.70	3.69	0.1%	Single cell
	5	20 x 4	21.16	21.09	3.52	3.51	0.3%	Single cell
20^0	*0.25*	*1 x 4*	*7.47*	*20.86*	*1.24*	*3.47*	***-64.2%***	***Multi cell***
	0.5	*2 x 4*	*21.03*	*26.55*	*3.50*	*4.41*	***-20.8%***	***Multi cell***
	0.625	2.5 x 4	24.28	23.96	4.04	3.98	1.3%	Single cell
	0.75	3 x 4	25.09	24.67	4.17	4.10	1.7%	Single cell
	1	4 x 4	25.73	25.59	4.28	4.25	0.5%	Single cell
	2	8 x 4	24.60	24.51	4.09	4.08	0.4%	Single cell
	4	16 x 4	20.31	20.37	3.38	3.39	0.3%	Single cell
	5	*20 x 4*	*19.14*	*18.93*	*3.18*	*3.15*	***1.1%***	***Multi cell***

APPENDIX C:

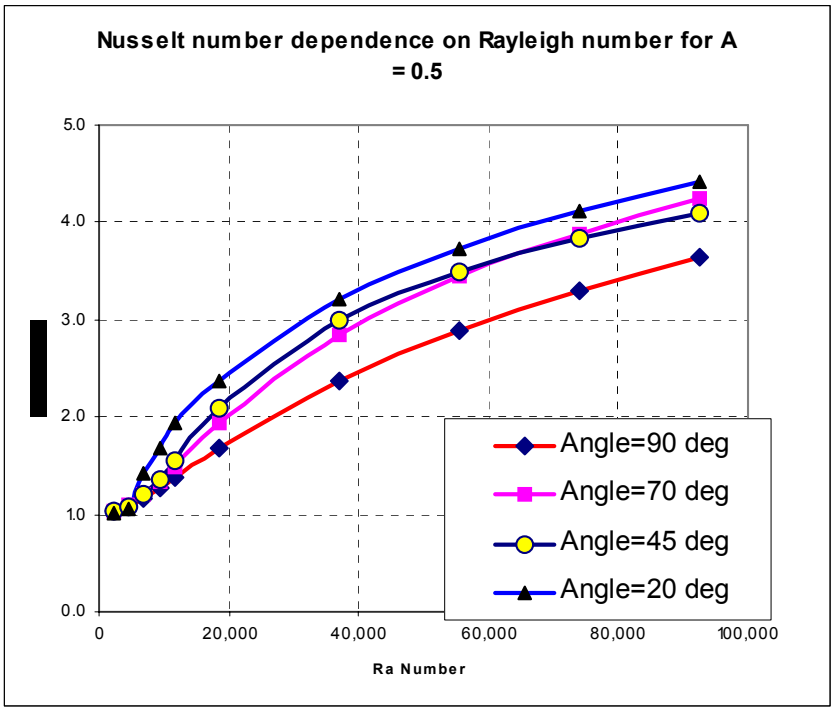


Figure C1: Frame sill cavity – *Nu* vs. *Ra* for A = 0.5 and $\Theta = 90^0, 70^0, 45^0, 20^0$

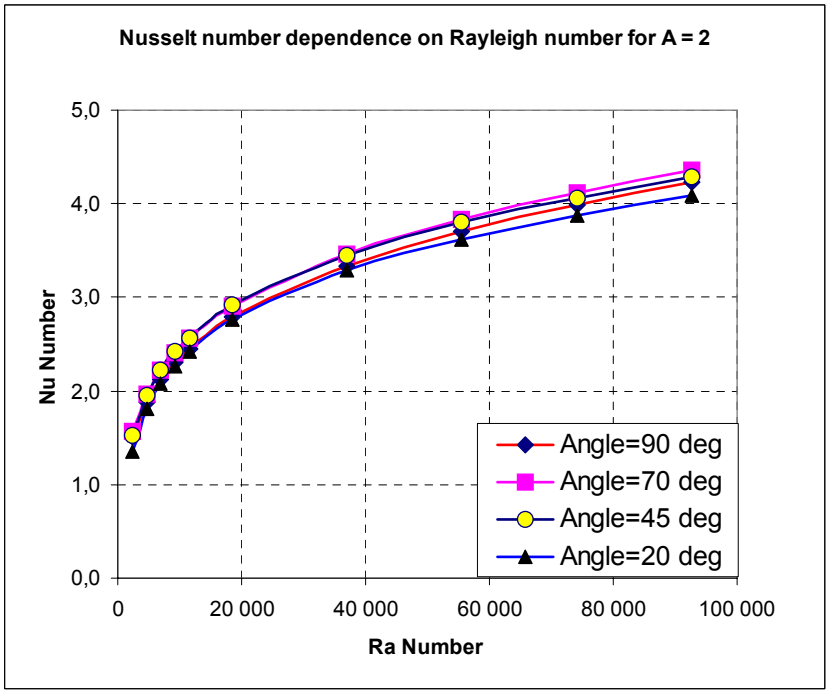


Figure C2: Frame sill cavity – *Nu* vs. *Ra* for A = 2.0 and $\Theta = 90^0, 70^0, 45^0, 20^0$

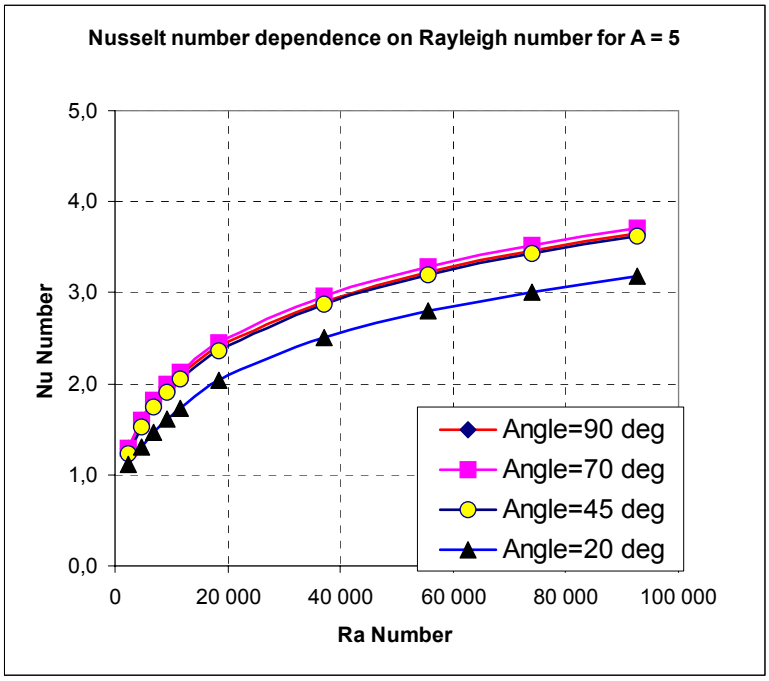


Figure C3: Frame sill cavity – *Nu* vs. *Ra* for A = 5.0 and $\Theta = 90^0, 70^0, 45^0, 20^0$

APPENDIX D:

Jamb cavities. Source data for diagrams on Figures 4.30, 4.31, and 4.32.

Table D1: *Nu* for $\theta = 90^0$ from the New Correlation Equation for the Three Cavities Modeled

Ra	A=25:1, A_h=1:1	A=25:1, A_h=2:1
18,525	1.3437	1.5245
37,050	1.6694	1.8859
55,575	1.9265	2.1463
74,100	2.1304	2.3368
92,625	2.2944	2.4767

Ra	A=20:1, A_h=1:2
27,136	1.3959
36,181	1.5298
72,363	1.9607
108,544	2.2747
144,726	2.5170

Table D2: *Nu* for $\theta = 45^0$ and 20^0 for Cavity A=25:1, A_h=1:1

Ra number	Current Study - 45^0	Proposed Correlation - 45^0	Current Study - 20^0	Proposed Correlation - 20^0
18,525	2.25	2.34	2.46	2.59
37,050	2.67	2.70	2.91	2.92
55,575	2.92	2.93	3.20	3.17
74,100	3.12	3.13	3.40	3.38
92,625	3.30	3.29	3.56	3.54

Table D3: Nusselt number for $\theta = 45^0$ and 20^0 for cavity A=25:1, A_h=2:1

Ra	Current Study - 45^0	Proposed Correlation - 45^0	Current Study - 20^0	Proposed Correlation - 20^0
18,525	2.34	2.42	2.66	2.67
37,050	2.91	2.79	3.09	3.03
55,575	3.05	3.05	3.16	3.29
74,100	3.12	3.24	3.46	3.48
92,625	3.40	3.38	3.60	3.62

Project 1.1.7

Project Name:	Development of a Procedure and a Model for U-factor Rating of Domed Skylights
Date:	December 27, 2007
Purpose:	The main purpose of this project was to develop heat transfer correlations for domed skylights, leading to the development of simulation method for U-factors and SHGC of domed skylights and other products that incorporate similar geometries.

Project Summary:

Literature review of the published numerical and experimental studies on convection heat transfer in curvilinear spaces was done to present current state-of-the-art and to identify potentially useful body of work for this study. Most of the identified work had limited usability and confirmed the need for the development of new set of heat transfer correlations that would be used in NFRC rating process.

3-D numerical modeling, utilizing laminar viscous convection heat transfer model and 3-D view-factor based radiation model were developed for Type-A and Type-B domed skylight glazing cavities and detailed heat transfer results, based on runs with range of boundary conditions and geometry parameters were presented and used in the development of generalized heat transfer correlations.

Experimental validation of numerical results were carried out for both Type-A and Type-B domed skylight glazing systems using innovative experimental technique for obtaining local heat transfer fluxes and temperatures. Experimental results agreed very well with the numerical models, giving confidence to the full numerical study used for the development of convective heat transfer correlations.

Click here for final report

C E E R E

Center for Energy Efficiency and Renewable Energy

Building Energy Efficiency Program



University of Massachusetts

Engineering Laboratory Building
160 Governor's Dr
Amherst, MA 01003-9265

Final Report:

Development of a Procedure for U-Factor Rating of Domed Skylights

Submitted by: *Dr. Alexander Fomichev*
Dr. D. Charlie Curcija

December 27, 2007

TABLE OF CONTENTS

1. Executive Summary 4

2. Introduction 4

2.1 Background 4

2.2 Objectives 5

3. Literature Review 5

4. Basic Parameters and Geometrical Consideration for Domed Skylights 6

4.1 Results and Validation of the numerical model 8

4.2 Summary 13

4. Analysis of Domed Skylight Glazing Configurations and Geometry 14

4.1 Domed Skylight Glazing Type-A 14

4.2 3-D Numerical Modeling of Convection Heat Transfer in Type-A Glazing Cavity. 16

4.2.1 Description of boundary conditions and numerical model. 16

4.2.2 Results and discussion 18

4.3 Heat transfer correlations for domed glazing cavity of a Type-A 26

4.3.1 Heat transfer correlations for Type-A domed skylight glazing cavities in vertical orientation 26

4.3.2 Heat transfer correlation for Type-A domed skylight glazing cavities in tilted orientation 29

4.4 Domed Skylight Glazing Type-B 30

Figure 22. Cross-Section of the Type-B Domed Skylight Glazing Cavity 31

4.5 3-D Numerical Modeling of Convection Heat Transfer in Type-B Glazing Cavity. 32

4.5.1 Description of boundary conditions and numerical model. 32

4.5.2 Results and discussion 34

4.6 Heat transfer correlations for domed glazing cavity of a Type-B 41

4.6.1 Heat transfer correlations for Type-B domed skylight glazing cavities in vertical orientation 41

4.6.2 Heat transfer correlations for Type-B domed skylight glazing cavities in tilted orientation 43

4.7 Summary 45

5. Experimental Study and Validation of Heat Transfer in Domed Skylight Glazing Cavities 45

5.1 Experiment Description 45

5.2 Calculation of the heat transfer (film) coefficient 48

5.3 Numerical model for Validation 49

5.4 Domed Skylight Glazing Type-A 49

5.5 Domed Skylight Glazing Type-B 56

5.5 Summary 60

6. Conclusions 61

7. Recommendations 62

8. References 63

1. EXECUTIVE SUMMARY

This research was undertaken under the grant with National Fenestration Rating Council in an effort to develop heat transfer correlations for domed skylights, leading to the development of simulation method for U-factors and SHGC of domed skylights and other products that incorporate similar geometries.

Literature review of the published numerical and experimental studies on convection heat transfer in curvilinear spaces was done to present current state-of-the-art and to identify potentially useful body of work for this study. Most of the identified work had limited usability and confirmed the need for the development of new set of heat transfer correlations that would be used in NFRC rating process.

Survey of the market and current practices in North America identified three distinct types of domed skylight glazing systems so they were categorized in Type-A, Type-B, and Type-C. Type-A and Type-B are double glazing layer configurations, while Type-C were triple and quadruple configurations. It was concluded that Type-C glazing systems can be constructed by combining Type-A and/or Type-B glazing cavities, so the detailed heat transfer analysis was done for Type-A and Type-B only.

Before numerical modeling was done, rules were developed for generating domed skylight glazing cavities by using geometrical primitives, which led to the identification of basic geometric parameters, radius of curvature, glazing base, maximum gap width and combination of those (e.g., aspect ratio, etc.). Formulas based on geometry analysis were developed to construct 3-D numerical models.

Preliminary numerical analysis indicated that it will be necessary to develop 3-D numerical models, as 2-D models were not adequate in capturing all of the flow and heat transfer details in non-uniform domed skylight glazing cavities.

3-D numerical modeling, utilizing laminar viscous convection heat transfer model and 3-D view-factor based radiation model were developed for Type-A and Type-B domed skylight glazing cavities and detailed heat transfer results, based on runs with range of boundary conditions and geometry parameters were presented and used in the development of generalized heat transfer correlations.

Experimental validation of numerical results were carried out for both Type-A and Type-B domed skylight glazing systems using innovative experimental technique for obtaining local heat transfer fluxes and temperatures. Experimental results agreed very well with the numerical models, giving confidence to the full numerical study used for the development of convective heat transfer correlations.

2. INTRODUCTION

2.1 Background

Domed skylights represent broad range of products in which transparent portion of the product is comprised of curvilinear geometry, forming uneven glazing cavities. These

products are typically manufactured from polymer materials which are easier to form into the curvilinear shapes. These products are very different from the standard fenestration products incorporating plane glazing, separated by a uniform gap. The reason for their curvilinear geometry is to maximize their visible transmittance at of-normal angles. This is due to their primary purpose, which is to provide daylighting in spaces. Often, these products are arranged in double or triple configurations (rarely quadruple configurations), where each dome roughly corresponds to the section of sphere. The space between them often resembles geometry that would be obtained if two spheres with the same or different radii are intersected. When the sphere has same radii, then space with uniform distance is obtained, while in the former case variable gap width space is obtained. Also, some domed skylight glazing products are formed by using one or more flat glazing in combination with one or more curvilinear glazing.

Currently NFRC, as well as other relevant domestic and international standards (NFRC 100, ISO 15099, ISO 10077, etc.) do not provide any heat transfer correlations for these non-uniform curvilinear geometries, so the only way to rate such products at NFRC is to measure their thermal and solar-optical performance. These systems can be oriented horizontally, or at an angle. NFRC rates skylights at an angle of 20º, but validates simulations at vertical orientation. For these reasons all simulations were carried at vertical orientations and 20º tilt from horizontal. Experimental validation was done for vertical glazing only.

2.2 Objectives

The main objective of this research project is to develop set of convection heat transfer correlations for equidistant or variable spacing domed skylight glazing cavities found in typical North American domed skylights. These correlations are intended to be in a form that is easily incoporated into the NFRC rating tools WINDOW and THERM.

.

3. LITERATURE REVIEW

There are currently very limited numerical or experimental studies of the convection heat transfer in curvilinear spaces with varying cavity width between glazing layers. These are the geometries and configurations that are typical of domed skylights.

Laouadi and Atif (2001) completed a numerical study on the heat transfer by steady-state laminar natural convection within multi-layer domes with uniform spacing. These models assumed heating from the above. They were able to develop correlations for heat transfer as a function of both the dome shape and the gap spacing between the layers. They define the term, δ as the dimensionless gap spacing between dome layers. By performing numerical analysis of both, the low profile and fully hemispherical domes both with various values of δ, they were able to reach the following conclusions: (1) Convection heat transfer is more that 10% higher for hemispherical domes as compared to low profile domes with

small values of δ (<0.1) and (2) convection heat transfer is more than 100% higher for hemispherical domes as compared to low profile domes with large values of δ (>0.3). These results are related to the flow patterns they observed in this analysis. For fully hemispheric domes, the flow patters were consistently in a form of single cell for all values of δ. However, for low profile domes, large gap spaces produced two cells. Finally, their research also suggests the existence of a critical gap space for each dome analyzed. The convection heat transfer increases to a maximum at this critical value of δ and then decreases upon further increases of the gap spacing.

Also relevant are the assumptions, boundary conditions, and modeling techniques employed by Laouadi and Atif (2001). The primary numerical assumptions employed are as follows: the fluid is incompressible, the buoyancy-driven flow within the dome gap is laminar, the physical properties of the fluid are constant except for density, and fluid density is given by the Boussinesq's approximation. The boundary conditions assume no-slip and uniform temperature conditions at the dome walls. Furthermore, symmetry and adiabatic conditions can be employed at the axis of revolution and the edges respectively. Finally, most relevant to the current study the observation made by Lauoadi and Atif (2001) with regards to the case when the interior dome wall is hotter than the exterior. This case, which was not the major focus of their research, yielded unsteady, periodic flow, particularly for small values of the gap spacing.

The results of numerical modeling were compared to numerical research of Garg (1991) and to correlation developed by Raithby and Hollands (1975), in which experimental data of Bishop (1965) was used. The results of Laouadi and Atif (2001) are in good agreement with numerical results obtained by Garg (1991). However, only horizontal orientation of the dome was investigated in (2001).

4. BASIC PARAMETERS AND GEOMETRICAL CONSIDERATION FOR DOMED SKYLIGHTS

Figure 1 shows simplified view of a domed skylight glazing system with uniform spacing between two concentric spheres. The basic geometrical parameters (dimensions and radii) as defined for a domed skylight glazing cavity are:

- R_i and R_o – inner and outer radii of spheres;
- H – Curvature of the glazing cavity;
- L – gap spacing between spherical surfaces of glazing cavity;
- Aspect Ratio $A_L = H/L$;
- Aspect Ratio $A_H = H/R_i$.

The parameter $A_H = 1$ for a fully hemispherical domed skylight, $0 < A_H < 1$ for low profile domed skylights and $A_H = 0$ for concentric disks.

Domed skylights often incorporate non-uniform gap widths and these will be presented later in this report.

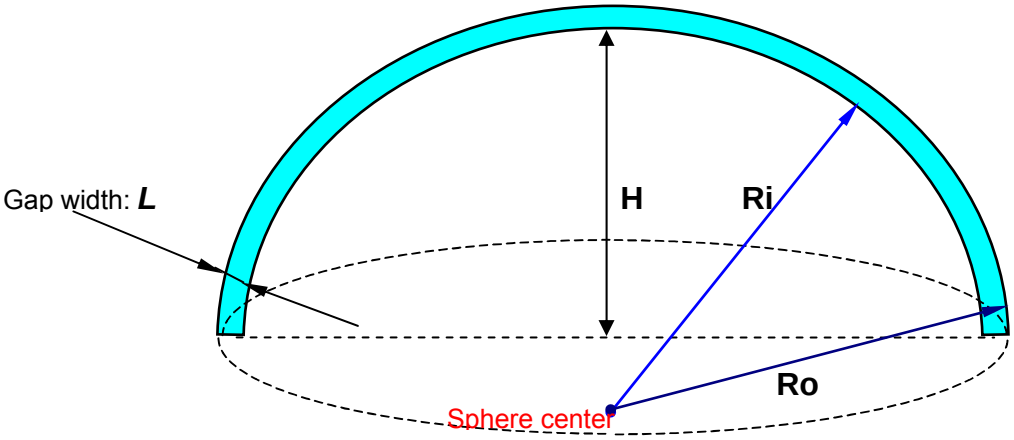


Figure 1. Schematic of Domed Skylight Glazing System with Uniform Gap Width

Table 1 presents the parameters for the example domed skylight for the 3-D heat transfer simulation in the range of Raleigh number from Ra = 4,000 to Ra = 80,000.

Table 1. Matrix of Glazing Cavity Configurations and Sizes

Inner radius R_i = 0.8 m								**Inner radius R_i = 1.2 m**							
A_H = 1		A_H = 1		A_H = 0.5		A_H = 0.5		A_H = 1		A_H = 1		A_H = 0.5		A_H = 0.5	
L = 16 mm		L = 25 mm		L = 16 mm		L = 25 mm		L = 16 mm		L = 25 mm		L = 16 mm		L = 25mm	
Tilt angle from horizontal direction															
20°	**90°**	**20°**	**90°**	**20°**	**90°**	**20°**	**90°**	**20°**	**90°**	**20°**	**90°**	**20°**	**90°**	**20°**	**90°**

In order to develop an effective 3-D model of heat transfer in a gap of the domed skylight, it is necessary to perform mesh study first. The initial study involved the diameter of the dome of D = 0.6m and gap spacing of L = 0.025m. Figure 2 shows 3-D mesh model of fully hemispherical domed skylight glazing cavity created from T-Grid elements (detailed description of T-Grid elements is provided in FDI (2003)). The details of boundary layer mesh within glazing cavity model are shown in Figure 3.

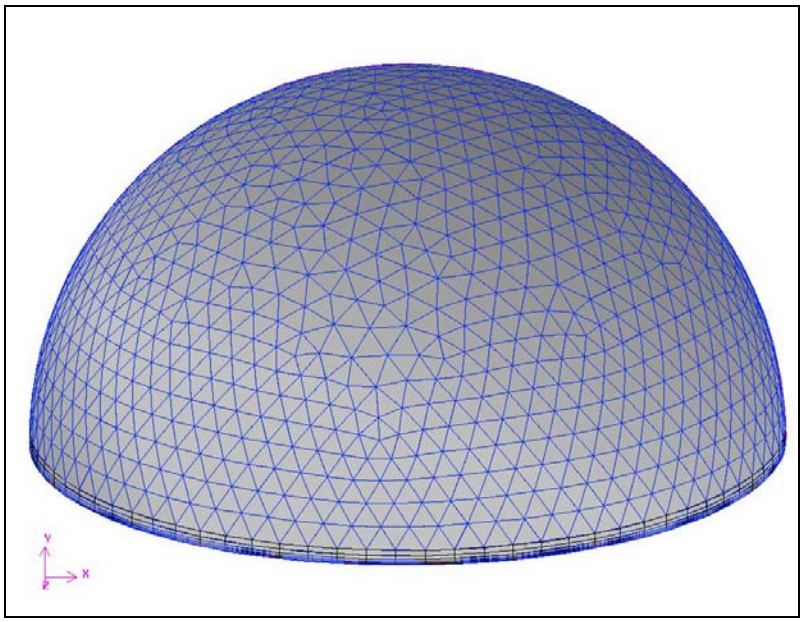


Figure 2. T-Grid Mesh of the Hemispherical Glazing Cavity of a Domed Skylight. Outer Diameter is 0.6 m; Glazing Gap Spacing is 0.025 m.

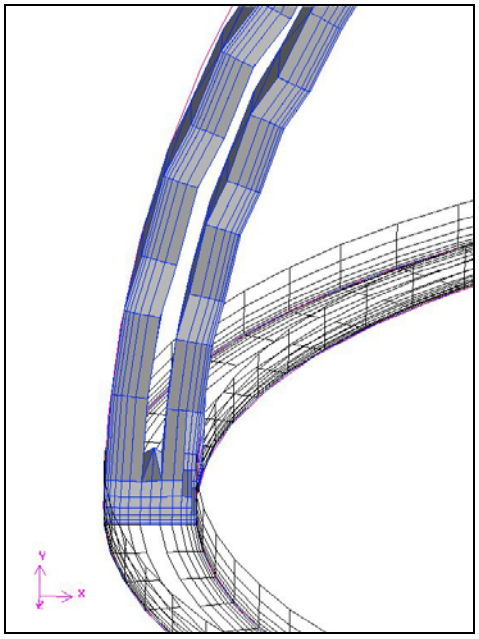


Figure 3. Boundary Layer Mesh Structure of 3-D Glazing Cavity Formed by Two Concentric Spheres

4.1 Results and Validation of the numerical model

A Fluent segregated solver (FDI 2003) was used with the following settings:

- Implicit equation formulation,
- Steady state model,
- Laminar viscous model;
- Solution controls: under-relaxation factors (RF) for all equations (variables) were defined with default settings and for energy equation as RF = 0.98,
- Method of discretization: pressure equation – PRESTO; pressure-velocity coupling – SIMPLEC; momentum – First Order; energy – First Order Scheme,
- Thermo-physical properties of air were treated as constants and were evaluated at the temperature of 0^{o}C,
- Boussinesq approximation was used in viscous laminar model.

With these settings, for this 3-D model the solution reached convergence after approximately 120 iterations.

For the purposes of comparison, the following model was created; the case when the exterior dome wall is at higher temperature than the interior one because the prior published work included this configuration (Laouadi and Atif 2001). Predicted temperature and velocity fields in the cavity for the heated outside wall case are shown in Figure 4 and Figure 5. From these distributions it is obvious that convection does not play significant role in the top part of the cavity, where the majority of heat transfer happens by conduction. This would mean that for the opposite heat flux direction, the heat transfer rate should increase.

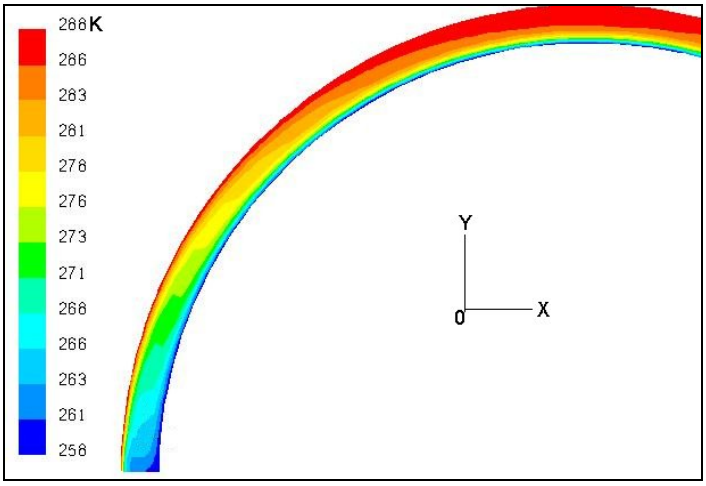


Figure 4. Temperature Distribution in a Centerline Cross-Section of the 3-D Glazing Cavity Formed by Two Concentric Spheres. Heat Flow Direction is Down. Ra = 68,000.

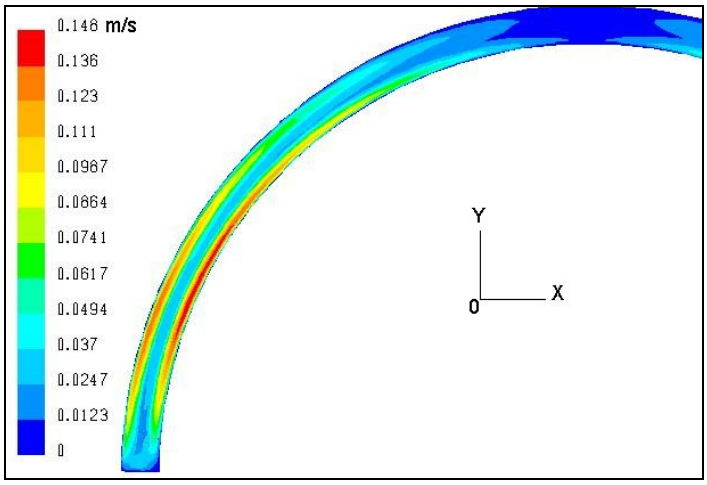


Figure 5. Velocity Field Magnitude in a Centerline Cross-Section of the 3-D Glazing Cavity Formed by Two Concentric Spheres. Heat Flow Direction is Down. Ra = 68,000.

The results of this modeling are compared with those published in the literature about heat transfer in concentric spheres by Raithby and Hollands (1975) and Garg (1991) and with numerical modeling results of Laouadi and Atif (2001). Raithby and Hollands (1975) developed a correlation for the Nusselt number under steady state conditions. The correlation is expressed as follows:

$$Nu = \max\left\{1, c\left(Ra^{x}\right)^{\frac{1}{4}}\right\} \tag{1}$$

Where:

c = Empirical coefficient based on the experimental data of Bishop et al. (1965);

Ra^{x} = Modified Rayleigh number.

Modified Rayleigh number is expressed as:

$$Rax = \frac{Ra \cdot 0.5 \cdot \delta}{\left[\left(1+\delta\right)^{-0.6} + \left(1+\delta\right)^{0.8}\right]^{5}}, \tag{2}$$

Where:

$\delta = L/R_i$

δ = Dimensionless gap spacing width (see Figure 1).

Dimensionless gap spacing for this model was $\delta = 0.091$.

According to Laouadi (2001) the coefficient c may also be expressed as a function of gap spacing δ for hemispherical domes using the following relation:

$$c = 0.7493 - 0.2461 \cdot \delta + 0.1129 \cdot \delta^2 - 0.0162 \cdot \delta^3 \quad (3)$$

The comparison between numerical modeling results of this study and calculations according to correlation (1) is presented in Figure 6 in terms of dimensionless convection heat transfer rate (i.e. Nusselt number, *Nu*). The maximum difference between compared values is 4.6% (for Ra = 90,500), which is within the accuracy limits of the correlation. Thus, the proposed numerical procedure and 3-D model results show complete conformity with results of existing published studies.

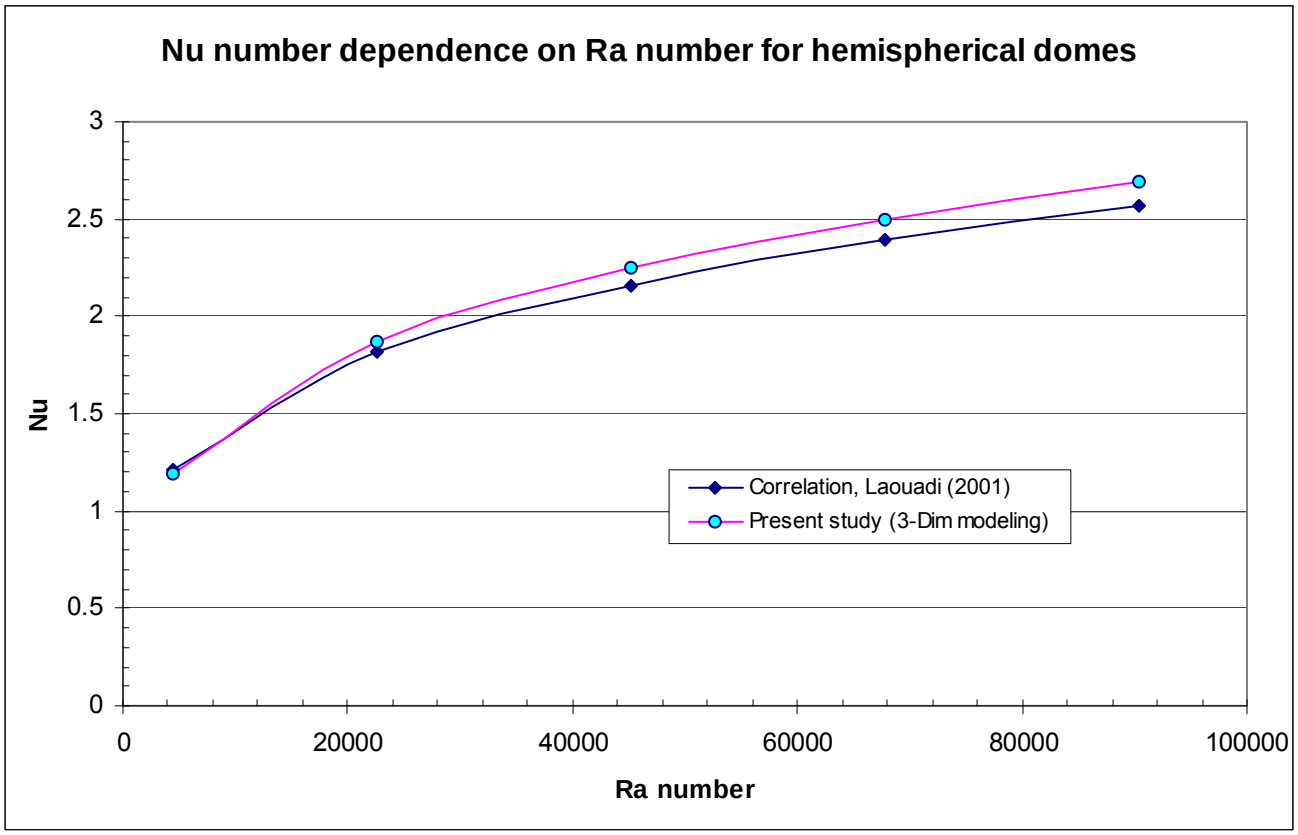


Figure 6. Comparison of Numerical Model with Correlation from Raithby and Hollands (1975).

However, for the prediction of nighttime thermal performances of domed skylights (also known as "Winter Standard Conditions", which is used for determining U-factors in NFRC rating) it is necessary to model laminar convection in domed skylight glazing cavity heated from the indoor facing surface (i.e., heat flow up). In this case, in the top region of the glazing cavity, the flow regime is similar to the convection heat transfer in the horizontal rectangular cavity heated from the bottom. Because of the expected multi vortices (or multi-cell) convection regime and flow pattern and based on previous studies (Yang 2004), only

full 3-D modeling can be used in this case. Predicted temperature field in the domed glazing cavity for the heat flow up case is shown in Figure 7.

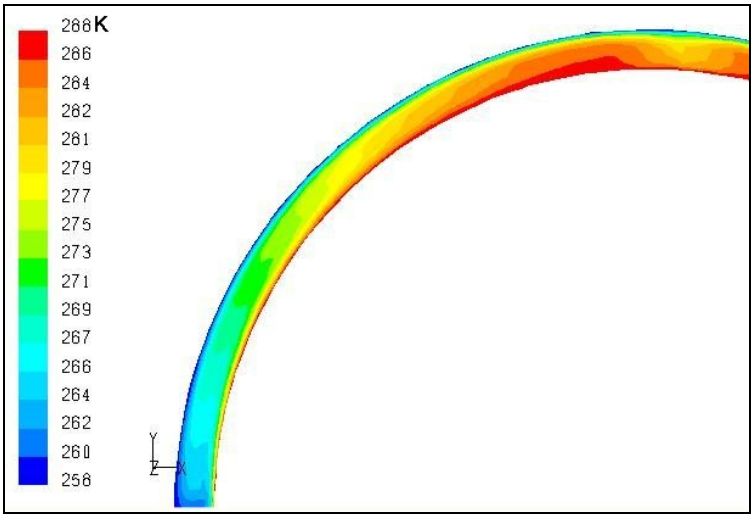


Figure 7. Temperature Distribution in a Centerline Cross-Section of the 3-D Glazing Cavity Formed by Two Concentric Spheres. Heat Flow Direction is Up. Ra = 68,000.

The comparison of convection heat transfer rates between the two cases, heat flow up and heat flow down, is given in Figure 8. *Nu* increases by 5% on average for the case of cavity heated from inside surface (heat flow up) when comparing to the cavity heated from outside (heat flow down).

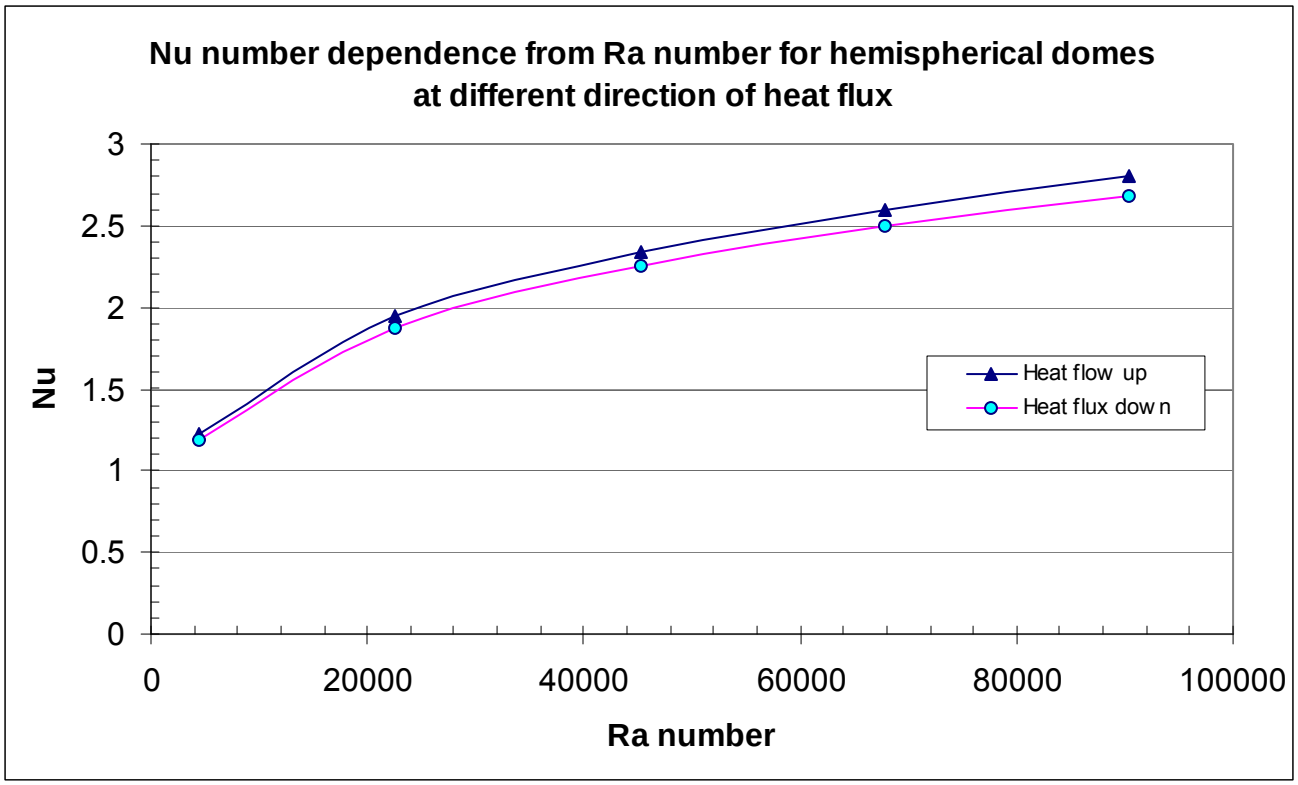


Figure 8. Comparison of Heat Transfer Rates for the 3-D Glazing Cavity Formed by Two Concentric Spheres with Different heat Flow Directions.

4.2 Summary

- The 3-D numerical model of natural convection heat transfer in domed skylight glazing cavity formed by two concentric spheres, is developed. The following geometric parameters were employed in order to compare to published results; diameter D_o = 0.78 m and spacing gap width L = 0.0325 m,.
- The 3-D numerical model results of heat transfer in domed skylight glazing cavity formed by two concentric spheres agreed well with the published studies, consisting of experimental and numerical results. The difference between compared Nusselt numbers is less than 4.6% for the case of cavity heated from outside (heat flow down).
- The 3-D numerical modeling and assumptions can be used for simulation of convection heat transfer in a full range of domed skylight glazing cavities under consideration.

4. ANALYSIS OF DOMED SKYLIGHT GLAZING CONFIGURATIONS AND GEOMETRY

In this section, realistic domed skylight geometry and configuration are analyzed (Vistawall 1994, BOCA 1997, ODL 1998, Crystalite 2006). These skylights include double and triple domed units constructed from sheets of acrylic or polycarbonate. The purpose is to select representative products for this research project.

Three main configurations, representative of domed skylights manufactured and sold in North America, are considered;

1) Type-A: Double domed glazing with both surfaces curvilinear
2) Type-B: Double domed glazing with one curvilinear and one flat surface
3) Type-C: Triple domed glazing with two curvilinear and one flat surface

The schematic of the three configurations are shown in Figure 9 .

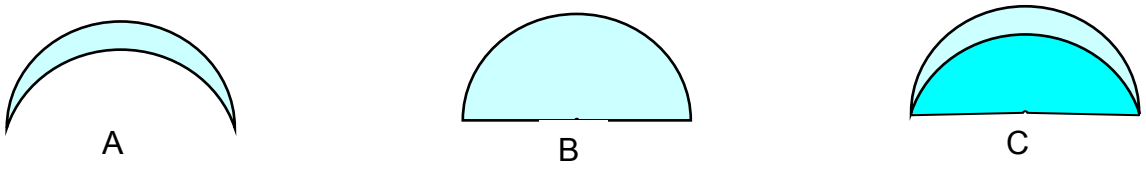


Figure 9. Types of Domed Skylight Glazing Configurations.

Because of the substantial differences in geometry, it is anticipated that one generalized convection heat transfer correlation couldn't be derived for Type-A and Type-B of domed skylight glazing cavity and that is why they will be considered separately. Convection heat transfer in the Type-C glazing can be derived as combined heat transfer through the glazing of Type-A and Type-B and will not be studied separately.

4.1 Domed Skylight Glazing Type-A

For this glazing type and for the purpose of better generalization, it is assumed that dome surfaces are close enough to two intersecting spherical surfaces. Therefore, the three main dome dimensions are:

- The diameter of the glazing base: $Ø = 2r$;
- The height of the dome: H;
- The maximum thickness of the gap between dome layers, d.

These dimensions could be obtained from drawings or by measuring physical skylight samples. Figure 10 shows the geometry and four main parameters of the Type-A glazing system.

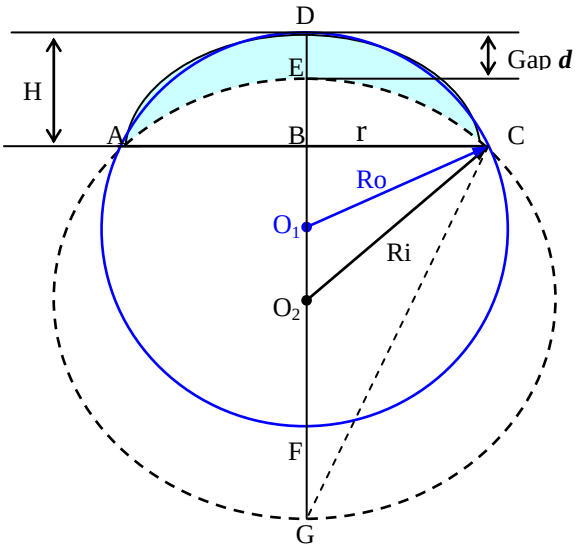


Figure 10. Geometry of the Double Domed Skylight Glazing System with Non-Uniform Gap Width.

The basic model dimensions can be expressed through the use of the well-known geometrical relations:

$$r^2 = BC^2 = BD \cdot BF = H \cdot (2 \cdot R_o - H) \tag{4}$$

$$r^2 = BE \cdot BG = (H - d) \cdot (2 \cdot R_i - H + d) \tag{5}$$

Where:

$$r = \frac{Ø}{2} = \frac{AC}{2}$$

r = radius of the glazing

R_i = radius of the inner sphere of the domedskylight glazing,

R_o = radius of the outer sphere of the domedskylight glazing.

From (4) and (5) and Figure 10, it folows:

$$R_i = \frac{\frac{r^2}{(H-d)} + H - d}{2} \tag{6}$$

$$R_o = \frac{\frac{r^2}{H} + H}{2} \tag{7}$$

$$O_1O_2 = R_i - R_o + d \tag{8}$$

Where:

O_1O_2 = distance between centers of inner and outer spheres.

Equations (6) to (8) give all necessary information for creating numerical model from specified domed skylight glazing system dimensions.

From the review of typical domed skylights used in buildings in North America and from the standard NFRC size we can deduce the following range of the main domed skylight glazing dimensions in this study:

- The range of glazing base diameter (Ø) is from 0.6 m to 1.2 m;
- The ratio of dome height to glazing base diameter (*H*/Ø) is from 0.12 to 0.3;
- The range of maximum thickness of the gap (*d*) is from 0.05 m to 0.07 m.

Table 2 presents domed skylight parameters selected for 3-D heat transfer simulation in the range of Raleigh number from *Ra* = 11,000 to Ra = 70,000 (temperature difference from 5K to 30K).

Table 2. Matrix of Dome Skylight Glazing Cavity Configurations and Sizes.

Glazing base diameter Ø = 0.6 m								Glazing base diameter Ø = 1.2 m					
H/Ø = 0.1		H/Ø = 0.2		H/Ø = 0.3		H/Ø = 0.3		H/Ø = 0.15		H/Ø = 0.3		H/Ø = 0.3	
d = 50 mm		*d* = 50 mm		*d* = 50 mm		*d* = 75 mm		*d* = 50 mm		*d* = 50 mm		*d* = 75 mm	
Tilt angle from horizontal direction													
90°	20°	90°	20°	90°	20°	90°	20°	90°	20°	90°	20°	90°	20°

4.2 3-D Numerical Modeling of Convection Heat Transfer in Type-A Glazing Cavity.

4.2.1 Description of boundary conditions and numerical model.

Figure 11 shows geometry and boundary conditions for the 3-D numerical model of Type-A domed skylight glazing cavity that was created using geometrical parameters obtained from equations (6) to (7). Two isothermal walls with temperature T_h and T_c are modeled as the inside (hot) and outside (cold) spherical surfaces of the glazing cavity.

For the simulation of natural convection heat transfer in a cavity we used a laminar viscous model with Boussinesq approximation. Thermo-physical properties of air were treated as constants and were evaluated at the temperature of $0^{o}C$ as the representative mean temperature in the glazing cavity.

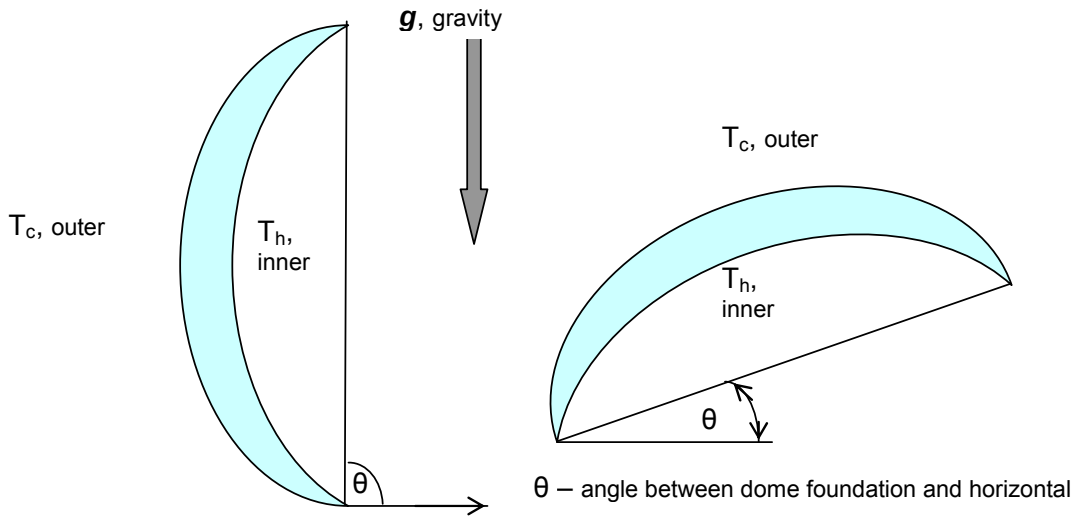


Figure 11. Orientation and Boundary Conditions for the Type-A Domed Skylight Glazing Cavity.

Figure 12 shows 3-D mesh of domed skylight glazing cavity Type-A with boundary layers created from T-Grid elements using Fluent software (FDI 2003).

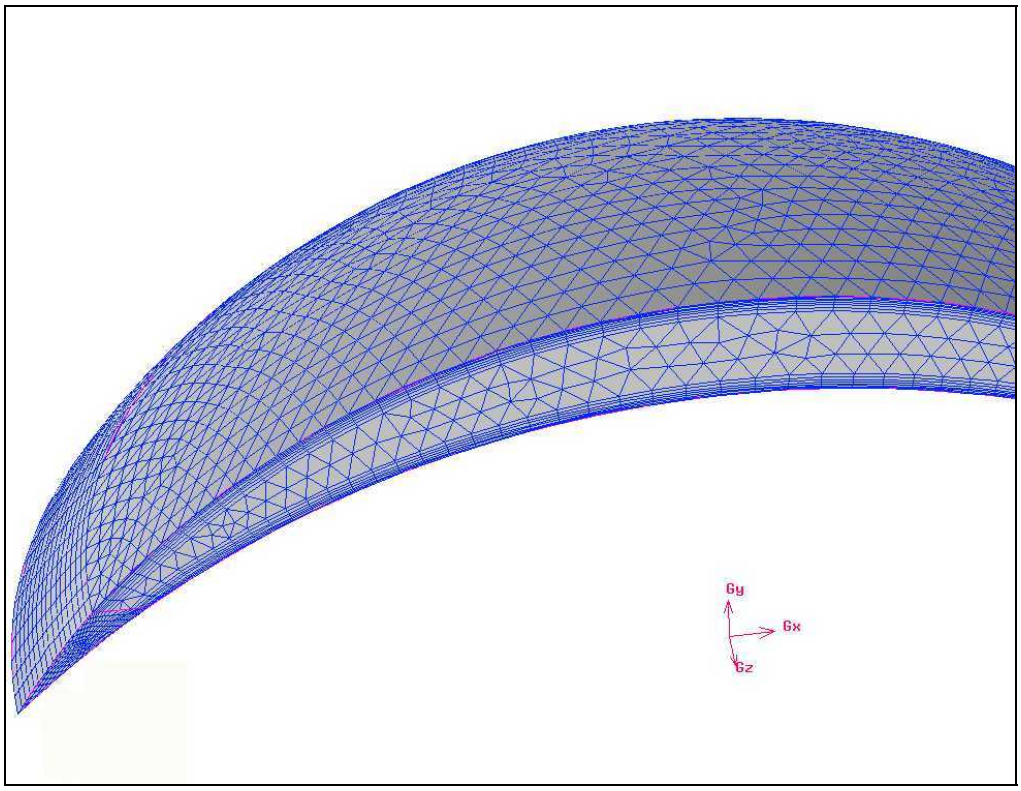


Figure 12. Numerical Mesh for the Type-A Domed Skylight Glazing Cavity.

4.2.2 Results and discussion

Predicted temperature and velocity fields in the Type-A domed skylight glazing cavity (Ø = 60 cm, H/Ø =0.3, maximum gap *d* = 50 mm) in vertical position (θ = 90^{o}) are shown in Figure 13 and for tilt orientation (θ = 20^{o}) are shown in Figure 14.

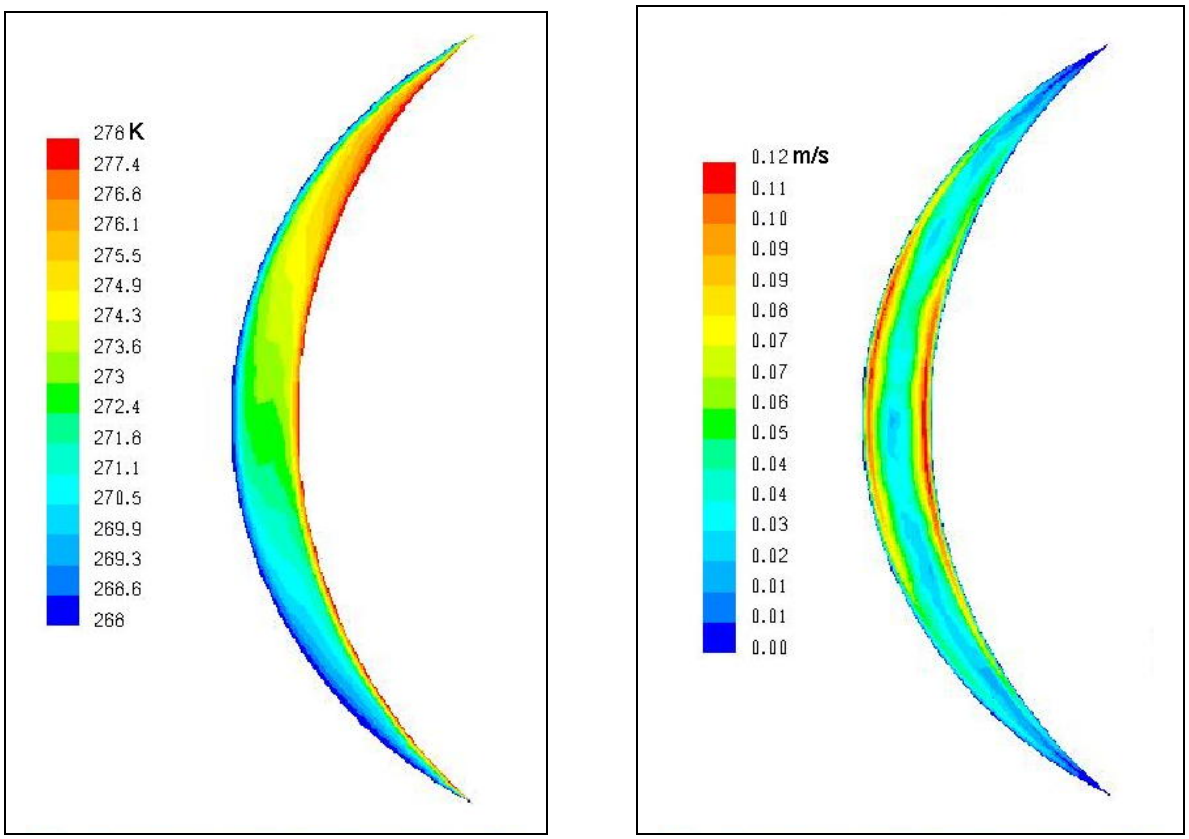
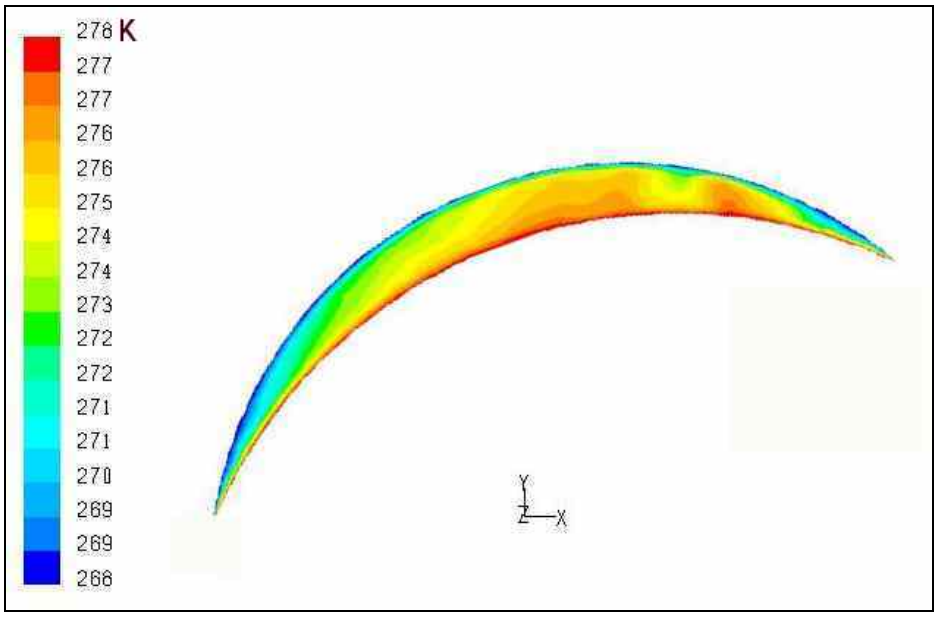


Figure 13. Temperature and Velocity Magnitude Distributions in a Symmetry Plane of the Type-A Domed Skylight Glazing Cavity at Vertical Orientation. Ra = 23,000 (ΔT = 10K).

a)



b)

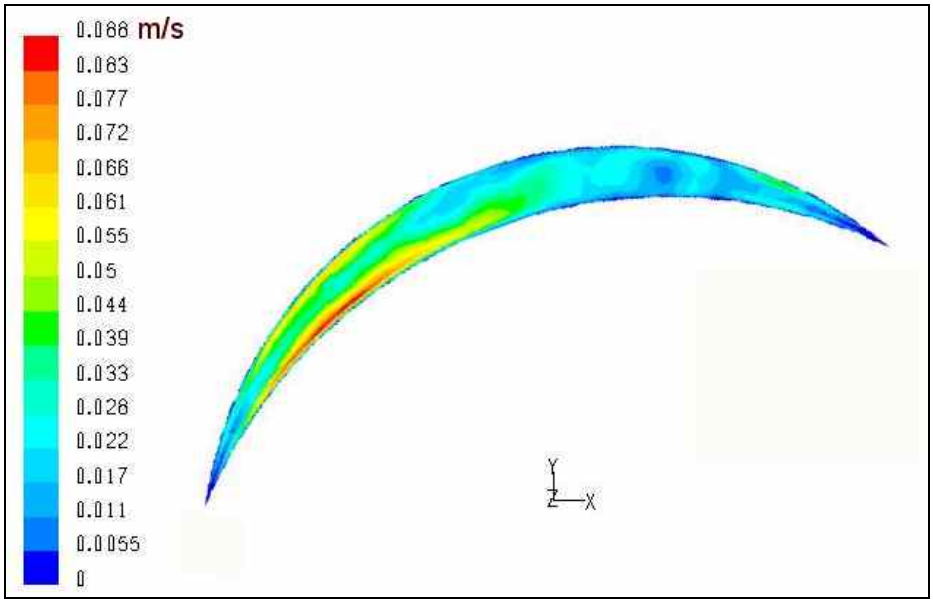


Figure 14. Temperature (a) and Velocity Magnitude (b) Distributions in a Symmetry Plane of the Type-A Domed Skylight Glazing Cavity at a tilt angle $\theta = 20^{o}$. Ra = 23,000 (ΔT = 10K).

Modified Nusselt number for cavities with irregular gap and curved walls

Nusselt number, *Nu*, is dimensionless average heat flux on the indoor cavity wall and usually applies to convection heat transfer rate in enclosures. In general *Nu* is ratio of the heat flux due to combined convection and conduction to the heat flux due to conduction only under the same conditions. For pure conduction it follows that *Nu* = 1. For rectangular cavities *Nu* is expressed as follows:

$$Nu = \frac{q_{conv}}{q_{cond}} = \frac{q_{conv}}{\frac{k \cdot \Delta T}{L}} \tag{9}$$

Where:

q_{conv} = heat flux caused by combined convection and conduction heat transfer in a cavity;

q_{cond} = heat flux caused by conduction only heat transfer in a cavity;

L = characteristic size of a cavity in the direction of the heat flux, usually it is the thickness of the cavity gap;

k = thermal conductivity at of air at the average temperature in the cavity;

ΔT= temperature difference between cavity walls.

However the *Nu* expression (9) is not applicable for cavities with irregular gap and curved walls as in the case of glazing cavity of domed skylights. Simulation results are summarized in Table 3 in terms of thermal conductance (surface to surface heat transmission) in domed glazing cavity models for selected configurations and parameters.

Table 3. Thermal Conductance C_{cond} for the 3-D domed glazing cavity.

Glazing base diameter Ø = 0.6 m				Glazing base diameter Ø = 1.2 m		
H/Ø = 0.1	H/Ø = 0.2	H/Ø = 0.3	H/Ø = 0.3	H/Ø = 0.15	H/Ø = 0.3	H/Ø = 0.3
d = 50 mm	*d* = 50 mm	*d* = 50 mm	*d* = 75 mm	*d* = 50 mm	*d* = 50 mm	*d* = 75 mm
Cavity Thermal Conductance $\underline{C}_{cond}$, W/(m^{2}K)						
2.93	3.02	2.84	2.08	2.75	2.76	1.81

As a comparison, the layer of still air with thickness of 50 mm has thermal conductance of 0.481 W/(m2K) and at thickness of 75 mm has thermal conductance of 0.321 W/(m^{2}K) under the same temperature conditions.

The following expression, derived from the present numerical study expresses heat flux q_{cond} due to conduction on inside cavity surface with errors less than 3% for most cases in

comparing with numerical modeling of conduction heat transfer (Table 3) in domed skylight glazing cavity

$$q_{cond} = \frac{\beta \cdot k \cdot \Delta T}{\frac{d}{2}} \tag{10}$$

Where:

$$\beta = 2.784 + 3.0 \cdot \frac{d}{Ø} \tag{11}$$

β = Form-factor of Type-A dome skylight glazing cavity heat transfer;
k = thermal conductivity of air at average temperature in the cavity;

ΔT= Temperature difference between cavity walls;

d = Maximum thickness of the glazing gap.

Using equation (10) the modified Nusselt number, Nu_m for domed glazing cavity can be expressed as:

$$Nu_m = \frac{q_{conv}}{\frac{2 \cdot \beta \cdot k \cdot \Delta T}{d}} = \frac{d \cdot q_{conv}}{2 \cdot \left(2.784 + 3.0 \cdot \frac{d}{Ø}\right) \cdot k \cdot \Delta T} \tag{12}$$

All heat transfer results are summarized in Table 4 and Figure 15 to Figure 18.

Table 4. Nusselt vs. Raleigh number Dependence for Type-A Domed Skylight Glazing Cavities

Glazing base diameter Ø = 0.6 m									Glazing base diameter Ø = 1.2 m					
H/Ø	H/Ø = 0.1		H/Ø = 0.2		H/Ø = 0.3		H/Ø = 0.3		H/Ø = 0.15		H/Ø = 0.3		H/Ø = 0.3	
d =	50 mm		50 mm		50 mm		75 mm		50 mm		50 mm		75 mm	
θ =	90°	20°	90°	20°	90°	20°	90°	20°	90°	20°	90°	20°	90°	20°
Ra	Nu number (Nu = q_{conv} / q_{cond})													
11300	1.14	1.19	1.14	1.17	1.12	1.14	1.28	1.33	1.07	1.13	1.08	1.12	1.24	1.27
22600	1.19	1.30	1.19	1.23	1.19	1.24	1.39	1.48	1.11	1.21	1.13	1.18	1.33	1.38
45200	1.26	1.47	1.26	1.29	1.28	1.35	1.55	1.63	1.18	1.29	1.18	1.25	1.45	1.52
67800	1.30	1.53	1.31	1.35	1.34	1.42	1.65	1.74	1.24	1.36	1.23	1.30	1.54	1.61

In Figure 15, modeling results in terms of modified Nu number are presented for two glazing cavities (glazing base diameter Ø =0.6 m and Ø = 1.2 m) with the same parameter H/Ø in vertical (θ = 90°) and tilted orientations (θ = 20°). From numerical results we can conclude that increasing base diameter of domed glazing cavity from 0.6 m to 1.2 m results in

decrease of convection heat transfer by about 8% on average. For tilted cavities the convection heat transfer is on the other hand 6-7% higher on average than for vertical cavities.

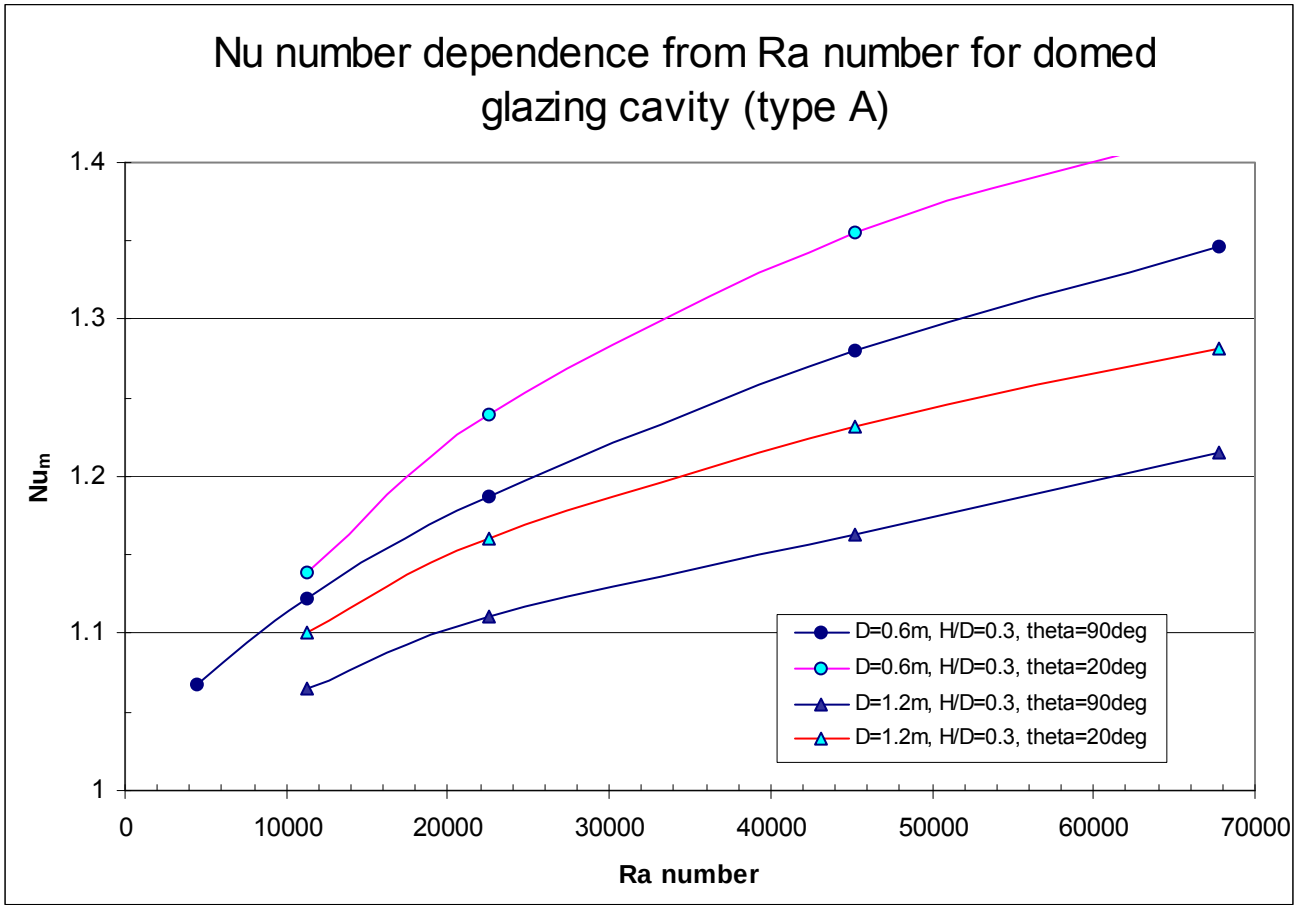


Figure 15. Comparison of Heat Transfer Rates for Two Type-A Domed Skylight Glazing Cavities (Glazing Base Diameter Ø =0.6 m and Ø = 1.2 m).

Figure 16 shows comparison of heat transfer rates for domed skylight glazing cavities vs. rectangular cavities, typical of standard fenestration products, such as windows. The rectangular glazing cavity configuration was *H* x *W* x *L* = 1m x 0.8m x 0.025m. Rectangular cavity gap of 0.025m is equal to the average gap of domed glazing cavity under the same boundary conditions, so to facilitate “apple to apple” type of comparison.

From this comparison we can conclude that the heat transfer rate (thermal conductance) of domed glazing cavities exceeds heat transfer rate of the rectangular glazing cavity by almost 200%.

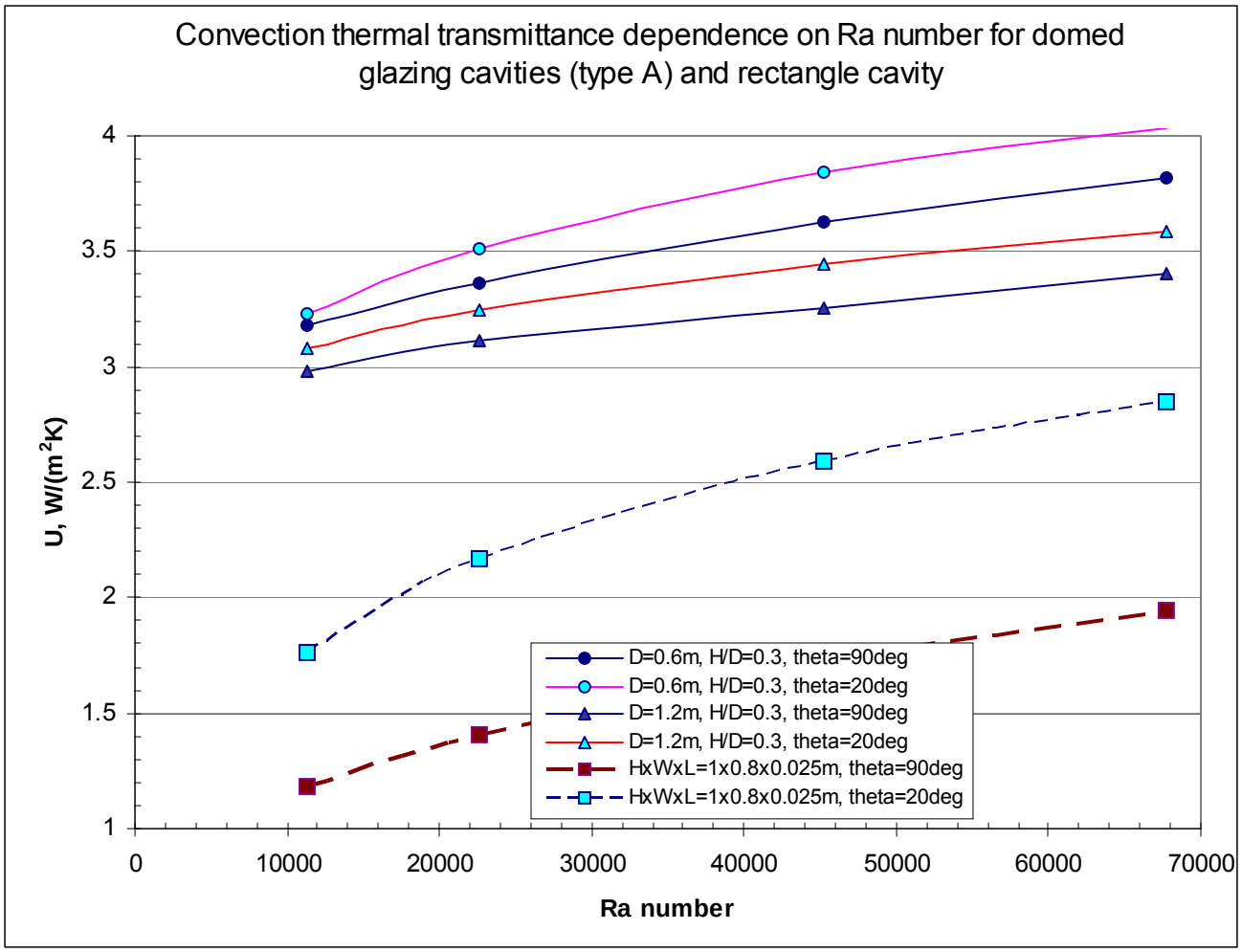


Figure 16. Comparison of Heat Transfer Rates for Type-A Domed Skylight Glazing Cavities and Rectangular Glazing Cavity (*H* x *W* x *L* = 1m x 0.8m x 0.025m).

Figure 17 shows heat transfer rates of domed skylight glazing cavities in vertical position (θ = 90°) with different parameter H/Ø (ratio of the dome height to the dome base diameter). The difference between predicted *Nu* does not exceed 3% and heat transfer rate for this case can therefore be considered as independent from parameter *H*/Ø.

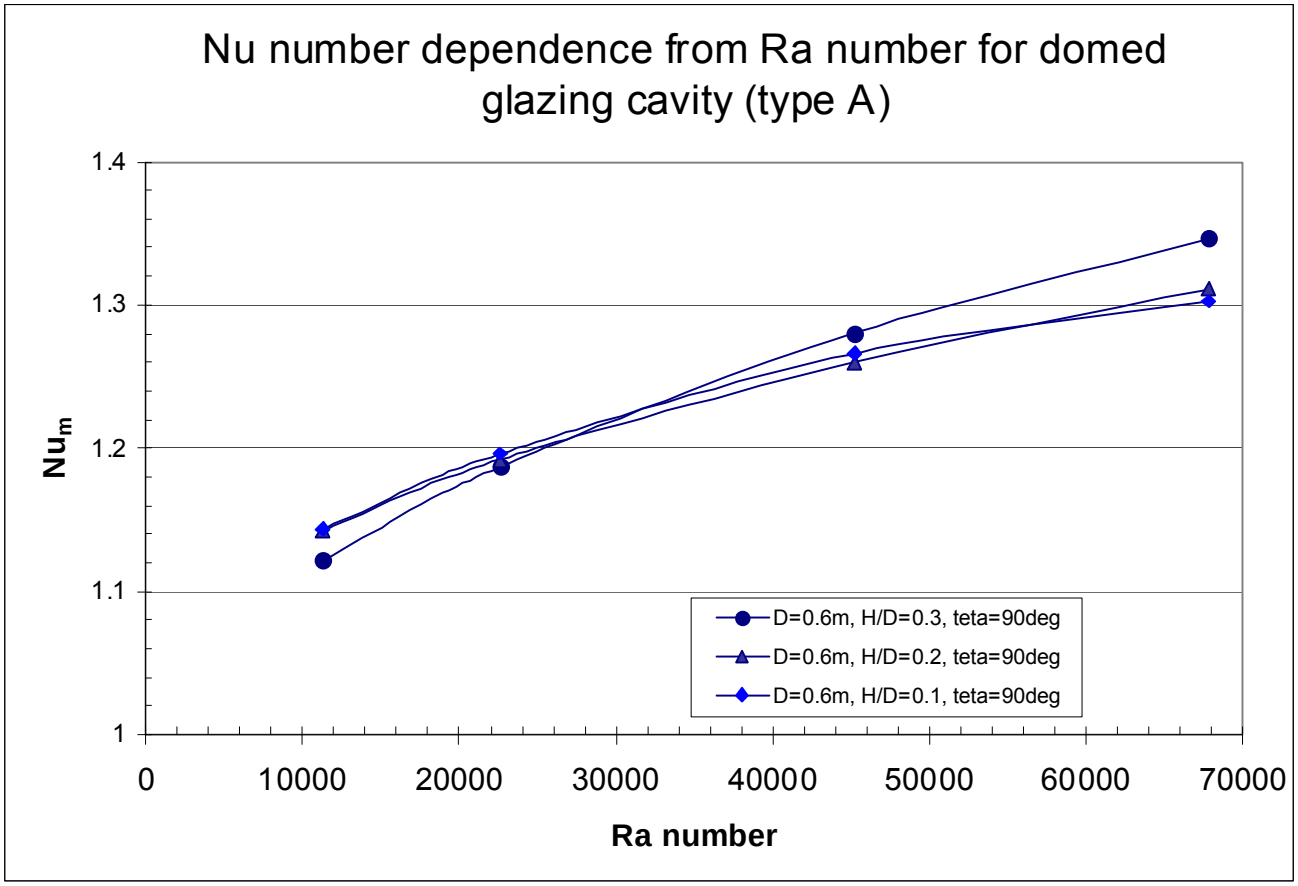


Figure 17. Heat Transfer Rate Comparison for Type-A Domed Skylight Glazing Cavities in Vertical Orientation with Different Parameter *H*/Ø.

More complicated *Nu* dependence was obtained in the case of tilted domed skylight glazing cavities with different parameter *H*/Ø as it is shown in Figure 18. The difference between predicted *Nu* for different parameter *H*/Ø in this case is up to 8%. The heat transfer rate for this case should be considered as dependent on the parameter *H*/Ø.

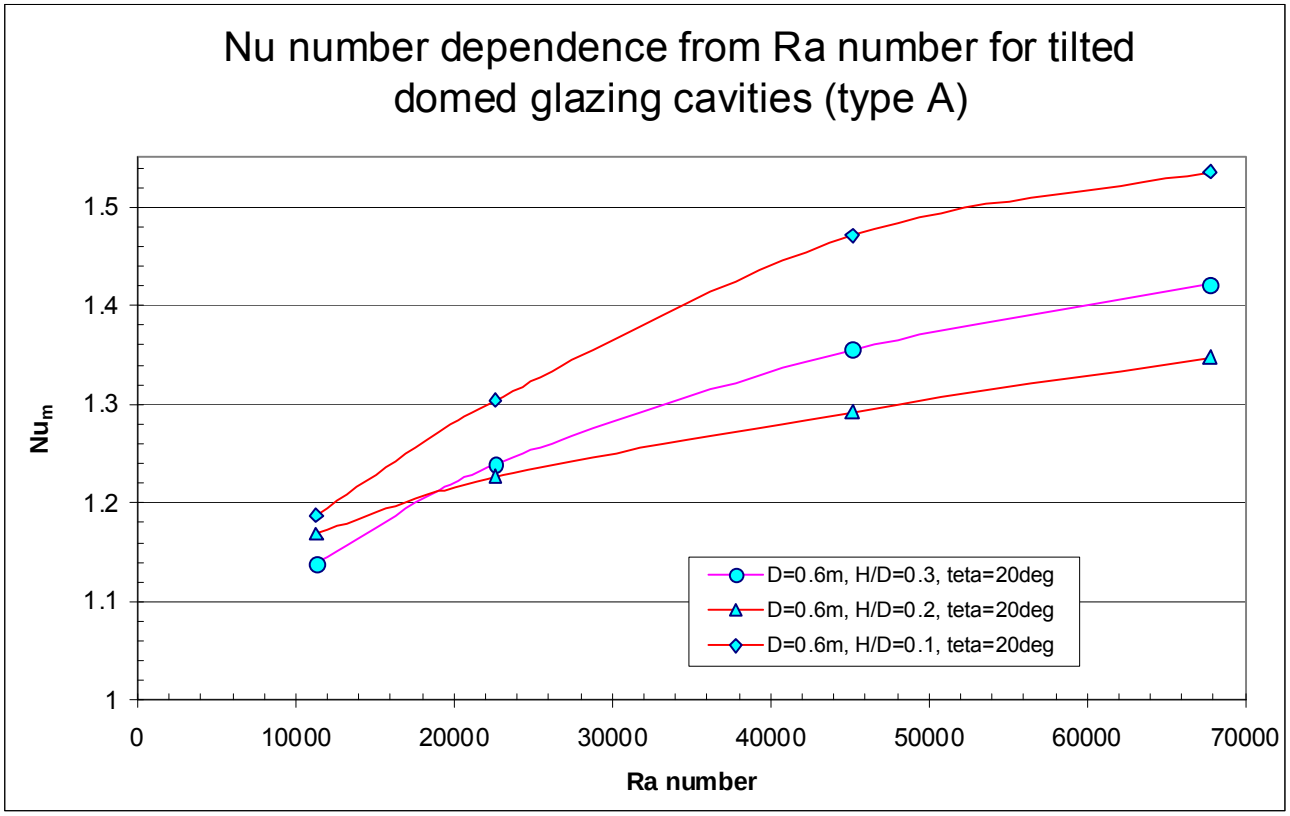


Figure 18. Heat Transfer Rate Comparison for Type-A Tilted Domed Skylight Glazing Cavities with Different Parameter *H*/Ø.

4.3 Heat transfer correlations for domed glazing cavity of a Type-A

4.3.1 Heat transfer correlations for Type-A domed skylight glazing cavities in vertical orientation

The following convection heat transfer correlations for Nu_m were derived from numerical modeling results for domed glazing cavities in vertical orientation ($\theta = 90^o$) as a function of Ra, *d*, and Ø:

a) Correlation for domed glazing cavities with maximum glazing cavity gap *d* = 0.05m and glazing base diameter in the range from Ø = 0.6m to Ø = 1.2m

$$Nu_{90} = 0.95 \cdot \left(0.01 \cdot Ra \cdot \frac{d}{Ø} \right)^{0.08} ; \quad d \le 0.05 \text{ m} \tag{13}$$

$$Nu_{90} = 0.95 \cdot \left(0.00125 \cdot Ra \right)^{0.12} ; \quad d = 0.075 \text{m} \ \textit{and} \ Ø \le 0.6 \text{m} \tag{14}$$

$$Nu_{90} = 0.95 \cdot \left(0.000625 \cdot Ra \right)^{0.13} ; \quad d = 0.075 \text{ m} \ \textit{and} \ Ø = 1.2 \text{ m} \tag{15}$$

Where:

d = Maximum gap of glazing cavity, m;

Ø = Glazing base diameter, m.

Correlations (13) to (15) are used as endpoints in linear interpolation for determining modified *Nu* for specified Ra number in the range of maximum glazing gap from 0.05m to 0.075m and glazing base diameter from Ø = 0.6m to Ø = 1.2m.

Figure 19 and Figure 20 show how proposed correlations (13) to (15) compare with numerical modeling results. The maximum difference between correlations and modeling results is less than 4%.

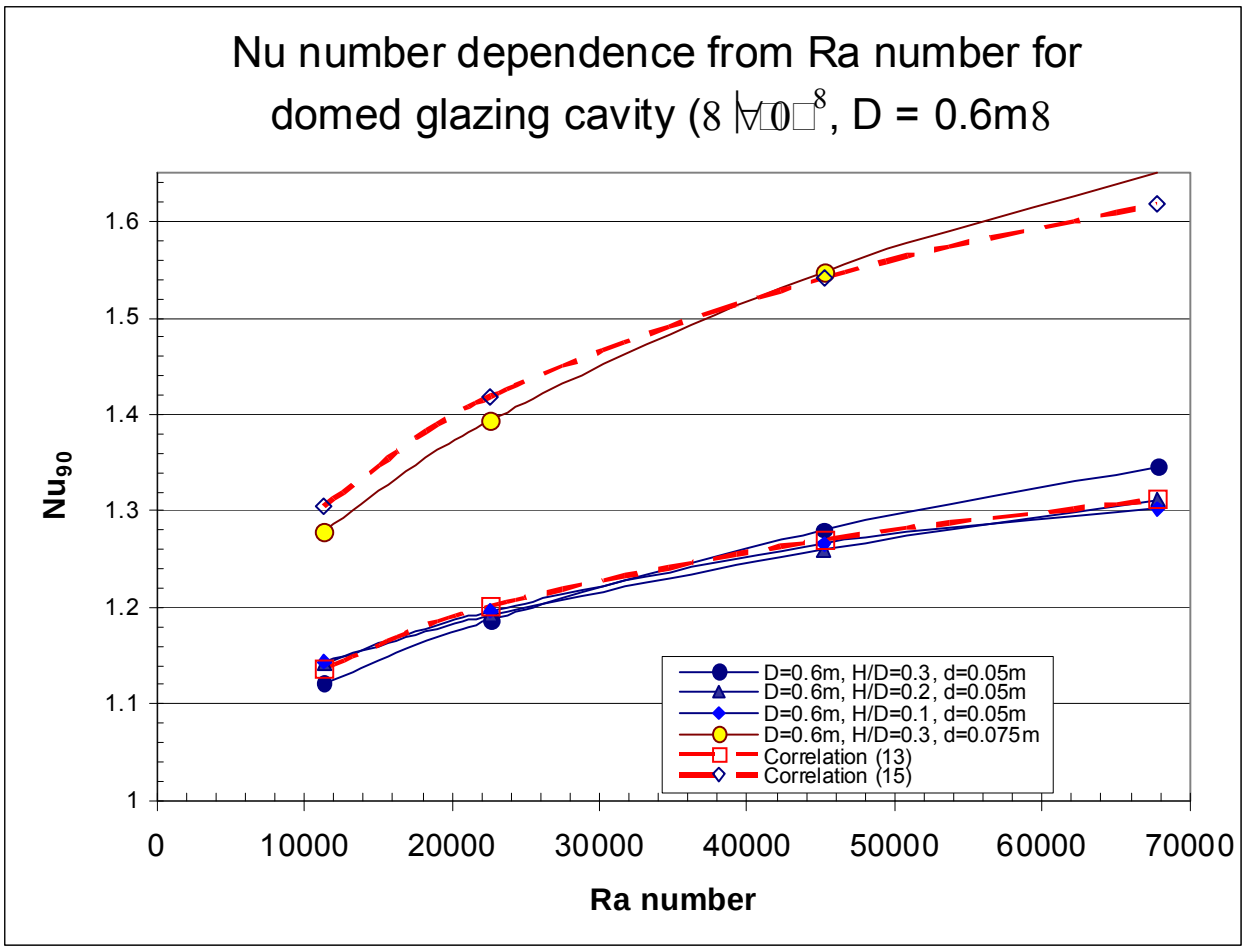


Figure 19. Comparison of Convective Heat Transfer Rates Predicted by Numerical Modeling and Correlations for Type-A Domed Glazing Cavity With Glazing Base Diameter Ø = 0.6 m.

.

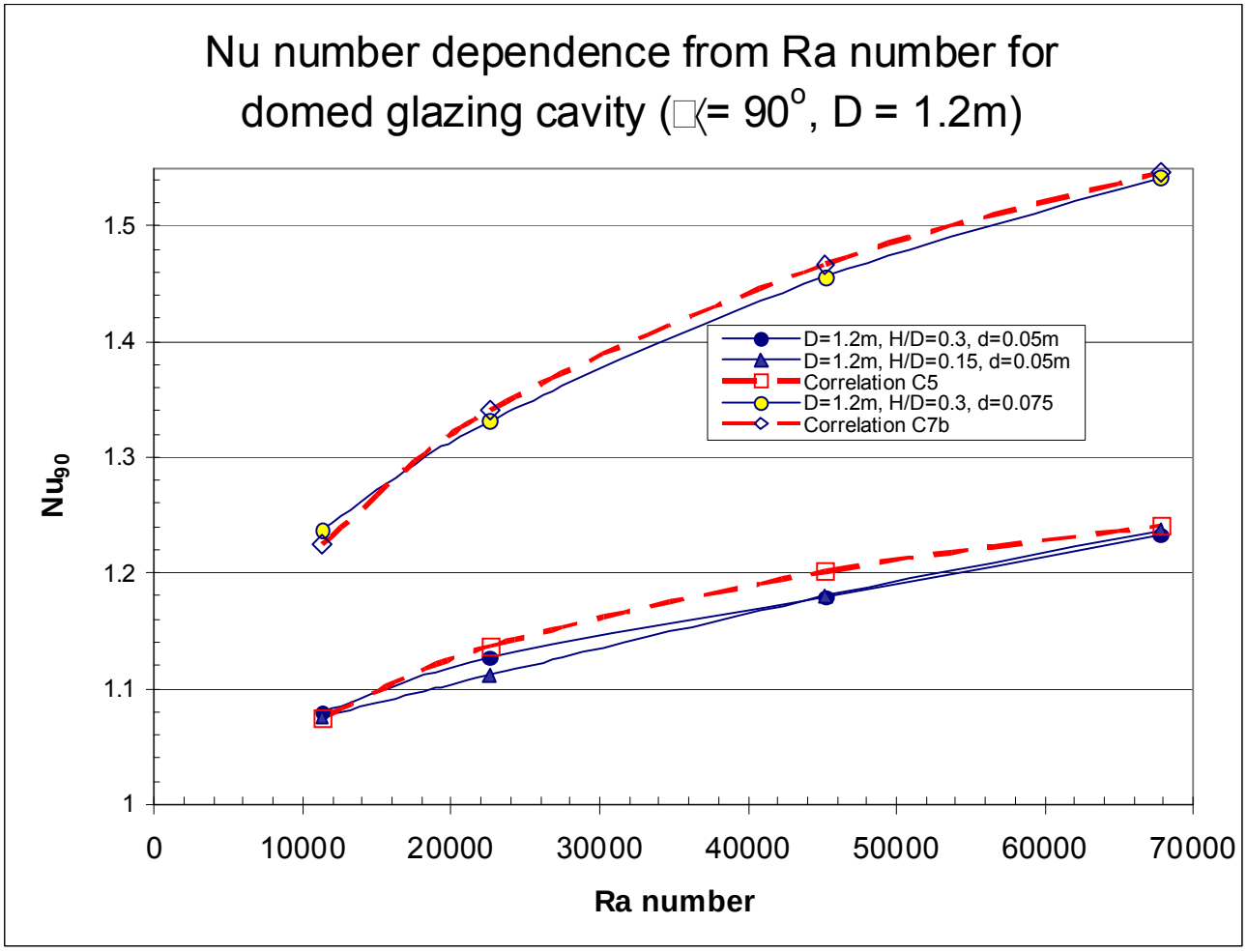


Figure 20. Comparison of Convective Heat Transfer Rates Predicted by Numerical Modeling and Correlations for Type-A Vertical Domed Glazing Cavity with Glazing Base Diameter Ø = 1.2 m.

Convective heat transfer coefficient is calculated from the Nu_m using the following relation:

$$h_c = Nu_m \frac{2 \cdot k}{d}$$

For intermediate values, linear interpolation can be used. The following is an example of the usage of correlations (13) to (15), when interpolation is applied.

***Example of using correlations (13)-(15) for Nu number calculation*:**

Calculate Nu number for vertical domed skylight cavity at the following conditions: Ra = 30000; maximum cavity gap *d* = 0.06 m and glazing base diameter Ø = 1 m.

Step 1. From equation (13) we find for values Ra = 30000, *d* = 0.05 m and Ø = 1 m:

$Nu_1 = 1.1798.$

Step 2. From equation (15) we find for values Ra = 30000, *d* = 0.075 m and Ø = 1.2 m:

$Nu_2 = 1.3906.$

Step 3. From equation (14) we find for values Ra = 30000, *d* = 0.075 m and Ø = 0.6 m:

$Nu_3 = 1.4676.$

Step 4. Applying linear interpolation on parameter Ø to values Nu_2 and Nu_3 for diameter Ø = 1.0 m we find:

$Nu_{2,3} = 1.4162.$

Step 5. Applying linear interpolation on parameter *d* to values Nu_1 and $Nu_{2,3}$ for cavity gap *d* = 0.06 m we find:

$Nu_m = 1.2743.$

4.3.2 Heat transfer correlation for Type-A domed skylight glazing cavities in tilted orientation

The following convection heat transfer correlation for Nu_{20} was derived from numerical modeling results for domed glazing cavities in titled orientation ($\theta = 20^o$) as a function of Ra, *d*, and Ø:

$$Nu_{20} = Nu_{90} \cdot \left[1.03 + 2.3 \cdot 10^{-5} \cdot Ra \cdot \left(\log 10 \left(\frac{H}{Ø} \right) + 0.7 \right)^2 \right];$$

$$d \le 0.075m;\ Ø \le 1.2\,\text{m};\ H/Ø \le 0.3 \qquad (16)$$

Where:

Nu_{90} - Nusselt number for vertical orientation obtained using correlations (13) - (15)

Figure 21 show how proposed correlation (16) compare with numerical modeling results. The maximum difference between correlations and modeling results is less than 3%

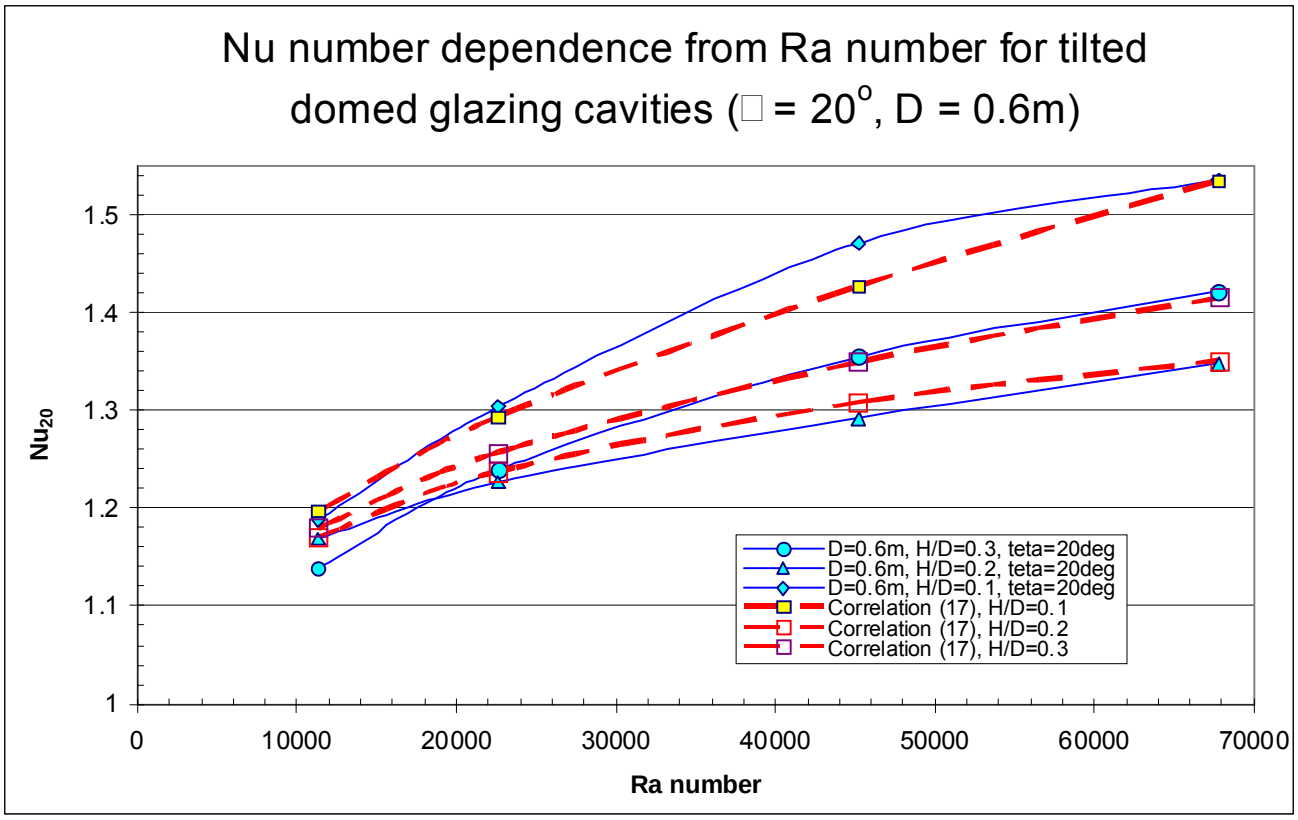


Figure 21. Comparison of Convective Heat Transfer Rates Predicted by Numerical Modeling and Correlations for Tilted Type-A Domed Skylight Glazing Cavity (θ=20°).

4.4 Domed Skylight Glazing Type-B

Type B domed skylight glazing cavity has one curved wall and other flat wall that is usually coinciding with skylight base as it is shown in Figure 22. For this glazing cavity type and for the purpose of better generalization, it is assumed that dome surfaces are close enough to an intersecting spherical and plane surfaces. Therefore, the two main dome dimensions are:

- The diameter of the glazing base: Ø = 2*r*;
- The height of the dome: H;

These dimensions could be obtained from drawings or by measuring physical skylight samples.

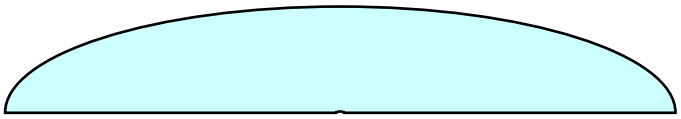


Figure 22. Cross-Section of the Type-B Domed Skylight Glazing Cavity.

Figure 23 shows the geometry abd geometric parameters of the Type-B domed skylight glazing cavity, which will be used to generate 3-D numerical model.

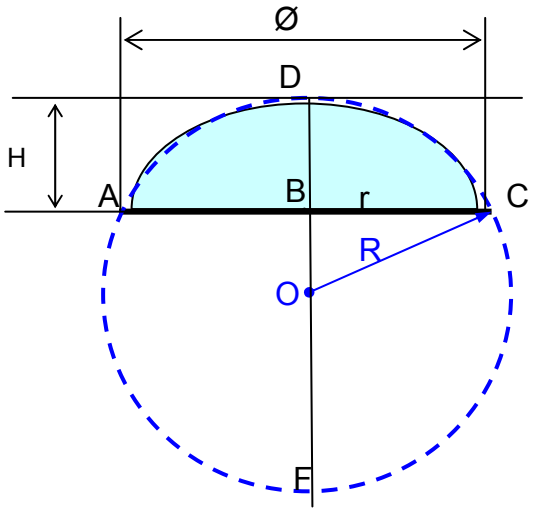


Figure 23. The Geometry of the Type-B Double Domed Skylight Glazing Cavity.

The basic model dimensions can be expressed through the use of the well-known geometrical relation:

$$r^2 = BC^2 = BD \cdot BF = H \cdot (2 \cdot R - H) \qquad (17)$$

where:

r = Ø /2 = AC/2

r = radius of the glazing base

R = radius of the sphere,

H = Height of the dome

From equation (17) and Figure 36 it follows:

$$R = \frac{\frac{r^2}{H} + H}{2} \tag{18}$$

Equations (17) and (18) give all the necessary information for creating numerical model from the Type-B domed skylight glazing dimensions: *H* and Ø.

Table 5 presents domed skylight glazing cavity (type B) parameters selected for 3-D heat transfer simulation in the range of Raleigh number from Ra = 11000 to Ra = 70000 (temperature difference from 5K to 30K).

Table 5. Matrix of Type-B Domed Skylight Glazing Cavity Configurations and Sizes.

Glazing base diameter Ø = 0.6 m						Glazing base diameter Ø = 1.2 m					
H/Ø = 0.1		H/Ø = 0.2		H/Ø = 0.3		H/Ø = 0.1		H/Ø = 0.2		H/Ø = 0.3	
Tilt angle from horizontal direction, θ											
90°	20°	90°	20°	90°	20°	90°	20°	90°	20°	90°	20°

4.5 3-D Numerical Modeling of Convection Heat Transfer in Type-B Glazing Cavity.

4.5.1 Description of boundary conditions and numerical model.

Figure 24 shows geometry and boundary conditions for the 3-D numerical model of Type-B domed skylight glazing cavity that was created using geometrical parameters obtained from equations (17) and (18). Two isothermal walls with temperature T_h and T_c are modeled as the inside (hot) flat surface and outside (cold) spherical surface of the glazing cavity.

For the simulation of natural convection heat transfer in a cavity we used a laminar viscous model with Boussinesq approximation. Thermo-physical properties of air were treated as constants and were evaluated at the temperature of 0°C as the representative mean temperature in the glazing cavity.

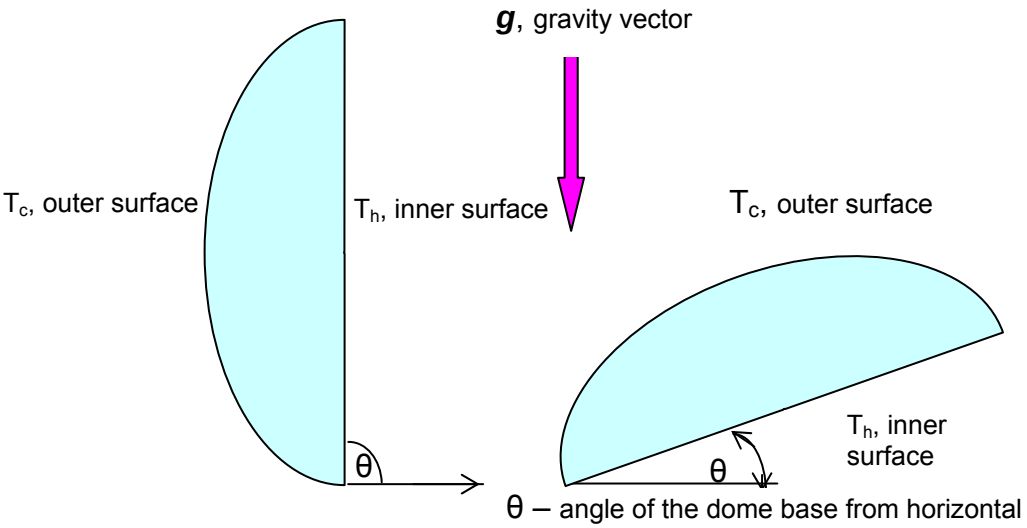


Figure 24. Orientation and Boundary Conditions for the 3-D Glazing Cavity Type-B.

Figure 25 shows 3-D mesh of domed skylight glazing cavity Type-B with boundary layers created using Fluent software (FDI 2000 and FDI 2003).

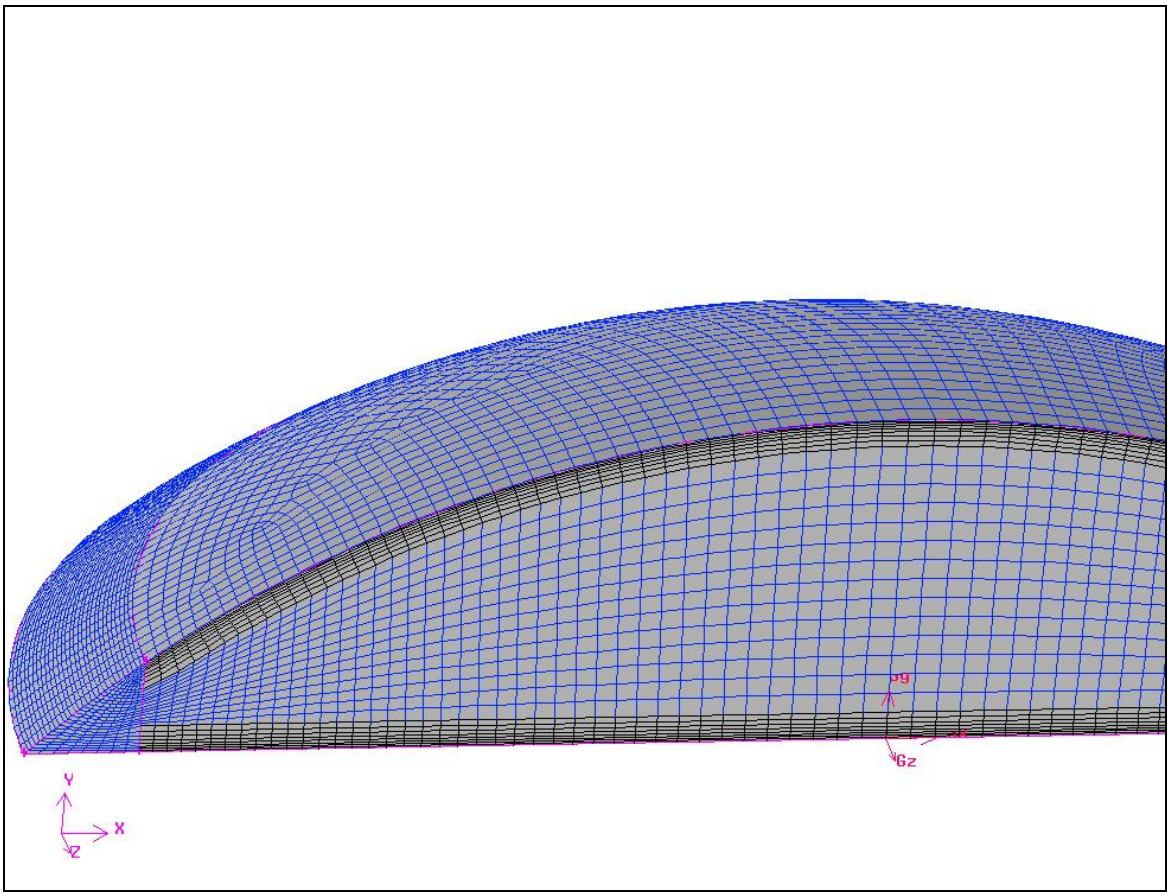


Figure 25. Numerical Mesh for the Type-B Domed Skylight Glazing Cavity.

4.5.2 Results and discussion

Predicted temperature and velocity fields in the cavity for the case of domed skylight glazing cavity Type-B (Ø = 60 cm, H/Ø =0.2) in vertical position (θ = 90^{o}) are shown in Figure 26 and for tilt angle (θ = 20^{o}) are shown in Figure 27.

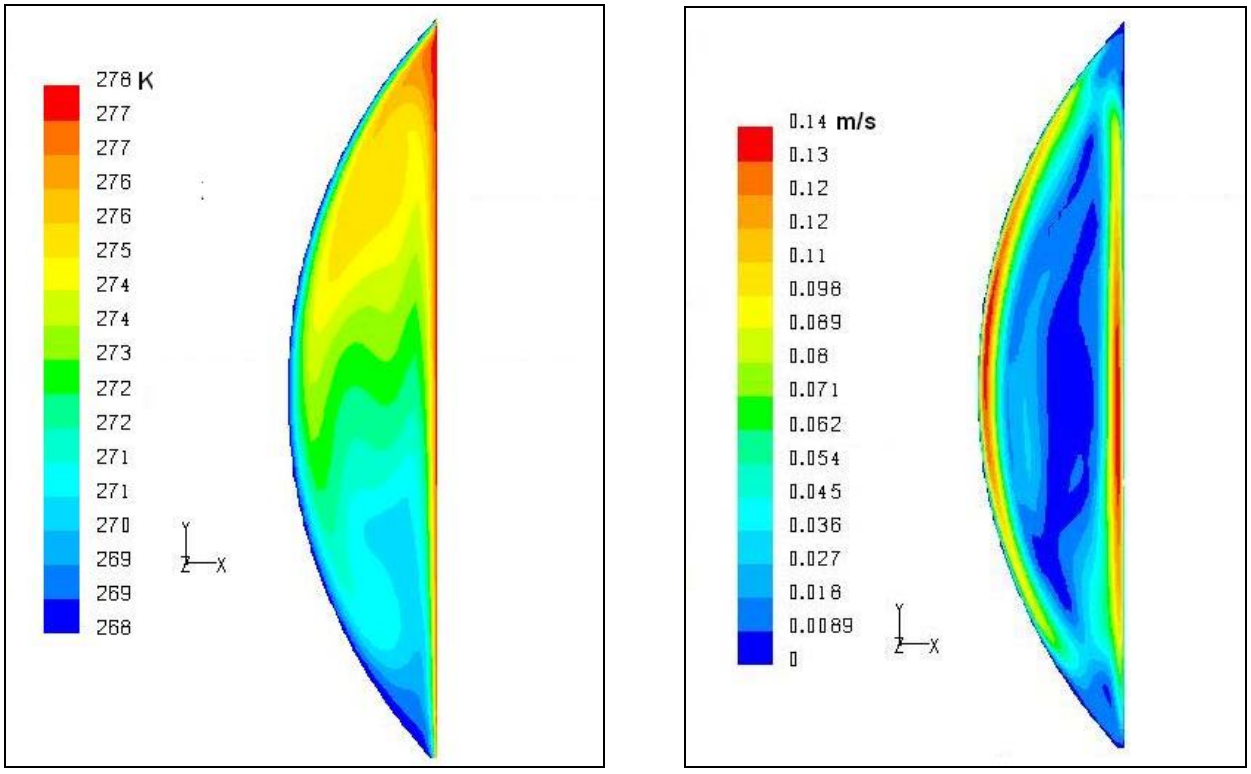
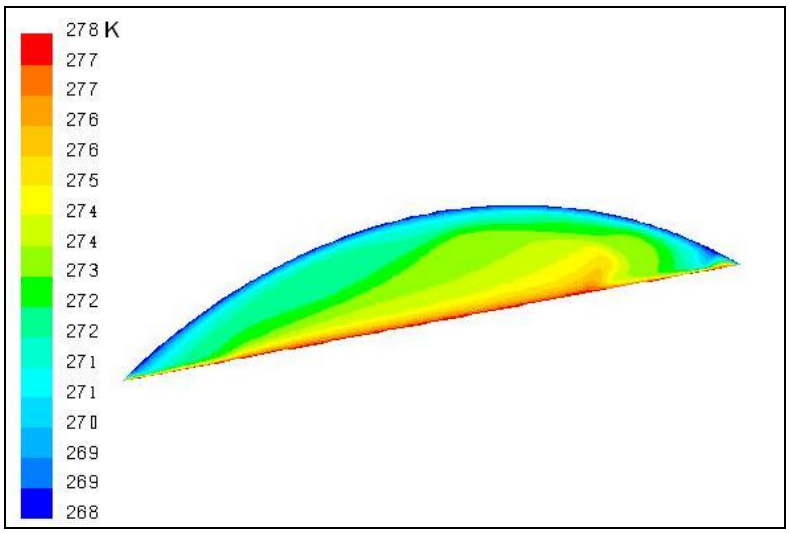


Figure 26. Temperature and Velocity Magnitude Distributions in a Symmetry Plane of the Type-B Domed Skylight Glazing Cavity at Vertical Orientation. Ra = 23,000 (ΔT = 10K).

a)



b)

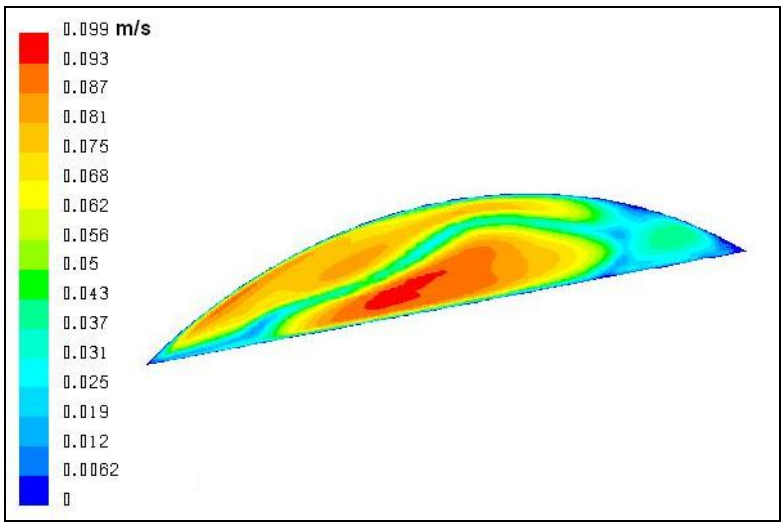


Figure 27. Temperature (a) and Velocity Magnitude (b) Distributions in a Symmetry Plane of the Type-B Domed Skylight Glazing Cavity at a tilt angle $\theta = 20^{o}$. Ra = 23,000 (ΔT = 10K).

Simulation results are summarized in Table 6 in terms of thermal conductance (surface to surface heat transmission) in Type-B domed glazing cavity models for selected configurations and parameters.

Table 6. Thermal Conductance C_{cond} for the 3-D domed glazing cavity (Type-B).

Glazing base diameter Ø = 0.6 m			Glazing base diameter Ø = 1.2 m		
H/Ø = 0.1	H/Ø = 0.2	H/Ø = 0.3	H/Ø = 0.1	H/Ø = 0.2	H/Ø = 0.3
Cavity Thermal Conductance $\underline{C}_{cond}$, W/(m^{2}K)					
2.015	1.146	0.912	0.990	0.568	0.421

The following expression, derived from the present numerical study expresses heat flux q_{cond} due to conduction on inside cavity surface with errors less than 3% for most cases in comparing with numerical modeling of conduction heat transfer (Table 3) in domed glazing cavity

$$q_{cond} = \frac{\beta \cdot k \cdot \Delta T}{\frac{H}{2}} \tag{19}$$

Where:

β = Form-factor of dome glazing cavity heat transfer;

$$\beta = 2.0 + 4.9 \cdot \frac{H}{Ø};\ Ø = 0.6\text{m} \tag{20}$$

$$\beta = 0.92 + 2.25 \cdot \frac{H}{Ø};\ Ø = 1.2\text{m} \tag{21}$$

k = Air thermal conductivity at average temperature in the cavity;

ΔT= Temperature difference between cavity walls;

H = Height of the dome.

Using equation (20) the modified Nusselt number for the Type-B domed skylight glazing cavity can be expressed as:

$$Nu_m = \frac{q_{conv}}{\frac{2 \cdot \beta \cdot k \cdot \Delta T}{H}} \tag{22}$$

All heat transfer results are summarized in Table 7 and Figure 28 to Figure 31.

Table 7. Nusselt vs. Raleigh number Dependence for Type-B Domed Skylight Glazing Cavities

Glazing base diameter Ø = 0.6 m							Glazing base diameter Ø = 1.2 m					
H/Ø	H/Ø = 0.1		H/Ø = 0.2		H/Ø = 0.3		H/Ø = 0.1		H/Ø = 0.2		H/Ø = 0.3	
θ =	90°	20°	90°	20°	90°	20°	90°	20°	90°	20°	90°	20°
Ra	Nu number (Nu = q_{conv} / q_{cond})											
11300	1.247	1.3	1.76	1.81	2.18	2.28	1.677	1.786	2.55	2.67	3.45	3.76
22600	1.355	1.44	1.99	2.05	2.477	2.60	1.89	2.02	3.00	3.11	4.13	4.37
45200	1.48	1.6	2.28	2.22	2.84	2.91	2.177	2.33	3.49	3.52	4.89	5.18
67800	1.574	1.63	2.47	2.5	3.15	3.18	2.37	2.536	3.84	3.87	5.47	5.6

Modeling results in terms of modified Nu number, Nu_m are presented in Figure 28 for two glazing cavities (glazing base diameter Ø =0.6 m and Ø = 1.2 m) with the same parameter *H*/Ø = 0.2 in vertical (θ = 90°) and tilted position (θ = 20°). From numerical results we can conclude that increasing base diameter of domed skylight glazing cavity from 0.6 m to 1.2 m results in increase of convection heat transfer by about 50% on average. This is true for vertical and tilted cavities. The intensity of convection heat transfer in tilted cavity under angle 20° differs by less than 4% when compared to the cavity in vertical position (θ = 90°) and that is why it can be considered as independent from tilt angle. It is also true for parameter *H*/Ø = 0.3.

However, in the case of parameter *H*/Ø = 0.1, the discrepancy of heat transfer intensity between two differently oriented cavities is about 8%. Comparison for the parameter *H*/Ø = 0.1 is shown in Figure 51.

Figure 30 shows heat transfer rate of domed skylight glazing cavities in vertical position (θ = 90°) with different parameter *H*/Ø (ratio of the dome height to the dome base diameter). The difference between predicted *Nu* for glazing cavities in vertical orientation (θ = 90°) for different *H*/Ø parameters is from 40% to 50%. Similar difference was observed in the case of tilted glazing cavities (θ = 20°) with different parameter *H*/Ø as shown in Figure 31.

For these reasons the heat transfer rate for these cases should be considered as dependent from parameter *H*/Ø.

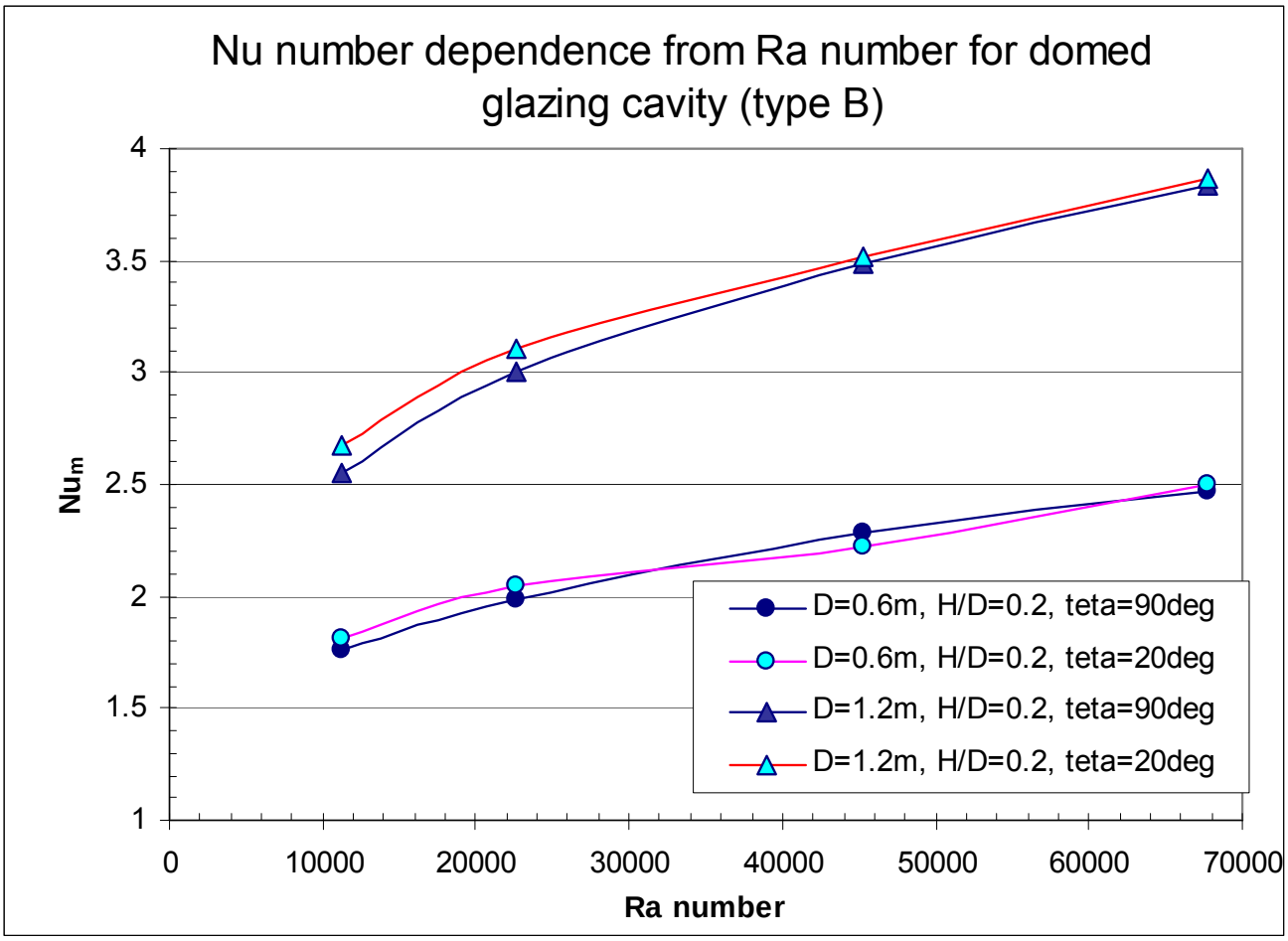


Figure 28. Comparison of Heat Transfer Rate for Type-B Domed Skylight Glazing Cavity with Base Diameters Ø =0.6 m and Ø = 1.2 m. and *H*/Ø = 0.2

.

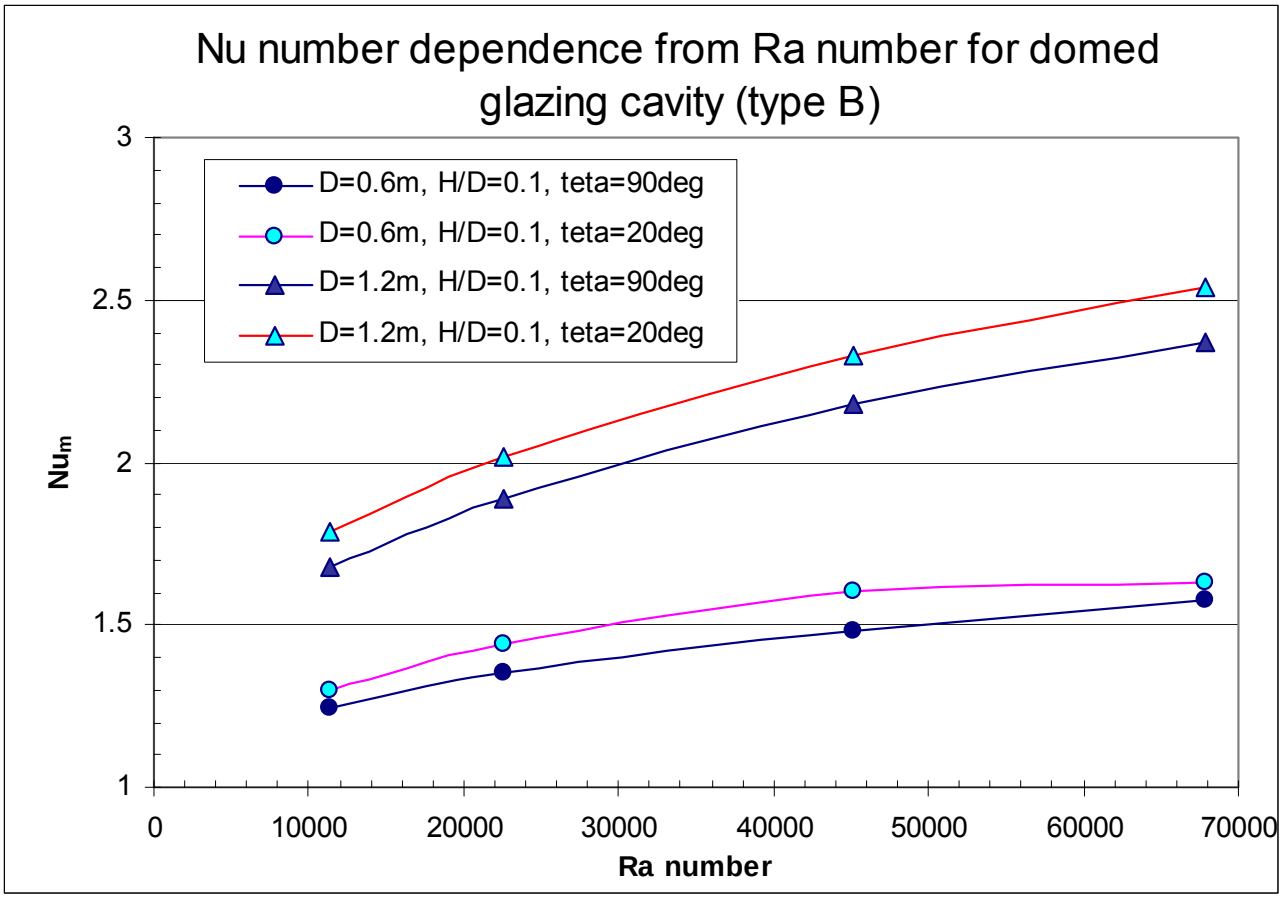


Figure 29. Comparison of Heat Transfer Rate for Type-B Domed Skylight Glazing Cavity with Base Diameters Ø =0.6 m and Ø = 1.2 m. and *H*/Ø = 0.1.

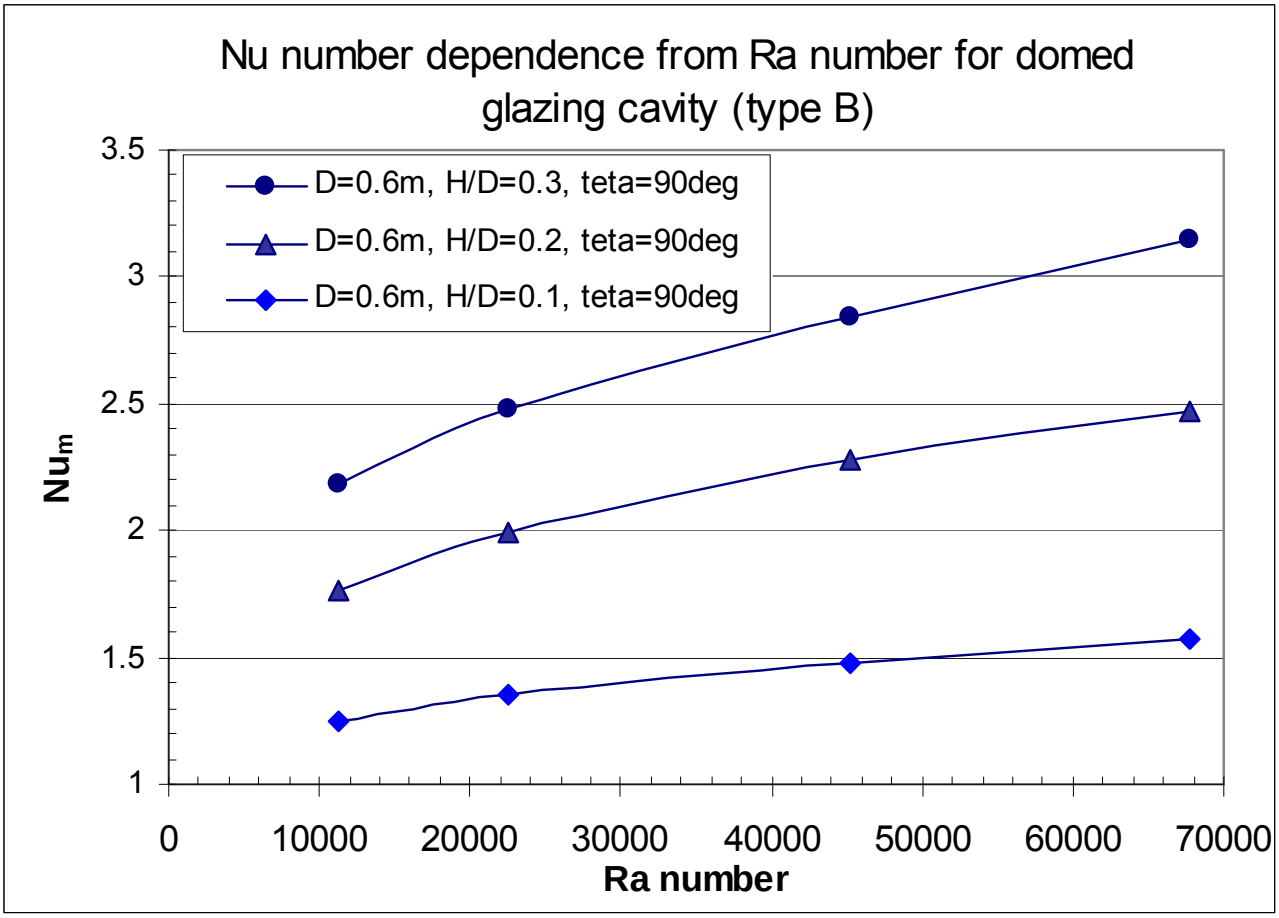


Figure 30. Heat transfer Rate Comparison for Type-B Domed Skylight Glazing Cavities in Vertical Orientation with Different Parameter *H*/Ø.

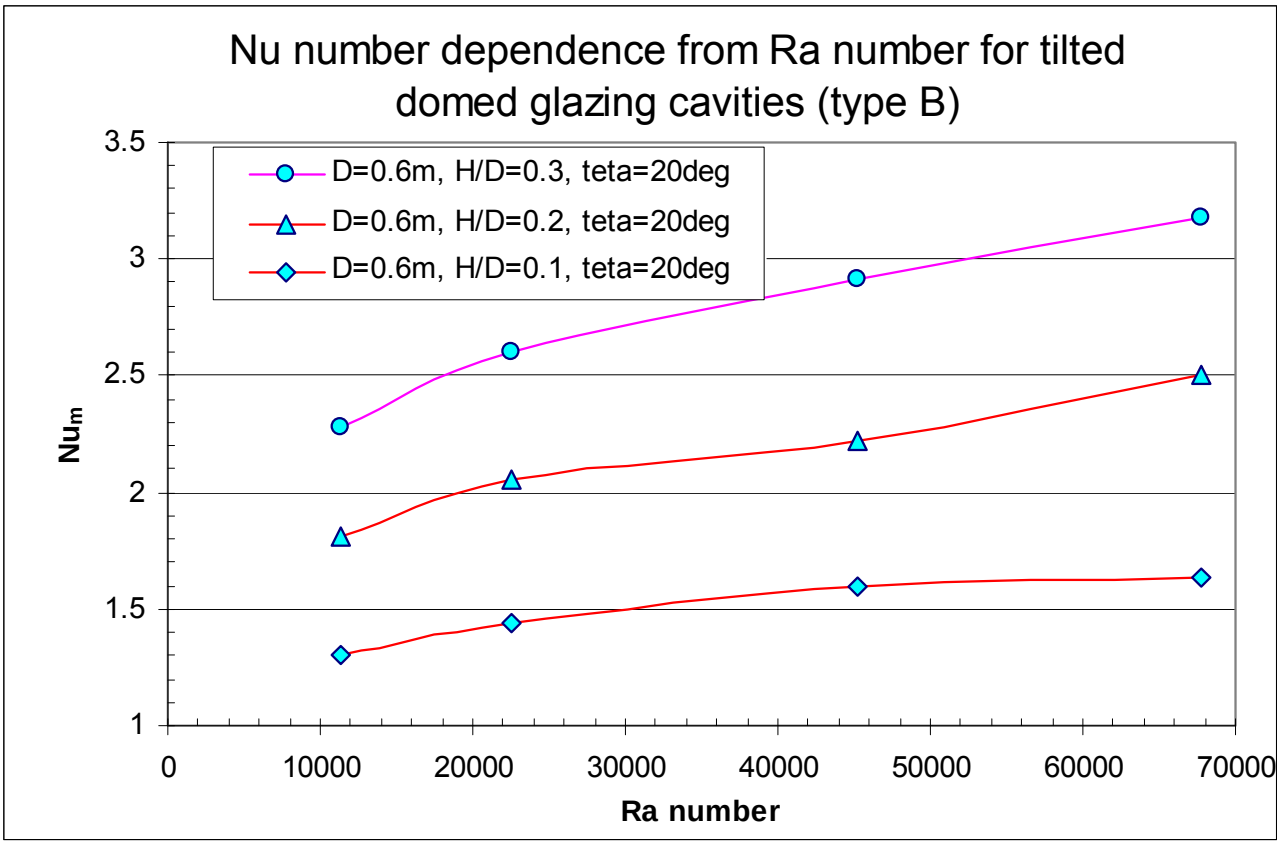


Figure 31. Heat transfer Rate Comparison for Type-B Domed Skylight Glazing Cavities in Tilted Orientation with Different Parameter *H*/Ø.

4.6 Heat transfer correlations for domed glazing cavity of a Type-B

4.6.1 Heat transfer correlations for Type-B domed skylight glazing cavities in vertical orientation

The following convection heat transfer correlations for Nu_m were derived from numerical modeling results for domed glazing cavities in vertical orientation ($\theta = 90^o$) as a function of *Ra*, *H*/Ø, and Ø:

a) Correlation for domed skylight glazing cavities with glazing base diameter Ø = 0.6 m:

$$Nu_{90} = -0.2 + (0.002 \cdot Ra)^{0.12}; \quad \frac{H}{\text{Ø}} = 0.1 \tag{23}$$

$$Nu_{90} = -0.1 + (0.002 \cdot Ra)^{0.19}; \quad \frac{H}{\text{Ø}} = 0.2 \tag{24}$$

$$Nu_{90} = 0.2 + (0.002 \cdot Ra)^{0.22}; \quad \frac{H}{\text{Ø}} = 0.3 \tag{25}$$

b) Correlation for domed glazing cavities with glazing base diameter Ø = 1.2m:

$$Nu_{90} = (0.002 \cdot Ra)^{0.17}; \quad \frac{H}{Ø} = 0.1 \tag{26}$$

$$Nu_{90} = 0.3 + (0.002 \cdot Ra)^{0.26}; \quad \frac{H}{Ø} = 0.2 \tag{27}$$

$$Nu_{90} = 0.8 + (0.002 \cdot Ra)^{0.31}; \quad \frac{H}{Ø} = 0.3 \tag{28}$$

Correlations (23) to (28) are used as endpoints in linear interpolation for determining modified Nu number for specified Ra number in the range of aspect ratio from *H*/Ø = 0.1 to *H*/Ø = 0.3 and glazing base diameter from Ø = 0.6 m to Ø = 1.2 m. Figure 32 show how proposed correlations (23) to (25) are compare with numerical modeling results. Figure 33 show how proposed correlations (26) to (28) are compare with numerical modeling results The maximum difference between correlations and modeling results is less than 2%.

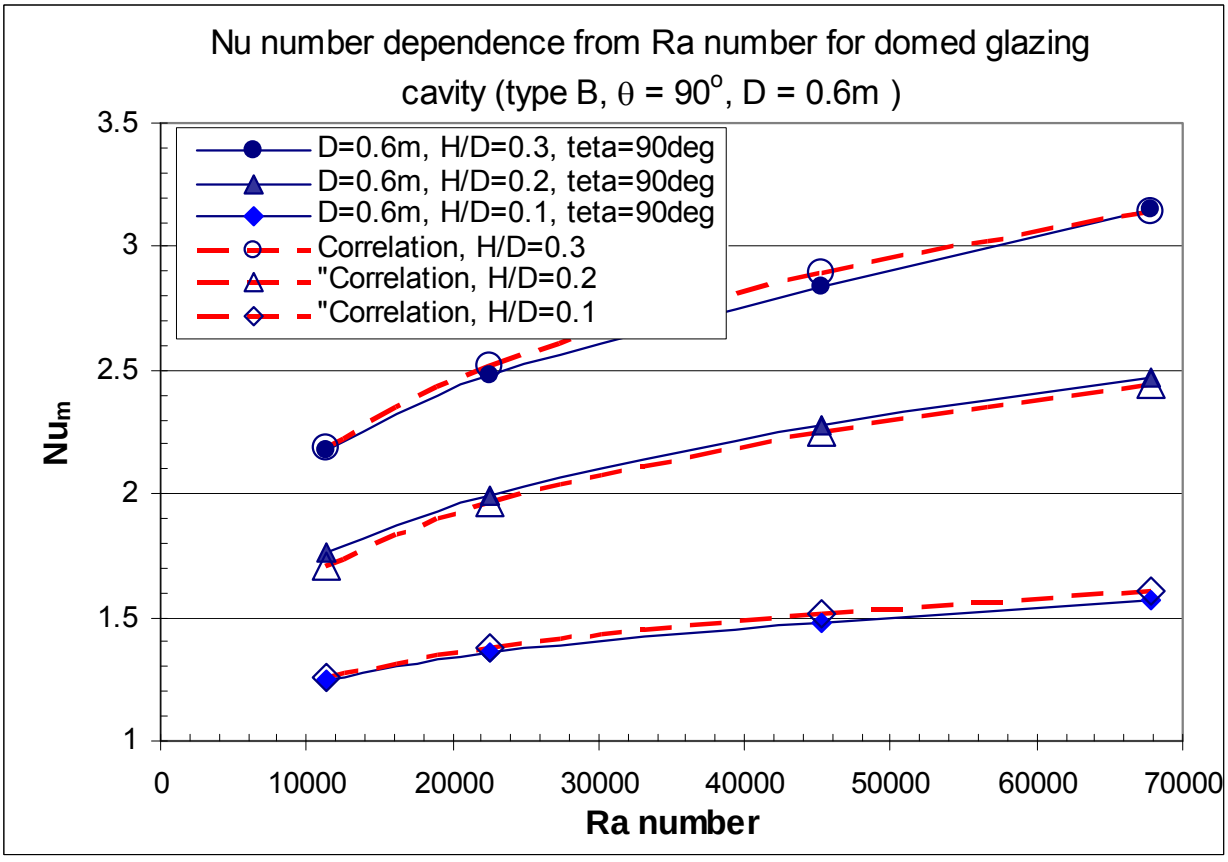


Figure 32. Comparison of Convective Heat Transfer Rates Predicted by Numerical Modeling and Correlations for Type-B Domed Glazing Cavity With Glazing Base Diameter Ø = 0.6 m.

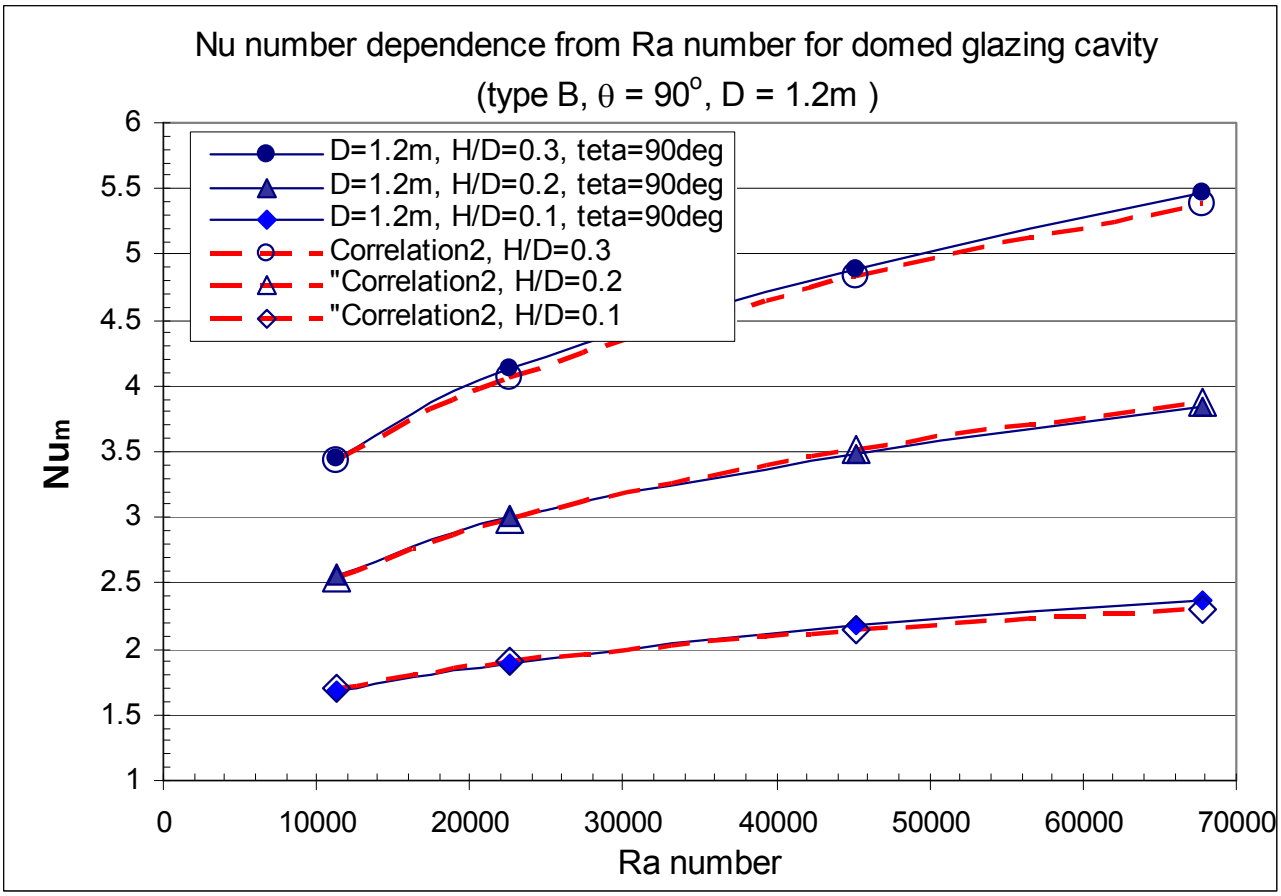


Figure 33. Comparison of Convective Heat Transfer Rates Predicted by Numerical Modeling and Correlations for Type-B Domed Glazing Cavity With Glazing Base Diameter Ø = 1.2 m.

Convective heat transfer coefficient is calculated from the Nu using the following relation:

$$h_c = Nu\frac{2 \cdot k}{d}$$

4.6.2 Heat transfer correlations for Type-B domed skylight glazing cavities in tilted orientation

The following convection heat transfer correlations for Nu_{20} were derived from numerical modeling results for domed skylight glazing cavities in titled orientation (θ = 20°) as a function of *Ra*, Ø, and *H*/Ø:

a) Correlation for Type-B domed skylight glazing cavities with the glazing base diameter in the range of aspect ratio *H*/Ø = 0.2 to *H*/Ø = 0.3.

$$Nu_{20} = Nu_{90};\ 0.2 \le \frac{H}{Ø} \le 0.3 \tag{29}$$

Where:

Nu_{90} = Nusselt number for the same glazing cavity in vertical orientation.

b) Correlation for Type-B domed glazing cavities with the glazing base diameter aspect ratio $H/Ø$ = 0.1:

$$Nu_{20} = -0.17 \cdot (0.002 \cdot Ra)^{0.12};\quad Ø = 0.6\,\text{m} \tag{30}$$

$$Nu_{20} = (0.002 \cdot Ra)^{0.19};\quad Ø = 1.2\,\text{m} \tag{31}$$

To calculate *Nu* for intermediate values of the glazing base diameter Ø and glazing base diameter aspect ratio $H/Ø$, linear interpolation between correlations (29) to (31) is used.

Figure 34 shows how proposed correlations (29) to (31) compare with numerical modeling results. The maximum difference between correlations and modeling results is less than 2%.

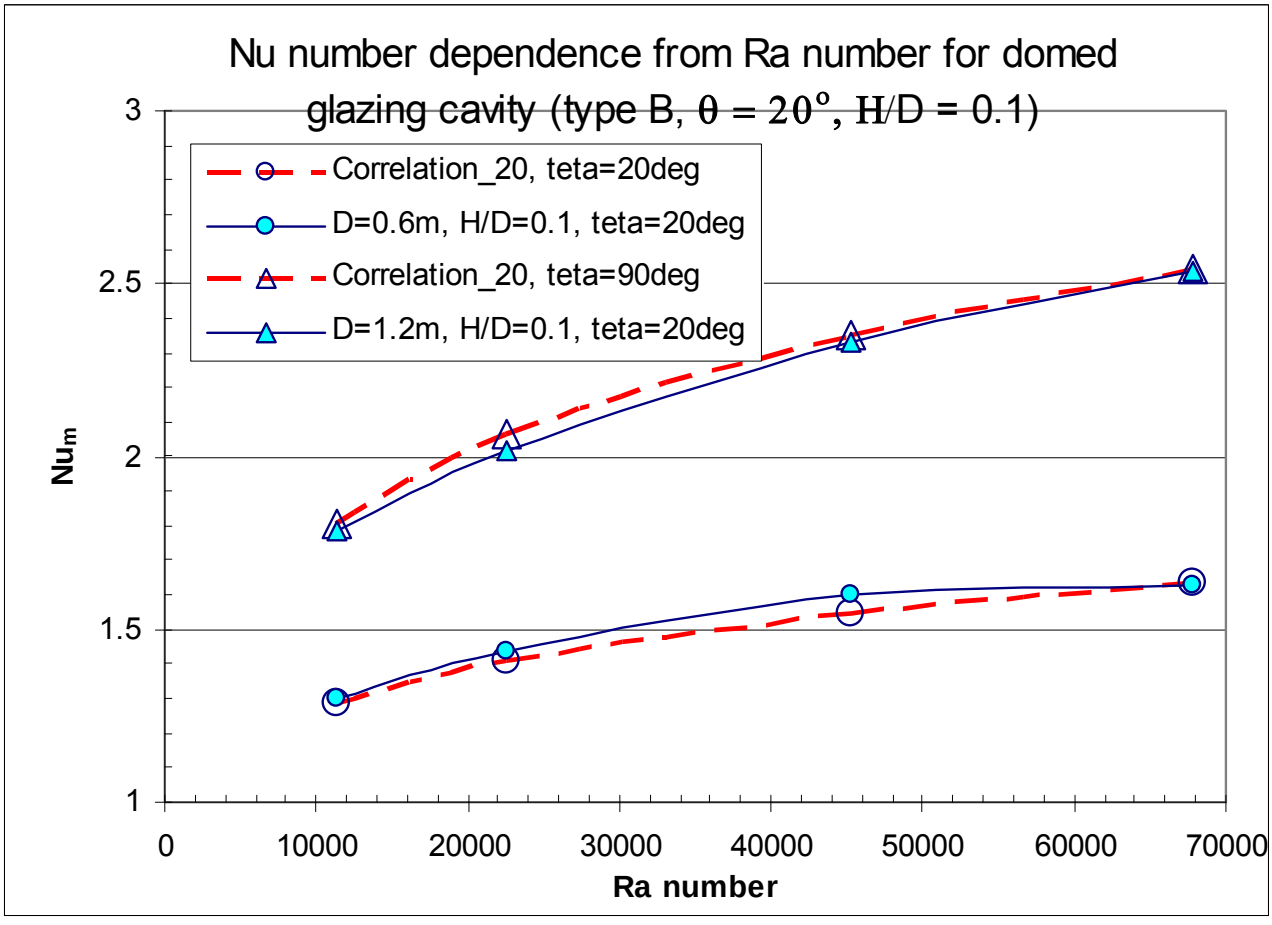


Figure 34. Comparison of Convective Heat Transfer Rates Predicted by Numerical Modeling and Correlations for Type-B Domed Glazing Cavity at Tilt angle θ=20º.

4.7 Summary

1) Domed skylight glazing cavities classification and formulas for creating 3-D numerical models of domed glazing cavities with non-uniform gap were developed. In particular, typical domed skylight glazing cavities can be categorized as Type-A, Type-B, or their combination (i.e., triple or quadruple glazed cavity).
2) Formulas for generating appropriate 3-D geometries using common geometry parameters, such as glazing base dimension, radius of curvature, and maximum gap width were developed.
3) The 3-D numerical models are developed for simulation of natural convection and detailed radiation heat transfer in domed skylight glazing cavities in vertical orientation (90º from horizontal) and tilted orientation (20º from horizontal).
4) The results of numerical modeling were expressed in terms of heat transfer rates and temperature distributions and presented in tabular and graph format.
5) Modified Nusselt number, Nu_m was developed to account for varying cavity gap widths.
6) Heat transfer correlations for domed skylight glazing cavities of a Type-A and Type-B were developed for vertical orientation ($\theta = 90º$) and tilted orientation ($\theta = 20º$).
7) Heat transfer for triple or quadruple dome skylight glazing cavities can be calculated using correlations for Type-A and Type-B cavities, by applying appropriate correlation to each cavity

5. EXPERIMENTAL STUDY AND VALIDATION OF HEAT TRANSFER IN DOMED SKYLIGHT GLAZING CAVITIES

This section presents results of experimental study of selected domed skylight glazing cavities, covering both Type A and Type B configurations. The goal of this study was to validate results of numerical 3-D modeling convection heat transfer in the vertical oriented domed skylight cavities against experiment results. The numerical modeling gives us information about temperature and heat flux distribution on glazing cavity walls that could be compared with test values under the same conditions. Thus, by verifying some of the numerical results, we are validating the subsequent correlations that are developed from these numerical results.

5.1 Experiment Description

Figure 35 shows a schematic drawing of the skylight glazing sample installation in insulation panel opening and locations of the attached heat flux meters and thermocouples.

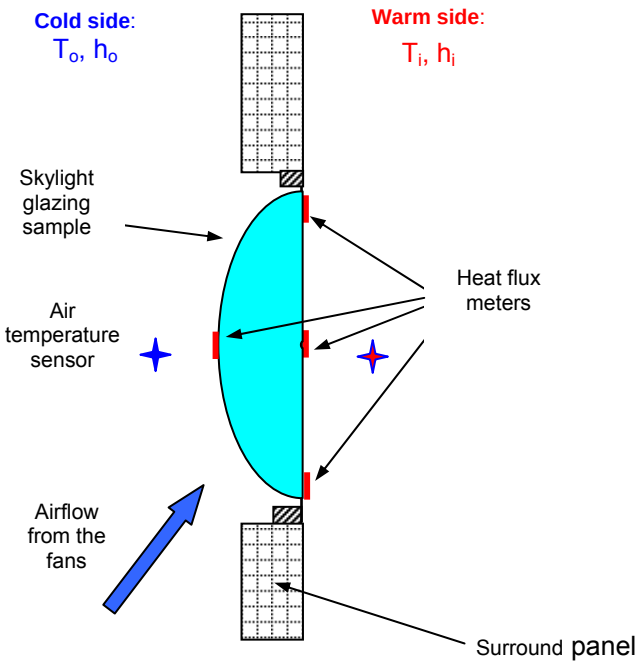


Figure 35. Schematic of Dome4d Skylight Glazing Sample Installation in the Surround Panel.

Test equipment

Experimental portion of the research work was done in a custom built measurement apparatus, consisting of the climatic chamber and measurement section. This measurement apparatus will be called Thermal Transmittance Apparatus.

Climatic chamber was constructed from the large size freezer, which was adapted and modified for this purpose. Inside dimensions of the freezer are *H* x *W* = 115cm x 86cm. The opening 114cm x 85cm was cut in the freezer door and insulation panel consisting of polyisocyanurate board was installed in the opening. This climatic chamber is shown in Figure 36



Figure 36. Thermal Transmittance Apparatus with the Surround Panel and Specimen Opening in Place**.**

Thermal conductivity of the surround panel was measured using the LaserComp FOX 304 instrument (LaserComp 2003). This thermal conductivity was utilized in a calibration procedure for the Thermal Transmittance Apparatus. The FOX 304 instrument is calibrated using NIST SRM 1450b (Standard Reference Material of National Institute of Standards and Technology). Accuracy (total uncertainty) for the FOX 304 apparatus and measurement conditions is 1% (FOX304 instrument's specification).

Temperature sensors

The type-T thermocouples have been used for the temperature measurement. Six thermocouples were fabricated from gage 30 copper-constantan wires. The accuracy and quality of thermocouples were checked using Omega thermometer/calibrator (model CL23A) and the method of comparing with standard type-T thermocouple at three temperature points: -18C^{o}, 0C^{o} and 24C^{o}.

Heat flux sensors

Four heat flux meters (transducers) have been used for the measurements of heat flux on domed skylight glazing surfaces. The heat flux meters of the integrating type with thickness of 2 mm were used. Two different sensor geometries were used; 1) Rectangular active measurement area with the overall sensor size of 40mm x 8mm; and 2) Circular active measurement area with the diameter of Ø =20mm. The heat flux meters incorporate type-T thermocouples arranged in thermo par fashion.

From the calibration procedure, the total uncertainty of these heat flux meters was estimated as 4.9%.

Data Acquisition System

Agilent (model 34970A) Data Acquisition/Switch Unit was used for reading and storing temperature and electrical signals from thermocouples and heat flux meters.

Figure 37 shows skylight glazing sample installed in the surround panel opening, ready for testing.

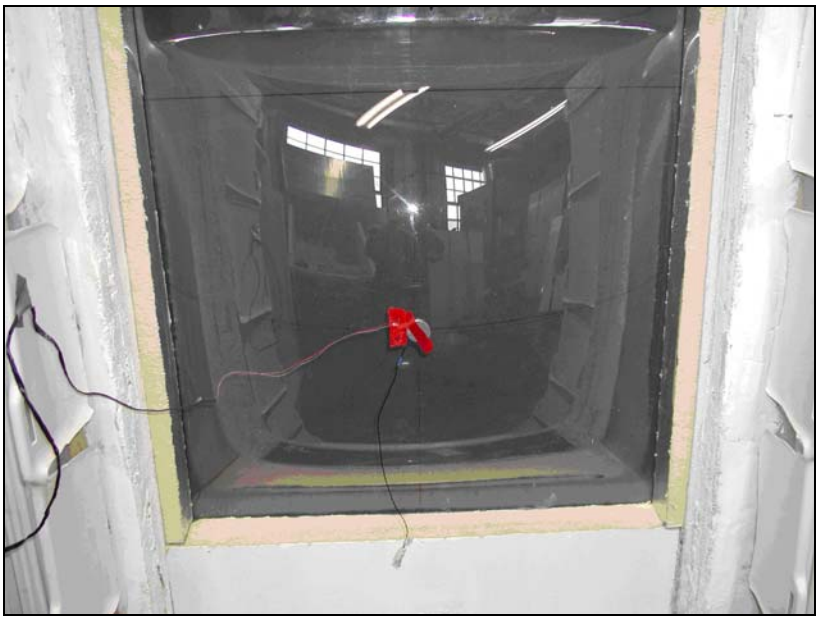


Figure 37. Domed Skylight Glazing Sample Installed in the Surround Panel Opening.

5.2 Calculation of the heat transfer (film) coefficient

The indoor and outdoor local surface heat transfer coefficients (also known as local film coefficients) h_i *and* h_o on glazing surfaces along the centerline were calculated from the following equation:

$$h_i = \frac{q_{HF_i}}{t_i - t_{si}} \tag{32}$$

$$h_o = \frac{q_{HF_o}}{t_o - t_{so}} \tag{33}$$

Where:

q_{HF_i} - heat flux measured by heat flux meter on indoor surface, W/m^2;

q_{HF_o} - heat flux measured by heat flux meter on outdoor surface, W/m^2;

t_i - air temperature measured on indoor side, ºC;

t_i - air temperature measured on outdoor side, ºC;

t_{si} - surface temperature measured on indoor specimen surface, ºC.

t_{si} - surface temperature measured on outdoor specimen surface, ºC.

5.3 Numerical model for Validation

In order to validate numerical model used for generating results for the full set of domed skylight configurations, selected fixed configuration is numerically modeled and experimentally tested and results compared. Local values of heat flux and surface temperatures are measured and compared to the equivalent values in a numerical model. The boundary conditions applied to the numerical model are based on the values obtained during the measurement (see Section 5.2).

5.4 Domed Skylight Glazing Type-A

Type-A glazing for domed skylights has two curved walls. Figure 38 and Figure 39 depict the Type-A test sample, prepared for thermal testing. The convex-concave glazing is fabricated from two 2.5 mm sheets of acrylic (polymetilmetacrilate) with the maximum gap thickness of 25 mm. The height of the glazing is 16 cm. The base of the sample has the size 56 cm x 56 cm (22”x22”). Figure 40 shows a schematic representation of the domed skylight glazing sample installation in surround panel opening and locations of the attached heat flux meters and thermocouples.



Figure 38. Test Sample for the Type-A Domed Skylight Glazing.

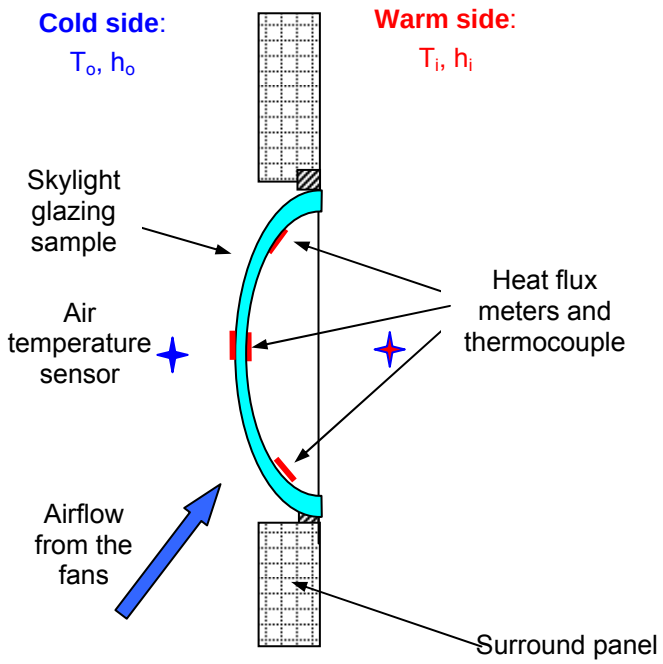


Figure 39. Schematic of the Domed Skylight Glazing Installation in a Surround Pannel.

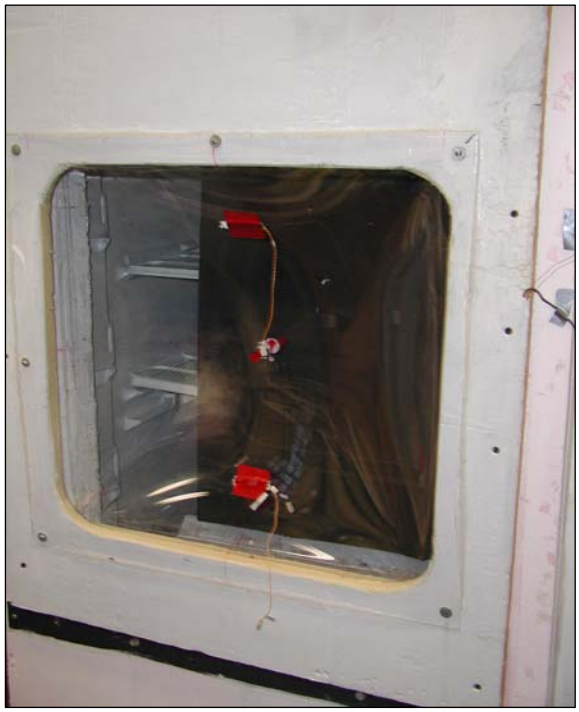


Figure 40. Schematic of the Type-A Domed Skylight Glazing Sample Installation in the Surround Panel.

***Description of boundary conditions and numerical model*.**

Figure 41 and Figure 42 show boundary conditions and geometry of the 3-D Type-A domed glazing cavity numerical model. The model was created using geometrical parameters for the dome glazing cavity sample that was measured in a thermal transmittance apparatus. The following dimensions were used: base diameter Ø = 0.56 m, ratio of glazing height to the base diameter $H/Ø$ =0.28 and gap width 25 mm. Temperatures t_h and t_c were recorded during an experiment and applied to the numerical model. Surface heat transfer coefficients h_h and h_c were calculated using equations in Section 5.2.

For the simulation of convection heat transfer in a domed glazing cavity a laminar viscous model with Boussinesq approximation was used. Thermo-physical properties of air were treated as constants and were evaluated at the temperature of 0°C using standard gas correlations (ISO 2003). Radiation heat transfer was modeled using Fluent DTRM radiation model. Emissivity of surfaces participating in a heat transfer (domed glazing cavity surfaces facing the cavity) were defined as ε =0.9.

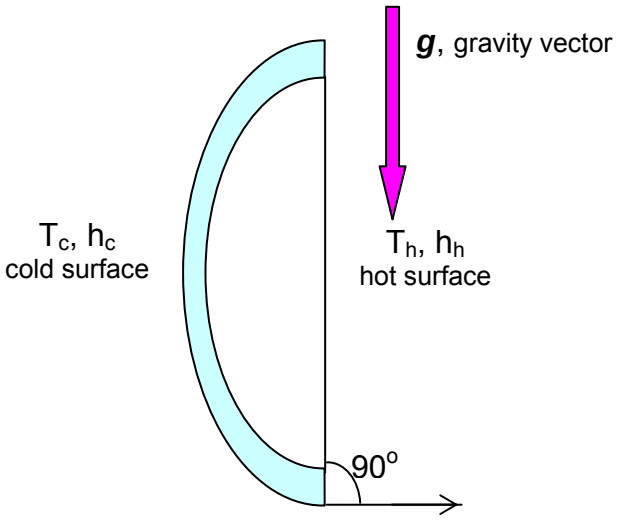


Figure 41. Boundary Conditions and Configuration for the Type-A Domed Skylight Glazing Cavity Numerical Model in Vertical Position.

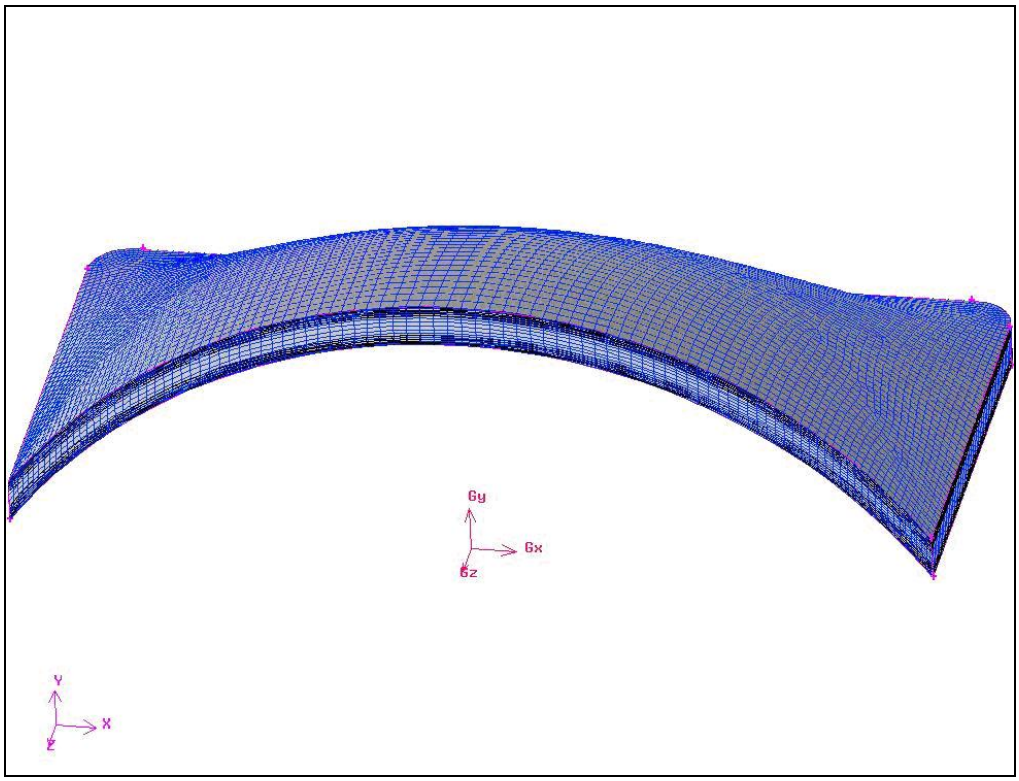


Figure 42. Finite Volume Mesh for the Type-A Domed Skylight Glazing Cavity (Ø = 0.56 m, *H*/Ø = 0.28, gap *d* = 25 mm).

Simulation Results and Comparison to the Experimental Results:

Results of numerical model include detailed heat flux, temperature and velocity fields for every region of the model. Figure 43 shows temperature and velocity fields in the vertical Type-A domed skylight glazing cavity.

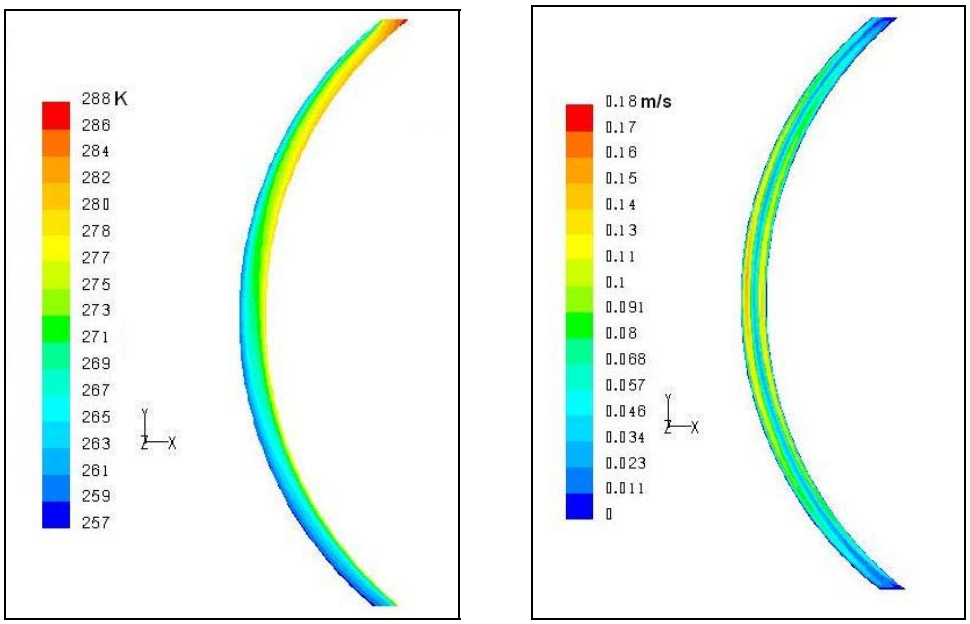


Figure 43. Predicted Temperature and Velocity Magnitude Distributions in a Symmetry Plane of a Type-A Domed Skylight Glazing Cavity.

Heat flux and temperature results for the predetermined locations, coinciding with the measurement locations, are presented in Table 8 and in Figure 44. These results are compared with the results of experimental measurements. Comparison of results shows that 3-D numerical model makes good prediction of the heat flow magnitudes and temperatures. The difference between measured and predicted average heat fluxes is within 3% for the most of the glazing surface and only in the bottom part the difference is 7%. The maximum difference in surface temperatures in the central area of glazing is 0.5 ^{o}C, which is excellent.

Table 8. The comparison Between Experimental and Numerical Results for the Domed Skylight Glazing, Type-A

Method	Boundary conditions: T, ^{o}C; h, W/(m^{2}K)				Hot wall surface temperature T_h, ^{0}C	Heat flux on hot wall, W/m^2		
						Location (Fig. 7)		
	T	h	T	h		1	2	3
Test	20.8	8.3	-19.0	22.0	8.1	128.6	107.6	107.9
Simulation	20.8	8.3	-19.0	22.0	7.6	129.5	115.7	100.7
Difference, %						-0.7	-7.0	+6.7

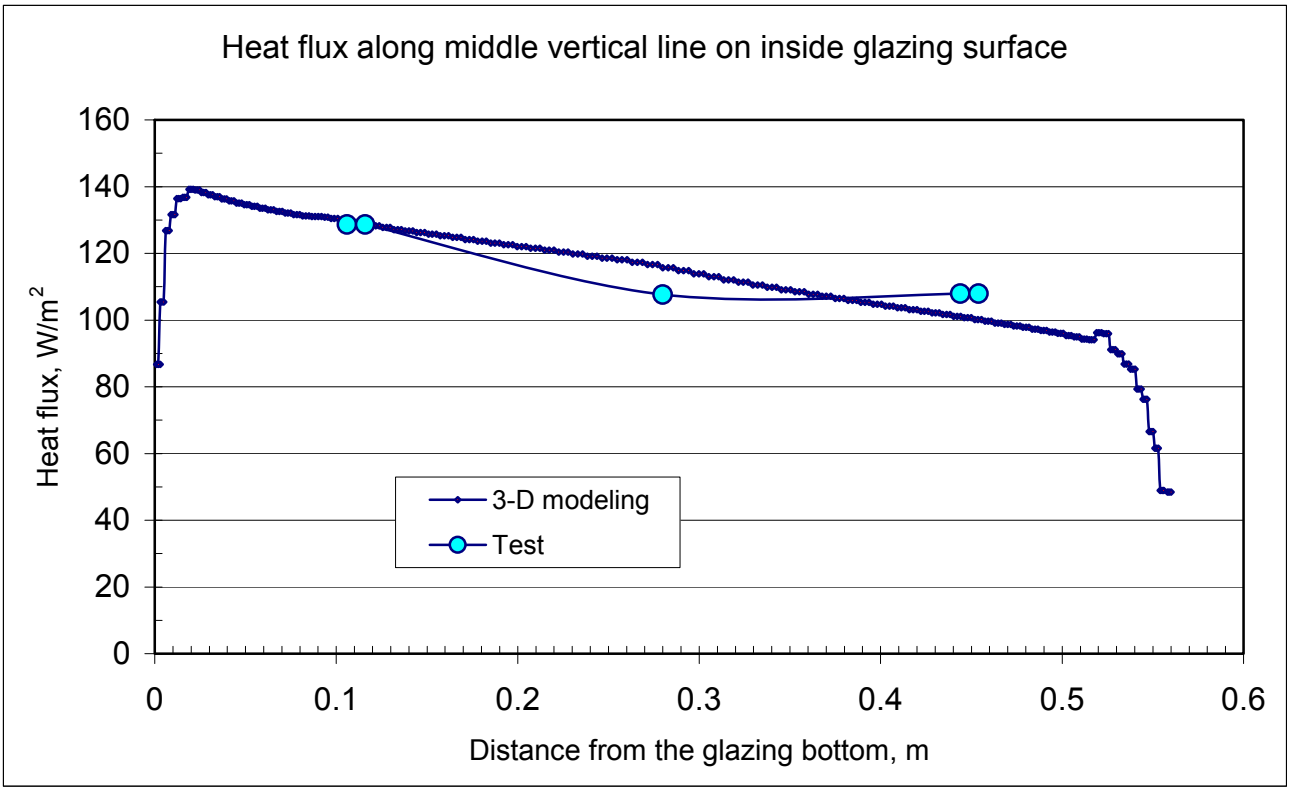


Figure 44. Comparison of Heat Flux Distribution Along the Vertical Symmetry Line on the Warm Glazing Surface of the Type-A Domed Skylight Glazing

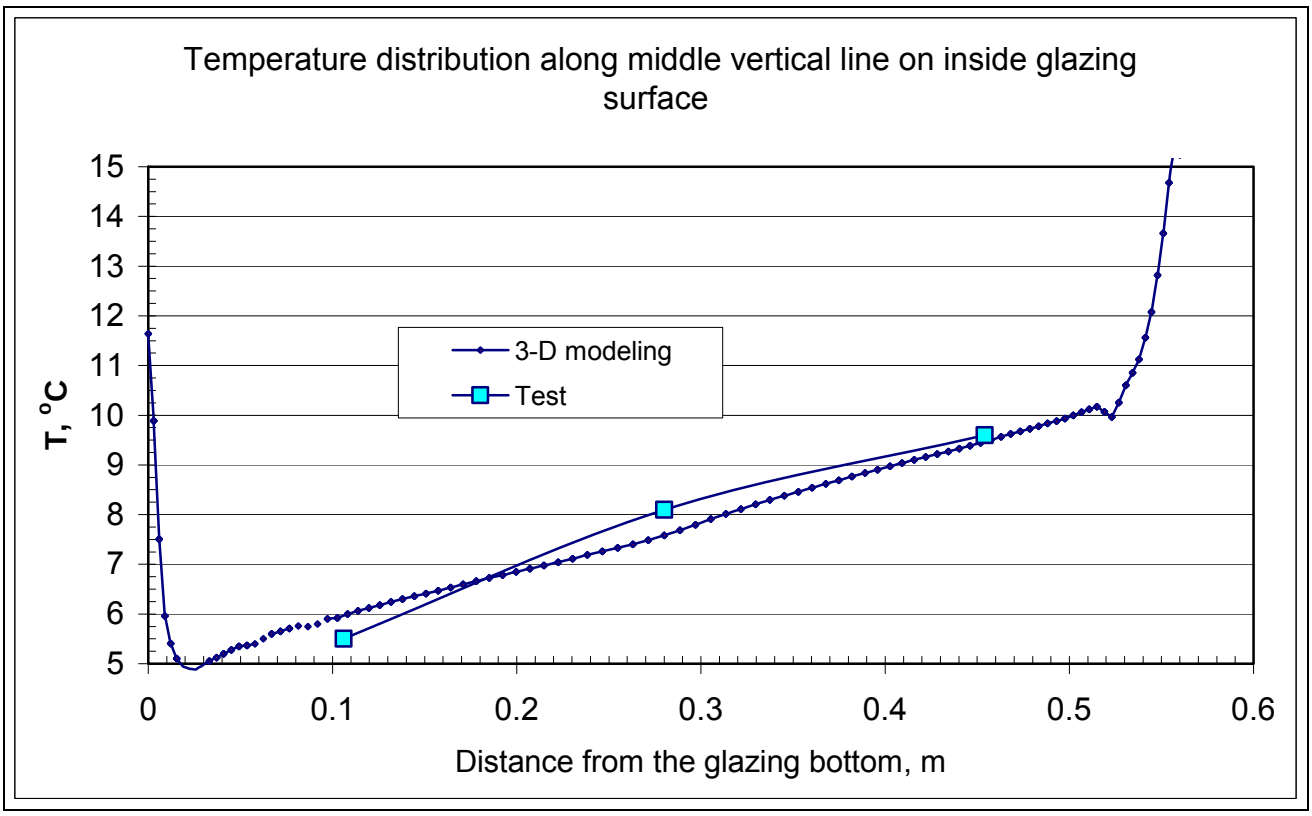


Figure 45. Comparison of Temperature Distribution Along the Vertical Symmetry Line on the Warm Glazing Surface of the Type-A Domed Skylight Glazing

Effect of the Surface Heat Transfer Coefficient Magnitude on the Warm Surface

To estimate range and dependence of indoor surface heat transfer coefficient on curved glazing surface temperature facing indoors, two measurements were done using different temperature differential. Heat fluxes and surface temperatures were measured in three locations under steady state conditions for two temperature differences $\Delta = T_h - T_c = 39.8^oC$ and $\Delta = 37.7^oC$. Results are presented in Figure 46.

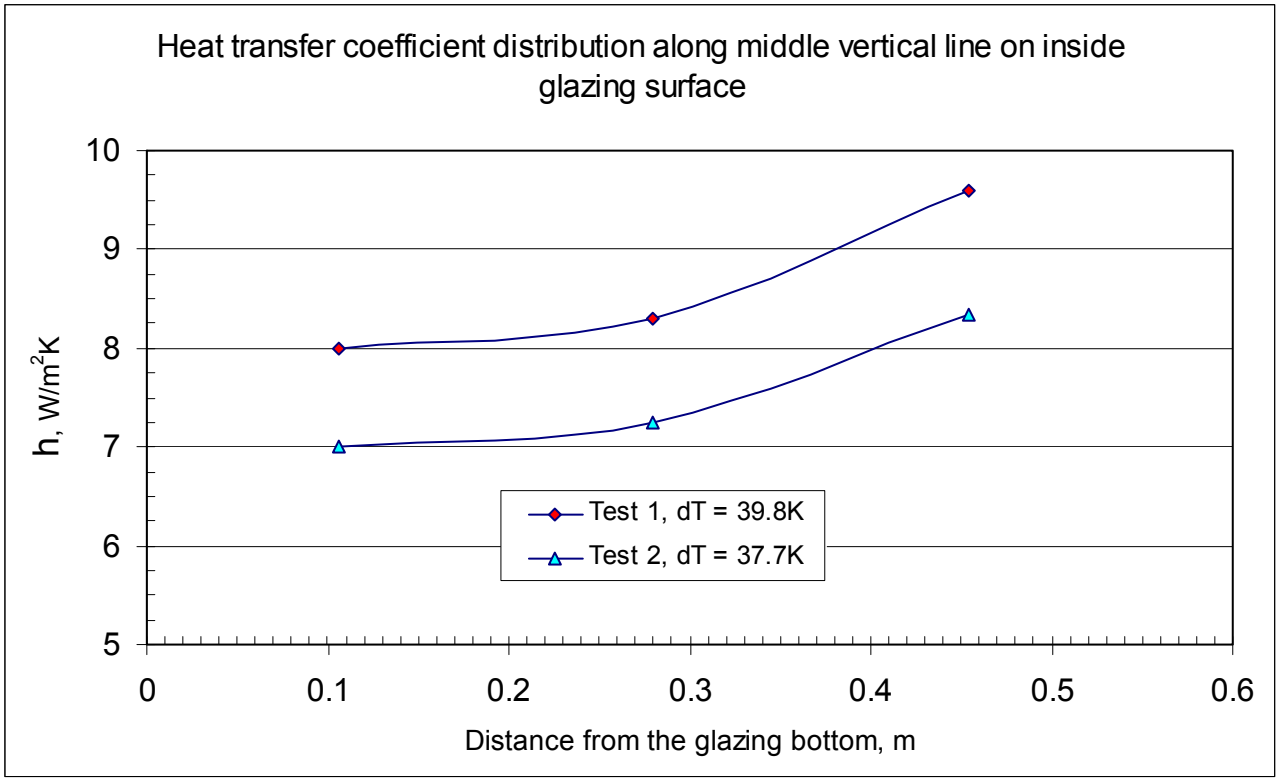


Figure 46. Heat Transfer Coefficient Distribution on the Warm Glazing Surface of the Type-A Domed Skylight Glazing

5.5 Domed Skylight Glazing Type-B

Type B glazing for domed skylights has one curved wall and other flat wall (flat wall oriented towards indoor side). Figure 47 depicts the type B test sample, prepared for thermal testing. The convex glazing is fabricated from 2.5 mm sheet of acrylic (polymetilmetacrilate) sheet. The maximum gap and the height of the glazing is 13.5 cm. The base of the sample has the size 56 cm x 56 cm (22”x22”). For testing purposes the convex acrylic sheet was attached to flat rigid PVC 3.2 mm sheet that plays the role of the second glazing layer in the experiment.

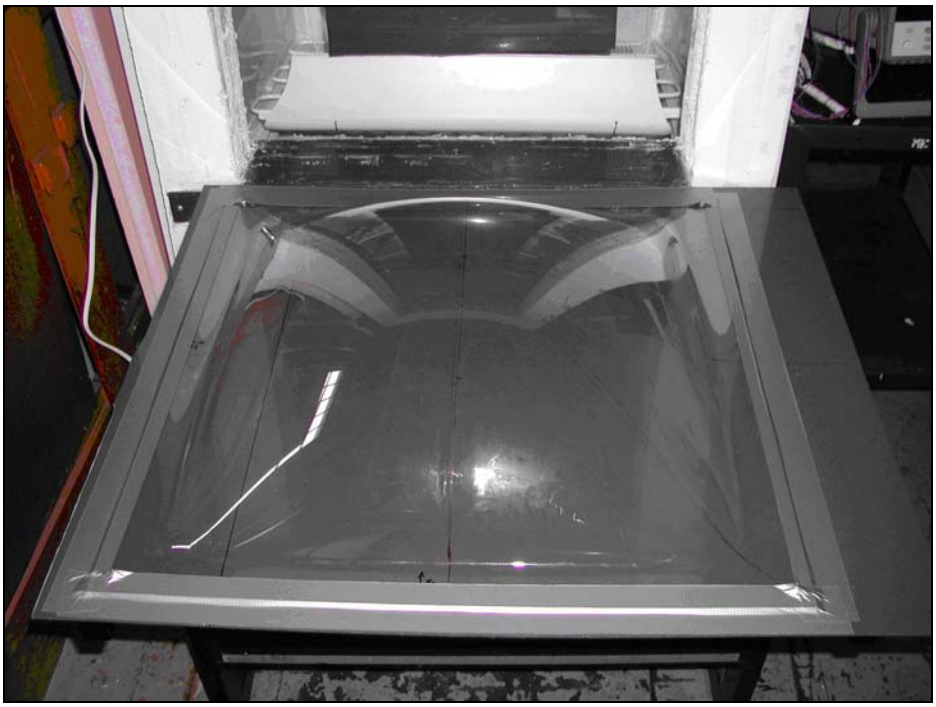


Figure 47. Test Sample for the Type-B Domed Skylight Glazing.

***Description of boundary conditions and numerical model*.**

Figure 48 and Figure 49 show boundary conditions and geometry of the 3-D Type B domed glazing cavity numerical model. The model was created using geometrical parameters for the dome glazing cavity sample that was measured in a Heat Transmittance apparatus. The following dimensions were used: base diameter Ø = 0.56 m, ratio of glazing height to the base diameter $H/Ø$ =0.24. temperatures t_h and t_c were recorded during an experiment and applied to the numerical model. Surface heat transfer coefficients h_h and h_c were calculated using equations in Section 5.2.

For the simulation of convection heat transfer in a domed glazing cavity a laminar viscous model with Boussinesq approximation was used. Thermo-physical properties of air were treated as constants and were evaluated at the temperature of 0^oC using standard gas correlations (ISO 2003). Radiation heat transfer was modeled using Fluent DTRM radiation model. Emissivity of surfaces participating in heat transfer (domed glazing cavity surfaces facing the cavity) were defined as ε =0.9.

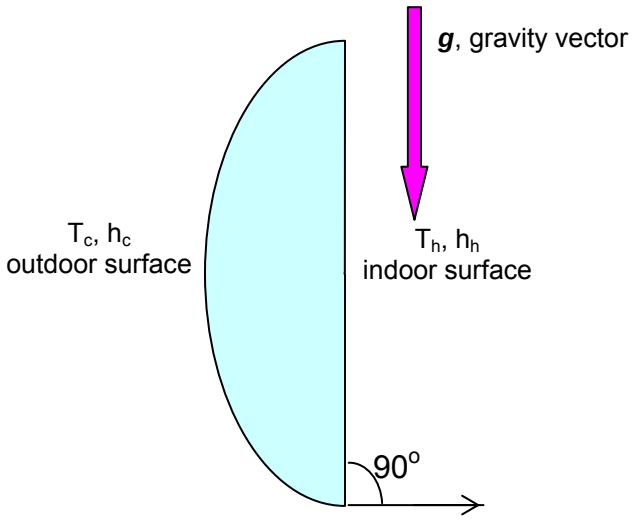


Figure 48. Boundary Conditions and Configuration for the Type-B Domed Skylight Glazing Cavity Numerical Model in Vertical Position.

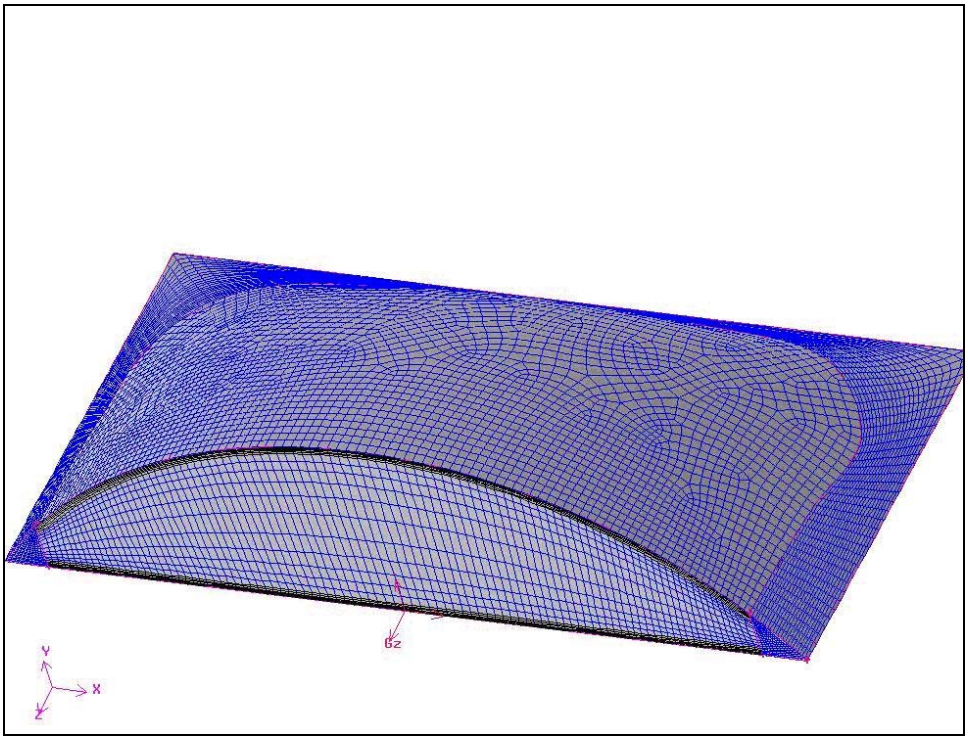


Figure 49. Finite Volume Mesh for the Type-B Domed Skylight Glazing Cavity (Ø=0.56 m, *H*/Ø=0.24).

Simulation Results and Comparison to the Experimental Results:

Results of the numerical model include detailed heat flux, temperature and velocity fields for every region of the model. Figure 50 shows temperature and velocity fields in the vertical domed skylight glazing cavity.

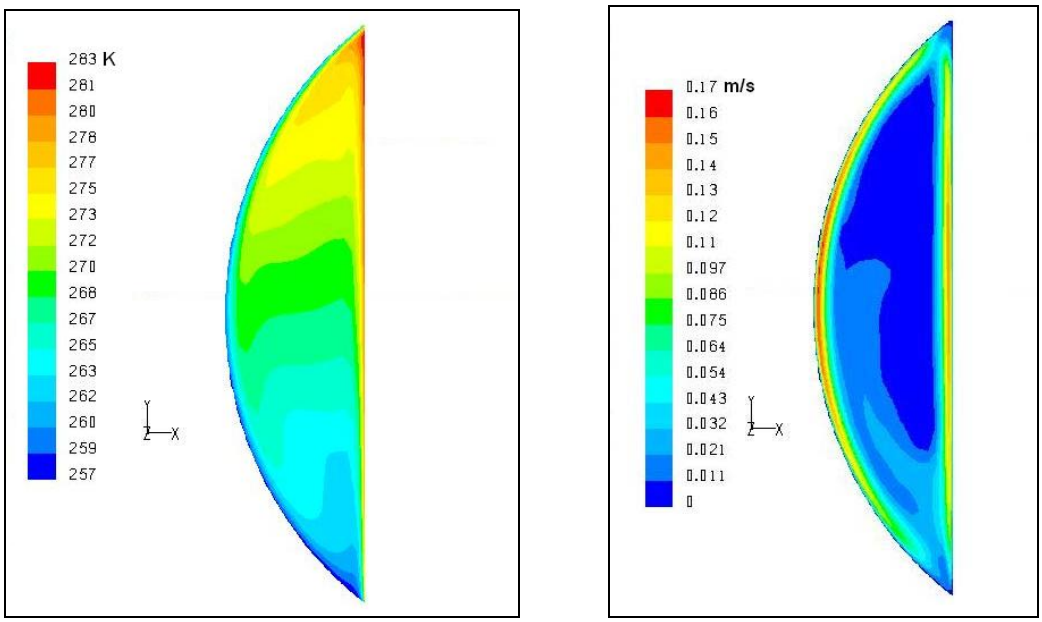


Figure 50. Predicted Temperature and Velocity Magnitude Distributions in a Symmetry Plane of a Domed Glazing Cavity.

Heat flux and temperature results for the predetermined locations, coinciding with the measurement locations, are presented in Table 9 and in Figure 51. These results are compared with the results of experimental measurements. Comparison of results shows that 3-D numerical model makes good prediction of the heat flow magnitudes and temperatures. The difference between measured and predicted average heat fluxes is within 3% for the most of the glazing surface and only in the bottom part the difference is 7.2%. The difference in surface temperatures in the central area of glazing is 1.5 ^{o}C, which is also very close.

Table 9. The comparison Between Experimental and Numerical Results for the Domed Skylight Glazing, Type-B

Source of Data	Boundary conditions: T, °C; h, W/(m²K)				Hot wall surface temperature T_h, °C	Heat flux on hot wall, W/m²		
						Location (Fig. 7)		
	T	h	T	h		1	2	3
Test	22.2	11.1	-18.6	21.3	11.0	166.3	125.5	109.2
Simulation	22.2	11.1	-18.6	21.3	9.5	154.2	128.2	111.8
Difference, %	0.0		0.0			+7.2	-3.0	-2.4

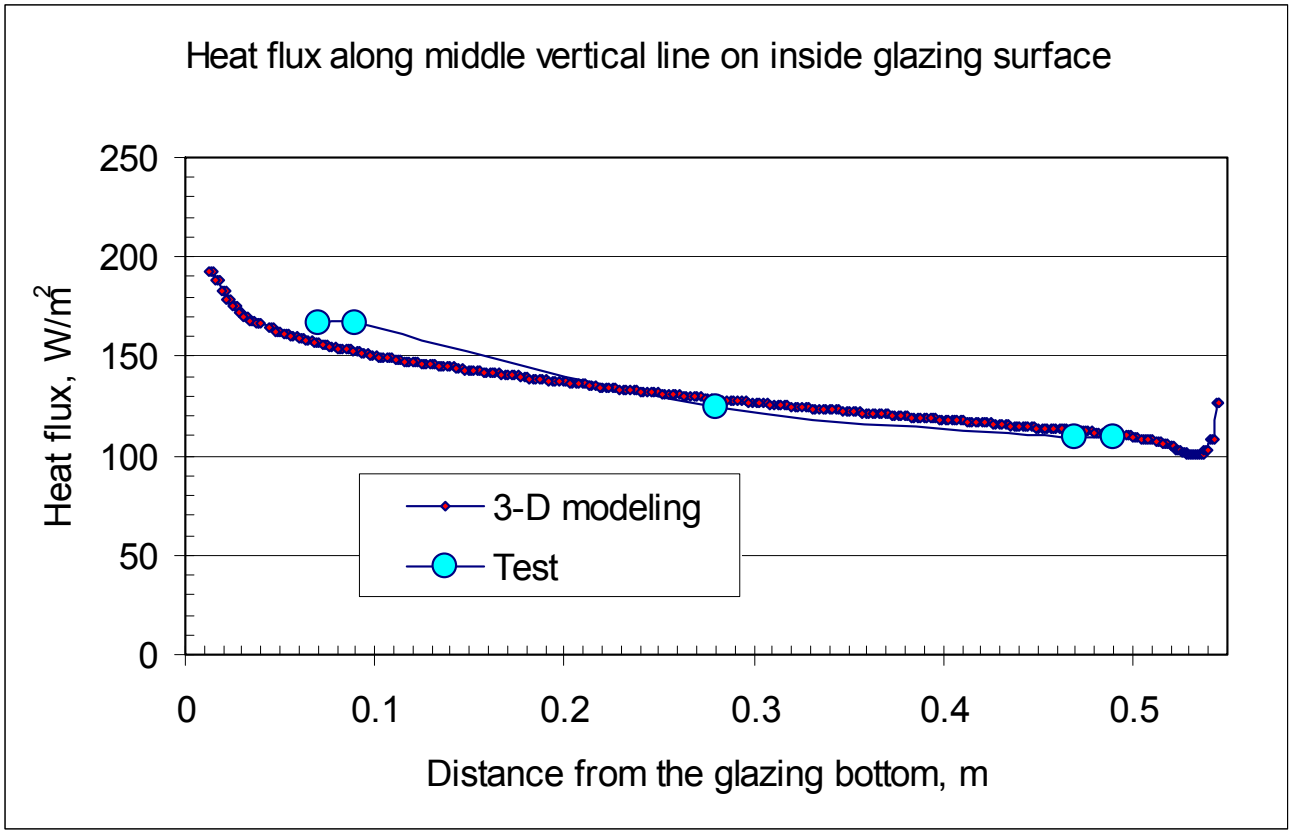


Figure 51. Comparison of Heat Flux Distribution Along the Vertical Symmetry Line on the Warm Glazing Surface of the Domed Skylight Glazing Type-B.

5.5 Summary

1) Experimental validation of numerical modeling for domed skylight glazing cavities using Thermal Transmittance Apparatus was developed for this research project.

This experimental validation can lead to the development of the alternative experimental technique for measuring and validating numerical modeling of heat transfer in fenestration products,

2) Measurements were done on Type-A and Type-B domed skylight glazing cavities for the purpose of validating numerical model. One sample (type B with one convex and other flat glass sheet) has base size 56 cm x 56 cm (22"x22") and height 13.5 cm; Second sample (type A with one convex and other concave glass sheet and with gap between them 25 mm) has base size 56 cm x 56 cm (22"x22") and height 16 cm.
3) The distribution of heat transfer coefficient on curved warm (indoor) glazing surface was obtained from test results for two different air to surface temperature differences.
4) Results of measuring heat flux through the warm wall of the domed skylight glazing and surface temperature were compared with 3-D numerical simulation results under the same boundary conditions. From the comparison it can be concluded that 3-D numerical model predicts well heat fluxes and surface temperatures on the glazing surface. Average difference in predicted and measured average heat fluxes is within 5% and maximum difference is 7.2% and average temperature difference is within 0.5^{o}C at maximum difference of 1.5^{o}C.
5) 3-D numerical model can be used with confidence to generate full set of results for all configurations and to generate heat transfer correlations.

6. CONCLUSIONS

1. Measurements of heat flux rates using surface heat flux transducers can be used to validate numerical modeling of complex convection and radiation heat transfer models and can lead to the development of a measurement standard for these kind of measurements,
2. Experimental validation of numerical modeling for all types of domed skylight glazing cavities produced very good to excellent agreement and gives high degree of confidence in the numerical modeling results,
3. 3-D numerical models of convection and radiation heat transfer in domed skylight glazing cavities were required to capture fluid flow details in domed skylight glazing cavities and to provide adequate accuracy of numerical modeling,
4. Domed skylight glazing cavities were categorized in three distinct groups, labeled Type-A, Type-B, and Type-C. Type-C, consisting of three glazing layers, can be constructed by combining Type-A and Type-B, so its heat transfer rates can be calculated by combining Type-A and/or Type-B cavities and applying appropriate correlations for these cavities.
5. Heat transfer correlations for calculating convective heat transfer rates in domed skylight glazing cavities were developed for Type-A and Type-B cavities for all relevant geometric parameters.

7. RECOMMENDATIONS

1. New heat transfer correlations for all types of domed skylight glazing cavities are proposed to be used for computer modeling of domed skylights and presented below:

Glazing Cavity	Tilt angle	Correlation
Type-A	θ = 90°	$Nu_{90} = 0.95 \cdot \left(0.01 \cdot Ra \cdot \frac{d}{Ø} \right)^{0.08}$; $d \le 0.05$ m
		$Nu_{90} = 0.95 \cdot (0.00125 \cdot Ra)^{0.12}$; $d = 0.075$ m *and* $Ø \le 0.6$ m
		$Nu_{90} = 0.95 \cdot (0.000625 \cdot Ra)^{0.13}$; $d = 0.075$ m *and* $Ø = 1.2$ m
		Linear interpolation for d and Ø in-between above values
	θ = 20°	$Nu_{20} = Nu_{90} \cdot \left[1.03 + 2.3 \cdot 10^{-5} \cdot Ra \cdot \left(\log 10 \left(\frac{H}{Ø} \right) + 0.7 \right)^2 \right]$; $d \le 0.075m$; $Ø \le 1.2$ m; H/Ø ≤ 0.3
Type-B	θ = 90°	$Nu_{90} = -0.2 + (0.002 \cdot Ra)^{0.12}$; $\frac{H}{Ø} = 0.1$ and $Ø = 0.6$ m
		$Nu_{90} = -0.1 + (0.002 \cdot Ra)^{0.19}$; $\frac{H}{Ø} = 0.2$ and $Ø = 0.6$ m
		$Nu_{90} = 0.2 + (0.002 \cdot Ra)^{0.22}$; $\frac{H}{Ø} = 0.3$ and $Ø = 0.6$ m
		$Nu_{90} = (0.002 \cdot Ra)^{0.17}$; $\frac{H}{Ø} = 0.1$ and $Ø = 1.2$ m
		$Nu_{90} = 0.3 + (0.002 \cdot Ra)^{0.26}$; $\frac{H}{Ø} = 0.2$ and $Ø = 1.2$ m
		$Nu_{90} = 0.8 + (0.002 \cdot Ra)^{0.31}$; $\frac{H}{Ø} = 0.3$ and $Ø = 1.2$ m
		Linear interpolation for values of H/Ø in-between 0.1 and 0.3 and for values of Ø in-between 0.6 m and 1.2 m.
	θ = 20°	$Nu_{20} = Nu_{90}$; $0.2 \le \frac{H}{Ø} \le 0.3$
		$Nu_{20} = -0.17 \cdot (0.002 \cdot Ra)^{0.12}$; $\frac{H}{Ø} = 0.1$ and $Ø = 0.6$ m
		$Nu_{20} = (0.002 \cdot Ra)^{0.19}$; $\frac{H}{Ø} = 0.1$ and $Ø = 1.2$ m
		Linear interpolation for values of H/Ø in-between 0.1 and 0.3 and for values of Ø in-between 0.6 m and 1.2 m.

2. Initiate the development of a new standard for measuring heat transfer rates in building products. This standard can be used to augment the existing ASTM hot box standards C1363, C1199, and E1324. This new experimental standard can improve the ability of experimental methods to be used in research level measurements and for validating numerical models.
3. Apply knowledge gained in this work to extend the range of correlations to products such as large commercial curvilinear products (e.g., barrel-vault skylights, very large domed skylights, etc.)
4. Incorporate results of this research into the new revisions of NFRC technical standards (NFRC 100, NFRC 200) and ISO standards (ISO 15099, ISO 10077-1, ISO 10077-2, ISO 18294).

8. REFERENCES

ASTM. 1997. "ASTM C1363: Standard Test Method for the Thermal Performance of Building Assemblies by Means of a Hot Box Apparatus". ASTM.

ASTM. 1999. ASTM E1423: Standard Practice for Determining Steady State Thermal Transmittance of Fenestration Systems

ASTM. 2000. "ASTM C1199: Standard Test Method for Measuring the Steady-State Thermal Transmittance of Fenestration Systems Using Hot Box Methods." ASTM.

Bishop E. H., Mack L. R. and Scanian J. A., 1965, "Heat transfer by natural convection between concentric spheres", International Journal of Heat and Mass Transfer, Vol. 9, pp. 649-662.

BOCA 1997. "BOCA Research Report No. 92-35". BOCA Evaluation Services, Inc.

Crystalite. 2006. "Crystalite Skylight – Drawings and Specifications"

FDI 2000. "Gambit 2.0 Users and Reference Manual". Fluid Dynamics International, Fluid Dynamics Analysis Package Revision 1.3.2, Evanston, IL.

FDI 2003. FLUENT 6.5. Users and Reference Manual. Fluid Dynamics International, Fluid Dynamics Analysis Package. Fluent Inc.

Garg V. G., 1991,"Natural convection between concentric spheres", International Journal of Heat and Mass Transfer, 35(8), pp. 1935-1945.

ISO 15099, 2003, "Thermal Performance of Windows, Doors and Shading Devices – Detailed Calculations," ISO.

ISO. 2003. "ISO 10077-2: Thermal performance of windows, doors and shutters - Calculation of thermal transmittance - Part 2: Numerical method for frames". ISO.

ISO. 2005. "ISO 10077-1: Thermal performance of windows, doors and shutters — Calculation of thermal transmittance — Part 1: General." ISO.

ISO. 2007. “ISO/DIS 18292: Energy performance of fenestration systems - Calculation procedure”. ISO.

Laouadi, A., Atif, M.R., 2001, “Natural convection heat transfer within multi-layer domes”, International Journal of Heat and Mass Transfer, Vol. 44, pp. 1973-1981.

LaserComp. 2003. “LaserComp FOX 304 Thermal Conductivity Apparatus User’s Manual”

NFRC 100-2004. “ Procedure for Determining Fenestration Product U-factors”. National Fenestration Rating Council. 2004.

NFRC 200-2004. “Procedure for Determining Fenestration Product Solar Heat Gain Coefficient and Visible Transmittance at Normal Incidence”. *National Fenestration Rating Council*. 2004.

ODL 1998. “ODL Skylights – Drawings and Specifications”.

Omega. 2005. Digital Calibrator/Thermometer CL23A, 24, 25, 26, 27. User’s Guide. http://www.omega.com.

Raithby G. D., Hollands K. G. T., 1975, “A general method of obtaining approximate solutions to laminar and turbulent free convection problems”, 11, pp. 266-315.

Vistawall. 1994. Vistawall Skylights - Drawings and Descriptions.

Yang, Y. 2004. *Natural Convective Flow and Heat Transfer in Vertical and Inclined Glazing Cavities*. Master Thesis. University of Massachusetts. September 2003.

Project 1.1.8

Project Name: Tubular Daylighting Devices U-factor Rating

Date: July 19, 2009

Purpose: The purpose of this project was to provide physical product validation testing for the current NFRC computer simulation rating approach for Tubular Daylighting Devices (TDD's).

Project Summary:

The U-Factor ratings for the current computer simulation procedure are performed unlike any other fenestration product and do not require a validation test to be performed. Due to the lack of facilities to run an accurate test on this type of product, the current procedure was put in place to allow these products to be rated without a validation test. At the time of implementation of this procedure there was very little data available for TDD's to validate the accuracy of the procedure.

This project consisted of construction of a TDD Hot Box Apparatus capable of accurately testing and measuring the thermal transmittance of a TDD in a horizontal orientation. Testing consisted of seven (7) different product configurations in a residential style installation and five (5) different products in a commercial style installation. Each unit was physically tested in the TDD Hot Box Apparatus and then simulated with all requirements specified in the NFRC's Simulation Manual: Section 8.6 – Modeling Tubular Daylighting Devices, with slight acceptable modifications necessary to perform the commercial configuration simulation.

The physical testing and simulation results are compared for differences in both the thermal transmittance and the temperature distributions. This analysis has been provided as an informative guide for changes that need to be implemented in both simulation and physical test procedures in order to provide the most accurate U-Factor ratings for TDD's.

Click here for final report

Final Technical Report
(Revised)

Experimental U-Factor Research To Validate NFRC Simulation Procedure for Tubular Daylighting Devices (TDD)

Report Prepared For

National Fenestration Rating Council
8484 Georgia Avenue, Suite 320
Silver Spring, Maryland 20910

Prepared By

Architectural Testing, Inc.
130 Derry Court
York, Pennsylvania 17402

July 19, 2009

Table of Contents

Executive Summary 3
Specimens 4
Equipment 7
Summary of Results 9
Conclusion 18
Recommendations 18
Physical Test Results 19
Simulation Results 45

Executive Summary

This technical report provides final results from the research project entitled: "Experimental U-Factor Research To Validate NFRC Simulation Procedure for Tubular Daylighting Devices (TDD)." This research project was initiated to provide physical product validation testing for the current NFRC computer simulation rating approach for Tubular Daylighting Devices (TDD's). The U-Factor ratings for the current computer simulation procedure are performed unlike any other fenestration product and do not require a validation test to be performed. Due to the lack of facilities to run an accurate test on this type of product, the current procedure was put in place to allow these products to be rated without a validation test. At the time of implementation of this procedure there was very little data available for TDD's to validate the accuracy of the procedure.

This project consisted of construction of a TDD Hot Box Apparatus capable of accurately testing and measuring the thermal transmittance of a TDD in a horizontal orientation. Testing consisted of seven (7) different product configurations in a residential style installation and five (5) different products in a commercial style installation. Each unit was physically tested in the TDD Hot Box Apparatus and then simulated with all requirements specified in the NFRC's Simulation Manual: Section 8.6 – Modeling Tubular Daylightling Devices, with slight acceptable modifications necessary to perform the commercial configuration simulation.

The physical testing and simulation results are compared for differences in both the thermal transmittance and the temperature distributions. This analysis has been provided as an informative guide for changes that need to be implemented in both simulation and physical test procedures in order to provide the most accurate U-Factor ratings for TDD's.

Specimens

The project utilized twelve (12) different specimens: seven (7) residential configuration and five (5) commercial configuration. The specimens were chosen to represent the simplest configurations on the market and to cover the variety of products available. Specifically, small (14") / large (21") samples, rigid / flexible tubes, single / double dome, and single / double diffusers were tested. The test matrix is included in Table 1.

Table 1: Test Matrix

Unit	Configuration	Size	Tube	Dome	Diffuser
1	Residential	Large	Rigid	Single	Single
2	Residential	Large	Rigid	Single	Double
3	Residential	Small	Flexible	Single	Single
4	Residential	Small	Flexible	Single	Double
5	Residential	Small	Rigid	Single	Single
6	Residential	Small	Rigid	Double	Single
7	Residential	Small	Rigid	Single	Double
8	Commercial	Large	Rigid	Single	Single
9	Commercial	Large	Rigid	Double	Single
10	Commercial	Large	Flexible	Single	Single
11	Commercial	Small	Rigid	Single	Single
12	Commercial	Small	Rigid	Double	Single

The configuration refers to the installation style of the product. The residential and commercial configurations, shown in Figure 1 & 2, not only illustrate the installation style but also further show each of the respective temperature regions with the surface coefficients for the installation style.

The specific individual components used to make up each test unit with the respective configuration are listed in Table 2 with further detailed descriptions of these individual components located in Table 3.

Figure 1: Residential Configuration

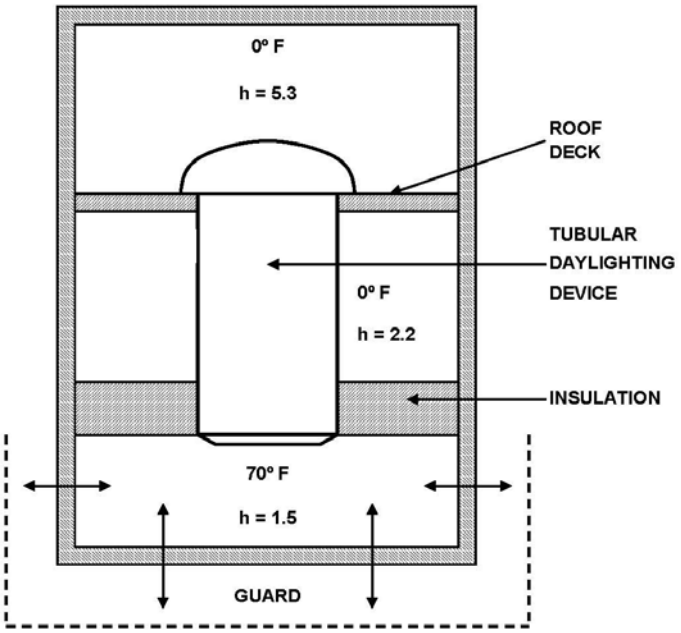


Figure 2: Commercial Configuration

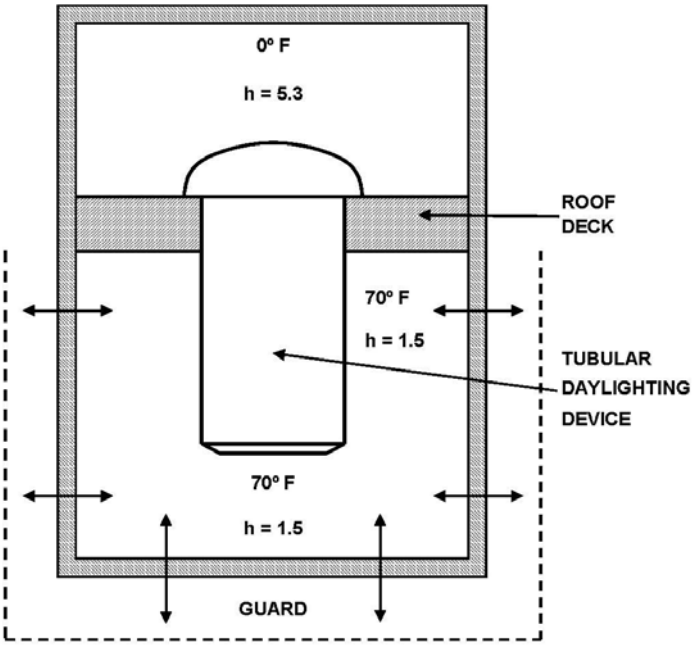


Table 2: Test Unit Components

Unit	Tube	Dome	Diffuser
1	A	Single A	Single A
2	A	Single A	Double A
3	B	Single B	Single B
4	B	Single B	Double B
5	C	Single C	Single C
6	C	Double C	Single C
7	C	Single C	Double C
8	E	Single D	Single D
9	E	Double D	Single D
10	D	Single D	SingleD
11	C	Single C	Single C
12	C	Double C	Single C

**Single Dome includes only the exterior dome*
**Single Diffuser includes only the Interior diffuser*

Table 3: Component Descriptions

Tubes

A	21" Rigid - Alanod Miro™ - 0.020" thick aluminum with a reflectance of 95%
B	14" Flexible - Metalized polyester, fiberglass scrim and spring steel wire
C	14" Rigid - Alanod Miro™ - 0.020" thick aluminum with a reflectance of 95%
D	22" Flexible - Metalized polyester, fiberglass scrim and spring steel wire
E	22" Rigid - Alanod PVD - 0.020" thick coated aluminum with a reflectance of 95%

Domes

A	Exterior - 0.177" Hyzod 'SL' clear polycarbonate dome, 21" Size
	Interior - 0.030" Hyzod clear polycarbonate flat panel, 21" Size
B	Exterior - Plexiglass, MC Grade A, acrylic or polycarbonate Clear Dome, 14" Size
C	Exterior - 0.177" Hyzod 'SL' clear polycarbonate dome, 14" Size
	Interior - 0.030" Hyzod clear polycarbonate flat panel, 14" Size
D	Exterior - Plexiglass, MC Grade A, acrylic or polycarbonate Clear Dome, 22" Size
	Interior - 0.125" Lexan clear polycarbonate flat panel, 22" Size

**Exterior indicates the primary dome in contact with the weather environment*
**Interior indicates the secondary dome in contact with the tube environment*

Diffusers

A	Interior - Modified Acrylic Lens (Crepe), 21" Size
	Exterior - 0.030" clear polycarbonate lens, 21" Size
B	Interior - Clear lens, 14" Size
	Exterior - Clear prizmatic lens, 14" Size
C	Interior - Modified Acrylic Lens (Crepe), 14" Size
	Exterior - 0.030" clear polycarbonate lens, 14" Size
D	Exterior - Clear prizmatic lens, 22" Size

**Exterior indicates the secondary diffuser in contact with the tube environment*
**Interior indicates the primary diffuser in contact with the room environment*

Equipment

A test apparatus was designed and constructed to measure the thermal transmittance of TDD products at ASHRAE standard winter conditions. The test apparatus includes three major spaces to install the test specimen and establish steady-state test conditions. These spaces include: a) guarded metering chamber on the bottom of the test apparatus; b) attic plenum space with the tube of the test specimen installed vertically in a 10-inch thick surround panel (EPS material) on the bottom and a half-inch plywood roof deck on the top; c) weather chamber on top of the roof deck with the dome of the test specimen installed.

Additionally a commercial specimen installation was designed and constructed by changing part b) above to attic space with the tube of the test specimen installed vertically in a half-inch plywood ceiling on the bottom and a 10-inch thick surround panel (EPS material) roof deck on top. For both installations, 6-row air surface thermocouples were placed inside the tube with the first row at the bottom of the tube, and 5-inch apart for each row from the first.

The guarded metering chamber provides natural convection conditions to the bottom of the tube with or without a diffuser. A metering chamber baffle was installed 6 inches away from the surround panel. The total energy input to all heaters and fans inside the metering chamber was measured and recorded.

The attic plenum was conditioned to 0^{o}F and natural convection conditions were established. The heat transfer through the tube sidewall was obtained using the measured surface temperature difference and the tube material thermal conductivity value. The material thermal conductivity of the surround panel and plywood roof deck was measured using ASTM C 518 guarded hot plate.

The weather chamber contains a blower, an evaporator of the refrigeration system, and a baffle to provide ASHRAE standard outdoor forced convection winter conditions of 15 mph wind and 0^{o}F air temperature.

The hot box incorporates three independent fan systems to maintain the correct surface coefficient on the diffuser, tubular wall and dome. The air velocity in all three areas is monitored during testing. Figures 3 and 4 show the schematics of the test apparatus.

The test apparatus incorporates separate thermopiles for measuring wall heat loss in the “attic” and “interior” spaces. Furthermore the test apparatus was calibrated in both residential and commercial configurations as required utilizing a 3-D CTS panel, pyramidal in shape.

Figure 3: TDD Hot Box Apparatus

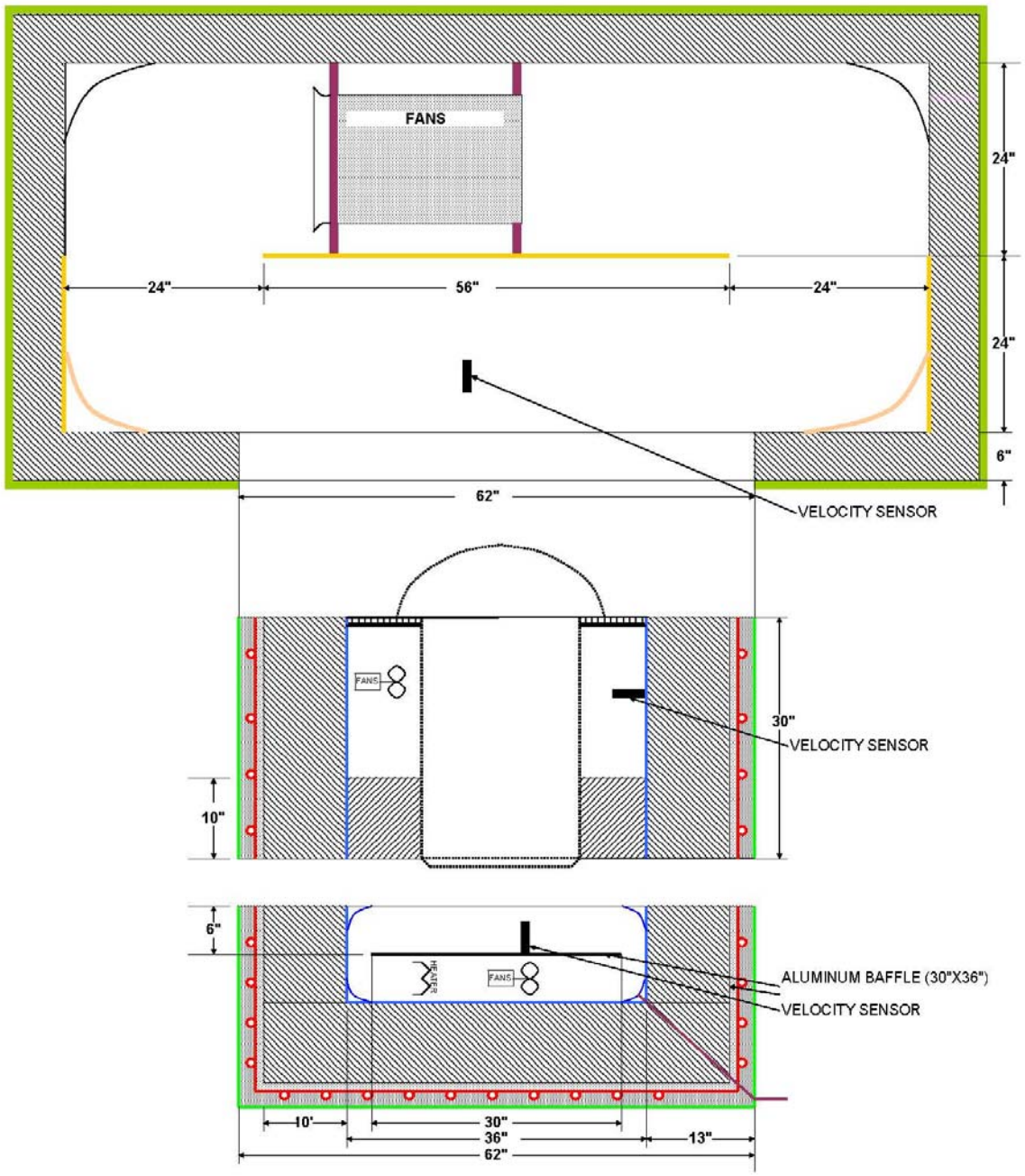
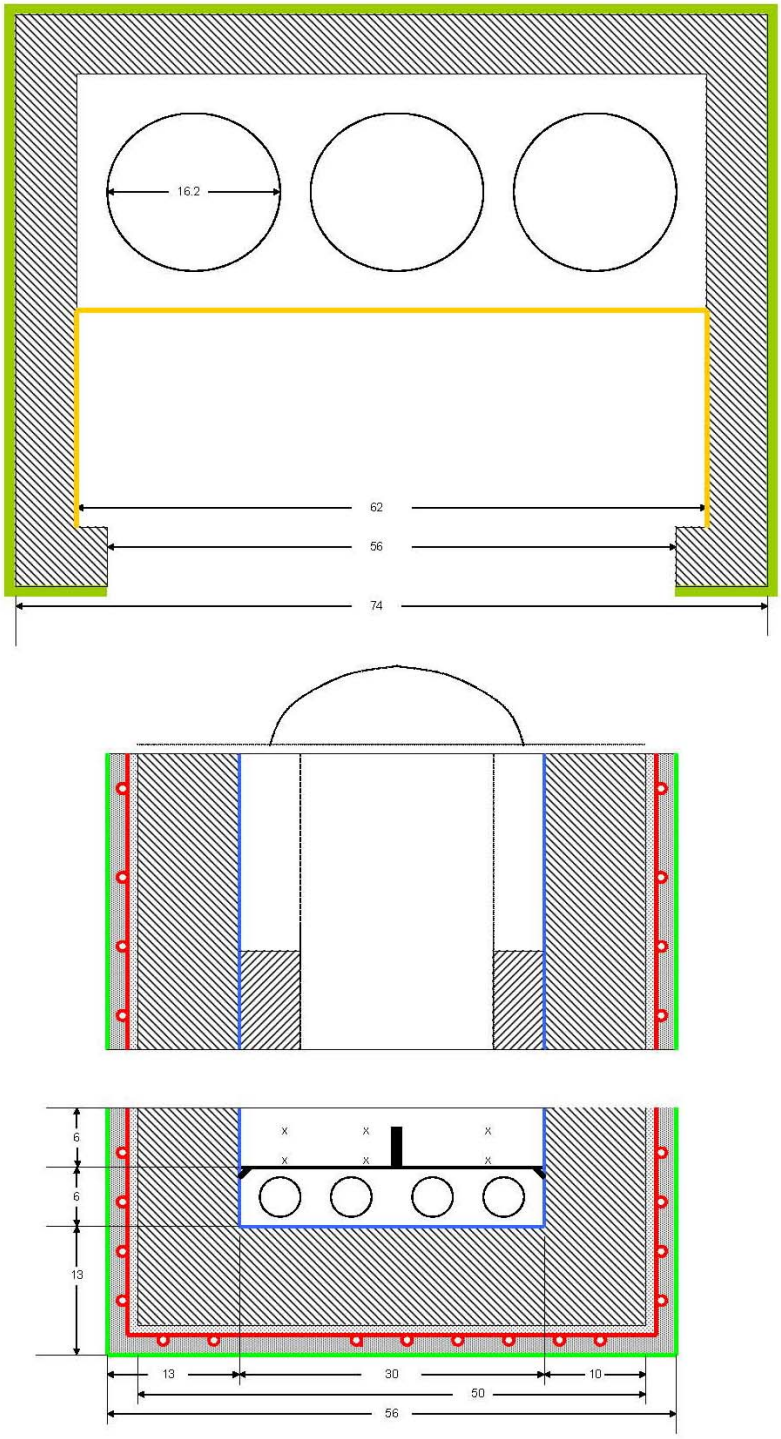


Figure 4: TDD Hot Box Apparatus



Summary of Results

The comparative thermal transmittance (U-Factor) results for this study of simulated and tested products are listed in Tables 4 & 5 inclusive of both residential and commercial configurations. The sample components, product U-factors and sample sizes are reported for all tested cases. A comprehensive set of calculations and test information is located in Appendix A and Appendix B of this report detailing component configurations, temperature distributions, and any relevant properties for the thermal transmittance calculations. In all cases, the simulated product size represents the same size as was tested for the product. This is a deviation from the standard rating procedure, which fixes the tube diameter at 14 inches. This was done to allow for an accurate comparison with tested results.

Table 4: Summary of Residential Thermal Transmittance

Unit	Size	Tube	Dome	Diffuser	Simulation	Test	Δ
Residential Configuration					BTU/Hr-Ft^2-°F	BTU/Hr-Ft^2-°F	
1	Large	Rigid	Single	Single	0.694	0.716	3%
2	Large	Rigid	Single	Double	0.412	0.593	44%
3	Small	Flexible	Single	Single	0.738	0.930	26%
4	Small	Flexible	Single	Double	0.503	0.673	34%
5	Small	Rigid	Single	Single	0.732	0.946	29%
6	Small	Rigid	Double	Single	0.724	0.805	11%
7	Small	Rigid	Single	Double	0.422	0.667	58%

Figure 5: Residential Thermal Transmittance

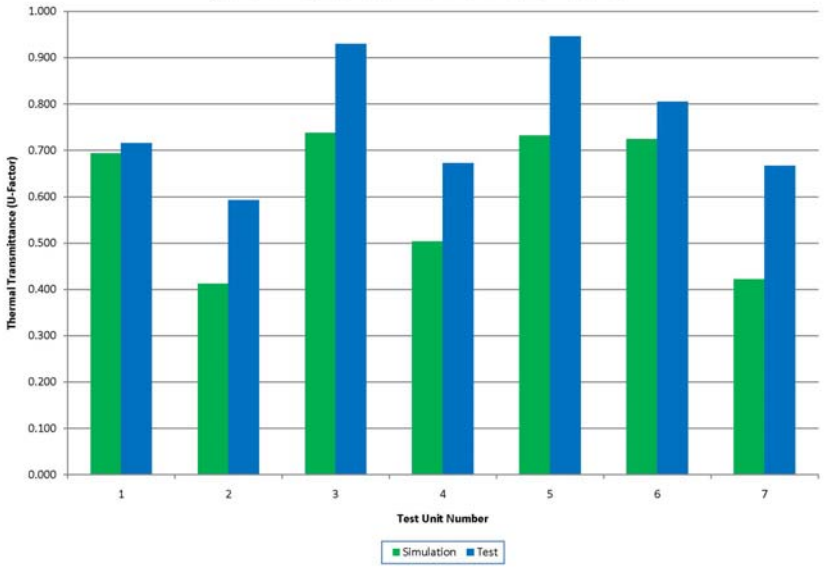
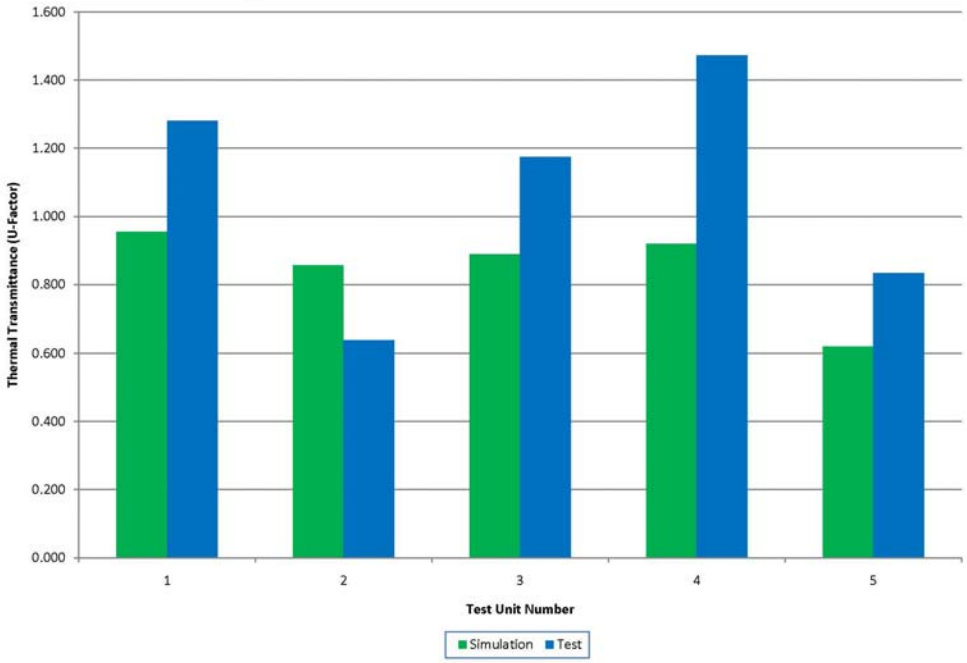


Table 5: Summary of Commercial Thermal Transmittance

Unit	Size	Tube	Dome	Diffuser	Simulation	Test	Δ
Residential Configuration					BTU/Hr-Ft^2-°F	BTU/Hr-Ft^2-°F	
8	Large	Rigid	Single	Single	0.955	1.280	34%
9	Large	Rigid	Double	Single	0.857	0.639	-25%
10	Large	Flexible	Single	Single	0.889	1.174	32%
11	Small	Rigid	Single	Single	0.920	1.473	60%
12	Small	Rigid	Double	Single	0.620	0.833	34%

Figure 6: Commercial Thermal Transmittance



The average temperature distribution results between the computer simulation and the physical testing have been listed in Tables 6 & 7 and plotted in Figures 7, 8, 9, 10, 11 & 12 for each of the unit configurations.

Table 6: Residential Average Temperature Distributions

Dome					Interior Surface Temperature Distributions		
Unit	**Size**	**Tube**	**Dome**	**Diffuser**	**Simulation**	**Test**	**ΔT**
Residential Configuration					**°F**	**°F**	**°F**
1	Large	Rigid	Single	Single	2.26	4.27	2.00
2	Large	Rigid	Single	Double	1.45	2.77	1.31
3	Small	Flexible	Single	Single	0.38	2.20	1.82
4	Small	Flexible	Single	Double	0.22	1.77	1.55
5	Small	Rigid	Single	Single	1.42	3.03	1.62
6	Small	Rigid	Double	Single	4.28	8.13	3.85
7	Small	Rigid	Single	Double	0.82	2.23	1.42

Tube - Top					Interior Air Temperature Distributions		
Unit	**Size**	**Tube**	**Dome**	**Diffuser**	**Simulation**	**Test**	**ΔT**
Residential Configuration					**°F**	**°F**	**°F**
1	Large	Rigid	Single	Single	4.40	17.80	13.40
2	Large	Rigid	Single	Double	4.00	14.20	10.20
3	Small	Flexible	Single	Single	4.60	8.60	4.00
4	Small	Flexible	Single	Double	4.40	7.93	3.53
5	Small	Rigid	Single	Single	4.20	12.97	8.77
6	Small	Rigid	Double	Single	8.30	14.57	6.27
7	Small	Rigid	Single	Double	4.00	12.53	8.53

Tube - Bottom					Interior Air Temperature Distributions		
Unit	**Size**	**Tube**	**Dome**	**Diffuser**	**Simulation**	**Test**	**ΔT**
Residential Configuration					**°F**	**°F**	**°F**
1	Large	Rigid	Single	Single	33.50	17.53	-15.97
2	Large	Rigid	Single	Double	19.60	16.33	-3.27
3	Small	Flexible	Single	Single	30.60	9.53	-21.07
4	Small	Flexible	Single	Double	21.10	8.10	-13.00
5	Small	Rigid	Single	Single	32.70	14.33	-18.37
6	Small	Rigid	Double	Single	32.80	15.30	-17.50
7	Small	Rigid	Single	Double	19.50	13.83	-5.67

Diffuser					Interior Surface Temperature Distributions		
Unit	**Size**	**Tube**	**Dome**	**Diffuser**	**Simulation**	**Test**	**ΔT**
Residential Configuration					**°F**	**°F**	**°F**
1	Large	Rigid	Single	Single	38.12	41.30	3.18
2	Large	Rigid	Single	Double	51.62	31.00	-20.62
3	Small	Flexible	Single	Single	38.66	38.40	-0.26
4	Small	Flexible	Single	Double	50.72	21.50	-29.22
5	Small	Rigid	Single	Single	37.04	39.45	2.41
6	Small	Rigid	Double	Single	37.40	41.15	3.75
7	Small	Rigid	Single	Double	51.26	30.40	-20.86

Tube – Overall Average					Interior Air Temperature Distributions		
Unit	**Size**	**Tube**	**Dome**	**Diffuser**	**Simulation**	**Test**	**ΔT**
Residential Configuration					**°F**	**°F**	**°F**
1	Large	Rigid	Single	Single	18.91	17.87	-1.05
2	Large	Rigid	Single	Double	11.80	14.93	3.13
3	Small	Flexible	Single	Single	17.57	8.78	-8.79
4	Small	Flexible	Single	Double	12.76	8.14	-4.62
5	Small	Rigid	Single	Single	18.48	13.64	-4.83
6	Small	Rigid	Double	Single	20.56	14.97	-5.59
7	Small	Rigid	Single	Double	11.76	13.13	1.37

Figure 7: Residential Average Dome Temperature Distributions

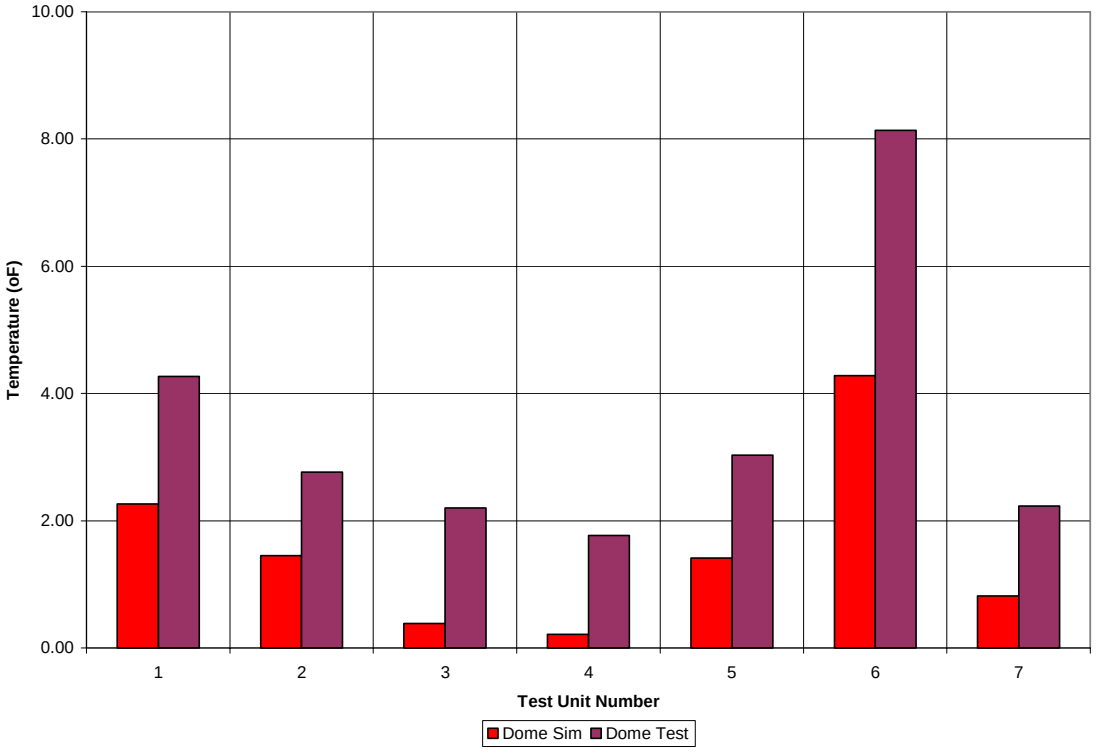


Figure 8: Residential Average Diffuser Temperature Distributions

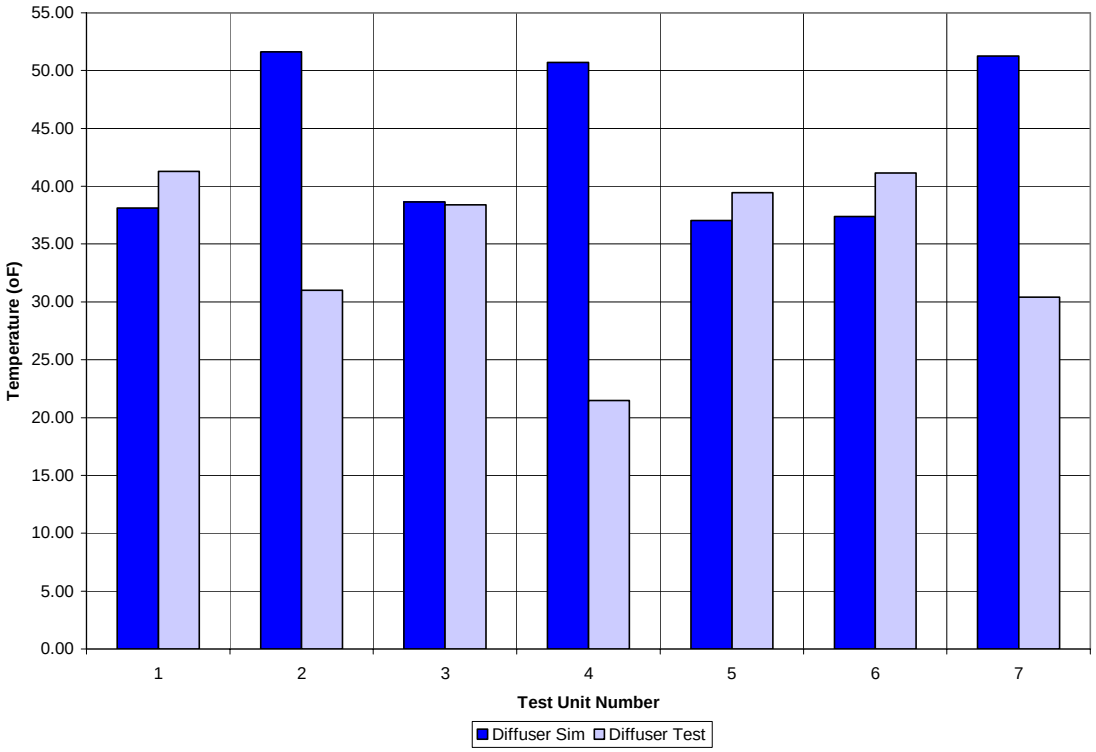


Figure 9: Residential Average Tube Temperature Distributions

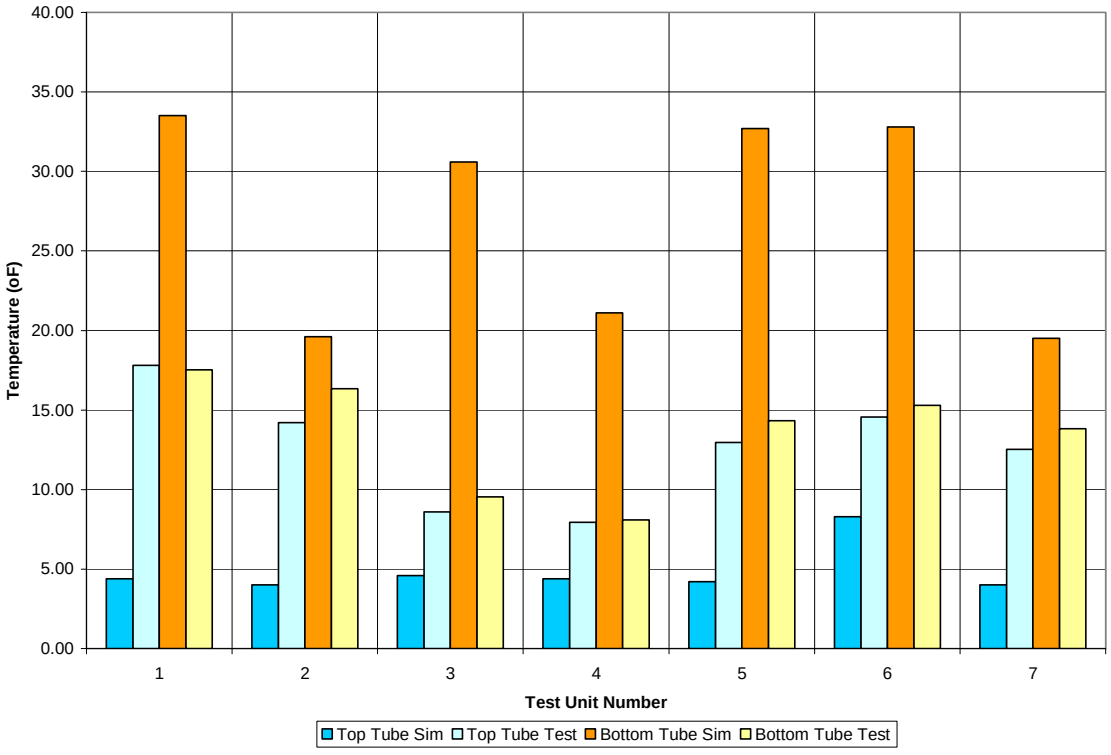


Table 7: Commercial Average Temperature Distributions

Dome					Interior Surface Temperature Distributions		
Unit	**Size**	**Tube**	**Dome**	**Diffuser**	**Simulation**	**Test**	**ΔT**
Commercial Configuration					**°F**	**°F**	**°F**
8	Large	Rigid	Single	Single	6.44	10.57	4.13
9	Large	Rigid	Double	Single	18.50	33.23	14.73
10	Large	Flexible	Single	Single	6.46	9.83	3.37
11	Small	Rigid	Single	Single	13.45	10.27	-3.18
12	Small	Rigid	Double	Single	36.68	35.63	-1.05

Tube - Top					Interior Air Temperature Distributions		
Unit	**Size**	**Tube**	**Dome**	**Diffuser**	**Simulation**	**Test**	**ΔT**
Commercial Configuration					**°F**	**°F**	**°F**
8	Large	Rigid	Single	Single	19.30	37.23	17.93
9	Large	Rigid	Double	Single	28.80	54.70	25.90
10	Large	Flexible	Single	Single	23.90	37.30	13.40
11	Small	Rigid	Single	Single	24.10	43.00	18.90
12	Small	Rigid	Double	Single	38.80	55.87	17.07

Tube - Bottom					Interior Air Temperature Distributions		
Unit	**Size**	**Tube**	**Dome**	**Diffuser**	**Simulation**	**Test**	**ΔT**
Commercial Configuration					**°F**	**°F**	**°F**
8	Large	Rigid	Single	Single	52.40	37.93	-14.47
9	Large	Rigid	Double	Single	57.40	54.53	-2.87
10	Large	Flexible	Single	Single	52.20	40.13	-12.07
11	Small	Rigid	Single	Single	57.40	43.93	-13.47
12	Small	Rigid	Double	Single	62.80	56.00	-6.80

Diffuser					Interior Surface Temperature Distributions		
Unit	**Size**	**Tube**	**Dome**	**Diffuser**	**Simulation**	**Test**	**ΔT**
Commercial Configuration					**°F**	**°F**	**°F**
8	Large	Rigid	Single	Single	58.82	54.97	-3.85
9	Large	Rigid	Double	Single	59.90	62.30	2.40
10	Large	Flexible	Single	Single	58.82	60.30	1.48
11	Small	Rigid	Single	Single	62.60	53.83	-8.77
12	Small	Rigid	Double	Single	65.12	61.90	-3.22

Tube – Overall Average					Interior Air Temperature Distributions		
Unit	**Size**	**Tube**	**Dome**	**Diffuser**	**Simulation**	**Test**	**ΔT**
Commercial Configuration					**°F**	**°F**	**°F**
8	Large	Rigid	Single	Single	37.53	37.78	0.25
9	Large	Rigid	Double	Single	40.73	54.68	13.96
10	Large	Flexible	Single	Single	35.70	39.04	3.34
11	Small	Rigid	Single	Single	40.74	43.65	2.91
12	Small	Rigid	Double	Single	50.80	56.04	5.24

Figure 10: Commercial Average Dome Temperature Distributions

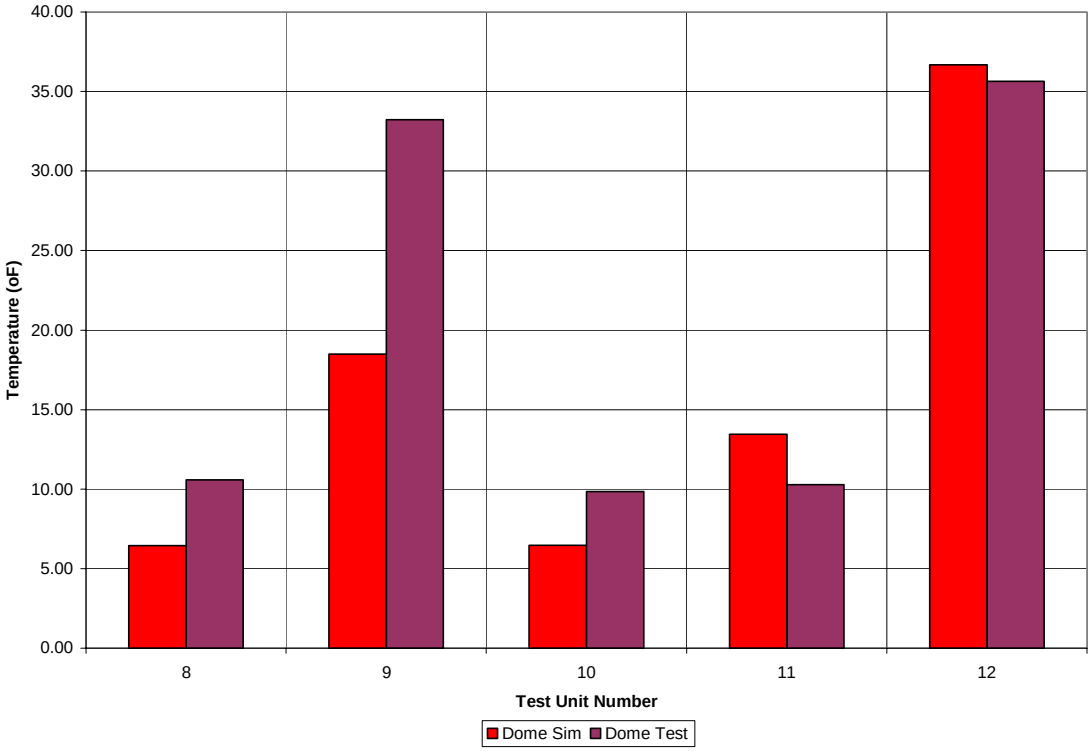


Figure 11: Commercial Average Diffuser Temperature Distributions

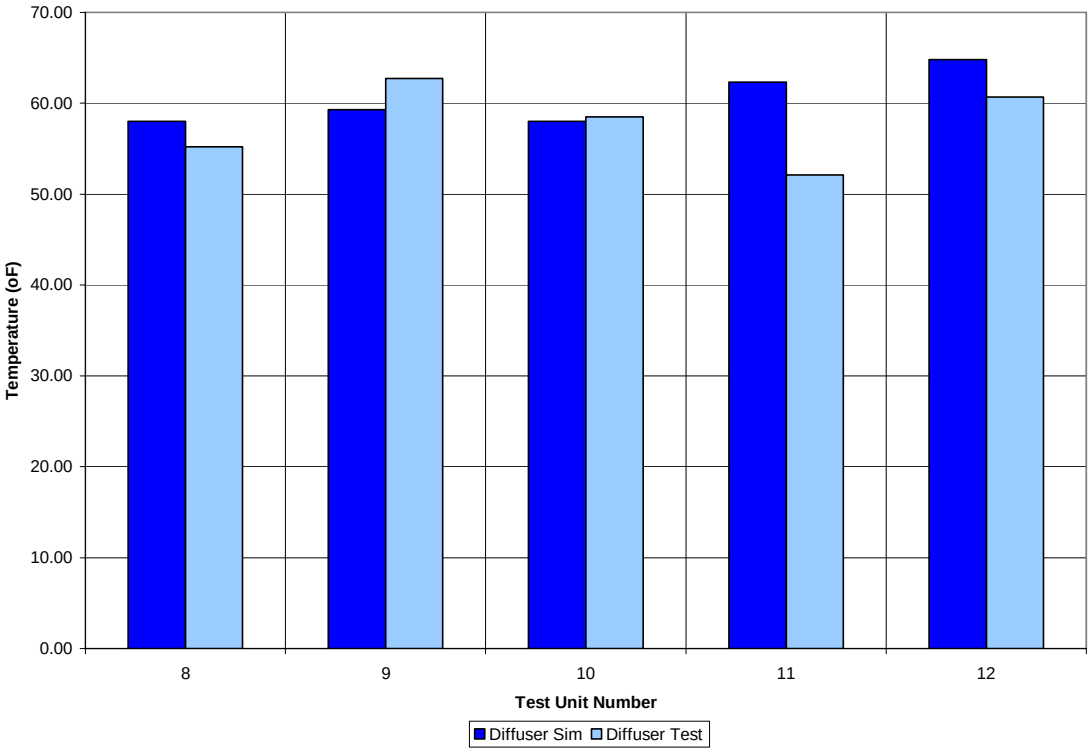
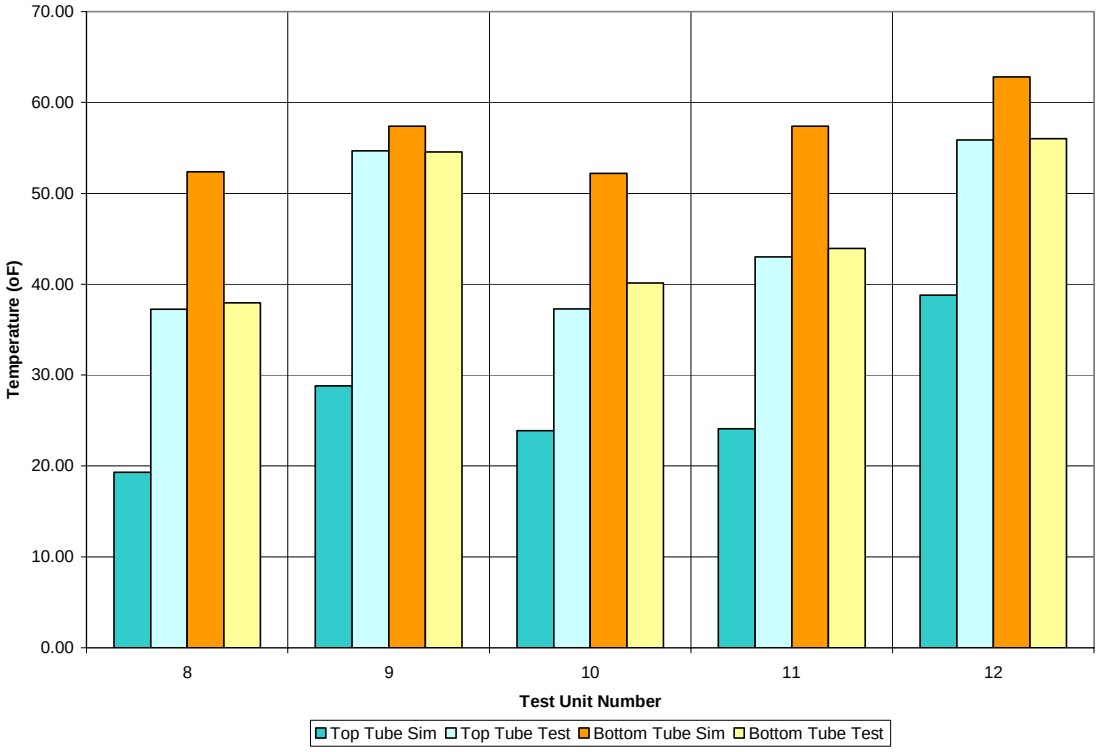


Figure 12: Commercial Average Tube Temperature Distributions



Conclusion

Examination of the physical test data with the computer simulation data clearly shows that there is no correlation between the two procedures with respect to the thermal transmittance and the temperature distribution values. Only three of twelve configurations were within the acceptable validation error from physical test to computer simulation. The data also reveals that there are no trends developed between the two procedures.

The physical test apparatus was constructed and operated in compliance with ASTM C1363 and C1199 procedures. The apparatus was verified and calibrated as required by the ASTM procedures. The results comparison points to deficiencies in the current simulation technique.

Further examination of the deficiencies in the computer simulation procedure is required, especially in areas such as the air circulation inside the TDD tube. The extremely dynamic air situation in the tube of the TDD is not handled by the simulation methodology. The current THERM program assumes that the air stratifies and creates a large temperature gradient from top to bottom of the tube. As can be readily seen in Figures 9 and 12, the actual air temperatures are very nearly equal at the top and bottom of the tube. In order to properly simulate this situation, a computational fluid dynamic model must be used. Another error in the methodology is that the simulation model does not represent a circular tube, but a cross-section of an infinitely long tunnel. The two-dimensional model, assuming static fluids, which is currently utilized by THERM, is not capable of truly representing the performance of this type of product. Both temperature and U-factor prediction are compromised by the limitations of THERM. Therefore, the simulation procedure does not give the TDD manufacturer accurate results for U-Factor rating of their products.

Recommendations

- The ASTM C1363 and C1199 procedures have been proven to provide accurate thermal transmittance test data when used for fenestration products in the vertical direction for many years. Therefore, in order to provide accurate U-Factor test results for NFRC rating purposes, it is recommended that the NFRC adopt a test-only procedure for TDD's in lieu of the current simulation-only approach.
- Additional research into advanced simulation techniques should be pursued, investigating advanced axial 2-D modeling, 3-D modeling, and computational fluid dynamics models to determine the correct techniques for simulation.

References

Arasteh, D.; Carmody, J.; Curcija, D.; Huizenga, C. 2003. "THERM 5 / WINDOW 5 NFRC Simulation Manual". Section 8.6. pp. 43-62.

Appendix A

Physical Test Results

U-factors have been calculated and all heat flows documented as required. Each sample was instrumented with thermocouples throughout the tube and on inner and outer surfaces of the domes and diffusers. The temperatures of the monitored surfaces are reported.

Physical Test Results

Test Unit Number 1

Unit Configuration Details

Test Configuration	**Residential**	
Tube Size	**Large**	
Tube Type	**Rigid**	**Tube A**
Dome (Single / Double)	**Single**	**Dome A**
Diffuser (Single / Double)	**Single**	**Diffuser A**

Bottom Box Fan Power (Watts) =	1.103
Bottom Box Heater Power (Watts) =	35.436
BB Box Thermopile (EMF, mv) =	1.902
Enter Specimen Diameter (Inches) =	21.040
Specimen Area (Ft2) =	2.414
Enter Thermopile Intercept =	-5.980
Enter Thermopile Slope =	1.108
Enter Surround Panel R-Value (Hr/BTU-F-Ft2) =	44.683
Enter Surround Panel Width (Inches) =	30.000
Enter Surround Panel Height (Inches) =	36.000
Surround Panel Area (Ft2) =	5.086
Surround Panel Cold Temperature (F) =	2.871
Surround Panel Warm Temperature (F) =	69.970
Top Box Air Temperature (F) =	-0.003
Middle Box Air Temperature (F) =	1.632
Bottom Box Air Temperature (F) =	69.995

Bottom Box Fan Power (BTUH) =	3.764
Bottom Box Heater Power (BTUH) =	120.978
Thermopile Wall Loss - Bottom Box (BTUH) =	-3.873
Surround Panel Heat Transfer (BTUH) =	7.637
Total Energy Input (BTUH) =	120.978

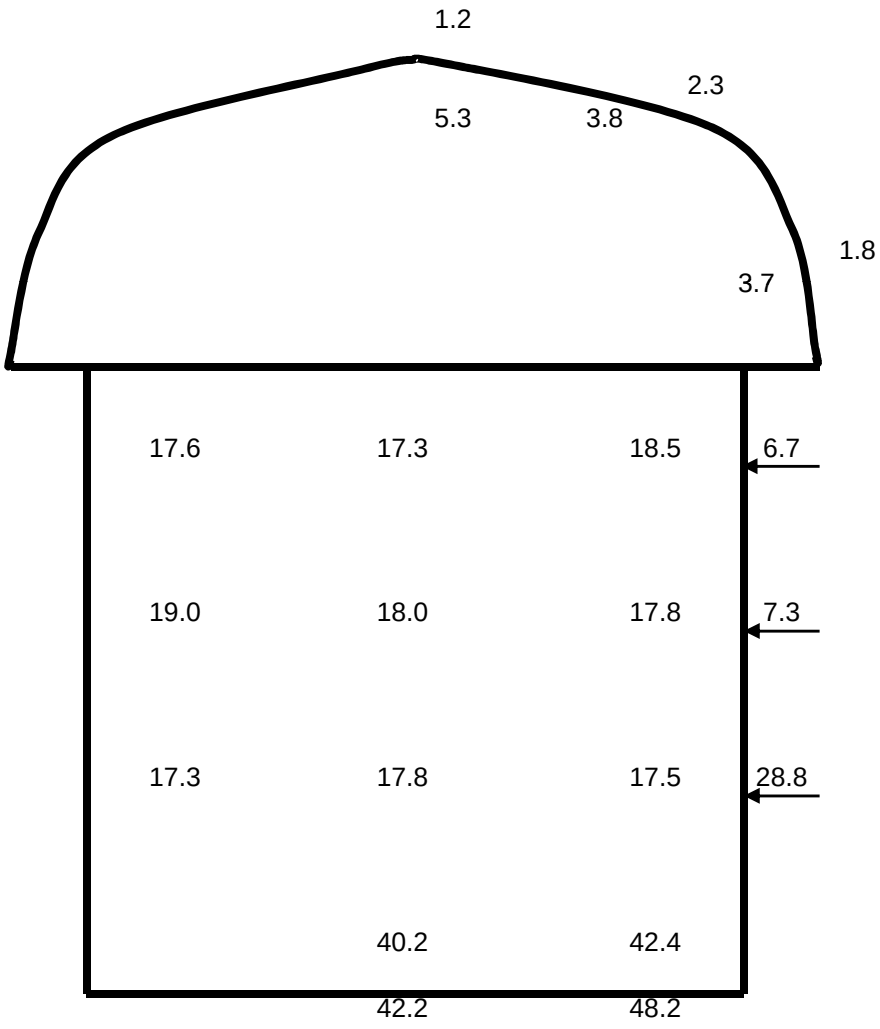
U-Factor (BTU/Hr-Ft2-F) =	**0.716**

Physical Test Temperature Distribution

Test Unit Number 1

Unit Configuration Details

Test Configuration	**Residential**	
Tube Size	**Large**	
Tube Type	**Rigid**	**Tube A**
Dome (Single / Double)	**Single**	**Dome A**
Diffuser (Single / Double)	**Single**	**Diffuser A**



All Temperatures reported in °F

Physical Test Results

Test Unit Number 2

Unit Configuration Details

Test Configuration	**Residential**	
Tube Size	**Large**	
Tube Type	**Rigid**	**Tube A**
Dome (Single / Double)	**Single**	**Dome A**
Diffuser (Single / Double)	**Double**	**Inner Diffuser A, Outer Diffuser A**

Bottom Box Fan Power (Watts) =	1.109
Bottom Box Heater Power (Watts) =	29.266
BB Box Thermopile (EMF, mv) =	1.829
Enter Specimen Diameter (Inches) =	21.040
Specimen Area (Ft2) =	2.414
Enter Thermopile Intercept =	-5.980
Enter Thermopile Slope =	1.108
Enter Surround Panel R-Value (Hr/BTU-F-Ft2) =	44.683
Enter Surround Panel Width (Inches) =	30.000
Enter Surround Panel Height (Inches) =	36.000
Surround Panel Area (Ft2) =	5.086
Surround Panel Cold Temperature (F) =	2.871
Surround Panel Warm Temperature (F) =	69.376
Top Box Air Temperature (F) =	0.038
Middle Box Air Temperature (F) =	1.218
Bottom Box Air Temperature (F) =	70.000

Bottom Box Fan Power (BTUH) =	3.787
Bottom Box Heater Power (BTUH) =	99.914
Thermopile Wall Loss - Bottom Box (BTUH) =	-3.954
Surround Panel Heat Transfer (BTUH) =	7.569
Total Energy Input (BTUH) =	100.085

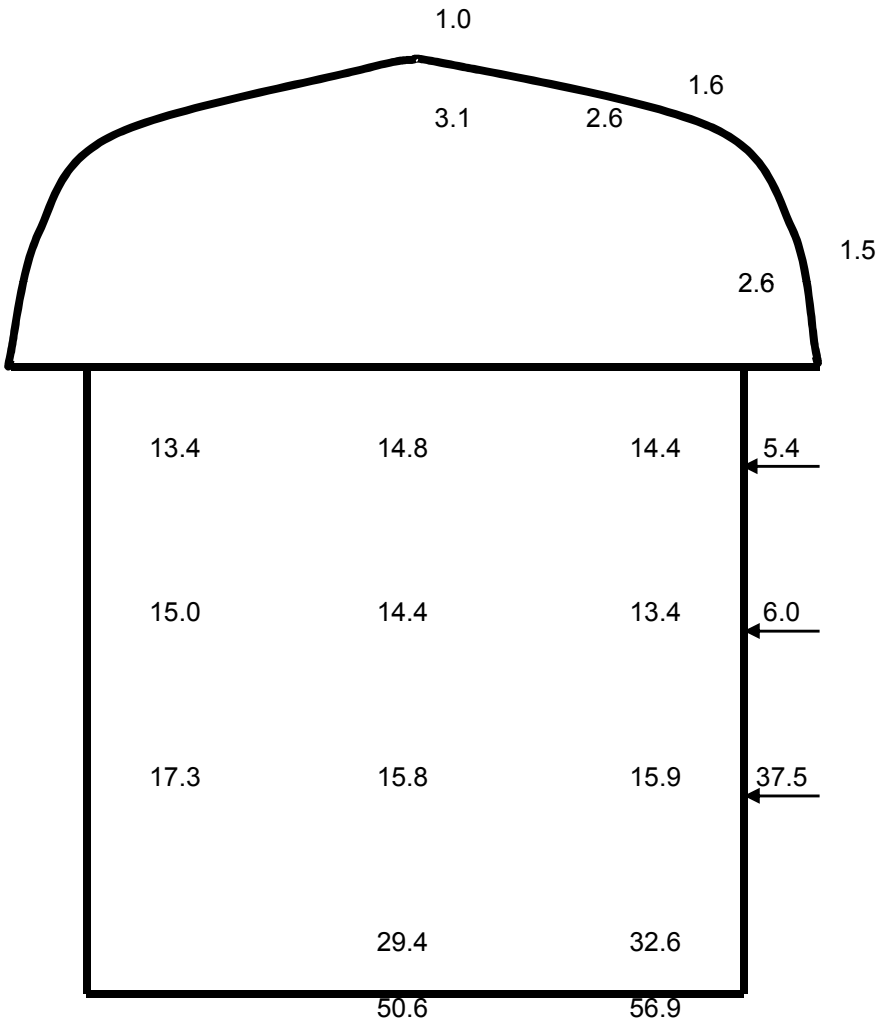
U-Factor (BTU/Hr-Ft2-F) =	**0.593**

Physical Test Temperature Distribution

Test Unit Number 2

Unit Configuration Details

Test Configuration	**Residential**	
Tube Size	**Large**	
Tube Type	**Rigid**	**Tube A**
Dome (Single / Double)	**Single**	**Dome A**
Diffuser (Single / Double)	**Double**	**Inner Diffuser A, Outer Diffuser A**



All Temperatures reported in °F

Physical Test Results

Test Unit Number 3

Unit Configuration Details

Test Configuration	**Residential**	
Tube Size	**Small**	
Tube Type	**Flexible**	**Tube B**
Dome (Single / Double)	**Single**	**Dome B**
Diffuser (Single / Double)	**Single**	**Diffuser B**

Bottom Box Fan Power (Watts) =	1.128
Bottom Box Heater Power (Watts) =	19.633
BB Box Thermopile (EMF, mv) =	2.123
Enter Specimen Diameter (Inches) =	13.510
Specimen Area (Ft2) =	0.995
Enter Thermopile Intercept =	-5.980
Enter Thermopile Slope =	1.108
Enter Surround Panel R-Value (Hr/BTU-F-Ft2) =	44.683
Enter Surround Panel Width (Inches) =	30.000
Enter Surround Panel Height (Inches) =	36.000
Surround Panel Area (Ft2) =	6.505
Surround Panel Cold Temperature (F) =	2.344
Surround Panel Warm Temperature (F) =	69.087
Top Box Air Temperature (F) =	0.014
Middle Box Air Temperature (F) =	1.729
Bottom Box Air Temperature (F) =	69.998

Bottom Box Fan Power (BTUH) =	3.850
Bottom Box Heater Power (BTUH) =	67.026
Thermopile Wall Loss - Bottom Box (BTUH) =	-3.628
Surround Panel Heat Transfer (BTUH) =	9.716
Total Energy Input (BTUH) =	64.788

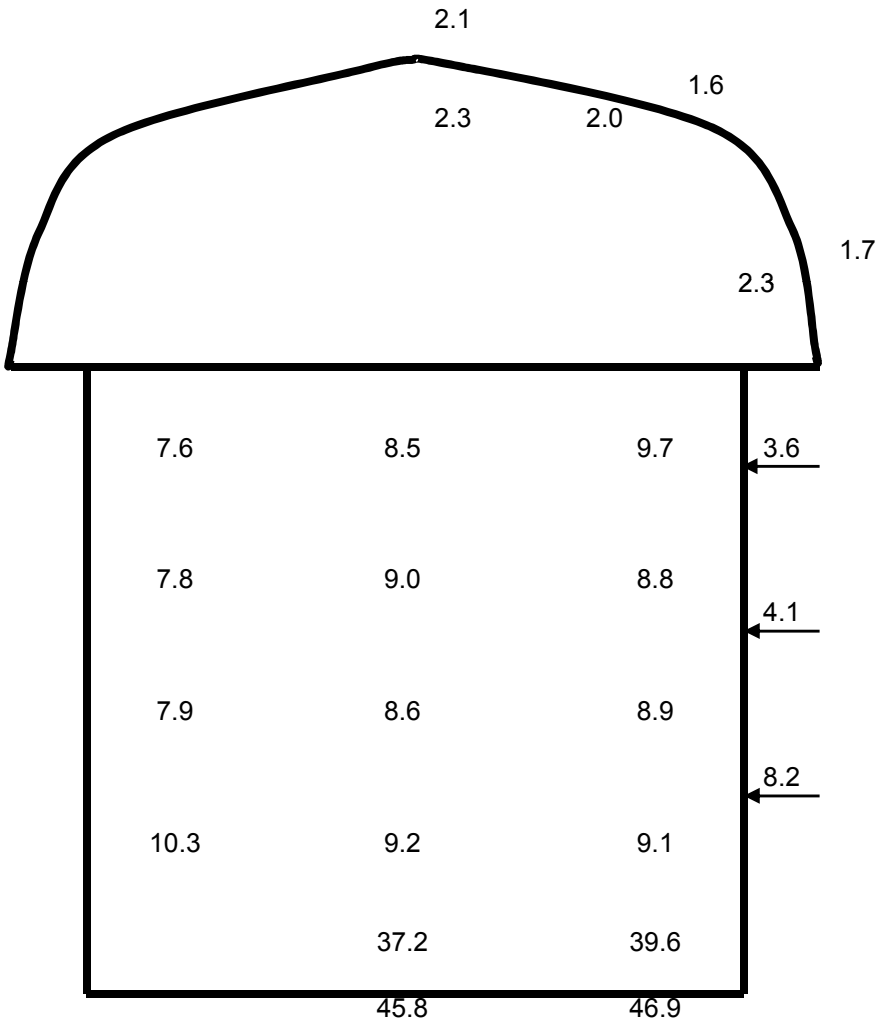
U-Factor (BTU/Hr-Ft2-F) =	**0.930**

Physical Test Temperature Distribution

Test Unit Number 3

Unit Configuration Details

Test Configuration	**Residential**	
Tube Size	**Small**	
Tube Type	**Flexible**	**Tube B**
Dome (Single / Double)	**Single**	**Dome B**
Diffuser (Single / Double)	**Single**	**Diffuser B**



All Temperatures reported in °F

Physical Test Results

Test Unit Number 4

Unit Configuration Details

Test Configuration	**Residential**	
Tube Size	**Small**	
Tube Type	**Flexible**	**Tube B**
Dome (Single / Double)	**Single**	**Dome B**
Diffuser (Single / Double)	**Double**	**Inner Diffuser B / Outer Diffuser B**

Bottom Box Fan Power (Watts) =	1.127
Bottom Box Heater Power (Watts) =	14.452
BB Box Thermopile (EMF, mv) =	2.390
Enter Specimen Diameter (Inches) =	13.510
Specimen Area (Ft2) =	0.995
Enter Thermopile Intercept =	-5.980
Enter Thermopile Slope =	1.108
Enter Surround Panel R-Value (Hr/BTU-F-Ft2) =	44.683
Enter Surround Panel Width (Inches) =	30.000
Enter Surround Panel Height (Inches) =	36.000
Surround Panel Area (Ft2) =	6.505
Surround Panel Cold Temperature (F) =	3.491
Surround Panel Warm Temperature (F) =	69.584
Top Box Air Temperature (F) =	0.002
Middle Box Air Temperature (F) =	2.156
Bottom Box Air Temperature (F) =	70.001

Bottom Box Fan Power (BTUH) =	3.849
Bottom Box Heater Power (BTUH) =	49.339
Thermopile Wall Loss - Bottom Box (BTUH) =	-3.332
Surround Panel Heat Transfer (BTUH) =	9.621
Total Energy Input (BTUH) =	46.898

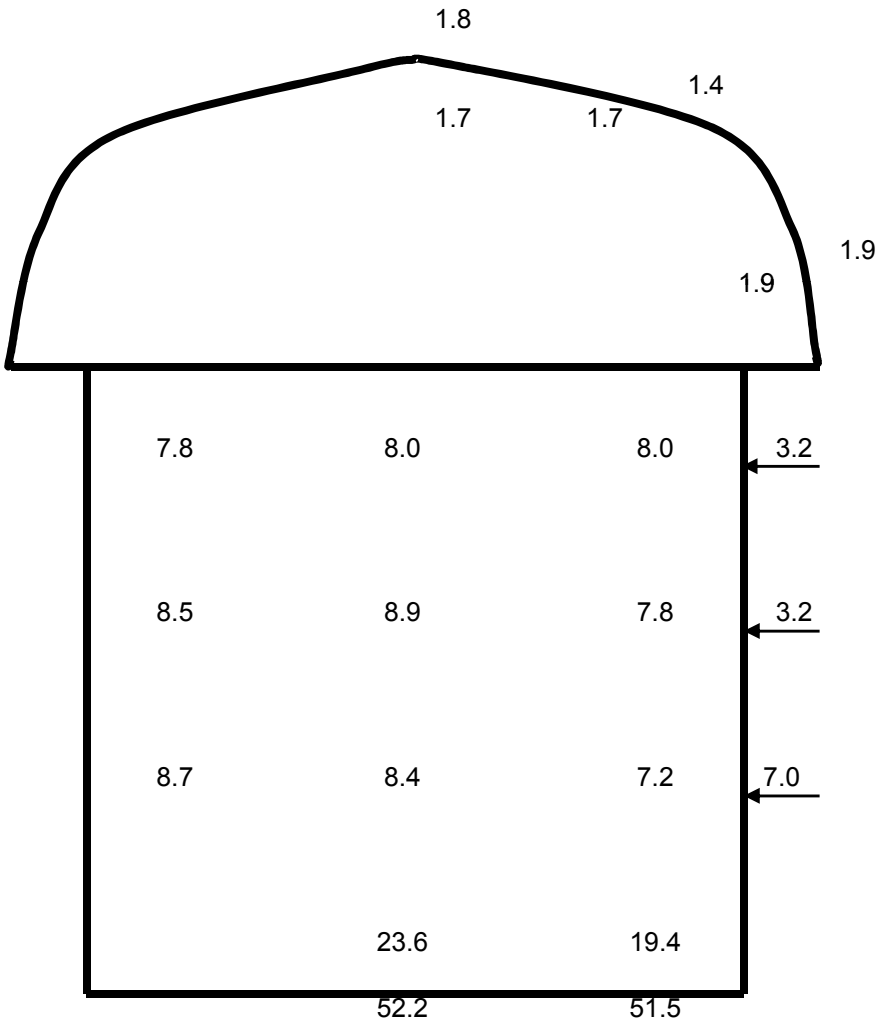
U-Factor (BTU/Hr-Ft2-F) =	**0.673**

Physical Test Temperature Distribution

Test Unit Number 4

Unit Configuration Details

Test Configuration	**Residential**	
Tube Size	**Small**	
Tube Type	**Flexible**	**Tube B**
Dome (Single / Double)	**Single**	**Dome B**
Diffuser (Single / Double)	**Double**	**Inner Diffuser B / Outer Diffuser B**



All Temperatures reported in °F

Physical Test Results

Test Unit Number 5

Unit Configuration Details

Test Configuration	**Residential**	
Tube Size	**Small**	
Tube Type	**Rigid**	**Tube C**
Dome (Single / Double)	**Single**	**Outer Dome C**
Diffuser (Single / Double)	**Single**	**Diffuser C**

Bottom Box Fan Power (Watts) =	1.107
Bottom Box Heater Power (Watts) =	21.608
BB Box Thermopile (EMF, mv) =	2.634
Enter Specimen Diameter (Inches) =	14.040
Specimen Area (Ft2) =	1.075
Enter Thermopile Intercept =	-5.980
Enter Thermopile Slope =	1.108
Enter Surround Panel R-Value (Hr/BTU-F-Ft2) =	44.683
Enter Surround Panel Width (Inches) =	30.000
Enter Surround Panel Height (Inches) =	36.000
Surround Panel Area (Ft2) =	6.425
Surround Panel Cold Temperature (F) =	3.423
Surround Panel Warm Temperature (F) =	69.603
Top Box Air Temperature (F) =	0.099
Middle Box Air Temperature (F) =	1.341
Bottom Box Air Temperature (F) =	70.001

Bottom Box Fan Power (BTUH) =	3.780
Bottom Box Heater Power (BTUH) =	73.769
Thermopile Wall Loss - Bottom Box (BTUH) =	-3.061
Surround Panel Heat Transfer (BTUH) =	9.516
Total Energy Input (BTUH) =	71.094

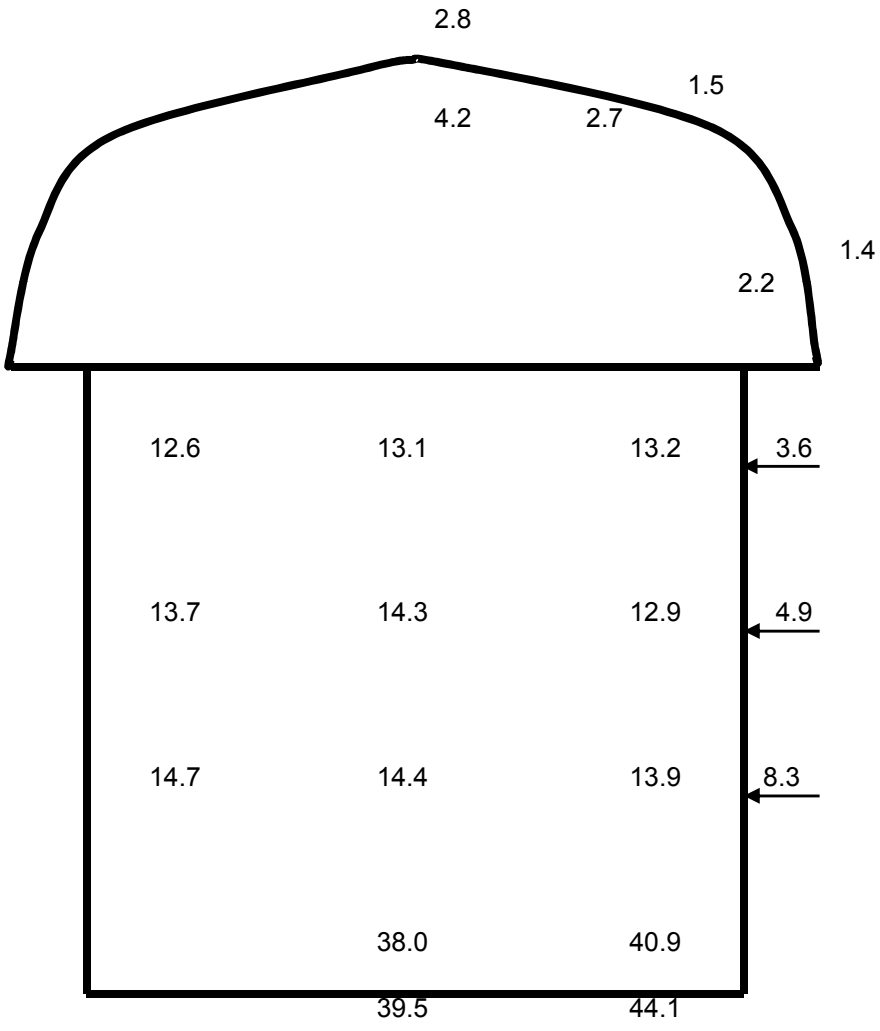
U-Factor (BTU/Hr-Ft2-F) =	**0.946**

Physical Test Temperature Distribution

Test Unit Number 5

Unit Configuration Details

Test Configuration	**Residential**	
Tube Size	**Small**	
Tube Type	**Rigid**	**Tube C**
Dome (Single / Double)	**Single**	**Outer Dome C**
Diffuser (Single / Double)	**Single**	**Diffuser C**



All Temperatures reported in °F

Physical Test Results

Test Unit Number 6

Unit Configuration Details

Test Configuration	**Residential**	
Tube Size	**Small**	
Tube Type	**Rigid**	**Tube C**
Dome (Single / Double)	**Double**	**Inner Dome C, Outer Dome C**
Diffuser (Single / Double)	**Single**	**Diffuser C**

Bottom Box Fan Power (Watts) =	1.108
Bottom Box Heater Power (Watts) =	18.494
BB Box Thermopile (EMF, mv) =	2.649
Enter Specimen Diameter (Inches) =	14.040
Specimen Area (Ft2) =	1.075
Enter Thermopile Intercept =	-5.980
Enter Thermopile Slope =	1.108
Enter Surround Panel R-Value (Hr/BTU-F-Ft2) =	44.683
Enter Surround Panel Width (Inches) =	30.000
Enter Surround Panel Height (Inches) =	36.000
Surround Panel Area (Ft2) =	6.425
Surround Panel Cold Temperature (F) =	1.924
Surround Panel Warm Temperature (F) =	68.747
Top Box Air Temperature (F) =	0.234
Middle Box Air Temperature (F) =	24.027
Bottom Box Air Temperature (F) =	70.000

Bottom Box Fan Power (BTUH) =	3.784
Bottom Box Heater Power (BTUH) =	63.139
Thermopile Wall Loss - Bottom Box (BTUH) =	-3.044
Surround Panel Heat Transfer (BTUH) =	9.608
Total Energy Input (BTUH) =	60.359

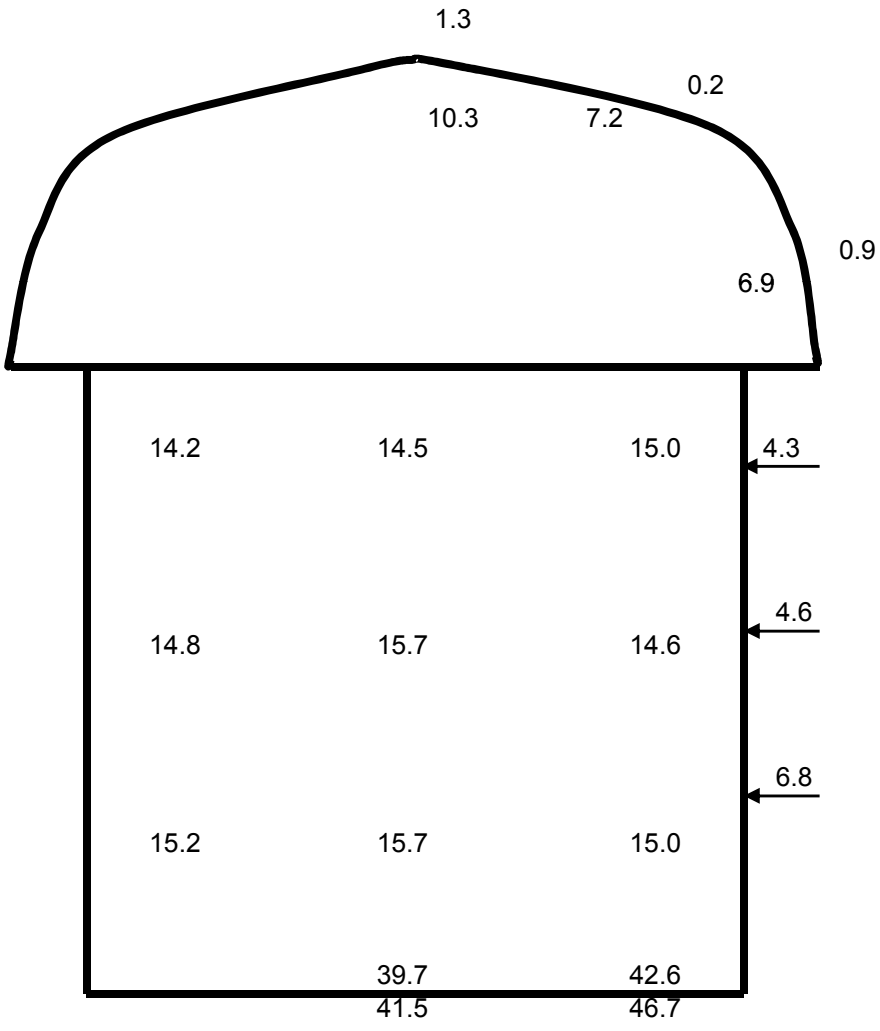
U-Factor (BTU/Hr-Ft2-F) =	**0.805**

Physical Test Temperature Distribution

Test Unit Number 6

Unit Configuration Details

Test Configuration	**Residential**	
Tube Size	**Small**	
Tube Type	**Rigid**	**Tube C**
Dome (Single / Double)	**Double**	**Inner Dome C, Outer Dome C**
Diffuser (Single / Double)	**Single**	**Diffuser C**



All Temperatures reported in °F

Physical Test Results

Test Unit Number 7

Unit Configuration Details

Test Configuration	**Residential**	
Tube Size	**Small**	
Tube Type	**Rigid**	**Tube C**
Dome (Single / Double)	**Single**	**Outer Dome C**
Diffuser (Single / Double)	**Double**	**Inner Diffuser C, Outer Diffuser C**

Bottom Box Fan Power (Watts) =	1.132
Bottom Box Heater Power (Watts) =	15.839
BB Box Thermopile (EMF, mv) =	3.849
Enter Specimen Diameter (Inches) =	14.040
Specimen Area (Ft2) =	1.075
Enter Thermopile Intercept =	-5.980
Enter Thermopile Slope =	1.108
Enter Surround Panel R-Value (Hr/BTU-F-Ft2) =	44.683
Enter Surround Panel Width (Inches) =	30.000
Enter Surround Panel Height (Inches) =	36.000
Surround Panel Area (Ft2) =	6.425
Surround Panel Cold Temperature (F) =	3.171
Surround Panel Warm Temperature (F) =	69.180
Top Box Air Temperature (F) =	-0.001
Middle Box Air Temperature (F) =	1.418
Bottom Box Air Temperature (F) =	69.997

Bottom Box Fan Power (BTUH) =	3.864
Bottom Box Heater Power (BTUH) =	54.073
Thermopile Wall Loss - Bottom Box (BTUH) =	-1.716
Surround Panel Heat Transfer (BTUH) =	9.491
Total Energy Input (BTUH) =	50.161

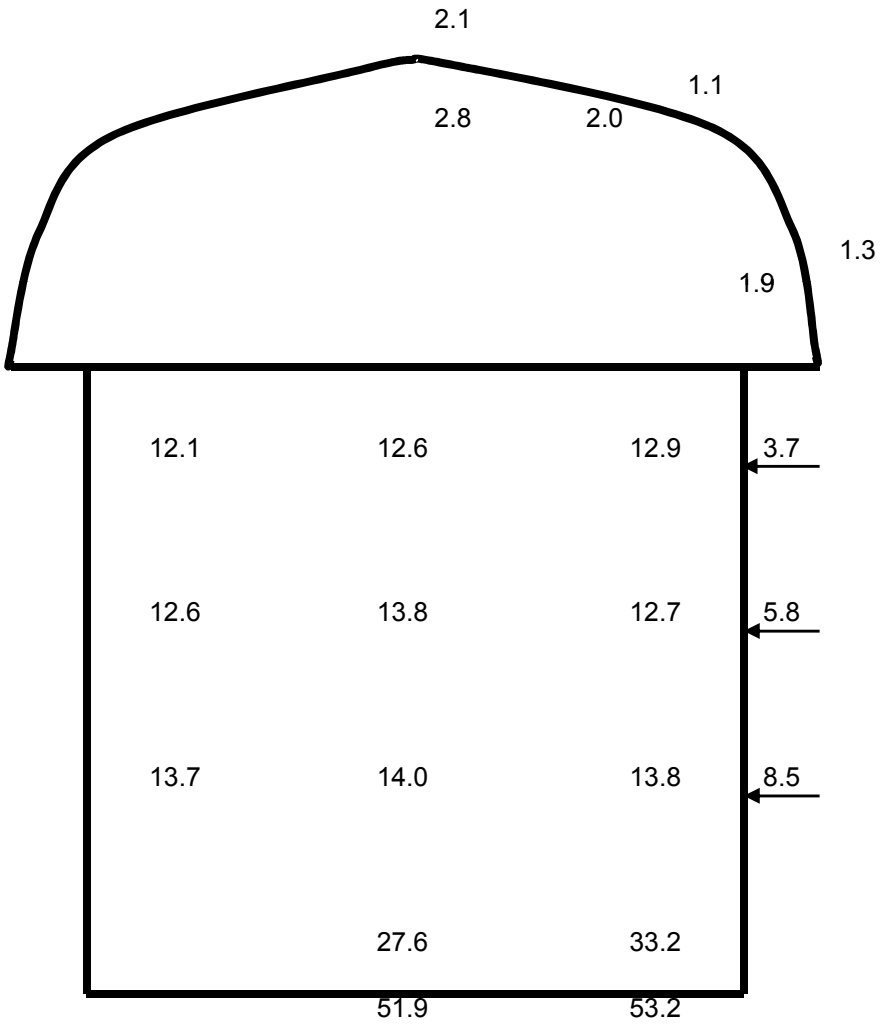
U-Factor (BTU/Hr-Ft2-F) =	**0.667**

Physical Test Temperature Distribution

Test Unit Number 7

Unit Configuration Details

Test Configuration	**Residential**	
Tube Size	**Small**	
Tube Type	**Rigid**	**Tube C**
Dome (Single / Double)	**Single**	**Outer Dome C**
Diffuser (Single / Double)	**Double**	**Inner Diffuser C, Outer Diffuser C**



All Temperatures reported in °F

Physical Test Results

Test Unit Number 8

Unit Configuration Details

Test Configuration	**Commercial**	
Tube Size	**Large**	
Tube Type	**Rigid**	**Tube E**
Dome (Single / Double)	**Single**	**Dome D**
Diffuser (Single / Double)	**Single**	**Diffuser D**

Bottom Box Fan Power (Watts) =	1.106
Bottom Box Heater Power (Watts) =	61.152
Bottom Box Thermopile (EMF, mv) =	4.673
Middle Box Fan Power (Watts) =	2.627
Middle Box Thermopile (EMF, mv) =	-5.102
Enter Specimen Diameter (Inches) =	21.510
Specimen Area (Ft2) =	2.524
Enter Bottom Box Thermopile Intercept =	-5.980
Enter Bottom Box Thermopile Slope =	1.108
Enter Middle Box Thermopile Intercept =	-5.979
Enter Middle Box Thermopile Slope =	1.036
Enter Surround Panel R-Value (Hr/BTU-F-Ft2) =	44.683
Enter Surround Panel Width (Inches) =	30.000
Enter Surround Panel Height (Inches) =	36.000
Surround Panel Area (Ft2) =	4.976
Surround Panel Cold Temperature (F) =	0.258
Surround Panel Warm Temperature (F) =	66.614
Top Box Air Temperature (F) =	-0.002
Middle Box Air Temperature (F) =	66.592
Bottom Box Air Temperature (F) =	69.999

Bottom Box Fan Power (BTUH) =	3.777
Bottom Box Heater Power (BTUH) =	208.774
Thermopile Wall Loss - Bottom Box (BTUH) =	-0.802
Middle Box Fan Power (BTUH) =	8.968
Thermopile Wall Loss - Middle Box (BTUH) =	-11.264
Surround Panel Heat Transfer (BTUH) =	7.390
Total Energy Input (BTUH) =	226.195

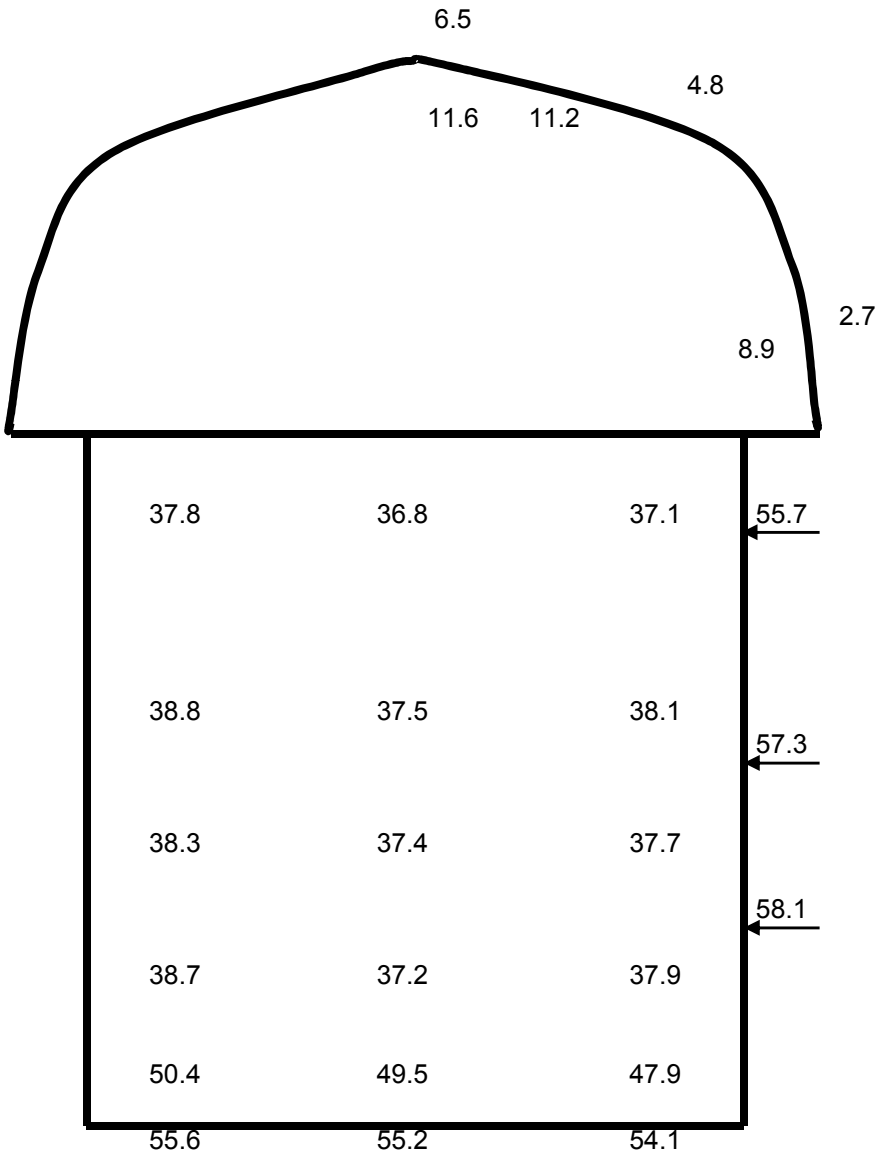
U-Factor (BTU/Hr-Ft2-F) =	**1.280**

Physical Test Temperature Distribution

Test Unit Number 8

Unit Configuration Details

Test Configuration	**Commercial**	
Tube Size	**Large**	
Tube Type	**Rigid**	**Tube E**
Dome (Single / Double)	**Single**	**Dome D**
Diffuser (Single / Double)	**Single**	**Diffuser D**



All Temperatures reported in °F

Physical Test Results

Test Unit Number 9

Unit Configuration Details

Test Configuration	**Commercial**	
Tube Size	**Large**	
Tube Type	**Rigid**	**Tube E**
Dome (Single / Double)	**Double**	**Outer Dome D, Inner Dome D**
Diffuser (Single / Double)	**Single**	**Diffuser D**

Bottom Box Fan Power (Watts) =	1.103
Bottom Box Heater Power (Watts) =	28.136
Bottom Box Thermopile (EMF, mv) =	3.402
Middle Box Fan Power (Watts) =	2.626
Middle Box Thermopile (EMF, mv) =	-3.232
Enter Specimen Diameter (Inches) =	21.510
Specimen Area (Ft2) =	2.524
Enter Bottom Box Thermopile Intercept =	-5.980
Enter Bottom Box Thermopile Slope =	1.108
Enter Middle Box Thermopile Intercept =	-5.979
Enter Middle Box Thermopile Slope =	1.036
Enter Surround Panel R-Value (Hr/BTU-F-Ft2) =	44.683
Enter Surround Panel Width (Inches) =	30.000
Enter Surround Panel Height (Inches) =	36.000
Surround Panel Area (Ft2) =	4.976
Surround Panel Cold Temperature (F) =	0.258
Surround Panel Warm Temperature (F) =	66.614
Top Box Air Temperature (F) =	0.000
Middle Box Air Temperature (F) =	68.685
Bottom Box Air Temperature (F) =	69.998

Bottom Box Fan Power (BTUH) =	3.766
Bottom Box Heater Power (BTUH) =	96.057
Thermopile Wall Loss - Bottom Box (BTUH) =	-2.210
Middle Box Fan Power (BTUH) =	8.966
Thermopile Wall Loss - Middle Box (BTUH) =	-9.327
Surround Panel Heat Transfer (BTUH) =	7.390
Total Energy Input (BTUH) =	112.936

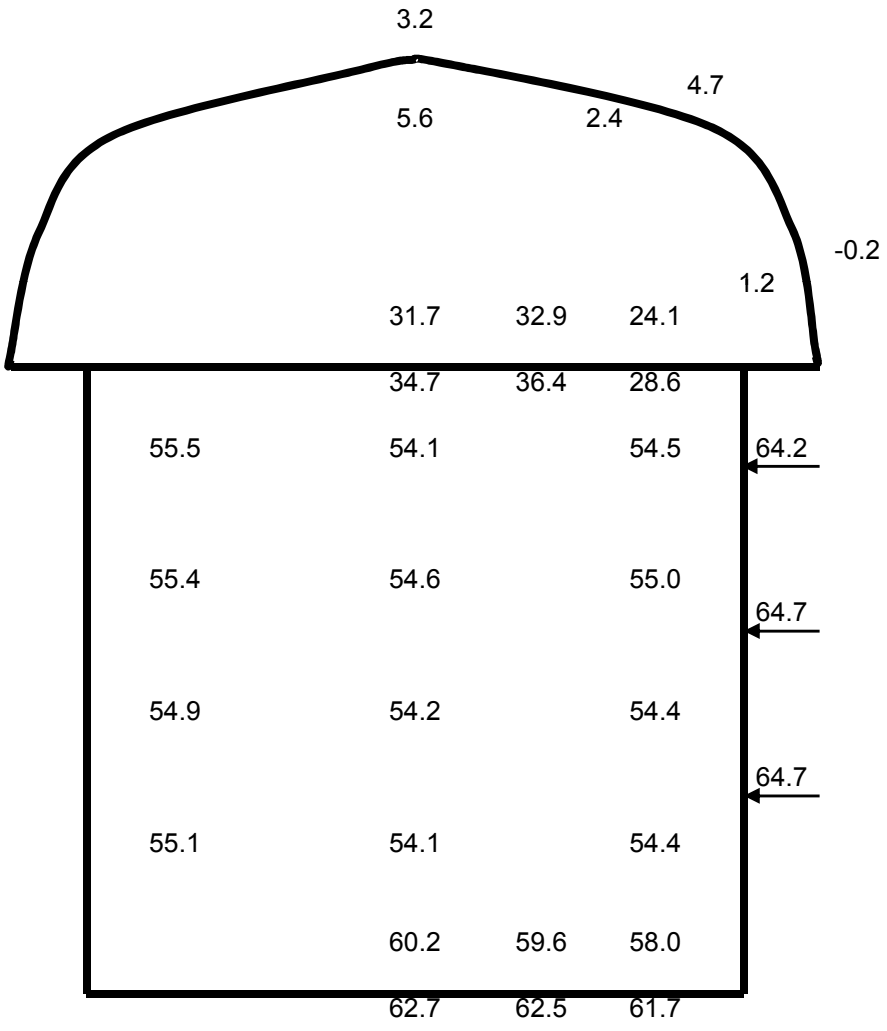
U-Factor (BTU/Hr-Ft2-F) =	**0.639**

Physical Test Temperature Distribution

Test Unit Number 9

Unit Configuration Details

Test Configuration	**Commercial**	
Tube Size	**Large**	
Tube Type	**Rigid**	**Tube E**
Dome (Single / Double)	**Double**	**Outer Dome D, Inner Dome D**
Diffuser (Single / Double)	**Single**	**Diffuser D**



All Temperatures reported in °F

Physical Test Results

Test Unit Number 10

Unit Configuration Details

Test Configuration	**Commercial**	
Tube Size	**Large**	
Tube Type	**Flexible**	**Tube D**
Dome (Single / Double)	**Single**	**Dome D**
Diffuser (Single / Double)	**Single**	**Diffuser D**

Bottom Box Fan Power (Watts) =	1.104
Bottom Box Heater Power (Watts) =	55.570
Bottom Box Thermopile (EMF, mv) =	4.351
Middle Box Fan Power (Watts) =	2.619
Middle Box Thermopile (EMF, mv) =	-5.102
Enter Specimen Diameter (Inches) =	21.510
Specimen Area (Ft2) =	2.524
Enter Bottom Box Thermopile Intercept =	-5.980
Enter Bottom Box Thermopile Slope =	1.108
Enter Middle Box Thermopile Intercept =	-5.979
Enter Middle Box Thermopile Slope =	1.036
Enter Surround Panel R-Value (Hr/BTU-F-Ft2) =	44.683
Enter Surround Panel Width (Inches) =	30.000
Enter Surround Panel Height (Inches) =	36.000
Surround Panel Area (Ft2) =	4.976
Surround Panel Cold Temperature (F) =	0.258
Surround Panel Warm Temperature (F) =	66.614
Top Box Air Temperature (F) =	-0.004
Middle Box Air Temperature (F) =	67.862
Bottom Box Air Temperature (F) =	70.004

Bottom Box Fan Power (BTUH) =	3.770
Bottom Box Heater Power (BTUH) =	189.718
Thermopile Wall Loss - Bottom Box (BTUH) =	-1.160
Middle Box Fan Power (BTUH) =	8.940
Thermopile Wall Loss - Middle Box (BTUH) =	-11.265
Surround Panel Heat Transfer (BTUH) =	7.390
Total Energy Input (BTUH) =	207.461

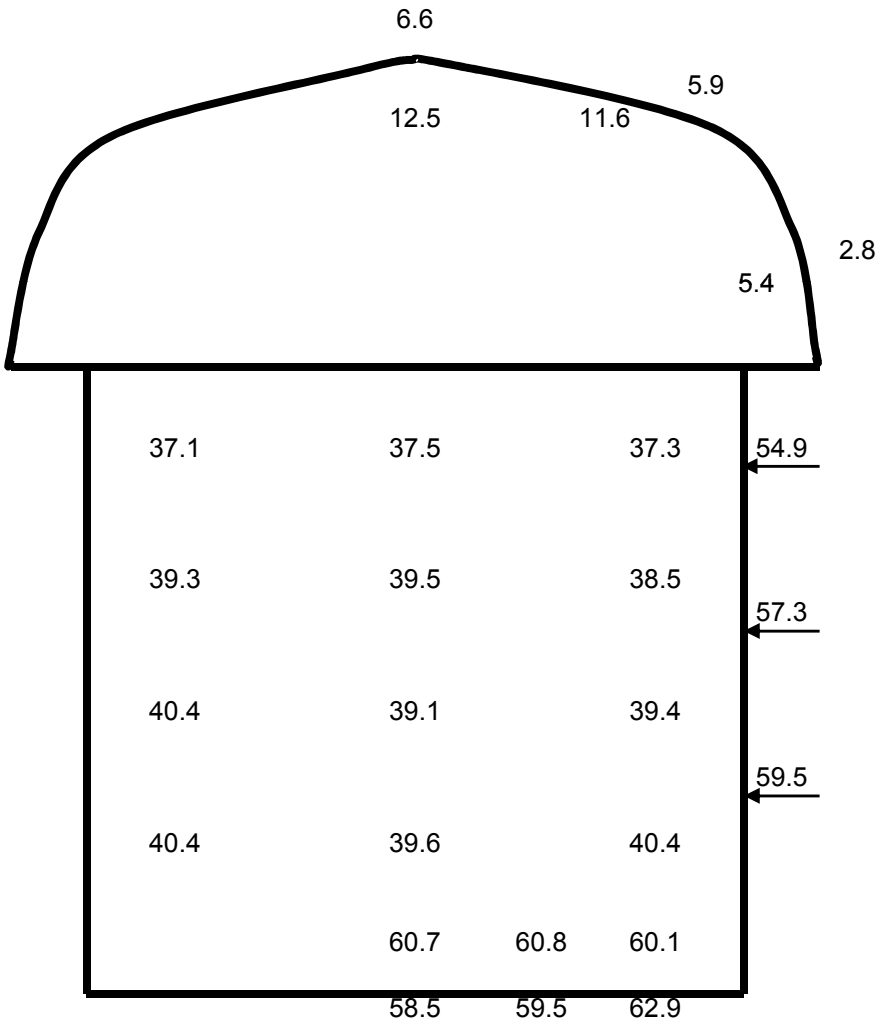
U-Factor (BTU/Hr-Ft2-F) =	**1.174**

Physical Test Temperature Distribution

Test Unit Number 10

Unit Configuration Details

Test Configuration	**Commercial**	
Tube Size	**Large**	
Tube Type	**Flexible**	**Tube D**
Dome (Single / Double)	**Single**	**Dome D**
Diffuser (Single / Double)	**Single**	**Diffuser D**



All Temperatures reported in °F

Physical Test Results

Test Unit Number 11

Unit Configuration Details

Test Configuration	**Commercial**	
Tube Size	**Small**	
Tube Type	**Rigid**	**Tube C**
Dome (Single / Double)	**Single**	**Dome C**
Diffuser (Single / Double)	**Single**	**Diffuser C**

Bottom Box Fan Power (Watts) =	1.104
Bottom Box Heater Power (Watts) =	28.727
Bottom Box Thermopile (EMF, mv) =	3.319
Middle Box Fan Power (Watts) =	2.612
Middle Box Thermopile (EMF, mv) =	-1.672
Enter Specimen Diameter (Inches) =	14.040
Specimen Area (Ft2) =	1.075
Enter Bottom Box Thermopile Intercept =	-5.980
Enter Bottom Box Thermopile Slope =	1.108
Enter Middle Box Thermopile Intercept =	-5.979
Enter Middle Box Thermopile Slope =	1.036
Enter Surround Panel R-Value (Hr/BTU-F-Ft2) =	44.683
Enter Surround Panel Width (Inches) =	30.000
Enter Surround Panel Height (Inches) =	36.000
Surround Panel Area (Ft2) =	6.425
Surround Panel Cold Temperature (F) =	0.426
Surround Panel Warm Temperature (F) =	69.138
Top Box Air Temperature (F) =	-0.003
Middle Box Air Temperature (F) =	69.838
Bottom Box Air Temperature (F) =	70.002

Bottom Box Fan Power (BTUH) =	3.770
Bottom Box Heater Power (BTUH) =	98.074
Thermopile Wall Loss - Bottom Box (BTUH) =	-2.303
Middle Box Fan Power (BTUH) =	8.919
Thermopile Wall Loss - Middle Box (BTUH) =	-7.711
Surround Panel Heat Transfer (BTUH) =	9.880
Total Energy Input (BTUH) =	110.897

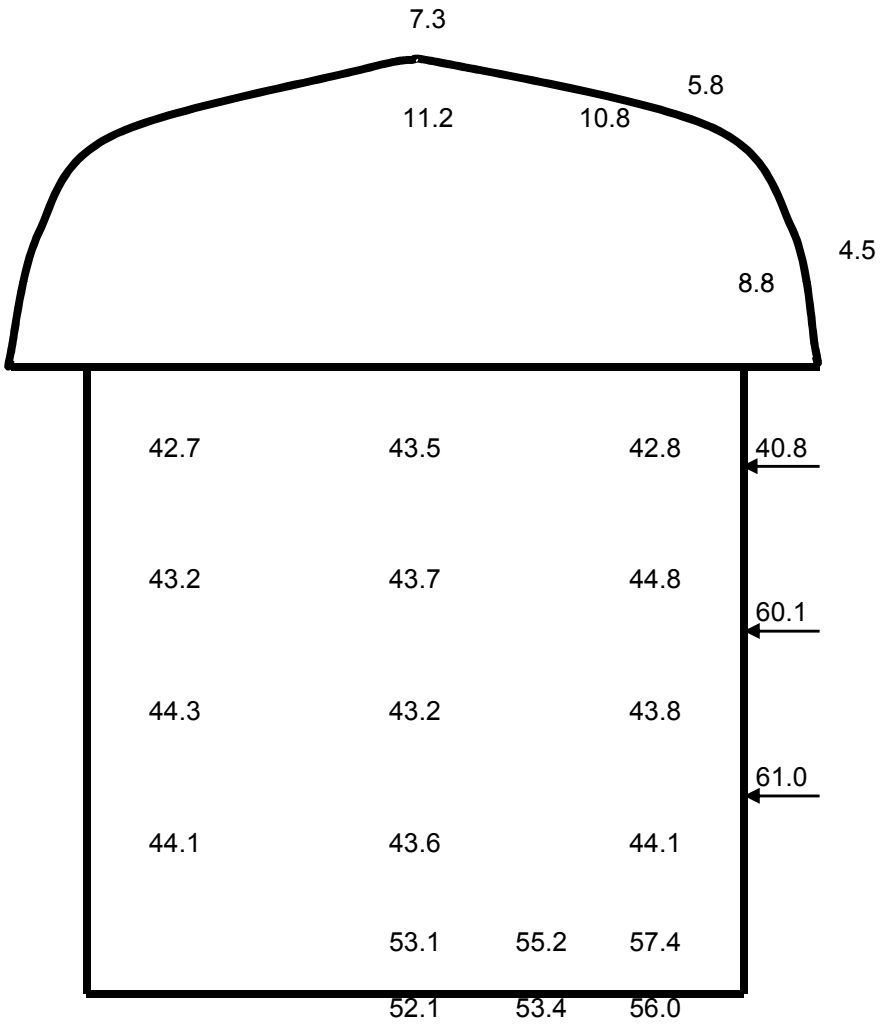
U-Factor (BTU/Hr-Ft2-F) =	**1.473**

Physical Test Temperature Distribution

Test Unit Number 11

Unit Configuration Details

Test Configuration	**Commercial**	
Tube Size	**Small**	
Tube Type	**Rigid**	**Tube C**
Dome (Single / Double)	**Single**	**Dome C**
Diffuser (Single / Double)	**Single**	**Diffuser C**



All Temperatures reported in °F

Physical Test Results

Test Unit Number 12

Unit Configuration Details

Test Configuration	**Commercial**	
Tube Size	**Small**	
Tube Type	**Rigid**	**Tube C**
Dome (Single / Double)	**Double**	**Outer Dome C, Inner Dome C**
Diffuser (Single / Double)	**Single**	**Diffuser C**

Bottom Box Fan Power (Watts) =	1.112
Bottom Box Heater Power (Watts) =	14.565
Bottom Box Thermopile (EMF, mv) =	3.158
Middle Box Fan Power (Watts) =	2.616
Middle Box Thermopile (EMF, mv) =	-1.662
Enter Specimen Diameter (Inches) =	14.040
Specimen Area (Ft2) =	1.075
Enter Bottom Box Thermopile Intercept =	-5.980
Enter Bottom Box Thermopile Slope =	1.108
Enter Middle Box Thermopile Intercept =	-5.979
Enter Middle Box Thermopile Slope =	1.036
Enter Surround Panel R-Value (Hr/BTU-F-Ft2) =	44.683
Enter Surround Panel Width (Inches) =	30.000
Enter Surround Panel Height (Inches) =	36.000
Surround Panel Area (Ft2) =	6.425
Surround Panel Cold Temperature (F) =	0.292
Surround Panel Warm Temperature (F) =	69.517
Top Box Air Temperature (F) =	0.001
Middle Box Air Temperature (F) =	70.104
Bottom Box Air Temperature (F) =	70.001
Bottom Box Fan Power (BTUH) =	3.796
Bottom Box Heater Power (BTUH) =	49.724
Thermopile Wall Loss - Bottom Box (BTUH) =	-2.481
Middle Box Fan Power (BTUH) =	8.930
Thermopile Wall Loss - Middle Box (BTUH) =	-7.701
Surround Panel Heat Transfer (BTUH) =	9.954
Total Energy Input (BTUH) =	62.678

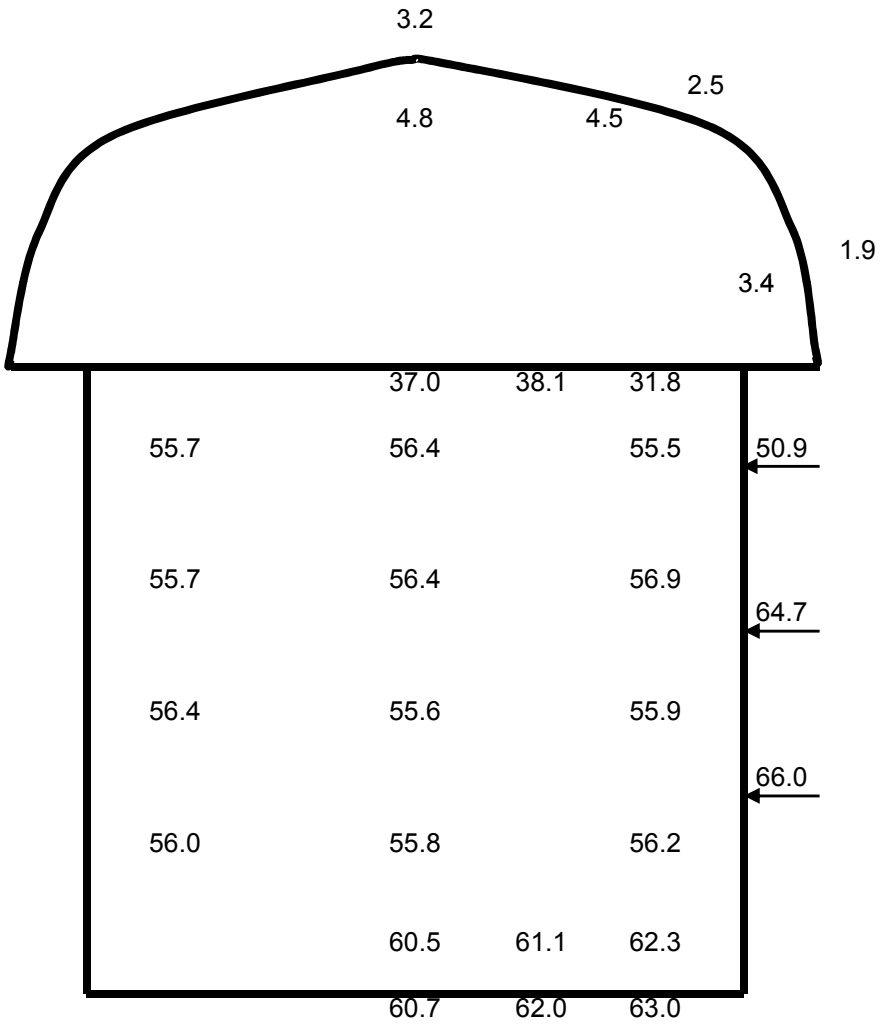
U-Factor (BTU/Hr-Ft2-F) =	**0.833**

Physical Test Temperature Distribution

Test Unit Number 12

Unit Configuration Details

Test Configuration	**Commercial**	
Tube Size	**Small**	
Tube Type	**Rigid**	**Tube C**
Dome (Single / Double)	**Double**	**Outer Dome C, Inner Dome C**
Diffuser (Single / Double)	**Single**	**Diffuser C**



All Temperatures reported in °F

Appendix B

Simulation Results

Each sample was simulated per NFRC guidelines, with the exception that actual product sizes as tested were utilized. This was necessary to provide an accurate comparison with tested values. For the commercial configurations, a modified NFRC approach was used which adapted to the differing installed configuration.

The simulation results are documented in the following tables. Isothermal graphs of the temperature distributions are included for comparison with tested results. Pertinent simulation input and output data is included in the following tables.

Simulation Results

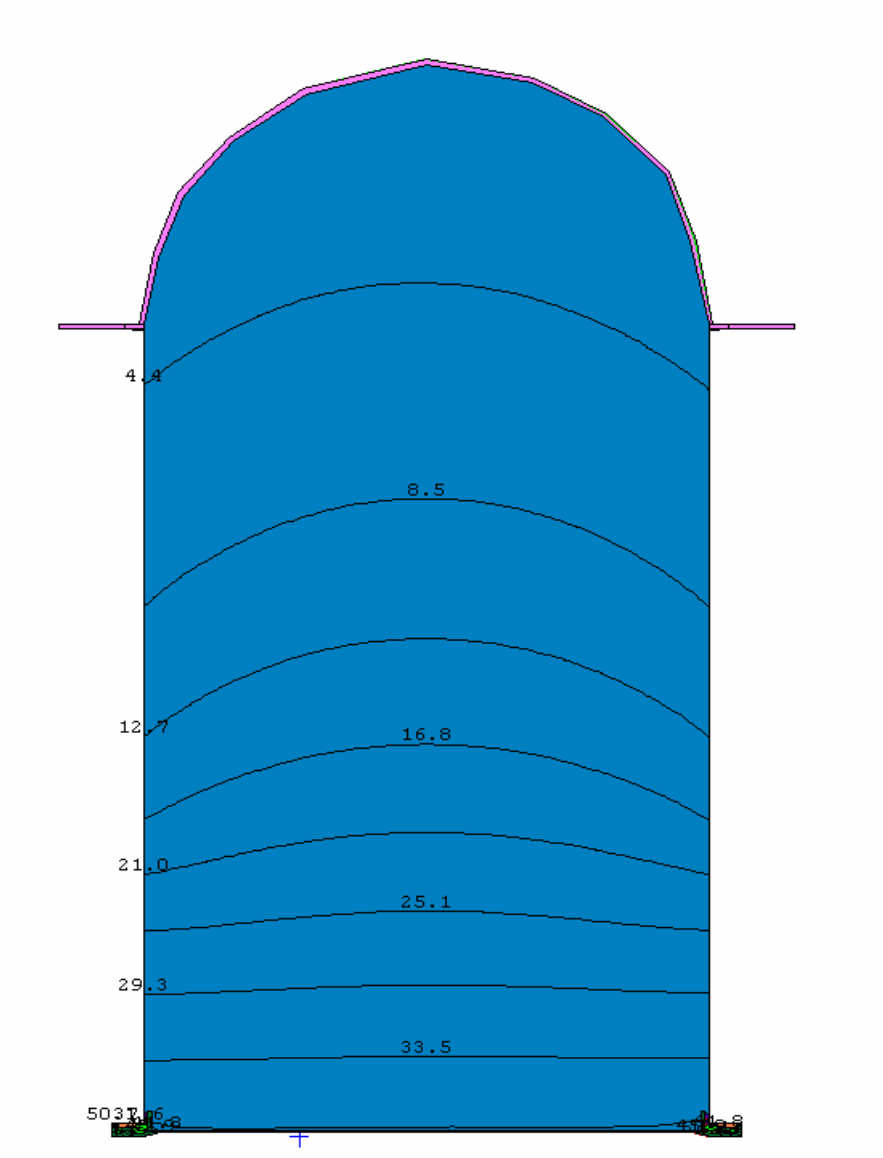
Test Unit Number 1

Unit Configuration Details

Test Configuration	**Residential**	
Tube Size	**Large**	
Tube Type	**Rigid**	**Tube A**
Dome (Single / Double)	**Single**	**Dome A**
Diffuser (Single / Double)	**Single**	**Diffuser A**

Frame Height = 21.036

U-Factor (BTU/Hr-Ft2-F) = 0.694



Simulation Results

Test Unit Number 1

Unit Configuration Details

Test Configuration	**Residential**	
Tube Size	**Large**	
Tube Type	**Rigid**	**Tube A**
Dome (Single / Double)	**Single**	**Dome A**
Diffuser (Single / Double)	**Single**	**Diffuser A**

Solid Materials

Name	Conductivity (Btu-in / Hr-Ft2-F)	Emissivity
Polyvinylchloride (PVC) / Vinyl - Rigid*	1.18	0.9
Foam Weather Stripping*	0.21	0.9
User Defined: Iron - Wrought	418.8	0.9
Steel (Rolled, Ground)*	346.67	0.6
Aluminum Alloys (Oxidized, Mill Finish)*	1109.36	0.2
Silicone*	2.43	0.9
Polycarbonate*	1.39	0.9
User Defined: Keff Tube - 4.486	31.1	0.9

Standard Boundary Conditions

Name	Temperature (F)	Film Coefficient (Btu / Hr-Ft2-F)
User Defined: Tubes - Attic	-0.4	2.201
User Defined: Tubes - Indoor	69.8	1.585
User Defined: Tubes - Exterior	-0.4	5.283

Simulation Results

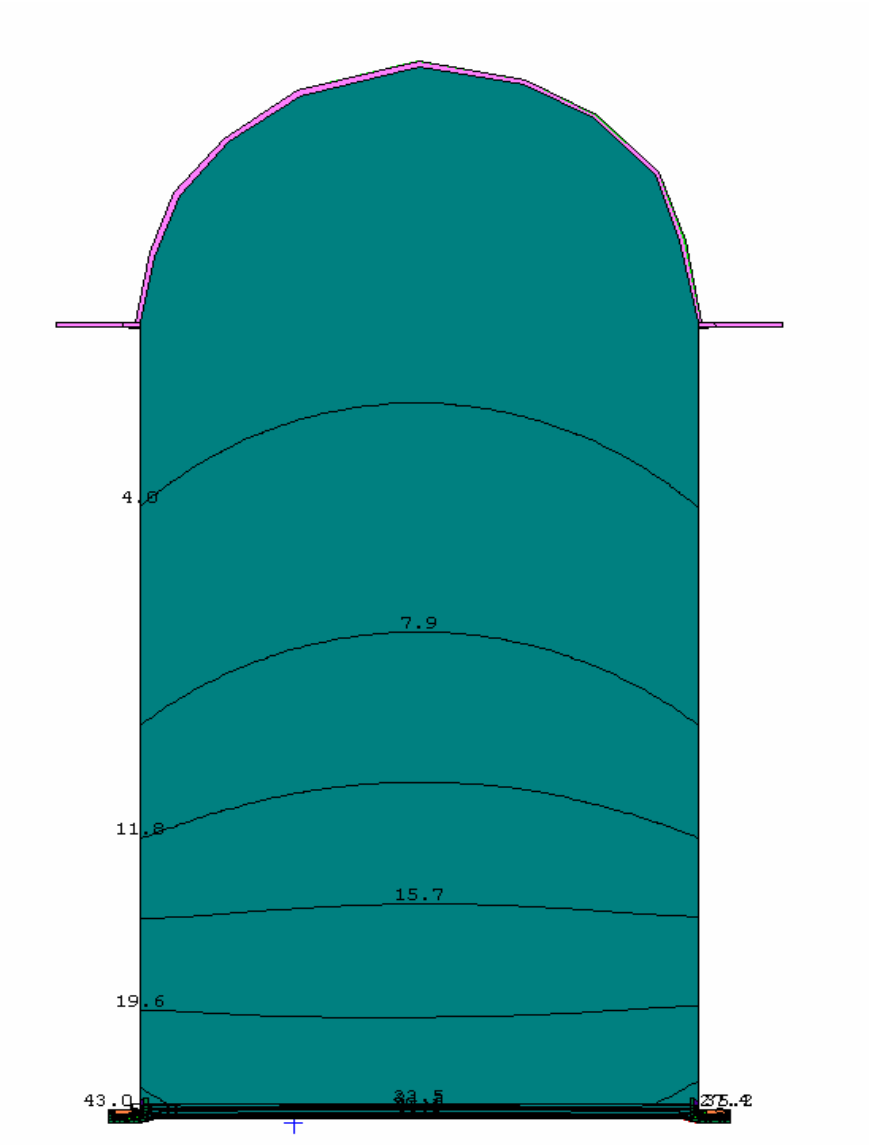
Test Unit Number 2

Unit Configuration Details

Test Configuration	**Residential**	
Tube Size	**Large**	
Tube Type	**Rigid**	**Tube A**
Dome (Single / Double)	**Single**	**Dome A**
Diffuser (Single / Double)	**Double**	**Inner Diffuser A, Outer Diffuser A**

Frame Height = 21.036

U-Factor (BTU/Hr-Ft2-F) = 0.412



Simulation Results

Test Unit Number 2

Unit Configuration Details

Test Configuration	**Residential**	
Tube Size	**Large**	
Tube Type	**Rigid**	**Tube A**
Dome (Single / Double)	**Single**	**Dome A**
Diffuser (Single / Double)	**Double**	**Inner Diffuser A, Outer Diffuser A**

Solid Materials

Name	Conductivity (Btu-in / Hr-Ft2-F)	Emissivity
Polyvinylchloride (PVC) / Vinyl - Rigid*	1.18	0.9
Foam Weather Stripping*	0.21	0.9
User Defined: Iron - Wrought	418.8	0.9
Steel (Rolled, Ground)*	346.67	0.6
Aluminum Alloys (Oxidized, Mill Finish)*	1109.36	0.2
Silicone*	2.43	0.9
Polycarbonate*	1.39	0.9
User Defined: Keff Tube - 4.773	33.09	0.9
User Defined: Keff - 0.0718	0.5	0.9

Standard Boundary Conditions

Name	Temperature (F)	Film Coefficient (Btu / Hr-Ft2-F)
User Defined: Tubes - Attic	-0.4	2.201
User Defined: Tubes - Indoor	69.8	1.585
User Defined: Tubes - Exterior	-0.4	5.283

Simulation Results

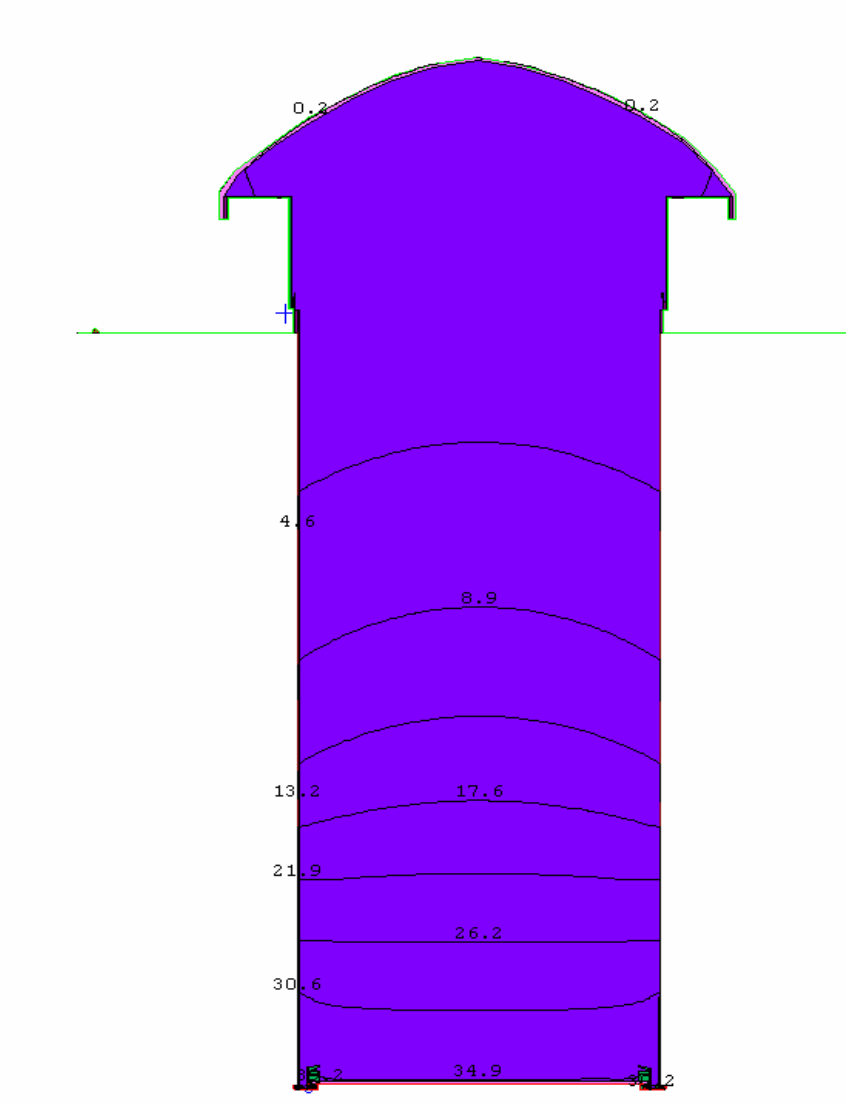
Test Unit Number 3

Unit Configuration Details

Test Configuration	**Residential**	
Tube Size	**Small**	
Tube Type	**Flexible**	**Tube B**
Dome (Single / Double)	**Single**	**Dome B**
Diffuser (Single / Double)	**Single**	**Diffuser B**

Frame Height = 13.776

U-Factor (BTU/Hr-Ft2-F) = 0.738



Simulation Results

Test Unit Number 3

Unit Configuration Details

Test Configuration	**Residential**	
Tube Size	**Small**	
Tube Type	**Flexible**	**Tube B**
Dome (Single / Double)	**Single**	**Dome B**
Diffuser (Single / Double)	**Single**	**Diffuser B**

Solid Materials

Name	Conductivity (Btu-in / Hr-Ft2-F)	Emissivity
Polyvinylchloride (PVC) / Vinyl - Rigid*	1.18	0.9
Polyvinylchloride (PVC) Flexible,with 40% Softener*	0.97	0.9
Polyester Fiber*	0.28	0.9
Aluminum Alloys (Painted)*	1109.36	0.2
Aluminum Alloys (Oxidized, Mill Finish)*	1109.36	0.2
Silicone*	2.43	0.9
Polycarbonate*	1.39	0.9
User Defined: Keff Tube - 4.500	31.2	0.9

Standard Boundary Conditions

Name	Temperature (F)	Film Coefficient (Btu / Hr-Ft2-F)
User Defined: Tubes - Attic	-0.4	2.201
User Defined: Tubes - Indoor	69.8	1.585
User Defined: Tubes - Exterior	-0.4	5.283

Simulation Results

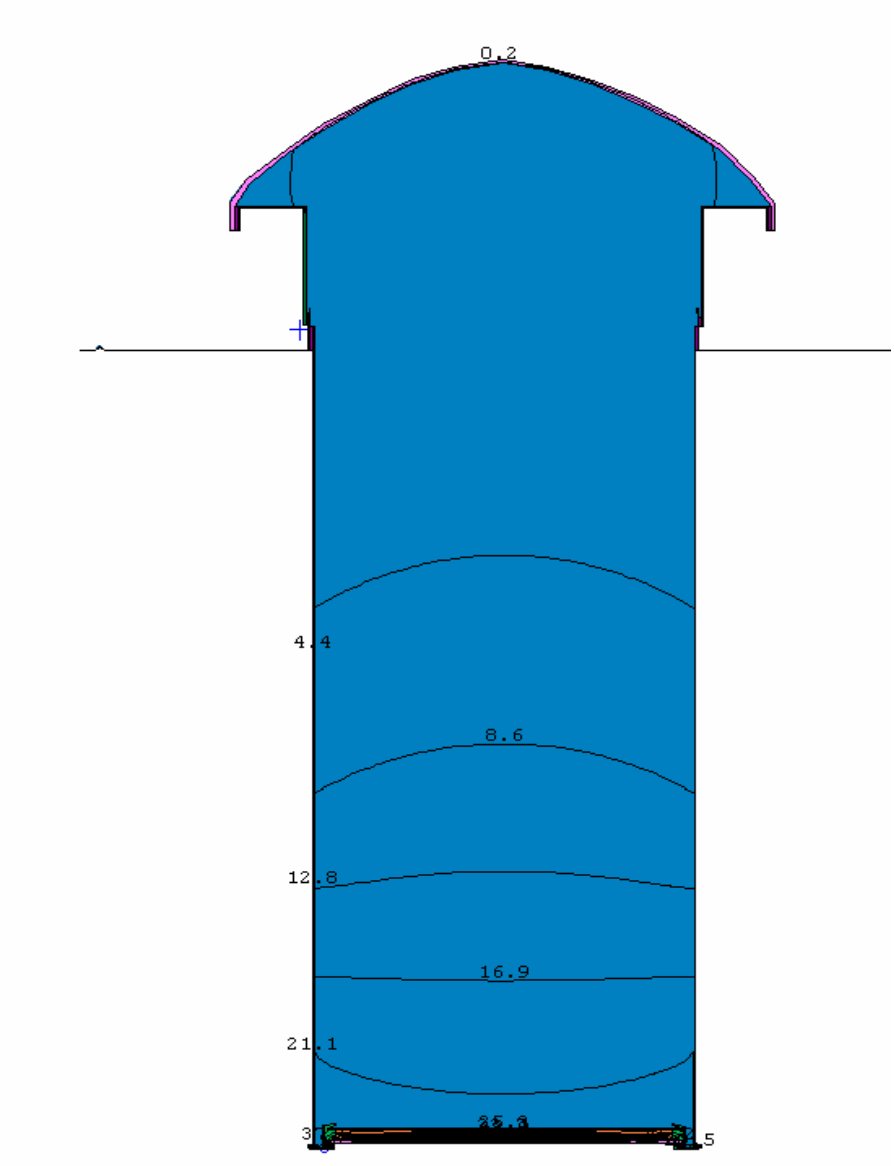
Test Unit Number 4

Unit Configuration Details

Test Configuration	**Residential**	
Tube Size	**Small**	
Tube Type	**Flexible**	**Tube B**
Dome (Single / Double)	**Single**	**Dome B**
Diffuser (Single / Double)	**Double**	**Inner Diffuser B / Outer Diffuser B**

Frame Height = 13.775

U-Factor (BTU/Hr-Ft2-F) = 0.503



Simulation Results

Test Unit Number 4

Unit Configuration Details

Test Configuration	**Residential**	
Tube Size	**Small**	
Tube Type	**Flexible**	**Tube B**
Dome (Single / Double)	**Single**	**Dome B**
Diffuser (Single / Double)	**Double**	**Inner Diffuser B / Outer Diffuser B**

Solid Materials

Name	Conductivity (Btu-in / Hr-Ft2-F)	Emissivity
Polyvinylchloride (PVC) / Vinyl - Rigid*	1.18	0.9
Polyvinylchloride (PVC) Flexible,with 40% Softener*	0.97	0.9
Polyester Fiber*	0.28	0.9
Aluminum Alloys (Painted)*	1109.36	0.2
Aluminum Alloys (Oxidized, Mill Finish)*	1109.36	0.2
Silicone*	2.43	0.9
Polycarbonate*	1.39	0.9
User Defined: Keff Tube - 4.766	33.04	0.9
User Defined: Keff - 0.058	0.41	0.9

Standard Boundary Conditions

Name	Temperature (F)	Film Coefficient (Btu / Hr-Ft2-F)
User Defined: Tubes - Attic	-0.4	2.201
User Defined: Tubes - Indoor	69.8	1.585
User Defined: Tubes - Exterior	-0.4	5.283

Simulation Results

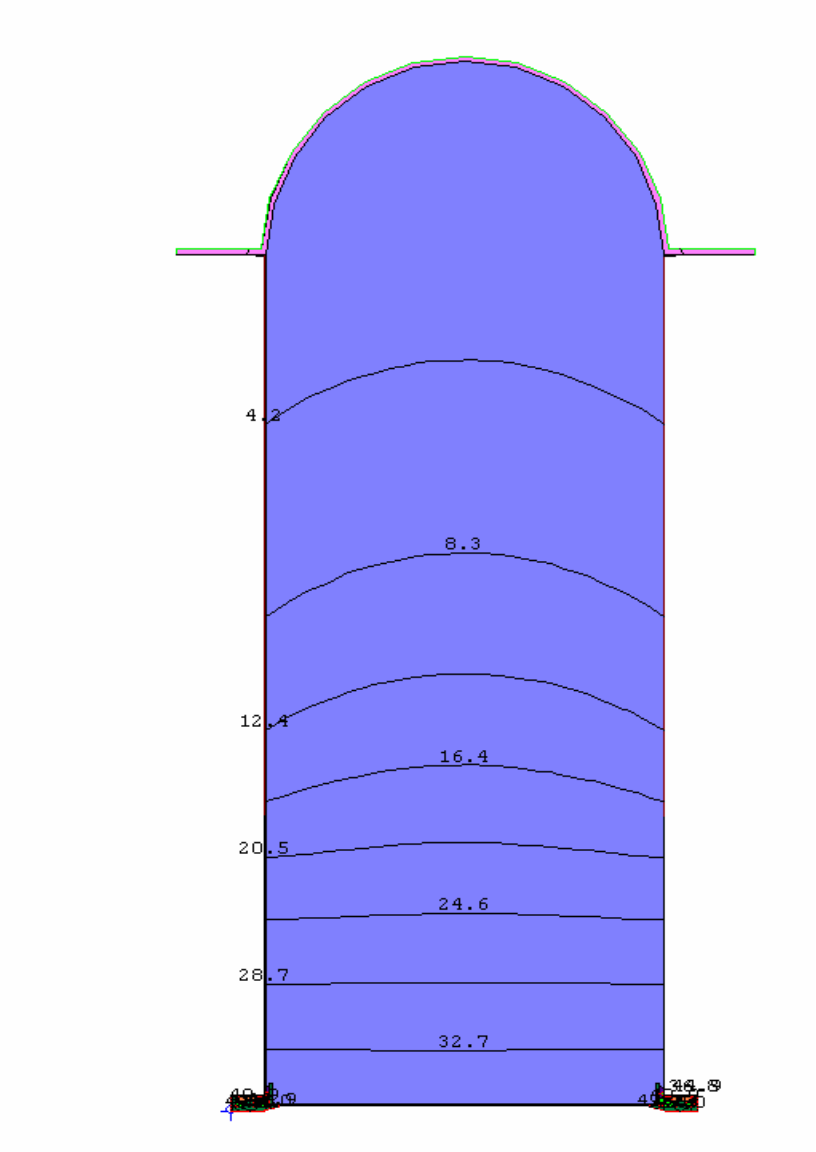
Test Unit Number 5

Unit Configuration Details

Test Configuration	**Residential**	
Tube Size	**Small**	
Tube Type	**Rigid**	**Tube C**
Dome (Single / Double)	**Single**	**Outer Dome C**
Diffuser (Single / Double)	**Single**	**Diffuser C**

Frame Height = 14.041

U-Factor (BTU/Hr-Ft2-F) = 0.732



Simulation Results

Test Unit Number 5

Unit Configuration Details

Test Configuration	**Residential**	
Tube Size	**Small**	
Tube Type	**Rigid**	**Tube C**
Dome (Single / Double)	**Single**	**Outer Dome C**
Diffuser (Single / Double)	**Single**	**Diffuser C**

Solid Materials

Name	Conductivity (Btu-in / Hr-Ft2-F)	Emissivity
Polyvinylchloride (PVC) / Vinyl - Rigid*	1.18	0.9
Foam Weather Stripping*	0.21	0.9
User Defined: Iron - Wrought	418.8	0.9
Steel (Rolled, Ground)*	346.67	0.6
Aluminum Alloys (Oxidized, Mill Finish)*	1109.36	0.2
Silicone*	2.43	0.9
Polycarbonate*	1.39	0.9
User Defined:Keff Tube - 4.450	30.85	0.9

Standard Boundary Conditions

Name	Temperature (F)	Film Coefficient (Btu / Hr-Ft2-F)
User Defined: Tubes - Attic	-0.4	2.201
User Defined: Tubes - Indoor	69.8	1.585
User Defined: Tubes - Exterior	-0.4	5.283

Simulation Results

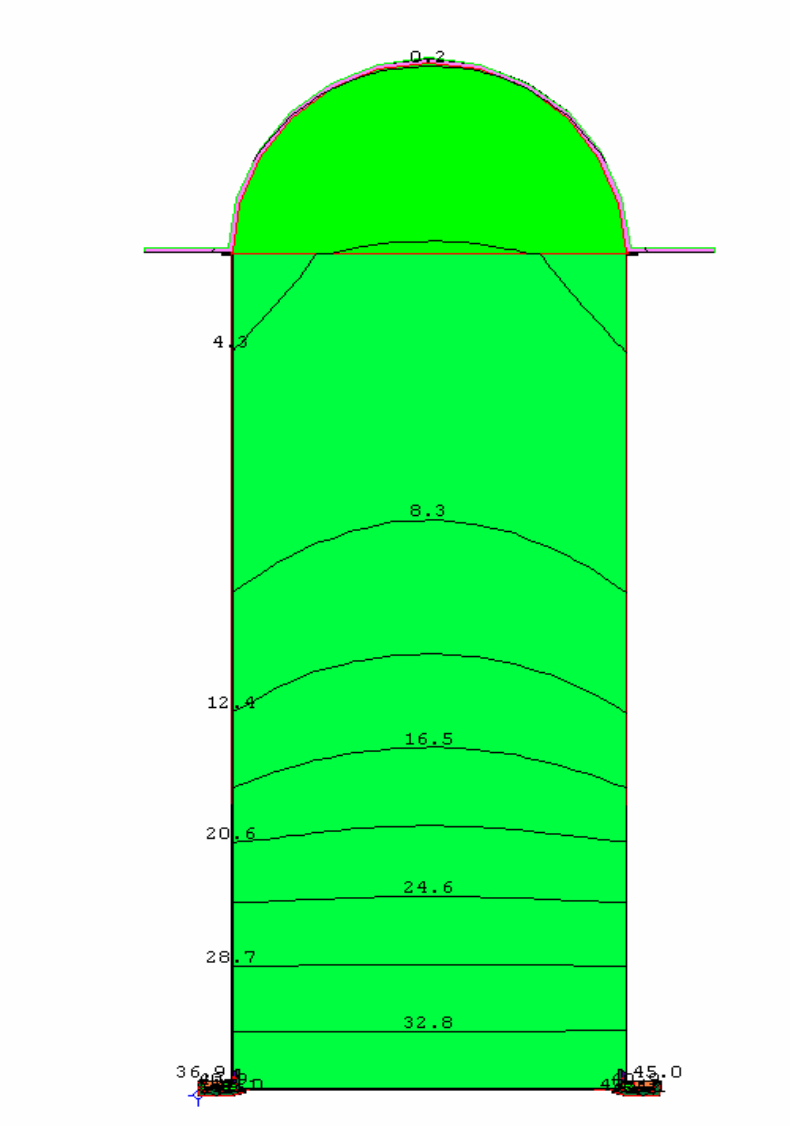
Test Unit Number 6

Unit Configuration Details

Test Configuration	**Residential**	
Tube Size	**Small**	
Tube Type	**Rigid**	**Tube C**
Dome (Single / Double)	**Double**	**Inner Dome C, Outer Dome C**
Diffuser (Single / Double)	**Single**	**Diffuser C**

Frame Height = 14.041

U-Factor (BTU/Hr-Ft2-F) = 0.724



Simulation Results

Test Unit Number 6

Unit Configuration Details

Test Configuration	**Residential**	
Tube Size	**Small**	
Tube Type	**Rigid**	**Tube C**
Dome (Single / Double)	**Double**	**Inner Dome C, Outer Dome C**
Diffuser (Single / Double)	**Single**	**Diffuser C**

Solid Materials

Name	Conductivity (Btu-in / Hr-Ft2-F)	Emissivity
Polyvinylchloride (PVC) / Vinyl - Rigid*	1.18	0.9
Foam Weather Stripping*	0.21	0.9
User Defined: Iron - Wrought	418.8	0.9
Steel (Rolled, Ground)*	346.67	0.6
Aluminum Alloys (Oxidized, Mill Finish)*	1109.36	0.2
Butyl rubber, (Isobutene), Solid / Hot Melt*	1.66	0.9
Polycarbonate*	1.39	0.9
User Defined:Keff Tube - 4.417	30.63	0.9

Standard Boundary Conditions

Name	Temperature (F)	Film Coefficient (Btu / Hr-Ft2-F)
User Defined: Tubes - Attic	-0.4	2.201
User Defined: Tubes - Indoor	69.8	1.585
User Defined: Tubes - Exterior	-0.4	5.283

Simulation Results

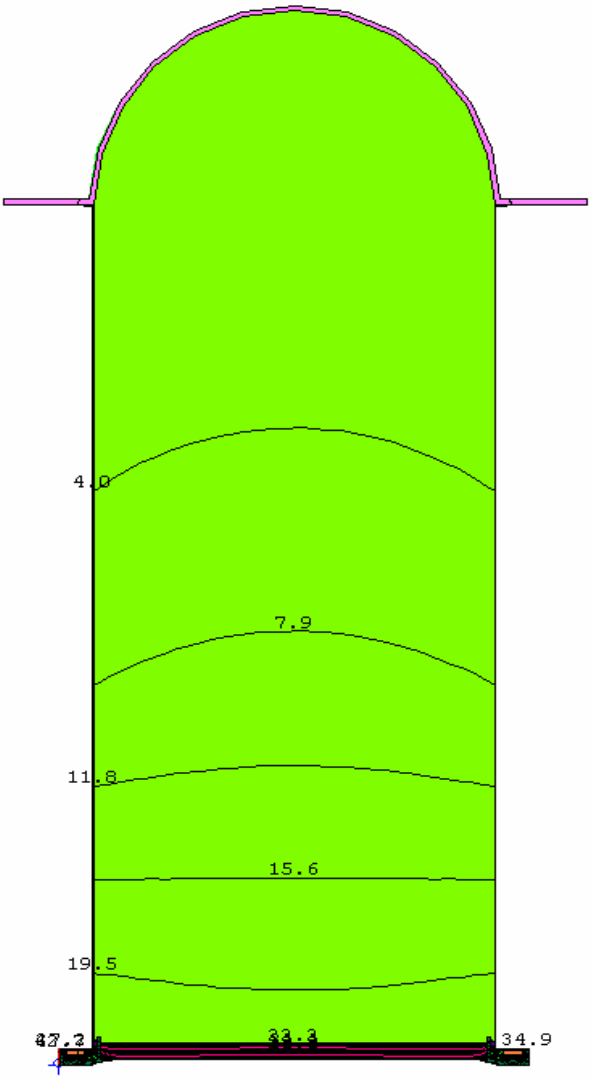
Test Unit Number 7

Unit Configuration Details

Test Configuration	**Residential**	
Tube Size	**Small**	
Tube Type	**Rigid**	**Tube C**
Dome (Single / Double)	**Single**	**Outer Dome C**
Diffuser (Single / Double)	**Double**	**Inner Diffuser C, Outer Diffuser C**

Frame Height = 14.041

U-Factor (BTU/Hr-Ft2-F) = 0.422



Simulation Results

Test Unit Number 7

Unit Configuration Details

Test Configuration	**Residential**	
Tube Size	**Small**	
Tube Type	**Rigid**	**Tube C**
Dome (Single / Double)	**Single**	**Outer Dome C**
Diffuser (Single / Double)	**Double**	**Inner Diffuser C, Outer Diffuser C**

Solid Materials

Name	Conductivity (Btu-in / Hr-Ft2-F)	Emissivity
Polyvinylchloride (PVC) / Vinyl - Rigid*	1.18	0.9
Foam Weather Stripping*	0.21	0.9
User Defined: Iron - Wrought	418.8	0.9
Steel (Rolled, Ground)*	346.67	0.6
Aluminum Alloys (Oxidized, Mill Finish)*	1109.36	0.2
Silicone*	2.43	0.9
Polycarbonate*	1.39	0.9
User Defined: Keff Tube - 4.771	33.08	0.9
User Defined: Keff - 0.074	0.51	0.9

Standard Boundary Conditions

Name	Temperature (F)	Film Coefficient (Btu / Hr-Ft2-F)
User Defined: Tubes - Attic	-0.4	2.201
User Defined: Tubes - Indoor	69.8	1.585
User Defined: Tubes - Exterior	-0.4	5.283

Simulation Results

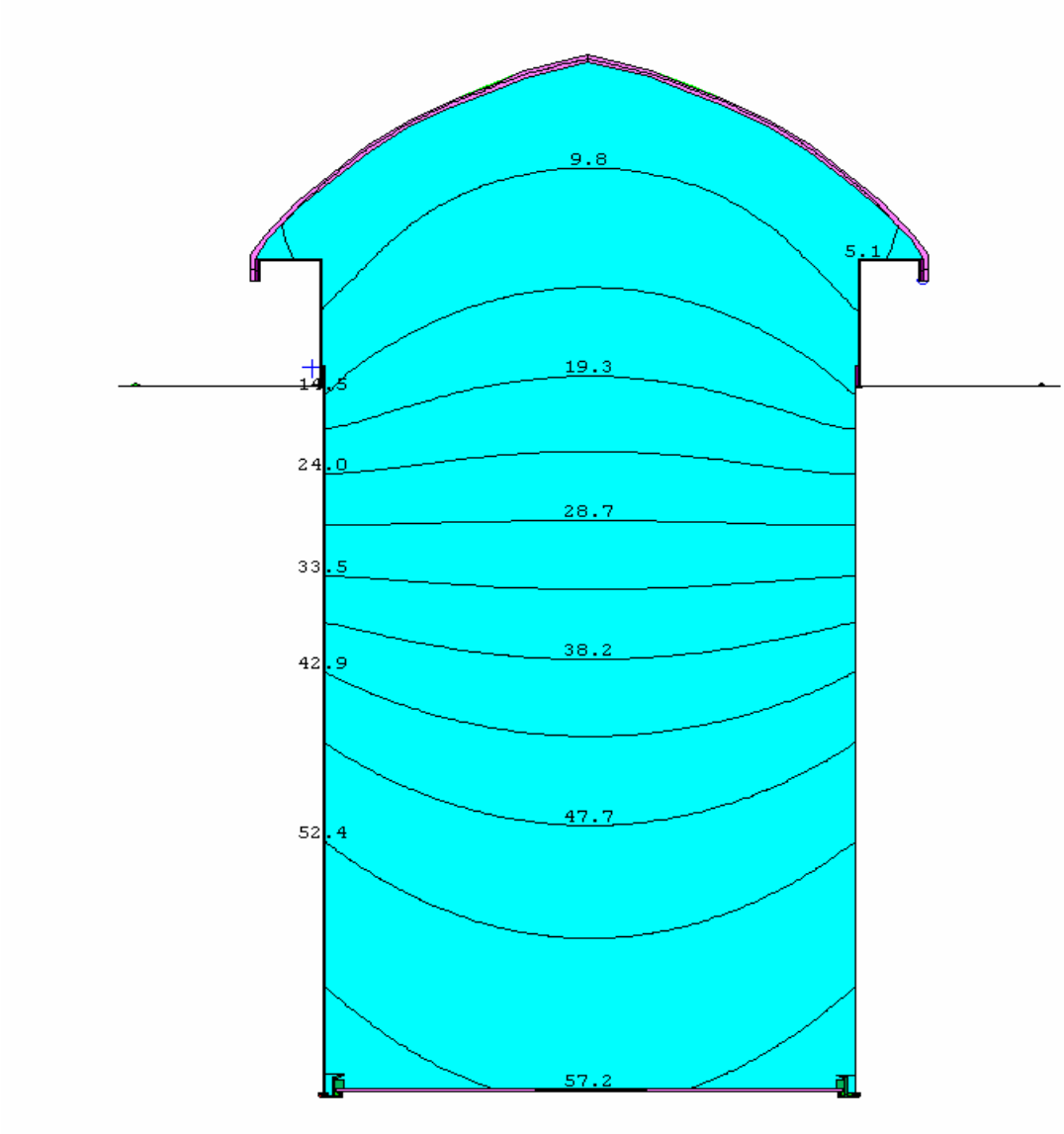
Test Unit Number 8

Unit Configuration Details

Test Configuration	**Commercial**	
Tube Size	**Large**	
Tube Type	**Rigid**	**Tube E**
Dome (Single / Double)	**Single**	**Dome D**
Diffuser (Single / Double)	**Single**	**Diffuser D**

Frame Height = 22.155

U-Factor (BTU/Hr-Ft2-F) = 0.955



Simulation Results

Test Unit Number 8

Unit Configuration Details

Test Configuration	**Commercial**	
Tube Size	**Large**	
Tube Type	**Rigid**	**Tube E**
Dome (Single / Double)	**Single**	**Dome D**
Diffuser (Single / Double)	**Single**	**Diffuser D**

Solid Materials

Name	Conductivity (Btu-in / Hr-Ft2-F)	Emissivity
Polyvinylchloride (PVC) / Vinyl - Rigid*	1.18	0.9
Polyvinylchloride (PVC) Flexible,with 40% Softener*	0.97	0.9
Aluminum Alloys (Painted)*	1109.36	0.2
Aluminum Alloys (Oxidized, Mill Finish)*	1109.36	0.2
Silicone*	2.43	0.9
Polycarbonate*	1.39	0.9
User Defined:Keff Tube - 4.898	33.96	0.9

Standard Boundary Conditions

Name	Temperature (F)	Film Coefficient (Btu / Hr-Ft2-F)
User Defined: Tubes - Indoor	69.8	1.585
User Defined: Tubes - Exterior	-0.4	5.283

Simulation Results

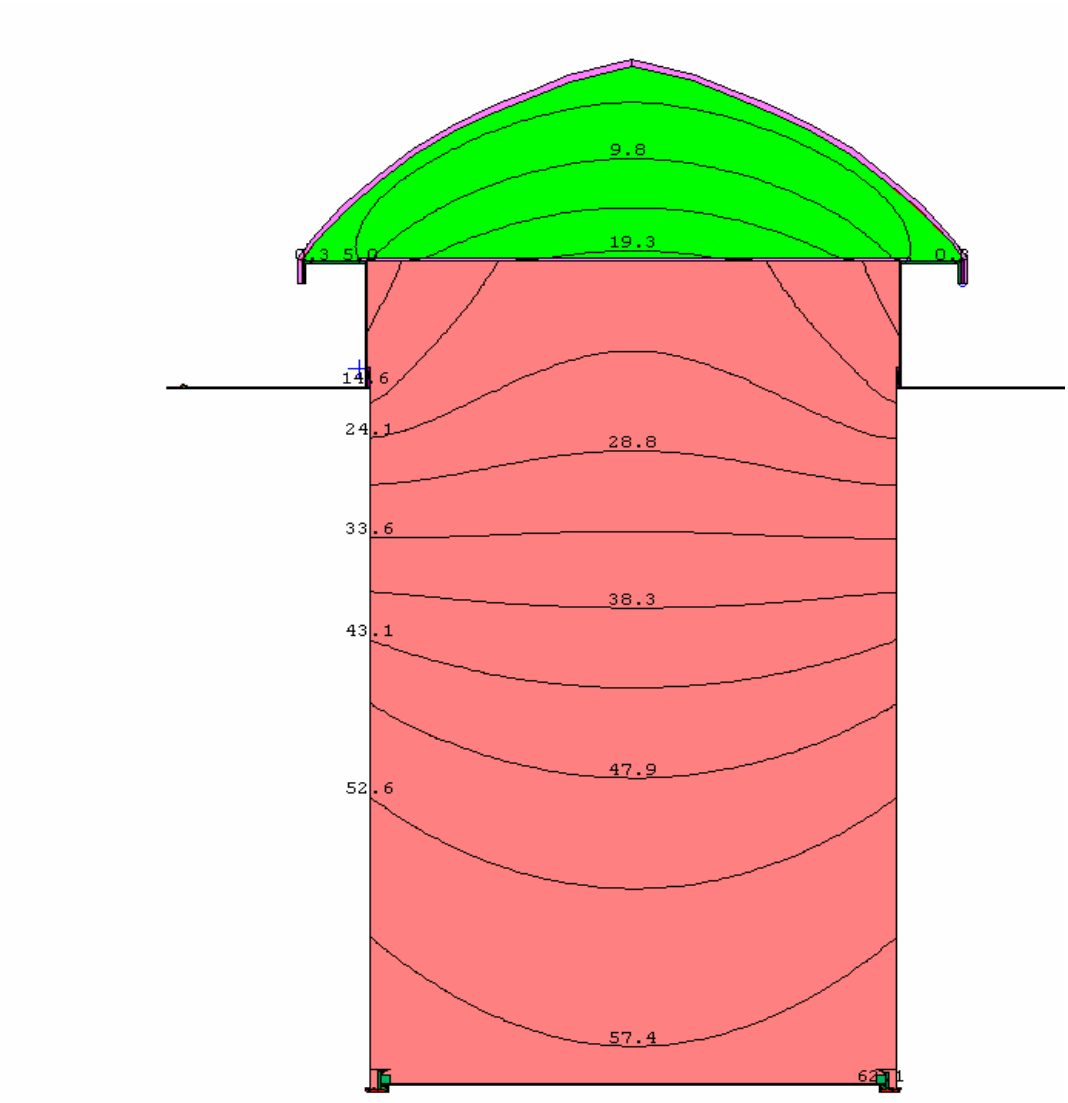
Test Unit Number 9

Unit Configuration Details

Test Configuration	**Commercial**	
Tube Size	**Large**	
Tube Type	**Rigid**	**Tube E**
Dome (Single / Double)	**Double**	**Outer Dome D, Inner Dome D**
Diffuser (Single / Double)	**Single**	**Diffuser D**

Frame Height = 22.154

U-Factor (BTU/Hr-Ft2-F) = 0.857



Simulation Results

Test Unit Number 9

Unit Configuration Details

Test Configuration	**Commercial**	
Tube Size	**Large**	
Tube Type	**Rigid**	**Tube E**
Dome (Single / Double)	**Double**	**Outer Dome D, Inner Dome D**
Diffuser (Single / Double)	**Single**	**Diffuser D**

Solid Materials

Name	Conductivity (Btu-in / Hr-Ft2-F)	Emissivity
Polyvinylchloride (PVC) / Vinyl - Rigid*	1.18	0.9
Polyvinylchloride (PVC) Flexible,with 40% Softener*	0.97	0.9
Aluminum Alloys (Painted)*	1109.36	0.2
Aluminum Alloys (Oxidized, Mill Finish)*	1109.36	0.2
Silicone*	2.43	0.9
Polycarbonate*	1.39	0.9
User Defined:Keff Tube - 4.815	33.38	0.9

Standard Boundary Conditions

Name	Temperature (F)	Film Coefficient (Btu / Hr-Ft2-F)
User Defined: Tubes - Indoor	69.8	1.585
User Defined: Tubes - Exterior	-0.4	5.283

Simulation Results

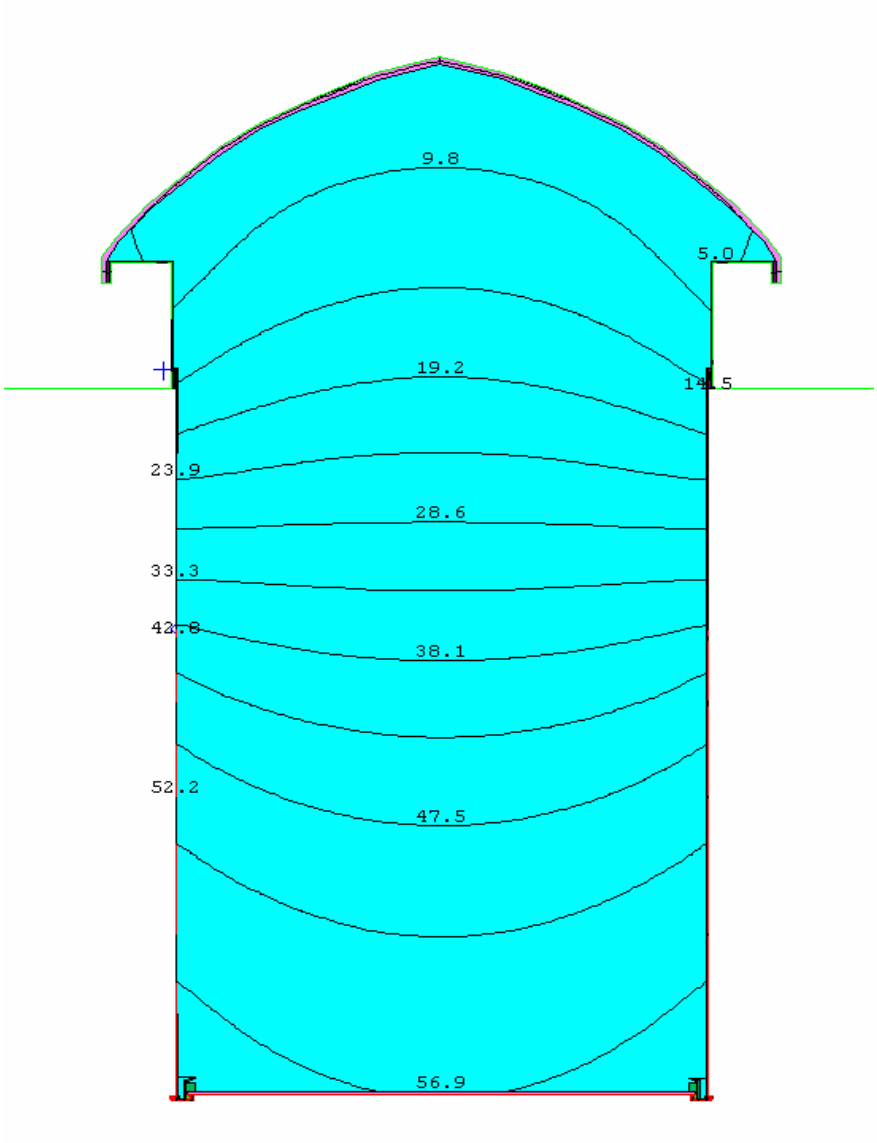
Test Unit Number 10

Unit Configuration Details

Test Configuration	**Commercial**	
Tube Size	**Large**	
Tube Type	**Flexible**	**Tube D**
Dome (Single / Double)	**Single**	**Dome D**
Diffuser (Single / Double)	**Single**	**Diffuser D**

Frame Height = 22.155

U-Factor (BTU/Hr-Ft2-F) = 0.889



Simulation Results

Test Unit Number 10

Unit Configuration Details

Test Configuration	**Commercial**	
Tube Size	**Large**	
Tube Type	**Flexible**	**Tube D**
Dome (Single / Double)	**Single**	**Dome D**
Diffuser (Single / Double)	**Single**	**Diffuser D**

Solid Materials

Name	Conductivity (Btu-in / Hr-Ft2-F)	Emissivity
Polyvinylchloride (PVC) / Vinyl - Rigid*	1.18	0.9
Polyvinylchloride (PVC) Flexible,with 40% Softener*	0.97	0.9
Polyester Fiber*	0.28	0.9
Aluminum Alloys (Painted)*	1109.36	0.2
Aluminum Alloys (Oxidized, Mill Finish)*	1109.36	0.2
Silicone*	2.43	0.9
Polycarbonate*	1.39	0.9
User Defined:Keff Tube - 4.898	33.96	0.9

Standard Boundary Conditions

Name	Temperature (F)	Film Coefficient (Btu / Hr-Ft2-F)
User Defined: Tubes - Indoor	69.8	1.585
User Defined: Tubes - Exterior	-0.4	5.283

Simulation Results

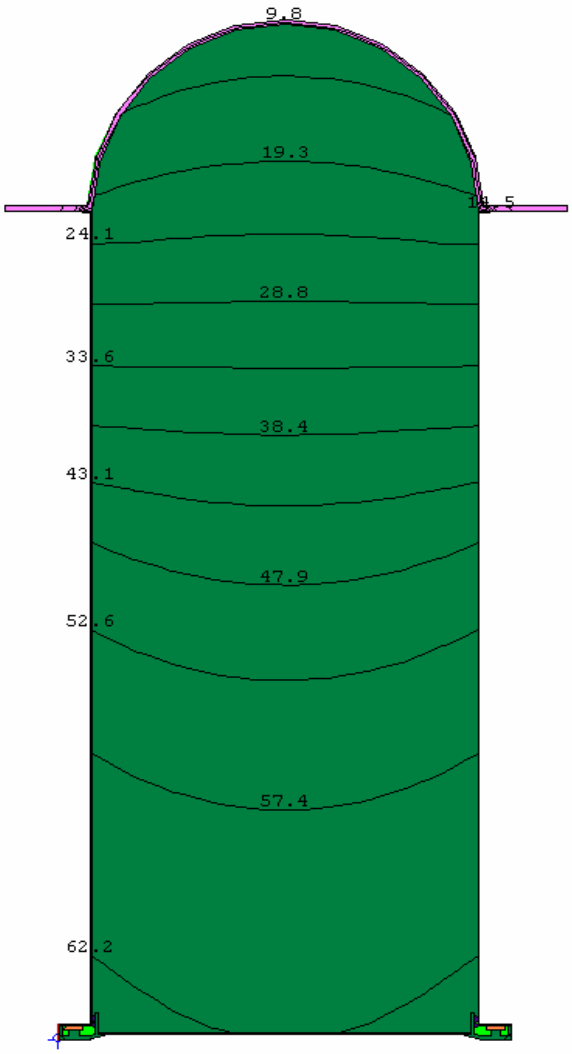
Test Unit Number 11

Unit Configuration Details

Test Configuration	**Commercial**	
Tube Size	**Small**	
Tube Type	**Rigid**	**Tube C**
Dome (Single / Double)	**Single**	**Dome C**
Diffuser (Single / Double)	**Single**	**Diffuser C**

Frame Height = 16.390

U-Factor (BTU/Hr-Ft2-F) = 0.920



Simulation Results

Test Unit Number 11

Unit Configuration Details

Test Configuration	**Commercial**	
Tube Size	**Small**	
Tube Type	**Rigid**	**Tube C**
Dome (Single / Double)	**Single**	**Dome C**
Diffuser (Single / Double)	**Single**	**Diffuser C**

Solid Materials

Name	Conductivity (Btu-in / Hr-Ft2-F)	Emissivity
Polyvinylchloride (PVC) / Vinyl - Rigid*	1.18	0.9
Foam Weather Stripping*	0.21	0.9
User Defined: Iron - Wrought	418.8	0.9
Steel (Rolled, Ground)*	346.67	0.6
Aluminum Alloys (Oxidized, Mill Finish)*	1109.36	0.2
Silicone*	2.43	0.9
Polycarbonate*	1.39	0.9
User Defined:Keff Tube - 4.92	34.11	0.9

Standard Boundary Conditions

Name	Temperature (F)	Film Coefficient (Btu / Hr-Ft2-F)
User Defined: Tubes - Indoor	69.8	1.585
User Defined: Tubes - Exterior	-0.4	5.283

Simulation Results

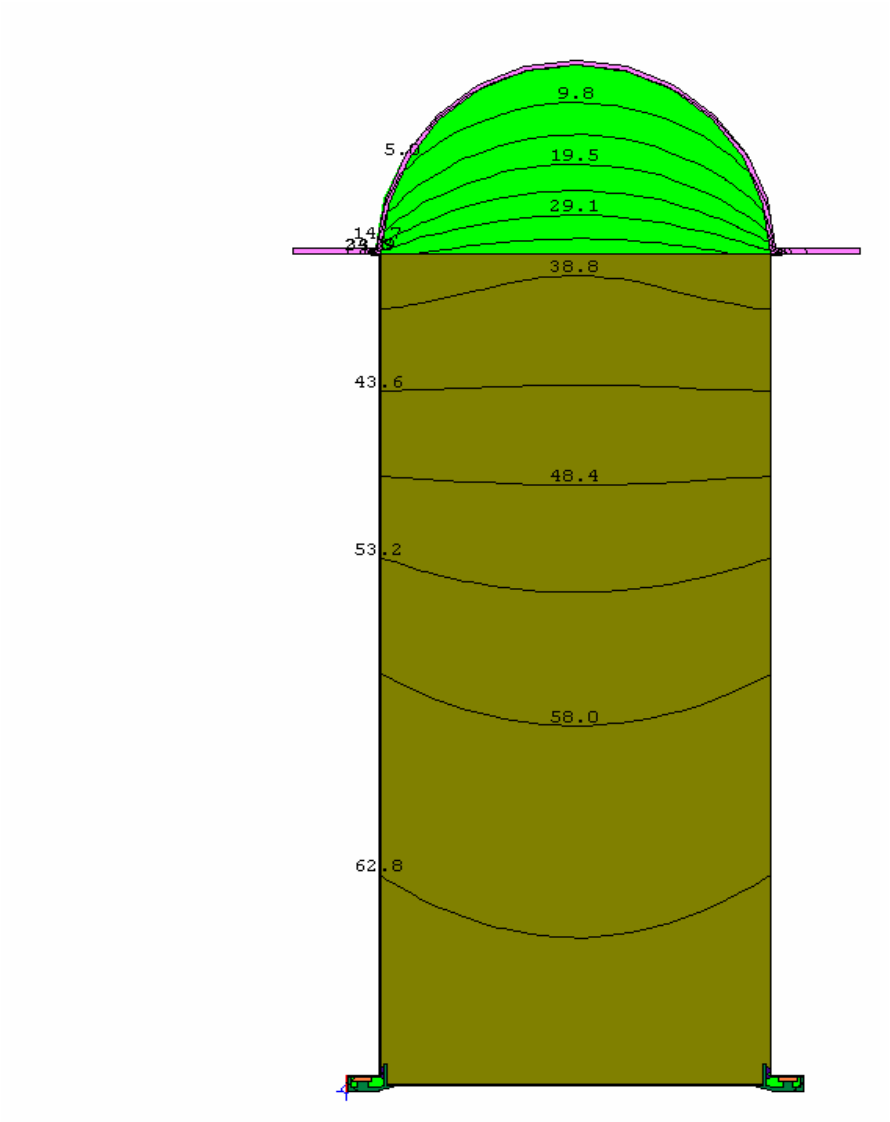
Test Unit Number 12

Unit Configuration Details

Test Configuration	**Commercial**	
Tube Size	**Small**	
Tube Type	**Rigid**	**Tube C**
Dome (Single / Double)	**Double**	**Outer Dome C, Inner Dome C**
Diffuser (Single / Double)	**Single**	**Diffuser C**

Frame Height = 16.390

U-Factor (BTU/Hr-Ft2-F) = 0.620



Simulation Results

Test Unit Number 12

Unit Configuration Details

Test Configuration	**Commercial**	
Tube Size	**Small**	
Tube Type	**Rigid**	**Tube C**
Dome (Single / Double)	**Double**	**Outer Dome C, Inner Dome C**
Diffuser (Single / Double)	**Single**	**Diffuser C**

Solid Materials

Name	Conductivity (Btu-in / Hr-Ft2-F)	Emissivity
Polyvinylchloride (PVC) / Vinyl - Rigid*	1.18	0.9
Foam Weather Stripping*	0.21	0.9
User Defined: Iron - Wrought	418.8	0.9
Steel (Rolled, Ground)*	346.67	0.6
Aluminum Alloys (Oxidized, Mill Finish)*	1109.36	0.2
Polycarbonate*	1.39	0.9
User Defined:Keff Tube - 4.725	32.76	0.9

Standard Boundary Conditions

Name	Temperature (F)	Film Coefficient (Btu / Hr-Ft2-F)
User Defined: Tubes - Indoor	69.8	1.585
User Defined: Tubes - Exterior	-0.4	5.283

Project ‘na’

Project Name: Entrance Door Systems Rating Simplification

Date: November 11, 2005

Purpose: The purpose of this research is to further streamline the process without inhibiting potential improvements in the energy efficiency of doors.

Project Summary:

The objective of this research project is to simplify door labeling. We reviewed existing NFRC door ratings to identify trends in the data and opportunities for simplifying the rating procedure. The following tasks describe the work that was completed in accordance with our contract; (1) Examine NFRC Door Data, (2) Collect Component Data, (3) Calculate U-factors for Generic Systems, (4) Trends in Data.

After reviewing the NFRC database and performance data for door components, we recognized that the best approach to simplifying door rating and labeling is to provide manufacturers with a set of equations from which they can calculate the door U-Factor, solar heat gain coefficient and visible light transmittance. This approach is similar to that used by window manufacturers for SHGC and VT.

Click here for final report

Prepared for:

National Fenestration Rating Council

SIMPLIFICATION OF DOOR LABELING

Final Report

November 11, 2005

Prepared by

Enermodal Engineering, Inc.
1554 Emerson Street
Denver, CO 80316, U.S.A
Tel: 303-861-2070
Fax: 303-830-2016
sreilly@enermodal.com
sgore@enermodal.com

Table of Contents

1. INTRODUCTION 3
1.1 Overview 3

2. Tasks 5
2.1 Task 1 Examine NFRC Door Data 5
2.2 Task 2 Collect Component Data 8
2.3 Task 3 Calculate U-Factors for Generic Systems 9
2.4 Task 4 Trends in Data 10
2.5 Glass Sizes 11

3. CONCLUSIONS 13
3.1 NFRC Swinging Door Size 13
3.2 Glass Sizes 14
3.3 Default Panel Sizes 15
3.4 U-Factor 19
3.5 SHGC 24
3.6 Visible Transmittance 25
3.7 Further Simplifications 26

1. INTRODUCTION

1.1 Overview

The current NFRC labeling procedure for doors is too cumbersome to implement. The industry needs a simplified procedure that can be more broadly applied. Although there is a wide variation in door types, NFRC has streamlined the rating process by establishing a rating size and glazing sizes for entry doors as well as default frames. The purpose of this research is to further streamline the process without inhibiting potential improvements in the energy efficiency of doors.

Simulation of doors is fairly simple as compared to that for windows because of the fixed glass sizes. A simulator models all opaque elements one time and then models all glazing options in their glazing gasket. So, the total product U-Factor and SHGC for all glazing options is based on the same component U-Factors for the opaque elements. The only component U-Factors that change are the edge-of-glass and center-of-glass U-Factors.

To simplify the rating and labeling of doors, Enermodal first analyzed existing NFRC door data to identify trends specific to door types. The data did not reveal any trends specific to the slab type and frame type.

We also requested component data from door manufacturers who have had their doors rated. We received a very small subset of data. Because of the variations in the total product values in the database, it was difficult to back out opaque-area trends that would allow us to simplify the ratings.

For SHGC and VT, the task is simpler in that NFRC 100 has already established one option for simplifying determination of SHGC and VT. The calculation of total product SHGC is a simple area-weighted calculation of opaque and glazing system SHGC's. The total product VT can be calculated directly from the glazing system VT since the glass areas are fixed.

We are proposing that simulators determine coefficients for a linear curve-fit of the U-Factor data, along with the individual center-of-glass values. Industry can use these to calculate total product values specific to products going out the door. It would be a simple calculation that utilizes product-specific data generated in accordance with NFRC procedures. A spreadsheet application could be developed for distribution to door fabricators that would calculate the total U-Factor, SHGC and VT for the product being built and generate an NFRC label.

We are further recommending that NFRC revisit the current door height for swing doors and revise it to 2100 mm (83 in). This is more representative of products with a 6'8" in tall slab. We are also recommending changes to the glass lite sizes. Based on the new lite sizes, default panel sizes are proposed as well. This will result in ratings that are more representative of products that are built, allow for default panel sizes to be established, and provide ratings that are comparable -- this is not currently the case for panel doors.

The monitoring committee also considered simulating only the no-glass, ½-glass and full-glass doors to simplify the rating and labeling procedures. This would reduce the confusion and potential for errors in labeling doors. However, it would also affect which doors can carry an EPA Energy Star label and possible limit the products that qualify. For this reason, this option was tabled.

2. TASKS

The objective of this research project is to simplify door labeling. We reviewed existing NFRC door ratings to identify trends in the data and opportunities for simplifying the rating procedure. The following tasks describe the work that was completed in accordance with our contract.

2.1 Task 1 Examine NFRC Door Data

Task 1 Examine NFRC Door Data

Enermodal extracted all swinging door data from the NFRC database. This data includes product U-Factor, and SHGC and VT if it is to current procedures. Also included is a description of the product and glazing system. Note that the NFRC data from the database does not include detailed information on component U-Factors.

Enermodal used Excel to sort this data according to product type. Our original proposal stated that the data would be separated into the following categories:

Slab	Panels	Sill
Wood	Flush	Default Wood
Steel	6-Panels	Default Steel
Composite		Wood
		Steel
		ADA

The distinctions between the products were not discernible from the database. We attempted to separate the data by frame type, either wood or steel, and glazing type. The glazing types included clear insulating glazing, clear insulating glazing with argon, low-E insulating glazing and low-E insulating glazing with argon. Within each of these glazing types, we were able to sort by glass-size (where identified), gap width, and any of the other variables included in the database. We screened out the units with grids in order isolate the door slab and door frame trends.

Table 2.1 below shows the general results for each glazing category. We did not include the clear insulating glazing units with argon because there are only a few such products. As

expected, as the insulating glazing unit improves, the U-factor decreases. As well, the doors with a steel frame have higher U-factors than those with a wood frame.

Table 2.1 Range of Door U-Factors in NFRC Database

	CLR IG	Low-E IG	Low-E, Arg IG
Steel Frame	0.20-0.49	0.27-0.43	0.20-0.43
Wood Frame	0.12-0.49	0.14-0.45	0.12-0.43

*Doors with grids not included.

Enermodal tried to categorize the doors by glass size. We found that wood frame, full-glass doors with clear insulating glazing vary from 0.33 to 0.42. There is one product with a U of 0.22; however, this product appears to be an outlier and the manufacturer's ¼-glass listing has the same U-factor. The full-glass doors, both wood and steel framed products, with low-E insulating glazing have a U-factor variation of 0.28-0.44. Wood frame, 1/4-glass doors with clear IG vary from 0.0.19 to 0.46. This information does not distinguish the products by door slab which explains the large variation in results.

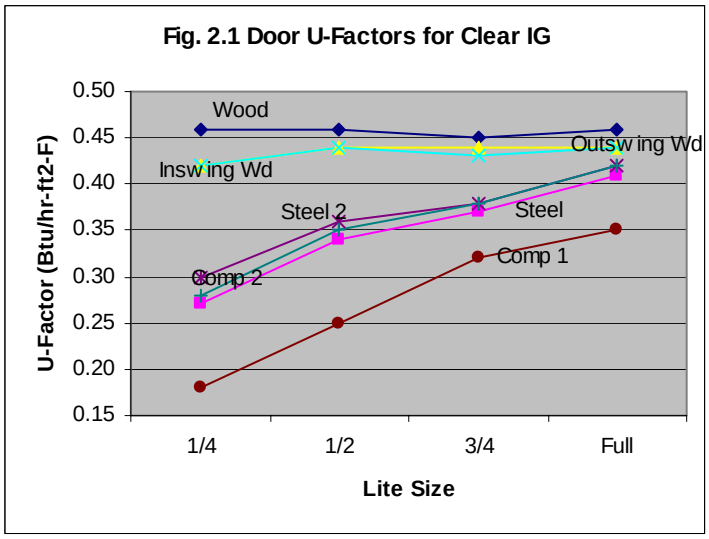


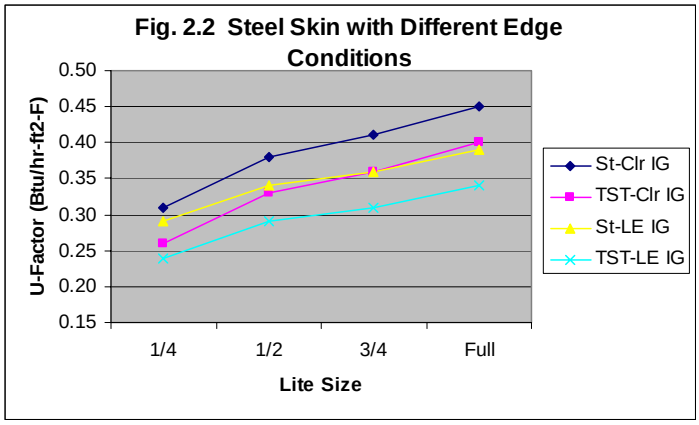
Figure 2.1 compares the total U-factor for three wood doors, two steel-skin doors and two composite doors (i.e. fiberglass skins). The inswing and outswing doors are made by the same manufacturer. For most of the products, it is unclear as to whether it is an outswing or inswing door. In general, we found the outswing doors have equal performance or are better by 0.01 than inswing doors.

Wood doors generally have higher U-factors than steel-skin and composite doors because of the rigid insulation in the core of the steel-skin and composite doors.

The difference in the steel doors is unclear from the database. These results are for doors from different manufacturers. The "Steel" door has a steel frame, whereas the "Steel 2" door has a wood frame. We anticipated that the results would be flipped with the "Steel 2" door outperforming the "Steel" door.

"Comp 1" and "Comp 2" represents two doors with composite material slabs and wood frames. They appear to have the same glazing and spacer. There is a significant difference in U-factors, although there is no clear explanation from the available information in the database.

Slab Edge

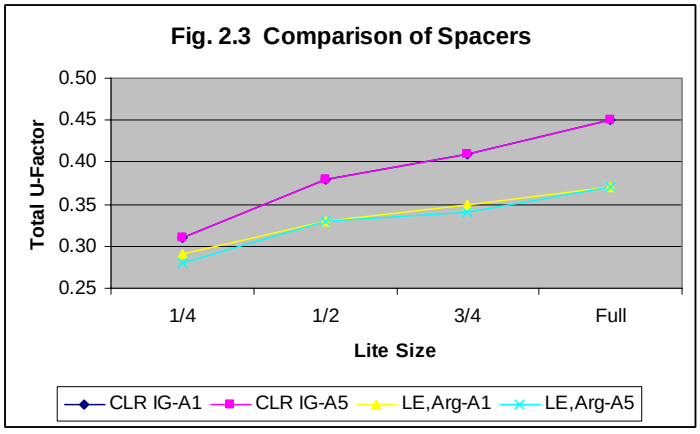


The slab edge is identified for a number of products. The edge condition appears to have a much greater influence on the product performance than whether the product is outswing or inswing and what type of spacer it is. Figure 2.2 compares two products from one manufacturer that just differ in the slab edge. There is a 0.05 difference in the U-factors for the same glass size and glazing option.

Frames

The database does not include data for doors with identical slab and slab edge conditions for which we could compare frame types.

Spacers



The database shows that different spacers make as much as a 0.01 difference in total U-factor. One manufacturer included aluminum spacer bar, Swiggle and silicone foam in clear insulating units. The units with the foam spacer were consistently 0.01 better than the metal spacers. In a door with low-E glass and argon fill, this difference may be as large as 0.02, but we could not confirm this.

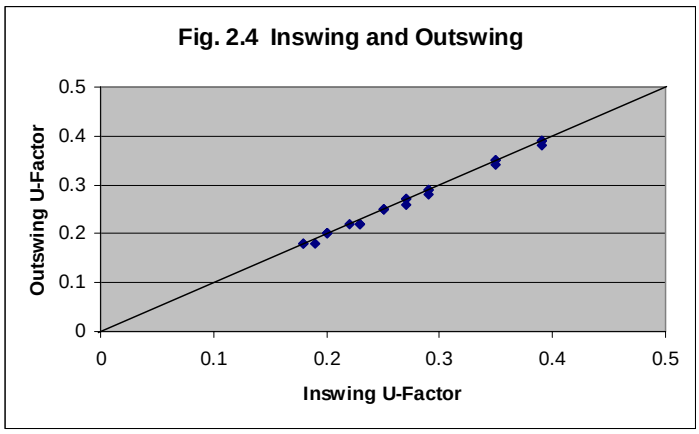
Grids and Dividers

Many of the product lines include internal grids with a 0.75" width. The products with grids have the same U-Factor as those without grids. The SHGC and VT values are lower than those for the units without grids. One product line lists true-divided glasss with a 1.5" width; however, we were unable to determine the make-up of the individual units in order to compare them with units without dividers.

Inswing and Outswing

For a few products it was possible to compare the inswing and outswing operators. It appears that the outswing performs as much as 0.01 better in U-Factor. Figure 2.3 compares the U-Factor results for one manufacturer's product line for which the inswing and outswing could be identified. For some of the units, the inswing and outswing units had equal U-Factors. For others, the outswing is 0.01 better.

Fig. 2.4 Inswing and Outswing



2.2 Task 2 Collect Component Data

To verify trends in the data, component U-Factors were obtained from a couple manufacturers. The data was too limited in its scope to draw any conclusions. While like products performed similarly, the data was only produced by two simulation laboratories and did not cover a broad enough range of door types to provide valuable comparisons.

2.3 Task 3 Calculate U-Factors for Generic Systems

Enermodal used the data collected in Tasks 1 and 2 to calculate total product U-Factors, SHGC and VT. These results are included in the Excel workbook containing the raw data. Originally, we intended to take the component U-Factors for similar products to arrive at generic component U-Factors for all opaque components. However, the data analysis in Task 1 demonstrated the wide variation in results and the unknowns in the database. So, we decided to attempt to curve-fit the data.

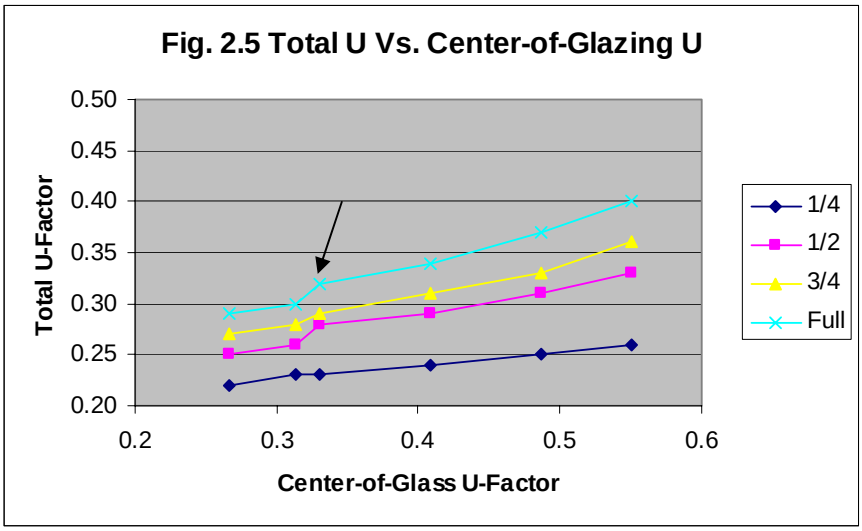


Figure 2.5 charts the total U-factor for different glass sizes versus the center-of-glazing U-factors for a steel door with a wood frame. This particular product includes a wide range of glazing options from a clear insulating unit with a 0.25 inch gap to a low-E insulating unit filled with argon and a gap of 0.75 inches. We took this data and fit the data for each glass size to an equation of a line. We used a simple interpolation approach between the data for the best and worst case glazing options. We then calculated the total U-Factor and compared it to the reported U-Factor. For 24 different glazing options, the results matched for 19 of the units and there is a 0.01 difference in the results for remaining 6 units. The data point with the arrow pointing to it in Figure 2.5 represents either a misrepresentation of the center-of-glazing U-Factor on our part, inaccurate data in the database or questionable ratings. Because this method of fitting data worked so well, we did not spend a significant amount of time trying to resolve the questions surrounding this one glazing option.

This same approach was used on a wide sampling of the products. The results were consistent with above. Very good agreement was seen, including the results for a product line with tripled-glazed units.

2.4 Task 4 Trends in Data

On the positive side, the fact that NFRC has fixed a number of door variables should allow us to identify trends in the data for U-Factor, SHGC and VT. The constants are listed below.

Constants

- Door Size: 1000mm x 2000 mm (39 in. x 79 in.)
- Door-glass size (none,1/4, ½, ¾, full)
  - ¼ glazing: 560 mm x 480 mm (22 in. x 19 in.)
  - ½ glazing: 560 mm x 10400 mm (22 in. x 41 in.)
  - ¾ glazing: 560 mm x 1270 mm (22 in. x 50 in.)
  - Full glazing: 560 mm x 1625 mm (22 in. x 64 in.)
- Frame Height: 63.5 mm (2.5 in.)
- Glass Frame Height: 63.5 mm (2.5 in.)
- Edge-of-glass Height: 63.5 mm (2.5 in.)
- Edge-of-Panel Height: Glass Frame Height: 25 mm (1 in.)

Based on the fixed sizes for the door and the door glass, we assembled the following table. Table 2.2 shows the corresponding dimensions, areas and fraction of total area for the individual components.

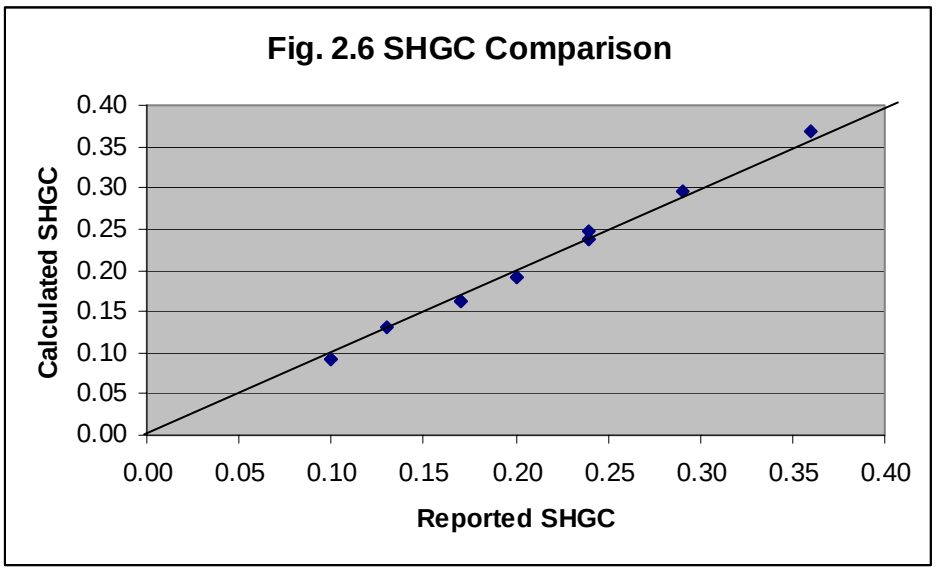
Table 2.2 Dimensions, Areas, and Fraction of Areas for Door Components

	Width (mm)	Height (mm)	Area (mm2)		Fraction
Door	1000	2000			
None (slab)					a
1/4-Lite	560	480	243029.16	incl edge	0.1215
1/2-Lite	560	1040	542405.16	incl edge	0.2712
3/4-Lite	560	1270	665363.16	incl edge	0.3327
Full Lite	560	1625	855146.16	incl edge	0.4276
Frame Ht		63.5			
Lite Frame Ht		63.5			
Edge-of-Lite Ht		63.5			
1/4-Lite					
1/2-Lite					
3/4-Lite					
Full Lite					
Edge-of-Panel Ht		25			

We attempted to identify trends in the U-Factor data. The large variation in the door constructions, particularly the slab edge, limited this effort. However, we were able to use the fraction of areas that include the edge-of-glass area with the center-of-glass area to arrive at trends in the SHGC and VT data.

Most notably, we found that by assuming a SHGC of 0.03 for the opaque elements of doors, that a total SHGC could be calculated from the center-of-glass SHGC and area fractions. Figure 2.6 compares the reported SHGC values with the calculated SHGC values for a door with a steel skin slab, steel edge and a wood frame. The calculated values agree with the reported values to within 0.0 to 0.01 for the range of glass sizes and glazing options in the product line. As for visible light transmittance, VT, the area fractions are sufficient for determine the total VT.

The equations resulting from this approach are given in section 3. This is the same approach as is used for SHGC and VT in NFRC 100. Doors are further simplified because the area of the door and the area of the door glass are fixed.



2.5 Glass Sizes

On option we considered for simplifying labeling was reducing the number of glass sizes at which results are reports. Table 2.3 compares the range of U-Factors for different doors. The

variation in door U-factors for wood products is 0.05 Btu/hr-ft2-F or less because the frame U-factor and glazing U-factor are close in value. The variation in U-Factor for the better insulating products is greater because the slab and frame have a lower U-Factor than the glazing.

Table 2.3 Comparison of Door U-Factors by Glass Size

Glass Size	Inswing Wood			Wood Entry		Fiberglass Entry		6-Panel Steel Skin	
	U=0.60	U=0.50	U=0.32	U=0.50	U=0.37	U=0.50	U=0.26	U=0.50	U=0.26
	0.42	0.42	0.42	0.45	0.45	0.12	0.12	0.21	0.21
1/4	0.44	0.42	0.40	0.46	0.45	0.19	0.16	0.27	0.24
1/2	0.47	0.44	0.39	0.46	0.42	0.26	0.19	0.34	0.28
3/4	0.47	0.43	0.37	0.45	0.41	0.29	0.21	0.37	0.29
Full	0.49	0.44	0.36	0.46	0.40	0.33	0.23	0.41	0.32

The variation in SHGC and VT is much greater because of the wide variation in glazing SHGC and VT. Table 2.4 compares the SHGC of the doors shown in Table 2.3. The center-of-glazing SHGC have been estimated and the results appear to be consistent for similar glazing options. The exception is the Inswing Wood door with a center-of-glazing U of 0.50. This must be a tinted insulating unit, but it is not identifiable from the NFRC database listing. If the glass areas actually corresponded to their names, e.g. a ¼-glass is one-fourth as tall as the full glass, etc., the change in SHGC between glass sizes would be the same. For instance, for clear insulating glazing, the difference in SHGC would be 0.06-0.07.

Table 2.4 Comparison of Door SHGC by Glass Size

Glass Size	Inswing Wood			Wood Entry		Fiberglass Entry		6-Panel Steel Skin	
	SHGC =0.78	SHGC=?	SHGC =0.42	SHGC =0.78	SHGC =0.42	SHGC =0.78	SHGC =0.42	SHGC =0.78	SHGC =0.42
	0.04	0.04	0.04	0.08	0.08	0.01	0.01	*	*
1/4	0.12	0.08	0.08	0.12	0.11	0.11	0.06	0.11	0.06
1/2	0.22	0.13	0.13	0.26	0.24	0.23	0.12	0.23	0.12
3/4	0.26	0.15	0.15	0.32	0.29	0.27	0.14	0.28	0.14
Full	0.32	0.18	0.18	0.39	0.35	0.35	0.15	0.35	0.18

Rating doors at three glass conditions: 1) No Glass; 2)½-Glass; and 3)Full-Glass, would demonstrate the same range as the existing ratings but would simplify the rating and labeling procedures and reduce the potential for errors in identifying the pertinent numbers.

3. CONCLUSIONS

After reviewing the NFRC database and performance data for door components, we recognized that the best approach to simplifying door rating and labeling is to provide manufacturers with a set of equations from which they can calculate the door U-Factor, solar heat gain coefficient and visible light transmittance. This approach is similar to that used by window manufacturers for SHGC and VT. A set of coefficients are determined by a simulator for each product line. These coefficients are based on the best and worst performing products in a product line. This approach would reduce the modeling considerably, because each glazing option does not need to be modeled in Therm. Each glazing option in a product line would be modeled in WINDOW 5 to determine the center-of-glass U-Factor, SHGC and VT.

A manufacturer must determine door ratings for both flush and panel doors, with and without door glasss. To further simply the door rating procedure, we are also proposing to change the default door height to be more consistent with products sold today and establish door glass sizes and panel sizes that are will allow for apples-to-apples comparison between products. Currently, simulators appear to be using different approaches to determining the panel areas; establishing default panel sizes will allow consumers to better compare products.

The conclusions are based on use of the proposed changed to the default door size, glass sizes and panel sizes. If the size changes are rejected, the simplified calculations can still be performed using the existing default sizes.

3.1 NFRC Swinging Door Size

The current swinging door size is 1000 mm by 2000 mm (39 in by 79 in) for a single door and 2000 mm by 2000 mm (79 in by 79 in) for a double door. This refers to the unit size and includes the door slab plus door frame. The history behind the swing door size is traced back to the U.S. and Canadian harmonization effort. The NFRC size was a 36x80 slab. When the standard moved to metric the unit size was fixed at 2000 mm.

While the overall unit width of 1000 mm is reasonable for a door slab that is 914 mm (36 in) wide, the height is too short. One of the most commonly produced door slabs is 914 mm by 2032 mm (36 in by 80 in). The addition of the head and sill height to the slab height results in a total height of approximately 2100 mm (83 in).

We are proposing that the NFRC 100 swinging door size be changed to 1000 mm by 2100 mm (39 in by 83 in). This modification will result in ratings that better represent products that are installed and simplify the rating process for door manufacturers.

3.2 Glass Sizes

Currently, glazed doors are rated at four different glass sizes: ¼, ½, ¾ and full. The width of the glass is the same for each size, 560 mm (22 in). The heights are 480 mm (19 in), 1040 mm (41 in), 1270 mm (50 in), and 1625 mm (64 in) respectively. The proposed glass sizes are based on typical half-lite sizes and fixing the panel sizes. Table 3.3 gives the proposed glass sizes and represents a revision to the existing Table 5-1 in NFRC 100-2004. The caming pattern has also been adjusted for the new lite sizes.

Table 3.3 Proposed Revision to Table 5-1 Glazing and Divider Patterns for Doors

Individual Product	For Doors with	Simulated or Test as	Glass inserts for a 6-panel door	Optional Caming Pattern for Flush and Panel Doors
1/4 glazing	0.118 m^2 (180 $in.^2$) or less	560 mm by 210 mm (22 in. by 8 in.)	replace upper two panels and upper intermediate stile	5 vertical 1 horizontal
1/2 glazing	0.118 to 0.512 m^2 (180 to 794 $in.^2$)	560 mm by 915 mm (22 in. by 36 in.)	replace upper four panels, upper and center intermediate stiles and upper rail	5 vertical 7 horizontal
3/4 glazing	0.512 m^2-0.725 m^2 (794-1124 $in.^2$)	560 mm by 1300 mm (22 in. by 51 in.)	replace lower four panels, center and lower intermediate stiles and lower rail	5 vertical 10 horizontal
Full glazing	0.725 m^2 (1124 $in.^2$) or more	560 mm by 1630 mm (22 in. by 64 in.)	replace all panels and all intermediate stiles and rails	5 vertical 13 horizontal

We struggled with defining the glass lite sizes. There are four constraints:

1) Half-lite height is 920 mm (36”). This is a change from the current standard.
2) Full-lite height is 1630 mm (64 in)
3) Height of upper and intermediates panels plus the upper rail needs to equal the half-lite height.
4) Height of all panels and intermediate rails needs to equal the full-lite height.

These constraints resulted in what appears to be a “short” quarter-lite height. We considered a broad range of possibilities, but the lite sizes presented in Table 3.3 correspond to the tallest upper panel height possible under these constraints.

3.3 Default Panel Sizes

Manufacturers must rate their flush and panel doors. In NFRC 100-2004, ratings for 6-panel doors are used to represent all panel door options. There are also a set of rules for rating panel doors with glass. Currently, glazed panel doors may have different glazing areas depending on the assumed panel sizes. This makes it difficult for consumers to compare like products.

We attempted to fix the panel sizes in accordance with the glass sizes to minimize the potential differences in simulations and to further simplify the door rating procedure. Figure 3.1, which is Figure 5-6 of the Typical 6-Panel Layout in NFRC 100-2004, shows the 6-panel door that is assumed for the panel-door simulations. As mentioned above, fixing the panel sizes is constrained by the ½-lite and full-lite sizes. If the existing ½-glass height of 1040 mm (41 in) was used, the upper, middle and lower panel heights would have to be nearly equal to add up to the ½-glass and full-glass heights.

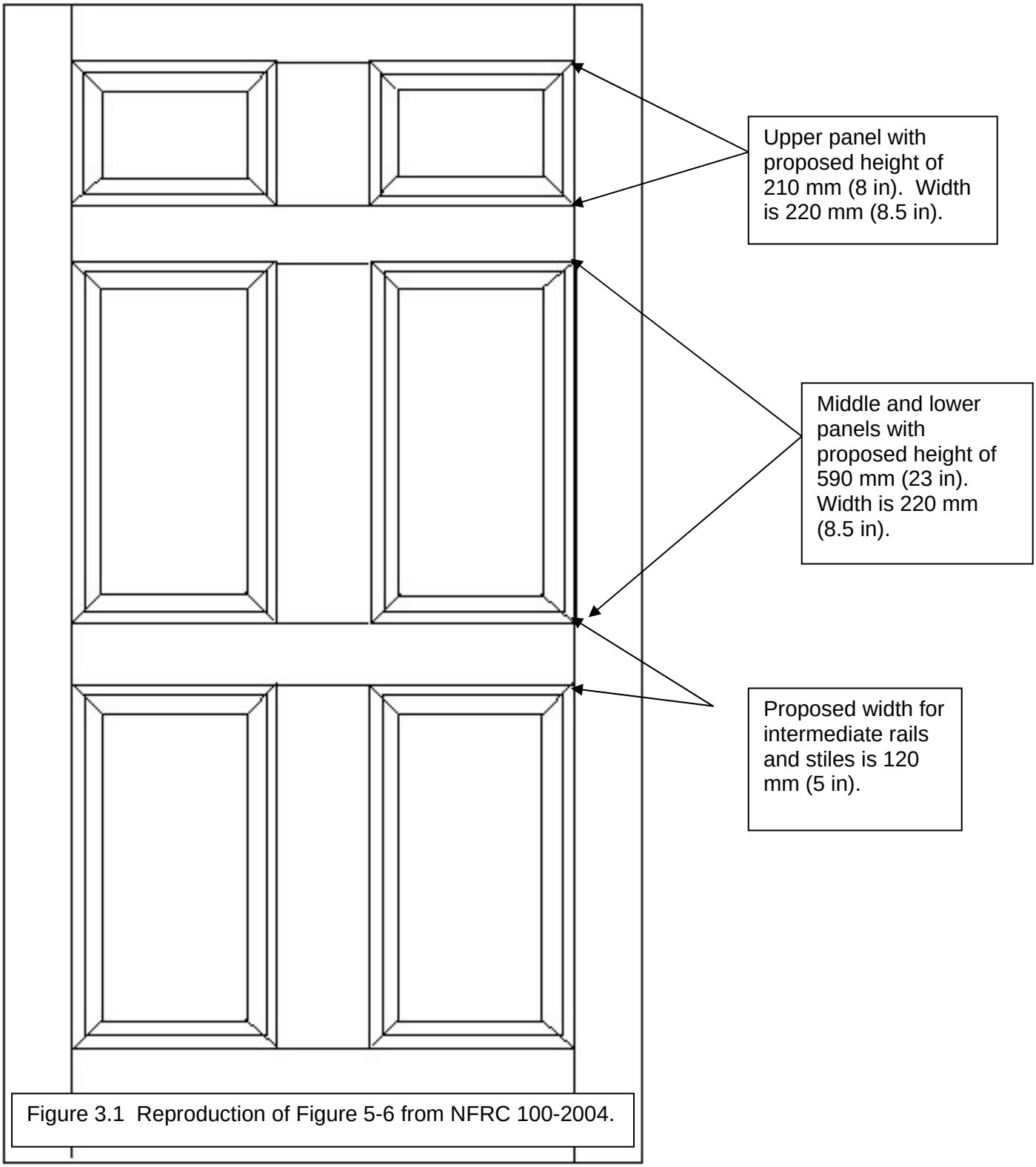


Figure 3.1 Reproduction of Figure 5-6 from NFRC 100-2004.

We looked at a number of alternatives for the panel sizes, but given the half-lite and full-lite constraints we arrived at the panel heights given in Tables 3.4a and 3.4b. Note that the heights we are proposing for the panels do not include the 25 mm (1 in) panel edges. The heights do include the approximate 12 mm (0.5 in) where the panel profile sits in the frame (Figure 3.2).

Table 3.4a Proposed ½-Glass Size and Panel Heights (SI)

Options	Height (mm)
Full Glass	1625
Half Glass	915
Upper Panel	205
Rail	125
Middle Panel	585
Rail	125
Lower Panel	585

Table 3.4b Proposed ½-Glass Size and Panel Heights (I-P)

Options	Height (mm)
Full Glass	64
Half Glass	36
Upper Panel	8
Rail	5
Middle Panel	23
Rail	5
Lower Panel	23

We are also proposing to fix the panel width. Based on a glass width of 560 mm (22 in), and a stile width of 120 mm (5 in), the panel width would be 220 mm (8.5 in).

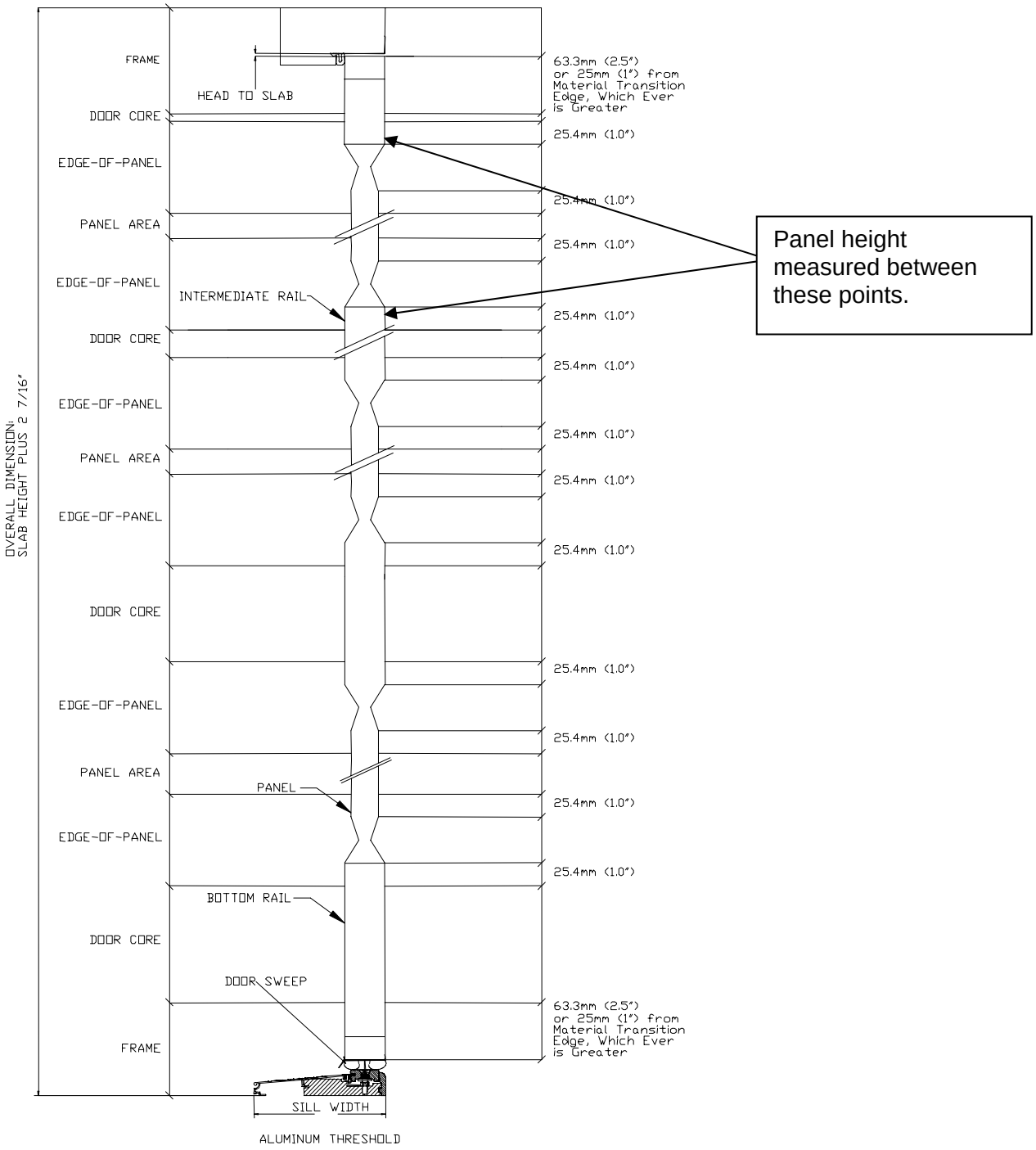


Figure 3.2 Example of proposed panel height reference points.

3.4 U-Factor

An NFRC simulator would perform the following simulations:

- Total door U-Factor for flush door
- Total door U-Factor for worst performing glazing option (not including single-glazed options that would be modeled separately) for each glass size
- Total door U-Factor for best performing glazing option for each glass size
- Center-of-glazing U-Factor, SHGC and VT for all glazing options

For each glass size, the following equation could be used to calculate the total product U-factor:

$$U = Coeff_Ua * U_{cog} + Coeff_Ub$$

The simulator determines the coefficients in the equation for each glass size from the U-Factor for the best performing and worst performing glazing options in a door product line. The worst performing glazing option should be a double-glazed unit. Single glazing should be modeled separately. The coefficients for each glass size is determined as follows:

$$Coeff_Ua = (U_{worst} – U_{best}) / (U_{cog\text{-}worst} – U_{cog\text{-}best})$$

$$Coeff_Ub = U_{best} – U_{cog\text{-}best} * Coeff\text{-}Ua$$

Where

- U_{best} is the door U-factor for the best-performing glazing option at a specific glass size
- U_{worst} is the door U-factor for the worst-performing glazing option at a specific glass size. This should be a double-glazed unit. Single glazing should be modeled separately.
- $U_{cogbest}$ is the center-of-glazing U-factor for the best performing glazing option.
- $U_{cog\text{-}worst}$ is the center-of-glazing U-factor for the worst performing glazing option. This should be a double-glazed unit. Single glazing should be modeled separately*.

*There is a very limited number of doors with single glazing in the database. In one product line, it was unclear what the difference between the single-glazed units was so that we could not evaluate the accuracy of the curve fit.

The following table lists the coefficients that must be determined for use by the manufacturer.

Door U-Factor Coefficients

	Coeff_Ua	Coeff_Ub
¼-Lite		
1/2-Lite		
¾-Lite		
Full Glass		

Because products may be sold with different spacers, door glass frames and installed in different frames, a manufacturer has the option of grouping these options as follows:

- Spacers may be grouped, but a manufacturer could also ask for a set of coefficients for each spacer type in the product line.
- The NFRC default door glass frame may be used to represent all door glass frame options
- The NFRC default steel door frame may be used to represent all door frames.
- Assume an inswing door and label outswing and inswing doors with outswing results.

These groupings ensure that a product will be labeled with U-Factors that are equal to or higher than the U-Factor simulated for a specific product.

As proof of this concept, the following tables demonstrate the application of this approach to existing products lines. The existing glass sizes were used for the calculations. At the top of each page on the right side, the calculated coefficients are shown. Directly below this table, the calculated U-factor is compared to the certified U-Factor. When the difference is more than 0.01, we deduce that there are errors in the input to the database or in the simulations.

Manufacturer	Product Name
Precision Entry	Steel Replacement Entry Door

Coefficients for Equations (ZF Spacer)

	Coeff-Ua	Coeff-Ub
1/4	0.12766	0.206298
1/2	0.255319	0.212596
3/4	0.340426	0.200128
Full	0.382979	0.218894

Key:
1) 2 values for U-Factor, SHGC, and VT indicates Res/Non-Res ratings.
2) * indicates that Certified SHGC/VT values are available from the Manufacturer.

186 records were returned.

CPD Number	Mfr Product Code	Frame/Sash Type	Glazing Layer	Low-E/Internal Film (Surface)	Gap Width(s)	Spacer Type	Fill	Grids	Dividers	Tint	U-Factor	SHGC	VT	Condensation Resistance		Ucog	U	Ucalc	Difference in U and Ucalc
RD-K-3-0005	6-Panel, No Lite	Steel / Steel	1			N		N			0.21	*	*						
RD-K-3-0005	6-Panel, No Lite	Steel / Steel	1			N		N			0.21	*	*			ZF Spacer			
RD-K-3-0005	DS 1/4 Lite	Steel	2		0.76400	ZF-S	Air	N			0.27	0.11	0.11			0.499	0.27	0.27	0.00
RD-K-3-0005	DS 1/4 Lite	Steel	2		0.76400	ZF-S	Air	N			0.27	0.11	0.11			0.499	0.27	0.27	0.00
K-3-00054-0	DS 1/4 Lite	Steel	2		0.76400	ZF-S	Air	G	0.75		0.27	0.10	0.09						
K-3-00054-0	DS 1/4 Lite	Steel	2		0.76400	ZF-S	Air	G	0.75		0.27	0.10	0.09						
RD-K-3-0005	DS 1/2 Lite	Steel	2		0.76400	ZF-S	Air	N			0.34	0.23	0.24			0.499	0.34	0.34	0.00
RD-K-3-0005	DS 1/2 Lite	Steel	2		0.76400	ZF-S	Air	N			0.34	0.23	0.24			0.499	0.34	0.34	0.00
K-3-00055-0	DS 1/2 Lite	Steel	2		0.76400	ZF-S	Air	G	0.75		0.34	0.20	0.21						
K-3-00055-0	DS 1/2 Lite	Steel	2		0.76400	ZF-S	Air	G	0.75		0.34	0.20	0.21						
RD-K-3-0005	DS 3/4 Lite	Steel	2		0.76400	ZF-S	Air	N			0.37	0.28	0.29			0.499	0.37	0.37	0.00
RD-K-3-0005	DS 3/4 Lite	Steel	2		0.76400	ZF-S	Air	N			0.37	0.28	0.29			0.499	0.37	0.37	0.00
K-3-00056-0	DS 3/4 Lite	Steel	2		0.76400	ZF-S	Air	G	0.75		0.37	0.24	0.25						
K-3-00056-0	DS 3/4 Lite	Steel	2		0.76400	ZF-S	Air	G	0.75		0.37	0.24	0.25						
RD-K-3-0005	DS Full Lite	Steel	2		0.76400	ZF-S	Air	N			0.41	0.35	0.37			0.499	0.41	0.41	0.00
RD-K-3-0005	DS Full Lite	Steel	2		0.76400	ZF-S	Air	N			0.41	0.35	0.37			0.499	0.41	0.41	0.00
K-3-00057-0	DS Full Lite	Steel	2		0.76400	ZF-S	Air	G	0.75		0.41	0.30	0.32						
K-3-00057-0	DS Full Lite	Steel	2		0.76400	ZF-S	Air	G	0.75		0.41	0.30	0.32						
RD-K-3-0005	6-Panel, No Lite	Steel / Steel	1			N		N			0.21	*	*						
RD-K-3-0005	6-Panel, No Lite	Steel / Steel	1			N		N			0.21	*	*			A5 Spacer			
RD-K-3-0005	DS 1/4 Lite	Steel	2		0.76400	A5-D	Air	N			0.28	0.11	0.11			0.499	0.28	0.27	0.01
RD-K-3-0005	DS 1/4 Lite	Steel	2		0.76400	A5-D	Air	N			0.28	0.11	0.11			0.499	0.28	0.27	0.01
K-3-00059-0	DS 1/4 Lite	Steel	2		0.76400	A5-D	Air	G	0.75		0.28	0.10	0.09						
K-3-00059-0	DS 1/4 Lite	Steel	2		0.76400	A5-D	Air	G	0.75		0.28	0.10	0.09						
RD-K-3-0006	DS 1/2 Lite	Steel	2		0.76400	A5-D	Air	N			0.35	0.23	0.24			0.499	0.35	0.34	0.01
RD-K-3-0006	DS 1/2 Lite	Steel	2		0.76400	A5-D	Air	N			0.35	0.23	0.24			0.499	0.35	0.34	0.01
K-3-00060-0	DS 1/2 Lite	Steel	2		0.76400	A5-D	Air	G	0.75		0.35	0.20	0.21						
K-3-00060-0	DS 1/2 Lite	Steel	2		0.76400	A5-D	Air	G	0.75		0.35	0.20	0.21						
RD-K-3-0006	DS 3/4 Lite	Steel	2		0.76400	A5-D	Air	N			0.38	0.28	0.29			0.499	0.38	0.37	0.01
RD-K-3-0006	DS 3/4 Lite	Steel	2		0.76400	A5-D	Air	N			0.38	0.28	0.29			0.499	0.38	0.37	0.01
K-3-00061-0	DS 3/4 Lite	Steel	2		0.76400	A5-D	Air	G	0.75		0.38	0.24	0.25						
K-3-00061-0	DS 3/4 Lite	Steel	2		0.76400	A5-D	Air	G	0.75		0.38	0.24	0.25						
RD-K-3-0006	DS Full Lite	Steel	2		0.76400	A5-D	Air	N			0.42	0.35	0.37			0.499	0.42	0.41	0.01
RD-K-3-0006	DS Full Lite	Steel	2		0.76400	A5-D	Air	N			0.42	0.35	0.37			0.499	0.42	0.41	0.01
K-3-00062-0	DS Full Lite	Steel	2		0.76400	A5-D	Air	G	0.75		0.42	0.30	0.32						
K-3-00062-0	DS Full Lite	Steel	2		0.76400	A5-D	Air	G	0.75		0.42	0.30	0.32						
RD-K-3-0006	6-Panel, No Lite	Steel / Steel	1			N		N			0.21	*	*						
RD-K-3-0006	6-Panel, No Lite	Steel / Steel	1			N		N			0.21	*	*			ZF Spacer			
RD-K-3-0006	DS 1/4 Lite, Solarban	Steel / Steel	2	0.03400 (2)	0.76400	ZF-S	Argon	N			0.24	0.06	0.10			0.264	0.24	0.24	0.00
RD-K-3-0006	DS 1/4 Lite, Solarban	Steel / Steel	2	0.03400 (2)	0.76400	ZF-S	Argon	N			0.24	0.06	0.10			0.264	0.24	0.24	0.00
K-3-00064-0	DS 1/4 Lite, Solarban	Steel / Steel	2	0.03400 (2)	0.76400	ZF-S	Argon	G	0.75		0.24	0.05	0.08			0.264			
K-3-00064-0	DS 1/4 Lite, Solarban	Steel / Steel	2	0.03400 (2)	0.76400	ZF-S	Argon	G	0.75		0.24	0.05	0.08			0.264			
RD-K-3-0006	DS 1/2 Lite, Solarban	Steel / Steel	2	0.03400 (2)	0.76400	ZF-S	Argon	N			0.28	0.12	0.21			0.264	0.28	0.28	0.00
RD-K-3-0006	DS 1/2 Lite, Solarban	Steel / Steel	2	0.03400 (2)	0.76400	ZF-S	Argon	N			0.28	0.12	0.21			0.264	0.28	0.28	0.00
K-3-00065-0	DS 1/2 Lite, Solarban	Steel / Steel	2	0.03400 (2)	0.76400	ZF-S	Argon	G	0.75		0.28	0.11	0.19			0.264			
K-3-00065-0	DS 1/2 Lite, Solarban	Steel / Steel	2	0.03400 (2)	0.76400	ZF-S	Argon	G	0.75		0.28	0.11	0.19			0.264			
RD-K-3-0006	DS 3/4 Lite, Solarban	Steel / Steel	2	0.03400 (2)	0.76400	ZF-S	Argon	N			0.29	0.14	0.26			0.264	0.29	0.29	0.00
RD-K-3-0006	DS 3/4 Lite, Solarban	Steel / Steel	2	0.03400 (2)	0.76400	ZF-S	Argon	N			0.29	0.14	0.26			0.264	0.29	0.29	0.00
K-3-00066-0	DS 3/4 Lite, Solarban	Steel / Steel	2	0.03400 (2)	0.76400	ZF-S	Argon	G	0.75		0.29	0.13	0.22			0.264			
K-3-00066-0	DS 3/4 Lite, Solarban	Steel / Steel	2	0.03400 (2)	0.76400	ZF-S	Argon	G	0.75		0.29	0.13	0.22			0.264			
RD-K-3-0006	DS Full Lite, Solarban	Steel / Steel	2	0.03400 (2)	0.76400	ZF-S	Argon	N			0.32	0.18	0.33			0.264	0.32	0.32	0.00
RD-K-3-0006	DS Full Lite, Solarban	Steel / Steel	2	0.03400 (2)	0.76400	ZF-S	Argon	N			0.32	0.18	0.33			0.264	0.32	0.32	0.00
K-3-00067-0	DS Full Lite, Solarban	Steel / Steel	2	0.03400 (2)	0.76400	ZF-S	Argon	G	0.75		0.32	0.16	0.28			0.264			
K-3-00067-0	DS Full Lite, Solarban	Steel / Steel	2	0.03400 (2)	0.76400	ZF-S	Argon	G	0.75		0.32	0.16	0.28			0.264			
RD-K-3-0006	6-Panel, No Lite	Steel / Steel	1			N		N			0.21	*	*						
RD-K-3-0006	6-Panel, No Lite	Steel / Steel	1			N		N			0.21	*	*		triple, grids				
RD-K-3-0006	DS 1/4 Lite, Caming	Steel / Steel	3		0.32300, 0.32300	A5-D	Air / Air	G	1.5		0.26	0.09	0.09			0.348			
RD-K-3-0006	DS 1/4 Lite, Caming	Steel / Steel	3		0.32300, 0.32300	A5-D	Air / Air	G	1.5		0.26	0.09	0.09			0.348			
RD-K-3-0007	DS 1/2 Lite, Caming	Steel / Steel	3		0.32300, 0.32300	A5-D	Air / Air	G	1.5		0.31	0.18	0.19			0.348			
RD-K-3-0007	DS 1/2 Lite, Caming	Steel / Steel	3		0.32300, 0.32300	A5-D	Air / Air	G	1.5		0.31	0.18	0.19			0.348			
RD-K-3-0007	DS 3/4 Lite, Caming	Steel / Steel	3		0.32300, 0.32300	A5-D	Air / Air	G	1.5		0.33	0.22	0.23			0.348			
RD-K-3-0007	DS 3/4 Lite, Caming	Steel / Steel	3		0.32300, 0.32300	A5-D	Air / Air	G	1.5		0.33	0.22	0.23			0.348			
RD-K-3-0007	DS Full Lite, Caming	Steel / Steel	3		0.32300, 0.32300	A5-D	Air / Air	G	1.5		0.36	0.28	0.29			0.348			
RD-K-3-0007	DS Full Lite, Caming	Steel / Steel	3		0.32300, 0.32300	A5-D	Air / Air	G	1.5		0.36	0.28	0.29			0.348			
RD-K-3-0007	6-Panel, No Lite	Steel / Steel	1			N		N			0.21	*	*						
RD-K-3-0007	6-Panel, No Lite	Steel / Steel	1			N		N			0.21	*	*			A1 Spacer			
RD-K-3-0007	DS 1/4 Lite	Steel	2		0.76400	A1-D	Air	N			0.28	0.11	0.11			0.499	0.28	0.27	0.01
RD-K-3-0007	DS 1/4 Lite	Steel	2		0.76400	A1-D	Air	N			0.28	0.11	0.11			0.499			
K-3-00074-0	DS 1/4 Lite	Steel	2		0.76400	A1-D	Air	G	0.75		0.28	0.10	0.09			0.499			
K-3-00074-0	DS 1/4 Lite	Steel	2		0.76400	A1-D	Air	G	0.75		0.28	0.10	0.09			0.499			
RD-K-3-0007	DS 1/2 Lite	Steel	2		0.76400	A1-D	Air	N			0.35	0.23	0.24			0.499	0.35	0.34	0.01
RD-K-3-0007	DS 1/2 Lite	Steel	2		0.76400	A1-D	Air	N			0.35	0.23	0.24			0.499			
K-3-00075-0	DS 1/2 Lite	Steel	2		0.76400	A1-D	Air	G	0.75		0.35	0.20	0.21			0.499			
K-3-00075-0	DS 1/2 Lite	Steel	2		0.76400	A1-D	Air	G	0.75		0.35	0.20	0.21			0.499			
RD-K-3-0007	DS 3/4 Lite	Steel	2		0.76400	A1-D	Air	N			0.38	0.28	0.29			0.499	0.38	0.37	0.01
RD-K-3-0007	DS 3/4 Lite	Steel	2		0.76400	A1-D	Air	N			0.38	0.28	0.29			0.499			
K-3-00076-0	DS 3/4 Lite	Steel	2		0.76400	A1-D	Air	G	0.75		0.38	0.24	0.25			0.499			
K-3-00076-0	DS 3/4 Lite	Steel	2		0.76400	A1-D	Air	G	0.75		0.38	0.24	0.25			0.499			
RD-K-3-0007	DS Full Lite	Steel	2		0.76400	A1-D	Air	N			0.43	0.35	0.37			0.499	0.43	0.41	0.02
RD-K-3-0007	DS Full Lite	Steel	2		0.76400	A1-D	Air	N			0.43	0.35	0.37			0.499			
K-3-00077-0	DS Full Lite	Steel	2		0.76400	A1-D	Air	G	0.75		0.43	0.30	0.32			0.499			
K-3-00077-0	DS Full Lite	Steel	2		0.76400	A1-D	Air	G	0.75		0.43	0.30	0.32			0.499			

Manufacturer	Product Name
Danvid Window Company	DOORCRAFT STEEL DOOR

Coefficients for Equations

	Coeff-Ua	Coeff-Ub
1/4	0.140845	0.182535
1/2	0.28169	0.17507
3/4	0.316901	0.185704
Full	0.387324	0.186972

Key:

1) 2 values for U-Factor, SHGC, and VT indicates Res/Non-Res ratings.
2) * indicates that Certified SHGC/VT values are available from the Manufacturer.

287 records were returned.

CPD Number	Mfr Product Code	Frame/Sash Type	Glazing Layer	Low-E/Internal Film (Surface	Gap Width(s)	Spacer Type	Fill	Grids	Dividers	Tint	U-Factor	SHGC	VT	Condensation Resistance	Ucog	U	Ucalc	Difference in U and Ucalc
CI-A-9-00003		none	2		0.25000	A1-D	Air	N			0.26	*	*		0.55	0.26	0.26	0.00
CI-A-9-00004		none	2		0.25000	A1-D	Air	N			0.33	*	*		0.55	0.33	0.33	0.00
CI-A-9-00005		none	2		0.25000	A1-D	Air	N			0.36	*	*		0.55	0.36	0.36	0.00
CI-A-9-00006		none	2		0.25000	A1-D	Air	N			0.4	*	*		0.55	0.4	0.40	0.00
CI-A-9-00007		none	2	(3)	0.25000	A1-D	Air	N			0.24	*	*		0.409	0.24	0.24	0.00
CI-A-9-00008		none	2	(3)	0.25000	A1-D	Air	N			0.29	*	*		0.409	0.29	0.29	0.00
CI-A-9-00009		none	2	(3)	0.25000	A1-D	Air	N			0.31	*	*		0.409	0.31	0.32	-0.01
CI-A-9-00010		none	2	(3)	0.25000	A1-D	Air	N			0.34	*	*		0.409	0.34	0.35	-0.01
CI-A-9-00011		none	2	(3)	0.25000	A1-D	Argon	N			0.23	*	*		0.333	0.23	0.23	0.00
CI-A-9-00012		none	2	(3)	0.25000	A1-D	Argon	N			0.28	*	*		0.333	0.28	0.27	0.01
CI-A-9-00013		none	2	(3)	0.25000	A1-D	Air	N			0.29	*	*		0.333	0.29	0.29	0.00
CI-A-9-00014		none	2	(3)	0.25000	A1-D	Argon	N			0.32	*	*		0.333	0.32	0.32	0.00
CI-A-9-00015		none	2		0.25000	A5-D	Air	N			0.26	*	*					
CI-A-9-00016		none	2		0.25000	A5-D	Air	N			0.33	*	*					
CI-A-9-00017		none	2		0.25000	A5-D	Air	N			0.35	*	*					
CI-A-9-00018		none	2		0.25000	A5-D	Air	N			0.40	*	*					
CI-A-9-00019		none	2	(3)	0.25000	A5-D	Air	N			0.24	*	*					
CI-A-9-00020		none	2	(3)	0.25000	A5-D	Air	N			0.29	*	*					
CI-A-9-00021		none	2	(3)	0.25000	A5-D	Air	N			0.31	*	*					
CI-A-9-00022		none	2	(3)	0.25000	A5-D	Air	N			0.34	*	*					
CI-A-9-00023		none	2	(3)	0.25000	A5-D	Argon	N			0.23	*	*					
CI-A-9-00024		none	2	(3)	0.25000	A5-D	Argon	N			0.27	*	*					
CI-A-9-00025		none	2	(3)	0.25000	A5-D	Argon	N			0.29	*	*					
CI-A-9-00026		none	2	(3)	0.25000	A5-D	Argon	N			0.32	*	*					
CI-A-9-00027		none	2		0.75000	A1-D	Air	G			0.25	*	*					
A-9-00027-00001		none	2		0.75000	A1-D	Air	N			0.25	*	*		0.486	0.25	0.25	0.00
CI-A-9-00028		none	2		0.75000	A1-D	Air	G			0.31	*	*					
A-9-00028-00001		none	2		0.75000	A1-D	Air	N			0.31	*	*		0.486	0.31	0.31	0.00
CI-A-9-00029		none	2		0.75000	A1-D	Air	G			0.33	*	*					
A-9-00029-00001		none	2		0.75000	A1-D	Air	N			0.33	*	*		0.486	0.33	0.34	-0.01
CI-A-9-00030		none	2		0.75000	A1-D	Air	G			0.37	*	*					
A-9-00030-00001		none	2		0.75000	A1-D	Air	N			0.37	*	*		0.486	0.37	0.38	-0.01
CI-A-9-00031		none	2	(3)	0.75000	A1-D	Air	G			0.23	*	*					
A-9-00031-00001		none	2	(3)	0.75000	A1-D	Air	N			0.23	*	*		0.313	0.23	0.23	0.00
CI-A-9-00032		none	2	(3)	0.75000	A1-D	Air	G			0.26	*	*					
A-9-00032-00001		none	2	(3)	0.75000	A1-D	Air	N			0.26	*	*		0.313	0.26	0.26	0.00
CI-A-9-00033		none	2	(3)	0.75000	A1-D	Air	G			0.28	*	*					
A-9-00033-00001		none	2	(3)	0.75000	A1-D	Air	N			0.28	*	*		0.313	0.28	0.28	0.00
CI-A-9-00034		none	2	(3)	0.75000	A1-D	Air	G			0.3	*	*					
A-9-00034-00001		none	2	(3)	0.75000	A1-D	Air	N			0.3	*	*		0.313	0.3	0.31	-0.01
CI-A-9-00035		none	2	(3)	0.75000	A1-D	Argon	G			0.22	*	*					
A-9-00035-00001		none	2	(3)	0.75000	A1-D	Argon	N			0.22	*	*		0.266	0.22	0.22	0.00
CI-A-9-00036		none	2	(3)	0.75000	A1-D	Argon	G			0.25	*	*					
A-9-00036-00001		none	2	(3)	0.75000	A1-D	Argon	N			0.25	*	*		0.266	0.25	0.25	0.00
CI-A-9-00037		none	2	(3)	0.75000	A1-D	Argon	G			0.27	*	*					
A-9-00037-00001		none	2	(3)	0.75000	A1-D	Argon	N			0.27	*	*		0.266	0.27	0.27	0.00
CI-A-9-00038		none	2	(3)	0.75000	A1-D	Argon	G			0.29	*	*					
A-9-00038-00001		none	2	(3)	0.75000	A1-D	Argon	N			0.29	*	*		0.266	0.29	0.29	0.00

Manufacturer	Product Name
Western Building Products	Doorcraft Alterna Door

Coefficients for Equations

	Coeff-Ua	Coeff-Ub
1/4	-0.387324	0.393028
1/2	0.140845	0.172535
3/4	0.28169	0.16507
Full	0.316901	0.175704

Key:

1) 2 values for U-Factor, SHGC, and VT indicates Res/Non-Res ratings.
2) * indicates that Certified SHGC/VT values are available from the Manufacturer.

290 records were returned.

CPD Number	Mfr Product Code	Frame/Sash Type	Glazing Layer	Low-E/Internal Film (Surface)	Gap Width(s)	Spacer Type	Fill	Grids	Dividers	Tint	U-Factor	SHGC	VT	Condensation Resistance	Ucog	U	Ucalc	Difference in U and Ucalc
WBP-M-3-00001		Wood /	1			N		N			0.17	0.04	0.00		0	0.17		slab
WBP-M-3-00002	Clear	Wood /	2		0.25000	A1-D	Air	N			0.18	0.13	0.10		0.55	0.18	0.18	0.00
WBP-M-3-00003	Clear	Wood /	2		0.25000	A1-D	Air	N			0.25	0.24	0.22		0.55	0.25	0.25	0.00
WBP-M-3-00004	Clear	Wood /	2		0.25000	A1-D	Air	N			0.32	0.28	0.27		0.55	0.32	0.32	0.00
WBP-M-3-00005	Clear	Wood /	2		0.25000	A1-D	Air	N			0.35	0.35	0.34		0.55	0.35	0.35	0.00
WBP-M-3-00006	CIG 172	Wood /	2		0.25000	A1-D	Air	N			0.39	0.09	0.09		0.409	0.39	0.23	0.16
WBP-M-3-00007	CIG 172	Wood /	2		0.25000	A1-D	Air	N			0.23	0.16	0.19		0.409	0.23	0.23	0.00
WBP-M-3-00008	CIG 172	Wood /	2		0.25000	A1-D	Air	N			0.28	0.19	0.24		0.409	0.28	0.28	0.00
WBP-M-3-00009	CIG 172	Wood /	2		0.25000	A1-D	Air	N			0.3	0.23	0.30		0.409	0.3	0.31	-0.01
WBP-M-3-00010	CIG 172	Wood /	2		0.25000	A1-D	Argon	N			0.33	0.09	0.09		0.333	0.33	0.26	0.07
WBP-M-3-00011	CIG 172	Wood /	2		0.25000	A1-D	Argon	N			0.22	0.16	0.19		0.333	0.22	0.22	0.00
WBP-M-3-00012	CIG 172	Wood /	2		0.25000	A1-D	Argon	N			0.27	0.19	0.24		0.333	0.27	0.26	0.01
WBP-M-3-00013	CIG 172	Wood /	2		0.25000	A1-D	Argon	N			0.28	0.23	0.30		0.333	0.28	0.28	0.00
WBP-M-3-00014	Clear	Wood /	2		0.25000	A5-S	Air	N			0.31	0.13	0.10					
WBP-M-3-00015	Clear	Wood /	2		0.25000	A5-S	Air	N			0.25	0.24	0.22					
WBP-M-3-00016	Clear	Wood /	2		0.25000	A5-S	Air	N			0.32	0.28	0.27					
WBP-M-3-00017	Clear	Wood /	2		0.25000	A5-S	Air	N			0.34	0.35	0.34					
WBP-M-3-00018	CIG 172	Wood /	2		0.25000	A5-S	Air	N			0.39	0.09	0.09					
WBP-M-3-00019	CIG 172	Wood /	2		0.25000	A5-S	Air	N			0.23	0.16	0.19					
WBP-M-3-00020	CIG 172	Wood /	2		0.25000	A5-S	Air	N			0.28	0.19	0.24					
WBP-M-3-00021	CIG 172	Wood /	2		0.25000	A5-S	Air	N			0.30	0.23	0.30					
WBP-M-3-00022	CIG 172	Wood /	2		0.25000	A5-S	Argon	N			0.33	0.09	0.09					
WBP-M-3-00023	CIG 172	Wood /	2		0.25000	A5-S	Argon	N			0.22	0.16	0.19					
WBP-M-3-00024	CIG 172	Wood /	2		0.25000	A5-S	Argon	N			0.26	0.19	0.24					
WBP-M-3-00025	CIG 172	Wood /	2		0.25000	A5-S	Argon	N			0.28	0.23	0.30					
WBP-M-3-00026	Clear	Wood /	2		0.75000	A1-D	Air	N			0.31	0.13	0.10		0.486	0.31	0.20	0.11
P-M-3-00026-000	Clear	Wood /	2		0.75000	A1-D	Air	G	0.75		0.31	0.12	0.09		0.486			
WBP-M-3-00027	Clear	Wood /	2		0.75000	A1-D	Air	N			0.24	0.24	0.22		0.486	0.24	0.24	0.00
P-M-3-00027-000	Clear	Wood /	2		0.75000	A1-D	Air	G	0.75		0.24	0.22	0.20		0.486			
WBP-M-3-00028	Clear	Wood /	2		0.75000	A1-D	Air	N			0.3	0.28	0.27		0.486	0.3	0.30	0.00
P-M-3-00028-000	Clear	Wood /	2		0.75000	A1-D	Air	G	0.75		0.3	0.26	0.25		0.486			
WBP-M-3-00029	Clear	Wood /	2		0.75000	A1-D	Air	N			0.32	0.35	0.34		0.486	0.32	0.33	-0.01
P-M-3-00029-000	Clear	Wood /	2		0.75000	A1-D	Air	G	0.75		0.32	0.33	0.32		0.486			
WBP-M-3-00030	CIG 172	Wood /	2		0.75000	A1-D	Air	N			0.36	0.09	0.09		0.313	0.36	0.27	0.09
P-M-3-00030-000	CIG 172	Wood /	2		0.75000	A1-D	Air	G	0.75		0.36	0.09	0.08		0.313			
WBP-M-3-00031	CIG 172	Wood /	2		0.75000	A1-D	Air	N			0.22	0.16	0.19		0.313	0.22	0.22	0.00
P-M-3-00031-000	CIG 172	Wood /	2		0.75000	A1-D	Air	G	0.75		0.22	0.15	0.18		0.313			
WBP-M-3-00032	CIG 172	Wood /	2		0.75000	A1-D	Air	N			0.25	0.19	0.24		0.313	0.25	0.25	0.00
P-M-3-00032-000	CIG 172	Wood /	2		0.75000	A1-D	Air	G	0.75		0.25	0.18	0.22		0.313			
WBP-M-3-00033	CIG 172	Wood /	2		0.75000	A1-D	Air	N			0.27	0.23	0.30		0.313	0.27	0.27	0.00
P-M-3-00033-000	CIG 172	Wood /	2		0.75000	A1-D	Air	G	0.75		0.27	0.22	0.28		0.313			
WBP-M-3-00034	CIG 172	Wood /	2		0.75000	A1-D	Argon	N			0.29	0.09	0.09		0.266	0.29	0.29	0.00
P-M-3-00034-000	CIG 172	Wood /	2		0.75000	A1-D	Argon	G	0.75		0.29	0.09	0.08		0.266			
WBP-M-3-00035	CIG 172	Wood /	2		0.75000	A1-D	Argon	N			0.21	0.16	0.19		0.266	0.21	0.21	0.00
P-M-3-00035-000	CIG 172	Wood /	2		0.75000	A1-D	Argon	G	0.75		0.21	0.15	0.18		0.266			
WBP-M-3-00036	CIG 172	Wood /	2		0.75000	A1-D	Argon	N			0.24	0.19	0.24		0.266	0.24	0.24	0.00
P-M-3-00036-000	CIG 172	Wood /	2		0.75000	A1-D	Argon	G	0.75		0.24	0.18	0.22		0.266			
WBP-M-3-00037	CIG 172	Wood /	2		0.75000	A1-D	Argon	N			0.26	0.23	0.30		0.266	0.26	0.26	0.00

3.5 SHGC

SHGC is simpler in that the manufacturer only needs the center-of-glass SHGC. We are proposing that the solar heat gain coefficient through the opaque elements by assumed to be 0.03. The total SHGC is then calculated based on the sum of the solar heat gain through the opaque area plus the solar heat gain through the glass area. Because the door glass sizes are set, it is straight forward to calculate the glazing and opaque area fractions and fix these values in the equations. The following set of equations reflects the current door size and glass sizes in NFRC 100-2004 and would apply only to flush doors:

$SHGC_{flush} = 0.03$

$SHGC_{1/4} = 0.0264 + 0.1215 * SHGC_{cog}$

$SHGC_{1/2} = 0.0219 + 0.2712 * SHGC_{cog}$

$SHGC_{3/4} = 0.0200 + 0.3327 * SHGC_{cog}$

$SHGC_{full} = 0.0172 + 0.4276 * SHGC_{cog}$

These equations would not apply to panel doors. The current approach to replacing panels with glasss does not result in the default glass sizes given for flush doors. A single set of equations that would apply to all panel doors cannot be determined using the current approach for panel doors.

Based on the proposed door height and glass sizes in sections 3.1 and 3.2, the equations would be as follows:

$SHGC_{flush} = 0.03$

$SHGC_{1/4} = 0.0286 + 0.457 * SHGC_{cog}$

$SHGC_{1/2} = 0.0232 + 0.2265 * SHGC_{cog}$

$SHGC_{3/4} = 0.0203 + 0.3232 * SHGC_{cog}$

$SHGC_{full} = 0.0178 + 0.4072 * SHGC_{cog}$

These equations would apply to both flush and panel doors.

3.6 Visible Transmittance

Visible light transmittance is the simplest. The manufacturer only needs to plug the center-of-glass VT into the equations. The total VT is then calculated from the visible light transmittance through the fraction of glass area. Again, because the door glass sizes are set, it is straight forward to calculate the glazing area fractions and fix these values in the equations. The equations for the existing sizes in NFRC 100-2004 are as follows:

$VT_{flush} = 0.0$

$VT_{1/4} = 0.1215 * VT_{cog}$

$VT_{1/2} = 0.2712 * VT_{cog}$

$VT_{3/4} = 0.3327 * VT_{cog}$

$VT_{full} = 0.4276 * VT_{cog}$

These equations would not apply to both flush and panel doors. The current approach to replacing panels with glass does not result in the default glass sizes given for flush doors. A single set of equations that would apply to all panel doors cannot be determined using the current approach for panel doors.

However, with the proposed lite sizes and panel sizes, it is possible to determine a set of equations that apply to both flush and panel doors:

$VT_{flush} = 0.0$

$VT_{1/4} = 0.0457 * VT_{cog}$

$VT_{1/2} = 0.2265 * VT_{cog}$

$VT_{3/4} = 0.3232 * VT_{cog}$

$VT_{full} = 0.4072 * VT_{cog}$

These equations assume the new door height as well.

3.7 Further Simplifications

Rather than having a set of equations for all options, we propose the following simplifications:

- Group spacers as per NFRC 100
- Group inswing and outswing with inswing the group leader
- Assume an add-on for doors installed in steel frames
- Provide an adjustment to SHGC and VT for grids and dividers

This approach could easily be implemented through a stand-alone spreadsheet that would be customized for each slab manufacturer. The coefficients for the equations for each product would be input by the NFRC simulator into the spreadsheet along with the center-of-glass results from WINDOW 5. The manufacturer could provide this spreadsheet to their fabricators, etc. The user would simply identify the product being built and print out the corresponding NFRC label.

Project 1.1.13

Project Name:	Component Modeling Approach Frame Grouping Research
Date:	December 4, 2007
Purpose:	To develop updated frame grouping rules to be used in CMA procedures.

Project Summary:

The objective of the project was to develop additional frame grouping rules, for nonresidential products and revisit existing frame grouping rules, so that the new set of frame grouping rules can uniformly be applied to the entire range of fenestration products, whether they are residential or non-residential. In addition to whole product grouping rules, investigate and develop frame grouping rules that are specific to frame component submission in the new CMA, being the basis for the new non-residential NFRC procedure, including the development of generic frame categories that can be used to simplify grouping of frame systems as components in CMA.

The research project consisted of three tasks, (1) Review, documentation and cataloguing of existing NFRC frame grouping rules, (2) Collection and cataloguing of major framing types and options in fenestration products and (3) Development of new and updated frame grouping rules.

Click here for final report

Web link:
http://www.nfrc.org/CMAFramegroupingrfpbrtg.aspx

Carli, Inc.

18 Tanglewood Rd.
Amherst, MA 01002

TEL: (413) 256-4647
FAX: (413) 256-4823

home@fenestration.com
http://www.fenestration.com

Technical Report:

DEVELOPMENT OF UPDATED FRAME GROUPING RULES

Report prepared for:

National Fenestration Rating Council, Inc.

6305 Ivy Lane, Suite 140
Greenbelt, MD 20770

December 4, 2007

TABLE OF CONTENTS:

Executive Summary 3
BACKGROUND 4
APPROACH 5
1.1 Review, Documentation and Cataloguing of Existing Frame Grouping Rules 5
1.2 Collection and Cataloguing of Major Framing Types and Options in Fenestration Products 5
1.3 Development of New and Updated Frame Grouping Rules 6
1.4 Default frame recommendation: 13
Conclusions and recommendations for technical documents: 17
Recommendations for technical committee 17
References 22
Appendix A . Current Frame grouping rules and their applicability to CMA 25
Appendix B: U factor variations for Various Parameters selected for frame grouping .. 27

Executive Summary

The purpose of this project was to develop updated frame grouping rules to be used in CMA procedures. The research project consisted of three tasks, (1) Review, documentation and cataloguing of existing frame grouping rules, (2) Collection and cataloguing of major framing types and options in fenestration products and (3) Development of new and updated frame grouping rules.

In task 1 current NFRC frame grouping rules were reviewed. The conclusion drawn based on the Component modeling approach being applicable to all the building types except single family houses and multi family structures of three stories or fewer above grade, which will deploy the standard punched opening products, was that all of the current NFRC frame grouping rules will be applicable to the CMA procedures as well. Therefore, the current NFRC 100 frame grouping rules including the latest addition/modification approved by NFRC membership meeting are recommended for CMA procedures as well. The rules are given in Appendix A.

In Task 2, to identify the listing of all major product types, including the listing and categories of prevalent existing framing cross sections and relevant manufacturers a list of manufacturer from NFRC was requested. Both punched opening and glazing façade manufacturers and products are considered for this project. Various parameters for frame grouping rules were identified for further analysis.

In task 3, based on our own findings and recommended frame grouping rules from the manufactures, a new set of frame grouping rules was developed. The parameters used in the analysis are: Projected Frame Depth (PFD), emissivity (external boundary conditions and internal frame cavity), glazing inset related to exterior, variation in frame width and/or frame height (frame cavity web addition causing cavity split), frame material thickness, changes in internal frame cavities and monotonous changes in the same parameter. The rules, derived from detailed THERM/WINODW modeling, are discussed in detail in the report. Order of priority for frame grouping rules was also established. The main advantage of this approach is that the manufacturers can determine the frame group leaders without performing any simulations as opposed to the current NFRC approach where the frame group leader needs to be determined by simulating all the frame cross sections involved.

One of the subtasks of this project was to recommend the generic frame systems for each of the product types. To achieve this goal, current NFRC certified product database was analyzed to determine the worst case U factors based on framing and operator type. Based on the information and analysis a default frame U factor in each category was developed -. These - values are given in Table 6.

BACKGROUND

The NFRC has identified frame groupings as the high priority technical issue that need to be resolved in order to successfully and effectively implement CMA.

The NFRC rating and certification process includes a number of grouping rules intended to simplify the process for manufacturers and make the rating process less burdensome. Current NFRC grouping rules are based on the assumption that different options can be grouped around the conservative (worst performing) option, if the overall difference in thermal performance is not large. Frame grouping rules are often intended to simplify the definition of a product line and to reduce number of individual product lines that a manufacturer has to certify. While the current rules in published NFRC 100 may help in reducing the modeling and validation (physical) test requirements, they do not reduce the number of product lines and the number of individual options within a product line. Current NFRC 100 grouping rules were developed with mainly residential products in mind and while many of them can be used for non-residential products, there are issues that are uniquely pertinent to non-residential and were additionally investigated, so that frame grouping rules can be applied to larger number of products. Additionally, the development and ongoing approval process for the component modeling approach (CMA), offers additional grouping and approval opportunities, where frame grouping could be applied first to a frame as a component and then to a more traditional whole product. The new grouping rules will potentially allow a frame manufacturer to have their frame cross-sections be assigned the thermal performance value from that of the matching generic frame cross-section.

The existing frame groupings, used in both residential and current non-residential NFRC procedures, are based on the similarities in framing design with the expectation that the thermal performance of the framing system will not differ significantly if frame groupings are employed. The current grouping procedures were developed over the years as NFRC rating procedures evolved and was fine-tuned during the standards, technical interpretations, and other methodology updates. This procedure is considered to be working well for the residential products and manufactured units where variations among product lines may not be substantial and the number of unique frame cross-sections may be limited. In non-residential products, this number is often described as *infinite* and manufacturers have called for the simplification of this process and for the reduction of unique frame cross-sections that would need to be modeled.

The new frame groupings rules, applicable to wider and more complete line of fenestration products will simplify, enhance and improve NFRC rating system. By providing less cumbersome rating system for non-residential products, which are currently not appropriately considered, NFRC will extend the reach into the non-residential market, which is currently only marginally covered. Also, the updated frame grouping rules will allow the new CMA rating system to be successfully implemented. Without the improved and updated frame grouping rules, CMA will not be able to fully deliver on its promise of simple and effective rating system.

APPROACH

The objective of the project was to develop additional frame grouping rules, for non-residential products and revisit existing frame grouping rules, so that the new set of frame grouping rules can uniformly be applied to the entire range of fenestration products, whether they are residential or non-residential. In addition to whole product grouping rules, investigate and develop frame grouping rules that are specific to frame component submission in the new CMA, being the basis for the new non-residential NFRC procedure, including the development of generic frame categories that can be used to simplify grouping of frame systems as components in CMA.

1.1 Review, Documentation and Cataloguing of Existing Frame Grouping Rules

Current frame grouping rules and language as outlined in NFRC 100 and 200 were reviewed especially in the light of their applicability for non-residential fenestration products. The conclusion drawn based on the Component modeling approach being applicable to all the building types except single family houses and multi family structures of three stories or fewer above grade, which will deploy the standard punched opening products, was that all of the current NFRC frame grouping rules will be applicable to the CMA procedures as well. Therefore, the current NFRC 100 frame grouping rules including the latest addition/modification approved by NFRC membership meeting are recommended for CMA procedures as well. The rules are given in Appendix A.

1.2 Collection and Cataloguing of Major Framing Types and Options in Fenestration Products

The number of unique frame cross section for non-residential products is often described as *infinite*; therefore, a simplification process of defining unique cross sections is required for the reduction of unique frame cross-sections that would need to be modeled. The aim was to identify the features such as variation in material thickness, appendages, monotonic variations of the same feature (e.g., depth of the reveal), and sort them out.

As a first step, the listing of all major product types, including the listing and categories of prevalent existing framing cross sections, and relevant manufacturers was identified. Inquiries were sent to selected group of manufacturers asking them to identify their unique framing types and also to indicate their recommendations for grouping rules, as that may be useful in the later part of the project. A list of manufacturer was obtained from NFRC. As current NFRC list did not contain a good representation of Non Residential manufacture, additional manufacturers were solicited from other organizations and personal contacts. The main emphasis was given to the Curtain Walls, Custom windows, Glazed wall/sloped glazing, Store Front and Commercial Skylights manufacturer.

Based on the review of various catalogs the potential parameters for analysis were identified as: Projected frame depth (PFD), emissivity (external boundary conditions and internal frame cavity), glazing inset related to exterior, variation in frame width and/or frame height (frame cavity web addition causing cavity split), frame material

thickness, changes in internal frame cavities and monotonous changes in the same parameter. In consultation with project monitoring task Group, the parameters given in Table 1were finalized for further study.

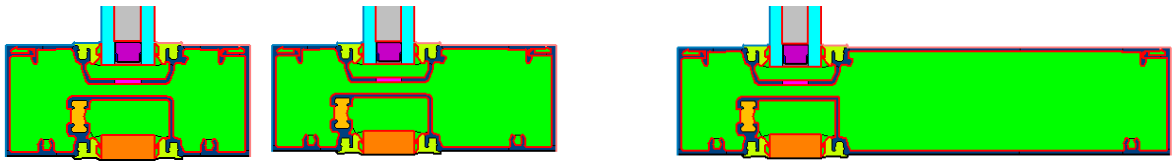
Table 1. Various Parameters selected for frame grouping criteria

	Variations
1	Change in length (X direction)
2	Emissivity (0.2, 0.8, 0.9)
3	Glass Location /Position (inward, centered and outward set)
4	Change in PFD
5	Material (wall) Thickness
6	Internal cavity (addition of web)- variations

1.3 Development of New and Updated Frame Grouping Rules

Detailed THERM and WINDOW modeling was performed for various parameters identified in Table 1. The analysis was carried out for different Product sizes and major framing material Aluminum (AL, AL-TI, AL-TB, Wood, Vinyl, and Fiberglass) materials to determine the group leader. A glazing system (clr-Arg-lowE) with c-o-g U factor of 1.37 W/m^{2}K (0.24 Btu/hr-ft^{2}F) was considered for the analysis. The calculations were performed for 3 product sizes of 600 mm x 1500 mm, 1200mm x 1500m and 2000mm and 200mm, representing casement, fixed and curtain wall/dual vision products.

The methodology is explained here with the help of an example for the parameter 1 (from Table 1). This example shows the effect of change in length in X direction. The cross section length in X direction was varied by 25mm, 50mm, 75mm, 125mm and 175 mm along the X-axis as shown in Figure 1 for the variation of 25 mm and 175 mm. The analysis was done for Aluminum and Thermally Improved (TI) Aluminum product type with emissivity of 0.8 (Anodized Aluminum) and 0.2 (Mill Finish Aluminum).



(a) Original (b) 25 mm (c) 175 mm

Figure 1: Variation of length in X-Axis

The U factor results are shown in Figures 2 to 6 below.

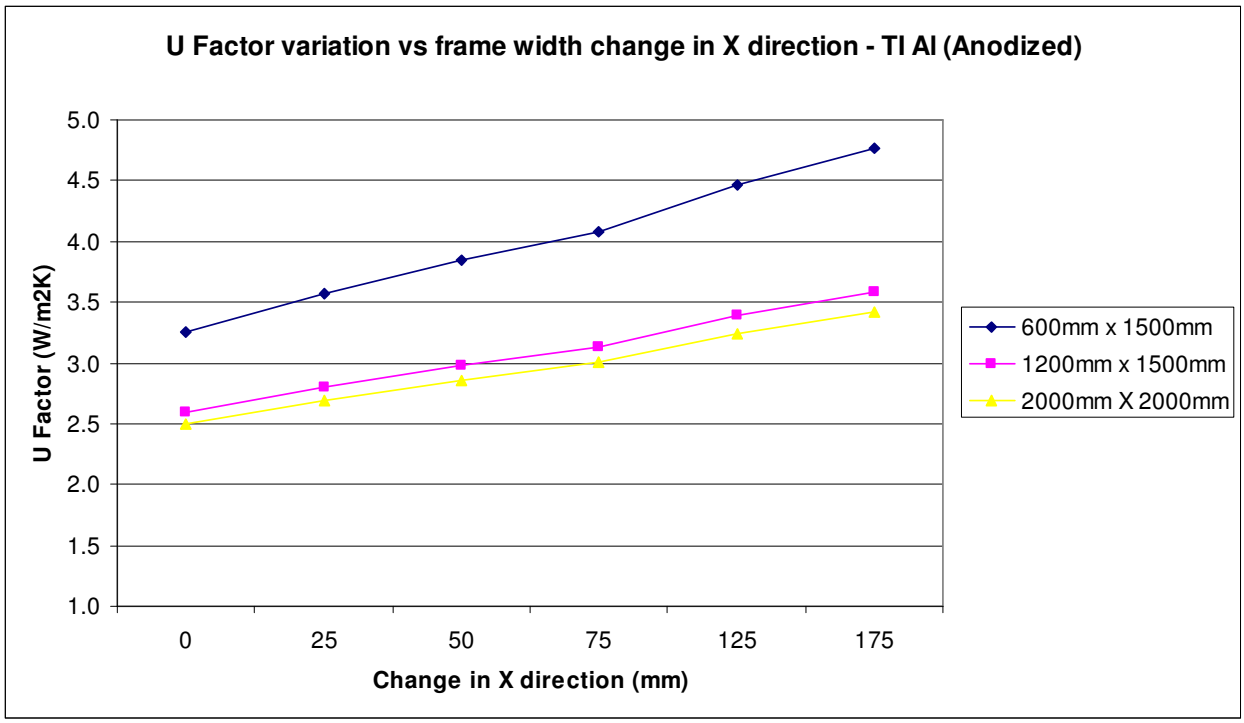


Figure 2: U factor variation with change in X direction for Thermally Improved Anodized Aluminum window

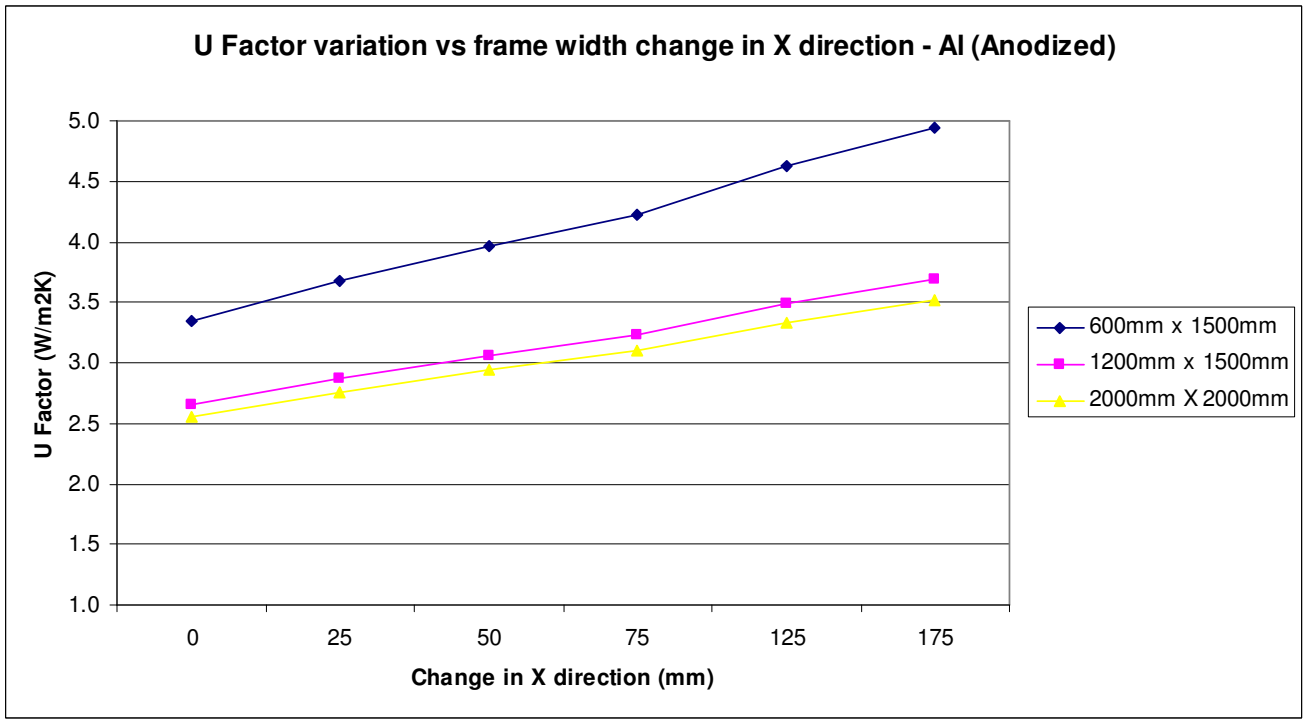


Figure 3: U factor variation with change in X direction for Anodized Aluminum window

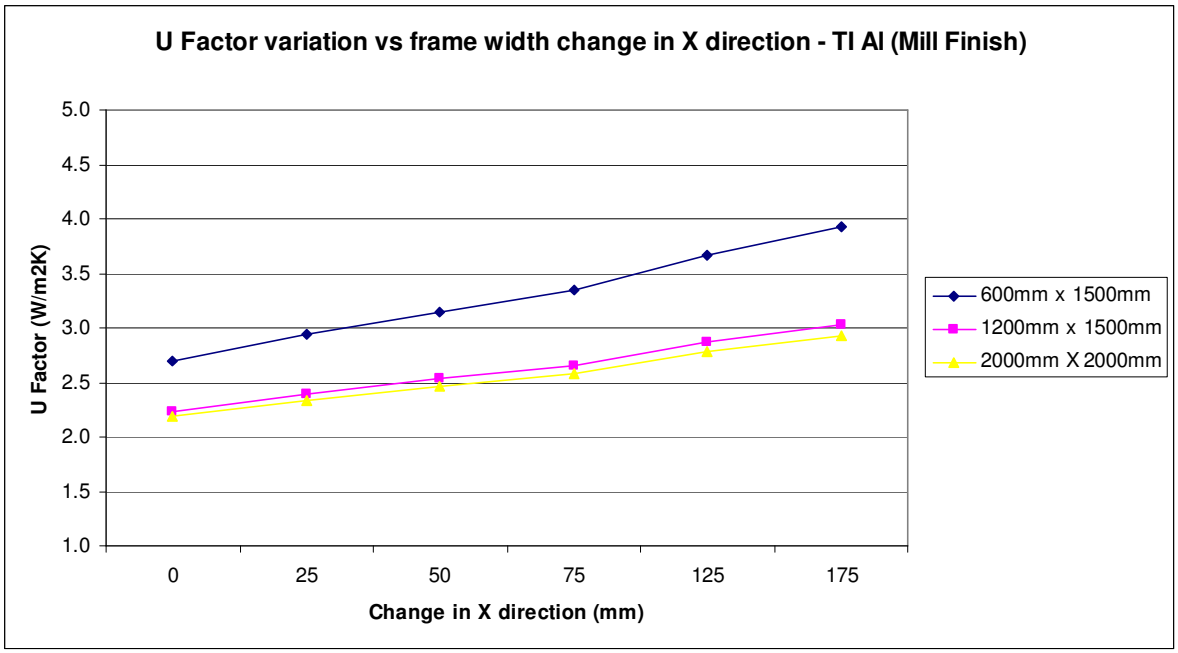


Figure 4: U factor variation with change in X direction for Thermally Improved Mill Finished Aluminum window

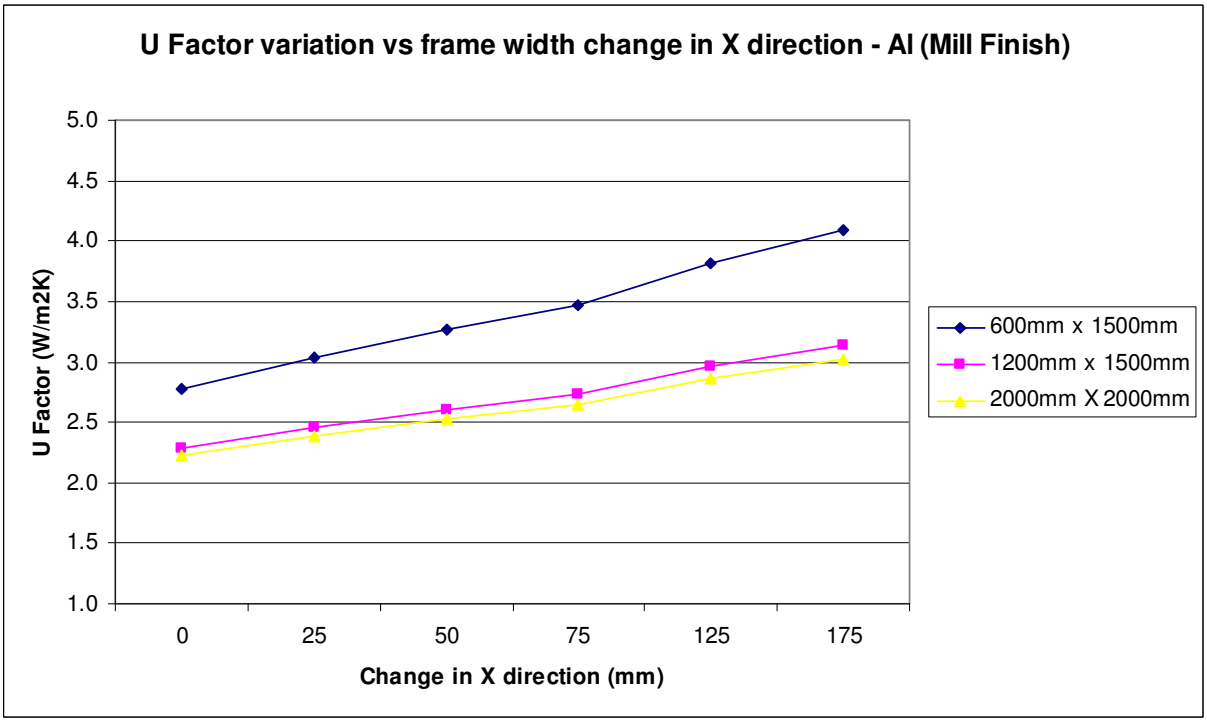


Figure 5: U factor variation with change in X direction for Mill Finished Aluminum window

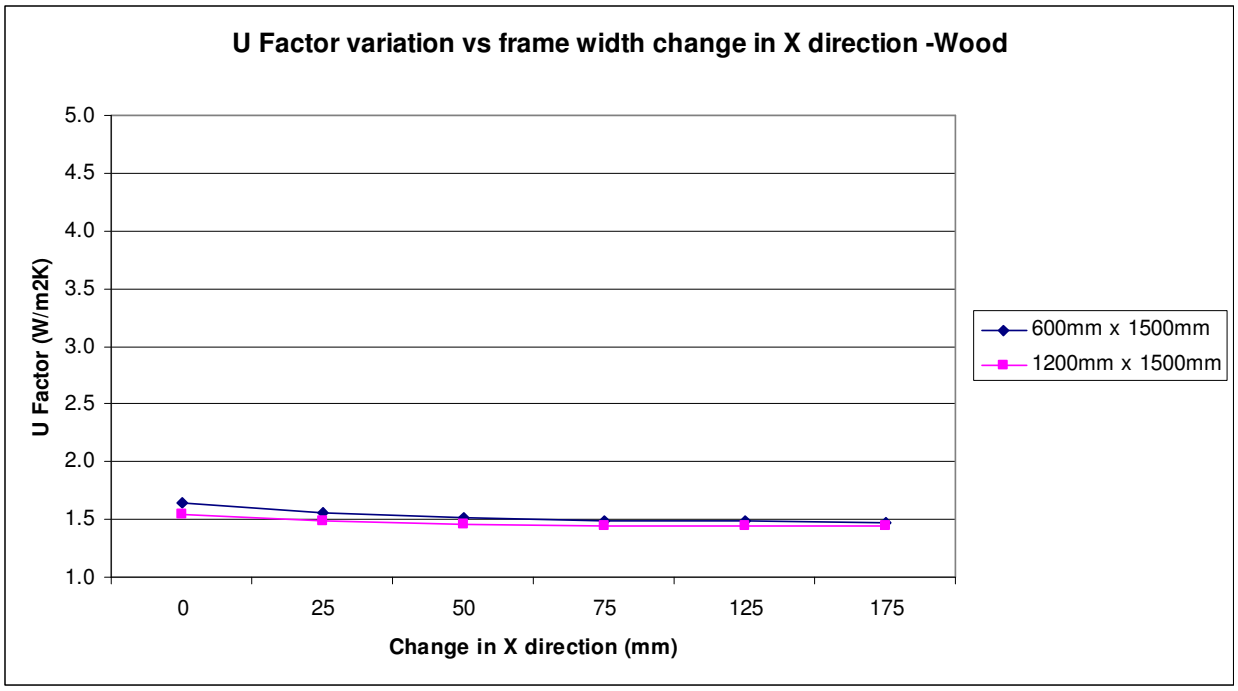


Figure 6: U factor variation with change in X direction for Wood window

It is evident from Figure 2-5 that U factor increases as the length along X-axis increases. The manufacture can choose the product having highest frame length in the X-direction as a group leader without simulating the product. The trend is reversed for the wood window, as is evident from Figure 6, though the variation is very small. The graphs for the rest of the parameters are given in Appendix B.

The results are summarized in Table 2for % U factor and SHGC changes. While frame grouping is important for U-factors, it is inconsequential for SHGC. This is because SHGC of frames is not modeled, but rather estimated from the ratio of wetted to projected area of outdoor frame surfaces. Therefore, the values for SHGC in Table 2 are shown only for reference. Table 2 below shows the maximum change with respect to minimum and maximum values for a particular variation. The main purpose of these results is to establish the order of priority for the variations in case of more than one variation being considered for the frame grouping.

Table 2. Change in U factor and SHGC for different frame variations

a. Thermally Broken -Aluminum

	Variations	**Description**	**% U factor change** (min–max /min)*100	**% SHGC change**
1	Glass Location /Position	Outside, center, inside set	-15	-3
2	Material (wall) Thickness	Increased by 2 , 4mm	-7	0
3	Change in length (X direction)	Increased by 25 mm upto 175 mm	-47	-3
4	Change in PFD	Increased by 10, 20 30 mm	-10	14
5	Emissivity (0.2, 0.8, 0.9)	0.2, 0.8 and 0.9	-25	-1
6	Internal cavity (addition of web)- variations	Addition of 1 and 2 cavities	-1	0

b. Aluminum

	Variations	**Description**	**% U factor change** (min–max /min)*100	**% SHGC change**
1	Glass Location /Position	Outside, center, inside set	-19	-3
2	Material (wall) Thickness	Increased by 2 , 4mm	-8	0
3	Change in length (X direction)	Increased by 25 mm upto 175 mm	-48	4
4	Change in PFD	Increased by 10, 20 30 mm	-13	13
5	Emissivity (0.2, 0.8, 0.9)	0.2, 0.8 and 0.9	-25	-1
6	Internal cavity (addition of web)- variations	Addition of 1 and 2 cavities	-2	0

c. PVC

	Variations	**Description**	**% U factor change** (min–max /min)*100	**% SHGC change**
1	Glass Location /Position	Outside, center, inside set	-4	0
2	Material (wall) Thickness	Increased by 2 , 4mm	4	0
3	Change in length (X direction)	Increased by 25 mm upto 175 mm	-9	0
4	Change in PFD	Increased by 10, 20 30 mm	-11	15
5	Emissivity (0.2, 0.8, 0.9)	0.2, 0.8 and 0.9		
6	Internal cavity (addition of web)- variations	Addition of 1 and 2 cavities	-3	0

Note: Fiberglass products show similar variations and therefore not considered separately

d. Wood

	Variations	**Description**	**% U factor change** (min–max /min)*100	**% SHGC change**
1	Glass Location /Position	Outside, center, inside set	-1.7	0.0
2	Material (wall) Thickness	Increased by 2 , 4mm		
3	Change in length (X direction)	Increased by 25 mm upto 175 mm	1.9	0.0
4	Change in PFD	Increased by 10, 20 30 mm	6.8	19
5	Emissivity (0.2, 0.8, 0.9)	0.2, 0.8 and 0.9		
6	Internal cavity (addition of web)- variations	Addition of 1 and 2 cavities		

Based on the results summarized from above, the following order of priority is established (Table 3).

Table 3. Order of priority for frame grouping

	Variations
1	Change in length (X direction)
2	Emissivity (0.2, 0.8, 0.9)
3	Glass Location /Position
4	Change in PFD
5	Material (wall) Thickness
6	Internal cavity (addition of web)- variations

The detailed results are presented in Appendix B. The group leaders for each of the variations are given in Table 4.

Table 4. Product Group Leaders

a. Frame types: Aluminum, Thermally Improved Aluminum and Thermally Broken Aluminum

	Variations	Description	Product Group leader
1	Change in length (X direction)	Increased by 25 mm upto 175 mm	Maximum length in X-direction
2	Emissivity (0.2, 0.8, 0.9)	0.2, 0.8 and 0.9	Hierarchy will be in the descending order of emissivity value, e.g. 0.9 will always be group leader
3	Glass Location /Position	Outside, center, inside set	Outside set is always the group leader (Center set is the group leader for inside and center set variation)
4	Change in PFD	Increased by 10, 20 30 mm	Highest PFD
5	Material (wall) Thickness	Increased by 2 , 4mm	Maximum wall thickness
6	Internal cavity (addition of web)- variations	Addition of 1 and 2 cavities	Maximum number of webs

b. Frame types: PVC and Fiberglass

	Variations	Description	Product Group leader
1	Change in length (X direction)	Increased by 25 mm upto 175 mm	Maximum length in X-direction
2	Glass Location /Position	Outside, center, inside set	Outside set (Center set in case of only inside and center set variation)
3	Change in PFD	Increased by 10, 20 30 mm	Highest PFD
4	Material (wall) Thickness	Increased by 2 , 4mm	Minimum wall thickness
5	Internal cavity (addition of web)- variations	Addition of 1 and 2 cavities	Minimum number of webs

c. Frame type: Wood

	Variations	Description	Product Group leader
1	Change in length (X direction)	Increased by 25 mm upto 175 mm	Minimum length in X-direction
2	Glass Location /Position	Outside, center, inside set	Outside set (Center set in case of only inside and center set variation)
3	Change in PFD	Increased by 10, 20 30 mm	Lowest PFD

In the current NFRC procedure (NFRC 100), the products are not eligible for frame grouping if PFD of the frame cross sections is different. The argument for not allowing difference in PFD is that if the product with higher PFD comes out to be the group leader, it will reduce the SHGC of the product which is against the intent of the grouping (group leader need to be worst performing and lower SHGC will be considered better especially with respect to cooling load reduction). However, In CMA procedure, the manufactures need to submit all the frame cross sections used for frame grouping and while only group leaders will be modeled for their actual U-factor and that U-factor will be used for all grouped frames; each of these products will be entered in the CMA frame database. Therefore, actual PFD of each grouped frame cross section will be available and will be considered for overall product SHGC calculations.

The trends for various parameters selected were very clear; therefore no building modeling is necessary as was proposed in the original proposal, which was envision for the scenario where the trends could not be established.

1.4 Determination of the Worst Case Frame U-factors:

One of the subtasks of this project was to determine the worst case frame performance for each of the product types to aid in the development of default frame U-factors. The default frame performance was not recommended as a part of this project for two reasons; 1) For several product and operator types, the data was either not available or sample was too small and/or unreliable; 2) there was no consensus what additional penalty in performance should be applied to produce default frame U-factors.

The data from NFRC CPD were utilized to develop the list of worst case frame performance. The data was obtained for clear argon lowE glazing units for all product types listed in the Table 5. The products that are not in NFRC CPD may have had worse performance, but because their data is unpublished this was not possible to determine. The worst case whole product U factors were extracted from current NFRC CPD for each of the product types. To obtain the Frame U Factors, the W5 mdb file for individual products which needed final analysis was requested from the simulation laboratories with the assistance from NFRC staff. The area weighted average frame U factors were extracted from the whole product U factors of the available W5 mdbs. Detailed report for the individual product with worst U factor from W5 MDB was extracted. The frame U factor was obtained by area weighting the frame U factors of various cross sections in that particular product. For example, for a fixed window, the area weighted frame U factor was calculated as follows:

$$U_{Frame} = \frac{A_{LJ} \cdot U_{LJ} + A_{RJ} \cdot U_{RJ} + A_S \cdot U_S + A_H \cdot U_H}{A_{LJ} + A_{RJ} + A_S + A_H}$$

Where, subscript LJ, RJ, S and H are left jam, right jamb, sill and head respectively and A is the area and U is the U Factor.

Data for some of the products were either not available or the data sample was not sufficient in the CPD. The missing products were not assigned any values and were denoted by **. Also, some of the products, which may not be manufactured currently in a specific product type category, were not assigned any values. For example, currently curtain walls are not manufactured with wood and vinyl framing materials and therefore default frame U factors are not assigned for wood and vinyl curtain walls. It is

recommended that these products shall be simulated and cannot use default generic frame U factors. The worst case frame U factors are shown in Table 5 (SI) and Table 6 (IP) . The unassigned categories are denoted by ** in. These unassigned categories may be filled in the future once the values are available.

Table 5. : Worst case frame U factors

S. No.	Description	Code	Definition	Worst case Frame U factor (W/m^{2}K))					
				Aluminum	Aluminum-TI	Aluminum-TB	Wood	Vinyl	FiberGlass
1	Casement	CSDV , CSOX, CSSV*, CSTH,	Double Vent, Vent/Fixed, Single	6.46	5.47	4.81	3.68	2.53	2.75
2	Dual Action	DAOT, DATT	Specify Configuration in Comment Field, Tilt	**	**	**	**	2.02	**
3	Double Door	DDFR	French-style Door (XX or OX)	**	**	**	**	2.10	**
4	Sliding Glass Door	DDSG	Sliding Glass Door (XX or OX)	8.44	7.04	5.00	2.86	2.50	3.28
5	Swinging Door	EDSL	Single Leaf Entrance Door	6.97	**	4.27	**	1.87	**
6	Fixed	FIGS, FIUN, FIXD*, FXEL,	Multiple Geometric, ShapeConfiguration,	6.75	6.19	4.68	*	2.53	2.49
7	Fixed	FXSL	Side-Lite	8.17	**	**	**	2.28	**
8	Fixed	FXTR	Transom	**	**	**	2.30	2.75	**
9	Glazed Wall System	GWCW	Curtain Wall	13.26	9.96	5.45	**	**	**
10	Glazed Wall System	GWSL	Solarium	**	**	5.31	**	**	**
11	Glazed Wall System	GWWW	Window Wall	**	10.10	6.12	**	**	**
12	Horizontal Slider	HSOX*, HSUN, HSXX**	Fixed/Operable, Configuration	8.32	5.69	4.55	2.58	2.15	2.74
13	Projected	PRAW*, PRFX, PROJ,	Awning, Fixed Over Projected, Vent Only,	6.86	6.56	4.79	**	1.68	2.75
14	Skylight	SKDM, SKFX*, SKOP, SKUN,	Domed, Fixed, Operable	**	**	17.18	12.79	12.04	16.64
15	Sloped glazing	SKSL	Sloped Glazing	**	**	11.19	**	**	**
16	Vertical Slider	VSDH, VSSH, VSUN	Double Hung, Single Hung, Configuration	9.16	7.94	5.57	2.48	2.75	2.82

***.Sufficient data is not available for this category*

Table 6. Worst Case frame U factors (IP – Units for reference only)

S. No.	Description	Code	Definition	Worst case U factor (Btu/hr-ft^{2}F)					
				Aluminum	Aluminum-TI	Aluminum-TB	Wood	Vinyl	FiberGlass
1	Casement	CSDV , CSOX, CSSV*, CSTH,	Double Vent, Vent/Fixed, Single	1.14	0.96	0.85	0.65	0.45	0.48
2	Dual Action	DAOT, DATT	Specify Configuration in Comment Field, Tilt	**	**	**	**	0.36	**
3	Double Door	DDFR	French-style Door (XX or OX)	**	**	**	**	0.37	**
4	Sliding Glass Door	DDSG	Sliding Glass Door (XX or OX)	1.49	1.24	0.88	0.50	0.44	0.58
5	Swinging Door	EDSL	Single Leaf Entrance Door	1.23	**	0.75	**	0.33	**
6	Fixed	FIGS, FIUN, FIXD*, FXEL,	Multiple Geometric, ShapeConfiguration,	1.19	1.09	0.82	*	0.45	0.44
7	Fixed	FXSL	Side-Lite	1.44	**	**	**	0.40	**
8	Fixed	FXTR	Transom	**	**	**	0.41	0.49	**
9	Glazed Wall System	GWCW	Curtain Wall	2.34	1.75	0.96	**	**	**
10	Glazed Wall System	GWSL	Solarium	**	**	0.93	**	**	**
11	Glazed Wall System	GWWW	Window Wall	**	1.78	1.08	**	**	**
12	Horizontal Slider	HSOX*, HSUN, HSXX**	Fixed/Operable, Configuration	1.47	1.00	0.80	0.45	0.38	0.48
13	Projected	PRAW*, PRFX, PROJ,	Awning, Fixed Over Projected, Vent Only,	1.21	1.16	0.84	**	0.30	0.48
14	Skylight	SKDM, SKFX*, SKOP, SKUN,	Domed, Fixed, Operable	**	**	3.03	2.25	2.12	2.93
15	Sloped glazing	SKSL	Sloped Glazing	**	**	1.97	**	**	**
16	Vertical Slider	VSDH, VSSH, VSUN	Double Hung, Single Hung, Configuration	1.61	1.40	0.98	0.44	0.49	0.50

***.Sufficient data is not available for this category*

Conclusions and recommendations for technical documents:

Current NFRC frame grouping rules were reviewed and recommended to be used in CMA procedures as well. Based on the review of various catalogs the potential parameters for analysis were identified and detailed THERM/WINDOW analysis were carried out to determine the frame group leader for the frame variations. The order of priority was established in case there are more than one variable that is changing in a particular frame cross section. The main advantage of this approach is that manufacturers can determine the frame group leaders without performing any simulations as opposed to the current NFRC approach where the frame group leader needs to be determined by simulating all the frame cross sections involved. As actual PFD will be used there would be no change in VT calculation procedure. .

Recommendations for the Frame Grouping

The following tables should be included in respective NFRC technical documents.

NFRC 100 Sections 5.6:

Table 7. Recommended Product Group Leaders

a. Frame type Aluminum, Thermally Improved Aluminum and Thermally Broken Aluminum

	Variations	**Description**	**Product Group leader**
1	Change in length (X direction)	Increased by 25 mm upto 175 mm	Maximum length in X-direction
2	Emissivity (0.2, 0.8, 0.9)	0.2, 0.8 and 0.9	Hierarchy will be in the descending order of emissivity value, e.g. 0.9 will always be group leader
3	Glass Location /Position	Outside, center, inside set	Outside set is always the group leader (Center set is the group leader for inside and center set variation)
4	Change in PFD	Increased by 10, 20 30 mm	Highest PFD
5	Material (wall) Thickness	Increased by 2 , 4mm	Maximum wall thickness
6	Internal cavity (addition of web)- variations	Addition of 1 and 2 cavities	Maximum number of webs

b. Frame type PVC and Fiberglass

	Variations	Description	Product Group leader
1	Change in length (X direction)	Increased by 25 mm upto 175 mm	Maximum length in X-direction
2	Glass Location /Position	Outside, center, inside set	Outside set (Center set in case of only inside and center set variation)
3	Change in PFD	Increased by 10, 20 30 mm	Highest PFD
4	Material (wall) Thickness	Increased by 2 , 4mm	Minimum wall thickness
5	Internal cavity (addition of web)- variations	Addition of 1 and 2 cavities	Minimum number of webs

c. Frame type Wood

	Variations	Description	Product Group leader
1	Change in length (X direction)	Increased by 25 mm upto 175 mm	Minimum length in X-direction
2	Glass Location /Position	Outside, center, inside set	Outside set (Center set in case of only inside and center set variation)
3	Change in PFD	Increased by 10, 20 30 mm	Lowest PFD

Table 8. Order of priority for frame grouping

	Variations
1	Change in length (X direction)
2	Emissivity (0.2, 0.8, 0.9)
3	Glass Location /Position
4	Change in PFD
5	Material (wall) Thickness
6	Internal cavity (addition of web)- variations

Recommendations for the Default Values

NFRC 100 - Section 5.6

Two options are recommended for the default frame U-factors. We recommend the following two options:

Option 1: Default frame U-factor for each of the categories in Table 5. Based on PMTG recommendations, 10% penalty was applied to the worst case U factors from Table 5 in order to create default frame U-factors. Results presented in Table 9 and Table **10**..

Option 2: Default frame U-factors for three broad-based categories.

I) Windows/Doors

II) Curtain Wall/Glazed Wall

III) Sloped products (i.e., skylights, sloped glazed wall, etc.)

For each of these categories, worst U-factor was chosen from Table 9 (SI) and Table **10** (IP) for appropriate products. The results are shown in Table 11 and Table 12.1

The following table(s) show recommended default U factors for the two options:

Table 9. Option 1: Recommended Default frame U factors (SI Units)

S. No.	Description	Code	Definition	Default U factor (Btu/hr-ft^{2}F)					
				Aluminum	Aluminum-TI	Aluminum-TB	Wood	Vinyl	FiberGlass
1	Casement	CSDV , CSOX, CSSV*, CSTH,	Double Vent, Vent/Fixed, Single	7.18	6.08	5.34	4.09	2.81	3.06
2	Dual Action	DAOT, DATT	Specify Configuration in Comment Field, Tilt	**	**	**	**	2.25	**
3	Double Door	DDFR	French-style Door (XX or OX)	**	**	**	**	2.33	**
4	Sliding Glass Door	DDSG	Sliding Glass Door (XX or OX)	9.37	7.83	5.56	3.18	2.77	3.64
5	Swinging Door	EDSL	Single Leaf Entrance Door	7.74	**	4.74	**	2.07	**
6	Fixed	FIGS, FIUN, FIXD*, FXEL,	Multiple Geometric, ShapeConfiguration,	7.50	6.88	5.20	*	2.81	2.77
7	Fixed	FXSL	Side-Lite	9.08	**	**	**	2.53	**
8	Fixed	FXTR	Transom	**	**	**	2.56	3.06	**
9	Glazed Wall System	GWCW	Curtain Wall	14.73	11.06	6.05	**	**	**
10	Glazed Wall System	GWSL	Solarium	**	**	5.90	**	**	**
11	Glazed Wall System	GWWW	Window Wall	**	11.22	6.80	**	**	**
12	Horizontal Slider	HSOX*, HSUN, HSXX**	Fixed/Operable, Configuration	9.24	6.32	5.06	2.87	2.39	3.05
13	Projected	PRAW*, PRFX, PROJ,	Awning, Fixed Over Projected, Vent Only,	7.62	7.29	5.32	**	1.87	3.06
14	Skylight	SKDM, SKFX*, SKOP, SKUN,	Domed, Fixed, Operable	**	**	19.09	14.21	13.38	18.49
15	Sloped glazing	SKSL	Sloped Glazing	**	**	12.44	**	**	**
16	Vertical Slider	VSDH, VSSH, VSUN	Double Hung, Single Hung, Configuration	10.18	8.82	6.18	2.75	3.06	3.13

***.Sufficient data is not available for this category*

Table 10. Option 1: Recommended Default frame U factors (IP Units – for reference only)

S. No.	Description	Code	Definition	Default U factor (Btu/hr-ft^{2}F)					
				Aluminum	Aluminum-TI	Aluminum-TB	Wood	Vinyl	FiberGlass
1	Casement	CSDV , CSOX, CSSV*, CSTH,	Double Vent, Vent/Fixed, Single	1.27	1.07	0.94	0.72	0.50	0.54
2	Dual Action	DAOT, DATT	Specify Configuration in Comment Field, Tilt	**	**	**	**	0.40	**
3	Double Door	DDFR	French-style Door (XX or OX)	**	**	**	**	0.41	**
4	Sliding Glass Door	DDSG	Sliding Glass Door (XX or OX)	1.65	1.38	0.98	0.56	0.49	0.64
5	Swinging Door	EDSL	Single Leaf Entrance Door	1.36	**	0.83	**	0.37	**
6	Fixed	FIGS, FIUN, FIXD*, FXEL,	Multiple Geometric, ShapeConfiguration,	1.32	1.21	0.92	*	0.50	0.49
7	Fixed	FXSL	Side-Lite	1.60	**	**	**	0.45	**
8	Fixed	FXTR	Transom	**	**	**	0.45	0.54	**
9	Glazed Wall System	GWCW	Curtain Wall	2.59	1.95	1.07	**	**	**
10	Glazed Wall System	GWSL	Solarium	**	**	1.04	**	**	**
11	Glazed Wall System	GWWW	Window Wall	**	1.98	1.20	**	**	**
12	Horizontal Slider	HSOX*, HSUN, HSXX**	Fixed/Operable, Configuration	1.63	1.11	0.89	0.50	0.42	0.54
13	Projected	PRAW*, PRFX, PROJ,	Awning, Fixed Over Projected, Vent Only,	1.34	1.28	0.94	**	0.33	0.54
14	Skylight	SKDM, SKFX*, SKOP, SKUN,	Domed, Fixed, Operable	**	**	3.36	2.50	2.36	3.26
15	Sloped glazing	SKSL	Sloped Glazing	**	**	2.19	**	**	**
16	Vertical Slider	VSDH, VSSH, VSUN	Double Hung, Single Hung, Configuration	1.79	1.55	1.09	0.49	0.54	0.55

***.Sufficient data is not available for this category*

Table 11. Option 2: Recommended Default frame U factors (SI Units)

	Default U factor (W/m2K)				
Fenestration Type	**Aluminum**	**Aluminum-TI**	**Aluminum-TB**	**Wood/Vinyl**	**Fiber Glass**
Windows	10.18	8.82	6.18	4.09	3.13
Curtain wall	14.73	11.22	6.80		
Skylights/Sloped glazing	*	*	19.09	14.21	18.49

***.Sufficient data is not available for this category*

Table 12. Option 2: Recommended Default frame U factors (IP Units – for reference only)

	Default Frame U factor (Btu/hr-ft^{2}F)				
Fenestration Type	**Aluminum**	**Aluminum-TI**	**Aluminum-TB**	**Wood/Vinyl**	**Fiber Glass**
Windows	1.79	1.55	1.09	0.72	0.64
Curtain wall	2.59	1.98	1.20		
Skylights/Sloped glazing	*	*	3.36	2.50	3.26

***.Sufficient data is not available for this category*

NFRC 200 – Section 4.7

Default SHGC will be calculated in accordance with ISO15099 Section 4.2.2. (as referenced in NFRC 200) with the listed assumption below:

$$SHGC_f = \alpha_f \frac{U_f}{\frac{A_s}{A_f} h_{ex}}$$

Where,

$SHGC_f$ = the frame SHGC

α_f = absorptivity of the frame

h_{ex} = exterior heat transfer coefficient, W/m^{2}K (Btu/hr-ft^2-F)

U_f = frame U factor, for this the default U factor from Table 9 (SI) / Table **10** (IP), or Table 11 (SI) / Table 12 (IP) will be used, W/m^{2}K (Btu/hr-ft^2-F), depending on which Option is adopted.

A_s = the developed (wetted) surface area of the frame, m^2 (ft^2)

A_f = the projected area of the frame, m^2 (ft^2)

For default $SHGC_f$, A_s/A_f is assumed to be 1.0. As per current NFRC guidelines α_f is assumed to be 0.5 for the non-residential products. A_s will always be greater than A_f therefore the assumption $A_s/A_f = 1$ is more conservative because the lower denominator value results in higher value of $SHGC_f$.

References

Curcija, D.C. 2003. "*C*omponent Model Approach In Modeling Non-Residential fenestration Products

ISO 15099 (2002) – Thermal Performance of Windows, Doors and Shading Devices - Detailed Calculations

LBNL. 2003. "THERM5 - A PC Program for Analyzing Window Thermal Performance of Fenestration Products", Berkeley CA: Windows and Daylighting Group, Lawrence Berkeley Laboratory, 2003.

LBNL 2003, "WINDOW5 - A PC Program for Analyzing Window Thermal Performance of Fenestration Products", Berkeley CA: Windows and Daylighting Group, Lawrence Berkeley Laboratory, 2003.

NFRC 100-2004. " Procedure for Determining Fenestration Product U-factors". National Fenestration Rating Council. 2004.

NFRC 200-2004. "Procedure for Determining Fenestration Product Solar Heat Gain Coefficient and Visible Transmittance at Normal Incidence". *National Fenestration Rating Council*. 2004.

NFRC 101-2004. "Procedure for Determining Thermo-Physical Properties of Materials For Use in NFRC-Approved Software Programs". National Fenestration Rating Council. 2004.

NFRC 102-2004. "Test Procedure for Measuring the Steady-State Thermal Transmittance of Fenestration Systems". *National Fenestration Rating Council*. 2004.

Appendix A. Current Frame grouping rules and their applicability to CMA

Current Frame grouping rules and their applicability to CMA

1. Changes to accommodate glazing unit variations. Limited to changes of geometry, number or material type to stops, beads, adhesives or gaskets designed to retain the glazing. Changes to frame and sash profiles are allowed to accommodate glazing unit variations. This provision does not allow for interior and exterior glazed products to be in the same product line. [Applicable to all product types]

2. Frame/sash modifications made to accommodate operating hardware and reinforcement for the purpose of addressing higher/lower loads and stresses. Limited to changes that do not change the exterior perimeter shape of the assembled cross section. [Applicable to high rise residential, motels]

3. Frame or sash changes where one component is replaced by another component of the same physical shape with a thermal conductivity that does not differ by more than ten times the thermal conductivity of the original material. [Applicable to high rise residential, motels]

4. Interior/exterior appendages added to the main web of the frame that is not exposed after product installation, i.e., nailing fins.[Applicable to high rise residential, motels]

5. Changes to the frame profiles to allow for different installations. Limited to the following:

    i. Any changes to interior/exterior appendages added to the main web of the frame that are removable or not exposed after product installation, i.e., nailing fins

    ii. Changes in the width (dimension perpendicular to the plane of the glazing) of the main frame or main frame components to allow for installation in different wall thicknesses.

    iii. Products manufactured in both in-swing and out-swing options.

6. Any sightline changes due to:

    i. Lengthening or shortening existing walls.

    ii. Components added or replaced for equal and unequal lite configuration options or;

    iii. For the installation of an Outside Air Ventilator Assembly (OAVA).

iv. Changes to the frame profiles to allow for different installations including pocket or sloped sill configuration options and sill height modifications. [Applicable to all the products]

7. Minor revisions made to the profiles for aesthetic purposes. Limited to changes in the size and shape of snap beads, stops, jamb extensions, dividers (including simulated and true divider lites), exterior trim caps on curtain walls, window walls and sloped glazing. Decorative elements such as grooves or beads formed in or applied to the frame or sash are also allowed. [Applicable to all the products]

8. Any changes to the exterior beyond the plane of the nailing fin, J-channel, or interior most point of exterior accessory groove, i.e. screen tracks, varying shapes of brickmold formed in (integral) or applied to the frame and that do not change the sightline. .[Applicable to high rise residential, motels]

9. Addition, deletion or changes in hardware and reinforcement .[Applicable to high rise residential, motels]

10. Changes to interior or exterior finishes or coatings [Applicable to all products]

11. Sealing characteristic variables and elements. Limited to changes in gaskets, sealants, adhesives or weather strips in the same profile. Profile changes to accommodate seal changes shall be allowed. [Applicable to all products]

12. Products manufactured in both in-swing and out-swing options. [Applicable to high rise residential, motels]

13. Pocket or sloped sill configuration options. [Applicable to high rise residential, motels]

14. Equal and unequal lite configuration options. [Applicable to all products]

15. Vinyl caps attached to the interior. [Applicable to high rise residential, motels]

16. Any changes to the internal cavities as long as the outside profile geometry does not change. [Applicable to all products]

17. Application of cladding to an unclad product line. [Applicable to high rise residential, motels]

18. Changes in the width (dimension perpendicular to the plane of the glazing) of the main frame or main frame components to allow for installation in different wall thicknesses, i.e., lengthening, shortening, and the addition of reinforcing web wall. [Applicable to all products]

Note: For the purpose of determining U-factors, frame groups shall consist only of frame/sash base profile variations consistent with the changes proposed above. The only allowable exceptions within a frame group are the individual products with different sightlines, simulated as separate individual products.

Appendix B: U factor variations for Various Parameters selected for frame grouping

A. Glazing Location

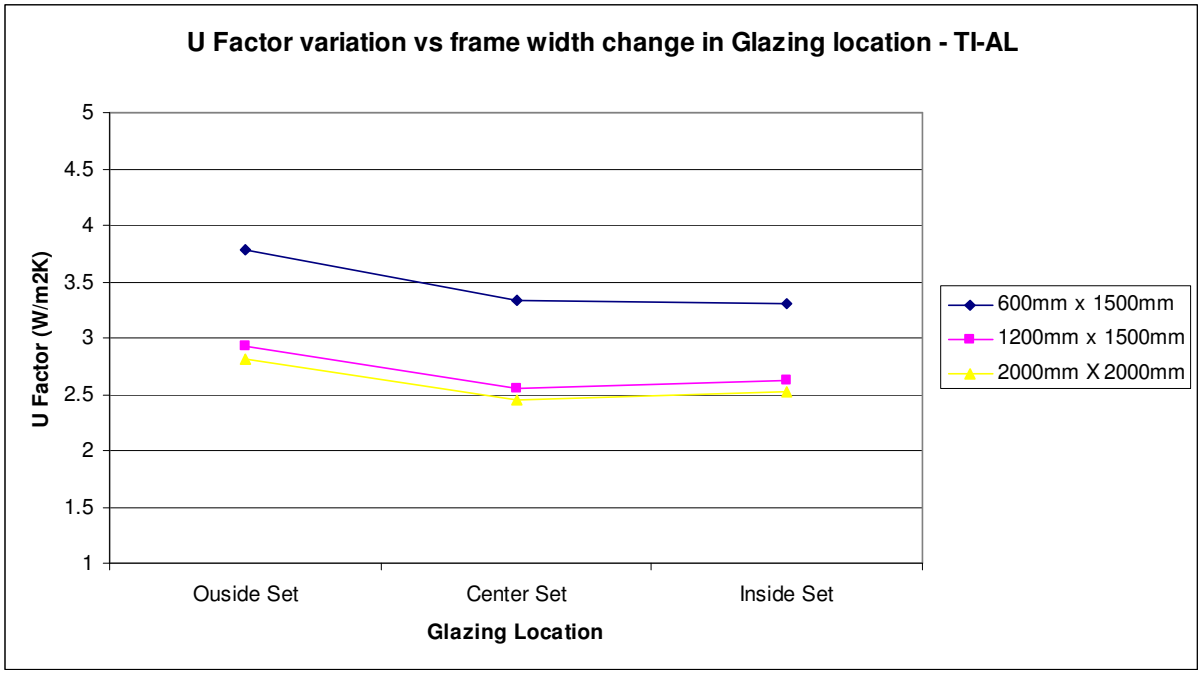


Figure B.1: U factor variation with glazing location for Thermally Improved Aluminum window

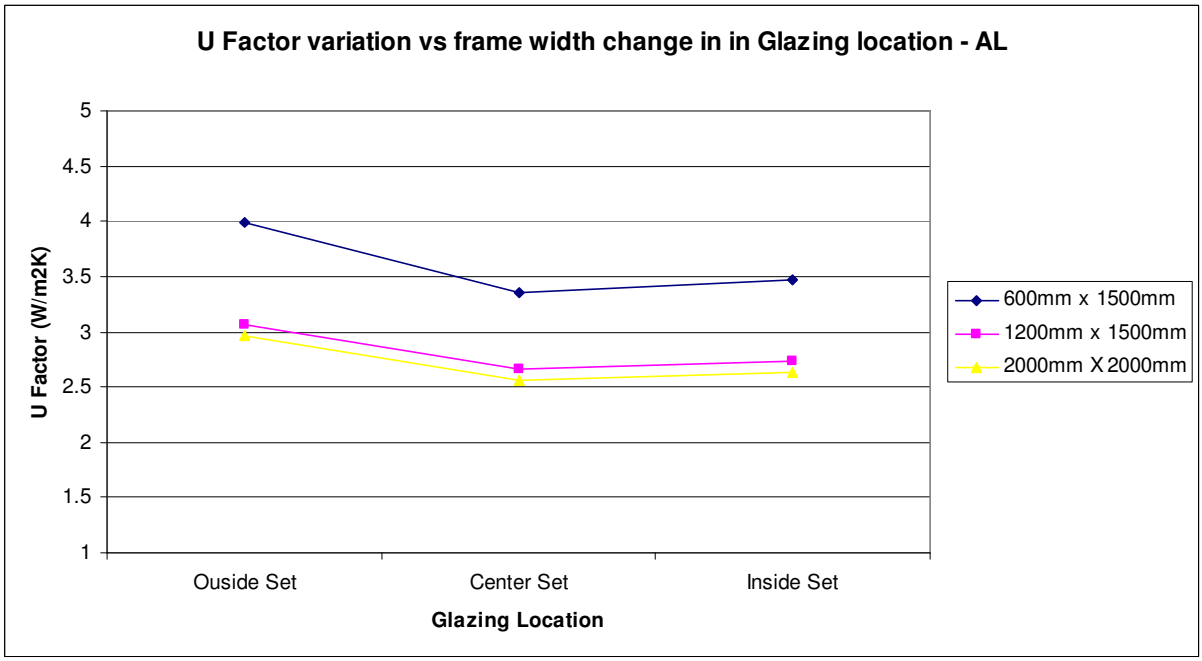


Figure B.2: U factor variation with glazing location for Aluminum window

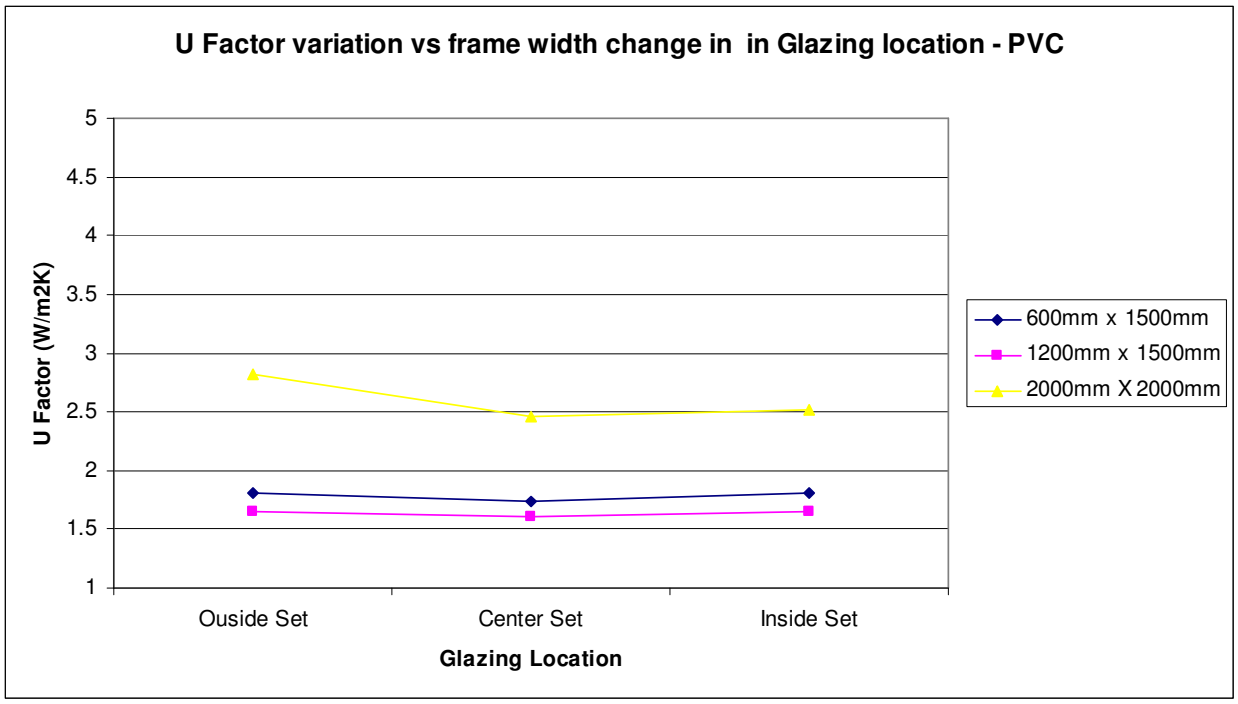


Figure B.3: U factor variation with glazing location for PVC window

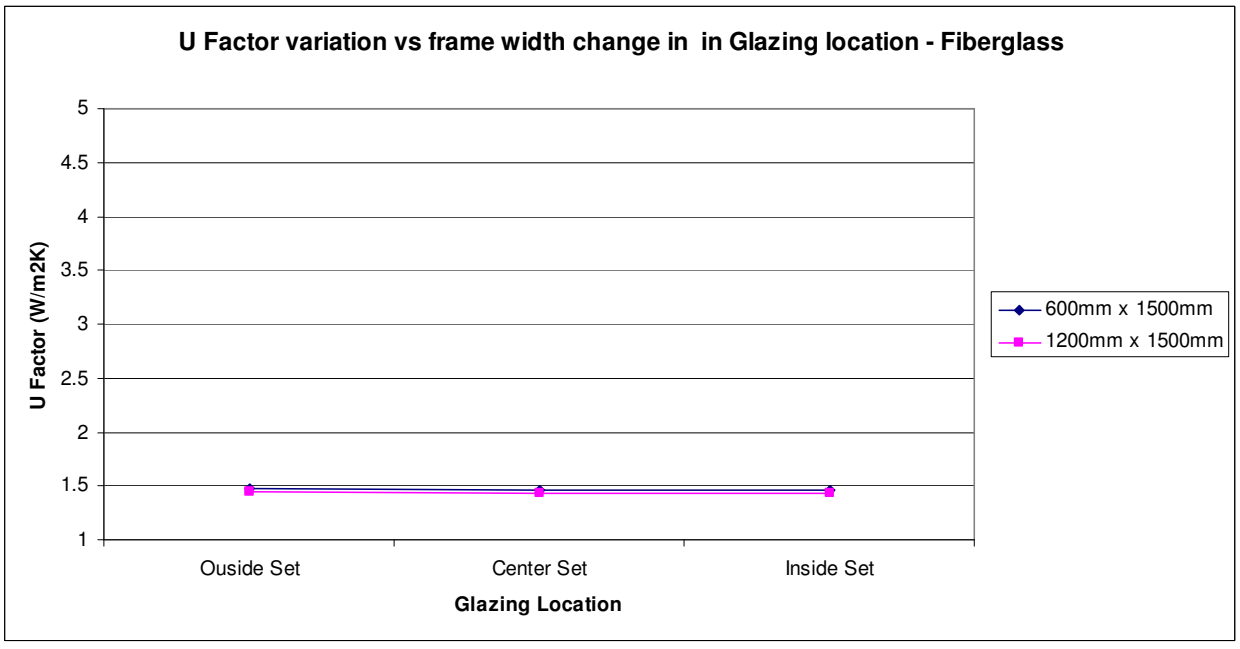


Figure B.4: U factor variation with glazing location for Wood window

B. Change in frame wall thickness

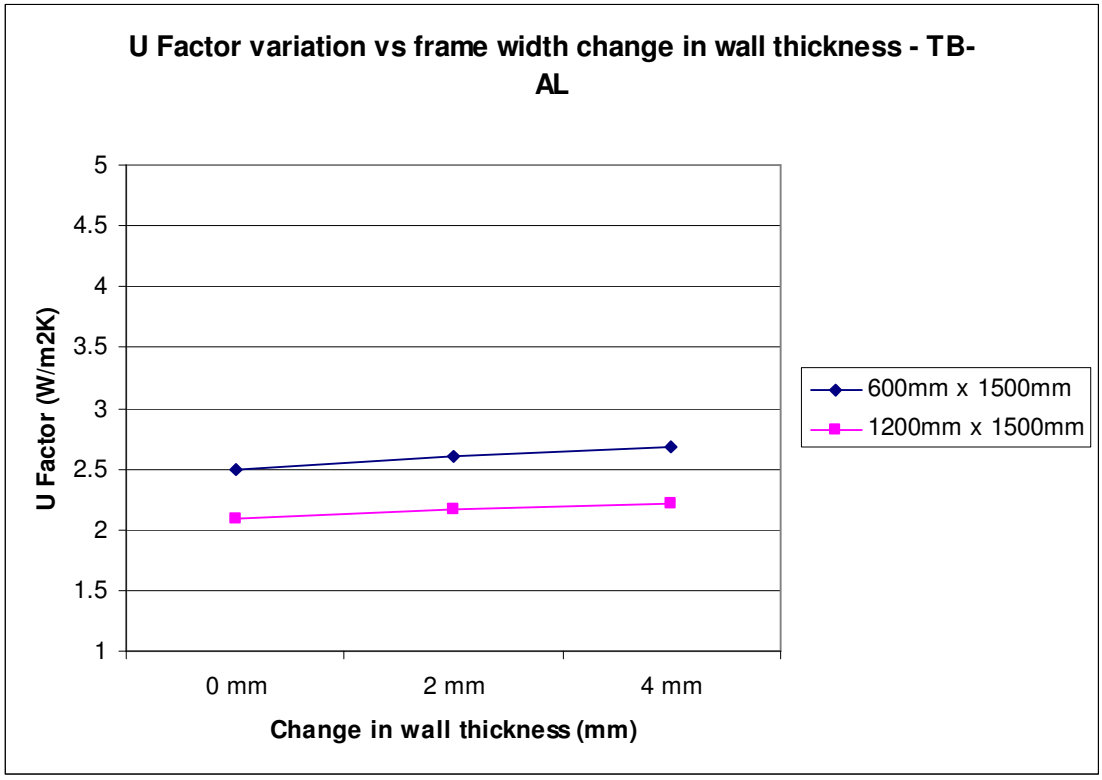


Figure B.5: U factor variation with frame wall thickness for Thermally Broken Aluminum Window

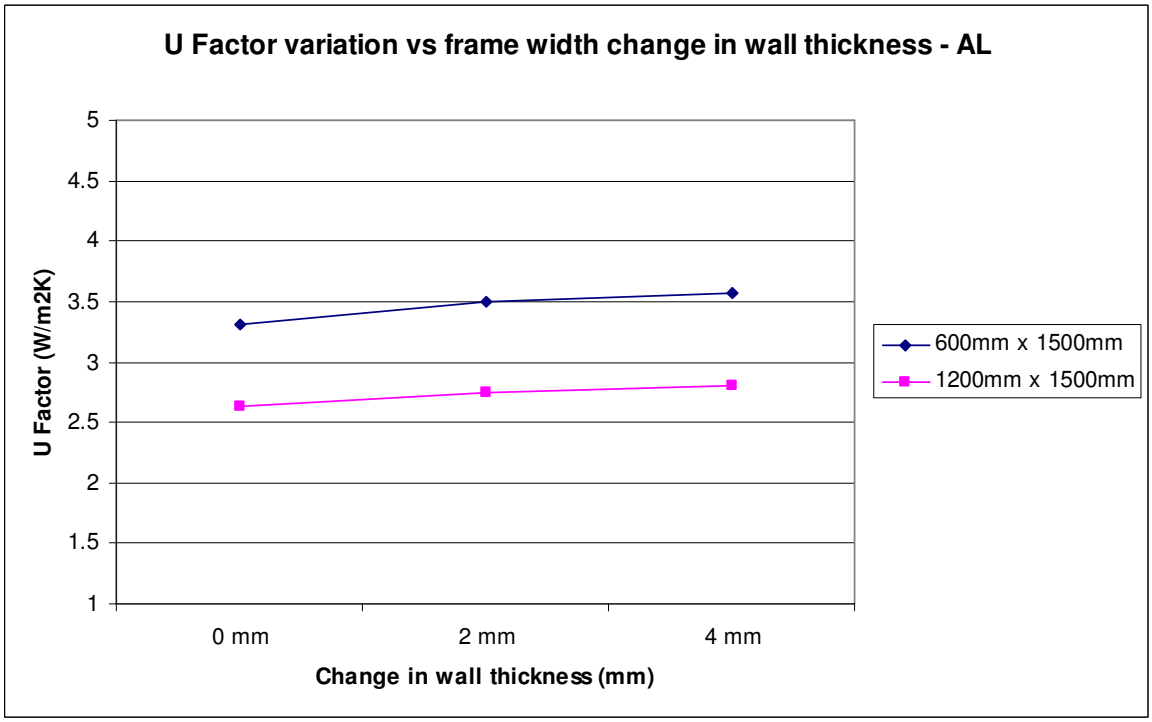


Figure B.6: U factor variation with frame wall thickness for Aluminum Window

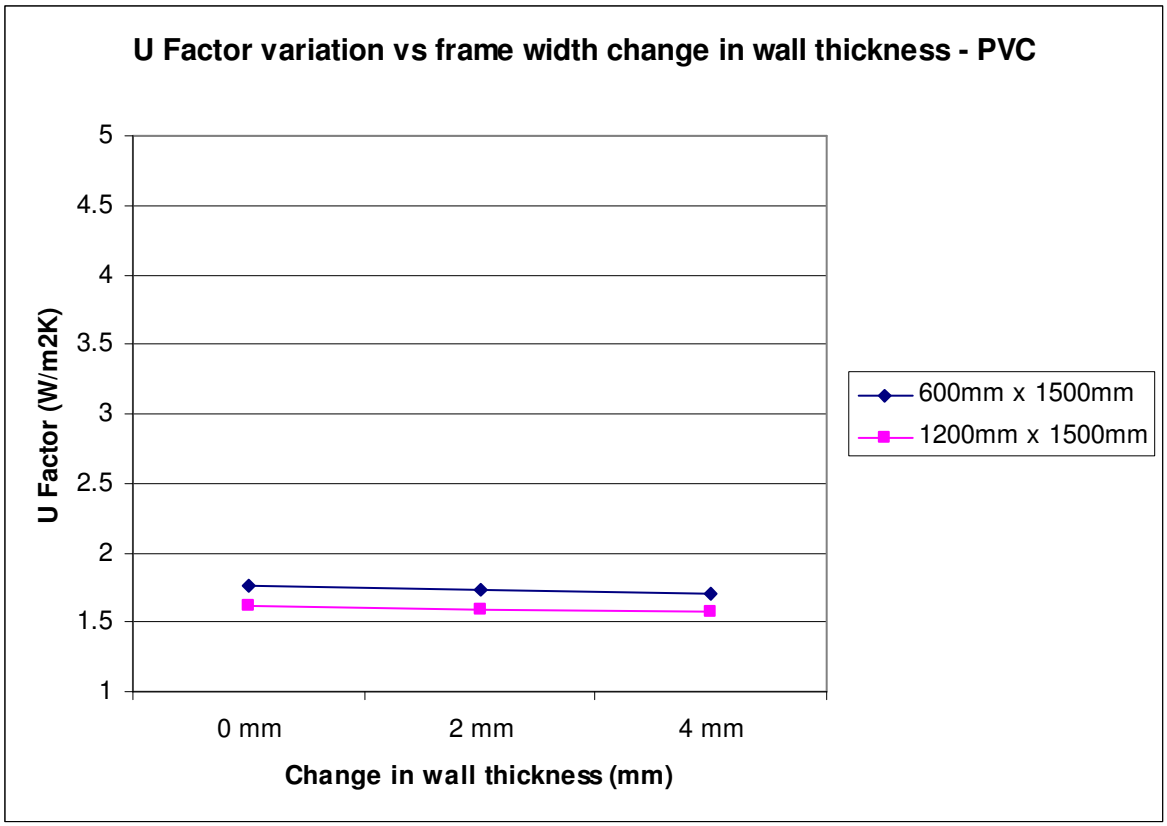


Figure B.7: U factor variation with frame wall thickness for PVC Window

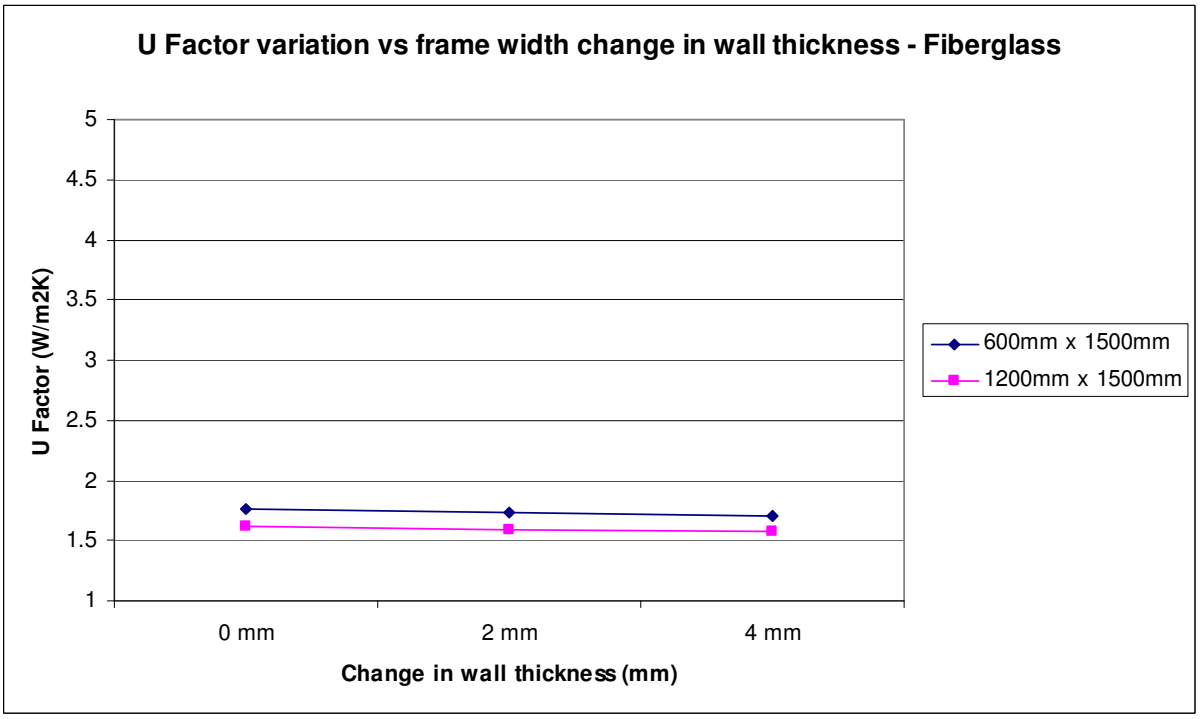


Figure B.8: U factor variation with frame wall thickness for Fiberglass Window

C. Change in Projected Frame Dimension (PFD)

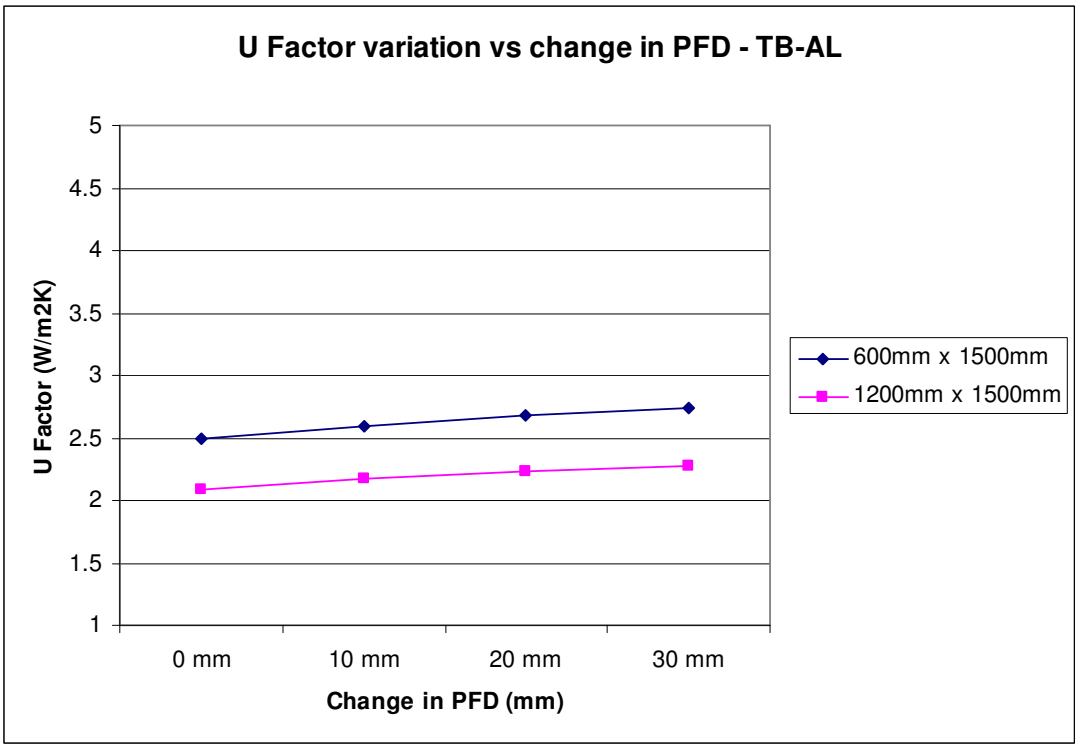


Figure B.9: U factor variation with change in PFD for thermally broken Aluminum window

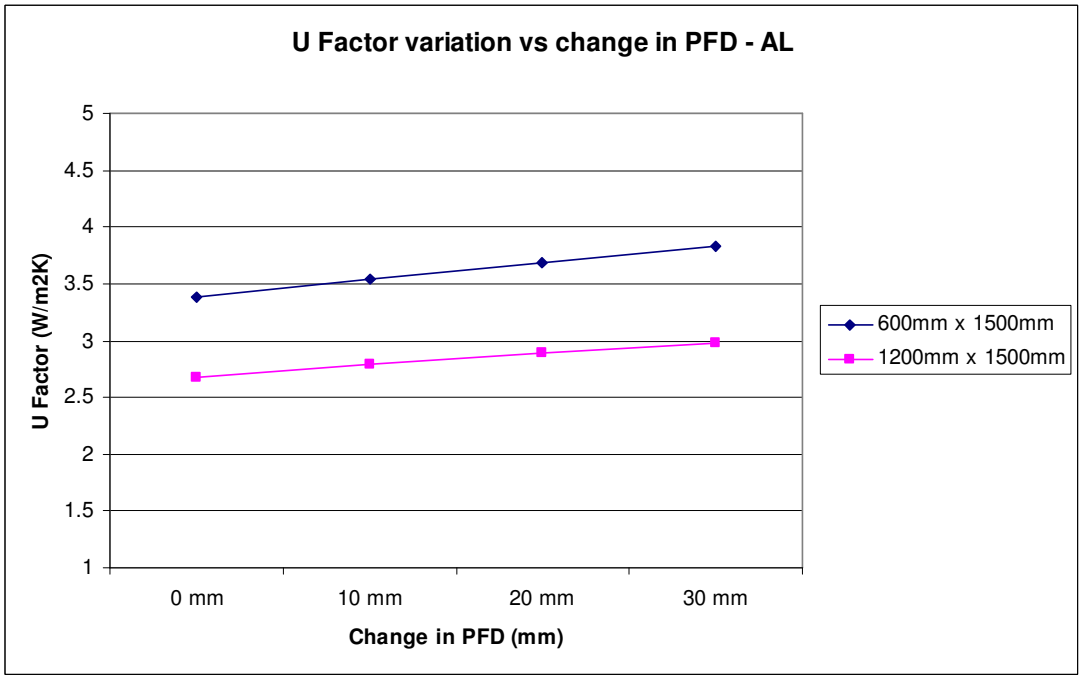


Figure B.10: U factor variation with change in PFD for Aluminum window

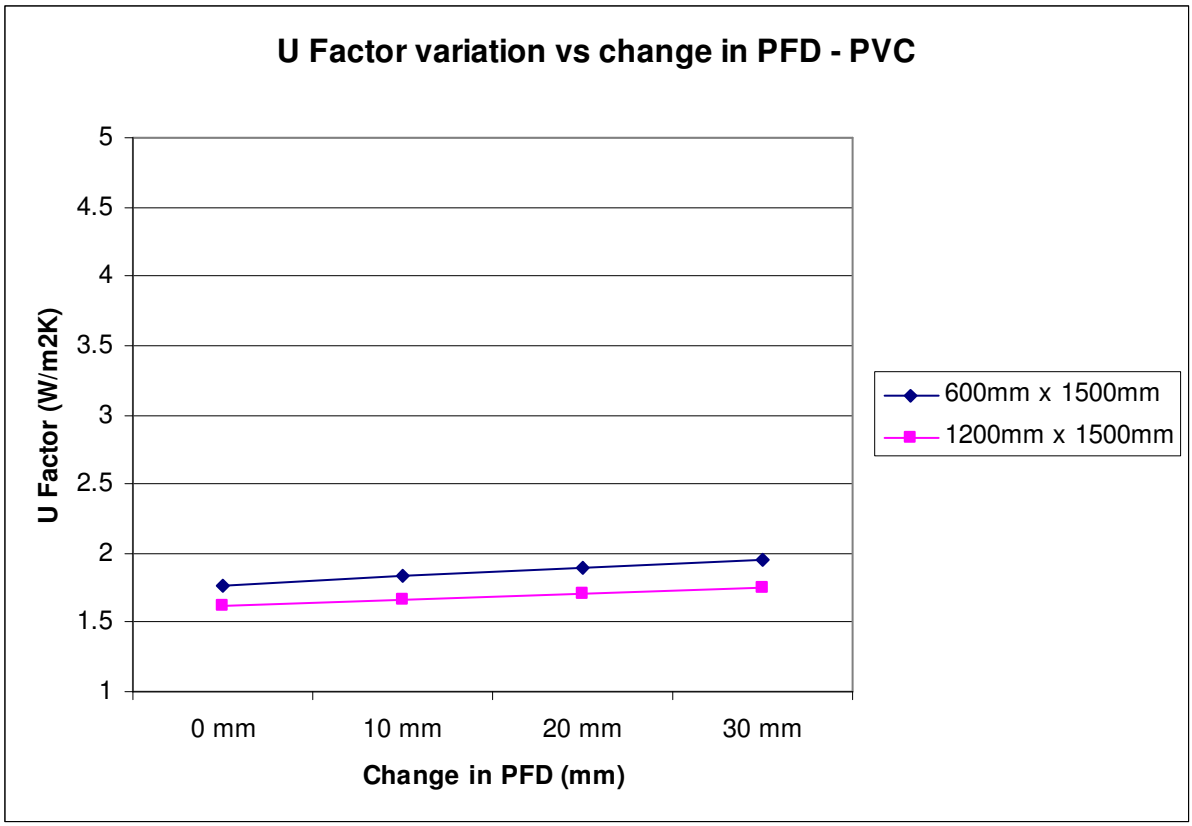


Figure B.11: U factor variation with change in PFD for PVC window

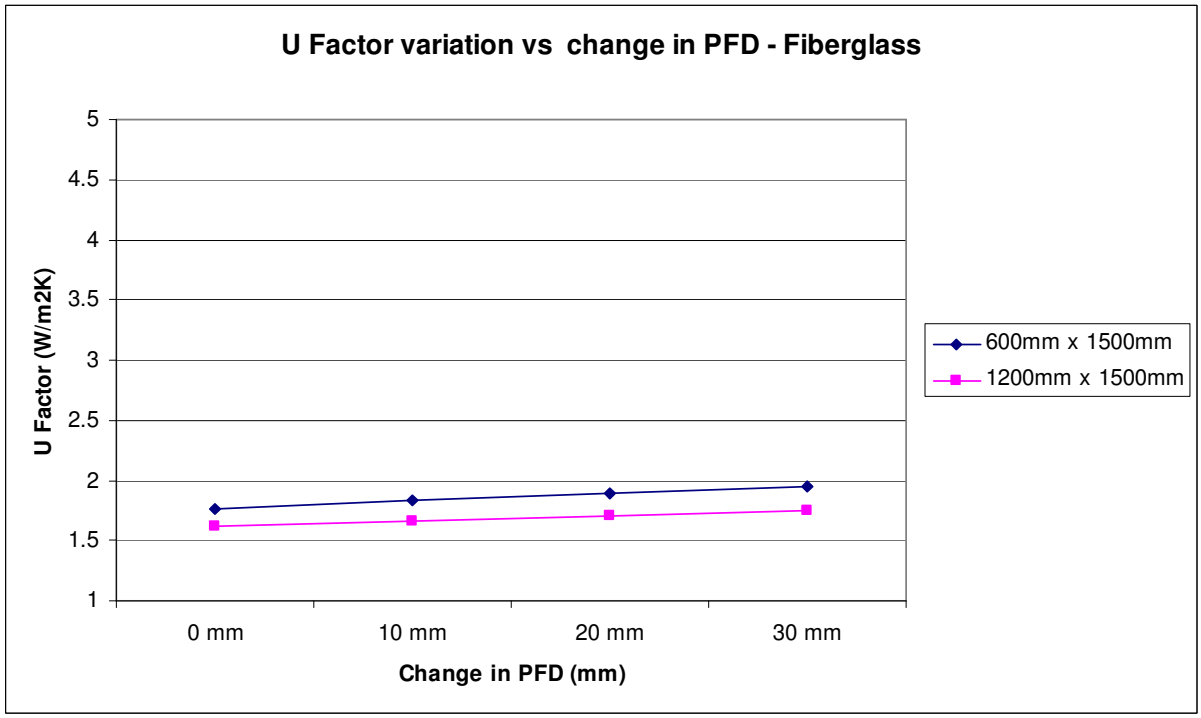


Figure B.12: U factor variation with change in PFD for Fiberglass window

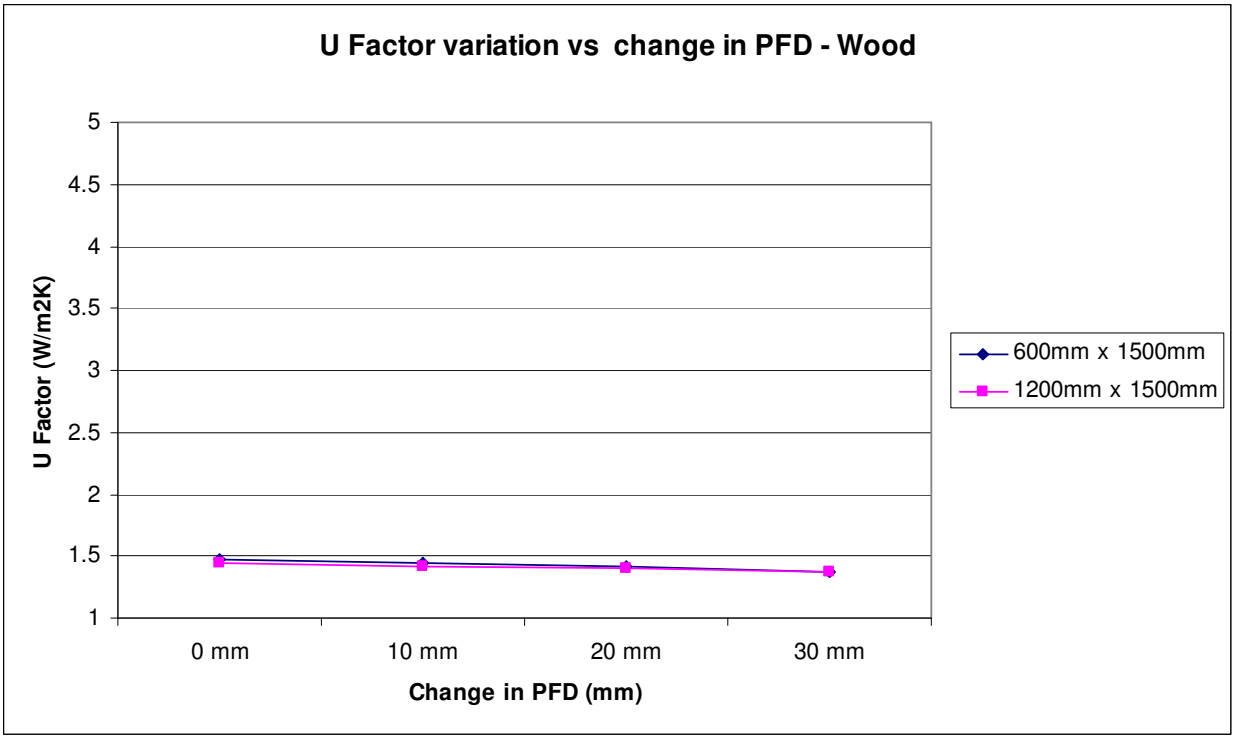


Figure B.13: U factor variation with change in PFD for Wood window

D. Change in frame emissivity

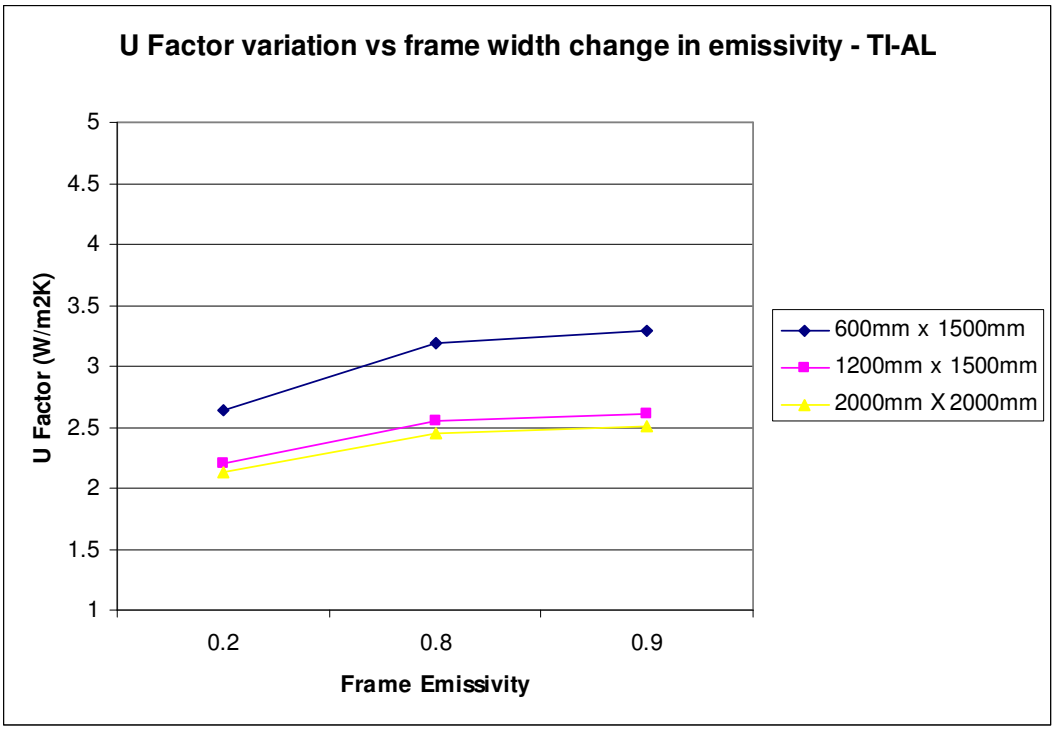


Figure B.13: U factor variation with change emissivity for thermally broken Aluminum window

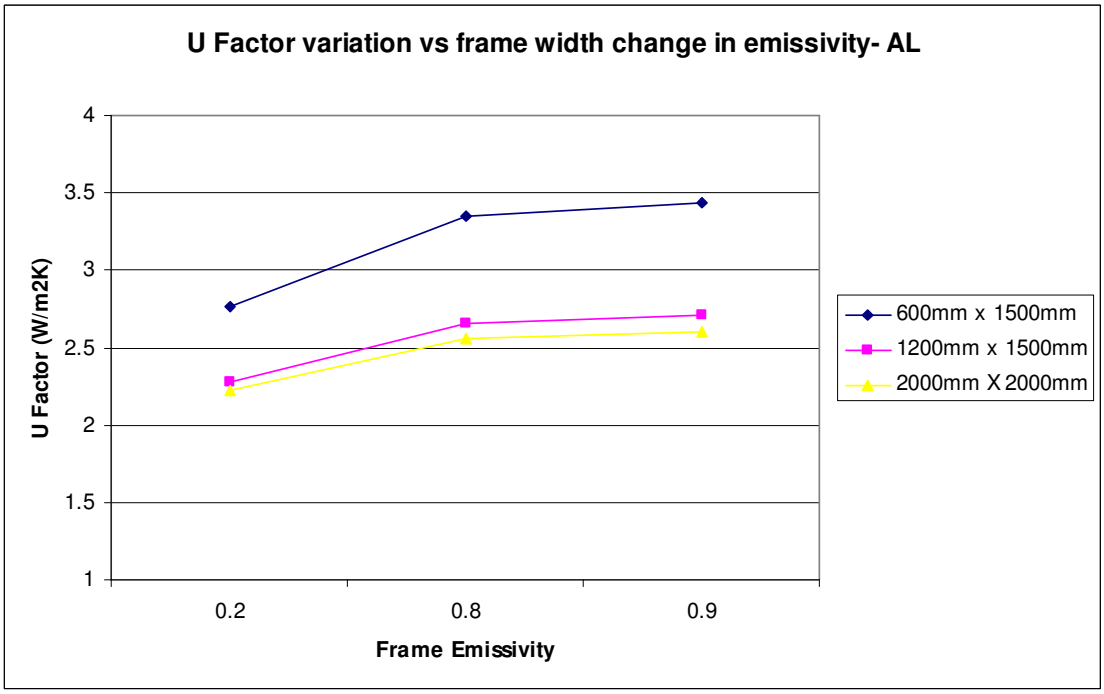


Figure B.14: U factor variation with change emissivity for Aluminum window

E. Webb Addition

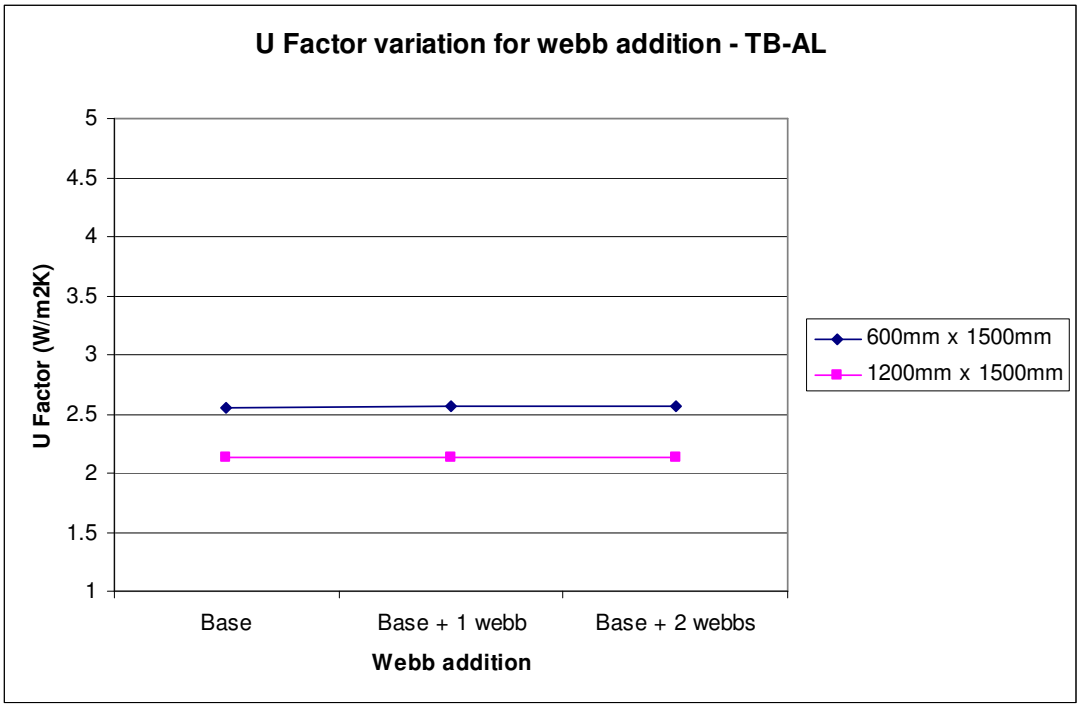


Figure B.15: U factor variation with variation of webb addition for thermally broken Aluminum window

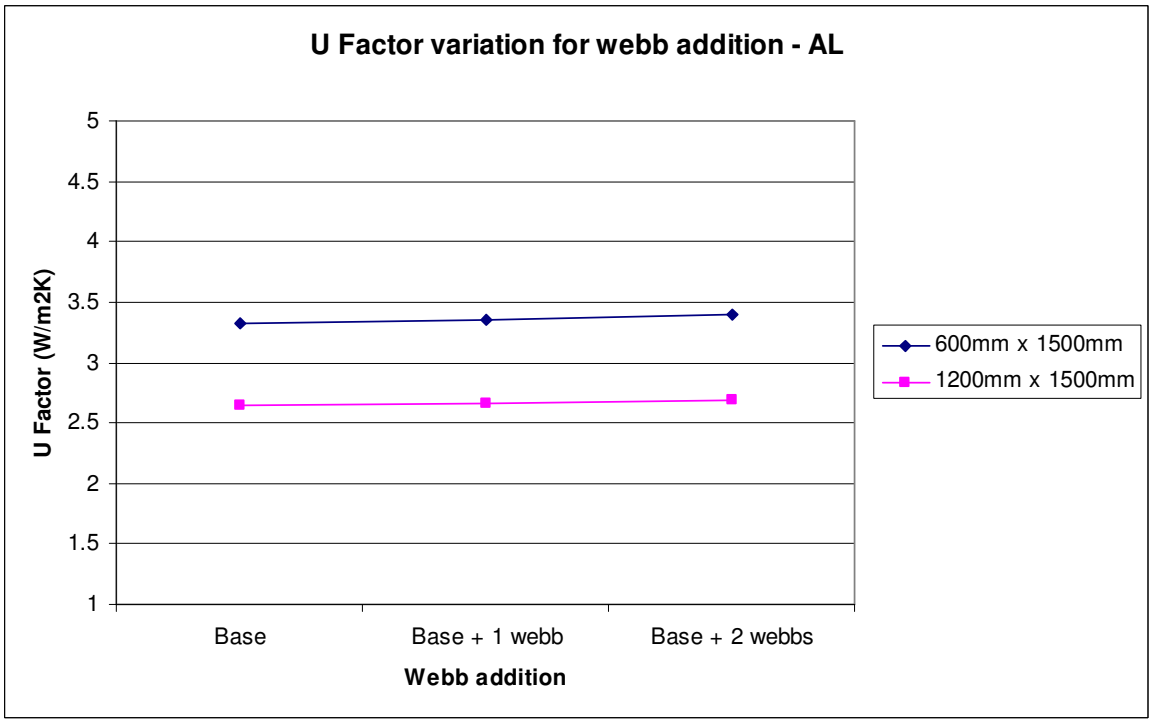


Figure B.16: U factor variation with variation of web addition for Aluminum window

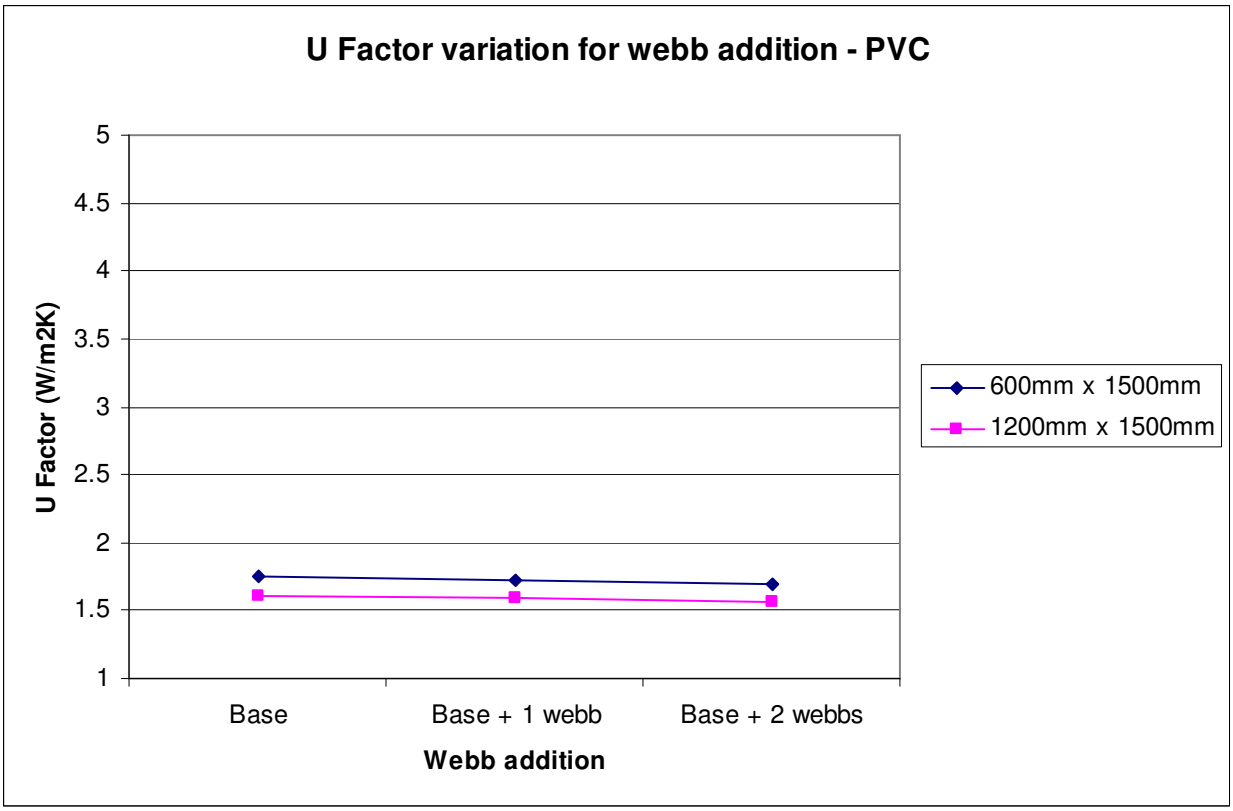


Figure B.17: U factor variation with variation of web addition for PVC window

Project 1.1.14

Project Name:	Component Modeling Approach Condensation Resistance Research
Date:	April 9, 2010
Purpose:	Develop a Component Modeling Approach (CMA) simulation procedure for Condensation Resistance so it can be used in conjunction with the CMA methodology currently being developed for U-factor, SHGC, and VT.

Project Summary:

- Identify leading factors used in the calculation of Condensation Resistance indices of fenestration products.
- Investigate similarities and differences between NFRC Condensation Resistance and AAMA *CRF*. The IG spacer plays an important role in the ability of a fenestration product to resist condensation.
- Investigation of how well the effective conductivity of the spacer assembly represents the local temperature distribution on the interior side of fenestration systems will be required.
- Evaluate if further assumptions need to be made in terms of spacer and spacer assembly representation for the purpose of Condensation Resistance calculations. Identify representative fenestration products that will be used in the validation of this procedure.
- The new Condensation Resistance procedure should be relatively easily implemented into existing computer tools so that the same *"bucket"* approach, used for U-factor, SHGC, and VT, can be utilized.
- Identify any potential issues with the existing algorithms in THERM and WINDOW, in terms of component calculations and recommended changes so that the new procedure could be implemented in the NFRC Product Certification Program.

Click here for latest interim report

Web link:
http://www.nfrc.org/CMACRBRTG.aspx

Carli, Inc.

18 Tanglewood Rd.
Amherst, MA 01002

TEL: (413) 256-4647
FAX: (413) 256-4823

carli@fenestration.com
http://www.fenestration.com

Progress Report:

Development of Condensation Resistance Procedure for the Component Modeling Approach

Report prepared for: **NFRC PMTG**

Report prepared by: **Dr. Charlie Curcija**

April 9, 2010

TABLE OF CONTENTS

TASK 1: IDENTIFICATION OF LEADING FACTORS FOR THE CALCULATION OF CONDENSATION RESISTANCE..... **Error! Bookmark not defined.**
SELECTION OF REPRESENTATIVE SPECIMENS ... **Error! Bookmark not defined.**
Framing Systems: ..... **Error! Bookmark not defined.**
Glazing Systems: ..... **Error! Bookmark not defined.**
Spacer Systems: ..... **Error! Bookmark not defined.**
STANDARD MODELING CONDITIONS ..... **Error! Bookmark not defined.**
SUMMARY OF THE CALCULATION PROCEDURES FOR CR **Error! Bookmark not defined.**
Frame CR (CR_f): ..... **Error! Bookmark not defined.**
Edge-of-Glass CR (CR_e): ..... **Error! Bookmark not defined.**
Center-of-Glass CR (CR_c): ..... **Error! Bookmark not defined.**
SUMMARY OF THE CALCULATION PROCEDURES FOR CMA.....**Error! Bookmark not defined.**
SELECTION OF RELEVANT PARAMETERS FOR CMA-CR .... **Error! Bookmark not defined.**
APPENDIX A: CALCULATION OF EFFECTIVE CONDUCTIVITIES (k_{eff}) of SPACER ASSEMBLIES: ..... **Error! Bookmark not defined.**

CORRELATION USING *S* VALUES

S values are used for developing correlations, after initial work and analysis showing their potential to be the good choice. S values are calculated from the temperatures where for each relative humidity, the following equation is used:

$$S = \frac{\sum_i \left(t_{dpp} - t\right)^{+} \cdot \Delta L_i}{\left(t_{dpp} - t_o\right) \cdot L} \qquad (1)$$

$^{+}$ = *positive values only*

In the above equations, the following quantities were used:

t_{dp} = Dew point temperatures at the given relative humidity (RH);

$t_{dp,1}$ = 2.9ºC (37.3ºF) @ RH = 30%

$t_{dp,2}$ = 10.3ºC (50.6ºF) @ RH = 50%

$t_{dp,3}$ = 15.4ºC (59.8ºF) @ RH = 70%

t_{dpp} = condensation reference point temperatures, $t_{dpp} = t_{dp} + 0.3^{o}C$ ($t_{dpp} = t_{dp} + 0.5^{o}F$)

$t_{dpp,1}$ = *3.2* ºC (37.8ºF)

$t_{dpp,2}$ = *10.6* ºC (51.1ºF)

$t_{dpp,3}$ = *15.7* ºC (60.3ºF)

t_o = exterior ambient temperature $-18^{o}C(0^{o}F)$

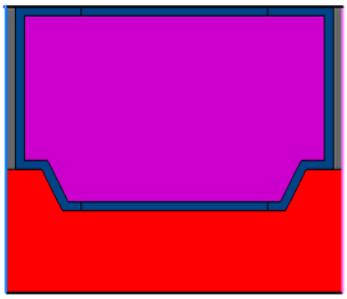
t_i = average temperature of the frame or edge of glazing segments, *i*

ΔL_i = length of subdivided segments

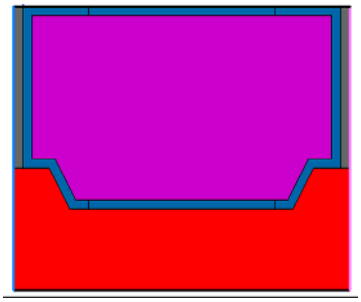
L = total (wetted) length of each section (i.e., frame, edge of glazing),

Note: all segments are located on the indoor facing boundary

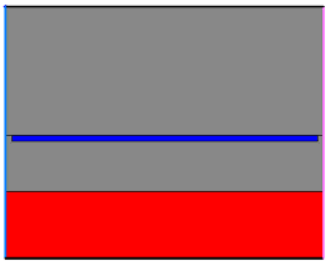
Spacer Systems:



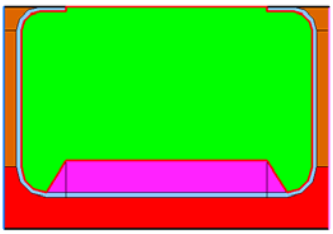
S1



S2



S3



S4



S5



S6

Framing System 1:

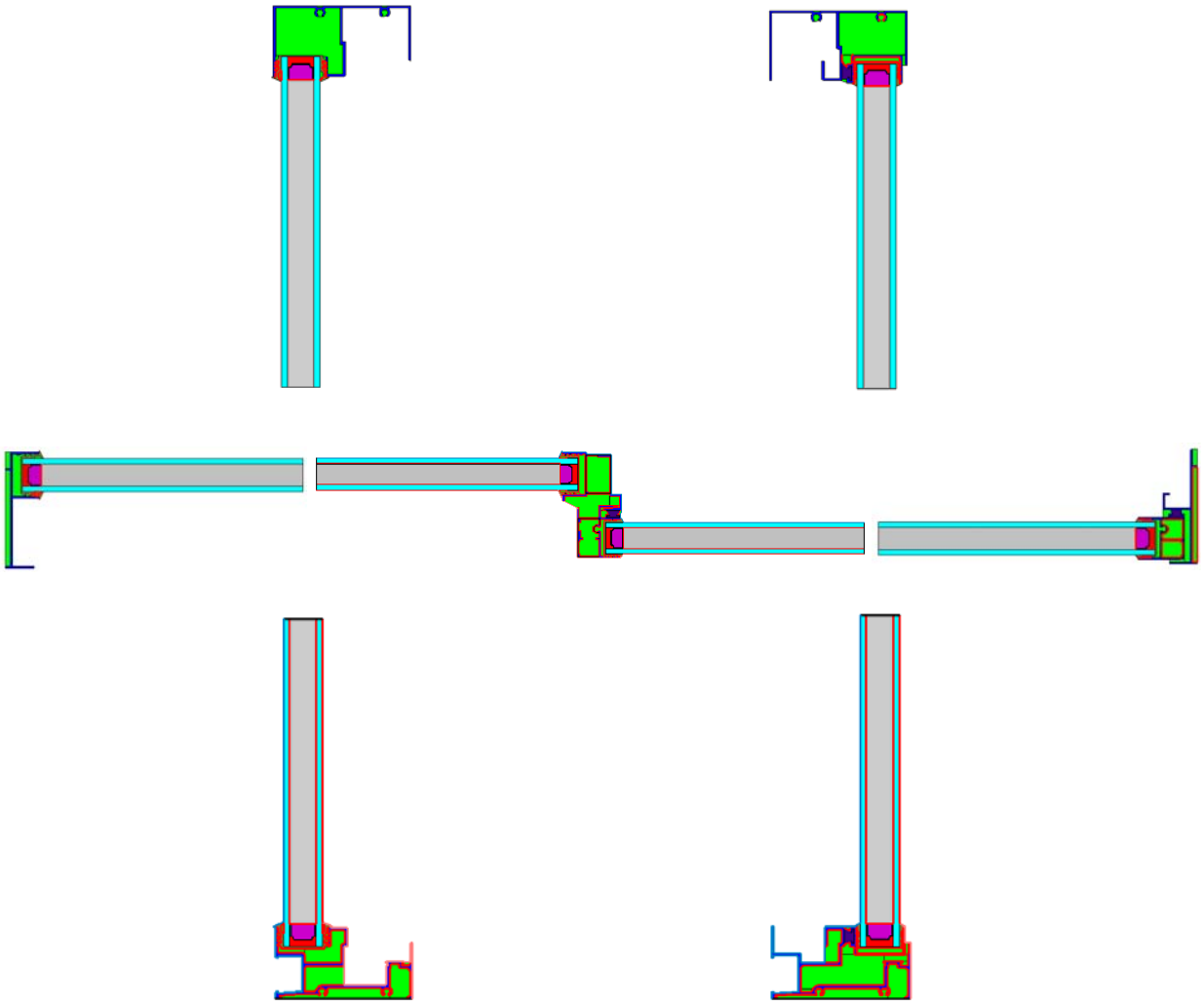


Figure 1. Framing System 1 (F1)

Spacer ID	DG k_{eff} W/m·K	TG k_{eff} W/m·K
S1	2.321	1.316
S2	1.757	1.124
S3	0.855	0.528
S4	0.402	0.346
S5	0.245	0.245
S6	0.181	0.181

Figure 2. Spacer Performance in Framing System 1 (F1)

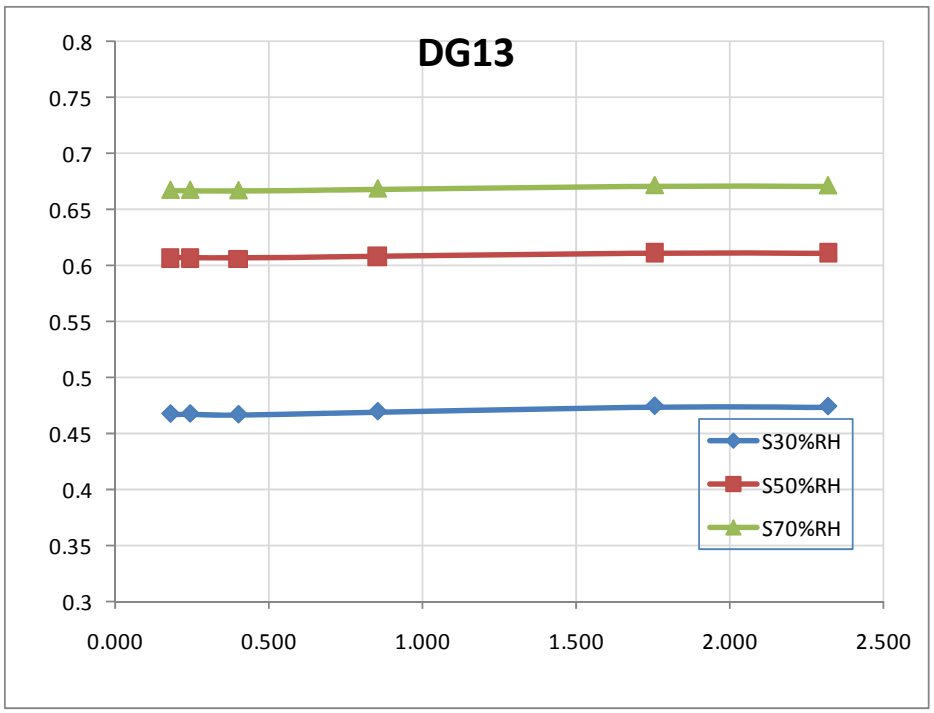


Figure 3. Plot of *S* vs. Spacer Effective Conductivity for Sill Fixed – Frame with Glazing System 3

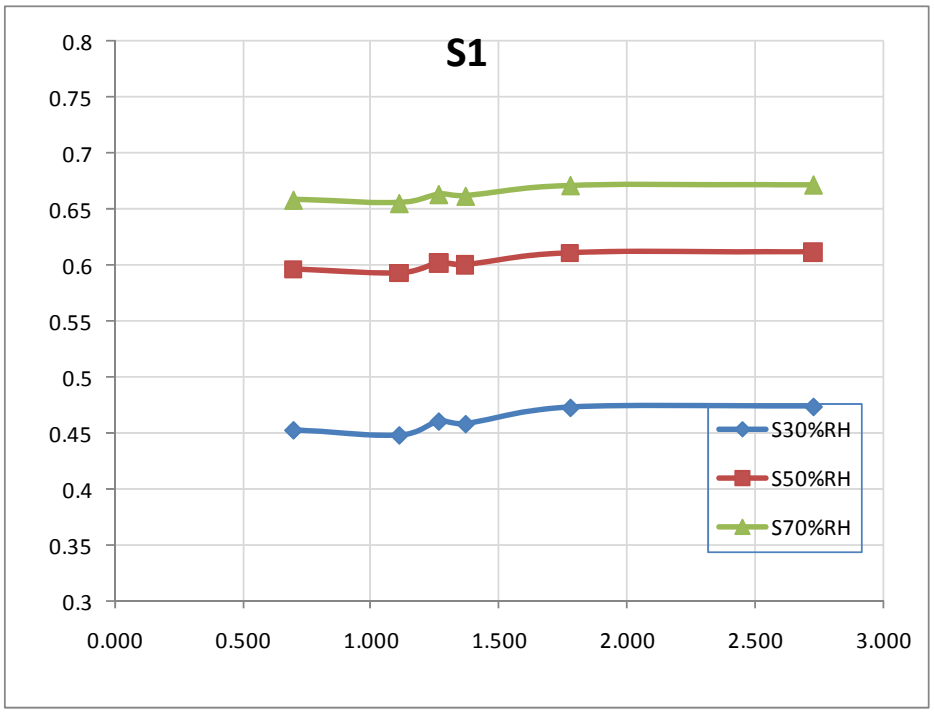


Figure 4. Plot of *S* vs. Glazing U-factor for Sill Fixed – Frame with Spacer System 1

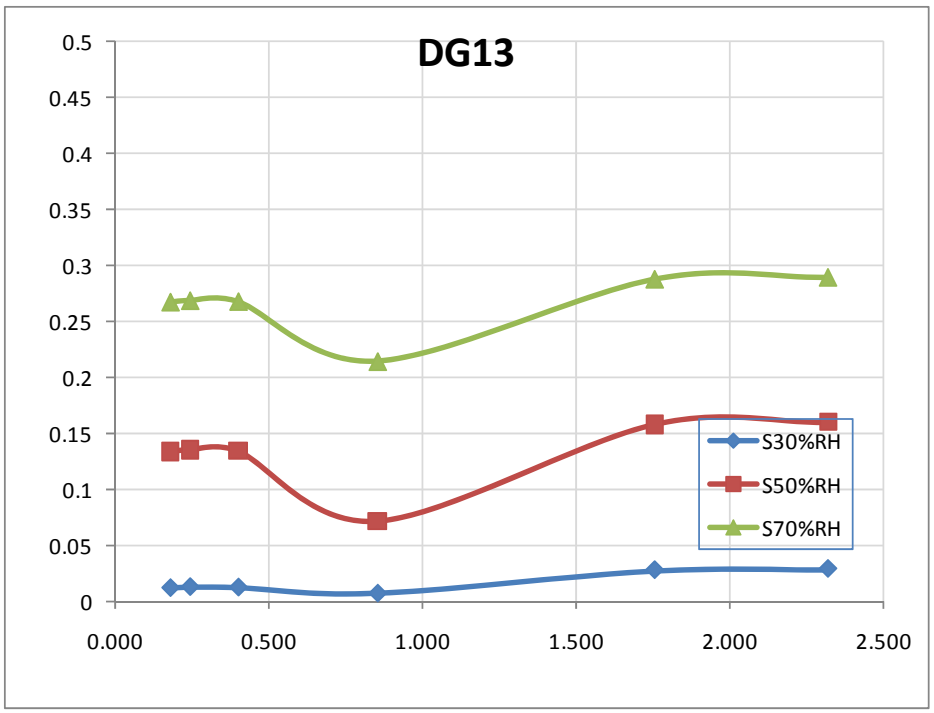


Figure 5. Plot of *S* vs. Spacer Effective Conductivity for Sill Fixed – Edge with Glazing System 3

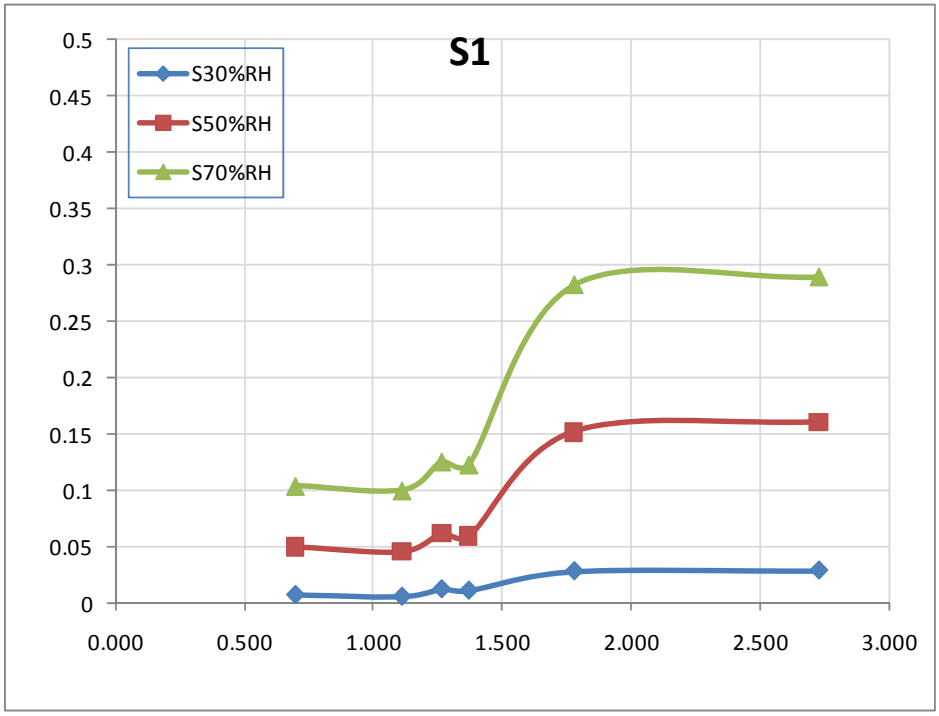


Figure 6. Plot of *S* vs. Glazing U-factor for Sill Fixed – Edge with Spacer System 1

Framing System 2:

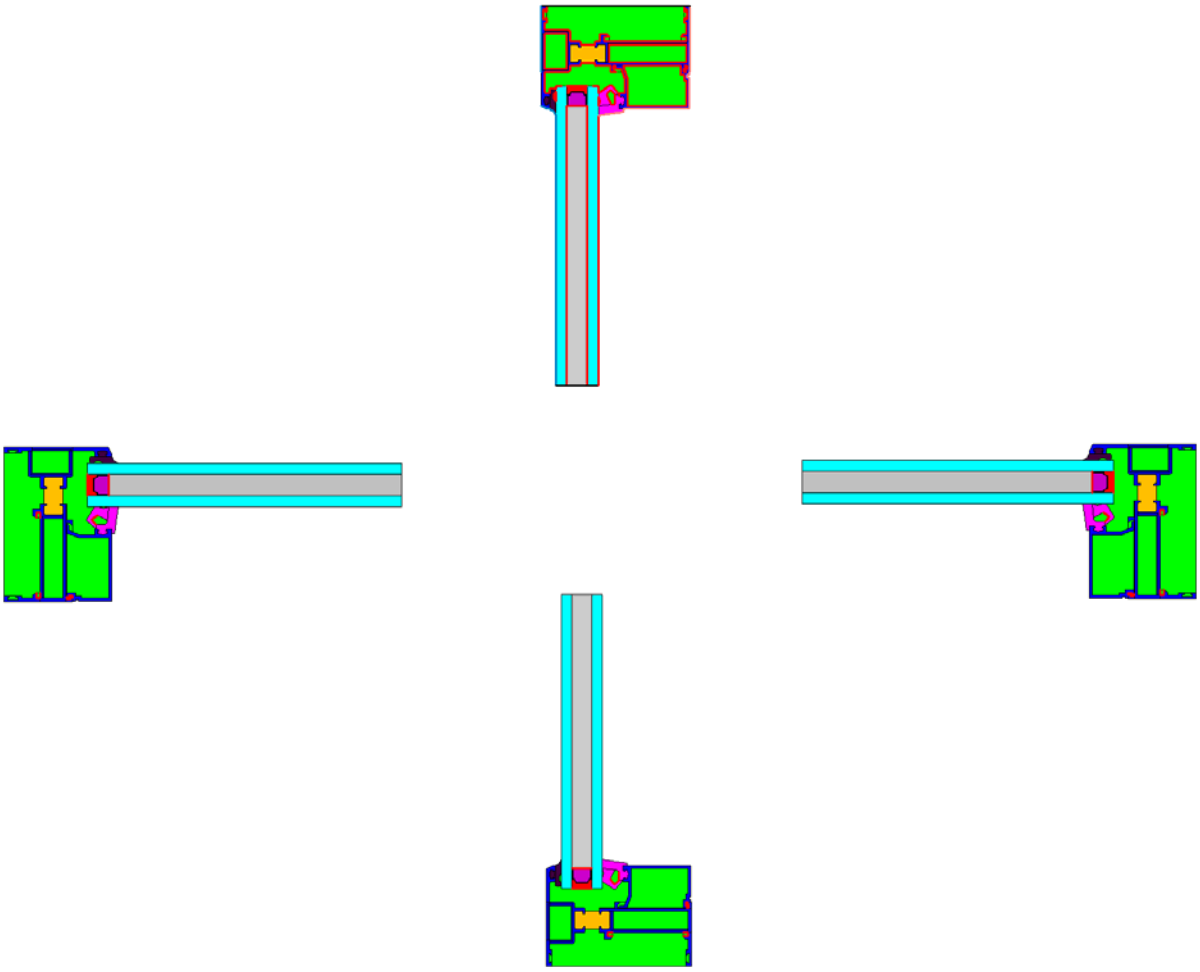


Figure 7. Framing System 2 (F2)

Spacer ID	DG k_{eff} W/m·K	TG k_{eff} W/m·K
S1	2.068	1.661
S2	1.612	1.359
S3	0.766	0.633
S4	0.391	0.369
S5	0.245	0.245
S6	0.181	0.181

Figure 8. Spacer Performance in Framing System 2 (F2)

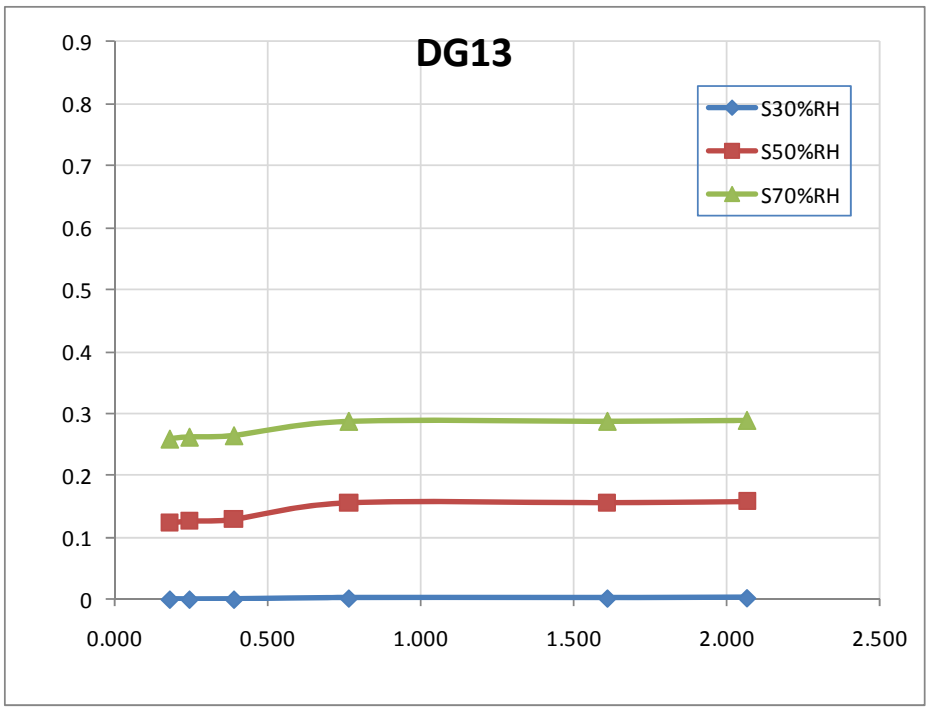


Figure 9. Plot of *S* vs. Spacer Effective Conductivity for Sill Fixed – Frame with Glazing System 3

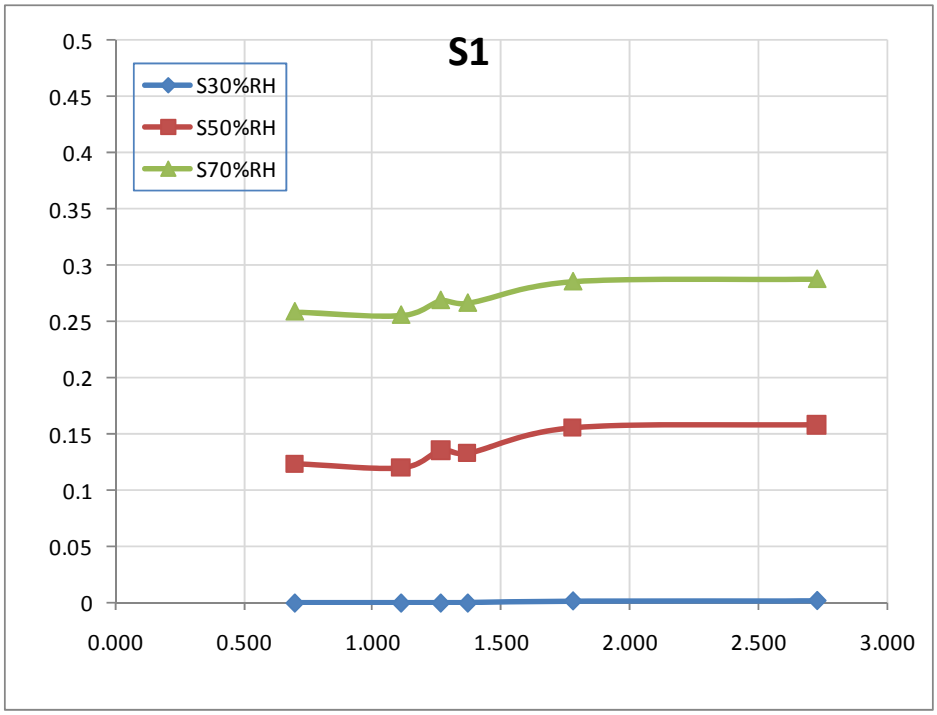


Figure 10. Plot of *S* vs. Glazing U-factor for Sill Fixed – Frame with Spacer System 1

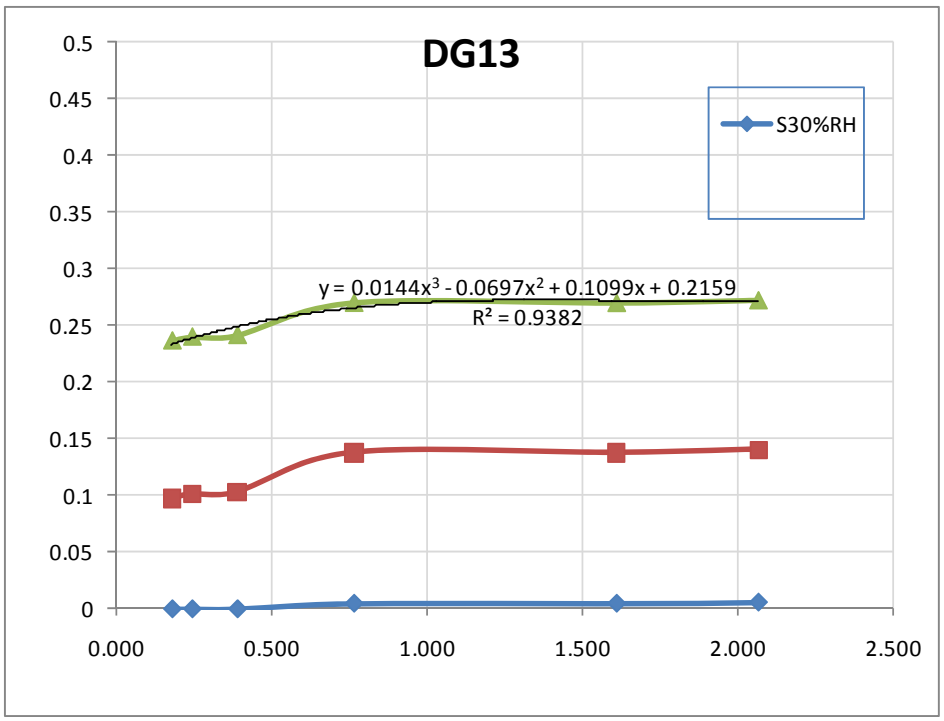


Figure 11. Plot of *S* vs. Spacer Effective Conductivity for Sill Fixed – Edge with Glazing System 3

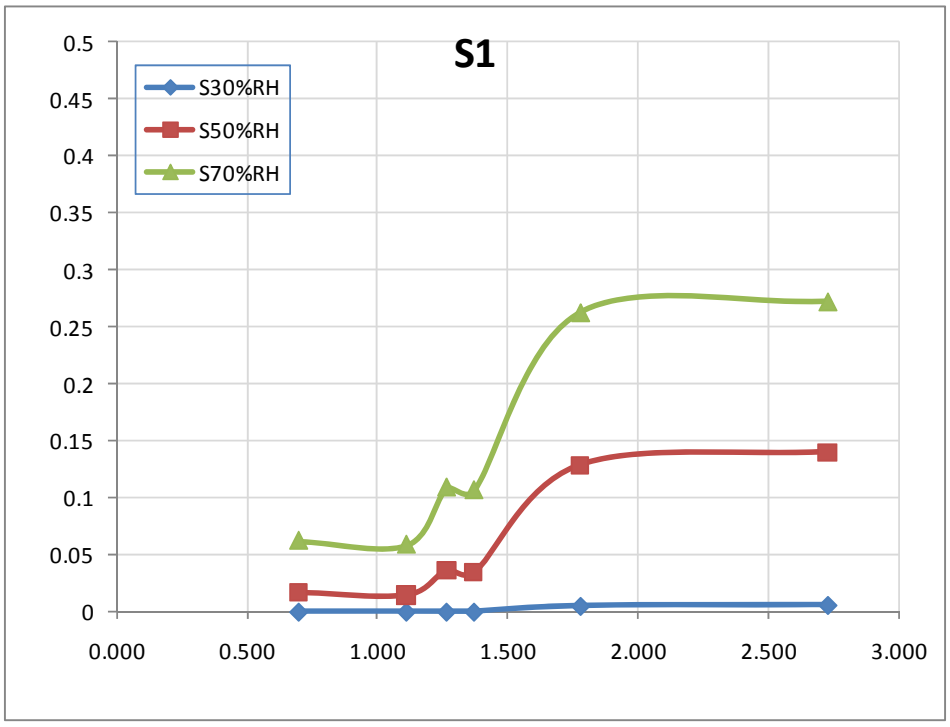


Figure 12. Plot of *S* vs. Glazing U-factor for Sill Fixed – Edge with Spacer System 1

Framing System 3:

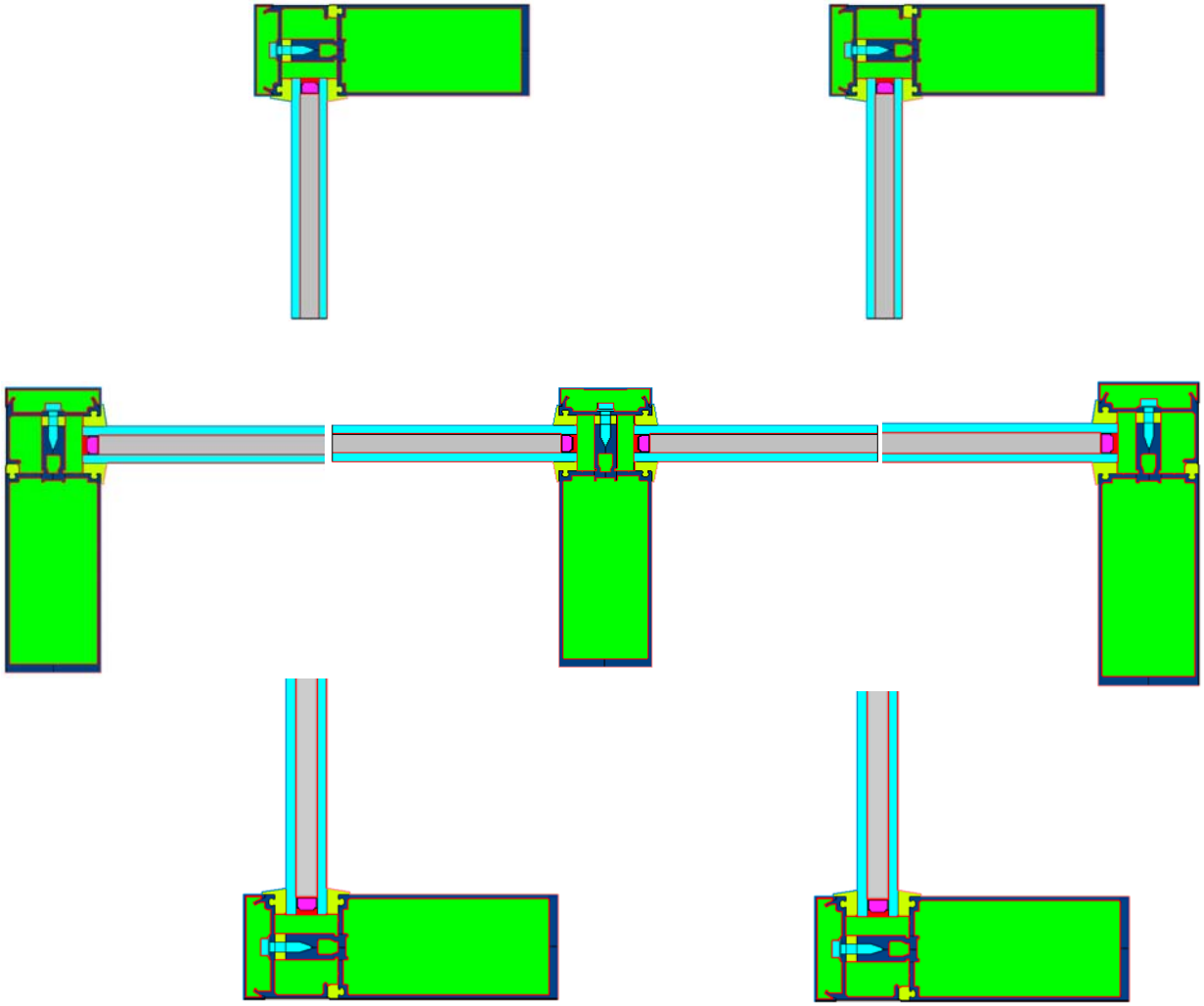


Figure 13. Framing System 3 (F3)

	DG	TG
Spacer ID	k_{eff}	k_{eff}
	W/m?K	W/m?K
S1	2.278	1.288
S2	1.744	1.109
S3	0.839	0.519
S4	0.400	0.344
S5	0.245	0.245
S6	0.181	0.181

Figure 14. Spacer Performance in Framing System 3 (F3)

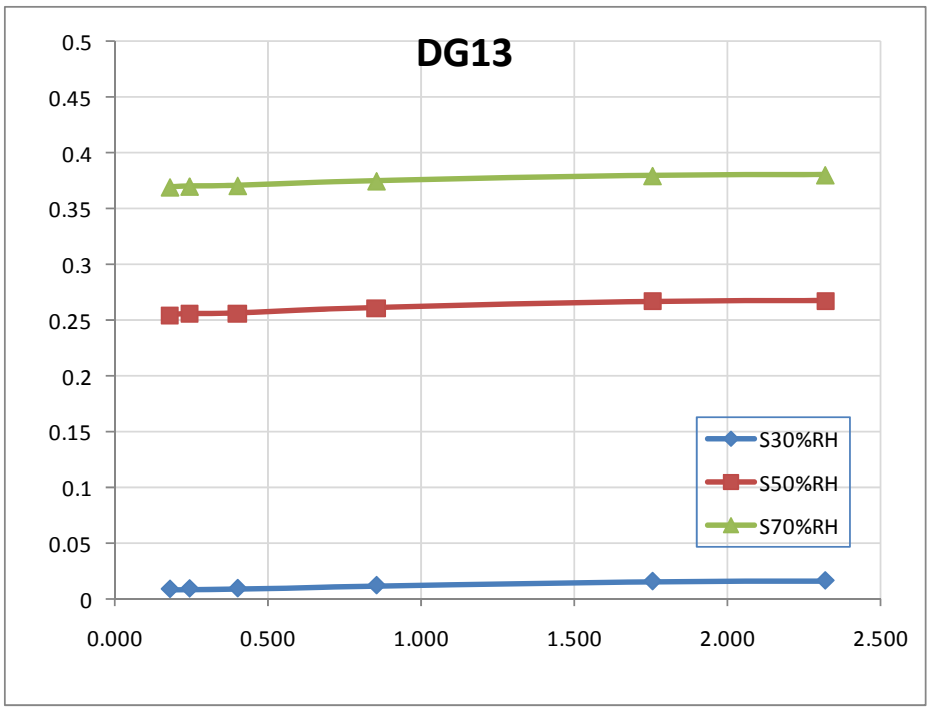


Figure 15. Plot of *S* vs. Spacer Effective Conductivity for Sill Fixed – Frame with Glazing System 3

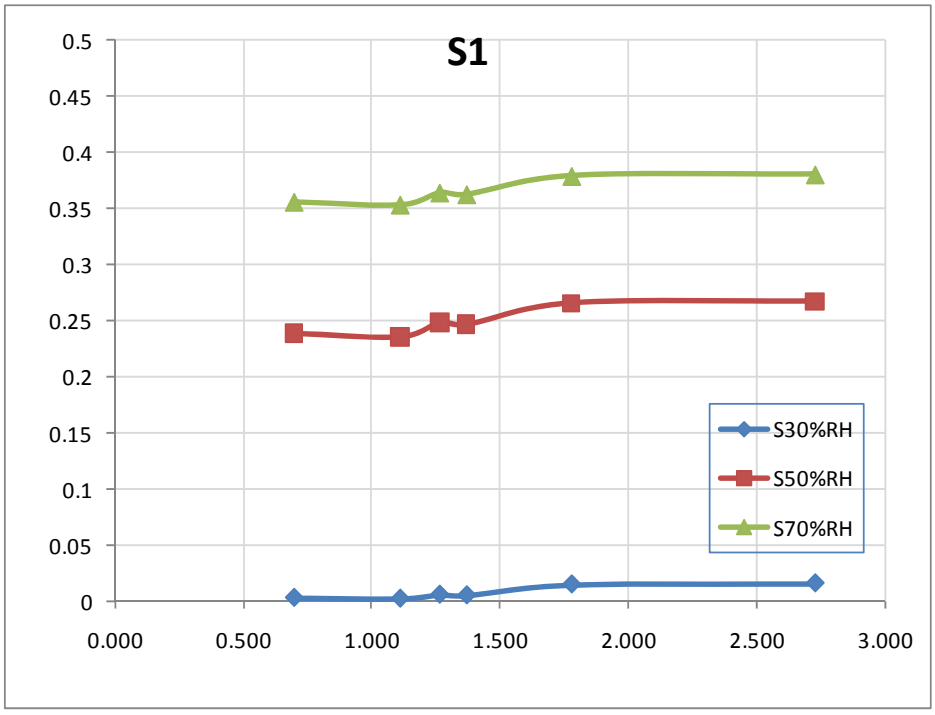


Figure 16. Plot of *S* vs. Glazing U-factor for Sill Fixed – Frame with Spacer System 1

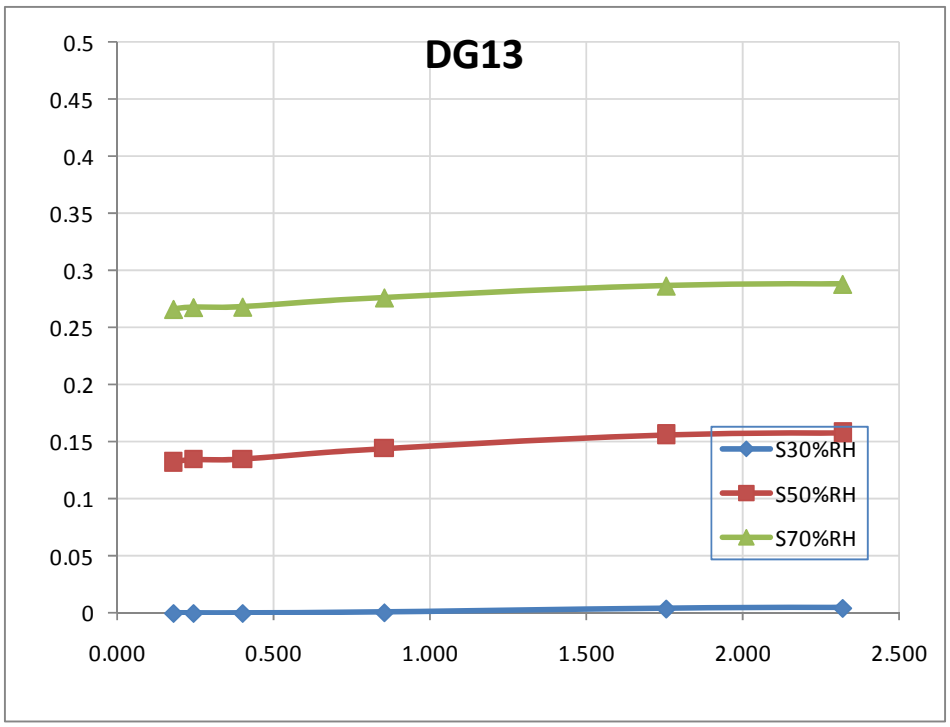


Figure 17. Plot of *S* vs. Spacer Effective Conductivity for Sill Fixed – Edge with Glazing System 3

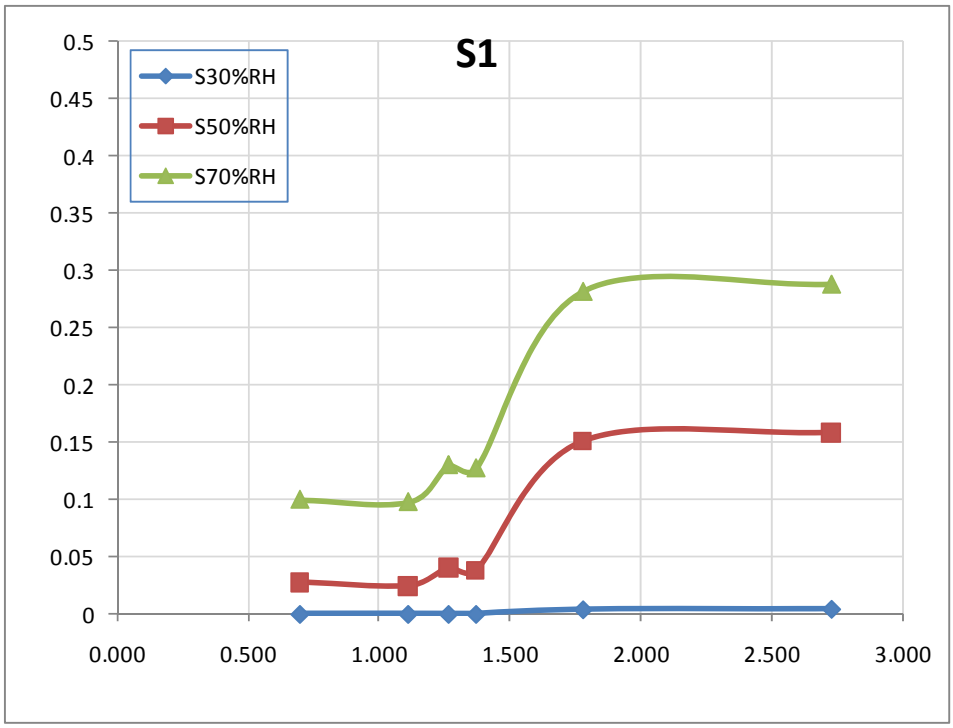


Figure 18. Plot of *S* vs. Glazing U-factor for Sill Fixed – Edge with Spacer System 1

Framing System 4:

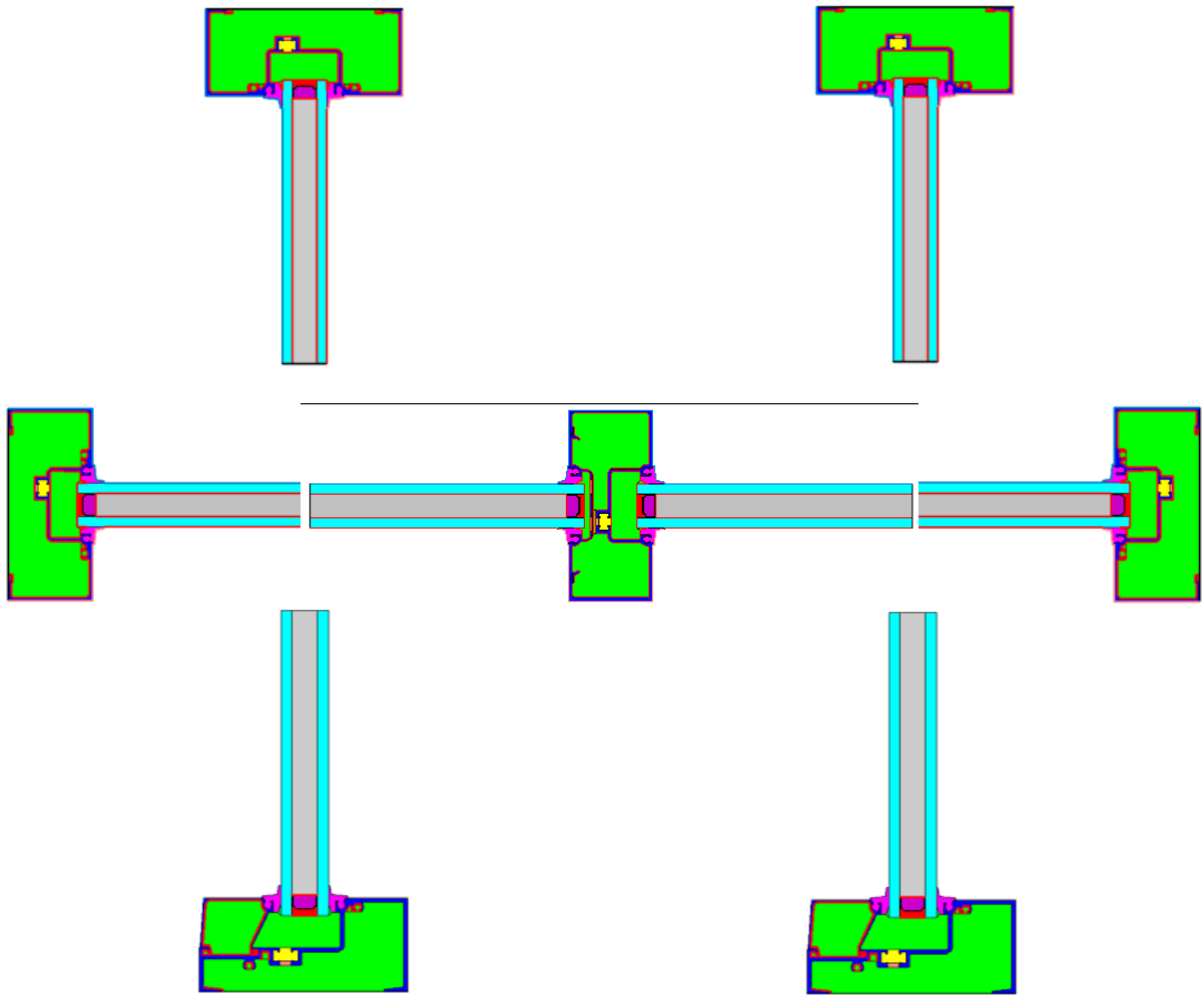


Figure 19. Framing System 4 (F4)

Spacer ID	k_{eff}	k_{eff}
	W/m·K	W/m·K
S1	2.451	1.394
S2	1.829	1.178
S3	0.900	0.550
S4	0.407	0.352
S5	0.245	0.245
S6	0.181	0.181

Figure 20. Spacer Performance in Framing System 4 (F4)

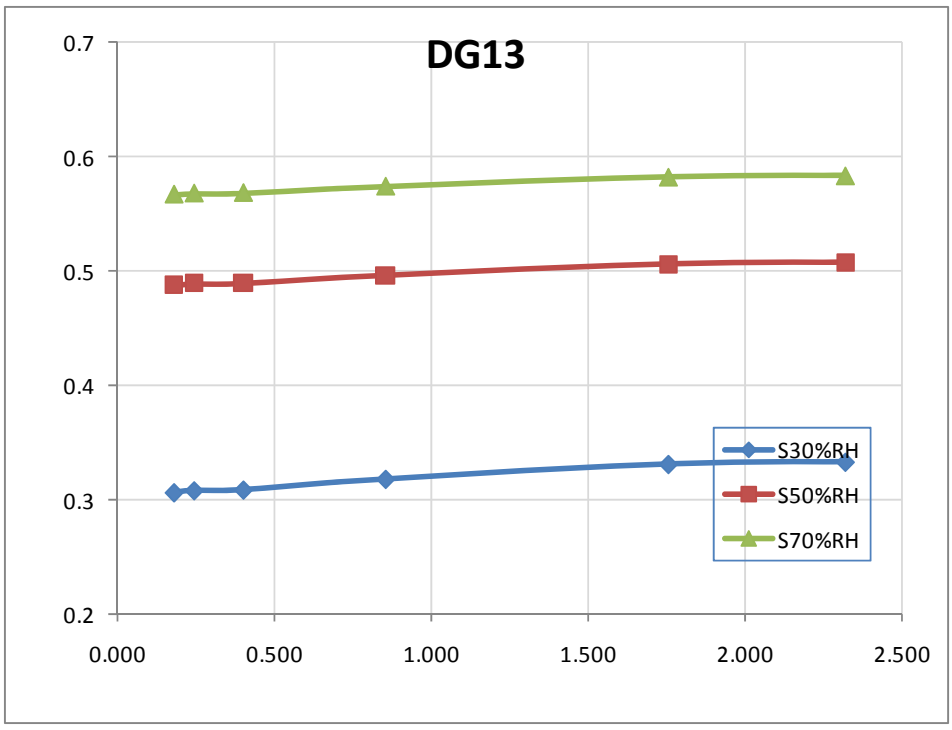


Figure 21. Plot of *S* vs. Spacer Effective Conductivity for Sill Fixed – Frame with Glazing System 3

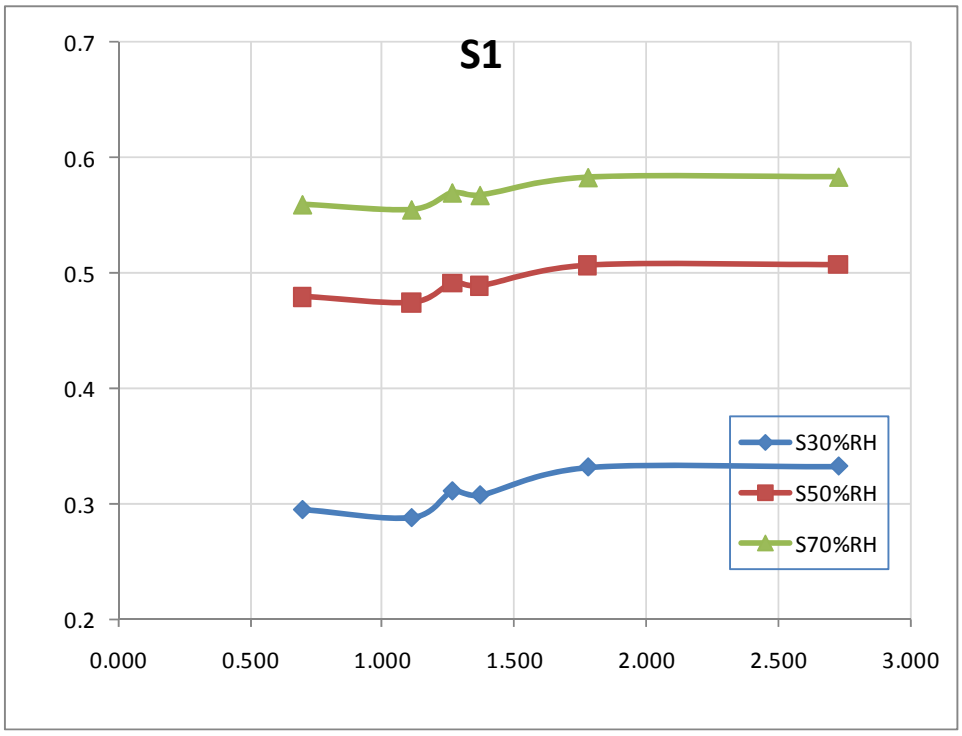


Figure 22. Plot of *S* vs. Glazing U-factor for Sill Fixed – Frame with Spacer System 1

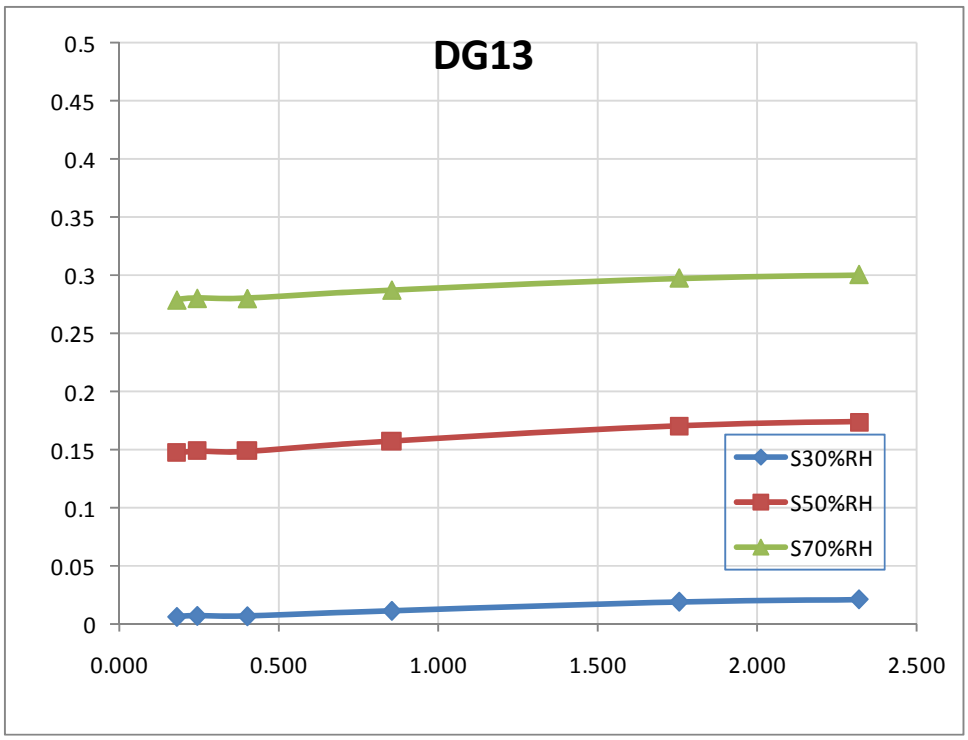


Figure 23. Plot of *S* vs. Spacer Effective Conductivity for Sill Fixed – Edge with Glazing System 3

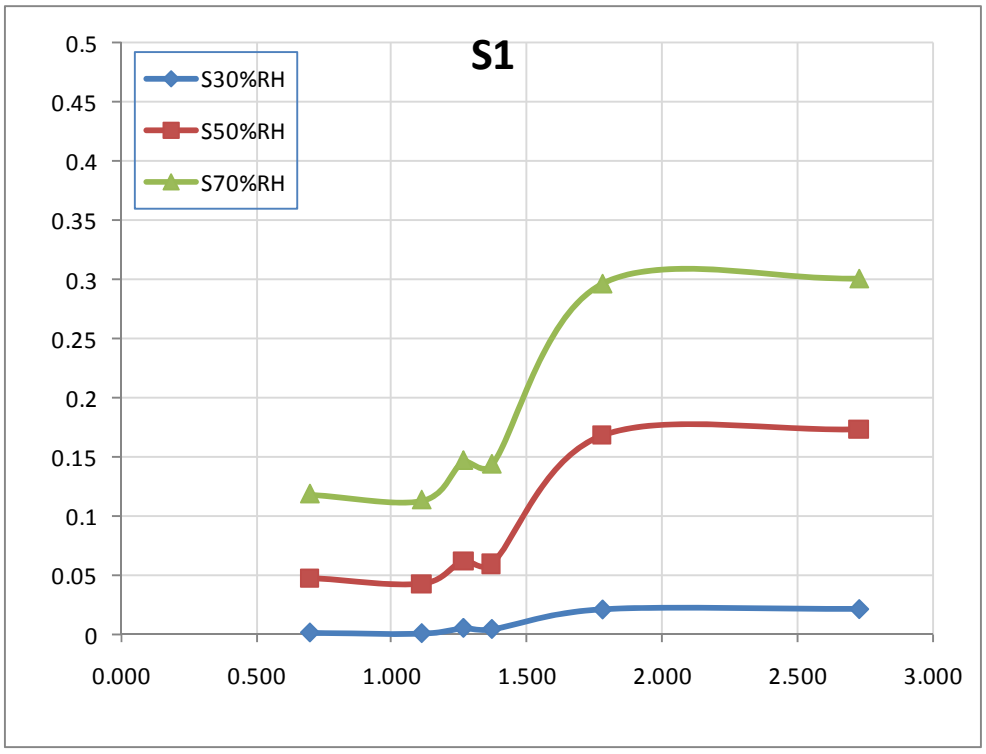


Figure 24. Plot of *S* vs. Glazing U-factor for Sill Fixed – Edge with Spacer System 1

Framing System 5:

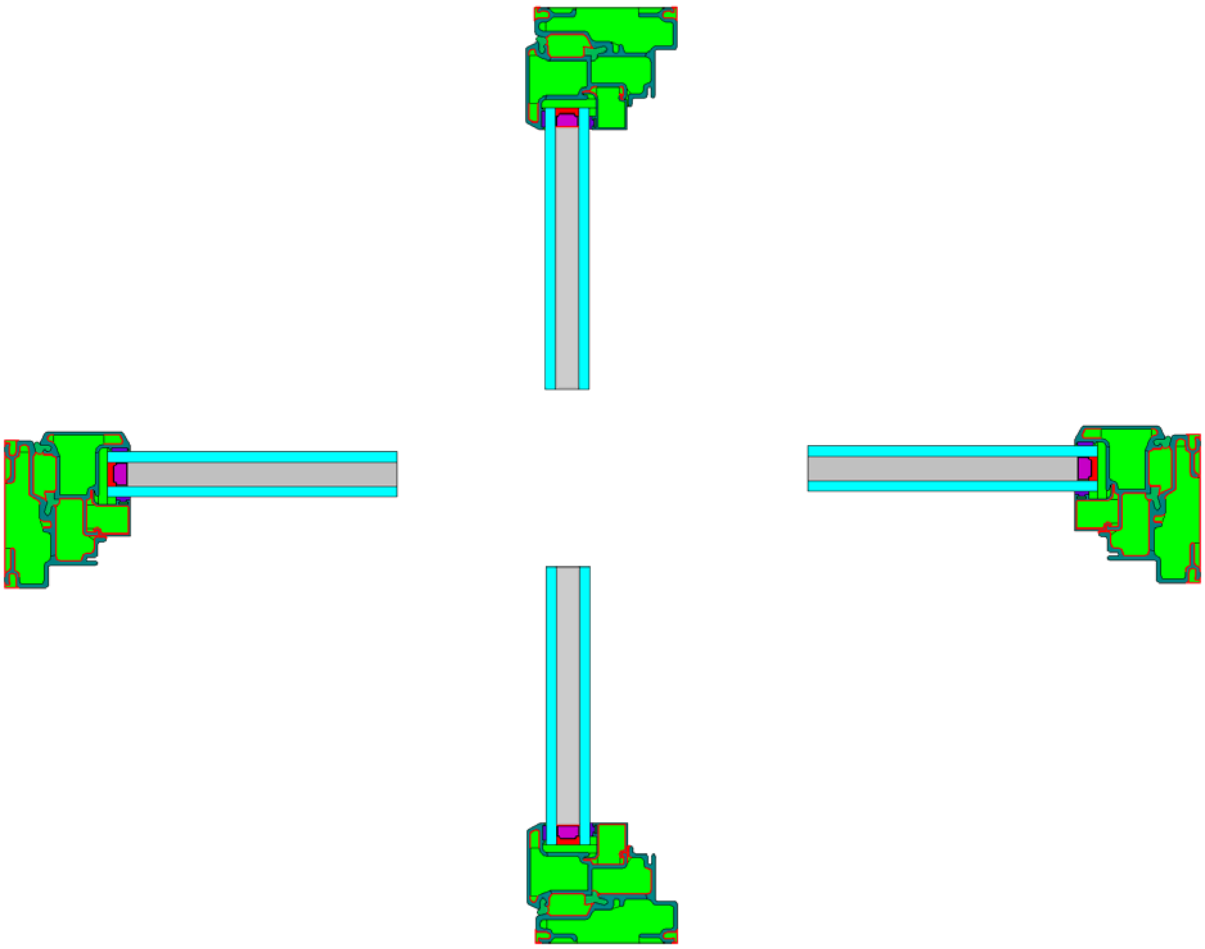


Figure 25. Framing System 5 (F5)

	DG	TG
Spacer ID	k_{eff}	k_{eff}
	W/m·K	W/m·K
S1	2.378	1.346
S2	1.789	1.145
S3	0.872	0.536
S4	0.407	0.348
S5	0.245	0.245
S6	0.181	0.181

Figure 26. Spacer Performance in Framing System 5 (F5)

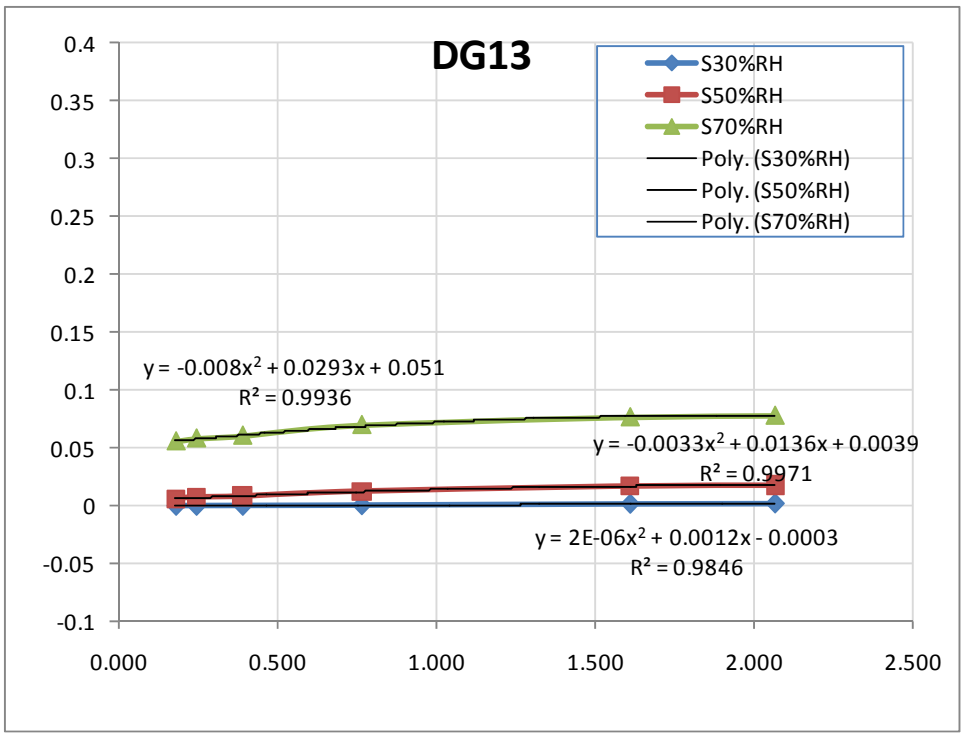


Figure 27. Plot of *S* vs. Spacer Effective Conductivity for Sill Fixed – Frame with Glazing System 3

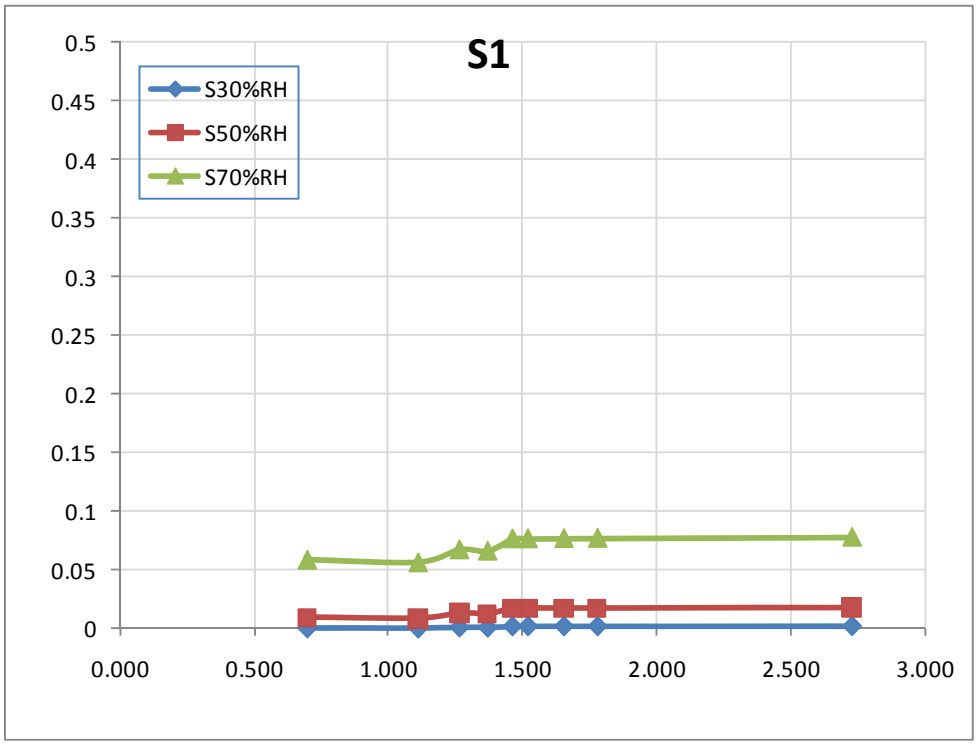


Figure 28. Plot of *S* vs. Glazing U-factor for Sill Fixed – Frame with Spacer System 1

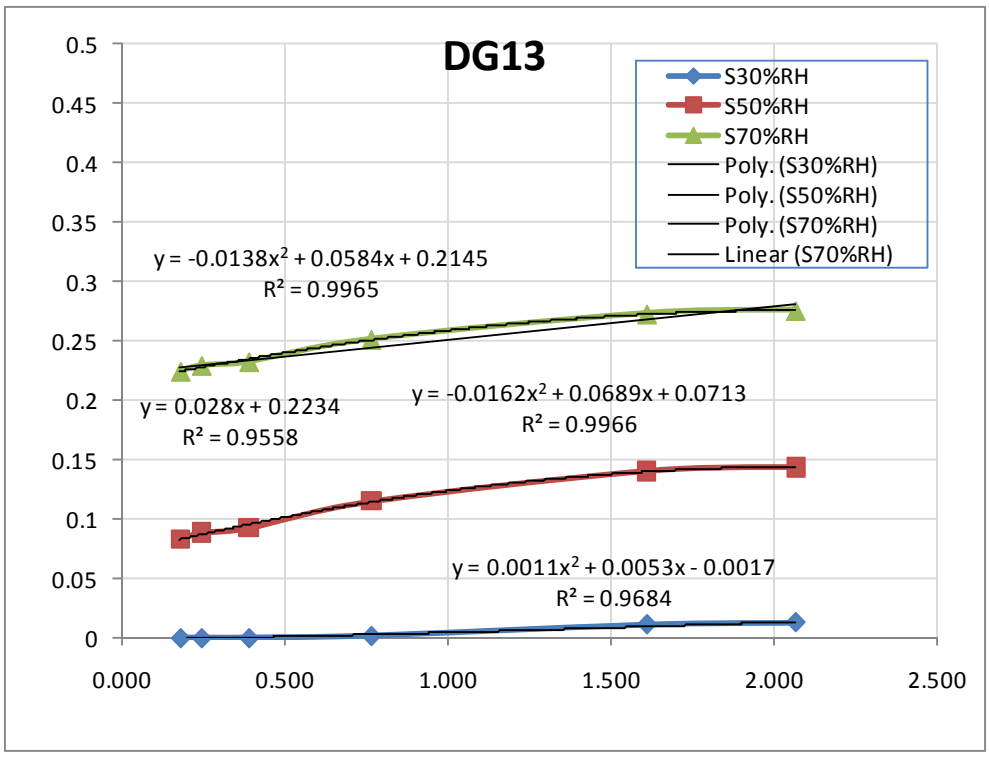


Figure 29. Plot of *S* vs. Spacer Effective Conductivity for Sill Fixed – Edge with Glazing System 3

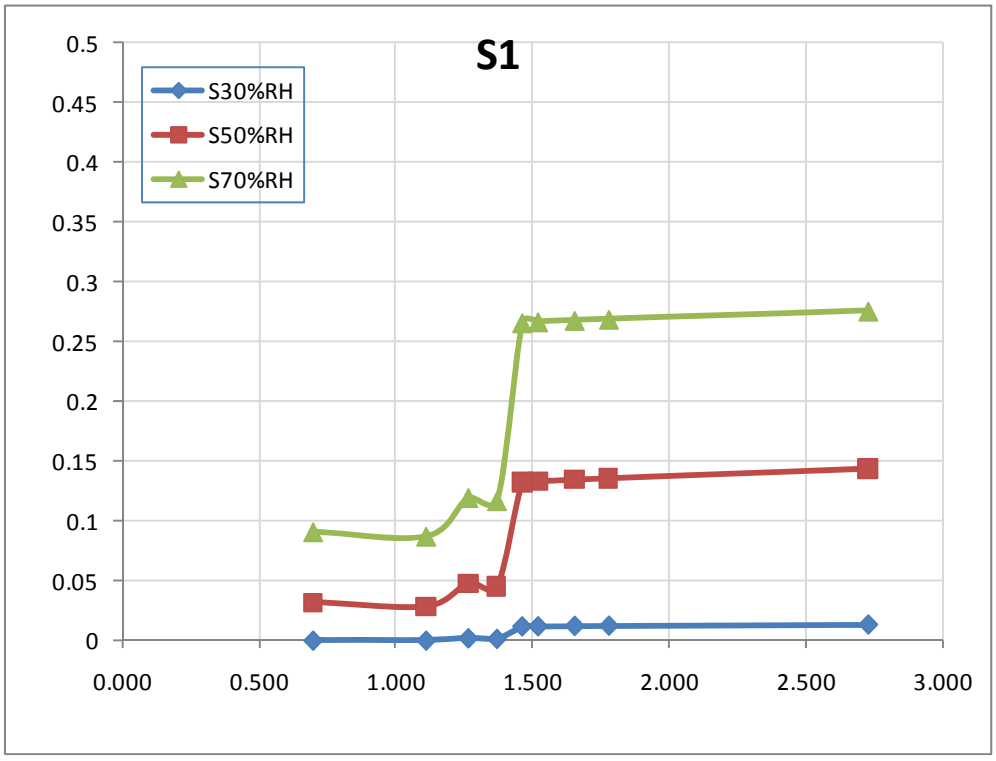


Figure 30. Plot of *S* vs. Glazing U-factor for Sill Fixed – Edge with Spacer System 1

Framing System 6:

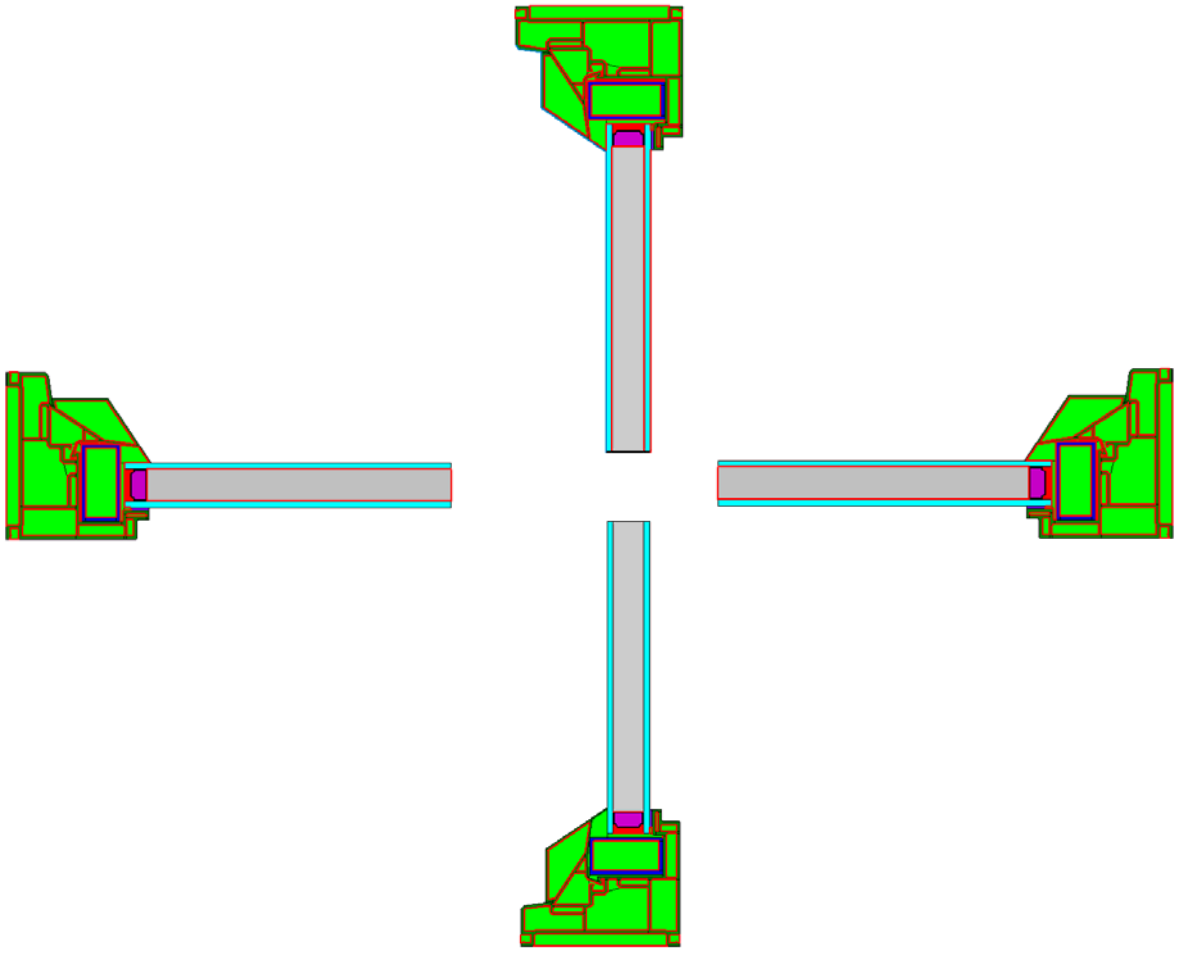


Figure 31. Framing System 6 (F6)

	DG	TG
Spacer ID	k_{eff}	k_{eff}
	W/m·K	W/m·K
S1	2.699	1.552
S2	1.960	1.287
S3	0.991	0.597
S4	0.418	0.362
S5	0.245	0.245
S6	0.181	0.181

Figure 32. Spacer Performance in Framing System 6 (F6)

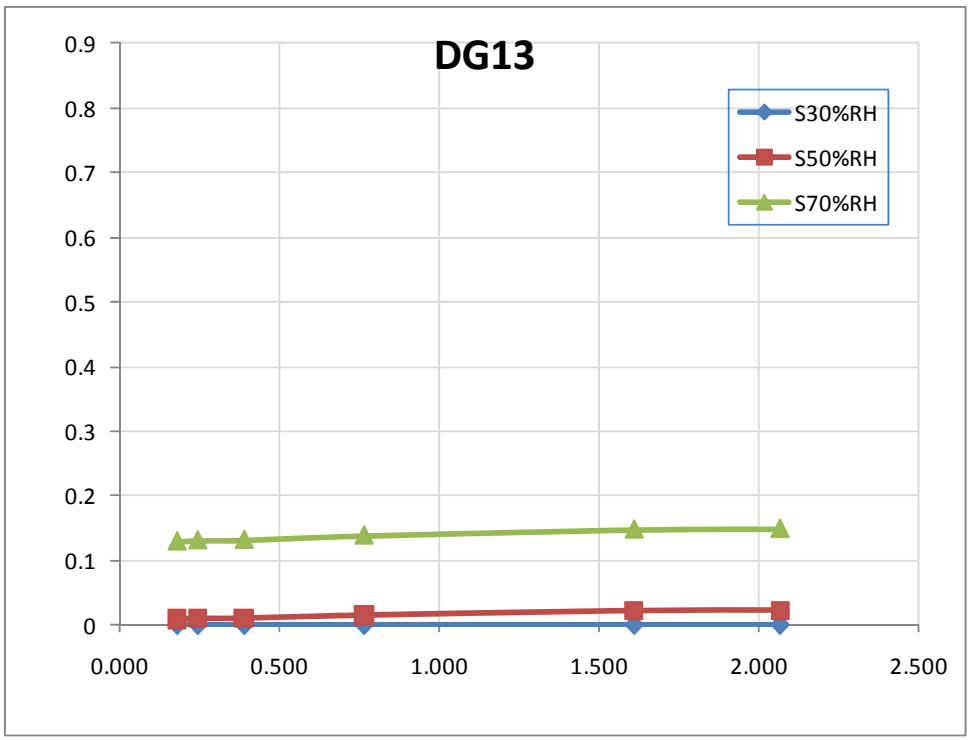


Figure 33. Plot of *S* vs. Spacer Effective Conductivity for Sill Fixed – Frame with Glazing System 3

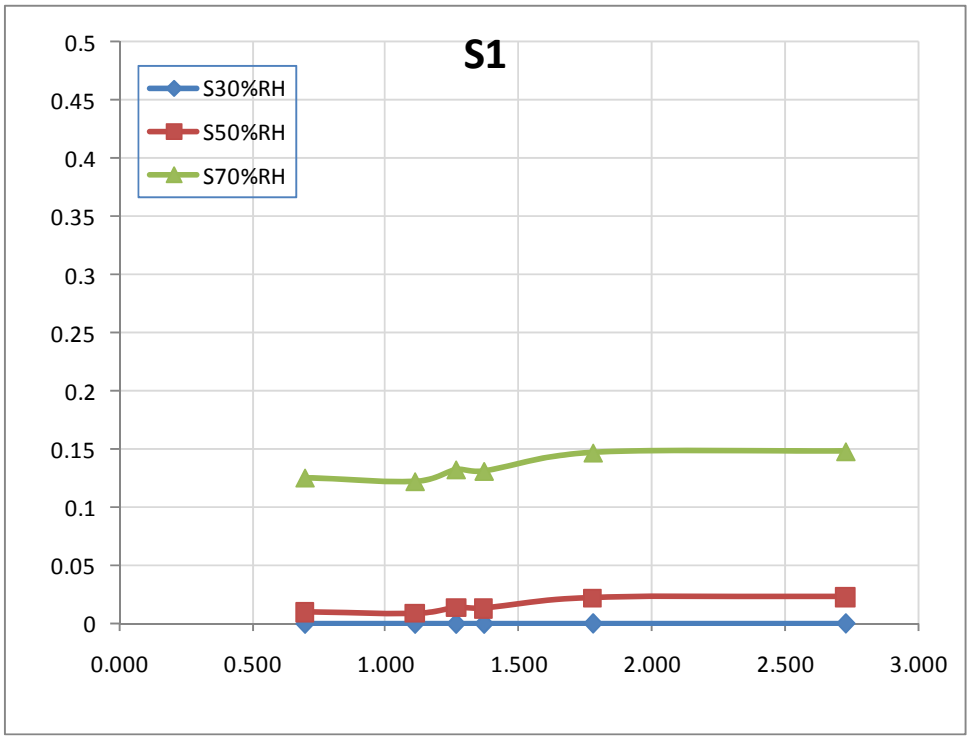


Figure 34. Plot of *S* vs. Glazing U-factor for Sill Fixed – Frame with Spacer System 1

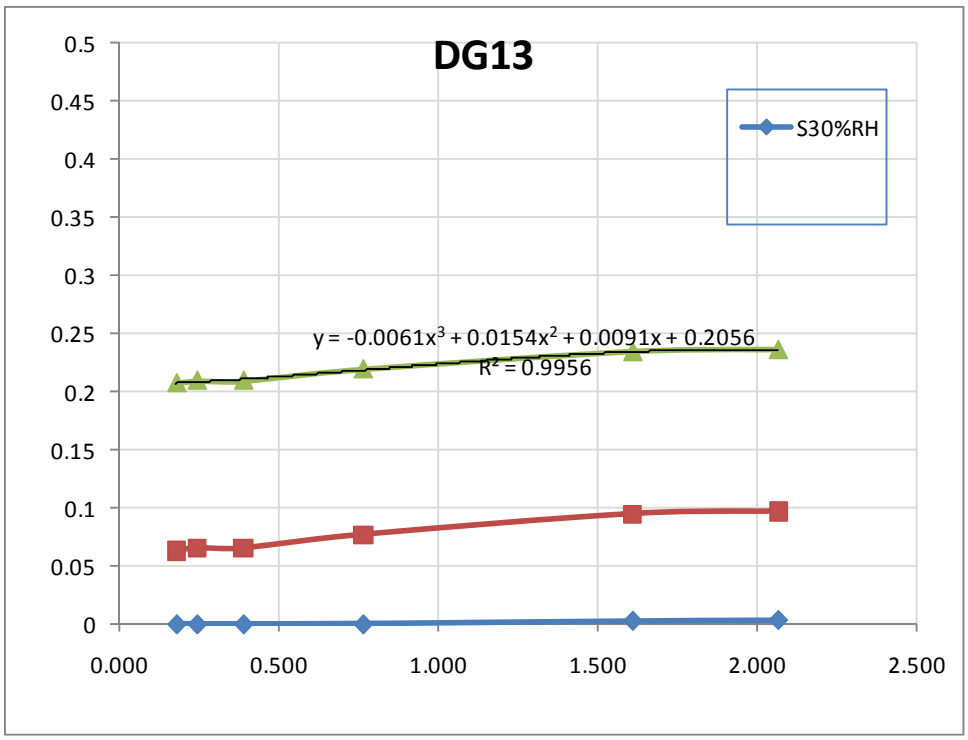


Figure 35. Plot of *S* vs. Spacer Effective Conductivity for Sill Fixed – Edge with Glazing System 3

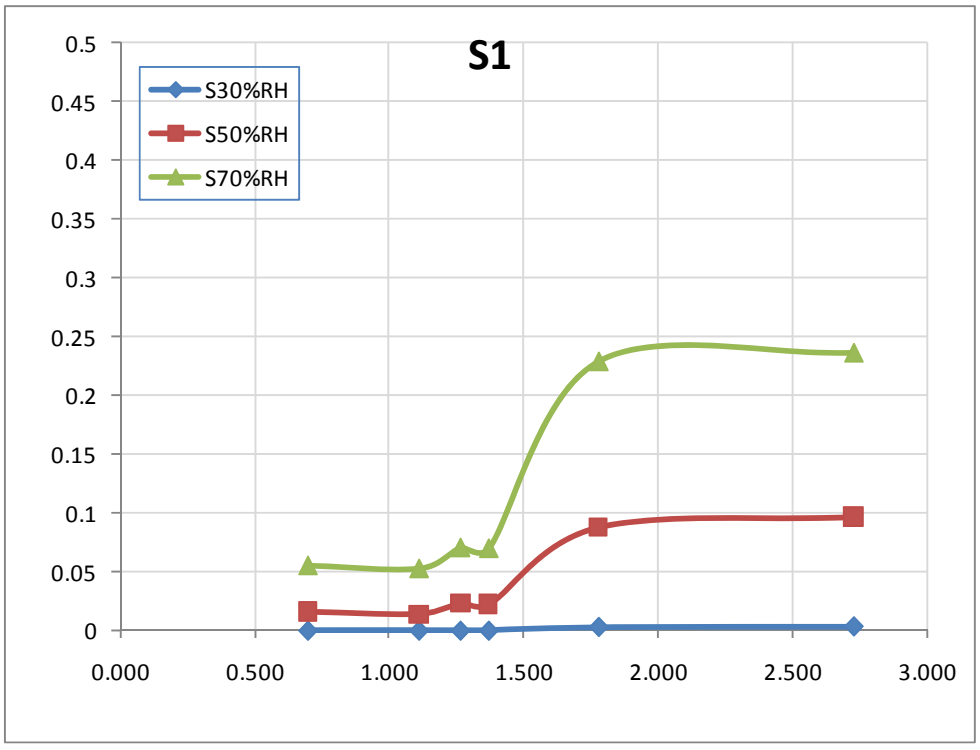


Figure 36. Plot of *S* vs. Glazing U-factor for Sill Fixed – Edge with Spacer System 1

Framing System 7:

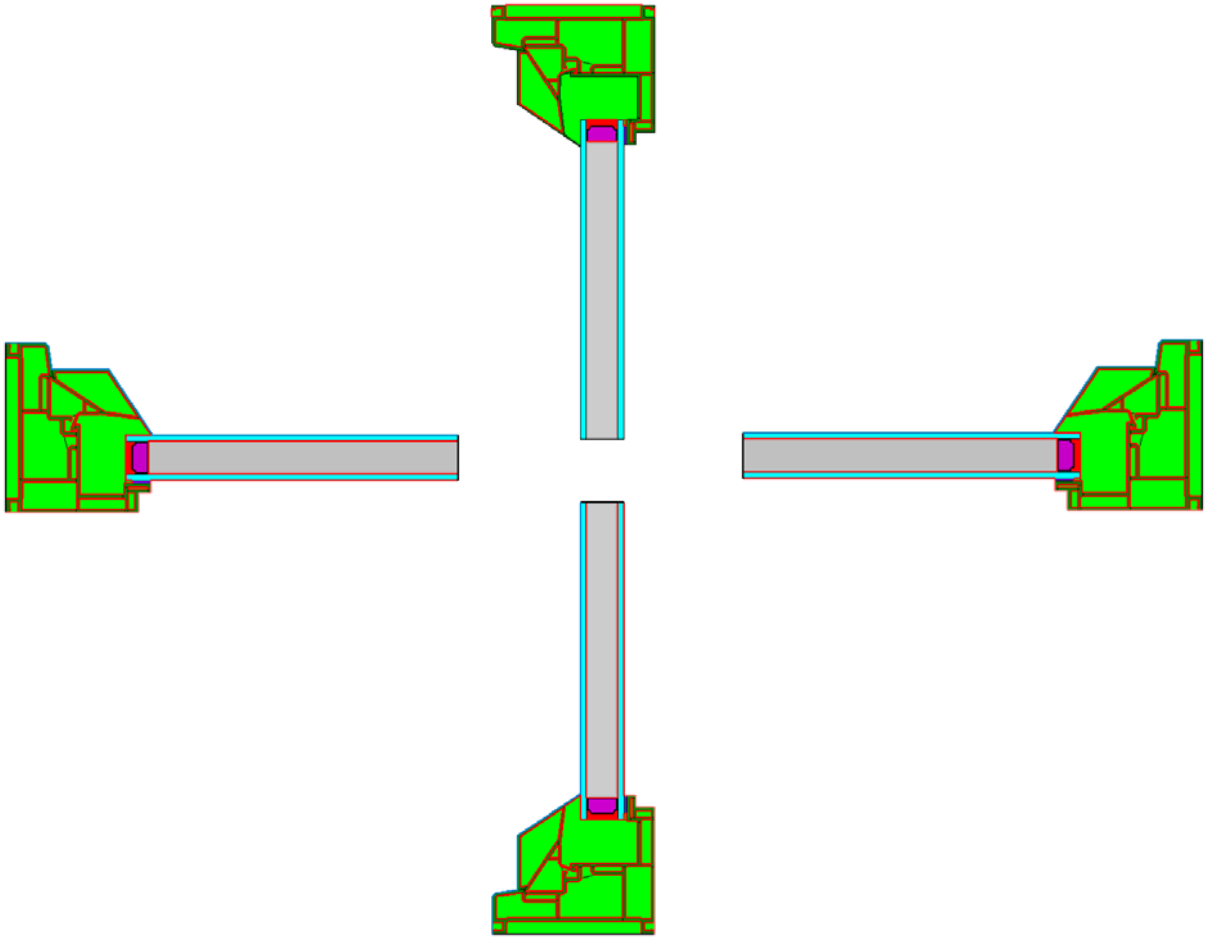


Figure 37. Framing System 7 (F7)

	DG	TG
Spacer ID	k_{eff}	k_{eff}
	W/m·K	W/m·K
S1	2.699	1.552
S2	1.960	1.287
S3	0.991	0.597
S4	0.418	0.362
S5	0.245	0.245
S6	0.181	0.181

Figure 38. Spacer Performance in Framing System 7 (F7)

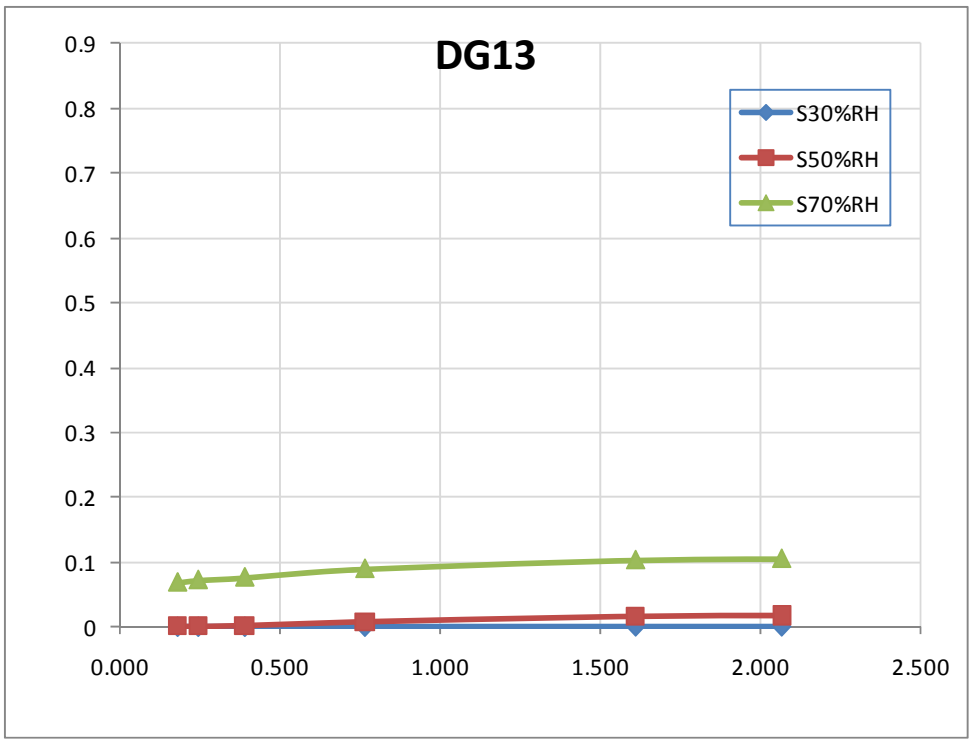


Figure 39. Plot of *S* vs. Spacer Effective Conductivity for Sill Fixed – Frame with Glazing System 3

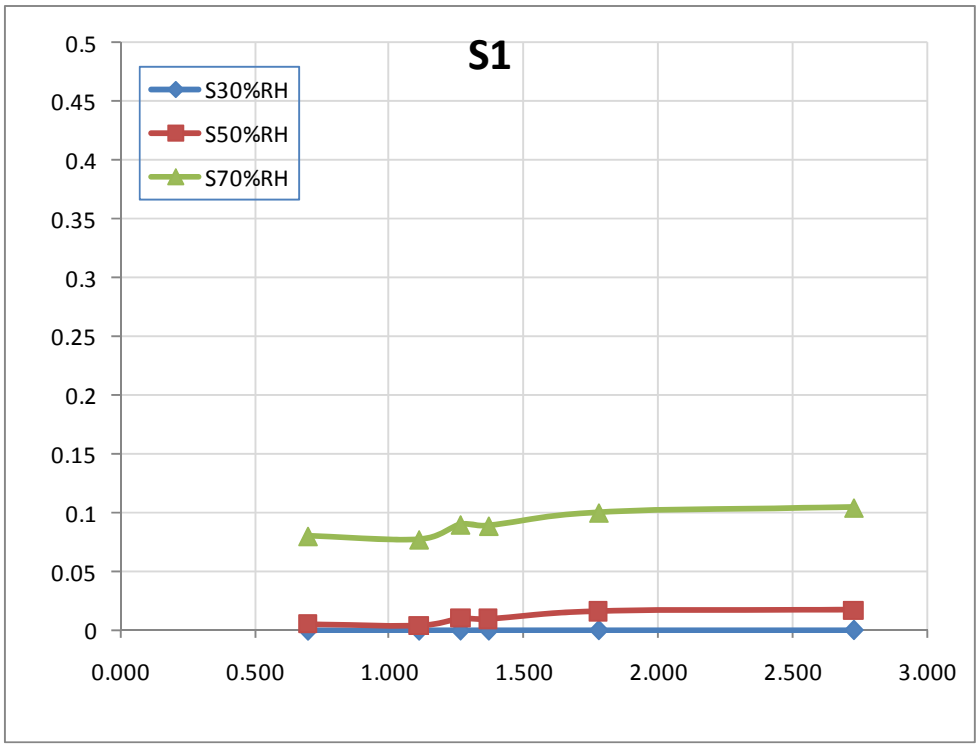


Figure 40. Plot of *S* vs. Glazing U-factor for Sill Fixed – Frame with Spacer System 1

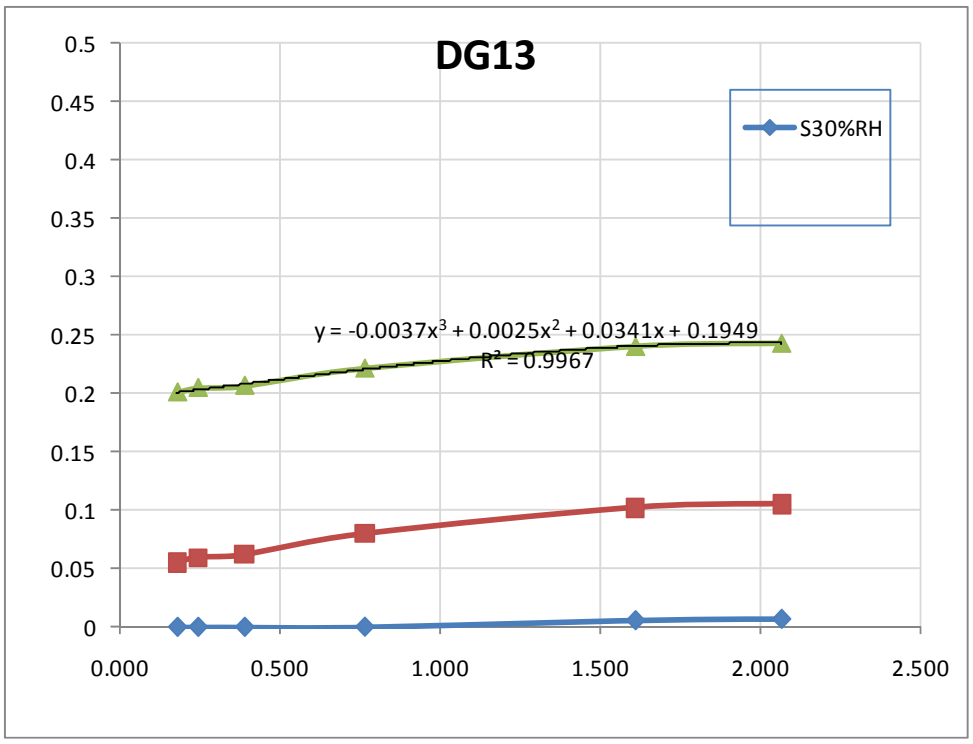


Figure 41. Plot of *S* vs. Spacer Effective Conductivity for Sill Fixed – Edge with Glazing System 3

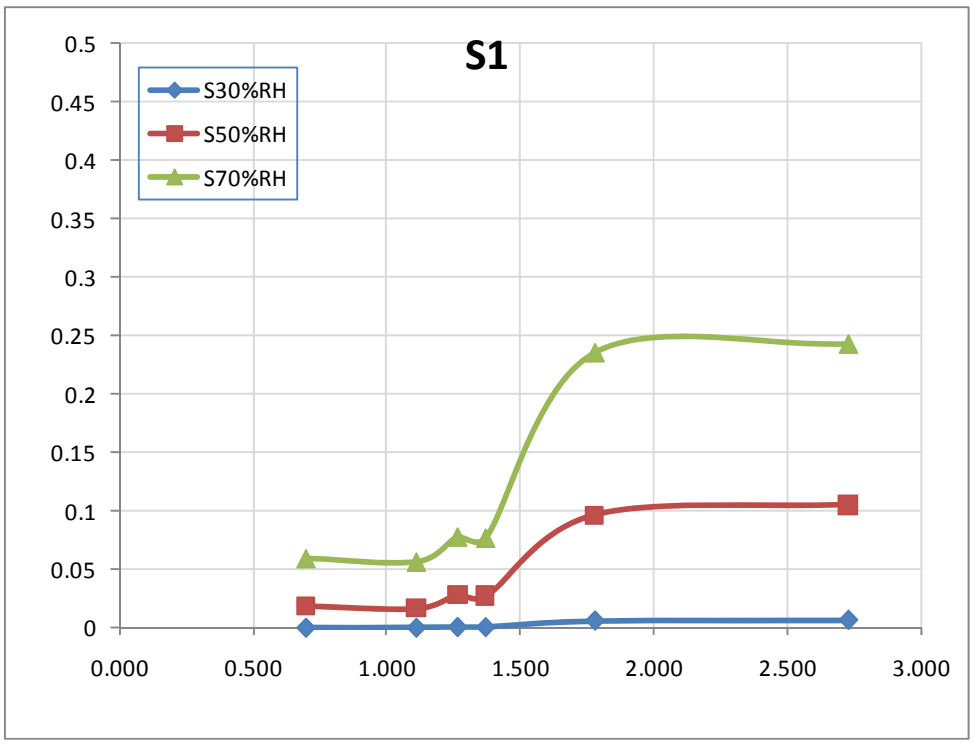


Figure 42. Plot of *S* vs. Glazing U-factor for Sill Fixed – Edge with Spacer System 1

Project 1.1.15

Project Name: Component Modeling Approach Non-Standard Products Research

Date: March 27, 2008

Purpose: The objective of this project is to simulate a selected group of non-standard products , namely, Single Glazing, Structural glazing, Sloped Glazing (slope of 20^{o} or less, IG incorporating a laminate layer and Double Sash Configurations, using both standard THERM/WINDOW and CMA methodologies to confirm that these products can be confidently simulated with the CMA methodology.

Project Summary:

The research project consisted of three tasks, (1) typical single glazing, structural glazing, sloped glazing, IG incorporating a laminated layer and double-sash fenestration products were identified and all necessary information required for simulation was collected, (2) the fenestration products from the finalize matrix, were modeled in THERM and WINDOW with all of the selected configurations, including all glazing options and (3) the THERM models from Task 2 were modified and modeled using the CMA methodology (i.e., Best/Worst options).

The results from the both conventional (THERM/WINDOW) and CMA based simulations were compared. From the results, it can be concluded that current CMA procedure can be confidently used for all the non-standard products identified in this project and no further investigation is necessary.

Click here for final report

Web link:
http://www.nfrc.org/documents/CMANonStandardProducts-FinalReport_040208.pdf

Carli, Inc.

18 Tanglewood Rd.
Amherst, MA 01002

TEL: (413) 256-4647
FAX: (413) 256-4823

home@fenestration.com
http://www.fenestration.com

Technical Report:

TREATMENT OF DOUBLE-SASH, SLOPED, SINGLE-GLAZED, AND STRUCTURAL GLAZING FENESTRATION PRODUCTS IN CMA METHODOLOGY

Report prepared for:

National Fenestration Rating Council, Inc.

6305 Ivy Lane, Suite 140
Greenbelt, MD 20770

March 27, 2008

TABLE OF CONTENTS:

EXECUTIVE SUMMARY 3
BACKGROUND 4
APPROACH 4
APPENDIX A. CONFIGURATIONS USED IN THE MODELING 8

EXECUTIVE SUMMARY

The objective of this project is to simulate a selected group of non-standard products , namely, Single Glazing, Structural glazing, Sloped Glazing (slope of 20^o or less, IG incorporating a laminate layer and Double Sash Configurations, using both standard THERM/WINDOW and CMA methodologies to confirm that these products can be confidently simulated with the CMA methodology.

In Task 1, typical single glazing, structural glazing, sloped glazing, IG incorporating a laminated layer and double-sash fenestration products were identified and all necessary information required for simulation was collected. A matrix of glazing and spacer options to be modeled with these fenestration products was proposed and sent to PMTG for review. Based on the suggestions from the PMTG, the matrix was modified and finalized. The matrix is given in Appendix 1.

In Task 2, the fenestration products from the finalize matrix, were modeled in THERM and WINDOW with all of the selected configurations, including all glazing options. Simulated thermal and solar optical performance for each product and associated options were tabulated.

In Task 3, the THERM models from Task 2 were modified and modeled using the CMA methodology (i.e., Best/Worst options). The modeling data was entered into the FENSIZE, which incorporates the CMA methodology. After the CMA based simulations were completed, the values for the same matrix of options and products were tabulated and the results compared with conventional modeling results obtained in Task 2.

The results from the both conventional (THERM/WINDOW) and CMA based simulations were compared. All of the U Factor results are within the expected discrepancies (i.e., less than 0.02 Btu/(hr-ft^2-F), with the majority being below 0.01. SHGC results are all within 0.01 while VT results are identical in both the procedures. The results are summarized in Table 1.

From the results, it can be concluded that current CMA procedure can be confidently used for all the non standard products identified in this project and no further investigation is necessary.

BACKGROUND

The NFRC CMA methodology (NFRC 2004, Curcija 2004) covers a majority of fenestration products. This procedure is being developed with a focus on typical non-residential products with a target implementation date of early 2009. It is believed that this methodology applies equally well to a smaller number of non-standard systems; however this has not been proven yet. It is important that as many fenestration products as possible are covered by this procedure to minimize exceptions and special cases. These systems have been identified by a Technical Issues Task Group as potentially problematic and solutions have been sought. The aim of this project is to investigate if the non standard products proposed here can be satisfactorily handled by current CMA methodology or not.

The objective of this project is to simulate a selected group of non-standard products (listed below) using both standard THERM/WINDOW and CMA methodologies to confirm that these products can be confidently simulated with the CMA methodology. If the CMA methodology does not produce satisfactory results for some or all of these products, the proposed alternate course(s) of action will be suggested and recommendations for further research to resolve any discrepancies will be provided.

The products considered in this project include:

- Single Glazing
  - This is to take into account products with a low emissivity coating on the interior glazing surface as well as glass / polycarbonate composite products with low conductivity.
- Structural glazing
  - These applications can utilize deep sightlines on the glazing as well as deep structural joints.
- Sloped Glazing (slope of 20^{o} or less)
  - By code, laminated glass is required for single glazing or the interior pane of an IG.
- IG incorporating a laminate layer
  - One or both panes may be laminated due to security/acoustic considerations.
- Double Sash Configuration
  - This must consider installations with IG or single glazed exterior, a wide airspace, and single glazed interior pane (including interior/exterior storms and standard triple glazing). Any of these panes may be laminated/lowE.

APPROACH

Based on the specific requirements in the bid document, this research project will be divided into the following 4 tasks:

1. Identification of typical fenestration products
2. THERM and WINDOW modeling of typical fenestration products
3. Modeling of typical fenestration products using CMA methodology
4. Conclusions and final report

Identification of representative fenestration products
Typical single glazing, structural glazing, sloped glazing, IG incorporating a laminated layer and double-sash fenestration products were identified and all necessary information required for simulation was collected. A matrix of glazing and spacer options to be modeled with these fenestration products was proposed and sent to PMTG for review. Based on the suggestions from the PMTG, the matrix was modified and finalized. The matrix is given in Appendix 1.

THERM and WINDOW modeling of fenestration products
The fenestration products from the finalize matrix, were modeled in THERM and WINDOW with all of the selected configurations, including all glazing options. Simulated thermal and solar optical performance for each product and associated options were tabulated.

Modeling of fenestration products using CMA methodology
The THERM models from Task 2 were modified and modeled using the CMA methodology (i.e., Best/Worst options). The modeling data was entered into the FENSIZE, which incorporates the CMA methodology. During the investigation we found out that for calculating the total product U factor, the current CMA procedure was not using actual product height for the center of glass U factor calculations instead nominal height was being used for this calculation. This was causing differences in results, mainly for the single glazed products. The results, shown in Table 1, using CMA methodology were recalculated using the actual product height. It is therefore recommended to use actual product height for center of glass calculations during the product U-factor calculation in CMA. After the CMA based simulations were completed, the values for the same matrix of options and products were tabulated and the results compared with conventional modeling results obtained in Task 2.

Conclusions
The results from the both conventional (THERM/WINDOW) and CMA based simulations were compared. All of the U Factor results are within the expected discrepancies (i.e., less than 0.02 Btu/(hr-ft^2-F), with the majority being below 0.01 Btu/(hr-ft2-F). SHGC results are all within 0.01 while VT results are identical in both procedures. The results are summarized in Table 1.

From the results, it can be concluded that current CMA procedure can be confidently used for all the non standard products identified in this project and no further investigation is necessary.

Recommendations
As the results are within the expected discrepancies for all the non-standard products considered in this project, no changes in the NFRC standard documents are necessary. However, it is recommended to use actual product height for the center of glass calculations during the whole product U Factor calculations in CMA and this may need to be clarified in NFRC 100, section 5.6, if needed. .

Table 1: Comparison of Results

Product Ref.	Product Type	Material: Frame / Spacer	Glazing System	Size		U (Btu/h-ft^2-F)				SHGC (-)				VT (-)			
				Width (in)	Height (in)	T5/W5	CMA	DIFF	DIFF (%)	T5/W5	CMA	DIFF	DIFF (%)	T5/W5	CMA	DIFF	DIFF (%)
P1	Single Glazed	AL / N/A	G1-103(clear)	78.740	78.740	1.110	1.099	-0.011	-0.99	0.750	0.749	0.000	-0.01	0.787	0.787	0.000	0.00
			G2-910(HClowE)			0.801	0.803	0.002	0.23	0.650	0.649	-0.001	-0.20	0.731	0.731	0.000	0.00
			G3-6162(Laminate)			0.748	0.760	0.012	1.63	0.441	0.441	0.000	0.06	0.618	0.618	0.000	0.00
			G4-30001(Film)			0.888	0.886	-0.002	-0.17	0.214	0.215	0.001	0.35	0.155	0.155	0.000	0.00
P2	Laminate Glazing	TI AL / AL 1/2"	G5-103-Arg-6162	78.740	78.740	0.456	0.454	-0.002	-0.37	0.451	0.450	-0.001	-0.25	0.518	0.518	0.000	0.00
			G6-103-Arg-6162-Flipped			0.436	0.433	-0.003	-0.67	0.550	0.550	0.000	-0.04	0.518	0.518	0.000	0.00
		TI AL / AL 7/32"	G7-Laminate-Air-Laminate			0.597	0.598	0.001	0.18	0.500	0.500	0.000	-0.04	0.607	0.607	0.000	0.00
P2	Sloped Orientation	TI AL / AL 1/2"	G8-103-Air-103	78.740	78.740	0.816	0.812	-0.003	-0.39	0.681	0.681	0.000	-0.03	0.753	0.753	0.000	0.00
			G9-103-Arg-5284(SClowE)			0.632	0.638	0.006	0.99	0.437	0.437	0.000	-0.03	0.672	0.672	0.000	0.00
P3	Structural Glazed	AL / AL 1/2"	G10-103-Air-103	78.740	78.740	0.516	0.505	-0.011	-2.14	0.695	0.690	-0.005	-0.69	0.728	0.728	0.000	0.00
			G11-103-Argon-5284(SClowE)			0.322	0.307	-0.015	-4.52	0.459	0.454	-0.005	-1.14	0.650	0.650	0.000	0.00
P4	Structural Glazed	AL / AL 1/2"	G10-103-Air-103	78.740	78.740	0.536	0.524	-0.011	-2.14	0.688	0.682	-0.005	-0.77	0.706	0.706	0.000	0.00
			G11-103-Argon-5284(SClowE)			0.344	0.330	-0.015	-4.26	0.459	0.453	-0.006	-1.21	0.630	0.630	0.000	0.00
P5	Double Sash	TB AL / AL 1/4"	G12-103-Air-103-Air-103-Air-103	47.244	59.055	0.340	0.336	-0.004	-1.05	0.431	0.431	0.000	0.01	0.493	0.493	0.000	0.00
			G13-5284-Arg-103-Air-5284-Arg-103			0.264	0.254	-0.010	-3.79	0.227	0.227	0.000	-0.11	0.390	0.390	0.000	0.00
P6	Double Sash	TB AL / N/A	G14-103-Air-103	59.055	47.244	0.678	0.678	0.001	0.09	0.445	0.445	0.001	0.11	0.469	0.469	0.000	0.00
			G15-910-Air-103			0.600	0.600	0.000	0.02	0.395	0.396	0.001	0.24	0.436	0.436	0.000	0.00

REFERENCES:

NFRC. 2004. “NFRC 100: Procedure for Determining Fenestration Product U-factors”. National Fenestration Rating Council. 2004.

NFRC. 2004. “NFRC 200: Procedure for Determining Fenestration Product Solar Heat Gain Coefficient and Visible Transmittance at Normal Incidence”. National Fenestration Rating Council. 2004.

LBNL. 2003. “THERM5 - A PC Program for Analyzing Window Thermal Performance of Fenestration Products”, Berkeley CA: Windows and Daylighting Group, Lawrence Berkeley Laboratory, 2003.

LBNL 2003, “WINDOW5 - A PC Program for Analyzing Window Thermal Performance of Fenestration Products”, Berkeley CA: Windows and Daylighting Group, Lawrence Berkeley Laboratory, 2003.

Curcija, D.C.; Manteghi, M.; Bhandari, M.S.; and Shah, B.V. 2004. “Component Modeling Methodology for Predicting Thermal Performance of Non-Residential Fenestration Systems”. *Thermal Performance of Building Envelopes IX Conference*. Clearwater Beach, FL. December 2004.

DBS. 2006. “FENSIZE: A Windows Based PC Program for Rapid Calculation of Thermal Performance of Fenestration Products in Accordance with Component Modeling Procedure”. *User’s Manual and Program Description*. DesignBuilder Software. 2006.

NFRC. 2004. “NFRC 100, Section 5.6: 5.6 Non Residential and High Rise Residential Building Fenestration Products”. *National Fenestration Rating Council*. 2004.

APPENDIX A. CONFIGURATIONS USED IN THE MODELING

Table A1. Glazing and spacer Systems

Glazing Systems to be Used							
	Glazing ID						
Single Glazing							
G1 – Single: clear - 6mm	103						
G2 – Single: Low-e (HC) - 6mm	910						
G3 –Single: Laminate	6162						
G4 –Single clear with applied film	103	2598 (aplied film)					
		[30001]					
IG Incorporating Laminates							
G5 – Double: Laminate Air Clear	103	Air (0.5")	6162				
G6 – Double: Clear Air Laminate	103	Air (0.5")	6162	Flipped (lowe on interior surface)			
G7 – Double: Laminate Air Laminate	laminate	Air (0.25")	laminate				
Laminate: 3mm clr - SGP 90 mil - 3mm clr	30002		3002				
(Total thickness - 0.4328 in)							
Sloped glazing (20 degeee tilt)							
G8 - Double: Clear Air Clear	103		103	20 degree			
G9 - Double: Clear- Argon Low-e (SC)	103	Argon	5284	20 degree			
Structured glazing							
G10 - Double: Clear Air Clear	103		103				
G11 - Double: Clear- Argon Low-e (SC)	103	Argon	5284				
Double sash							
G12 - Double/Double: Clear Air Clear	103		103	Air	103		103
G13 - Double/Double: Clear- Argon Low-e (SC)	5284	Argon	103	Air	5284	Argon	103
G14 - Single/Single: Clear- AIR-clear	103	AIR	103				
G15 - Single/Single: LowE- AIR-clear	910	AIR	103				
Spacer							
S1 – Standard Aluminum bar single seal							

Table A2. Optical properties of glasses

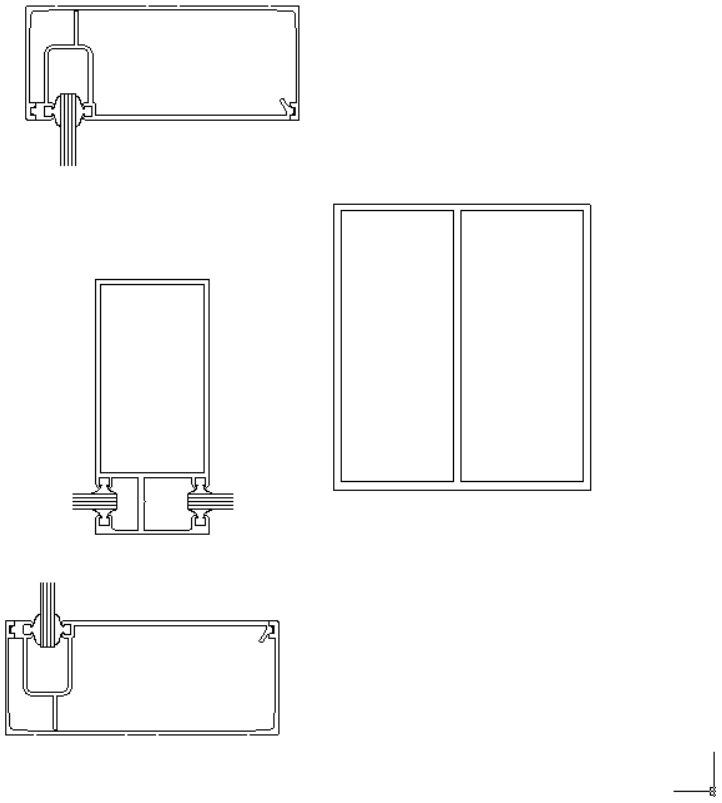
Glass ID	Name	Product Description	Thick in.	Tsol -	Rsol1 -	Rsol2 -	Tvis -	Rvis1 -	Rvis2 -	emis1 -	emis2 -
103	CLEAR_6.DAT	Generic Clear Glass	0.2250	0.771	0.070	0.070	0.884	0.080	0.080	0.840	0.840
724	C120.AFG	Copper on Clear	0.2220	0.112	0.623	0.474	0.224	0.327	0.354	0.026	0.840
910	CMFTE2_6.AFG	Comfort E² on Clear	0.2220	0.662	0.107	0.092	0.821	0.097	0.086	0.202	0.840
5000	SB70XL Strph-6.PPG	Solarban® 70XL on Starphire®	0.2230	0.281	0.513	0.562	0.720	0.077	0.059	0.841	0.018
5284	SB60 Clear-6.PPG	Solarban 60® on Clear	0.2230	0.386	0.272	0.455	0.790	0.059	0.049	0.840	0.035
6162	BGLE-lam.vir	Blue Green LowE laminated	0.5059	0.368	0.055	0.091	0.694	0.077	0.088	0.840	0.154
30001	2598-On-103.usr	Generic Applied Film	0.2262	0.122	0.430	0.625	0.174	0.537	0.589	0.840	0.371
30002	102/90SGP6/102.usr	Generic Laminate	0.4328	0.616	0.062	0.062	0.848	0.078	0.078	0.840	0.840

Table A3. Thermal and Optical properties of glazing systems (At Nominal Height)

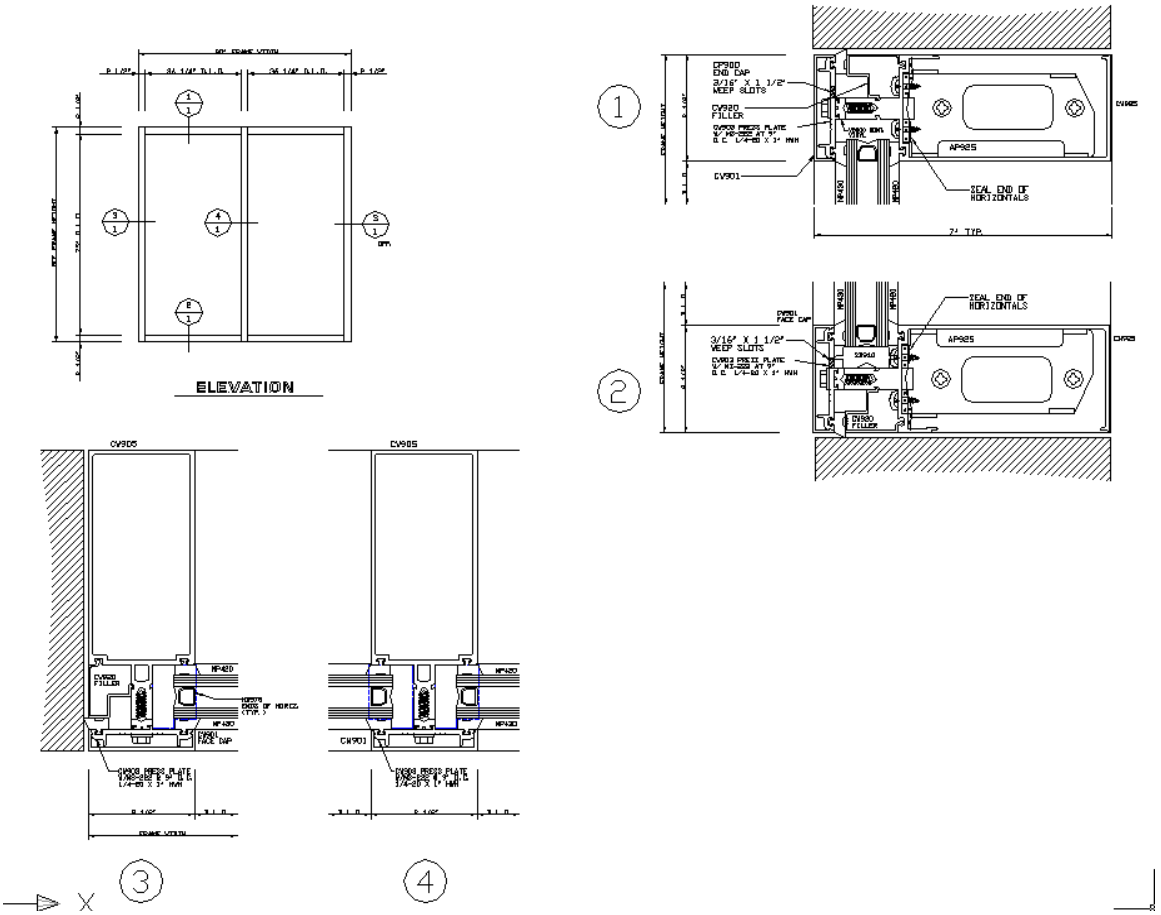
W5 ID	Reference - Name	# of layers	Thick in.	U Btu/h-ft2-F	SHGC -	Tvis
1	G1-103(clear)	1	0.236	1.023	0.816	0.884
2	G2-910(HClowE)	1	0.236	0.670	0.704	0.821
3	G3-6162(Laminate)	1	0.472	0.612	0.477	0.694
4	G4-30001(Film)	1	0.236	0.769	0.218	0.174
11	G5-103-ARG-6162	2	1.229	0.325	0.527	0.618
12	G6-103-ARG-6162-Flip	2	1.229	0.283	0.636	0.618
13	G7-Laminate-AIR-Lami	2	1.116	0.499	0.576	0.724
21	G8-103-Air-103 (20 degree)	2	0.992	0.558	0.705	0.786
22	G9-103-Argon-5284(SC) (20 degree)	2	0.992	0.355	0.450	0.701
25	G10-103-Air-103	2	0.992	0.472	0.702	0.786
26	G11-103-Argon-5284(SC)	2	0.992	0.246	0.449	0.701
31	G12-103-Air-103-AIR-103-Air-103	4	4.185	0.255	0.544	0.632
32	G13-5284-Arg-103-AIR-5284-Arg-103	4	4.185	0.149	0.282	0.499
33	G14-103-AIR-103	2	1.292	0.480	0.703	0.786
33	G15-910-AIR-103	2	1.292	0.359	0.620	0.731
41	Low Glazing - IGU	2	0.972	0.080	0.184	0.165
42	High Glazing - IGU	2	0.972	0.473	0.702	0.786
43	Low Glazing - Single	1	0.236	0.561	0.170	0.224
44	High Glazing - Single	1	0.236	1.023	0.816	0.884

Table A4. Product Configurations used in the modeling

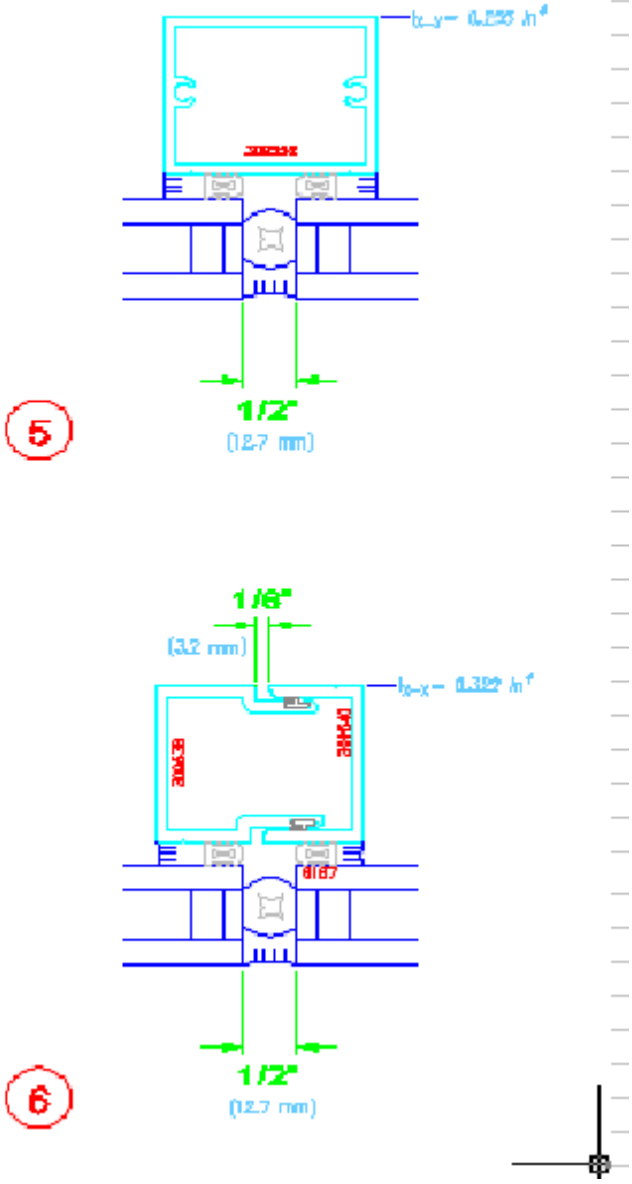
1. Product Details [Window Wall] – Single glazing option [P1]

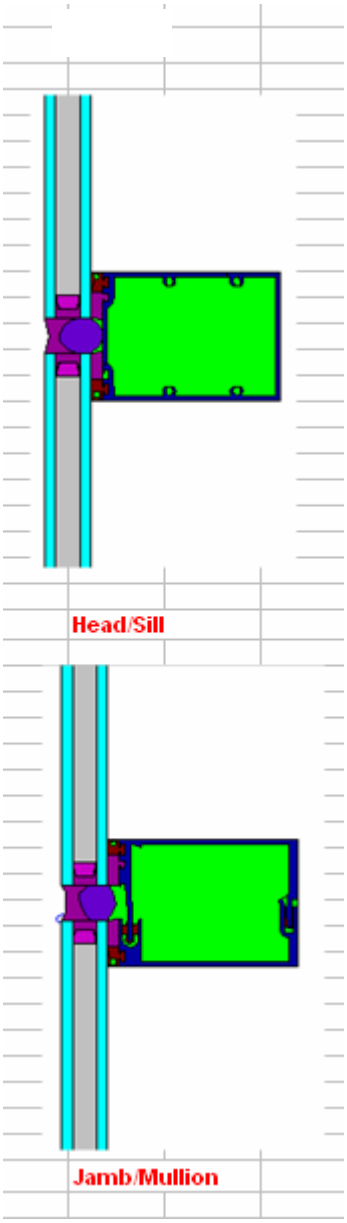


2. Product Details [Window Wall] – Laminate and sloped glazing options [P2]



3. Product Details [Curtain Wall] – Structural glazed options [P3, P4]

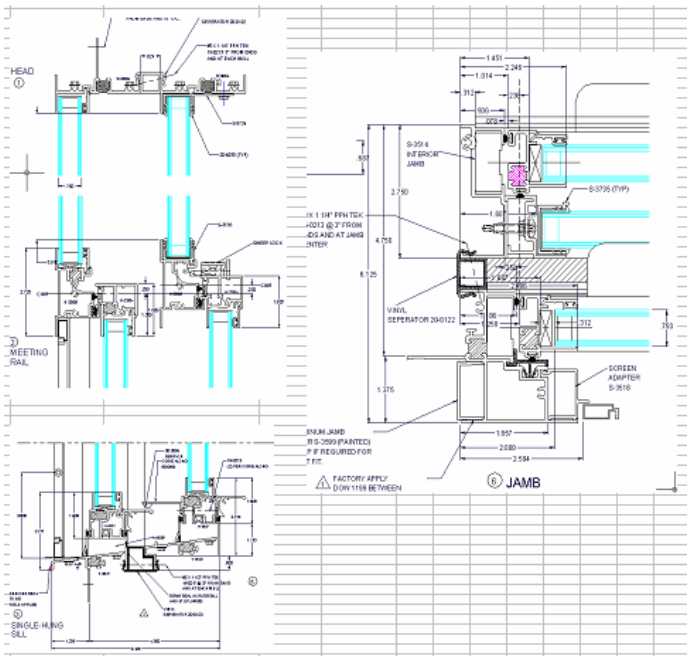




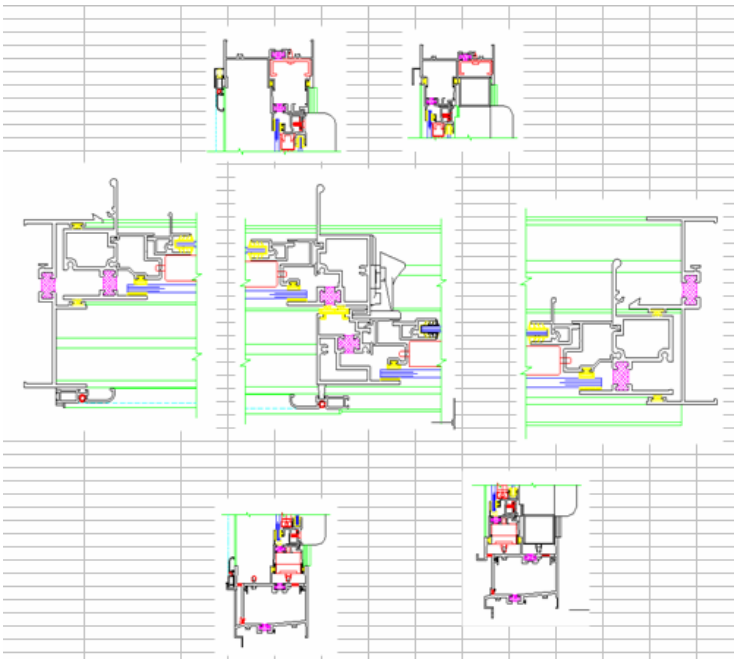
Note: Cross section 5 would be used as Head and Sill and 5 would be used for Jamb and mullion

P3 **P4**

4. Product Details [Double Hung] – Double Sash Configurations [P5, P6]



P5



P6

Project 1.1.16

Project Name:	Revision of Standard Spectral Weighting Function for Calculation of Solar Optical Properties and Solar Heat Gain
Date:	March 3, 2008; rev. March 22, 2008
Purpose:	The intent of this research project is to provide a *recommended solar spectrum* to NFRC by assessing the impact of a potential change in the reference spectrum that is used to weigh the spectral transmission calculations through glazing.

Project Summary:

It is therefore proposed

(i) to evaluate the effect that adopting one of the new possible spectra would have on the optical properties, SHGC and VT ratings of typical fenestration systems;

(ii) to follow closely the progress of the standardization work at ASTM and CIE with the help of a liaison; and

(iii) to orient their work so that NFRC's needs for a single spectrum (specifically applicable to fenestration rating) are fully taken into consideration.

The research project consisted of four tasks, (1) Selection of Glazing Systems, (2) Calculate and Analyze Optical Properties and SHGC with Different Spectra, (3) the THERM models from Task 2 were modified and modeled using the CMA methodology (i.e., Best/Worst options Monitor CIE Technical Committee 2.17 and (4) Reports on CIE Activities, Final Report, and Technical Paper.

Click here for final report

Final Report

REVISION OF STANDARD SPECTRAL WEIGHTING FUNCTION FOR CALCULATION OF SOLAR OPTICAL PROPERTIES AND SOLAR HEAT GAIN

Submitted to:

NFRC Project Monitoring Task Group, and
NFRC Research Subcommittee

Submitted by:

Chris A. Gueymard/Solar Consulting Services, and
William C. duPont/Sunergy Consulting

March 3, 2008

Revised, March 22, 2008

Table of Contents

Table of Contents 2

Background 3

Objectives 4

Scope 4

Task 1 – Selection of Glazing Systems 5

Task 2 – Evaluation of Rated Optical Properties Using Various Spectral Weighting Functions 10

Task 3 – Report ASTM Activities and Represent NFRC at ASTM G-03.09 Meetings 25

Task 4 – Reports on CIE Activities, Final Report, and Technical Paper 27

Recommendations 28

References 29

Appendix 1 — Instructions for Calculating Solar and Optical Properties of Select Glazing Systems Using Alternate Spectra in WINDOW 5.2 31

Appendix 2 — Proposed Methodology to Adjust Solar Calorimeter Test Results Based on a Known Source Spectrum 40

Background

NFRC 200 and NFRC 300 use a standard spectrum for the purpose of weighting the spectral calculations of solar transmission performed by appropriate fenestration analysis software (e.g., WINDOW and OPTICS). Since the inception of these NFRC documents, the spectrum used for this task has always been the ASTM E 891 standard spectrum [*Tables for Terrestrial Direct Normal Solar Spectral Irradiance Tables for Air Mass 1.5* (E891)], which was initially adopted 25 years ago (ASTM 1982), and later elevated to international status (ISO 1992). This is a *direct irradiance* spectrum at an air mass of 1.5. The use of a single standard spectrum is necessary for rating purposes, and therefore needs to be carefully chosen and validated.

ASTM E891 was withdrawn in 1999 and is now *obsolete*. It has been replaced by ASTM G173 [*Standard Tables for Reference Solar Spectral Irradiances: Direct Normal and Hemispherical on 37° Tilted Surface* (G173)] in 2003 (ASTM 2003). This new standard has marked differences; its overall direct irradiance is more intense, its spectral balance is blue-shifted compared to E891, and its resolution is an order of magnitude finer than that of E891. The adoption of this new standard was also backed by a careful validation process based on comparison to actual measurements and other state-of-the-art atmospheric computer models. It is anticipated that international standards organizations, such as CIE, ISO and the International Electrotechnical Commission (IEC), will follow suit and adopt G173 or similar spectra as the standard spectrum for their practices. In particular, IEC is currently in the final steps of adopting a revised version of its standard 60904-3 for photovoltaic applications. The revised IEC reference spectrum consists of a slightly modified version of the global spectrum of G173. Similarly, CIE has established a Technical Committee (TC 2.17) to prepare new spectral standards based on the same radiative model as specified in G173, but for purposes other than those of the ASTM Standard.

With the E891 standard now withdrawn, the NFRC procedures are currently without the proper standard-backing umbrella, and can therefore be considered outdated and obsolete. There is an opportunity to develop new standard spectra in either ASTM or CIE that are more appropriate for the window industry. These new standard spectra would include *global irradiance on vertical surfaces*, which for vertical fenestration, is closer to reality than direct irradiance. It is important that NFRC can be represented in the ASTM or CIE technical discussions so that the standard spectra they eventually adopt respect the specific needs of NFRC. For instance, a particularly sensitive case is the rating of skylights, which can be improved by relying on a specific spectrum corresponding to a tilted—rather than vertical—surface. ASTM and/or CIE should address the issue of non-vertical surfaces in their deliberations, using their own expertise to offer NFRC some educated choices. All these developments would offer NFRC the opportunity to participate in the replacement of the currently outdated weighting function with more accurate data, and to insure that tilted products, such as skylights, are represented too. It is anticipated that, through the use of more accurate solar spectral data, simulation software will generate Solar Heat Gain Coefficients (SHGC) that are in better agreement with actual solar calorimeter test results, thus removing a source of uncertainty in SHGC calculations.

In order to keep up with the latest and more accurate procedures, NFRC 200 and NFRC 300 need to update the standard spectrum used in those procedures. To accomplish this goal, NFRC needs

to decide if it should reference ASTM G173, or a potentially more appropriate spectrum from ASTM or CIE. Knowledge about how this change will affect the current SHGC and Visible Transmittance (VT) ratings is crucial in order to select a new solar spectral weighting function (SWF) for NFRC's use.

Furthermore, it is anticipated that the current standardization process at ASTM and CIE will have a ripple effect in Europe, with the likely result of changes into ISO standards and European rating procedures. Therefore, this project provides a timely opportunity of finally harmonizing the North American and European rating methodologies, at least regarding the spectral issues.

Objectives

The intent of this research project is to provide a *recommended solar spectrum* to NFRC by assessing the impact of a potential change in the reference spectrum that is used to weigh the spectral transmission calculations through glazing. It is therefore proposed

(i) to evaluate the effect that adopting one of the new possible spectra would have on the optical properties, SHGC and VT ratings of typical fenestration systems;
(ii) to follow closely the progress of the standardization work at ASTM and CIE with the help of a liaison; and
(iii) to orient their work so that NFRC's needs for a single spectrum (specifically applicable to fenestration rating) are fully taken into consideration.

Scope

This research project consists of four inter-related tasks, which were originally defined as:

Task 1 – Selection of Glazing Systems

Task 2 – Calculate and Analyze Optical Properties and SHGC with Different Spectra

Task 3 – Monitor CIE Technical Committee 2.17

Task 4 – Reports on CIE Activities, Final Report, and Technical Paper.

Details on how these tasks have been accomplished are reported as follows.

Task 1 – Selection of Glazing Systems

It is anticipated that a change in the spectral weighting function will affect some glazing systems more than others. For instance, negligible change in the SHGC of clear glass should occur because the latter's transmittance is essentially flat over the most important part of the shortwave spectrum. Conversely, glazing systems characterized by strong spectral selectivity due to their use of coatings, films, etc., are more likely to be affected in one way or another. At this stage, it would not be productive or cost-effective to analyze all possible glazing systems that can be invented by combining various elements. Hundreds of thousand such combinations might exist.

To explore the effect of a change in the spectral weighting function, the Principal Investigators (PI) worked in close contact with the assigned Project Monitoring Task Group (PMTG) to develop an appropriate and manageable methodology. The PI proposed, and the PMTG approved, to analyze combinations of glazing and coatings that would be representative of a large range of optical properties and glazing system types. Because of the anticipated key role that would be played by spectral selectivity, the PI selected glazing systems of different types of glass and coatings, using one to three layers, as well as specific glazing systems used for skylights. The PI defined six categories:

1. Window Films on Glazing
2. Laminates and Laminated Glazing
3. Reference Glazing
4. Double Glazing—Low-E
5. Double Glazing—Electrochromic
6. Triple Glazing—Clear, Heat Mirror & Low-E.

These categories were populated with glazing systems that appeared to be either "typical" or "extreme" in various ways, and to respect a few important criteria, which are detailed below. The third category ("Reference Glazing") was created to represent specific systems from the technical literature, known to the PI or members of the PMTG for their special characteristics or scientific value.

The following criteria and objectives were used to develop the specimen list in Table 1.

LSG Ratio: The intent was to select different glazing systems that would create a large scatter in a "T_{vis} *vs* SHGC" plot (see Figure 1). Spectral selectivity can be characterized by the Light-to-Solar-Gain ratio, LSG, which is simply the ratio of the Visible Transmittance (VT, or T_{vis}) and SHGC. The importance of LSG in characterizing the performance of glazings vis-à-vis solar heat gains and energy conservation in buildings has been studied extensively in the literature (see, e.g., McCluney, 1993, 1996). Hopefully, this deliberate large scatter in LSG will ensure that the broadest range of both non-spectrally selective and spectrally selective glazing systems is chosen. The LSG of the selected specimens spans from 0.058 to 2.381 (Table 2), indicating glazing systems of very diverse properties and performance.

Manufacturer Representation: Although it was impossible to include all manufacturers listed in the Glazing Library, there was an effort to have each of the NFRC Members' and major

United States manufacturers' products represented. To that end, there was also an attempt to include the most common product types.

Reference Glazing: Some of the glazing systems were selected because they were used in previous research projects, such as those by McCluney (1993, 1996) and McCluney and Gueymard (1993). The results for these reference systems can be used for comparison and verification purposes, or future scientific research.

A list of the 37 glazing systems analyzed in this project is presented in Table 1. A plot of the visible transmittance *vs.* the Solar Heat Gain Coefficient (SHGC) for each glazing system is presented in Figure 1. Both Table 1 and Figures 1–3 are also included in a separate spreadsheet file. [In that file, moving the cursor over a symbol in the original Figure (in the "Figure 1" tab, reproduced here also as Figure 1) helps to identify that point.]

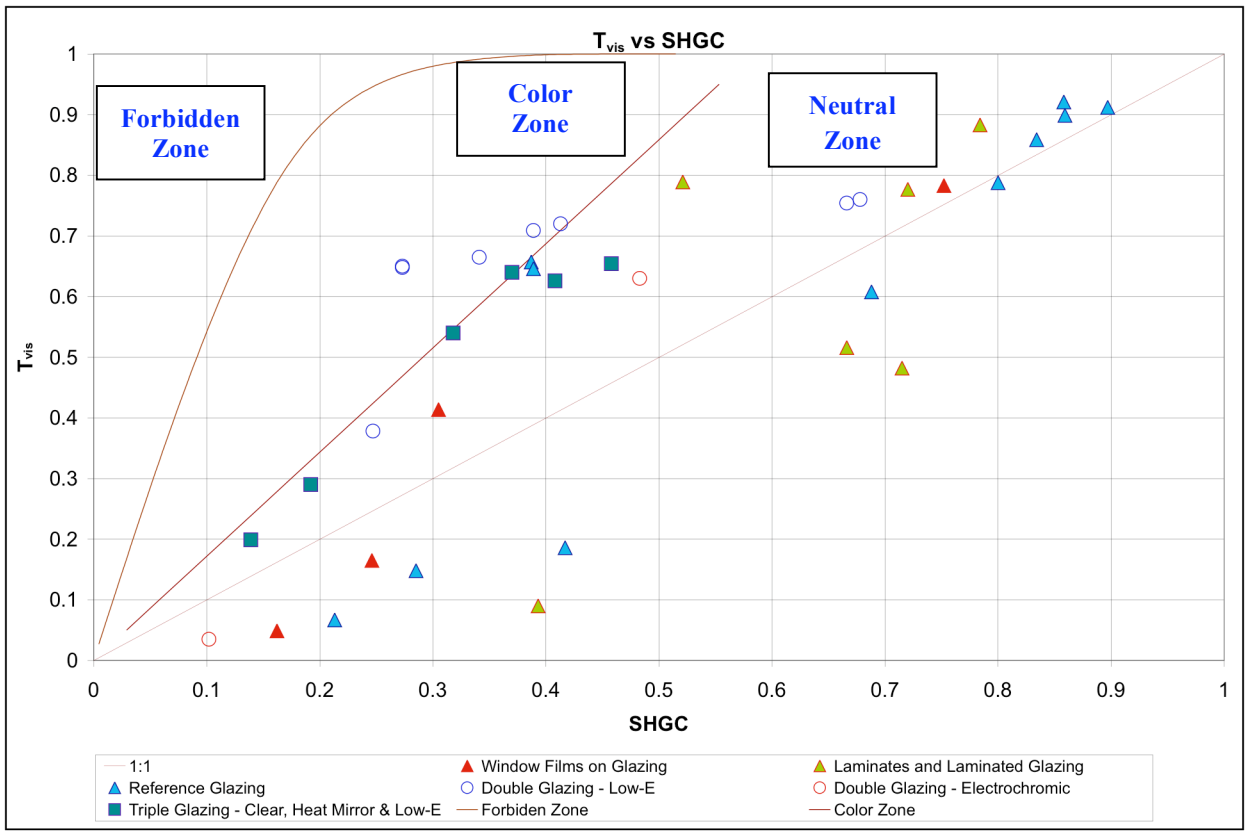


Fig. 1 Visible transmittance (T_{vis}) *vs* SHGC for the 37 specimens

Figure 1 also indicates some properties of glass, such as the limits of the "Color Zone", "Forbidden Zone", and "Neutral Zone", as defined by Mike Rubin and explained in McCluney and Gueymard (1993).

Table 1 Summary statistics for the optical properties of the 37-specimen dataset.

		WINDOW 5.2.17a Glazing Library Data															Center-of-Glass Results				
Glazing ID	OPTICS 5.1 Layers	Glass ID	Name	Product Name	Manufacturer	Source	Mode	Thick. mm	Tsol	Rsol1	Rsol2	Tvis	Rvis1	Rvis2	Tir	emis1	emis2	U-Factor W/(m²·K)	SHGC	Tvis	LSG	Comment
Window Films on Glazing																						
10	BRONZE_6.AFG + Sunbelt LowE	775	ESB4.AFG	Sunbelt LowE on Bronze	AFG Industries	IGDB v11.4	#	5.613	0.215	0.170	0.524	0.414	0.106	0.177	0.000	0.840	0.025	3.187	0.305	0.414	**1.357**	LowE Low Transmittance
11	GRAY_6.AFG + Gold	792	G308.AFG	Gold on Grey	AFG Industries	IGDB v11.4	#	5.639	0.026	0.189	0.712	0.049	0.172	0.576	0.000	0.840	0.124	3.538	0.162	0.049	**0.302**	Low Transmittance
45	CLEAR_6.PPG + RE15SIARXL	2751	RE15SIARXL.mmm	Scotch Tint Sun Control	3M Corporation	IGDB v14.6	#	5.648	0.115	0.439	0.628	0.165	0.557	0.610	0.000	0.840	0.840	5.817	0.246	0.165	**0.671**	Lowest Transmittance 3M Coating
25	CLEAR_6.PPG + SunClean	5306	SN-6.ppg	SunClean on Clear	PPG Industries	IGDB v14.1	#	5.664	0.712	0.145	0.131	0.783	0.191	0.184	0.000	0.837	0.842	5.825	0.752	0.783	**1.041**	SunClean
Laminates and Laminated Glazing																						
15	015_8050.SOL	1815	015_8050.SOL	Vanceva Ruby Red	Solutia	IGDB v11.4	#	6.380	0.623	0.063	0.064	0.482	0.060	0.061	0.000	0.840	0.840	5.723	0.715	0.482	**0.674**	Red Glazing
16	015_8178.SOL	1817	015_8178.SOL	Vanceva Sahara Sun	Solutia	IGDB v11.4	#	6.380	0.632	0.067	0.069	0.777	0.084	0.085	0.000	0.840	0.840	5.723	0.720	0.777	**1.079**	Yellow Glazing
17	015_8250.SOL	1819	015_8250.SOL	Vanceva Sapphire	Solutia	IGDB v11.4	#	6.380	0.553	0.062	0.061	0.516	0.061	0.059	0.000	0.840	0.840	5.723	0.666	0.516	**0.775**	Blue Glazing
46	BRN_Dark.DUP	1112	BRN_Dark.DUP	Butacite 0360900	DuPont	IGDB v11.4	#	6.760	0.151	0.068	0.068	0.090	0.079	0.079	0.000	0.840	0.840	5.687	0.393	0.090	**0.229**	Low Transmittance Interlayer
18	030cl3_0.SOL	1845	030cl3_0.SOL	Saflex Clear	Solutia	IGDB v11.4	#	6.760	0.724	0.069	0.068	0.883	0.079	0.079	0.000	0.840	0.840	5.663	0.784	0.883	**1.126**	Laminated Clear
19	CLR-3.CIG + X4	2059	X4-3.cig	X4 LoE 2-Lami on Clear	Cardinal IG	IGDB v12.4	#	2.972	0.486	0.262	0.348	0.789	0.082	0.093	0.000	0.840	0.065	3.367	0.521	0.789	**1.514**	Laminated LowE
Reference Glazing																						
20	Acrylic	2604	236MCATO	Plexiglas MC	ATOFINA Chemicals, Inc.	IGDB v11.4		5.994	0.825	0.069	0.069	0.921	0.073	0.073	0.000	0.900	0.900	5.167	0.858	0.921	**1.073**	Clear Plexiglass
66	Polycarbonate	3501	LXCL_3.GEC	Lexan XL	General Electric Company	IGDB v11.4	#	2.997	0.801	0.086	0.085	0.859	0.087	0.087	0.000	0.892	0.892	5.644	0.834	0.859	**1.030**	Thin Lexan
67	Polycarbonate	3504	LXCL_13.GEC	Lexan XL	General Electric Company	IGDB v11.4	#	12.700	0.737	0.078	0.079	0.788	0.080	0.080	0.000	0.892	0.892	4.386	0.800	0.788	**0.985**	Thick Lexan
71	Glass	9831	GREY3.LOF	Optifloat Grey	Pilkington North America	IGDB v11.4	#	3.200	0.585	0.059	0.059	0.608	0.061	0.061	0.000	0.840	0.840	5.907	0.688	0.608	**0.884**	Thin Grey Glass
72	Glass	9837	GREY12.LOF	Optifloat Grey	Pilkington North America	IGDB v11.4	#	12.497	0.171	0.044	0.044	0.186	0.045	0.045	0.000	0.840	0.840	5.592	0.417	0.186	**0.446**	Thick Grey Glass
24	Glass	5004	STRPH_6.PPG	Starphire	PPG Industries	IGDB v14.6	#	5.664	0.888	0.079	0.081	0.912	0.083	0.084	0.000	0.840	0.840	5.820	0.897	0.912	**1.017**	Clear Glass (Highest Transmittance)
27	Azurl_6.ppg + VE785	6080	VE785.VIR	LowE on Azuria	Viracon	IGDB v14.0	#	5.660	0.278	0.053	0.249	0.657	0.057	0.049	0.000	0.840	0.088	3.413	0.387	0.657	**1.698**	Gueymard Reference
28	Evgrn6.lof + VE855	6085	VE885.VIR	LowE on Evergreen	Viracon	IGDB v11.4	#	5.660	0.282	0.059	0.243	0.646	0.058	0.043	0.000	0.840	0.088	3.413	0.389	0.646	**1.661**	Gueymard Reference
44	Azurl_6.ppg + VS708	6109	VS708.VIR	Stainless Steel on Azurlite	Viracon	IGDB v11.4	#	5.660	0.029	0.145	0.478	0.067	0.295	0.374	0.000	0.840	0.354	4.317	0.213	0.067	**0.315**	McCluney ASES 93
43	Evgrn6.lof + VS820	6114	VS820.VIR	Stainless Steel on Evergreen	Viracon	IGDB v11.4	#	5.660	0.068	0.087	0.387	0.148	0.154	0.319	0.000	0.840	0.531	4.886	0.285	0.148	**0.519**	McCluney ASES 93
57	CLEAR_3.DAT	102	CLEAR_3.DAT	Generic Clear Glass	Generic	IGDB v11.4	#	3.048	0.834	0.075	0.075	0.899	0.083	0.083	0.000	0.840	0.840	5.912	0.859	0.899	**1.047**	Double & Triple Clear Reference
Double Glazing - Low-E																						
73	BRONZE_6.AFG + Sunbelt LowE	775	ESB4.AFG	Sunbelt LowE on Bronze	AFG Industries	IGDB v11.4	#	5.613	0.215	0.170	0.524	0.414	0.106	0.177	0.000	0.840	0.025	1.740	0.247	0.378	**1.530**	Double Clear & AFG LowE
	CLEAR_3.DAT	102	CLEAR_3.DAT	Generic Clear Glass	Generic	IGDB v11.4	#	3.048	0.834	0.075	0.075	0.899	0.083	0.083	0.000	0.840	0.840					
70	CLR-3.CIG + LoE2-272	2011	EE272-3.CIG	LoE2-272 on 3 mm Clear	Cardinal IG	IGDB v14.5	#	2.970	0.429	0.325	0.418	0.793	0.056	0.043	0.000	0.840	0.042	1.784	0.413	0.720	**1.743**	Double Clear & Cardinal LowE Reference
	CLR-3.CIG	2001	CLR-3.CIG	Float Glass	Cardinal IG	IGDB v11.4	#	2.970	0.848	0.076	0.076	0.904	0.082	0.082	0.000	0.840	0.840					
80	CLR-2.CIG + LoE^3-366	2153	E366-2.CIG	LoE^3 366 on Clear	Cardinal IG	IGDB v14.5	#	2.200	0.277	0.451	0.549	0.717	0.066	0.044	0.000	0.840	0.022	1.749	0.273	0.648	**2.374**	Double Clear & Cardinal LowE
	CLEAR_3.DAT	102	CLEAR_3.DAT	Generic Clear Glass	Generic	IGDB v11.4	#	3.048	0.834	0.075	0.075	0.899	0.083	0.083	0.000	0.840	0.840					
81	Clear_23.GRD + RLE 71/38	3232	RLE71382.grd	ClimaGuard RLE 71/38 Low-E on clear	Guardian	IGDB v14.2	#	2.286	0.405	0.353	0.437	0.786	0.048	0.040	0.000	0.840	0.027	1.758	0.389	0.709	**1.823**	Double Clear & Guardian LowE
	CLEAR_3.DAT	102	CLEAR_3.DAT	Generic Clear Glass	Generic	IGDB v11.4	#	3.048	0.834	0.075	0.075	0.899	0.083	0.083	0.000	0.840	0.840					
82	CLEAR2.LOF + Energy Advantage LoE	9920	LOW-E_2.LOF	Energy Advantage Low-E	Pilkington North America	IGDB v11.4	#	2.235	0.713	0.110	0.121	0.831	0.107	0.113	0.000	0.840	0.159	1.990	0.666	0.754	**1.132**	Double Clear & Pilkington LowE
	CLEAR_3.DAT	102	CLEAR_3.DAT	Generic Clear Glass	Generic	IGDB v11.4	#	3.048	0.834	0.075	0.075	0.899	0.083	0.083	0.000	0.840	0.840					
77	STRPH_6.PPG + Solarban 70XL	5000	SB70XL Stph-6.PPG	Solarban 70XL on Starphire	PPG Industries	IGDB v14.5	#	5.664	0.281	0.513	0.562	0.720	0.077	0.059	0.000	0.841	0.018	1.727	0.273	0.650	**2.381**	Double Clear & PPG LowE
	CLEAR_3.DAT	102	CLEAR_3.DAT	Generic Clear Glass	Generic	IGDB v11.4	#	3.048	0.834	0.075	0.075	0.899	0.083	0.083	0.000	0.840	0.840					
83	CLEAR_2.PPG + Sungate 500	5240	S500CL_2.PPG	Sungate 500 on Clear	PPG Industries	IGDB v11.4	#	2.261	0.727	0.112	0.127	0.838	0.109	0.113	0.000	0.840	0.215	2.079	0.678	0.760	**1.121**	Double Clear & PPG Sungate LowE
	CLEAR_3.DAT	102	CLEAR_3.DAT	Generic Clear Glass	Generic	IGDB v11.4	#	3.048	0.834	0.075	0.075	0.899	0.083	0.083	0.000	0.840	0.840					
79	ip024004.ipe + 33600	7117	ip6734naipe	ipaol natura 67734	Interpane Glass Industries	IGDB v14.6	#	6.000	0.346	0.334	0.460	0.737	0.064	0.046	0.000	0.840	0.024	1.738	0.341	0.665	**1.950**	Double Clear & Interpane LowE
	CLEAR_3.DAT	102	CLEAR_3.DAT	Generic Clear Glass	Generic	IGDB v11.4	#	3.048	0.834	0.075	0.075	0.899	0.083	0.083	0.000	0.840	0.840					
Double Glazing - Electrochromic																						
58	CLEAR_3.DAT	102	CLEAR_3.DAT	Generic Clear Glass	Generic	IGDB v11.4	#	4.000	0.018	0.103	0.103	0.039	0.059	0.024	0.000	0.840	0.148	1.964	0.102	0.035	**0.343**	Double Electrochromic Dark
	Unknown + SageGlass EC	1200	SageGlass_4_0.SAG	SageGlass tinted state	SAGE Electrochromics, Inc	IGDB v11.2	#	3.048	0.834	0.075	0.075	0.899	0.083	0.083	0.000	0.840	0.840					
59	CLEAR_3.DAT	102	CLEAR_3.DAT	Generic Clear Glass	Generic	IGDB v11.4	#	4.000	0.498	0.180	0.131	0.696	0.167	0.081	0.000	0.840	0.148	1.964	0.483	0.630	**1.304**	Double Electrochromic Light
	Unknown + SageGlass EC	1201	SageGlass_4_1.SAG	SageGlass untinted state	SAGE Electrochromics, Inc	IGDB v11.2	#	3.048	0.834	0.075	0.075	0.899	0.083	0.083	0.000	0.840	0.840					
Triple Glazing - Clear, Heat Mirror & Low-E																						
60	CLEAR_3.DAT	102	CLEAR_3.DAT	Generic Clear Glass	Generic	IGDB v11.4	#	5.700	0.409	0.264	0.417	0.781	0.055	0.042	0.000	0.840	0.042	1.242	0.370	0.640	**1.730**	Triple Clear LowE
	CLEAR_3.DAT	102	CLEAR_3.DAT	Generic Clear Glass	Generic	IGDB v11.4	#	3.048	0.834	0.075	0.075	0.899	0.083	0.083	0.000	0.840	0.840					
	CLR-6.CIG + LoE^3-272	2014	EE272-6.CIG	LoE^3-272 on 6 mm Clear	Cardinal IG	IGDB v14.5	#	3.048	0.834	0.075	0.075	0.899	0.083	0.083	0.000	0.840	0.840					
61	CLEAR_3.DAT	102	CLEAR_3.DAT	Generic Clear Glass	Generic	IGDB v11.4	#	3.048	0.834	0.075	0.075	0.899	0.083	0.083	0.000	0.840	0.840	1.206	0.139	0.199	**1.432**	Triple Clear Heat Mirror 22
	Unknown + Heat Mirror 22	1500	HM22 SWT	Heat Mirror 22 Suspended Film	Southwall Technologies	IGDB v11.4		0.076	0.103	0.832	0.811	0.218	0.705	0.724	0.000	0.019	0.755					McCluney ASES 93
	CLEAR_3.DAT	102	CLEAR_3.DAT	Generic Clear Glass	Generic	IGDB v11.4	#	3.048	0.834	0.075	0.075	0.899	0.083	0.083	0.000	0.840	0.840					
62	CLEAR_3.DAT	102	CLEAR_3.DAT	Generic Clear Glass	Generic	IGDB v11.4	#	3.048	0.834	0.075	0.075	0.899	0.083	0.083	0.000	0.840	0.840	1.204	0.192	0.290	**1.510**	Triple Clear Heat Mirror 33
	Unknown + Heat Mirror 33	1501	HM33 SWT	Heat Mirror 33 Suspended Film	Southwall Technologies	IGDB v11.4		0.076	0.157	0.766	0.744	0.323	0.588	0.608	0.000	0.017	0.755					
	CLEAR_3.DAT	102	CLEAR_3.DAT	Generic Clear Glass	Generic	IGDB v11.4	#	3.048	0.834	0.075	0.075	0.899	0.083	0.083	0.000	0.840	0.840					
63	CLEAR_3.DAT	102	CLEAR_3.DAT	Generic Clear Glass	Generic	IGDB v11.4	#	3.048	0.834	0.075	0.075	0.899	0.083	0.083	0.000	0.840	0.840	1.263	0.458	0.654	**1.428**	Triple Clear Heat Mirror 77
	Unknown + Heat Mirror 77	1505	HM77 SWT	Heat Mirror 77 Suspended Film	Southwall Technologies	IGDB v11.4	#	0.076	0.478	0.410	0.391	0.786	0.128	0.147	0.000	0.070	0.755					McCluney ASES 93
	CLEAR_3.DAT	102	CLEAR_3.DAT	Generic Clear Glass	Generic	IGDB v11.4	#	3.048	0.834	0.075	0.075	0.899	0.083	0.083	0.000	0.840	0.840					
64	CLEAR_3.DAT	102	CLEAR_3.DAT	Generic Clear Glass	Generic	IGDB v11.4	#	3.048	0.834	0.075	0.075	0.899	0.083	0.083	0.000	0.840	0.840	1.247	0.408	0.626	**1.534**	Triple Clear Heat Mirror Solar Control 75
	Unknown + Heat Mirror Single Coat 75	1510	HMSC75 SWT	Heat Mirror Solar Control 75 Suspended Film	Southwall Technologies	IGDB v14.6	#	0.076	0.375	0.460	0.460	0.756	0.107	0.128	0.000	0.055	0.755					
	CLEAR_3.DAT	102	CLEAR_3.DAT	Generic Clear Glass	Generic	IGDB v11.4	#	3.048	0.834	0.075	0.075	0.899	0.083	0.083	0.000	0.840	0.840					
65	CLEAR_3.DAT	102	CLEAR_3.DAT	Generic Clear Glass	Generic	IGDB v11.4	#	5.700	0.409	0.264	0.417	0.781	0.055	0.042	0.000	0.840	0.042	1.208	0.318	0.540	**1.698**	Triple Clear LowE w/Heat Mirror
	Unknown + Heat Mirror Single Coat 75	1510	HMSC75 SWT	Heat Mirror Solar Control 75 Suspended Film	Southwall Technologies	IGDB v14.6	#	0.076	0.375	0.460	0.460	0.756	0.107	0.128	0.000	0.055	0.755					
	CLR-6.CIG + LoE2-272	2014	EE272-6.CIG	LoE2-272 on 6 mm Clear	Cardinal IG	IGDB v14.5	#	3.048	0.834	0.075	0.075	0.899	0.083	0.083	0.000	0.840	0.840					

Figure 2 presents the distribution of LSG for all of the glazing systems, in increasing order of LSG. The frequency distribution of LSG (in number of cases per bin of 0.2 LSG) appears in Figure 3. These figures demonstrate the large range of spectral selectivity of all the specimens. For the whole dataset, the range in LSG, U-factor, Tvis and SHGC is quite large (Table 2).

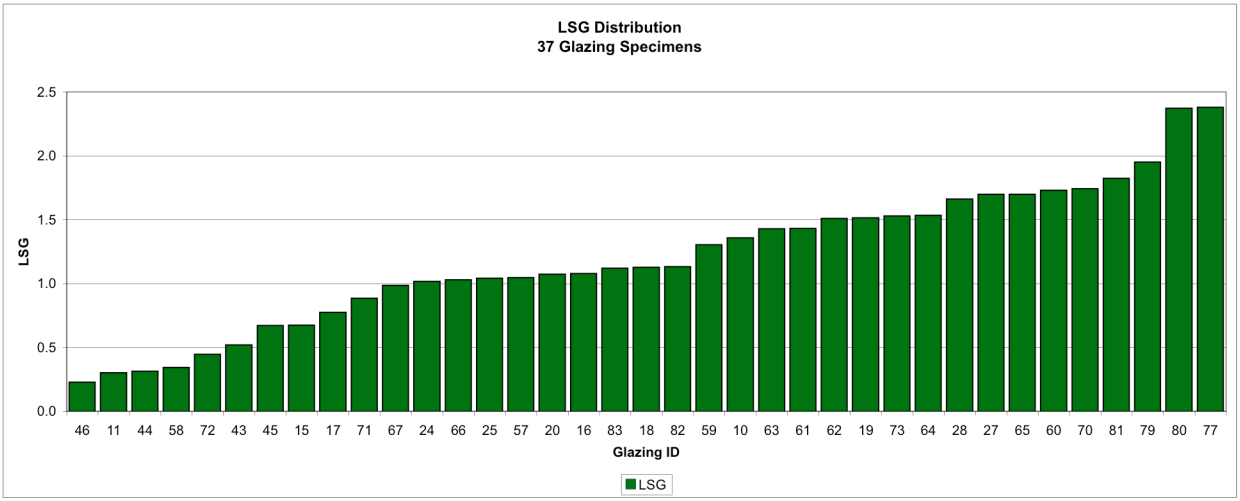


Fig. 2 Distribution of LSG (=Tvis/SHGC) among the 37 specimens, in increasing order of LSG

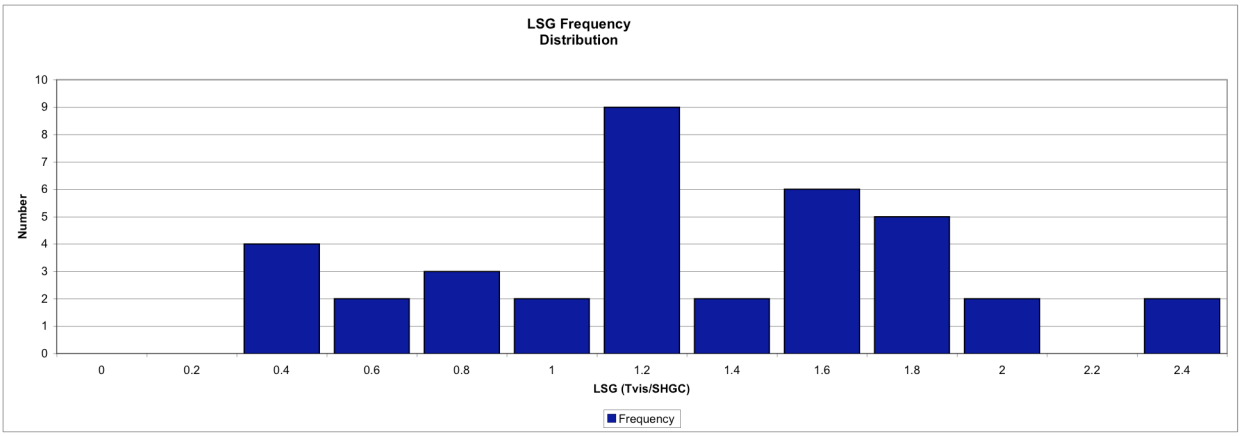


Fig. 3 Frequency distribution of LSG, i.e., number of specimens per bin of 0.2 LSG

Table 2 Summary statistics for the optical properties of the 37-specimen dataset.

Variable	U-Factor	SHGC	Tvis	LSG
Unit	W/(m^2 • K)	-	-	-
Minimum	1.204	0.102	0.035	0.229
Mean	3.529	0.477	0.555	1.202
Maximum	5.912	0.897	0.921	2.381
Std. Dev.	1.868	0.236	0.273	0.550

Some details need to be stressed for a proper interpretation of Table 1.

Center-of-Glass: All of the thermal and optical properties are listed for the center-of-glass region as calculated by WINDOW 5.2.17a. Although edge and spacer effects may affect the U-factor, they do not affect the visible transmittance or solar heat gain of the glazing system, and therefore were omitted from the scope of this analysis.

Glazing Thickness: Most of the glazing samples have a nominal thickness of 6 mm. (The exact thickness varies between 5.613 and 6.760 mm.) Two monolithic substrates (e.g., polycarbonate and bronze glass) of vastly different thicknesses (e.g., 3 and 12 mm) are included in the "Reference Glazing" category to show the combined effects of the spectral weighing function and glazing thickness on SHGC. All the clear glass layers in double and triple glazing systems are 3-mm thick. Finally, the thickness of the Heat Mirror suspended films (#61–65), of one laminate (#19), and of the electrochromic systems (#58 and 59) is less than 6 mm.

Gas Fill and Cavity Thicknesses: The gas-fill thicknesses are always 19.5 mm in the double-glazing systems, and 12.7 mm in triple-glazing specimens. The clear-glass layer in double- and triple-glazing systems is always the same 3-mm Generic Clear Glass. Air is used as the gas fill in all of the specimens as none of the gasses used to fill cavities in typical glazing systems are spectrally selective at these thicknesses.

U-Factor: The values listed in Tables 1 and 2 correspond to a vertical glazing system. This study considers that the same systems could also be mounted on a roof, whose standard tilt is 20° (NFRC 100). Under such conditions, the U-factor is larger (sometimes significantly) than in the vertical case. This effect has been considered in all of the simulations performed at a 20° tilt.

Orientation of Films/Coatings: The single glazed systems always have applied films facing indoors except for the SunClean on Clear (#25), which has the film facing outside. All of the double- and triple- glazed systems have the low-e coating or film applied to the inner surface of the outer pane (Surface 2), which is inside of the glazing cavity. The heat mirror films are all oriented in the same direction, with the lower-emittance surface facing toward the outside (Surface 3).

Software and Naming Convention: All of the thermal and optical properties in Table 1 were generated using WINDOW 5.2.17a and OPTICS 5.1. The Glass ID, Name, Product Name and other information in Table 1 was directly copied from the Glazing Library (15.5) in the WINDOW 5 program.

Task 1 Deliverables: The original Work Statement required that a list 20 specimens be provided to the PMTG, of which 16 would be selected for analysis.

In actuality, the PI analyzed 37 specimens after the list was approved by the PMTG.

Task 2 – Evaluation of Rated Optical Properties Using Various Spectral Weighting Functions

Using WINDOW and OPTICS (the current NFRC 200 and NFRC 300 approved computer modeling software) the SHGC and VT ratings of the glazing systems identified in Task 1 were determined, successively for various spectral weighting functions not currently available in these computer programs.

The PMTG approved the following seven spectra to be used to analyze the 37 test specimens chosen in Task 1. The first three spectra have already been standardized by ASTM. The last four are in the process (see Task 3), and have been given a temporary ASTM Work Item Number, WK 17196.

1. ASTM E891 Spectrum (used by default in WINDOW 5.2), as prescribed by NFRC 200 & NFRC 300. This is the "base case" scenario, to which all other results will be compared. The calculations in Table 1 use this default spectrum.
2. ASTM G 173 Direct Irradiance at Normal Incidence (2003)
3. ASTM G 173 Global Irradiance for a 37º Tilt (2003)
4. Proposed ASTM Direct Irradiance Spectrum for a 20º Tilt
5. Proposed ASTM Global Irradiance Spectrum for a 20º Tilt
6. Proposed ASTM Direct Irradiance Spectrum for a Vertical Surface
7. Proposed ASTM Global Irradiance Spectrum for a Vertical Surface.

Discussion on Diffuse Radiation
It is important to stress that NFRC 200 and NFRC 300 specify a *direct* spectrum, whereas Europeans specify a *global* spectrum. In general terms, a global spectrum is a combination of a direct and a diffuse spectrum. The diffuse spectrum is always richer in blue wavelengths than a direct spectrum, but overall has a far lower intensity than the direct spectrum. This is illustrated in Figure 4, which refers to the proposed ASTM spectra mentioned above.

Another difference between a direct and diffuse spectrum is that the former is associated with a quasi-point source (the sun's disc), whereas the latter originates from the whole sky vault and/or the ground (by reflection). Moreover, the spatial distribution of diffuse radiation is not homogeneous over the sky. This considerably complicates the analysis of diffuse solar heat gains.

Currently, WINDOW 5.2 calculates the SHGC and VT for direct irradiance *only*. The proposed ASTM Standard (see Task 3 below) includes spectra separately for direct and diffuse solar irradiance for both vertical and 20º-tilted surfaces. [The 20° tilt angle has been standardized by NFRC to define the tilt of skylights used on roofs.]

There is ongoing discussion related to the importance of considering the diffuse radiation incident on fenestration. The PI has been in negotiation with LBNL concerning the implementation of this desirable new capability in WINDOW (i.e., addressing the calculation of SHGC and VT for incident diffuse radiation, in addition to direct radiation). Unfortunately, LBNL's staff was not able to implement that modification in time to be included in this research project.

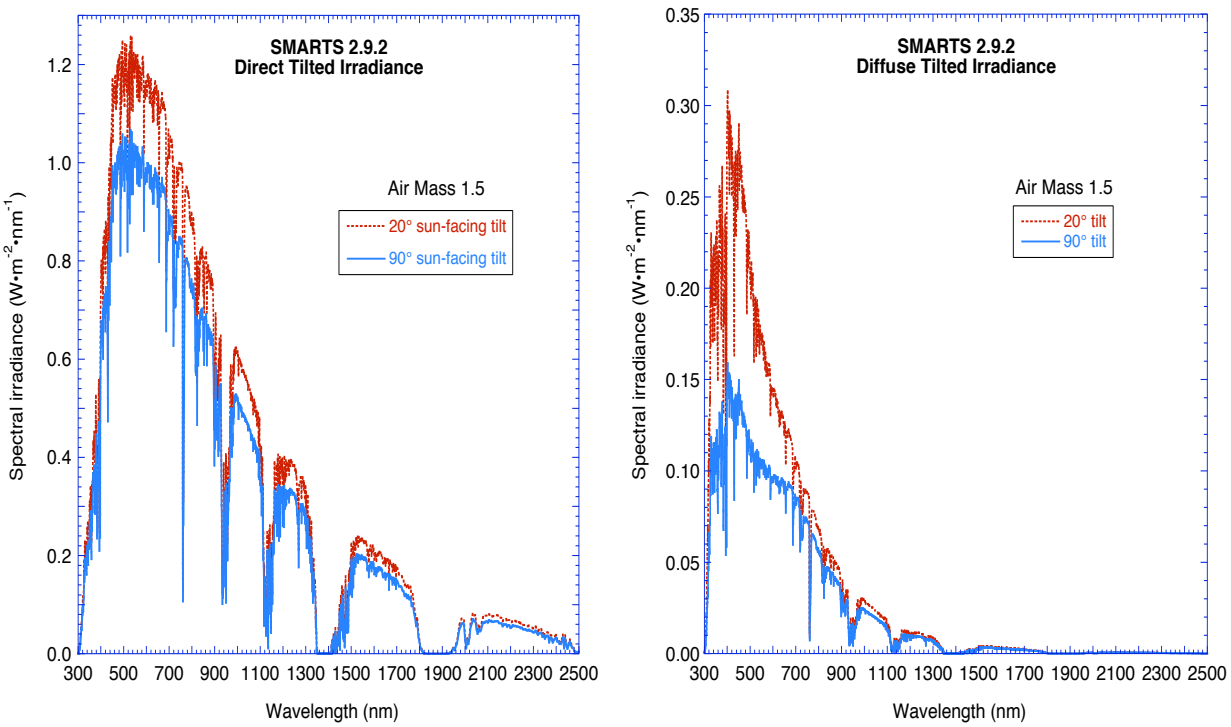


Fig. 4 Direct and diffuse reference spectral irradiance distributions as proposed to ASTM. Note the change in Y-axis scale.

The proposed spectra separate direct and diffuse irradiance because it is anticipated that WINDOW and other fenestration analysis software will eventually calculate the transmission of diffuse radiation. This would be particularly important for diffusing fenestration systems (i.e., frits, frosted glass, etc.), and for an eventual annual energy rating, since most windows are exposed to significant diffuse radiation for long periods during the year. The total diffuse irradiance might even have to be separated into *sky diffuse* and *ground-reflected diffuse*, because both their spectral *and* angular distributions are different. This might come into play in a future version of WINDOW, per our discussions with LBNL.

Since WINDOW cannot currently consider point sources of diffuse radiation, each associated with a different incidence angle, the only possible way to use a diffuse or global spectral weighting function is by assimilating them to a direct spectrum, i.e., by ignoring the multi-directional aspect of diffuse radiation. This normally does not introduce too much error because diffuse irradiance is generally a small fraction of direct irradiance, as mentioned above (Fig. 4). The notable exception, however, is in the UV and at blue wavelengths, where the diffuse fraction is significant. As mentioned earlier, the European methodology uses a global spectrum as if it were purely direct radiation. Until a true calculation of diffuse SHGC and VT calculations can be done reliably, we think this pragmatic approach is the best compromise.

A provision is made in the proposed ASTM standard that the tabulated *diffuse* spectral irradiance can be used solely to represent cases when a surface is shaded from the sun, and therefore no direct radiation impinges on fenestration. This is a very common case under realistic conditions.

Alternate Spectra

The comparison between the existing NFRC spectrum (i.e., ASTM E891) and the proposed direct and global spectra for vertical and 20° tilts are presented in Figures 5–7. Interestingly, these figures show that the four proposed spectra are *less* different from the current NFRC weighting function than the two existing ASTM G173 standard spectra.

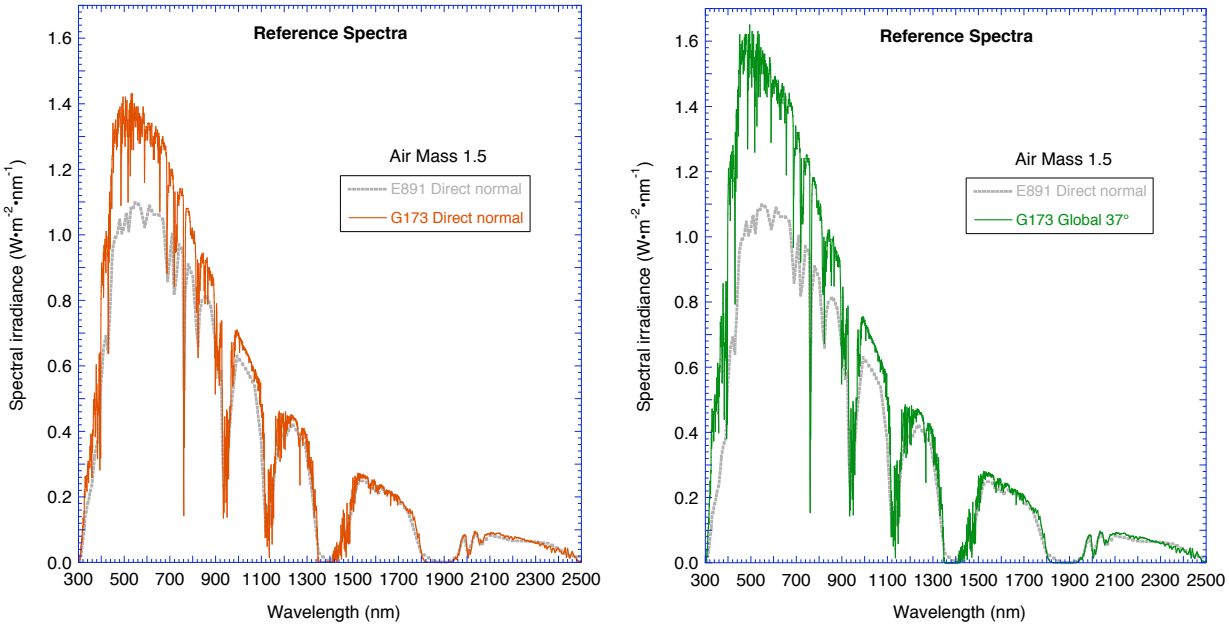


Fig. 5 Direct and global reference spectral irradiance distributions from ASTM G173 compared to the current NFRC distribution, per ASTM E891

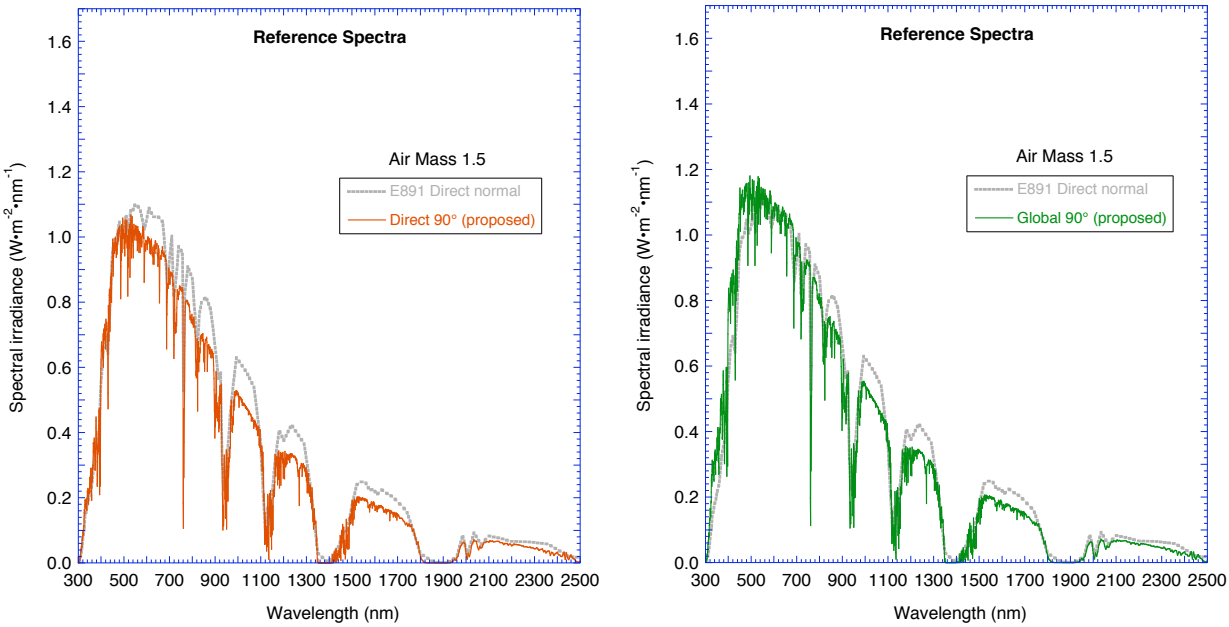


Fig. 6 Direct and global reference spectral irradiance distributions for vertical surfaces from the proposed ASTM standard compared to the current NFRC distribution, per ASTM E891

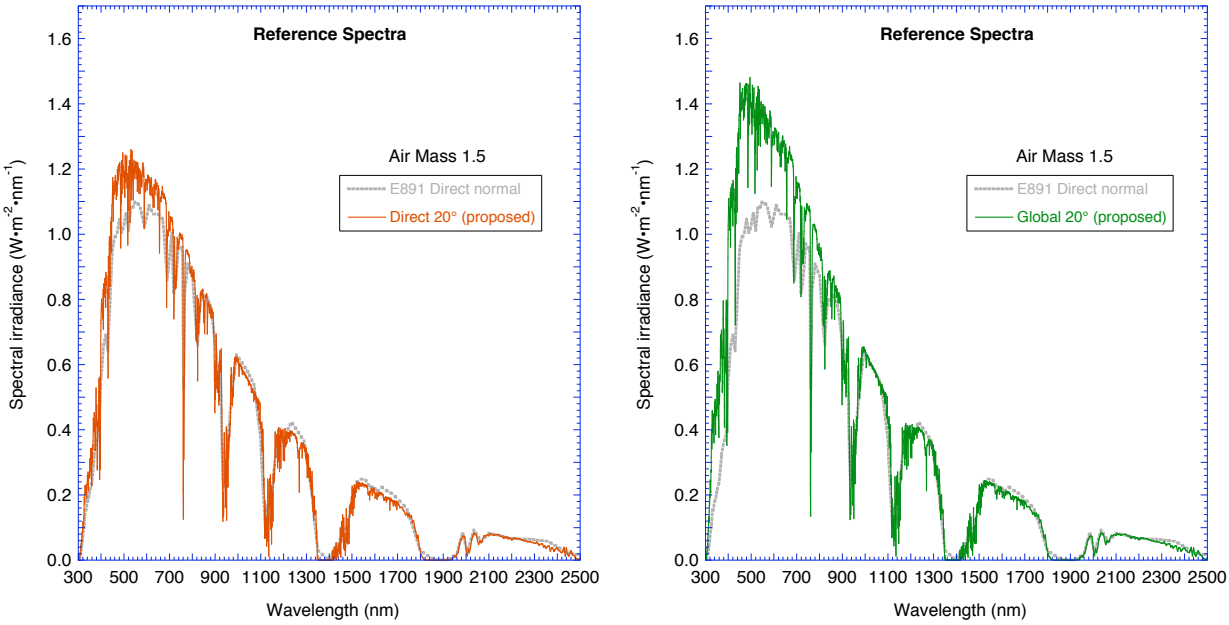


Fig. 7 Direct and global reference spectral irradiance distributions for 20°-tilted surfaces from the proposed ASTM standard compared to the current NFRC distribution, per ASTM E891

U-Factor and Tilt Effects

This study considers the spectral effects affecting both vertical fenestration and roof-mounted skylights. Although it is likely that not all of the 37 selected specimens would constitute good skylights, we have simulated them all anyway for both a 90° and a 20° tilt. Note, however, that a change in tilt also affects the convection heat transfer, and hence the U-factor. Our results show that, for our 37 specimens, the U-factor increases by 8–34% when moving from a 90° tilt to a 20° tilt (Figure 8). The largest percent changes normally correspond to the lowest U-factors.

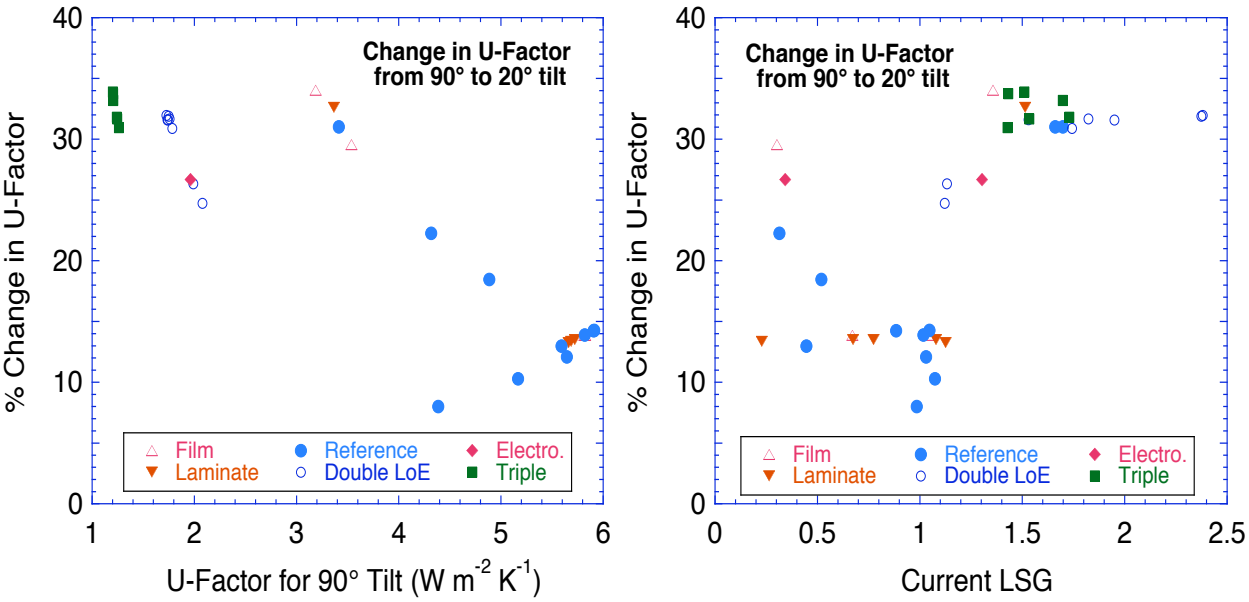


Fig. 8 Percent change in U-factor for a 20°-tilt *vs.* a 90°-tilt, for varying U-factor (left) or LSG (right).

To serve as the base case for all 20°-tilt simulations, we have first evaluated SHGC with the default E891 spectrum at a 20° tilt, and have calculated the percent change in SHGC from the more usual results at the 90° tilt. These results are illustrated in Figure 9 and show that, even without modifying the default spectrum, increases in SHGC of up to 20% occur because of the tilt effect alone. The largest increase occurs with specimen #11, a film-on-glass system, whose response to various environmental changes will be singled out and discussed further in what follows.

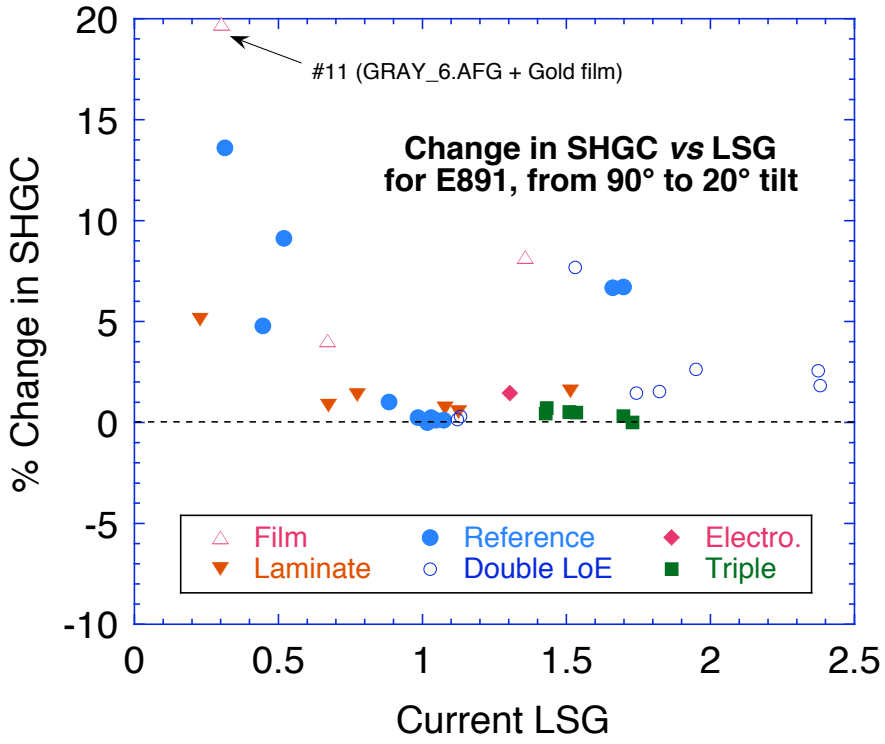


Fig. 9 Percent change in SHGC for a 20°-tilt compared to a 90°-tilt, with the default spectrum

Methodology

For each of the 37 specimens of Table 1, the WINDOW software has been run in "non-standard" mode, once for each of the six alternate spectra defined above. Such runs require some tweaking since WINDOW does not currently store these spectra, and does not offer a user-friendly way to switch from one spectrum to another, while at the same time transparently change the environmental conditions (which include the tilt and the total irradiance corresponding to the spectral weighting function). Files in the appropriate format had to be prepared and added to the appropriate folders.

WINDOW is currently limited in the number of wavelengths a spectral file can contain. The original files prepared with the SMARTS radiative code (Gueymard, 2001) for Task 3 and the proposed ASTM standard were of too high resolution for WINDOW. Therefore, degraded spectra (down to only 671 wavelengths from the original 2002 wavelengths) were obtained, at 1 nm resolution (rather than 0.5 nm) between 300 and 400 nm, at 5 nm resolution (rather than 1 nm) up to 2500 nm, and 10 nm beyond (rather than 5 nm). The "environmental conditions" setting in WINDOW, which particularly includes the total integrated irradiance in the spectrum,

also had to be changed consistently. In particular, this means that the calculations involving the two 20°-tilt spectra were done for the geometry of a 20°-tilt roof. In these two instances, the base case spectrum was also used with a 20°-tilt geometry.

Instructions for glazing and coating manufacturers to calculate the solar and optical properties of any glazing system using these six alternate spectra in WINDOW are provided in Appendix 1 and as a separate document. The intent is to allow NFRC to post a folder containing these files and instructions on their website so that NFRC Members can perform these calculations on their own.

SHGC Sensitivity Results

A statistical analysis of the data has been performed to determine whether the change in SHGC ratings of any glazing system resulting from a change in spectral weighting function can be predicted. Such a prediction would be easy if a relationship could be shown to exist between the glazing system's degree of spectral selectivity (usually described by LSG) and the expected relative change in SHGC and VT ratings.

Percent changes in SHGC have been calculated for each specimen and alternate spectrum. They are consolidated in Table 3, which is extracted from a detailed spreadsheet. The latter is also made available separately for further reference. The columns in Table 3 correspond to the alternate spectra listed on p. 10.

Among the four newly proposed ASTM spectra, the 20°-tilt global spectrum is the one that deviates most from the base case (Figure 7), nearly as much as the global G173 spectrum (#3, Figure 5). The percent change in SHGC due to using the 20°-tilt global spectrum rather than the current E891 is illustrated in Figure 10. All specimens are color coded per their category in Table 1. There is no clear dependence of the change in SHGC on the specimen category, except that electrochromics display little change, and triple glazings consistently display moderate to high changes (5–8%). Double low-e systems exhibit a linear increase of the change in SHGC with increasing LSG. Below an LSG of about 1, all specimens exhibit very limited changes, in the range -2 to +3%. This is the case, for instance, of specimen ID #11 with a 3.1% change. Changes tend to be larger at higher LSGs, up to +11% for double low-e specimens.

Figure 11 is similar to Figure 10, but for the global vertical spectrum (#7). The changes in SHGC are significantly less than in Figure 10. This could be expected since this spectrum is closer to the base case (Figure 6). The magnitude of the changes is nearly half of that in Figure 10, for all specimens. It ranges from -1 to +7%. For low LSGs (<1), the changes are very limited, from -1 to 2%, and do not seem to depend on LSG. Changes are also only marginally affected by LSG for LSGs greater than1.8. The main sensitivity area is clearly for glazing systems that have LSGs between 1 and 1.8.

Figure 12 shows the percent change in SHGC for all alternate spectra and all specimens. System #11 deviates again from the general trend, but is not alone. An upward trend of increasing percent change in SHGC with increasing LSG clearly appears, but the scatter is relatively large. This scatter precludes the possibility of accurately predicting, from LSG alone, by how much the SHGC of any glazing system would change. Considering, however, the wide range of optical

properties in the specimen list, it is unlikely that excursions beyond -3 and +11% would result from such a change.

Table 3 Percent change in U-factor, SHGC, Tvis and LSG due to a change in the spectral weighting function and tilt. The six alternate spectra are defined on p. 10.

			%Chnge	Percent change in SHGC							Percent change in Tvis							Percent change in LSG						
		Spctrm	U-Fact.	1 E891	2 G173D	3 G173G	4 WK20D	5 WK20G	6 WK90D	7 WK90G	1 E891	2 G173D	3 G173G	4 WK20D	5 WK20G	6 WK90D	7 WK90G	1 E891	2 G173D	3 G173G	4 WK20D	5 WK20G	6 WK90D	7 WK90G
Glazing ID	OPTICS 5.1 Layers	Tilt LSG	20°	20°	90°	90°	20°	20°	90°	90°	20°	90°	90°	20°	20°	90°	90°	20°	90°	90°	20°	20°	90°	90°
Window Films on Glazing																								
10	BRONZE_6.AFG + Sunbelt LowE	**1.357**	34.0	8.2	3.3	4.9	2.4	4.5	2.3	3.3	0.0	0.2	0.0	0.2	0.0	0.2	0.2	-7.6	-2.9	-4.7	-2.1	-4.3	-2.0	-2.9
11	GRAY_6.AFG + Gold	**0.302**	29.6	19.8	2.5	4.3	1.0	3.1	-0.6	1.2	0.0	-2.0	-2.0	-2.0	-2.0	-2.0	-2.0	-16.5	-4.4	-6.1	-3.0	-5.0	-1.4	-3.2
45	CLEAR_6.PPG + RE15SIARXL	**0.671**	13.9	4.1	1.2	2.4	0.8	2.3	0.4	1.6	0.0	-0.6	-0.6	-0.6	-0.6	-0.6	-0.6	-3.9	-1.8	-3.0	-1.4	-2.9	-1.0	-2.2
25	CLEAR_6.PPG + SunClean	**1.041**	13.9	0.3	-0.3	-0.8	-0.3	-0.9	-0.3	-0.7	0.0	0.1	0.1	0.1	0.1	0.1	0.1	-0.3	0.4	0.9	0.4	1.1	0.4	0.8
Laminates and Laminated Glazing																								
15	015_8050.SOL	**0.674**	13.5	0.8	-0.6	-1.4	-0.6	-1.5	-0.7	-0.6	0.0	3.5	2.9	3.5	2.9	3.5	4.8	-0.8	4.1	4.4	4.1	4.5	4.3	5.4
16	015_8178.SOL	**1.079**	13.5	0.7	-0.8	-2.1	-0.7	-2.2	-1.0	-1.1	0.0	0.8	0.6	0.8	0.5	0.8	0.9	-0.7	1.6	2.8	1.5	2.8	1.8	2.0
17	015_8250.SOL	**0.775**	13.5	1.4	-0.3	-0.8	-0.6	-1.0	-0.6	-1.1	0.0	-3.7	-2.9	-3.7	-2.9	-3.7	-4.7	-1.3	-3.4	-2.2	-3.1	-1.9	-3.1	-3.6
46	BRN_Dark.DUP	**0.229**	13.4	5.1	-0.5	-0.8	-1.0	-1.2	-1.8	-1.3	0.0	1.1	1.1	1.1	1.1	1.1	1.1	-4.8	1.6	1.9	2.1	2.4	2.9	2.4
18	030cl3_0.SOL	**1.126**	13.3	0.5	0.5	0.1	0.4	0.0	0.4	0.3	0.0	0.0	0.0	0.0	0.0	0.0	-0.1	-0.5	-0.5	-0.1	-0.4	0.0	-0.4	-0.4
19	CLR-3.CIG + X4	**1.514**	32.6	1.5	3.6	5.4	3.4	5.7	3.5	4.4	0.0	0.0	0.0	0.0	0.0	0.0	0.0	-1.5	-3.5	-5.1	-3.3	-5.4	-3.3	-4.2
Reference Glazing																								
20	Acrylic	**1.073**	10.3	0.1	0.5	0.1	0.5	0.1	0.3	0.5	0.0	0.0	0.0	0.0	0.0	0.0	0.0	-0.1	-0.5	-0.1	-0.5	-0.1	-0.3	-0.5
66	Polycarbonate	**1.030**	12.1	0.2	0.1	-0.7	0.0	-1.0	0.0	0.0	0.0	0.0	0.0	0.0	0.0	0.0	0.0	-0.2	-0.1	0.7	0.0	1.0	0.0	0.0
67	Polycarbonate	**0.985**	8.0	0.3	0.1	-0.4	0.2	-0.5	0.1	0.3	0.0	0.0	0.0	0.0	0.0	0.0	0.0	-0.2	-0.1	0.4	-0.2	0.5	-0.1	-0.2
71	Glass	**0.884**	14.3	1.0	0.1	0.0	0.1	0.0	-0.1	-0.1	0.0	0.0	0.0	0.0	0.0	0.0	0.0	-1.0	-0.1	0.0	-0.1	0.0	0.1	0.1
72	Glass	**0.446**	13.0	4.8	0.7	1.2	0.2	0.7	-0.5	0.0	0.0	0.0	0.0	0.0	0.0	0.0	0.0	-4.6	-0.7	-1.2	-0.2	-0.7	0.5	0.0
24	Glass	**1.017**	13.9	0.0	-0.1	-0.3	0.0	-0.3	-0.1	-0.2	0.0	0.0	0.0	0.0	0.0	0.0	0.0	0.0	0.1	0.3	0.0	0.3	0.1	0.2
27	Azurl_6.ppg + VE785	**1.698**	31.0	6.7	4.4	7.2	3.6	7.0	3.4	3.9	0.0	-0.9	-0.8	-0.9	-0.8	-0.9	-1.2	-6.3	-5.1	-7.5	-4.4	-7.3	-4.1	-4.9
28	Evgrn6.lof + VE855	**1.661**	31.0	6.7	3.6	5.7	2.9	5.3	2.8	3.3	0.0	-0.5	-0.3	-0.5	-0.3	-0.5	-0.6	-6.3	-3.9	-5.6	-3.3	-5.3	-3.2	-3.8
44	Azurl_6.ppg + VS708	**0.315**	22.3	13.6	0.9	1.4	-0.4	0.4	-1.4	0.0	0.0	0.0	0.0	0.0	0.0	0.0	0.0	-12.0	-0.9	-1.4	0.4	-0.4	1.4	0.0
43	Evgrn6.lof + VS820	**0.519**	18.5	9.1	1.4	2.1	0.6	1.6	-0.7	0.4	0.0	0.0	0.0	0.0	0.0	0.0	0.0	-8.4	-1.4	-2.1	-0.6	-1.6	0.7	-0.3
57	CLEAR_3.DAT	**1.047**	14.3	0.1	0.1	0.1	0.2	0.2	0.1	0.0	0.0	0.0	0.0	0.0	0.0	0.0	0.0	-0.1	-0.1	-0.1	-0.2	-0.2	-0.1	0.0
Double Glazing - Low-E																								
73	BRONZE_6.AFG + Sunbelt LowE	**1.530**	31.6	7.7	4.0	5.7	3.0	5.3	2.8	4.0	0.0	0.0	0.0	0.0	0.0	0.0	0.0	-7.1	-3.9	-5.4	-2.9	-5.0	-2.8	-3.9
70	CLR-3.CIG + LoE2-272	**1.743**	30.9	1.5	4.6	6.8	4.3	7.2	4.4	5.1	0.0	0.0	0.0	0.0	0.0	0.0	0.0	-1.4	-4.4	-6.3	-4.1	-6.7	-4.2	-4.8
80	CLR-2.CIG + LoE^3-366	**2.374**	31.9	2.6	6.6	9.9	6.4	10.7	6.2	6.2	0.0	-0.3	-0.3	-0.3	-0.3	-0.3	-0.5	-2.5	-6.5	-9.3	-6.3	-10.0	-6.2	-6.3
81	Clear_23.GRD + RLE 71/38	**1.823**	31.7	1.5	5.1	8.0	5.1	8.6	5.1	5.9	0.0	-0.1	-0.1	-0.1	-0.1	-0.1	-0.1	-1.5	-5.0	-7.5	-5.0	-8.1	-5.0	-5.7
82	CLEAR2.LOF + Energy Advantage LoE	**1.132**	26.3	0.3	1.2	1.7	1.0	1.6	1.2	1.7	0.0	0.0	0.0	0.0	0.0	0.0	0.0	-0.3	-1.2	-1.6	-1.0	-1.6	-1.2	-1.6
77	STRPH_6.PPG + Solarban 70XL	**2.381**	32.0	1.8	6.6	10.3	6.8	11.2	6.6	6.6	0.0	0.0	0.0	0.0	0.0	0.0	-0.2	-1.8	-6.2	-9.3	-6.4	-10.0	-6.2	-6.3
83	CLEAR_2.PPG + Sungate 500	**1.121**	24.7	0.1	1.0	1.3	1.0	1.5	0.9	1.3	0.0	0.1	0.0	0.1	0.0	0.1	0.1	-0.1	-0.9	-1.3	-0.9	-1.5	-0.7	-1.2
79	ip024004.ipe + 33600	**1.950**	31.6	2.6	5.6	7.9	5.1	8.6	5.3	5.9	0.0	-0.2	-0.2	-0.2	-0.2	-0.2	-0.2	-2.6	-5.4	-7.5	-5.0	-8.0	-5.2	-5.7
Double Glazing - Electrochromic																								
58	Unknown + SageGlass EC	**0.343**	26.7	23.5	2.9	4.9	1.6	3.2	-1.0	2.0	0.0	-2.9	0.0	-2.9	0.0	-2.9	-2.9	-19.0	-5.6	-4.7	-4.4	-3.1	-1.9	-4.7
59	Unknown + SageGlass EC	**1.304**	26.7	1.4	1.7	1.7	1.4	1.6	1.4	2.1	0.0	0.2	0.0	0.2	0.0	0.2	0.2	-1.4	-1.5	-1.6	-1.3	-1.6	-1.3	-1.9
Triple Glazing - Clear, Heat Mirror & Low-E																								
60	CLR-6.CIG + LoE^2-272	**1.730**	31.8	0.0	4.6	6.8	4.6	7.6	4.3	5.1	0.0	-0.2	-0.2	-0.2	-0.2	-0.2	-0.2	0.0	-4.5	-6.5	-4.5	-7.2	-4.3	-5.0
61	Unknown + Heat Mirror 22	**1.432**	33.7	0.7	5.0	7.2	4.3	7.9	4.3	5.0	0.0	-0.5	-0.5	-0.5	-0.5	-0.5	-0.5	-0.7	-5.3	-7.2	-4.6	-7.8	-4.6	-5.3
62	Unknown + Heat Mirror 33	**1.510**	33.9	0.5	4.7	7.3	4.7	7.8	4.7	5.2	0.0	-0.7	-0.7	-0.7	-0.7	-0.7	-0.7	-0.5	-5.1	-7.4	-5.1	-7.9	-5.1	-5.6
63	Unknown + Heat Mirror 77	**1.428**	31.0	0.4	3.5	5.0	3.0	5.2	3.3	3.9	0.0	-0.3	-0.3	-0.3	-0.2	-0.3	-0.3	-0.4	-3.7	-5.1	-3.3	-5.1	-3.5	-4.1
64	Unknown + Heat Mirror Single Coat 75	**1.534**	31.7	0.5	4.9	7.6	4.9	8.3	4.7	5.6	0.0	-0.3	-0.2	-0.3	-0.2	-0.3	-0.3	-0.5	-5.0	-7.2	-5.0	-7.8	-4.8	-5.6
65	Unknown + Heat Mirror Single Coat 75	**1.698**	33.2	0.3	5.3	7.9	5.0	8.5	5.0	5.3	0.0	-0.2	-0.2	-0.2	-0.2	-0.2	-0.2	-0.3	-5.3	-7.5	-5.0	-8.0	-5.0	-5.3

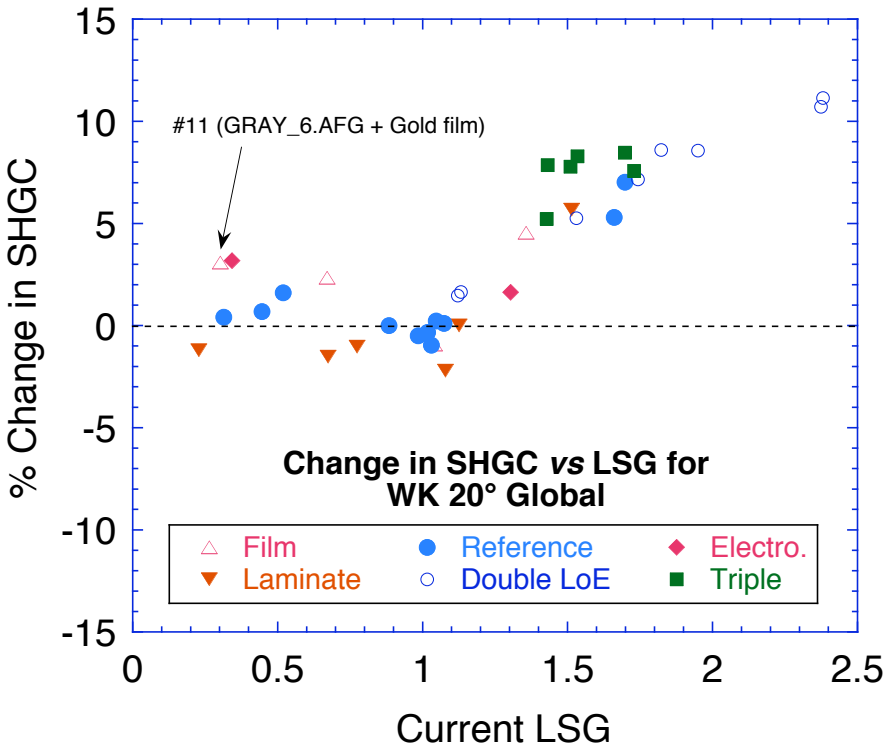


Fig. 10 Percent change in SHGC *vs* LSG for each specimen of Table 1, using the proposed 20°-tilt global spectrum. Results are color coded by specimen category.

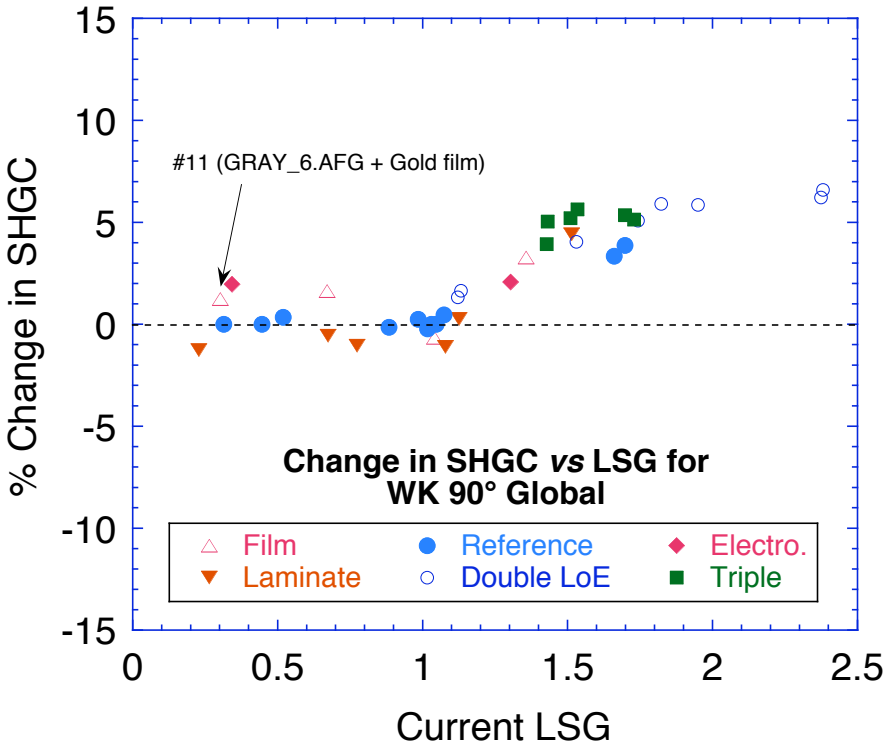


Fig. 11 Same as Fig. 10, but for the proposed 90°-tilt global spectrum

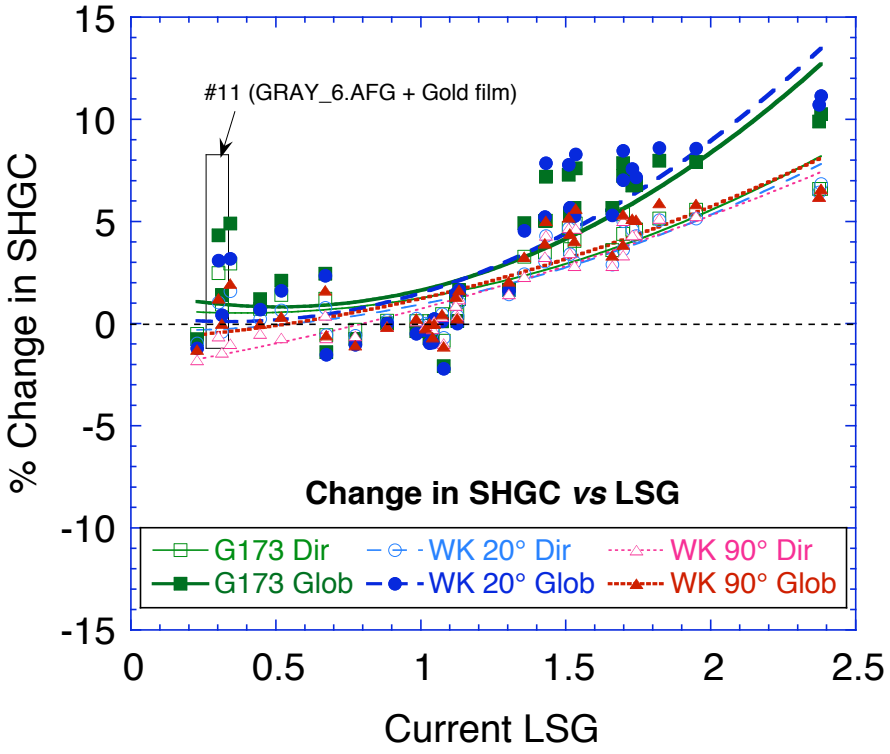


Fig. 12 Percent change in SHGC *vs* LSG for each specimen of Table 1, for each alternate spectrum

Interestingly, the calculated changes are normally the lowest (between about -2 and +7%) for spectra #6 and 7, which are the ASTM-proposed direct and global spectra for vertical tilts, respectively. These numbers are comparable to, if not lower than, the percent differences typically obtained when comparing modeled and experimentally measured SHGC values. This finding supports the notion that, for better agreement between modeled and measured data, the variable effect of the incident spectrum should be taken into account. See Appendix 2 for a discussion of a theoretical methodology to adjust test results from solar calorimeters for differences in the source spectrum, provided that the source spectrum can be identified.

Predicting Changes in SHGC

Figure 12 shows the upward trend of the change in SHGC *vs.* LSG. The curves indicate least-squares fits using simple quadratics. The scatter around these curves complicates the prediction of the change in SHGC. Although nothing would replace the actual calculation of SHGC with WINDOW, we have investigated the prediction possibilities a little further. Much can be gained by analyzing the reason behind the very presence of outliers. Since the only change in this case is in the incident spectrum, the reason must be spectral in nature, even though it does not appear to be related to LSG. Figure 13 compares the spectral transmittances of two different systems: ID #11 (film-on-glass) and ID #73 (double glazing with low-E). For the latter specimen, the change in SHGC is 5.3% in the case of Fig. 10 and 4.0% in the case of Fig. 11, compared to 3.1% and 1.2%, respectively, for the former (Table 3). The figure also shows the relative distributions of the current spectral weighting function (E891) and of the alternate spectrum #7, after normalization to 0.3 at 555 nm, for clarity. Whereas the peak of the transmittance of specimen #73 (at 560 nm) is close to that of the incident spectra, the peak of #11's transmittance is at a far

smaller wavelength, namely 400 nm. The transmittance of specimen #73 is typical of the advanced systems that try to maximize VT while minimizing SHGC. From Table 1, these numbers are 0.378 and 0.247, respectively. These numbers change to 0.049 and 0.162 for specimen #11. It is likely that a bivariate fit, using both LSG and the peak-to-peak distance as the independent variables, would predict the change in SHGC with relatively better accuracy than a fit based on LSG alone, but this has not been attempted yet.

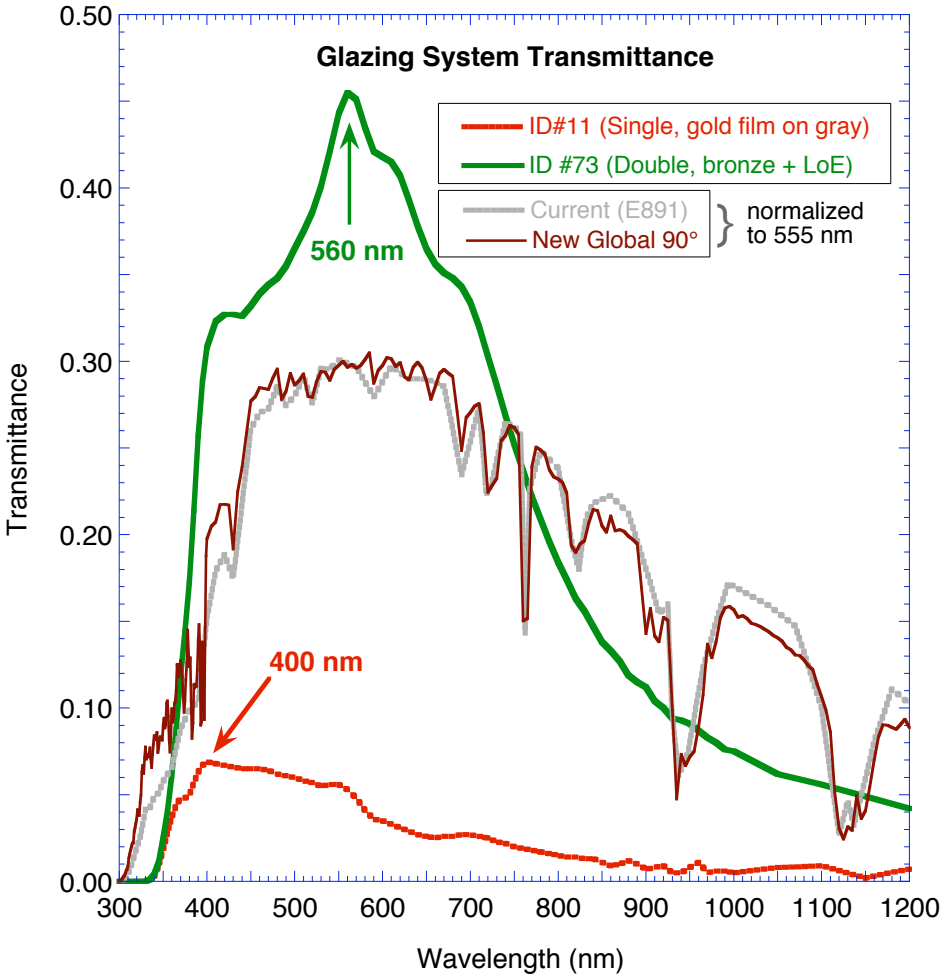


Fig. 13 Spectral transmittance of two specimens (ID#11 and ID#73), compared to two spectral weighting functions, normalized to 0.3 at 555 nm for clarity.

Visible Transmittance and LSG Sensitivity

The Work Statement specifically called for an analysis of the change in VT induced by a change in the spectral weighting function. After this analysis started, it became clear that the VT ratings would *not* be affected by a change in the solar spectrum since NFRC 300 specifies another spectral weighting function for VT, namely CIE's standard illuminant (D65). The latter attempts to reproduce the typical spectral distribution of daylight at a correlated color temperature of 6500 K. It is based entirely on spectral measurements obtained in the early '60s (Judd et al., 1964).

Having to rely on two different spectra for the calculation of SHGC and VT appears as a source of inconsistency. The visible spectrum (300–830 nm in D65) is obviously a significant part of the solar spectrum used for SHGC (300–2500 nm), and should not be a separate entity. Furthermore, this discrepancy translates into an inconsistent definition of LSG = VT/SHGC.

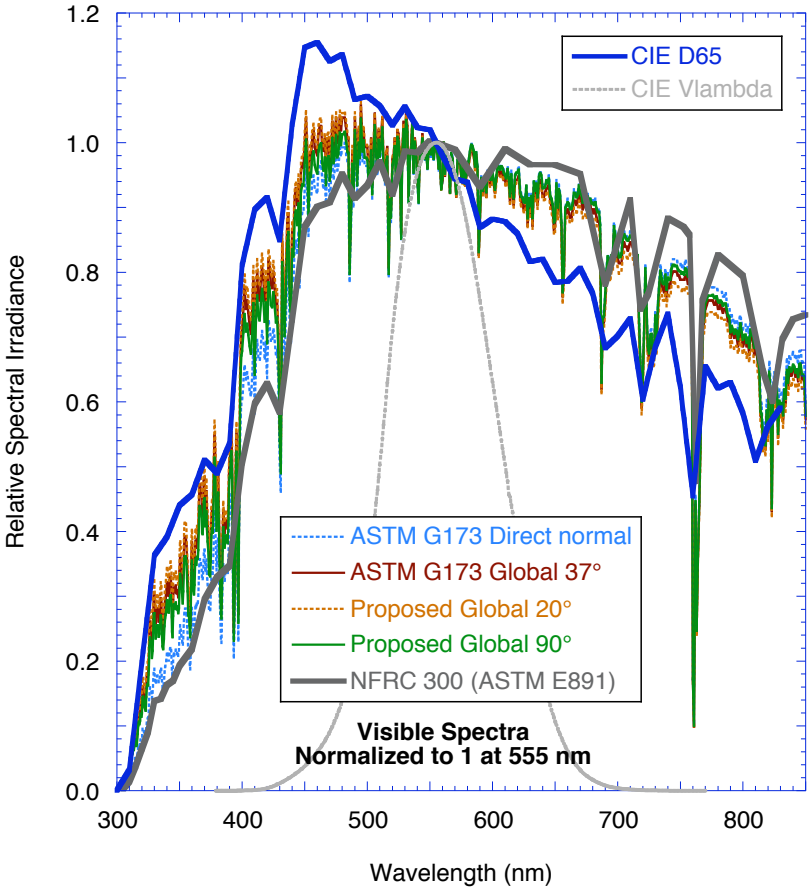


Fig. 14 Relative spectral distributions of some solar spectra and of CIE D65. All spectra are normalized to their value at 555 nm, which is the peak of CIE's photopic response curve, also shown.

After discussion with the PMTG, it was agreed that this part of Task 2 would be modified to analyze what changes in VT would occur if D65 was replaced by the same solar spectra weighting function as for SHGC.

Preliminary calculations showed that, in the visible, there were noticeable differences between the spectral distribution in D65 and some other solar spectra considered here (Figure 14). It can be hypothesized that these differences are in great part the result of the correlated temperature constraint. Close examination of Figure 14 reveals that the largest difference is between D65 and the current NFRC 300 solar weighting function. This can be explained by the fact that D65 is a daylight spectrum, which mixes direct and diffuse radiation, whereas the E891/NFRC 300 spectrum is for direct radiation only. If D65 could be used as a weighting function for SHGC in replacement of E891, it is obvious that far larger SHGC changes than those reported in the previous section would occur. Nevertheless, it can be argued that the role of the photopic curve is essential here to attenuate these differences.

VT is obtained by convolving the glazing's spectral transmittance results with both the spectral weighting function (e.g., D65) and the photopic response curve (also shown in Fig. 14). Since the latter is highly peaked, it remains to be seen whether the spectral discrepancy observed in Figure 14 would survive the latter convolution. The result of convolving all spectra in Figure 14 with the photopic curve appears in Figure 15. The resulting "reduced" spectral distributions now appear in relatively close agreement, although D65 is perceptibly shifted towards bluer wavelengths than the other distributions.

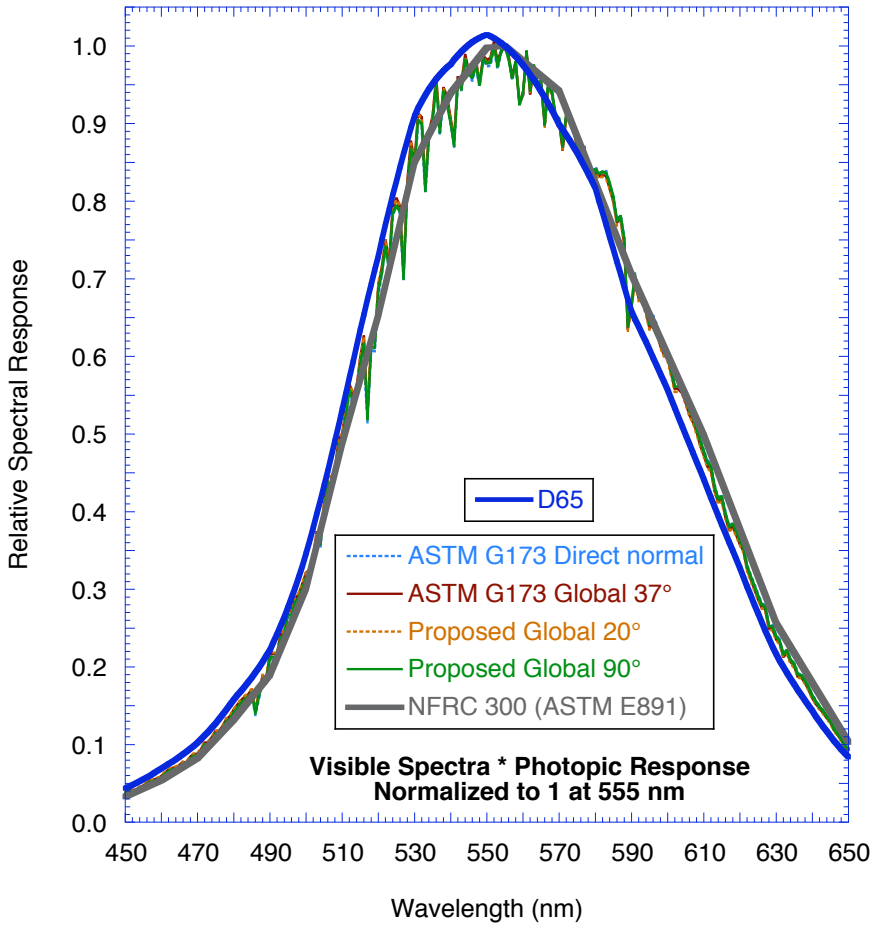


Fig. 15 Normalized spectra of Fig. 10, after convolution with the photopic curve.

As could be expected from the findings just described, the effect of changing from D65 to any one of the six alternate spectra defined above is significantly reduced compared to the effect on SHGC, due to the strong filtering effect of the photopic curve. As shown in Figure 16, these changes are typically well within ±2% for most specimens, with specimen #11 right at the limit of -2%. There are three outliers (two laminates and an electrochromic) in the -5 to +5% range. Curiously, these two laminates display significant and unmatched variability in VT from one spectrum to the other. Since many glazing systems have a VT lower than 0.5, a change in VT less than ±2% results in an absolute change of less than 0.01, which would only affect the third decimal.

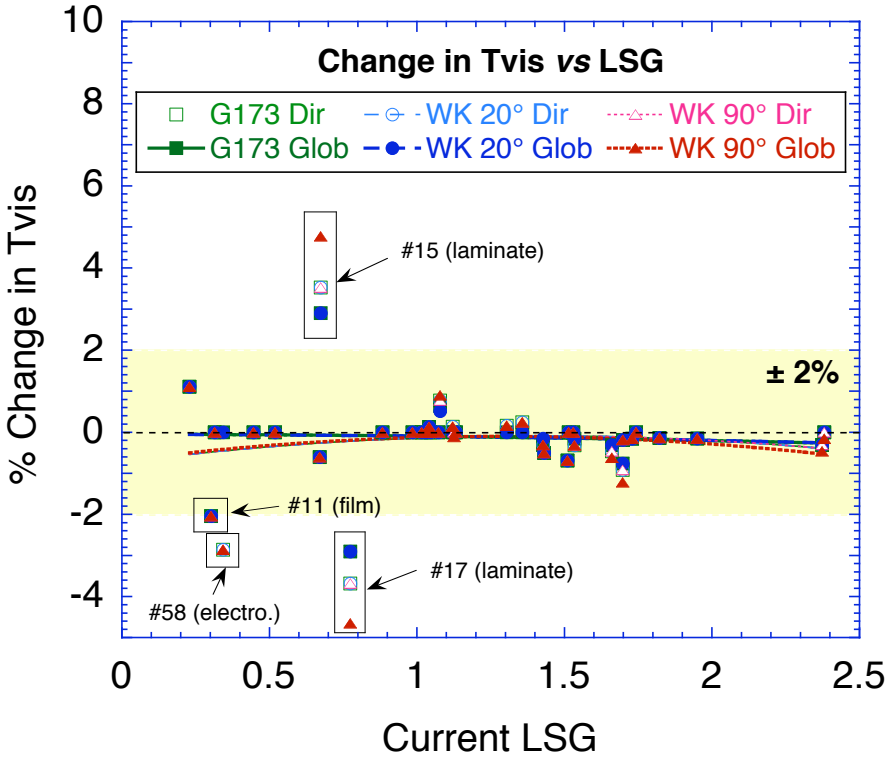


Fig. 16 Percent change in Tvis *vs* LSG for each specimen of Table 1, for each alternate spectrum

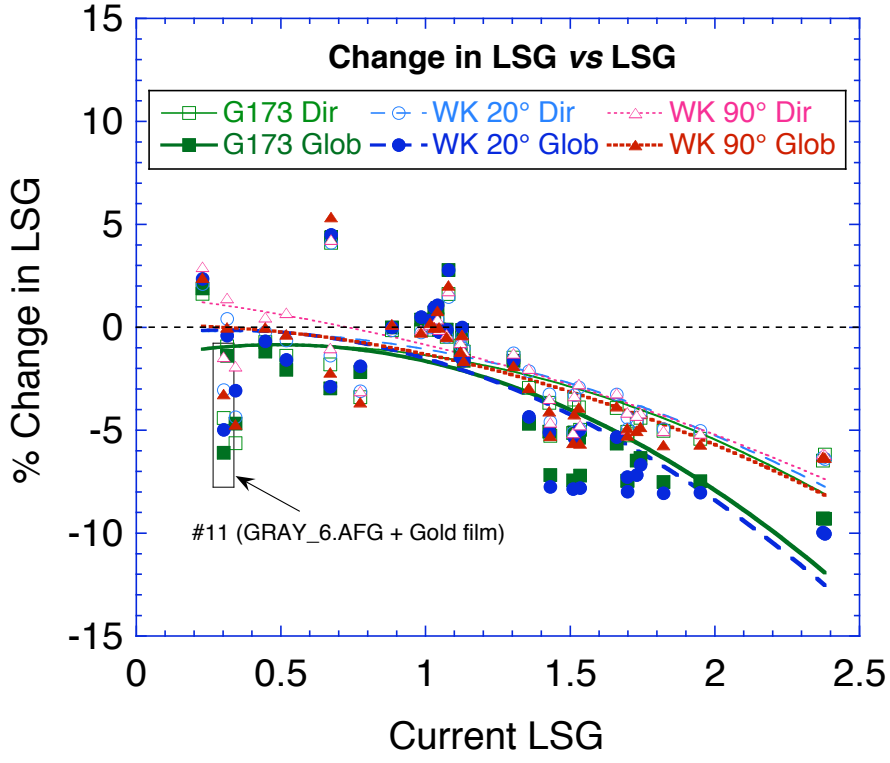


Fig. 17 Percent change in LSG *vs* current LSG for each specimen of Table 1, for each alternate spectrum

Finally, Figure 17 shows how the adoption of an alternate spectrum would affect LSG. VT being significantly less sensitive to the weighting function than SHGC, and LSG being inversely proportional to SHGC, it is clear that the spectral effect on LSG is close to be the reverse of what it is on SHGC (Figure 12).

During our discussions with the PMTG, it has been argued that VT was a variable to consider in colorimetry. Colorimetric calculations are based on D65 and are not likely to change soon. To respect the integrity of this application, it has been proposed that the color properties continue to be based on D65. This implies that new columns be added to the "Color Properties" tab in WINDOW to report the visible transmittance and reflectances based on D65.

Task 2 Deliverables: The original Work Statement requires that a minimum of four spectra be selected for analysis. It also stipulates that a method to adjust calorimeter test results for spectral effects be explored.

In actuality, the PI produced results for six alternate spectra. The effect of changing the spectral weighting function for the calculation of VT (currently disconnected from that of SHGC) was investigated. The relationship between the glazing system's degree of spectral selectivity and the expected relative change in SHGC and VT ratings was analyzed and reported. A methodology of adjusting solar calorimeter test results based on a known source spectrum has been explored and presented (see Appendix 2).

Task 3 – Report ASTM Activities and Represent NFRC at ASTM G-03.09 Meetings

At the time the work statement was written, it was thought that the best venue for developing NFRC-oriented solar spectra would be through CIE TC 2.17. A general meeting in Europe was then being organized by the TC chairman. Various organizational problems occurred, however, and that meeting could not take place as anticipated.

Following the discussions we had at previous ASTM and CIE meetings and with confirmation from the PMTG, we finally elected to develop the new standard spectra through ASTM instead of CIE.

ASTM G-03.09 subcommittee on Radiometry had produced various reference spectra in the last few years (e.g., ASTM G173 and ASTM G177) with the help of the first PI, and therefore was considered the appropriate ASTM Subcommittee to develop this new standard.

ASTM Activity: ASTM G-03.09 was approached, and accepted, to develop standard direct normal and diffuse spectra for fenestration at vertical and 20º tilted orientations. The first PI prepared a draft standard, which he presented at the ASTM G-03.09 subcommittee meeting in Cleveland, Ohio in June 2007, chaired by Gene Zerlaut. The draft standard has some similarities with the existing G173 standard (adopted in 2003), but is tailored for fenestration applications. Spectral calculations are made with the same SMARTS code (Gueymard, 2001; Gueymard et al., 2002) that was used to develop G173, as well as a spectral heat gain calculation procedure for ASHRAE (Gueymard, 2007). The tabulated data include the direct and diffuse irradiance incident on vertical and 20°-tilted sun-facing planes, under predetermined atmospheric and environmental conditions. The global irradiance is simply obtained by summing the direct and diffuse components. The data tables extend from 280 to 4000 nm, with a total of 2002 wavelengths. Three spectral steps are used: 0.5 nm in the UV (280–400 nm), 1 nm between 400 and 1700 nm, and 5 nm beyond. The SMARTS code, which has been recognized as an adjunct standard by ASTM in 2003, can be used to degrade these spectra to accommodate a variety of lower spectral resolutions. It can also be used to separate the sky and ground-reflected diffuse components if so desired.

Shortly after this meeting in June 2007, a revised draft for this proposed ASTM standard was balloted at subcommittee level, under the ASTM Work Item number WK 17196. The single negative and the few editorial comments from that ballot were resolved by the first PI at the following ASTM meeting in Fort Lauderdale, Florida on January 22, 2008. The revised draft is now being finalized, and will be submitted for full G-03 Committee ballot shortly.

CIE Activity: Immediately following both ASTM G-03.09 meetings mentioned above, there were also CIE TC 2-17 “limited” meetings. The North American representation to CIE TC 2.17 is modest compared to the European one, but the latter does not attend the North American meetings such as these, thus creating a difficult situation. Gene Zerlaut has tried to convene a CIE TC 2.17 meeting in Europe, but this has not materialized yet. This state of affair appears to us as a confirmation that the projected “NFRC-friendly spectrum” will be standardized by ASTM much faster than it would have been by CIE. It is possible, however, that CIE eventually

adopts some variant of the draft ASTM standard for its own use, which would make these new reference spectra known by the glazing industry in Europe and elsewhere.

Task 3 Deliverables: The original Work Statement required that new spectrum standards be developed by CIE, and that the PI attend the NFRC meetings.

With permission from the PMTG, these standard spectra were developed and balloted at ASTM G-03.09 instead of CIE. If the next G-03 ballot goes smoothly as anticipated, the new standard should be adopted by ASTM later this year.

The second PI attended all NFRC meetings. In addition, the first PI (Chris Gueymard) attended the NFRC Meeting in Tempe, Arizona in November 2007, as also stipulated by the Work Statement.

Task 4 – Reports on CIE Activities, Final Report, and Technical Paper

Three status reports (including this final report), and three presentations, were given at all of the NFRC Research Subcommittee meetings since the initiation of this research project. These reports and presentations described the status of the project, as well as our activities within ASTM and CIE.

The peer-reviewed paper will be derived from this final report upon its approval by the PMTG. The current plan is to submit it to *Solar Energy*. This journal already published important papers on NFRC-related methodologies (e.g., Karlsson et al., 2001; Rubin et al, 1998, 1999).

Task 4 Deliverables: The original Work Statement required that the status of the project and the activities within CIE be reported to the PMTG and the NFRC Membership. In addition, a peer-reviewed paper describing the project and conclusions had to be developed and submitted for publication.

The PI indeed reported the progress and standardization activities to the PMTG and NFRC meetings (see also Task 3 Deliverables). Although the required reports and presentations have been delivered, the peer-reviewed paper is still under development. An important step in the process will be the acceptance of this Final Report by the PMTG.

Recommendations

Based on the results from this research project, the PI recommends that the NFRC peruse the following future activities.

Adopt the new (draft standard) ASTM G-03.09 Spectrum for Global Irradiance on Vertical Surfaces for Windows

Not only is this new standard spectrum more accurate than the current default spectrum, it does not significantly change the listed solar and optical properties of most glazing systems. By adopting this new spectrum, it will also become easier to correct spectrum-induced discrepancies between modeled and experimentally determined SHGC data.

If this new spectrum is adopted, the spectral weighting functions in future versions of WINDOW, OPTICS (NFRC 200), and the ASTM E 903 Test Method (NFRC 300) will need to be modified. These modifications should be balloted and approved for each calculation methodology and test method by the NFRC Membership.

Adopt the new (draft standard) ASTM G-03.09 Spectrum for Global Irradiance on 20°-Tilt Surfaces for Skylights

For consistency, the SHGC procedure for skylights should adopt the global 20°-tilt spectrum draft standard, which has been developed specifically for that application. The change in SHGC would be slightly larger than with the 90°-tilt spectrum recommended above, but on the other hand, this change would most likely lead to more accurate numbers, and better agreement between modeled and experimental data.

Use Identical Solar and Visible Spectrum in WINDOW

NFRC 300 currently specifies that the visible transmittance be calculated using a different spectrum (CIE D65) than SHGC (ASTM E891). This discrepancy is confusing, and does not permit the Light-to-Solar-Gain (LSG) ratio to be properly determined. To remove this inconsistency and to simplify and update the procedure, we recommend that the spectral weighting function for VT be identical to that for SHGC.

Upgrade WINDOW to Use the ASTM G-03.09 Spectrum for Direct & Diffuse Irradiance

Once the WINDOW software is capable of performing SHGC calculations using direct and diffuse irradiance separately, the Direct and Diffuse spectral irradiance standards should be adopted and specified. Fortunately, the adoption of this methodology and spectra should not produce significant variations in the solar and optical performance in all but a few glazing systems as compared with the results from the current spectral weighting function or the recommended global spectrum.

References

ASTM, Standard for Terrestrial Direct Normal Solar Spectral Irradiance Tables for Air Mass 1.5, Standard E891, American Society for Testing and Materials, Philadelphia, PA (1982).

ASTM, Standard Tables for Reference Solar Spectral Irradiances: Direct Normal and Hemispherical on 37° Tilted Surface, Standard G173-03, American Society for Testing and Materials, Philadelphia, PA (2003).

Gueymard C.A., Parameterized Transmittance Model for Direct Beam and Circumsolar Spectral Irradiance. *Solar Energy,* 71: 325-346 (2001).

Gueymard C.A., D.R. Myers and K. Emery, Proposed Reference Irradiance Spectra for Solar Energy Systems Testing. *Solar Energy,* 73: 443-467 (2002).

Gueymard C.A., Advanced Solar Irradiance Model and Procedure for Spectral Solar Heat Gain Calculation (RP-1143). *ASHRAE Trans.*, DA-07-016 (2007).

International Organization for Standardization. ISO 9845-1: Solar Energy—Reference Solar Spectral Irradiance at he Ground at Different Receiving Conditions, part 1, Geneva (1992).

Judd D.B., MacAdam D.L., Wyszecki G., Budde H.W., Condit, H.R., Henderson S.T., and Simonds J.L., Spectral Distribution of Typical Daylight as A Function of Correlated Color Temperature. *J. Opt. Soc. Amer.*, 54, 1031-1040 (1964).

Karlsson J., Rubin M. and Roos A., Evaluation of Predictive Models for the Angle-Dependent Total Solar Energy Transmittance of Glazing Materials. *Solar Energy*, 71, 23-31 (2001).

Lawrence Berkeley National Laboratory, WINDOW 5.2.17a, Berkeley, CA (2005), http:// windows.lbl.gov/software/window/window.html.

McCluney R., Sensitivity of Optical Properties and Solar Gain of Spectrally Selective Glazing Systems to Changes in Solar Spectrum. Proc. Passive Solar Conf., Washington, DC, American Solar Energy Society (1993).

McCluney W.R., Sensitivity of Fenestration Solar Gain to Source Spectrum and Angle of Incidence. *ASHRAE Trans*., 102 (2): 112-122 (1996).

McCluney R. and Gueymard C., Selecting Windows for South Florida Residences. Rep. FSEC-CR-1691-93, Florida Solar Energy Center, Cocoa, FL (1993). Available from http://www.fsec.ucf.edu/en/publications/pdf/FSEC-CR-1691-93.pdf.

National Fenestration Rating Council, NFRC 100-2004: Procedure for Determining Fenestration Product U-Factors, Silver Spring, MD (2004).

National Fenestration Rating Council, NFRC 200-2004: Procedure for Determining Fenestration Product Solar Heat Gain Coefficient and Visible Transmittance at Normal Incidence, Silver Spring, MD (2004).

National Fenestration Rating Council, NFRC 300-2004: Test Method for Determining the Solar Optical Properties of Glazing Materials and Systems, Silver Spring, MD (2004).

Rubin M., Von Rottkay K. and Powles R., Window Optics. *Solar Energy,* 62, 149-161 (1998).

Rubin M., Powles R. and Von Rottkay K., Models for the Angle-Dependent Optical Properties of Coated Glazing Materials. *Solar Energy,* 66, 267-276 (1999).

Appendix 1 — Instructions for Calculating Solar and Optical Properties of Select Glazing Systems Using Alternate Spectra in WINDOW 5.2

Overview—Researchers, window and glazing manufacturers may want to determine whether the solar and optical properties of any glazing system are significantly affected by the use of any of the alternate spectra presented in the NFRC SWF Research Project. These instructions provide guidance on how to create a separate WINDOW 5.2 Glazing System Library that will reference alternate environmental conditions, namely Spectral Data and Standard files (*.ssp & *.std) within WINDOW. The differences in the solar and optical properties using different spectra can then be easily determined by comparing the results from repetitive calculations on the same Glazing System Library. Comprehensive step-by-step instructions are provided in this document.

1. Create Glazing System Library

Although it is not essential, it is recommended that a separate WINDOW database be created that contains only those glazing systems in the Glazing System Library to be considered for comparison. This can be performed in two different ways. One is to save the entire database as another name (click on **File**|**Save As** in the menu bar). This will copy all the records from the original database into the new database. Another option is to make a separate "Project" database, by exporting records from one database into another. To make a Project database from a master database from the Glazing System Library, create the desired glazing systems, and then use the "Ctrl" and "Shift" keys to highlight those glazing systems in the **[List]** view of the WINDOW Glazing Library. As shown in Fig. 1, use the **[Export]** button to copy those selected glazing systems into a new WINDOW database file (*.mdb) with a different name and/or location.

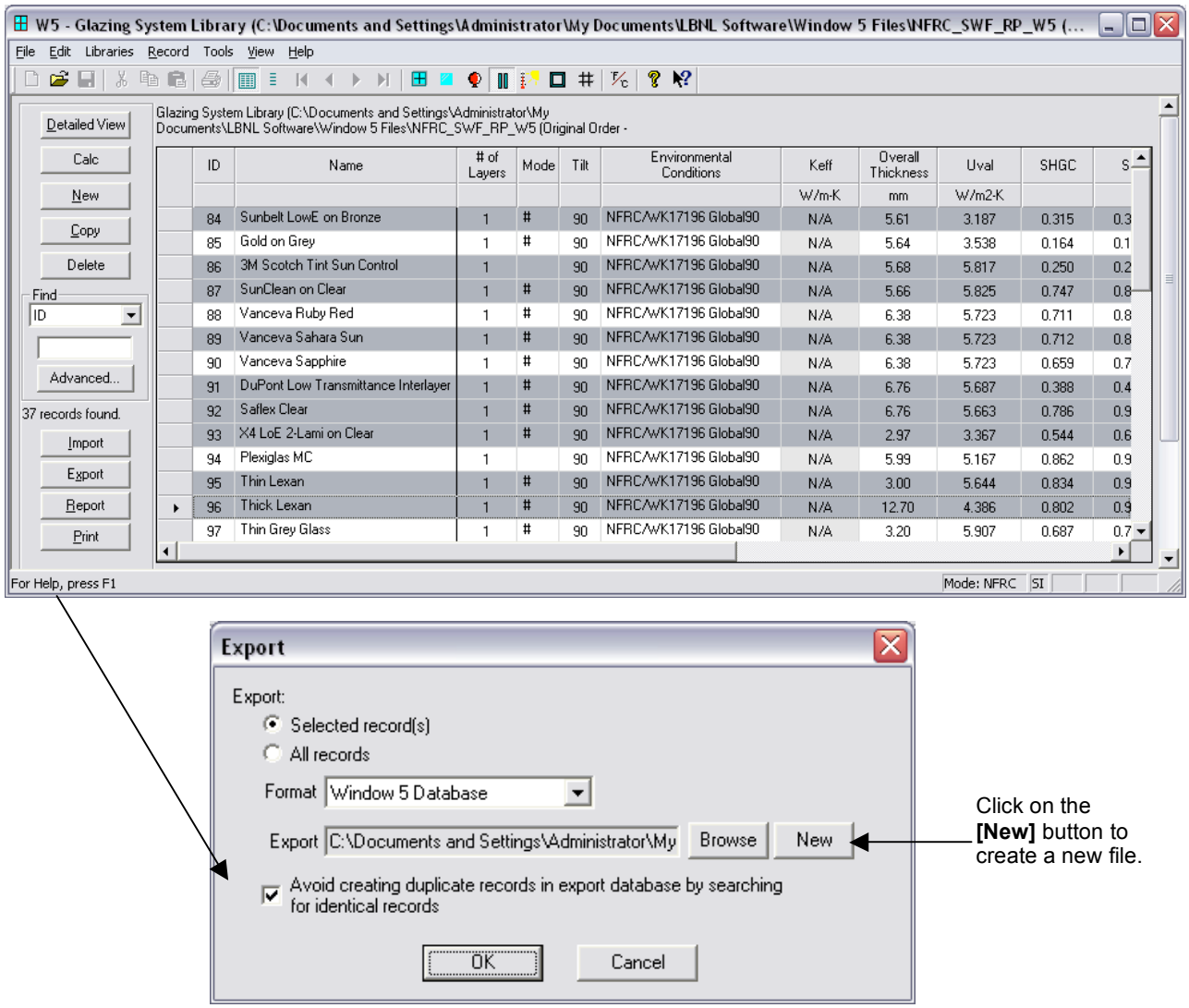


Figure 1 - Select Glazing Systems for Export to New WINDOW database

2. Copy Spectral Data and Standard Files into the WINDOW Standards Folder

Copy the following pairs of files[1] from the attached folder to the WINDOW Standards folder[2]:

ASTM G 173-03, Air Mass of 1.5, Direct Normal Irradiance
"ASTM G173 AM1_5 Direct Normal.ssp"
"W5_NFRC_2003 G173 AM1_5 Direct Normal.std"

ASTM G 173-03, Air Mass of 1.5, Global Irradiance on a Surface at a 37° Tilt
"ASTM G173 AM1_5 37 Tilt Global.ssp"
"W5_NFRC_2003 G173 AM1_5 37 Tilt Global.std"

ASTM WK17196, Air Mass of 1.5, Direct Irradiance on a Surface at a 20° Tilt
"ASTM WK17196 AM1_5 20 Tilt Direct.ssp"
"W5_NFRC_2003 WK17196 AM1_5 20 Tilt Direct.std"

ASTM WK17196, Air Mass of 1.5, Global Irradiance on a Surface at a 20° Tilt
"ASTM WK17196 AM1_5 20 Tilt Global.ssp"
"W5_NFRC_2003 WK17196 AM1_5 20 Tilt Global.std"

ASTM WK17196, Air Mass of 1.5, Direct Irradiance on a Surface at a 90° Tilt (Vertical)
"ASTM WK17196 AM1_5 90 Tilt Direct.ssp"
"W5_NFRC_2003 WK17196 AM1_5 90 Tilt Direct.std"

ASTM WK17196, Air Mass of 1.5, Global Irradiance on a Surface at a 90° Tilt (Vertical)
"ASTM WK17196 AM1_5 90 Tilt Global.ssp"
"W5_NFRC_2003 WK17196 AM1_5 90 Tilt Global.std"

As shown in Fig. 2, the default location for the WINDOWS 5.2 Standards folder is:

```
C:\Program Files\LBNL\LBNL Shared\Standards
```

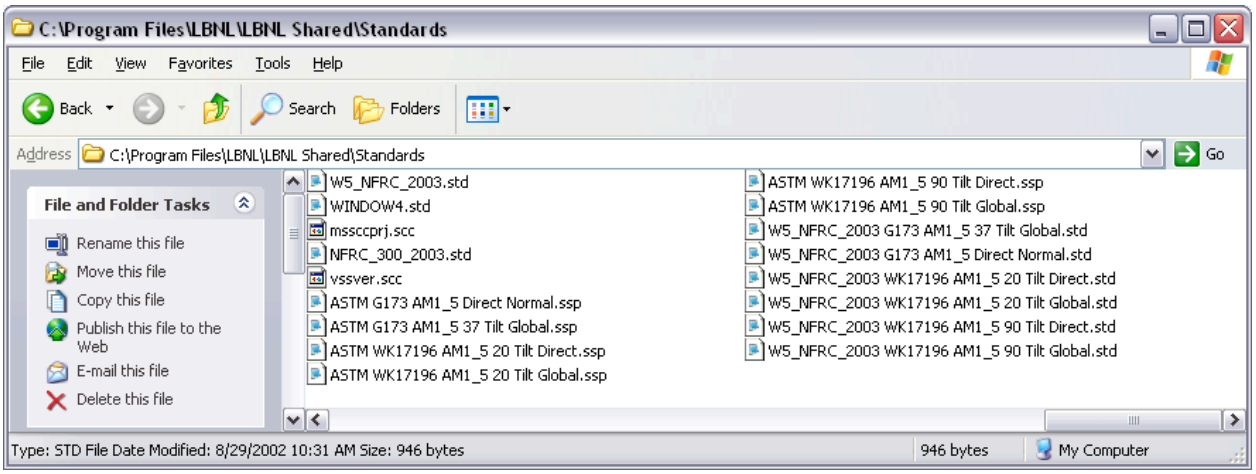


Figure 2 - Copy Spectral Data and Standard Files to WINDOW Standards Folder

[1] Although it is recommended that all the files be copied into the WINDOW 5.2 Standards folder, one can limit their selection to specific spectra from the list. Make sure that the Spectral Data files (*.ssp), and the associated Standard files (*.std) are copied in pairs, as the Standards file calls upon a specific Spectral Data file.

[2] Copy all these files directly into the Standards folder *without* making a subfolder.

3. Open the Glazing System Glazing Library in the Newly Created WINDOW Database

Open WINDOW, and then use the **[Glazing System Library]** toolbar button (or the **Libraries|Glazing System** menu choice) to open the new Glazing System Library that was previously created in Step 1 (Fig. 3).

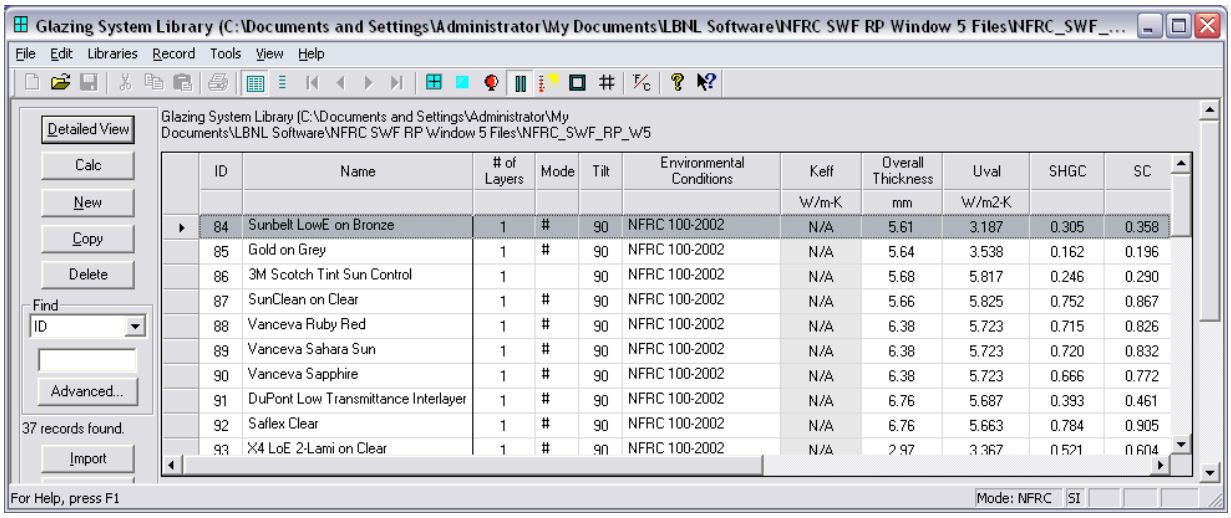


Figure 3 - Open New Glazing System Library for Analysis

4. Change the WINDOW Standards File Reference

Open the *Preferences* box in WINDOW (on the Menu Bar, click on **File|Preferences**), and then click on the "Optical Data" Tab. Click on the **[Browse]** button under the "Standards File" section near the bottom (Fig. 4). Select the Standards file (*.std) representing the spectrum in question. Click on the **[Open]** button to select the file, and then click on the **[OK]** button to close the *Preferences* box. The WINDOW Spectral Data file (*.ssp) is referenced by the WINDOW Standards file, and so the Spectral Data file reference is not directly specified within WINDOW.

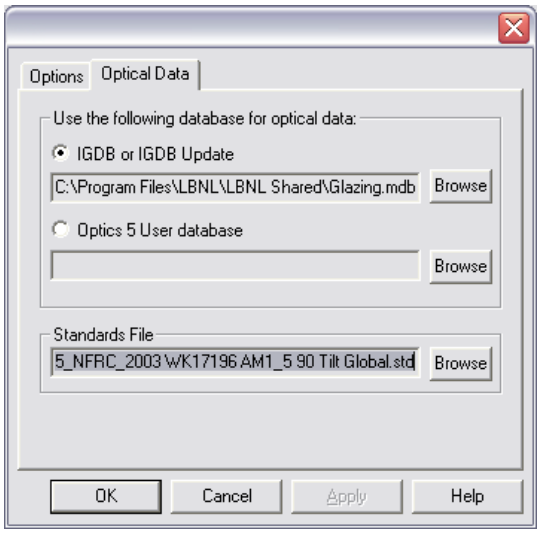


Figure 4 - Specify Location of the New Standards File in *Preferences*

5. Change the WINDOW Environmental Conditions

Click on the **[Environmental Conditions Library]** button to open that library (on the Menu Bar, click on **Libraries|Environmental Conditions**). From within the **[List]** view of the Environmental Conditions Library, highlight the first ID record, titled "NFRC 100-2002," and use the **[Copy]** button to make a copy of that environmental condition[3] (Fig. 5). Select this new environmental condition, and click on the **[Detailed View]** button to edit this condition.

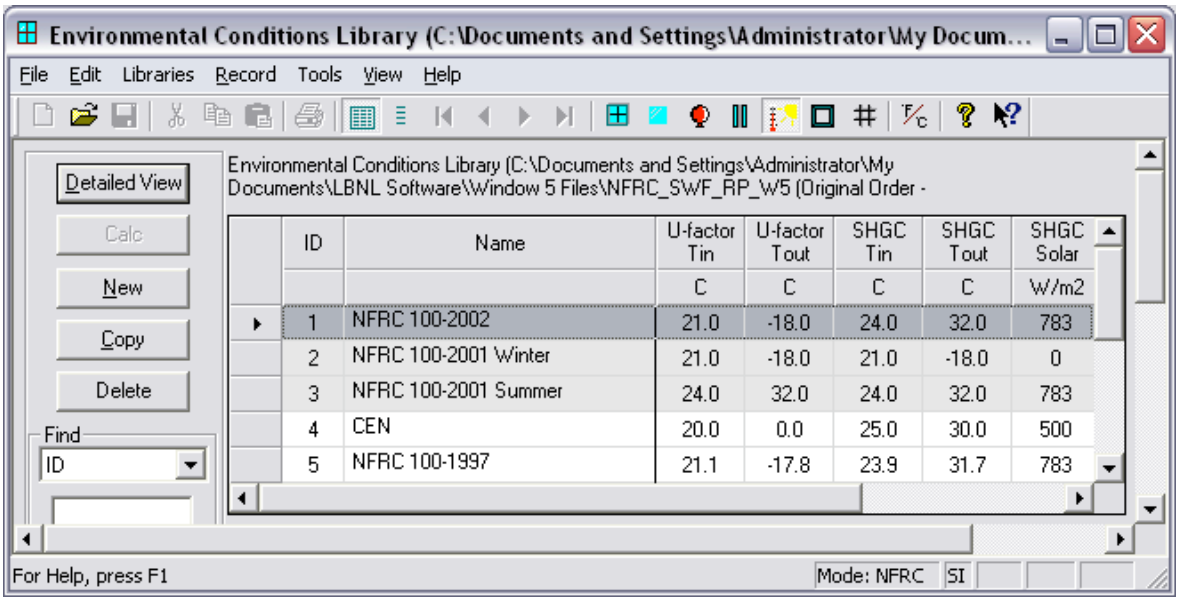


Figure 5 - Copy NFRC 100-2002 Environmental Conditions to Edit

By editing a copy of the NFRC 100-2002 Environmental Conditions, all of the specific environmental parameters (i.e., temperatures, emissivity, wind speed and direction, solar irradiance, and surface conductance coefficient models) for U-factor and SHGC will be initially defined. Only two fields need to be modified. First, change the environmental condition *Name* to reflect the use of the new spectrum, (i.e., "NFRC/ASTM G173 Global37"). Second, click on the "SHGC Outside" Tab, and change the *Direct Solar Radiation* value[4] based on the last column of Table 1 (Fig. 6).

[3] If the NFRC 100-2002 Condition is not available, use the **[Import]** button to copy it from the original "w5.mdb" file initially supplied with WINDOW 5.2.

[4] The term "Direct Solar Radiation" is not exactly correct since some new spectra refer to global radiation, but is used in these instructions to be consistent with the current version of WINDOW.

Table 1 – *Direct Solar Radiation* Values for WINDOW 5.2 Standards Files

Spectrum	Standards File	Direct Solar Radiation, W/m^2
ASTM E 891 (NFRC 300)	W5_NFRC_2003.std	783.0
ASTM G 173, Direct Normal	W5_NFRC_2003 G173 AM1_5 Direct Normal.std	900.1
ASTM G 173, Global, 37° Tilt	W5_NFRC_2003 G173 AM1_5 37 Tilt Global.std	1000.4
ASTM WK17196, Direct, 20° Tilt	W5_NFRC_2003 WK17196 AM1_5 20 Tilt Direct.std	791.1
ASTM WK17196, Global, 20° Tilt	W5_NFRC_2003 WK17196 AM1_5 20 Tilt Global.std	889.0
ASTM WK17196, Direct, 90° Tilt	W5_NFRC_2003 WK17196 AM1_5 90 Tilt Direct.std	669.7
ASTM WK17196, Global, 90° Tilt	W5_NFRC_2003 WK17196 AM1_5 90 Tilt Global.std	810.3

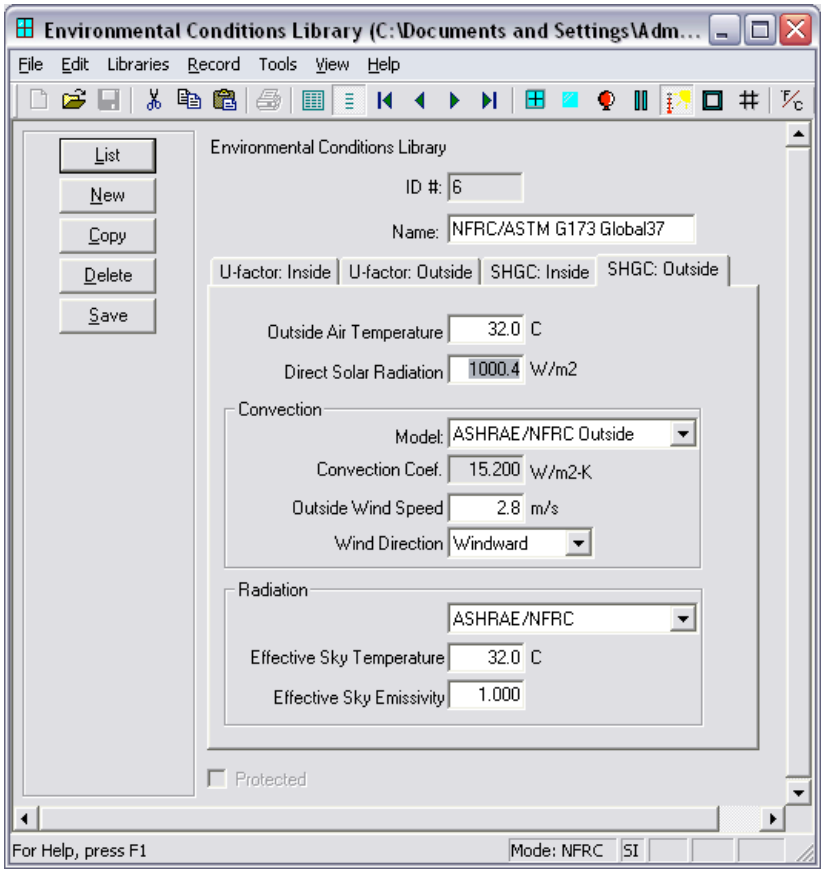


Figure 6 – Rename and Edit Copy of Existing NFRC 100-2002 Environmental Conditions

Click on the **[Save]** button to save the changes to this new Environmental Conditions file.

Once new Environmental Conditions have been created, the referenced Environmental Conditions must be individually changed for each glazing system by selecting the appropriate *Environmental Conditions* designation in the **[Detailed View]** of the Glazing System Library (Fig. 7). All of the *Environmental Conditions* entries in the Glazing System Library can be easily changed by scrolling through each glazing system using the **[Next Record]** button. This also a convenient time to change the tilt angle as described in the next step if necessary. To speed up the process of changing multiple records, press the **[Calc]** and **[Save]** button after each record is changed.

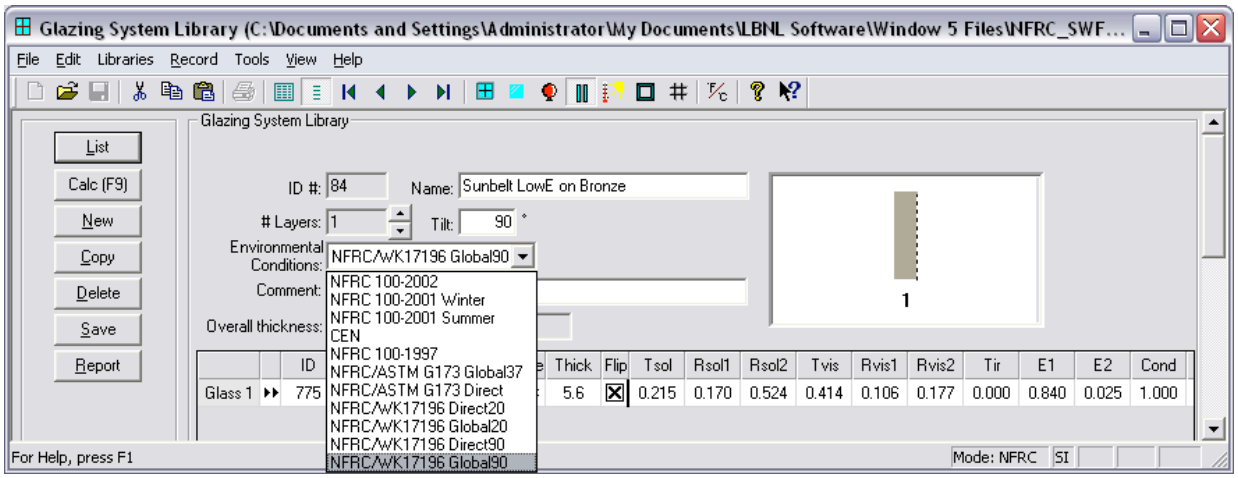


Figure 7 - Select Environmental Conditions for Each Individual Glazing System

6. Change the Tilt of the Glazing System (20° Tilted Spectra Only)

The outdoor and indoor surface heat transfer coefficients and the effective conductivity of glazing cavities vary with the tilt of the glazing system. Their effect on SHGC may appear small in many cases, but they can be of the same magnitude as those that result from a change in spectral distribution. Proper calculation of the SHGC therefore requires that the tilt of each glazing system be changed from 90° to 20° when using spectra for surfaces tilted at 20°. This modification must be performed individually for each glazing system by changing the *Tilt* value to 20 in the **[Detailed View]** (Fig. 8). All of the *Tilt* values in the Glazing Library can be easily changed by scrolling through each glazing system using the **[Next Record]** button. Remember to press the **[Calc]** and **[Save]** button after each record is changed.

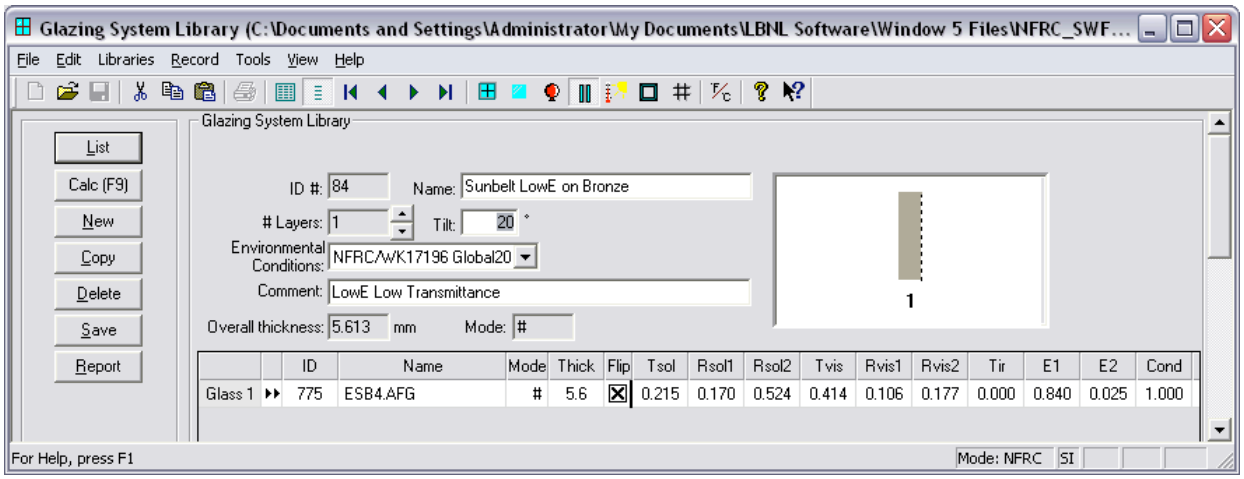


Figure 8 – Change the Tilt Angle for Each Glazing System

7. Calculate

If you have not recalculated the results for all of the glazing systems while modifying the Environmental Conditions or tilt, then results may need to be calculated. From the Glazing Library **[List]** view, click on the **[Calc]** button, and check the *All records* option before clicking on the **[OK]** button to calculate new solar and optical properties of all the glazing systems in the library. This will calculate new results for all the glazing systems using the new Spectral Data file referenced by the Standards file specified in the *Preferences* box[5]. Changing the Standards file is a program setting, so all records are affected by those settings[6].

Use the **[Report]** button to create a text file of the results (Fig. 9). After deselecting *Use default column widths*, and *Wrap column* boxes in the "Text file options" section, press **[OK]** in the *Report* box to generate the report for *All records*. This report can then be saved as a comma delimited file (*.csv) using a name identifying the spectrum by pressing the **[Save]** button in the *Report* window. The comma delimited file needs to be specified in the *Save as type* field in the *Save As* box before pressing the **[Save]** button.

[5] The variations in the ultra-violet (UV) results calculated by WINDOW in the "Optical Data" tab are not reported in this research project. By specifying the Standards files provided with these instructions, the spectra used to calculate the Krochman Damage Weighted Average (Tdw-K), the UV Damage Weighted Transmittance based on CIE 89/3 (Tdw-ISO), and the Unweighted UV Average (Tuv) are all calculated using the new spectra instead of ASTM E891.
[6] For this reason, it is important that the new Standards file be replaced with the original "W5_NFRC_2003.std" file once this analysis is complete as this initial Standards file will not be restored when opening your original database.

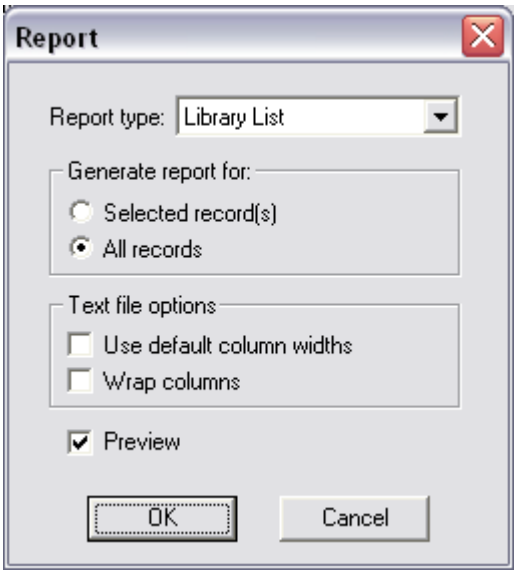
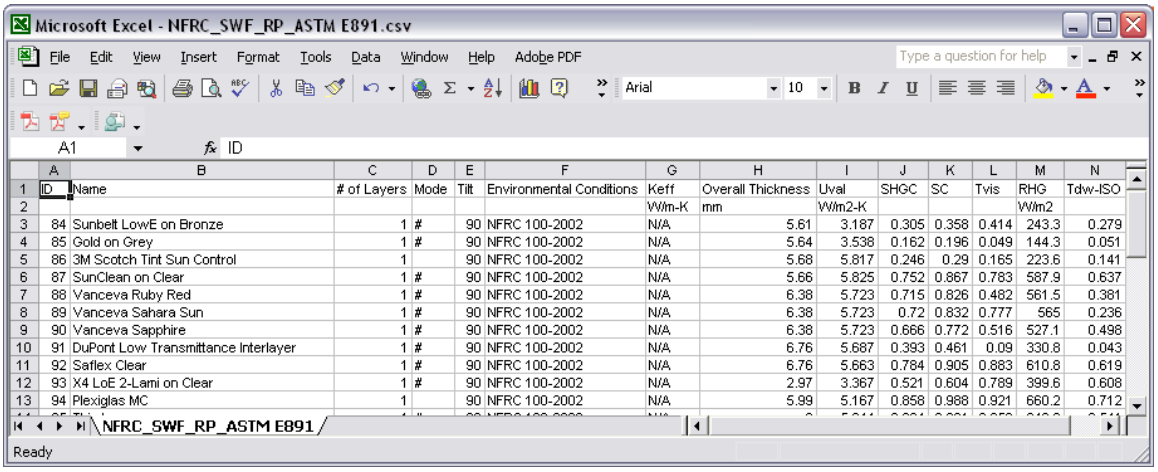


Figure 9 - Create Text File Using WINDOW 5.2 [Report] Button

8. Compare

Repeat Steps 4 through 7 for each spectrum under consideration. The results from calculations of all the spectra can be easily compared by opening each of the comma-delimited files (*.csv) in a spreadsheet (Fig. 10), and copying the appropriate data from each file into the same worksheet.



	A	B	C	D	E	F	G	H	I	J	K	L	M	N
1	ID	Name	# of Layers	Mode	Tilt	Environmental Conditions	Keff	Overall Thickness	Uval	SHGC	SC	Tvis	RHG	Tdw-ISO
2							W/m-K	mm	W/m2-K				W/m2	
3	84	Sunbelt LowE on Bronze	1	#	90	NFRC 100-2002	N/A	5.61	3.187	0.305	0.358	0.414	243.3	0.279
4	85	Gold on Grey	1	#	90	NFRC 100-2002	N/A	5.64	3.538	0.162	0.196	0.049	144.3	0.051
5	86	3M Scotch Tint Sun Control	1		90	NFRC 100-2002	N/A	5.68	5.817	0.246	0.29	0.165	223.6	0.141
6	87	SunClean on Clear	1	#	90	NFRC 100-2002	N/A	5.66	5.825	0.752	0.867	0.783	587.9	0.637
7	88	Vanceva Ruby Red	1	#	90	NFRC 100-2002	N/A	6.38	5.723	0.715	0.826	0.482	561.5	0.381
8	89	Vanceva Sahara Sun	1	#	90	NFRC 100-2002	N/A	6.38	5.723	0.72	0.832	0.777	565	0.236
9	90	Vanceva Sapphire	1	#	90	NFRC 100-2002	N/A	6.38	5.723	0.666	0.772	0.516	527.1	0.498
10	91	DuPont Low Transmittance Interlayer	1	#	90	NFRC 100-2002	N/A	6.76	5.687	0.393	0.461	0.09	330.8	0.043
11	92	Saflex Clear	1	#	90	NFRC 100-2002	N/A	6.76	5.663	0.784	0.905	0.883	610.8	0.619
12	93	X4 LoE 2-Lami on Clear	1	#	90	NFRC 100-2002	N/A	2.97	3.367	0.521	0.604	0.789	399.6	0.608
13	94	Plexiglas MC	1		90	NFRC 100-2002	N/A	5.99	5.167	0.858	0.988	0.921	660.2	0.712

Figure 10 - Open Exported Text File in Spreadsheet

Appendix 2 — Proposed Methodology to Adjust Solar Calorimeter Test Results Based on a Known Source Spectrum

Overview – Although the calculation of SHGC is typically performed using a unique standard spectrum, the measurement of the SHGC of windows, door and skylights using solar calorimeters is seldom—if ever—performed using a light source emitting a spectrum that is the same as this standard spectrum. This is often a source of discrepancy when comparing simulated SHGC with measurements from solar calorimeters. In the process of performing this research project, the investigators cultivated a methodology to correct the differences between test and simulation results. If the spectral characteristics of the light source are known, such as with an electric artificial light source, or by measurement or inference of the incident solar spectrum outdoors, it becomes possible to adjust the solar calorimeter test results to more closely match simulation at a standard spectrum. This Appendix outlines a methodology to perform that adjustment.

Characterize Source Spectrum – Measurement or estimation of the actual spectrum emitted from a light source such as the sun or an electric light is not a trivial task. A discussion of methods of obtaining the spectral response curves of light sources that might be used to illuminate solar calorimeters follows:

> Indoor Solar Calorimeters – Electric Artificial Light Source: The spectral output from an electric light may be the easiest to obtain, especially if it can be provided by the manufacturer of the lamp. Manufacturers of large-scale lamps, like those used to simulate sunlight, are often able to provide the spectral output from their lamps in sufficient detail. For instance, Figure A2 shows the output from a Vortek Lamp used by Bodycote Materials Testing[7] for their indoor solar calorimeter compared with the ASTM E891 spectrum and the proposed ASTM Global 90°-tilt spectrum.
>
> If the spectral response of the electric light source cannot be provided by the manufacturer, or the source has been altered by additional lamps or filters, then the spectrum of the incident irradiation on the face of the indoor solar calorimeter may need to be directly measured. Although instrumentation and testing methodologies are available to perform this measurement, it is not an easy or inexpensive task.
>
> Outdoor Solar Calorimeters – Natural Sunlight: The spectral composition of the irradiance from the sun, the sky or the ground is considerably more variable than that of indoor lamps, but it can be measured or estimated. As in the measurement of the spectral characteristics of electric lamps, the measurement of the spectrum of incident solar and diffuse irradiation is difficult and expensive to perform. The sensors must be rugged enough to withstand exposure to the outdoor environment, and the angular distribution of the diffuse irradiation from the ground and the sky must be taken into account. Accurate,

[7] Bodycote Materials Testing Canada, Inc. 2395 Speakman Drive, Mississauga, ON L5K 1B3, Contact: Alfred Brunger (905) 822-4111 Ex 544

laboratory-grade equipment can be expensive to purchase and maintain. Nevertheless, acceptable measurements can generally be performed by commercially available sensors and software that may be adequate for this task.

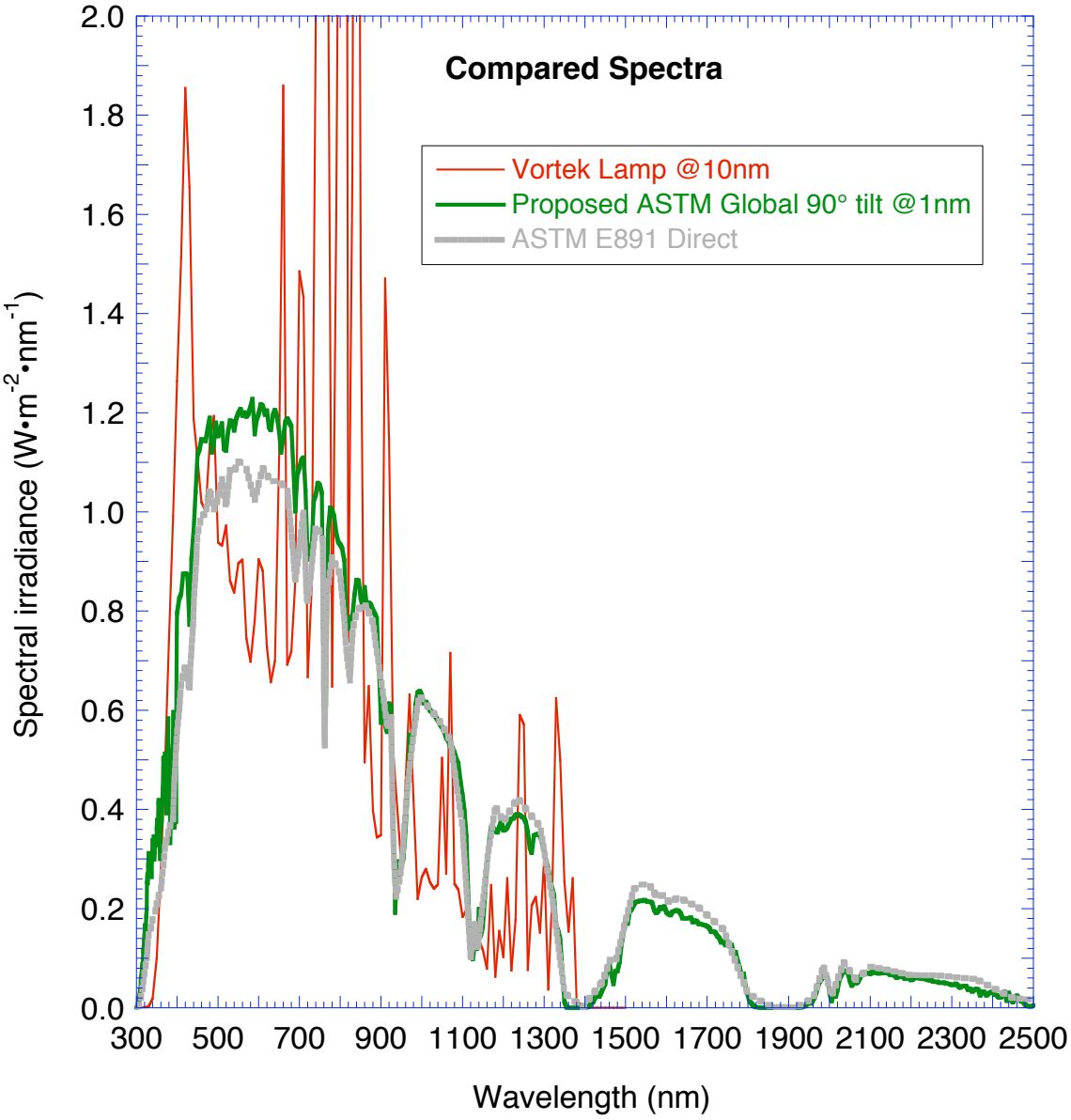


Figure A2 Spectral response from Vortek Lamp (smoothed to 10-nm resolution) compared to ASTM E891 Direct spectrum and proposed ASTM Global spectrum

Another way to estimate the spectral composition of the incident spectrum is to use SMARTS software[8] to calculate the direct irradiance from the sun, and the diffuse irradiance emanating from the sky or reflected by the ground. This can be done for a specific time, date and location, given that certain atmospheric parameters can be determined or estimated. Some of these atmospheric parameters may be measured by

[8] Available from http://www.nrel.gov/rredc/smarts/.

nearby airports, universities or government laboratories, and are generally available to the public. In addition, these atmospheric parameters may be estimated from other sources (such as satellite data) by qualified technicians and scientists.

Select Similar Glazing System Specimen – Select or construct a glazing system from the WINDOWS 5.2 Glazing System Library that most closely resembles the test specimen installed in the solar calorimeter. Most importantly, the spectral characteristics and the SHGC of the glazing system selected in the Glazing System Library must be as close as possible to the test specimen.

Methodologies to Calculate SHGC of Glazing System Using Measured and Standard Spectra

1. Approximate (Short) Method

Use WINDOW to calculate the SHGC of the selected glazing system using the standard spectrum, $SHGC_{STD}$. Since these calculations are attempting to mimic the conditions experienced during solar calorimeter tests, it may be necessary to change the Environmental Conditions within WINDOW from the standard NFRC conditions, to conditions that more closely resemble the actual environmental conditions experienced during testing.

Using the same environmental conditions, recalculate the SHGC using WINDOW, but replace the standard spectrum with the source spectrum measured or estimated by the previously described methodology, $SHGC_{ALT}$. The source spectrum will have to be converted into a WINDOW spectral file (*.ssp), which typically means that the resolution is degraded to 1 nm resolution between 300 and 400 nm, 5 nm resolution up to 2500 nm, and 10 nm beyond. Use the Instructions provided in Appendix 1 of this report as guidance in performing WINDOW 5.2 calculations with alternate spectra.

Correct the Measured SHGC – Simply use the ratio of the SHGC calculated using the standard spectrum, $SHGC_{STD}$ to the SHGC calculated using the actual spectrum, $SHGC_{ALT}$, to adjust the measured SHGC. The corrected SHGC, $SHGC_{SPEC}$, is a function of the measured SHGC, $SHGC_{TEST}$, as follows:

$$\frac{SHGC_{ALT}}{SHGC_{STD}} = \frac{SHGC_{TEST}}{SHGC_{SPEC}} \quad (1)$$

2. Detailed (Long) Method

This alternate method is derived from the technique known as "spectral mismatch correction" in the field of photovoltaic (PV) cell testing[9]. This method is more general and accurate than the short method above, but also involves more calculation.

[9] See, e.g., D. Myers and C. Gueymard, Description and availability of the SMARTS spectral model for photovoltaic applications. 49th SPIE Annual Meeting, Denver, CO (2004).

The definition of *SHGC* is

$$SHGC = T_s + A_s N_i \tag{2}$$

where T_s is the fraction of incident flux transmitted through the glazing to the interior (i.e., its transmittance), A_s is the glazing system's absorptance, and N_i is the fraction of the absorbed radiation that is re-emitted to the interior. For any glazing system, the calculation described by Eq. (2) is actually performed wavelength by wavelength in WINDOW. Therefore, for each wavelength λ,

$$SHGC_\lambda = T_{s\lambda} + A_{s\lambda} N_i. \tag{3}$$

Note that N_i does not depend on the wavelength of the incident *shortwave* (or "solar") spectrum, since it is only a function of the convection, conduction and *longwave* ("infrared" or "thermal") radiation heat transfer characteristics of the glazing system. The limit between the shortwave and longwave domains is 4–5 μm, approximately.

When all individual spectral calculations are completed, WINDOW performs the final step, by convolving the calculated SHGC spectrum defined by Eq. (3) with the *standard* SWF, i.e.,

$$SHGC_{STD} = \int SHGC_\lambda E_{STD\lambda} d\lambda / \int E_{STD\lambda} d\lambda \tag{4}$$

where $E_{STD\lambda}$ is the standard spectral solar irradiance at wavelength λ. The denominator in Eq. (4) simply represents the integrated incident solar irradiance, per the last column of Table A1 in Appendix 1.

Using Eq. (3), Eq. (4) can be developed into

$$SHGC_{STD} = [\int T_{s\lambda} E_{STD\lambda} d\lambda + N_i \int A_{s\lambda} E_{STD\lambda} d\lambda] / \int E_{STD\lambda} d\lambda. \tag{5}$$

If the actual spectral irradiance during the experimental tests is $E_{ALT\lambda}$ (obtained either by measurement or prediction with, e.g., SMARTS, as discussed above), the SHGC that WINDOW *would* predict under the spectral test conditions is

$$SHGC_{ALT} = [\int T_{s\lambda} E_{ALT\lambda} d\lambda + N_i \int A_{s\lambda} E_{ALT\lambda} d\lambda] / \int E_{ALT\lambda} d\lambda. \tag{6}$$

The $T_{s\lambda}$ and $A_{s\lambda}$ spectra are important characteristics of the glazing system, which can be exported from WINDOW. Therefore, $SHGC_{ALT}$ can be easily calculated from Eq. (6) in a spreadsheet if N_i is known. Whenever N_i is not known beforehand, it can be derived from Eq. (3), such as

$$N_i = (SHGC - T_s) / A_s. \tag{7}$$

$SHGC_{ALT}$ thus obtained from Eq. (6) should be the same as if WINDOW was actually used to calculate it when using the procedure described in Appendix 1 (to change the standard spectrum for an alternate spectrum—in this case, $E_{ALT\lambda}$).

NOTES

1. Rather than correcting the measured value of SHGC as in the short method, the intent of the long method is, conversely, to obtain the theoretical SHGC that would correspond to the spectral test conditions.

2. The detailed methodology would also have to include cases where the tested fenestration system includes glazing layers whose spectral characteristics are close, but not necessarily identical to, the data in WINDOW. This case has not been discussed in the overview of the long method for conciseness.

3. The equations involving integrals are given in mathematical form for further reference, and may look intimidating. In practice, they are easily calculated as summations of columnar values in a spreadsheet.

Project 1.1.17

Project Name: Complex Product VT Rating Research

Date: March 2009

Purpose: Develop a methodology for determining Visible Transmittance (VT) for products with complex glazings.

Project Summary:

The following research project is designed to test TDDs for Visible Transmission (VT) with two existing goniophotometers (owned by TDD manufacturers) at various incident angles. The results will be compared with test results using integrating sphere currently in use at LBNL.

Click here for latest interim report

Review documents on this web link:
http://www.nfrc.org/complexprodvtrfpbrtg.aspx

V_t Algorithm

Legend

V_{t20} = Visible Transmission at 20 degrees solar altitude (i.e.)

ZT_{20} = Zonal Time, percent of time spent in zone that number falls into (i.e. ZT_{20} is for 15-25 range from chart)

Vt Yearly = (Vt10*ZT10)+(Vt20*ZT20)+(Vt30*ZT30)+(Vt40*ZT40)+(Vt50*ZT50)+(Vt60*ZT60)+(Vt70*ZT70)

Hypothetical V_t data		**OPTION #1 (sunrise to sunset)**		**OPTION #2 (10° to 10°)**		**OPTION #3 (15° to 15°)**	
SALT	**Vt**	SALT range	**ZT**	SALT range	**ZT**	SALT range	**ZT**
10	**0.20**	<15°	0.247				
20	**0.25**	15°-25°	0.176	**10º - 25º**	**0.307**	15°-25°	0.234
30	**0.35**	25-35	0.1895	25-35	0.2275	25-35	0.252
40	**0.38**	35-45	0.1365	35-45	0.164	35-45	0.182
50	**0.42**	45-55	0.111	45-55	0.133	45-55	0.147
60	**0.45**	55-65	0.086	55-65	0.103	55-65	0.114
70*	**0.48**	>65°	0.054	>65°	0.065	>65°	0.072
			1		0.9995		1.001

OPTION # 1

Yearly efficiency (**sunrise**) = (0.20*0.247)+(0.25*0.176)+(0.35*0.1895)+(0.38*0.1365)+(0.42*0.111)+(0.45*0.086)+(0.48*0.054) = **0.32**

OPTION # 2

Yearly efficiency (**10 deg**) = (0.25*0.307)+(0.35*0.2275)+(0.38*0.164)+(0.42*0.133)+(0.45*0.103)+(0.48*0.065) = **0.35**

OPTION # 3

Yearly efficiency (**15 deg**) = (0.25*0.234)+(0.35*0.252)+(0.38*0.182)+(0.42*0.147)+(0.45*0.114) +(0.48*0.072)= **0.36**

NOTE 1:

Yearly efficiency starting at different points of day, depending on levels of usable amount of light

NOTE # 2: 70* we could use the efficiency for 60° SALT if agreeable, in order to reduce the cost of the tests
Presently we considered only 5 data points for Vt (20, 30, 40, 50 and 60)

NOTE # 3:

For the second Zonal Time, the lower range is 10° to 25° , using Vt20 and combined ZT10+ZT20

Project 1.1.18

Project Name:	Window 6 and THERM 6 Validation Research
Date:	March 2008
Purpose:	Perform and coordinate the data collection, research, and testing to evaluate the new features within Window 6 and THERM 6

Project Summary:

The research project consisted of four tasks, (1) Literature search, (2) Perform tests and simulations, (3) Compare and evaluate results and (4) Status reports and papers.

Click here for the latest interim report

Web link:
http://www.nfrc.org/window6therm6validationresearch.aspx

Validation of WINDOW 6 and THERM 6 for Use in Determining the Solar Heat Gain Coefficients and U-Factors of Complex Glazing Systems Research Project

NFRC Project Number: 07-101-RP

NFRC 2010 Spring Membership Conference

William C. duPont/Sunergy Consulting

W. Ross McCluney/Sun Pine Consulting

Background

- WINDOW 6 and THERM 6 are currently under development with new capabilities
- Calculate the SHGC and U-Factor of
  - Woven Shades,
  - Venetian Blinds, and
  - Fritted Glass
- Shading Systems Can Be Located
  - Indoor
  - Between Glazing
  - Outdoor

Project Objectives

- Perform and coordinate the data collection, research, and testing to evaluate the new features within WINDOW 6 and THERM 6

Project Tasks and Deliverables

- **Task 1 – Literature Search** ***(3 Months)***
  - Compile and Evaluate Existing SHGC and U-Factor Test Results
  - Describe Existing Methods of Calculating SHGC and U-Factors
- **Task 2 – Perform Tests and Simulations** ***(7 Months)***
  - Identify and Procure Test Specimens
  - Perform SHGC and U-Factor Tests
  - Perform SHGC and U-Factor Simulations
- **Task 3 – Compare and Evaluate Results** ***(2 Months)***
  - Test and Simulation Results from Literature Search
  - SHGC and U-Factor Test Results
- **Task 4 – Status Reports & Papers** ***(3 Months)***

Task 2b Overview



- Perform SHGC Tests
  - Architectural Testing, Inc. in Fresno, CA (ATI) performed SHGC Testing between October 6, 2008 and September 3, 2009
  - PI Visit ATI during the week of October 6-10, 2008
  - All 26 SHGC Test Reports Received

Task 2b Overview (Continued)

- Perform U-Factor Tests
  - Architectural Testing, Inc. in Fresno, CA (ATI) performed tests between October 3, 2008 and July 12, 2009
  - PI Visit ATI during the week of October 6-10, 2008
  - All 20 U-Factor Tests Reports Received



Task 2c Overview

- Perform SHGC and U-Factor Simulations
  - Carli, Inc. is performing NFRC 100 and NFRC 200 Simulations.
  - Simulations At Standard Conditions
    - Window Manufactures Have Donated WINDOW and THERM Files
    - Have Measured Optical Properties of Shade Materials (LBNL Donation)
    - Have Procured Adequate Working Drawings and Bill of Materials of All Windows and Shading Systems
  - Simulated as Tested
    - At Environmental Conditions Experienced During Testing
    - As Installed in Solar Calorimeter or Thermal Chamber

Task 2c Overview

- Perform Computer Simulations
  - Carli, Inc. is providing:
    - SHGC and U-Factors at
    - Standard and Actual Conditions
    - Modeled Using 5 Computational Methodologies
      - ISO 15099
      - University of Waterloo
      - LBNL Scalar 0.0
      - LBNL Scalar 0.5
      - LBNL Scalar 1.0
    - Many Simulations Completed
      - 15 Sets of ISO 15099 Results
      - 8 Sets of All Models (12 Total)

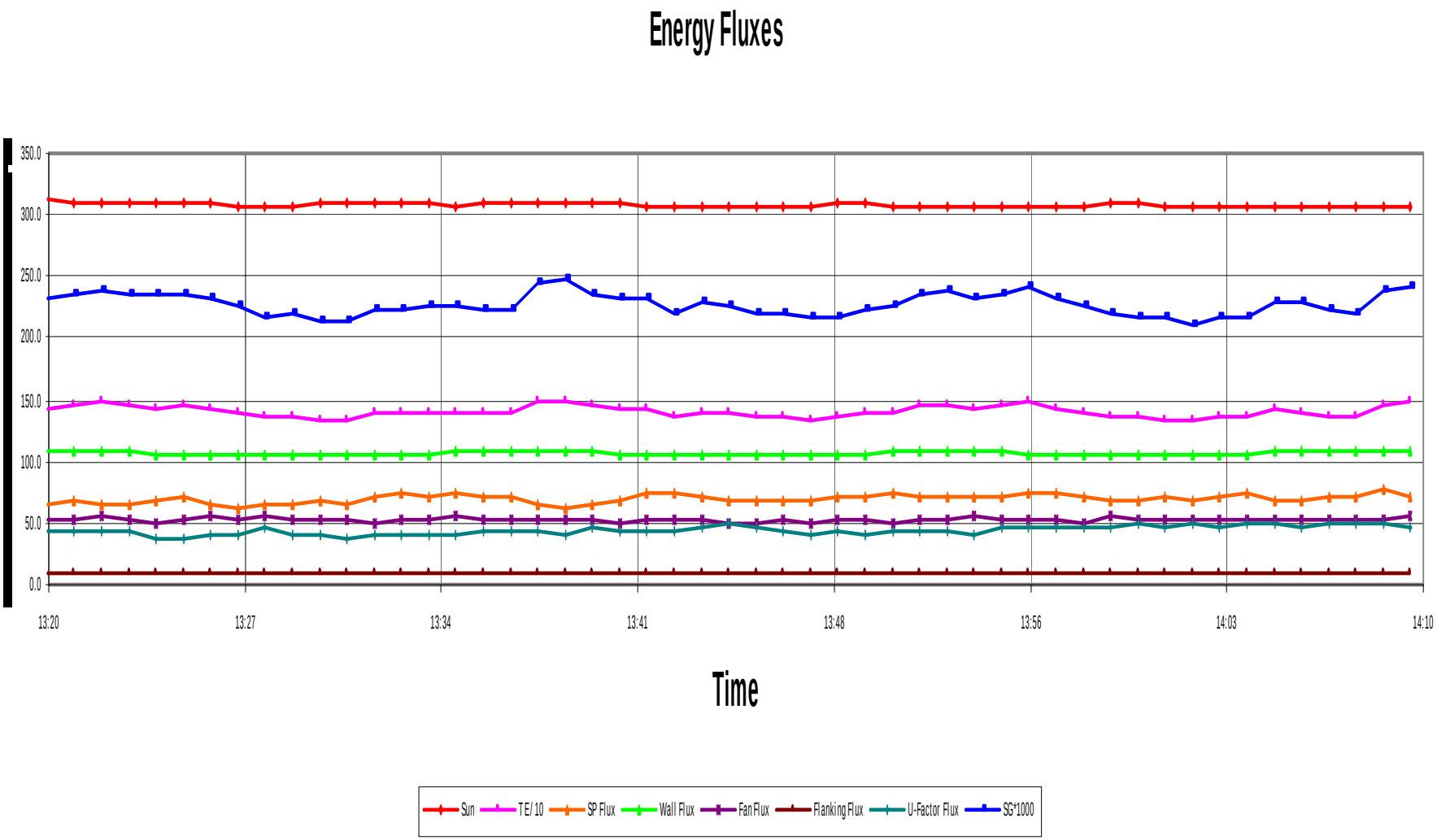
Current Tasks

- Provide Carli, Inc. with…
  - Information from Architectural Testing, Inc.
    - Identify Environmental Conditions of SHGC Tests
    - Identify Exterior Color of Specimen Frame of SHGC Tests (10 Tests)
    - Identify Exact Location and Dimensions of Frames Used to Mount Woven Shades (5-7 Tests)
    - Perform Area-Weighting U-Factor Standardization of High Conductance and Interior Blinds Specimens (8 Tests)

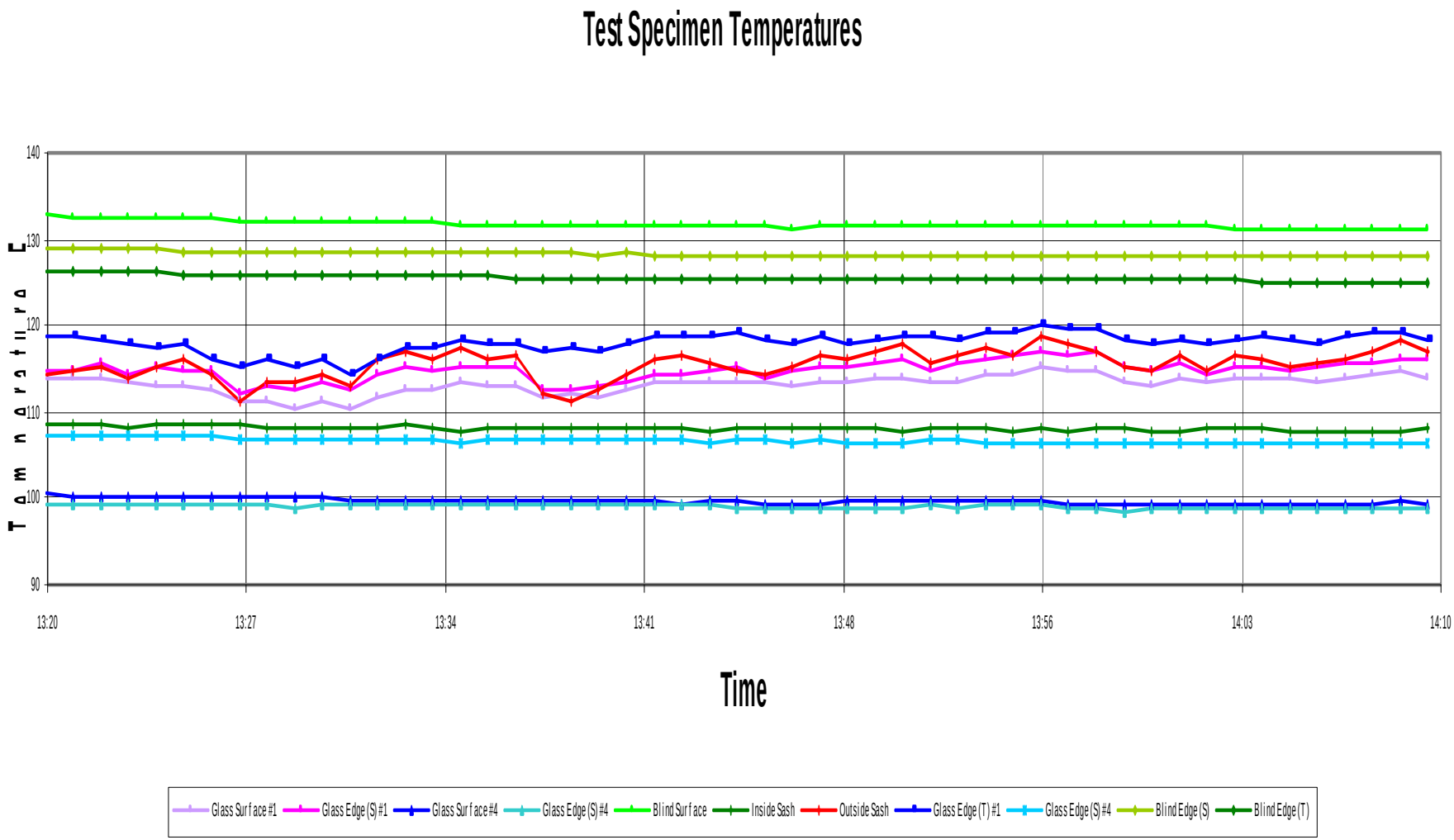
Current Tasks

- Environmental Conditions of SHGC Tests
  - Developed MS EXCEL spreadsheets for Raw Data from ATI (Templates)
    - Statistical Analysis of Measured Data
    - Graph Heat Flux
    - Graph Wind Speed
    - Graph Solar Calorimeter Temperatures
    - Graph Test Specimen Temperatures
    - Graph Temperature Differences

Current Tasks



Current Tasks



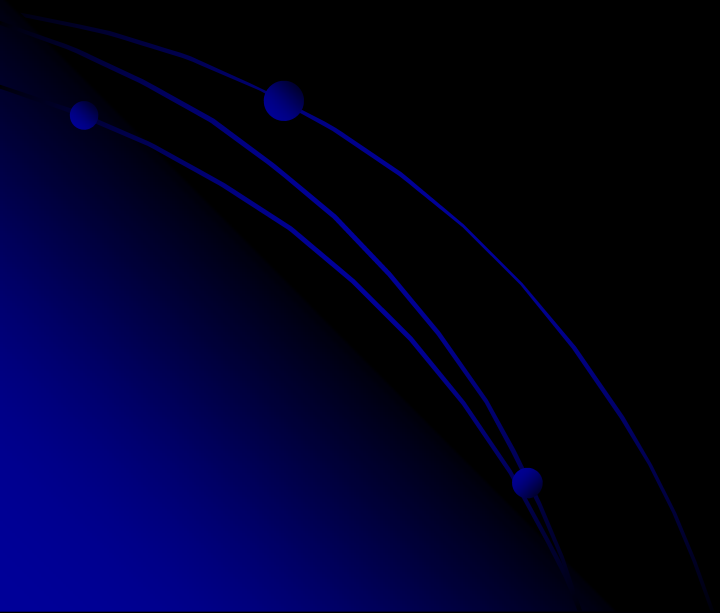
Current Tasks

- Analysis of Test Reports
  - U-Factor Test Omission and Errors (20 Tests)
    - Surface Temperatures and Corresponding Areas
      - Perform Area-Weighting U-Factor Standardization
    - Raw Data In Electronic Format (MS EXCEL)
    - Location and Methodology Used to Mount Blinds and Shades
    - Verify Air-Filled Cavities
    - CTS Calibration Test Results

Current Tasks

- Analysis of Test Reports *(Continued)*
  - SHGC Test Omission and Errors (26 Tests)
    - Inquiry Consisted of over 64 Issues
      - Surface Temperatures and Corresponding Areas
        - Perform Area-Weighting U-Factor Standardization
      - Raw Data In Electronic Format (MS EXCEL)
      - Location and Methodology Used to Mount Blinds and Shades
      - Verify Air-Filled Cavities
      - CTS Calibration Test Results

Questions or Comments?



Project 2

Project Name:	Development of NFRC 101-Thermophysical Properties of Materials
Date:	Ongoing
Purpose:	The purpose of this project shall be to provide a uniform method for determining the thermophysical properties of glazing (thermal conductivity only), framing, and other opaque materials used in the construction and manufacture of fenestration products.

Project Summary:

Materials covered by this document:

- All frame materials, either single component or composite,
- All glazing materials, thermal conductivity only,
- All sealants and adhesives,
- Weather-stripping materials,
- Thermal barrier materials,
- Cladding materials,
- Spacer materials,
- Desiccant materials

Click here for the May 2010 NFRC-101 document



National Fenestration Rating Council Incorporated

NFRC 101-2010 [E2A5]

Procedure for Determining Thermophysical Properties of Materials For Use in NFRC-Approved Software Programs

© 2010 NATIONAL FENESTRATION RATING COUNCIL, INC.

PREPARED BY:
National Fenestration Rating Council
6305 Ivy Lane, Suite 140
Greenbelt, MD 20770-6323
Voice: (301) 589-1776
Fax: (301) 589-3884
Email: info@nfrc.org
Website: www.nfrc.org

FOREWORD

The National Fenestration Rating Council, Incorporated ("NFRC") has developed and operates a uniform rating system for energy and energy-related performance of fenestration products. The Rating System determines the U-factor, Solar Heat Gain Coefficient (SHGC), and Visible Transmittance (VT) of a product, which are mandatory ratings for labeling NFRC certified products and are mandatory ratings for inclusion on label certificates, and are supplemented by procedures for voluntary ratings of products for Air Leakage (AL), and Condensation Resistance. Together, these rating procedures, as set forth in documents published by NFRC, are known as the NFRC Rating System.

The Rating System employs computer simulation and physical testing by NFRC-accredited laboratories to establish energy and related performance ratings for fenestration product types. The Rating System is reinforced by a certification program under which NFRC-licensed responsible parties claiming NFRC product certification shall label and certify fenestration products to indicate those energy and related performance ratings, provided the ratings are authorized for certification by an NFRC-licensed certification and Inspection Agency (IA).

The requirements of the rating, certification, and labeling program (the "Certification Program") are set forth in the most recent versions of the following as amended, updated or interpreted from time to time:

- NFRC 700 Product Certification Program (the "PCP")
- NFRC 705 Component Modeling Approach ("CMA") Product Certification Program (the "CMA-PCP").

Through the Certification Programs and the most recent versions of its companion programs as amended, updated or interpreted from time to time:

- The laboratory accreditation program (the "Accreditation Program"), set forth in the NFRC 701 Laboratory Accreditation Program (the "LAP")
- The IA licensing program (the "IA Program"), set forth in NFRC 702 Certification Agency Program (the "CAP")
- The CMA Approved Calculation Entity ("ACE") licensing program (the “ACE Program”) as set forth in the NFRC 708 Calculation Entity Approval Program (the

"CEAP"),

NFRC intends to ensure the integrity and uniformity of NFRC ratings, certification, and labeling by ensuring that responsible parties, testing and simulation laboratories, and IAs adhere to strict NFRC requirements.

In order to participate in the Certification Programs, a manufacturer / responsible party shall rate a product whose energy and energy-related performance characteristics are to be certified in accordance with mandatory NFRC rating procedures. At present, a manufacturer/responsible party may elect to rate products for U-factor, SHGC, VT, Air Leakage, Condensation Resistance, or any other procedure adopted by NFRC, and to include those ratings on the NFRC temporary label affixed to its products, or on the NFRC Label Certificate. U-factor, SHGC and VT, AL, and Condensation Resistance rating reports shall be obtained from a laboratory, which has been accredited by NFRC in accordance with the requirements of the NFRC 701.

The rating shall then be reviewed by an IA which has been licensed by NFRC in accordance with the requirements of the NFRC 702. NFRC-licensed IAs also review label format and content, conduct in-plant inspections for quality assurance in accordance with the requirements of the NFRC 702, and issue a product Certification Authorization Report (CAR), or approve for issuance an NFRC Label Certificate for site-built or CMA products and attachment products. The IA is also responsible for the investigation of potential violations (prohibited activities) as set forth in the NFRC 707 Compliance and Monitoring Program.

Ratings for products that are labeled with the NFRC Temporary and Permanent Label, or products that are listed on an NFRC Label Certificate, in accordance with NFRC requirements, are considered to be NFRC-certified. NFRC maintains a Certified Products Directory (CPD), listing product lines and individual products selected by the manufacturer/responsible party for which certification authorization has been granted.

NFRC manages the Rating System and regulates the Product Certification Program (PCP), Laboratory Accreditation Program (LAP) and Certification Agency Program (CAP) in accordance with the NFRC 700 (PCP), the NFRC 701 (LAP), the NFRC 702 (CAP), the NFRC 705 (CMA-PCP), and the NFRC 708 (CEAP) procedures, and conducts compliance activities under all these programs as well as the NFRC 707 Compliance and Monitoring Program (CAMP). NFRC continues to develop the Rating System and each of the programs.

NFRC owns all rights in and to each of the NFRC 700, NFRC 701, NFRC 702, NFRC 705, NFRC 707, NFRC 708 and each procedure, which is a component of the Rating System, as well as each of its registration marks, trade names, and other intellectual property.

The structure of the NFRC program and relationships among participants are shown in Figure 1, Figure 2, and Figure 3. For additional information on the roles of the IAs and laboratories and operation of the IA Program and Accreditation Program, see the NFRC 700 (PCP), NFRC 701 (LAP), and NFRC 702 (CAP) respectively.

Figure 1

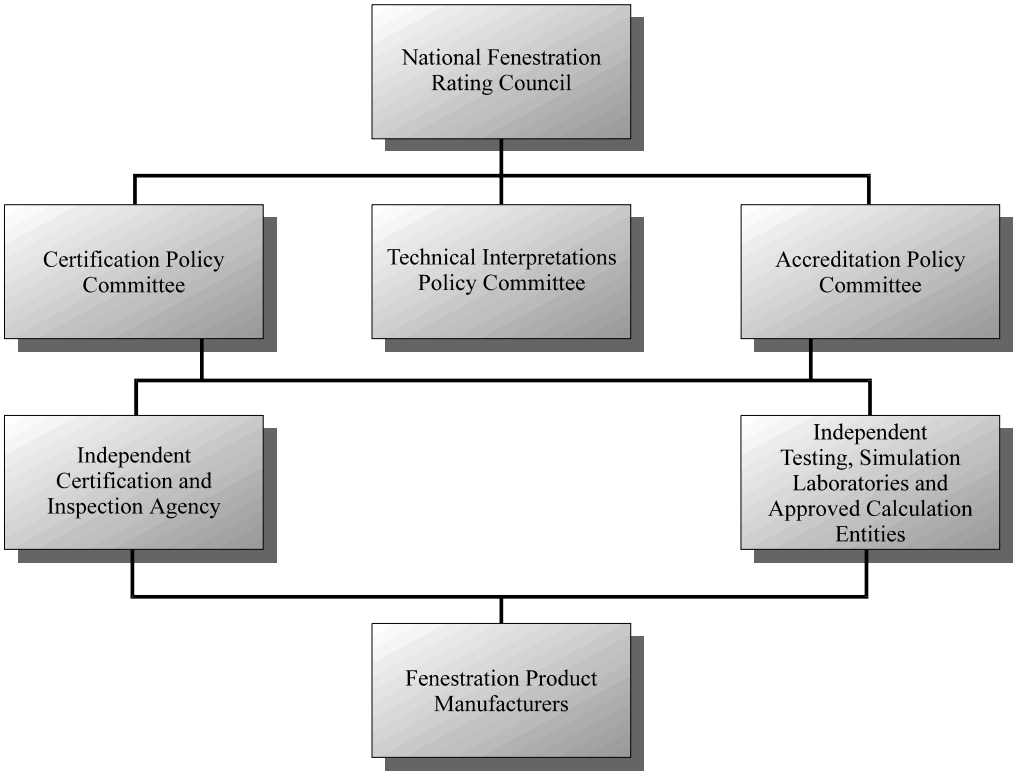


Figure 2

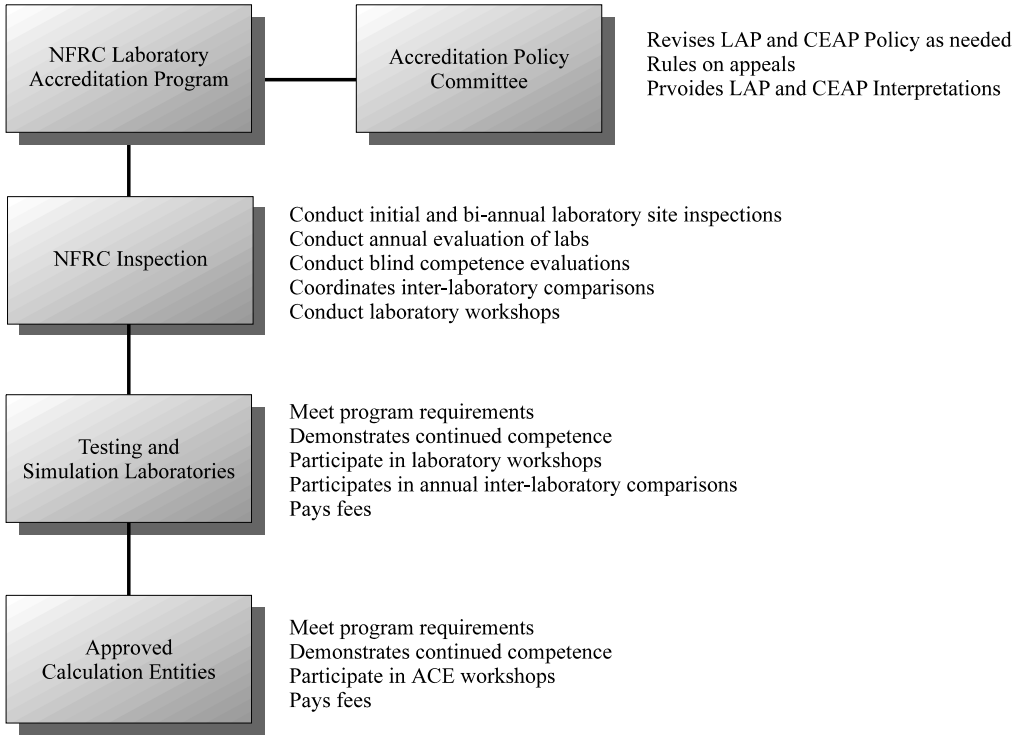
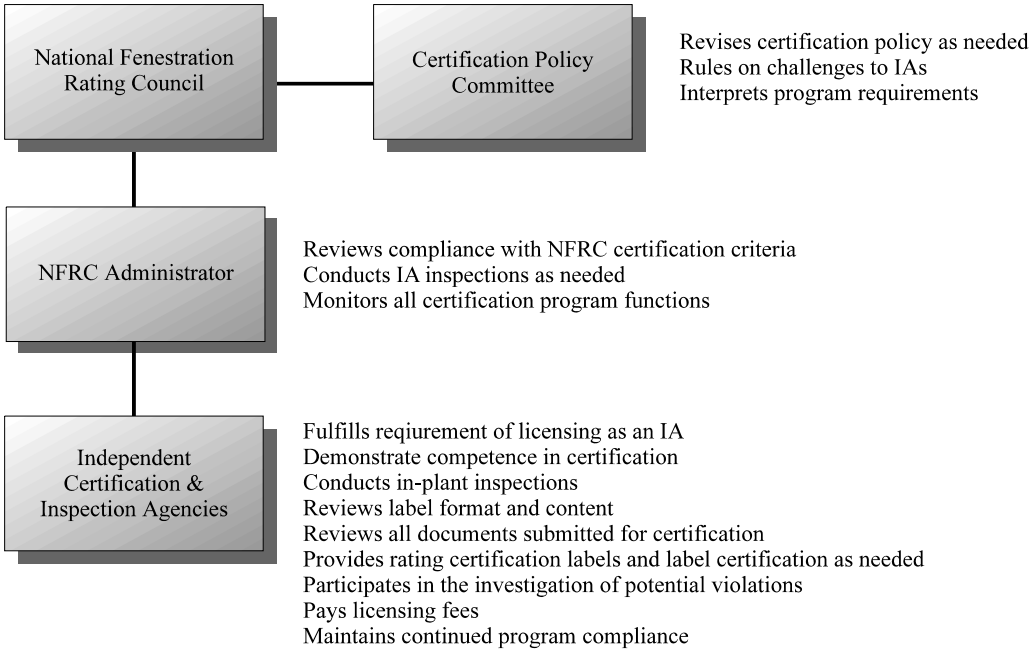


Figure 3



Questions on the use of this procedure should be addressed to:

National Fenestration Rating Council
6305 Ivy Lane, Suite 140
Greenbelt, MD 20770
Voice: (301) 589-1776
Fax: (301) 589-3884
Email: info@nfrc.org
Website: www.nfrc.org



DISCLAIMER

NFRC certification is the authorized act of a manufacturer/responsible party in: (a) labeling a fenestration or related attachment product with an NFRC Permanent Label and NFRC Temporary Label, or (b) generating a site built or CMA label certificate, either of which bears one or more energy performance ratings reported by NFRC-accredited simulation and testing laboratories and authorized for certification by an NFRC-licensed IA. Each of these participants acts independently to report, authorize certification, and certify the energy-related ratings of fenestration and related attachment products.

NFRC does not certify a product and certification does not constitute a warranty of NFRC regarding any characteristic of a fenestration or fenestration-related attachment product. Certification is not an endorsement of or recommendation for any product or product line or any attribute of a product or product line. NFRC is not a merchant in the business of selling fenestration products or fenestration-related products, and therefore cannot warrant products as to their merchantability or fitness for a particular use.

NFRC THEREFORE DISCLAIMS ANY AND ALL LIABILITY THAT MAY ARISE FROM OR IN CONNECTION WITH SERVICES PROVIDED BY, DECISIONS MADE BY OR REPORTS OR CERTIFICATIONS ISSUED OR GRANTED BY ANY NFRC-ACCREDITED LABORATORY, NFRC-LICENSED IA OR ANY PRODUCT MANUFACTURER/ RESPONSIBLE PARTY; RELIANCE ON ANY NFRC PRODUCT DESCRIPTION, SPECIFICATION, RATING, TEST OR CERTIFICATION, WHETHER APPEARING IN A REPORT, A PRODUCT CERTIFICATION AUTHORIZATION OR A PRINTED OR ELECTRONIC DIRECTORY, OR ON A LABEL, OR ON A LABEL CERTIFICATE; OR THE SALE OR USE OF ANY NFRC-RATED OR CERTIFIED PRODUCT OR PRODUCT LINE; INCLUDING BUT NOT LIMITED TO DAMAGES FOR PERSONAL OR OTHER INJURY, LOST PROFITS, LOST SAVINGS OR OTHER CONSEQUENTIAL OR INCIDENTAL DAMAGES.

NFRC program participants are required to indemnify NFRC from and against such liability.

National Fenestration Rating Council®

Table of Contents

Foreword ..... **ii**

Figure 1 v
Figure 2 v
Figure 3 vi

Disclaimer ..... **vii**

1. Introduction **1**

2. Purpose and Scope **1**

2.1 PURPOSE 1
2.2 SCOPE 1

3. Terminology **2**

4. Representative Thermophysical Properties **2**

4.1 GENERIC THERMOPHYSICAL PROPERTIES 2
4.2 MANUFACTURER SPECIFIC THERMOPHYSICAL PROPERTIES 4
4.2.1 Manufacturer Supplied Test Data ...**Error! Bookmark not defined.**

5. Thermophysical Properties Test Methods **5**

5.1 THERMAL CONDUCTIVITY 5
5.1.1 Mean temperatures 6
5.1.2 Specimen thickness 6
5.1.3 Non-homogenous specimens 7
5.2 EMISSIVITY 7
5.2.1 Cleanness of the surface 7
5.2.2 Finishes 7
5.3 SOLAR ABSORPTIVITY 7
5.3.1 Finishes 7
5.3.2 Specularity 8
5.3.3 Cleanness of the surface 8
5.4 LABORATORY ACCREDITATION 8

6. References 8

6.1 STANDARDS 8
6.2 OTHER DOCUMENTS 10

Appendix A Basic Set of Generic Thermophysical Property Values of Materials 12

TABLE A.1: THERMOPHYSICAL PROPERTIES OF SOLIDS 12
TABLE A.2: THERMOPHYSICAL PROPERTIES OF GASES 15

Appendix B Extended Set of Generic Thermophysical Property Values of Materials 17

TABLE B.1: THERMOPHYSICAL PROPERTIES OF SOLIDS 17

Appendix C Manufacturer Specific Thermophysical Property Values of Materials 20

TABLE C.1: THERMOPHYSICAL PROPERTIES OF SOLID MATERIALS 20

1. INTRODUCTION

The National Fenestration Rating Council has developed a uniform national rating system for fenestration product energy performance.

a product certification program reinforces the rating system by requiring ratings are determined by NFRC accredited laboratories and then reviewed and authorized by NFRC licensed independent certification and inspection agencies (IA's) and conform to NFRC requirements.

This procedure has been developed to provide uniform and credible tables (libraries) of thermophysical properties of materials used in the construction and manufacture of fenestration products in approved software tool(s). The following thermophysical properties, currently considered, are: thermal conductivity, long-wave surface emissivity, and solar surface absorptivity hereafter referred to as thermophysical properties.

In this procedure, a table of generic materials and their associated thermophysical properties is provided, as well as a process of introducing custom materials or new, manufacturer specific materials. This procedure should improve the credibility of the values used in simulating thermal performance indices of fenestration systems.

This procedure may involve hazardous materials, operations and equipment. This procedure does not purport to address all of the safety problems associated with its use. It is the responsibility of the user of this procedure to establish appropriate health and safety practices and to determine the applicability of any regulatory limitations prior to use.

The values stated in metric (SI) units shall be regarded as the standard. The inch-pound (IP) units shown in parenthesis shall be for reference only.

2. PURPOSE AND SCOPE

2.1 Purpose

The purpose of this procedure shall be to provide a uniform method for determining the thermophysical properties of glazing (thermal conductivity only), framing, and other opaque materials used in the construction and manufacture of fenestration products. These thermophysical properties shall be used in NFRC approved software tools for the simulation of thermal performance indices of fenestration products.

2.2 Scope

2.2.1. Materials Covered By This Document

- All frame materials, either single component or composite,
- All glazing materials, thermal conductivity only,

- All sealants and adhesives,
- Weather-stripping materials,
- Thermal barrier materials,
- Cladding materials,
- Spacer materials,
- Desiccant materials.

2.2.2. Materials and/or Properties Not Covered By This Document

- Thermal conductivity of finishes
- Glass coatings
- Solar-optical properties of glazing and other transparent materials. (See NFRC 300 and NFRC 301and solar-optical database).

3. TERMINOLOGY

See NFRC Glossary and Terminology of all definitions.

4. REPRESENTATIVE THERMOPHYSICAL PROPERTIES

All materials used in the design and fabrication of a fenestration product shall have either generic thermophysical properties assigned from the list in Appendices A or B, or a manufacturer shall supply thermophysical properties determined by an approved test procedure(s) (see Section 5) and shall be listed in Appendix C.

4.1 Generic Thermophysical Properties

Those materials determined by NFRC to be generic in nature shall be identified and listed in Appendix A (Basic Set of Generic Materials), or Appendix B (Extended Set of Generic Materials). NFRC may add or remove materials as needed.

All simulators shall use Appendix A, unless the simulator's client requests the use of Appendix B or the material is not represented in Appendix A.

If the simulator's client requests the use of material properties from Appendix B, then the client shall provide the simulator with appropriate product drawings and/or material specifications verifying that the requested material properties are representative of the material(s) specified.

If such documentation is not provided to the simulator, then the simulator shall use the applicable material property value(s) from Appendix A.

If a component's cross-sectional material properties vary along the length of the component, and the client wishes to use material property values from Appendix B, then for purposes of simulation, the cross-section shall be assigned the highest conductivity of all the materials used in that component.

For example, consider a wood frame member composed of multiple individual pieces of wood finger-jointed together along the length of the frame member. Some of the wood pieces are Sugar Pine (k=0.099 W/m•K), some are Ponderosa Pine (k=0.122 W/m•K), and some are Radiata Pine (k=0.128 W/m•K). The cross-section for this frame member would be assigned a conductivity of 0.128 W/m•K. See Figure 1.

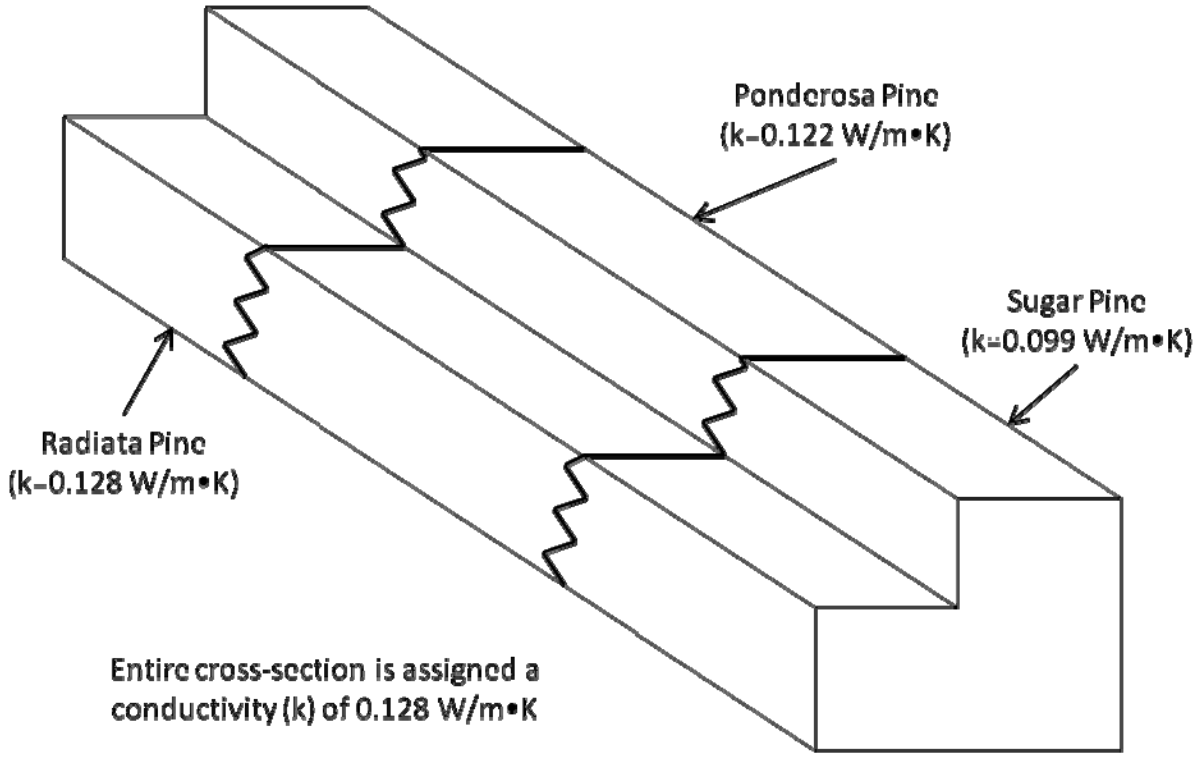


Figure 1

Note: If a product is simulated using material properties from Appendix B, then additional requirements will apply during annual inspections of Product Certification Program licensees. See NFRC 700 for details.

The NFRC Thermophysical Properties Subcommittee shall review the list of generic materials and update the thermophysical properties, as necessary. Each update shall be announced and promptly posted on the NFRC website for easy retrieval by NFRC-accredited simulation laboratories, NFRC-certified simulators, NFRC IAs, and other interested parties. The update shall have its version number clearly identified and NFRC shall post the date when this new material library becomes effective. Upon the effective date of the new material property file as posted by NFRC, old versions of the material library are deemed obsolete.

If the material data are not in the generic material library, and an interested party believes that the material in question is generic, the interested party may request in writing that NFRC include said material in Appendix A or Appendix B. Such requests shall be handled as outlined in NFRC 103 Sections 2.4 through 2.6. If the interested party disagrees with a published Generic Thermophysical Property, the interested party may request, in writing, testing of representative samples to determine a corrected thermophysical property. In such a case, a minimum of three different samples of the same generic material, preferably supplied by three different manufacturers, shall be tested. The verification of the tested data shall be done according to NFRC 103. If the difference between any individual sample value and the average value of all samples is more than 10% or 0.003 W/(m•K) (0.02 Btu•in./(hr•ft^2•°F)), whichever is greater, of the average value, the materials shall not be considered to be the same, and the reasons for outlier(s) shall be determined. The average of the measured thermophysical properties shall be compared to the currently used generic thermophysical property. If the difference is less than 10%, or 0.003 W/(m•K) (0.02 Btu•in./(hr•ft^2•°F)), whichever is greater, the current thermophysical property shall be considered valid. If the average of the three individual thermophysical property values is more than 10%, or 0.003 W/(m•K) (0.02 Btu•in./(hr•ft^2•°F)), whichever is greater, different from the current generic thermophysical property, this new thermophysical property shall be peer-reviewed, and upon acceptance, shall become the new thermophysical property of that generic material and be included in the updated material database.

4.2 Manufacturer Specific Thermophysical Properties

If the material is not considered generic and is not part of generic material library, its thermophysical properties shall be determined in accordance with Section 5. The manufacturer is responsible for providing typical samples for testing.

The Manufacturer may use its own equipment or hire a third party laboratory to determine thermophysical properties and submit test data to the NFRC Thermophysical Properties Subcommittee for verification. The testing shall be done according to the procedure(s) outlined in Section 5. In addition, the testing laboratory shall retain the three original test samples for the duration of the peer review challenge period and so that they may be sent to NFRC for verification according to NFRC 103.

Emissivity and solar absorptance of materials is not required to be determined if the manufacturer accepts default values of 0.9 for emissivity and NFRC default values for solar absorptance.

5. THERMOPHYSICAL PROPERTIES TEST METHODS

Thermophysical properties shall be determined according to appropriate ASTM standards, as indicated in Sections 5.1, 5.2, and 5.3. A minimum of three samples shall be measured and the mean value reported.

5.1 Thermal Conductivity

For the determination of thermal conductivity, the test shall be done according to ASTM C177, C518, C1114, E1225, E1530, E1461 or E1952, as applicable for the specific material. The test equipment shall be calibrated at least once each year as per the recommendations in the appropriate ASTM document(s).

Note: The specimen conductance should be less than 16 W/m^2•K (thermal resistance greater than 0.0625 m^2•K/W) if the test is done using C177. C518 may be used for a specimen with thermal conductance less than 10 W/m^2•K (thermal resistance greater than 0.10 m^2•K/W). For either of these tests, the temperature difference across the specimen shall not be less than 10 K. C1114 is applicable to a low conductance specimen only and the specimen shall be thermally homogeneous. Apparatus of the type covered by C1114 apply to the study of thermal properties of specimens containing moisture because of the use of small temperature differences and the low thermal capacity of the heat source. E1530 is similar in concept to C518 and is especially useful for materials in sheet and similar forms having a thermal resistance in the range from 20 x10-4 to 400x10-4 m^2•K/W over the approximate temperature range from 150 to 600 K. Reduced accuracy will be achieved for thicker specimens and for thermal conductivities up to 10 W/m•K. E1225 uses a steady state technique for the determination of thermal conductivity of homogeneous, opaque solids with effective conductivities in the approximate range of 0.2 to 200 W/m•K over the approximate temperature range between 90 and 1300 K. E1952 covers the determination of thermal conductivity of homogeneous, non-porous solid materials in the range of 0.10 to 1.0 W/m•K by modulated temperature differential scanning calorimeter. ASTM E1461 is a flash diffusivity method

used for thin gage highly conductive materials such as sheet metals. Use of ASTM E1461 for NFRC thermophysical properties requires following specific heat capacity measurement and thermal conductivity measurement per ASTM E1461's Appendix X2.

Test method information is summarized in Table 1.

Table 1. Summary of thermal conductivity standards and their applicability

ASTM Standard	Conductivity Range (W/m•K)	Conductance Range (W/m^2•K)	Min ΔT (K)	Remarks
C177		< 16	10	Thermally homogeneous
C518		< 10	10	Thermally homogeneous
C1114			None	Thermally homogeneous, for specimens with moisture
E1225	0.2-200		90-1300	Thermally homogeneous, Opaque
E1530		25-500	150-600	Thermally homogeneous
E1952	0.1-1.0		None	Thermally homogeneous
E1461	NA	NA	NA	Primarily homogeneous isotropic solid materials. Thermal diffusivity values ranging from 10^{-7} to 10^{-3} m^2/s ; temperature range: 75 to 2800 K (appendix X2 use mandatory)

5.1.1 Mean temperatures

The test shall be conducted at a mean temperature of 2±1ºC (35±2ºF) unless otherwise specified by the applicable ASTM test method. ASTM E1461 is conducted at 25±1°C (77±2°F).

5.1.2 Specimen thickness

The thickness of the specimen shall be chosen based on the standard procedure selected. With ASTM E1530, the thickness of specimen is required to be less than 12 mm. ASTM C177 and ASTM C1114 recommend that maximum specimen thickness depends on several parameters, including the size of the apparatus, thermal resistance of the specimen and the accuracy desired. ASTM E1461 specimen thickness ranges from 1.0 mm to 6 mm. For more specific quantitative information on thickness limitation see Refs (1), (2), (3) and (4).

5.1.3 Non-homogenous specimens

Non-homogeneities normal to the heat flux direction, such as layered structures, can be evaluated using ASTM C177. However, for testing specimens with non-homogeneities in the heat flux direction, such as an insulation system with thermal bridges, see test method ASTM C1363 for guidance. To use ASTM E1225 for composites or heterogeneous systems consisting of slabs of plates bonded together, the specimen shall be more than 20 units wide and 20 units thick, respectively, where a unit is the thickness of the thickest slab or plate.

5.2 Emissivity

For the determination of long wave surface emissivity, the test shall be done according to ASTM E1933 or ASTM C1371. ASTM E1933 requires the specimen to be at a temperature at least 10 K warmer or cooler than the ambient temperature while ASTM C1371 provides a comparative means of quantifying the emittance of opaque, highly thermally conductive materials near room temperature. The long wave range is considered from 2.5 μm to 40 μm.

Emissivity for non-metallic materials is defaulted to 0.90 without actual measurements.

5.2.1 Cleanness of the surface

ASTM C1371 recommends that the procedure used should ensure minimum alteration of the specimen surface. For example, if the emittance of a dust-covered specimen is desired, the dust shall not be removed. However, if the surface is intended to be clean and free of any residue, it shall be visually inspected for signs of contamination prior to the measurement and, if necessary, cleaned with the appropriate solution and dried.

5.2.2 Finishes

For painted or finished specimens, the paint or finish shall be fully cured and in good contact with the substrate (i.e., no bubbles, peeling, or scratches). For further instructions see ASTM D3359.

5.3 Solar Absorptivity

For the determination of surface solar absorptivity, the test shall be done according to ASTM E903 or ASTM C1549.

Solar absorptance of all frame materials is defaulted to 0.50 for commercial products and to 0.30 for residential products without actual measurements.

5.3.1 Finishes

The painted or finished surfaces shall be treated as in the case of emissivity measurement. See Section 5.2.2.

5.3.2 Specularity

This test method has been found practical for materials having both specular and diffuse optical properties.

5.3.3 Cleanness of the surface

Surfaces that are measured shall be clean and free of any residue.

4.1. Density

The density of the material shall be determined by dividing its weight by its volume. Table 2 describes allowable density measurement methods for various materials.

Table 2. Density Standards and their applicability

Material	Procedure
Polymer or plastic based materials	ASTM D792, ASTM D1505, ASTM D4883, ISO 1183-1, ISO 1183-2, or ISO 1183-3
Timber based	ASTM D2395
Fine aggregates	ASTM C128
Any other	Must report density measurement standard used

6. REFERENCES

6.1 Standards

NFRC PCP: Product Certification Program

NFRC 100-2004: Procedure for Determining Fenestration Product U-Factors.

NFRC 200-2004: Procedure for Determining Fenestration Product Solar Heat Gain Coefficient and Visible Transmittance at Normal Incidence.

NFRC 300-2004: Test Method for Determining the Solar Optical Properties of Glazing Materials and Systems.

NFRC 400-2004: Procedure for Determining Fenestration Product Air Leakage

NFRC 500-2004: Procedure for Determining Fenestration Product Condensation Resistance Values

ASTM C128 - 07a Standard Test Method for Density, Relative Density (Specific Gravity), and Absorption of Fine Aggregate

ASTM C177-04: Standard Test Method for Steady-State Heat Flux Measurements and Thermal Transmission Properties by Means of the Guarded-Hot-Plate Apparatus

ASTM C518-04: Standard Test Method for Steady-State Thermal Transmission Properties by Means of the Heat Flow Meter Apparatus

ASTM C1114-00: Standard Test Method for Steady-State Thermal Transmission Properties by Means of the Thin-Heater Apparatus

ASTM C1363-97: Standard Test Method for the Thermal Performance of Building Assemblies by Means of a Hot Box Apparatus

ASTM C1371-04a: Standard Test Method for Determination of Emittance of Materials near Room Temperature Using Portable Emissometers

ASTM C1549-04-Standard Test Method for Determination of Solar Reflectance near Ambient Temperature Using a Portable Solar Reflectometer

ASTM E1461-07: Standard Test Method for Thermal Diffusivity of Solids by the Flash Method.

ASTM D792-00 Standard Test Methods for Density and Specific Gravity (Relative Density) of Plastics by Displacement

ASTM D1505 - 03 Standard Test Method for Density of Plastics by the Density-Gradient Technique

ASTM D2395 - 07ae1 Standard Test Methods for Specific Gravity of Wood and Wood-Based Materials

ASTM D3359-02: Standard Test Methods for Measuring Adhesion by Tape Test

ASTM D4883-08 Standard Test Method for Density of Polyethylene by the Ultrasound Technique

ASTM E903-96: Standard Test Method for Solar Absorptance, Reflectance, and Transmittance of Materials Using Integrating Spheres

ASTM E1225-04: Standard Test Method for Thermal Conductivity of Solids by Means of the Guarded-Comparative-Longitudinal Heat Flow Technique

ASTM E1530-04: Standard Test Method for Evaluating the Resistance to Thermal Transmission of Materials by the Guarded Heat Flow Meter Technique

ASTM E1933-99a (2005) e1: Standard Test Methods for Measuring and Compensating for Emissivity Using Infrared Imaging Radiometers

ASTM E1952-01: Standard Test Method for Thermal Conductivity and Thermal Diffusivity by Modulated Temperature Differential Scanning Calorimetry

ISO 1183-1:2004 Plastics - Methods for determining the density of non-cellular plastics - Part 1: Immersion method, liquid pyknometer method and titration method

ISO 1183-2:2004 Plastics - Methods for determining the density of non-cellular plastics - Part 2: Density gradient column method

ISO 1183-3:1999 Plastics -- Methods for determining the density of non-cellular plastics -- Part 3: Gas pynometer method

IEEE / ASTM SI10-02: American National Standard for Use of the International System of Units (SI): The Modern Metric System

6.2 References for Table A.1 and Table B1.

1. prEn 12524: Building material and products-Hygrothermal properties-Tabulated design values , November 1999 (and B.R. Anderson, et al., Final Report of the Thermal Values Group, March 1999)
2. ASHRAE Fundamentals Handbook
3. Wright, J. L. and H. F. Sullivan (1989). “Thermal Resistance Measurement of Glazing System Edge-Seal and Seal Materials Using a Guarded Heater Plate Apparatus.” At. 95-2.
4. NRCC report, No. A3090.1, March 24, 1994
5. ASHRAE Fundamentals Handbook (SI), 2001

6. THERM program material library

7. D.F. Miner and J.B. Seastone, Handbook of Engineering Materials, 1955

8. F.P. Incropera and D.P. Dewitt, Fundamental of Heat and Mass Transfer(Third edition), 1990

9. Kuzman Raznjevic, Handbook of Thermodynamic Tables and Charts, McGraw-Hill Book Company

10. NIST Heat Transmission Properties of Insulation and Building Materials Database

11. FRAME program material library

12. M. Loffler, Glazing Edge-Seal Using Foamglass as Spacer and Frameless Window Design, Solar Energy, Oct., 1997, pp303-312

13. Azon. Thermal Break Material Test Report

14. Maier, C.; and Calafut, T. 1998. "Polypropylene: The Definitive User's Guide and Databook". Plastics Design Library, div. Of William Andrew. P. 124

15. Harper, C.A. Modern Plastics Handbook. McGraw-Hill. P. C51.

16. Bankvall, C.G., "Mechanisms of Heat Transfer in Permeable Insulation and Their Investigation in a Special Guarded Hot Plate", Heat Transmission Measurements in Thermal Insulations, ASTM STP 544, Edited by R.P. Tye, 1974, pp 34-48.

17. Frank M. White, Heat and Mass Transfer, Addison-Wesley, 1991

18. Solutia. 1989. Saflex Interlayer Physical Properties.

19. DuPont Glass Laminating Products

20. Ro, S.T.; and Kim, C.L. International Journal of Heat and Mass Transfer, Vol. 40, 1997. pp. 3899-3907.

21. Kim, H.S.; Kim, C.J.; and S.T. International Journal of Heat and Mass Transfer, Vol. 39, 1996. pp. 2267-2270.

22. IS. Emissivity Values for Common Materials. Infrared Services Co.; 2000.

23. Exergen. Tech Note 69. Exergen Co. 2002.

Table A.1: Thermophysical Properties of Solid Materials

Name	Density ρ	Conductivity *k*			Source	Emissivity
	kg/m^3	W/m•K	Btu/hr•ft•F	Btu•in/hr•ft^2•^{o}F	-	-
Rubbers						
Butadiene	980	0.250	0.144	1.733	1	0.9
Butyl rubber (isobutene, solid/hot melt)		0.240	0.139	1.664	1,6,11	0.9
Expanded rubber (rigid)	72	0.032	0.018	0.222	2	0.9
Ethylene propylene diene monomer (EPDM)	1150	0.250	0.144	1.733	1	0.9
Foam Rubber	60-80	0.060	0.035	0.416	1	0.9
Neoprene (polychloroprene)	1,240	0.230	0.133	1.595	1	0.9
Polyisobutylene (PIB)	930	0.200	0.116	1.387	1	0.9
Polysulphide	1,700	0.400	0.231	2.773	1	0.9
Polymers						
PVB		0.221	0.128	1.536	21	0.9
Polycarbonate	1,200	0.200	0.116	1.387	1	0.9
Polyethylene/polythene HD (high density)	980	0.500	0.289	3.467	1	0.9
Polyethylene/polythene LD (low density)	920	0.330	0.191	2.288	1,6	0.9
Polypropylene	910	0.22	0.127	1.525	1	0.9
Polystyrene	1,050	0.160	0.092	1.109	1	0.9
Polytetrafluoroethylene(PTFE)	2,200	0.250	0.144	1.733	1	0.9
Polyurethane	1,200	0.250	0.144	1.733	1	0.9
Polyurethane foam	70	0.050	0.029	0.347	1	0.9
Polyvinylchloride (PVC) flexible, with 40% softener	1,200	0.140	0.081	0.971	1	0.9
PVC/Vinyl (rigid)	1,390	0.170	0.098	1.179	6,11	0.9
Silicone		0.350	0.202	2.427	1	0.9
Silicone foam		0.170	0.098	1.179	6,11	0.9

Name	Density ρ	Conductivity *k*			Source	Emissivity
	kg/m^3	W/m•K	Btu/hr•ft•F	Btu•in/hr•ft^2•^{o}F	-	-
Polymers - Continued						
Silicone, filled		0.500	0.289	3.467	1	0.9
Urethane-thermal break		0.121	0.070	0.839	13	0.9
Urethane/polyurethane		0.210	0.121	1.456	1	0.9
Composites						
Fiberglass		0.300	0.173	2.080	6,11	0.9
Polyamide 6.6 with 25% glass fiber		0.300	0.173	2.080	1	0.9
Timbers						
Coniferous woods (Softwoods)		0.140	0.081	0.971	6,11	0.9
Deciduous woods (Hardwoods)		0.160	0.092	1.109	6,8,11	0.9
Wood based panels						
Hardboard (medium density)	800	0.110	0.064	0.763	11	0.9
Particleboard, Plywood (low density)	300	0.100	0.058	0.693	1	0.9
Particleboard, Plywood (medium density)	700	0.170	0.098	1.179	1	0.9
Particleboard, Plywood (high density)	1,000	0.240	0.139	1.664	1	0.9
Metals						
Aluminum (oxidized, mill finish)		237.000	136.936	1643.235	8	0.2
Aluminum alloys (oxidized, mill finish)	2,800	160.000	92.446	1109.357	1,6,11	0.2
Aluminum (anodized)		237.000	136.936	1643.235	8	0.8
Aluminum alloys (anodized)	2,800	160.000	92.446	1109.357	1,6,11	0.8
Steel (oxidized)	7,800	50.000	28.890	346.674	1	0.8
Steel (rolled, ground)	7,800	50.000	28.890	346.674	1	0.6
Steel Stainless (oxidized)	7,900	17.000	9.822	117.869	1	0.8
Steel Stainless (buffed)	7,900	17.000	9.822	117.869	1	0.2
Steel- galvanized sheet (0.14%C)		62.000	35.823	429.876	11	0.2

Name	Density ρ	Conductivity *k*			Source	Emissivity
	kg/m^3	W/m•K	Btu/hr•ft•F	Btu•in/hr•ft^2•^{o}F	-	-
Glazing Materials						
Glass (Plate or Float)		1.000	0.578	6.933	1,6,11	0.84
Glass mosaic	2,000	1.200	0.693	8.320	1	0.84
Glass-Flint (lead), Pyrex	4,280	1.400	0.809	9.707	5	0.84
Glass-Quartz		1.400	0.809	9.707	1	0.90
Plexiglass (PMMA) / Lucite		0.200	0.116	1.387	11	0.90
Insulating Materials						
Cellulosic fiber, Cotton fiber	56	0.042	0.023	0.277	11	0.9
Expanded perlite, organic bonded	16	0.052	0.030	0.361	2	0.9
Polystyrene-expanded	15	0.038	0.022	0.263	11,1	0.9
Extruded polystyrene (XPS) with CFC and HCFC	25-65	0.029	0.017	0.201	11, 1	0.9
Extruded polystyrene (XPS) with CO2	30-50	0.034	0.020	0.236	1	0.9
Felt	330	0.050	0.029	0.347	5	0.9
Glass fiber (semi-rigid) Sheathing		0.034	0.020	0.236	11	0.9
Glass fiber (spray applied)		0.039	0.023	0.270	11	0.9
Glass fiber (rigid) Roof insulation		0.047	0.027	0.326	11	0.9
Glass wool	52	0.038	0.022	0.263	5	0.9
Insulation Fiberboard (Ceiling Tile, Lay-in Panel)		0.061	0.035	0.423	11	0.9
Insulation Fiberboard (Roof Board)		0.055	0.032	0.381	11	0.9
Insulation Fiberboard		0.050	0.029	0.347	11	0.9
Mineral fiber-low density (rock, slag, glass)		0.042	0.024	0.291	11	0.9
Mineral fiber-loose fill (rock, slag, glass)		0.050	0.029	0.347	11	0.9
Perlite		0.053	0.031	0.367	11	0.9
Polyester fibre	15	0.040	0.023	0.279	1	0.9
Polyisocyanurate/polyurethane-Unfaced Board		0.020	0.012	0.139	11	0.9
Polyisocyanurate/Polyurethane-Faced Sheathing		0.024	0.014	0.166	11	0.9
Polyurethane Foam Insulation (Spray Applied)		0.024	0.014	0.166	11	0.9
Ureaformaldehyde foam	11--26	0.040	0.023	0.277	2	0.9
Vermiculite	179	0.077	0.044	0.534	10	0.9

Name	Density ρ	Conductivity *k*			Source	Emissivity
	kg/m^3	W/m•K	Btu/hr•ft•F	Btu•in/hr•ft^2•^{o}F	-	-
Miscellaneous						
Foam glass		0.040	0.023	0.277	1,12	0.9
Mohair		0.140	0.081	0.971	6,11	0.9
Desiccant-desiccated matrix	-	0.290	0.168	2.011	24	-
desiccant–loose fill	-	0.030	0.017	0.208	6,11,24	0.9
Silicone Foam		0.170	0.098	1.179	11	0.9
Miscellaneous - Continued						
Foam weather stripping		0.030	0.017	0.208	6,11	0.9
Paints		N/A	N/A	N/A	-	0.9

Table A.2: Thermophysical Properties of Gases

	Conductivity $k = a + bT+cT^2$ [W/m•K]			Dynamic Viscosity $\mu = a + bT+cT^2$ [kg/m•s]		
Gas	**Coefficient a** [W/m•K]	**Coefficient b** [W/m•K^2]	**Coefficient b** [W/m•K^3]	**Coefficient a** [kg/m•s]	**Coefficient b** [kg/m•s•K]	**Coefficient c** kg/m•s•K^2
Air*	$2.873x10^{-3}$	$7.760x10^{-5}$	0	$3.723x10^{-6}$	$4.94x10^{-8}$	0
Argon	$2.285x10^{-3}$	$5.149x10^{-5}$	0	$3.379x10^{-6}$	$6.451x10^{-8}$	0
Krypton	$9.443x10^{-4}$	$2.826x10^{-5}$	0	$2.213x10^{-6}$	$7.777x10^{-8}$	0
Xenon	$4.538x10^{-4}$	$1.723x10^{-5}$	0	$1.069x10^{-6}$	$7.414x10^{-8}$	0
CO_2	$-5.8181x10^{-3}$	$7.4714x10^{-5}$	0	$8.5571x10^{-7}$	$4.7143x10^{-8}$	0

*Note: Nitrogen shall be treated as air.

	Specific Heat $Cp = a + bT + cT^2$ [J/kg•K] -				**Molecular Masses**
Gas	**Coefficient a** [W/m•K]	**Coefficient b** [W/m•K^2]	**Coefficient c** [W/m•K^3]		Mass [kg/kmol]
Air*	1.00274×10^{3}	1.2324×10^{-2}	0		28.97
Argon	5.21929×10^{2}	0	0		39.948
Krypton	2.48091×10^{2}	0	0		83.80
Xenon	1.58340×10^{2}	0	0		131.30
CO_2	5.76903×10^{2}	9.18088×10^{-1}	0		44.01

*Note: Nitrogen shall be treated as air.

APPENDIX B EXTENDED SET OF GENERIC THERMOPHYSICAL PROPERTY VALUES OF MATERIALS

Table B.1: Thermophysical Properties of Solid Materials

Name	Density ρ	Conductivity *k*			Source	Emissivity
	kg/m^3	W/m•K	Btu/hr•ft•F	Btu•in/hr•ft^2•°F	-	-
Rubbers						
Neoprene(polychloroprene)	146	0.036	0.021	0.246	10	0.9
Neoprene(polychloroprene)	1290	0.237	0.137	1.643	10	0.9
Polymers						
Polyurethane foam	24-40	0.026	0.015	0.180		0.9
ABS	1,020-1,210	0.190			Web	0.9
Timbers						
Redwood (California)	392-448	0.118	0.068	0.818	2	0.9
Cedars (western, red)	247-502	0.130	0.075	0.901	2	0.9
Cypress (southern)	502-514	0.132	0.076	0.915	2	0.9
Elm (soft)	521	0.131	0.076	0.909	7	0.9
Fir (white)	430	0.120	0.069	0.832	5	0.9
Fir (Douglas)	529	0.111	0.064	0.769	7	0.9
Hemlock (eastern)	457	0.115	0.067	0.799	7	0.9
Larch (western)	625	0.143	0.082	0.988	7	0.9
Mahogany	550	0.130	0.075	0.901	5	0.9
Maple (sugar)	720	0.187	0.108	1.297	5	0.9
Oak (red)	721	0.173	0.1	1.198	7	0.9
Oak (white)	745-750	0.176	0.102	1.218	5,7	0.9
Pine (sugar)	409	0.099	0.057	0.689	7	0.9
Pine (white)	430	0.110	0.064	0.763	5	0.9
Pine (Norway)	441	0.120	0.069	0.829	7	0.9

Name	Density ρ	Conductivity *k*			Source	Emissivity
	kg/m^3	W/m•K	Btu/hr•ft•F	Btu•in/hr•ft^2•^{o}F	-	-
Timbers - Continued						
Pine (northern white)	481	0.121	0.070	0.839	7	0.9
Pine (ponderosa)	489	0.122	0.071	0.849	7	0.9
Pine (Radiata)	504	0.128	0.074	0.887	10	0.9
Pine (longleaf)	609	0.138	0.080	0.958	7	0.9
Pine (shortleaf)	545	0.141	0.082	0.978	7	0.9
Pine (southern, yellow)	659	0.161	0.093	1.116	2	0.9
Alder (Red)	440	0.114	0.066	0.791	10	0.9
Spruce (Sitka)	425	0.098	0.057	0.679	7	0.9
Wood based panels						
Particleboard, Plywood	500	0.130	0.075	0.901	1	0.9
Particleboard, Plywood	600	0.140	0.081	0.971	1	0.9
Insulating Materials						
Cellulose	48	0.039	0.023	0.273	10	0.9
Cellulose	54	0.057	0.033	0.395	5	0.9
Cellulosic fiber	96	0.049	0.028	0.340	1	0.9
Polystyrene expanded (EPS)	50-60	0.031	0.018	0.218	1	0.9
Polystyrene expanded (EPS)	35-45	0.032	0.019	0.223	1	0.9
Polystyrene expanded (EPS)	30	0.033	0.019	0.227	1	0.9
Polystyrene expanded (EPS)	25	0.034	0.020	0.236	1	0.9
Polystyrene expanded (EPS)	20	0.035	0.020	0.243	1	0.9
Polystyrene expanded (EPS)	10	0.043	0.025	0.300	1	0.9
Polystyrene expanded, molded beads	16	0.037	0.021	0.257	1	0.9
Polystyrene expanded, molded beads	24	0.035	0.020	0.243	1	0.9
Polystyrene expanded, molded beads	32	0.033	0.019	0.229	1	0.9
Extruded polystyrene(XPS) CO2	30-50	0.034	0.020	0.236	1	0.9
Mineral fiber with resin binder		0.042	0.024	0.291	2	0.9
Polyester fiber	25	0.035	0.020	0.243	1	0.9

Name	Density ρ	Conductivity *k*			Source	Emissivity
	kg/m^3	W/m•K	Btu/hr•ft•F	Btu•in/hr•ft^2•^{o}F	-	-
Insulating Materials-continued						
Polyester fiber	35	0.033	0.019	0.230	1	0.9
Polyester fiber	45	0.032	0.019	0.225	1	0.9
Silica Aerogel	73	0.024	0.014	0.166	10	0.9
Polyurethane foam, HCFC blown		0.021	0.012	0.146	11	0.9
Masonry Materials						
Concrete – medium density	1,800	1.15	0.66	7.97		0.90
Concrete – high density	2,400	2.00	1.16	13.87		0.90
Concrete – reinforced (2% steel)	2,400	2.50	1.44	17.33		0.90
Brick, Fired clay – high density	2,400	1.47	0.85	10.19		0.90
Brick, Fired clay – medium density	1,600	0.74	0.43	5.13		0.90
Brick, Fired clay – low density	1,120	0.45	0.26	3.12		0.90
Gypsum plasterboard	900	0.25	0.14	1.73		0.90
Metals						
Bronze	8,700	65	37.56	450	1,9	0.20
Brass	8,400	120	69.34	832	1,9	0.20
Copper	8,900	380	219.56	2634	1,9	0.80
Gold	19,290	310	179.12	2149	9	0.50
Iron, cast	7,500	50	28.89	346	1,9	0.80
Lead	11,300	35	20.22	242	1,9	0.30
Nickel	8,800	93	53.74	644	9	0.40

APPENDIX C MANUFACTURER SPECIFIC THERMOPHYSICAL PROPERTY VALUES OF MATERIALS

Table C.1: Thermophysical Properties of Solid Materials

Name	Density ρ	Conductivity *k*			Emissivity [1]
	kg/m^3	W/m•K	Btu/hr•ft•F	Btu•in/hr•ft^2•^{o}F	-
Aspen Aerogel-IM-Green-100F (4mm)	124.94	0.012	0.007	0.085	-
Aspen Aerogel-IM-Green-100P (3mm)	123.34	0.011	0.006	0.011	-
Aspen Aerogel-Spaceloft	137.1	0.015	0.009	0.103	-
ADCO PIB-8 HSNB Gray	1,060	0.155	0.089	1.073	-
ADCO Kömmerling - TPS Material	1,243	0.245	0.141	1.70	0.9
Advanced Environmental Recycling Technologies-Moisture Shield	1,000	0.198	0.114	1.373	0.9
Cabot Nanogel Translucent Aerogel	81.4	0.019	0.011	0.134	0.9
Cardinal Stainless Steel	7,808	14.187	8.197	98.37	-
Chelsea Building Products-composite PVC	1,698	0.292	0.169	2.023	-
Colonial Warmetal-SST	7,688	12.933	7.473	89.673	-
Colonial Metal-tin plated steel	7,660	50.2	29.05	348.6	-
CW Ohio-Wood Flour Polystyrene Material	587.9	0.077	0.044	0.533	0.9
Eagle Window and Doors-Eagle Composite	1,349	0.190	0.110	1.317	-
Edgetech- Silicone foam spacer, S1	968	0.159	0.092	1.104	-
Edgetech- Silicone foam spacer, S2	690	0.102	0.059	0.704	-
Edgetech- Super Spacer Material nXt	493	0.114	0.066	0.789	-
Edgetech-Super Spacer Standard (EPDM)	820	0.127	0.074	0.883	-
Edgetech-Triseal Premium/Slimline	702	0.108	0.063	0.752	-
Ensinger, Inc.- Insulbar Material	1,292	0.251	0.145	1.74	0.9
Fibrex EB-vinyl coated composite material	1,389	0.199	0.115	1.38	0.9
Futura Coatings-ITW Foamseal E-Z Fill Foam	51.9	0.03	0.018	0.211	-
GED-Intercept Ultra Stainless Steel	7,473	13.63	7.877	94.52	-

[1] Emissivity for non-metallic materials is defaulted to 0.90 without actual measurements

Name	Density ρ	Conductivity *k*			Emissivity [1]
	kg/m^3	W/m•K	Btu/hr•ft•F	Btu•in/hr•ft^2•ºF	-
Glasslam Air-Tight foam spacer	826	0.143	0.083	0.995	-
Gossen Cellular PVC	653	0.066	0.038	0.459	-
ICT, Inc. - Cellulosic Thermoplastic Composite	1,057	0.244	0.141	1.693	0.71
JeldWen-LFI Door Skin sample-30% CaCO3	1,353	0.134	0.077	0.929	-
Jeld-Wen-LFI Door Skin sample-no CaCO3	1464	0.170	0.098	1.18	-
Jeld-Wen EPS Door Core Material	18.58	0.033	0.019	0.229	-
Kalwall Insulation A	4.54	0.115	0.066	0.794	-
Kalwall Insulation B	4.06	0.093	0.054	0.648	-
Kalwall Insulation C	12.82	0.047	0.027	0.327	-
Kalwall Insulation D	38.98	0.032	0.019	0.222	-
Kalwall Insulation E	8.0	0.04	0.023	0.277	0.9
Lakeside Radiant SST	7,461	14.1	8.16	97.9	-
Leading Edge SST coil	7,576	14.33	8.262	99.149	-
Major Industries - Translucent Thermal Insulation 15	6.94	0.079	0.046	0.549	0.9
Major Industries - Translucent Thermal Insulation 24	4.31	0.098	0.057	0.680	0.9
Major Industries - Ultimate Series FRP	1,236	0.143	0.083	0.993	0.9
Major Industries- 10 Light Transmitting Insulation	9.58	0.07	0.041	0.487	-
Major Industries-IMG 125 Light Transmitting Insulation	6.92 (@ 1.25“)	0.037	0.021	0.258	-
Mikron-EnergyCore Fusion Insulated System	134	0.032	0.019	0.225	-
Mikron XTD composite (updated, 2009)	493	0.052	0.030	0.362	-
Milgard Polyethylene	38.9	0.053	0.031	0.366	-
Nan Ya Plastics-Neuma Door-foam PVC material	999	0.082	0.048	0.570	-
Plast Pro-cellular PVC framing material	999	0.096	0.055	0.665	-
Ply Gem Windows-Ply Gem G-Force	916	0.093	0.054	0.646	-
Royal Moldings- cellular PVC	635	0.066	0.038	0.456	-
Serious Materials-Ultem 2300	1,522	0.223	0.129	1.549	-
Trinity Glass International - Wood Flour Resin	45.80	0.081	0.047	0.559	0.9
TrueSeal Technologies - Butyl 761-71X		0.231	0.133	1.603	0.9

Project 3.1

Project Name: International Standard Organization

Date: March 2008

Purpose: Carli, an NFRC contractor, maintains an ISO relationship for the NFRC and monitors developments with the ISO18292 procedure to enable NFRC to consider similar process related to its comparable standard

Project Summary:

Carli, an NFRC contractor, attended two ISO TC163/SC2/WG11 meetings each year from 05 to 09 regarding ISO 18292- *Energy performance of fenestration systems - Calculation procedure*. This procedure calculates the energy consumption of a window based on how it is used in a typical home. Carli maintains an ISO relationship for the NFRC and monitors developments with the ISO18292 procedure to enable NFRC to consider similar process related to its comparable standard, NFRC 901-*Guidelines to Estimate the Effects of Fenestration on Heating and Cooling Energy Consumption in Single Family Residences*.

Click here for the latest draft of ISO 18292

DRAFT INTERNATIONAL STANDARD ISO/DIS 18292

ISO/TC **163**/SC **2** Secretariat: **SN**

Voting begins on: **2009-03-09** Voting terminates on: **2009-08-09**

INTERNATIONAL ORGANIZATION FOR STANDARDIZATION • МЕЖДУНАРОДНАЯ ОРГАНИЗАЦИЯ ПО СТАНДАРТИЗАЦИИ • ORGANISATION INTERNATIONALE DE NORMALISATION

Energy performance of fenestration systems — Calculation procedure

Performance énergétique des systèmes de fenêtrage — Mode opératoire de calcul

ICS 91.120.10

In accordance with the provisions of Council Resolution 15/1993 this document is circulated in the English language only.

Conformément aux dispositions de la Résolution du Conseil 15/1993, ce document est distribué en version anglaise seulement.

To expedite distribution, this document is circulated as received from the committee secretariat. ISO Central Secretariat work of editing and text composition will be undertaken at publication stage.

Pour accélérer la distribution, le présent document est distribué tel qu'il est parvenu du secrétariat du comité. Le travail de rédaction et de composition de texte sera effectué au Secrétariat central de l'ISO au stade de publication.

THIS DOCUMENT IS A DRAFT CIRCULATED FOR COMMENT AND APPROVAL. IT IS THEREFORE SUBJECT TO CHANGE AND MAY NOT BE REFERRED TO AS AN INTERNATIONAL STANDARD UNTIL PUBLISHED AS SUCH.

IN ADDITION TO THEIR EVALUATION AS BEING ACCEPTABLE FOR INDUSTRIAL, TECHNOLOGICAL, COMMERCIAL AND USER PURPOSES, DRAFT INTERNATIONAL STANDARDS MAY ON OCCASION HAVE TO BE CONSIDERED IN THE LIGHT OF THEIR POTENTIAL TO BECOME STANDARDS TO WHICH REFERENCE MAY BE MADE IN NATIONAL REGULATIONS.

RECIPIENTS OF THIS DRAFT ARE INVITED TO SUBMIT, WITH THEIR COMMENTS, NOTIFICATION OF ANY RELEVANT PATENT RIGHTS OF WHICH THEY ARE AWARE AND TO PROVIDE SUPPORTING DOCUMENTATION.

© International Organization for Standardization, 2009

PDF disclaimer

This PDF file may contain embedded typefaces. In accordance with Adobe's licensing policy, this file may be printed or viewed but shall not be edited unless the typefaces which are embedded are licensed to and installed on the computer performing the editing. In downloading this file, parties accept therein the responsibility of not infringing Adobe's licensing policy. The ISO Central Secretariat accepts no liability in this area.

Adobe is a trademark of Adobe Systems Incorporated.

Details of the software products used to create this PDF file can be found in the General Info relative to the file; the PDF-creation parameters were optimized for printing. Every care has been taken to ensure that the file is suitable for use by ISO member bodies. In the unlikely event that a problem relating to it is found, please inform the Central Secretariat at the address given below.

Copyright notice

This ISO document is a Draft International Standard and is copyright-protected by ISO. Except as permitted under the applicable laws of the user's country, neither this ISO draft nor any extract from it may be reproduced, stored in a retrieval system or transmitted in any form or by any means, electronic, photocopying, recording or otherwise, without prior written permission being secured.

Requests for permission to reproduce should be addressed to either ISO at the address below or ISO's member body in the country of the requester.

ISO copyright office
Case postale 56 • CH-1211 Geneva 20
Tel. + 41 22 749 01 11
Fax + 41 22 749 09 47
E-mail copyright@iso.org
Web www.iso.org

Reproduction may be subject to royalty payments or a licensing agreement.

Violators may be prosecuted.

© ISO 2009 – All rights reserved

Contents

Page

Foreword v

Introduction vi

1 Scope 1

2 Normative references 1

3 Terms and definitions 2

4 Symbols and units 2

5 Principle 5
5.1 Introduction 5
5.2 Heating energy performance 5
5.3 Cooling energy performance 6

6 Methodology and basic equations 7
6.1 General 7
6.2 The window energy performance for heating 10
6.3 The window energy performance for cooling 10
6.4 The heat balance elements 11
6.4.1 Heat transfer 11
6.4.2 Solar gain 12
6.5 Assessment of the solar control potential of the rated window 13
6.5.1 Principle 13
6.5.2 Procedure 13

7 Climate data 14
7.1 Introduction 14
7.2 External air temperature 14
7.3 Solar radiation 14
7.4 Wind speed 14

8 Basic thermal and solar-optical fenestration properties 14
8.1 Introduction 14
8.2 Thermal transmittance, U-value 15
8.3 Total solar energy transmittance or solar factor, g-value 15
8.4 Daylight potential 15
8.5 Air infiltration (air permeability) and ventilation 16
8.5.1 Air infiltration 16
8.5.2 Natural ventilation through deliberate opening of the window 17

9 Reference building 17
9.1 Introduction 17
9.2 Overview of data 17

10 Reporting 18

Annex A (informative) **Explanation of gain/loss utilization factor method used in ISO 13790 for the window energy balance equation** 19
A.1 Building energy balance 19
A.2 Accumulated temperature difference versus degree day method 21
A.3 Monthly method: correction factor for season length 23

Annex B (informative) **Assessment of the solar control potential of the rated window** 24
B.1 Introduction 24
B.1.1 Principle 24
B.1.2 Procedure 24

© ISO 2009 – All rights reserved

B.2 Reference solar control provision 25
B.3 Window properties with the fictitious reference solar control provision 25
B.4 Recommended approach 25
B.5 Examples of assessment of solar control potential 25

Annex C (informative) **Example of reference buildings 27**

Annex D (informative) **Example of the calculation of $EP_{C,w}$ and $EP_{H,w}$ - Using a detailed hourly method 31**

Annex E (informative) **Example of the calculation of $EP_{C,w}$ and $EP_{H,w}$ - Using a monthly method 36**

Bibliography 37

 © ISO 2009 – All rights reserved

Foreword

ISO (the International Organization for Standardization) is a worldwide federation of national standards bodies (ISO member bodies). The work of preparing International Standards is normally carried out through ISO technical committees. Each member body interested in a subject for which a technical committee has been established has the right to be represented on that committee. International organizations, governmental and non-governmental, in liaison with ISO, also take part in the work. ISO collaborates closely with the International Electrotechnical Commission (IEC) on all matters of electrotechnical standardization.

International Standards are drafted in accordance with the rules given in the ISO/IEC Directives, Part 2.

The main task of technical committees is to prepare International Standards. Draft International Standards adopted by the technical committees are circulated to the member bodies for voting. Publication as an International Standard requires approval by at least 75 % of the member bodies casting a vote.

ISO 18292 was prepared by Technical Committee ISO/TC 163, *Thermal performance and energy use in the built environment*, Subcommittee SC 2, *Calculation methods*.

© ISO 2009 – All rights reserved

Introduction

This International Standard describes a procedure for the determination of energy rating of window and door products and other products that are installed in building envelope openings, also known as fenestration products. As the fenestration industry and their clients move towards using energy performance instead of thermal transmittance to assess their products, the acceptance of this approach is being hampered by the wide variety of procedures being adopted. There is a need to produce a simple, clear, accurate and transparent procedure that enables the energy performance of these products to be assessed using National Climate data and Nationally selected reference buildings.

One of the most important aims of the world community is to reduce the consumption of energy with the associated reduction in CO_2 production; considered by many to be a vital perquisite of reducing the harmful effects of global warming. Ensuring that fenestration products are selected on the basis of optimizing their energy performance in their specific environment will have a significant impact on achieving that goal. The accumulated additional energy loss through poorly selected fenestration products, over their lifetime, is truly enormous, and any steps that can help reduce that loss must be taken as soon as possible.

The task of developing procedure for determining energy performance of fenestration products, in specific climatic environments, is very important. The drive to assess these products by considering the net energy flows through them is growing (e.g., the European Building Energy Performance Directive, North American efforts and others) and unless we can produce a reliable and acceptable standardized methodology, many countries will develop their own procedures that will constitute new free trade barriers.

This International Standard gives detailed procedures for calculating the energy performance of fenestration products. Converting that value into a Window Energy Rating is the responsibility of each country's appropriate national body. The details of that rating system should be published in a publicly available document. These procedures require the use of reference conditions, which may be different for different countries and may represent conditions different than actual conditions. The rationale for allowing different reference conditions is to allow the use of nationally specified reference conditions, which allows each country to determine their own reference conditions. As long as these conditions are publicly available and the calculation is based on standardized procedures, as specified in this standard, it will be possible to easily calculate energy performance of a specific product to the desired national reference conditions.

© ISO 2009 – All rights reserved

Energy performance of fenestration systems — Calculation procedure

1 Scope

This standard gives a procedure to calculate the energy performance of fenestration systems for rating of windows, doors and skylights, including the effects of frame, sash, glazing and shading components. The standard is to take into account the heating and cooling energy use in residential buildings, internal and external climatic conditions and relevant building characteristics.

2 Normative references

The following referenced documents are indispensable for the application of this document. For dated references, only the edition cited applies. For undated references, the latest edition of the referenced document (including any amendments) applies.

ISO 6613, *Windows and door height windows — Air permeability test*

ISO 7345, *Thermal insulation — Physical quantities and definitions*

ISO 9050, *Glass in building — Determination of light transmittance, solar direct transmittance, total solar energy transmittance, ultraviolet transmittance and related glazing factors*

ISO 9972, *Thermal performance of buildings — Determination of air permeability of buildings — Fan pressurization method*

ISO 9288, *Thermal insulation — Heat transfer by radiation — Physical quantities and definitions*

ISO 10077-1, *Thermal performance of windows, doors and shutters — Calculation of thermal transmittance — Part 1: General*

ISO 10077-2, *Thermal performance of windows, doors and shutters — Calculation of thermal transmittance — Part 2: Numerical method for frames*

ISO 12567-1, *Thermal performance of windows and doors — Determination of thermal transmittance by hot box method — Part 1: Complete windows and doors*

ISO 12567-2, *Thermal performance of windows and doors — Determination of thermal transmittance by hot box method — Part 2: Roof windows and other projecting windows*

ISO 13790:2008, *Energy performance of buildings — Calculation of energy use for space heating and cooling*

ISO 15099, *Thermal performance of windows, doors and shading devices — Detailed calculations*

ISO 15927-1, *Hygrothermal performance of buildings — Calculation and presentation of climatic data — Part 1: Monthly means of single meteorological elements*

ISO 15927-4, *Hygrothermal performance of buildings — Calculation and presentation of climatic data — Part 4: Hourly data for assessing the annual energy use for heating and cooling*

© ISO 2009 – All rights reserved

EN 410, *Glass in building — Determination of luminous and solar characteristics of glazing*

EN 1026, *Windows and doors — Air permeability — Test method*

EN 13363-1, *Solar protection devices combined with glazing — Calculation of solar and light transmittance — Part 1: Simplified method*

EN 13363-2, *Solar protection devices combined with glazing — Calculation of total solar energy transmittance and light transmittance — Part 2: Detailed calculation method*

3 Terms and definitions

For the purposes of this document, the terms and definitions in ISO 7345 and ISO 9288 and the following apply.

3.1
SHGC
an abbreviation for solar heat gain coefficient

NOTE SHGC is also denoted total solar energy transmittance, solar factor or g-value

3.2
visible transmittance
the glazing to window area ratio and on the view factor from the glazing to the sky

4 Symbols and units

Symbols and units used are in accordance with ISO 7345 and ISO 9288. The quantities, which are specific to this standard, are also defined in Table 1.

Table 1 — Symbols and units

Symbol	Quantity	Unit
A	area	m^2
a	numerical parameter in utilization factor	-
b	correction factor for an unconditioned adjacent space	-
C	effective heat capacity of a conditioned space	J/K
c	specific heat capacity	J/(kg·K)
d	layer thickness	m
E	energy	MJ
F	factor	-
g	total solar energy transmittance of a building element	-
H	heat transfer coefficient	W/K
h	surface coefficient of heat transfer	$W/(m^2 \cdot K)$
I_{sol}	solar irradiance	W/m^2
Q	quantity of heat	MJ/kWh
q	heat flow density	W/m^2
q_v	(volumetric) airflow rate	m^3/s

© ISO 2009 – All rights reserved

Symbol	Quantity	Unit
R	thermal resistance	$m^2 \cdot K/W$
T	thermodynamic temperature	K
t	time, period of time	Ms [a]
U	thermal transmittance	$W/(m^2 \cdot K)$
V	volume of air in a conditioned zone	m^3
α	absorption coefficient of a surface for solar radiation	-
γ	heat balance ratio	-
ε	emissivity of a surface for long-wave thermal radiation	-
η	efficiency, utilization factor	-
θ	Celsius temperature	°C
κ	heat capacity per area	$J/(m^2 \cdot K)$
ρ	density	kg/m^3
σ	Stefan-Boltzmann constant ($\sigma = 5{,}67 \times 10^{-8}$)	$W/(m^2 \cdot K^4)$
τ	time constant	h
Φ	heat flow rate, thermal power	W
χ	point thermal transmittance	W/K
Ψ	linear thermal transmittance	W/(m·K)

NOTE These symbols are in line with the symbols used in ISO 13790:2008.

[a] Hours can be used as the unit of time instead of seconds for all quantities involving time (i.e. for time steps or periods as well as for air change rates), in which case the unit of energy is watt-hours [Wh] instead of joules. In most equations, MJ are used instead of J for quantities of heat or energy and Ms instead of s for time.

The subscripts indicated in Table 2 are used.

© ISO 2009 – All rights reserved

Table 2 — Subscripts

a	air	ht	heat transfer	rvd	recovered
A	appliances	*i,j,k,m,n*	dummy integers	*s*	designated space
adj	adjusted	in	input		
an	annual	i	internal (temperature)	seas	seasonal
AO	accumulated overtemperature	int	Internal (heat)		
alt	altitude	interm	intermittent	se	surface external
at	coupling term	is	conductance term [a)]	sol	solar (heat gains)
aux	auxiliary	L	lighting (system)	set	setpoint
avg	time-average	lat	latent	sh	shading
bh	boost heating	ls	loss	shut	shutter
c	structure, construction element	m, *m*	monthly, designated month	si	surface internal
d	design; daily, direct	m	mass related conductance or capacitance	ss	surface-sky average
C	cooling, capacity	met	metabolic	sup	supply (of air)
C,nd	cooling need, or building need for cooling			sys	system
c	convective	mn	mean (time or space)		
calc	calculated	ms	conductance term [a)]	T	Thermal
corr	corrected	nd	need	tb	Thermal bridge
ctr	control	noc	unoccupied period	Tot	Total (system)
cont	continuous	nrbl	non-recoverable	tot	total
day	daily	nrvd	non-recovered	tr	transmission (heat transfer)
dif	diffuse	nren	non-renewable	u	unconditioned
dis	distribution	nut	non-utilized	ut	utilised
e	external, exterior, envelope	ob	obstacles	p	partition wall
el	electricity	Oc	occupants	pp	peak power
em	emission	occ	occupied period	ps	permanent shading
F	frame	off	off	V	ventilation (system)
f	floor	on	on	v	volume
		op	opaque	ve	ventilation (heat transfer)
gl	glazing, glazed element	o	overall	W	hot water (system or need)
gn	gains	P	related to power	w	window
g	ground	r	radiative	*y, z*	zone number
h	hourly	rvd	recovered		
hem	hemispherical	rbl	recoverable	⊥	perpendicular
H	Heating, or horizontal	red	reduced	0	base; reference
H,nd	heating need, or building need for heating	ren	renewable		
HC,nd	heating and/or cooling need; building need for heating and/or cooling				

NOTE 1 These subscripts are in line with the subscripts used in ISO 13790:2008.

NOTE 2 Variables are also defined when they appear for the first time.

© ISO 2009 – All rights reserved

5 Principle

5.1 Introduction

Energy performance of the fenestration products is expressed through energy performance indices, EP, one representative of the heating season and one representative of the cooling season:

The $EP_{H,w}$, and $EP_{C,w}$ values are the energy needs per unit area of the window per year that is the contribution of window to the energy need of the reference building for heating and cooling:

where

$EP_{H,w}$ is the fenestration heating energy performance index, expressed in kWh/m^2;

$EP_{C,w}$ is the fenestration cooling energy performance index, expressed in kWh/m^2.

Different calculation procedures are possible as given in ISO 13790:2008:

— monthly energy balance calculation method;

— seasonal energy balance calculation method;

— hourly energy balance calculation method.

The energy need of the window can be converted to energy use by considering the efficiency of the HVAC system.

5.2 Heating energy performance

Monthly method:

$$EP_{H,w,i} = \sum_{m=1}^{12} q_{H,nd,w,m,i} \quad (1)$$

Seasonal method:

$$EP_{H,w,i} = q_{H,nd,w,seas} \quad (2)$$

Hourly method:

$EP_{H,w,i}$ is the annual heating energy associated with the windows, expressed in kWh/m^2.

NOTE For the hourly method, separating cooling and heating components is a complex task which may involve multiple steps, see ISO 13790:2008 clause 15.3.1.2.

where

$EP_{H,w,i}$ is the energy performance value of the window facing i-orientation for the heating season, expressed in kWh/m^2;

i is the orientation of the window, expressed in degrees;

$q_{H,nd,w,m}$ is the net heat loss through the window, for the heating mode, per m^2 of (projected) window area A_w, per month, m, determined in accordance with clause 6.2, expressed in kWh/m^2;

© ISO 2009 – All rights reserved

$q_{H,nd,w,seas}$ is the net heat loss through the window, for the heating mode, per m^2 of (projected) window area A_w, per season, *seas*, determined in accordance with clause 6.2, expressed in kWh/m^2.

For situations where windows are placed in more than one position:

$$EP_{H,w} = \frac{\sum_i EP_{H,w,i}}{N_i} \quad (3)$$

where

N_i is the total number of orientations.

NOTE When calculating EP using detailed dynamic methods it is necessary to consider changes in U-values due to the exposure to actual environmental conditions and angle dependency of g-value (SHGC) and visible transmittance. It is unacceptable to use fixed values for U-value, g-value (SHGC) and visible transmittance as provided from performance rating where products are compared only. Same building assumptions and boundary conditions have to be used for both simplified and dynamic calculation methods to ensure compatibility.

5.3 Cooling energy performance

Monthly method:

$$EP_{C,w,i} = \sum_{m=1}^{12} q_{C,nd,w,m,i} \quad (4)$$

Seasonal method:

$$EP_{C,w,i} = q_{C,nd,w,seas} \quad (5)$$

Dynamic method:

$EP_{C,w,i}$ is the annual cooling energy associated with the windows, expressed in kWh/m^2.

NOTE For the dynamic method, separating cooling and heating components is a complex task which may involve multiple steps, see ISO 13790:2008 clause 15.3.1.2.

where

$EP_{C,w,i}$ is the energy performance value of the window facing i-orientation for the cooling season, expressed in kWh/m^2;

i is the orientation of the window, expressed in degrees;

$q_{C,nd,w,m}$ is the net heat loss through the window, for the cooling mode, per m^2 of (projected) window area A_w, per month, m, determined in accordance with clause 6.3, expressed in kWh/m^2;

$q_{C,nd,w,seas}$ is the net heat loss through the window, for the cooling mode, per m^2 of (projected) window area A_w, per season, *seas*, determined in accordance with clause 6.3, expressed in kWh/m^2.

For situations where windows are placed in more than one position:

© ISO 2009 – All rights reserved

$$EP_{C,w} = \frac{\sum_i EP_{C,w,i}}{N_i} \quad (6)$$

where

N_i is the total number of orientations.

NOTE Calculation of $EP_{H,w}$ and $EP_{C,w}$ can be accomplished using detailed dynamic energy simulation methods, as specified in Bibliography. When calculating EP using detailed dynamic methods it is necessary to consider changes in U-values due to the exposure to actual environmental conditions and angle dependency of g-value (SHGC) and visible transmittance. It is unacceptable to use fixed values for U-value, g-value (SHGC) and visible transmittance as provided from performance rating where products are compared only. Same building assumptions and boundary conditions have to be used for both simplified and dynamic calculation methods to ensure compatibility. Detailed dynamic calculation programs need to comply with validation and verification tests as specified in Bibliography.

6 Methodology and basic equations

6.1 General

For the evaluation of energy performance for windows, all data used should be for the same tilt angle either a typical situation for that window or the one given in national regulations.

The procedure presented in this standard includes two different parts that should be distinguished:

Part 1: Preparation of the national or regional window energy rating procedures

The following actions described in this standard have to be performed only once, by the responsible bodies, as part of the overall preparation of the national or regional window energy rating procedures:

— the calculation of the energy use of a reference building in order to obtain the building dependent parameters needed for the rating of the window;

— the choice of representative climate and other relevant data needed as parameters in the calculation of the energy performance of the window, including all conversions that are independent of the specifications of the window to be rated;

— establishing procedures and templates for the conversion from calculated energy performance for heating, and cooling into a classification (rating);

— establishing procedures and templates for the conversion from the day-lighting performance of the window (characterised by a daylight potential) into a classification (rating).

Part 2: Calculation of the energy performance of a specific window

The user applying this standard shall calculate the energy performance of a specific window according to steps outlined here. The energy rating can be carried out either in a specific orientation or as a weighted average of a number of orientations. The user will follow the successive steps 1, 2 and 3 detailed below.

The calculation procedure consists of three steps. Each step involves the gathering of a specific set of input data, followed by specific 'pre-processing' calculations.

Figure 1 gives a detailed schematic overview of the calculation steps and the data are needed as input. Also the main sources of the data are given. The detailed procedures are given in the clauses 6.2 to 6.5. This clause only provides the general principles.

© ISO 2009 – All rights reserved

Step 1: Climate
Input data: Select appropriate nationally or regionally representative climate data, such as external temperature and the intensity of solar radiation incident on the window with given orientation and tilt.

Step 2: Building
Input data: Select appropriate data on one (or a set of) nationally specified reference building(s) and reference occupancy, including reference services (heating, cooling and ventilation) and their control.

Step 3: Window
Input data: Obtain the window properties, thermal transmittance, solar and light transmittance and heat transfer due to air leakage.

Step 4: Calculation procedure: from the building related data (step 2), together with the window data (step 3) and the climate data (step 1) the gain and loss utilisation factors for heating and cooling respectively are calculated.

Finally, with all input data available and all 'pre-processing' calculations done, the energy performance of the window can be calculated, for the heating mode, $EP_{H,w}$, and for the cooling mode, $EP_{C,w}$, separately. This procedure is given in clause 5.

NOTE It may be decided at a national level to present one annual energy performance value, combining the value for heating with the value for cooling. The energy performance value may be used as a basis for classification, using a continuous or discrete scale and benchmarks, e.g. in a way similar to EN 15217 for the energy performance classification for buildings.

© ISO 2009 – All rights reserved

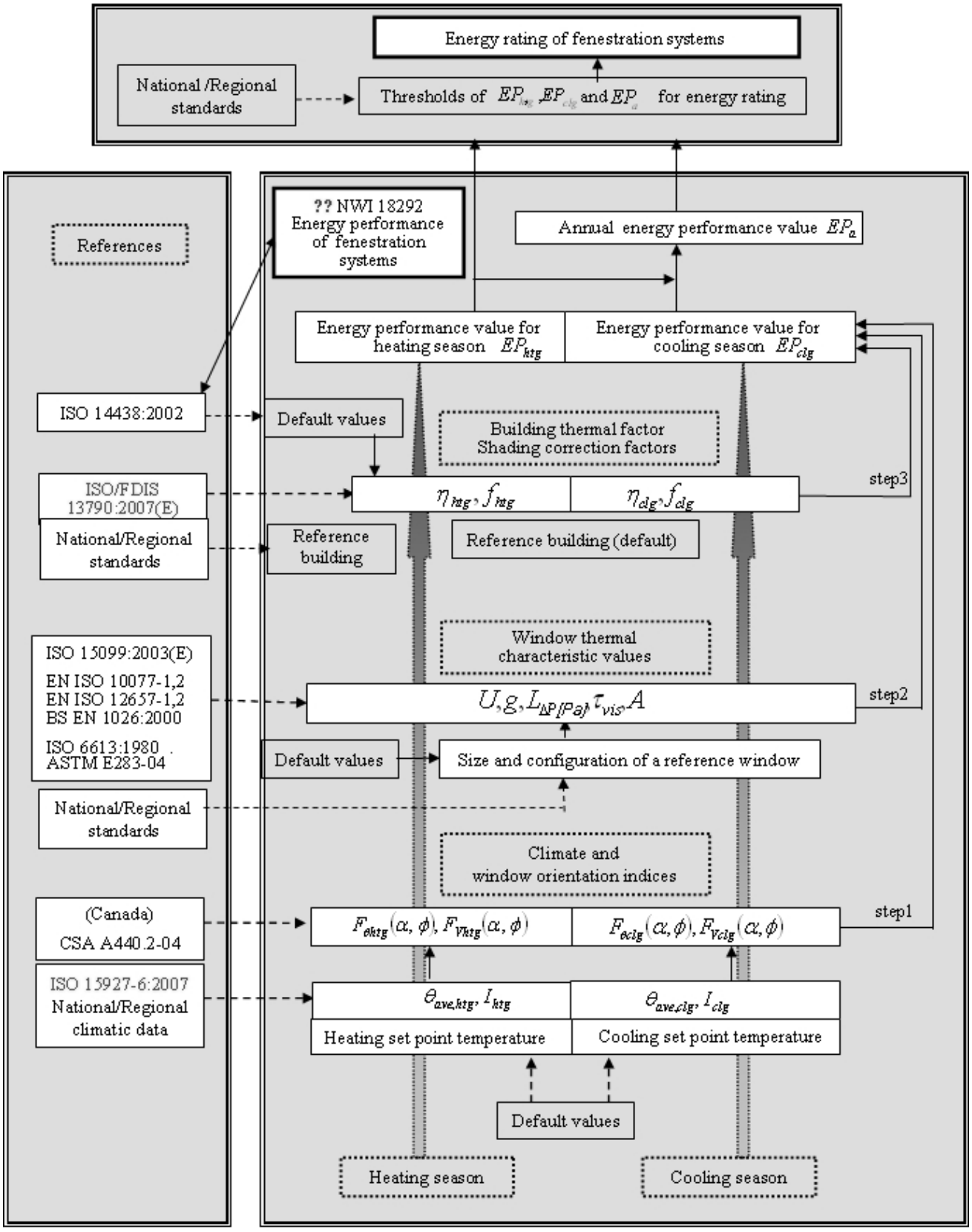


Figure 1 — Calculation procedure for energy performance values (simplified method using monthly climate indices and utilization factors)

© ISO 2009 – All rights reserved

6.2 The window energy performance for heating

The window energy performance for heating is the annual sum of the monthly contributions or the seasonal weighted average for the seasonal utilisation factor method, from the window to the energy need for space heating.

The monthly contributions from the window to the energy needs for space heating are calculated according to:

$$q_{\mathrm{H,nd,w}} = f_{\mathrm{H},m}\left(q_{\mathrm{H,ht,w}} - \eta_{\mathrm{H,gn}}\, q_{\mathrm{H,gn,w}}\right) \tag{7}$$

where

$q_{\mathrm{H,nd,w}}$ is the net heat loss through the window, for the heating mode, per m^2 of (projected) window area A_{w}, expressed in kWh/m^2;

$q_{\mathrm{H,ht,w}}$ is the overall heat transfer by transmission and infiltration through the window, for the heating mode, expressed in kWh/m^2, determined according to clause 6.4;

$q_{\mathrm{H,gn,w}}$ is the overall solar heat gain through the window, for the heating mode, expressed in kWh/m^2, determined according to clause 6.4;

$f_{\mathrm{H},m}$ is the fraction of the month that is part of the heating season;

$\eta_{\mathrm{H,gn}}$ dimensionless gain utilization factor for heating, determined according to the procedure outlined in Annex A.

The fraction of the month, that is part of the heating season, shall be calculated for each month m as:

$$f_{\mathrm{H},m} = \frac{Q_{\mathrm{H,nd},m}}{\left(Q_{\mathrm{H,nd},m} + Q_{\mathrm{C,nd},m}\right)} \tag{8}$$

NOTE 1 Since there are no internal heat gains coming in via the window, $q_{\mathrm{H,gn,w}}$ is equal to $q_{\mathrm{H,sol,w}}$.

NOTE 2 $f_{\mathrm{H},m}$ is already part of the calculation of the energy balance of the reference building according to ISO 13790:2008.

6.3 The window energy performance for cooling

The window energy performance for cooling equals the annual sum of the monthly contributions or the seasonal weighted average for the seasonal utilisation factor method, from the window to the energy need for space cooling.

The monthly contributions from the window to the energy need for space cooling shall be calculated according to:

$$q_{\mathrm{C,nd,w}} = \left(1 - f_{\mathrm{H},m}\right)\left(q_{\mathrm{C,gn,w}} - \eta_{\mathrm{C,ls}}\, q_{\mathrm{C,ht,w}}\right) \tag{9}$$

where

$q_{\mathrm{C,nd,w}}$ is the net heat gain through the window, for the cooling mode, per m^2 of (projected) window area A_{w}, expressed in kWh/m^2;

© ISO 2009 – All rights reserved

$q_{C,ht,w}$ is the overall heat transfer by transmission and infiltration through the window, for the cooling mode, expressed in kWh/m^2, determined according to clause 6.4;

$q_{C,gn,w}$ is the overall solar heat gain through the window, for the cooling mode, expressed in kWh/m^2, determined according to clause 6.4;

$\eta_{C,ls}$ dimensionless loss utilisation factor for cooling, determined according to the procedure outlined in Annex A;

$(1 - f_{H,m})$ is the fraction of the month that is part of the cooling season, $f_{H,m}$.is given by equation (8).

NOTE Since there are no internal heat gains coming in via the window, $q_{C,gn,w}$ is equal to $q_{C,sol,w}$.

6.4 The heat balance elements

6.4.1 Heat transfer

The overall heat transfer by transmission and air leakage shall be calculated as:

For the heating mode:

$$q_{H,ht,w} = \left(U_{H,w} + \frac{H_{H,ve,w}}{A_w} \right) \left(\theta_{int,set,H} - \theta_{e,avg} \right) \frac{t}{1\,000} \quad (10)$$

where

$U_{H,w}$ is the thermal transmittance (U-value) of the window for the heating mode, expressed in W/(m^2·K), determined according to clause 8.2;

NOTE There may be a difference in U-value between heating and cooling mode if the window is adaptive to the time period over which the calculation is made (e.g. season, day) and day and night (e.g. movable solar blind, curtains, seasonal add-ons).

$H_{H,ve,w}$ is the heat transfer coefficient due to air leakage of the window, expressed in W/K, determined according to clause 8.5;

NOTE Normally there will be no difference between heating and cooling mode with respect to the value of the heat transfer coefficient due to air leakage.

$\theta_{int,set,H}$ is equal to the set point temperature for heating, expressed in degrees Celsius, to be determined according to clause 9;

$\theta_{e,avg}$ is equal to the time-average external air temperature, expressed in degrees Celsius, to be determined according to clause 7;

t is the total length of the considered time period, expressed in hours.

NOTE 1 The divisor of 1 000 is to convert Wh to kWh.

NOTE 2 For more details of this approach see Annex A.

© ISO 2009 – All rights reserved

For the cooling mode:

$$q_{C,ht,w} = \left(U_{C,w} + \frac{H_{C,ve,w}}{A_w} \right) \left(\theta_{int,set,C} - \theta_{e,avg} \right) \frac{t}{1\,000} \quad (11)$$

where

$U_{C,w}$ is the thermal transmittance (U-value) of the window for the cooling mode, expressed in W/(m^2·K), determined according to clause 8.2;

NOTE There may be a difference in U-value between heating and cooling mode if the window is adaptive to the time period over which the calculation is made (e.g. season, day) and day and night (e.g. movable solar blind, curtains, seasonal add-ons).

$H_{C,ve,w}$ is the heat transfer coefficient due to air leakage of the window, expressed in W/K, determined according to clause 8.5;

NOTE Normally there will be no difference between heating and cooling mode with respect to the value of the heat transfer coefficient due to air leakage.

$\theta_{int,set,C}$ is equal to the set point temperature for cooling, expressed in degrees Celsius, to be determined according to clause 9;

$\theta_{e,avg}$ is equal to the time-average external air temperature, expressed in degrees Celsius, to be determined according to clause 7;

t is the total length of the considered time period, expressed in hours.

NOTE 1 The divisor of 1 000 is to convert Wh to kWh

NOTE 2 For more details of this approach see Annex A.

6.4.2 Solar gain

The overall solar heat gain through the window shall be calculated as:

For the heating mode:

$$q_{H,gn,w} = F_{sh,ob}\, g_{H,w}\, I_{sol} \frac{t}{1\,000} \quad (12)$$

where

$F_{sh,ob}$ is the factor due to glazing maintenance and shading effects during the heating season, determined according to clause 8.3;

$g_{H,w}$ is the dimensionless total solar energy transmittance of the window, for the heating mode, determined according to clause 8.3;

NOTE There may be a difference in g-value between heating and cooling mode if the window is adaptive to the season (e.g. movable solar blind, curtains, seasonal add-ons).

t is the total length of the considered time period, expressed in hours;

© ISO 2009 – All rights reserved

I_{sol} the average solar irradiance for the considered time period on the window plane, expressed in W/m^2, determined according to clause 7.3.

For the cooling mode:

$$q_{C,gn,w} = g_{C,w}\, I_{sol}\, \frac{t}{1\,000} \tag{13}$$

where

$g_{C,w}$ is the dimensionless total solar energy transmittance of the window, for the cooling mode, determined according to clause 8.4.

NOTE There may be a difference in g-value between heating and cooling mode if the window is adaptive to the season (e.g. movable solar blind, seasonal add-ons etc).

6.5 Assessment of the solar control potential of the rated window

6.5.1 Principle

The rated window may have proper solar control provisions incorporated (e.g. solar control glazing, incorporated blinds, *etc.*); or the rated window is an assembly of glazing, frame and e.g. an add-on solar control provision (film, blind, etc.); or the rated window has no solar control provision.

The energy performance for cooling, $EP_{C,w}$, will reflect the differences. But the differences will not appear unless a series of different windows, with different solar control quality are compared.

This clause provides a procedure to assess the solar control potential of a rated window, without the need to compare serried of different windows.

This is done by comparing the rating of the window against the rating of the same window provided with a fictitious reference high performance solar control provision.

NOTE As a black box the rated window has already proper solar control provisions incorporated (e.g. solar control glazing, incorporated blinds, etc); or the rated window is an assembly of glazing, frame and e.g. an add-on solar control provision (film, blind, etc.); or the rated window has no solar control provision, etc.

If the difference in rating is small, the energy performance of the window for cooling is apparently efficient, for the given conditions: adding a high performing solar control provision will not lead to significant improvement of the energy performance of the window for cooling.

If the difference in rating is large, the energy performance of the window for cooling is apparently inefficient for the given conditions and hence subject to significant improvement by adding a solar control provision.

6.5.2 Procedure

The following procedure can be used to assess the solar control potential of the rated window as described in more detail in Annex B.

— a fictitious reference high performance solar control provision is defined;

— a formula is given to calculate the new properties of the window with this added fictitious reference solar control provision;

— the energy performance is calculated for the window without and with this added fictitious reference solar control provision;

© ISO 2009 – All rights reserved

— a recommendation is given to national or regional window energy rating schemes to rate the "solar control potential" of the window in the given conditions on the basis of the difference between the energy performance as calculated for the window without and with this added fictitious reference solar control provision.

The g-value for the combination of a window with additional external solar shading device is derived using the simplified method given in EN 13363-1, EN 13363-2 and ISO 15099. This standard gives conservative values for the summer situation (assuming no ventilation between shading and window).

NOTE See Annex B for background information and example.

7 Climate data

7.1 Introduction

This clause specifies the procedure shown as step 1 in the block diagram described in clause 6.

The procedures in ISO 13790:2008 Annex F should be used. Definitions and procedures to develop these data are specified in ISO 15927-1 and ISO 15927-4.

Typical data should be defined on a regional or national basis.

7.2 External air temperature

The value for the external air temperature, θ_e, shall be the appropriate time period mean external air temperature, expressed in degrees Celsius.

NOTE Averaged over the appropriate time period, see Annex B for the difference with the degree day method.

7.3 Solar radiation

Follow procedures in ISO 13790:2008 Annex F.

Validated theoretical models of solar radiation on vertical and tilted surfaces, at different orientations and geographic places and times can also be used.

7.4 Wind speed

Wind speed (air velocity) is only needed when dynamic calculation methods are used. It is a parameter to calculate the external surface heat transfer coefficient as specified in ISO 15099. Standard national values can also be used.

NOTE ISO 6946:2007 contains standard values for the surface resistances.

8 Basic thermal and solar-optical fenestration properties

8.1 Introduction

Fundamental thermal and solar-optical fenestration properties are thermal transmittance, U, total solar energy transmittance or solar factor, g, light transmittance, τ_v, and air leakage, L_x, where x is the pressure difference in expressed in pascals.

© ISO 2009 – All rights reserved

8.2 Thermal transmittance, *U*-value

The thermal transmittance, U-value, is determined for the whole fenestration product. The procedure to calculate the U-value is specified in ISO 15099, and in ISO 10077-1 and ISO 10077-2. The U-value can also be determined by laboratory measurement according to the procedures specified in ISO 12567-1 and ISO 12567-2.

8.3 Total solar energy transmittance or solar factor, *g*-value

Total solar energy transmittance or solar factor, g, (also called solar heat gain coefficient (SHGC)), shall be calculated as follows:

— whole window (frame + glazing) with or without shading devices: ISO 15099 or ISO 13790:2008;

— glazing: ISO 9050 and EN 410;

— glazing with shading devices: EN 13363-1 and EN 13363-2.

The effect of the following can be defined at a national level:

— influence of incident angle of solar radiation;

— influence of the frame component.

In the case where no agreed national guidance for the two effects above is available, use the values defined in ISO 13790:2008.

For sloped windows it is allowed to use the g-values obtained in the vertical position.

8.4 Daylight potential

The daylight potential of a window indicates its potential to supply a building with daylight and depends on the visible transmittance, the glazing to window area ratio and on the view factor from the glazing to the sky. The latter parameter is used to determine the effect of different window slope angle.

The visible transmittance, τ_{vis}, shall be calculated for the glazing as specified in ISO 15099, ISO 9050 and EN 410. For shading devices it can also be calculated using the procedures in EN 13363-1 and EN 13363-2.

Quantify daylight potential of the window and quote this figure with the energy rating. Daylight potential is an important parameter for window selection but is not used in the energy rating procedure.

In this standard, the daylight potential of the window as a building component is treated as independent of parameters such as the window height over floor, building overhangs and of the interior of the building. These will all affect the daylight performance in practical situations.

The daylight potential, DP, is expressed as:

$$DP = \tau_{vis}\left(F_{g-s} + 0{,}2 \times F_{g-g}\right)\frac{A_{gl}}{A_w} \tag{14}$$

where

τ_{vis} is the visible transmittance of the glazing;

$F_{g\text{-}s}$ is the view factor from the glazing to the sky;

$F_{g\text{-}g}$ is the view factor from the glazing to the ground;

© ISO 2009 – All rights reserved

0,2 is the albedo of the ground;

A_{gl} is the visible glazing area of the window, expressed in m^2;

A_w is the area of the window, expressed in m^2.

The view factor from the glazing to the sky depends on the type of the rated window: façade window (vertical), roof window and skylight (sloped) or roof light (horizontal). Self-shading effects from frame and sash may be neglected if frame and sash rebate is small compared to the dimensions of the window (< 1/20).

View factor depending on installation angle can be determined from:

$$F_{g-s} = \frac{(1+\cos\alpha)}{2} \tag{15}$$

$$F_{g-g} = \frac{(1-\cos\alpha)}{2} \tag{16}$$

where

α is the angle between the glazing plane and horizontal, where a horizontal plane is $\alpha = 0$ degrees.

If the given window comprises a movable shading device that blocks direct solar radiation (e.g. venetian blind), give values for the complete dynamic range (fully open and fully closed)

8.5 Air infiltration (air permeability) and ventilation

8.5.1 Air infiltration

Overall air infiltration (air permeability) rate L is measured for the whole fenestration product at the reference pressure difference and is denoted $L_{p,ref}$. The procedure to measure $L_{p,ref}$ is specified in EN 1026 or ISO 6613.

NOTE The procedure to recalculate L to an other pressure difference, L_p is specified in EN 12207, and is incorporated into equation below.

The heat transfer coefficient due to air infiltration of the window is given by:

$$H_{ve,w} = \left(\frac{\Delta p}{\Delta p_{ref}}\right)^{\frac{2}{3}} \left(\frac{\rho C_p}{3{,}6}\right) L_{p,ref} \tag{17}$$

where

$H_{ve,w}$ is the heat transfer coefficient due to air infiltration of the window, expressed in W/K;

Δp is the average pressure difference in the building, expressed in pascal. (If no national value is defined, use Δp = 6 Pa);

Δp_{ref} is the reference pressure difference that was used for the measurement of the air leakage rate of the window, expressed in pascal;

ρC_p is the thermal capacitance of air (ρC_p= 1,24), expressed in kJ/(m^3·K);

© ISO 2009 – All rights reserved

$L_{p,\text{ref}}$ is the air leakage rate of the window at a pressure difference Δp_{ref}, expressed in m^3/h.

8.5.2 Natural ventilation through deliberate opening of the window

Use the procedures given in ISO 13790:2008 for calculating free cooling and night time ventilation during cooling mode.

9 Reference building

9.1 Introduction

This clause describes step 2 of the block diagram presented in clause 6.

It describes the set of data needed on one (or a set of) nationally specified reference building(s) and reference occupancy, including reference services (heating, cooling and ventilation) and their control.

ISO 13790:2008 shall be used as the basis for specifying the reference building.

The energy performance of the window shall be determined using one of the following options of mounting the window being evaluated into the reference building:

a) one window type in one specific orientation;

b) area weighted average results from one window type placed in each of the four cardinal orientations;

c) defined by national regulations.

NOTE Ensure ratio of window area to reference building floor area is as specified by national regulations or use a "typical" ratio.

9.2 Overview of data

A reference building must be specified. This could be on a national or regional level and should represent a building typical for the region relevant for the rating – an example is given in informative Annex D. Parameters for calculating the energy performance of windows are specified in ISO 13790:2008. The reference building must define:

— the geometry of the building including the distribution of windows in different orientations and slopes and effects of shading and surroundings;

  — the same reference building that is used to evaluate vertical windows can be used to evaluate sloped windows installed in their correct orientation;

— the thermal properties of the building envelope (U-value, thermal conductivity, specific heat, mass);

— internal gains (e.g. define the standard number of people, usage etc or use data given in National regulations);

— to calculate the utilization factors the reference building will have to have a reference window;

— building operating parameters such as set point temperature and operating schedule;

— all other input data required for the seasonal, monthly, or hourly method.

© ISO 2009 – All rights reserved

10 Reporting

The report giving an assessment of the energy performance of the fenestration product in accordance with this standard shall include at least the following information.

- a technical description of the product;
- name of person responsible for calculation;
- all input data, especially that associated with the reference building shall be listed and justified, e.g. by reference to international or national standards, or by reference to the appropriate annexes to this standard or to other documents. Specifically the data reported should be sufficient to enable the calculation to be replicated;
- a note indicating which method (detailed simulation, simple hourly, monthly or seasonal) was used and, if seasonal, the assumed fixed length of the heating and cooling season;
- a reference to this standard;
- energy performance values for the heating and cooling season;
- day-lighting potential.

© ISO 2009 – All rights reserved

Annex A
(informative)

Explanation of gain/loss utilization factor method used in ISO 13790 for the window energy balance equation

A.1 Building energy balance

Main equations from ISO 13790:2008 (summarized, monthly method) or seasonal weighted average for the seasonal utilisation factor method:

The monthly energy need for space heating is calculated according to:

$$Q_{H,nd} = Q_{H,ht} - \eta_{H,gn}\, Q_{H,gn} \quad \text{(A.1)}$$

The monthly energy need for space cooling is calculated according to:

$$Q_{C,nd} = Q_{C,gn} - \eta_{C,ls}\, Q_{C,ht} \quad \text{(A.2)}$$

where

$Q_{H,ht}$ is the total heat transfer by transmission and ventilation of the building for the heating mode, expressed in MJ;

$Q_{C,ht}$ is the total heat transfer by transmission and ventilation of the building for the cooling mode, expressed in MJ;

$Q_{H,gn}$ is the total solar and internal heat gains of the building for the heating mode, expressed in MJ;

$Q_{C,gn}$ are the total solar and internal heat gains of the building for the cooling mode, expressed in MJ;

$\eta_{H,gn}$ is the dimensionless gain utilisation factor for heating;

$\eta_{C,ls}$ is the dimensionless loss utilisation factor for cooling.

NOTE kWh may be used as alternative unit instead of MJ.

Leaving out the index H for heating and C for cooling:

The total monthly heat transfer of the building by transmission and ventilation, Q_{ht}, is given by:

$$Q_{ht} = Q_{tr} + Q_{ve} \quad \text{(A.3)}$$

where

Q_{tr} is the total heat transfer of the building by transmission, expressed in MJ;

Q_{ve} is the total heat transfer of the building by ventilation, expressed in MJ.

The total monthly heat gains, Q_{gn}, of the building by internal and solar gains are:

© ISO 2009 – All rights reserved

$$Q_{gn} = Q_{int} + Q_{sol} \quad \text{(A.4)}$$

where

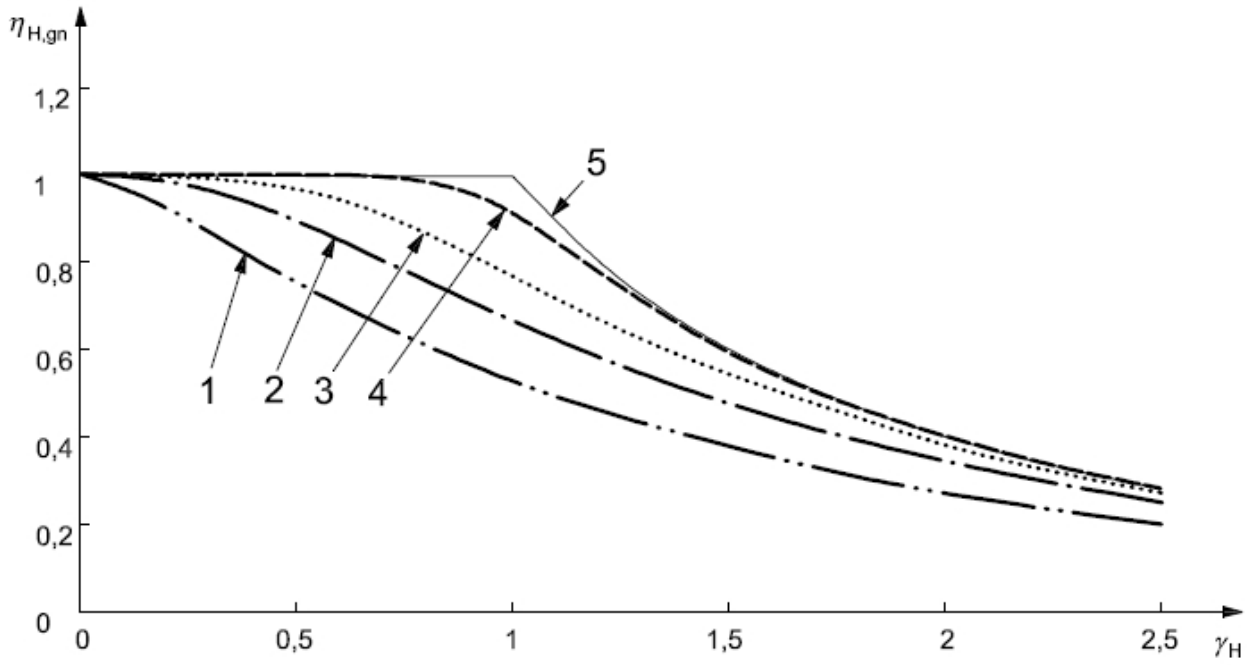
Q_{int} is the sum of internal heat gains of the building, expressed in MJ;

Q_{sol} is the sum of solar heat gains of the building, expressed in MJ.

Values for the gain utilization factor for heating, $\eta_{H,gn}$, are obtained by curves depending on the heat balance ratio for heating, γ_H,and the time constant of the building, as shown in the following illustration.

The heat balance ratio for the heating mode, γ_H, is given by:

$$\gamma_H = \frac{Q_{H,gn}}{Q_{H,ht}} \quad \text{(A.5)}$$



Key

1 time constant of 8 h (low inertia)
2 time constant of 1 d
3 time constant of 2 d
4 time constant of 7 d
5 time constant infinite (high inertia)

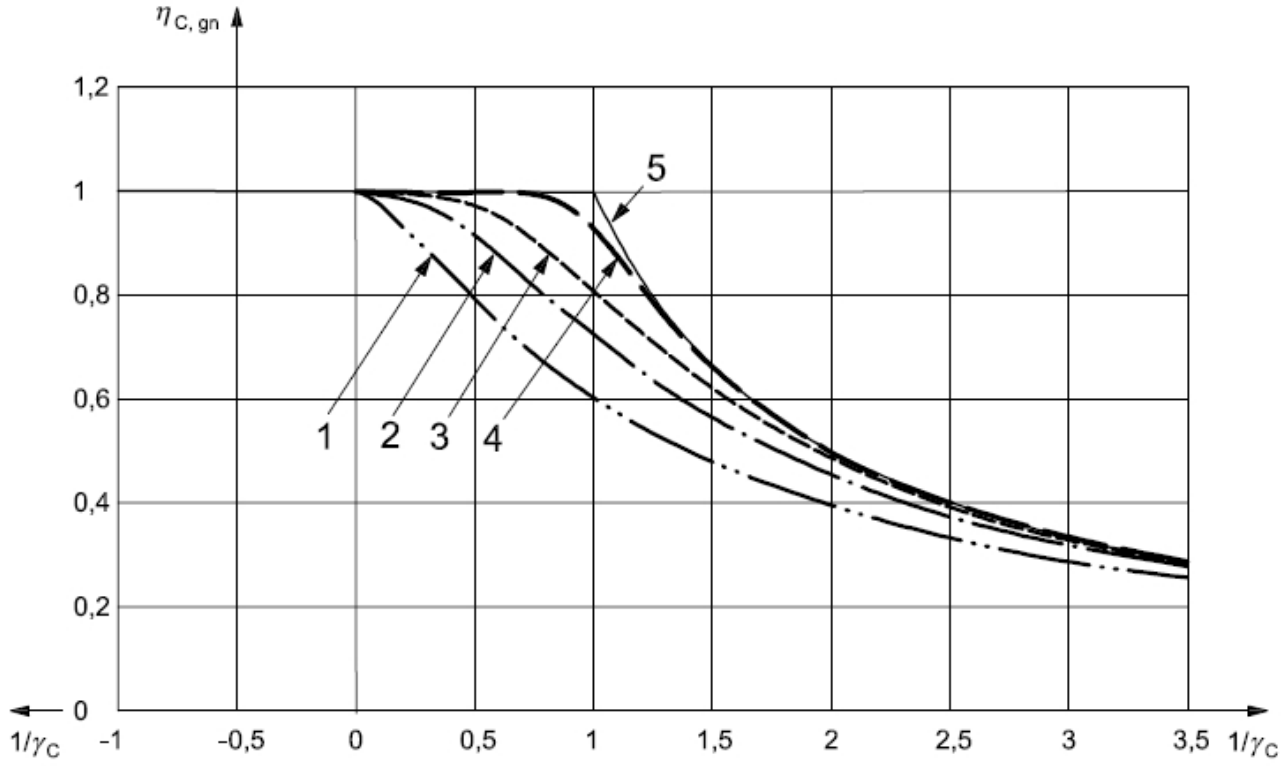
Figure A.1 — Illustration of gain utilization factor for heating mode, for 8 hours, 1 day, 2 days, 1 week and infinite time constants, valid for monthly calculation method

Values for the loss utilization factor for cooling, $\eta_{C,ls}$, are obtained by curves depending on the heat balance ratio for cooling, γ_C and the time constant of the building, as shown in the following illustration.

© ISO 2009 – All rights reserved

The heat balance ratio for the cooling mode, γ_C, is given by:

$$\gamma_C = \frac{Q_{C,gn}}{Q_{C,ht}} \quad \text{(A.6)}$$



Key

1 time constant of 8 h (low inertia)
2 time constant of 1 d
3 time constant of 2 d
4 time constant of 7 d
5 time constant infinite (high inertia)

Figure A.2 — Illustration of loss utilization factor for cooling mode, for 8 hours, 1 day, 2 days, 1 week and infinite time constants, valid for monthly calculation method

A.2 Accumulated temperature difference versus degree day method

The monthly or seasonal weighted average for the seasonal utilisation factor method, in ISO 13790:2008 is a so called utilization factor approach. In the utilization factor approach, the energy needs for heating are calculated as the difference between the heat transfer by transmission and ventilation and the sum of gains from internal and solar sources, multiplied by a gain utilization factor, monthly or seasonal weighted average for the seasonal utilisation factor method.

In equation:

© ISO 2009 – All rights reserved

$$Q_{H,nd} = (H_{tr} + H_{ve}) \sum (\theta_{int,set,H} - \theta_e) - \eta_{H,gn} Q_{H,gn} \quad (A.7)$$

subject to $Q_{H,nd} \geq 0$

where

$\theta_{int,set,H}$ is the set point temperature for heating, expressed in degrees Celsius;

θ_e is the external air temperature, degrees Celsius.

$\sum (\theta_{int} - \theta_e)$ is equal to $(\theta_{int,set,H} - \theta_e) t$. The difference between the set point and monthly or seasonal weighted average for the seasonal utilisation factor method, average external air temperatures, multiplied by the (total) period length.

If, during the given month or seasonal weighted average for the seasonal utilisation factor method, there are intervals with zero energy needs for heating, these are implicitly taken into account by (a lower value of) the utilization factor, as explained in more detail in ISO 13790:2008, Annex I.

NOTE This approach shall not be confused with the degree day method, such as described in ISO 15927-6, which also uses an accumulated temperature difference.

In the degree day method, the energy needs for heating are calculated without explicitly taking into account the effect of internal and solar gains. This defect is compensated by taking only a subset of the number of days (degree days method) or hours (degree hour method) when calculating the heat transfer by transmission and ventilation.

In equation, for the degree day method:

$$Q_{H,nd} = (H_{tr} + H_{ve}) \sum_{pos} (\theta_{int,base} - \theta_e) \quad (A.8)$$

where

$\sum_{pos}$ is the sum over only the days when $\theta_e < \theta_{int,base}$;

$\theta_{int,base}$ is a pre-defined temperature, lower than the indoor set point temperature, expressed in degrees Celsius.

This reduction in temperature difference and the reduction in the number of days is needed because the (utilized) internal and solar gains are disregarded in the equations.

NOTE The reduction is a reduction without knowledge of the specific heat balance ratio (ratio between gains and heat transfer). This shows that the degree day method is a more rough and simple method compared to the utilization factor method.

Concluding:

— in the utilization factor method all hours of the considered month, or seasonal weighted average for the seasonal utilisation factor method, shall be included in the calculation of the accumulated temperature difference;

— no distinction shall be made between days or hours with external temperature higher or lower than a certain base temperature as in a degree day method;

— the indoor temperature shall be defined by the set point temperature and not by a base temperature as known for a degree day method.

© ISO 2009 – All rights reserved

For the cooling mode, a similar reasoning applies.

A.3 Monthly method: correction factor for season length

If we extract the window energy balance from the overall energy balance of the building or building zone, the utilization factor will not be enough to distinct the months which are part of the heating season (resp. cooling season) from the months that are outside the heating season (resp. cooling season).

The solution for this is to use the parameter given in 7.4.1 of ISO 13790:2008:

where

$f_{H,m}$ is the fraction of the month that is part of the heating season;

(1 - $f_{H,m}$) is the fraction of the month that is part of the cooling season.

Where the fraction of the month that is part of the heating season, is calculated for each month m as:

$$f_{H,m} = \frac{Q_{H,nd,m}}{\left(Q_{H,nd,m} + Q_{C,nd,m}\right)} \quad \text{(A.9)}$$

Following the monthly calculation method according to ISO 13790:2008, $f_{H,m}$ will be automatically calculated.

NOTE Normally, $f_{H,m}$ is used to determine the number of hours of operation of certain season-length dependent provisions (e.g. pumps, fans, central pre-heating). For the window energy performance calculation this factor is appropriate to weight whether a month is fully, partly or zero part of the heating season (resp. cooling season).

In case of central pre-heating and/or pre-cooling in the reference building the full equation reads:

$$f_{H,m} = \frac{Q_{H,nd,m,d}}{\left(Q_{H,nd,m} + Q_{C,nd,m} + Q_{V,pre\text{-}heat,m} + Q_{V,pre\text{-}cool,m}\right)} \quad \text{(A.10)}$$

NOTE Equation (11) in ISO 13790:2008 which, if applicable, is not an additional complication, because it is an intrinsic part of the calculation of the reference building according to ISO 13790:2008.

© ISO 2009 – All rights reserved

Annex B
(informative)

Assessment of the solar control potential of the rated window

B.1 Introduction

B.1.1 Principle

As stated in clause 6.5, the rated window may have proper solar control provisions incorporated (e.g. solar control glazing, incorporated blinds etc.) or the rated window is an assembly of glazing, frame and e.g. an add-on solar control provision (film, blind, etc.); or the rated window has no solar control provision.

The energy performance for cooling, $EP_{C,w}$ will reflect the differences.

But the differences will not appear unless a series of different windows, with different solar control quality are compared.

This section provides a procedure to assess the solar control potential of a rated window, without the need to compare serried of different windows.

This is done by comparing the rating of the window against the rating of the same window provided with a fictitious reference high performance solar control provision.

NOTE As a black box the rated window has already proper solar control provisions incorporated (e.g. solar control glazing, incorporated blinds, etc.); or the rated window is an assembly of glazing, frame and e.g. an add-on solar control provision (film, blind, etc.); or the rated window has no solar control provision, etc.

If the difference in rating is small, the energy performance of the window for cooling is apparently efficient, for the given conditions: adding a high performing solar control provision will not lead to significant improvement of the energy performance of the window for cooling.

If the difference in rating is large, the energy performance of the window for cooling is apparently inefficient for the given conditions and hence subject to significant improvement by adding a solar control provision.

B.1.2 Procedure

As stated in clause 6.5, the following procedure can be used to assess the solar control potential of the rated window:

- a fictitious reference high performance solar control provision is defined;
- a formula is given to calculate the new properties of the window with this added fictitious reference solar control provision;
- the energy performance is calculated for the window without and with this added fictitious reference solar control provision;
- a recommendation is given to national or regional window energy rating schemes to rate the "solar control potential" of the window in the given conditions on the basis of the difference between the energy performance as calculated for the window without and with this added fictitious reference solar control provision.

© ISO 2009 – All rights reserved

In the following sections these procedures are presented in more detail.

B.2 Reference solar control provision

The properties resemble a reference external shading device.

NOTE The properties are used for the summer (cooling mode) situation.

For the cooling calculation with reference solar shading we use a reference shading with the following properties:

— solar transmittance: τ_e = 0,2;

— solar absorptance: α_e = 0,4.

B.3 Window properties with the fictitious reference solar control provision

The g-value for the combination of window with additional fictitious solar control provision is derived using the simplified method given in EN13363-1.

This standard gives conservative values for the summer situation (assuming no ventilation between shading and window).

We assume that the change in U-value can be ignored.

B.4 Recommended approach

Recommendation to national or regional window energy rating schemes to rate the "solar control potential" of the window on the basis of the difference between the energy performance calculated for the window without and with an added fictitious reference solar control provision.

B.5 Examples of assessment of solar control potential

For a certain country (+orientation, etc.) we obtain for instance the following rating:

Table B.1 — Example window A

Energy performance for heating of window A:	$EP_{H,w}$ = 9,8 kWh/m^2
Energy performance for cooling of window A:	$EP_{C,w}$ = 1,2 kWh/m^2
Energy performance for cooling of window A, provided with the reference solar shading device:	$EP_{C,w+ref.shad}$ = 1,0 kWh/m^2

So, for window A the difference between $EP_{C,w}$ and $EP_{C,w+ref.shad}$ is only 20 %.

Conclusion on window A: for the given conditions (reference building, climate and given orientation), the addition of a high performing solar control provision to window A will not lead to a significant improvement of the energy performance of the window for cooling.

© ISO 2009 – All rights reserved

The energy performance of the window for cooling is apparently efficient, for the given conditions. This is either due to proper properties of the window A itself, or due to the given conditions.

Table B.2 — Example window B

Energy performance for heating of window B:	$EP_{H,w}$ = 7,3 kWh/m^2
Energy performance for cooling of window B:	$EP_{C,w}$ = 3,6 kWh/m^2
Energy performance for cooling of window B, provided with the reference solar shading device:	$EP_{C,w+ref.shad}$ = 1,0 kWh/m^2

So, for window B the difference between $EP_{C,w}$ and $EP_{C,w+ref.shad}$ is very large.

Conclusion on window B: for the given conditions (reference building, climate and given orientation), the window B is apparently inefficient for cooling. The addition of a high performing solar control provision to window B will lead to highly improved energy performance of the window for cooling.

Consequently, it is worth considering to add a solar control provision in this case.

© ISO 2009 – All rights reserved

Annex C
(informative)

Example of reference buildings

Table C.1 gives an example of a reference building from North America.

Table C.1 — User Input and Fixed Parameters for a Typical House and a Specific House

PARAMETER	Typical House	Specific House
Floor Area	Fixed: 2000 square feet.	User Inputs actual floor area to the nearest 100 square feet
House Construction	User Choice of: - New Construction (Frame, 1-Story) or - Existing Construction (Frame, 1-Story). Choice defines many other parameters (see Table 2)	User Choice of: - New Construction, Frame, 1-story - New Construction, Frame, 2-story - New Construction, Masonry, 1-story - New Construction, Masonry, 2-story - Existing Construction, Frame, 1-story - Existing Construction, Frame, 2-story - Existing Construction, Masonry, 1-story - Existing Construction, Masonry, 2-story Choice defines many other parameters (see Table 2)
Foundation	Fixed: Foundation is based on location and is one of the following (see Table 2): ▪ Basement ▪ Slab-on-Grade ▪ Crawlspace	User Input: Choice of: - Basement - Slab-on-Grade - Crawlspace
Fenestration Type	User Defined.	User Defined.
Fenestration Area and Distribution	Fixed: 15 % of total floor area (300sf), equally distributed on all four cardinal orientations.	User Defined for each cardinal orientation.
Solar Gain Reduction	Fixed: Typical [a] : to represent a statistically average solar gain reduction for a typical house, this option includes all of the following: ▪ Interior shades (Seasonal SHGC multiplier, summer value = 0,80, winter value = 0,90); ▪ 1' overhang; ▪ a 67 % transmitting same-height obstruction 20' away intended to represent adjacent buildings. ▪ To account for other sources of solar heat gain reduction (insect screens, trees, dirt, building and fenestration self-shading), the SHGC multiplier was further reduced by 0,1. This results in a final winter SHGC multiplier of 0.8 and a final summer SHGC multiplier of 0,7.	User Defined from one of the following choices: ▪ **None:** No solar gain reduction ▪ **Overhang:** 2' Exterior Overhangs ▪ **Obstruction:** Exterior Obstructions, a completely opaque (τ=0.0), same-height obstruction 20 feet away, intended to represent adjacent buildings. ▪ **Interior:** Interior shades with a Seasonal SHGC multiplier, summer value = 0,80, winter value = 0,90. ▪ **Int+Ovh:** Interior shades and 2' overhangs ▪ **Ovh+Obs:** 2' overhangs & obstructions ▪ **All:** Interior shades, 2' overhangs, and obstructions ▪ **Typical**[(a)]**:** to represent a statistically average solar gain reduction for a typical house, this option includes: ▪ Interior shades (Seasonal SHGC multiplier, summer value = 0,80, winter value = 0,90);

© ISO 2009 – All rights reserved

PARAMETER	Typical House	Specific House
		▪ 1' overhang; ▪ a 67 % transmitting same-height obstruction 20' away intended to represent adjacent buildings. To account for other sources of solar heat gain reduction (insect screens, trees, dirt, building and fenestration self-shading), the SHGC multiplier was further reduced by 0,1. This results in a final winter SHGC multiplier of 0,8 and a final summer SHGC multiplier of 0,7.
Insulation	Fixed: Envelope insulation levels are based on location: ▪ **New construction:** See Table 2. ▪ **Existing construction:** See Table 3.	Fixed: Same as typical house.
Infiltration	Fixed: **New Construction:** ELA=0,77 ft^2 (0,58 ACH) **Existing Construction:** ELA=1,00 ft^2 (0,70 ACH)	Fixed: Same as typical house.
Structural Mass (lb/ft^2)	Fixed: 3,5 lb/ft^2 of floor area, in accordance with the Model Energy Code and NFRC Annual Energy Performance Subcommittee recommendation (September 1998).	Fixed: Same as typical house.
Internal Mass Furniture (lb/ft^2)	Fixed: 8,0 lb/ft^2 of floor area, in accordance with the Model Energy Code and NFRC Annual Energy Performance Subcommittee recommendation (September 1998).	Fixed: Same as typical house.
HVAC System	Fixed: Gas Furnace and A/C,	User Defined Heating: Gas Furnace or Electric Heat Pump Fixed Cooling: Air Conditioner.
HVAC System Sizing	Fixed: For each climate, system sizes are fixed for all fenestration options. Fixed sizes are based on the use of DOE-2 auto-sizing for the same house as defined in the analysis, with the most representative fenestration for that specific climate. An auto-sizing multiplier of 1,3 used to account for a typical safety factor.[b]	Fixed: Same as typical house.
HVAC Efficiency	Fixed: New Construction: ▪ AFUE = 0,78, A/C SEER=10.0 Existing Construction: ▪ AFUE = 0,70, A/C SEER= 8.0	Fixed: Same as typical house.
Duct Losses	Fixed: Heating: 10 % (fixed) Cooling: 10 % (fixed)	Fixed: Same as typical house.
Part-Load Performance	Fixed: New part-load curves for DOE2 (Henderson 1998) for both new and existing house types	Fixed: Same as typical house.
Thermostat Settings	Fixed: Heating: 70 ^oF, Cooling: 78 ^oF Basement (partially conditioned): Heating 62^oF, Cooling 85^oF	Fixed: Same as typical house.
Night Heating Setback	Fixed: 65 ^oF (11 PM – 6 AM[c])	Fixed: Same as typical house.
Internal Loads	Fixed: Sensible: 43,033 Btu/day + (floor area * 8,42 Btu/ft^2-day for lighting) Latent: 12,2 kBtu/day	Fixed: Same as typical house.
Natural Ventilation	Fixed: Enthalpic – Sherman-Grimsrud (78 ^oF / 72 ^oF based on 4 days' history)	Fixed: Same as typical house.

© ISO 2009 – All rights reserved

PARAMETER	Typical House	Specific House

[a] A one-foot overhang is assumed on all four orientations in order to represent the average of a two-foot overhang and no overhang.

[b] A 67 % transmitting obstruction 20 feet away on all four orientations represents the average of obstructions (such as neighboring buildings and trees) 20 feet away on one-third of the total fenestration and no obstructions in front of the remaining two-thirds of fenestration products.

[c] An interior shade is assumed to have a Solar Heat Gain Coefficient multiplier of 0,9 during the winter and 0,8 during the summer. To account for solar heat gain reducing effects from other sources such as screens, trees, dirt, and self-shading of the building, the SHGC multiplier was further reduced by 0,1 throughout the year. This amounts to a 12,5 % decrease in the summer and an 11,1 % decrease in the winter. The final SHGC multipliers (0,8 in the winter and 0,7 in the summer) thus reflect the combined effects of shading devices and other sources.

Table C.2 — New Construction Insulation Values (Representative cities given as an example)

State	City	Climate Zone	HDD 65	CDD 50	Glz %	Fenestr. U-factor	Ceiling R-value	Wall R-value	Floor R-value	Basem. R-value	Slab R-value	Crawl R-value
FL	Miami	1	115	9405	15	1,100	19	11	11	--	0	--
AZ	Phoenix	2	1130	8323	15	0,900	30	11	11	--	0	--
AL	Birmingham	3A,3B	2685	5068	15	0,700	38	14	19	6	6	7
CA	San Francisco	3C	3285	2208	15	0,700	38	14	19	6	6	7
DC	Washington	4	3733	4440	15	0,550	38	19	19	9	--	--
IL	Chicago	5	6003	3304	15	0,400	38	19	30	14	--	--
MN	Minneapolis	6	7736	2716	15	0,400	38	19	30	15	--	--
AK	Anchorage	7	10099	689	15	0,400	38	19	30	30	--	--
AK	Barrow	8	20059	0	15	0,700	38	19	30	30	6	7

Table C.3 — Existing Construction Insulation Values. (Ritschard, et. al. 1992)

State	City	Climate Zone	HDD 65	CDD 50	Glz %	Fenestr. *U*-factor	Ceiling R-value	Wall R-value	Floor R-value	Basem. R-value	Slab R-value	Crawl R-value
FL	Miami	1	115	9405	15	0,650	11	7	0	0	0	0
AZ	Phoenix	2	1130	8323	15	0,650	11	7	0	0	0	0
AL	Birmingham	3A,3B	2685	5068	15	0,650	19	7	0	0	0	0
CA	San Francisco	3C	3285	2208	15	1,100	11	7	0	0	0	0
DC	Washington	4	3733	4440	15	0,650	11	7	0	0	0	0

© ISO 2009 – All rights reserved

State	City	Climate Zone	HDD 65	CDD 50	Glz %	Fenestr. *U*-factor	Ceiling R-value	Wall R-value	Floor R-value	Basem. R-value	Slab R-value	Crawl R-value
IL	Chicago	5	6003	3304	15	0,650	19	7	0	0	0	0
MN	Minneapolis	6	7736	2716	15	0,650	22	7	0	0	0	0
AK	Anchorage	7	10099	689	15	0,650	22	7	0	0	0	0
AK	Barrow	8	20059	0	15	?	?	?	?	?	?	?

Table C.4 — Definition of climate zones

Climate Zone	Heating Degree Days *HDD*	Cooling Degree Days *CDD*
1	N/A	$\infty > CDD > 9{,}000$
2	N/A	$9{,}000 \geq CDD > 6{,}300$
3A	$HDD < 5400$	$6{,}300 \geq CDD > 4{,}500$
3B	$HDD < 5400$	$6{,}300 \geq CDD > 4{,}500$
3C	$3{,}600 \geq HDD \geq 0$	$CDD \leq 4{,}500$
4	$5{,}400 \geq HDD > 3{,}600$	N/A
5	$7{,}200 \geq HDD > 5{,}400$	N/A
6	$9{,}000 \geq HDD > 7{,}200$	N/A
7	$12{,}600 \geq HDD > 9{,}000$	N/A
8	$\infty > HDD > 12{,}600$	N/A

© ISO 2009 – All rights reserved

Annex D
(informative)

Example of the calculation of $EP_{C,w}$ and $EP_{H,w}$ - Using a detailed hourly method

The following example uses the data from the worked example in ISO 13790:2008, annex J.

A spreadsheet has been prepared with the monthly method according to ISO 13790:2008 (input sheet. result sheet, plus supporting sheets), with an additional worksheet containing the input data, equations and output data for the energy performance of windows.

With this spreadsheet it is possible to specify the reference building (monthly method according to ISO 13790:2008) including climate and operation conditions and the energy performance of a specific window ("Demo_window_rating"), as a function of window properties and orientation(s) and reference climate, building and operation conditions. Also the calculation of the EP of the window with reference solar shading is included.

Reference building and climate:

See ISO 13790:2008 Annex J. Chosen climate: Paris

Calculated monthly energy needs for heating and cooling (per m^2 floor area) is shown in Figure D.1.

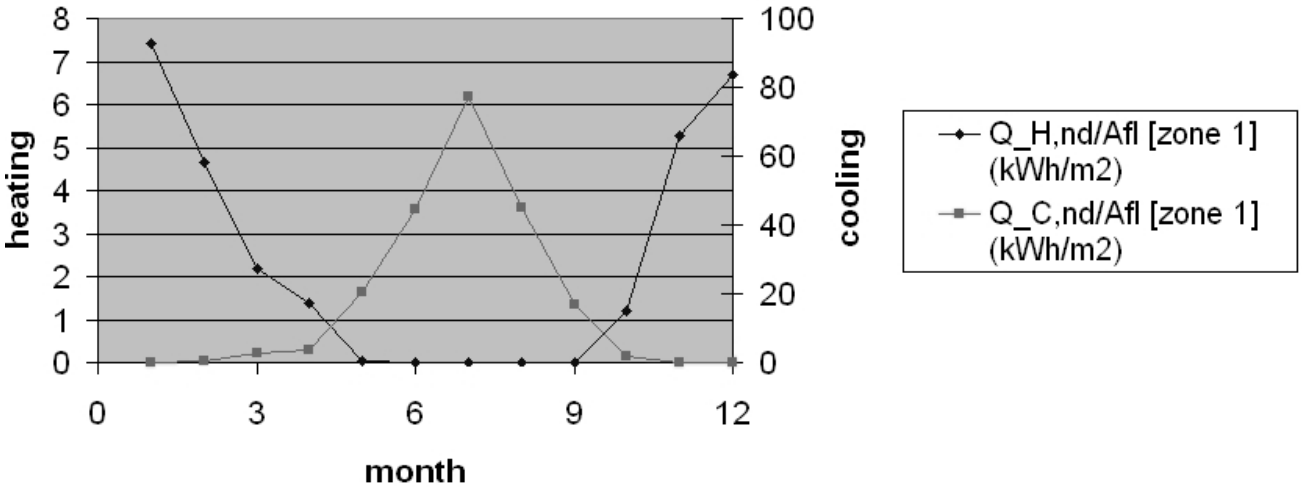


Figure D.1 — Calculated monthly energy needs for heating and cooling

Fraction of the month that is part of the heating season or cooling season, see clauses 6.2 and 6.3.

© ISO 2009 – All rights reserved

Table D.1 — Fraction of the month

Month	$f_{H,m}$ fraction of the month is heating season	$(1-f_{H,m})$ fraction of the month is cooling season
Jan	1,00	0,00
Feb	1,00	0,00
Mar	0,94	0,06
Apr	0,89	0,11
May	0,03	0,97
Jun	0,00	1,00
Jul	0,00	1,00
Aug	0,00	1,00
Sep	0,01	0,99
Oct	0,92	0,08
Nov	1,00	0,00
Dec	1,00	0,00

Note Single zone; otherwise one of the zones has to be defined for the window energy rating.

Table D.2 — Window input data

Window properties Description	**Quantity**	**Value**	**Unit**	**Remarks**
Window area, per orientation	$A_{w,hor}$	0,00	m^2	for weighting EPwindow over hor,E,S,W,N
	$A_{w,East}$	1,00	m^2	
	$A_{w,South}$	1,00	m^2	
	$A_{w,West}$	1,00	m^2	
	$A_{w,North}$	1,00	m^2	
Heating mode (all values incl. window frame):				To be most general: properties distinguished for H vs C
U-value	$U_{H,w}$	1,50	$W/(m^2 \cdot K)$	
Infiltr. and ventil. coeff.	$H_{H,ve,w}/A_w$	0,30	$W/(m^2 \cdot K)$	per m^2 window
g-value (total solar energy transmittance)	$g_{H,w}$	0,50	-	for given orient./slope resp. weighted mean over orientation(s)
visual transmittance	$\tau_{H,w,vis}$	0,60	-	for given orient./slope resp. weighted mean over orientation(s)
factor due to glazing maintenance and shading effects	$F_{shad,ob,H}$	1,00	-	for given orient./slope resp. weighted mean over orientation(s)
Cooling mode (all values incl. window frame)				
U-value	$U_{C,w}$	1,50	$W/(m^2 \cdot K)$	
Infiltr. and ventil. coeff.	$H_{C,ve_w}/A_w$	0,30	$W/(m^2 \cdot K)$	per m^2 window
solar transmittance	$g_{C,w}$	0,50	-	for given orient./slope resp. weighted mean over orientation(s)
	$\tau_{C,vis}$	0,60	-	for given orient./slope resp. weighted mean over orientation(s)

© ISO 2009 – All rights reserved

Window properties Description	Quantity	Value	Unit	Remarks
factor due to glazing maintenance and shading effects	$F_{shad,ob,C}$	1,00	-	for given orient./slope resp. weighted mean over orientation(s)

Window energy rating results:

Heating:

Annual:

$\tau_{H,w,vis}$	0,60	-
$EP_{H,w}$	17	kWh/m^2
NOTE Result depends on window in combination with orientation(s), climate and ref. building.		

Monthly:

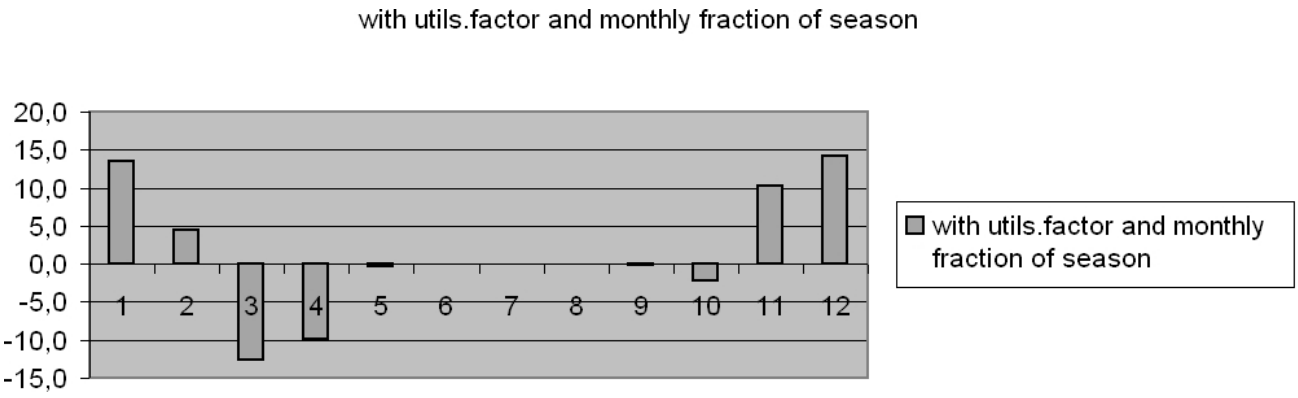


Figure D.2 — Results for window, heating

Cooling:

Annual:

$\tau_{C,w,vis}$	0,60	-
$EP_{C,w}$	122	kWh/m^2
$EP_{C,w,ref.shading}$	31	kWh/m^2
NOTE 1 Result depends on window in combination with orientation(s), climate and ref. building.		

© ISO 2009 – All rights reserved

NOTE 2 If EP_C with ref.shading device << EP_C without:

— then: for given window, in given climate and orientation(s) there is room for improvement by adding a solar shading protection;

— else: for given window, in given climate and orientation(s) there is no need for adding a solar shading protection.

Per month:

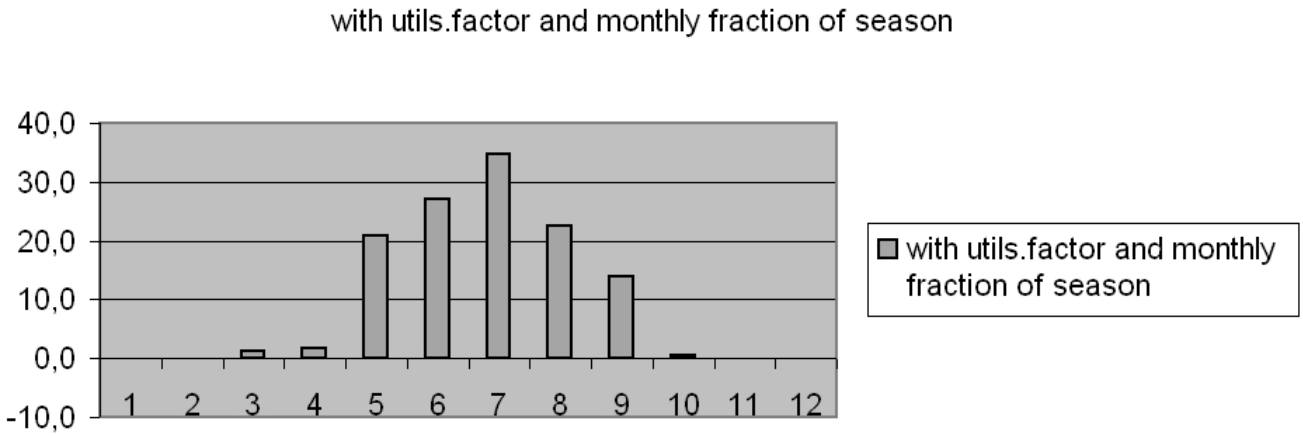


Figure D.3 — Results for window, cooling

Compare same window with reference solar shading:

Annual:

$\tau_{C,w,vis}$	0,60	-
$EP_{C,w}$	122	kWh/m^2
$EP_{C,w,ref.shading}$	31	kWh/m^2

NOTE 1 Result depends on window in combination with orientation(s), climate and ref. building.

NOTE 2 If EP_C with ref.shading device << EP_C without:

— then: for given window, in given climate and orientation(s) there is room for improvement by adding a solar shading protection;

— else: for given window, in given climate and orientation(s) there is no need for adding a solar shading protection.

Conclusion: the comparison between the window and the same window with the reference solar shading shows that for given window, in given climate and orientation(s) there is room for improvement by adding a solar shading protection

© ISO 2009 – All rights reserved

Results for window with reference shading, monthly:

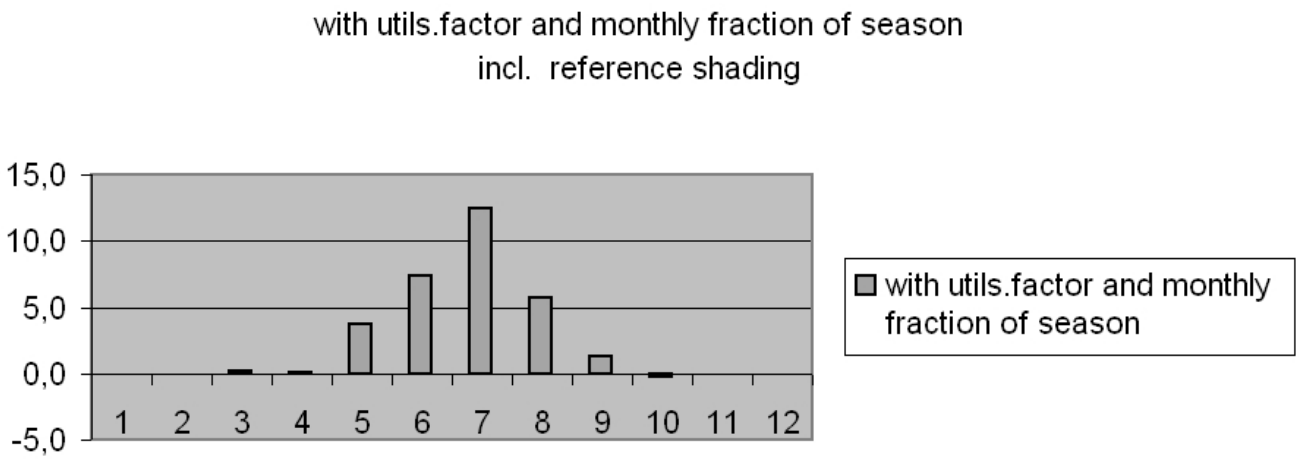


Figure D.4 — Results for window with reference shading, monthly

© ISO 2009 – All rights reserved

Annex E
(informative)

Example of the calculation of $EP_{C,w}$ and $EP_{H,w}$ - Using a monthly method

For the single story wood frame house, new construction, located in Tampa, FL calculate $EP_{C,w}$ and $EP_{H,w}$ using detailed dynamic method of the following window:

Double glazing: 3 mm clear, Argon 90 %, gap fill 12,7 mm wide, 3 mm hard coat Low-e from Pilkington LOF (IGDB ID #: 9921). Window to floor ratio for each orientation is 15 %.

The thermal and solar-optical performance indices for this window are:

Glazing: U_C = 1,665 W/(m^2·K); g_C = 0,713; τ_{vc} = 0,748

Window: U = 2,074 W/(m^2·K); g = 0,529; τ_v = 0,540

The floor area of the house is 186 m^2. Heating is provided with direct fired gas furnace and cooling is provided by central AC. The foundation type is slab-on-grade.

Using RESFEN program, which incorporates assumptions for the typical house from Table C.1, $EP_{C,w}$ and $EP_{H,w}$ for each orientation is calculated from the cooling and heating energy associated with windows. The following is cooling and heating energy for each orientation:

	N	E	S	W
Cooling [kWh]	268,31	603	494	543
Heating [kWh]	116,67	-25,00	-213,89	13,89
Area [m^2]	6,967	6,967	6,967	6,967

From the results for each orientation, average value can be calculated by area weighting each orientation:

	N	E	S	W	Average
Cooling [kWh]	268,31	603	494	543	477,08
Heating [kWh]	116,67	-25,00	-213,89	13,89	-27,08
Area [m^2]	6,967	6,967	6,967	6,967	6,97

After dividing window heating and cooling energy by the window area, we get the EP values:

	N	E	S	W	Average
$EP_{C,w}$ [kWh/m^2]	39	87	71	78	68
$EP_{H,w}$ [kWh/m^2]	17	-4	-31	2	-4

So,

$EP_{C,w}$ = 68 kWh/m^2

$EP_{H,w}$ = -4 kWh/m^2

© ISO 2009 – All rights reserved

Bibliography

[1] ISO 6613:1980, *Windows and door height windows — Air permeability test*

[2] ISO 6946:2007, *Building components and building elements — Thermal resistance and thermal transmittance — Calculation method*

[3] ISO 8990:1994, *Thermal insulation -- Determination of steady-state thermal transmission properties -- Calibrated and guarded hot box*

NOTE The “temperature of the surroundings” is taken as the “environmental temperature” which in turn is defined in ISO 8990:1994 Annex A.

[4] ISO 10291:1994, *Glass in building — Determination of steady-state U values (thermal transmittance) of multiple glazing — Guarded hot plate method*

[5] ISO 10292:1994, *Glass in building — Calculation of steady-state U values (thermal transmittance) of multiple glazing*

[6] ISO 10293:1997, *Glass in building — Determination of steady-state U values (thermal transmittance) of multiple glazing — Heat flow meter method*

[7] ISO 15927-6, *Hygrothermal performance of buildings — Calculation and presentation of climatic data — Part 6: Accumulated temperature differences (degree-days)*

[8] EN 673:1997, *Glass in building — Determination of thermal transmittance (U value) — Calculation method*

[9] EN 12207:1999, *Windows and doors — Air permeability — Classification*

[10] EN 15217:2007, *Energy performance of buildings — Methods for expressing energy performance and for energy certification of buildings*

[11] Canadian Standard Association, A440.2-98, *Energy Performance of Windows and Other Fenestration Systems*, p20, 1998.

[12] ASTM E283-04, *Standard Test Method for Determining Rate of Air Leakage Through Exterior Windows, Curtain Walls, and Doors Under Specified Pressure Differences Across the Specimen*

[13] ASTM E1424-91(2000), *Standard Test Method for Determining the Rate of AIR Leakage Through Exterior Windows, Curtain Walls, and Doors Under Specified Pressure and Temperature Differences Across the Specimen*

[14] ASTM E2319-04, *Standard Test Method for Determining Air Flow Through the Face and Sides of Exterior Windows, Curtain Walls, and Doors Under Specified Pressure Differences Across the Specimen*

[15] RESFEN, *Software for predicting the energy performance of residential window systems*: Lawrence Berkeley National Laboratory, http://windows.lbl.gov/software/resfen/resfen.html

CALCULATION OF WINDOW *U*-VALUES

[16] EN ISO 10077-1:2006, *Thermal performance of windows, doors and shutters — Calculation of thermal transmittance — Part 1: General*

[17] EN ISO 10077-2:2003, *Thermal performance of windows, doors and shutters — Calculation of thermal transmittance — Part 2: Numerical method for frames*

© ISO 2009 – All rights reserved

[18] ISO 15099:2003, *Thermal Performance of Windows, Doors and Shading Devices — Detailed Calculation*

MEASUREMENT OF WHOLE WINDOW AND WINDOW FRAME U-VALUES

[19] EN ISO 12567-1:2000, *Thermal performance of windows and doors — Determination of thermal transmittance by hot box method — Part 1: Complete windows and doors*

[20] EN ISO 12567-2:2005, *Thermal performance of windows and doors — Determination of thermal transmittance by hot box method — Part 2: Roof windows and other projecting windows*

[21] EN 12412-2:2003, *Thermal performance of windows, doors and shutters — Determination of thermal transmittance by hot box method — Part 2: Frames*

[22] ASTM C1199-00 Standard, *Test Method for Measuring the Steady-State Thermal Transmittance of Fenestration Systems Using Hot Box Methods*

[23] ASTM E1423 Standard, *Practice for Determining the Steady State Thermal Transmittance of Fenestration Systems*

CALCULATION OF SOLAR GAIN

[24] EN 410:1998, *Glass in building — Determination of luminous and solar characteristics of glazing*

Total solar energy transmittance (solar factor, g) is defined in EN 410 as:

The total solar energy transmittance g is calculated as the sum of the solar direct transmittance τ_e and the secondary heat transfer factor q_i of the glazing towards the inside, the latter resulting from heat transfer by convection and longwave IR-radiation of that part of the incident solar radiation which has been absorbed by the glazing: $g = \tau_e + q_i$

NOTE The ratio of the amount of total solar energy in the full solar wavelength range (300 - 2,100 nanometers) that is allowed to pass through a glazing system to the amount of total solar energy falling on that glazing system. Value is usually expressed as a percent.

[25] ISO 3538:1997, *Road vehicles — Safety glazing materials — Test methods for optical properties*

[26] EN 1096-3:2001, *Glass in building — Coated glass — Part 3: Requirements and test methods for class C and D coatings*

NOTE Glass, Coated materials, Construction materials, Construction systems parts, Buildings, Glazing, Coatings, Durability, Conformity, Artificial ageing tests, Solar radiation, Electromagnetic radiation, Performance testing, Grades (quality), Classification systems, Reflection factor, Transmittance.

[27] EN 2155-5:1989, *Aerospace series — Test methods for transparent materials for aircraft glazing — Part 5: Determination of visible light transmission*

NOTE Uses a photometer employing a defined light source and a photocell matched to the response of the human eye.

[28] EN 12758:2002, *Glass in building — Glazing and airborne sound insulation — Product descriptions and determination of properties*

NOTE Glass, Construction materials, Glazing, Transparency, Opacity, Airborne sound insulation, Acoustic properties and phenomena, Performance

[29] EN 12898:2001, *Glass in building — Determination of the emissivity*

[30] EN 13363-1:2003, *Solar protection devices combined with glazing — Calculation of solar and light transmittance — Part 1: Simplified method*

 © ISO 2009 – All rights reserved

[31] EN 13363-2:2005, *Solar protection devices combined with glazing — Calculation of total solar energy transmittance and light transmittance — Part 2: Detailed calculation method*

CIE - INTERNATIONAL COMMISSION ON ILLUMINATION

As its name implies, the International Commission on Illumination - abbreviated as CIE from its French title Commission Internationale de l'Eclairage - is an organization devoted to international cooperation and exchange of information among its member countries on all matters relating to the science and art of lighting. The CIE is a technical, scientific and cultural, non-profit autonomous organization. It has grown out of the interests of individuals working in illumination.

[32] ISO 10526:2007, CIE Standard, *Illuminants for Colorimetry*

GLAZING ENERGY PERFORMANCE

[33] EN ISO 14438:2002, *Glass in building — Determination of energy balance value — Calculation method*

© ISO 2009 – All rights reserved

Project 3.2
South Africa

Project Name:	International Harmonization – South Africa
Date:	November 6, 2006
Purpose:	NFRC has a license agreement with the Association of Architectural Aluminum Manufacturers of South Africa (AAAMSA) to begin developing NFRC ratings for fenestration products.

Project Summary:

NFRC conducted fenestration simulation training and accredited Thermal Testing Labs in South Africa (a thermal testing facility for fenestration), an important first step towards a full NFRC certification program.

Click here for a copy of the NFRC-AAAMSA license agreement

Web link:
http://www.nfrc.org/testinglabs.aspx

License and Support Agreement

Between

National Fenestration Rating Council

and

Association of Architectural Aluminum Manufacturers of South Africa-Group trading as South African Fenestration & Insulation Energy Rating Association

This License and Support Agreement (the "Agreement") is made this 15st day of May, 2007 by and between National Fenestration Rating Council, Incorporated, a not-for-profit U.S. corporation organized in the State of Maryland ("NFRC") and the ["The Association of Architectural Aluminum Manufacturers of South Africa Group (The AAAMSA Group) trading as South African Fenestration & Insulation Energy Rating Association (SAFIERA) "].

RECITALS

A. NFRC owns and controls the use of procedures for rating thermal performance and other performance attributes of fenestration products as set forth in Exhibit A hereto, as such procedures are amended and supplemented from time to time (the "Rating System").

B. NFRC owns and controls the program for rating (by computer simulation and physical testing), certification and labeling of fenestration products for thermal performance and other attributes (the "Certification Program"), including as set forth in the documents entitled NFRC PCP: Product Certification Program, the NFRC LAP: Laboratory Accreditation Program and the NFRC CAP: Compliance Assurance Program (collectively, the "Program Documents"), as the Program Documents are amended from time to time by NFRC.

C. NFRC employs and/or contracts with individuals with knowledge and experience with the Rating System, Certification Program and the Program Documents, including administration of the labeling program used in connection with the Rating System.

D. NFRC operates a database of certified residential fenestration products of manufacturers who are NFRC licensees (the "Database"). NFRC owns the software used to create and operate the Database (the "Database Software").

E. The AAAMSA Group trading as SAFIERA is an organization which wishes to establish a system for rating, certification and labeling of fenestration products in South Africa (the "South Africa Rating System") that will employ NFRC's Rating System. The AAAMSA Group trading as SAFIERA desires to use, reproduce and

modify some or all of the Rating System, Certification System, Program Documents, and the Database Software for the development of the South Africa Rating System and seeks professional training and assistance from NFRC employees and agents in creating and implementing the South Africa Rating System.

F. NFRC is willing to assist The AAAMSA Group trading as SAFIERA in the development of the South Africa Rating System on the terms set forth below.

NFRC and The AAAMSA Group trading as SAFIERA hereby agree as follows:

SECTION 1
COPYRIGHT LICENSE

(a) NFRC hereby grants to The AAAMSA Group trading as SAFIERA a non-exclusive, non-assignable license, during the term of this Agreement to reproduce, make and distribute copies of the Rating System, Certification Program and Program Documents (collectively, the "NFRC Materials") in South Africa and the right to make derivative works of the NFRC Materials, in each case in connection with The AAAMSA Group trading as SAFIERA development and operation of the South Africa Rating System. NFRC agrees to provide to The AAAMSA Group trading as SAFIERA all updates or modifications to the NFRC Materials created by NFRC from time to time.

(b) The AAAMSA Group trading as SAFIERA shall have the right to prepare derivative works based on the NFRC Materials including the right to maintain, update, modify or utilize the derivative works in any manner The AAAMSA Group trading as SAFIERA chooses. The AAAMSA Group trading as SAFIERA shall own all right, title and interest in the derivative works, subject to NFRC's retention of its copyright ownership in the NFRC Materials.

(c) The AAAMSA Group trading as SAFIERA shall indicate in any written materials in which all or part of the NFRC Materials appear that the NFRC Materials and the copyright in the NFRC Materials are the exclusive property of NFRC and are used by The AAAMSA Group trading as SAFIERA pursuant to a license from NFRC.

(d) This Agreement does not grant to The AAAMSA Group trading as SAFIERA any right to use any trademarks, service marks, collective marks, or certification marks owned by NFRC in any manner.

(e) The AAAMSA Group trading as SAFIERA hereby acknowledges NFRC's exclusive ownership and proprietary rights in the NFRC Materials and agrees to take no action inconsistent with such rights or with the terms of this Agreement.

(f) NFRC and The AAAMSA Group trading as SAFIERA agree to work cooperatively in good faith to assure that the South Africa Rating System recognizes and utilizes the NFRC Rating System.

SECTION 2
TRAINING

(a) NFRC shall develop a training program to instruct The AAAMSA Group trading as SAFIERA designated individuals on the conduct of computer simulation of fenestration products under NFRC's simulation program under the Rating System. NFRC agrees from time to time to conduct the training programs in South Africa at times and locations agreed to by both parties. Individuals who have attended and successfully completed the simulation training program in accordance with NFRC requirements will be accredited by NFRC to conduct simulation training programs for The AAAMSA Group trading as SAFIERA.

(b) The AAAMSA Group trading as SAFIERA agrees to send at least one accredited trainer for an NFRC conducted mandatory workshop training to be conducted by NFRC annually. The AAAMSA Group trading as SAFIERA also agrees to require a The AAAMSA Group trading as SAFIERA designated trainer who has been accredited by NFRC to participate in NFRC conducted "round robin" testing programs. The AAAMSA Group trading as SAFIERA agrees to allow only NFRC accredited trainers to conduct simulation training programs for the South Africa Rating System.

SECTION 3
OTHER SERVICES

The parties recognize that from time to time The AAAMSA Group trading as SAFIERA may request consultation with NFRC personnel for advice or other input on technical and other matters relating to the South Africa Rating System that are not otherwise provided by NFRC pursuant to the other provisions of this Agreement. NFRC will use reasonable commercial efforts to provide such additional services in a timely, cost effective manner and The AAAMSA Group trading as SAFIERA shall pay NFRC for such services based on NFRC's standard hourly charge for the time expended by NFRC personnel and contractors in providing those services. Any reasonable travel, lodging or other out-of-pocket expenses incurred by the NFRC in providing these services shall be reimbursed by The AAAMSA Group trading as SAFIERA, provided those expenses are approved by The AAAMSA Group trading as SAFIERA in advance.

SECTION 4
LICENSE TO DATABASE SOFTWARE

NFRC hereby grants to The AAAMSA Group trading as SAFIERA a non-exclusive, non-assignable license to use the Database Software during the term of this Agreement for the South Africa Rating System. If required the Database Software shall be provided in object code form and may not be modified by The AAAMSA Group trading as SAFIERA without NFRC's consent. NFRC makes no representation or warranty regarding the Database Software, including its fitness for a particular purpose or that the Database Software is error free. NFRC shall have no obligation to maintain or support the Database Software but shall provide any updates or enhancements to the

Database Software that is completed during the term of this Agreement. This license shall not include a license to software developed following the date of this Agreement for use in NFRC's non-residential fenestration rating program.

SECTION 5
TERM OF THE AGREEMENT

(a) This Agreement shall take effect on 1st day of June 2007 and shall continue until terminated as provided below. This agreement will be subjected to review by NFRC every 3 years.

(b) Either party may terminate this Agreement without cause, at any time on not less than 180 days prior written notice to the other party.

(c) Either party may terminate this Agreement on written notice if the other party breaches any of its obligations under this Agreement and fails to cure such breach within 30 days after receipt of a written notice detailing that breach.

(d) Any amounts that were due to NFRC prior to termination of the Agreement shall be paid promptly following the termination of the Agreement. Upon termination of this Agreement, all licenses granted hereunder to The AAAMSA Group trading as SAFIERA to the NFRC Materials and Database shall terminate.

SECTION 6
FEES AND EXPENSES

The AAAMSA Group trading as SAFIERA agrees to make the following payments to NFRC during the term of this Agreement. All payments are designated in and shall be paid in U.S. dollars.

(a) The AAAMSA Group trading as SAFIERA shall pay an annual fee of $20,000 USD to a maximum value of ZAR 160000 to NFRC as a membership fee to become and remain a member of NFRC, with commencement date 1st January 2008. The AAAMSA Group trading as SAFIERA shall make the non-refundable one time license fee of $10,000 USD to a maximum value of ZAR 80000 payment on 1 June 2007, and thereafter shall make an annual membership fee payment, with commencement date of 1st January 2008, of $20,000 USD to a maximum value of ZAR 160000 on the successive anniversary dates of January 1st.

(b) The AAAMSA Group trading as SAFIERA shall pay non-refundable one time license fee of $10,000 USD to a maximum value of ZAR 80000 payment on 1 June 2007 in consideration for the licenses granted pursuant to Sections 1 and 4 above. The AAAMSA Group trading as SAFIERA shall make the initial license fee payment on execution of this Agreement and thereafter shall make the annual license fee payment of $10,000 USD on the successive anniversary dates of this Agreement.

(c) The AAAMSA Group trading as SAFIERA shall pay a training fee of $2,500 USD for each person designated by The AAAMSA Group trading as SAFIERA to attend the NFRC simulation training program conducted in South Africa by NFRC from time to time as referenced in Section 2 above. The fee shall be payable for each such training program attended by such individual.

(d) The AAAMSA Group trading as SAFIERA shall pay the actual out-of-pocket travel and lodging expenses incurred by one NFRC designated observer to conduct the initial simulation training course in South Africa. The AAAMSA Group trading as SAFIERA shall also pay NFRC for the time expended by that NFRC observer at NFRC's standard hourly rate up to a maximum of $5,000 USD. NFRC's initial hourly billing rate under this Agreement is $100 USD. The hourly rate may be increased no more frequently than once per year and may not increase more than 15% per year.

(e) The AAAMSA Group trading as SAFIERA shall pay NFRC for any additional services provided by NFRC at The AAAMSA Group trading as SAFIERA request pursuant to Section 3 above at NFRC's standard hourly billing rates.

(f) All amounts owed by The AAAMSA Group trading as SAFIERA to NFRC hereunder (other than payment due upon execution of this Agreement) shall be due within 15 days after receipt of an NFRC invoice for such amount.

(g) Except as expressly provided in this Section 6, each party shall be responsible for its own fees and expenses incurred in connection with this Agreement.

SECTION 7
MISCELLANEOUS

(a) Any notices required to be given to a party hereunder shall be deemed given when received by that party at the address set forth on the signature page to this Agreement.

(b) This Agreement shall be construed in accordance with the federal and state laws of the United States, including, but not limited to the U.S. Copyright Act.

(c) NFRC is an independent contractor to The AAAMSA Group trading as SAFIERA and neither party is the agent, partner or joint venturer of the other party and neither party has the right to legally bind or contract for the other party.

(d) Neither party shall have the right to assign this Agreement to any other entity or person without the prior written consent of the other party.

(e) This Agreement constitutes the entire agreement between the parties and supersedes and replaces any prior oral or written agreements regarding the subject matter hereof.

(f) This Agreement may be executed in counterparts.

SO AGREED:

National Fenestration Rating Council	**South Africa Fenestration Rating Council**
8484 Georgia Avenue Suite 320 Silver Spring, MD 20910	
By:_____ Executive Director	By: _____ Title: _____

Exhibit A

NFRC owns and controls the use of procedures for rating performance and other attributes of fenestration products (the "Rating System") set forth in *NFRC 100: Procedure for Determining Fenestration Products U-factors ("NFRC 100") and NFRC 200: Procedure for Determining Fenestration Product Solar Heat Gain Coefficients and Visible Transmittance at Normal Incidence ("NFRC 200"), et seq.,* as amended and updated from time to time, *NFRC 400: Procedure for Determining Fenestration Product Air Leakage ("NFRC 400"), NFRC 500: Procedure for Determining Fenestration Product Condensation Resistance Value ("NFRC 500"), NFRC 101: Procedure for Determining Thermo-Physical Properties of Materials for Use in NFRC-approved Software Programs ("NFRC 101"), NFRC 102: Test Procedure for Measuring the Steady-State Thermal Transmittance of Fenestration Systems ("NFRC 102"), NFRC 201: Procedure for Interim Standard Test Method for Measuring the Solar Heat Gain Coefficient of Fenestration Systems Using Colorimeter Hot Box MethodS ("NFRC 201"), NFRC 300: Test method for Determining the Solar Optical Properties of Glazing Materials and Systems ("NFRC300"), and NFRC 301: Standard Test Method for Emittance of Specula Surfaces Using Spectrometric Measurements ("NFRC 301")* and *NFRC 400: Procedure for Determining Fenestration Product Condensation Resistance Values and NFRC 500: Procedure for Determining Fenestration Product Condensation Resistance Values,* copies of which have previously been provided to Licensee.

Project 3.2
Australia (a)

Project Name: International Harmonization – Australia

Date: November 2006

Purpose: The Australian Fenestration Rating Council (AFRC) was established to provide an energy rating system for windows and doors that is fair, accurate and credible in application. The AFRC is the Australian operator of the NFRC.

Project Summary:

NFRC continues to work with the Australian Fenestration Rating Council (AFRC, a new NFRC licensee) as they begin to certify fenestration products according to NFRC procedures. The ARFC website contains numerous technical documents that were jointly developed with NFRC: www.afrc.org.au NFRC works with the Australian Window Association (AWA) closely to continue work toward NFRC harmonization.

Click here for the current Australian Fenestration Rating Council procedures

Chapter 1

Introduction

The Australian Fenestration Rating Council (AFRC) was established to provide an energy rating system for windows and doors that is fair, accurate and credible in application. The AFRC is the Australian operator of the NFRC.

The establishment of the AFRC is an attempt by the fenestration industry to take control of its own future.

The Government is interested in the development of a comprehensive and credible system to fairly evaluate fenestration products for more efficient energy performance. Insulation has been a primary energy saving component improved energy efficiency for some years but now other building components (such as windows) are seen as having a role to play in energy conservation and CO_2 emission reductions.

It is not within the AFRC remit to establish 'performance targets', that is the responsibility of the appropriate authorities. The role of the AFRC is to make sure that uniform methods of independently evaluating fenestration performance are available and employed so that any manufacturer's products can be compared and contrasted.

NFRC Process Background

The National Fenestration Rating Council Incorporated (NFRC) operates a uniform national rating system for energy performance of fenestration products. The Rating System determines the U-value (this is synonymous with U-factor), Solar Heat Gain Coefficient (SHGC) and Visible Transmittance (VT) of a product, and is supplemented by procedures for the ratings of products for Air Leakage (AL) and Condensation Resistance (CR). Together, these rating procedures, as set forth in documents published by NFRC, are known as the NFRC Rating System. The Rating System is expected to be supplemented by additional procedures for rating energy performance characteristics including annual energy performance, long term energy performance, ultra-violet (UV) and comfort.

The Rating System employs computer simulation and physical testing by NFRC-accredited laboratories to establish energy performance ratings for fenestration product types.

NFRC ensures the integrity and uniformity of NFRC ratings, certification and labeling by ensuring that responsible parties, testing and simulation laboratories and Independent Auditors (IAs) adhere to strict NFRC requirements.

In order to participate in the Certification Program, a responsible party shall rate a product to be certified for mandatory NFRC rating procedures. At present, a responsible party may elect to rate products for U-factor, solar heat gain coefficient, visible transmittance, air leakage, condensation resistance, or any other procedure adopted by NFRC, and to include those ratings on a label affixed to its products (or Certificate for site-built products).

U-factor, SHGC and VT, AL, and CR rating reports shall be obtained from a laboratory, which has been accredited by NFRC in accordance with the requirements of the Laboratory Accreditation Program (LAP).

NFRC maintains a Certified Products Directory, listing product lines and individual products selected by the responsible party for which product certification authorisation has been granted and listing all NFRC-licensed IAs and NFRC-accredited testing simulation laboratories.

NFRC manages the Rating System and regulates the Product Certification Program (PCP) , Laboratory Accreditation Program (LAP) and Certification Agency Program (CAP) in accordance with the PCP, the LAP and the CAP procedures, and conducts compliance activities under all these programs as well as the Compliance and Monitoring Program. NFRC continues to develop the Rating System and each of the programs.

NFRC owns all rights in and to each of the PCP, LAP, CAP, Compliance and Monitoring Program, and each procedure, which is a component of the Rating System, as well as each of its certification marks, trade names, and other intellectual property.

Approved Simulation Software

- Therm 5.2
- Window 5.2
- Optics 5.1.02

Approved Simulation Documentation

The following documents are to be used in conjunction with the exceptions in this manual:

- NFRC Simulation Manual
- Current 2001/2004 Technical Interpretations (ie. NFRC TIPC Interpretations)
- Creating a Laminate in Optics for NFRC

Chapter 2

Scope

This AFRC User Manual provides guidelines and explains the procedure to AFRC-licensed users in Australia to obtain thermal performance ratings for fenestration products within product lines from AFRC-accredited simulation and testing laboratories, and obtain a certification authorisation report (CAR) for these ratings, and authorisation to label products from AFRC-licensed independent agencies (IAs).

This manual specifically documents the Australian variations and rules and should be read in conjunction with the PCP, the LAP, the CAP and the technical procedures of the NFRC.

Each participant of this program acts independently to report, authorise for certification, and certify a rating.

AFRC and NFRC do not certify a product and certification does not constitute a warranty of AFRC or NFRC regarding any characteristic of a fenestration product. Certification is not an endorsement of or recommendation for any fenestration product or product line or any attribute of a product or product line. AFRC and NFRC are not merchants in the business of selling fenestration products and therefore cannot warrant products as to their merchantability or fitness for a particular use.

AFRC and NFRC therefore disclaim any and all liability that may arise from or in connection with services provided by, decisions made by, or reports or certifications issued or granted by any NFRC-accredited laboratory, NFRC-licensed IA or any product manufacturer; reliance on any NFRC product description, specification, rating, test or certification, whether appearing in a report, a product certification authorisation or a printed or electronic directory, or on a label; or the sale or use of any NFRC-rated or certified fenestration product or product line; including but not limited to damages for personal or other injury, lost profits, lost savings or other consequential or incidental damages.

AFRC program participants are required to indemnify AFRC from and against such liability.

Chapter 3

Approved Glass Library

REFERENCES

NFRC Simulation Manual
2001/2004 Technical Interpretations (NFRC TIPC Interpretations)
Creating a Laminate in Optics for NFRC

3.1 GENERAL

The **only** sources of glass spectral data are:

- The International Glazing Database (IGDB) as issued by Lawrence Berkeley National Laboratory (LBNL). The current version of the IGDB is located at http://windows.lbl.gov/materials/IGDB/default.htm
- NFRC approved spectral data is identified by a # sign in the IGDB.
- Laminates constructed by an accredited simulator in accordance with NFRC procedure "Creating a Laminate in Optics for NFRC".

3.2 AUSTRALIAN EXCEPTION

Australia only permits the use of IGDB certified data including, but not limited to, NFRC data with the # sign and laminated glass constructions as defined above. To be classified as IGDB certified data, the data must have a valid IGDB version number. This number is found in the Source column of the Glass Library in Window5.

3.2.1 Non-Valid IGDB Data

- Data with the Source 'User' with the exception of laminates as described above.
- Data with the Source 'Optics5 vx.x' where 'x' indicates the version number of Optics5 with the exception of laminates as described above.
- Data with the Source 'IGDB v12.2' with the exceptions of IGDB ID 1343 and 1344 with the exception of laminates as described above. (IGDB 1343 and 1344 are permitted because they are identified as NFRC approved (or #) products.)

3.2.2 Additional Notes

a. Glazing with an applied film is to be measured as a spectral data file on the appropriate substrate (3mm clear, 6mm clear and 6mm grey) and have an approved IGDB number.
b. Obscure and patterned glass products are modelled as their base glass properties (refer TI-2004-13)
c. Glass blocks and blinds are not currently included.
d. The nominal glass thickness used in the IGDB and by the NFRC is based on imperial thicknesses found in ASTM C1036-97. Glass intended for use in the Australian market should be represented by metric nominal thickness as stated in AS 4667:2000 and AS2208:1996. If a product falls outside the metric nominal thickness range, only a thinner product may be substituted.

Chapter 4

Simulation Process

REFERENCES

NFRC 100-2004
NFRC 200-2004
NFRC 500-2004
NFRC Simulation Manual
NFRC Approved Simulation Computer Programs
2001/2004 Technical Interpretations (NFRC TIPC Interpretations)
Creating a Laminate in Optics for NFRC
NFRC PCP-2005

4.1 GENERAL

All simulations are to be performed using NFRC Approved Software, NFRC Approved Simulation Documentation (see Chapter 1) and NFRC technical documents (NFRC 100-2004, NFRC 200-2004, NFRC 500-2004).

4.1.1 Overview

Receive Manufacturer's Documentation

a. Create Glazing Library with any Product Grouping using Approved Simulation Software (see Chapter 1) and the Approved Glass Library (see Chapter 3)
b. Create frame component files using Approved Simulation Software (see Chapter 1)
c. Create complete window file using the data from steps 1 and 2 and Approved Simulation Software (see Chapter 1)

4.2 ENVIRONMENTAL CONDITIONS

The glazing, frames and whole windows are modelled using NFRC 100-2001 environmental conditions.

4.3 SIMULATION SOFTWARE

Simulations are to be performed using Approved Software. For the current list of approved software see Chapter 1.

4.4 MANUFACTURER'S DOCUMENTATION

The minimum documentation that a manufacturer shall provide to the simulator is as follows:

- Manufacturer's Details (name, address, contact details)
- General Product Description (Series or model type, operator type, size, framing type, glazing type, spacer type)
- Accurate scale assembly drawings including frame component/part numbers

- Dimensioned frame component drawings (including material types)
- Glazing Material including:
    - thickness,
    - coatings and films (if present) with location identified (surface),
    - gap width (insulated glass units),
    - gas fill (type of gas and fill method)
    - spacers – materials, construction, drawings

4.5 CREATION OF GLAZING LIBRARY

The Glazing Library is created using Approved Simulation Software and the Approved Glass Library. Nominal glass thickness is to be used when modelling. After the creation of the Glazing Library, similar products can then be grouped, as per the NFRC product grouping rules, to minimise the total number of simulations to be performed.

4.6 PRODUCT GROUPING FOR GLAZING

The rules for product grouping by U-value are present in NFRC 100-2004.

4.7 CREATION OF FRAME COMPONENT FILES

The frame component files are to be created using Approved Simulation Software following the guidelines of the NFRC Approved Simulation Manual. The Simulation Manual details how frame sections should be modelled including, but not limited to, frame cavities, boundary conditions, U-value tags. The default frame absorptance for residential products is 0.30. The default frame absorptance for commercial products is 0.50.

4.8 CREATION OF COMPLETE WINDOW FILE

To create a complete window file, the following is required:
- Glazing components (modelled using Approved Simulation Software)
- Frame components (modelled using Approved Simulation Software)
- Product Model Size
- An Approved Simulation software program

4.9 PRODUCT MODEL SIZE AND CONFIGURATIONS

The product model size and configurations used are given in NFRC 100-2004 Table 4-3. It is recognised that the standard simulation configurations are not representative of the typical window configurations found in Australian housing. The Approved Simulation Software is currently only able to simulate one or two light windows. For a multi-light product, the product shall be modelled as a single or two light window following the notes accompanying table in Section 4.10 below. This rule is applicable because some studies have shown that it is valid to extrapolate the values calculated with one and two light windows to multi-light windows.

4.10 EXTRACT FROM NFRC 100-2004 Table 4-3

(Using Australian nomenclature, with Model Size as height by width, SI units)

WINDOW PRODUCTS

Product Type	Opening (X) Non-operating (O)	Model Size (height by width) SI units
Awning, Single (Projecting)	X	600mm by 1500mm
Awning, Dual (Projecting)	XX	1200mm by 1500mm
Casement – Single	X	1500mm by 600mm
Casement – Double[1]	XX	1500mm by 1200mm
Double Hung (Vertical Slider)	XO or XX	1500mm by 1200mm
Fixed (incl. non-standard shapes)	O	1500mm by 1200mm
Folding Window	XX	1500mm by 1200mm
Horizontal Slider	XO or XX	1200mm by 1500mm
Louvre windows (Jal/Jal awning)	X	1500mm by 1200mm
Pivoted	X	1500mm by 1200mm
Tilt'n'Turn	X	1500mm by 600mm

DOOR PRODUCTS

Product Type	Opening (X) Non-operating (O)	Model Size (height by width) SI units
Door Transom	X	600mm by 2000mm
Folding Door[2]	XX	2000mm by 2000mm
Garage Door	X	2400mm by 3000mm
Sliding Patio Door with Frame[2]	XO or XX	2000mm by 2000mm
Swinging Door with Frame[3]	O, X, XO or XX	2000mm by 1000mm or 2000mm by 2000mm

OTHER FENESTRATION PRODUCTS

Product Type	Opening (X) Non-operating (O)	Model Size (height by width) SI units
Glazed Wall/Sloped Glazing	OO[4]	2000mm by 2000mm
Sidelight	X	2000mm by 600mm
Skylight/Roof Window	X[5]	1200mm by 1200mm
Tubular Daylighting Device (TDD)	O	350mm diameter

Notes:

1. Double Casements are to be rated only in the case where a single casement is not manufactured.
2. The double door shall be used to represent all door assemblies (OXO, OXXO). Where a multi panel door is required to be modelled, it shall be modelled as a two light door using the head, sill, jamb and mullion cross sections with the most 'finning'.
3. The single door shall be used to represent all door assemblies (single, double, multiple) unless the manufacturer does not produce a single door. In that case, the double door shall be used to represent double and multiple door assemblies.
4. Two lights with one vertical mullion. Curtain walls shall be simulated and tested with intermediate verticals as jambs and intermediate horizontals as head/sill frame members. Window walls shall be simulated and tested with intermediate verticals as jambs and standard head and sill members. For rating of curtain walls and window walls, area weight intermediate members based on centreline dimensions. Glazed wall and sloped glazing shall be simulated and tested with standard jamb, head and sill members. Refer to NFRC 100-2004, Section 5.6.
5. Fits over an 1180 mm by 1180 mm opening.

4.11 EXCLUDED PRODUCTS

The following products cannot be calculated for SHGC using NFRC 200-2004 simulation techniques:

- Tubular Daylighting Devices (TDD)
- Dome Skylights
- Prismatic diffusers
- Glass Blocks
- Translucent Glazings

4.12 SPECIFIC PRODUCT CONSIDERATIONS

4.12.1 What is Not Modelled

NFRC 100-2004 specifically excludes certain details which are not modelled in Therm. These include:

- Screens
- Optional interior trim
- Colonial Bars which are applied to the surface of the glass. Internal dividers between glass layers must be modelled as per NFRC 100-2004.
- Optional jamb, head and sill extensions.
- Interior or exterior shading devices.
- Non-continuous components such as hinges, locks, balances, operators, setting blocks, shear blocks and corner stakes.
- Reveal linings. Frames with removable reveal fins shall be modelled with the fins removed. Permanent reveal fins shall be modelled as per NFRC Technical Interpretation TI-2005-08.

Chapter 5

Reporting Formats

REFERENCE

NFRC LAP

5.1 GENERAL

The simulator shall produce both a test report for the client and for assessment by the auditor. Details are given below. All reported units to be SI (metric).

5.2 UNITS

Data reporting in the public domain shall be to one decimal place for U-value and to two decimal places for SHGC and VT, with a leading zero in the case of SHGC and VT. All results shall be reported in SI units. U-value shall be reported in W/m^2K.
(Example of Results: U-value = 5.6W/m^2K, SHGC = 0.39, VT = 0.56)

5.3 SIMULATION AND TEST REPORT CONTENTS

5.3.1 Administration

a. Name, address, telephone number and email address of simulation/test laboratory
b. Simulation date
c. Name, address and all contact details of the client
d. Unique report number for each product/product line
e. Simulation/test methods employed (eg; NFRC 100-2004)
f. Software versions used
g. Version of AFRC Protocols and Procedures User Manual used
h. A statement that the simulations/tests were conducted in full compliance with the applicable requirements
i. Rating size [height (mm) x width (mm)]
j. A statement that the report relates only to the fenestration products simulated/ tested
k. Name and signature of the Simulator-in-responsible-charge.

5.3.2 Product Description

A detailed written description and/or drawing(s) of the specimen including, where applicable:

- Manufacturer and model number
- General description of product (i.e. operator type, frame type)
- A window elevation identifying frame cross sections
- Scale drawings of cross-sections of the window system (keyed to the window elevation) identifying hardware, frame gasket and weather-stripping locations
- A bill of materials if full material descriptions are not included on the cross sectional drawings

- Individual product glazing characteristics, including IGDB numbers and version, local identification name, thickness, coatings and/or films and their location (surface number, starting from the outside)
- Gap characteristics including width, gas fill, type and design concentration
- Spacer drawing(s) identifying profiles and materials (spacer, sealants and desiccants)
- All continuous hardware
- Solar absorptance of frames and dividers if other than the default values

5.3.3 Simulation Results

- Total Product Area Weighted U-value (U), Solar Heat Gain Coefficient (SHGC) and Visible Transmittance (VT)
- Centre of Glass U-value (Ucog), Solar Heat Gain Coefficient (SHGCcog) and Visible Transmittance (VTcog)
- A table of the 0 and 1 Solar Heat Gain Coefficient and Visible Transmission SHGC/VT 0 & 1 values for no dividers and, if the manufacturer specifies that the product may have dividers, values with the standard default dividers
- ISO Damage Weighted Transmittance TdwISO
- Identification of each individual product within the product line simulated, if using grouping.
- For roof windows, Luminous Efficacy (VT/SHGC) (optional for other products)
- For commercial applications only, the following additional properties for both frame and edge-of-glazing are required: average and individual U-values, SHGCs and areas.

5.4 AUSTRALIAN VARIATION – WHOLE OF HOUSE SOFTWARE PROGRAM REQUIREMENTS

Note: These requirements are currently subject to review.

- Average outdoor and indoor Projected Frame Dimension (PFD), indoor frame total length and SHGC exterior total length
- Interior convective and radiative film coefficients
- Exterior convective and radiative film coefficients

Chapter 6

Australian Variation – Physical Testing

REFERENCES

NFRC 100-2004
NFRC 101-2004
NFRC 200-2004
NFRC 201-2004
Memorandum of Understanding

6.1 GENERAL

Testing is not currently required for U-value and Solar Heat Gain Coefficient except for products where these properties cannot be simulated. In such circumstances the following test procedures shall be adopted.

6.2 U-VALUE

NFRC 100-2004 Section 4.3.5 procedures shall be followed using relevant Australian model sizes. (Refer to Chapter 4.10) Physical Testing procedures are specified in NFRC 101-2004.

6.3 SHGC

The product shall be tested in accordance with NFRC 201-2004 to the standard conditions specified in NFRC 200-2004 Section 4.3. Relevant Australian model sizes shall be used. (Refer to Chapter 4.10)

Chapter 7

Simulator Training & Accreditation

REFERENCES

NFRC LAP
NFRC PCP-2005

7.1 GENERAL

The AFRC administer and provide the training and accreditation for all simulation and test laboratories. This training generally occurs at the NFRC office in the United States of America. The NFRC Laboratory Accreditation Program (LAP) details the requirements of simulation and test laboratories. To reduce the cost involved in the training and accreditation of Australian simulators, local training and accreditation procedures are based on the NFRC procedures and protocols.

7.2 AUSTRALIAN EXCEPTION

All simulators are to be trained in the use of the currently NFRC approved simulation software programs and technical procedures including the current Australia variations (as presented in this document). Membership of the NFRC is not mandatory for simulators or trainers. An individual may have both trainer and simulator status if all accreditation requirements are met for each category.

7.3 TRAINER REQUIREMENTS & ACCREDITATION

The individual shall have successfully attended and completed all the necessary examinations of the NFRC Simulator Accreditation or Train the Trainer Workshop and shall meet the following requirements:

- Participate in annual round robins as required (both internationally through the NFRC and on a national basis through the AFRC)
- Participate in annual workshops or training inline with NFRC requirements with respect to the AFRC
- Participate in random checks of other accredited trainers and be randomly checked by other accredited trainers
- Actively participate in the training of simulators to maintain status (timeframe)
- An active member of the AFRC Technical Protocols Committee
- Participate in the development of training procedures
- Participate in the evaluation of Simulator's examinations
- Meet the minimum simulation equipment requirements (refer to NFRC LAP for details)
- Meet the minimum operations manual requirements (refer to NFRC LAP for details)
- Meet the minimum record keeping requirements (refer to NFRC LAP for details)

7.4 SIMULATOR REQUIREMENTS & ACCREDITATION

The individual shall have successfully attended and completed all the necessary examinations of an Australian Accredited Training Course or the NFRC Simulator Accreditation or Train the Trainer Workshop and shall meet the following requirements:

- Meet the independence criteria
- Participate in national annual round robins
- Participate in any annual workshop/training and successfully complete any examination resulting from this workshop.
- Participate in random checks of other simulators and be randomly checked by other accredited simulators
- Participate in annual reviews
- Meet the minimum simulation equipment requirements (refer to NFRC LAP for details)
- Meet the minimum operations manual requirements (refer to NFRC LAP for details)
- Meet the minimum record keeping requirements (refer to NFRC LAP for details)

7.5 AUSTRALIAN ACCREDITED TRAINING COURSE

This training course involves learning how to perform simulations using the currently AFRC approved simulation software programs and technical procedures including the current Australia variations. It will be developed by the AFRC TAC. The course involves the successful completion of two test problems within a given time period (to be determined). The accuracy of the results is required to be within (to be determined) of the calculated value. The examination is assessed by an Australian trainer and may be cross-checked by another accredited trainer or simulator. The successful completion of this examination is required as part of the process to be successfully accredited as a simulator in Australia.

7.6 INDEPENDENCE CRITERIA

In order for a simulator/simulation laboratory to become or remain accredited the laboratory shall meet the laboratory independence requirements set out in this section, so that services are rendered objectively and without bias.

1. No accredited simulator, laboratory, owner, owners, officers, directors, managers or employees or any affiliated person may:
   a. Have any financial interest in any fenestration product or component manufacturer, supplier or vendor,
   b. Recommend the use of any product (or product component) for which the accredited simulator/laboratory provides simulation services,
   c. Recommend the use of a particular thermal performance certification agency,
   d. Be involved in the commercial design or fabrication of fenestration products or components.

2. No accredited laboratory shall accept any payment or consideration of any kind, from any person, in exchange for the laboratory's reporting a rating or simulation result that appears to meet or comply with the requirements of the Australian Supplement AFRC documents when the testing or simulation was in fact not conducted and reported in compliance with those requirements.

3. Each accredited simulator/laboratory shall keep confidential all product information, test data and other proprietary information developed for or acquired from the simulator/laboratory's clients to the extent required by such clients, except as may be expressly required by auditors or through the simulator and trainer cross checking process (for simulator and trainer reviews).

Chapter 8

Independent Auditor (IA)

REFERENCES

NFRC CAP-2005
NFRC PCP-2005
NFRC Certification and Inspection Agency (IA) Operations Manual.

8.1 GENERAL

An AFRC-licensed Independent Auditor (IA) is responsible for reviewing simulation laboratory reports and data files and certifying their validity. The IA shall comply with the requirements of the AFRC Certification Agency Program (CAP) with the following Australian exceptions.

8.2 ANNUAL IN-PLANT INSPECTIONS

Where a manufacturer participates in an independent certified Inspection Accreditation Program there is no requirement for such inspections by an IA. In such circumstances their role shall be limited to certification of simulation data. Otherwise, inspections shall be carried out as specified in the NFRC CAP-2005.

8.3 TECHNICAL AUDITING OF SIMULATIONS

In order to manage a system without auditing of all products, products shall be randomly selected and auditing shall be subcontracted out by the Gatekeeper. The Gatekeeper data upload fee shall contain an audit provision to allow for auditing of 30% of product lines on average across the industry, comprising a mix of random audits for practicing simulators and mandatory audits for new simulators

For a new accredited simulator the first 20 product lines simulated shall be audited. Where more than 5 glazing systems or glazing product groups are simulated within a product line, only 5 glazing systems or glazing product groups (if product grouping has been used) need to be audited per product line if no errors are found. If the first 20 product lines are found to be without error, the frequency of audit shall reduce to nominally 20% of product lines selected at random by the Gatekeeper.

In the event of a subsequent failed audit, the frequency shall increase to all product lines until 5 consecutive error-free ratings are generated. The simulator shall also review all intervening ratings since the last audit for the same type of error and submit a written report to the IA outlining the findings and any necessary remediation. The IA shall forward this report to the AFRC Board for their action.

In the event of an audit failure rate of 1 in 3 audits or greater, the AFRC Board shall review the accreditation status of the simulator. If any remedial action is not undertaken or is unsatisfactory or ineffective the Board reserves the right to suspend accreditation.

8.3.1 Auditing Checklist

The following is an overview of the items to be checked when auditing simulations. An exhaustive checklist is contained in the NFRC Certification and Inspection Agency (IA) Operations Manual.

Manufacturers Documentation

- Check documentation for completeness: manufacturers' details / product description.
- Check Assembly drawings: scale / frame, component part numbers.
- Check frame component drawings.
- Check glazing matrix: thickness, coatings & films, gas, spacers etc.

Glazing Library

- Check IGDB ID number, thickness, coatings & films (surface), gap width, gas fill.
- Check groupings (if used).

Frame Component Files

- Check Therm file properties: ID / cross section type.
- Check gravity vector.
- Check frame component materials against drawings.
- Check frame cavities: Nu number, slightly ventilated exterior cavities, taped edge cavities, frame cavity surface emissivity (hollow aluminium sections).
- Check Glazing library / ID / CR cavity height / options.
- Check Glazing Sight line / spacer height / edge of glass dimension / glazing system height.
- Check boundary conditions / tags.
- Check U-value is set to 'projected Y'

Complete Window File

- Check window type / mode / conditions.
- Check glazing system.
- Check frame elements.

Simulation Report

- Check manufacturer's details.
- Check client details
- Check window type / mode / conditions.
- Check results / units.
- Check window report file.

8.4 INDEPENDENCE CRITERIA

An IA shall satisfy the independence criteria stipulated for simulators. An IA may also perform the role of simulator provided they do not act as Simulator and IA on any given simulation.

8.5 IA TRAINING AND ACCREDITATION

IA's must meet the training and accreditation requirements of a Simulator. In particular they must participate in annual round robins and annual workshops and any related examinations. In addition an IA must submit to an initial inspection by two members of the NFRC Technical Committee to verify compliance with the requirements of the NFRC CAP-2005.

Chapter 9

Technical Interpretations Policy Committee (TIPC)

REFERENCE

2001/2004 Technical Interpretations (NFRC TIPC Interpretations)

9.1 GENERAL

Technical Interpretations Policy Committee (TIPC) is a standing NFRC committee that provides supplementary technical advice and rulings to NFRC participants. It was created because existing NFRC technical procedures and documents do not always provide clear guidance, especially regarding modelling procedures. The NFRC Simulation Manual is replete with worked examples and TIPC complements that document. TIPC rulings are contained in *2001-4TechnicalInterpretations071006.pdf.* The benefits of TIPC are i) a quicker turnaround on questions requiring interpretation, and ii) more time available during regular committee and membership meetings for the development of new procedures.

TIPC meets once a month by teleconference. Because most TI requests are from highly experienced simulators, TIPC requires that a request be accompanied by a suggested answer. If TIPC members agree with the proposed answer the committee will simply answer 'yes'. If they do not agree, the committee will provide a workaround or a solution.

Totally new language issued by TIPC is not automatically added to the relevant technical procedure(s). That action occurs during the normal cycle of document revision which is normally four years but can be shorter in the case of urgent issues. For this reason, NFRC simulators and test labs are expected to be familiar with and to refer to the latest version of the TIPC document when carrying out ratings.

9.2 AusTIPC

For practical reasons, it is recommended that the AFRC Technical Advisory Committee function as a local TIPC ('AusTIPC'). Rulings shall be considered by that committee and finalised by consensus. The current NFRC TIPC request form ('TIR') shall be used and forwarded to the AFRC Board. Once an AusTIPC ruling has been issued, if it is related to current NFRC procedures it shall be forwarded to NFRC TIPC for peer review and approval. If the AusTIPC request relates to non-NFRC (i.e. Australia-only) provisions, the AusTIPC ruling may be optionally forwarded to AFRC Board, depending on the judgment of AusTIPC.

National Fenestration Rating Council

ATIR-year-*xx*
00/00/00

NFRC Technical Interpretation-2001 (AFRC)

Interpretation Requested:

Date Requested:	***Initial Interpretation Date:***	***Final TIPC Approval Date:***

Pertinent Document:	
Referenced Sections:	***Referenced Pages:***

Interpretation :

Technical Committee Revisions to Initial Interpretation:

Chapter 10

Software Validation

REFERENCE

NFRC Software Approval Guidelines

10.1 GENERAL

The NFRC Software Approval Guidelines document sets out the procedure for the approval of software by the NFRC. The process involves the formation of a task group to review the software. The task group consists of a minimum of three NFRC members and one NFRC Staff member. This group reviews and evaluates the software and any additional manuals and validation data provided by the software author/vendor. The task group then forms a report based on the NFRC Software Approval Guidelines document for discussion and review by the Software Review Subcommittee.

The NFRC Software Approval Guidelines document shall be followed for Software Validation in Australia with the following exceptions.

10.2 AUSTRALIAN EXCEPTION

An Australian Software Approval Task Group consisting of a minimum of three members will be appointed by the AFRC Board to evaluate new software. The members of this task group shall be independent of the Software author/vendor and consist of at least two AFRC-accredited simulators and an auditor engaged to assess the software. The validation input data should be based on recommendations from NFRC but shall also include data for products considered typical of Australian manufacture.

The Software author/vendor is required to present documentation and supporting evidence to meet the requirements set out in the NFRC Software Approval Guidelines including all algorithms used for calculations.

A report on the accuracy and stability of the software and any other pertinent observations shall be provided to the Board for evaluation with a copy returned to the developer. This report may be forwarded to the NFRC Software Approval Task Group for their recommendations at the discretion of the Board.

Upon Board approval, the software will be added to the list of Australian Approved Software Programs for subsequent inclusion into AFRC Protocols.

Chapter 11

Dispute Resolution

REFERENCES

AS 4608-2004 Dispute Management Systems
AS ISO 10002-2006 Customer Satisfaction-Complaints Handling Guidelines
NFRC CAP-2005

11.1 AFRC COMPLAINTS PROCEDURE GUIDELINES

11.1.1 General

Adherence to the guiding principles set out in 11.1.2 to 11.1.6 is recommended for effective handling of complaints or challenges.

11.1.2 Visibility

Information about how and where to complain should be well publicised to customers, personnel and other interested parties.

11.1.3 Accessibility

Information should be made available on the details of making and resolving complaints. The complaints-handling process and supporting information should be easy to understand and use. The information should be in clear language. For information and assistance in making a complaint refer 11.2.1

11.1.4 Responsiveness

Receipt of each complaint should be acknowledged to the complainant immediately. Complaints should be addressed promptly in accordance with their urgency.

11.1.5 Objectivity

Each complaint should be addressed in an equitable, objective and unbiased manner through the complaints-handling process referred to in 11.2.2.

11.1.6 Charges

Access to the complaints-handling process should be free of charge to the complainant.

11.2 AFRC COMPLAINTS PROCEDURES

11.2.1 Making a Complaint

A complaint shall be noticed in writing and shall be sent by a method which provides evidence of delivery to the Secretary of the AFRC and shall specify the basis for the complaint. Complaints shall be specific and include supporting documentation, contact details and the resolution being sought.

Upon receipt of the complaint the Secretary shall log the correspondence and forward the details, including action to be considered, to the appropriate party and advise the complainant of the course of action to be taken and an approximate time for redress:

a. The chair of the TAC will be responsible for processing technical issues
b. The board of the AFRC will be responsible for all other issues

11.2.2 Handling a Complaint

In the event of a complaint being received by the Secretary of the AFRC, the following process shall be followed:

a. Details of the complaint entered into complaints register
b. Notification of receipt sent to complainant
c. Complaint and request for action forwarded to the appropriate AFRC committee
d. Resolution, including recommended actions, returned to the Secretary. This must include supporting documentation for the committee's decision.
e. Approval from the AFRC board.
f. Recommendations actioned and recorded
g. Notify complainant in writing

11.3 AFRC LICENSING AND APPEALS PROCEDURE

11.3.1 Grounds for Suspension of Licensing

An IA's license may be suspended by the AFRC Board pursuant to the express provisions of the AFRC.

11.3.2 Grounds for Revocation of Licensing

An IA's license shall be revoked by AFRC in any of the following circumstances:

a. Pursuant to the non-fulfillment of the provisions contained in the CAP within the required time period;
b. Upon the expiration of an IA's right to appeal a suspension of licensing;
c. Upon a determination by the AFRC Board that an IA has acted in such a manner as to
   - Impair the objectivity or integrity of the Certification Agency Program or harm the reputation of AFRC, including, but not limited to, submission of false information to AFRC, or failure to submit to AFRC any material information required to be submitted, in connection with obtaining or maintaining licensing;
   - Knowingly or negligently issue reports that fail to meet all of the requirements of applicable testing or simulation methods; or
   - Make misrepresentations in advertising or promotional materials of its license status in general or with respect to any service that the IA offers.

11.3.3 Appeals Procedure

a. In the event that AFRC licensing has been denied, suspended or revoked the IA shall have the right to appeal to the AFRC under the rules detailed in NFRC CAP-2005.
b. An appeal shall be noticed in writing and shall be sent by a method which provides evidence of delivery to the Chair of the AFRC or the Board of Directors, as the case may be, with a copy to the AFRC Inspector, and shall specify the basis for the appeal.
c. An IA may also appeal a suspension of the IA License Agreement pursuant to this section.
d. An applicant for IA licensing may also appeal a denial of licensing to the AFRC Board of Directors pursuant to this section.

Chapter 12

Non-Residential Glazing

REFERENCE

NFRC 100-2004

12.1 GENERAL

Non-residential glazing is currently considered under NFRC 100-2004 Section 5.6. This section currently covers but is not limited to the following product types:

- Glazed wall support and framing systems
- Products of any size or design
- Products with single or multiple glazing layers
- Products with spacer systems between glazings
- Horizontal, vertical and sloped systems
- Products that, by design, may have multiple framing components and/or glazing combinations
- Fenestration systems using unitised construction, where a system is field assembled from factory-assembled sub-units

The systems not covered include:

- Totally opaque walls, including spandrels.

The standard size for a Glazed Wall is 2000mm by 2000mm consisting of two lights with one vertical mullion. See Section 4.10 for further details.

12.2 AUSTRALIAN EXCEPTION

Pre-assembled or pre-glazed fenestration products can be simulated, eg. unitised curtain walls.

Glazed spandrel panels are currently excluded but may be considered for inclusion in a future revision.

Project 3.2
Australia (b)

Project Name: International Harmonization - Australia

Date: November 2006

Purpose: The Australian Fenestration Rating Council (AFRC) was established to provide an energy rating system for windows and doors that is fair, accurate and credible in application. The AFRC is the Australian operator of the NFRC.

Project Summary:

NFRC continues to work with the Australian Fenestration Rating Council (AFRC, a new NFRC licensee) as they begin to certify fenestration products according to NFRC procedures. The ARFC website contains numerous technical documents that were jointly developed with NFRC: www.afrc.org.au NFRC works with the Australian Window Association (AWA) closely to continue work toward NFRC harmonization.

Click here for the NFRC-AFRC license agreement

License and Support Agreement

Between

National Fenestration Rating Council

and

Australian Fenestration Rating Council

This License and Support Agreement (the "Agreement") is made this ___ day of _____, 2006 by and between National Fenestration Rating Council, Incorporated, a not-for-profit U.S. corporation organized in the State of Maryland ("NFRC") and the [Australian Fenestration Rating Council, a _____ ("AFRC")].

RECITALS

A. NFRC owns and controls the use of procedures for rating thermal performance and other performance attributes of fenestration products as set forth in Exhibit A hereto, as such procedures are amended and supplemented from time to time (the "Rating System").

B. NFRC owns and controls the program for rating (by computer simulation and physical testing), certification and labeling of fenestration products for thermal performance and other attributes (the "Certification Program"), including as set forth in the documents entitled NFRC PCP: Product Certification Program, the NFRC LAP: Laboratory Accreditation Program and the NFRC CAP: Compliance Assurance Program (collectively, the "Program Documents"), as the Program Documents are amended from time to time by NFRC.

C. NFRC employs and/or contracts with individuals with knowledge and experience with the Rating System, Certification Program and the Program Documents, including administration of the labeling program used in connection with the Rating System.

D. NFRC operates a database of certified residential fenestration products of manufacturers who are NFRC licensees (the "Database"). NFRC owns the software used to create and operate the Database (the "Database Software").

E. AFRC is an organization which wishes to establish a system for rating, certification and labeling of fenestration products in Australia (the "Australian Rating System") that will employ NFRC's Rating System. AFRC desires to use, reproduce and modify some or all of the Rating System, Certification System, Program Documents, and the Database Software for the development of the Australian Rating System and seeks professional training and assistance from NFRC employees and agents in creating and implementing the Australian Rating System.

F. NFRC is willing to assist AFRC in the development of the Australian Rating System on the terms set forth below.

NFRC and AFRC hereby agrees as follows:

SECTION 1
COPYRIGHT LICENSE

(a) NFRC hereby grants to AFRC a non-exclusive, non-assignable license, during the term of this Agreement to reproduce, make and distribute copies of the Rating System, Certification Program and Program Documents (collectively, the "NFRC Materials") in Australia and the right to make derivative works of the NFRC Materials, in each case in connection with AFRC's development and operation of the Australian Rating System. NFRC agrees to provide to AFRC all updates or modifications to the NFRC Materials created by NFRC from time to time.

(b) AFRC shall have the right to prepare derivative works based on the NFRC Materials including the right to maintain, update, modify or utilize the derivative works in any manner AFRC chooses. AFRC shall own all right, title and interest in the derivative works, subject to NFRC's retention of its copyright ownership in the NFRC Materials.

(c) AFRC shall indicate in any written materials in which all or part of the NFRC Materials appear that the NFRC Materials and the copyright in the NFRC Materials are the exclusive property of NFRC and are used by AFRC pursuant to a license from NFRC.

(d) This Agreement does not grant to AFRC any right to use any trademarks, service marks, collective marks, or certification marks owned by NFRC in any manner.

(e) AFRC hereby acknowledges NFRC's exclusive ownership and proprietary rights in the NFRC Materials and agrees to take no action inconsistent with such rights or with the terms of this Agreement.

(f) NFRC and AFRC agree to work cooperatively in good faith to assure that the Australian Rating System recognizes and utilizes the NFRC Rating System.

SECTION 2
TRAINING

(a) NFRC shall develop a training program to instruct AFRC designated individuals on the conduct of computer simulation of fenestration products under NFRC's simulation program under the Rating System. NFRC agrees from time to time to conduct the training programs in Australia at times and locations agreed to by both parties. Individuals who have attended and successfully completed the simulation training

program in accordance with NFRC requirements will be accredited by NFRC to conduct simulation training programs for AFRC.

(b) AFRC agrees to send at least one accredited trainer for an NFRC conducted mandatory workshop training to be conducted by NFRC annually. AFRC also agrees to require an AFRC designated trainer who has been accredited by NFRC to participate in NFRC conducted "round robin" testing programs. AFRC agrees to allow only NFRC accredited trainers to conduct simulation training programs for the Australian Rating System.

SECTION 3
OTHER SERVICES

The parties recognize that from time to time AFRC may request consultation with NFRC personnel for advice or other input on technical and other matters relating to the Australian Rating System that are not otherwise provided by NFRC pursuant to the other provisions of this Agreement. NFRC will use reasonable commercial efforts to provide such additional services in a timely, cost effective manner and AFRC shall pay NFRC for such services based on NFRC's standard hourly charge for the time expended by NFRC personnel and contractors in providing those services. Any reasonable travel, lodging or other out-of-pocket expenses incurred by the NFRC in providing these services shall be reimbursed by AFRC, provided those expenses are approved by AFRC in advance.

SECTION 4
LICENSE TO DATABASE SOFTWARE

NFRC hereby grants to AFRC a non-exclusive, non-assignable license to use the Database Software during the term of this Agreement for the Australian Rating System. The Database Software shall be provided in object code form and may not be modified by AFRC without NFRC's consent. NFRC makes no representation or warranty regarding the Database Software, including its fitness for a particular purpose or that the Database Software is error free. NFRC shall have no obligation to maintain or support the Database Software but shall provide any updates or enhancements to the Database Software that are completed during the term of this Agreement. This license shall not include a license to software developed following the date of this Agreement for use in NFRC's non-residential fenestration rating program.

SECTION 5
TERM OF THE AGREEMENT

(a) This Agreement shall take effect on the date set forth above and shall continue until terminated as provided below.

(b) Either party may terminate this Agreement without cause, at any time on not less than 180 days prior written notice to the other party.

(c) Either party may terminate this Agreements on written notice if the other party breaches any of its obligations under this Agreement and fails to cure such breach within 30 days after receipt of a written notice detailing that breach.

(d) Any amounts that were due to NFRC prior to termination of the Agreement shall be paid promptly following the termination of the Agreement. Upon termination of this Agreement, all licenses granted hereunder to AFRC to the NFRC Materials and Database shall terminate.

SECTION 6
FEES AND EXPENSES

AFRC agrees to make the following payments to NFRC during the term of this Agreement. All payments are designated in and shall be paid in U.S. dollars.

(a) AFRC shall pay an annual fee of $20,000 USD to NFRC as a membership fee to become and remain a member of NFRC. AFRC shall make the initial fee payment on execution of this Agreement and thereafter shall make an annual membership fee payment of $20,000 USD on the successive anniversary dates of this Agreement.

(b) AFRC shall pay an annual license fee of $10,000 USD in consideration for the licenses granted pursuant to Sections 1 and 4 above. AFRC shall make the initial license fee payment on execution of this Agreement and thereafter shall make the annual license fee payment of $10,000 USD on the successive anniversary dates of this Agreement.

(c) AFRC shall pay a training fee of $2,500 USD for each person designated by AFRC to attend the NFRC simulation training program conducted in Australia by NFRC from time to time as referenced in Section 2 above. The fee shall be payable for each such training program attended by such individual.

(d) AFRC shall pay the actual out-of-pocket travel and lodging expenses incurred by one NFRC designated observer to conduct the initial simulation training course in Australia. AFRC shall also pay NFRC for the time expended by that NFRC observer at NFRC's standard hourly rate up to a maximum of $5,000 USD. NFRC's initial hourly billing rate under this Agreement is $100 USD. The hourly rate may be increased no more frequently than once per year and may not increase more than 15% per year.

(e) ARFC shall pay NFRC for any additional services provided by NFRC at AFRC's request pursuant to Section 3 above at NFRC's standard hourly billing rates.

(f) All amounts owed by AFRC to NFRC hereunder (other than payment due upon execution of this Agreement) shall be due within 15 days after receipt of an NFRC invoice for such amount.

(g) Except as expressly provided in this Section 6, each party shall be responsible for its own fees and expenses incurred in connection with this Agreement.

SECTION 7
MISCELLANEOUS

(a) Any notices required to be given to a party hereunder shall be deemed given when received by that party at the address set forth on the signature page to this Agreement.

(b) This Agreement shall be construed in accordance with the federal and state laws of the United States, including, but not limited to the U.S. Copyright Act.

(c) NFRC is an independent contractor to AFRC and neither party is the agent, partner or joint venturer of the other party and neither party has the right to legally bind or contract for the other party.

(d) Neither party shall have the right to assign this Agreement to any other entity or person without the prior written consent of the other party.

(e) This Agreement constitutes the entire agreement between the parties and supersedes and replaces any prior oral or written agreements regarding the subject matter hereof.

(f) This Agreement may be executed in counterparts.

SO AGREED:

National Fenestration Rating Council	**Australian Fenestration Rating Council**
8484 Georgia Avenue Suite 320 Silver Spring, MD 20910	
By:_____	By: _____
Executive Director	Title: _____

Exhibit A

NFRC owns and controls the use of procedures for rating performance and other attributes of fenestration products (the "Rating System") set forth in *NFRC 100: Procedure for Determining Fenestration Products U-factors ("NFRC 100") and NFRC 200: Procedure for Determining Fenestration Product Solar Heat Gain Coefficients and Visible Transmittance at Normal Incidence ("NFRC 200"), et seq.,* as amended and updated from time to time, *NFRC 400: Procedure for Determining Fenestration Product Air Leakage ("NFRC 400"), NFRC 500: Procedure for Determining Fenestration Product Condensation Resistance Value ("NFRC 500"), NFRC 101: Procedure for Determining Thermo-Physical Properties of Materials for Use in NFRC-approved Software Programs ("NFRC 101"), NFRC 102: Test Procedure for Measuring the Steady-State Thermal Transmittance of Fenestration Systems ("NFRC 102"), NFRC 201: Procedure for Interim Standard Test Method for Measuring the Solar Heat Gain Coefficient of Fenestration Systems Using Colorimeter Hot Box MethodS ("NFRC 201"), NFRC 300: Test method for Determining the Solar Optical Properties of Glazing Materials and Systems ("NFRC300"), and NFRC 301: Standard Test Method for Emittance of Specula Surfaces Using Spectrometric Measurements ("NFRC 301")* and *NFRC 400: Procedure for Determining Fenestration Product Condensation Resistance Values and NFRC 500: Procedure for Determining Fenestration Product Condensation Resistance Values,* copies of which have previously been provided to Licensee.

Project 3.2
India (a)

Project Name: International Harmonization - India

Date: December 2008

Purpose: National Fenestration Rating Council (NFRC) along with several partner companies is to participate in the ZAK Door and Window Trade show in New Delhi, December 5-7, 2008. NFRC and US-DOE will also host Building Envelope (Window Systems, Wall and Roof) Energy Efficiency Technology Conference to help introduce USA manufacturers energy efficient products in the Indian market place.

Project Summary:

At these events it is intended to provide information about the NFRC ratings and certification process, education literature for disseminating the advantages of using high energy performance. US-DOE activities of supporting development of high performance windows which will be highlighted by displaying product samples and simulation programs like EnergyPlus, THERM and WINDOW.

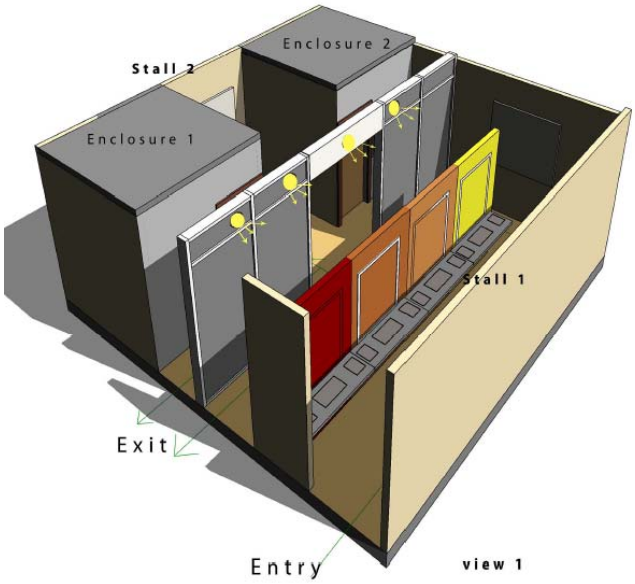
In the end, by participating we will achieve the Asia Pacific Partnership goal of encouraging high energy performance technology transfer, promotion of quality products in the market place and hence reductions in energy use resulting in less green gas emissions.

Click here for US- Pavilion and Building Envelope Conference summary and booth description

US- Pavilion and Building Envelope Conference - India:

National Fenestration Rating Council (NFRC) along with several partner companies is to participate in the ZAK Door and Window Trade show in New Delhi, December 5-7, 2008. NFRC and US-DOE will also host Building Envelope (Window Systems, Wall and Roof)Energy Efficiency Technology Conference to help introduce USA manufacturers energy efficient products in the Indian market place.
US-DOE has supported these events and will be participating at the show booth and conference along with NFRC. At these events it is intended to provide information about the NFRC ratings and certification process, education literature for disseminating the advantages of using high energy performance. US-DOE activities of supporting development of high performance windows which will be high lighted by displaying product samples and simulation programs like EnergyPlus, THERM and WINDOW.

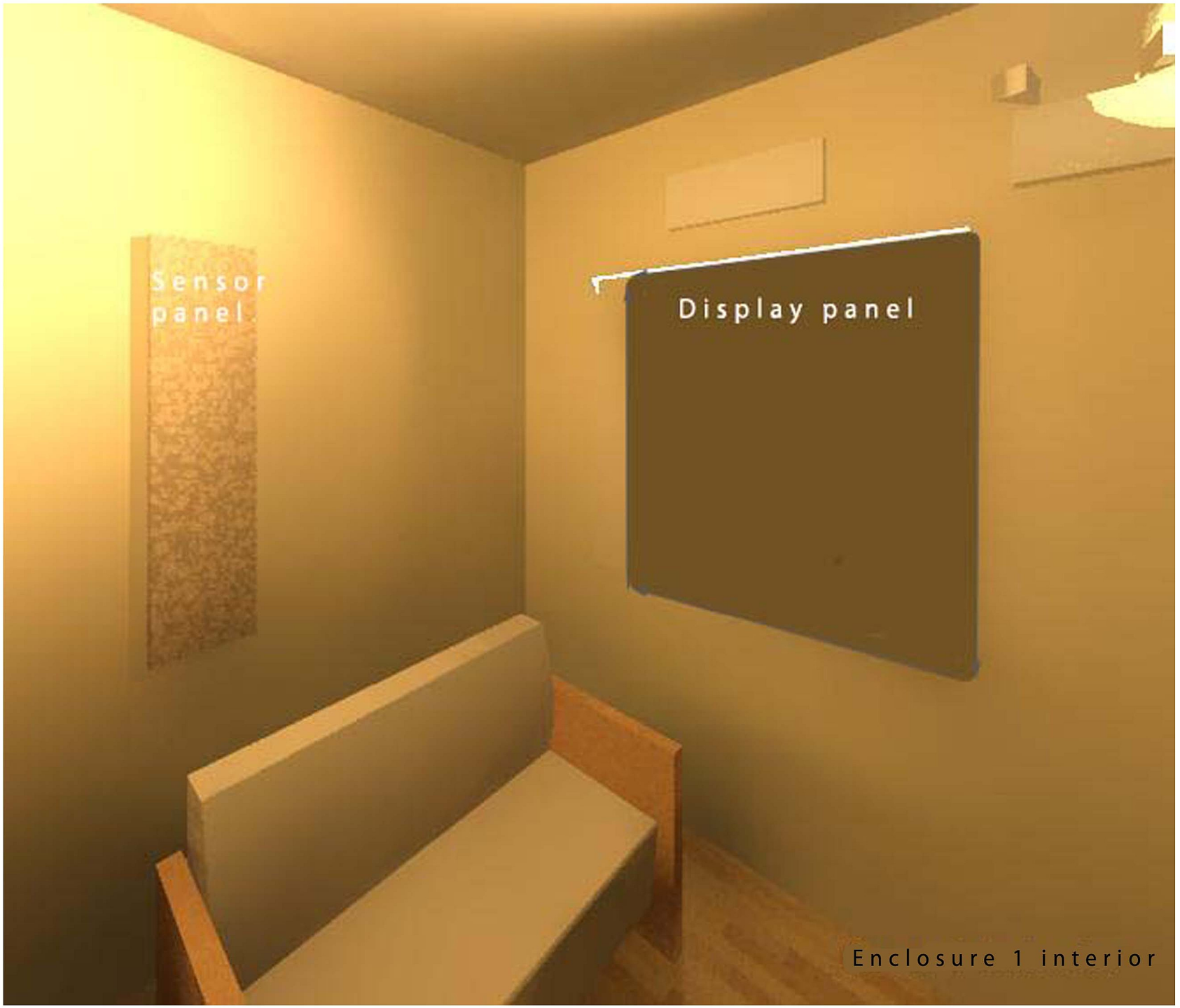
Major windows and glass industry companies in the USA are interested in developing Fenestration rating program and building capacity by setting up of test & simulation laboratories to launch national labeling and certification programs. This helps them to have a level plain field in the Asia Pacific Partner countries market place, especially India. NFRC has been actively assisting Center for environmental Planning and Technology (CEPT) in establishment of Regional Energy Efficiency Center which will have state of art simulation, testing and research facilities to support implementation of Energy Conservation Building Code (ECBC) of India

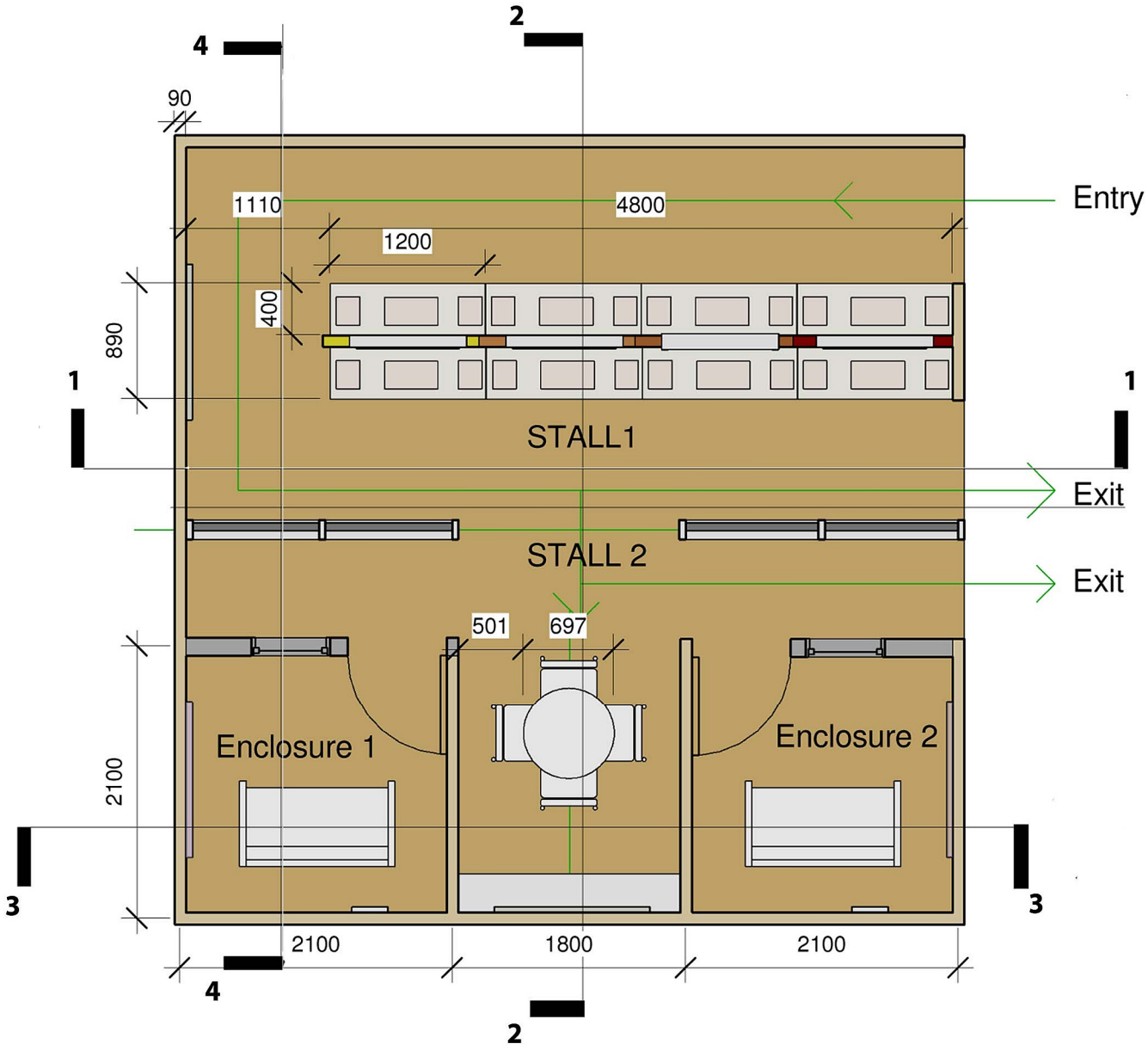


Further more it is in the USA interest to have North American standards be adopted by India so that duplication of certification cost and effort is reduced for the US companies.

ZAK Door and Window Trade show is the largest show for the fenestration industry in India and provide high visibility. Several countries, especially EU countries have been actively participating in the show for last 2 years. USA participation is for the first time and NFRC and US-DOE participation will help promote the US –companies and more energy efficient products in the Indian market place.

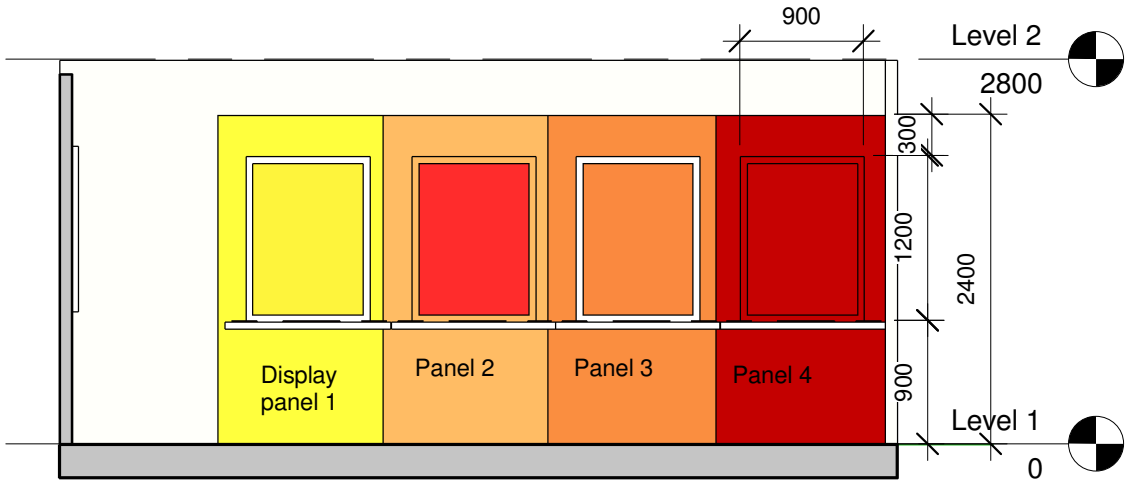
In the end, by participating we will achieve the Asia Pacific Partnership goal of encouraging high energy performance technology transfer, promotion of quality products in the market place and hence reductions in energy use resulting in less green gas emissions.


Sensor panel
Display panel
Enclosure 1 interior

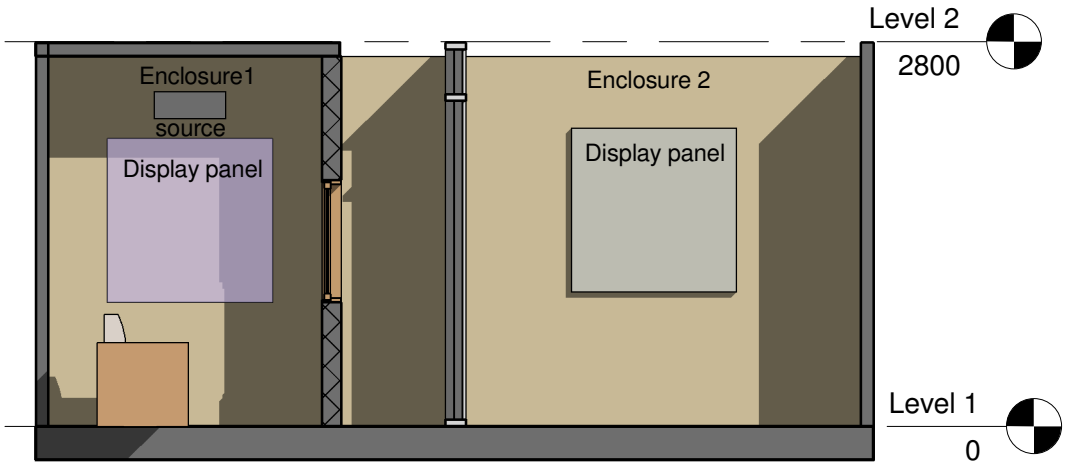


PLAN
SCALE 1:50

ALL DIMENSIONS ARE IN MM



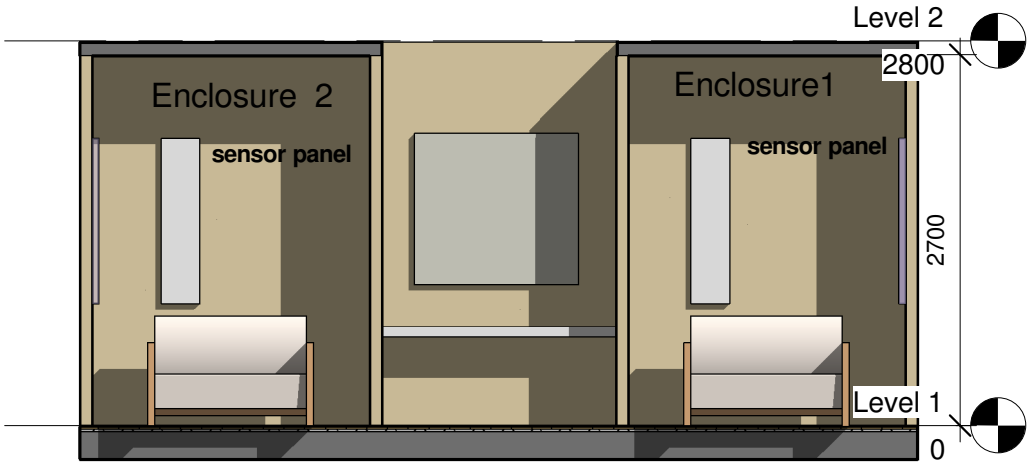
SECTION 1



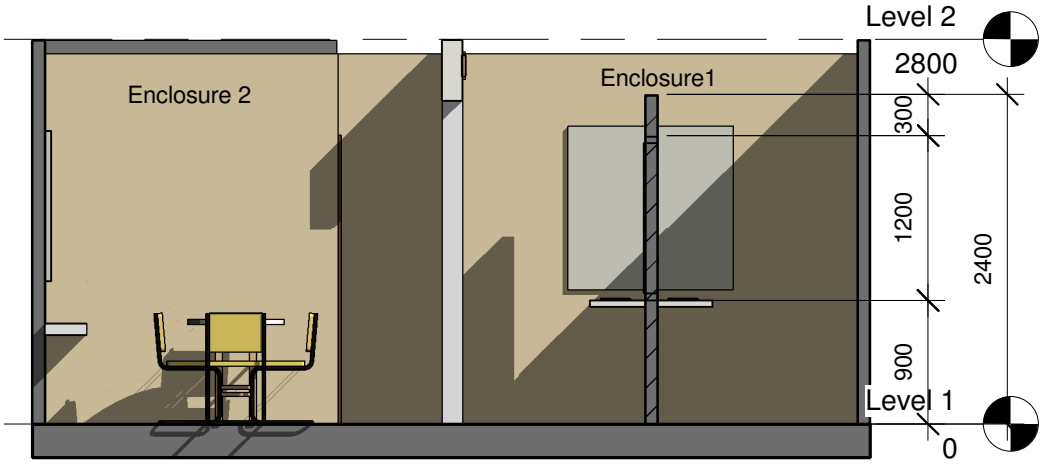
SECTION 2

Scale 1:50

All dimensions are in mm



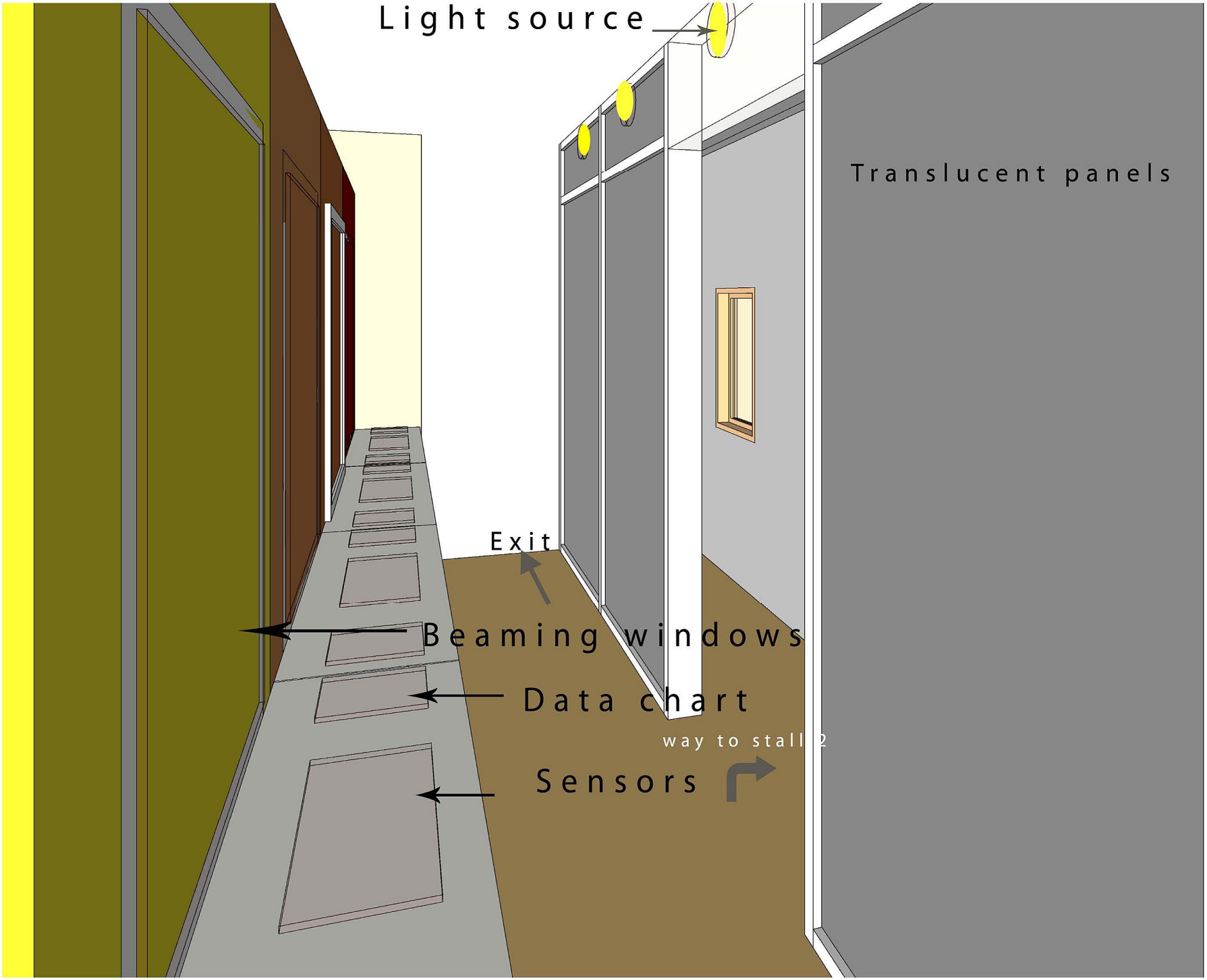
SECTION 3

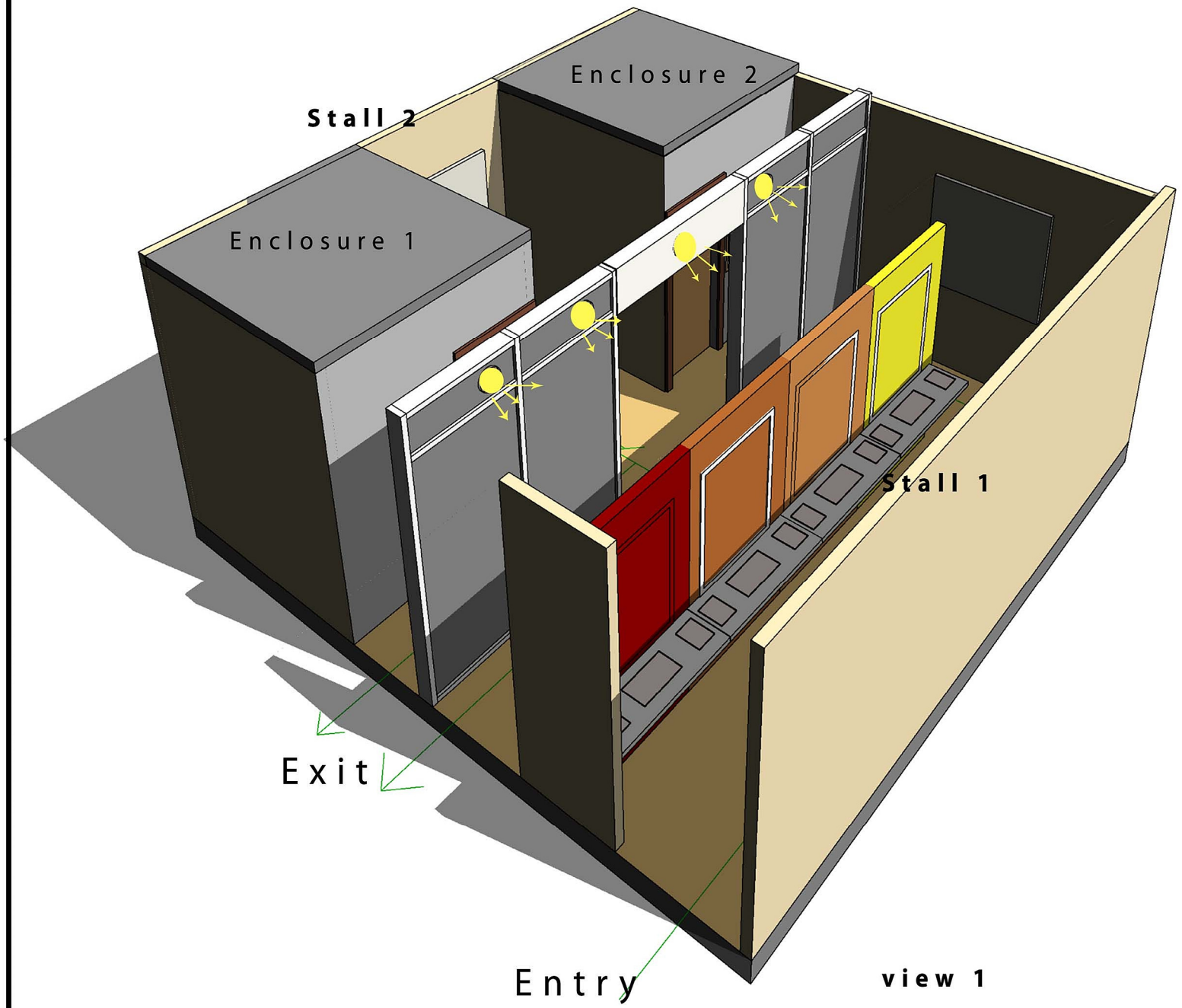


SECTION 4

Scale 1:50

All dimensions are in mm


Light source
Translucent panels
Exit
Beaming windows
Data chart
way to stall 2
Sensors



view 1



Project 3.2
India (b)

Project Name: International Harmonization - India

Date: December 2008

Purpose: National Fenestration Rating Council (NFRC) along with several partner companies is to participate in the ZAK Door and Window Trade show in New Delhi, December 5-7, 2008. NFRC and US-DOE will also host Building Envelope (Window Systems, Wall and Roof) Energy Efficiency Technology Conference to help introduce USA manufacturers' energy efficient products in the Indian market place.

Project Summary:

At these events it is intended to provide information about the NFRC ratings and certification process, education literature for disseminating the advantages of using high energy performance. US-DOE activities of supporting development of high performance windows which will be highlighted by displaying product samples and simulation programs like EnergyPlus, THERM and WINDOW.

In the end, by participating we will achieve the Asia Pacific Partnership goal of encouraging high energy performance technology transfer, promotion of quality products in the market place and hence reductions in energy use resulting in less green gas emissions.

Click here for a WinBuild presentation for Indian Visitors to the NFRC in the US

Supporting Infrastructure Required for Energy Ratings of Building Envelope Components (Windows, Wall & Roof)



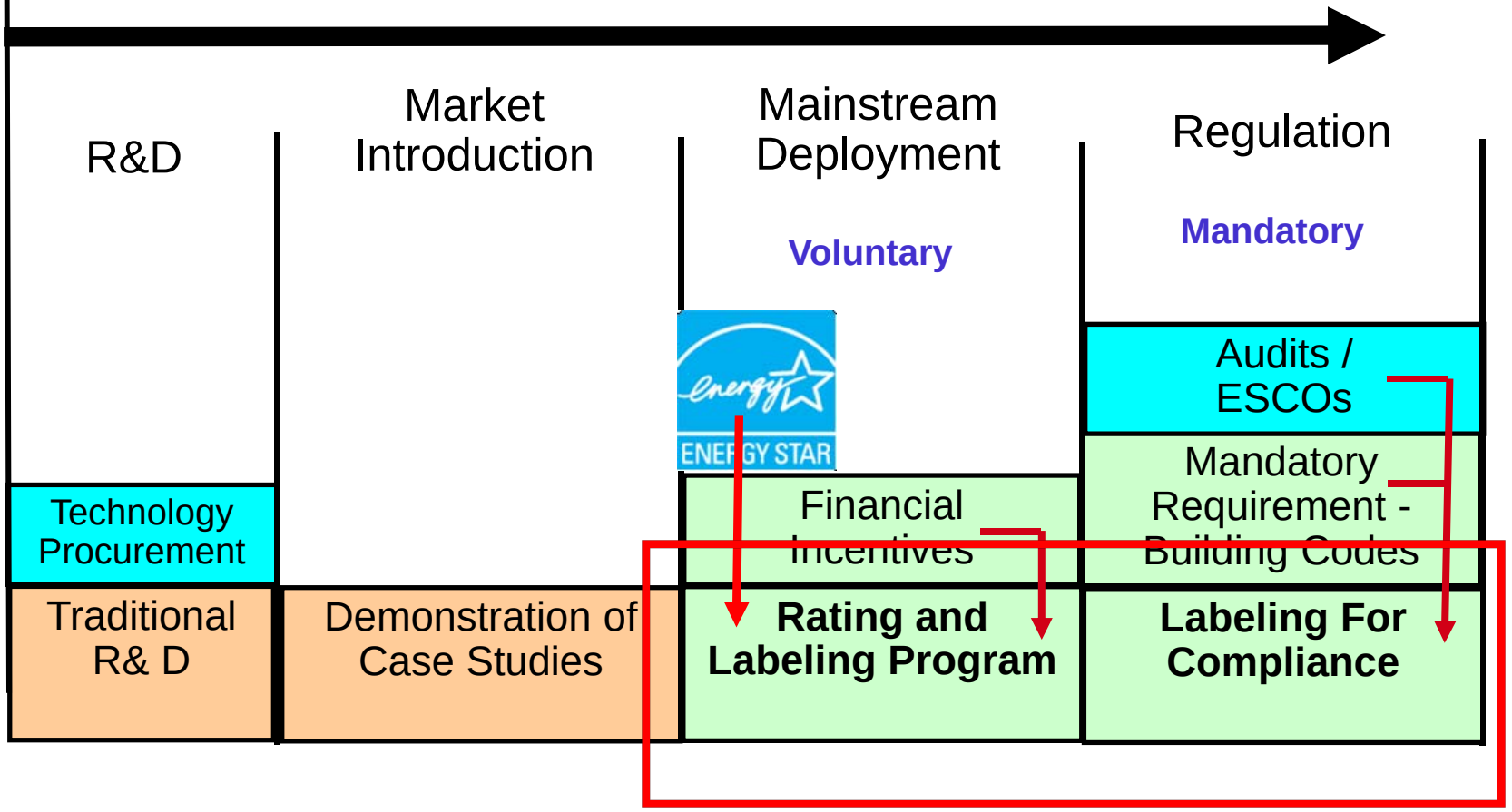




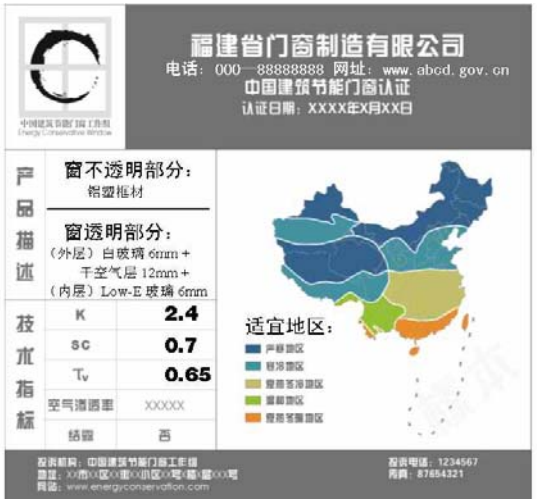


Bipin Shah
WinBuild Inc.
US DOE International Consultant
National Fenestration Rating Council – International Program Coordinator

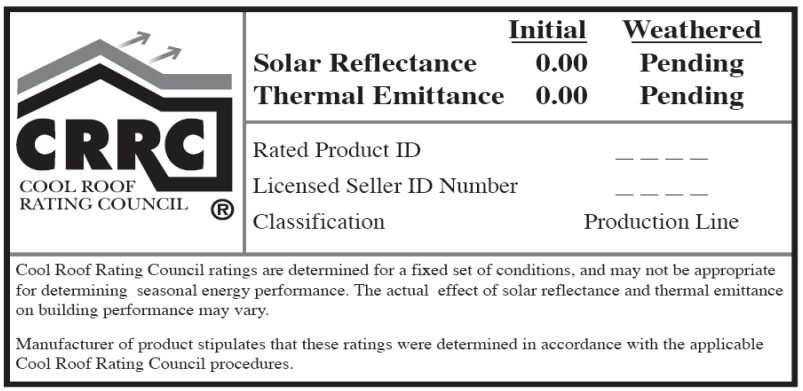
Policies – Commercialization Path



Rating and Certification









- **Label helps Verify the Compliance**
- **Helps consumer to distinguish products**

Testing Used for Product Certification

Fenestration:

- Simulation of U-factor, Solar Heat Gain Factor and Visible transmittance - ISO 15099
- U-factor testing - ASTM C 1363, C1199, NFRC 102
- Solar Heat Gain Testing – NFRC 201
- Spectral Optical Property – ASTM E903, NFRC 300, 301
- Air Leakage – ASTM E283, NFRC 400

Cool Roof

- Solar Reflectance Testing - ASTM E903, ASTM C1549, ASTM E1918 and CRRC-1
- Thermal emittance - ASTM C1371

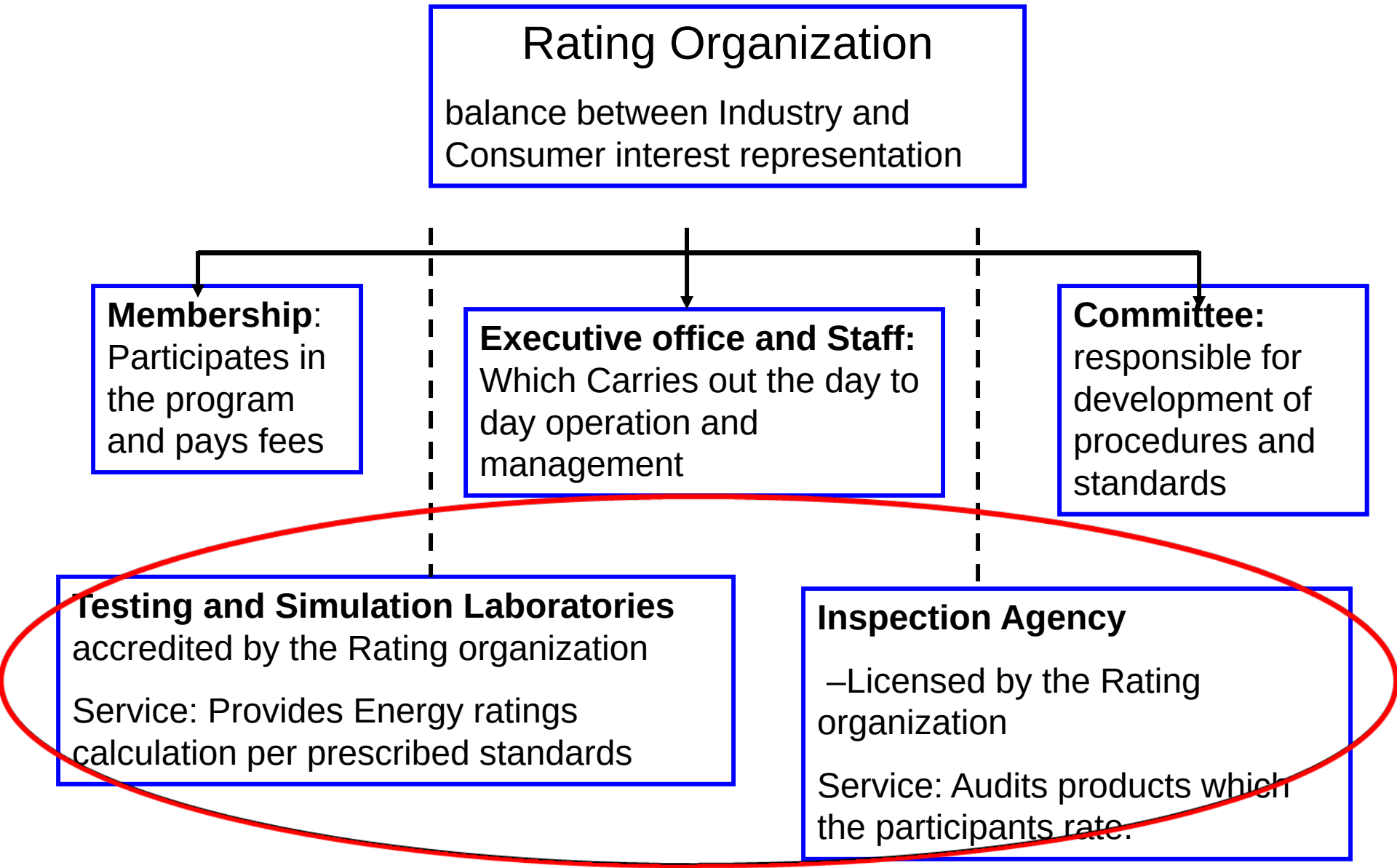
Wall Insulation

- ASTM C 518, C 177

Wall System

- ASTM C1363, ASTM C1155

Infrastructure Of A Rating Organization



Infrastructure

Rating organization should be a consensus and membership based:

- Executive Director appointed by Board of Directors assist in the implementation of the ratings program as developed by the rating organization.
  - Day to day operation.
  - Publish Standards and Procedures for Rating and labeling program.
  - Ensure quality control of accredited simulation & testing laboratories and the Inspection Agencies.
    - Organize Round Robin
    - Inspection of Laboratories and Inspection agencies
  - Provide training, accreditation and Licensing service
  - Maintain Database of the Certified Products

Simulation Laboratory

- Simulation Laboratory has to employ an accredited simulator who has pass simulation examination.
- Perform Simulation for product rating and labeling in accordance with the approved standard and procedures
- Demonstrate initial and continued technical competence
- Meet program requirements
- Participate in annual laboratory training workshops
- Participate in annual round robins
- Pay participation fees

Minimum Equipment Needs for Building Envelope Testing Laboratory

- Spectrophotometer for Spectral Data Testing: Data is used for calculating Thermal transmittance, Solar heat Gain and Visible transmittance in accordance with ISO 15099
- Hot box for thermal transmittance of wall assembly and fenestration
- Solar Calorimeter for Solar heat gain testing
- Air leakage testing Chamber
- Guarded plate Heat flow meter: determine material conductivity

Testing Laboratory Requirements

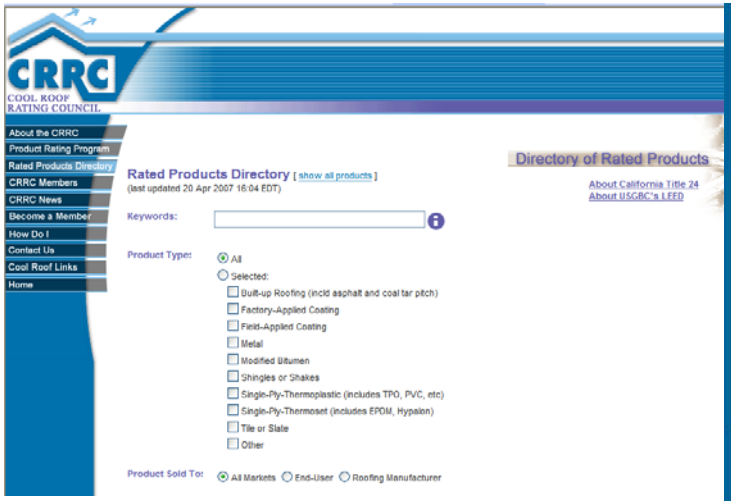
- Perform Testing for product rating or certification in accordance with the approved standard and procedures
- demonstrate initial and continued technical competence
- Calibrate and Maintain Equipments to provide accurate and consistent results.
- participate in annual laboratory training workshops
- participate in annual International round robins
- pay participation fees

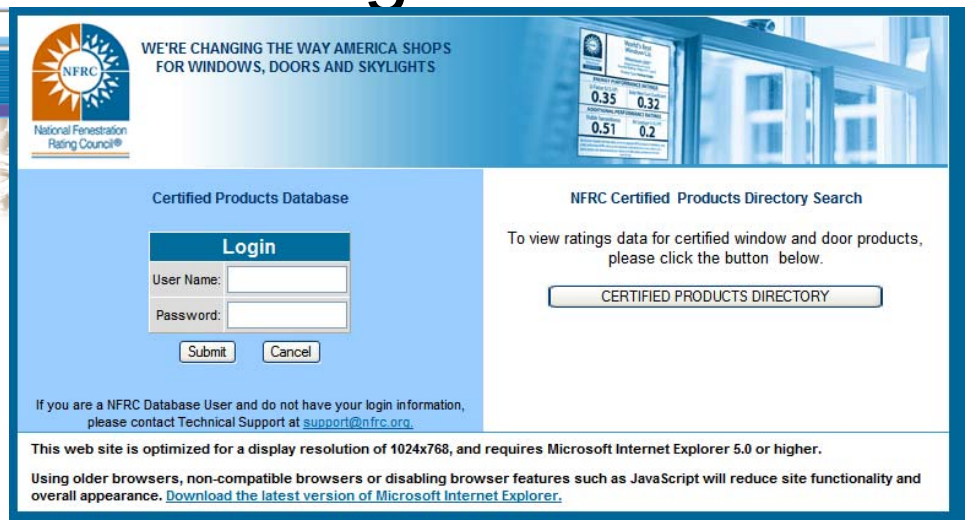
Inspection Agencies - responsible to carry out audits

- Inspection Agencies have to be licensed by rating organization.
- Verify simulation and testing reports
- Inspect products at manufacturing facility for compliance
- Issue certification authorization and labels
- Input certified product information to database.

Database of Certified Products

- Should list all products certified by rating organization for public view.
- Maintain information to verify certified values in case of a challenge



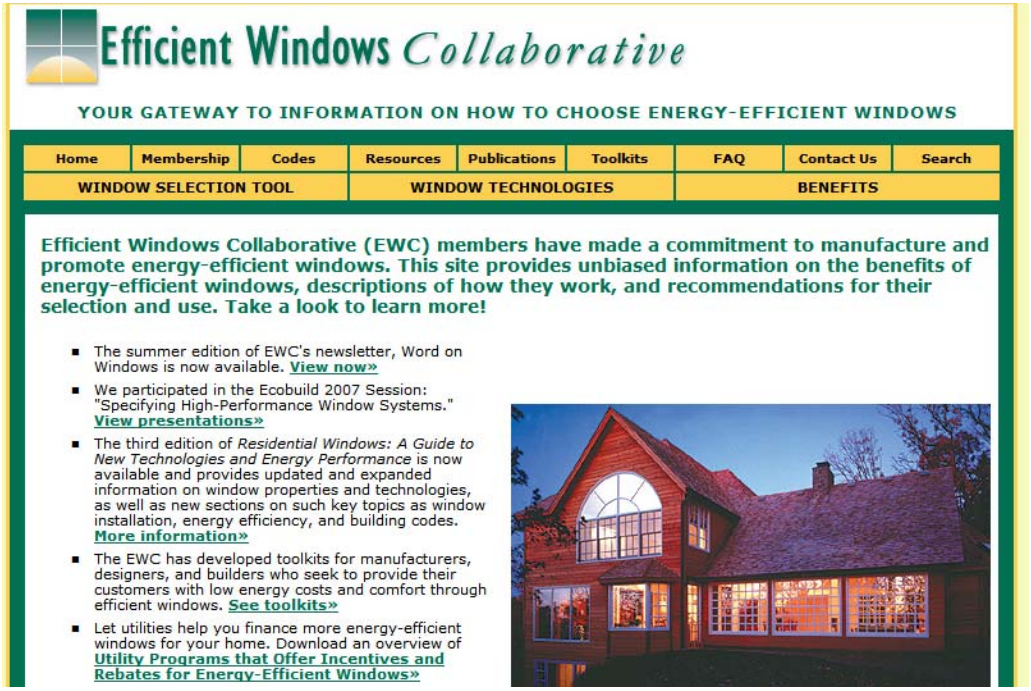


http://www.coolroofs.org/products/search.php

http://cpd.nfrc.org/login.asp

Education website

- Help educate consumer and stake holders



http://www.efficientwindows.org/index.cfm

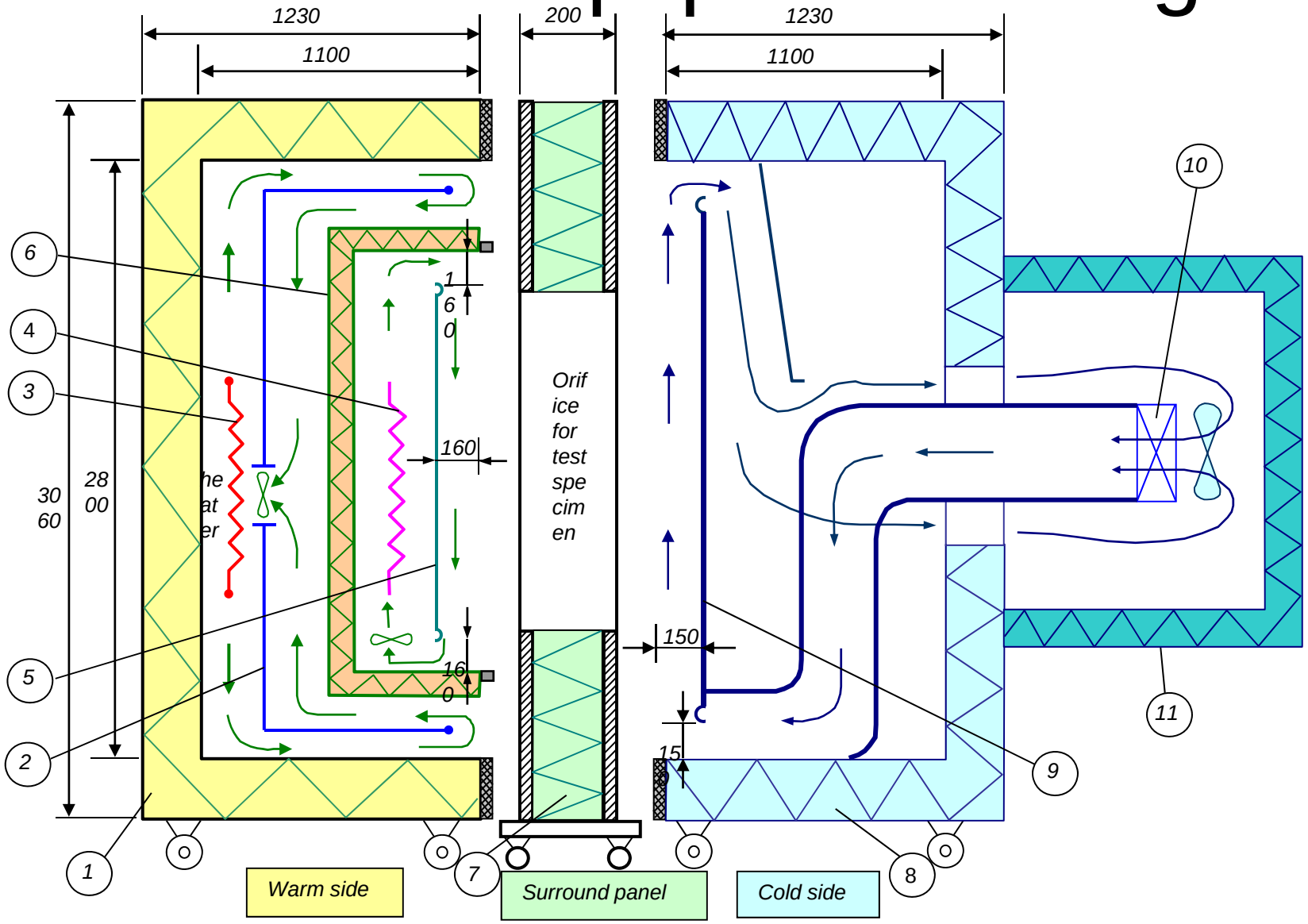
Collaboration Opportunities

- Phase I:

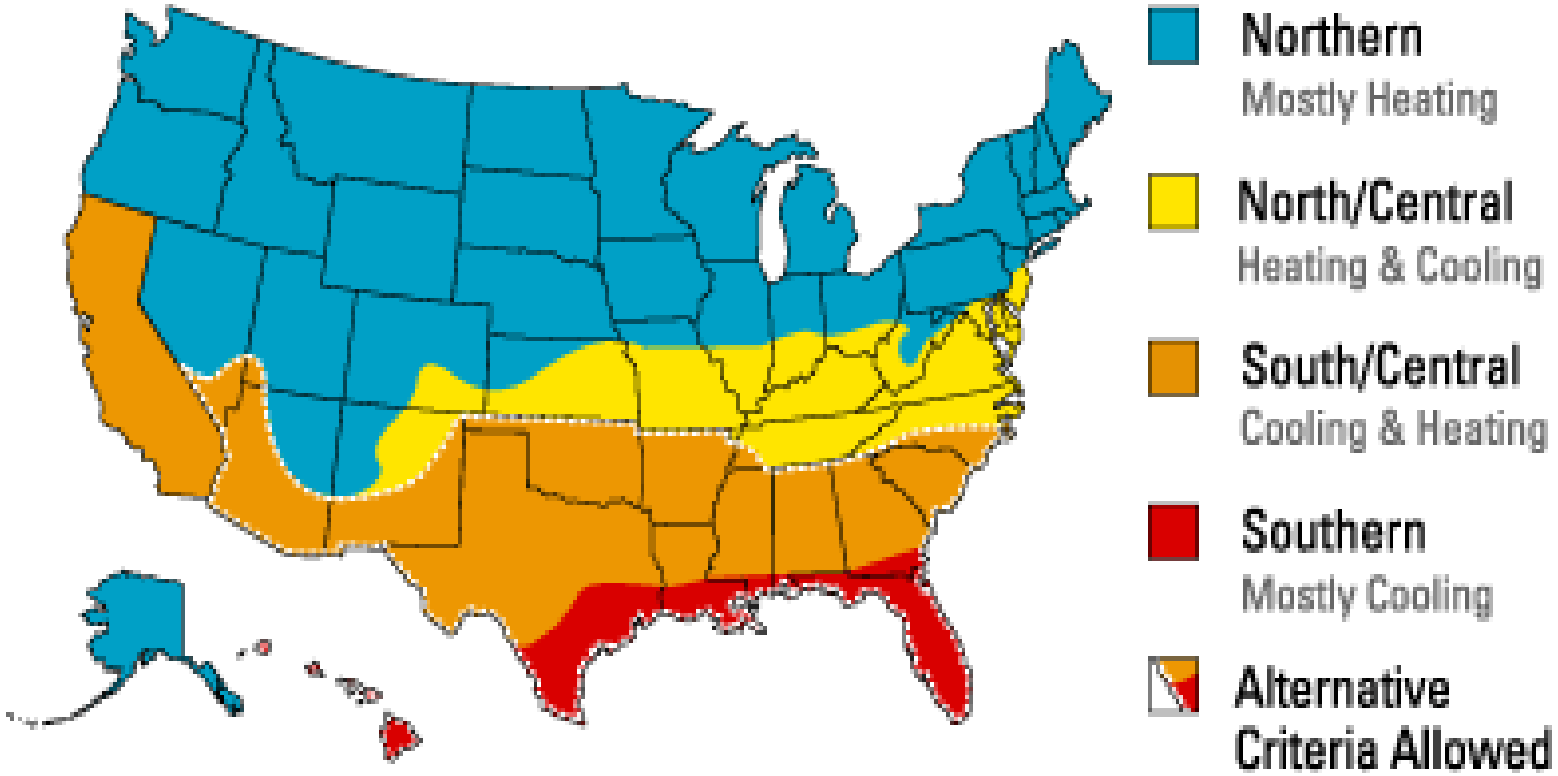
  Capacitate building

  - Conduct simulation train the trainers workshop:
  - Build Spectral data testing capabilities
  - Build Product and Component testing capabilities
  - Develop Auditing and quality control.
- Phase II
  - Work with Government, Industry associations and Research Institutes to Develop a Building Envelope Component rating council
  - Energy Star program
  - Building Envelope Component next generation product development and research

Assistance in Equipment Design



ENERGY STAR Program Establishment:



Our Successes

- Help Establish British Fenestration Rating Council
- Help Establish Australian Fenestration Rating Council
- Help Establish South African Fenestration and Insulation Ratings
- Help Establish Simulation Laboratory in India
- Assisting Chinese to Develop and Establish Window Energy Rating Organization
- Assisting to Establish Energy Efficiency Center in India
- Assisting to Establish Energy Efficiency Center in Jordan
- Assisted Bureau of Energy Efficiency India to develop Energy Conservation Building Code and for its implementation
- Working With Chinese Institutes on Product Standards Development



?

Thank You

Project 3.2
China (a)

Project Name: International Harmonization - China

Date: April 2008

Purpose: NFRC attended several events in China working towards window labeling harmonization.

Project Summary:

NFRC attended several events in China working towards window labeling harmonization.

Click here for Glass Processing Days in China-08

GPD

GLASS PERFORMANCE DAYS

GPD China 2008

8-9 April, 2008

Call for Papers

GPD continues its successful series of state-of-the-art presentations for builders, designers, professional producers and users of glass in Beijing 8-9 April 2008. The 10th GPD Conference in Finland in June 2007 made it clear that glass has a major role to play in supporting sustainable development and the lead theme for Beijing next spring is Climate Change and its Effect on the Glass Industry.

Organizers:

glaston seeing it through

China Building Materials Academy

Co-organizers:

ctc

China Building Material Test & Certification Center

Main Sponsors:

TROSIFOL

Supporters:

China

10-13 April 2008

Official Media Partners:

asianglass

万汇筑业

ECC





GPD China 2008, arranged in conjunction with the China Glass Expo (10-13 April), will be built on Practical and Processing Sessions as well as Architectural, Façade and Market Trends Sessions. A Float session is introduced for the first time. We are now calling for papers to address the lead theme. See the session overview part for details about the subjects.

Session overviews

Practical and Processing Session - papers to include

» hands on presentations – practical examples
» production efficiency
» process case studies
» handling and processing coated glass
» laminating & tempering process and products
» standards and regulations

Float Session - papers to include

» cooling, cutting & quality inspection
» float handling, transport & services
» material and machinery supplies
» melting & simulations
» all process control systems

Architectural, Facade and Market Trends Session - papers to include

» building case studies
» how new designs or processes can affect the use of glass - an ideal educational possibility for architects, facade builders & glass company management
» what architects & facade builders want from glass processors
» what glass technology can offer architects and facade builders
» energy efficiency

Workshop possibilities

We are also inviting proposals for practical workshops on specific subjects. Workshops will be held either before or after conference.

How to be a
GPD China Speaker

The following items must be submitted on time and in the required format:

» abstracts: December 17, 2007
» final manuscripts: March 3, 2008 (They must be both in English and Chinese languages)
» GPD will, in return, issue 'speaker fee' invoices against the abstracts
» notification of acceptance or rejection of presentations will be sent on January 15, 2008
» refunds in full will be given for the rejected presentations
» PowerPoint presentations: March 25, 2008

Abstract submission form available at:
http://www.gpd.fi/Abstract

In case you may have difficulty with submitting your abstract online, please contact us and we will send you a separate form for you to fill and send back to us. The deadline for submitting abstracts is **December 17, 2007**.

GPD China 2008 conference proceedings book will be published in March 2008. Manuscripts not delivered on time will not be included in the book.

Speaker Fee

A speaker fee is charged. If interested, please contact us for more information.

The speaker fee will include the following:

» 30-40 minute presentation time
» a company table for promotion
» the company logo published in different mailings and publicity materials
» A4 sized advertisement in the Proceedings Book
» plus more!

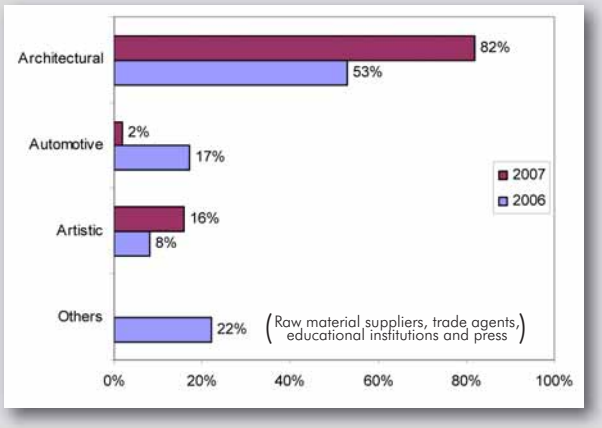




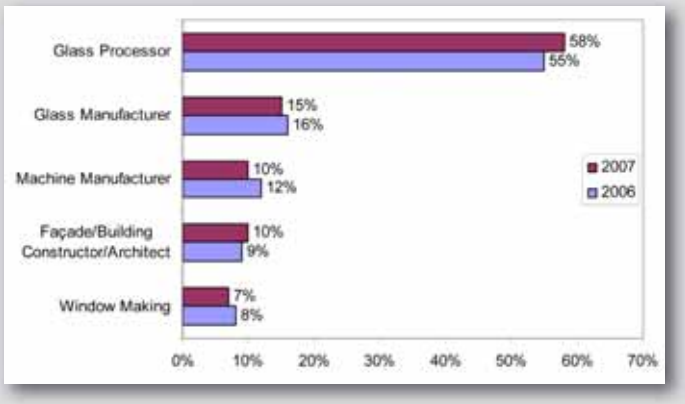


GPD China 2006 & 2007 Participant Profiles

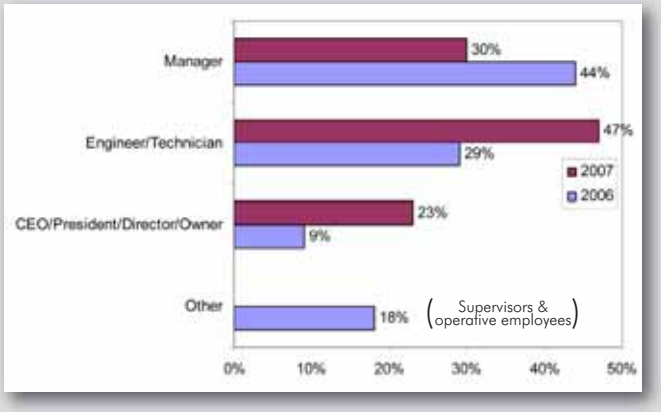
Company Profile



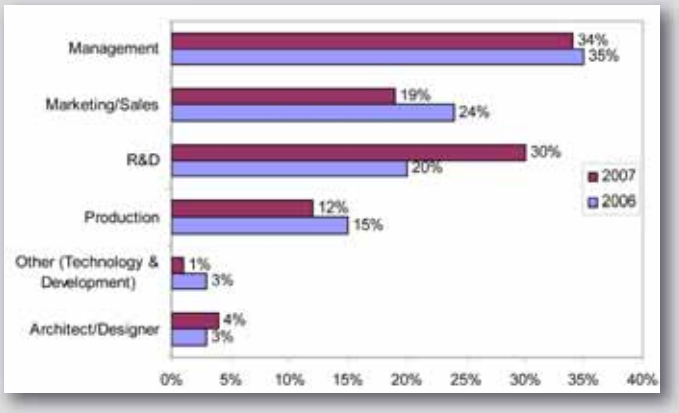
Company Activity



Level



Department



Details at **www.gpd.fi/china** or contact:

Mr Brown Onduso
GPD China Coordinator
Glaston Services Ltd. Oy
Vehmaistenkatu 5
33730 Tampere
Finland

Tel. +358 10 500 6246
Fax. +358 10 500 6180
Mobile: +358 40 773 9313
E-Mail: brown.onduso@glassfiles.com
Internet: http://www.gpd.fi

Project 3.2
China (b)

Project Name: International Harmonization - China

Date: April 2008

Purpose: NFRC attended several events in China working towards window labeling harmonization.

Project Summary:

NFRC attended several events in China working towards window labeling harmonization.

NFRC CEO Presentation at the Building Envelope click here for Energy Efficiency Conference

Windows, Energy and Certification Programs

U.S – China Conference on Building Envelope Energy Efficiency
April 12, 2008

James C. Benney, CAE
NFRC Executive Director



Global Warming

Introduction to NFRC

The NFRC's mission:

NFRC develops and administers comparative energy and related rating programs that serve the public and satisfy the needs of its private sector partners by providing fair, accurate and credible, user-friendly information on fenestration product performance.

Introduction to NFRC



Energy Efficiency

FAST FACTS

- Created in 1989; as a 501(c) 3
- Unique, educational non-profit public/private organization representing:
  - **Industry (fenestration and building)**
  - **State energy offices**
  - **Design Professionals**
  - **Representatives from Higher Education**
  - **Utilities**
  - **Consumer Organizations**

Why Certified Ratings?

- Help meet the code requirements
- Provides means to compare products
- Provides a base line for product development and improvement
- Help consumers to make informed decision
- International Harmonization
- Promote energy efficiency



Why Certified Ratings?

For Market Transformation

Which requires:

- Free Exchange of Information
- Credible, Validated Data
- A Means to Demonstrate Performance



Windows, Energy and Certification

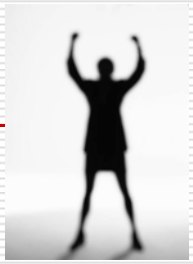
Save Money through Energy Efficiency



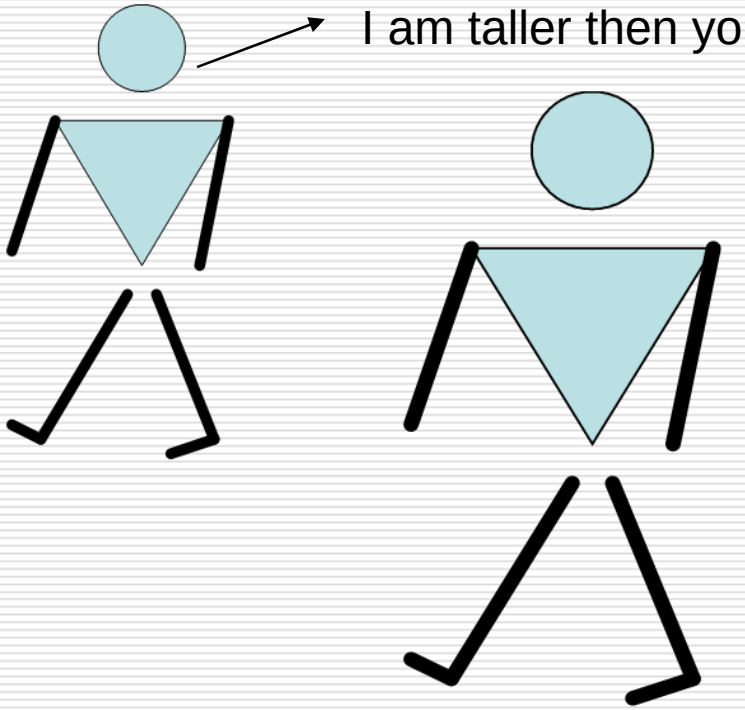
Certified Ratings Assists:

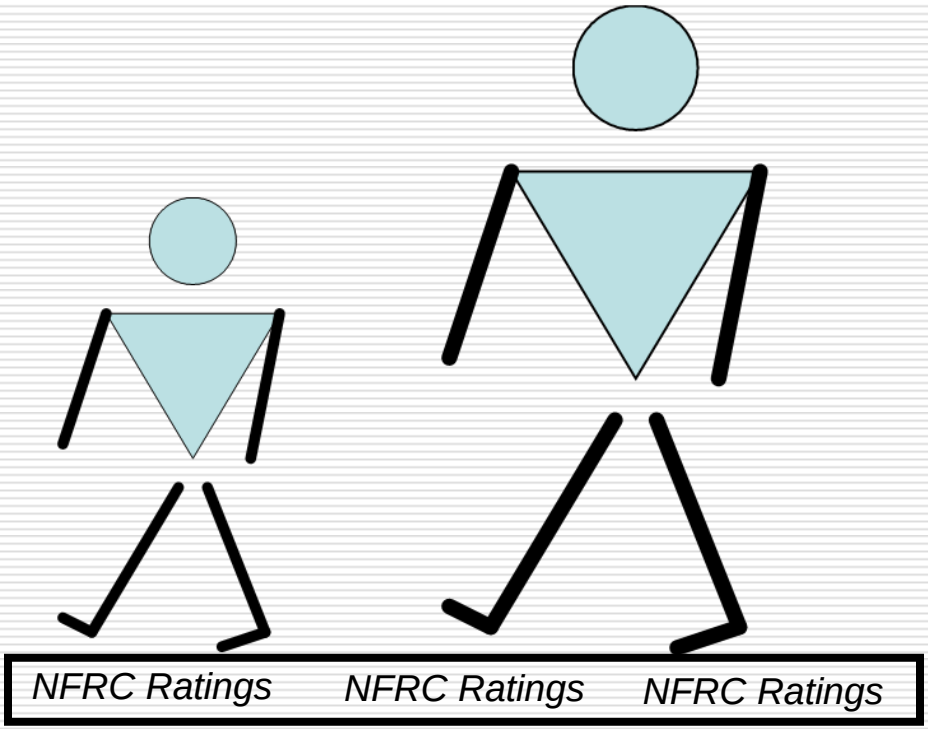
- **Architects, builders, contractors, homeowners – to make informed decisions when purchasing, specifying energy efficient products.**
- **Building officials, state government employees - effective code implementation and enforcement**
- **Government and utility run energy efficiency programs - to be sure they were getting the benefits they paid for.**
- **Manufacturers -a method to fairly compete and to take credit for all the new technology**

Certified Ratings ensure a "Level Playing Field"



Consumer is the winner







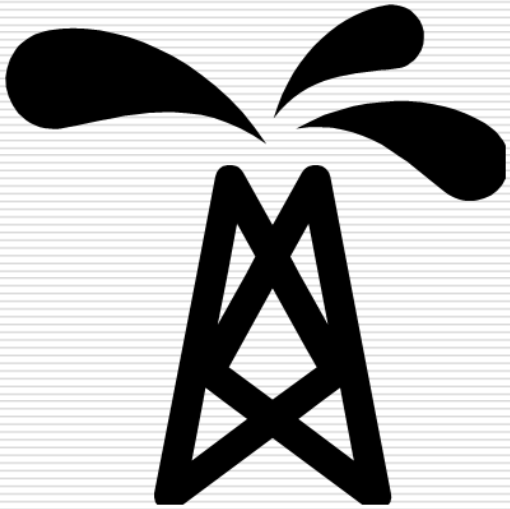
Consumer

If Fair Rating is available

Certified Ratings = Market Transformation = Energy Efficiency = Energy Savings



=



NFRC Certified Ratings are required for Energy Star ® Windows

In 2003 alone Energy Star ® Windows Saved 7 Billion BTU's of energy

For a successful certification program

Product Certification Program (PCP)

- establishes rules for certified ratings

Laboratory Accreditation Program (LAP)

- Maintains credibility of simulation and test laboratories

Certification and Inspection Agency Program (CAP)

- Maintains credibility of third-party program

Compliance Assurance and Monitoring Program

- Provides assistance to building officials, enforces program requirements

Research Program

Marketing and Education Program

National Fenestration Rating Council®
CERTIFIED

World's Best Window Co.

Millennium 2000+
Vinyl-Clad Wood Frame
Double Glazing • Argon Fill • Low E
Product Type: **Vertical Slider**

ENERGY PERFORMANCE RATINGS

U-Factor (U.S./I-P)	Solar Heat Gain Coefficient
0.35	**0.32**

ADDITIONAL PERFORMANCE RATINGS

Visible Transmittance	Air Leakage (U.S./I-P)
0.51	**0.2**

Manufacturer stipulates that these ratings conform to applicable NFRC procedures for determining whole product performance. NFRC ratings are determined for a fixed set of environmental conditions and a specific product size. NFRC does not recommend any product and does not warrant the suitability of any product for any specific use. Consult manufacturer's literature for other product performance information.
www.nfrc.org

NFRC Label

NFRC Label Certificate
(For Buildings with 10,000 sq ft. of glazing area)

NFRC Label Certificate

(for Site-Built Products)



PROJECT LOCATION
Street address:
City, state, zipcode:
Project name (optional): Designer (optional):

PRODUCT LINE INFORMATION
Operator type (per NFRC 100, Table 1):
Product line ID number: Individual product ID number:
How many of this individual product: Location in building:
Elevation drawing page: Fenestration (window & door) schedule page:

FRAME MATERIAL SUPPLIER
Company name, address:
City, state zipcode:
Contact person, phone & fax number:

GLAZING MATERIAL SUPPLIER
Company, name, address:
City, state, zipcode:
Contact person, phone & fax number:

GLAZING CONTRACTOR/INSTALLER
Company, name, address:
City, state, zipcode:
Contact person, phone & fax number:

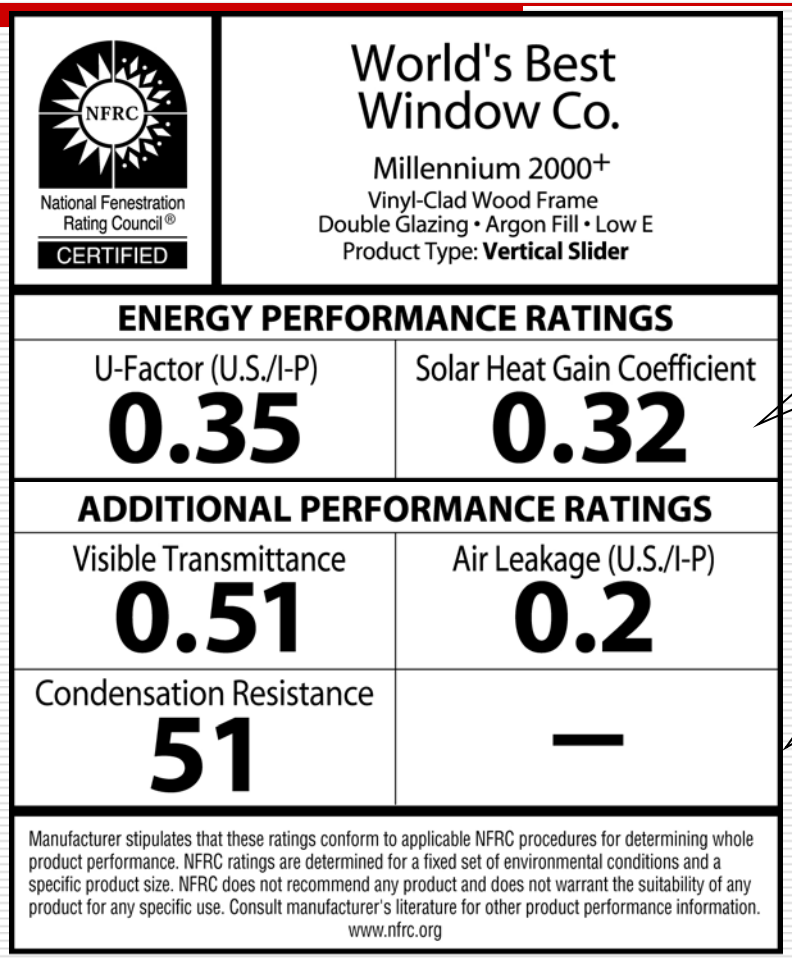
CERTIFICATION AUTHORIZATION
Independent Certification and Inspection Agency (IA):
Date Certification Authorization Issued:

NFRC Temporary Label

NFRC logo indicates licensure by NFRC

Remains attached to fenestration product through product installation and Code inspection

Details on NFRC rating procedures, disclaimer, & NFRC web address



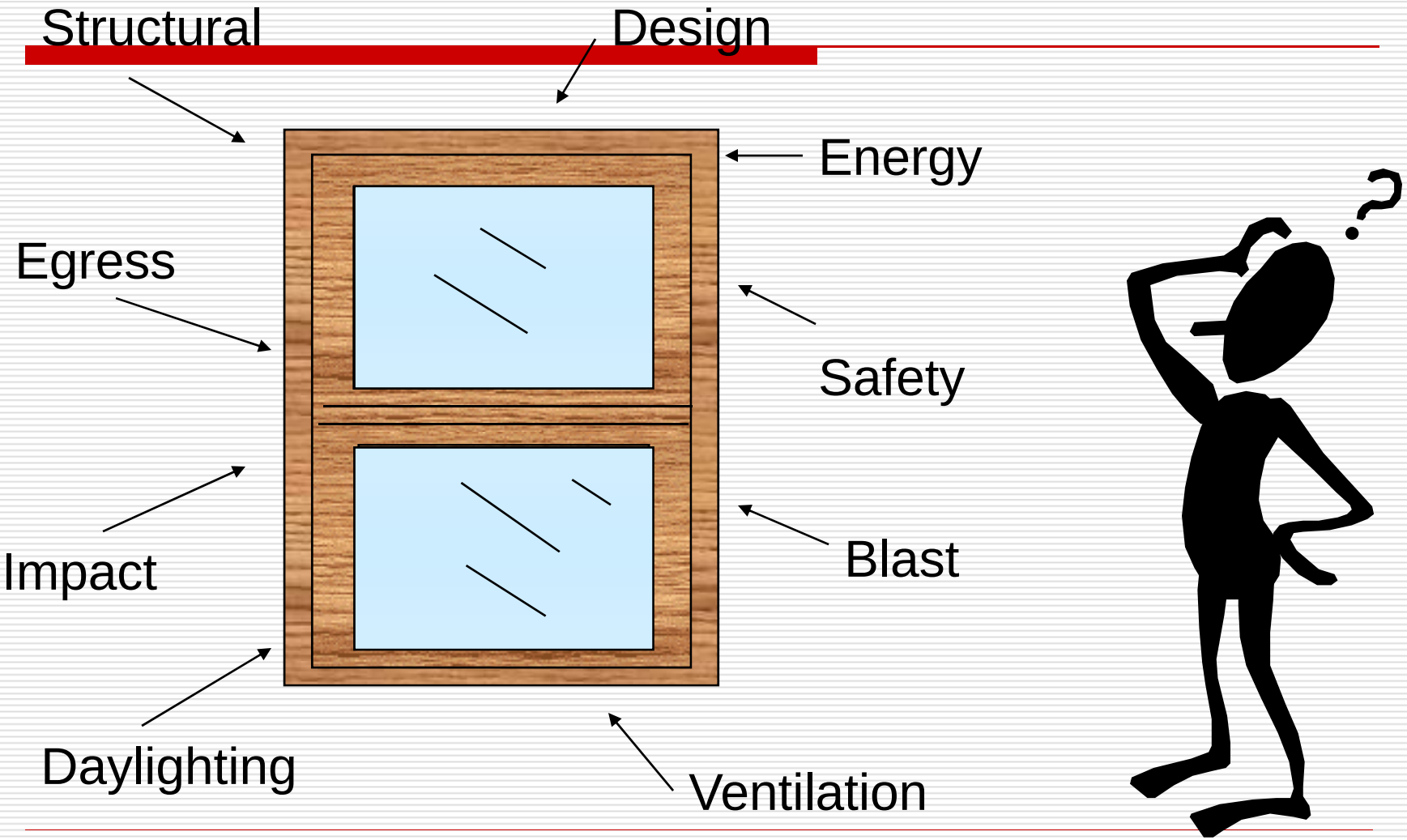
Mfr. Name/ID & Product Description

Ratings are product-specific

If the label contains a box without a rating, the box is left blank except for a dash

NFRC
National Fenestration Rating Council®

Why Certified Ratings?
Because Windows are Complicated



Certification Formats

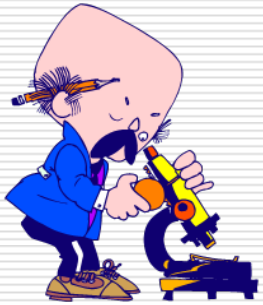
- Self Certification (buyer beware)
- 2 Party Certification - **Common Format –client/customer relationship.**
- 3 Party Certification - **Independent Format.**



MANUFACTURING



ADMINISTRATION



CERTIFICATION

Self Certification

- The lowest level of certification is self certification.
- Uses testing to an industry standard to enhance what is essentially a product warranty.
- The manufacturer administers his own testing and certification program and performs his own in-house inspections as a part of his Quality Control process.
- When you only specify test procedures, you are accepting self-certification
- Building codes allow self-certification with independent test reports

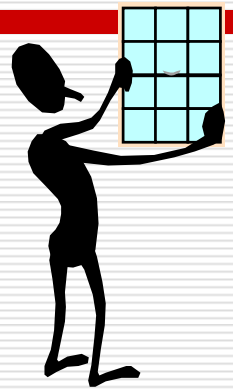
2 Party Certification

- Tested at an independent laboratory
- Certification is granted by a 2nd party, often a trade association to which the manufacturer may belong.
- The trade association staff performs both the administrative and inspection functions.
- This is the most popular form of certification
- Potential exists for influencing the staff of the association if the manufacturer is a member. This level of certification is offered by some trade associations.

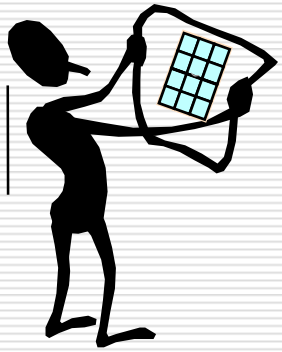
3 Party Certification

- The highest level of product certification
- The certifying or inspection agency is independently under contract to the administering agency, often a trade association to which the manufacturer may belong.
- There is no direct link between the certifying/inspection agency and the manufacturer.

Third Party Certification







FENESTRATION PRODUCER
- Drawings
- Bill of Material

LABORATORY
Provides testing

VALIDATOR
- Plant Inspections
- Review Test Data
- Obtain Test Units
- Review QC Tests

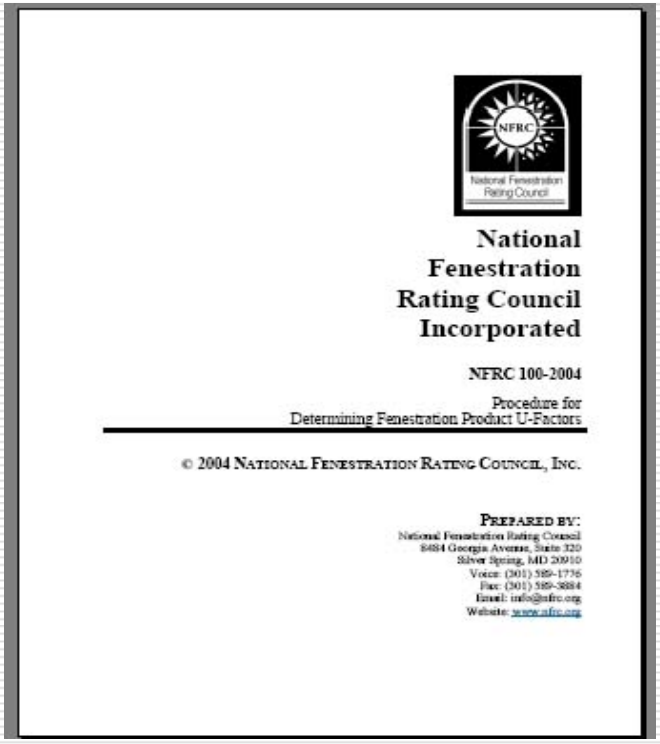


Plant Inspection Reports

Quality Control Reports

Secret of Success
National Fenestration Rating Council

- Performance based standards
- Material neutral
- Required by national recognized codes (IECC and ASHRAE)
- Recognized by Government (EPAct 1992)



National
Fenestration
Rating Council
Incorporated

NFRC 100-2004

Procedure for
Determining Fenestration Product U-Factors

© 2004 National Fenestration Rating Council, Inc.

Prepared by:
National Fenestration Rating Council
8484 Georgia Avenue, Suite 320
Silver Spring, MD 20910
Voice: (301) 589-1776
Fax: (301) 589-3884
Email: info@nfrc.org
Website: www.nfrc.org

Why is third-party certification so important?

The checks and balances are designed to ensure

- Product design intent and performance
- Standardized communication tool

THANK YOU!

301-589-1776

jbenney@nfrc.org

WWW.NFRC.ORG

Project 3.2
China (c)

Project Name: International Harmonization - China

Date: April 2008

Purpose: NFRC attended several events in China working towards window labeling harmonization.

Project Summary:

NFRC attended several events in China working towards window labeling harmonization.

USA-China Building Conference on Energy Efficiency



USA - China Conference on Energy Efficiency in Building Envelope

April 12th 2008 – Beijing China

Conference Goal

GENERAL INFORMATION

PURPOSE AND STRATEGY

PARTICIPANTS

PROGRAM AND HIGHLIGHT

CONFERENCE LOGISTICS

AGENDA FOR THE CONFERENCE

General Information



PURPOSE AND STRATEGY

Objective:

- Establishment of Rating System for Building Envelope Components (i.e. Windows and Insulation)
- Build up a platform to Implement Window Energy Rating and labeling with leadership of CCMSA.

Strategy:

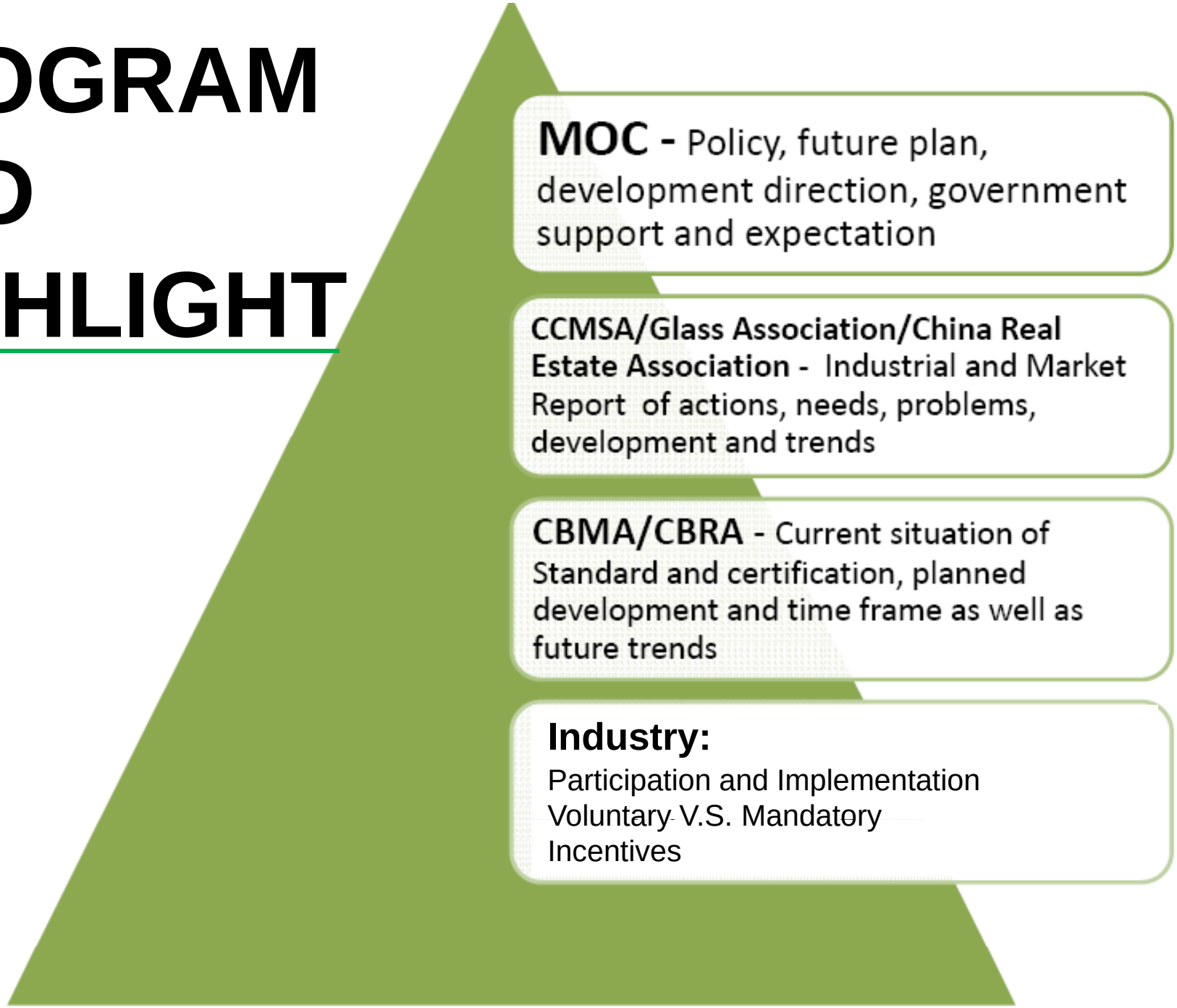
- Have Key Decision Makers to Participate in the Conference.
- Promotion of Energy Labeling Concept for the Chinese Market. Current focus on Window and Wall Insulation
- Understand concern/needs of the Government and the Industry for Implementation of Such Ratings.
- Road Map development to establish window Rating and labeling for China Market.
- Harmonization of Standards for Building Envelop components, namely Wall Insulation, Fenestration and its Components .

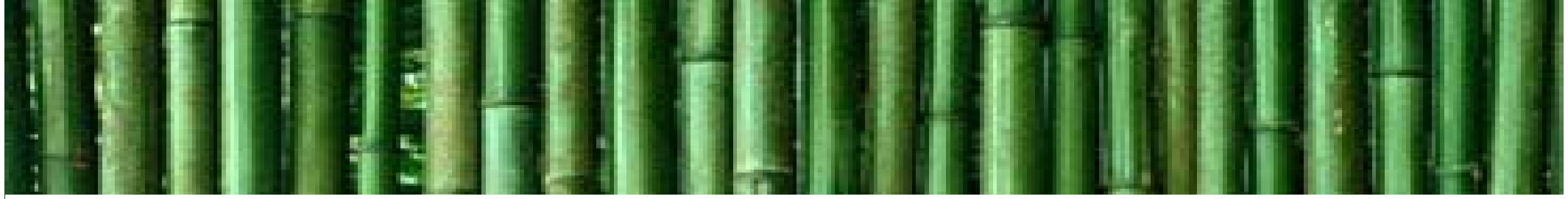
Participants List

US – DOE
Marc Lafrance
MOC
Chen YiMing
Chen GuoYi
NFRC
Jim Benney -
Executive director of NFRC
Bipin Shah -
International Liaison
IWFA
Darrell Smith
China Construction Metal Structure Association - CCMSA
Du ZongHan
Huang Qi
Glass Association
Zhang BaiHeng
China Real Estate Association
Song ChunHua
Zhu ZhongYi

CBMA – China Building Material Academy
Yao Yan
Ma ZhenZhu
Rocky Shi
CBRA – China Building Research Academy
Lin HaiYan
Wang HongTao
Jiang Ren
Industry:
Wall Insulation
Window, Glass and Components
Curtain Walling
Engineering
Magazine and Press:
Intelligent Glass and Architecture

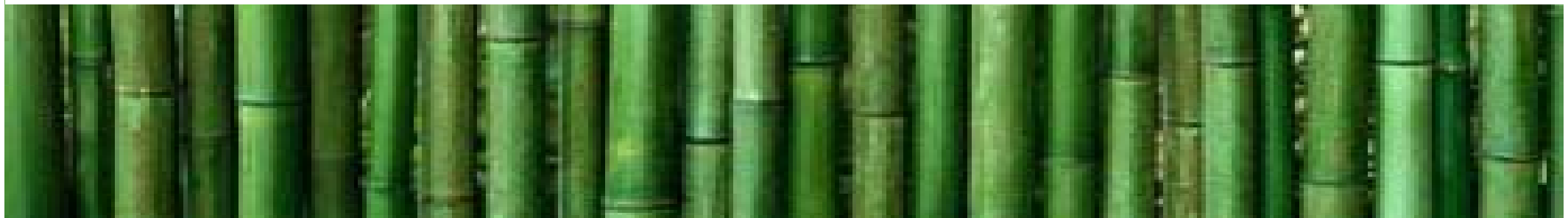
PROGRAM AND HIGHLIGHT



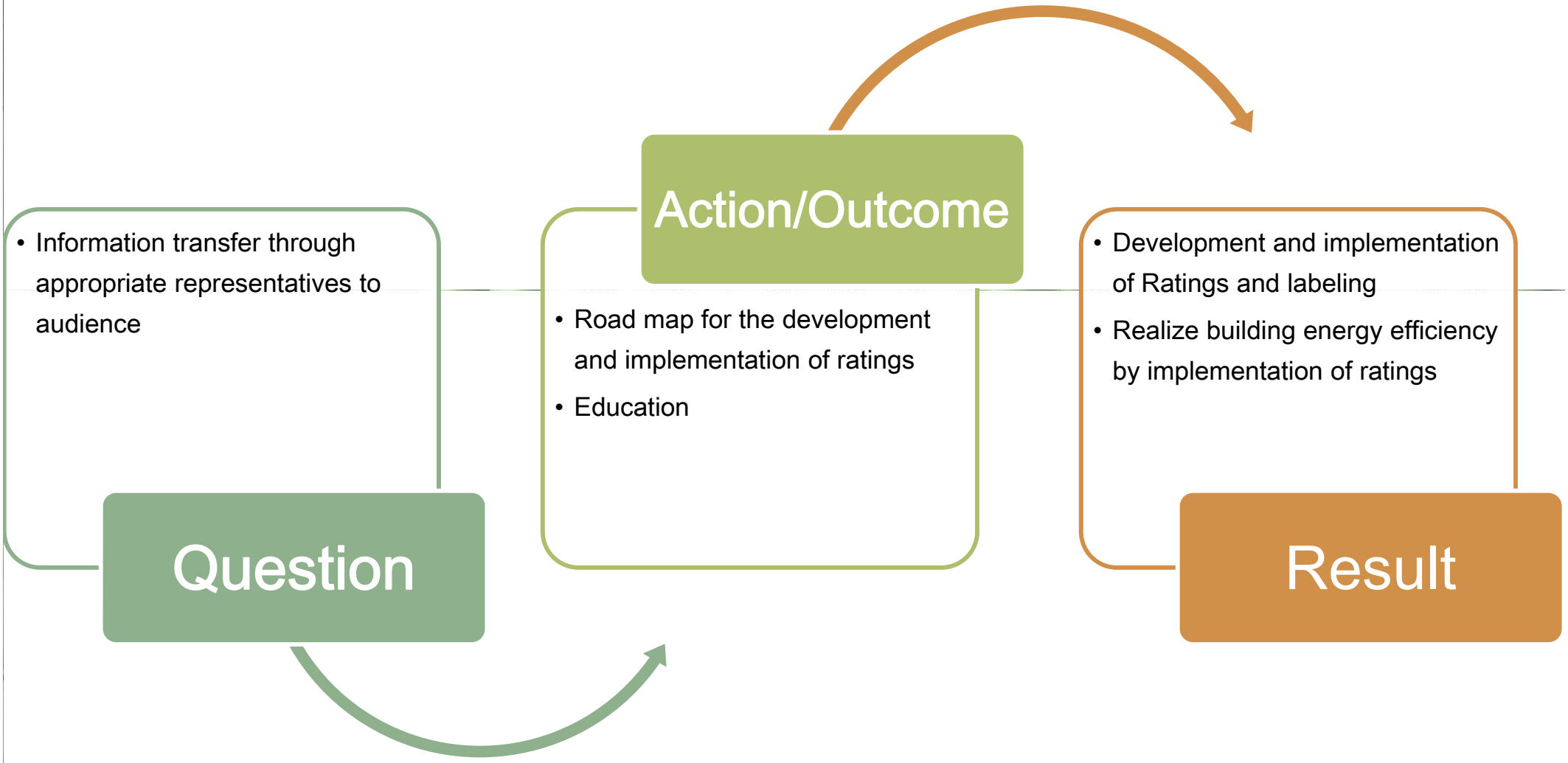


Conference Logistics:

- Representative speakers will have 30 minute to present and inform the audience on specific subjects.
- Other speakers and audience can ask question and/or request more information. 10 minutes
- Organizer will record all the questions and answers
- Sort out action plan and to develop a road map for implementation



Conference Logistics:



Agenda For the Conference

The main objectives :

- Establishment of Rating and Labeling of Building Envelop Components.
- Understanding the barriers and illustrate ways to overcome the barriers
- Delineate approaches of how to establish and implement rating and labeling of windows in China.
- Agenda:
- Policy, Implementation and Incentives for Energy Ratings of Building Envelop Components
  Ministry of Construction China
  US- Department of Energy
- Fenestration and Glass industry view points
  China Construction Metal Structure Association - CCMSA
  China Glass Association
- Experience of Rating in the USA
  National Fenestration Rating Council
  International Window Film Association
- Energy Efficiency Code requirements for Building Envelop Sector in China
  CBMA- China Building Material Academy
  CBRA- China Building Research Academy
- Builders perspective of Energy Efficiency
  China Real Estate Chamber of Commerce
- General Discussion.

- Dinner: (7:00 pm onwards)
- Attendees will have an opportunity to meet with the Chinese official

Project 3.2
China (d)

Project Name: International Harmonization - China

Date: April 2008

Purpose: NFRC attended several events in China working towards window labeling harmonization.

Project Summary:

NFRC attended several events in China working towards window labeling harmonization.

US Green Building Technology Seminar agenda and invitation-09

14、美国绿色技术论坛

US Green Building Technology Seminar

时间：2009 年 3 月 28 日下午 13：30-17：3 地点： 2 floor

主持人： Mark Ginsberg，Senior Executive Board Member, EERE Board of Directors, U.S. Department of Energy 美国能源部执行委员会高级成员

Elizabeth Shieh, Commercial Officer, Embassy of the United States of America, 美国使馆商务处商务官员

编号	时 间	演 讲 题 目	演 讲 人	职称 / 职务
主持人：Mark Ginsberg 美国能源部执行委员会高级成员				
1	13:20	美国能源部领导祝词 USDOE Welcome	Mark Ginsberg	美国能源部高级执行官 Senior Executive，US Department of Energy
2	13:25	美国商务部领导祝词 USDOC Welcome	William Brekke	美国使馆商务参赞 Minister-Counselor for Commercial Affairs
3	13:30	美国联合技术公司 UTC Welcome	Sandy Diehl	美国联合技术公司全球副总裁 Vice President of UTC
4	13:35	美国门窗测评委员会 NFRC Welcome	Nils Peterman	美国门窗测评委员会主任 NFRC Board of Directors
5	13:40	**零能耗建筑正在兴起** **On the Road to High Performance, Net-Zero Energy Buildings**	Brian Castelli	美国节能联盟项目发展执行副总裁 Executive Vice President for Programs and Development，Alliance to Save Energy
6	13:55	北京的金色建筑：奥运村和科技部 21 世纪节能建筑 Gold Buildings in Beijing: Agenda 21 and Olympic Village	Joe Huang	White Box Technologies
主持人：Elizabeth Shieh 美国使馆商务处商务官员				
7	14:10	可持续发展企业 Corporate Sustainability	李红宇 博士 Dr. Li Hongyu 汪宏 先生 Mr. Wang Hong	AECOM 公司

8	14:30	地源热泵技术 Geothermal Technologies	吴展豪 Alfred Ng	美意（上海）空调设备有限公司总裁 P.Eng, President & CEO, Mammoth (Shanghai) Air Conditioning Ltd
9	14:50	来自美国的绿色保温隔热产品 Green Insulation Products From the USA	邵磊 Leon Shao	首席代表，美国佳殿建筑产品公司亚洲代表处 Chief Representative，Guardian Building Products Asia Rep. Office
10	15:10	**支持可持续发展: 清洁能源解决方案** Fueling Sustainable Development: Clean Energy Solutions	刘军亮 Liu Junliang	尤尼索拉津能(天津)能源有限责任公司总经理 United Solar Ovonic Jinneng Limited，General Manager
11	15:30	**普通照明的应用** Energy Saving - LED general lighting application	刘锋 Liu Feng	霍尼韦尔朗能电气系统技术(广东)有限公司销售总监 Honeywell Lonon Sales Director，Honeywell Lonon
12	15:50	节能空调系统 Energy Efficient Air Conditioning Systems	**PHILIP C.H. YU**, PhD RPE CEng 余中海博士	特灵公司 Trane Co.
13	16:10	欧文斯科宁保温节能产品 Insulation & Energy Efficiency	徐凯讯 Xu Kaixun	亚太科技中心，规范与测试部主任，欧文斯科宁 Owens-Corning
14	16:30	The Role of Daylight and Solatube Daylighting Systems in China's Sustainable Future 日光及索乐图日光照明系统在中国可持续发展中的作用	Neall Digert	苏州中节能索乐图日光科技有限公司国际市场开拓部副总裁 Ph.D., MIES，Vice President of International Market Development Solatube International, Inc
15	16:50	Q & A 问答		
16	17:20-17:30	USDOE Closing Remarks 美国能源部总结发言	Mark Ginsberg	

主办：美国能源部 & 美国商务部 Hosted by U.S. Department of Energy & U.S. Department of Commerce

The Fifth International Conference on Intelligent, Green & Energy Efficient Building & New Technologies and Products Expo

March 31-April 2, 2009 Beijing, China

Greetings from China Beijing!

The U.S. Commercial Service in Beijing is pleased to invite American firms to participate in our U.S. Pavilion at the Conference on Intelligent Green and Energy Efficient Building & New Technologies and Products Expo to promote American energy efficient construction, building materials products and services to China's emerging construction market!

Organized and supported by the Ministry of Housing & Urban-Rural Development, National Development and Reform Commission, and the Ministry of Science and Technology, the 5th International Conference on Intelligent Green and Energy Efficient Building & New Technologies and Products Expo will be held from March 31 –April 2, 2009 at the Beijing International Conference Center. The event will focus on improving the energy efficiency of buildings in China and is the best venue to showcase products, services and new technologies in this field. Vice Minister Qiu Baoxing of the Ministry of Housing & Urban-Rural Development will host this conference. The U.S. Department of Energy, and governments of European and Asian countries will send delegations to attend this event.

We are eager to work with you to promote your American products and services in China. We look forward to hearing from you before the end of February18, 2009.

Sincerely,

William Brekke
Minister-Counselor for
Commercial Affairs

Exhibitors at the U.S. Pavilion Receive:

- **Fully furnished, nine square-meter booth in a prime location**
- **On-site counseling & matchmaking throughout the show**
- **Free introduction of U.S. Pavilion members to VIPs at the show**

All for a Local exhibition fee of RMB12,000 per booth (Listed price RMB 15,000)!!

For more information:
Ms. Merry (Shujuan) Cao
Commercial Specialist,
Foreign Commercial Service, U.S. Embassy, Beijing, China.
Email: Shujuan.cao@mail.doc.gov
Tel :(86-10) 8529-6655 x861

or

Ms. Vicky Liu
Email: Yinglin.liu@mail.doc.gov
Tel: (86-10) 8529-6655x857
Fax :(86-10) 8529-6558

Official Website: http://www.Chinagb.net

Project 3.2
Jordan (a)

Project Name: International Harmonization – Jordan

Date: March - April 2009

Purpose: The National Fenestration Rating Council (NFRC) participated at the GCREEDER-2009 conference in Amman Jordan, March 31st -April 2nd, 2009.

Project Summary:

NFRC attended several events in Jordan working towards window labeling harmonization.

Click here for the Global Conference on Renewables and Energy Efficiency for Desert Regions brochure

Conference Fees and Registration Fees:

$400 for early registration (prior to 15/03/2009)
$450 for late registration (after 1/03/2009)
$100 for students, (Please provide proof)
Payment should be made in USD by wire bank transfer, quoting:

University of Jordan /GCREEDER 2009
CAIRO AMMAN BANK
University of Jordan branch
Account: 0253014042000
Swift Code: CAABJOAMXXX

Registration will be valid upon reception of a copy of the bank transfer by either
Fax: +962 6 53 429 69, or by email to
gcreeder2009@ju.edu.jo

The registration fees include: reception banquet, refreshments, conference handouts, and CD-Rom Proceedings, and Book of Abstracts.

For inclusion of an accepted paper in the conference proceedings, at least one author of the paper must register for the conference.

Conference Proceedings

Conference proceedings will include keynote addresses and papers.

CD-Rom of the conference proceedings will be delivered on the conference first day at the registration desk.

Correspondence

Dr. Ahmed Al Salaymeh,
Energy Center - University of Jordan
Phone +962-6-5355000 Ext. 23937
Fax: +962-6-5342969
Gcreeder2009@ju.edu.jo
http://gcreeder2009.ju.edu.jo

The University of Jordan

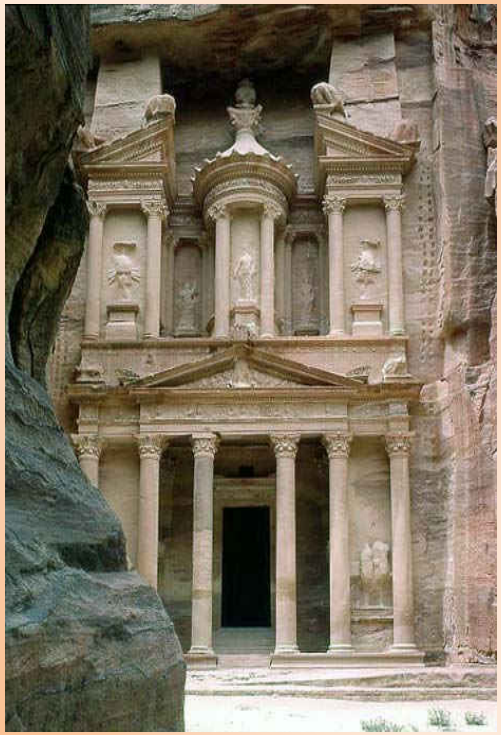
ENERGY CENTER JORDAN UNIVERSITY

Ministry of Higher Education and Scientific Research

Global Conference on Renewables and Energy Efficiency for Desert Regions

GCREEDER 2009

March 31st -April 2nd, 2009
Amman - Jordan



GCREEDER 2009 conference was originally planned to be held in October 28-31, 2008 in Amman, Jordan. But, due to numerous requests from participants, it was decided to postpone it until March 31st to April 2nd, 2009. It is organized by the Energy Center at the University of Jordan, in cooperation with International Research Centre for Renewable Energy e.V. Germany (IFEED), The Jordan Europe Business Association in addition to a number of institutions known for their innovative and collaborative efforts in the area of energy. An exhibition on renewable energy will be held at the site of the conference to encompass companies and institutions concerned with the subject. The past conference of (GCREADER) has attracted professionals from both the industry and academia worldwide.



GCREEDER 2009 Objectives

The primary objective of GCREADER2009 is to provide a forum for thoughtful evaluations and discussions regarding up-to-date developments of solar, wind, bio-mass, energy efficiency and other sources of renewable energy including basic research, technologies and applications in desert regions. The conference is a perfect forum for academics and power industries to get to common grounds of discussions in the area.

GCREEDER 2009 Exhibition

A supporting exhibition will be held in conjunction with the conference. This will be free of charge for visitors to acquire knowledge about the most recent technologies in the field of renewable energy and its applications.

Sponsors

The conference is sponsored by the University of Jordan, Amman, Jordan, and is organized with a support from the Ministry of Higher Education and Scientific Research / Scientific Research Support Fund.

Venue

Sessions of the conference will be held at the University of Jordan, and a five star hotel, Amman, Jordan.

Important Dates

Deadline for paper submission	February 2nd 2009
Paper acceptance notification	March 1st 2009

Subject Coverage

Subjects in the conference include but not limited to the following topics:

I- Energy Sources in Desert
II- Green Buildings
III- III-Basic Research

Papers are being solicited in the following topic areas:

- Solar Thermal applications
-Photovoltaic applications
-Passive solar systems
-Wind energy
-Energy storage
-Geothermal
-Fuel cells
-Alternative fuels
-Bio-fuels
-Hydrogen

IV- Energy Management
-Grid connected and off-grid systems.
-Monitoring
-Maintenance
-Policy and legislation for renewable energy
-Environmental issues

V- Energy Efficiency

VI- Technologies and applications
-Power generation
-Heating, Cooling and air conditioning
-Water pumping and desalination
-Food preservation
-Industrial technologies

VII- System Integration
-Remote areas and rural sites
-Communities
-Agricultural applications

VIII- Underground Water in Desert

Information for Authors

PAPERS

Authors are kindly asked to submit their papers in full manuscript to the conference either at: gcreeder2009@ju.edu.jo, or using online submission on the conference website: http://gcreeder2009.ju.edu.jo, by February 2nd 2009; indicating title, author(s) name(s), position, affiliation, telephone, fax and e-mail. Upon reviewing by the conference peers, the final paper including revisions based on reviewer's comments should be submitted by March 1st 2009.

A template format for full paper is available on the conference website.

PEER REVIEW

The acceptance of the conference papers will be subject to blind peer review.

LANGUAGE

The official language for abstracts, papers, and discussions is English.

PUBLICATIONS AND SPECIAL ISSUES

Selected 25-30 papers will be considered for publication in the Energy Conversion and Management journal as a "Special Issue".

Project 3.2
Jordan (b)

Project Name: International Harmonization - Jordan

Date: March - April 2009

Purpose: The National Fenestration Rating Council (NFRC) hosted Jordanian visitors to work towards window labeling harmonization.

Project Summary:

NFRC attended several events in Jordan working towards window labeling harmonization.

Click here for a presentation Rating and Certification System in the USA for Jordanian visitors

Rating and Certification Programs in USA
International Activity with Jordan





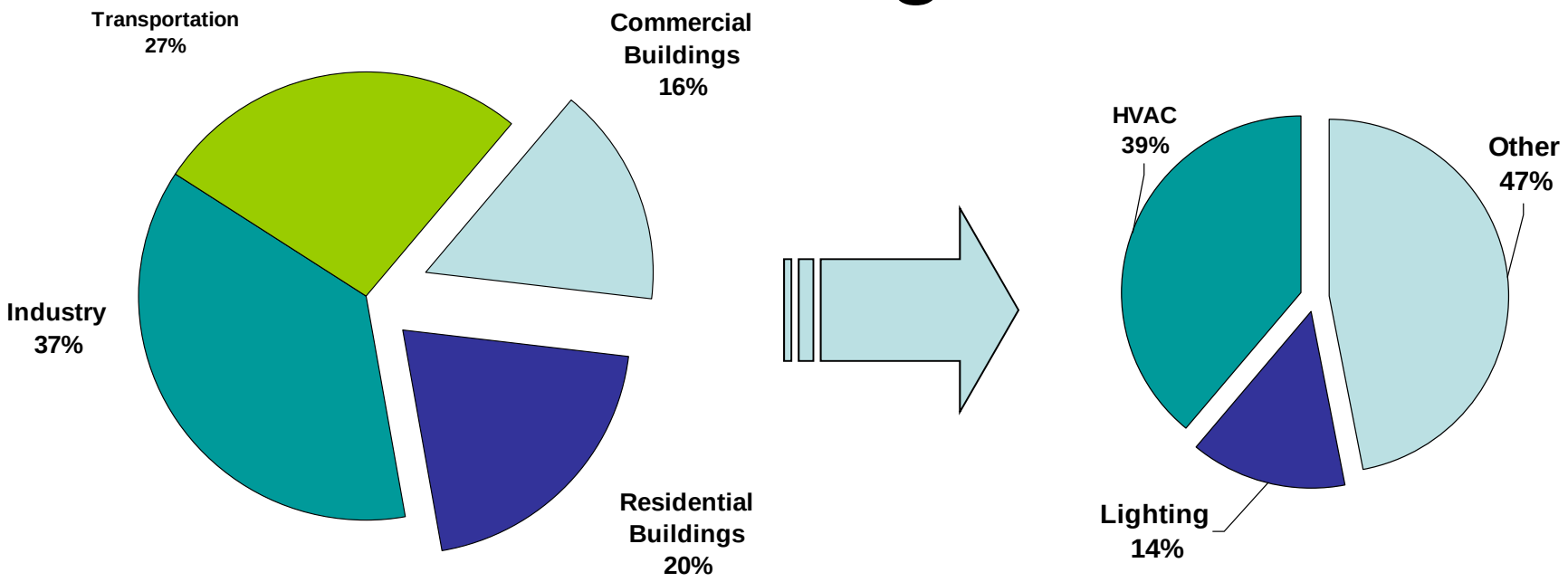






John Lewis - National Fenestration Rating Council

US Energy Consumption in Buildings



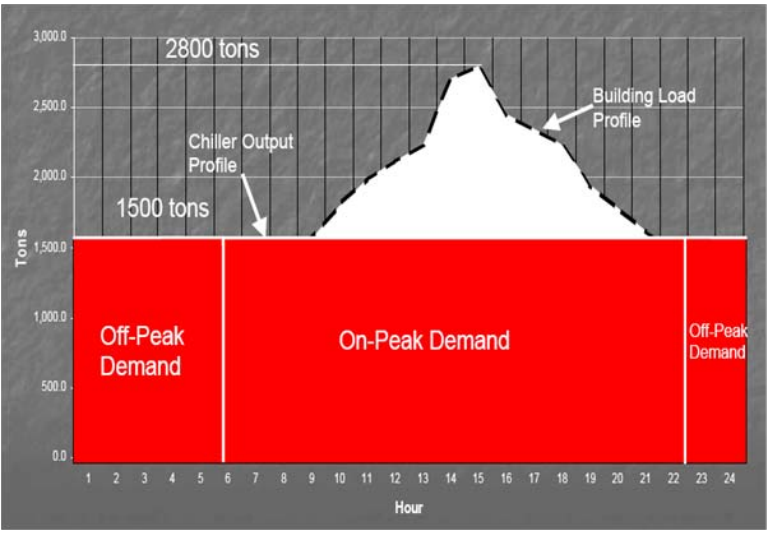
US Building Energy:

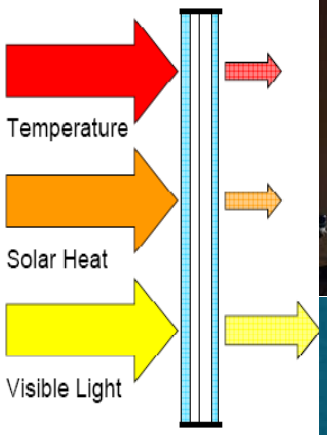
Over 1/3 of US Economy

Over 70 percent of electricity

Building space conditioning ~ 18 percent of US Economy

Holistic Energy Solution for Building Envelope





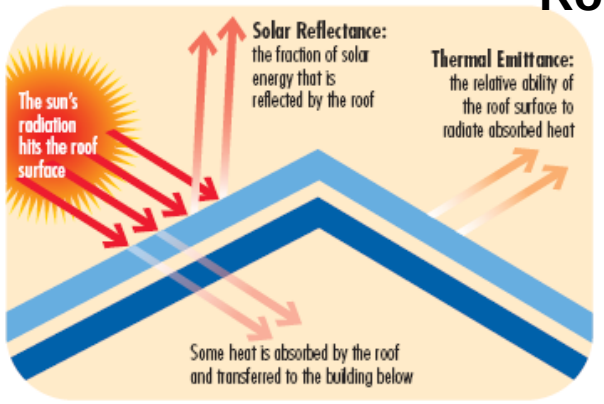


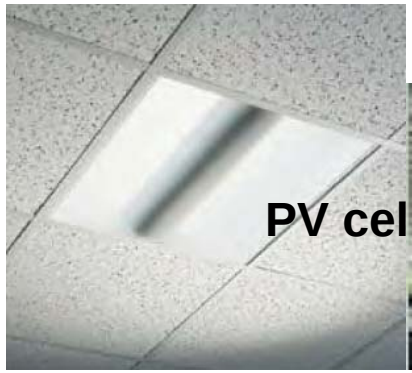
Windows



Wall

Roof





PV cell





- ***Whole Building Solutions:***
  - ***High Performance Glazing***
  - ***Efficient Lighting and Day Lighting, Green Roofs***
  - ***Renewable Energy Sources / Cogeneration***
  - ***Heat Recovery, Thermal Energy Storage, Efficient Distribution***

Energy Efficiency and Renewable Source Energy

- **Primary focus** has to be **Energy Efficiency**

- **Secondary Emphasis** Should be to provide **Renewable** Source Energy.

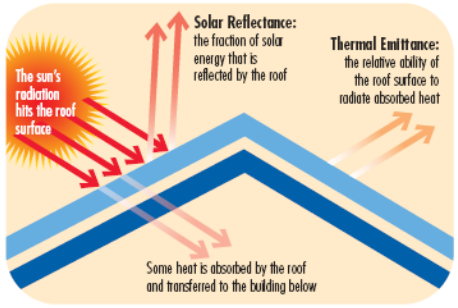


These strategy will be a win win Green Solution as it Makes renewable (first cost) more cost effective.

Rating Organization in USA

- National Fenestration Rating Council (NFRC)
  - Rates Fenestration Products
- Cool Roof Rating Council (CRRC)
  - Rates Roofs.
- North American Insulation Manufactures Association (NAIMA)
  - Rates Insulation







Testing Used for Product Certification

Fenestration:

- Simulation for U-factor, Solar Heat Gain Factor and Visible transmittance - ISO 15099
- U-factor testing - ASTM C 1363, C1199, NFRC 102
- Solar Heat Gain Testing – NFRC 201
- Spectral Optical Property – ASTM E903, NFRC 300
- Air Leakage – ASTM E283

Cool Roof

- Solar Reflectance Testing – ASTM E903, ASTM C1549, ASTM E1918 and CRRC-1
- Thermal emittance – ASTM C1371

Wall Insulation

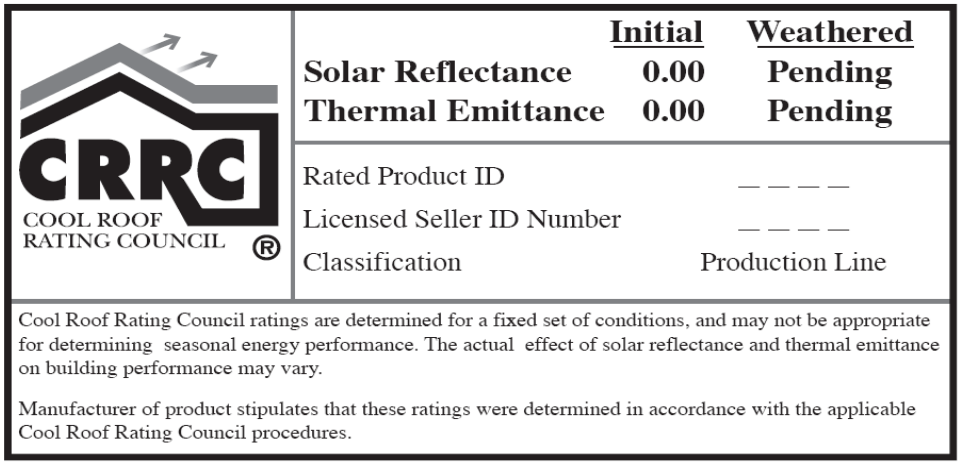
- ASTM C 518

Wall Systems

- ASTM C 1363, ASTM C1155

Why Rating and Labeling





- **Label helps Verify the Compliance**
- **Helps consumer to distinguish products**
- **Promotes competition and drives innovation**
- **Code Compliance**

Policies - Regulations

- Policy and Regulation are difficult to implement and enforce unless one has infrastructure to support products performance verification that are being installed (i.e.ratings, certification, product compliance, whole building integrated performance, and validation)
- Can be highly effective in achieving energy savings and carbon reduction



NFRC Window Energy Rating Process



Simulation Laboratory
Simulate All Option

Testing Laboratory
(Test One Base Line Product)

Inspection Agency (IA)
Issue Certificate authorization, Plant inspection

NFRC Label or Label Certificate

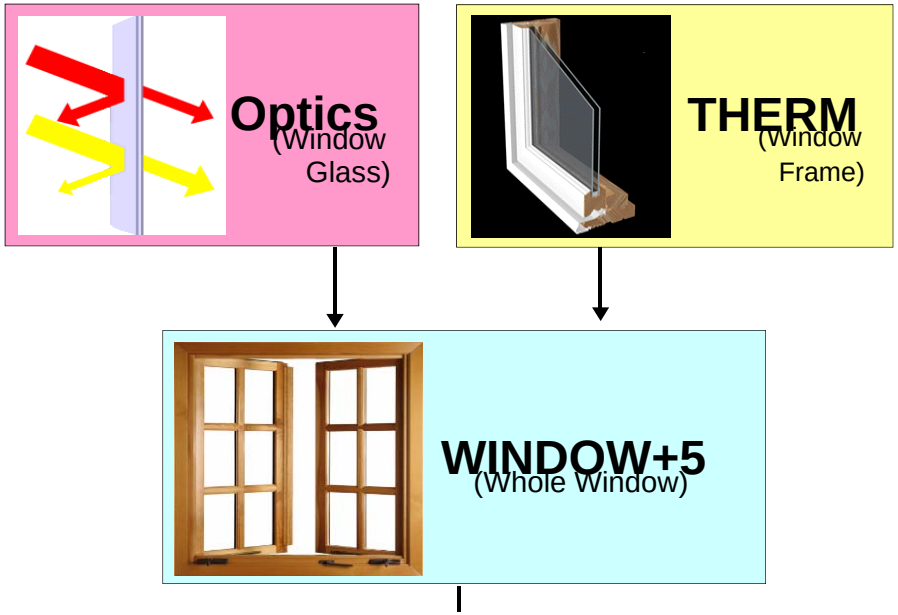
Market Place
Responsible Party Label Product

Compliance Assurance and Penalties for non-compliance

Simulation Workshop

Simulation Tools Provide Consistency and reliability

- WINDOW
- THERM
- OPTICS



Computer Programs are ISO-15099 compliant

Applicable ISO Standards

- **ISO – 15099** -Thermal Performance of Windows, Doors and Shading Devices — Detailed Calculations
- **ISO 12567**: Thermal performance of windows and doors -Determination of thermal transmittance by hot box method —
  - Part 1: Complete windows and doors and
  - Part II: Roof windows and other projecting windows
- **ISO 9050 -** Glass in building-Determination of light transmittance, solar direct transmittance, total solar energy transmittance, ultraviolet transmittance and related glazing factors

WINDOW 5.2

- Current version WINDOW 5.2
- Calculates center of glass and total product U-factors.
- Relies on THERM (or compatible) program to determine frame and divider U-factors.
- Incorporates libraries of glass products, gas fillings and environmental conditions
- Has Certified (NFRC) mode and Design mode

Window Library (C:\User\BEEP_Shared\Round Robins\TRR99\TRR99_W5-T5\w502b.mdb)

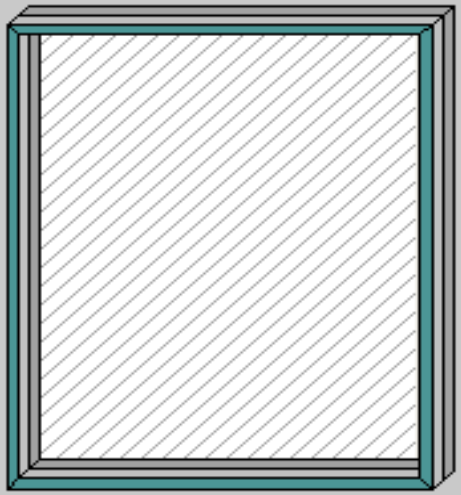
File Edit Libraries Record Tools View Help

List
Calc
New
Copy
Delete
Save
Report

Dividers
Dividers

Display mode:
Normal

ID # 11
Name Al Winter
Mode NFRC
Type Casement - Doubl >>
Width 47.244 inches
Height 59.055 inches
Area 19.38 ft2
Tilt 90
Environmental Conditions
NFRC 100-2002



Total Window Results

U-factor	0.456	Btu/h-ft2-F
SHGC	0.642	
VT	0.675	
CR	N/A	

Detail...
Detail...

Click on a component to display characteristics below

Glazing System

Name Al_winter >>

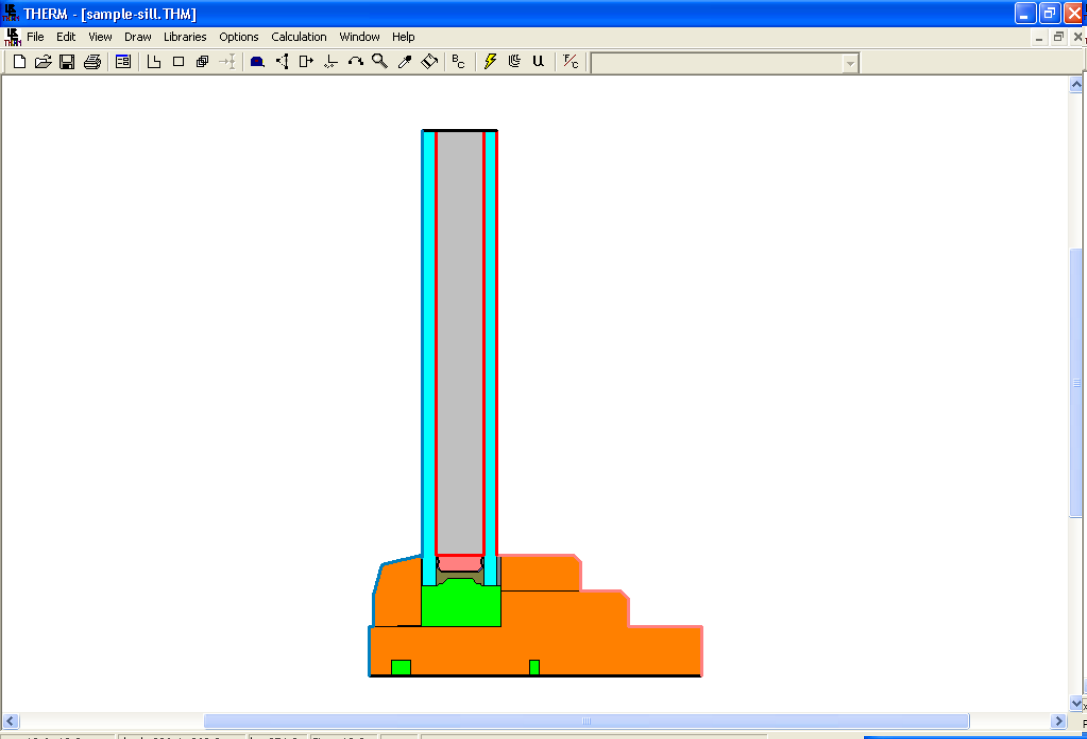
ID	12	Ucenter	0.351	Btu/h-ft2-F
Nlayers	2	SC	0.809	
Area	13.99 ft2	SHGC	0.702	
Edge area	3.32 ft2	Vtc	0.756	

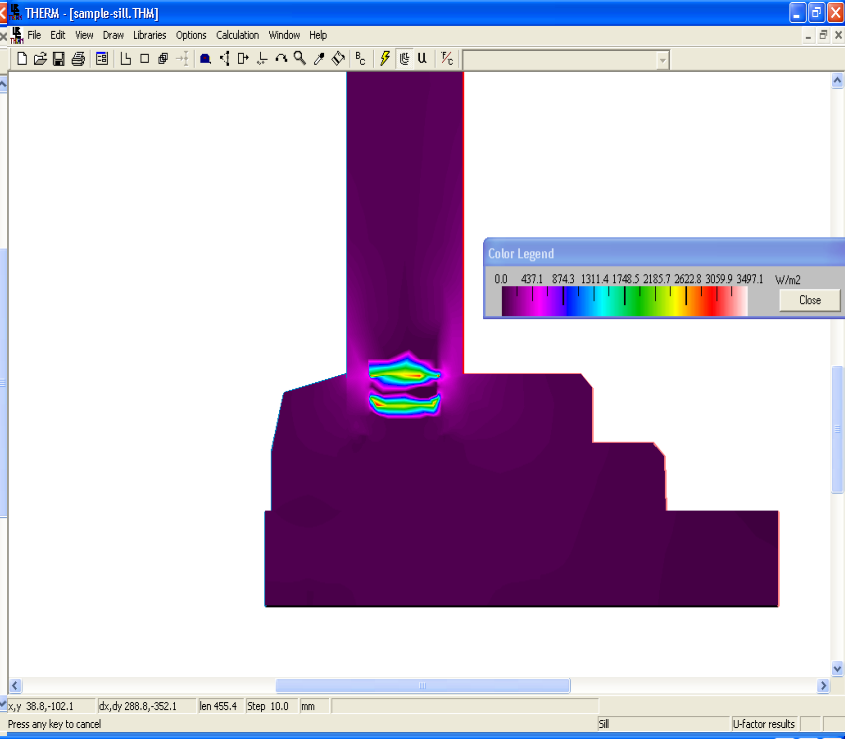
For Help, press F1

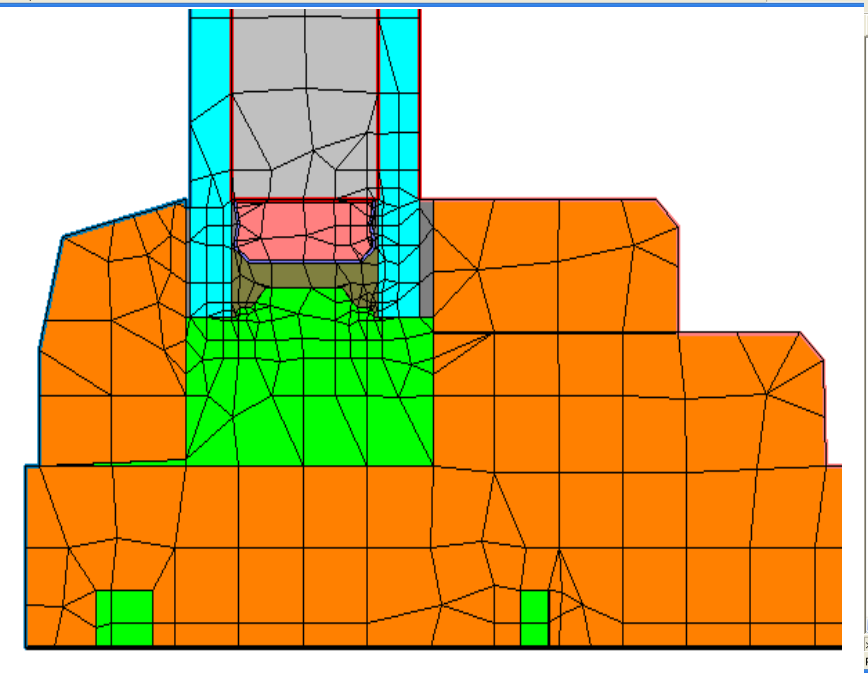
Mode: NFRC IP

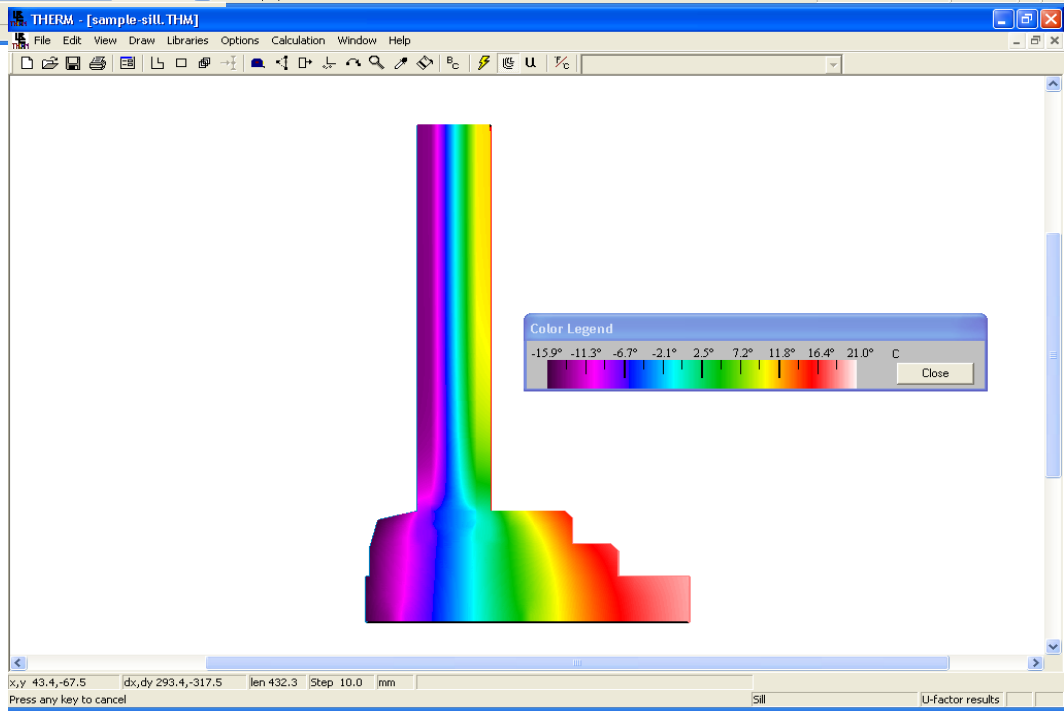
THERM

- Current version 5.2
- Two-Dimensional conduction and radiation heat transfer program
- Finite Element Method (FEM)
- Glazing cavity convection modeling (correlat.)
- Powerful drawing tool for preparing model geometry
- View-factor radiation modeling
- Automatic meshing
- Error estimation and auto re-meshing


THERM - [sample-sill.THM]
File Edit View Draw Libraries Options Calculation Window Help
x,y -13.6,-13.8 dx,dy 236.4,-263.8 len 354.2 Step 10.0 mm
Ready
Sill


THERM - [sample-sill.THM]
File Edit View Draw Libraries Options Calculation Window Help
Color Legend
0.0 437.1 874.3 1311.4 1748.5 2185.7 2622.8 3059.9 3497.1 W/m2
Close
x,y 38.8,-102.1 dx,dy 288.8,-352.1 len 455.4 Step 10.0 mm
Press any key to cancel
Sill
U-Factor results




THERM - [sample-sill.THM]
File Edit View Draw Libraries Options Calculation Window Help
Color Legend
-15.9° -11.3° -6.7° -2.1° 2.5° 7.2° 11.8° 16.4° 21.0° C
Close
x,y 43.4,-67.5 dx,dy 293.4,-317.5 len 432.3 Step 10.0 mm
Press any key to cancel
Sill
U-Factor results

OPTICS

- Current version 5.2
- Virtual Glass Laboratory
- Hundreds of records of glass products with detailed solar-optical properties
- Change glazing thickness
- Switch glazing coating
- Construct glazing with applied films
- Construct glazing with laminate
- International glass product database

Optics

File Edit Database View Tools Graph Help

Main Database (IGDB)

Glazing System | Laminate

Add Glazing | Edit Glazing System | View All | Schematic

Layer:	#1	#2	#3	System
Filename	CMFTE	CLR_3.		GlzSys.
solar, T	0.695	0.859		0.604
solar, Rf	0.115	0.079		0.156
solar, Rb	0.101	0.078		0.154
photopic, T	0.830	0.904		0.755
photopic, Rf	0.096	0.077		0.149
photopic, Rb	0.087	0.077		0.148
EmitF	0.204	0.840		0.204
EmitB	0.840	0.840		0.840

<-- Outside

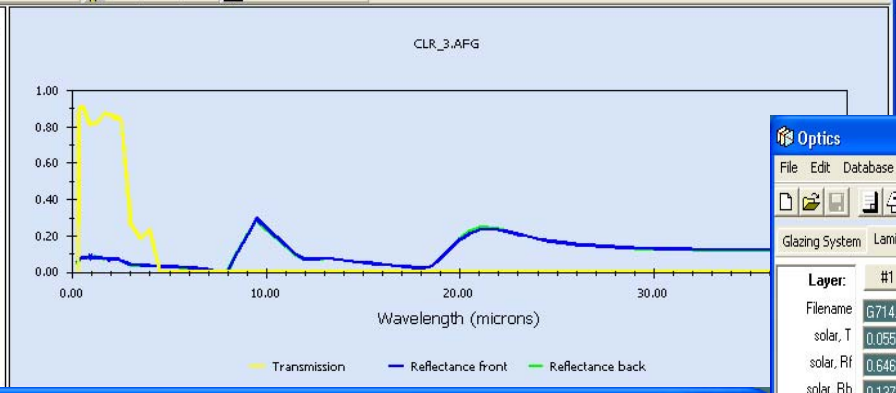
3.1 mm

---- Coating / Applied Film

CLR_3.AFG | Float Glass | W5_NFRC_2003 | IGDB version 12.4

Spectral Properties:

Filename	CLR_3.AFG
solar, T	0.859
solar, Rf	0.079
solar, Rb	0.078
photopic, T	0.904
photopic, Rf	0.077
photopic, Rb	0.077
EmitF	0.840
EmitB	0.840



Type

Type	FileName	ProductName	Nominal (m...	Nominal (in)	Thickness	Manufacturer	NFRC_
Monolithic	118MCW.ATO	Plexiglas® MC	3 mm	double - 1/8 "	2.9972	ATOFINA C...	2602
Monolithic	177MC.ATO	Plexiglas® MC	N/A	no match	4.4958	ATOFINA C...	2603
Monolithic	236MC.ATO	Plexiglas® MC	6 mm	1/4 "	5.9944	ATOFINA C...	2604
Monolithic	ARCBL10.LOF	Arctic Blue™	10 mm	3/8 "	9.4488	Pilkington N...	9929
Monolithic	ARCBL4.LOF	Arctic Blue™	4 mm	5/32 "	3.937	Pilkington N...	9927
Monolithic	ARCBL6.LOF	Arctic Blue™	6 mm	1/4 "	5.6388	Pilkington N...	9928
Monolithic	ASBRNZ6.PGL	Pilkington Optiflo...	6 mm	1/4 "	5.9	Pilkington	4001

Optics

File Edit Database View Tools Graph Help

Main Database (IGDB)

Glazing System | Laminate

Add Glazing | Add Interlayer | Add Embedded Coating | Edit Laminate | View All | Schematic | Warnings!

Layer:	#1	#2	#3	Lamin.
Filename	G714.A	30PVB6	CLR_6.	s1_lam.
solar, T	0.055	0.946	0.801	0.051
solar, Rf	0.646	0.000	0.069	0.646
solar, Rb	0.137	0.000	0.069	0.121
photopic, T	0.140	0.996	0.883	0.134
photopic, Rf	0.488	0.000	0.076	0.487
photopic, Rb	0.299	0.000	0.076	0.276
EmitF	0.155	0.000	0.840	0.155
EmitB	0.840	0.000	0.840	0.840

<-- Outside

Inside -->

G714.AFG ; 5.7 mm

5.7 mm

0.8 mm

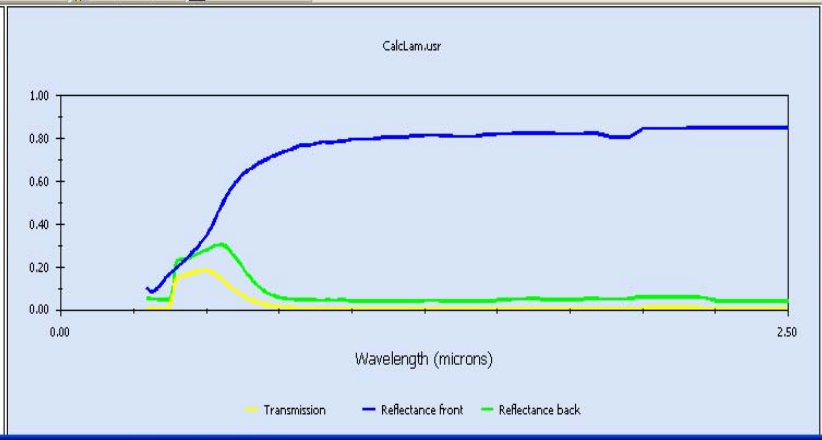
5.7 mm

---- Coating / Applied Film

CalcLam.usr | W5_NFRC_2003 | IGDB version 12.4

Spectral Properties:

Filename	CalcLam.usr
solar, T	0.051
solar, Rf	0.646
solar, Rb	0.121
photopic, T	0.134
photopic, Rf	0.487
photopic, Rb	0.276
EmitF	0.155
EmitB	0.840



Spectral data

Wl. (µm)	T	Rf	Rb
0.300	0.000	0.099	0.049
0.305	0.000	0.093	0.049
0.310	0.000	0.087	0.049
0.315	0.000	0.084	0.048
0.320	0.000	0.086	0.048
0.325	0.000	0.090	0.047
0.330	0.000	0.095	0.047
0.335	0.000	0.102	0.047
0.340	0.000	0.109	0.046
0.345	0.000	0.117	0.045
0.350	0.000	0.128	0.045
0.355	0.000	0.137	0.044
0.360	0.000	0.146	0.044
0.365	0.001	0.153	0.044
0.370	0.003	0.160	0.044
0.375	0.024	0.167	0.050
0.380	0.047	0.174	0.068

OK

Rating of Products

- Temporary



- Permanent



CRRC's Ratings Program

	Initial	Weathered
Solar Reflectance	**0.00**	**Pending**
Thermal Emittance	**0.00**	**Pending**

Rated Product ID	_ _ _ _
Licensed Seller ID Number	_ _ _ _
Classification	Production Line

Cool Roof Rating Council ratings are determined for a fixed set of conditions, and may not be appropriate for determining seasonal energy performance. The actual effect of solar reflectance and thermal emittance on building performance may vary.

Manufacturer of product stipulates that these ratings were determined in accordance with the applicable Cool Roof Rating Council procedures.







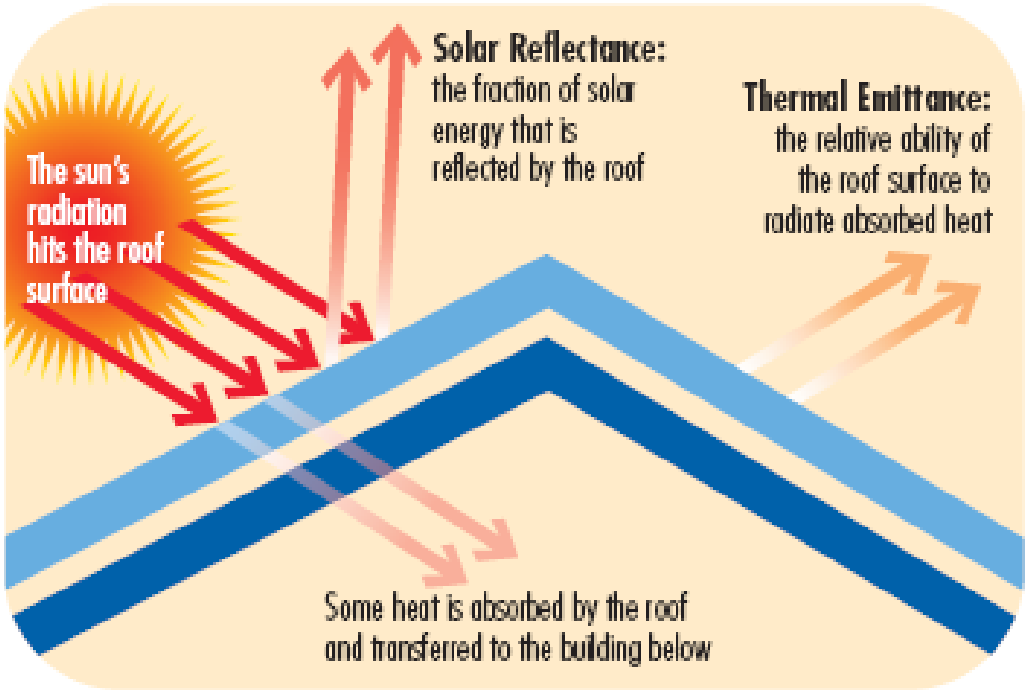
- Measures *reflectance* and *emittance* values
- Initial and three year values
- Actual weather exposure in 3 sites:
  - Hot/Humid (Florida)
  - Cold/ Temperate (Ohio)
  - Hot/Dry (Arizona)
- Directory and Product Label

What is a Cool Roof?

CRRC only looks at **surface** properties:

- Solar Reflectance
- Thermal Emittance

CRRC does **not** set minimum requirements



Cool Roof Case Study

Jefferson Houston Elementary School - Alexandria, VA
White EP Single-ply Insulated Roofing System
Re-roof Application Total Roof Area: 83,000 ft^2

Project Costs	**Total Expenditures**	**$330,000**
	Dollars per ft^2	**$3.87**
	Extra Costs for High-Efficiency	**$0**
Cost Savings	**Annual Dollar Savings**	**$31,000**
	Dollar Savings Per ft^2	**$0.37**
Energy Savings	**Annual Energy Savings**	**514,000 kWh**
Pollution Prevention	**Annual CO_2 Emissions**	**1,217,000 lbs**
	Car Pollution Equivalent	**122 cars**

CRRC Approved Test Methods

Solar Reflectance

- Reflectometer (ASTM C1549)
- Spectrometer (ASTM E903)
- CRRC-1 Test Method 1
- Pyranometer (ASTM E1918 and E1918A)









CRRC Approved Test Methods

Thermal Emittance

- Emissometer (ASTM 1371)



NAIMA

NORTH AMERICAN INSULATION MANUFACTURERS ASSOCIATION

Wall Insulation

ASTM C 518

Wall Systems

ASTM C 1363, ASTM C1155



NAIMA Member Plant Locations – Canada, United States and Mexico

Members:

Aislantes Minerales, S.A.

Amerrock Products, LP

CertainTeed Corp.

FiberTEK Insulation, LLC

Fibrex Insulations Inc.

Industrial Insulation Group, LLC

Isolatek International

Johns Manville

Knauf Insulation

Owens Corning

Rock Wool Manufacturing Co.

Roxul Inc.

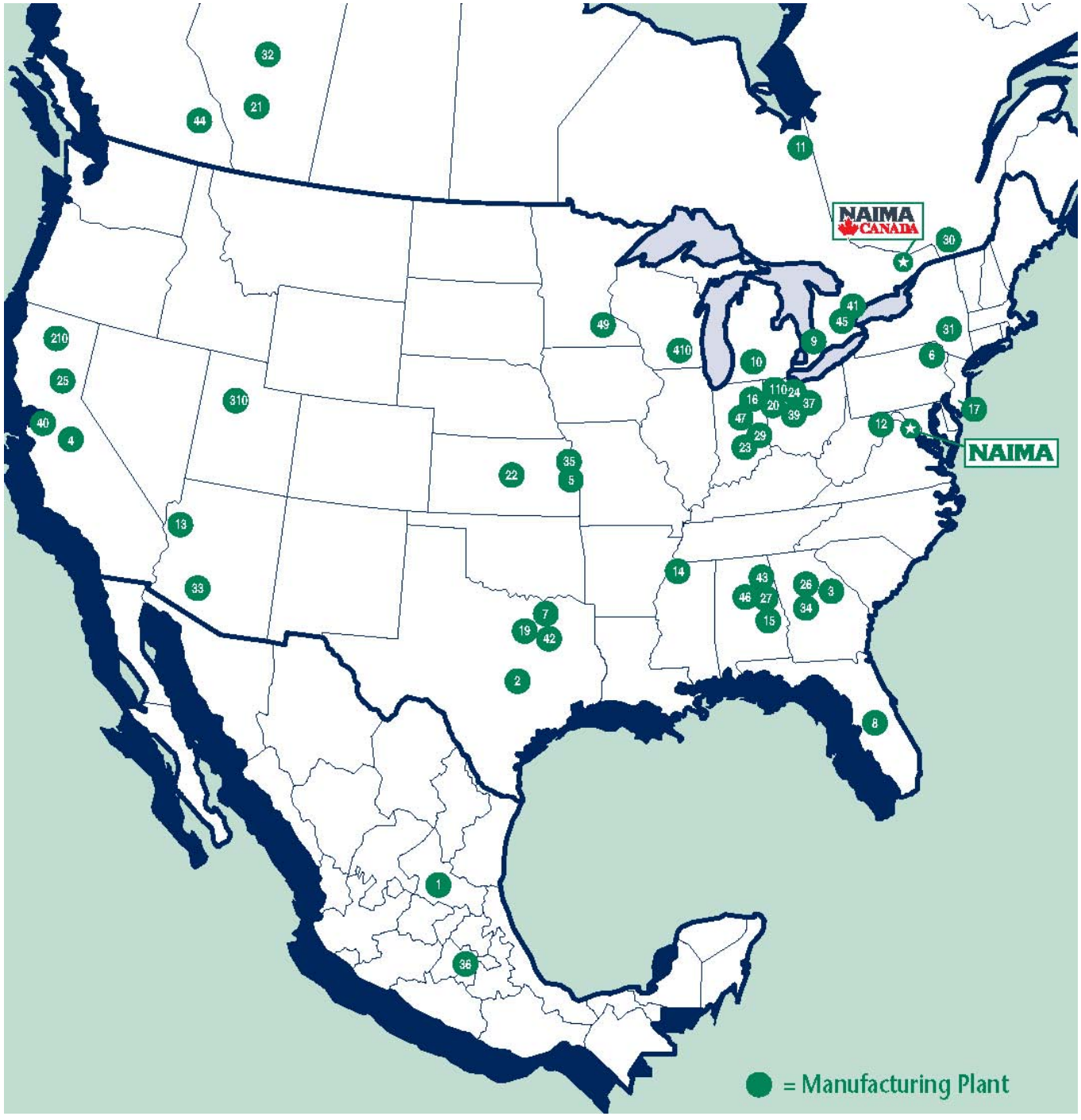
Sloss Industries Corp.

Thermafiber, Inc.

USG Interiors, Inc.

INSULATE TODAY 1933-2008 SAVE TOMORROW

Celebrating 75 Years of Energy Efficiency



Collaboration / opportunities - Jordan

- Phase I: (October 2008) - Completed
  - Workshop on Window Energy Rating – Involving key stake holders (Government officials, Institutes, associations, public interest and manufactures)
  - Provide Basic Training for THERM, Windows and OPTICS Software.

Collaboration opportunities

- Phase II: (2009 - 2010) Capacitate building:

  (Collaboration with Higher Council for Science and Technology (HCST), and Royal Scientific Society (RSS)
  - Computer Software Simulation training workshop (2009)
    - Building simulation (DesignBuilder, Energy Plus)
    - WUFI – moisture migration analysis program
    - THERM, WINDOW and OPTICS – fenestration analysis program:
  - Spectral data testing (2010)
  - Establishment of Regional Energy Product and Component testing Center (2009 – 2010)
  - New Jordan Energy Code implementation and Pilot project Crystalle Building, Abdali, Jordan - (2009)
- Phase III (2011 and 2012)
  - Develop a Middle East Building Energy Efficiency Unified Code
  - Work with Governments, Industry associations and Research Institutes to Develop a fenestration rating council
  - Energy Star program

Our Successes

- Help Establish British Fenestration Rating Council
- Help Establish Australian Fenestration Rating Council
- Help Establish South African Fenestration and Insulation Ratings
- Help Establish Simulation Laboratory in India
- Working to Establish Energy Center in India
- Assisted Bureau of Energy Efficiency India to develop Energy Conservation Building Code and for its implementation
- Working With Chinese Institutes on Standards Development
- Assisting Chinese to Develop and Establish Window Energy Rating Organization
- Assisting Kuwait Institute of Scientific Research for Establishment of Testing Laboratory

Helpful Links

- http://www.eere.energy.gov/buildings/
- www.NFRC.org
- www.naima.org
- www.PipeInsulation.org
- www.SimplyInsulate.com
- www.coolroofs.org
- http://windows.lbl.gov
- http://www.ornl.gov/sci/eere/tech_building.shtml



?

Thank You

Project 3.2
Jordan (c)

Project Name: International Harmonization – Jordan

Date: March 31 - April 2, 2009

Purpose: The National Fenestration Rating Council (NFRC) participated in events to work towards window labeling harmonization.

Project Summary:

NFRC attended several events in Jordan working towards window labeling harmonization.

Click here for a Building Envelop Energy Efficiency Technology Cooperation Workshop agenda





INVITATION
To Attend

Jordan - USA
Building Envelop Energy Efficiency Technology Cooperation Workshop

Building construction in Jordan is experiencing a boom, which has put an additional burden on the government to generate more electricity to meet the demand. Buildings account for major portion of electricity consumption in the region and most of it is spent on meeting the Air Conditioning and lighting load. As oil is the main fuel source used for generating electricity, any significant reduction in use of electric consumption will result in reduced demand in the market place and stress on the economy. This demand can effectively be reduced by selecting energy efficient building envelope components especially fenestration system. Cool roof technology will also be an effective technology to be adopted especially in the residential market.

This workshop effort resulted from the initial meeting of the U.S.-Jordanian Joint Committee Meeting (JCM) on Science & Technology (S&T) Cooperation, July 9 – 10, in Amman. As part of the outcome, the Department of Energy's (DOE) Office of African and Middle Eastern Affairs reviewed potential opportunities for partnering in energy with two key umbrella organizations, the Jordanian Higher Council for Science & Technology (HCST) and the State Department's Office of Oceans, International Environment and Scientific Affairs.

The workshop is a first step to initiate a discussion to developing a building envelope rating system which will help consumers to identify energy saving products against less efficient alternatives in windows, insulation and other energy intensive market products.

DOE along with the National Fenestration Ratings Council (NFRC) is committed to assist Jordan counterparts to develop the rating program and provide basic training in specialized computer software program THERM, WINDOWS and OPTICS used for analyzing the products energy performance.

Objectives:

- **Establishment of Rating and Labeling of Building Envelope Components.**
- **Understanding the barriers and illustrate ways to overcome the barriers for procurement of energy efficient products**
- **Energy efficiency codes and their implementation**

Venue: Amman Chamber of Commerce , Second Circle – Zahran Street, Amman 11118. Telephone #: (962) 6 464 3001. www.aci.org.jo

Time/Date: 9:00 to 17:30 October 25th, 2008

Sponsors: Jordanian Higher Council for Science & Technology (HCST) and the State Department's Office of Oceans, International Environment and Scientific Affairs, US-Department of Energy and National Fenestration Rating Council





Agenda:

9:00-9:30: Registration

9:30-10:00: Opening and Welcome speech

Prof. Anwar Battikhi /Secretary General of the Higher Council for Science and Technology

10:00-11:00: Policy, Implementation and Incentives for Energy Ratings of Building Envelop Components

Speaker (Jordan): Eng.Tala Awadalla
Title: Policy, Implementation and Incentives for Energy Ratings of Building Envelop in Jordan
Organization: Royal Scientific Society

Speaker (USA): Mr. Mark Lafrance Technology Development Program Manager- US-DOE
Title: US-DOE Policies to Promote Energy Efficiency in Building Envelop and Focused Effort to Achieve Net Zero Energy Buildings.
Organization / Company: US-Department of Energy.

Discussion: Question and answers

11:00-11:15: Coffee Break

11:15-12:15: Energy Efficiency Code requirements for Building Envelop Sector in Jordan

Speaker (#1): Prof. Ali Badran
Title: Present Status of Research on Building Envelop in Jordan
Organization: University of Jordan

Speaker (#2): Eng. Nizar Qaqish
Title: Codes, Manuals, Industry and Testing Facilities on Building Envelop in Jordan
Organization: Royal Scientific Society

Discussion: Question and answers

Lunch Break:: 12:15 to 13:30

13:30-14:30: Energy Rating in the USA – means to promote energy efficient products

Speaker (USA): Bipin Shah
Title: International Programs Coordinator for National Fenestration Rating Council - USA
Organization / Company: WinBuild Inc.

Speaker (USA): Stephanie Stern
Title: Energy Ratings for Cool Roof
Organization / Company: Cool Roof Rating Council - USA.

Speaker (USA): Joe Huang
Title: Role of Building Energy Simulation for Development of Energy Codes and Incentive Programs - USA
Organization / Company: White Box Technologies.





Discussion: Question and answers

14:30 – 15:00: Fenestration, Glass and Real Estate industry view points

Speaker (#1 -Fenestration): Karunakaran. A P, Sales Manager Middle East,
Title: How Green Are Your Windows?" – Window Film and its role in reducing energy consumption
Organization: Solar Gard® Window Films manufactured by Bekaert Specialty Films LLC

Speaker (#2 - Insulation): Glen Runagall, Managing Director, Dryvit - Europe, Middle East, Africa & India
Title: Wall Insulation and Energy efficiency
Organization: Dryvit UK Ltd

15:00-15:15: Coffee Break

15:15-16:00: Fenestration, Glass and Real Estate industry view points (Continue)

Speaker (#3 – Fenestration): Leon Davids (Marketing & Business Development)
Title: "Window Film Industry - Improving Energy Efficiency in Glazing Systems'
Organization: Hanita Coatings

Speaker (#4 – Fenestration): Alex Dantziguian
Title: Thermal Break Systems – The Answer to New Market Needs in Energy Saving Windows
Organization: Technoform Middle East

Speaker (#5 – Lighting,): Khaled Masri
Title: Lighting Controls and Equipments the Next Step After Building Envelope Energy Efficiency
Organization: Representing National Electrical Manufacturer Association (NEMA)

16:00-17:30: General Discussion

Next Steps

Project 3.2
Japan (a)

Project Name: International Harmonization - Japan

Date: September 2008

Purpose: NFRC hosted a Japanese delegation in September 2008.

Project Summary:

NFRC attended several events in Japan working towards window labeling harmonization.

NFRC overview presented to Japanese Visitors

The National Fenestration Rating Council

National Fenestration Rating Council®

To rate the energy efficiency of windows, doors, & skylights and other Fenestration products

Why was NFRC Created?

- To provide standardized methods for determining the windows, doors and skylights energy performance



NFRC Mission

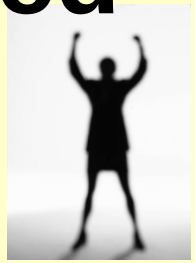


Global Warming

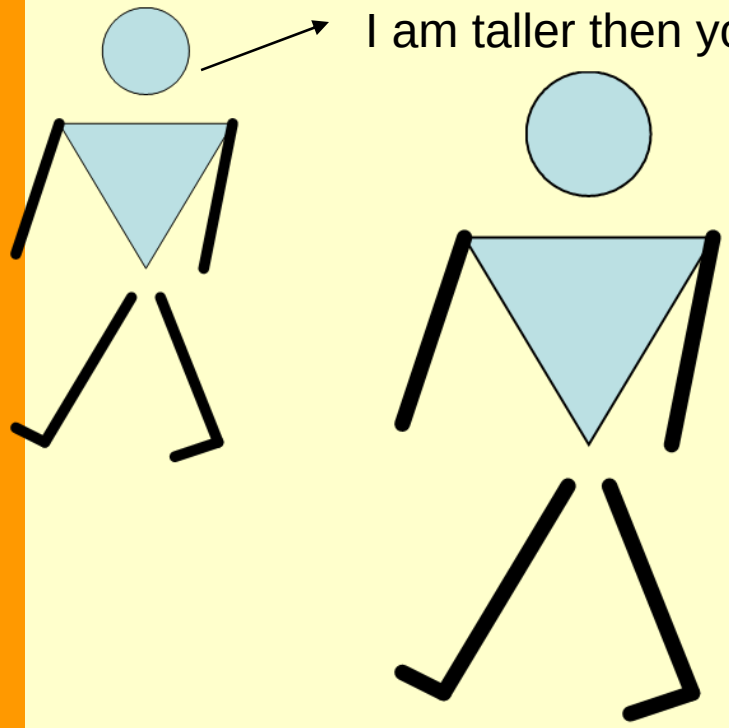
NFRC develops and administers comparative energy and related rating programs that serve the public and satisfy the needs of its private sector partners by providing fair, accurate and credible, user-friendly information on fenestration product performance.

In Rating and Codes a

Level Playing Field is Required

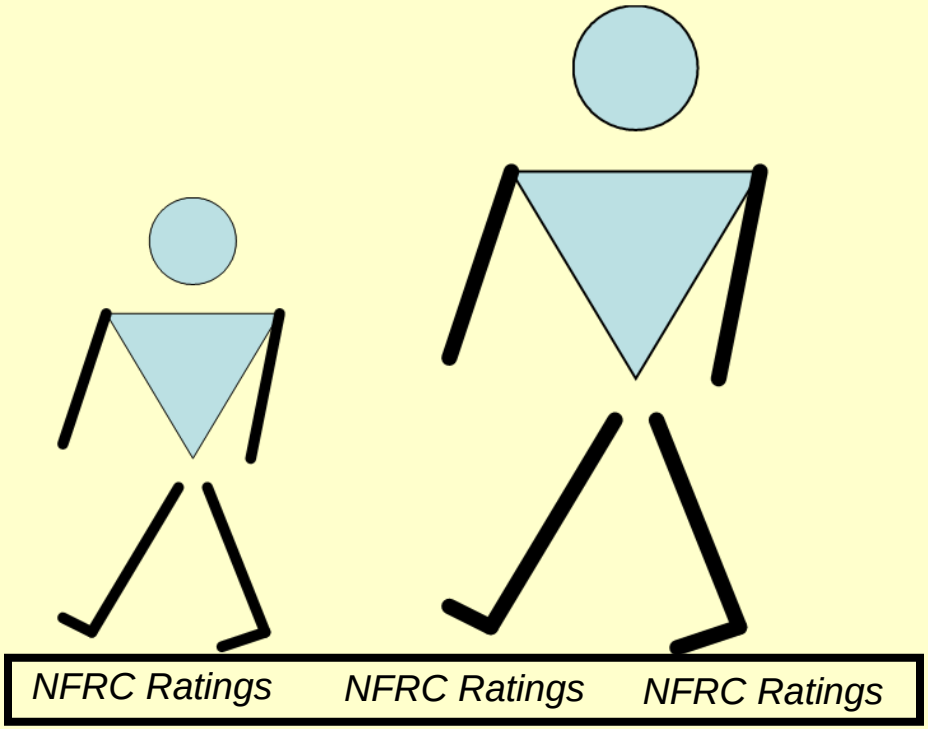


Consumer is the winner





Consumer



If Fair Rating is available

Introduction to NFRC



Energy Efficiency

FAST FACTS

- Created in 1989, by industry
- Unique, educational non-profit public/private organization representing:
  - **Industry (fenestration and building)**
  - **State energy offices**
  - **Design Professionals**
  - **Representatives from Higher Education**
  - **Utilities**
  - **Consumer Organizations**

(Not a trade association)

NFRC Members and Participants

- 650 participants
  - Window manufacturers
  - Use labeling system
- 210 members
  - Manufacturers and others
  - Can vote
- Can be both participant and member
  - About 140 Voting manufacturers

World Window/Door Market

- North America: $36.8 billion
- Western Europe: $32.4 billion
- Asia/Pacific: $36.1 billion
- Rest of world: $8.2 billion
- Total: $117.5 billion

- 2011 forecast: $150 billion worldwide

Buildings Use Most Energy in US (05 stats)

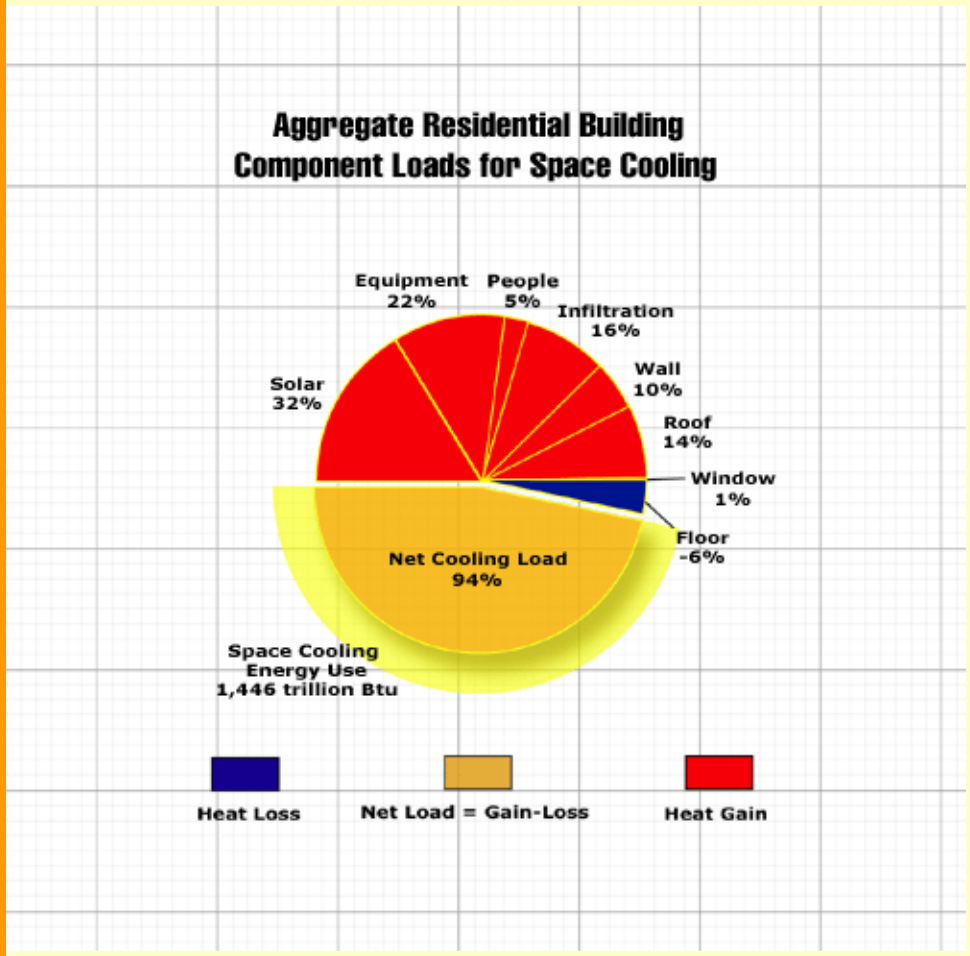
- Buildings: 40%
  - Residential: 22%
  - Commercial: 18%
- Industry: 32%
- Transportation: 28%
- Total US Consumption: 100 Quadrillion BTUS! (1/4 of world's energy)
  - US Buildings consume about 10% of world energy

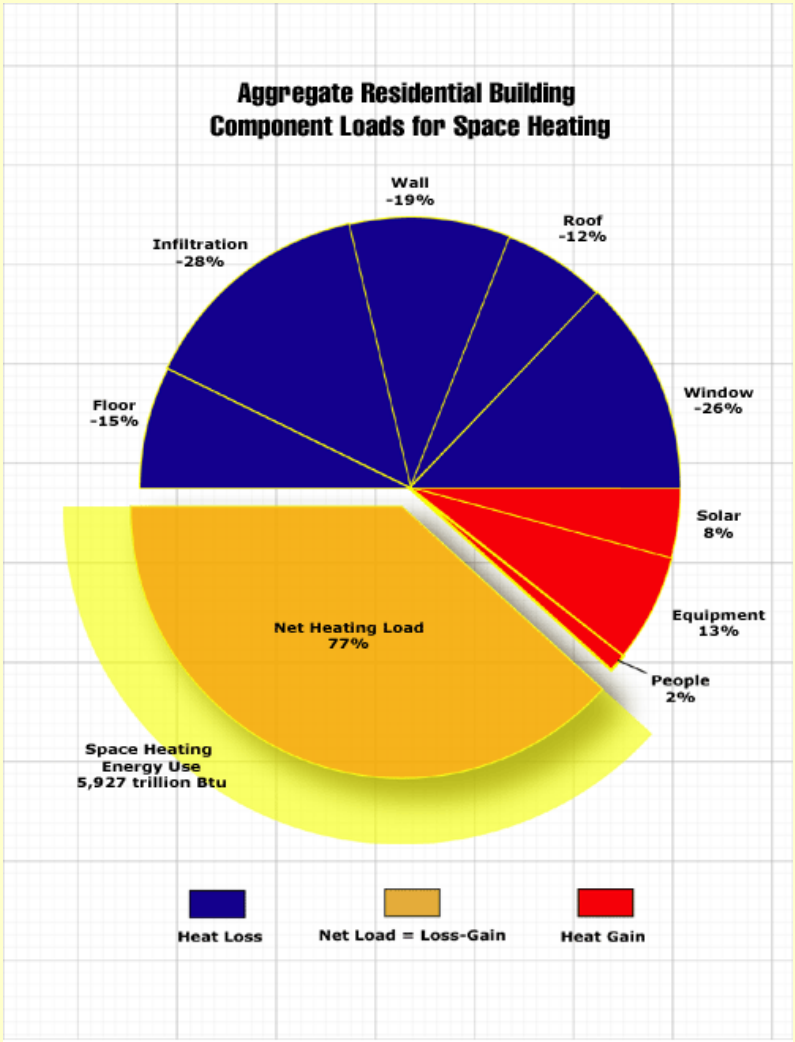
Buildings Use Most Electricity in US

- Buildings: 72%
  - Commercial: 35%
  - Residential: 37%
- Industry: 28%

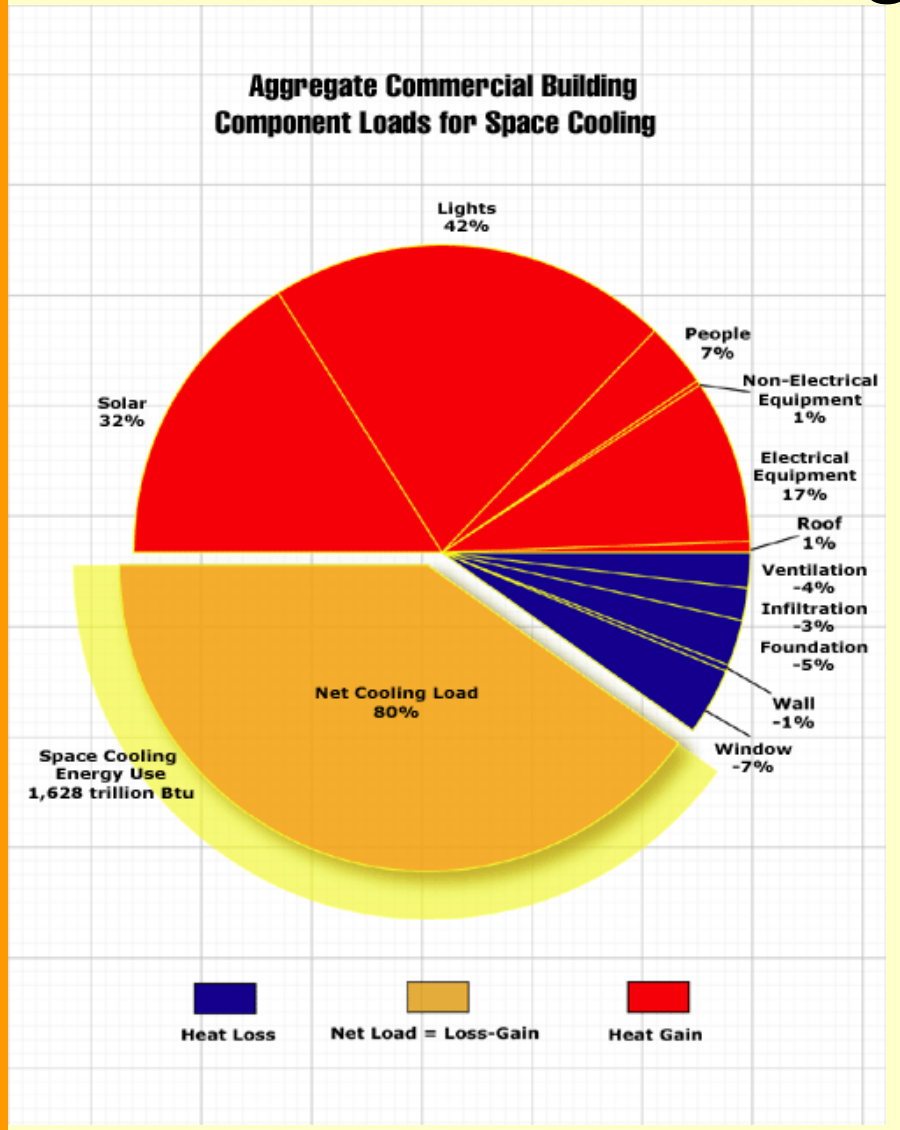
- 3.6 quadrillion kwhs consumed by buildings
  - releasing 9 quadrillion pounds $C0_2$

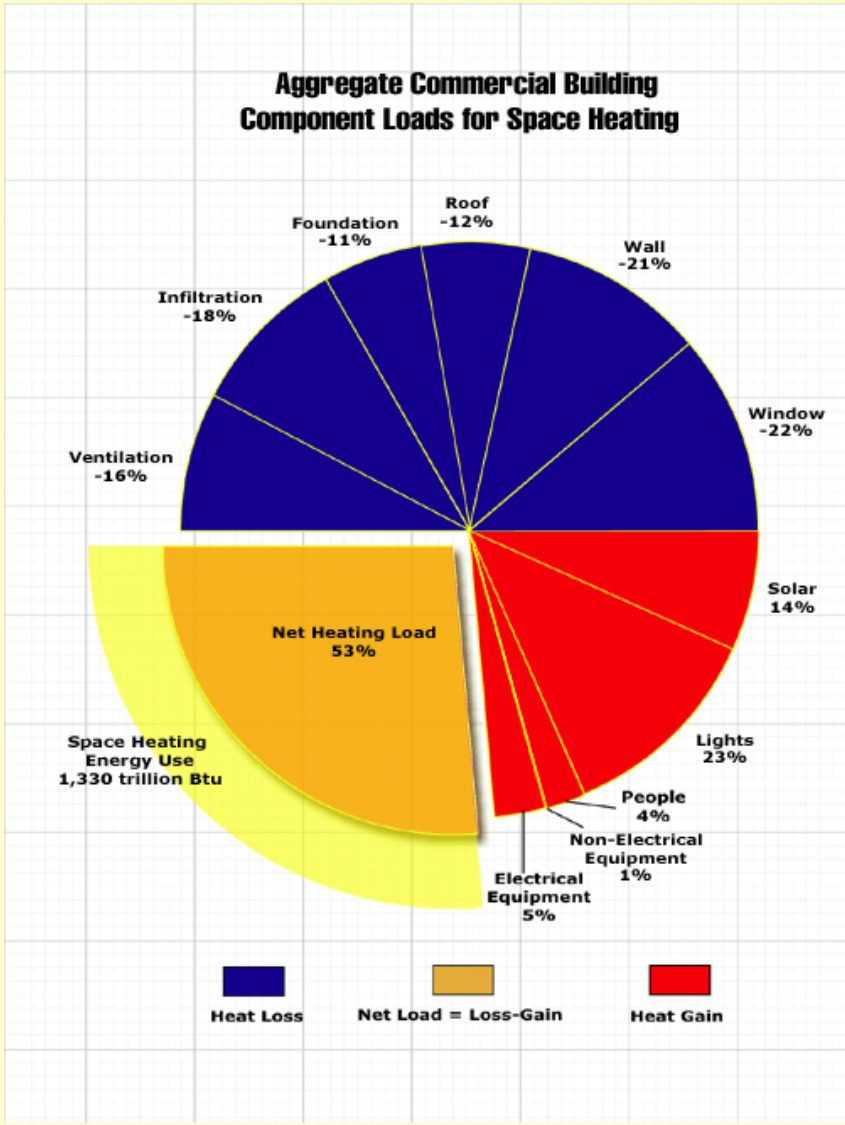
Aggregate Residential Building Loads





Aggregate Commercial Building Loads

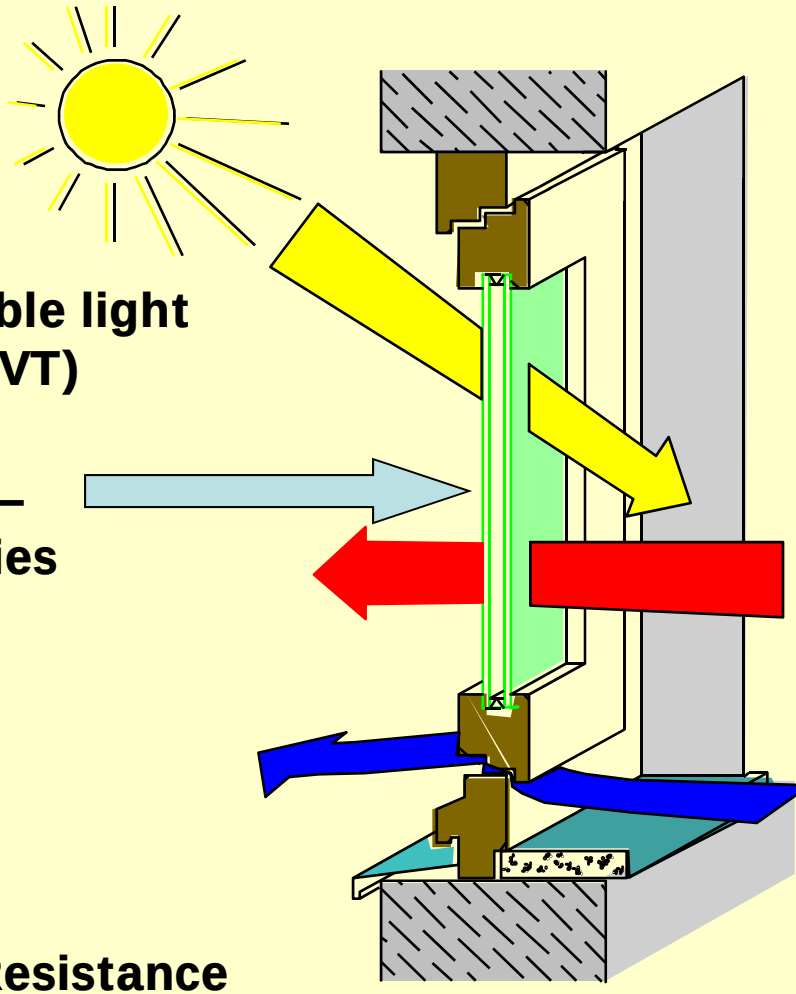




NFRC Energy Performance Ratings

NFRC 200 – Solar heat gain coefficient, Visible light transmittance (VT)

NFRC 300/301 – Optical Properties (Emissivity)



NFRC 100 - U-factor

NFRC 400 - Air Leakage

NFRC 500 – Condensation Resistance

The NFRC "Rating Process"



Simulation Laboratory
Simulate All Options

Testing Laboratory
(Test One Base Line Product)

Inspection Agency (IA)
Issue Certificate authorization, Plant inspection

NFRC Label or Label Certificate

Market Place
Responsible Party Label Product

Simulations

- Performed by NFRC accredited personnel
- 15 accredited labs in US and Canada
  - International simulators pending
- Use WINDOW and THERM software
  - Developed by University of CA-Lawrence Berkeley National Labs
  - Based on ISO 15099 algorithms/equations
  - Use ISO 9050 spectrum

Testing

- Performed by NFRC accredited labs
- 7 accredited labs across US and Canada
  - International labs under construction
- Use ASTM C1199 and ASTM C1423 procedures
- Must test one product per product line every four years

Inspection Agency

- Accredited by NFRC
- Compare simulations to tests
- Allow manufacturer to use NFRC labels
- Inspect manufacturing plants for NFRC compliance once/year
  - Includes international participants

National Fenestration Rating Council®
CERTIFIED

World's Best Window Co.

Millennium 2000+
Vinyl-Clad Wood Frame
Double Glazing • Argon Fill • Low E
Product Type: **Vertical Slider**

ENERGY PERFORMANCE RATINGS

U-Factor (U.S./I-P)	Solar Heat Gain Coefficient
0.35	**0.32**

ADDITIONAL PERFORMANCE RATINGS

Visible Transmittance	Air Leakage (U.S./I-P)
0.51	**0.2**

Manufacturer stipulates that these ratings conform to applicable NFRC procedures for determining whole product performance. NFRC ratings are determined for a fixed set of environmental conditions and a specific product size. NFRC does not recommend any product and does not warrant the suitability of any product for any specific use. Consult manufacturer's literature for other product performance information.
www.nfrc.org

NFRC Label

NFRC Label Certificate

(for Site-Built Products)



PROJECT LOCATION

Street address: _____

City, state, zipcode: _____

Project name (optional): _____ Designer (optional): _____

PRODUCT LINE INFORMATION

Operator type (per NFRC 100, Table 1): _____

Product line ID number: _____ Individual product ID number: _____

How many of this individual product: _____ Location in building: _____

Elevation drawing page: _____ Fenestration (window & door) schedule page: _____

FRAME MATERIAL SUPPLIER

Company name, address: _____

City, state zipcode: _____

Contact person, phone & fax number: _____

GLAZING MATERIAL SUPPLIER

Company, name, address: _____

City, state, zipcode: _____

Contact person, phone & fax number: _____

GLAZING CONTRACTOR/INSTALLER

Company, name, address: _____

City, state, zipcode: _____

Contact person, phone & fax number: _____

CERTIFICATION AUTHORIZATION

Independent Certification and Inspection Agency (IA): _____

Date Certification Authorization Issued: _____

National Fenestration Rating Council®

NFRC Labeling Requirements

an Overview….

Temporary Label – Ratings Information

- ***Required Ratings* –*** Appear in the order listed:
  - U-factor (to two decimal places for IP units & one decimal place for SI units)
  - Solar Heat Gain Coefficient (to two decimal places)
  - Visible Transmittance (to two decimal places)
- ***Optional Ratings*-*** Appear in alphabetical order, moving left to right:
  - Air Leakage (to one decimal place)
  - Condensation Resistance (whole number)

****** For ratings less than 1, a leading "0" shall be used*

Temporary Label Required Information

In product description box:

- Manufacturer name, code, or numeric ID
- Frame Type
- Product Type
- Glazing Description, including
  - Gas fill and/or
  - Low E, if present

Temporary Label
Optional Information

In product description box:

- Certified Products Directory number (to individual product ID); e.g.,
  - CPD# 000 – X - 001- 001
  - *[Mfr.ID] [IA] [PL#] [individual product #]*
  - *HIGHLY RECOMMEND ADDING!!!*
- Air space width
- Coating emissivity
- Spacer type (generic or CPD code)
- Glazing tint or reflective coating (generic or CPD code)
- Manufacturer contact information

Permanent Certification Label

In General,

- Label remains permanently affixed to the authorized product.
- Label shall be affixed to ensure legibility and visibility from the interior after installation
- Label shall be affixed at the time and place of final manufacture and prior to shipment

Permanent Certification Label

May be in the form of a

- ***Label***, stand alone label
- ***Tab***, extension to existing certification label
- ***Series of marks or etchings***, indelible markings on product

Shall contain

- NFRC logo or wordmark
- Licensee's identification
- Product line identification number (CPD # to product line level)

May contain

- IA identification
- Series/Model name

Permanent Certification Label
Location

- **Operable products** – visible and legible from either its open or closed position, and located on a surface not subject to exterior weather when closed.
- **Non-operable products (fixed**) – visible and legible and located on a portion of either the frame, glazing, spacer, or other interior surface. Maybe located on the exterior surface of the product that is protected from exposure to direct sunlight and moisture (e.g., window/door head).
- **Attachment Products** – visible and legible, and located on the box or packaging used to contain the product.
- **See Section 6.5, PCP-2006**

Permanent Certification Label
Suggested Location



Plant Qualification

Each plant location must physically test at least one production line unit every 4 years.

- The production line unit can be any individual product option within a product line that is manufactured at the plant location.
- Tested U-factor is compared with the equivalent U-factor of the individual product option within the simulation matrix.
- Product line is validated if the simulated and tested U-factor meets NFRC 100 equivalence criteria.

Plant Qualification continued….

- Each plant location on Schedule I
- If a manufacturer has only one location:
  - then recertification satisfies plant qualification requirements.

Plant Qualification continued….

- If a manufacturer has more than one plant location, additional testing is required to cover those additional locations.
  - If the number of authorized product lines is greater than the number of plants, then each plant is required to test a different production line unit.
  - If the number of plant locations is greater than the number of authorized product lines, then the same product line is tested in more than one plant location.
  - When an additional plant location is added to Schedule I, that added location is required to test a production line unit for plant qualification within 6 months of being added to the schedule.

Fenestration & Code

- Each state legislates a code
  - IECC (residential)
  - ASHRAE 90.1 (commercial)
- Some states develop own code-based on IECC/ASHRAE
  - California has Title 24
  - Maine, Michigan has independent code
  - Mississippi has no energy code

Fenestration and Code

- **NFRC required by:**
  - **IECC**
  - **ASHRAE**
  - **ENERGY STAR (voluntary program)**

IECC Directly References NFRC

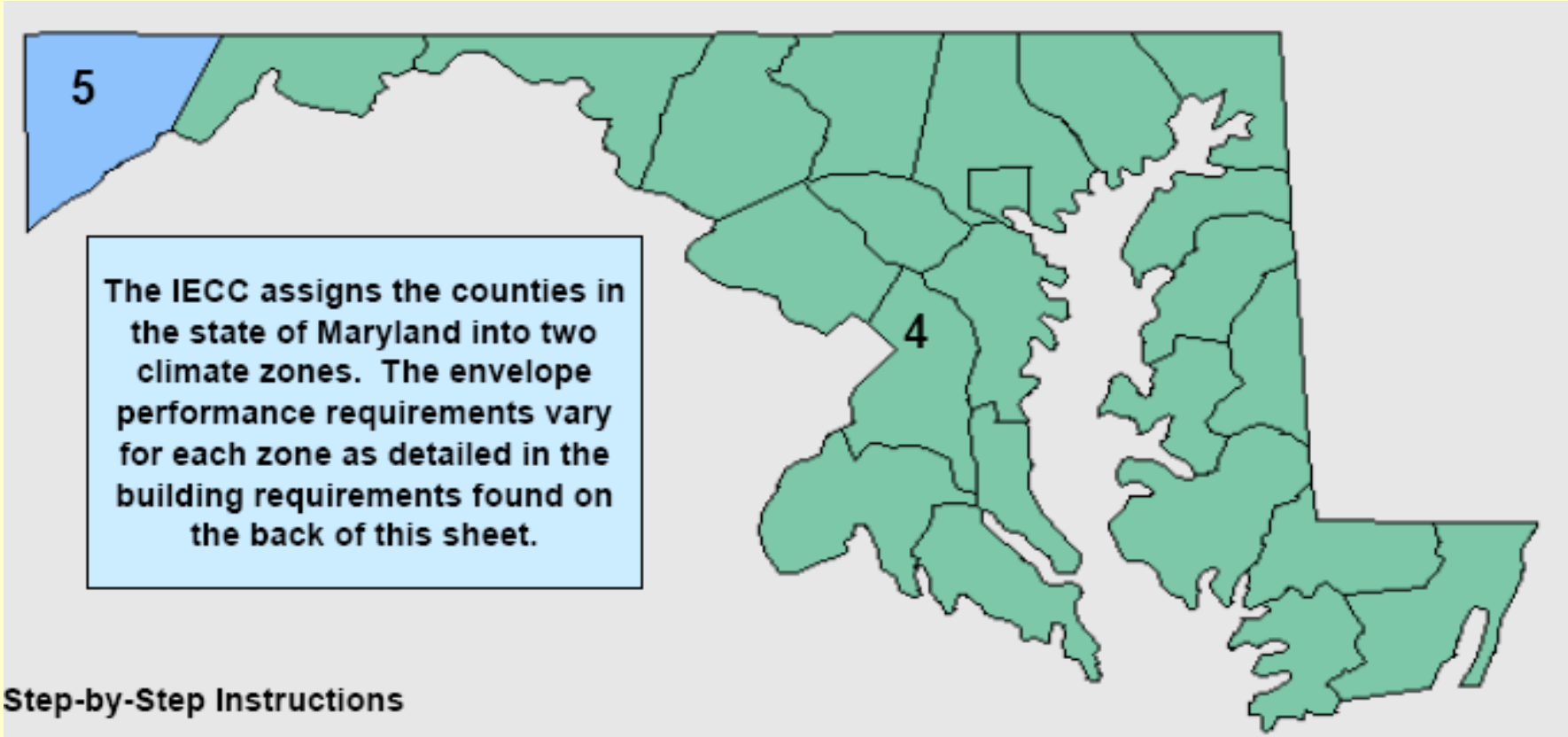
102.5.2 Fenestration product rating, certification and labeling. *U*-factors of fenestration products (windows, doors and skylights) shall be determined in accordance with NFRC 100 by an accredited, independent laboratory, and labeled and certified by the manufacturer. The solar heat gain coefficient (SHGC) of glazed fenestration products (windows, glazed doors and skylights) shall be determined in accordance with NFRC 200 by an accredited, independent laboratory, and labeled and certified by the manufacturer. Where a shading coefficient for a fenestration product is used, it shall be determined by converting the product's SHGC, as determined in accordance with NFRC 200, to a shading coefficient, by dividing the SHGC by 0.87. Such certified and labeled *U*-factors and SHGCs shall be accepted for purposes of determining compliance with the building envelope requirements of this code.

When a manufacturer has not determined product *U*-factor in accordance with NFRC 100 for a particular product line, compliance with the building envelope requirements of this code shall be determined by assigning such products a default *U*-factor in accordance with Tables 102.5.2(1) and 102.5.2(2). When a SHGC or shading coefficient is used for code compliance and a manufacturer has not determined product SHGC in accordance with NFRC 200 for a particular product line, compliance with the building envelope requirements of this code shall be determined by assigning such products a default SHGC in accordance with Table 102.5.2(3). Product features must be verifiable for the product to qualify for the default value associated with those features. Where the existence of a particular feature cannot be determined with reasonable certainty, the product shall not receive credit for that feature. Where a composite of materials from two different product types is used, the product shall be assigned the higher *U*-factor.

Residential Energy Codes

- IECC governs
- MD and VA require IECC 2006
- Window must display NFRC certificate

IECC MD Climate Zones



IECC MD Fenestration Requirements

WINDOWS AND INSULATION

Package	Window U-factor	Skylight U-Factor	Ceiling R-Value	Wood Frame Wall R-Value	Mass Wall R-Value
Climate Zone 4	0.40	0.60	R-38	R-13	R-5
Climate Zone 5	0.35	0.60	R-38	R-19 or 13+5	R-13

If No NFRC Rating

- Default tables in IECC must be used
  - Unlikely window complies!
- Default tables penalize all window performance

IECC defaults

TABLE 102.1.3(1)
DEFAULT GLAZED FENESTRATION *U*-FACTOR

FRAME TYPE	SINGLE PANE	DOUBLE PANE	SKYLIGHT	
			Single	Double
Metal	1.20	0.80	2.00	1.30
Metal with Thermal Break	1.10	0.65	1.90	1.10
Nonmetal or Metal Clad	0.95	0.55	1.75	1.05
Glazed Block	0.60			

TABLE 102.1.3(3)
DEFAULT GLAZED FENESTRATION SHGC

SINGLE GLAZED		DOUBLE GLAZED		
Clear	Tinted	Clear	Tinted	GLAZED BLOCK
0.8	0.7	0.7	0.6	0.6

Commercial Fenestration Requirements

- ASHRAE 90.1 NFRC References:

5.8.2.4 U-factor. U-factors shall be determined in accordance with NFRC 100. U-factors for skylights shall be determined for a slope of 20 degrees above the horizontal.

5.8.2.5 Solar Heat Gain Coefficient. *SHGC* for the overall *fenestration area* shall be determined in accordance with NFRC 200.

A8 Fenestration. All *fenestration* with *U-factors, SHGC,* or visible light transmittance determined, certified, and labeled in accordance with NFRC 100, 200, and 300, respectively, shall be assigned those values.

MD, VA in Climate Zones 4,5

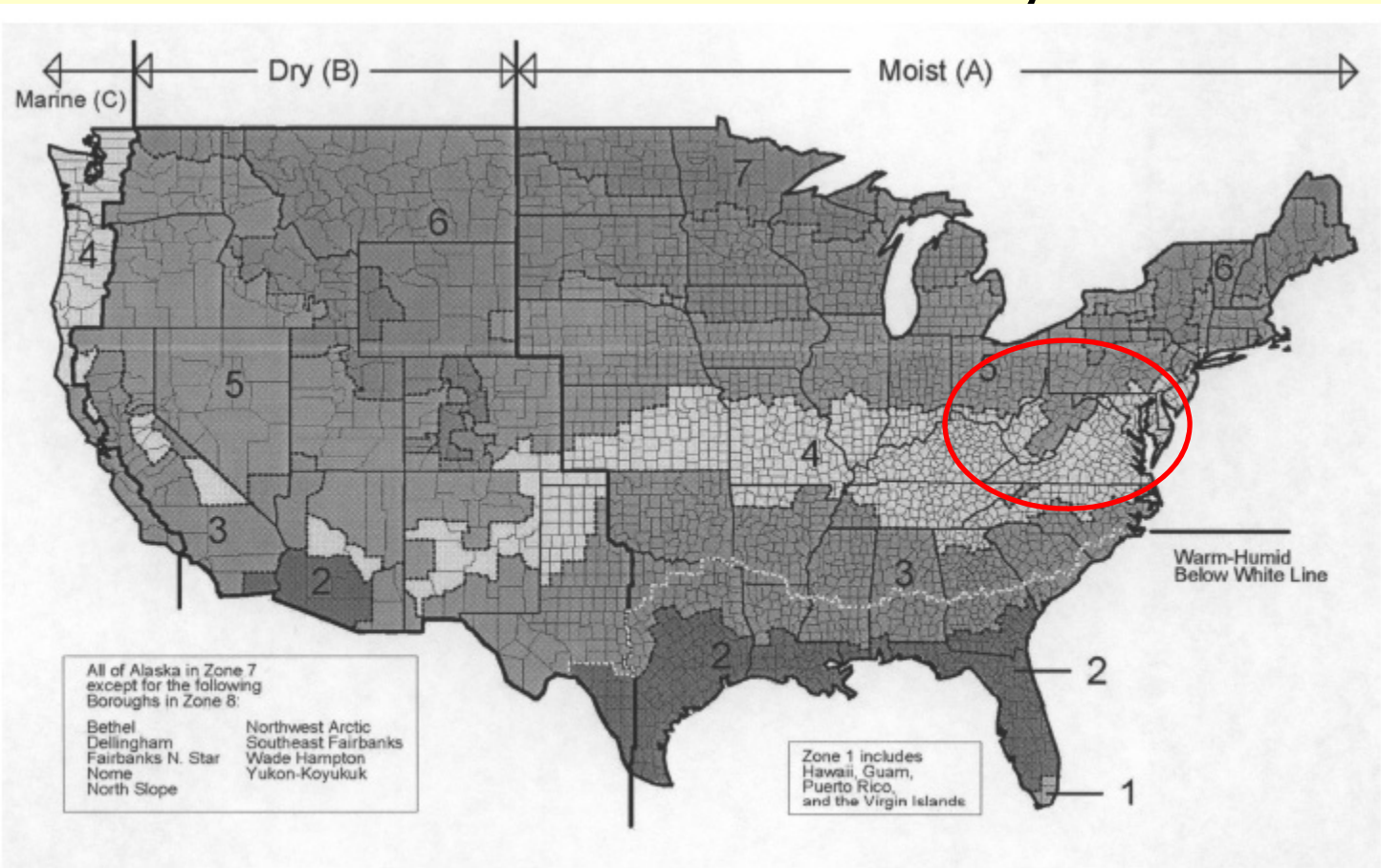


Figure B-1 Climate zones for United States locations.

IECC Commercial Requirement, < 40% WWR

TABLE 502.3
BUILDING ENVELOPE REQUIREMENTS: FENESTRATION

CLIMATE ZONE	1	2	3	4 except Marine	5 and Marine 4	6	7	8
Vertical Fenestration (40% maximum of above-grade wall)								
***U*-Factor**								
Framing materials other than metal with or without metal reinforcement or cladding								
U-Factor	1.20	0.75	0.65	0.40	0.35	0.35	0.35	0.35
Metal framing with or without thermal break								
Curtain Wall/Storefront *U*-Factor	1.20	0.70	0.60	0.50	0.45	0.45	0.45	0.45
Entrance Door *U*-Factor	1.20	1.10	0.90	0.85	0.80	0.80	0.80	0.80
All Other *U*-Factor[a]	1.20	0.75	0.65	0.55	0.55	0.55	0.50	0.50
SHGC-All Frame Types								
SHGC: PF < 0.25	0.25	0.25	0.25	0.40	0.40	0.40	NR	NR
SHGC: 0.25 ≤ PF < 0.5	0.33	0.33	0.33	NR	NR	NR	NR	NR
SHGC: PF ≥ 0.5	0.40	0.40	0.40	NR	NR	NR	NR	NR
Skylights (3% maximum)								
Glass								
U-Factor	1.60	1.05	0.90	0.60	0.60	0.60	0.60	0.60
SHGC	0.40	0.40	0.40	0.40	0.40	0.40	NR	NR
Plastic								
U-Factor	1.90	1.90	1.30	1.30	1.30	0.90	0.90	0.60
SHGC	0.35	0.35	0.35	0.62	0.62	0.62	NR	NR

ASHRAE Prescription Reqs < 40% WWR.

TABLE 5.5-4 Building Envelope Requirements For Climate Zone 4 (A, B, C)*

Opaque Elements	Nonresidential		Residential		Semiheated	
	Assembly Maximum	Insulation Min. R-Value	Assembly Maximum	Insulation Min. R-Value	Assembly Maximum	Insulation Min. R-Value

Fenestration	Assembly Max. U	Assembly Max. SHGC
Vertical Glazing, 0%–40% of Wall		
Nonmetal framing (all)[b]	U-0.40	SHGC-0.40 all
Metal framing (curtainwall/storefront)[c]	U-0.50	
Metal framing (entrance door)[c]	U-0.85	
Metal framing (all other)[c]	U-0.55	
Skylight with Curb, Glass, % of Roof		
0%–2.0%	U_{all}-1.17	$SHGC_{all}$-0.49
2.1%–5.0%	U_{all}-1.17	$SHGC_{all}$-0.39
Skylight with Curb, Plastic, % of Roof		
0%–2.0%	U_{all}-1.30	$SHGC_{all}$-0.65
2.1%–5.0%	U_{all}-1.30	$SHGC_{all}$-0.34
Skylight without Curb, All, % of Roof		
0%–2.0%	U_{all}-0.69	$SHGC_{all}$-0.49
2.1%–5.0%	U_{all}-0.69	$SHGC_{all}$-0.39

ASHRAE Performance Method

- If WWR > 40%
  - Use full building energy simulation to demonstrate compliance
  - Energy Plus or other approved software

ASHRAE Fenestration Defaults (unlabeled products)

TABLE A8.2 Assembly U-Factors, Assembly SHGCs, and Assembly Visible Light Transmittances (VLTs) for Unlabeled Vertical Fenestration

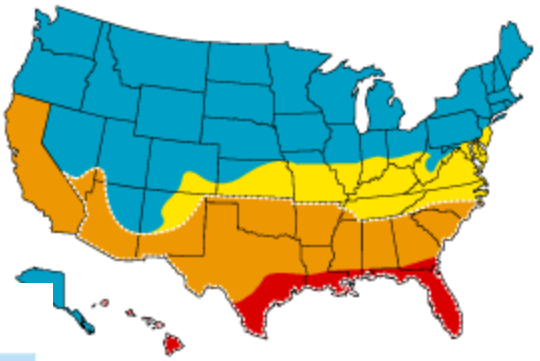
Frame Type	Glazing Type	Unlabeled Vertical Fenestration					
		Clear Glass			Tinted Glass		
		U-Factor	SHGC	VLT	U-Factor	SHGC	VLT
All frame types							
	Single glazing	1.25	0.82	0.76	1.25	0.70	0.58
	Glass block	0.60	0.56	0.56	n.a.	n.a.	n.a.
Wood, vinyl, or fiberglass frames							
	Double glazing	0.60	0.59	0.64	0.60	0.42	0.39
	Triple glazing	0.45	0.52	0.57	0.45	0.34	0.21
Metal and other frame types							
	Double glazing	0.90	0.68	0.66	0.90	0.50	0.40
	Triple glazing	0.70	0.60	0.59	0.70	0.42	0.22

Will not meet code in most cases!!!

ENERGY STAR and Fenestration

- ENERGY STAR labels over 40 products
  - Usually qualifies top 25% energy performers in product category
- Residential windows included
  - Extremely popular with public and manufacturers
  - Performance levels changing in 2009
  - NFRC ratings required to qualify
  - Assists replacement market tremendously

ENERGY STAR windows



Windows & Doors

Climate Zone	U-Factor[1]	SHGC[2]	
Northern	≤ 0.35	Any	
North/Central	≤ 0.40	≤ 0.55	
South/Central	≤ 0.40	≤ 0.40	Prescriptive
	≤ 0.41	≤ 0.36	Equivalent Performance *(Excluding CA)*
	≤ 0.42	≤ 0.31	
	≤ 0.43	≤ 0.24	*Products meeting these criteria also qualify in the Southern zone.*
Southern	≤ 0.65	≤ 0.40	Prescriptive
	≤ 0.66	≤ 0.39	Equivalent Performance
	≤ 0.67		
	≤ 0.68	≤ 0.38	
	≤ 0.69	≤ 0.37	
	≤ 0.70		
	≤ 0.71	≤ 0.36	
	≤ 0.72	≤ 0.35	
	≤ 0.73		
	≤ 0.74	≤ 0.34	
	≤ 0.75	≤ 0.33	

Skylights

Climate Zone	U-Factor[1] 2001 NFRC rated at 20°[3]	U-Factor[1] RES97 rated at 90°[4]	SHGC[2]
Northern	≤ 0.60	≤ 0.45	Any
North/Central	≤ 0.60	≤ 0.45	≤ 0.40
South/Central	≤ 0.60	≤ 0.45	≤ 0.40
Southern	≤ 0.75	≤ 0.75	≤ 0.40

[1] *Btu/h.ft².°F*

[2] *Fraction of incident solar radiation.*

[3] *U-Factor qualification criteria based on 2001 NFRC simulation and certification procedures that rate skylights at a 20-degree angle. Although reported U-Factor is higher than RES97 rated products, energy performance at the ENERGY STAR minimum qualifying level is equivalent.*

[4] *NFRC certification using the 1997 NFRC procedures for residential windows (RES 97) that rated skylights at a 90-degree angle. Skylights rated under this procedure may be present in the marketplace until March 31, 2008. NFRC labels for products using this procedure state: "RES97 rated at 90 degrees."*

NFRC and USGBC-LEED

- US Green Building Council administers LEED
- LEED = Leadership in Energy Efficient Design
  - new and popular program
  - LEED rated buildings now required in some states and cities
    - New York, Maryland
- NFRC is US Green Building Council member since 07

LEED 2.2 Minimum Energy Requirement

- Meet ASHRAE 90.1-04
- Requires NFRC Ratings for fenestration
  - Without NFRC rating, use defaults

LEED Scoring

- Fenestration scoring possible under energy and atmosphere section
- Scoring based on improvement over ASHRAE baseline
- Low-e products reduce load, improve score
- Reduce window sizes may increase score
- Shading may contribute also

NFRC's New Commercial Initiative: Component Modeling Approach



To rate the energy efficiency of windows, doors, & skylights in Commercial Buildings



Component Modeling Approach-CMA

- Existing commercial fenestration energy ratings not fully implemented
- New online calculation tool for fenestration energy performance
- Under development for last seven years
- CMA software tool being tested now
- CMA pilot in CA early next year
- Full CMA implementation in 2009

Component-Based Fenestration Product Certification Program

Applicable for projects and for commercial buildings

National Fenestration Rating Council®

DRAFT

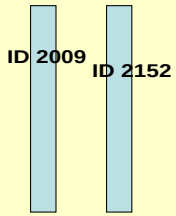
COMPONENT APPROVAL PROCESS

GLASS

SPECTRAL DATA APPROVAL PER 302

UPON APPROVAL, UPLOADED INTO GLASS LIBRARY
Upload will be made by NFRC

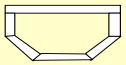
Glass



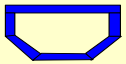
SPACER

SUBMISSION OF DRAWINGS AND BASE THERM MODEL TO NFRC IN ACCORDANCE WITH SPACER LIBRARY PER 303

Spacer



Spacer
Therm Model



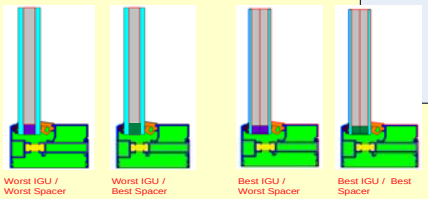
PEER REVIEW OF SUBMISSIONS

UPON APPROVAL, UPLOADED INTO SPACER LIBRARY
Upload will be made by NFRC

FRAMING SYSTEM

CONTRACT WITH ACCREDITED SIMULATION LAB TO MODEL BASE FRAMING SYSTEM
(Four Best and Worst Cases per NFRC 100 section 5.6)

- submit drawings
- bill of materials
- material properties



ACCREDITED SIMULATION LAB WILL SUBMIT RESULTS AND REPORT TO LICENSED IA SELECTED BY THE FRAMING SYSTEM MANUFACTURER

- NFRC LICENSED IA REVIEWS THE RESULTS AND REPORT FOR ACCURACY
- APPROVES & UPLOADS FRAMING SYSTEM DATA INTO THE FRAMING SYSTEM LIBRARY

Approved GLASS LIBRARY

Approved SPACER LIBRARY

Approved FRAMINING SYSTEM LIBRARY

Future Component Based Rating

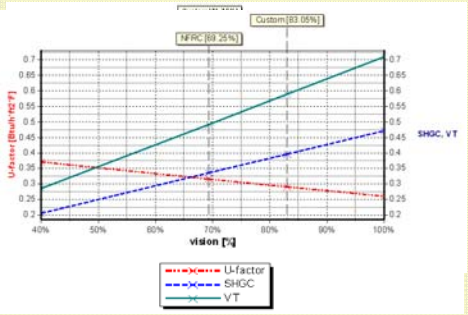
NFRC Label Certificate

NFRC Label Certificate

National Fenestration Rating Council
CERTIFIED

World's Best Window Co.

Millennium 2000+
Vinyl-Clad Wood Frame
Double Glazing • Argon Fill • Low E
Product Type: **Vertical Slider**



ENERGY PERFORMANCE RATINGS

U-Factor (U.S./I-P)	Solar Heat Gain Coefficient
0.34	**0.25**

ADDITIONAL PERFORMANCE RATINGS

Visible Transmittance	Air Leakage (U.S./I-P)
0.41	**0.2**

Manufacturer stipulates that these ratings conform to applicable NFRC procedures for determining whole product performance. NFRC ratings are determined for a fixed set of environmental conditions and a specific product size. Consult manufacturer's literature for other product performance information.
www.nfrc.org

DRAFT

PROJECT LOCATION
Street Address: _____
City:_____State:_____Zipcode_____

PRODUCT LINE INFORMATION
Operator Type (per NFRC 100, Table 1): _____Product Line ID Number:_____
Individual Product ID number _____How many of this individual product: _____
Elevation drawing page: _____Fenestration (window & door) schedule page: _____

FRAME MATERIAL SUPPLIER
Company name: _____
Product Certification ID Number:_____

GLAZING MATERIAL SUPPLIER
Company name: _____
Product Certification ID Number:_____

SPACER SUPPLIER
Company name: _____
Product Certification ID Number:_____

GLAZING CONTRACTOR/INSTALLER
Company name:_____
Address:_____
City, State, Zipcode:_____
Contact person:_____Phone:_____Facsimile:_____

CERTIFICATION AUTHORIZATION
Independent Certification and Inspection Agency (IA):_____
Date Certification Authorization Issued:_____

BENEFITS OF THE COMPONENT APPROACH…

- REDUCED COSTS
- WEB BASED
- BENCHMARKING & COMPETITION
- FASTER TURN AROUND
- INCREASED SPECIFIERS

NFRC's Newest Ratings

- Applied films (aftermarket)
  - Only SHGC and VT
  - Three participants so far
  - Several other applying
- Tubular daylighting devices changing
  - Simulation method only now
  - Likely change to testing only
  - New simulation software to be developed

NFRC Potential Ratings

- Attachments
  - Major focus of membership currently
  - Internal
  - External

NFRC Potential Ratings

- Garden House windows
  - Research RFP being presented in November
- Dome skylight simulation
  - Currently test only
  - New software enables simulation
  - Research RFP being presented in November

NFRC-International

- NFRC licenses in:
  - Australia
  - South Africa
- NFRC working towards implementation in
  - China
  - India
  - ASEAN countries (pending)
  - Middle East
    - Jordan, Kuwait, Bahrain, Saudi Arabia

NFRC government support

- Grants from
  - $1.3 million from US Department of Energy-Building Technologies Department over five years
    - Support research and international harmonization
  - $250,000 from US Department of State-Office of Environment (part of Asian Pacific Partnership) over two years
    - Supports energy efficiency, clean environment

NFRC Government Support

- US Trade Development Agency
  - standards transfer to other countries: China
- US Department of Commerce-National Institute of Standards (pending)
  - Support standards transfer to ASEAN Countries: Thailand, Malaysia, Indonesia, etc.
- US Agency for International Development (pending)

Summary

- NFRC is only recognized fenestration energy rating entity in US
- NFRC becoming recognized in other countries
- NFRC enables
  - Code compliance
  - Competition
  - Voluntary programs
  - Innovation

Thank you for your time!

QUESTIONS??

Ray McGowan

240-821-9510

rmcgowan@nfrc.org

www.nfrc.org

National Fenestration Rating Council

Project 3.2
Japan (b)

Project Name: International Harmonization - Japan

Date: September 2008

Purpose: NFRC hosted a Japanese delegation in September 2008.

Project Summary:

NFRC attended several events in Japan working towards window labeling harmonization.

Excel Shannon presentation on Japanese vinyl market

Shanon window

Advanced PVC window

Hamburg, February 17, 2000

SHANON
株式会社 シャノン

Introduction

Shanon Corporation is affiliated company of Tokuyama Corporation. “Shanon window” is a top brand of PVC(polyvinyl chloride) window in Japan.
We started making PVC window from 1976 as a pioneer in Japan.
Every year since then we’ve added new design and style to our production line, and every year we’ve increased our capacity to produce them.
We have been the top makers of PVC windows in Japan over thirty years.

Hamburg, February 17, 2000

SHANON
株式会社 シャノン

Tokuyama Corporation Overview

Net Sales : US$2,795 Million (07)
Operating Income : US$321 Million (07)
Net Income : US$ 171 Million(07)
Employees : 5,057 (Mar/08)

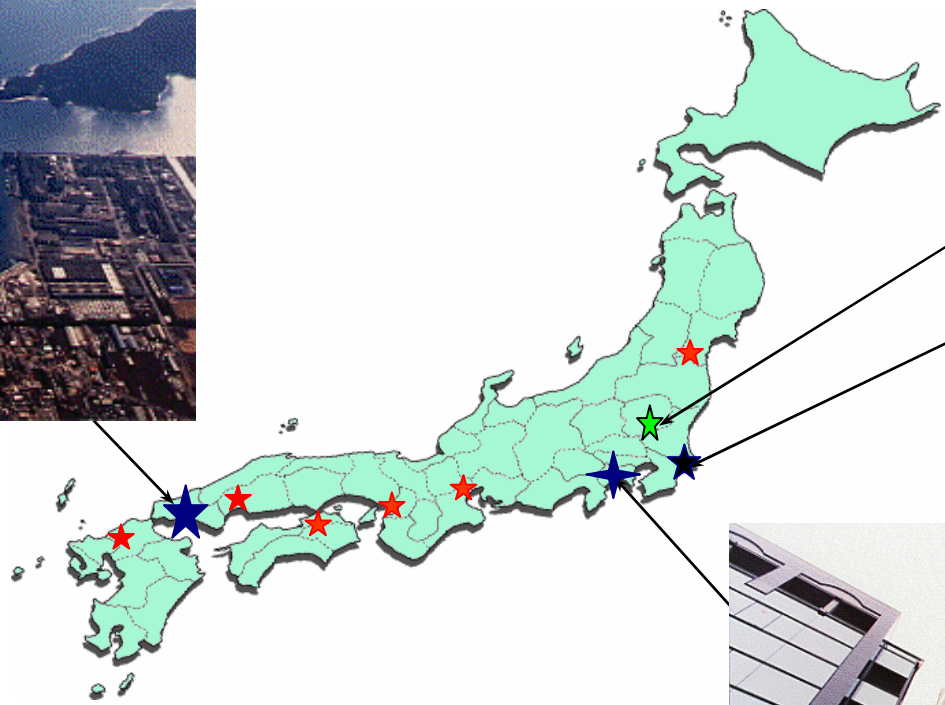
Corporate Overview
Product Lines

- Chemicals& Plastics : Chloralkali, Soda Ash, **PVC**
  Microporous PP & PE sheets, OPP films...
- Electronic Materials: Polycrystalline Silicon, ALN Ceramics,
  Silica, Ion Exchange Membranes,
  ULSI Chemicals, Gas Sensors,
  High Purity Chemicals for electronics manufacturing,…
- Medical Products: Dental Materials,
  Diagnostic Reagents & Systems…
- Cement and Building Materials :
  Portland Cement, **Shanon Window** ,…

Corporate Overview
Domestic Locations



Tokuyama Factory,
Tokuyama Laboratory
RC Laboratory



Tsukuba Research Laboratory

Kashima Factory

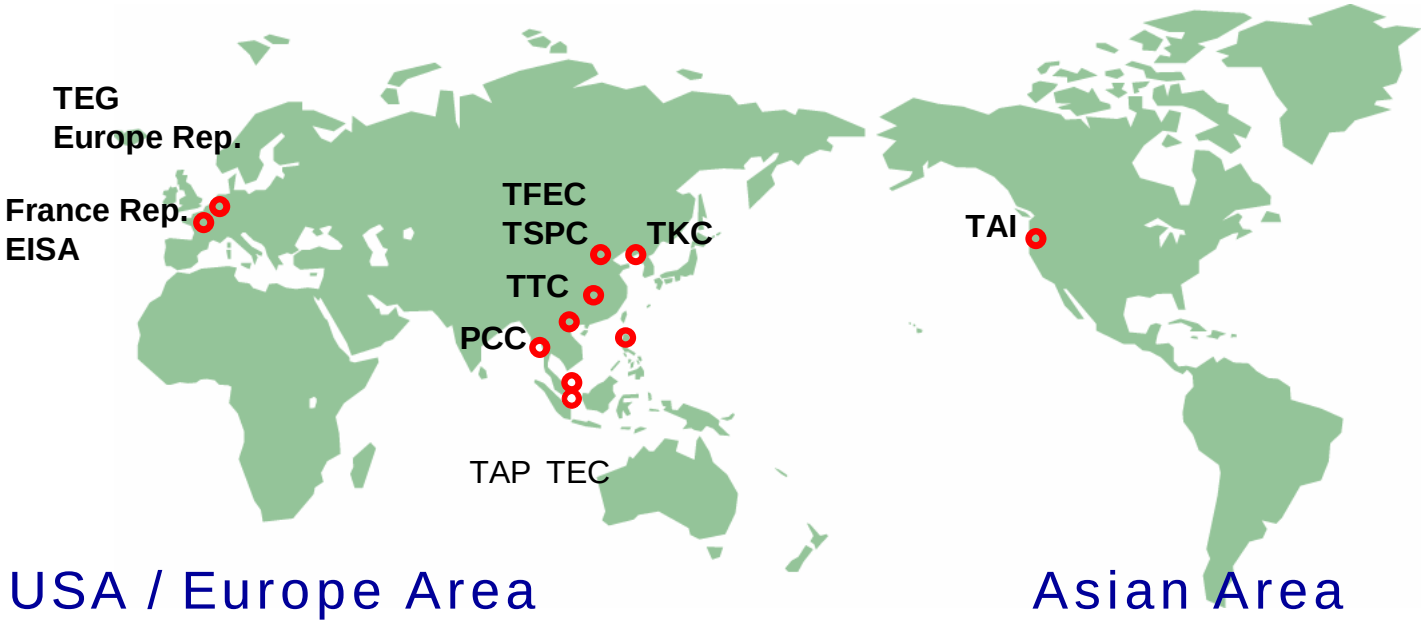


Tokyo Head Office

Chemistry with a heart
TOKUYAMA

Hamburg, February 17, 2000

Corporate Overview
Worldwide Locations



USA / Europe Area

TAI : Tokuyama America Inc.
TEG : Tokuyama Europe GmbH
EISA : Eurodia Industrie S.A.

Asian Area

TFEC : Tianjin Figaro Electronics Co.
TSPC : Tianjin Sunshine Plastic Co.
PCC : Pornpat Chemicals Co.
TKC : Tokuyama Korea Co.
TTC : Tokuyama Trading Corporation
TAP : Tokuyama Asia Pacific Pte. Ltd.
TEC : Tokuyama Electronics Chemicals

Chemistry with a heart
TOKUYAMA

Shanon Corporation

Overview

1. President Tatsumi Nakamura

2. Capital US＄¥4,500,000-

3. Share Holder Tokuyama Corporation

4. Establishment April 1st, 2000

5. Number of Employees 294

6. Outline of Business

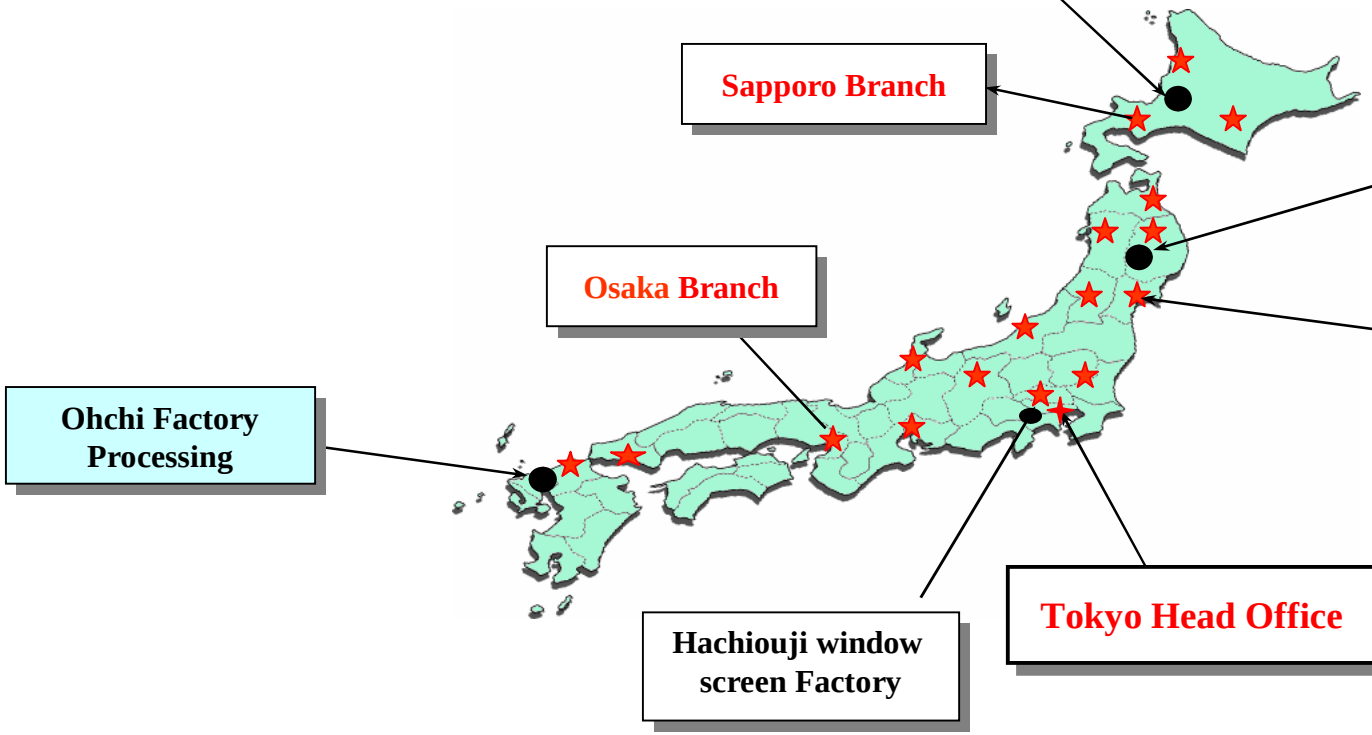
1) Produce, assemble and sell plastic window and products.
2) Construction, supervision and design to support above subjects.
3) Sell other products for home use
4) Other business to support above subjects.

Hamburg, February 17, 2000

SHANON
株式会社 シャノン

Corporate Overview
Domestic Locations

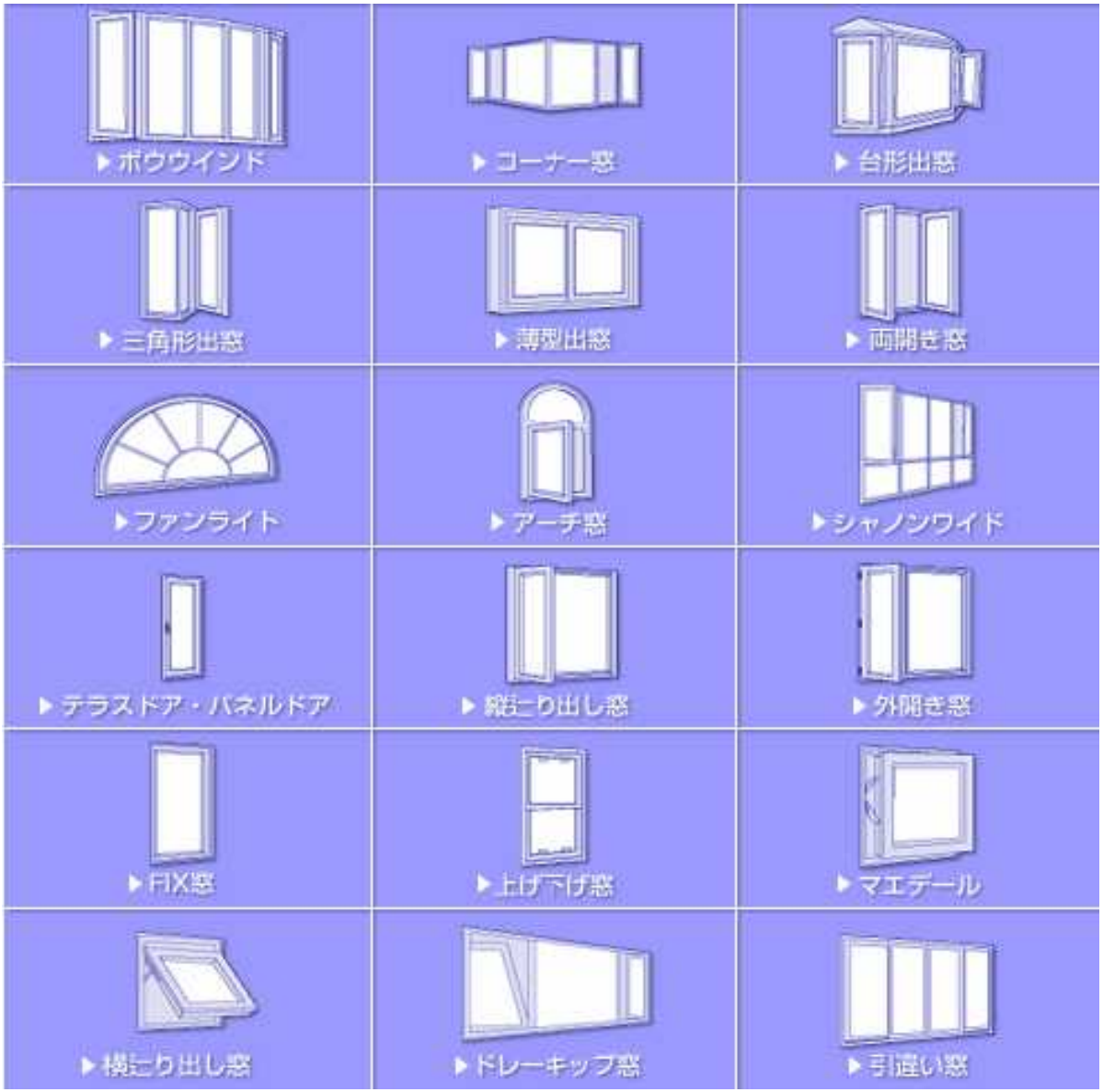




Hamburg, February 17, 2000

SHANON
株式会社 シャノン

Product line up



Hardware & Option



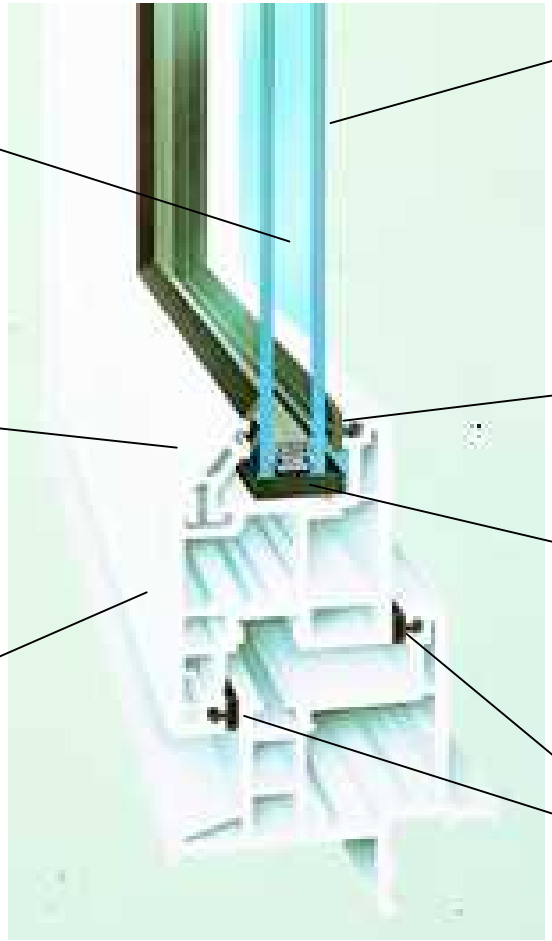








Specifications



12mm Air space (argon gas option)

Double glazing -3mm glass panels- (Low-emissive and anti-solar heat glass panels option)

Glazing stop

Glazing bead

Aluminium spacer or Warm-Edge spacer

PVC frames that is highly heat resistance

Dual air sealant

Hamburg, February 17, 2000

SHANON 株式会社 シャノン

Performance

- Energy saving(insulation performance)
- Air tightness
- Sound insulation
- Wind-Pressure Resistance
- Watertightness
- Fire retarding performance

SHANON
株式会社 シャノン

Energy saving
Insulation performance

- 2.4W/m^2･K **thermal transmittance**(JIS H-4 grade)
  - …with standard double glazing
- 1.8W/m^2･K **thermal transmittance** (JIS H-5 grade)
  - …optional Low-emissive double glazing
- 1.2W/m^2･K **thermal transmittance** (JIS H-5 grade)
  - …optional Low-emissive triple glazing

    Ar gas

SHANON 株式会社 シャノン

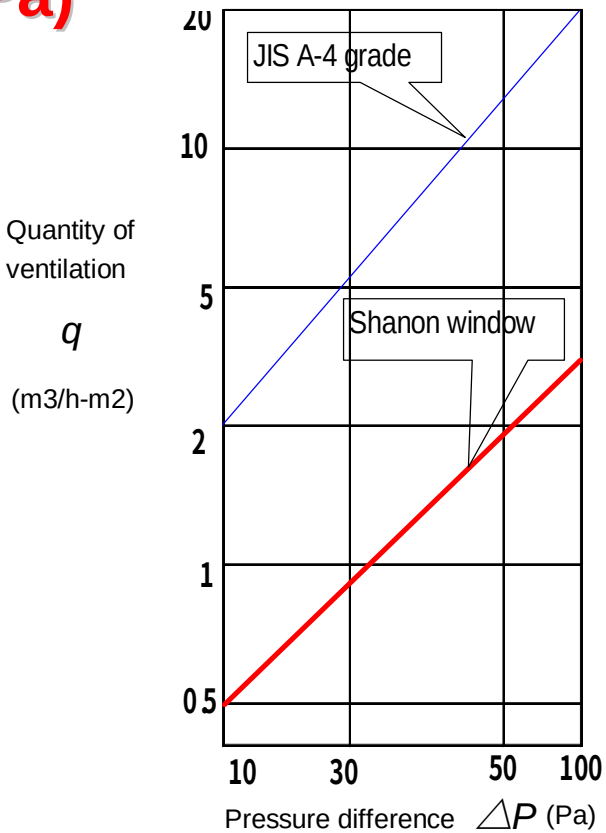
Air tightness

air leakage efficiency

(air infiltration level at 10-100Pa)

・2 $m^3/h・m^2$

(JIS A-4 grade)



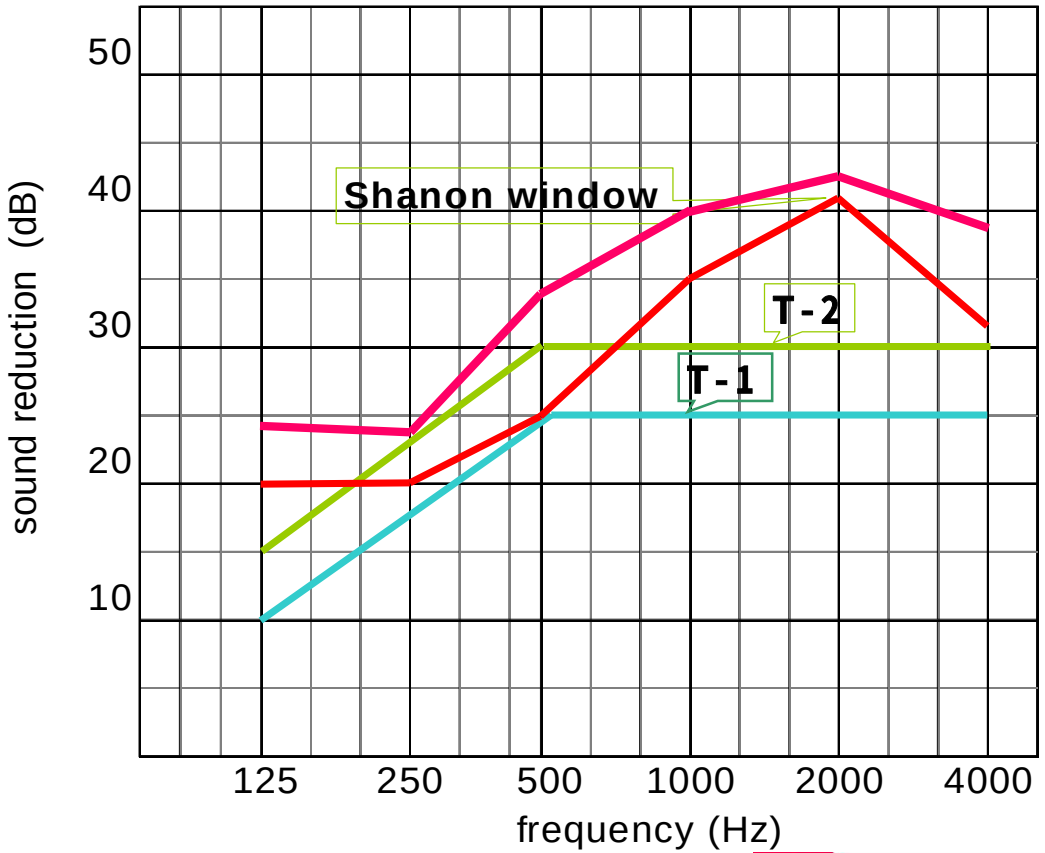
Hamburg, February 17, 2000

SHANON
株式会社 シャノン

Sound Insulation

sound reduction level from 125Hz to 4000Hz

- **25dB** reduction (JIS T-1 grade)
  - …with standard glass panel
- **30dB** reduction (JIS T-2 grade)
- **35dB** reduction (JIS T-3 grade)
  - …optional sound-proof glazing panel



SHANON
株式会社 シャノン

Wind-Pressure Resistance

–strength test

- **1200Pa** (JIS S-2 grade)

Water tightness

–no water infiltration against wind and rain

- **350Pa**(JIS W-4 grade) sliding sash
- **500Pa**(JIS W-4 grade) casement sash

SHANON
株式会社 シャノン

Fire retarding performance

- retardation in fire Optionally Side hung out open and Fixed light windows can take measure to fire-retarding structure

  (**20minutes fire-proof**)

Eco-friendly

- We are ready to recycle used PVC windows through our technology.
  - We started to sell our products 30years ago first in Japan and yet now recycle-needs is not substantial issue in Japan.
- We have been already recycling PVC materials inside our factory.



SHANON 株式会社 シャノン

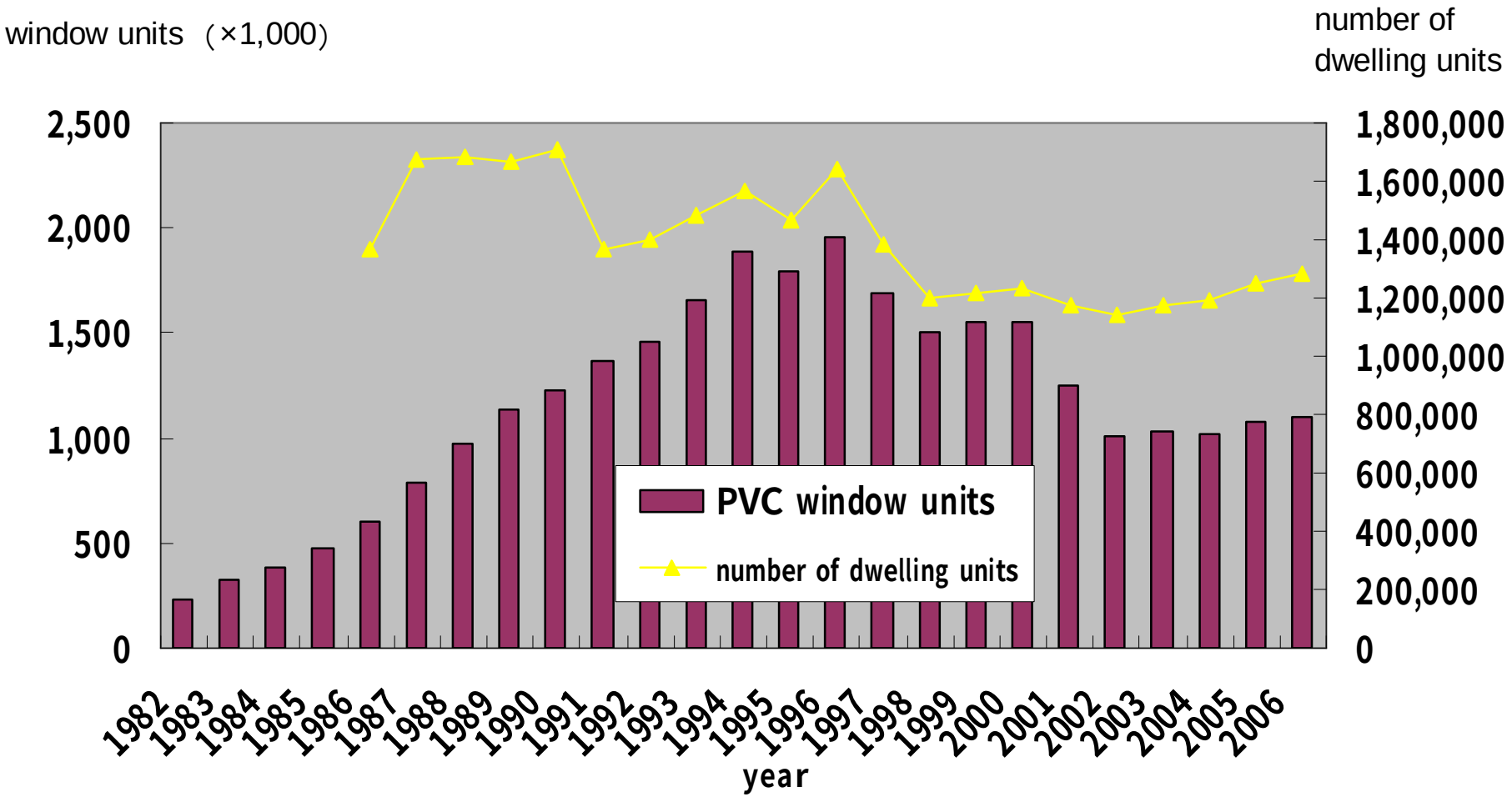
Quality Control

- ISO9001 (Kuriyama Factory,
  Tohoku Shanon Corporaion)
- ISO14001(Tohoku Shanon Corporaion)

SHANON
株式会社 シャノン

Japanese market

Number of PVC windows

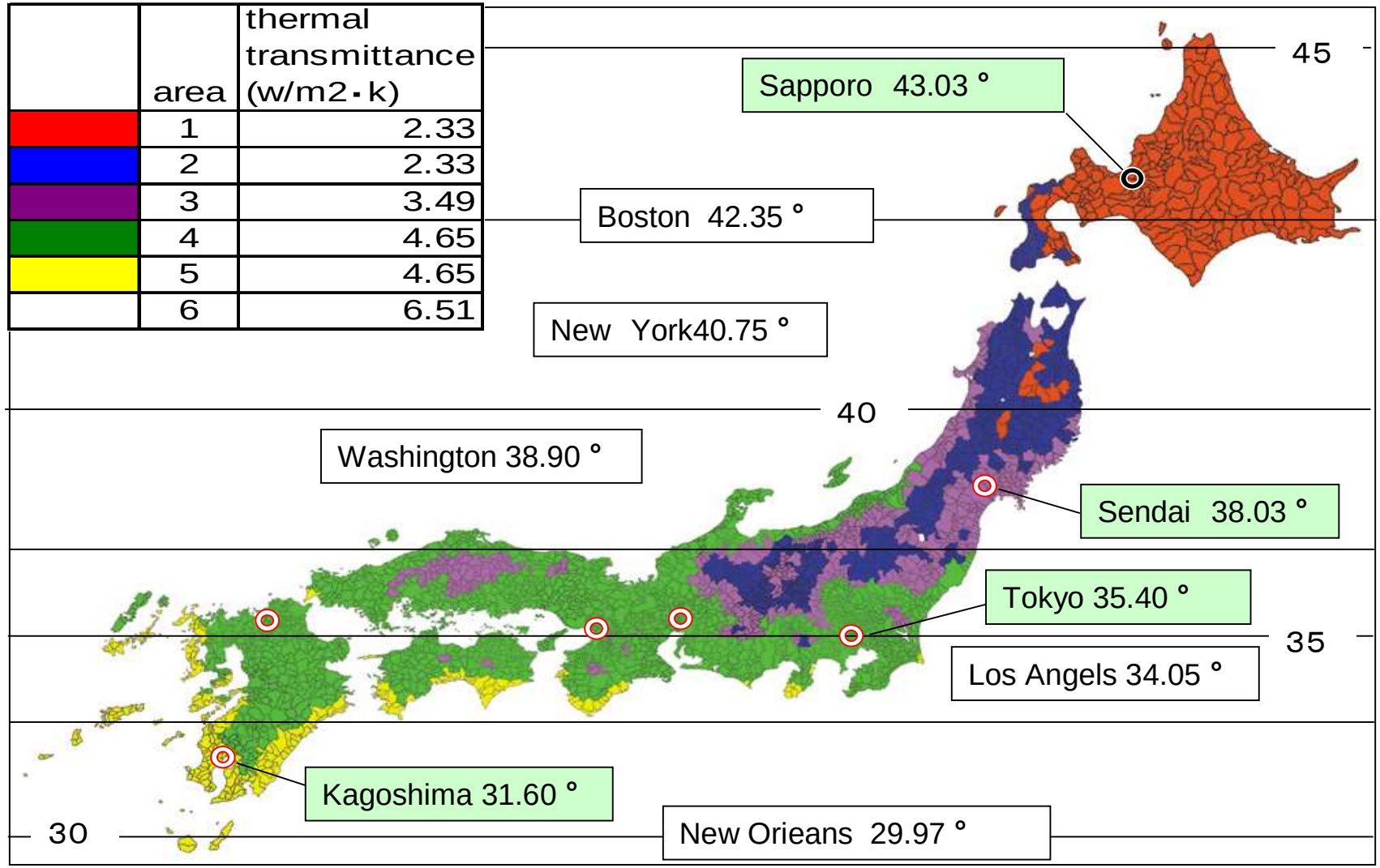


Hamburg, February 17, 2000

SHANON
株式会社 シャノン

Japanese housing insulation standard

	area	thermal transmittance (w/m2・k)
	1	2.33
	2	2.33
	3	3.49
	4	4.65
	5	4.65
	6	6.51

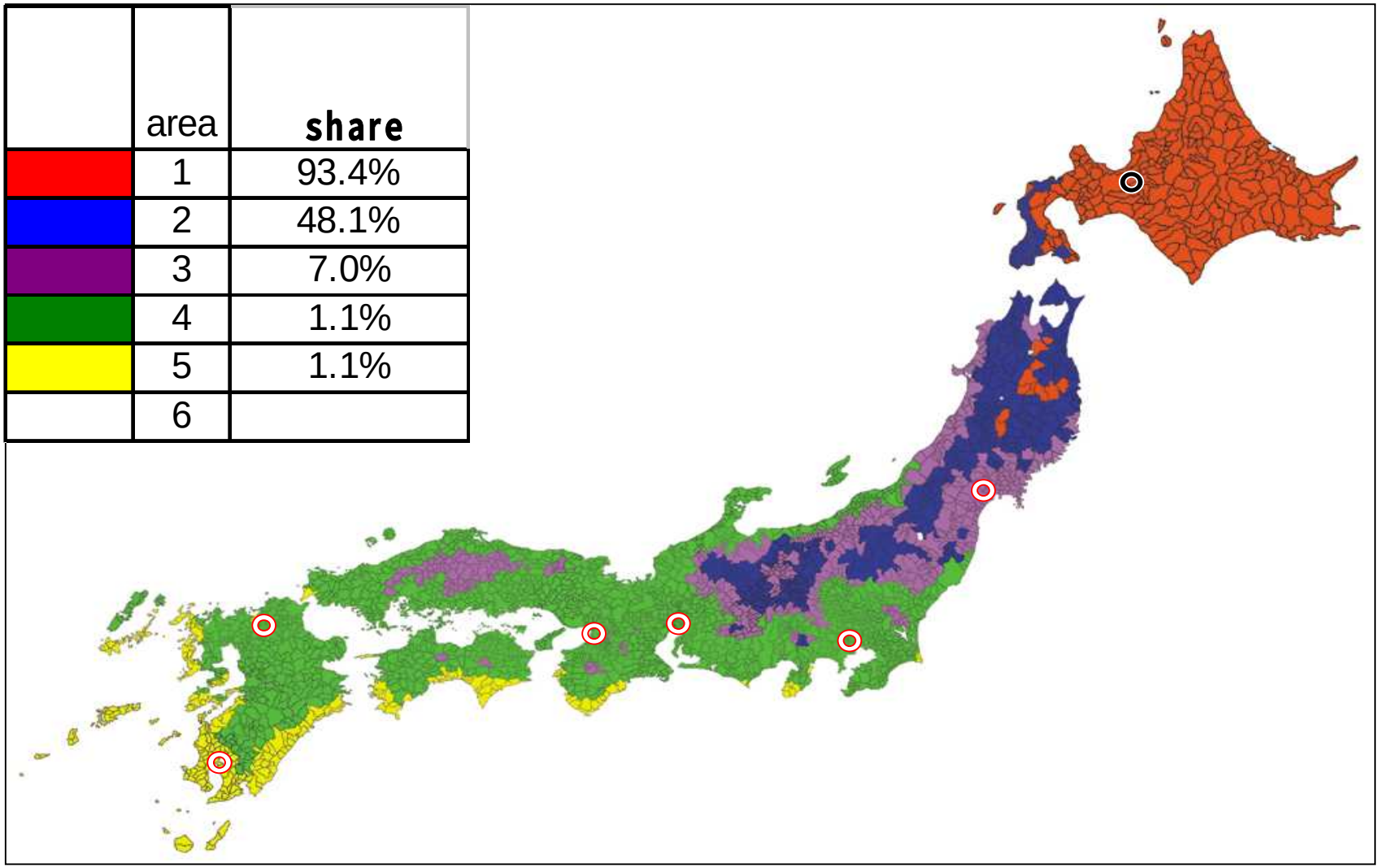


Hamburg, February 17, 2000

SHANON
株式会社 シャノン

Area share of PVC windows

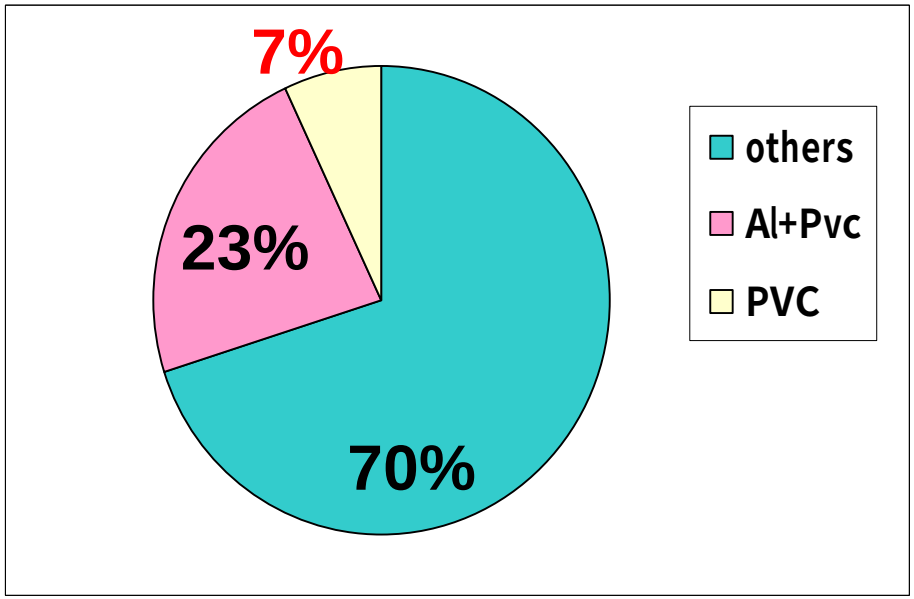
	area	share
	1	93.4%
	2	48.1%
	3	7.0%
	4	1.1%
	5	1.1%
	6	

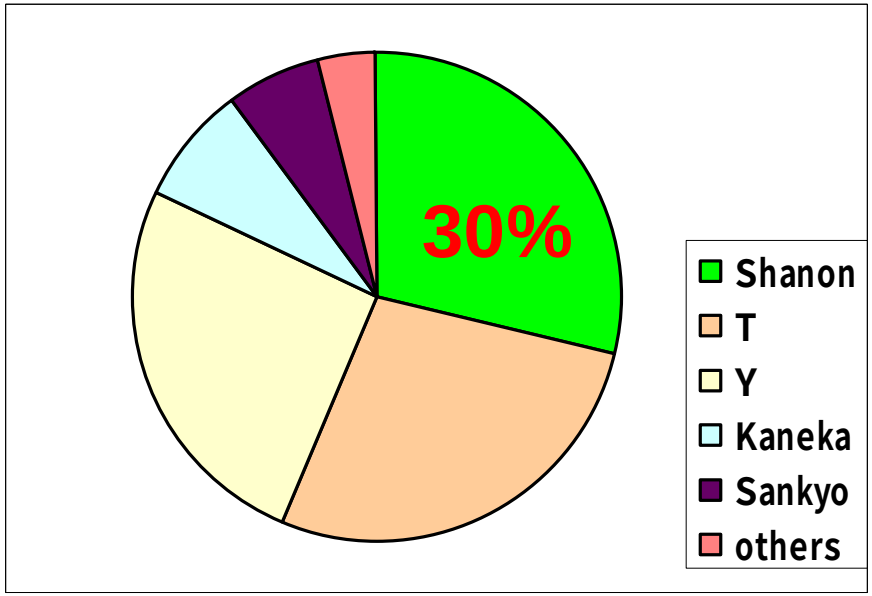


Hamburg, February 17, 2000

SHANON
株式会社 シャノン

Domestic share of PVC windows





SHANON
株式会社 シャノン

Japanese market
Feature

1.The ratio of the double sliding windows is high.
50% or more

2.The ratio of the colors is high.
Sten-color,black,brown,etc 50% or more

3.Few standard products and Many special orders

4.The demand for the outside quality is severe.

SHANON
株式会社 シャノン

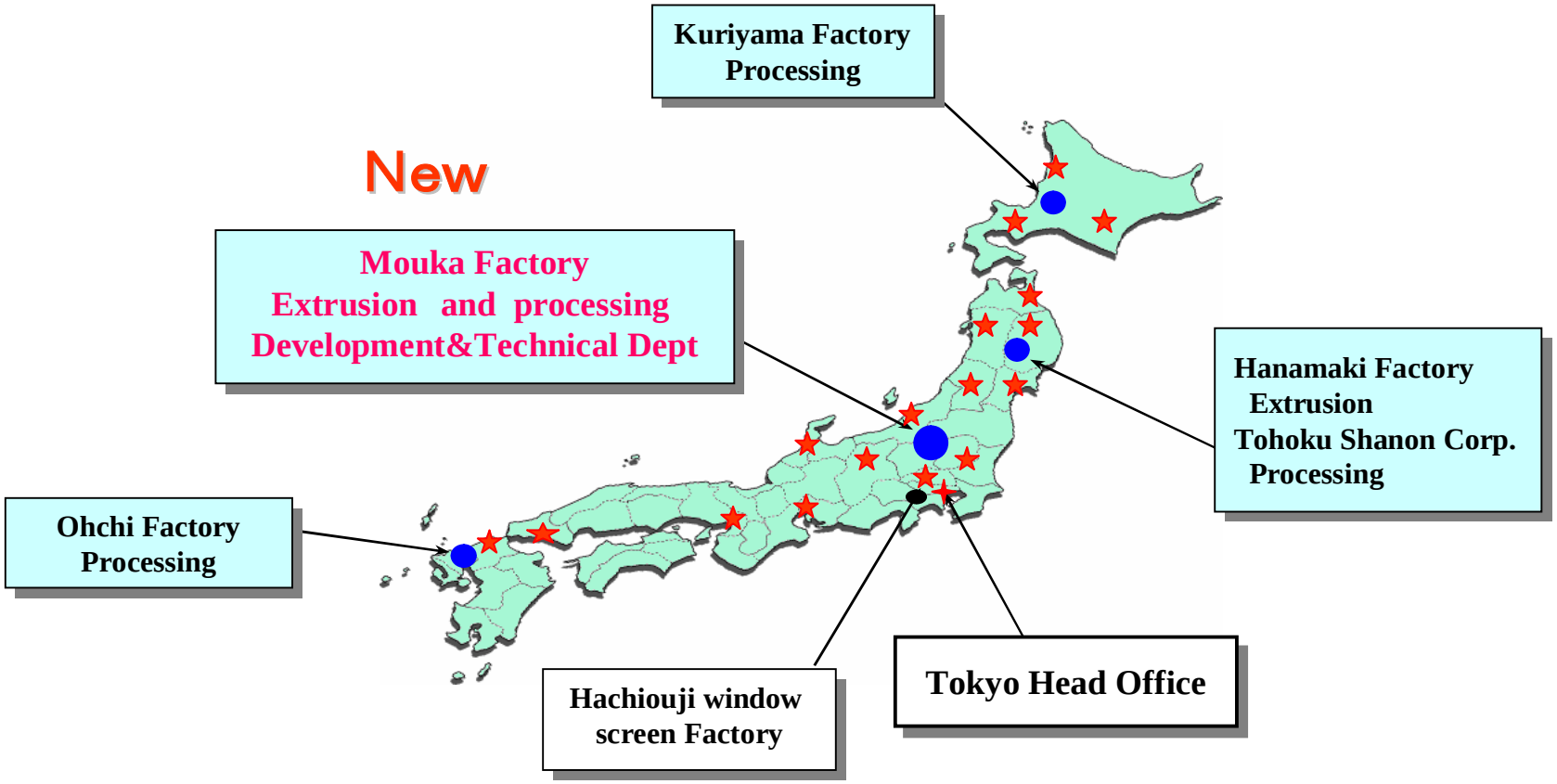
SHANON merge with PVC Window Department of KANEKA CORP.

1.Company Name	EXCELSHANON CORP.	
2.Date	01／Oct／2008	
3.President	Tatsumi Nakamura	
4.Share Holder	Tokuyama Corporation	67%
	Kaneka Corporation	33%

SHANON 株式会社シャノン

EXCEL SHANON 株式会社エクセルシャノン

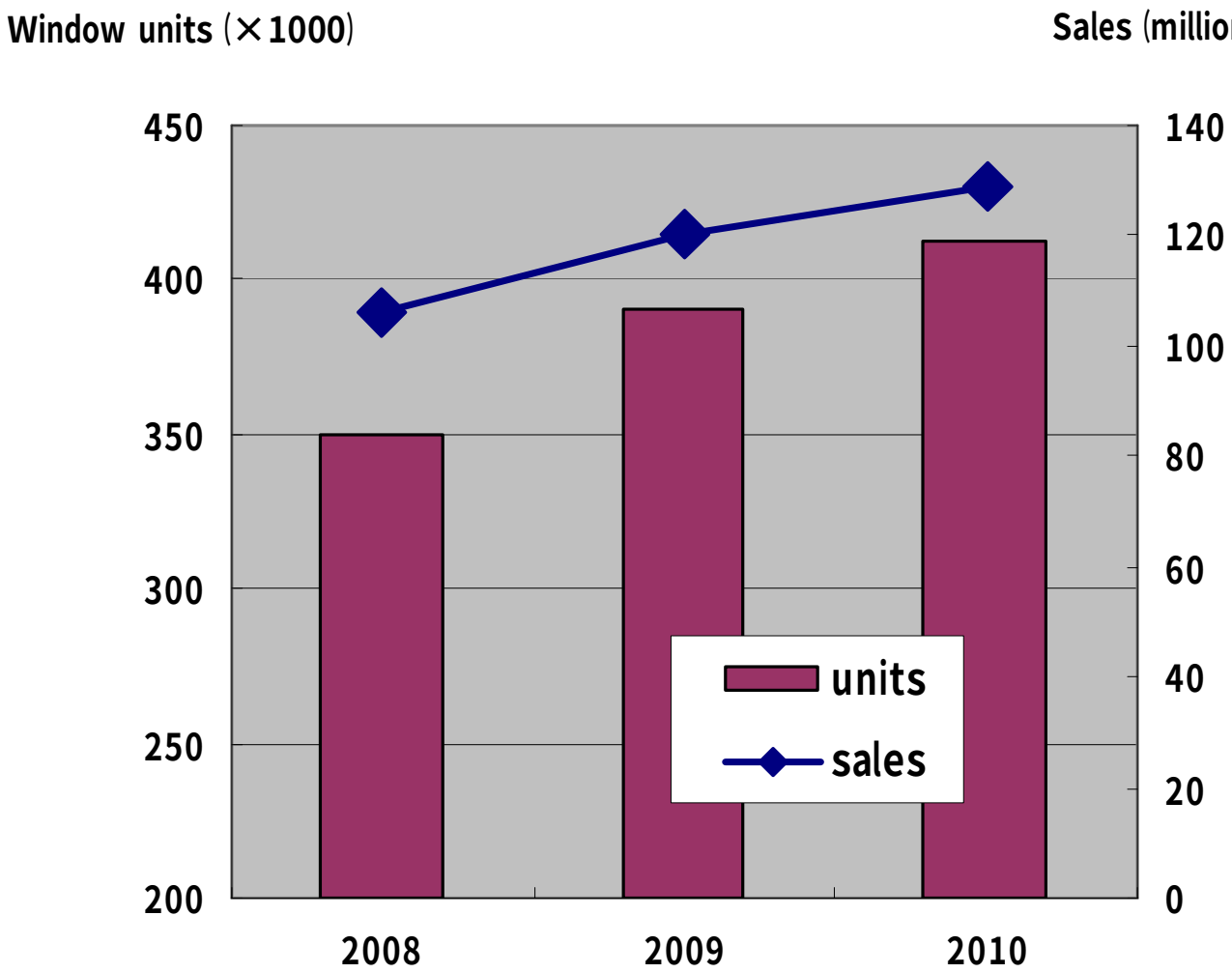
Domestic Locations



Hamburg, February 17, 2000

EXCEL SHANON
株式会社エクセルシャノン

Business plan



Hamburg, February 17, 2000

EXCEL SHANON
株式会社エクセルシャノン

We make a fresh as a leading company.

- We make the best use of the technology of the two companies and keep No1 market share in PVC windows in Japan.

- We try for PVC windows to prevalent in the central part of Japan by effectively using Mouka factory.

Hamburg, February 17, 2000

EXCEL SHANON
株式会社エクセルシャノン

Thanks for your attention

Sep 2008

Project 3.2
Japan (c)

Project Name: International Harmonization - Japan

Date: September 2008

Purpose: NFRC hosted a Japanese delegation in September 2008.

Project Summary:

NFRC attended several events in Japan working towards window labeling harmonization.

Japanese Window Market Presentation

Residential Window market in Japan



Goto Tomorrow.Co.Ltd.

Sept.24, ’08

Window Market Overview
New

- **market size : 10M windows**
  - Houses 1,060,741(-17.8% vs 2006)
- **trend**
  - slowly decreasing
- **Each window penetration(Mar. 2008)**



- **IGU penetration (2007):** **total : 15,493,000sqm**
  - Family house 80.1%(Low-E IGU 27.3%)
  - Condominium 44.7%(Low-E IGU 4.5%)

Window Market Overview
Renovation

- **Renovation market size(‘06)**
  - Renovated Houses 277,499
  - Average expenditure
    3,270,000yen(31,000US$)@house



- **Window related renovation.**
  - Burglar resistance glass is increased.
  - House insulation has been seen in family houses in last few years as government encourages households but not big.

Governmental Energy saving actions for upgrading windows

- **There are some programs for households**

<New>

- Mortgage interest reduction (0.3% reduction)

< Renovation >

- property tax reduction (one third)
- Income tax reduction(max 1,100US$/year)
- Special subsidy for renovation
  - One third of total cost
  - Government's total budget 11M US$ in 2008

Energy Saving Regulation

- Not mandatory
- Current regulation's recommendation is very low.

  Top class window's U-value is **only 2.33**.

  – Thermal test for Windows/Doors (JIS A 4706:2000・ JIS A 4702:2000)



  - U-value (sqm・ K/W)

H1	H2	H3	H4	H5
4.65	4.07	3.48	2.90	2.33 (top class)

  – Even for the coldest area, recommended U-value is 2.33

Issues

- No mandatory energy saving regulation is existed.
- No standard size window is available. All are tailor made, hence windows is expensive.



Issues

- Official marking system is available but very complicated and recommended U-value is very low.
- Mark for window is used by Shanon but not others.
- Others marked glass and sash&frame separately.

<Window>(W/m2･K)

U-value under 2.33	U-value 2.33-3.49	U-value 3.49-4.65	U-value over 4.65
 ★★★★	 ★★★	 ★★	 ★

Issues

- <Sash&frame>

Wood,PVC, PVC(or Wood) clad aluminum	Insulated Aluminum	Aluminum For IGU	Aluminum for monolitic
 ★★★★	 ★★★	 ★★	 ★

- <Glass>(W/m2・K)

U-value under 2.33	U-value 2.33-2.7	U-value 2.7-4	U-value over 4
 ★★★★	 ★★★	 ★★	no mark

What is needed?

- Awareness creation **" Window is the key factor to upgrade energy saving level of their houses"** among end-users
- Awareness creation **"Japanese energy saving level is needed to upgrade to US/EU level"** among government/local authorities
- System for end-users to select suitable windows
  - Accurate Window Rating system
  - Visual recognition

Welcome NFRC to Japan!!

- With introducing US codes and NFRC system
  - End-users will notice "**Window is the key factor to upgrade energy saving level of their houses.**"
  - Government/local authorities will notice **"Japanese energy saving level is needed to upgrade to US/EU level"**
  - We will have **the System for end-users to select suitable windows**
    - **Window Rating system**
    - **Visual recognition**

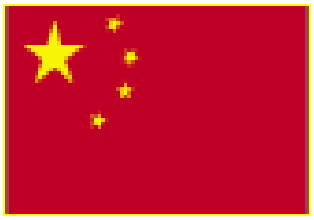
Project 4 (a)
(2008 only)

Project Name:	IG Durability and Applied Film Status Harmonization
Date:	April 13, 2008
Purpose:	NFRC attempted to develop an IGU and Applied Film Standard with China

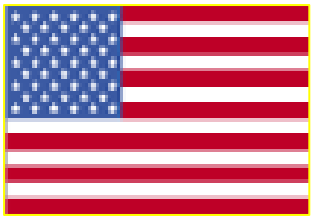
Project Summary:

China has adopted the European procedure for testing Insulated Glazing units (IGU). The contractor participated in several experts meeting, and concluded that the efforts to convince the Chinese to adopt North American practice is futile, and therefore recommends ending the efforts for IGU standards harmonization with China.

Click here for IG Durability and Applied Film Meeting Agenda







INVITATION

USA – China: Insulating Glass Unit and Applied Film Standards Development meeting

Meeting Details and Agenda:

Conference: USA-China collaboration and the Chinese Insulating Glass Unit Durability and Applied Film Standard development:

Venue: Meeting will be hosted at SAS Hotel: 6A, East Beisanhuan Road, Chaoyang District, 100028, Beijing, P.R. China. (Tel: +86 10 5922 3388),

Time: Meeting will Held on 13th of April, 2008 from 9:00am to 5:00 pm

Agenda:

Opening Note: 9:00 am to 9:15 am - Chinese
9:15 am to 9:30 am - USA

Insulating Glass Unit standard:

Chinese Side: (9:30 am to 11:00 am)

- Report by Mr. Huang JianBin on ISO 160 working group 4 meeting.
- Current status of GB11944
- Issues which needs to be resolved by joint committee.

USA side: (11:15 am to 12:30 pm)

- Report by Mr. Bill Lingnell Chair of the ISO 160 working group 4 meeting
- ASTM Standard Test Method for Determining Argon Concentration in Sealed Insulating Glass Units Using an Argon Gas Analyzer.

Lunch Break: 12:30 pm to 1:30 pm.

Applied Film Standard:

Chinese Side: (1:30 am to 2:30 am)

- Current status of JC/T xxxx standard Functional Film of Building Glass
- Issues which needs to be resolved by joint committee.

USA side: (2:30 pm to 3:00 pm)

- Report by Darrel Smith (Executive Director), IWFA on current USA standards.

Open Session (3:00 pm to 5:00 pm)

- Update on the meeting proceedings to USA manufacturers
- Future cooperation, identification of action plan and needs
- Next meeting

Project 4 (b)
(2008 only)

Project Name: International Window Film Harmonization

Date: April 13, 2008

Purpose: NFRC attempted to develop an IGU and Applied Film Standard with China

Project Summary:

China has adopted the European procedure for testing Insulated Glazing units (IGU). The contractor participated in several experts meeting, and concluded that the efforts to convince the Chinese to adopt North American practice is futile, and therefore recommends ending the efforts for IGU standards harmonization with China.

Click here for the International Window Film Harmonization presentation

U.S. Window Film Industry Experience with Ratings

Darrell Smith

Executive Director
International Window Film Association
&
Window Film Committee Manager
Association of Industrial Metalizers, Coaters & Laminators

Window Film New to Ratings

- Films used prior to 1970, but major increase started in late 1970s
- U.S. oil shortages in late 1970s and again in early 1990s created more demand
- Until mid-1990s, window film industry not affected by regulation in building use except as safety enhancement to existing glass
- As more states adopted model energy codes, window films viewed as way to retrofit existing windows to meet energy requirements

Industry Re-Defined

- Window film industry associations began to attend glazing industry meetings
- Building code consultants hired; first for safety use issues, then asked to monitor energy
- Active participation with NFRC begun
- Involvement in energy codes started
- Result was that window film industry began to be part of the larger fenestration industry

Need for Involvement in Building Codes

- Window films can improve safety performance of existing glazing to match or exceed full replacement windows
- Window films can improve energy performance of existing glazing to match or exceed full replacement windows
- Window films may be more affordable, more timely, and “greener” than replacing windows which otherwise have more life
- Without code participation, paths for compliance using window films may be omitted

Need to Have Films Rated

- Small number of quality manufacturers and converters in window film industry
- Consumers cannot distinguish between films designed for different uses
- Local dealers do not have the technical expertise to test published specifications
- Without a rating system, party responsible for performance claims unknown

Need for Basic Standardization

- The public needs to see actual differences in product performance, not differences in the way performance is stated
- Manufacturers should agree on definitions of commonly used and published terms
- Manufacturers should agree on specific testing procedures
- Consumer confusion causes mistrust; in many cases, mistrust means missed opportunities
  - For energy savings
  - For industry sales

At the Intersection

- Enforced building codes give ***real value*** for materials and services purchased
- Basic standardization, at least within industries, give ***real meaning*** to the performance specifications published
- Rating systems give the public ***real differences*** on which to evaluate market choices
- All of these three items work together to insure ***long-term and stable growth*** in an industry
- The window film industry is actively involved and supports all these functions

Status of Films in U.S. Today

- Agreement on definitions, applicable standards, and test procedures
- Safety and energy code compliance can be demonstrated by the use of window films on existing glazing
- NFRC certification and labeling of window films has begun
- Energy analysis of commercial buildings based on DOE-2 available now
- New analysis program for residential and commercial buildings based on EnergyPlus (called E*Film*) will be available next year

Results Seen

- Local code officials praise having NFRC label to demonstrate compliance
- Rebate and incentive programs for energy reduction will require labeling, proof of industry compliance, as minimum
- U.S. Department of Energy assisting us in development of EnergyStar Window Film Program
- ESCOs, large contractors, and government agencies all using energy analyses on projects
- Manufacturers not previously involved in industry programs applying for certification and labeling, asking about EnergyStar programs, and becoming more industry involved

Project 6 (a)
(2008 only)

Project Name: Component Modeling Approach

Date: April 13, 2008

Purpose: NFRC has completed and launched its new rating procedure, the Component Modeling Approach.

Project Summary:

The calculation tool named the Component Modeling Approach Software Tool (CMAST), is found on the NFRC web site and is available for commercial use. It may be downloaded here: http://cmast.nfrc.org/ . Below are links to several materials developed to support the CMA program.

Click here to view the CMAST User Manual

Project 6 (b)
(2008 only)

Project Name: Component Modeling Approach

Date: April 13, 2008

Purpose: NFRC has completed and launched its new rating procedure, the Component Modeling Approach.

Project Summary:

The calculation tool named the Component Modeling Approach Software Tool (CMAST), is found on the NFRC web site and is available for commercial use. It may be downloaded here: http://cmast.nfrc.org/ . Below are links to several materials developed to support the CMA program.

Click here for the CMA Marketing Plan

Component Modeling Approach



Bridging the Gap between Theory and Reality to Create Demand

Component Modeling Approach
Marketing and Promotional Assistance
Working Document

Jim Benney
Executive Director
National Fenestration Rating Council

Abstract

This marketing plan discusses the implementation of the Component Modeling Approach for the rating and certification of fenestration products in nonresidential buildings. This plan outlines priorities and actions for aggressively pursuing various target audiences and details how the implementation will begin in California. This plan also describes a "push/pull" strategy that will have strong appeal among architects, contractors, code officials, and the fenestration industry. Furthermore, this plan explains the need for a strong educational program to promote interest and increase awareness and concludes by discussing the need for an enforcement component, designed to ensure compliance with energy codes.

Preface

It's no secret that we live in an increasingly competitive and complex world. Consumer tastes and preferences are changing rapidly, and organizations everywhere must find new and innovative ways to meet their needs. The CMA initiative enables NFRC to provide architects and HVAC engineers with a powerful tool they can use to obtain the energy performance data required to perform their jobs most effectively. It is the hope of this organization that this document will answer the following:

- How do we successfully introduce CMA into a somewhat dormant market?
- What should we do to give CMA the best possible chance to succeed?

The greatest challenge *any* high-tech product faces, CMA included, is making the transition from an early market dominated by a few visionary customers, which are called innovators and early adopters, to a mainstream market dominated by a large block of customers who we'll refer to as pragmatists. These are known as the early majority and the late majority. These two groups are followed by a final group known as laggards. These are the people that defy a given change until they are left with no other alternatives. These concepts are adapted from Geoffrey Moore's seminal work, *Crossing the Chasm*.

The gap between the innovators and early adopters and the early majority and late majority is so wide that it can be called a chasm. It may be useful to think of this chasm as a gulf that lies between the two distinctly different marketplaces for technology products. In order for CMA to be successful, it must cross this chasm because doing so represents acceptance of the product into the mainstream market. This, then, is the goal of this marketing plan – for CMA to win acceptance in the mainstream market.

Technology Adoption Life Cycle

To this point, we have referenced Moore (2002) and his theory about how technology products enter the market. It may be useful here to examine his theory, and how it applies to CMA, in greater detail. Moore refers to his theory as the Technology Adoption Life Cycle. He cautions that crossing the chasm involves undertaking immense and radical efforts. The marketing plan that follows offers a number of such actions for crossing the chasm and establishing CMA as a viable and credible product.

By using Moore's Technology Adoption Life Cycle as a template to promote CMA, NFRC can more clearly identify precisely the target market it should pursue. This, in turn, will give CMA the best possible chance of succeeding. Our first goal is for CMA, therefore, is to successfully cross the chasm by winning the approval of the innovators and the early adopters. Once we have done this, they will help push CMA out into the mainstream through word-of-mouth-advertising. NFRC, however, will not rely solely on word-of-mouth advertising conducted by others. We intend to engage in other aggressive forms of promotion, which will be described in more detail in the following sections.

Before we delve into the marketing plan proper, it will be helpful to identify and define some of the terms it refers to. First, for the purposes of promoting CMA, we will define the term "marketing" as taking actions to create, grow, maintain, and defend the product.

It is important to note that each one of the following groups can be clearly distinguished by the way it responds to advances in technology. The five groups involved in the Technology Adoption Life Cycle are as follows:

Innovators – *The Technology Enthusiasts*. These are the first people to adopt a new technology because they appreciate technology for its own sake.

Early Adopters – *The Visionaries*. These are the people who have the insight to match an emerging technology to a strategic opportunity and the charisma to get the rest of their organization to buy into their enthusiasm about it.

Early Majority – *The Pragmatists*. These are people who typically do not like to take giant leaps forward. Instead, they prefer to make incremental, measurable, and predictable progress.

Late Majority – *The Conservatives*. These are the people who prefer tradition over progress. When they find something that works for them, they stick with it.

Laggards – *The Skeptics*. Barely participate in the high-tech marketplace except to attempt to block purchases. Laggards struggle to find reasons not to like high-technology products.

Foreword

As we can see, each of Moore's categories enters the market at a specific time and for a specific reason. As we apply this theory to CMA, it appears reasonable that we can't simply launch CMA and hope for the best. What we need, instead, is a strategic and carefully-crafted incremental approach.

Our objective, therefore, should be to target strictly those we are able to identify as innovators and early adopters. After we win over these two groups, we can then begin to approach the other three. In all likelihood, the innovators and the early adopters will have already helped pave the way to succeeding with these other three groups.
In general, NFRC views component suppliers as the innovators and contractors/installers as the early adopters. On the other hand, the NFRC considers architects, contractors, and installers to be members of the early majority, the group to target after we have established solid ground by appealing to the innovators and early adopters. Our goal is that by providing specific examples of innovators and early adopters we will be able to build a persuasive case to take to the other groups. Once we have used the case studies to attract the innovators and the early adopters, we will shift our focus toward education to appeal to the early majority.

Possibly one of the most important things to keep in mind is that there exists a vast difference in the mindset of innovators and early adopters when compared to the early majority and late majority.

For example, Moore (2002) explains that innovators and early adopters enjoy being the first to implement change in their industries. This is because they expect that doing so will give them a jump on the competition. This may come from lower product costs, faster time to market, more complete customer service, or some other comparable business advantage. These two groups expect a radical discontinuity between the old ways and the new ways, and they are prepared to champion this cause against any resistance. Because they enjoy being the first, they are prepared to bear with the inevitable glitches that accompany any innovation that is just coming into the market.

Moore (2002) goes on to explain that the early majority and the late majority, on the other hand, see things a lot differently. These two groups want to buy a productivity improvement for their existing operations. They want to minimize the discontinuity with the old ways. They want evolution, not revolution. In other words, they want technology to enhance, not overthrow, the established ways of doing business. Above all, they do not want to have to spend any of their own time debugging someone else's product. By the time they adopt it, they want it to work properly and to integrate appropriately with their existing technology base.

The glaring differences in these attitudes toward accepting new technology provide NFRC with critical insight about proceeding with its plan to win widespread acceptance for CMA.

Executive Summary

The successful deployment of the Component Modeling Approach (CMA) for the nonresidential fenestration industry depends upon three important factors:

- **Marketing**. A highly-focused marketing program aimed at "innovators" and "early adopters" in the technology market that will promote the benefits of the CMA program to architects, contractors, and the fenestration industry.

- **Education**. An educational program to increase the awareness and understanding of how CMA works among industry and code officials.

- **Enforcement**. An enforcement plan to ensure enforcement of code compliance with state and local energy codes.

As with the residential NFRC program almost 20 years ago, California currently represents the most fertile ground for the introduction and advancement of the CMA program. The California Energy Commission is in support the program, Title 24 already incorporates requirements for NFRC certification in nonresidential buildings, and the utility community is especially supportive of energy efficiency programs, incentives, and educational initiatives

As a result, NFRC staff recommends that the strategy for implementing the CMA program begin in California. In addition to the factors listed above, financial assistance and cooperation from California Energy Service providers will be key to the success of this strategy, as will cooperation and involvement from the following entities: NFRC staff and Potomac Communications Group; the California Energy Commission, Southern California Edison (SCE); Pacific Gas and Electric (PG&E); the West Wall Group; and other relevant parties.

Introduction

The success of NFRC's Component Modeling Approach will depend on both market pull and market push. A successful marketing strategy must have the means to accomplish both and will be initiated by commissioning a series of case study/demonstration projects:

- Commission a series of case study/demonstration projects in which processes will be documented and used in the marketing, education, and enforcement strategies. These demonstration projects will get an NFRC certified rating and will aid in the assessment of CMA's value and help to set priorities of all marketing, education and enforcement efforts.

- Market pull will provide incentives for industry participation, including financial assistance for early adopters, Demand Side Energy Management programs that require NFRC-certified products for program acceptance and educational programs.

Market push will depend upon proper code enforcement, which also requires educational and marketing programs to raise awareness among those responsible for compliance.

Specific Marketing Approach

At this point in its evolution, CMA is largely theoretical simply because many of us have yet to see it in action. Accordingly, one of our main tasks will be to bridge the gap between theory and reality. In order to accomplish this, NFRC will commission a number of case studies. These real-time examples will establish the credibility of CMA and also lend validation to the program. The case studies will essentially serve as testimonials from satisfied users. Findings from these studies will be targeted towards the innovators and early adopter groups, as promotion of the CMA will rely heavily on the theory that it will be of immediate interest only to these members of the early market. Other groups such as the "early majority," "late majority," and the "laggards" are the people who simply will not purchase technology of any kind until it has already proven successful with an early market.

Case Study/Demonstration Projects

1. ***Arcadia*** (and site-built) will use CMA prototype to validate.

Goal: To remove any negative connotations that NFRC takes a long time to get things done and to use the numbers from the simulation process to show consistency. Also, to show overall consistency between Site Build and CMA

Lead: Jim Benney and Jessica Ferris

Desired Outcome: To achieve favorable press, particularly among code officials at the IECC

Further Details: First, Arcadia will obtain a Site-Built certificate on a building project in Las Vegas, Nevada. Accordingly, Arcadia will do all testing and simulations required and use an NFRC accredited IA to obtain the certificate.

Furthermore, Arcadia will keep a record of the start date(s) and end date(s) for all steps involved in the project. Upon completion, an article will be prepared to show the timelines needed for Site-Built Certification, provided the timeline is "positive."

NFRC will then work with the CMA template (to be tested in May/June) to determine the energy rating of the site-built project (using the accredited simulation lab) and add that information to the article, again, if the results are positive. Finally, Arcadia will work with NFRC staff and Potomac Design Group to craft an article to be published in a trade magazine. Note - SCE has expressed interest in this project and may be able to provide funding and/or communication channels promoting same.

2. TRACO Building Project. Mike Manteghi of TRACO will contribute to this effort by going through the process on an actual building project with an NFRC volunteer. Additionally, TRACO will use one of its projects in the Fall for the testing phase of the CMA network. Again, NFRC plans to promote the success of this initiative by crafting an article to be published in one or more trade publications.

3. Benson Industries Project. Katharine Best of Benson Industries will go through the process on an actual building project while working with an NFRC volunteer. The goal here is to work with Benson during the fall of 2008 on a project for which they are getting NFRC certified. Upon completion, NFRC will again conduct a study, similar to the Arcadia study mentioned above. Financial support may be provided through Southern California Electric (SCE) or Pacific Gas & Electric (PGE).

As noted above, industry participation in CMA is critical for a successful marketing and promotional campaign. In addition to providing case studies and demonstration projects, NFRC will offer a component library to provide supplemental materials for those who want to learn more about CMA and how it works. Those most likely to make use of the component libraries are the innovators and early adopters.

Component Library

CMA will be effective only if it maintains meaningful data of fenestration components, especially the frame library. In order to get frame suppliers to get products in the frame library in 2008, we will show them that the component library is not only viable but a robust resource that reinforces the viability of the case studies and demonstrations projects. NFRC's goal here is that the component library will help users better understand CMA and reveal why it is the next logical step for NFRC to take.

The component library offers comprehensive resources that will answer nearly any questions potential users have regarding CMA. In fact, it may be helpful to think of the component library at something of a "user's manual" for CMA.

Goal: To work with TRACO and other organizations to stock the frame library and show that the CMA process works

Lead: Jessica Ferris

Desired Outcome: To publish articles verifying the success of CMA. These articles are intended to serve as a model to attract the attention of the early adopters.

Further Details: One of the primary ideas here is to provide financial assistance to frame suppliers in 2008. This may be done through cost-sharing for additions that strengthen the validity of the CMA frame library. NFRC plans additional means of gathering data. These include the following:

- Once the procedures for entering data into the component libraries are confirmed, NFRC will be better prepared to offer a realistic budget for simulation and validation testing
- Provide incentives, in the form of lower costs, to frame suppliers in 2008
- Recognition, in the form of articles in state and national trade publications and the NFRC newsletters, of suppliers who get accepted in the libraries. Suppliers will also be recognized on the NFRC Web site.

Educational Program

There are multiple opportunities to increase the success of CMA's implementation through educational programs. Specifically, we will focus this training on members of the early majority and late majority, those members of the marketplace that typically exhibit skepticism early in the Technology Adoption Lifecycle.

Goal: This is the point where NFRC is attempting to win over members of the mainstream market

Lead: Jessica Ferris and Cornerstone Professional Group

Desired Outcome: Clearly informing the early majority and late majority of the benefits that the innovators and early adopters have enjoyed by implementing CMA

Further Details: One of the fundamental objectives of the educational program is to develop concise and effective help files for software to make the CMA software tool easy to use. Another objective is to develop a clearly-defined set of instructions, an online help desk, and a "live" help desk. NFRC will further educate the public on how to use CMA in the following ways:

- Live seminars for users in California. This effort will receive financial support from SCE, PGE, and SMUD
- The publication of technical briefs at www.energydesignresources.org
- The creation of handout materials aimed at attracting framing suppliers, contractors, architects, and others deemed to be innovators and early adopters. The CMA marketing committee will take on this initiative.
- The development of a Title 24 user's manual, which will involve NFRC and its partners in determining how to use CMA to meet Title 24 compliance. NFRC staff, CEC, PGE, and SCE will be responsible for this effort.
- The establishment of NFRC-certified and rated fenestration products as a requirement for any Savings by Design Program buildings.
- Referencing http://www.savingsbydesign.com in the Daylighting and HVAC Systems sections
- Development of a user's manual, handbook, or educational program, which thoroughly explains how CMA fits into the Savings By Design Program. The NFRC staff will work in conjunction with SCE and PGE in on this project.

Cooperation with CEC to Promote CMA

The NFRC believes gaining the support of the CEC is integral to its efforts to effectively promote CMA. NFRC also plans to work closely with the Office of the State Architect of California and the General Services Administration to spread favorable publicity, win acceptance, and gain endorsements from top officials for CMA. Nelson Pena will manage this project.

NFRC will also launch an aggressive promotional campaign program within California. The campaign will target architects, contractors, and code officials (all widely viewed as innovators and early adopters) with the following message: *Look for the NFRC logo!* Potential communications channels include CALBO meetings, its newsletter and Web site, training sessions, direct mail, and NFRC's internal newsletters.

Enforcement Program

The true key to CMA success in California (and elsewhere) will be appropriate enforcement of the requirements in Title 24. This will ensure that the majority of the buildings in California use only fenestration products that have NFRC-certified ratings. To improve code compliance, NFRC will take the following actions:

- Develop an educational program specifically for code officials, targeting the Association of California Building Officials and the Association of California County Building Code Officials. This educational program will explain the details of CMA, including plan checking and label certification.
- Become published in "Blueprint," a prominent trade publication among members of our target audience. The main idea here is to produce an article that provides an in-depth discussion of the benefits of CMA. The article will also emphasize that CMA will simplify the code official's job.
- Work with CEC to ensure that default values are punitive in order to push the industry toward NFRC-certified ratings. The concentration will be on bigger, more high-profile project. NFRC will also reinforce the loophole for breaking up a single project into smaller pieces. For example, less than 10,000 square feet is no longer available.

Return on Investment

The expenditures associated with introducing CMA to the marketplace may appear significant. Nevertheless, they promise a considerable return on investment. Once the development of CMA is complete, all of NFRC's stakeholder groups will experience the following benefits, which will represent a substantial return on the investment. These include, but are not limited to, the following:

- The nonresidential glazing industry will be able to show validated energy performance ratings for its products, which will help them to show compliance with local and state energy codes
- The CMA software will provide architects with a user-friendly tool to verify performance and give them assurance that bids and estimates are done using a validating methodology for determining energy performance
- HVAC engineers and energy consultants can obtain uniform energy data from WINDOW and THERM that is needed for advanced building design software
- International partners will be able to adopt harmonized software based on recognized standards
- The public at-large will benefit from increased use of higher performance fenestration systems that will in turn reduce energy use in the U.S.

Goal: To realize the most substantial return on investment possible

Leads: Jim Benney, Jessica Ferris

Desired Outcome: NFRC plans to use the Potomac Group to assist in realizing this goal. NFRC will work with Potomac to develop white papers, newsletter articles, press releases, and other promotional pieces to help spread the word about CMA among innovators and early adopters.

Further Details: NFRC will focus on the strategic placement of articles. It will research the most favorable publications and Web sites that are likely to appeal innovators and early adopters of technology products. In particular, NFRC will aggressively promote success stories through various trade publications. In addition to using the resources of the Potomac Group, the NFRC communications staff will also play an integral role in this promotional effort.

NFRC believes getting the word out about innovators and early adopters that are using CMA will go a long way toward helping the product/service cross the chasm and reach the mainstream markets because of the prevalent and widespread phenomenon that people like to follow a leader.

Springboard Projects

Goal: Successfully crossing the chasm and establishing solid ground for NFRC to launch further projects aimed at conserving energy in the U.S. and abroad

Lead: Tom Herron

Desired Outcome: Crossing the chasm and reaching the mainstream market with such impact that it spurs related projects for NFRC

Further Details: While the majority of the work described in this marketing plan is aimed at California and Title 24, this is merely a starting point. NFRC ultimately intends to take CMA nationwide and international. The following are some of the endeavors that the acceptance of CMA is likely to create:

- Establish NFRC-certified and rated fenestration products as a requirement for LEED and other "green" rating and certification programs
- The development of an NFRC "Green Team"
- Incorporate NFRC, CMA ratings as in integral part of any code-compliant building design software
- Encourage the establishment of a Federal commercial Energy Star windows program that requires NFRC-certified ratings for approval

Budget

$100,000 has been earmarked for CMA marketing projects.

Conclusion

As noted earlier, the point of greatest peril in the development of a high-tech market lies in making the transition from an early market, which is dominated by a few visionary customers to a mainstream market, which is dominated by a large block of customers who are far more practical in their thinking. The gap between these two markets is so large that it is referred to as a chasm. Crossing the chasm must be the primary focus of any long-term high-tech marketing plan.

The very foundation of our success with CMA lies in our ability to effectively target the innovators and early adopters. Once these two groups realize the value of CMA then a new mainstream market will emerge, and the product will be successful. This should, therefore, be the focus of our work – making that mainstream market emerge. Relying on the Technology Adoption Life Cycle to turn CMA into a viable product holds out the most promise for NFRC and all of its stakeholders.

The various groups we have discussed are clearly distinguished from each other by their characteristic response to a discontinuous innovation. This is an innovation that causes people to think in new and different ways rather than simply expanding their thinking on an existing product or service. Each group represents a unique psychographic profile. This is a combination of psychology and demographics, and it makes each group's marketing response different from the others'. Thoroughly understanding each profile and its relationship to its neighbors is the critical component of this marketing plan.

NFRC believes strongly in the efficacy of this plan because it is based on the results of scientific study of the technology adoption life cycle, and it provides us with a specific marketing approach to reach that will enable us to target our market with laser-like focus rather than using a "scattershot" approach and hoping for the best.

Appendix "A"

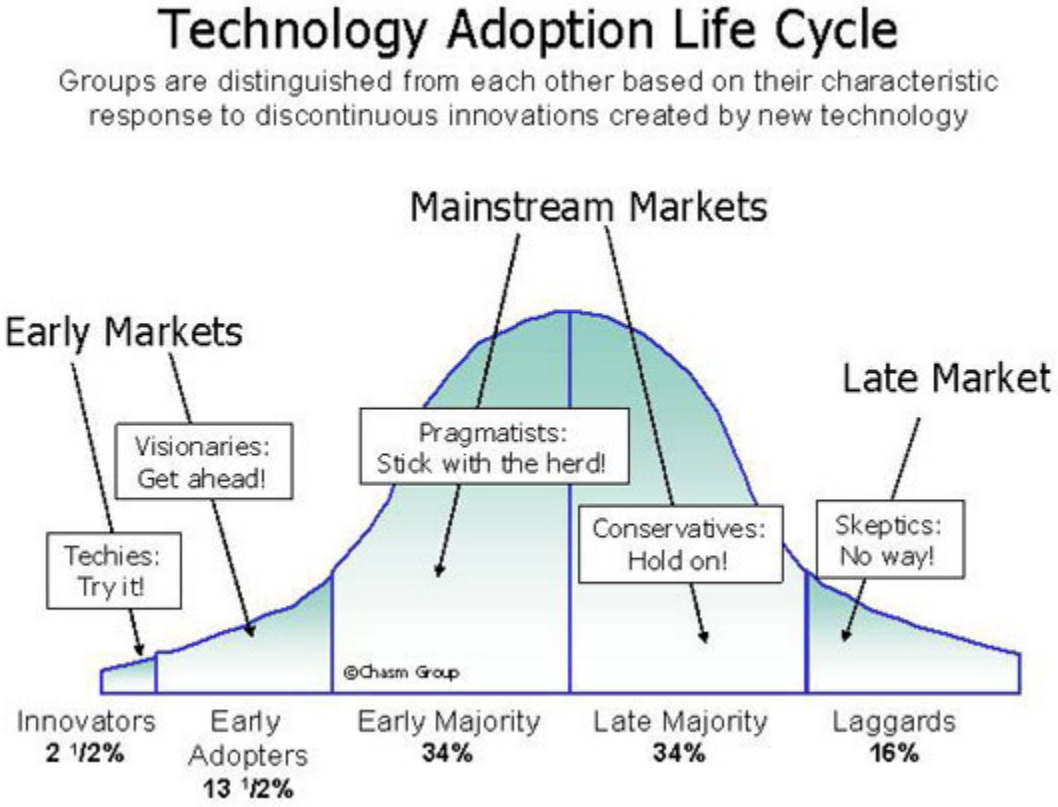
Twelve-Month Implementation Forecast

The following forecast shows the areas NFRC will focus on during certain months of the year. As indicated, we foresee the initial appeal to the innovators and early adopters to run from June through September. From October until January, we will emphasize our promotional efforts in the early majority, and from February until April, we will reach out to the late majority. The laggards will be the last to adopt CMA and really should not be the focus of any of our marketing efforts. This is because these are the kind of people that will use CMA only after they have no other choice.

Below is a graphical representation of everything we have discussed to this point. It shows the percentages of the various groups that comprise the technology adoption lifecycle. The chasm lies between the early adopters and the early majority. This is the critical area that we must navigate effectively to make CMA successful.

Before we look at the graphic, NFRC will more clearly define what it means when it refers to a "market." For the purpose of promoting CMA, NFRC refers to a market as a set of actual or potential customers for a given set of products or services who have a common set of needs or wants, and who refer to each other when making buying decisions. This is critical to point out at this stage because word-of-mouth advertising among the innovators and early adopters will play an integral role in pushing CMA out into the mainstream markets.

June July Aug Sept Oct Nov Dec Jan Feb March April May



Note: The chasm lies between the early adopters and the early majority. This may also be thought of as the "make or break" point.

As you can see from the timeline above the graphic, NFRC anticipates it will take approximately four to five months to build a strong foundation with the innovators and early adopters. NFRC will accomplish this using the specific marketing techniques discussed in the next section.

For the moment, however, it will help us to better understand the graphic by pointing out that NFRC intends to conduct case studies and demonstration projects with the innovators and the early adopters. It will then use the results of these studies and projects to reach out to the mainstream markets, which are made up of the early majority and the late majority. None of our marketing efforts, however, will be targeted toward the laggards as this group will eventually adopt CMA, but not until they are forced to.

Project 6 (c)
(2008 only)

Project Name: Component Modeling Approach

Date: April 13, 2008

Purpose: NFRC has completed and launched its new rating procedure, the Component Modeling Approach.

Project Summary:

The calculation tool named the Component Modeling Approach Software Tool (CMAST), is found on the NFRC web site and is available for commercial use. It may be downloaded here: http://cmast.nfrc.org/ . Below are links to several materials developed to support the CMA program.

Click here for the CMA Informational Brochure

LEARN MORE ABOUT COMPONENT MODELING APPROACH

AT A WEBINAR ON CMA AND CALIFORNIA'S TITLE 24

December 3rd 2009 or January 28th 2010

Component Modeling Approach (CMA) determines energy-related performance ratings for nonresidential fenestration products.

This webinar is targeted to California's code enforcement agencies and energy professionals.

To register for this **free** webinar:

www.h-m-g.com/cma

Sophia Hartkopf, Heschong Mahone Group, Inc.
hartkopf@h-m-g.com
916-962-7001

Space is limited...register now!

Commercial Site-Built Fenestration

Three Ways to Comply with 2008 Title 24:

1. **CEC Default Values**
   - ***Worst Approach*** (least energy credit)
   - Nonresidential Standards: Tables 116-A, 116-B
2. **Calculated Thermal Performance**
   - ***Barely Acceptable Approach*** (less energy credit)
   - <10,000sf only, Nonresidential Appendices NA6
3. **NFRC Certified Label Certificate**
   - ***Best Approach*** (most energy credit)
   - Nonresidential Compliance Manual Section 3.2

Component Modeling Approach

- **What is it?**

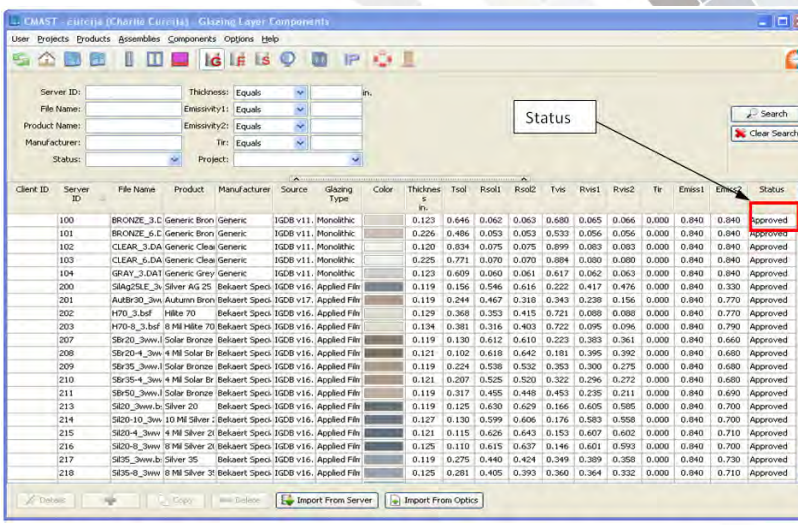
  National Fenestration Rating Council's (NFRC) Component Modeling Approach (CMA) lets designers create a window product "virtually" on an NFRC approved software (CMAST) and generate its certified performance ratings (U-Factor, SHGC, VT) for use in energy compliance

- **What can it be used for?**

  1. **Site-built fenestration** only (in CA)
  2. **Commercial projects** only (except HR residential)
  3. **Any size fenestration** (irrespective of whether total fenestration area is < or > than 10,000sf)

CMA Software Tool (CMAST)

- **Quick turn-around**
  no lab testing
- **Real-time**
  web-based access
- **Bidding, quoting**
  research capability
- **Create a CMA LC**
  Label Certificate





Download: http://cmast.nfrc.org
Use for 6 months FREE
Support Desk: http://support.nfrc.org
E: cmast_support@designbuildersoftware.com
P: 1 866-411-6845

CMA Label Certificate

- **Use In lieu of FC-1/FC-2**
  - Fenestration Certificates for CEC's Default Values
- **Make available on site**
  - for field inspection
- **NOT required for permit submittal**

NATIONAL FENESTRATION RATING COUNCIL
LABEL CERTIFICATE
PRODUCT LISTING

Enforcement Agency Collects Form

FOR CODE COMPLIANCE

LABEL CERTIFICATE ID: *XYZ-001* Issuance Date: mm/dd/yyyy

NFRC CERTIFIED PRODUCT RATING INFORMATION:*
The NFRC Certified Product Rating Information listed here is to be used to verify that the ratings meet applicable energy code requirements.

PRODUCT LISTING:

Responsible Party Verifies

CPD ID	Total Area ft²	Name	Framing Ref	Glazing Ref	Spacer Ref	CERTIFIED Performance Rating at NFRC Model Size U** Btu/hr-ft²-°F	SHGC** -	VT** -
P-PL-010	88.89	PL-2200 / PL-2210	FA-PL2210	GA-TT-001	SA-AM-001	0.53	0.58	0.66
P-PL-005	192.67	PL-3400 / PL-3401	FA-PL3401	GA-TT-001	SA-AM-002	0.56	0.57	0.65
P-PL-012	362.22	PL-5700 / PL-5720	FA-PL5720	GA-TO-002	SA-AM-00	0.52	0.21	0.30
P-PL-002	60.00	PL-1100 / PL-1152	FA-PL1152	GA-TT-001	SA-AM-001	0.42	0.51	0.62
P-PL-022	525.00	PL-9900 / PL-9915	FA-PL9915	GA-TO-003	SA-AM-002	0.45	0.15	0.19

FRAME, GLAZING and SPACER ASSEMBLIES:

FRAMING LISTING:

FRAMING REF	SUPPLIER ID	DESCRIPTION
FA-PL2210		Single Casement Thermally Broken Aluminum
FA-PL3401		Projecting (Awning) Thermally Broken Aluminum
FA-PL5720		Vertical Slider PVC reinforced with Steel
FA-PL1152		Vertical Slider Thermally Broken Aluminum
FA-PL9915		Fixed Thermally Broken Aluminum

GLAZING LISTING:

GLAZING REF	SUPPLIER ID	DESCRIPTION
GA-TT-001		1" Double Glazed, 1/4" HC Low-e, 1/4" Clear, Argon (90%), 1/2" gap
GA-TT-002		1" Triple Glazed, 1/8"Clear, Coated film, 1/8"SC, Argon (90%), 3/8" gap
GA-TT-003		1" Double Glazed, 1/4" Bronze, 1/4" SC Low-e, Argon (90%), 1/2" gap

SPACER LISTING:

SPACER REF	SUPPLIER ID	DESCRIPTION
SA-AM-001		250P Mill Finish Aluminum Low profile (1/2")
SA-AM-002		15A Polymer Spacer (3/8")

© 2009 National Fenestration Rating Council

Certificate of Compliance (ENV-1C)

- **Documentation Author indicates "Source" as NFRC**
  - under "Fenestration Surface Details"
- **Plan Checker checks consistency w/plans**
  - "Max SHGC" and "Max U-factor"

Documentation Author to indicate source as "NFRC"

CERTIFICATE OF COMPLIANCE AND FIELD INSPECTION ENERGY CHECKLIST — ENV-1C (Page 1 of 4)

Project Name:	Date:	Climate Zone:
Project Address:		Conditioned Floor Area:

General Information

Building Type: ☐ Nonresidential ☐ High-Rise Residential ☐ Hotel/Motel Guest Room
☐ Schools (Public School) ☐ Relocatable Public School Bldg. ☐ Conditioned Spaces ☐ Unconditioned Spaces
☐ Skylight Area for Large Enclosed Space ≥ 8000 ft² (If checked include the ENV-4C with submittal)

Phase of Construction: ☐ New Construction ☐ Addition ☐ Alteration

Approach of Compliance: ☐ Component ☐ Overall Envelope ☐ Unconditioned (file affidavit)

Front Orientation: N, E, S, W or in Degrees:

FIELD INSPECTION ENERGY CHECKLIST

OPAQUE SURFACE DETAILS

Tag/ ID	Assembly Name[1]	Frame Type[2]	Furring framing Material	Surface Area	Surface Orientation N, S, W, E	Cavity R-Value		Furring	Furring framing R-	Condition Status[5]	Special Feature[6]	Pass	Fail[7]
											☐	☐	☐
											☐	☐	☐
											☐	☐	☐
											☐	☐	☐
											☐	☐	☐
											☐	☐	☐

1. Indicate the identifying name of the frame type (i.e. Wall -1, Ceiling-1, Roof -1, and Floor- 1).
2. Indicate type of Assembly Type such as Wood 2x4 or LW CMU 8". For additional other assembly types see Reference Joint Appendix, JA4-1.
3. If furring is checked refer to ENV-2C Furring Strips Construction worksheet.
4. Indicate furring R-value when furred wall are being used.
5. Indicate Status of fenestration (New, Existing or Upgrade).
6. Indicate Special Feature on Page 2 of the Inspection Checklist Form below.
7. If Fail, then describe on Page 2 of the Inspection Checklist Form and take appropriate action to correct. Verify building plans if necessary.

FENESTRATION SURFACE DETAILS

Tag /ID[1]	Fenestration Type[2]	Surface Area	Surface Orientation N, S, W, E	# of Panes	Max U-Factor	Max SHGC	Source[3]	Overhang	Condition Status[4]	Special Feature[5]	Pass	Fail[6]
							NFRC	☐		☐	☐	☐
								☐		☐	☐	☐
								☐		☐	☐	☐
								☐		☐	☐	☐
								☐		☐	☐	☐
								☐		☐	☐	☐

1. Indicate the identifying name of the frame type (i.e. Window #1).
2. Indicate type of construction Type such, Window, Glass Door, Curtain wall, Skylight, or other
3. Indicate if the efficiency values are from the NFRC Label Certificate or from the CEC Default Values. Enter NFRC or CEC (FC-1 and FC-2).
4. Indicate Status of fenestration (New, Existing or Upgrade).
5. Indicate Special Feature on Page 2 of the Inspection Checklist Form below.
6. If Fail then describe on Page 2 of the Inspection Checklist Form and take appropriate action to correct. Verify building plans if necessary.

Certificate of Acceptance (ENV-2A)

- **Responsible Party checks "NFRC CMA Label Certificate"**
  - under "Building Information" - "Label Certificate"
- **Fills out NFRC Label Certificate ID #s**

CERTIFICATE OF ACCEPTANCE — ENV-2A
Fenestration Acceptance Certificate — (Page 1 of 2)

Project Name/Address:

Enforcement Agency Collects Form

System Name or Identification/Tag:	System Location or Area Served:
Note: A maximum of 4 NFRC Product Listings for each Certificate of Acceptance.	Enforcement Agency Use: Checked by/Date

Note: The Enforcement Agency may choose to verify the Fenestration Certified Products Directory number that matches the CPD-ID number at http://cpd.nfrc.org/search/search_cpdnum.aspx.

BUILDING INFORMATION

Date of Permit:	Building Permit #	Label Certificate Issuance Date:	Climate Zone:
BUILDING TYPE:	☐ NONRESIDENTIAL/COMMERCIAL/SCHOOL	☐ HIGH RISE RESIDENTIAL	☐ HOTEL/MOTEL GUEST ROOM
PHASE OF CONSTRUCTION:	☐ NEW CONSTRUCTION	☐ ADDITION	☐ ALTERATION
LABEL CERTIFICATE:	☐ **NFRC CMA** LABEL CERTIFICATE ID #_____ *(Attach an NFRC Label Certificate for each product listing and enter the Label Certificate ID in each column below)*	☐ **NA7 or CEC** Default Values Use FC-1/FC-2 < 10,000 ft² (Attach FC-1/FC-2 and Enter information in *Row1 through 4*)	☐ **CEC** Default Values Use FC-1/FC-2 ≥ 10,000 ft² (Attach FC-1/FC-2 and Enter information in *Row1 through 4*)

STATEMENT OF ACCEPTANCE

This Certificate of Acceptance summarizes the results of the Acceptance test related to building fenestration requirements as per Title 24, Part 6. Verify that each fenestration product meets the Reference Nonresidential Appendix, NA7.4. In accordance with Sections 10-103(a)3B, 10-111, 116(a)5 of the Energy Standards.

SUMMARY OF FENESTRATION VERIFICATION AND INSPECTION BY RESPONSIBLE PARTY

The Responsible Party shall verify the thermal performance (U-factor and SHGC) of each specified fenestration product being installed matches the fenestration label certificate, energy compliance documentation and building plans.

	1	2	3	4
NFRC Label Certificate ID #				

CEC Default Fenestration Information:

1	Manufactured Fenestration Description (i.e. Bluegreen/ air/clear-6mm)				
2	Manufactured Product ID #				
3	Glazing Layers	☐ Single ☐ Double ☐ Other	☐ Single ☐ Double ☐ Other	☐ Single ☐ Double ☐ Other	☐ Single ☐ Double ☐ Other
4	Verification (Verify each product with…)	☐ Delivery Receipt(s) ☐ Purchase Order or ☐ Detailed Receipt	☐ Delivery Receipt(s) ☐ Purchase Order or ☐ Detailed Receipt	☐ Delivery Receipt(s) ☐ Purchase Order or ☐ Detailed Receipt	☐ Delivery Receipt(s) ☐ Purchase Order or ☐ Detailed Receipt
		☐ Cross Reference and Matches Building Plans	☐ Cross Reference and Matches Building Plans	☐ Cross Reference and Matches Building Plans	☐ Cross Reference and Matches Building Plans

Responsible Party completes these fields

N/A

Acceptance Requirements (NA7.4.1)

- **Responsible Party verifies that U-factor and SHGC of installed window match:**
  - NFRC CMA Label Certificate
  - Energy compliance documentation
  - Building plans
- **On job site, Enforcement Agency (Inspector) collects:**
  - NFRC CMA Label Certificate
  - ENV-2A form (signed by the Responsible Party)
  - ENV-INST form (signed by the Window Installer)
  - and may verify that thermal efficiencies of installed window are equal or better than values on NFRC CMA LC

Learn more about CMA
at a FREE webinar on CMA & Title 24
Dec. 3rd 2009 or Jan. 28th 2010

Register: www.h-m-g.com/cma

Contact: Sophia Hartkopf
916.962.7001
hartkopf@h-m-g.com

- **NFRC Website**
  - www.nfrc.org/CMAProgram.aspx
- **NFRC Staff**
  - Jessica Ferris: CMA Program Manager, jferris@nfrc.org
- **CMAST Support**
  - http://support.nfrc.org
    cmast_support@designbuildersoftware.com, 1.866.411.6845
- **CEC Energy Hotline**
  - 1.800.772.3300

UPCOMING EVENTS

CALIFORNIA EVENTS

CMA & Title 24 Webinar #1
December 3, 2009 Register now!
www.h-m-g.com/cma

CMA & Title 24 Webinar #2
January 28, 2010 Register now!
www.h-m-g.com/cma

NATIONAL EVENTS

NFRC Webinar
November 11, 2009
www.nfrc.org/CMA-Training-Page.aspx

ACE (Approved Calculation Entity) Training
November 15, 2009
San Antonio, Texas

NFRC Regional Meeting
November 16-19, 2009
San Antonio, Texas

NFRC Webinar
December 9, 2009
www.nfrc.org/CMA-Training-Page.aspx

ADDITIONAL RESOURCES

WEBSITES

NFRC:
www.nfrc.org

CMA:
www.nfrc.org/CMAProgram.aspx

CMAST Support:
http://support.nfrc.org

DOWNLOADS

Free 6-month CMAST trial period!
http://cmast.nfrc.org

FOR MORE INFORMATION

NFRC

Jessica Ferris
CMA Program Manager
National Fenestration Rating Council
301.589.1776, ext. 204
jferris@nfrc.org

HMG

Mudit Saxena, Sr. Project Manager
Sophia Hartkopf, Associate Manager
Heschong Mahone Group
916.962.7001
Mudit.Saxena@h-m-g.com

CALIFORNIA ENERGY COMMISSION

California Energy Commission's Energy Standards Hotline
800.772.3300 (CA only)
916.772.3300 (National)
Title24@energy.state.ca.us

FSC Mixed Sources
Product group from well-managed forests, controlled sources and recycled wood or fiber
www.fsc.org Cert no. SCS-COC-001248
© 1996 Forest Stewardship Council

COMPONENT MODELING APPROACH

Information about a new provision in Title 24 2008 for site-built fenestration in non-residential buildings

Wall poster inside!

COMPONENT MODELING APPROACH

CMA MAKES IT SIMPLE!

CMA IN TITLE 24 ENERGY STANDARDS

Rating Site-Built Fenestration: The 2008 update of California's Building Energy Standard (Title 24) approved the use of CMA to determine energy-related performance ratings for site-built fenestration in nonresidential buildings.

CMA, or "Component Modeling Approach," is a Product Certification Program from the National Fenestration Rating Council (NFRC) which enables energy-related performance ratings for nonresidential fenestration products.

CMAST, or CMA Software Tool, is NFRC approved software which allows a user to create a fenestration product "virtually," and generate its energy-related performance ratings (U-Factor, SHGC, VT).

BENEFITS OF CHOOSING CMA

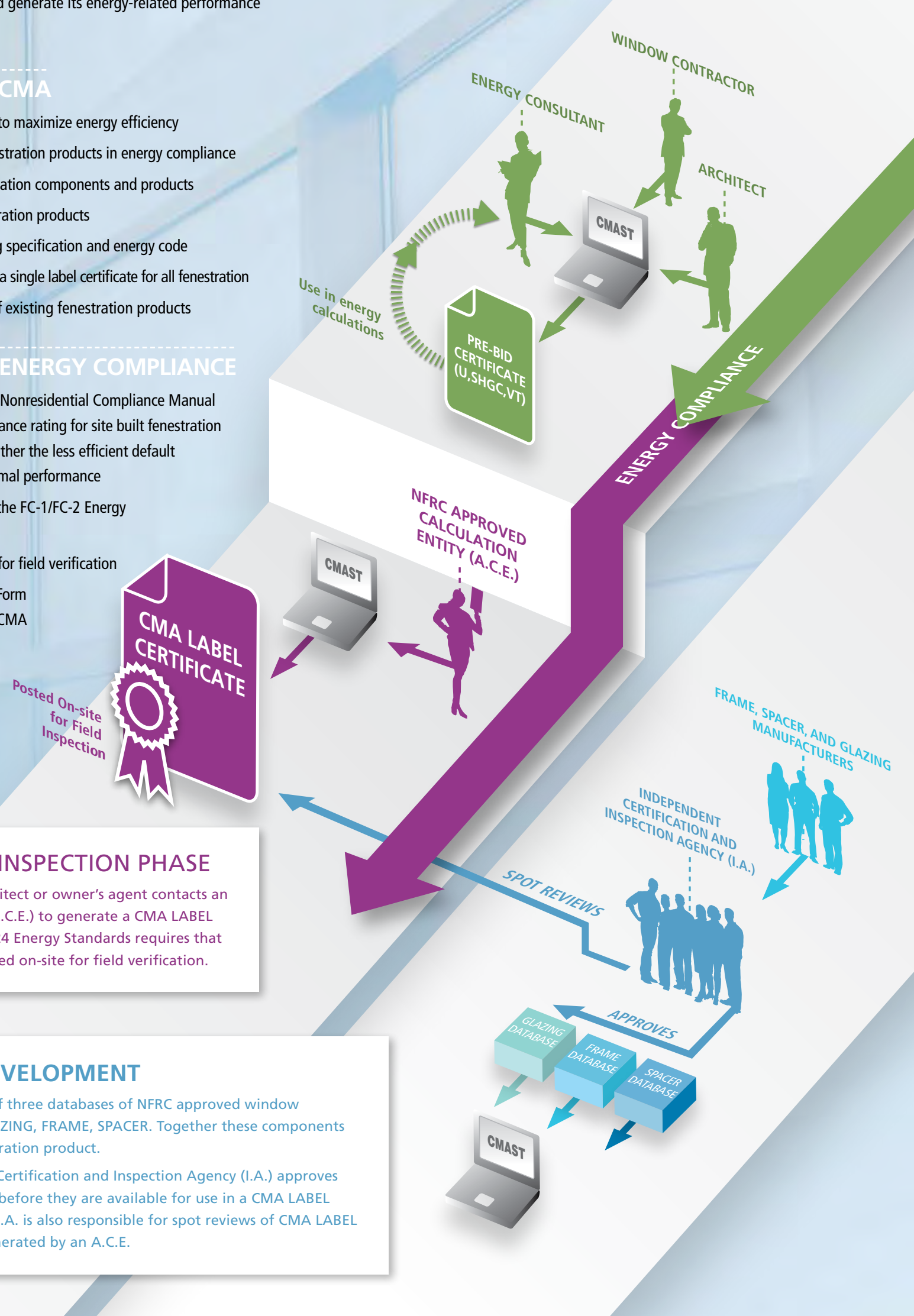
- Design envelope/fenestration products to maximize energy efficiency
- Obtain credit for high performance fenestration products in energy compliance
- Compare energy performance of fenestration components and products
- Eliminate lab-testing of site-built fenestration products
- Standardize bid reports to meet building specification and energy code
- Simplify compliance documentation with a single label certificate for all fenestration
- Create label certificates from a library of existing fenestration products

USING CMA FOR TITLE 24 ENERGY COMPLIANCE

- New to 2008 is the option to use CMA (Nonresidential Compliance Manual Section 3.2). Previously, energy performance rating for site built fenestration in Title 24 has been determined using either the less efficient default tables or Appendix NA6 calculated thermal performance
- CMA Label Certificate is used in lieu of the FC-1/FC-2 Energy Commission Label Certificates
- CMA Label Certificate is posted on-site for field verification
- Responsible party completes and signs Form ENV-2A and provides it along with the CMA Label Certificate to the building owner and field inspector

CMA PROCESS: DESIGN PHASE

During DESIGN PHASE, an architect, a window contractor and an energy consultant use CMAST to create a virtual model of the proposed window. A PRE-BID CERTIFICATE can be generated at this time for use in energy calculations by the energy consultant.



CMA PROCESS: FIELD INSPECTION PHASE

During COMPLIANCE PHASE, an architect or owner's agent contacts an NFRC Approved Calculation Entity (A.C.E.) to generate a CMA LABEL CERTIFICATE from CMAST. The Title 24 Energy Standards requires that the CMA LABEL CERTIFICATE be posted on-site for field verification.

CMAST DEVELOPMENT

CMAST consists of three databases of NFRC approved window components: GLAZING, FRAME, SPACER. Together these components make up a fenestration product.

An Independent Certification and Inspection Agency (I.A.) approves each component before they are available for use in a CMA LABEL CERTIFICATE. An I.A. is also responsible for spot reviews of CMA LABEL CERTIFICATES generated by an A.C.E.

Project 6 (d)
(2008 only)

Project Name: Component Modeling Approach

Date: April 13, 2008

Purpose: NFRC has completed and launched its new rating procedure, the Component Modeling Approach.

Project Summary:

The calculation tool named the Component Modeling Approach Software Tool (CMAST), is found on the NFRC web site and is available for commercial use. It may be downloaded here: http://cmast.nfrc.org/ . Below are links to several materials developed to support the CMA program.

Click here for the CMA Informational Packet



COMPONENT MODELING APPROACH

Informational Packet

COMPONENT MODELING APPROACH

Index

1. Background information regarding CMAST page 3
2. CMA Brochure page 5
3. Flow-Charts page 6
4. Contacts Page page 12

The Facts about the Component Modeling Approach (CMA)

For the past 20 years, the National Fenestration Rating Council (NFRC) has provided a fair, accurate, and credible rating and labeling system for windows, doors, and skylights used in residential construction. Now NFRC is providing the non-residential market with a powerful and exciting online program known as the Component Modeling Approach (CMA).

What is CMA?

CMA is a groundbreaking concept in the non-residential fenestration industry. It offers performance information on fenestration components through an online database. This is essentially a library that houses data on a wide variety of fenestration components and is available all the time from anywhere in the world.

CMA shows how changing one component affects overall energy efficiency and provides information on which components can be combined. Ultimately, the information obtained from CMA can be used to determine a whole product energy performance rating for a fenestration system.

This rating information is incorporated into a CMA Label Certificate for product validation. The label certificate lists the performance for all fenestration systems for a given building project.

Furthermore, any products certified for a particular project can be used in subsequent projects without recertification. Finally, components and certified products are maintained indefinitely in CMA.

How is CMA organized?

CMA is organized into three primary components:

Glazing	Frame	Spacer
Optical/spectral data from the International Glazing Database	Thermal performance data of frame cross-sections	Thermal performance of spacer component materials

Why did NFRC create CMA?

NFRC developed CMA to:

- Ease market transformation in the commercial fenestration industry by encouraging broad access and use of CMA.
- Provide a fair, level playing field among competitors for marketing energy-efficient fenestration products and components.
- Assist the building code community through the use of the CMA for determining the compliance of fenestration products to state and local energy codes.

(Over)

NFRC provides accurate, credible energy performance ratings for windows, curtain walls, doors, skylights, and fenestration attachments. For more information on NFRC, please visit our Web site at www.nfrc.org or contact NFRC directly at 301-589-1776.

What's in it for me?

Architects and builders:

- Designing envelope/fenestration systems for maximum energy efficiency – whether for solar control, energy efficiency, daylighting, or passive solar design
- Comparing the energy performance of different fenestration components and products, and making more informed choices
- Enforcing – relate specified performance to installed performance

Building officials, state government employees, and others involved in code development and enforcement:

- Establishing realistic prescriptive energy codes for fenestration products (windows, doors, curtain walls, skylights)
- Determining if fenestration products meet local energy codes

Government- and utility-run energy-efficiency programs:

- Promoting advanced building technology
- Establishing demand-side management programs based on fenestration product performance
- Determining if the products installed meet the performance requirements of those voluntary programs

Manufacturers/contractors:

- Standardizing bid reports, showing that your products meet both the building specification and the local energy code requirements
- Determining and reporting the energy benefits of new designs or technology accurately
- Utilizing the most efficient components using a reliable design tool

How can I learn more about CMA?

Please contact NFRC's CMA Program Manager, Jessica Ferris, at jferris@nfrc.org for more details.



June 2009

COMPONENT MODELING APPROACH

CMA MAKES IT SIMPLE!

CMA IN TITLE 24 ENERGY STANDARDS

Rating Site-Built Fenestration: The 2008 update of California's Building Energy Standard (Title 24) approved the use of CMA to determine energy-related performance ratings for site-built fenestration in nonresidential buildings.

CMA, or "Component Modeling Approach," is a Product Certification Program from the National Fenestration Rating Council (NFRC) which enables energy-related performance ratings for nonresidential fenestration products.

CMAST, or CMA Software Tool, is NFRC approved software which allows a user to create a fenestration product "virtually," and generate its energy-related performance ratings (U-Factor, SHGC, VT).

BENEFITS OF CHOOSING CMA

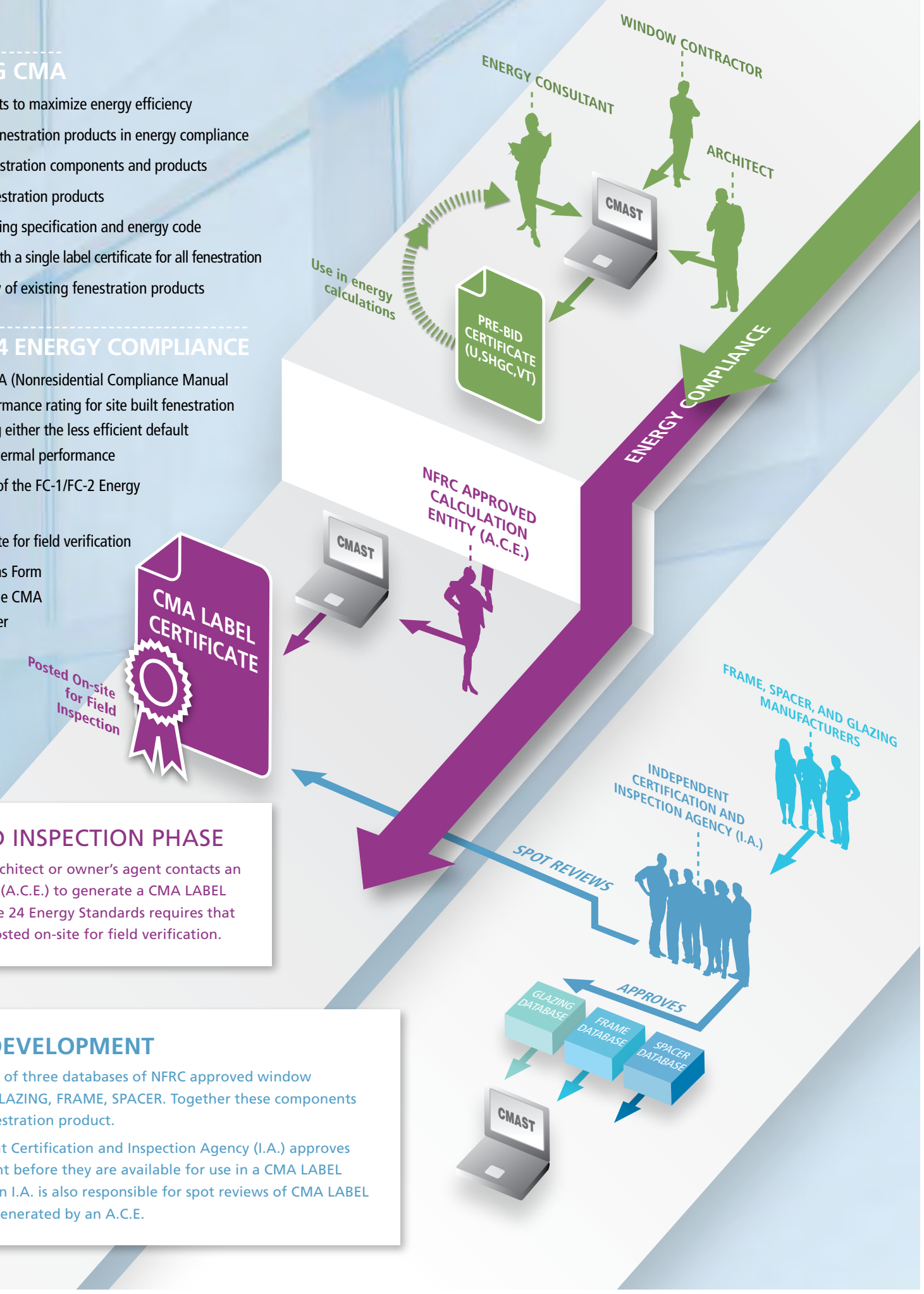
- Design envelope/fenestration products to maximize energy efficiency
- Obtain credit for high performance fenestration products in energy compliance
- Compare energy performance of fenestration components and products
- Eliminate lab-testing of site-built fenestration products
- Standardize bid reports to meet building specification and energy code
- Simplify compliance documentation with a single label certificate for all fenestration
- Create label certificates from a library of existing fenestration products

USING CMA FOR TITLE 24 ENERGY COMPLIANCE

- New to 2008 is the option to use CMA (Nonresidential Compliance Manual Section 3.2). Previously, energy performance rating for site built fenestration in Title 24 has been determined using either the less efficient default tables or Appendix NA6 calculated thermal performance
- CMA Label Certificate is used in lieu of the FC-1/FC-2 Energy Commission Label Certificates
- CMA Label Certificate is posted on-site for field verification
- Responsible party completes and signs Form ENV-2A and provides it along with the CMA Label Certificate to the building owner and field inspector

CMA PROCESS: DESIGN PHASE

During DESIGN PHASE, an architect, a window contractor and an energy consultant use CMAST to create a virtual model of the proposed window. A PRE-BID CERTIFICATE can be generated at this time for use in energy calculations by the energy consultant.



CMA PROCESS: FIELD INSPECTION PHASE

During COMPLIANCE PHASE, an architect or owner's agent contacts an NFRC Approved Calculation Entity (A.C.E.) to generate a CMA LABEL CERTIFICATE from CMAST. The Title 24 Energy Standards requires that the CMA LABEL CERTIFICATE be posted on-site for field verification.

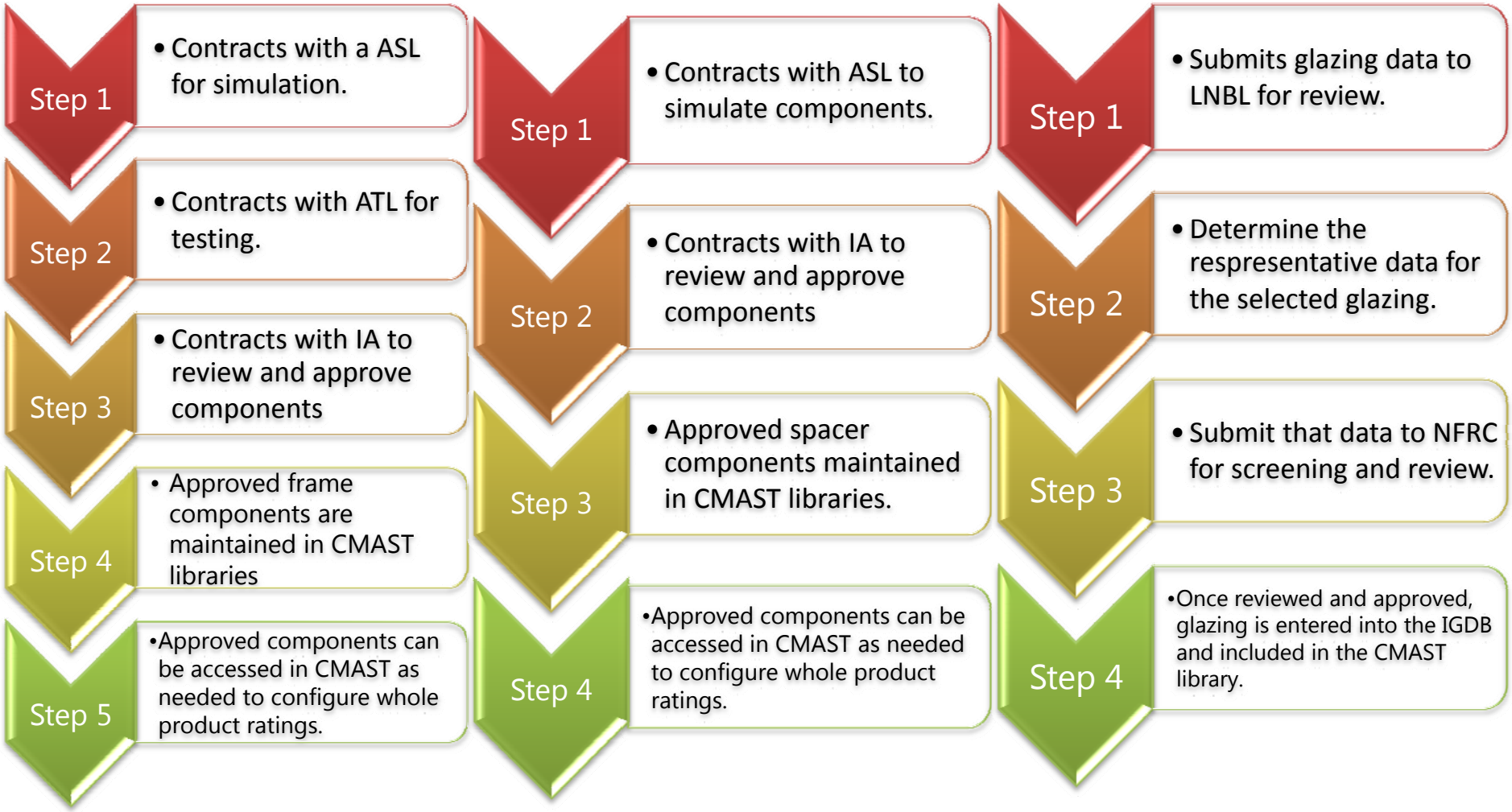
CMAST DEVELOPMENT

CMAST consists of three databases of NFRC approved window components: GLAZING, FRAME, SPACER. Together these components make up a fenestration product.

An Independent Certification and Inspection Agency (I.A.) approves each component before they are available for use in a CMA LABEL CERTIFICATE. An I.A. is also responsible for spot reviews of CMA LABEL CERTIFICATES generated by an A.C.E.

Component Modeling Approach

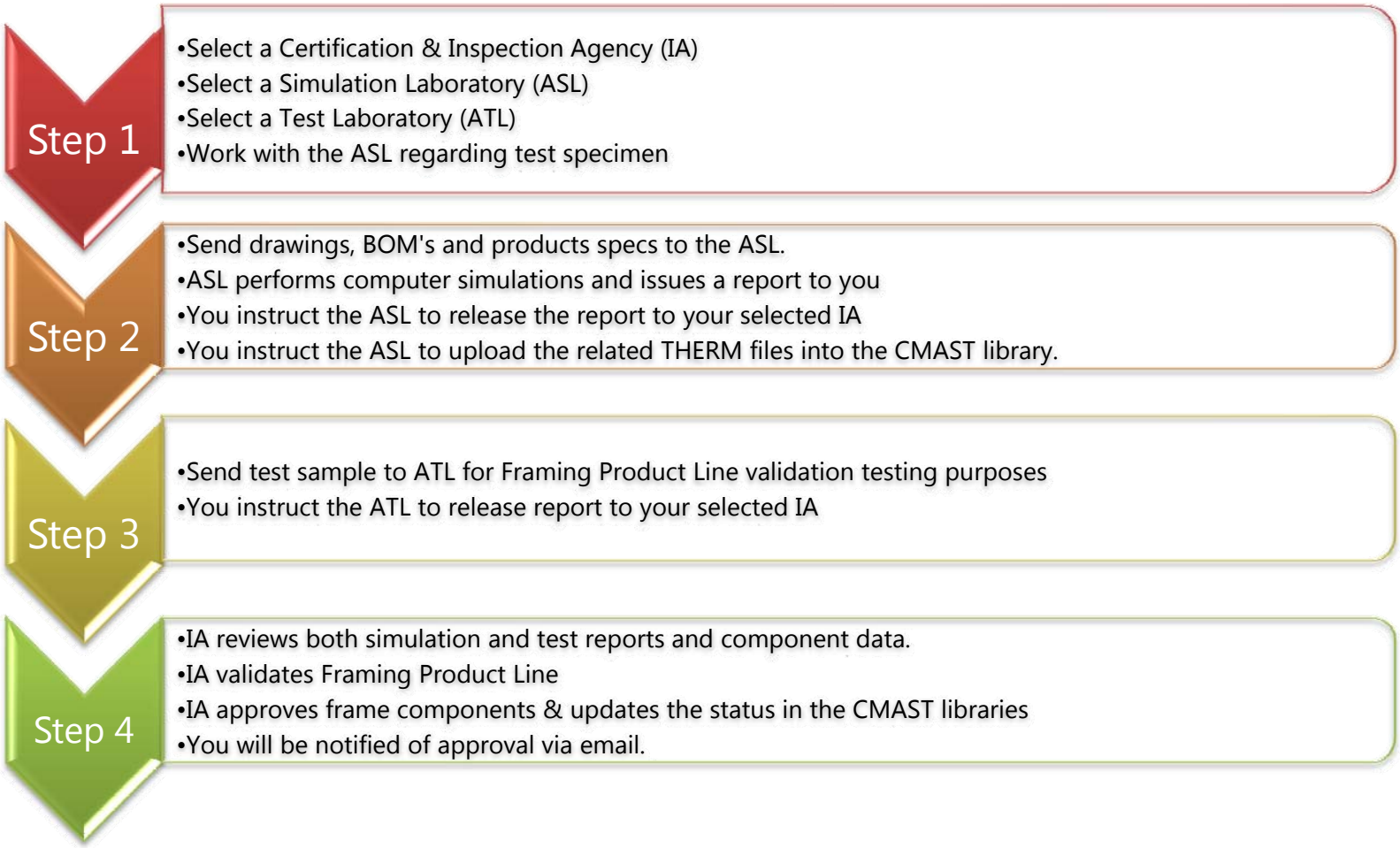
Component Approval Process



For the appropriate fee schedule and a more detailed step by step procedure of how to submit your product for approval in the CMA PCP, please visit our website.
http://www.nfrc.org/CMAprogram.aspx

Component Modeling Approach

How to submit my Frame Component for CMA Approval

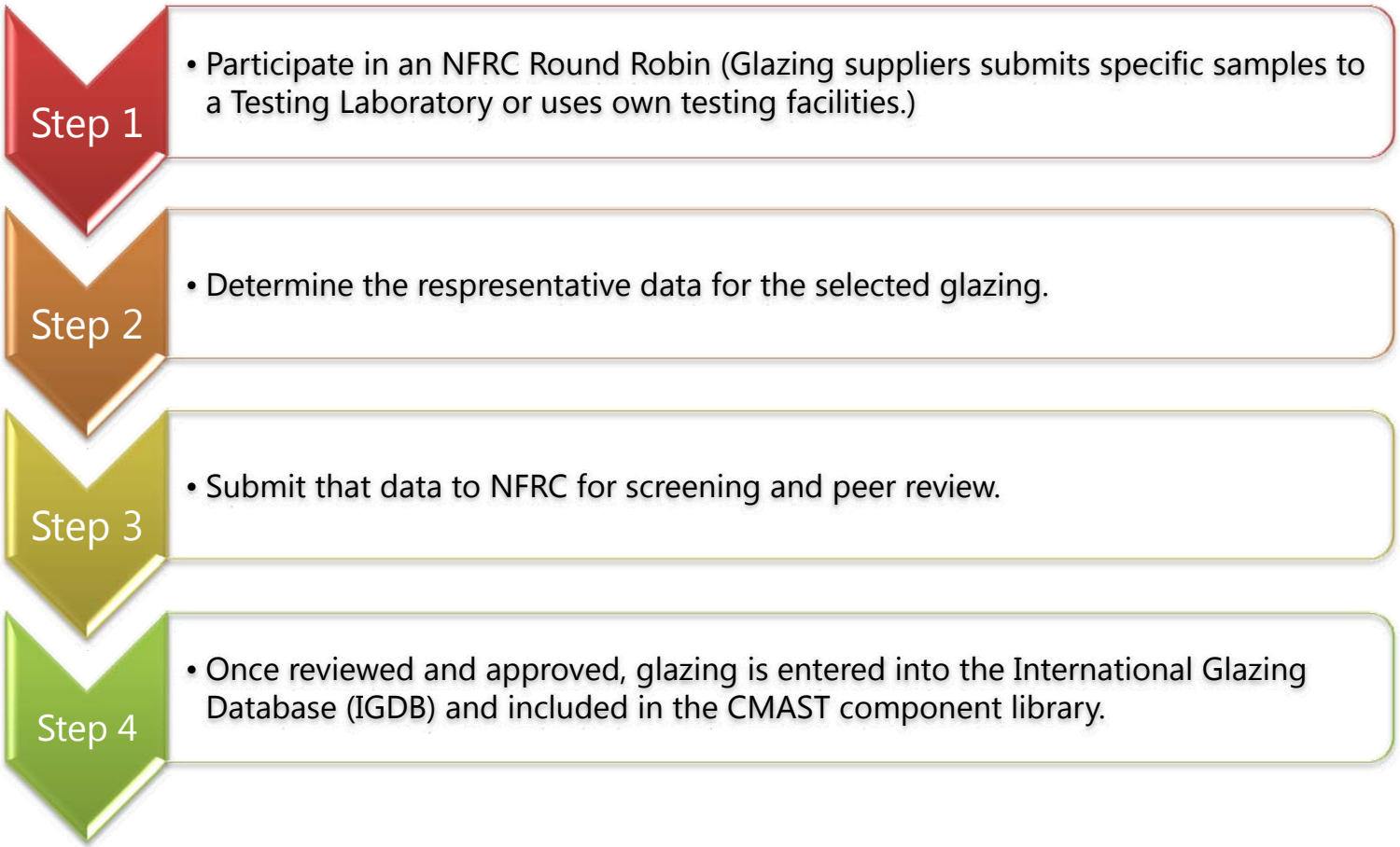


For the appropriate fee schedule and a more detailed step by step procedure of how to submit your product for approval in the CMA PCP, please visit our website.
http://www.nfrc.org/CMAprogram.aspx

Component Modeling Approach

How to submit my Glazing for CMA Approval

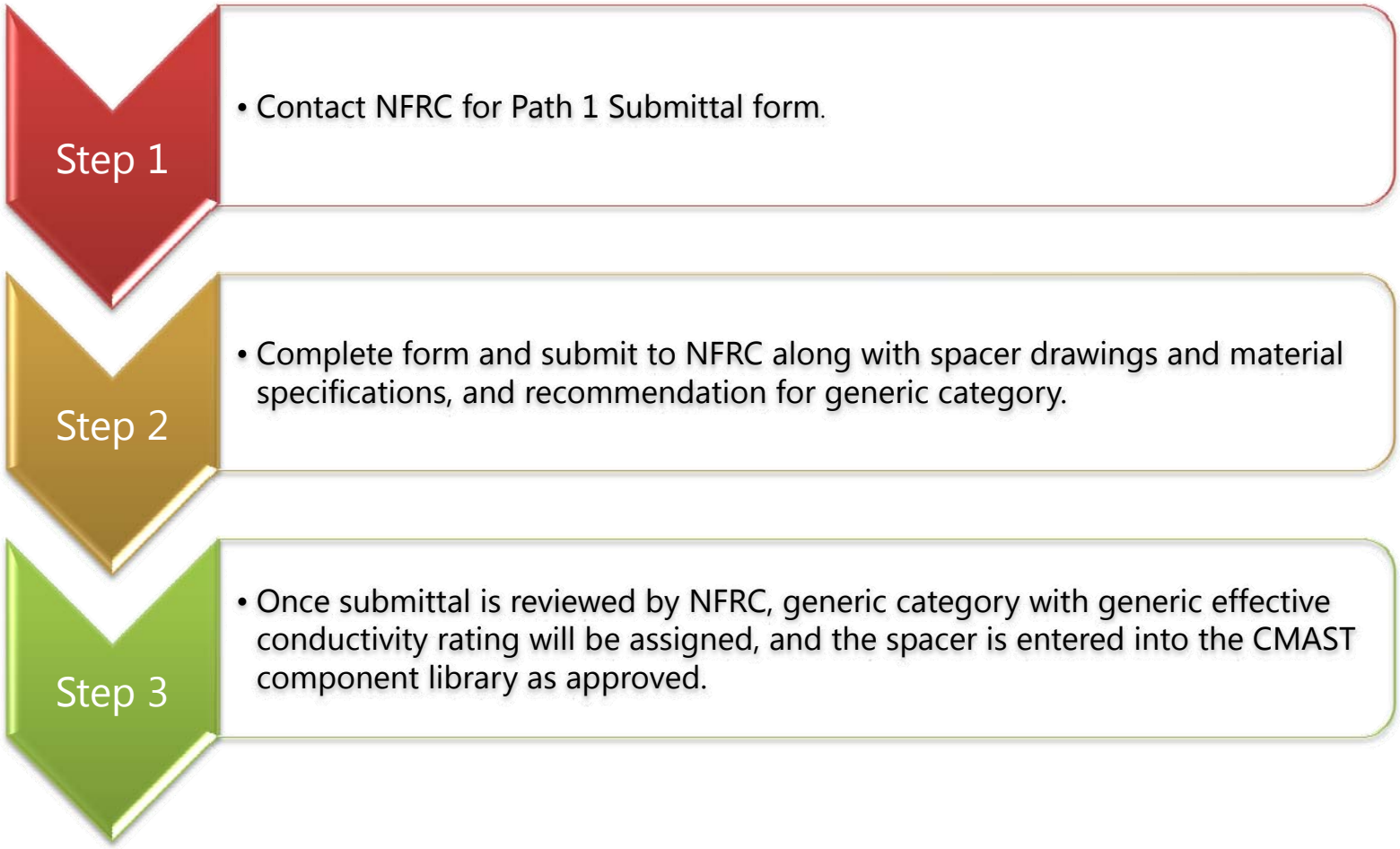
Glazing is approved through NFRC's Spectral Data Program (NFRC 300)



For the appropriate fee schedule and a more detailed step by step procedure of how to submit your product for approval in the CMA PCP, please visit our website.
http://www.nfrc.org/CMAprogram.aspx

Component Modeling Approach

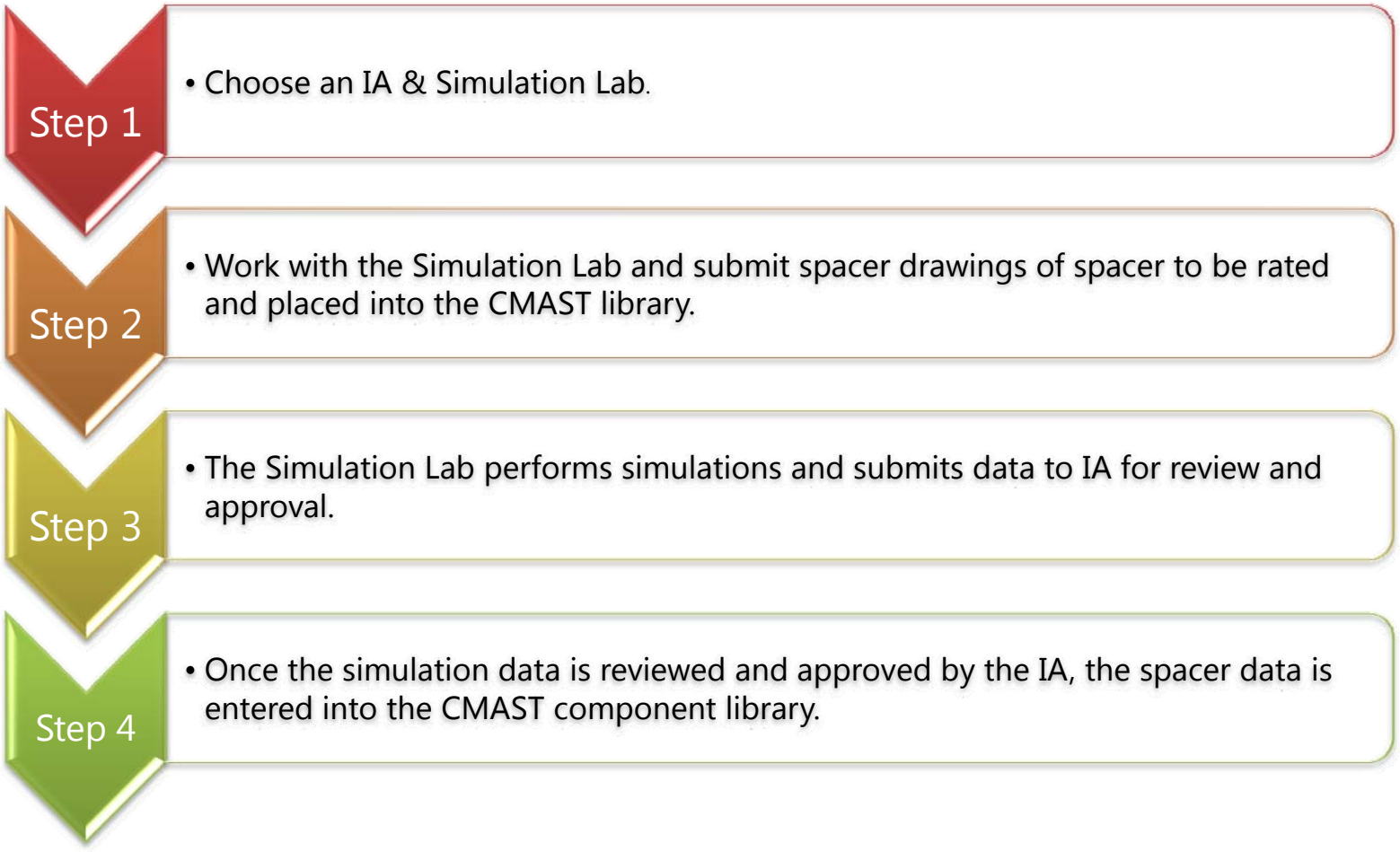
How to submit my Spacer, Path 1 for CMA Approval



For the appropriate fee schedule and a more detailed step by step procedure of how to submit your product for approval in the CMA PCP, please visit our website.
http://www.nfrc.org/CMAprogram.aspx

Component Modeling Approach

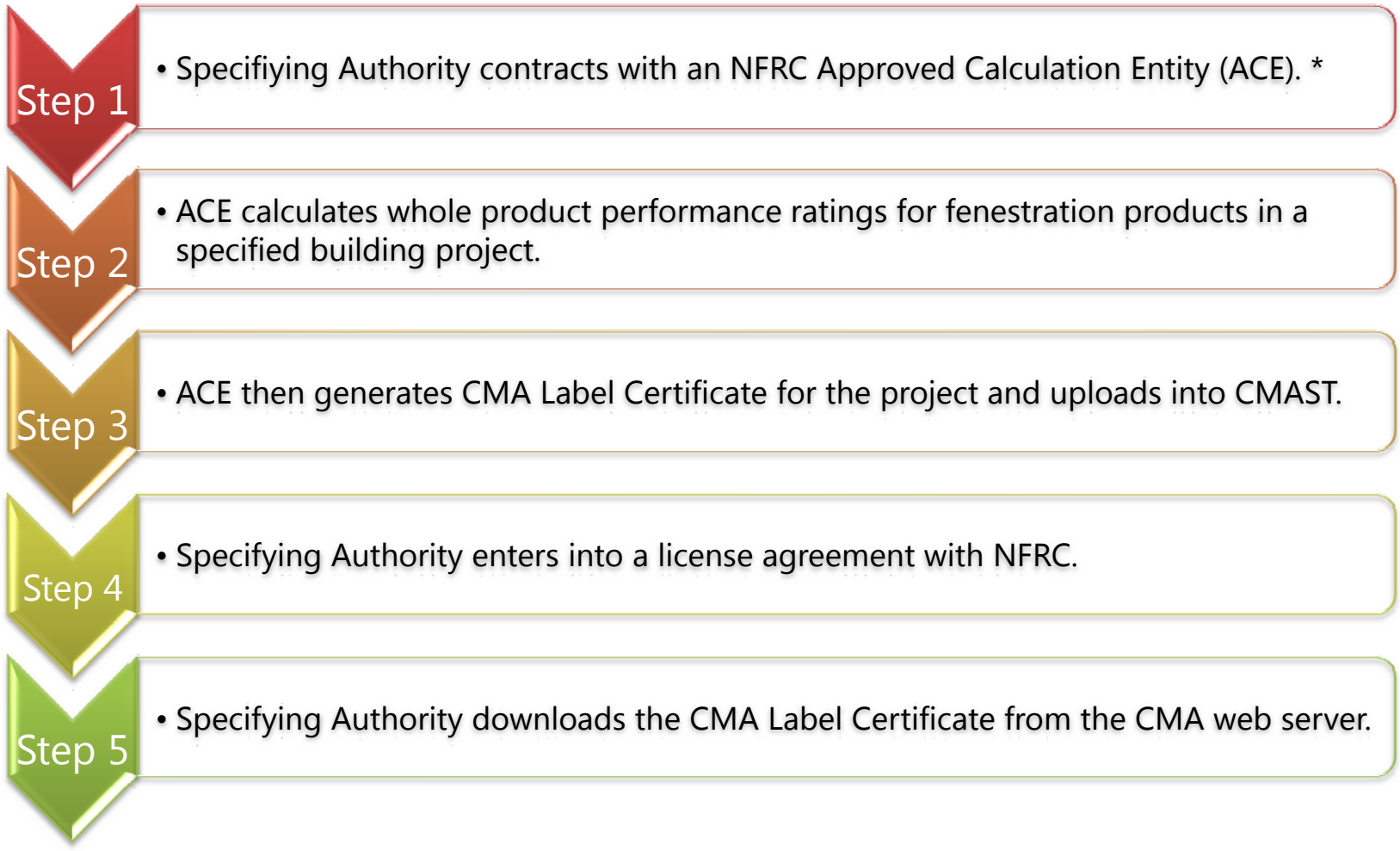
How to submit my Spacer, Path 2 & 3 for CMA Approval



For the appropriate fee schedule and a more detailed step by step procedure of how to submit your product for approval in the CMA PCP, please visit our website.
http://www.nfrc.org/CMAprogram.aspx

Component Modeling Approach

How to obtain a Label Certificate



* Note: ACE Organization refers to both the Manufacturer ACE Organization & Independent ACE Organization.

For the appropriate fee schedule and a more detailed step by step procedure of how to submit your product for approval in the CMA PCP, please visit our website.
http://www.nfrc.org/CMAprogram.aspx

COMPONENT MODELING APPROACH

CMA Contacts Page:
John Lewis
Director, New Programs
Voice: (301) 589-1776, ext. 217
jlewis@nfrc.org

Jen Padgett
CMA Program Coordinator
Voice: (301) 589-1776, ext. 215
jpadgett@nfrc.org